

Mike Marlowe

WITHDRAWN

Geodynamics of the Western Pacific

Geodynamics of the Western Pacific

Edited by
B. J. H. van der Meulen
R. J. P. van der Meulen
C. J. van der Meulen

ADVANCES IN EARTH AND PLANETARY SCIENCES

General Editor:

T. RIKITAKE (Tokyo Institute of Technology)

Editorial Board:

S. AKASOFU (University of Alaska)

S. AKIMOTO (University of Tokyo)

Y. HAGIWARA (University of Tokyo)

H. KANAMORI (California Institute of Technology)

C. KISSLINGER (University of Colorado)

A. MASUDA (University of Kobe)

A. NISHIDA (University of Tokyo)

M. OZIMA (University of Tokyo)

R. SATO (University of Tokyo)

S. UYEDA (University of Tokyo)

I. YOKOYAMA (Hokkaido University)

Advances in Earth and Planetary Sciences 6

Supplement Issue of Journal of Physics of the Earth

Geodynamics of the Western Pacific

**Proceedings of the International Conference on
Geodynamics of the Western Pacific-Indonesian Region
March 1978, Tokyo**

**Edited by
S. Uyeda
R. W. Murphy
K. Kobayashi**



**Center for Academic Publications Japan
Japan Scientific Societies Press
Tokyo**

© CENTER FOR ACADEMIC PUBLICATIONS JAPAN, 1979

All rights reserved. No part of this publication may be reproduced or transmitted in any form or by any means, electronic or mechanical, including photocopy, recording, or any information storage and retrieval system, without permission in writing from the publisher.

Published by:

CENTER FOR ACADEMIC PUBLICATIONS JAPAN

JAPAN SCIENTIFIC SOCIETIES PRESS

2-10, Hongo 6-chome, Bunkyo-ku, Tokyo 113, Japan

Sole distributor for the outside Japan:

BUSINESS CENTER FOR ACADEMIC SOCIETIES JAPAN

20-6, Mukogaoka 1-chome, Bunkyo-ku, Tokyo 113, Japan

JSSP No. 01862-1104

Printed in Japan

PREFACE

Physical and chemical studies of the earth and planets along with their surroundings are now developing very rapidly. As these studies are of essentially international character, many international conferences, symposia, seminars and workshops are held every year. To publish proceedings of these meetings is of course important for tracing development of various disciplines of earth and planetary sciences though publishing is fast getting to be an expensive business.

It is my pleasure to learn that the Center for Academic Publications Japan and the Japan Scientific Societies Press have agreed to undertake the publication of a series "Advances in Earth and Planetary Sciences" which should certainly become an important medium for conveying achievements of various meetings to the academic as well as non-academic scientific communities. It is planned to publish the series mostly on the basis of proceedings that appear in the Journal of Geomagnetism and Geoelectricity edited by the Society of Terrestrial Magnetism and Electricity of Japan, the Journal of Physics of the Earth by the Seismological Society of Japan and the Volcanological Society of Japan, and the Geochemical Journal by the Geochemical Society of Japan, although occasional volumes of the series will include independent proceedings.

Selection of meetings, of which the proceedings will be included in the series, will be made by the Editorial Committee for which I have the honour to work as the General Editor. I and the members of the Editorial Committee will certainly welcome any suggestions that will promote the series. Whenever the convener of a meeting related to earth and planetary sciences is in a position to have to look for a medium for publishing the proceedings please contact us.

Tsuneji Rikitake
General Editor

PREFACE TO VOLUME 6

An international geodynamics conference was held on the 13th to 17th of March, 1978 in Tokyo as a part of the activities of the Geodynamics Project. The Geodynamics Project is an international programme of research on the dynamics and dynamic history of the Earth with emphasis on deep-seated foundations of geological phenomena. This includes investigations related to movements and deformations, past and present, of the lithosphere, and all relevant properties of the Earth's interior and especially any evidence for motions at depth. The programme is an interdisciplinary one, coordinated by the Inter-Union Commission on Geodynamics (I.C.G.) established by the I.C.S.U. at the request of I.U.G.G. and I.G.S.,U. with rules providing for the active participation of all interested I.C.S.U. Unions and Committees.

The Tokyo Conference consisted of two parts. The organization of the Conference was as follows:

Part I.

Geodynamics of the Western Pacific-Indonesian Region

Convenor: S. Uyeda (Tokyo) Co-convenor: R. Murphy (Houston)

Part II.

Physics and Chemistry of Magma Genesis

Convenor: K. Yagi (Sapporo) Co-convenor: S. Akimoto (Tokyo)

Organizer: Inter-Union Commission on Geodynamics, Working Group I (Geodynamics of the Western Pacific-Indonesian Region: chairman, S. Uyeda) and Working Group 5 (Properties and Processes in the Earth's Interior: chairman, O.L. Anderson)

Local Organizing Committee:

Chairman: T. Asada (Tokyo) Secretary General: K. Kobayashi (Tokyo)

Co-sponsored by:

International Association of Seismology and Physics of the Earth's Interior (IASPEI)

International Association of Volcanology and Chemistry of the Earth's Interior (IAVCEI)

International Association of Physical Science of Ocean (IAPSO)

International Union of Geological Sciences—Commission on Experimental Petrology at High Temperatures and Pressures (IUGS-CEP)

Science Council of Japan

Supported by:

The Japan Society for the Promotion of Science

The Seismological Society of Japan

The Volcanological Society of Japan

The Oceanographical Society of Japan

The Society of Terrestrial Magnetism and Electricity of Japan

The Geodetic Society of Japan

The Geological Society of Japan

The Japanese Association of Mineralogists, Petrologists and Economic Geologists

The Mineralogical Society of Japan
The Geochemical Society of Japan
Japan Association for Quaternary Research
Japan Geothermal Energy Association

The Conference was held at the Science Council of Japan, Tokyo, where sessions of the two parts were run simultaneously. The Conference was attended by approximately 300 scientists, including 100 overseas participants from over 17 nations.

At the present stage of solid earth science, great interest is focused on the tectonics of the Western Pacific and Indonesian Region. The interest is indeed two-fold: the tectonics of the oldest part of the ocean floor and that of the subduction zones of great complexity. The exposition of papers and succeeding discussions were naturally extremely lively.

The present volume is the collection of some of the papers presented to Part I, the proceedings of Part II being published in a volume of the *Bulletin Volcanologique*.

Since some important papers are published elsewhere and hence unable to be included in this volume, the number of papers dealing with the Japanese area in this volume became somewhat disproportionately large for the title of the volume. We, however, preferred to keep the original title of the Conference for this volume.

We are grateful to the Ministry of Education, Science and Culture of Japan for its continuous financial support to the Geodynamics Project as well as the organization of this Conference and publication of this volume. Financial support to this Conference by the Japan Society for the Promotion of Science, Inter-Union Commission on Geodynamics and U.N.E.S.C.O. is greatly appreciated.

We would like to express our hearty thanks to the contributors to this volume and to Mr. K. Oshida of the Center for Academic Publications, Japan, for his assistance in compiling this volume. Our thanks are also due to those colleagues who kindly reviewed the papers. Lastly on behalf of the Local Organizing Committee of the Conference, we would like to thank ESSO Sekiyu K.K. and Amoco Japan Exploration Co. for their generous financial assistance to the post-conference field excursion to the Izu-Hakone-Oshima volcanic area.

Seiya Uyeda
Richard Murphy
Kazuo Kobayashi

CONTENTS

Preface.....	v
Preface to Volume 6	vii
Plate Tectonic Evolution of North Pacific Rim	W.R. DICKINSON 1
Speculations on Mountain Building and the Lost Pacifica Continent	A. NUR and Z. BEN-AVRAHAM 21
Benioff Zones, Absolute Motion and Interarc Basin	F.T. WU 39
Oceanic Crust in the Dynamics of Plate Motion and Back-Arc Spreading. .Y. IDA	55
Basic Types of Internal Deformation of the Continental Plate at Arc-Arc Junctions	K. SHIMAZAKI, T. KATO, and K. YAMASHINA 69
Fault Patterns in Outer Trench Walls and Their Tectonic Significance	G.M. JONES, T.W.C. HILDE, G.F. SHARMAN, and D.C. AGNEW 85
Motion of the Pacific Plate and Formation of Marginal Basins: Asymmetric Flow Induction	R.C. BOSTROM 103
The Relationship between Volcanic Island Genesis and the Indo-Australian Pacific Plate Margins in the Eastern Outer Islands, Solomon Islands, South-West Pacific.	G. Wyn HUGHES 123
Upper Mantle Velocity Structure in the New Hebrides Island Arc Region	K.L. KAILA and V.G. KRISHNA 139
Upper Mantle Velocity Structure in the Tonga-Kermadec Island Arc Region ..	K.L. KAILA and V.G. KRISHNA 155
Morphology and Structure of the Southern Part of the New Hebrides Island Arc System	J. DANIEL 181
Palaeomagnetic Evidence for the Rotation of Seram, Indonesia.....	N.S. HAILE 191
A Late Miocene K-Ar Age for the Lavas of Pulau Kelang, Seram, Indonesia	R.D. BECKINSALE and S. NAKAPADUNG RAT 199
A Survey of Paleomagnetic Data on Mexico	S. PAL 203
Southeast Asian Tin Granitoids of Contrasting Tectonic Setting. .C.S. HUTCHISON	221
Seismicity, Gravity and Tectonics in the Andaman Sea	R.K. VERMA, Manoj MUKHOPADHYAY, and N.C. BHUIN 233
Focal Mechanisms and Tectonics in the Taiwan-Philippine Region	T. SENO and K. KURITA 249
Recent Tectonics of Taiwan.....	F.T. WU 265
Tectonics of the Ryukyu Island Arc	K. KIZAKI 301
Explosion Seismic Studies in South Kyushu Especially around the Sakurajima Volcano	K. ONO, K. ITO, I. HASEGAWA, K. ICHIKAWA, S. IIZUKA, T. KAKUTA, and H. SUZUKI 309
Two Types of Accretionary Fold Belts in Central Japan	Y. OGAWA and K. HORIUCHI 321

Permian and Triassic Sedimentary History of the Honshu Geosyncline in the Tamba Belt, Southwest Japan . . .	D. SHIMIZU, N. IMOTO, and M. MUSASHINO	337
Thermal Structure of the Sanbagawa Metamorphic Belt in Central Shikoku . . .	S. BANNO, T. HIGASHINO, M. OTSUKI, T. ITAYA, and T. NAKAJIMA	345
Shimanto Geosyncline and Kuroshio Paleoland . . .	T. HARATA, K. HISATOMI, F. KUMON, K. NAKAZAWA, M. TATEISHI, H. SUZUKI, and T. TOKUOKA	357
Magnetic Stratigraphy of the Japanese Neogene and the Development of the Island Arcs of Japan . . .	N. NIITSUMA	367
Regional Characteristics and Their Geodynamic Implications of Late Quaternary Tectonic Movement Deduced from Deformed Former Shorelines in Japan . .	Y. OTA and T. YOSHIKAWA	379
Magnetic Anomalies and Tectonic Evolution of the Shikoku Inter-Arc Basin . .	K. KOBAYASHI and M. NAKADA	391
A Compilation of Magnetic Data in the Northwestern Pacific and in the North Philippine Sea . . .	N. ISEZAKI and H. MIKI	403
Collision of the Izu-Bonin Arc with Central Honshu: Cenozoic Tectonics of the Fossa Magna, Japan . . .	T. MATSUDA	409
Flow under the Island Arc of Japan and Lateral Variation of Magma Chemistry of Island Arc Volcanoes . . .	M. TORIUMI	423
Seismic Activity and Pore Pressures across Island Arcs of Japan . . .	N. FUJII and K. KURITA	437
Aseismic Belt along the Frontal Arc and Plate Subduction in Japan . . .	K. YAMASHINA, K. SHIMAZAKI, and T. KATO	447
Tsunamicity of Sanriku Depends on Subduction Tectonics . . .	Wm. M. ADAMS	459
Seismic Studies of the Upper Mantle beneath the Arc-Junction at Hokkaido: Folded Structure of Intermediate-Depth Seismic Zone and Attenuation of Seismic Waves . . .	T. MORIYA	467
Sedimentary Patterns in Apparent Back-Arc Basins: A Case Study of the Neogene Sequence in Northwestern Hokkaido, Japan . . .	H. OKADA	477
Velocity Anisotropy in the Sea of Japan as Revealed by Big Explosions . . .	H. OKADA, T. MORIYA, T. MASUDA, T. HASEGAWA, S. ASANO, K. KASAHARA, A. IKAMI, H. AOKI, Y. SASAKI, N. HURUKAWA, and K. MATSUMURA	491
Geodynamics of the North-Eastern Asia in Mesozoic and Cenozoic Time and the Nature of Volcanic Belts . . .	L.M. PARFENOV, I.P. VOINOVA, B.A. NATAL'IN, and D.F. SEMENOV	503
The Crustal Structure and Origin of the Basins of Japan Sea and Some Other Seas of the Circum-Pacific Mobile Belt . . .	P.N. KROPOTKIN	527
Major Strike-Slip Faults and Their Bearing on Spreading in the Japan Sea . . .	K. OTSUKI and M. EHIRO	537
Significant Eruptive Activities Related to Large Interplate Earthquakes in the Northwestern Pacific Margin . . .	M. KIMURA	557
A Mechanism to Explain the Earthquakes around Japan by the Process of Partial Melting . . .	M. HAYAKAWA and S. IIZUKA	571
The Formation of Intermediate and Deep Earthquake Zone in Relation to the Geologic Development of East Asia since Mesozoic . . .	Y. SUZUKI, K. KODAMA, and T. MITSUNASHI	579
Subject Index . . .		585
Geographical Index . . .		591

PLATE TECTONIC EVOLUTION OF NORTH PACIFIC RIM

William R. DICKINSON

Geology Department, Stanford University, Stanford, California, U.S.A.

(Received May 22, 1978)

The North Pacific Rim is a segment of the circum-Pacific orogenic belt lying along the great circle between Mesoamerica and Indochina. Paleotectonic reconstructions rely upon integration of information about rocks exposed on land, crustal thicknesses, paleolatitudes of crustal blocks, sediment layers cored at sea, and geomagnetic anomalies. Continental margins have been modified by accretion of oceanic materials during subduction, suturing of continental blocks by collision, and opening or trapping of marginal seas. Prior to the breakup of Pangaea, a vast Paleopacific seafloor was built by spreading coeval with the subduction that elsewhere assembled Pangaea. After the breakup of Pangaea, circum-Pacific subduction accreted deformed increments of the Paleopacific seafloor to the edges of continental blocks now along the North Pacific Rim. Cretaceous crustal collisions closed the North Pacific Rim and isolated the Arctic Ocean. Paleogene accretion of the continental Okhotsk block caused subduction to shift from the Bering shelf edge to the Aleutian chain. The elbow in the Emperor-Hawaii hotspot track records a change in Pacific plate motion at about the same time. Current circum-Pacific arcs include east-facing island arcs and west-facing continental arcs in a consistent pattern that implies net westward drift of continental lithosphere with respect to underlying asthenosphere.

1. *Introduction*

The northern margin of the Pacific Ocean extends from Central America on the east to the Philippine Sea on the west, and has the Bering Sea at its northern extremity. This North Pacific Rim lies along a global great circle upon which Japan and California are spaced about 90° apart. A continuation of the same great circle down the western side of the Americas leads to Chile, which lies about the same angular distance from California as does Japan. In the study of circum-Pacific tectonics, we must thus apply to the geology of the North Pacific Rim the same kind of integrated view that we should apply also to the western Cordilleras of the Americas. For example, British Columbia, Alaska, and Kamchatka form a single continuous segment of the circum-Pacific belt as surely as do the Latin American countries from Mexico through Columbia to Ecuador and Peru.

The purpose of this paper is to review the general status of our understanding about the plate tectonic history of the North Pacific Rim. Many details of present knowledge are omitted to allow a focus on broad relationships. My interest in the questions discussed was stimulated especially by my trip to Japan in 1976 as a visitor at the Earthquake Research Institute of the University of Tokyo, where I was a participant in the scientist exchange program sponsored by the American Geophysical Union and supported by the U.S. National Science Foundation under the U.S.-Japan Cooperative Science Program in liaison with the Japan Society for the Promotion of Science. My subsequent work was supported by the U.S. National Science Foundation with Grants EAR75-14568 and EAR77-27542.

2. Overview

The present configuration of the Pacific borders of North America and Eurasia, and the present geologic relationships of rock assemblages within the continental margins, is the result of long-continued processes of tectonic evolution within the circum-Pacific orogenic belt. Valid paleogeographic and paleogeologic reconstructions of these lands that are now part of the North Pacific Rim must be based on the integration of several kinds of data:

- a) distribution and age of diagnostic rock assemblages mapped on land,
- b) varying crustal thicknesses on land and at sea,
- c) paleomagnetic data on paleolatitudes for different continental blocks,
- d) patterns of geomagnetic anomalies on the deep-sea floor,
- e) information on sediment thicknesses and facies from deep-sea drilling.

Data from the deep sea applies directly only to times since the mid-Mesozoic, for no pre-Jurassic seafloor is known in the Pacific Ocean. In common with those in the Atlantic and Indian oceans, Pacific seafloor anomalies thus provide some record of events since the breakup of Pangaea, but not before.

The major types of tectonic events that have affected the Pacific Rim since the Mesozoic breakup of Pangaea include:

- a) the subduction and accretion of oceanic materials during plate consumption at various bounding trenches,
- b) the collision and suturing of microcontinental blocks against the surrounding continental margins,
- c) the opening of interarc basins to form or expand marginal seas lying mainly on the western side of the open ocean,
- d) the cancellation of spreading centers (or belts) by rise-trench encounters occurring mainly on the eastern side of the ocean,
- e) the development of marginal and intracontinental transforms causing strike slip either longitudinal or transverse to associated continental margins.

Prior to the breakup of Pangaea, the world ocean Panthalassa was mainly a paleo-Pacific realm (DICKINSON, 1977a, b), and the Tethys Sea can be regarded as a gulf of the Paleopacific Ocean (Fig. 1) during Permo-Triassic time. In Permo-Carboniferous time, the earlier assembly of Pangaea (IRVING, 1977) presumably required subduction of ocean floor to allow Laurasia and Gondwana to be sutured together west of the Tethyan gulf. Late Paleozoic subduction can be inferred along both the Hercynian-Variscan (and Appalachian-Ouachita) orogenic belts of Laurasia and the Gondwanide-Tasmanide orogenic trend of Gondwana (see Fig. 1). Coeval spreading within the Paleopacific Ocean was presumably required to maintain a global mass balance. Subduction at continental margins facing the Paleopacific Ocean was apparently not required prior to the later breakup of Pangaea.

The oldest granitic components in batholiths of the circum-Pacific orogenic belt do not date much beyond about 200 my, which was near the Triassic-Jurassic boundary. This fact suggests that the present regime of subduction beneath continental margins now facing the Pacific Ocean was not established before about mid-Triassic time. Since then, circum-Pacific and Alpine-Himalayan subduction have been paired in time with opening of the Atlantic and Indian oceans. Widespread mid-Carboniferous to mid-Triassic

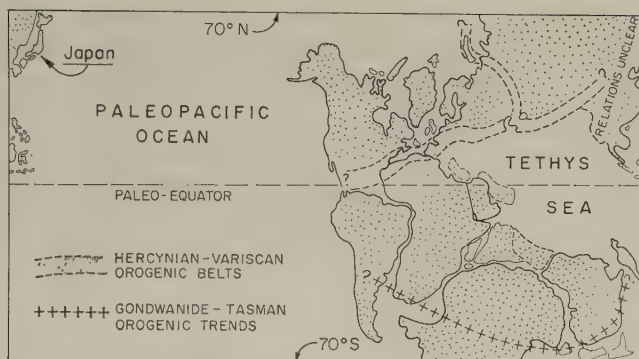


Fig. 1. Inferred Triassic world map (Mercator projection) showing Pangaea and the large Paleopacific Ocean. Japan is restored against Eurasia but remnant oceans within Eurasia are not shown (Indonesian islands depicted in present configuration for orientation only). From DICKINSON (1977b).

oceanic facies exposed now within the circum-Pacific orogenic belt of the North Pacific Rim apparently represent deformed increments of the old Paleopacific seafloor now incorporated into the margins of continental blocks. They were accreted tectonically to the edges of North America and Eurasia by Mesozoic subduction as seafloor spreading generated younger Pacific seafloor farther offshore. No vestige of the once vast Paleopacific seafloor remains within the confines of the present Pacific Ocean.

The enclosed outline of the North Pacific Rim did not attain its present overall shape until the closure of late Mesozoic suture belts welded the Eurasian and American continental blocks together across the Alaska-Bering-Yakutia region (CHURKIN, 1972). Full details of this complex process will not be known until the plate tectonic evolution of the Arctic Ocean is better documented.

3. Current Tectonics

Figure 2 is a sketch map showing key tectonic features of the North Pacific Rim and the adjacent Pacific Ocean. Volcanic chains that mark active magmatic arcs stand parallel to active subduction zones at trenches, but are absent elsewhere around the periphery of the ocean. Young seafloor marks the crests of active midoceanic rises and forms the floor of active interarc basins. The Emperor Seamounts chain and the Hawaiian Ridge form linked segments of a hotspot track generated by the hotspot now beneath Hawaii (MORGAN, 1972). The Emperor-Hawaii elbow evidently records a marked change in the motion of the Pacific plate with respect to the hotspot about 40 mybp (DALRYMPLE and CLAGUE, 1976).

On Fig. 2, Japan and California appear to lie on opposite sides of an intervening ocean, but this erroneous impression reflects distortion that is inherent in the customary Mercator projection used as a base map. In reality, the North Pacific Rim is a belt that approximates a great circle (see Fig. 2, inset). Figure 3 is a tectonic sketch map showing much the same information as Fig. 2, but drawn using a projection upon which that great circle plots as a straight line. Japan and California are thus shown correctly as lying on the

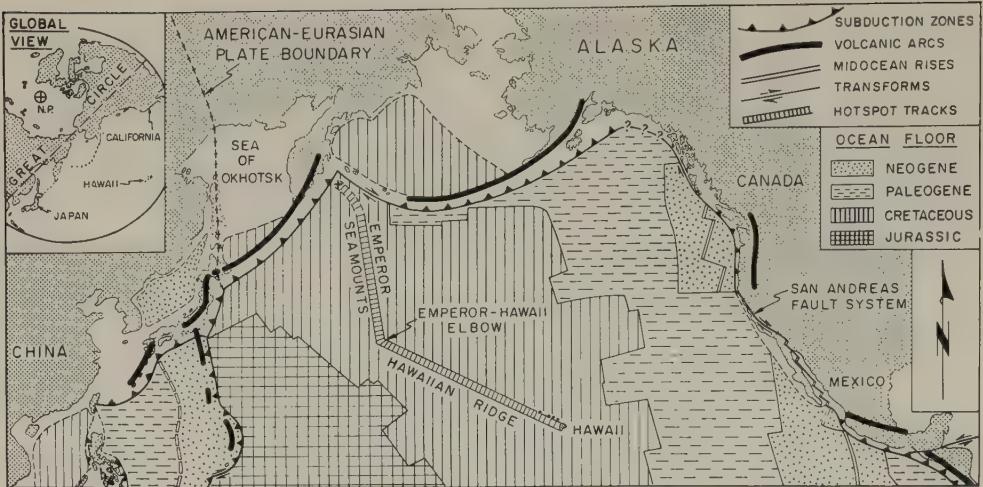


Fig. 2. Current tectonic elements of the North Pacific Rim and the northern Pacific Ocean shown on a standard Mercator projection. Seafloor ages modified after PITMAN *et al.* (1974) and HILDE *et al.* (1977). American-Eurasian plate boundary after CHAPMAN and SOLOMON (1976).

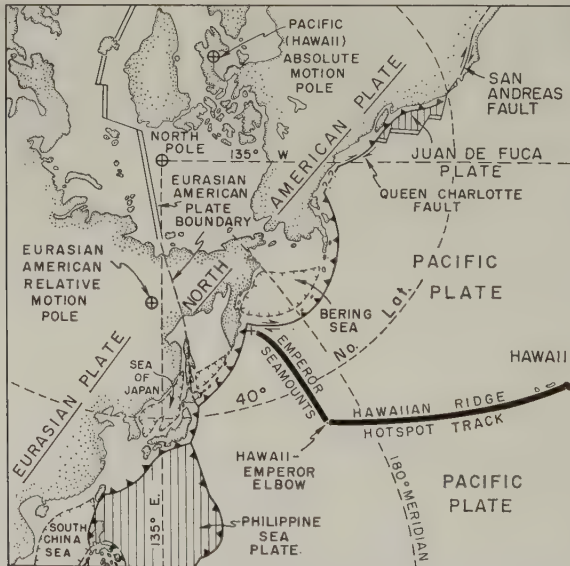


Fig. 3. Current tectonic framework of the North Pacific Rim plotted on a projection showing that segment of the circum-Pacific great circle as a linear belt bordering the northern Pacific Ocean. Double line denotes Atlantic spreading center; subduction zones shown as on Fig. 2.

same continuous margin of the Pacific Ocean. The ocean in reality has no "sides" because its whole periphery approximates the great circle that delimits the watery hemisphere of the earth.

Nevertheless, Figs. 2 and 3 both reflect a distinct east-west asymmetry in Pacific

tectonics (NELSON and TEMPLE, 1972). In the open ocean, spreading centers lie well to the east of the central meridian within the oceanic region. The continental margins with subduction zones also have different characters. On the western "side" of the ocean, east-facing island arcs are associated with marginal seas formed by interarc spreading. On the eastern "side" of the ocean, west-facing magmatic arcs stand on the edges of intact continental blocks. These differences imply some fundamental distinction between subduction systems where seafloor is being subducted either eastward or westward beneath continental margins that have generally meridional orientations.

4. *Backarc Behavior*

Although the rates of tectonic and sedimentary accretion vary in the forearc region between the trench and the volcanic chain, evolutionary trends are similar in all arc-trench systems (DICKINSON, 1973a). In the backarc region, however, two opposite extremes of behavior are noted (DICKINSON, 1972, 1973b, 1974a, b):

a) Behind some intra-oceanic arcs, seafloor spreading within an interarc basin widens the marginal sea that separates the island arc from the nearby continental margin; this process involves separation of lithosphere and upwelling of asthenosphere to form new oceanic lithosphere in the backarc region.

b) Behind some continental-margin arcs, fold-thrust belts form a subsidiary mountain chain that rises between the volcanic chain and the adjacent continental interior; this process involves contraction of lithosphere, crustal thickening within the mountain belt, and the development of a retroarc foreland basin on a depressed part of the continental block in the backarc region.

For a third and intermediate style of backarc behavior, neither process occurs.

Several workers have discussed the probable plate motions associated with backarc spreading and backarc thrusting (HAVEMANN, 1972; HYNDMAN, 1972; MOBERLY, 1972; WILSON and BURKE, 1972). In general, advective heat flow associated with arc magmatic activity apparently softens the lithosphere along the trend of the arc, and thus allows lithosphere in the backarc region to move independently of the narrow sliver of lithosphere occupying the band between arc and trench. The arc structure itself remains in place above the descending slab of lithosphere being subducted. The sliver plate in the arc-trench gap is thus constrained to maintain its position relative to the flexure where lithosphere bends at the subduction zone to descend into the mantle. Meanwhile, backarc lithosphere is able to shift position with respect to that flexure.

Two fundamental causes of relative motion between the backarc lithosphere and the flexure in the subducted slab of lithosphere have been suggested (e.g., MOLNAR and ATWATER, 1978; UYEDA and KANAMORI, 1979):

a) One mechanism considers the tendency of the descending slab to sink into the asthenosphere. Where the sinking slab is old and thick, with a high bulk density, the rate of sinking is fast in relation to the rate of plate convergence across the arc-trench system; the flexure in the descending slab thus tends to migrate oceanward, and backarc spreading accommodates the resulting extension as the arc-trench system pulls away from backarc lithosphere. Where the sinking slab is young and thin, with a low bulk density, the rate of sinking is slow in relation to the rate of plate convergence across the arc-trench system; the flexure in the descending slab thus tends to migrate landward, and backarc

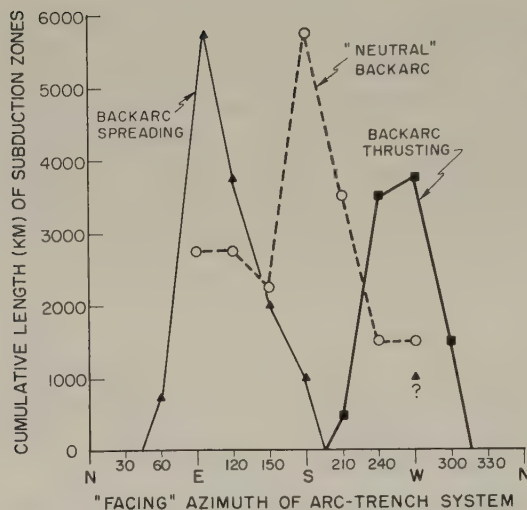


Fig. 4. Plot showing relationship between Cenozoic backarc tectonics and geographic orientation of associated arc-trench systems. "Facing" azimuth is given by a line drawn normal to the subduction zone and leading away from the trench side of the system. See text for discussion.

thrusting accommodates the resulting contraction as the arc-trench system presses against the backarc lithosphere.

b) The other mechanism considers potentially independent motions of the backarc lithosphere with respect to underlying asthenosphere. The descending slab is held to anchor the arc-trench system with respect to the part of the asthenosphere into which the slab is being inserted. Backarc spreading then occurs where backarc lithosphere is skidding away from the flexure in the descending slab, and backarc thrusting occurs where backarc lithosphere is skidding toward the flexure in the descending slab.

The two mechanisms are not mutually exclusive, and each may serve to reinforce or counteract the effect of the other in a particular case.

A census of modern arc-trench systems (Fig. 4) shows that backarc spreading is characteristic of those that face eastward (subduction downward to the west), whereas backarc thrusting is most widespread in those that face westward (subduction downward to the east). Although "neutral" systems that lack either backarc spreading or backarc thrusting are known to face both eastward and westward, they are most typically southward-facing (northward-facing arcs are absent on the modern earth). Consequently, backarc spreading is typical for arcs along the western periphery of the Pacific and backarc thrusting is common for arcs along the eastern periphery of the Pacific. Figure 5 is a schematic diagram of standard relations across the modern Pacific.

The east-west dichotomy of current arc behavior and the east-west asymmetry of the modern Pacific Ocean may be wholly fortuitous products of plate motions that are currently suitable for that pattern but are directionally random over the long term. How-

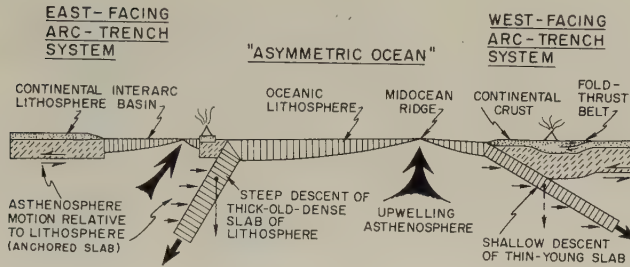


Fig. 5. Diagram showing characteristic east-west asymmetry of placement of midoceanic rise and east-west dichotomy of backarc behavior. See text for discussion.

ever, several workers have suggested that the present relationships are the systematic result of net shear between lithosphere and asthenosphere (BOSTROM, 1971; KNOPOFF and LEEDS, 1972; MOORE, 1973). Such shear may be inherent between these two loosely coupled layers of the outer earth as the rotation of the earth decelerates. Westward lag of the lithosphere layer above asthenosphere that rotates faster could account for both the dichotomy of arc behavior and the asymmetry of the ocean (see Fig. 5):

a) For east-facing subduction zones (subduction downward to the west), backarc lithosphere would move away from the arc-trench system, which would be anchored by a steepened slab.

b) For west-facing subduction zones (subduction downward to the east), backarc lithosphere would move toward the arc-trench system, which would be anchored by a slab being entrained beneath overriding lithosphere.

c) Gradual eastward migration of midocean rises relative to bounding continental margins might occur in response to the interaction between asthenosphere and the portions of plates of lithosphere that are inserted into the asthenosphere as descending slabs. West-facing continental margins would tend to override and entrain eastward-subducting plates, and thus to encroach upon the eastern flanks of midocean rises. Slabs of differing age, thickness, and consequent negative buoyancy would thus come to descend on eastern and western borders of the ocean. The contrast would be such as to reinforce the behavioral tendencies established for east-facing and west-facing arc-trench systems (see Fig. 5). Moreover, interaction between lithosphere and asthenosphere would help to steepen the angle of descent of westward-subducting plates and to press the zone of plate flexure away from associated east-facing continental margins, whereas the angle of descent of eastward-subducting plates could be reduced and their zones of flexure pressed toward associated west-facing continental margins.

The relationships depicted by Fig. 4 seem too clearcut to be wholly coincidental, and hence suggest that the rotational effects are real.

5. Late Cenozoic Tectonics

For tectonic reconstructions during the Cenozoic, the key feature in the northern Pacific Ocean is the Emperor-Hawaii hotspot track (Figs. 2, 3). During the past 40 my, the Hawaiian Ridge has been generated by movement of the Pacific plate over the Hawaii hotspot at an essentially constant rate (DALRYMPLE *et al.*, 1977). Figure 6 shows inferred

relationships in the northern Pacific Ocean during that time span. Prior to 40 mybp, back to about 70 mybp, movement of the Pacific plate over the Hawaii hotspot at a similar rate, but in a more northerly direction, generated the Emperor Seamounts. Both paleomagnetic and paleoecologic data confirm the requisite northward motion of the seamounts during the Cenozoic (MARSHALL, 1978; GREENE *et al.*, 1978).

Figure 6 indicates that the existence of the Meiji sediment tongue of Neogene terrigenous clay (SCHOLL *et al.*, 1977) cannot be used as a valid argument against such motion of the Pacific seafloor. The area near Meiji seamount has occupied positions close to

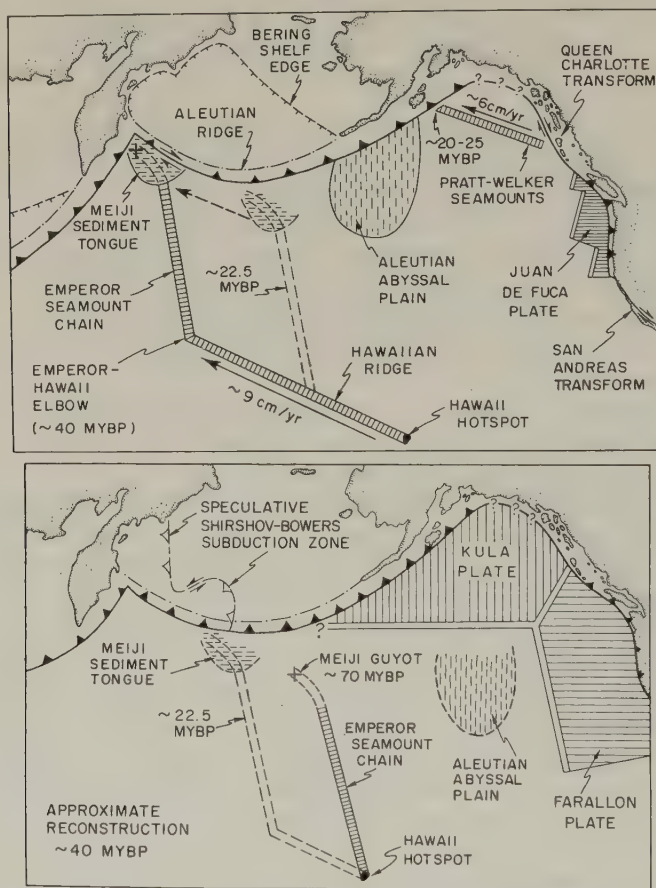


Fig. 6. Sketch maps showing key tectonic elements in the northern Pacific Ocean at present (above) and 40 mybp (below). Approximate position of Emperor Seamount chain is shown also at 22.5 mybp (Oligocene-Miocene boundary) on each plot. Rates of generation of Hawaiian and Pratt-Welker hotspot tracks modified after DUNCAN and McDougall (1976), JARRARD and CLAGUE (1977), and DALRYMPLE *et al.* (1977). Plate boundaries and continental configurations at 40 mybp modified after COOPER *et al.* (1976), STONE and PACKER (1977), and PITMAN and TALWANI (1972).

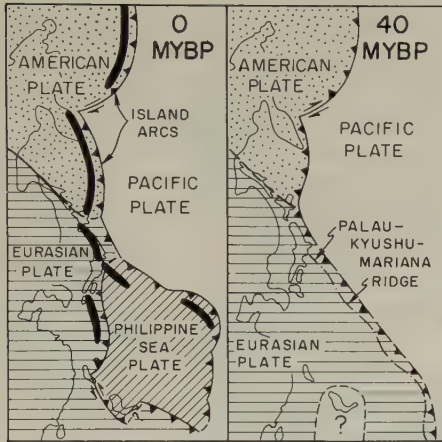


Fig. 7. Configurations of western North Pacific plate boundaries and island arcs at present (left) and 40 mybp (right). See text for discussion.

sediment sources along the Aleutian Ridge since the sediment tongue first began to form. However, the restored position of the Aleutian abyssal plain is problematical (MARLOW *et al.*, 1973; SCHOLL *et al.*, 1975, 1977), because the source terrane for its mid-Cenozoic turbidites lay somewhere along the continental margin between Vancouver Island and Kodiak Island (STEWART, 1976). The reconstruction of Fig. 6 implies that unsuspected complexities in the configuration of plate boundaries may have existed in the northeastern corner of the mid-Cenozoic Pacific. BYRNE (1978) has recently argued that the Kula-Pacific spreading center ceased operating about 57.5 mybp. If this idea is confirmed, the Kula plate is incorrectly included in Fig. 6 (below) for 40 mybp, and no plate boundary would have been present to block the delivery of mid-Tertiary turbidites from sources along the northeastern margin of the Pacific to the Aleutian abyssal plain on the Pacific plate.

In the western Pacific, interarc seafloor spreading (KARIG, 1970) behind east-facing island arcs has opened the Sea of Japan (MATSUDA and UYEDA, 1971; SILLITOE, 1977) and broadened the Philippine Sea (TOMODA *et al.*, 1975; WATTS *et al.*, 1977) since the early Cenozoic. Figure 7 shows the changing configuration of island arcs within this region during the time span represented by Fig. 6. At 40 mybp, the Marianas frontal arc and the Palau-Kyushu remnant arc were united as a single ancestral island arc (KARIG, 1971). Past plate configurations in the area of the Philippine Islands are problematical (KARIG, 1973). In Taiwan and the Ryukyus along the western side of the Philippine Sea, no subduction was underway in the middle parts of the Cenozoic (MURPHY, 1973). Complex strike slip is implied for the Sakhalin region during formation of the Sea of Japan, but the restoration depicted in Fig. 7 is schematic only.

Along the American border of the North Pacific (Fig. 8), the major events during the late Cenozoic were (a) ridge or rise subductions that occurred as the asymmetry of the ocean basin was accentuated by consumption of the Kula plate and most of the Farallon plate, (b) generation of the San Andreas and Queen Charlotte transform systems as the Pacific plate came into contact finally with the American plate, and (c) development of the extensional Basin and Range province by incipient disruption of the American plate in the region adjacent to the San Andreas transform.

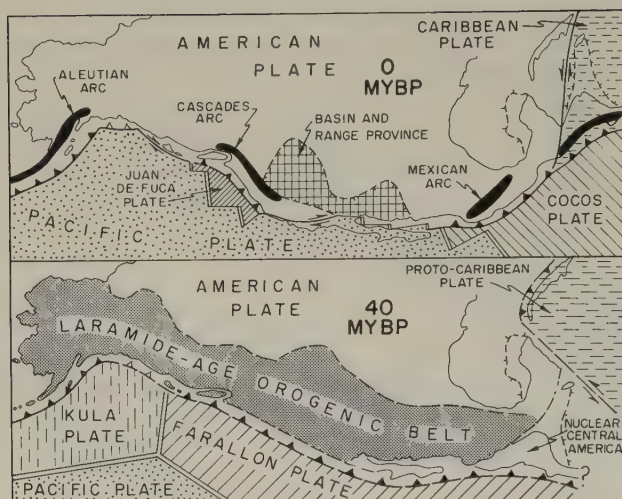


Fig. 8. Configurations of eastern North Pacific plate boundaries and subduction zones at present (above) and 40 mybp (below). See text for discussion.

6. Rise-Trench Encounter

So-called ridge or rise subduction is better described as rise-trench encounter. Generation of new lithosphere is the dominant process at a rise or ridge crest, but can occur only near the surface of the earth. Only there does plate separation involve the kind of pressure release required to trigger partial melting of the asthenosphere on a large scale, and only there can heat loss be rapid enough to chill upwelling material sufficiently to form new lithosphere. When a rise and a trench meet after the intervening plate has been consumed, the zone of plate separation that is marked by a discrete ridge crest at the surface will no longer form such a discrete belt where it becomes subterranean. The overall plate kinematics do require that the wholly consumed plate descend into the mantle faster than the plate on the other side of the rise or ridge crest (else no plate separation occurs!). As the zone of separation between the two is drawn into a subterranean position, however, it is marked by a broad and expanding region of sublithospheric mantle upwelling, and not by a belt of steady-state width where new lithosphere is created, as would occur at the surface.

Rise-trench encounter can cause two different but related results depending upon whether the plate beyond the rise or ridge crest is subducted or not following the encounter:

a) Where it is subducted, as happened along the Aleutian trench following a mid-Cenozoic encounter with the Kula-Pacific ridge (DeLong *et al.*, 1978), several distinct but simultaneous events punctuate the geologic history of the arc-trench system. These serve to record the rise-trench encounter as a discontinuity in the evolution of the Aleutian Ridge. The genetically related effects stem either from the temporary absence of a descending slab beneath the arc-trench system, or from the high heat flow and thermal expansion imposed across the arc-trench system while the cold subterranean slab was absent (DeLong and Fox, 1977). The changing thermal regime was reflected by an episode of broad uplift affecting the whole arc-trench system, and by a pulse of metamorphism at

crustal levels. A temporary cessation of arc magmatism extinguished the volcanic chain while no subducted slab was present.

b) Where it is not subducted, the trench is converted to a transform like the modern San Andreas, which lengthens as the triple junctions at either end migrate away from one another. In this case, a gradually expanding region that lacks a subducted slab develops in a triangular form adjacent to the transform (DICKINSON and SNYDER, 1979b). This no-slab region occupies the space above a gradually enlarging window or hole in the descending slab. Arc magmatism is extinguished where a descending slab is absent, and upwelling of asthenosphere to occupy the slab-window can contribute also to uplift and extensional tectonics within a region of triangular shape adjacent to the transform. Figure 9 depicts these relationships for the San Andreas transform system and the Basin-and-Range province adjacent to it. Note the following geometric relationships shown: (a) the gradual shortening of the Cascades volcanic arc as the expansion of the no-slab region above the slab-window in the descending Farallon plate expanded to extinguish the southern extension of the arc in progressive fashion through the Neogene, (b) the overall coincidence between the inferred extent of the modern no-slab region and the known extent

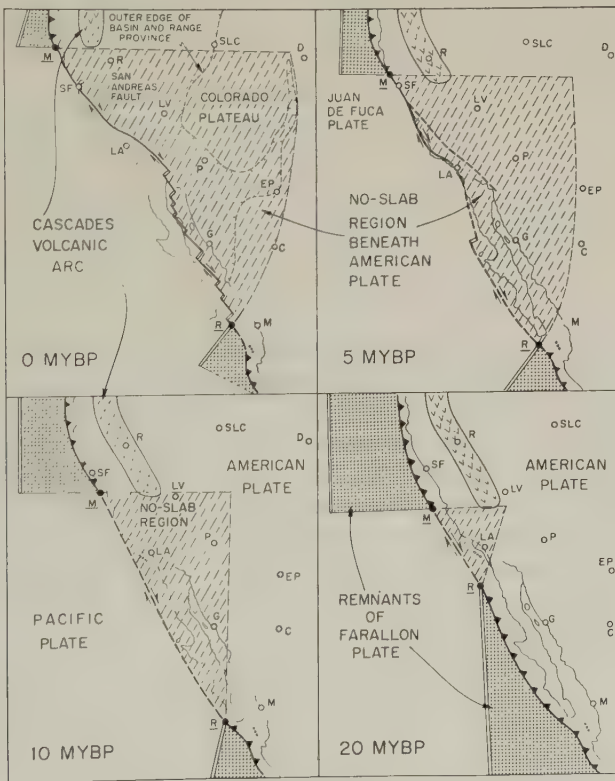


Fig. 9. Sketch maps showing evolution of the San Andreas coastal transform system and an adjacent subcontinental region of triangular shape lacking a subducted slab. After DICKINSON and SNYDER (1979a, b). See text for discussion. Points *M* and *R* are Mendocino and Rivera triple junctions, respectively.

of uplifted and block-faulted continental crust underlying the Basin-and-Range province and Colorado Plateau where mantle upwelling through the slab-window is to be expected, and (c) the manner in which the site of the San Andreas transform boundary between Pacific and American plates has shifted gradually inland from an original position near the continental slope to its present location along the San Andreas fault proper.

In either scenario for events that follow rise-trench encounter, thermal effects near triple junctions that terminate rise crests at the trench may promote anatectic melting of otherwise cold subduction complexes (MARSHAK and KARIG, 1977). This effect can give rise to magmatism at sites anomalously close to the trench. Small plutons and volcanic fields of Cenozoic age in the coastal regions of California, Alaska, and Japan may all stem from this potential effect of rise-trench encounter.

7. *Early Cenozoic Tectonics*

Latest Cretaceous and earliest Cenozoic tectonics in the western Cordillera of North America were dominated by the Laramide Orogeny. In the central part of the Cordillera where the deformation was most characteristic, fault-bounded uplifts and intervening sediment-filled depressions developed across a broad arc massif that was essentially dormant magmatically. This style of diastrophism occurred during the period from 70 to 40 mybp, and was most intense at about 55 mybp in the Wyoming and Colorado Rockies. The classic Laramide orogenic style, essentially amagmatic with basement involvement in contractional structures, can be attributed to underthrusting of a subducted plate at a low angle beneath the continental plate (CONEY, 1976, 1978). This inference is based on the areal distribution of subduction-related igneous suites having varied alkalinity and potassicity (LIPMAN *et al.*, 1971). This shallow mode of plate consumption contrasts with the more normal steep mode that generates arc magmatism (see Fig. 10). Where the descending plate dives steeply into the asthenosphere, magmas are generated (BARAZANGI and ISACKS, 1976), and a standard type of arc orogen develops. Where the descending plate scrapes along beneath the overriding plate, magmatism is suppressed and buckling of the overriding plate causes the basement-cored uplifts of a Laramide-style orogen (DICKINSON and SNYDER, 1978).

Pacific asymmetry that dictates the presence of spreading centers in comparative proximity to the American coasts means that relatively young lithosphere is subducted beneath the Americas (see Fig. 8). Plate buoyancy may thus commonly promote Laramide-type phases of evolution for west-facing American arc massifs, whereas similar deformation may never or seldom affect east-facing Eurasian island arcs. In this sense, Laramide-style deformation is akin genetically to backarc thrusting and is incompatible with backarc spreading (CONEY, 1972).

The prominent elbow in the Emperor-Hawaii hotspot track (Figs. 2, 3, and 6) reflects an abrupt change in the direction of Pacific plate motion across the Hawaii hotspot at about 40 mybp. The movement of a subducting plate is governed mainly by the descending slabs attached to it at subduction zones (FORSYTH and UYEDA, 1975; CHAPPLE and TULLIS, 1977). In effect, the pull of the slab as it falls into the mantle causes the plate to skid over the asthenosphere. Consequently, the most direct way to affect the overall motion of the Pacific plate is to change the configuration of the subduction zones at its boundaries.

Tectonic relations across northeastern Eurasia between the Bering Sea and the Hok-

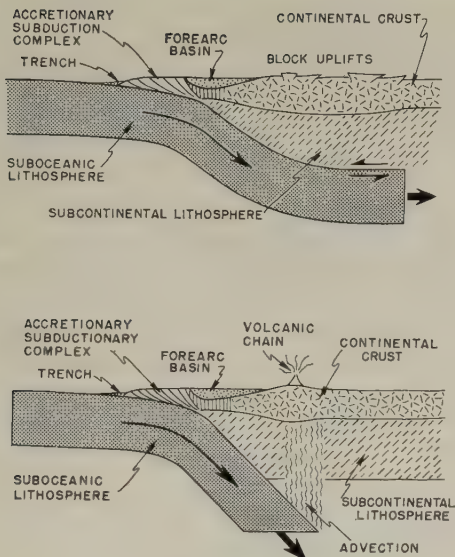


Fig. 10. Diagrams illustrating amagmatic Laramide-style shallow subduction (above) and more ordinary steeper subduction (below) that generates arc magmatism. After DICKINSON and SNYDER (1978).

kaido-Sakhalin region suggest a major change in plate boundaries during the early Cenozoic. Most of the Sea of Okhotsk is underlain by continental crust at least twice as thick as standard oceanic crust (BURK and GNIBIDENKO, 1977). Despite this, a calc-alkalic volcano-plutonic belt lay west and north of the present Sea of Okhotsk during the Late Cretaceous and early Cenozoic (ZONENSHAIN *et al.*, 1974). These relations suggest that a microcontinental Okhotsk block of unknown origin lodged against the margin of Eurasia during the early Cenozoic (DEN and HOTTA, 1973). Previously, an unknown width of ocean intervened between Eurasia and the Okhotsk block.

Figure 11 shows the key relationships of the Okhotsk block in map view. Prior to the accretion of the Okhotsk block to Eurasia, the subduction system forming the North Pacific Rim lay farther west and north than it does now. The subduction zone lay through Taiwan, the Shimanto belt of outer Japan, central Hokkaido, Sakhalin, the Magadan coast, and the Koryak Mountains at the root of Kamchatka; thence along the continental slope of the Bering Sea and the Shumagin-Kodiak-Chugach trend in southern Alaska. The parallel magmatic arc lay in coastal China, peninsula Korea, parts of inner Japan, Sikhote-Alin in coastal Primorye, the Okhotsk belt, and northeasternmost USSR; thence along the Bering shelf and coastal Alaska. After accretion of the Okhotsk block, subduction shifted eastward and southward to the Izu-Mariana arc east of the Philippine Sea, the Kuril-Kamchatka arc along the edge of the accreted Okhotsk block, and the Aleutian arc south of the Bering Sea.

The Bering Sea contains north-south geomagnetic anomalies formed at the Kula-Farallon plate boundary during the Early Cretaceous (COOPER *et al.*, 1976). This Mesozoic seafloor was trapped behind the Aleutian Ridge when subduction and arc magmatism jumped from the Bering shelf edge to the Aleutian trend (SCHOLL *et al.*, 1975). Accretion of the Okhotsk block directly choked the segment of the pre-accretion subduction zone that lay along the Magadan coast parallel to the Okhotsk volcano-plutonic belt, and southward through Sakhalin to Hokkaido. Abandonment of the subduction system

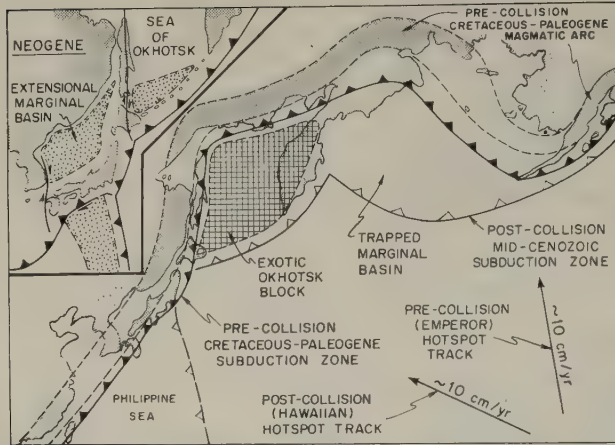


Fig. 11. Sketch map showing inferred evolution of subduction systems before and after accretion of the Okhotsk block by crustal collision followed by a subduction jump.

through the Koryak Mountains and along the Bering shelf edge was evidently an indirect effect of Okhotsk accretion. Attachment of the Okhotsk block to Eurasia left the Koryak-Bering segment of the pre-accretion subduction zone adjacent to a deep re-entrant in the continental margin. Rather than mold itself in a tight flexure following the outline of the re-entrant, the Pacific plate apparently broke across the re-entrant to connect post-accretion subduction along the southeast edge of the Okhotsk block with continuing subduction in southern Alaska by way of the newly established Aleutian trend. The oldest well dated rocks exposed on the Aleutian Ridge are Eocene (MARLOW *et al.*, 1973), and the oldest arc volcanics on Kamchatka are of similar age (AVDEIKO, 1971). The completion of Okhotsk accretion was thus timed closely with the change in Pacific plate motion at about 40 mybp. The reasons for the initiation of subduction along the Izu-Mariana trend to create the Philippine Sea plate are still uncertain (UYEDA and BEN-AVRAHAM, 1972; UYEDA and MIYASHIRO, 1974), but the oldest arc volcanics in the Marianas are also Eocene. Termination of Laramide deformation in the North American Cordillera and of subduction in the Greater Antilles is even more difficult to relate to either the accretion of the Okhotsk block or the formation of the Emperor-Hawaii elbow, but these other events also took place at about 40 mybp (CONEY, 1971). Some linkage of plate interactions throughout the North Pacific region is seemingly implied by the widespread significance of that date (cf. CONEY, 1971).

8. Crustal Collision-Accretion

Accretion of exotic crustal blocks to the continental margins that now form the North Pacific Rim has occurred repeatedly throughout the Mesozoic and the Cenozoic. Both equant microcontinental blocks and elongate island arcs or aseismic oceanic ridges have been involved. In both cases, accretion occurs by crustal collision when the buoyancy of lithosphere capped by a thick crustal profile resists subduction. The accretion of discrete

crustal masses by such crustal collision is a process apart from the incremental accumulation of a growing subduction complex formed of offscrapings from the seafloor.

Two main kinds of crustal collision provide accretionary additions to continental margins (Fig. 12). In one case, an active island arc collides with a passive continental margin, which it partially subducts. The arc structure is thus attached to the continental margin. Such an event occurred in Taiwan in the late Cenozoic (CHAI, 1972). If the overall pattern of plate kinematics induces subduction to resume following such arc-continent collision, then subduction beneath the opposite side of the accreted arc structure may generate an active continental margin following accretion.

Such a sequence of events was involved in the onset of circum-Pacific subduction in California (Fig. 13). An east-facing island arc of late Paleozoic age collided with the Cordilleran margin to produce an episode of Permo-Triassic deformation called the Sonoma Orogeny, during which the Havallah-Pumpnickel subduction complex was

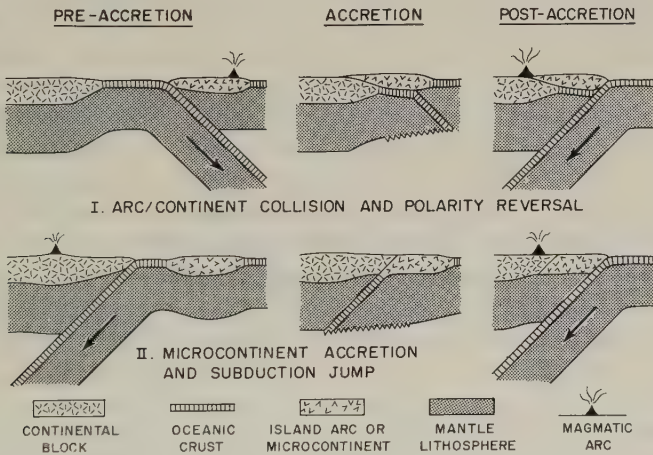


Fig. 12. Diagrams depicting main variants of accretionary events involving crustal collision at continental margins.

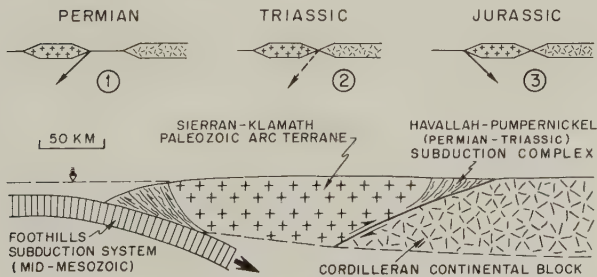


Fig. 13. Regional geologic relations of the Sierran-Klamath arc terrane at the onset of Mesozoic subduction, which was initiated by polarity reversal following accretion of the terrane to the continental margin by crustal collision during the Sonoma Orogeny near the close of the Paleozoic.

emplaced across the continental margin as an allochthonous mass atop the Golconda thrust (DICKINSON, 1977a). Following accretion of the island arc by crustal collision in the mid-Triassic, reversal of arc polarity allowed Jura-Triassic subduction to continue along the western side of the accreted arc terrane in the Sierra Nevada foothills (SCHWEICKERT and COWAN, 1975). This was the earliest inception of the continental-margin Cordilleran arc-trench system.

In the kind of accretion represented by the attachment of the Okhotsk block to Eurasia, the continental margin is active and draws a passive block against its bounding subduction zone from a position at sea. Following crustal collision, subduction jumps to the opposite side of the accreted block. Not only may microcontinental blocks be accreted in this way, but also dormant island arcs, oceanic seamount chains, and aseismic oceanic ridges (DICKINSON, 1976). Extensive terranes in the Cordillera of North America have been accreted in this general fashion.

Figure 14 depicts inferred crustal relations along a generally east-west profile across the Hidaka collision orogen in Hokkaido. During the early Cenozoic, a southern extremity of the Okhotsk block was sutured against a western terrane then attached to Eurasia prior to the opening of the Sea of Japan. Prior to collision, the Cretaceous and early Cenozoic orogen was an east-facing arc-trench system on the Eurasian mainland (OKADA, 1974). Clastics shed eastward from the igneous terrane to the west fill an old forearc basin where they rest on ophiolitic rocks. This ophiolitic substratum is tilted up and faulted against strongly deformed but weakly metamorphosed oceanic facies representing the subduction complex. Along a fault contact interpreted here as the main suture belt, these strata are in contact with a belt of amphibolites, gabbros, migmatites, and gneisses (HASHIMOTO, 1975). These strongly metamorphosed rocks are taken here to be part of the basement of the Okhotsk block that lodged against the old subduction zone. Subduction then jumped eastward to the new subduction zone along the Kuril trend. During the late Cenozoic, sediments were shed westward from the collision orogen to mask parts of the old forearc basin.

Late Mesozoic crustal collisions across the Alaska-Bering-Yakutia region welded together for the first time the crustal blocks that form the North Pacific Rim (Fig. 15). The positions and ages of the various suture belts involved is not yet well known. Large tracts are accretionary collages of oceanic rock assemblages. Closure of the most signifi-

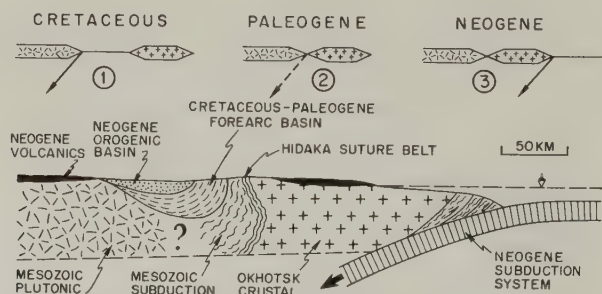


Fig. 14. Inferred structural relations in Hokkaido where Paleogene accretion of the Okhotsk block along the Hidaka suture belt triggered a subduction jump that initiated the Kuril trench.

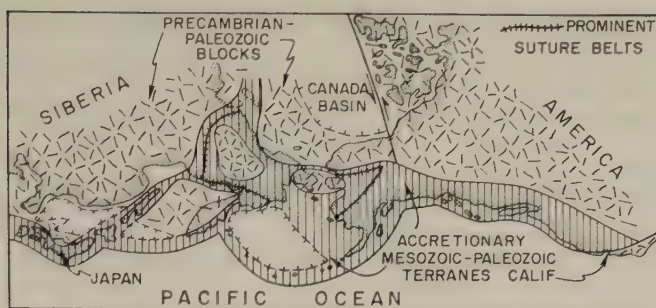


Fig. 15. Sketch map showing main crustal sutures joining North America and Eurasia across the Alaska-Bering-Yakutia region to form the North Pacific Rim.

cant oceanic regions probably occurred between mid-Jurassic and mid-Cretaceous time (CHURKIN, 1972), but some contraction across the region was still underway in the Cenozoic (PITMAN and TALWANI, 1972).

9. Review

The major points made are these:

- 1) The North Pacific Rim is a continuous great-circle belt on the globe.
- 2) Prominent east-west asymmetry of the Pacific Ocean and systematic east-west dichotomy of arc behavior both probably stem from rotational influences on plate tectonics.
- 3) Late Cenozoic tectonics around the North Pacific Rim involved mainly the opening of interarc basins behind east-facing Eurasian arcs and rise-trench encounters at west-facing American subduction zones.
- 4) The formation of the Emperor-Hawaii elbow at about 40 mybp was roughly coeval with accretion of the Okhotsk block to Eurasia by crustal collision and with termination of the classic Laramide deformation, which was caused by plate descent at an abnormally shallow angle beneath America.
- 5) The North Pacific Rim lacked geographic continuity prior to the late Mesozoic closure of remnant ocean basins along suture belts within the land bridge between America and Eurasia, and even circum-Pacific subduction itself was probably not underway prior to the early Mesozoic.

REFERENCES

- AVDEIKO, G.P., Evolution of geosynclines on Kamchatka, *Pac. Geol.*, **3**, 1-15, 1971.
- BARAZANGI, Muawia and B.L. ISACKS, Spatial distribution of earthquakes and subduction of the Nazca plate beneath South America, *Geology*, **4**, 686-692, 1976.
- BOSTROM, R.C., Westward displacement of lithosphere, *Nature*, **234**, 536-538, 1971.
- BURK, C.A. and H.S. GNIBIDENKO, The structure and age of acoustic basement in the Okhotsk Sea, in *Island Arcs, Deep Sea Trenches, and Back-Arc Basins*, edited by Manik Talwani and W.C. Pitman, III, pp. 451-462, Am. Geophys. Union Maurice Ewing Ser. 1, 1977.
- BYRNE, Tim, Early Tertiary demise of the Kula-Pacific spreading center, *Geol. Soc. Am. Abstr. with Programs*, **10**, 98, 1978.
- CHAI, B.H.T., Structure and tectonic evolution of Taiwan, *Am. J. Sci.*, **262**, 389-422, 1972.
- CHAPMAN, M.C. and S.C. SOLOMON, North American-Eurasian plate boundary in northeast Asia, *J. Geophys. Res.*, **81**, 921-930, 1976.

- CHAPPLE, W.M. and T.E. TULLIS, Evaluation of the forces that drive the plates, *J. Geophys. Res.*, **82**, 1967–1984, 1977.
- CHURKIN, Michael, Jr., Western boundary of the North American continental plate in Asia, *Geol. Soc. Am. Bull.*, **83**, 1027–1036, 1972.
- CONEY, P.J., Cordilleran tectonic transitions and motion of the North America plate, *Nature*, **233**, 462–465, 1971.
- CONEY, P.J., Cordilleran tectonics and North America plate motion, *Am. J. Sci.*, **262**, 603–628, 1972.
- CONEY, P.J., Plate tectonics and the Laramide orogeny, in *Tectonics and Mineral Resources of Southwestern North America*, edited by L.A. Woodward and S.A. Northrop, New Mex. Geol. Soc. Spec. Publ. No. 6, pp. 5–10, 1976.
- CONEY, P.J., Mesozoic-Cenozoic Cordilleran plate tectonics, *Geol. Soc. Am. Mem.*, **152**, 33–50, 1978.
- COOPER, A.K., D.W. SCHOLL, and M.S. MARLOW, Plate tectonic model for the evolution of the eastern Bering Sea basin, *Geol. Soc. Am. Bull.*, **87**, 1119–1126, 1976.
- DALRYMPLE, G.B. and D.A. CLAGUE, Age of the Emperor-Hawaii bend, *Earth Planet. Sci. Lett.*, **31**, 313–329, 1976.
- DALRYMPLE, G.B., D.A. CLAGUE, and M.A. LANPHERE, Revised age for Midway volcano, Hawaiian volcanic chain, *Earth Planet. Sci. Lett.*, **37**, 107–116, 1977.
- DELONG, S.E. and P.J. FOX, Geological consequences of ridge subduction, in *Island Arcs, Deep Sea Trenches, and Back-Arc Basins*, edited by Manik Talwani and W.D. Pitman, III, Am. Geophys. Union Maurice Ewing Ser. 1, pp. 221–228, 1977.
- DELONG, S.E., P.J. FOX, and F.W. McDOWELL, Subduction of the Kula ridge at the Aleutian trench, *Geol. Soc. Am. Bull.*, **89**, 83–95, 1978.
- DEN, N. and H. HOTTA, Seismic refraction and reflection evidence supporting plate tectonics in Hokkaido, *Pap. Meteorol. Geophys.*, **24**, 31–54, 1973.
- DICKINSON, W.R., Evidence for plate-tectonic regimes in the rock record, *Am. J. Sci.*, **272**, 551–576, 1972.
- DICKINSON, W.R., Widths of modern arc-trench gaps proportional to past duration of igneous activity in associated magmatic arcs, *J. Geophys. Res.*, **78**, 3376–3389, 1973a.
- DICKINSON, W.R., Reconstruction of past arc-trench systems from petrotectonic assemblages in the island arcs of the western Pacific, in *The Western Pacific; Island Arcs, Marginal Seas, Geochemistry*, edited by P.J. Coleman, pp. 569–601, Univ. Western Australia Press, Perth, 1973b.
- DICKINSON, W.R., Sedimentation within and beside ancient and modern magmatic arcs, in *Modern and Ancient Geosynclinal Sedimentation*, edited by R.H. Dott, Jr. and R.H. Shaver, Soc. Econ. Paleontol. Mineral. Spec. Publ. No. 19, pp. 230–239, 1974a.
- DICKINSON, W.R., Plate tectonics and sedimentation, in *Tectonics and Sedimentation*, edited by W.R. Dickinson, Soc. Econ. Paleontol. Mineral. Spec. Publ. No. 22, pp. 1–27, 1974b.
- DICKINSON, W.R., Sedimentary basins developed during evolution of Mesozoic-Cenozoic arc-trench system in western North America, *Can. J. Earth Sci.*, **13**, 1268–1287, 1976.
- DICKINSON, W.R., Paleozoic plate tectonics and the evolution of the Cordilleran continental margin, in *Paleozoic Paleogeography of the Western United States*, edited by J.H. Stewart, C.H. Stevens, and A.E. Fritsche, Pac. Sec. Soc. Econ. Paleontol. Mineral. Pac. Coast Paleogeogr. Symp. 1, pp. 137–156, 1977a.
- DICKINSON, W.R., Subduction tectonics in Japan, *EOS, Trans. Am. Geophys. Union*, **58**, 948–952, 1977b.
- DICKINSON, W.R. and W.S. SNYDER, Plate tectonics of Laramide Orogeny, *Geol. Soc. Am. Mem.*, **151**, 355–366, 1978.
- DICKINSON, W.R. and W.S. SNYDER, Geometry of triple junctions related to San Andreas transform, *J. Geophys. Res.*, **84**, 1979a (in press).
- DICKINSON, W.R. and W.S. SNYDER, Geometry of subducted slabs related to San Andreas transform, *J. Geol.*, **87**, 1979b (in press).
- DUNCAN, R.A. and Ian McDougall, Linear volcanism in French Polynesia, *J. Volcanol. Geotherm. Res.*, **1**, 197–227, 1976.
- FORSYTH, Donald and S. UYEDA, On the relative importance of the driving forces of plate motion, *Geophys. J. R. Astr. Soc.*, **43**, 163–200, 1975.
- GREENE, H.G., G.B. DALRYMPLE, and D.A. CLAGUE, Evidence for northward movement of the Emperor Seamounts, *Geology*, **6**, 70–74, 1978.
- HASHIMOTO, S., The basic plutonic rocks of the Hidaka metamorphic belt, *J. Fac. Sci. Hokkaido Univ.*, Ser. IV, **16**, 367–420, 1975.
- HAVEEMANN, H., Displacement of dipping slabs of lithosphere, *Earth Planet. Sci. Lett.*, **17**, 129–134, 1972.
- HILDE, T.W.C., S. UYEDA, and L. KROENKE, Evolution of the western Pacific and its margin, *Tectonophysics*, 145–165, 1977.
- HYNDMAN, R.D., Plate motions relative to the deep mantle and the development of subduction zones, *Nature*, **238**, 263–265, 1972.

- IRVING, E., Drift of the major continental blocks since the Devonian, *Nature*, **270**, 304–309, 1977.
- JARRARD, R.D. and D.A. CLAGUE, Implications of Pacific island and seamount ages for the origin of volcanic chains, *Rev. Geophys. Space Phys.*, **15**, 57–76, 1977.
- KARIG, D.E., Ridges and basins of the Tonga-Kermadec island arc system, *J. Geophys. Res.*, **75**, 239–255, 1970.
- KARIG, D.E., Structural history of the Mariana island arc system, *Geol. Soc. Am. Bull.*, **82**, 323–344, 1971.
- KARIG, D.E., Plate convergence between the Philippines and the Ryukyu Islands, *Mar. Geol.*, **14**, 153–168, 1973.
- KNOPOFF, LEON and A. LEEDS, Lithospheric momenta and the deceleration of the earth, *Nature*, **237**, 93–95, 1972.
- LIPMAN, P.W., H.J. PROSKA, and R.L. CHRISTIANSEN, Evolving subduction zones in the western United States, as interpreted from igneous rocks, *Science*, **174**, 821–825, 1971.
- MARLOW, M.S., D.W. SCHOLL, E.C. BUFFINGTON, and T.R. ALPHA, Tectonic history of the central Aleutian arc, *Geol. Soc. Am. Bull.*, **84**, 1555–1574, 1973.
- MARSHAK, R.S. and D.E. KARIG, Triple junctions as a cause for anomalously near-trench igneous activity between the trench and volcanic arc, *Geology*, **5**, 233–236, 1977.
- MARSHALL, Monte, The magnetic properties of some DSDP basalts from the North Pacific and inferences for Pacific plate tectonics, *J. Geophys. Res.*, **83**, 289–308, 1978.
- MATSUDA, T. and S. UYEDA, On the Pacific-type orogeny and its model—Extension of the paired belts concept and possible origin of marginal seas, *Tectonophysics*, **11**, 5–27, 1971.
- MOBERLY, R., Origin of lithosphere behind island arcs, with reference to the western Pacific, *Geol. Soc. Am. Mem.*, **132**, 35–55, 1972.
- MOLNAR, Peter and Tanya ATWATER, Interarc spreading and Cordilleran tectonics as alternates related to the age of subducted oceanic lithosphere, *Earth Planet. Sci. Lett.*, **41**, 330–340, 1978.
- MOORE, G.W., Westward tidal lag as the driving force of plate tectonics, *Geology*, **1**, 99–100, 1973.
- MORGAN, W.J., Plate motions and deep mantle convection, *Geol. Soc. Am. Mem.*, **132**, 7–21, 1972.
- MURPHY, R.W., The Manila Trench-West Taiwan foldbelt, a flipped subduction zone, *Geol. Soc. Malaysia Bull.*, No. 6, 27–42, 1973.
- NELSON, T.H. and P.G. TEMPLE, Mainstream mantle convection; a geologic analysis of plate motion, *Am. Assoc. Pet. Geol. Bull.*, **56**, 226–246, 1972.
- OKADA, H., Migration of ancient arc-trench systems, in *Modern and Ancient Geosynclinal Sedimentation*, edited by R.H. Dott, Jr. and R.H. Shaver, Soc. Econ. Paleontol. Mineral. Spec. Publ. No. 19, pp. 311–320, 1974.
- PITMAN, W.C., III, R.L. LARSON, and E.M. HERRON, The age of the ocean basins, *Geol. Soc. Am. Map*, 1974.
- PITMAN, W.C., III and Manik TALWANI, Sea-floor spreading in the North Atlantic, *Geol. Soc. Am. Bull.*, **83**, 619–646, 1972.
- SCHOLL, D.W., E.C. BUFFINGTON, and M.S. MARLOW, Plate tectonics and the structural evolution of the Aleutian-Bering Sea region, *Geol. Soc. Am. Spec. Pap.*, **151**, 1–31, 1975.
- SCHOLL, D.W., J.R. HEIN, M.S. MARLOW, and E.C. BUFFINGTON, Meiji sediment tongue; North Pacific evidence for limited movement between the Pacific and North American plates, *Geol. Soc. Am. Bull.*, **88**, 1567–1576, 1977.
- SCHWEICKERT, R.A. and D.S. COWAN, Early Mesozoic tectonic evolution of the western Sierra Nevada, California, *Geol. Soc. Am. Bull.*, **86**, 1329–1336, 1975.
- SILLITOE, R.H., Metallogeny of an Andean-type continental margin in South Korea; implications for opening of the Japan Sea, in *Island Arcs, Deep Sea Trenches, and Back-Arc Basins*, edited by Manik Talwani and W.C. Pitman, III, Am. Geophys. Union Maurice Ewing Ser. 1, pp. 303–310, 1977.
- STEWART, R.J., Turbidites of the Aleutian abyssal plain: Mineralogy, provenance, and constraints for Cenozoic motion of the Pacific plate, *Geol. Soc. Am. Bull.*, **87**, 793–808, 1976.
- STONE, D.B. and D.R. PACKER, Tectonic implications of Alaska Peninsula paleomagnetic data, *Tectonophysics*, **37**, 183–201, 1977.
- TOMODA, Y., J. KOBAYASHI, M. SEGAWA, M. NOMURA, K. KIMURA, and T. SAKI, Linear magnetic anomalies in the Shikoku basin, northern Philippine Sea, *J. Geomag. Geoelectr.*, **28**, 47–56, 1975.
- UYEDA, S. and Zvi BEN-AVRAHAM, Origin and development of the Philippine Sea, *Nature*, **240**, 176–178, 1972.
- UYEDA, S. and H. KANAMORI, Back-arc opening and the mode of subduction, 1979 (in press).
- UYEDA, S. and A. MIYASHIRO, Plate tectonics and the Japanese Islands, *Geol. Soc. Am. Bull.*, **85**, 1159–1170, 1974.
- WATTS, A.B., J.K. WEISSEL, and R.L. LARSON, Sea-floor spreading in marginal basins of the western Pacific, *Tectonophysics*, **37**, 167–181, 1977.
- WILSON, J.T. and Kevin BURKE, Two types of mountain building, *Nature*, **239**, 448–449, 1972.
- ZONENSHAIN, L.P., M.I. KUZMIN, V.I. KOVALENKO, and A.J. SALTYSKY, Mesozoic structural-magmatic pattern and metallogeny of the western part of the Pacific belt, *Earth Planet. Sci. Lett.*, **22**, 96–109, 1974.

SPECULATIONS ON MOUNTAIN BUILDING AND THE LOST PACIFICA CONTINENT

Amos NUR* and Zvi BEN-AVRAHAM**

**Department of Geophysics, Stanford University,
Stanford, California, U.S.A.*

***Department of Mathematics, Weizmann Institute of Science, Rehovot and
the Israel Oceanographic and Limnological Ltd., Haifa, Israel*

(Received October 6, 1978)

Extensive geological and geophysical evidence suggests that numerous fragments of continents, miniplates, and so called "island arcs" have been incorporated into the Circum Pacific continents. The old rocks exposed on these bodies bear strong evidence for continental origins. This leads to the speculation that a large continental mass existed once in what is now the Pacific Ocean. This mass—which we call the Pacifica continent—could have been part of the Pangea Super Continent, adjacent to Australia and Antarctica. When this continent broke into fragments, they drifted toward continental collision in South America, North America, Alaska, Kamchatka, Japan and East Asia. Submerged platforms in the Pacific Ocean, such as the Ontong Java area, the Shatsky rise, and the Manihiki plateau, may also be remnants of Pacifica. The thick crusts of these plateaus, with velocities typical of continents, are thus predicted to be continental crusts.

Although the details of the breakup and collision of Pacifica cannot be resolved very well at present, the postulated existence of this continent supports a large generalization: We suggest that all spreading centers on earth may originate underneath continental masses. Without Pacifica of course, the present day east Pacific rise is without associated continents. If continents account for all spreading, it may be because the continental crust acts as thermal blanket, warming the lower lithosphere and upper asthenosphere.

Adding to this the further hypothesis and that subducted ridges are responsible for back arc rifting and spreading, we obtain the typical trench-continent-ridge sequences, containing volcanism, uplifted blocks, metamorphism, and rifting. Multiple collisions involving several continental slivers and ridges may result in several consecutive sequences juxtaposed on one another. Such complexities with geological record are common in belts such as Western North America.

On the basis of the similarities of (a) the geophysical aspects-seismicity and crustal thickness, (b) morphology, and (c) geological complexities, we propose in this paper that the circum Pacific mountain belts may be at least in part the result of past continental collisions, quite similar to those associated with the Alpine belts.

The notion of Pacifica and its breakup may provide an explanation for the similarities of flora, fauna, and rock sequences in widely separated locations in the mountain belts across the Pacific, and may tie in divergent paleomagnetic data.

1. Introduction

There are two puzzling phenomena associated with the crust in the Western Pacific Ocean and the Circum Pacific continental margins: (1) the presence of a large number of old allochthonous continental fragments throughout the entire Pacific continental rim, and (2) submerged thick-crustal platforms, in the Western Pacific Ocean. We will first review the evidence for the continental nature of the embedded fragments in the Circum

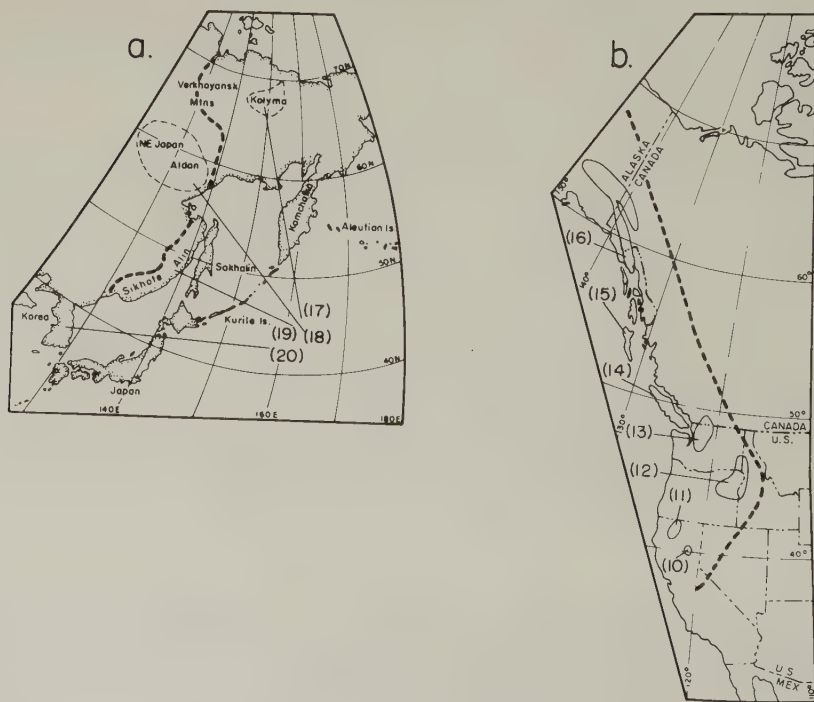
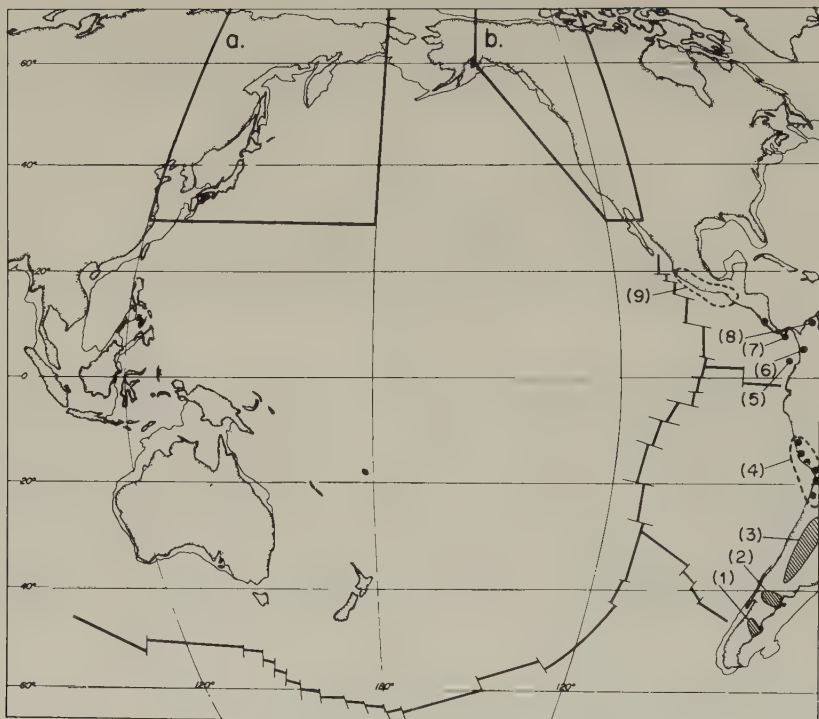


Fig. 1(a)



Fig. 1(b)

Fig. 1(a). The distribution of some of the old continental masses around the Pacific Ocean. The insets a and b mark the location of enlarged maps on the bottom. 1, Deseado massif (HERRERO-DUCLOUX, 1963); 2, Patagonian massif (HERRERO-DUCLOUX, 1963); 3, Pampean massif (HERRERO-DUCLOUX, 1963); 4, small blocks in the coastal range of Peru and Chile (JAMES, 1971 a); 5, Gorgona Island and the continental shelf off Columbia (MACDONALD and HURLEY, 1969; CASE *et al.*, 1971; MEYER *et al.*, 1976; LLOYD, 1963; GUZMAN and DE CSERNA, 1963); 6, small blocks in the Serrania de Baudo in Columbia (MACDONALD and HURLEY, 1969; CASE *et al.*, 1971; MEYER *et al.*, 1976; LLOYD, 1963; GUZMAN and DE CSERNA, 1963); 7, Nicoya complex in Costa Rica and Panama (MACDONALD and HURLEY, 1969; CASE *et al.*, 1971; MEYER *et al.*, 1976; LLOYD, 1963; GUZMAN and DE CSERNA, 1963); 8, Santa Marta Mountain in Columbia (MACDONALD and HURLEY, 1969; CASE *et al.*, 1971; MEYER *et al.*, 1976; LLOYD, 1963; GUZMAN and DE CSERNA, 1963); 9, small block in the Sierra Madre del Sur in Mexico (MACDONALD and HURLEY, 1969; CASE *et al.*, 1971; MEYER *et al.*, 1976; LLOYD, 1963; GUZMAN and DE CSERNA, 1963). *Inset a*—In the Far East: 17, Kolyma block in Siberia (McELHINNY, 1973; HAMILTON, 1970); 18, Aldan block in Siberia (McELHINNY, 1973; HAMILTON, 1970); 19, Sikhote Alin in Siberia (McELHINNY, 1973; HAMILTON, 1970); 20, The Precambrian in Korea (KAWAI *et al.*, 1969). *Inset b*—In northwestern America: 10, Plumas Terrane, Sierra Nevada, California (CHURKIN and EBERLEIN, 1977); 11, Eastern Klamath Mountains (HAMILTON, 1969); 12, Hells Canyon in eastern Oregon, western Idaho and southeastern Washington (JONES *et al.*, 1977); the Supplee-Izee areas, central Oregon (CHURKIN and EBERLEIN, 1977); the Ochoco terrain; 13, San Juan and northern Cascade Treanes Butte area and the Juan Island, Washington (CHURKIN and EBERLEIN, 1977); 14, Vancouver Island (CHURKIN and EBERLEIN, 1977); 15, Queen Charlotte Islands (JONES *et al.*, 1977); 16, Alexander Archipelago, Alaska (CHURKIN and EBERLEIN, 1977) and the Wrangell Mountains, Alaska (JONES *et al.*, 1977). The dashed line in *inset b* indicates limit of Triassic continental shelf (JONES *et al.*, 1977).

Fig. 1(b). Submarine plateaus and ridges in the western Pacific Ocean. The dashed line marks the boundary between highs which were part of Australia to the south, to those which may be part of Pacifica to the north.

Pacific, the paleomagnetic and geologic data related to their origins and age. We will then reconstruct a possible migration of these fragments with Cenozoic and Mesozoic plate motion in the Pacific. Independently, we will review the evidence for the continental character of the Western Pacific platforms, which may have originated, like the other fragments, in a large, ancient continental mass in the paleopacific—a mass we call *Pacifica*. We will then consider some implications of the *Pacifica* speculation, among them the origin of spreading and nature of continental collision.

2. *Continental Fragments in the Pacific Margins*

In Fig. 1(a) we have summarized evidence in support of past continental masses in the Pacific Ocean: HOLMES (1965) presents a compelling case for late Paleozoic to early Tertiary continental landmasses, such as Cascadia and Llanoria, to the west of present-day North America (SCHUCHERT and DUNBAR, 1950). The land includes conglomerates derived from crystalline Sialic rocks which have since disappeared. HAMILTON (1969) refined this notion, specifying that “old arcs presumably have been swept into the (North America) continent.” This is necessary to explain, for example, the Klamath-Sierran arc geology (BURCHFIELD and DAVIS, 1975; SCHWEICKERT and COWAN, 1975; ANDERSON, 1976). Most recently, Davis and Armstrong (in FISHER, 1976) suggested “that the Klamaths were originally some distance off shore to the west and that the Permo-Triassic Sonoma Orogeny results from an arc continent collision.”

Several investigators (MONGER and ROSS, 1971; JONES *et al.*, 1972; RICHARDS, 1974) have suggested a large scale collision of Alaska with a continental fragment during Paleozoic and early Mesozoic, while masses finally coalesced in late Jurassic-early Cretaceous time. HAMILTON (1969) has proposed that Permian terranes bearing Tethyan fusulinids may have formed in the central Pacific, on island arcs which were subsequently swept into the North American continent. These North American terranes share Jurassic and Cretaceous faunas and floras with New Zealand, Caledonia, the Antarctica peninsula, and Chile (HAMILTON, 1969). This is consistent with several paleomagnetic studies which suggest that large fragments in the western U.S., Canada, and Alaska were located near the equator, perhaps at Triassic times (SYMONS, 1971; IRVING and YOLE, 1972). HILLHOUSE (1977) found that tholeiitic flows in the Wrangell mountain area were formed at 15° north of the equator during Triassic time. Other paleomagnetic evidence is summarized in Table 1.

JONES *et al.* (1977) have shown convincingly that a large continental block—Wrangellia—was incorporated into northwestern North American in late Mesozoic time. The block or blocks extending over 2,000 km from Alaska to Oregon could not have been contiguous to central Alaska in the Jurassic period. Warm water Carbonate rocks, with no evidence of faunas, have been found at high latitudes in western Canada. This is typical of North American or north Asian regions.

Most remarkably, JONES *et al.* (1977) have pointed out that the displaced Wrangellia block received “enormous quantities of Triassic tholeiitic basalts—to become one of the largest domains of non oceanic basalts.” “Presumably, rifting initiated this volcanism, but where it occurred and what was rifted remain enigmatic.” This rifting, as well as the subsequent synchronous subsidence through Wrangellia, could be the result of a pre-Triassic continental breakup in the South Pacific. In central and South America, there are numerous old basement inclusions within the mobile belts, some of which extend well into the

Table 1. Paleomagnetic evidence for large scale migration of continental fragments now embedded in the Pacific margins.

Region	Position and age	Reference
Part of East Siberia	<i>U. Carb.-Perm.</i> —50° away from computed pole; 20° further away from pole	Creer (in Tarling and Runcorn (1970))
East Siberia	<i>Triassic</i> —Distance to pole ~30° further away than computed. <i>Jurassic</i> —Poles coincide. Implies a 3,000 km northward migration in Triassic time, at a rate of 30°/30 my=10 cm/year.	Creer (see above)
Sikhote-Alin	<i>Permian</i> —50° away from computed pole. <i>Cretaceous</i> —10° away from computed pole. Moved 4,000 km (40°) in ~ 50 my or 8 cm/year.	McElhinny (in Tarling and Runcorn, 1970)
Kolyma	<i>Permo-Triassic</i> —45° away from computed pole. <i>Cretaceous</i> —5° away from computed pole. Implies a 4,000 km northward migration between Permo-Triassic and Cretaceous.	McElhinny (see above)
Insular belt, Western Canada	Insular belt has moved 4,000 km northward since Triassic.	Irving and Yole (1967)
Southern Alaska	Low paleolatitudes in <i>Triassic</i> time. Upper Triassic Nikolai Greenstone was 15°N or 15°S of paleoequator. Thus 3,000 or 6,000 km south of computed position. Has moved 3,000 or 6,000 km since upper Triassic times.	HILLHOUSE (1977)
	<i>Ordovic-Pennsylv.</i> —The Prince Wales Isl. was at least 25° further south than computed.	Jones, Van der Voo, Churkin and Eberlein (1977)
	<i>Triassic or Mid Cenozoic</i> —Queen Charlotte Isl. has moved northward 25°.	Hicken and Irving (1977)
Japan	<i>Permian</i> —Southern Japan was situated near the paleoequator, and drifted northward during early Permian-late Cretaceous.	Minato and Fujiwara (1964) Hattori and Hirouka (in press) Adachi (1976)

Pacific Ocean itself and suggest past continental accretion. In Argentina, the Pampean, Patagonian, and Deseado massifs are composed of igneous and metamorphic rocks, of Precambrian and lower Paleozoic age; of unclear origin (HERRERO-DUCLOX, 1963). The Pampean massif, for example, is flanked by continental deposits ranging in origin from the Permo-Carboniferous to Tertiary period (HERRERO-DUCLOX, 1963). We do not know the original positions of these massifs, but WINDHAUSEN (1931) and MORRISON (1962) have suggested that Patagonia was a separate continental fragment before Cretaceous time. During the Jurassic, South America was bounded to the west by volcanic rocks "resting on strongly folded and metamorphosed rocks" off Ecuador, Peru, and Bolivia (WEEKS, 1947; MARKS, 1956; TSCHOPP, 1956; JENKS, 1956). Old Precambrian continental basement fragments, of unknown origins, have been identified in the Santa Marta mountains in

Columbia, the Serrania de Baudo in Panama and Columbia, the Pacific Ocean off Peru, and the Sierra Madre de Sur in Mexico (MACDONALD and HURLEY, 1969; CASE *et al.*, 1971; MEYER *et al.*, 1976; LLOYD, 1963; GUZMAN and DE CSERNA, 1963).

The situation is perhaps best summarized by JAMES (1973): "Jurassic volcanic rocks in southern Peru are wedged in among crystalline metamorphic rocks at least 400 my old. Just what these remnants of ancient sialic crust are doing some 300 km west of the currently exposed geosynclinal rocks of the continental margin is unknown. These rocks could be part of the paleozoic microcontinent that lay to the west of the South American coastline."

In northeast Asia, paleomagnetic data (McELHINNY, 1973) suggest that the Kolyma block and the Sikhote Alin region have been welded onto the Asian continent, probably in late Jurassic or Cretaceous time. The Verkhoyansk and Sikhote mountain belts, therefore, represent probable sites of continental collisions (HAMILTON, 1970). Other possible continental fragments from the Pacific Ocean are: the Sea of Ohotsk and surrounding areas in early tertiary time, almost all of China south of 40°, and Korea (KAWAI *et al.*, 1969; HURLEY, 1971). All this suggests that large fragments have collided with mainland Asia from the Triassic through, the Cretaceous periods. CHURKIN and EBERLEIN (1977) point out that "Permian rocks lie outboard of poorly known Paleozoic and Precambrian rocks in the Alaska range. Ancient rocks reappear west of the Bering Sea along the northwest rim of the Pacific, where similar terranes of Paleozoic age occur in northeastern USSR, in Japan, and discontinuously farther south along the west Pacific rim." Like North America and the Andes, Japan, East Siberia, and China show traces of mysterious continental masses in the Pacific.

DICKINSON (1971) suggests that "for western N. America...we are forced to contemplate the possibility of several collisions of the main North American Craton with other continents, microcontinents, or island arcs, and the initiation of several arc-trench systems..." We conclude that numerous fragments of the aforementioned land masses have been incorporated into the entire borders of the Circum Pacific continents, as summarized in Fig. 2.

3. *The Pacifica Continent*

Three processes have been proposed to account for the presence of old continental crust in the Circum Pacific belts: (1) separation, subsequent return and collision of continental slivers; (2) the transverse motion of irregular continental slivers along transform faults such as the San Andreas fault; (3) collision with and incorporation of island arcs. We envision a fourth process: the collision of large continental chunks with the Circum Pacific continents over at least the past few hundred million years. These chunks were part of a continental mass which disaggregated, in the manner of Gondawana and, currently, of Africa.

We may imagine the following future for the Indian Ocean and Africa: Assuming that the Carlsberg ridge continues to spread, India may eventually be consumed by the Himalayas and a trench may develop south of India to accommodate the continuously forming ocean plate. With this configuration, the Tibet-Himalaya-India orogen would become quite similar to a Circum Pacific orogen: a trench and ocean adjacent to the collision belts.

As an alternative to random migration of island arcs or haphazard recoallescence of

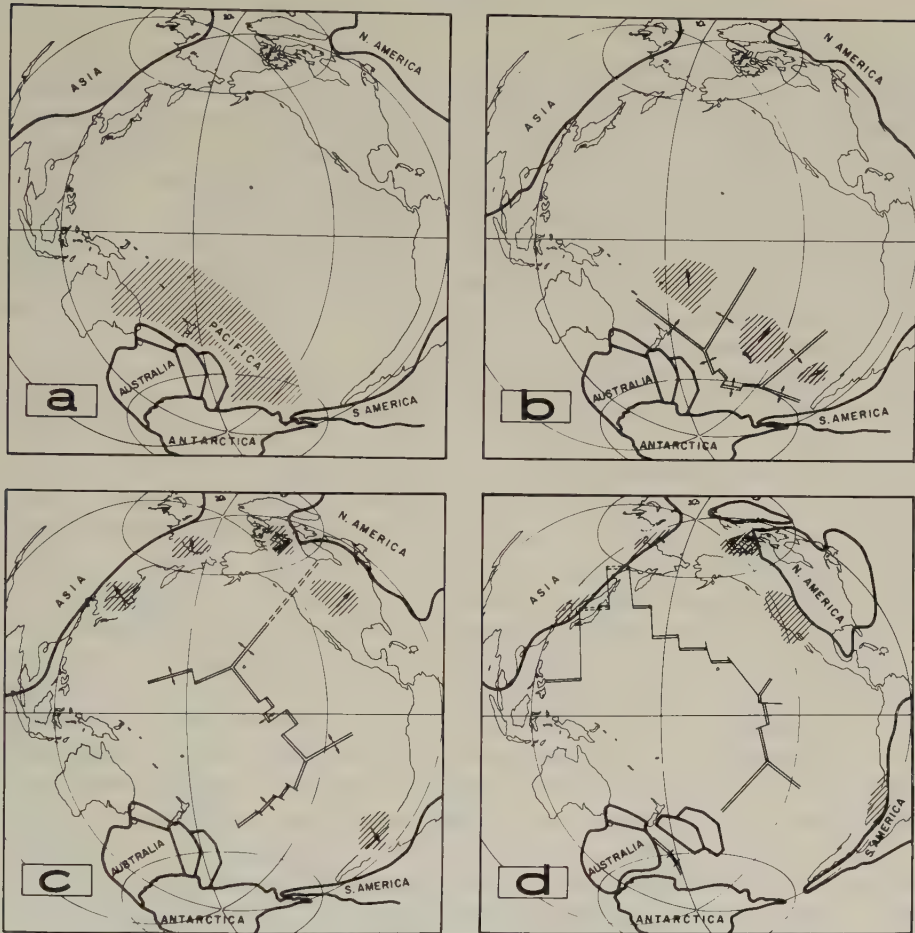


Fig. 2. Schematic model of the breakup of Pacifica and the resulting collision events. Possible ages of the reconstruction stages: (a) 225 my; (b) 180 my; (c) 135 my; (d) 65 my. Fine lines mark the present day continental outline. Heavy lines mark the location of the various continental areas through the geological evolution after DIETZ and HOLDEN (1970). Position of spreading centers simplified from LARSON and CHASE (1972), UYEDA and BEN-AVRAHAM (1972), BEN-AVRAHAM and UYEDA (1973), HILDE *et al.* (1976), and HAYES and RINGIS (1973).

continents, we suggest that the Circum Pacific fragments were embedded in, and moved with, the major plates of the Pacific Ocean. We may roughly reconstruct the motion of such fragments, back to 190 mybp, the paleomagnetically derived motions of the Kula, Farallon, Phoenix, and Pacific plates (LARSON and CHASE, 1972; HILDE *et al.*, 1976). In Fig. 2, we remove continental blocks from Alaska, western North America, the Andes, Kamchatka, and Japan, attaching them in a cartoon fashion to their corresponding plates. We note that the various fragments, as they migrate towards their respective spreading ridges, also approach each other. In fact, it appears that by late Jurassic time, the earliest for which magnetic data is available, these fragments are well on their way toward coa-

lescung into a single continental mass. We suggest that such a mass actually existed by approximately mid-Permian times.

We thus propose that a continental mass, intact before early Mesozoic time, was broken up by the complex spreading (LARSON and CHASE, 1972) which separated the Kula, Farallon, Pacific, and Phoenix plates. The fragments, divided into four groups associated with these plates, were presumably carried along toward subduction zones and eventually reached continental margins. Roughly speaking, the Kula fragments collided with Alaska and Eastern Siberia, the Farallon fragments with North America, and the Phoenix fragments with South America. There is no major continental collision region associated with the Pacific plate of LARSON and CHASE (1972); this fact may be related to the submerged platforms in the Western Pacific Ocean (Fig. 1(b)).

The oldest magnetic anomalies and sediments in the Pacific Ocean suggest that the continental fragments of Pacifica were already fully separated by late Jurassic or early Cretaceous times, approximately 120 mybp (LARSON and CHASE, 1972). It is quite likely that major continental collisions were already in advanced stages, and that a large part of the Pacific Ocean had been swept clean at this time of continental fragments. By reconstructing the spreading junction, we may locate the early Pacifica to the northeast of today's Australia (HILDE *et al.*, 1976).

The continent may either have continued as a distinct mass in the middle of the Pacific Ocean, or may originally have been attached to Pangea. A hypothetical configuration of Pacifica near Pangea, sometime during or before Permian time, is shown in Fig. 2(a).

We may estimate the time scale for migration of fragments to the Circum Pacific continental margins by taking typical distances as 4,000, 6,000 and 9,000 km, and typical plate convergence rates as the current Pacific 10 cm/year; resultant durations are 40, 60, and 90 my, respectively. These durations can be easily accommodated in the period from the Traissic to the Cretaceous.

We propose the following gross sequences of breakups and collisions: By late Permian to Triassic time, rifting and spreading have developed sufficiently to define the Kula, Farallon, and Phoenix plates (Fig. 2(b)). Each one of these plates now carries one or more fragments of the original Pacifica continent.

In the course of subduction near Proto North America, South America, Alaska, and East Asia, the three plates are consumed at their converging boundaries.

Towards late Jurassic time, the Pacifica fragments begin to collide with the surrounding continents. We assume that collision replaces subduction when a continental fragment approaches a subduction zone adjacent to a continent. In the Proto Japan and South America areas, a Pacifica fragment has totally coalesced with the East Asia continent. In Alaska, North America, the bulk of the continental mass is approaching rapidly; some collisions are already taking place (Fig. 2(c)).

By Cretaceous time, massive collisions have taken place in North America. New subduction zones have developed behind the various Pacifica segments, now part of their respective continental masses. In Cenozoic time, all continental fragments in the western and northern Pacific have coalesced with their respective continents; left behind is a purely oceanic crust with spreading centers (Fig. 2(d)).

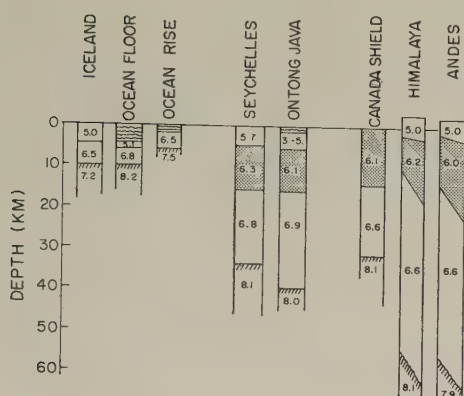


Fig. 3. Comparison of oceanic and continental crustal structures. Although morphologically slightly similar, the enigmatic Ontong-Java platform is totally dissimilar to Iceland (FURUMOTO *et al.*, 1973; PALMASON, 1971) or to typical oceanic crust. It is however, remarkably similar to typical shield structures, with thick 6.1 km/sec upper crust, and the Seychelles banks, known to be continental (LAUGHTON *et al.*, 1970). Typical orogenic roots are even thicker, with the Himalaya (NARAIN, 1973) of known continental collision. Note the similarity with the Andes (JAMES, 1971)—where no collision is known at present. Past collisions with Pacifica fragments may be the explanation.

4. Western Pacific Ocean Floor

One of the attractions of this hypothesis is that it may account for some of the submerged platforms in today's western Pacific Ocean. Typically, these platforms and blocks (Fig. 1(b)) are shallowly submerged and rise perhaps 2-3 km above the surrounding sea floor. Unlike the sea floor, they are devoid of magnetic lineations, and exhibit strikingly thicker crusts. In some places, these crusts have compressional velocity structures which approach continental values (Table 2). Of particular interest is the example of the Ontong Java plateau in the southwest Pacific Ocean; the thick crust ranges from 36 to 43 km. Remarkably, seismic velocity to 20 km depth is only 6.3 km/sec, typical of granitic basement (Fig. 3). The western margin of the plateau is rifted, whereas Joides drill-hole 64 penetrated 900 m through sediments without reaching basement rock.

A number of authors have suggested that the Ontong Java plateau, among others, consists of piles of volcanic flows, similar (MILSON and SMITH, 1975; WINTERER, 1976) to present-day Iceland. As shown in Fig. 3, the crustal velocity structures of Ontong Java and Iceland (FURUMOTO *et al.*, 1973; PALMASON, 1971) are drastically different. Iceland resembles a typical ocean floor and rises; the Ontong Java structure resembles a shield: the granite layer is 10-20 km thick with a P velocity of 6.1 km/sec. It is unlikely that basaltic piles at 15-20 km depth would have such a low velocity.

We propose that these platforms are continental crustal fragments of Pacifica. They are grossly similar to known submerged continental platforms in Melanesia (Table 1) and in the Indian Ocean: The exposed granitic basement of the Seychelles bank, for example, indicates its continental origin, as do the P velocities of 6.1-6.3 km/sec, which are typical of shallow "sialic" continental crust (KANAIEV and TURKO, 1976).

5. Spreading Underneath Continents

With the exception of the Pacific Ocean, essentially all known spreading centers originate under continental masses (e.g., the Mid Atlantic Ridge, Red Sea Rift, Carlsberg Ridge, Indian Ocean Ridges, the Balearic and Tyrrhenian Seas). SCHUILING (1973) has suggested that the thermal blanketing effect and the high radioactive heat generation in the continental crust may cause upwelling of partial melt and spreading. To date, this

Table 2. Water depth, crustal thickness and velocities in several submerged platforms in Western Pacific Ocean.

Area	Water depth (km)	Mantle depth (km)	"Sialic" velocity (km/sec)	Depth of "Sialic" layer (km)	Notes	Reference
Kermadac ridge	0.7-2.5	16-19			Generally assumed to be submerged continental fragments	SHORE <i>et al.</i> (1971)
Norfolk ridge	1-2	~22				
Lord Howe rise	1.2-1.6	18-29	6.0	16		
Coville ridge	1.7-2.3	14-20				WOOLLARD (1975)
Ontong Java plateau	2-2.5	40-42	6.1	17	Rifted margin to the west	MURAUCHI <i>et al.</i> (1973)
Manihiki rise	2.5	> 13.5	6.1	13	Moho not reached	FURUMOTO <i>et al.</i> (1976)
Okai Daito ridge	2.5	> 15	6.0	12	Moho not reached	SUTTON <i>et al.</i> (1971)
Eauripik-New Guinea rise	2-3	20 (?)	(6.9?)	?	Velocity data uncertain	MURAUCHI <i>et al.</i> (1968)
Bismark archipelago	1-2	25-35	6.1	10-15		DEN <i>et al.</i> (1971)
Shatski rise	1.4	> 24	(7.0)	(25)	Water depth is but velocity is not consistent with continental crust	WOOLLARD (1975) DEN <i>et al.</i> (1969)

In many cases, the velocities are typical of "Sialic" continental crust.

Table 3. Some examples of biogeographic problems associated with the Pacific basin and Pacifica.

Problem	Proposed source region	Reference	Notes
Origin of angiosperms	Southwest Pacific region (New Guinea, New Caledonia, China, etc.)	HALLIER (1912)	Suggested a "Pacifica" continental bridge
Origin of Angiosperms Glospteris and Gigantopteris flora Coal floras	Southwest Pacific region (New Guinea, New Caledonia, China, etc.) "Cathasia"	MELVILLE (1966) MELVILLE (1966)	Differences between European and east North America to west North America coals. Tropical in southern Alaska
Marsupial biogeography	New Guinea-New Caledonia Early Mesozoic	MARTIN (1977)	
Multituberculata	Migration from East Asia to North America, Early Mesozoic	KEILAN-JAWOROWSKA (1974)	Migration only from Asia to America, not reversed
Lizards, alligators	Migrated from China to America	WEGENER (1915), GREGORY (1925)	Suggested a continental transpacific link
Subtropical broad leaf forest in Western U.S. and China, Japan (Tertiary)	S.W. Asia?	Leopold and MacGinitie (1972)	Transpacific link

or similar thermal models have floundered on the east Pacific rise which, unlike the mid-Atlantic and Indian Ocean ridges, is associated with no apparent continental fragments.

The Pacifica model now allows us to extend the thermal model. The east Pacific rise and other ridge remnants in the Pacific Ocean began, according to the proposed reconstruction beneath Pangea and have been spreading ever since. The thermal blanket effect, in possible conjunction with subcontinental hot spots (BURKE and WILSON, 1976) may therefore be a major element in the driving mechanism of plates. The heat which accumulates under the blanket eventually causes spreading through the buoyancy of the melt phase in the upper mantle. The pre-shaped rifting phases of India and Australia from Antarctica lasted 170 and 110 my respectively (VEEVERS and McELHINNY, 1976). If the model is applicable, this indicates that there are long periods of heat accumulation preceeding spreading itself, which may be rapid and short lived.

We thus obtain a new constraint on the sequential development of plate consumption: Every coalescence between a ridge and a trench, with subsequent back arc rifting (UYEDA and MIYASHIRO, 1974), must be preceded by the consumption of a continental mass, separated from its other half by the ridge. Some hypothetical sequences are sketched schematically in Fig. 4. In the simplest case, that of an oceanic trench (Fig. 4), the leading continental fragment collides with the trench before moving with the subducted plate. Though the light continental mass cannot be subducted, spreading continues, and the trench may "jump" to the ridge side of the fragment, which is thus added to the overriding plate. During the trench jump, the fragment may undergo substantial deformation, the folding of geosynclinal sediments off its leading edge, metamorphism, volcanism, and

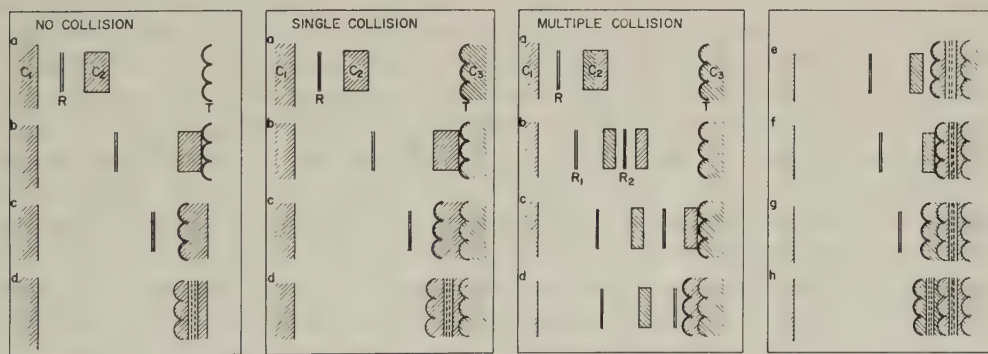


Fig. 4. Sequential development of plate consumption assuming that all spreading is initiated under continents: coalescence between ridge and trench with subsequent back arc rifting must be preceded by the consumption of a continental mass (C_2), which was separated from its other half (C_1) by the ridge (R). Some hypothetical sequences are: (a) *oceanic trench*. The leading continental fragment (C_2) which moves with the subducted plate first collides with the trench (T). Because the light continental mass cannot be subducted, while spreading continues, the trench may "jump" to the ridge side of the fragment, which is thus added to the overriding plate. The net result is perhaps an island like fragment in mid ocean, with a subducting trench. Eventually, the ridge is consumed by the trench, subducts and presumably causes back arc spreading (dashed lines). The final product is therefore a rifted island arc system. (b) *Trench at the edge of a continent* (C_3). Upon collision with the approaching continental fragment the trench jumps across the fragment to accommodate the continuing spreading. Eventually ridge consumption leads to spreading at the continental margin. (c) *Multiple rifting and collision*. The resultant structure in this case includes multiple collisions, subduction and spreading at the continental margin.

subsequent deformation of its tailing edge. The ridge behind the fragment is eventually consumed by the trench, is subducted, and presumably causes rifting and back arc spreading. The final product is therefore a rifted island arc system, containing the geological signature of subduction and trench jumping.

If the trench is situated at the edge of a continent, a collision with the approaching continental fragment occurs first (Fig. 4(b)). The trench, as before, may jump to the ridge side to the colliding fragment. Later, the ridge is consumed, leading again to a zone of rifting and spreading. The net result is a somewhat complex orogenic geology; possible volcanics from the initial subduction, uplift and strong folding from the continental collision, tensile faulting and volcanism from the ridge consumption. As shown in Fig. 4, secondary rifting and spreading like that observed in the western Mediterranean Sea, may result in very complicated orogenic structures: belts which record the multiple effects of subduction, collision, and rifting due to ridge submergence.

6. *Collision and Orogenic Deformation*

It thus appears that even simple continental collision, followed by ridge consumption, leads to very complex geology, even without the effects of sediment accumulation offshore, shape irregularities, and deformation in the orogenic belt during collision. The complex geology of the Circum Pacific mountain belts is therefore consistent with our hypothesis.

It was previously assumed that immobile sediment-filled geosynclines led to mountain building or orogeny by means of upheaval and deformation. This hypothesis could not quite explain the great crustal shortening implied by the deformation observed in mountain belts. It was plate tectonics which provided this essential element. Several investigators (DEWEY and BIRD, 1970; SMITH, 1976) have journalized the general features of orogeny in terms of continental collision, subduction, and rifting. As a result, the Alpine mountain chain is now generally agreed to be the product of continent-continent collisions. In this belt, particularly in the Tibet and Iran segments (BEN-AVRAHAM and NUR, 1976), the zone of recent tectonic activity is over 2,000 km wide. Crustal thicknesses are 1.5–2 times as great as the average continental crust; the light continental material has presumably been made to sink into the asthenosphere. Under the Himalayas, for example, the crust is 70 km thick (NARAIN, 1973). The active collision zone, as indicated by seismicity, includes not only the highly deformed Himalaya belt but also the entire width of the Tibet plateau. This great width is not accounted for at present, but may be closely related to the collision process.

The Circum Pacific mountain belts, with width and morphology similar to the Alpine belt, clearly do not experience continental collisions today. The crust in western North America, Alaska, East Siberia, and the Andes, is often as thick as 40 km (Fig. 5) (JAMES, 1971a). Even morphologically the elevated parts of the western U.S., Alaska and to some extent South America, Japan, and Kamchatka resemble the segments of the Alpine belts. All are seismically active, wide, highly deformed, and marked by high plateaus of various sizes. The Pacific hypothesis provides an explanation for the similarities and suggests that the more complex *Circum Pacific* mountain belts may be in part the result of past continental collisions similar to those associated with the Alpine belt.

7. *Biogeography and the Transpacific Connection*

A curious and possibly very important aspect of the drifting of the Pacifica fragments, is the question of the transpacific connection for fauna and flora. In this section we briefly and incompletely mention a few of the published works on the distribution of flora and fauna which suggest that some sort of continental link has existed between southeast Asia and western North America.

Following Wegener's publication of "The Origin of Continents and Oceans" GREGORY (1925) stated that "There is however similar (to the Atlantic) evidence of land connection across the Pacific." This is required to explain the distribution of the alligator, some lizards, amphibians, earthworms and various plants. HALLIER (1912) following earlier studies has already suggested "the birthplace of the angiosperms in the basin of the Pacific Ocean on the hypothetical continent of Pacifica" (TAKHTAJAN, 1969). This early suggestion for such a Pacifica continent, preceding WEGENER's (1915) continental drift theory, was to be abandoned because, as GREGORY (1925) points out "The existence of a land connection from America Westward across the Pacific is, however wholly inconsistent with the present form of (Wegener's continental) displacement theory." Several decades later, MELVILLE (1966, 1967) has forcefully resurrected the Pacifica continent notion—occupying the central Pacific over Menard's (1964) Darwin rise. Here the land connection was required to explain the distribution of Gigantopteris flora. MELVILLE (1967) suggests that "During carboniferous there were three continents in the northern hemisphere: Atlantica, consisting of western Europe and eastern North America; Pacifica, consisting of western North America and eastern Asia with adjacent Island arcs, and Angaraland. The uprising of the Darwin rise produced a land bridge, which connected Pacifica with the New Zealand platform in the Triassic..."

Melville's suggestion was immediately challenged by HALLAM (1967) and others. Most important is the conclusion by Menard and Hamilton (1963) "there is no possibility that sunken continents could have been in the area (of the Darwin rise) since the Middle Mesozoic..." TAKHTAJAN (1969) points out on the basis of Menard and Hamilton (1963) conclusions that a Pacifica land connection would be very attractive, but the marine geophysical evidence does not support this idea. Obviously, Takhtajan was not aware in 1969 that the structure and history of the Pacific Ocean floor has been totally reevaluated since Menard's earlier static interpretation. The measurement, interpretation and analysis of the magnetic anomalies in the Pacific established the mobilistic nature of its sea floor, with migrating spreading centers (VINE, 1966; HEIRTZLER *et al.*, 1968) leading to the conclusion that most parts of the Pacific floor have been in motion since late Jurassic time or earlier.

Our version of the Pacifica notion—namely that a late paleozoic continental mass has disaggregated, with fragments moving with the various mesozoic plates, provides therefore a renewed possibility for a continental transpacific link: The link is much more mobile than previous models, and does not require major inconsistencies with plate tectonics as known today. In fact the motion of the fragments of Pacifica are estimated on the basis of the motion of the plates, and are therefore generally consistent with plate tectonics. We suggest therefore that a mobile transpacific land connection could have existed, and may have played a role in determining the distribution of floras and faunas around the Pacific basin.

This may help in resolving some aspects of the bitter debate among biogeographers concerning not only the Pacific basin, but also the dominance of vicariance or dispersal in evolution in general (e.g., NELSON, 1975).

8. Conclusion

The mass we call *Pacifica*—to emphasize its centrality in Pacific geological history—could have been part of the Pangea Super Continent, adjacent to Australia and Antarctica. The breakup of this continent and the drift of its fragments resulted in continental collision with South America, North America, Alaska, Kamchatka, Japan, and East Asia. Submerged platforms in the Pacific Ocean, such as the Ontong Java area, the Shatsky rise, and the Manihiki plateau, may be further remnants of *Pacifica*. The thick crusts of these plateaus, with seismic velocities typical of continents, are thus predicted to be continental crusts.

Although the details of the breakup and collision of *Pacifica* cannot be resolved very well at present, we suggest two general features: (1) That *Pacifica* disaggregated in a manner similar to the current breakup of Africa, producing continental slivers which may appear in the collision zone perhaps as "island arcs"; (2) that all spreading centers on earth may have originated underneath continental masses.

If, in addition, subducted ridges are responsible for back arc rifting and spreading, we can account for the typical trench-continent-ridge sequences, containing volcanism, uplifted blocks, metamorphism, and rifting. In cases of multiple collisions with continental slivers and ridges, the geological record may contain several consecutive sequences juxtaposed on one another. Such complexities are common in belts such as western North America.

The notion for *Pacifica* and its breakup provides an attractive explanation for the similarities of faunas and rock sequences in widely separated locations in the mountain belts around the Pacific, and may tie in divergent paleomagnetic data. It may explain the curious geological history of Wrangellia (JONES *et al.*, 1977), where flood basalts and Triassic continental deposits are supplemented by strong evidence for continental rifting in an unknown location near the equator. The submergence of this fragment, and its subsequent emergence upon collision with North America, is almost a perfect example of the history we envision for the fragments of *Pacifica*.

The greatest difficulty which our hypothesis encounters is the scarcity of direct evidence. By the very nature of plate consumption, older lithosphere becomes very rare in the oceans, highly deformed and distorted in continental mountain belts. The validity of the proposed plate processes in the pre-mesozoic Pacific can be tested only through essentially second order effects which survive the subduction and consumption of older crusts. The *Pacifica* notion will remain speculative until the physical and geological nature of the submerged platforms in the western Pacific are revealed through geophysical and drilling activities. We have a general working hypothesis for reassessing the geological evidence in deformed orogenic belts: How strong is the evidence for the incorporation of large continental masses in the Circum Pacific and other mountain belts? Can some of the apparent complexity be resolved by the multiplicity of collisions? At present, we lack a basic understanding of the mechanics of continental collisions. We do not know what happens to lithospheric slabs below the colliding crusts: Do they, for example, override one another, or deform viscously into a thick fluid-like blob? We must investigate the role of small

density variations between colliding continents, variations due to either different thermal histories or rock types.

There is little doubt that the thermal history of continental regions is of the greatest importance in understanding the mechanics of plate motions. Major unresolved problems exist: Why do some large continental areas, such as the Canadian shield, remain immobile for long periods of time, while some small blocks, as in the western Mediterranean, spread? The Pacifica speculation leads to exciting generalizations about the nature and history of plate tectonics on earth; these generalizations in turn provide working hypotheses and experiments which address major existing questions about the nature of geological processes.

We are greatly indebted to G. Thompson for important discussions on crustal velocities, and to W. Dickinson for critical and insightful comments. The responsibility for the ideas and conclusions of this paper, however, are solely ours, and no one else should be held responsible for them. Research was supported in part by grant NO. NSF DES 75-04874 from the Earth Science Division, U.S. National Science Foundation, and by a grant from the Arthur L. Day Fund of the U.S. National Academy of Sciences.

REFERENCES

- ANDERSON, P., Oceanic crust and arc-trench gap tectonics in southwestern British Columbia, *Geology*, **4**, 443–446, 1976.
- BEN-AVRAHAM, Z. and A. NUR, Slip rates and morphology of continental collision belts, *Geology*, **4**, 661–664, 1976.
- BEN-AVRAHAM, Z. and S. UYEDA, The evolution of the China Basin and the mesozoic paleogeography of Borneo, *Earth Planet. Sci. Lett.*, **18**, 365–376, 1973.
- BURCHFIELD, B.C. and G.A. DAVIS, Nature and controls of Cordilleran Orogenesis, western United States: Extensions of an earlier synthesis, *Am. J. Sci.*, **275** (A), 363–396, 1975.
- BURKE, K.C. and J.T. WILSON, Hot spots on the earth's surface, *Sci. Am.*, **235**, 46–57, 1976.
- CASE, J.E., L.G. FURAN S., A. LOPEZ, and W.R. MOORE, Tectonic investigations in western Columbia and eastern Panama, *Geol. Soc. Am. Bull.*, **82**, 2685–2712, 1971.
- CHURKIN, M. and G.D. EBERLEIN, Ancient borderland terranes of the North American Cordillera: Correlation and microplate tectonics, *Geol. Soc. Am. Bull.*, **88**, 769–786, 1977.
- DEN, N., W.J. LUDWIG, S. MURAUCHI, J.I. EWING, H. HOTTA, N.T. EDGAR, T. YOSHII, T. ASANUMA, K. HAGIWARA, T. SATO, and S. ANDO, Seismic-refraction measurements in the northwest Pacific basin, *J. Geophys. Res.*, **74**, 1421–1434, 1969.
- DEN, N., W.J. LUDWIG, S. MURAUCHI, M. EWING, H. HOTTA, T. ASANUMA, T. YOSHII, A. KUBOTERA, and K. HAGIWARA, Sediments and structure of the Eauripik-New Guinea Rise, *J. Geophys. Res.*, **76**, 4711–4723, 1971.
- DEWEY, J.E. and J.M. BIRD, Mountain belts and the new global tectonics, *J. Geophys. Res.*, **75**, 2625–2647, 1970.
- DICKINSON, W.R., Plate tectonic models of geosynclines, *Earth Planet. Sci. Lett.*, **10**, 165–174, 1971.
- DIETZ, R.S. and J.C. HOLDEN, Reconstruction of Pangaea: Breakup and dispersion of continents, Permian to present, *J. Geophys. Res.*, **75**, 4939–4956, 1970.
- FISHER, J.F., Global tectonics and the Cordilleran Orocline, *Geotimes*, **21**, 18–19, 1976.
- FURUMOTO, A.S., W.A. WIEBENGA, J.P. WEBB, and G.H. SUTTON, Crustal structure of the Hawaiian archipelago, northern Melanesia, and the central Pacific Basin by seismic refraction methods, *Tectonophysics*, **20**, 153–164, 1973.
- FURUMOTO, A.S., J.P. WEBB, M.E. ODEGARD, and D.M. HUSSON, Seismic studies on the Ontong Java Plateau, 1970, *Tectonophysics*, **34**, 71–90, 1976.
- GREGORY, J.W., Continental drift, (review of *The Origin of Continents and Oceans*, by A. Wegener), *Nature*, **115**, 255–257, 1925.
- GUZMAN, Ed. J. and Z. DE CSERNA, Tectonic history of Mexico, in *Backbone of the Americas*, edited by Orlo E. Childs, pp. 113–129, Am. Assoc. Pet. Geol., Tulsa, Ok., 1963.
- HALLAM, A., A discussion, in *Aspects of Tethyan Biogeography (a Symposium on Systematics Association)*, Vol. 7, pp. 310–312, 1967.
- HALLIER, H., Über frühere Landbrücken pflanzen- und Wölkerwanderungen zwischen Australasien und Amerika, *Med. Rijksherb. (Leiden)*, **13**, 1–41, 1912.

- HAMILTON, W., Mesozoic California and the underflow of Pacific mantle, *Geol. Soc. Am. Bull.*, **80**, 2409–2430, 1969.
- HAMILTON, W., The Uralides and the motion of the Russian and Siberian platform, *Geol. Soc. Am. Bull.*, **81**, 2553–2576, 1970.
- HAYES, D.E. and J. RINGIS, Seafloor spreading in the Tasman Sea, *Nature*, **243**, 454–458, 1973.
- HEITZLER, J.R., G.O. DICKSON, E.M. HERRON, W.C. PITMAN, III, and X. LE PICHON, Marine magnetic anomalies, geomagnetic field reversals, and motions of the ocean floor and continents, *J. Geophys. Res.*, **73**, 2119–2136, 1968.
- HERRERO-DUCLOUX, A., The Andes of western Argentina, in *The backbone of the Americas*, edited by Orlo E. Childs, pp. 16–28, Am. Assoc. Pet. Geol., Tulsa, Ok., 1963.
- HILDE, T.W.C., S. UYEDA, and L. KROENKE, Evolution of the western Pacific and its margin in *Geodynamics: Progress and Prospects*, edited by C.L. Drake, pp. 1–15, Am. Geophys. Union, Washington, 1976.
- HILLHOUSE, J. W., Paleomagnetism of the Triassic Nikolai Greenstone, McCarthy Quadrangle, Alaska, *Can. J. Earth Sci.*, **14**, 2578–2592, 1977.
- HOLMES, A., Mountain building and orogenic belts, in *Principles of Physical Geology*, edited by A. Holmes, pp. 1109–1192, Ronald Press, New York, 1965.
- HOUTZ, R. and R. MEIJER, Structure of the Ross Sea shelf from profiler data, *J. Geophys. Res.*, **75**, 6592–6597, 1970.
- HOUTZ, R. and F.J. DAVEY, Seismic profiler and sonobuoy measurements in Ross Sea, Antarctica, *J. Geophys. Res.*, **78**, 3448–3468, 1973.
- HURLEY, P.M., Possible inclusion of Korea, central and western China, and India in Gondwanaland, *EOS, Trans. Am. Geophys. Union*, **52**, 356, 1971.
- IRVING, E. and R.W. YOLE, Paleomagnetism and kinematic history of mafic and ultramafic rocks in fold mountain belts, *Ottawa, Earth Phys. Branch Publ.*, **42**, 87–95, 1972.
- JAMES, D.E., Plate tectonic model for the evolution of the central Andes, *Geol. Soc. Am. Bull.*, **82**, 3325–3346, 1971a.
- JAMES, D.E., Andean crustal upper mantle structure, *J. Geophys. Res.*, **76**, 3246–3271, 1971b.
- JAMES, D.E., The evolution of the Andes, *Sci. Am.*, **229**, 61–69, 1973.
- JENKS, W.F., Peru, Handbook of South American Geology, *Geol. Soc. Am. Mem.*, **65**, 219–247, 1956.
- JONES, D.L., W.P. IRWIN, and A.T. OVENSHERE, Southeastern Alaska—A displaced continental fragment? *U. S. Geol. Surv. Prof. Pap.*, **800-B**, B211–B217, 1972.
- JONES, D.L., N.J. SILBERLING, and J. HILLHOUSE, Wrangellia—a displaced terrane in northwestern North America, *Can. J. Earth Sci.*, **14**, 2565–2577, 1977.
- KANAEV, V.F. and N.N. TURKO, Morphology and volcanism of the Indian Ocean Floor, in *Volcanoes and Tectonosphere*, edited by H. Aoki and S. Iizuka, pp. 35–60, Tokai University Press, Tokyo, 1976.
- KAWAI, N., K. HIROOKA, and T. NAKAJIMA, Paleomagnetic and Potassium-Argon age informations supporting Cretaceous-Tertiary hypothetical bend of the main island Japan, *Paleogeogr. Paleoclimatol. Paleocol.*, **6**, 277–282, 1969.
- KEILAN-JAWOROWSKA, Z., Migrations of the multituberculata and the late Cretaceous connections between Asia and North America, *Ann. S. Afr. Mus.*, **64**, 231–243, 1974.
- LARSON, R.L. and C.G. CHASE, Late Mesozoic evolution of the western Pacific ocean, *Geol. Soc. Am. Bull.*, **83**, 3627–3644, 1972.
- LAUGHTON, A.S., D.H. MATTHEWS, and R.L. FISHER, *The Sea*, Vol. 4, Part 2, 543 pp., Wiley, New York, 1970.
- LLOYD, J.L., Tectonic history of the South Central-American Orogen, in *Backbone of the Americas*, edited by O.E. Childs, pp. 88–100, Am. Assoc. Pet. Geol., Tulsa, Ok., 1963.
- MACDONALD, W.D. and P.M. HURLEY, Pre-Cambrian gneisses from northern Columbia, South America, *Geol. Soc. Am. Bull.*, **80**, 1867–1872, 1969.
- MCELHINNY, M.W., *Paleomagnetism and Plate Tectonics*, 358 pp., Cambridge University Press, Cambridge, 1973.
- MARKS, J.G., Pacific coast geologic province, Handbook of South American Geology, *Geol. Soc. Am. Mem.*, **65**, 277–288, 1956.
- MARTIN, P.G., Marsupial biogeography and plate tectonics, in *The Biology of Marsupials*, pp. 97–115, University Park Press, Baltimore, Md., 1977.
- MELVILLE, R., Continental drift, Mesozoic continents and the migrations of the angiosperms, *Nature*, **211**, 116–120, 1966.
- MELVILLE, R., The distribution of land around the Tethys Sea and its bearing on modern plant distribution, in *Systematics Association*, No. 7, Aspects of Tethyan Biogeography, edited by C.G. Adams and D.V. Ager, pp. 291–310, The Systematics Association, London, 1967.
- MEYER, R.P., W.D. MOONEY, A.L. HALES, C.E. HELSELY, G.P. WOOLLARD, D.M. HUSSONG, L.W. KROENKE, and J.E. RAMIREZ, Project Narino III: Refraction observations across a leading edge Malpelo Island to the Colombian Cordillera Occidental, in *The Geophysics of the Pacific Ocean Basin and Its Margin*, American Geophysical Union, Geophysical Monograph, No. 19, edited by G.H. Sutton, M. Manghani, and R. Moberly, pp. 105–132, AGU, Washington, 1976.

- MILSON, J. and I.E. SMITH, Southeastern Papua: Generation of thick crust in a tensional environment? *Geology*, **3**, 117–120, 1975.
- MONGER, J.W.H. and C.A. ROSS, Distribution of fusulinaceans in the western Canadian Cordillera, *Can. J. Earth Sci.*, **8**, 259–278, 1971.
- MORRISON, R.P., *A resume of the Geology of South America*, 146 pp., Toronto Univ. Inst. Earth Sci., 1962.
- MURAUCHI, S., W.J. LUDWIG, N. DEN, H. HOTTA, T. ASANUMA, T. YOSHII, A. KUBOTERA, and K. HAGIWARA, Seismic refraction measurements on the Ontong Java plateau northeast of New Ireland, *J. Geophys. Res.*, **78**, 8653–8663, 1973.
- MURAUCHI, A., N. DEN, S. ASANO, H. HOTTA, T. YOSHII, T. ASANUMA, K. HAGIWARA, K. ICHIKAWA, T. SATO, W.J. LUDWIG, J.I. EWING, N.T. EDGAR, and R.E. HOUTZ, Crustal structure of the Philippine Sea, *J. Geophys. Res.*, **73**, 3143–3171, 1968.
- NARAIN, H., Crustal structure of the Indian subcontinent, *Tectonophysics*, **20**, 249–260, 1973.
- NELSON, G., Reviews biogeography, the vicariance paradigm, and continental drift, *System. Zool.*, **24**, 499–501, 1975.
- PALMASON, G., Crustal structure of Iceland from explosion seismology, *Visindafelag Islend. (Rit)*, **40**, 187 pp. 1971.
- RICHARDS, H.G., Tectonic evolution of Alaska, *Am. Assoc. Pet. Geol. Bull.*, **58**, 79–105, 1974.
- SCHUCHERT, C. and C.O. DUNBAR, *Outlines of Historical Geology*, pp. 291, John Wiley and Sons, Inc., New York, 1950.
- SCHUILING, R.D., Active role of continents in tectonic evolution—geothermal models, in *Gravity and Tectonics*, edited by K.A. DeJong and R. Scholten, pp. 35–47, Wiley-Interscience, New York, 1973.
- SCHWEICKERT, R.A. and D.S. COWAN, Early Mesozoic tectonic evolution of the western Sierra Nevada, California, *Geol. Soc. Am. Bull.*, **86**, 1329–1336, 1975.
- SHORE, G.G., Jr., H.K. KIRK, and H.W. MENARD, Crustal structure of the Melanesian area, *J. Geophys. Res.*, **76**, 2562–2586, 1971.
- SMITH, A.G., Plate tectonics and orogeny: A review, *Tectonophysics*, **33**, 215–285, 1976.
- SUTTON, G.H., G.L. MAYNARD, and D.M. HUSSONG, Widespread occurrence of a high-velocity basal layer in the Pacific crust found with repetitive sources and sonobuoys (with discussion), in *Structure and Physical Properties of the Earth's Crust*, Am. Geophys. Monogr., No. 14, pp. 193–209, 1971.
- SYMONS, D.T.A., Paleomagnetic notes on the Karmutsen basalts, Vancouver Island, British Columbia, *Can. Geol. Surv. Pap.*, **71-24**, 11–24, 1971.
- TAKHTAJAN, A., *Flowering Plants, Origin and Dispersal*, 310 pp., Smithsonian Institution Press, City of Washington, 1969.
- TSCHOPP, H.J., Upper Amazon basin geological province, *Geol. Soc. Am. Mem.*, **65**, 253–266, 1956.
- UYEDA, S. and Z. BEN-AVRAHAM, Origin and development of the Philippine Sea, *Nature Phys. Sci.*, **240**, 176–178, 1972.
- UYEDA, S. and A. MIYASHIRO, Plate tectonics and the Japanese Islands: A synthesis, *Geol. Soc. Am. Bull.*, **85**, 1159–1170, 1974.
- VEEVERS, J.J. and M.W. McELHINNY, The separation of Australia from other continents, *Earth Sci. Rev.*, **12**, 139–159, 1976.
- VINE, J., Spreading of the ocean floor: New evidence, *Science*, **154**, 1405–1415, 1966.
- WEEKS, L.G., Paleogeography of South America, *Am. Assoc. Pet. Geol. Bull.*, **31**, 1194–1241, 1947.
- WEGENER, A., *The origin of Continents and Oceans*, 246 pp., Dover, New York, 1915.
- WINDHAUSEN, A., *Geologia Argentina*, Peuser and Co., Buenos Aires, 1931.
- WINTERER, E.L., Anomalies in the tectonic evolution of the Pacific, in Prog. with Abstr: *The Geophysics of the Pacific Ocean Basin and Its Margin, 8–10 Dec., 1974*, p. 23, Univ. of Hawaii, Honolulu, 1976.
- WOOLLARD, G.P., The interrelationships of crustal and upper mantle parameter values in the Pacific, *Rev. Geophys. Space Phys.*, **13**, 87–137, 1975.

BENIOFF ZONES, ABSOLUTE MOTION AND INTERARC BASIN

Francis T. Wu

*Department of Geological Sciences and Environmental Studies,
State University of New York, Binghamton, New York, U.S.A.*

(Received July 20, 1978; Revised October 9, 1978)

While in the Honshu region, the Benioff zone exhibits a straight profile, dipping west at about 30° , the Mariana arc has a curved zone changing into a very steeply dipping zone at depth, and the Peru-Chilean arc has a very extended and gently dipping zone at 16° . These can be interpreted as three type-cases where, correspondingly, the trenchline is at rest with respect to the deeper mantle and the trenchline is moving in the dip direction with respect to the deeper mantle. Where the direction of relative motion has changed, we can then expect sharper bends as in the cases of Central Bonin and the Peru-Chilean arcs.

This interpretation is consistent with the concept of the decoupling of plate motion across the asthenosphere and enables us to use the Benioff Zone to decipher the recent history of absolute plate motion.

The steepening of the Marianas Zone is closely related to the westward motion of the Philippine Sea Plate. The separation of the plates due to anchoring of the trenchline, after the subducted lithosphere reaches the mesosphere, and the continued westward motion of the Philippine Sea Plate is probably responsible for the formation of the back-arc basin and the lack of large shallow thrust-type earthquakes there. This could be one of the several mechanisms for the formation of the back-arc basin.

1. Introduction

Relative motions of tectonic plates have been studied in great detail (LEPICHON, 1968; MORGAN, 1968; MINSTER *et al.*, 1974; among others). Recently, attention has been turned to the "absolute" motion of plates (MORGAN, 1972; WILSON, 1973; MINSTER *et al.*, 1974; and others). Strictly speaking, "absolute" is with respect to the Earth's center. But since the upper mantle below the asthenosphere, the mesosphere, is often considered to be decoupled from the plate motion, and the motion of the mesosphere is probably of the order 1–2 cm/year (MOLNAR and FRANCHETEAU, 1975), slower than most of the plate velocities we are interested in, we may regard the mesosphere as stationary. Depending on the absolute motions of plates in a subduction regime, the subducted lithosphere may have to move through the asthenosphere. The resistant force exerted by the asthenosphere can conceivably modify the shape of the slab. Also, after the slab has been inserted into the mesosphere, the motion of the trenchline may be restricted; this restriction in motion of the trenchline may create tension on the upper plate side, if the upper plate is moving away from the trenchline.

Seismic data, in general, are of ephemeral nature in comparison to the time needed to create major geological expressions. Thus focal mechanism solution is reflecting the stress conditions and the orientation of the fault planes prevalent at the time of the earthquake and the present shallow seismicity may only have a vague memory of what has gone on millions of years before. The Benioff zone, interpreted as a subduction zone, bears

information regarding the motions of the plates associated with that boundary for the duration of its activity; when the length of the subduction is L and the velocity of subduction is V then the duration is L/V . In other words, under our assumptions, the varying slope of a Benioff zone as a function of depth coupled with velocity of subduction can be translated into time history of the absolute motions of the plates involved. Because most of the Benioff zones are continuous and the obvious breaks in some of them are short, the time resolution of our interpretation is finer than that based on discrete volcanic islands although only the recent 10 million years or so history can be studied this way.

Aspects of the relation of the shape of Benioff zone to the motion of plates (or more precisely the trenchlines) have been discussed by MCKENZIE and MORGAN (1969), LUYENDIK (1970), TULLIS (1972, 1976), WU (1971, 1972), KARIG (1971b), WILSON (1973), JACOBY (1973), and TOVISH and SCHUBERT (1978) among others. In this paper, we shall attempt to systematically examine the well-defined Benioff zones and explain the inclinations and the changes in inclination as a function of depth in terms of absolute motion and change in absolute motion in the past. We shall include in these discussions considerations regarding the generation of down-dip stresses (ISACKS and BARAZANGI, 1977; HASEGAWA *et al.*, 1978) as well as the magnitude and frequency of earthquakes.

A problem closely related to the subduction zone, namely the formation of interarc basin has received much attention (KARIG, 1971a, b; TOKSOZ and BIRD, 1977; UYEDA and KANAMORI, 1978; POEHL, 1978; and others). We shall briefly discuss the kinematics in terms of absolute motions of trenchlines and separation of plates.

2. Interpretation of Different Configurations of Benioff Zones

Along each island arc the configuration of Benioff zone varies, not only in the down-dip direction but also laterally. The lateral variations in some cases can be understood in terms of the variations of the absolute velocities of the plates involved. In this section we shall be concerned with the depth profiles only. But in our discussion of the actual arcs later, the variations of shapes along the arcs shall be taken into consideration.

ISACKS and MOLNAR (1971) and ISACKS and BARAZANGI (1977) have summarized the general shapes of the Benioff zones perpendicular to the trench as well as the down-dip stresses which has partly been updated by the works of HASEGAWA *et al.* (1978). Figure 1 is a reproduction of Isacks and Molnar's results.

Of the well-developed Benioff zones, we can distinguish three cases: (1) very straight and moderately dipping zone (example: Honshu), (2) steeply dipping zone (example: the lower portions of Marianas and Peru), (3) curved and very shallow dipping zones (example: the upper portions of Peru and Chile zones). Some of the zones can be recognized as a combination of 2 and 3 (example: Peru and Chile zones, deep parts included; New Hebrides).

Although ISACKS and MOLNAR (1971) believe that the irregularities in the Benioff profiles represent relative motion of the upper and the lower part of the slabs, they called the non-straightness of the profiles "contortions", and felt that both the contortion and the distribution of the down-dip stresses are not amenable to simple explanations. MCKENZIE and MORGAN (1969) however, in an attempt to match the slope of the Ryukyu Benioff zone to the average slope of the Bonin Benioff zone, postulated that the matching can be done by moving the Bonin trench eastward for about 200 km, implying that the steeper profile of the Bonin Benioff zone was a result of the westward motion of Bonin

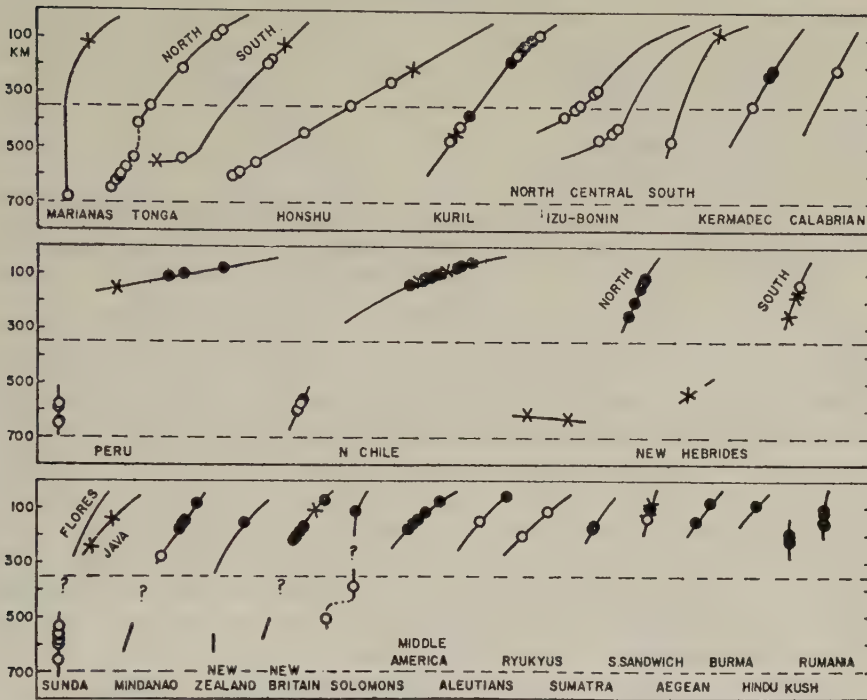


Fig. 1. Global summary of the distribution of down-dip stresses in inclined seismic zones. The stress axis that is approximately parallel to the dip of the zone is represented by an unfilled (open) circle for the compressional or P-axis and a filled (solid) circle for the tensional or T-axis; an X indicates that neither the P- nor the T-axis is approximately parallel to the dip. For each region the line represents the seismic zone in a vertical section aligned perpendicular to the strike of the zone. The lines show approximately the dips and lengths of the zones and gaps in the seismic activity as a function of depth. (After ISACKS and MOLNAR, 1971)

trench. KARIG (1971b) concluded that the slope of the upper portions of several Benioff zones are influenced heavily by interarc spreading. WU (1971, 1972) applied the concept of absolute motion of plates and explained the change of dip of Benioff zone along the Izu-Bonin-Marianas arc as a result of the clockwise rotation of Philippine Sea Plate. He also described the shallow dipping of the Benioff zone under South America as a result of overriding of the Nazca plate by South America. TULLIS (1972) thought that the deeper part of the Benioff zone may have an anchoring effect. WILSON (1973, 1974) had similar conclusions as cited above. Since the discovery of the double seismic zone (HASEGAWA *et al.*, 1976, 1978; ISACKS and BARAZANGI, 1977) the down-dip stresses in some cases have been understood much better.

In this section, we shall cast the ideas expressed in my earlier works cited above in a more systematic way and extend the arguments further toward a more complete presentation.

For two plates in contact, the absolute velocities V_1 and V_2 (let us consider only the components perpendicular to the arc) determine whether *initially* a subduction zone would form. The "truth table" is shown in Fig. 2. The conditions (1), (5), (6), and (7) represent situations where subduction can occur and (2), (3), (4), and (8) are cases where

	\vec{V}_2	\vec{V}_2
\vec{V}_1	(1) $V_1 > V_2$	(5) $V_1 > V_2$
	(2) $V_1 \leq V_2$	(6) $V_1 \leq V_2$
\vec{V}_1	(3) $V_1 \geq V_2$	(7) $V_1 < V_2$
	(4) $V_1 < V_2$	(8) $V_1 \geq V_2$

$V_1 \quad T \quad V_2$

Fig. 2. "Truth table." The arrows over V_1 in the table indicate the direction of the velocities V_1 of the plates as shown schematically below the table. Shaded areas indicate the subduction will occur under that condition.

spreading will occur. If conditions (1) or (7) persists after the initiation of subduction, at first the trenchline will attempt to follow the upper plate, but as the plate enters deeper into the asthenosphere and then the mesosphere, the motion of the trenchline will be greatly hindered due to the resistance exerted on the subducted slab by the asthenosphere and the mesosphere. Under these conditions, there will be a lack of compression and shallow seismicity near the plate boundary; backarc spreading can take place, and the Benioff zone is likely to be steep. If conditions (5) and (6) persist, on the other hand, the trenchline will be forced to migrate against the direction of subduction due to the overriding of the subducting plate by the upper plate; in this instance, the compression is high, therefore shallow, large earthquakes can take place. In cases (1), (5), (6), and (7), if one of the velocities becomes zero then the trenchline will be stationary.

Thus, based on the motion of the trenchline, we can distinguish three cases:

I. When the trenchline is stationary. FRANK'S (1968) attempt to explain the dip of Benioff zone assumed a rigid shell, then, on a sphere, the dip of the Benioff zone will be equal to two times the radius of the surface trace of the island arc in degrees. In vertical profile, such a zone will be a straight line. As TOVISH and SCHUBERT (1978) concluded however, the correlation of the dip angle with the radius of curvature is too poor for Frank's simple geometrical relation to be significant in determining the dip angle. JACOBY (1973) demonstrated by a simple model experiment that gravity sinking of a non-rigid slab also keeps a straight profile after it enters into the underlying liquid.

Because of the expected high viscosity of the mesosphere, the subduction zone can be expected to incline at the slope at which it emerges from under the asthenosphere to enter the mesosphere. Once this angle is established, the subduction will persist at that angle, unless there is substantial convection in the mantle, or if the subducted lithosphere has to move through the asthenosphere and/or the mesosphere.

Such profile exists—in its full form to the depth of 700 km only in one arc, i.e. Honshu (Fig. 1). Disregarding profiles that only extend to intermediate depths, whereby a good definition of the subducted zone is not possible, then we can determine one area on the globe where the relative velocity between the trenchline and the mesosphere is near zero. The time interval when this conclusion is applicable is from about 15 mybp to present.

ISACKS and MOLNAR (1971) show that the focal mechanisms for earthquakes indicate down-dip compressive stresses for earthquakes along the whole slab, although recent works by HASEGAWA *et al.* (1978) show a well-defined double-zone under northeastern Japan down to a depth of about 150 km and the mechanisms along the top zone indicate thrust faulting or down-dip compression while the bottom zone indicates down-dip tension. These results are consistent with the unbending of the Benioff zone going into the astheno-

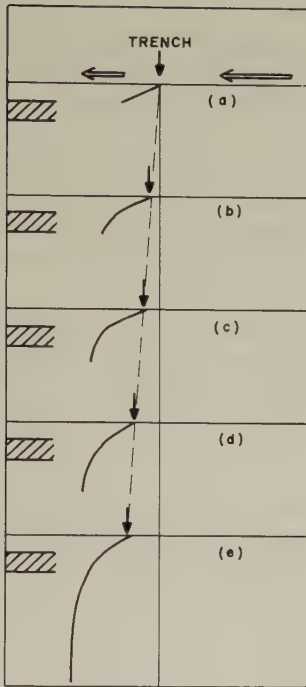


Fig. 3. The configuration of Benioff zone for a case where the upper plate is moving away from the trench line. See text for details. Hatched zone represents asthenosphere.

sphere (ISACKS and BARAZANGI, 1977; ENGDAHL and SCHOLZ, 1978; HASEGAWA *et al.*, 1978).

II. *Where the trenchline is migrating in the direction of subduction.* In Fig. 3, we have shown schematically the sequence of events that could lead to a configuration such as that under the Marianas (Fig. 1). As soon as the lithosphere dips into the asthenosphere, its advance through the asthenosphere will be resisted much as a vane moving through a viscous liquid would be resisted. As a consequence, the lithosphere will be bent further. The resistance will increase as a function of viscosity of the asthenosphere and the velocity at which the trenchline migrates.

If the bending force is such that when the tip of the subducted lithosphere is inclined at 90° or less from the horizontal, then it will enter the mesosphere; if the dip is greater than 90° , i.e., the lithosphere overturns, then the plate may be broken off and left behind.

Upon entering the mesosphere where the viscosity is expected to be high, it is likely that the subducted lithosphere acts as an anchor for the trenchline, although the anchoring could not be perfect because of the finite viscosity. If the upper plate keeps on moving after the subducted plate reaches the mesosphere, then near the plate boundary there will be a general lack of compression. We may observe two consequences. First, tension may occur behind the arc and the formation of back-arc basin may ensue. Secondly, due to the lack of compression, large shallow-thrust earthquakes may not occur.

For this case, the stress distribution will be quite different from that of the last case (with a stationary trenchline). Using the Marianas as an example (see next section), from 0 to 150 km, the curvature of the Benioff zone increases and we expect the down-dip tension type of mechanisms to be associated with earthquakes near the top of the lithosphere, and down-dip tension for events near the bottom of the lithosphere.

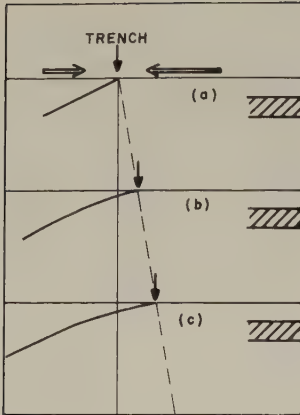


Fig. 4. The configuration of Benioff zone for a case where the upper plate is advancing over the trench. See text for detail.

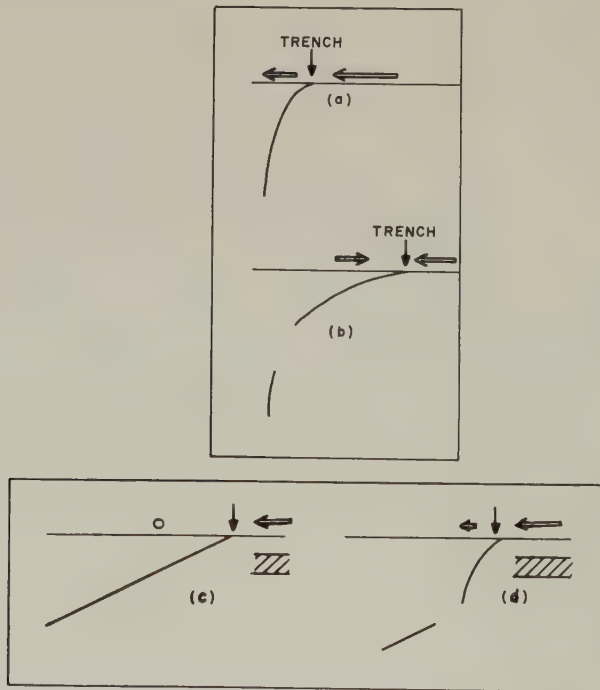


Fig. 5. The configurations of Benioff zone for cases where the absolute motions of plates changed during the course of subduction: a and b, from upper plate moving away from the trench to moving over the trench; c and d, from stationary upper plate to the upper plate moving away from the trench.

III. Where the trenchline is advancing against the direction of subduction. Assuming that the plate is subducting at an initial angle of 45° (Fig. 4(a)); as the trenchline is advancing in the direction opposite to that of subduction, a movement of the point at which the lithosphere enters will be applied at the point where the asthenosphere will occur, thus

the dip of the subduction zone will decrease. The viscous asthenosphere will resist the rotation of the subducted lithosphere and as the subduction continues and the lithosphere gets farther from the subduction point, the dip of the subduction will not be influenced further by the motion of the upper plate. Figure 4(b) and (c) show schematically the sequence of possible events in such a case.

The seismicity in this case will involve very large, shallow thrust type of earthquakes.

IV. Where in the past history of the formation of the subduction zone has the sense of motion changed. If the initial subduction is in any one of the three categories discussed above and changed later to any other category, then a discontinuity in curvature or a break may exist in the Benioff zone (Fig. 5(a) and (b)). Such discontinuity is seen in Chile, Peru, New Hebrides, South Tonga, etc. (see Fig. 1). While for Peru, Chile and New Hebrides there are actually discontinuities in Benioff zones, for Tonga the profile is without gaps.

3. Discussion of Examples

In the last section, we have discussed the possible consequences of absolute plate motions upon the shapes of the Benioff zones. In this section, we shall explain in some detail several examples for illustration. In the process, we will be able to provide another basis for determination of the sense of absolute motion (in addition to that provided by the "hot spot" theory).

3.1 Izu-Bonin-Marianas-Yap-Palau

The clearest example of case II is the eastern margin of the Philippine Sea Plate.

The Philippine Sea Plate itself is relatively simple; it has a typical oceanic crust in most parts (MURAUCHI *et al.*, 1968) and probably thin lithosphere of about 50 km (KANAMORI and ABE, 1968). There are some older structures in several parts of the Philippine Sea, such as Oki-Daito Ridge, the Central Philippine Basin Fault (HESS, 1946) and Palau-Kyushu Ridge that are not yet fully understood. Some of these structures apparently have not been active since mid-Miocene (MIZUNO *et al.*, 1978); therefore, for our purpose, they can be viewed as part of the inert plate. The formation of the Young Mariana Trough and the variations in subduction geometry of the eastern boundary are the problems that we shall attempt to address by using the concept described in the previous section (case II).

The seismicity along the eastern boundary of the Philippine Sea Plate, namely along the Izu-Bonin-Marianas-Yap-Palau arcs, has been studied by KATSUMATA and SYKES (1969) and more recently by ISACKS and BARAZANGI (1977). In the cross section (Fig. 6) based on KATSUMATA and SYKES (1969) the slope of the Benioff zone below 100 km steepens successively southward. The lengths of the Benioff zone under Izu-Bonin and the Marianas remain about 800 km, thus the depth of the zone increases toward the Marianas. The seismicity under the Volcano Islands (near 25°N) and the southern part of the long arc chain is low; although as pointed out by ISACKS and BARAZANGI (1977), the foci under the Volcano Islands do reach 500 km depth, the foci definitely shoal under the southern Marianas and only shallow (0–30 km) foci are found under the Yap and Palau. As shown in Fig. 7, adapted from ISACKS and BARAZANGI (1977), the 500 km foci lie directly under the 100 km foci near the Volcano Islands. The Benioff zone implied by Fig. 7 would have an increasingly steep profile starting from Izu Island going southward toward the Marianas, where the zone below 200 km becomes vertical; under the Volcano Islands and the northern Marianas the zone has overturned.

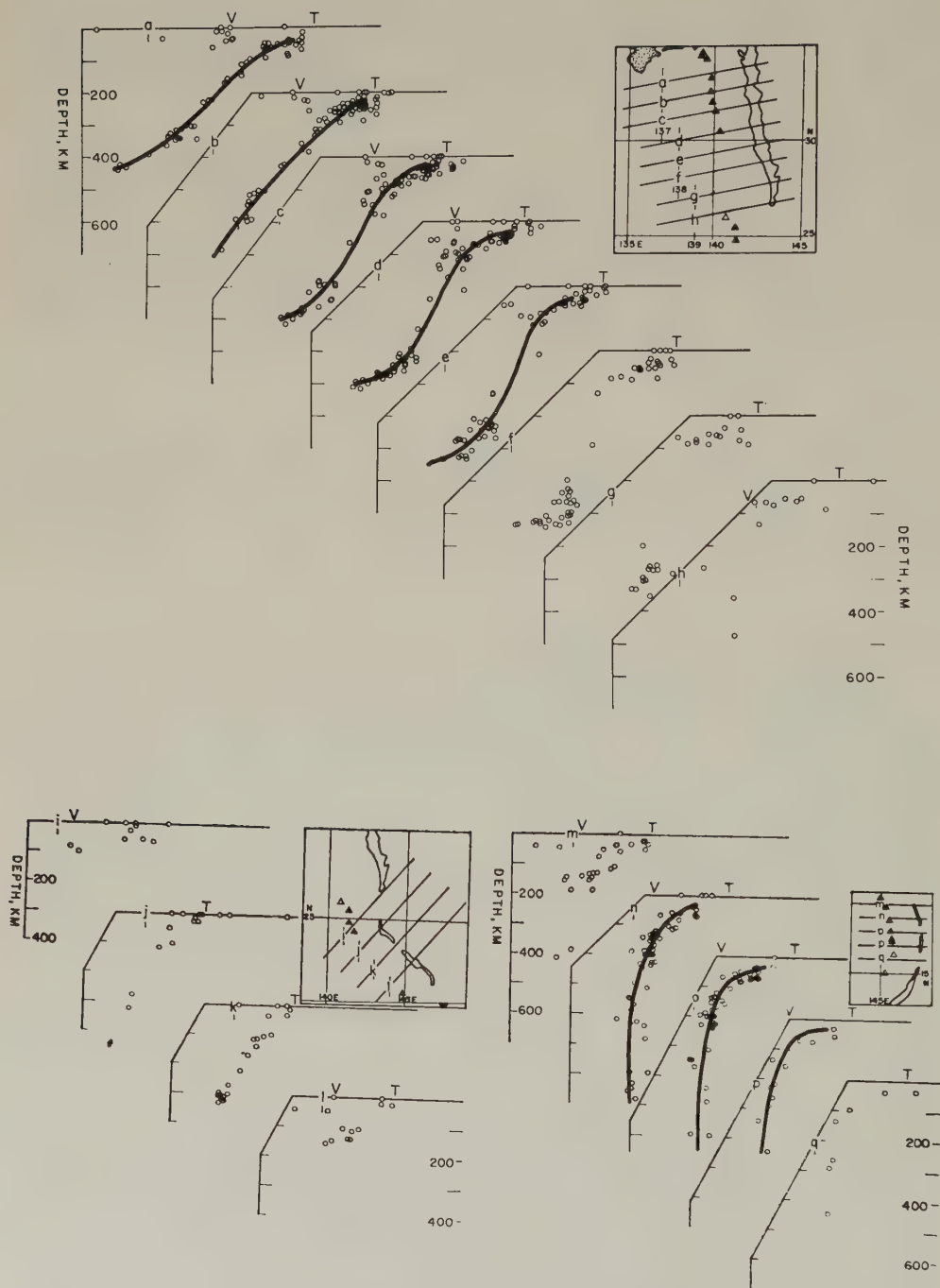


Fig. 6. Series of closely spaced vertical sections perpendicular to Izu-Bonin-Marianas trench showing changes in configuration and apparent thickness of deep focal zone. Orientation of sections shown in upper right corner. V denotes volcano and T denotes trench. (After KATSUMATA and SYKES, 1969)

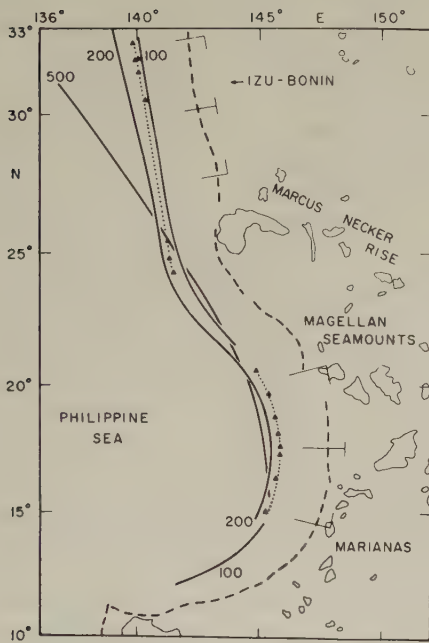


Fig. 7. The Benioff zone contours under Izu-Bonin and Marianas showing the overturn of Benioff zone near 25°N and 15°N. (After ISACKS and BARAZANGI, 1977)

In explaining the geometry of the eastern boundary of the Philippine Sea Plate, it is noted first that the Philippine Sea Plate itself is rotating clockwise (with respect to the lower mantle) around a pole close to the junction of the Izu-Bonin arc with the Honshu arc (Wu, 1971). As a result, the upper plate moves west at an increasing rate from Izu-Bonin toward the Marianas, Yap and Palau. In the north, the velocity of the Pacific plate is much higher than that of the Philippine Sea plate so the subduction takes place more or less normally. To the extreme south, across the Palau arc, the velocity of the Philippine Sea Plate almost matches that of the Pacific plate and little or no subduction is taking place there. Perhaps south of Palau the velocities match exactly and no hint of subduction is detected.

In between, the slope of the subduction zone increases southward as a consequence of the more rapid westward migration of the trenchline. Initially, the trenchline would follow the upper plate; as the subduction zone reaches beyond the mesosphere, however it provides at least a partial anchor for the trenchline. The continuous pulling away of the Philippine Sea then causes tension to occur west of the trenchline, thus the formation of the southward widening Mariana Trough. According to this scheme, the back-arc basin ought to widen starting from the junction of Honshu and Izu. As VOGT *et al.* (1976) have suggested however, the approach of the Marcus-Necker ridge has probably created the bend in the Izu-Bonin-Marianas chain. In our concept, this is equivalent to speeding up the westward migration of the trenchline at the bend, and thereby creating an overturn of the subduction zone and perhaps closing the back-arc basin there.

The seismicity in the Marianas is quite low and the lack of large shallow thrust-type earthquakes is especially noticeable along the whole eastern boundary of the Philippine Sea Plate. Such lack can be expected from the presence of a tensile regime behind the arc due to plate separation.

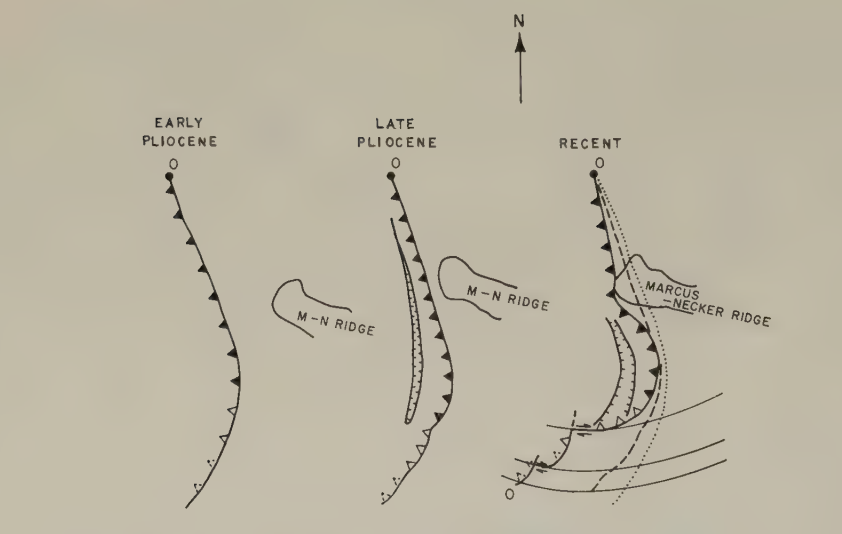


Fig. 8. Reconstruction of the tectonic history of the Marianas.

Because of the low seismicity, very few focal mechanism solutions are available by using world-wide data. There is the possibility that the double zone can be detected in the Marianas by using local high sensitivity stations. From the increase of the curvature of the Marianas subduction zone, the top down-dip tension and bottom down-dip compression may persist to greater depth than under the Honshu and the “unbending” should commence at a depth of about 150–250 km.

We shall now attempt to reconstruct the history of the eastern boundary of the Philippine Sea Plate since early Pliocene (KARIG, 1971b). The time that corresponds to this age is about 10 mybp, which is consistent with the length of the Benioff zone divided by the absolute velocity ($L=800$ km, $V=9$ cm/year, $L/V \sim 9 \times 10^6$ years). This perhaps represents the latest “pulse” of subduction activity along this boundary (KARIG, 1971b).

The reconstruction is shown schematically in Fig. 8. Beginning from early Pliocene, the subduction zone we see now started to form. The initial boundary could have been a broad arc. As the subduction proceeded because of the differential resistance to motion between sections, the arc began to tear along small circles around the rotation pole. This tear becomes more pronounced as the subduction zone reached the mesosphere. In late Pliocene, an interarc basin opened along the lithosphere weakened by thermal activity associated with the subduction because of the tension created by the pulling away of the Philippine Sea Plate and the anchoring of the trenchline. Then the Marcus-Necker Ridge that came in contact with the Philippine Sea Plate, started to push the subduction boundary in front of the ridge westward, closing partially the interarc basin north of it and overturning the Benioff zone directly in front of it. From then on, the basin behind the Marianas arc continued to open and the tear and bending of arcs continued until today.

3.2 Peru and Chile

Seismicity and focal mechanisms of the western margin of South America have been

discussed by ISACKS (1970), ISACKS and MOLNAR (1971), STAUDER (1973) and ISACKS and BARAZANGI (1977).

The main feature in both regions are a very shallow-dipping upper Benioff zone and a very steep-dipping lower Benioff zone. The two zones are apparently broken as shown by seismicity, but based on wave propagation studies, opinions differ. ISACKS and BARAZANGI (1973) believe that high frequency arrivals from deep earthquakes at the stations indicate a continuous slab; SNOKE *et al.* (1973) interpreted the high frequency arrivals as phases reflected at the top interface between the slab and the mantle, thereby negating the necessity of assuming a continuous slab from 650 km up to the trench. As far as our present discussion is concerned, the question of continuity of the slab is not so important as the change in dip between the shallow and the deep parts.

There are discernible differences among the Benioff profiles under Peru, northern Chile, central Chile and southern Chile as shown by BARAZANGI and ISACKS (1976) and ISACKS and BARAZANGI (1977). Barazangi and Isacks' profiles are adapted and shown in Fig. 9. While the lengths of the observable upper Benioff zones in these areas are about the same (~ 730 km), the northern and southern Chilean profiles (section C-C) appear to be concave downward, but the Peruvian and central Chilean profiles are concave upward between 100 and 300 km inland from the trench, then became flat further inland and finally became concave downward (sections B-B and D-D). The common feature for all these profiles is the small dip angle of the Benioff zones.

Section C-C can be interpreted as resulting from a westward-advancing South America over the Nazca plate based on the description in case III (Fig. 4). The length of the subduction divided by the average relative motion velocity gives an age of about 6.5 my. Then we can estimate the distance of the trench has migrated westward by multiplying the absolute velocity of South America moving west: $23 \text{ mm/year} \times 6.5 \text{ my} \cong 150 \text{ km}$.

The Peruvian and the central Chilean sections can be viewed as anomalous in that they are perturbed because of the subduction of aseismic ridges: the Nazca Ridge for Peru and Juan Fernandez Ridge in the case of central Chile (see for example VOGT *et al.*, 1976). The point at which the Nazca Plate contacts the South American Plate moved south, because the ridge is oblique to the direction of subduction. If the dip angle of the Benioff zone is proportional to the density of the subducted lithosphere, then the less dense aseismic ridge would form the low angle Benioff zone. The absence of a trench where the aseismic ridges come to the subduction boundary, whence not very much sediments are carried down to depth, will be responsible for the lack of recent volcanism over the subducted ridges.

The deeper part of the subduction zones have apparently very steep dips. It could mean that before 7 mybp, the sense of the absolute motions of the South American plate might have been different, i.e., it could have been moving east. The rather drastic change in the dip between the deeper Benioff zone and the shallower Benioff zone represents a change in the nature of the plate motions there.

3.3 Tonga-Kermadec

Along the Tonga-Kermadec zone, the Benioff zone, below about 100 km, steepens southward from about 45° in northern and southern Tonga and 60° in Kermadec (Fig. 1). According to our previous discussion, we would expect the trenchline to have moved westward with respect to the lower mantle in the southern part of this chain. One possible cause for this behavior is the slowing down of subduction in New Zealand due to the buoy-

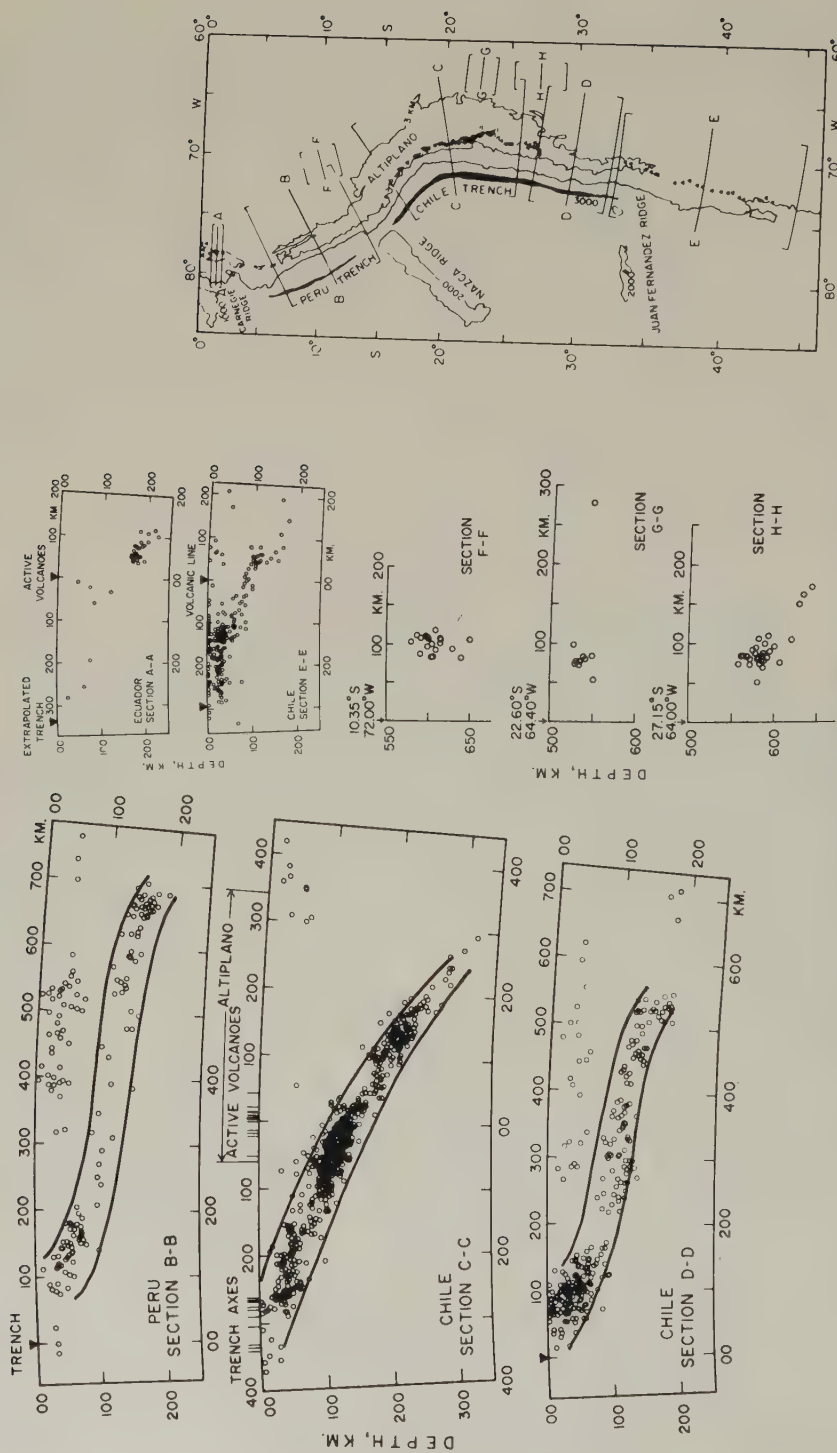


Fig. 9. Cross sections showing segments of inclined seismic zone (A, B, C, D, E) and deep seismic zone (F, G, H). See inset for locations and limits of sections. (After BARAZANGI and ISACKS, 1976)

ancy of the Chatham rise and the New Zealand Plateau and the push they exert on the Indian plate. The relative short subduction zone under New Zealand is fairly steep (65°).

Behind Tonga, we have one of the interarc basins that are considered to be active (KARIG, 1971). In contrast to the Marianas, here the map view of the trough is closely related to the configuration of the Benioff zone underneath where the subduction has a gentle dip, the interarc basin is wide, and vice versa.

4. *Back-Arc Basins*

Interarc basins are found behind some arcs (Marianas, Tonga, etc.) but not others (Aleutians, New Hebrides, Indonesia, etc.). They seem to form an integral part of some of the arc systems and are therefore important features to be understood in order to further our understanding of the global tectonics. UYEDA (1977) has summarized the possible mechanisms that operate to create the basins namely, ridge subduction, ocean basin entrapment, backarc opening ("Karig's process") and leaky transform faulting. It is difficult to envisage ridge subduction to be genetically related to the formation of interarc basin. Since the ridge represents a weakness, the subducted ridge may create a break in the subduction zone, but whether this could in turn cause a basin to open above this break is to be considered. The Gulf of California example can conceivably be explained by the northward propagation of the East Pacific Ridge rather than the eastward migration of it. The entrapment scheme will leave a basin behind the arc not genetically related to it. Back-arc opening and leaky transform faulting are still being actively studied (TOKSÖZ and BIRD, 1977; UYEDA, 1977).

In a previous paper (WU, 1972) and in the previous discussion in this paper, we have proposed another mechanism namely, the creation of interarc basin due to the tension resulting from plate separation and possibly the closing of parts of the basin due to the compression arisen from the forced migration of sections of the trench toward the basin. We have discussed the possible mode of formation of the Mariana Trough and closure of the Izu-Bonin Trough as well as the southern part of the Iau-Hauve Trough based on these reasonings. The plate-separation tension can explain the lack of large earthquakes in the Marianas (WU, 1972).

The northern part of the Lau-Havre Basin is more complicated. WEISSEL (1977) interprets the magnetic profiles based on the back-arc opening model, but the patterns are by no means clear. SCLATER *et al.* (1972) had earlier interpreted similar data quite differently. POEHLS (1978), using Sclater's model, hypothesized an opening of the Lau Basin through shear along the left-lateral fault separating the Fiji Plateau from the south Fiji Basin (see also WU, 1972). It is a question however, whether the lithosphere is rigid enough to transmit this stress for over 1,000 km. It is possible that the Pacific Plate is connected or coupled strongly through large-scale asperities on the plate boundary to the south Fiji Basin and the lithosphere behind the Tonga arc is torn apart at its weakest points, namely where the magma rises from the subduction zone. In fact, morphologically Lau Ridge and the Fiji Islands are continuous and the Fiji Islands have apparently undergone counter-clockwise rotation in the recent past (GREEN and CULLEN, 1973), indicating the nature of the deformation of the Fiji Plateau.

Another factor worth considering is that the descending slabs, especially those descending at higher rates are denser than the surrounding mantle material due to the lower temperature in the slabs (MINEAR and TOKSÖZ, 1970). SEGAWA and TOMODA (1976)

confirmed Minear and Toksoz's result by demonstrating that if the known crustal density structures near northeast Honshu and across the Shikoku Basin, Izu-Bonin Ridge and Izu-Bonin Trench are taken into account, then a heavier slab with $\Delta\rho\sim 0.05\text{ g/cm}^3$ is needed to fit the free-air anomaly data. In the presence of this denser slab, isostatic equilibrium is maintained if the material over the slab is less dense than the surrounding or if the column, i.e., with a depression over the slab, or a combination of both. According to the Airy principle (HEISKANEN, 1938), the elevation of anomalous column is related to the excess density in the slab ρ_s , the vertical thickness of the slab ΔR and the density of the average mantle ρ_0 by

$$h = \frac{\Delta R (\rho_s - \rho_0)}{\rho_s}.$$

If $\Delta R=100\text{ km}$, $\rho_s-\rho_0=0.05\text{ g/cm}^3$, $\rho_s=3.25\text{ g/cm}^3$, the $h=1.54\text{ km}$, i.e., if the density over the slab remains the same as the surrounding, the backarc trough should be 1.54 km deep; if the density is lower, as one would expect from the upward curved isotherms (TOKSÖZ and BIRD, 1977), then the trough would be shallower.

If isostatic readjustment is the mechanism for the formation of the interarc basin, then the isostatic anomaly over the interarc basin should approach zero and the width of the basin should be correlated with the presence of the slab underneath: the gentler the dip the wider the basin. The variation in width of the Lau-Havre Basin behind the Tonga-Kermadec arc can perhaps be explained this way. One could imagine that the adjustment would be more complete as the mantle material above the slab heats up and flows more readily.

5. Conclusion

By invoking the absolute motion of the plates, i.e. relative motion between the tectonic plates, and the more or less stationary mesosphere, we are able to explain the vertical profile of some of the Benioff zones. Although we are only making a qualitative correlation of the various factors involved, a numerical modelling of the situation is desirable. In fact, in order to deal with the details of the rather complex profiles of the different zones, one needs to do such modelling.

With regard to the interarc basins, we have proposed some additional mechanisms to explain their existence, recognizing that these mechanisms are probably neither universal nor complete. So far, the study of the interarc basins are limited to the use of magnetics, shallow seismic reflection method, heat flow and dredging. For further details of the deeper structures under the more interarc basins, seismic refraction profiles and/or reflection profiles are perhaps needed to yield additional critical data.

The support of NSF Grant EAR76-14457 and INT76-20073 during the course of the work is acknowledged.

REFERENCES

- BARAZANGI, M. and B. ISACKS, Spatial distribution of earthquakes and subduction of the Nazca plate beneath South America, *Geology*, **4**, 686-692, 1976.
- FRANK, F.G., Curvature of island arcs, *Nature*, **220**, 363, 1968.
- ENGDAHL, E. R. and C.H. SCHOLZ, Double planed Benioff zone beneath island arcs: An unbending of the lithosphere, Abstr., p. 22., Int. Geodyn. Conf., Tokyo, 1978.
- GREEN, D. and D.J. CULLEN, The tectonic evolution of the Fiji region in *The Western Pacific*, edited by Coleman, pp. 127-145, Crane, Russak and Co., New York, 1973.

- HASEGAWA, A., N. UMINO, and A. TAKAGI, Fine structure of deep seismic plane in northeast Japan, Abstr., Spring Meet. of Seismol. Soc. Jpn., 1976.
- HASEGAWA, A., N. UMINO, and A. TAKAGI, Double-planed deep seismic zone beneath the northeastern Japan arc, Abstr., p. 44, Int. Geodyn. Conf., Tokyo, Japan, 1978.
- HEISKANEN, W.A., New isostatic tables for the reduction of the gravity values calculated on the basis of Airy's hypothesis, Publ. Isostatic Inst., No. 2, 1938.
- HESS, H.H., Major structural features of the western north Pacific: An interpretation of H.O. 5485 Bathymetry chart, Korea to New Guinea, *Geol. Soc. Am. Bull.*, **59**, 417-446, 1946.
- ISACKS, B., Focal mechanisms of earthquakes in western South America, *EOS, Trans. Am. Geophys. Union*, **51**, 355, 1970.
- ISACKS, B. and M. BARAZANGI, High frequency shear waves guided by a continuous lithosphere descending beneath western South America, *Geophys. J. R. Astr. Soc.*, **33**, 129-139, 1973.
- ISACKS, B. and M. BARAZANGI, Geometry of Benioff zones: Lateral segments and downgoing bending of the subducted lithosphere, in *Island Arcs, Deep Sea Trenches, and Back Arc Basin*, Vol. 99, edited by Talwani and Pitman, p. 114, Am. Geophys. Union, 1977.
- ISACKS, B. and P. MOLNAR, Distribution of stresses in the descending lithosphere from a global survey of focal-mechanism solutions of mantle earthquakes, *Rev. Geophys. Space Phys.*, **9**, 103-174, 1971.
- JACOBY, W.R., Model experiment of plate movements, *Nature (Phys. Sci.)*, **242**, 130-134, 1973.
- KANAMORI, H. and K. ABE, Deep struture of island arcs as revealed by surface waves, *Bull. Earthq. Res. Inst., Tokyo Univ.*, **46**, 1001-1025, 1968.
- KARIG, D.E., Structural history of the Mariana arc system, *Geol. Soc. Am. Bull.*, **83**, 323-344, 1971a.
- KARIG, D.E., Origin and development of marginal basins, *J. Geophys. Res.*, **76**, 2542-2561, 1971b.
- KATSUMATA, W. and L.R. SYKES, Seismicity and tectonics of Western Pacific: Izu-Mariana-Caroline and Ryukyu-Taiwan Regions, *J. Geophys. Res.*, **74**, 5923-5948, 1969.
- LEPICHON, X., Sea-floor spreading and continental drift, *J. Geophys. Res.*, **73**, 3661-3697, 1968.
- LUYENDIK, B., Dips of downgoing lithospheric plates beneath island arcs, *Geol. Soc. Am. Bull.*, **81**, 3411-3416, 1970.
- MCKENZIE, D.P. and W.J. MORGAN, Evolution of triple junctions, *Nature*, **224**, 125-133, 1969.
- MINEAR, J. and M.N. TOKSÖZ, Thermal regime of a downgoing slab and new global tectonics, *J. Geophys. Res.*, **75**, 1397-1419, 1970.
- MINSTER, J.B., T.H. JORDAN, P. MOLNAR, and E. HAINES, Numerical modeling of instantaneous plate tectonics, *Geophys. J. R. Astr. Soc.*, **36**, 541-576, 1974.
- MIZUNO, A., Y. OKUDA, S. NAGUMO, H. KAGAMI, and N. NASU, Geology and subsidence history of the Daito ridge and associated basins, North Philippine Sea, Abstr. p. 102, Int. Geodyn. Conf., Tokyo, 1978.
- MOLNAR, P. and J. FRANCHETEAU, The relative motion of 'hot spots' in the Atlantic and Indian Oceans during the Cenozoic, *Geophys. J. Roy. Astron. Soc.*, **43**, 763-774, 1975.
- MORGAN, W.J., Rises, trenches, great faults and crustal blocks, *J. Geophys. Res.*, **73**, 1959-1981, 1968.
- MORGAN, W.J., Plate motions and deep mantle convection, *Geol. Soc. Am. Bull.*, **132**, 7-22, 1972.
- MURAUCHI, S., N. DEU, S. ASANO, T. HOTTA, T. YOSHII, K. ASANUMA, K. HAGIWARA, T. ICHIKAWA, W.J. SATO, J.I. EWING, N.T. EDGAR, and R.E. HONTZ, Crustal Structure of the Philippine Sea, *J. Geophys. Res.*, **73**, 3143-3171, 1968.
- POEHL, K.A., Inter-arc basins: A kinetic model, *Geophys. Res. Lett.*, **5**, 325-328, 1978.
- SEGAWA, J. and Y. TOMODA, Gravity measurements near Japan and study of the upper mantle beneath the oceanic trench-marginal sea transition zone, in *The Geophys. of the Pacific Ocean Basin and Its Margin*, pp. 35-52, The Woolard Vol., Am. Geophys. Union, 1976.
- SCLATER, J.G., J.W. HAWKINS, J. MAMMERICKX, and G.G. CHASE, Crustal extension between the Tonga and Lau ridges, Petrologic and geophysical evidence, *Bull. Geol. Soc. Am.*, **83**, 505-518, 1972.
- SNOKE, J.A., I.S. SACKS, and H. OKADA, A comparison of empirical model for explaining anomalous high-frequency arrivals from deep-focus South American earthquakes, *EOS, Trans. Am. Geophys. Union*, **54**, 1140, 1973.
- STAUDER, W., Mechanism and spatial distribution of Chilean earthquakes with relation to subduction of the oceanic plate, *J. Geophys. Res.*, **74**, 6696-6701, 1973.
- TOKSÖZ, M.N. and P. BIRD, Formation and evolution of marginal basins and continental plateaus, in *Island Arcs, Deep Sea Trenches and Back Arc Basin*, edited by Talwani and Pittman, pp. 1379-1394, Am. Geophys. Union, 1977.
- TOVISH, A. and G. SCHUBERT, Island arc curvature, velocity of convergence and angle of subduction, *Geophys. Res. Lett.*, **5**, 329-332, 1978.
- TULLIS, T.E., Evidence that lithospheric plates act as anchors (abstr.), *EOS, Trans. Am. Geophys. Union*, **53**, 522, 1972.

- TULLIS, T.E., Factors determining the dip of downgoing slabs, preprint, 1976.
- UYEDA, S., Some basic problems in the trench-back arc system, in *Island Arco, Deep Sea Trenches, and Back Arc Basins*, edited by Talwani and Pittman, pp. 1-14, Am. Geophys. Union, 1977.
- UYEDA, S. and H. KANAMORI, Back-arc opening and the mode of subduction, *J. Geophys. Res.*, 1978 (in press).
- VOGT, P.R., A. LOWRIE, D.R. BRACEY, and R.N. HEY, Subduction of aseismic oceanic ridges: Effects on shape, seismicity and other characteristics of consuming plate boundaries, *Geol. Soc. Am. Spec. Paper* 172, 1976.
- WEISSEL, J.K., Evolution of the Lau basin by the growth of small plates, in *Island Arcs, Deep Sea Trenches, and Back Arc Basins*, edited by Talwani and Pittman, pp. 429-436, Am. Geophys. Union, 1977.
- WILSON, J.T., Mantle plumes and plate motions, *Tectonophysics*, **19**, 149-164, 1973.
- WILSON, J.T., J.A. JACOBS, R.D. RUSSEL, and J.T. WILSON, *Physics and Geology*, Chap. 17, McGraw-Hill, New York, 1974.
- Wu, F.T., Structural history of the Mariana Island Arc System: Discussion, *Geol. Soc. Am. Bull.*, **82**, 2671-2672, 1971.
- Wu, F.T., The Philippine Sea Plate: "A sinking towel", *Tectonophysics*, **14**, 81-86, 1972.

OCEANIC CRUST IN THE DYNAMICS OF PLATE MOTION AND BACK-ARC SPREADING

Yoshiaki IDA

Ocean Research Institute, University of Tokyo, Tokyo, Japan

(Received July 25, 1978; Revised September 18, 1978)

Some of the fundamental features of plate tectonics are interpreted in connection with the behavior of oceanic crust. It is shown to be likely that the oceanic crust which is produced at the mid-ocean ridge by chemical differentiation may be removed from the down-going slab by melting at the depth of asthenosphere behind the deep-sea trench. The melting of crustal material after the subduction is made possible by an efficient supply of heat through the well-developed asthenosphere with a low-velocity and high-attenuation of seismic waves. The removal of subducted oceanic crust from the slab is consistent with the positive gravity anomaly behind trenches and the double Benioff zone recently discovered. We propose new type of driving forces of plate motion, which arises from the density contrast between the crust and mantle when the oceanic crust is either created or destructed. The proposed driving mechanism is consistent with the non-uniform size and shape of individual plates, the migration of mid-ocean ridges and compressional intraplate stress, while these facts are difficult to understand in the framework of conventional models. A continuous accumulation of basaltic magma beneath the trench-arc system results in a catastrophic overflow of material, which corresponds to back-arc spreading. The picture presented in this paper explains the evolution of marginal basins that is characterized by the presence of remnant arcs, the changes in stress field and the dip angle of the slab, and the anomalous depth-age relationships.

1. Introduction

Although the reality of plate tectonics leaves no room for doubt, the physical mechanism that governs the process is not clear. It is widely believed that some form of thermal convection in the earth's mantle is the ultimate origin of the driving forces of plate motion (e.g., TURCOTTE and OXBURGH, 1972; O'CONNELL, 1977). The validity of the convection hypothesis is, however, not totally convincing. Non-uniform size and shape of individual plates do not seem to reflect the regular cells that are expected from ordinary thermal convection. It is uncertain that mantle convection can penetrate into the mantle to the depth comparable to the large horizontal scales of the Pacific and Eurasian plates. The migration of a mid-ocean ridge relative to deep-sea trenches also puzzles us, if we identify the ridge and trench as the positions of upwelling and downgoing flow of mantle convection. It is really mysterious that a ridge is sometimes subducted under a trench (ATWATER, 1970; HILDE *et al.*, 1977).

Some investigators prefer to stress the gravitational effect of lithosphere, rather than the role of deeper mantle (HALES, 1969; JACOBY, 1970; RICHTER, 1977). According to them, the lithosphere is more dense than the asthenosphere, and it has the tendency to sink. Although such density reversal indeed produces a driving force of plate movement, it is difficult for the idea to explain the stability of large plates. As far as the ordinary rheological properties are assumed for the solid earth, the unstable lithosphere should be divided

into much smaller segments than actually observed, within very short time compared with the tectonic time scale of plate tectonics (RAMBERG, 1968). Sometimes it is assumed that the lithosphere becomes unstable only after it is sufficiently cooled. In this case, a negative bouyancy that the downgoing slab is subjected to is considered as the main driving force. This view predicts that all the plates should be subducted at nearly the same age determined by the thermal properties of the earth. In fact, however, some very old plates float stably in spite of the sinking of much younger plates. Furthermore it is expected that dominant extension should be generated by the negative bouyancy in most area of plates. This again contradicts compressional intraplate stresses actually observed (SYKES and SBAR, 1973).

We have thus several paradoxes, when we try to formulate the physical mechanism of plate tectonics, based on the effect of thermal expansion. These paradoxes seem to be serious enough to suggest that some important factors might have been neglected in conventional models. In this paper, we would like to evaluate a possible effect of chemical differentiation, particularly the differentiation of asthenospheric material into the oceanic crust and mantle. Although the Moho is one of the most distinctive boundaries in the earth's interior, the crust is usually neglected in the dynamics of plate motion. The crust is regarded as moving passively with the lithospheric plate, even if it may be sometimes involved in the phenomena that results from plate motion. In this paper, we would like to examine a possible role of the crust in the driving mechanism of plate motion, and we attempt to construct a picture of plate dynamics consistent with the known facts, based on the evolution of oceanic crust.

The trench-arc system contains some interesting features whose tectonic meaning has not yet been well understood (UYEDA, 1977). In particular, the evolution of marginal basins is determined not only by the nature of subductions, but also the mechanism to initiate and keep the activity of sea-floor spreading. Various models have been proposed to interpret the formation of marginal basins. They include the mechanisms of a mantle diapir (KARIG, 1971), a convection induced by the downgoing slab (TOKSÖZ and PETER, 1977), and relative motion between the continental and oceanic plate (UYEDA and KANAMORI, 1978). These theories, however, do not seem to give a definite answer to the following fundamental questions. (1) How does the process of subduction supply the heat and material that are necessary to the evolution? (2) What determines whether the volcanic activity involves the growth of continental lithospheres or back-arc spreading? To answer these problems, we propose a model of the evolution of trench-arc systems, which again involves the crustal material in most essential point of the mechanism.

2. *Creation and Destruction of Oceanic Crust*

The material in the crust is characterized by the melting point that is substantially lower than those of mantle minerals. This is the main reason why the oceanic crust forms a discrete part when the oceanic lithosphere is created at mid-ocean ridges. For the same reason, the oceanic crust would be melted again after the downgoing lithosphere is heated enough. We begin our study with considering the manner of such creation and destruction of oceanic crust.

2.1 *Creation*

The structure of mid-ocean ridges have been clarified fairly well by the observations

made there on magnetic anomaly, seismic velocities, heat flow and gravity (e.g., FORSYTH, 1977). The boundary between the lithosphere and asthenosphere reaches almost the ocean bottom beneath the ridge axis, and it becomes deeper with increasing distance from the ridge axis. Such a structure is usually understood as a result of gradual growth of the lithosphere (PARKER and OLDENBURG, 1973; YOSHII, 1973). Namely the lithosphere, which was born at the ridge, grows thicker by the solidification of asthenospheric material at its bottom, as it is moved sideways and cooled. The lithosphere has a distinctive layer of oceanic crust on its top, while similar layered structures may be also produced in deeper part of the lithosphere, as was suggested by YOSHII *et al.* (1976) and OXBURGH and PARMENTIER (1977). Here we consider only the effect associated with the oceanic crust whose structure is well known, even though any layered structure in the lithosphere should have similar effects. The oceanic crust is made from basaltic magma which has been squeezed by gravity from the asthenosphere. The crust is thus characterized by lower density as well as lower melting-point than the mantle part of oceanic lithosphere.

We should pay a special attention to the following points, when we consider the dynamical effect of mid-ocean ridges. First it is not only the crust but the entire lithosphere that is produced at the ridge. We may thus regard the formation of oceanic lithospheres as a process of chemical differentiation of asthenospheric material with the help of gravity. In the second place, isostatic balance is almost completed over the area including the ridge axis, since no remarkable free-air gravity anomaly is found there (KAULA, 1969). This means that the asthenosphere may be treated as a fluid layer in our discussion of mechanical properties.

2.2 Destruction

From the presence of active orogeny along trenches, it is expected that both heat and material should be supplied to the area behind trenches, directly or indirectly from the process of subduction. High heat-flow that is often observed in arcs and marginal basins (WATANABE *et al.*, 1977) can be understood in the same context. However it is not easy to find the actual mechanism to supply such heat and material. According to the calculations made by several authors (e.g., TOKSÖZ *et al.*, 1973; ANDERSON *et al.*, 1978), the sinking slab is expected to cool its environment so effectively that the subduction would rather hinder thermal activities of the trench-arc system. Abnormally high stress along the slab is required to obtain sufficient heat from the friction associated with the downgoing movement of slab (HASEBE *et al.*, 1970). The dehydration of hydrous minerals that occurs in the slab at a certain depth remarkably reduces the melting point, but the same reaction also absorbs substantial latent heat (ANDERSON *et al.*, 1976).

This difficulty is resolved if substantial heat is supplied through the asthenosphere adjacent to the slab. In fact, the low-velocity and high-attenuation zone of seismic wave observed below a very thin lithosphere (UTSU, 1971) means that the asthenosphere is well developed beneath island arcs and marginal basins. Although only conductive heat is taken into account in ordinary calculations of the thermal process of trench-arc systems, it is probable that heat is transferred much more effectively through the asthenosphere by the migration of magma and various small convections. Therefore the asthenosphere would bring sufficient heat from broad area surrounding the trench-arc system to melt the subducted oceanic crust. Once the melt of subducted crust is poured into the asthenosphere, the region occupied by the asthenosphere is further expanded, and heat transfer is made more efficient. Radioactive elements brought with the molten crustal material

also produce some amount of heat in the asthenosphere. It should be noted here that the melting of subducted crust and the growth of asthenosphere could strengthen each other in this mechanism, since a positive feedback works. As a result of such a cooperative interaction between the slab and asthenosphere, both the heat and material would be available to the active volcanism and the high heat-flow in the trench-arc systems.

We have shown that the melting of subducted basalt is made possible by the feedback mechanism mentioned above. It seems difficult to interpret the origin of thermal and volcanic activities behind the trenches without considering the role of molten crustal material. In fact, there is a big debate on whether or not subducted crust actually melts in the upper mantle. Some petrologists point out the evidence that supports the melting (e.g., RINGWOOD, 1977), but others have opposite opinions. Since such petrological discussions are too complicated to readily draw any definite conclusions, we here restrict ourselves to the examination of other geophysical problems that are related to the behavior of the subducted oceanic crust.

It is sometimes maintained that deep seismicities along Benioff zones mean the presence of unmelted oceanic crust on the slabs. Based on more accurate determination of seismic sources, however, it was made clear that the Benioff zone actually consists of two separate layers (UMINO and HASEGAWA, 1975; ENGDAHL and SCHOLZ, 1977), as is sketched in Fig. 1(a). The upper plane that may be identified as the layer of oceanic crust disappears below about 100 km depth. Therefore the seismological observation now supports the destruction of oceanic crust at about the depth corresponding to the top of asthenosphere.

Free-air gravity anomaly is dominantly positive behind trenches (KAULA, 1969; WATT and TALWANI, 1974; SEGAWA and TOMODA, 1976), as is shown in Fig. 1. This

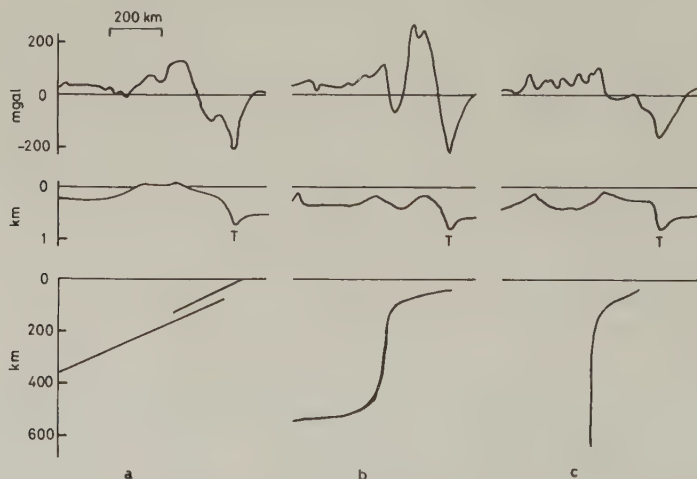


Fig. 1. A brief sketch of the distributions of free-air gravity anomaly (top), topography (center) and Benioff zone (bottom) in the trench-arc systems. The distribution in northeastern Japan (a) gives a typical example of the inactive arc. Bonin (b) and Mariana basins (c) are classified by KARIG (1971) as the regions with active back-arc spreading. Data after WATT and TALWANI (1974), SEGAWA and TOMODA (1976), UMINO and HASEGAWA (1975), and KATSUMATA and SYKES (1969) are reproduced.

anomaly is often explained by a density structure beneath arcs (e.g., SEGAWA and TOMODA, 1976). It is not reasonable, however, to attribute the whole anomaly to such a structure, because the scale of time and space involved is too long for the structure to resist against isostatic adjustment. For instance, the effect of dense lithosphere beneath the arc should have been compensated by isostatic sinking of island arcs regardless of the motion of slabs, as far as the thickness and dip angle of slab are kept unchanged. Instead we can attribute the gravity anomaly to non-isostatic pressure that is caused by the excessive crustal material continuously brought by the slab. The presence of excess material naturally causes a positive gravity anomaly. The observed gravity anomaly corresponds to the amount of crustal material that has been supplied by the subduction during about 0.5 my. Therefore we can easily explain the magnitude of anomaly by some tectonic process including the removal of basalt from the slab.

It is quite probable that some part of subducted oceanic crust rises as magmas to the orogenic belts. The magmas may either come directly from the downgoing slab, or indirectly after they are mixed with asthenospheric material adjacent to the slab. In any case, continuous subduction is able to give unlimited supply of basaltic magma. It is estimated, however, that only minor part of subducted crust is spent for the volcanism in arcs. If all the basaltic crust subducted were converted into the continental lithosphere of 100 km thickness, the continental area should grow at as high a rate as 600 km in 100 my for the subduction rate of 10 cm/year. In practice, we do not have any evidence of such a high growth-rate during recent 200 my. The estimate of volcanic extrusive material in arcs is also much less compared with the amount of subducted oceanic crust (NAKAMURA, 1974).

Therefore we have to conclude that material steadily accumulates in the upper mantle with the process of subduction. A catastrophic overflow of material may be expected from such a continuous accumulation. Later we propose that the catastrophe results in the opening of a marginal basin. It is also expected from the proposed behavior of oceanic crust that basaltic component should increase in the asthenosphere with continued subduction. Such a change of chemical composition must finally result in a process that involves the growth of continents. The author believes, however, that the formation of continents is not a stationary process associated with the subduction, but it takes place rather intermittently (Ida, manuscript prepared).

3. *Driving Forces of Plate Motion*

In this section, we consider the driving forces of plate motion that originate from the density contrast between the crust and mantle of oceanic lithosphere. We propose a new type of ridge push that is associated with the construction of oceanic crust. The trench pull considered here is caused by the increase in the density of slab due to the loss of the crustal component. The transfer of heat is necessary to realize either the ridge push or trench pull, particularly to solidify or melt crustal material. However the thermal effect is only implicit and the forces are formulated in terms of the density contrast and gravitational constant. To emphasize the role of oceanic crust, we neglect the volume change due to compression, thermal expansion and fusion. Since these factors have additional contributions to the pressure distribution in the earth's interior, we may include these effects simply by superimposing them to the value estimated here.

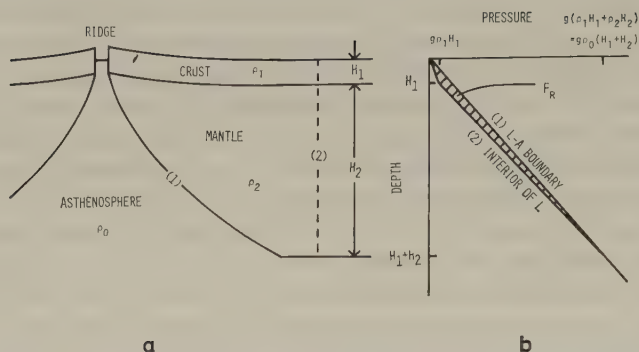


Fig. 2. The mechanism of ridge push associated with the gravitational differentiation of asthenospheric material. (a) The structure of oceanic lithosphere and asthenosphere in the area including the ridge axis. (b) The distribution of pressure as a function of depth at the lithosphere-asthenosphere boundary (1) and in the interior of lithosphere (2).

3.1 Ridge push

It is schematically illustrated in Fig. 2(a) that the oceanic lithosphere that consists of the crust of thickness H_1 and the mantle of thickness H_2 is generated as a result of the chemical differentiation of asthenospheric material. To pick up the effect of differentiation alone, let us assume that the asthenosphere is mixture of the crust and mantle materials so that the density ρ_0 of the asthenosphere is determined from the densities ρ_1 and ρ_2 of the crust and mantle, respectively, as

$$\rho_0 = (H_1\rho_1 + H_2\rho_2) / (H_1 + H_2). \quad (1)$$

We have already pointed out that isostasy approximately holds over the area including a ridge. In other words, the asthenosphere behaves like a fluid so that the pressure in the asthenosphere is everywhere the same at the same depth. Noting this, we obtain the pressure distributions in the interiors of lithosphere and asthenosphere, as are given as a function of depth in Fig. 2(b). The two distributions intersect each other at the bottom of the lithosphere because of isostasy, and also at the top of it on account of the assumption (1).

It should be noted that isostasy is concerned only with the balance of vertical forces. Let us consider the horizontal force that acts on the edge segment of lithosphere in Fig. 2(a). The forces involved are graphically displayed in similar method used by FRANK (1972). The total force is given by the push from the lithosphere-asthenosphere boundary minus the reaction from the interior of lithosphere. Each of these forces is obtained by integrating the pressure distribution given in Fig. 2(b) over the entire depth to the bottom of lithosphere. Clearly we have an unbalanced push F_R , which corresponds to the area of a hatched triangle on the pressure-depth plane, and which is mathematically expressed per unit length of the ridge axis as

$$F_R = (g/2)\phi(1-\phi)(\rho_2 - \rho_1)(H_1 + H_2)^2 \quad (2)$$

where $\phi = H_1/(H_1 + H_2)$ and g is the gravitational acceleration.

The force F_R works so as to move the plates away from the ridge axis. When the plate moves steadily, F_R should be balanced with the other forces, including other driving

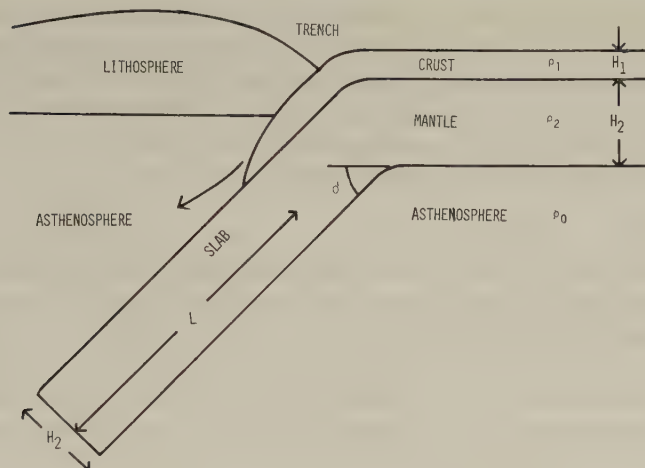


Fig. 3. A negative buoyancy force associated with the removal of the oceanic crust from the subducted slab.

forces, viscous drags, and frictional resistances. It is seen from Eq. (2) that F_R is positive only when ρ_1 is smaller than ρ_2 . This reflects that F_R originates from the effect of gravity that tends to reduce the energy by lifting up lighter material and sinking heavier deeper. As a representative value of F_R , we have 0.75×10^{15} dyn/cm, assuming $H_1=6$ km, $H_1+H_2=90$ km and $\rho_2-\rho_1=0.3$ g/cm³. This forces has the same effect as a uniform horizontal compression of 83 bar does across a vertical section of the plate.

It is pointed out that ridge push also plays an essential role in keeping the activity of the ridge itself. If the plates containing a ridge could not be moved aside by such a push, the solidification of asthenosphere would be made possible only by the retreat of asthenosphere. Therefore the effect of cooling would finally produce the structure that is nothing but a lithosphere of normal thickness. In other words, continuous reproduction of lithosphere is assured only under the action of ridge push. When ocean floor is spreading, upward flow in the asthenosphere brings the heat and keeps the asthenosphere in the state of partial melting.

3.2 Trench pull

A pull from downgoing slab is available, if the oceanic crust is removed from the slab at some depth beneath the trench (Fig. 3). Namely a negative buoyancy due to the increased density of the slab yields the following driving force F_T :

$$F_T = g(\rho_2 - \rho_0)H_2L \sin \theta \quad (3)$$

where θ is the dip angle of the slab, and L is the length of the slab which is free from the low-density crust. Based on the deep seismicity along Benioff zone, we may tentatively assume 600 km as a typical value of the vertical extension $L \sin \theta$. Then we have $F_T = 1.0 \times 10^{16}$ dyn/cm, using the same values of H_1 , H_2 and $\rho_2 - \rho_0$ as in the estimate of F_R . This value of F_T is equivalent to the uniform stress of 1.1 kbar working on the section of the slab.

It is emphasized that the numerical value estimated above gives only an idea of the magnitude of F_T . The process of subduction involves various complicated effects that

are difficult to evaluate correctly at present. The asthenospheric density ρ_0 may be smaller in the mantle wedge above the slab, because it may contain more abundant melt. The phase transformations occurring in the transition zone of the mantle may change the density contrast $\rho_2 - \rho_1$. When the basaltic crust is transformed into eclogite within the slab, we have an additional pull corresponding to the density increase. These factors should be carefully estimated in more advanced study.

3.3 Remarks

We have evaluated the driving forces of plate motion that are associated with the creation and destruction of oceanic crust. Besides the effects proposed here, many theories have provided with various specific mechanisms to cause the forces acting on the plates (HALES, 1969; JACOBY, 1970; ELSASEER, 1971; FRANK, 1972; ARTYUSHKOV, 1973; OXBURGH and PARMENTIER, 1977). Although we do not intend to critically review these theories, it does not seem that the paradoxes of plate motion that have been pointed out at the beginning of this paper are systematically resolved by any of them. Therefore we would like to go our own way and to examine if the idea that plate tectonics is subject mainly to the driving forces proposed here could overcome the paradoxes. We should first recall that our mechanism is able to produce as high stress as is believed to actually realize in the interior of plates. Compared with those theories referred to above, it is the most remarkable point that our mechanism works even if plates are gravitationally stable against the asthenosphere. Both ridge push and trench pull that are proposed here are effective regardless of the bulk density of lithosphere, as far as the crust has lower density than the mantle.

The mechanism that produces either F_R or F_T involves only localized area in the vicinity of a ridge or a trench. Therefore we may regard F_R and F_T as being independent of each other. This is a remarkable nature, compared with the mechanism of thermal origin in which we must consider heating and cooling simultaneously as complementary processes. The independence of F_R and F_T brings about a great flexibility of the plate dynamics. It turns out to be quite natural that some plates can move without any subduction. The driving mechanism does not give any a priori restriction on the size and shape of plates. A mid-ocean ridge is permitted to migrate on the global surface, and even to collide with a trench.

Let us note that our estimates yield $F_T/F_R = 13$. FORSYTH and UYEDA (1975), and CHAPPLE and TULLIS (1977) determined relative magnitude of various forces acting on the different type of plate boundaries, so as to interpret the distribution of absolute velocities of existing plates. The ratio F_T/F_R obtained by them falls between 10 and 20, being consistent with our value.

Since our trench pull does not require that the plate spontaneously sinks by its own weight, we should understand that the subduction of plates is enforced by a horizontal compression. This idea is consistent with observed compressional stress in the interior of lithosphere (SYKES and SBAR, 1973). Compression may be produced at least partly by pushes from ridges. Extensional stresses observed in some area are regarded as exceptional cases involved in particular deformations that are probably restricted to the layers close to the earth's surface. For instance, the oceanic crust stretched by sea-floor spreading involves extensional field in the vicinity of ridge crests. The extension seaward of deep-sea trenches is connected with the bending of lithosphere.

The pull F_T in Eq. (3) works only after the slab sinks to a certain depth. In the

circumstance where the continental and oceanic lithospheres push against each other at deep-sea trenches, large friction at the plate boundary would prevent the pull from acting effectively on the plate that has not yet been subducted. It is thus expected that such interplate interaction substantially reduces the effect of F_R as the driving mechanism. In fact, FROSYTH and UYEDA (1975) and CHAPPLE and TULLIS (1977) independently obtained at trenches such large resistance against plate motion as almost entirely cancels out the effect of the pull.

According to UMINO and HASEGAWA (1975) and ENGDAHL and SCHOLZ (1977), observed focal mechanisms of earthquakes indicate that there are compressional stress on the upper layer, and extensional on the lower layer along the two-layered structure of Benioff zone. There are several possibilities to interpret this, such as an unbending of the lithosphere during subduction (ENGDAHL and SCHOLZ, 1977). In connection with our model, the following mechanism also appears probable. Down-dip extension on the lower layer is caused by negative bouyancy F_T while down-dip compression on the upper layer corresponds to the resistance against the intrusion of oceanic crust into the mantle.

4. Evolution of Marginal Basins

4.1 Model

We would like to propose that the continuous supply of subducted crustal material should result in such an evolution of the trench-arc system as is displayed by a cartoon in Fig. 4. In the first stage of this figure, some part of the subducted crust is spent as rising

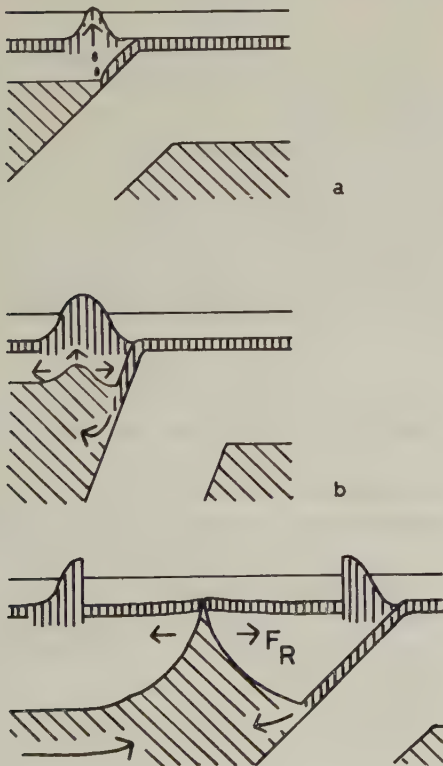


Fig. 4. The evolution of trench-arc system. (a) The formation and growth of an island arc. (b) The accumulation of material beneath the arc, accompanied by sharp bending of the slab, and by the extension in the arc. (c) The back-arc spreading after a catastrophic overflow of material.

magmas that grow island arcs (Fig. 4(a)). When the resultant volcanic material has almost occupied the whole space adjacent to the trench, further extrusion or intrusion is made difficult, and almost all the material is obliged to stay in the asthenosphere. Therefore excessive material gradually accumulates beneath the arc, accompanied by higher pressure in the asthenosphere than the isostatic value. Such pressure, which is observed as a positive free-air gravity anomaly, would push the slab aside so that the subducted slab may be bent steeply (Fig. 4(b)). The same effect should stretch the lithosphere overlying the asthenosphere, and thus extensional stress field appears in the arc. Finally the lithosphere along with the arc is torn away, and asthenospheric material rises to occupy cracked space (Fig. 4(c)). This is regarded as the opening of marginal basin.

In the story mentioned above, it is considered that the marginal basin is opened by the increased pressure of asthenosphere containing excess material. Alternatively it is possible to attribute back-arc opening to a gravitational effect. With the continuation of subduction, the asthenosphere contains more basaltic melt, and its mean density becomes smaller. When a density reversal is achieved between the lithosphere and asthenosphere, the structure is no longer gravitationally stable. Therefore the asthenosphere may rise, intruding into the lithosphere, in the same mechanism as salt domes.

In either case, the structure similar to the mid-ocean ridge that contains a shallow asthenosphere is brought about after the cracking of the arc. Therefore it follows the event that oceanic lithospheres are produced on both sides of the opening center, accompanied by ocean-floor spreading. It should be noted here that the rise of hot material does not always result in back-arc spreading. The spreading requires the action of ridge push and thus large-scale uplift of asthenosphere. This is an essential point to understand the difference of volcanism between the ridges and orogenic belts.

In the beginning of the spreading, the material that is necessary for the formation of new ocean basin is easily available from the store that has been accumulated. Once the source is exhausted, however, material must be brought from somewhere, probably by the flow through asthenosphere, in order to keep the activity. In the marginal basins, such flow may be obstructed by the presence of adjacent slabs and continents. Therefore the spreading would often be obliged to decelerate and even to stop. In this case, the lack of material must cause a suction and make the slab return to the position with smaller dip angle. Then we have a circumstance similar to the first stage, and we may expect that the process described above is repeated. Namely a cyclic evolution might take place in the trench-arc system.

4.2 Remarks

The following facts on the evolution of marginal basins can be interpreted by the picture described above:

- 1) The presence of frontal and remnant arcs surrounding the marginal sea is explained in this model by the cracking due to excessively accumulated material below the arc.
- 2) The Benioff zones beneath active marginal basins (Fig. 1(b) and (c) reproduced from KATSUMATA and SYKES, 1969) look as if they were bent by the push working on the slab in the depth of asthenosphere.
- 3) The stress field in active marginal basins is believed to be extensional, while compressional stress is observed in inactive arcs (KARIG, 1971; UYEDA and KANAMORI, 1978).

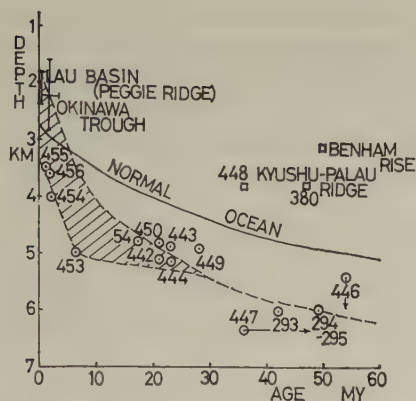


Fig. 5. The depth of marginal seas compared with the curve for normal oceans (after Kobayashi).

4) According to KOBAYASHI and NAKADA (1978), the depth of marginal sea is shallower for very young basins, compared with the depth of normal ocean with the same age (Fig. 5). The lifting of young ocean bottom is explained by the excessive material existing below. On the other hand, Fig. 5 points out that the sea with older basins becomes deeper than normal. This can be attributed either to the lack of asthenospheric material in the final stage of spreading, or to an isostatic adjustment to compensate the effect of dense slab.

5) It is observed in the Shikoku basin that the rate of spreading actually decreased from the initial high value (KOBAYASHI and NAKADA, 1978).

6) The evolution of island arcs and the back-arc spreading is actually repeated in the northwest Pacific.

According to our model, whether an island arc grows or ocean-floor spreads behind a deep-sea trench is determined by the depth of lithosphere-asthenosphere boundary. It is suggested that such picture is consistent with the difference of volcanic activities, as follows. During the stage in which arcs grow, magma must penetrate through long narrow conduits from deep asthenosphere. Chemical fractionations that possibly take place on the way to the surface produce various compositions, including andesitic and granitic magmas (RINGWOOD, 1977). When ocean-floor is spreading, original basaltic magma could extrude directly from shallow asthenosphere without appreciable fractionation. The resultant magma is considered to be abyssal tholeiite.

Some deep-sea trenches do not have any marginal sea attached to them. Let us consider the case of the Peru-Chile trench as one of the most typical examples. It is known that no clear low-velocity zone is found beneath Andes (JAMES, 1971). On the other hand, we have pointed out that the formation of marginal sea must be supported by the efficient transfer of heat through asthenosphere. Therefore our model interprets the connection between the absence of marginal basin and the undeveloped asthenosphere behind the Peru-Chile trench.

Then why has the asthenosphere been kept undeveloped there in spite of the long history of active subduction? One of the possible answers is that major part of subducted material may be supplied to the region below the Atlantic Ocean, passing beneath South America. Such process may be understood consistently with our model, if we regard the South Atlantic Ocean as a marginal sea of Peru-Chile trench. This means that we classify the Atlantic, and the other oceans except for the Pacific, into the same category

as ordinary marginal basins. Even if this may look too fantastic an idea, it may not be totally unsound, because these oceans do not have any deep-sea trenches on their own. If this idea is acceptable, we are led to an attractive hypothesis that the subduction along the rim of the old Pacific, created the other oceans, and gave rise to the continental drifts. This hypothesis seems to be worthy of further examination, because it could reduce the formation of most oceans to a single mechanism related to subduction.

5. Conclusions

We have shown that the oceanic crust should play an important role in the basic dynamics of plate motion, particularly in the tectonic activities of the trench-arc system. Main results obtained here are summarized as follows:

1) Shallow asthenospheres beneath the active spreading center of the oceans and marginal basins cause a gravitational differentiation of the oceanic lithosphere between the crust and mantle. The differentiation generates the force that drives the lithospheric plates aside and keeps the steady activity of the ridge itself.

2) Various pieces of evidence including seismology, heat flow and gravity support the idea that the subducted oceanic crust is melted and poured into the asthenosphere. The asthenosphere that has been developed as a result of the supply of basaltic magma works as a good conductor of heat.

3) The ridge push and trench pull that are respectively associated with the construction and destruction of the oceanic crust overcome some paradoxes involved in the dynamics of plate motion.

4) The evolution of trench-arc system including back-arc spreading is formulated as a cyclic process associated with the accumulation and dispersion of crustal material that is supplied from the subducted slab. The proposed model gives a dynamical picture that is consistent with known characteristics of the evolution.

I would like to thank Prof. K. Kobayashi who suggested to me that I might consider the problems discussed in this paper. Prof. S. Uyeda kindly read the first draft of this paper and gave me lots of valuable comments to improve it.

REFERENCES

- ANDERSON, R.N., S. UYEDA, and A. MIYASHIRO, Geophysical and geochemical constraints at converging plate boundaries. I. Dehydration in the downgoing slab, *Geophys. J. R. Astr. Soc.*, **44**, 333–357, 1976.
- ANDERSON, R.N., S.E. DELONG, and W.M. SCHWARZ, Thermal model for subduction with dehydration in the downgoing slab, *J. Geol.*, **86**, 731–739, 1978.
- ARTYUSHKOV, E.V., Stresses in the lithosphere caused by crustal thickness inhomogeneities, *J. Geophys. Res.*, **78**, 7675–7708, 1973.
- ATWATER, T., Implication of plate tectonics for the Cenozoic tectonic evolution of western North America, *Geol. Soc. Am. Bull.*, **81**, 3513–3536, 1970.
- CHAPPLE, W.M. and T.E. TULLIS, Evaluation of the forces that drive the plates, *J. Geophys. Res.*, **82**, 1967–1984, 1977.
- ELSASSER, W.M., Sea-floor spreading as thermal convection, *J. Geophys. Res.*, **76**, 1101–1112, 1971.
- ENGDAHL, E.R. and C.H. SCHOLZ, A double Benioff zone beneath the central Aleutians: An unbending of the lithosphere, *Geophys. Res. Lett.*, **4**, 473–476, 1977.
- FORSYTH, D.W., The evolution of the upper mantle beneath mid-ocean ridges, *Tectonophysics*, **38**, 89–118, 1977.
- FORSYTH, D. and S. UYEDA, On the relative importance of the driving forces of plate motion, *Geophys. J. R. Astr. Soc.*, **43**, 163–200, 1975.
- FRANK, F.C., Plate tectonics, the analogy with glacier flow, and isostasy, in *Flow and Fracture of Rocks*, pp. 285–292, Am. Geophys. Union, Washington, D.C., 1972.
- HALES, A.L., Gravitational sliding and continental drift, *Earth Planet. Sci. Lett.*, **6**, 31–34, 1969.

- HASEBE, K., N. FUJII, and S. UYEDA, Thermal processes under island arcs, *Tectonophysics*, **10**, 335–355, 1970.
- HILDE, T.W.C., S. UYEDA, and L. KROENKE, Evolution of the Western Pacific and its margin, *Tectonophysics*, **38**, 145–165, 1977.
- JACOBY, W.R., Instability in the upper mantle and global plate movements, *J. Geophys. Res.*, **75**, 5671–5680, 1970.
- JAMES, D.E., Andean crustal and upper mantle structure, *J. Geophys. Res.*, **76**, 3246–3271, 1971.
- KARIG, D.E., Origin and development of marginal basins in the western Pacific, *J. Geophys. Res.*, **76**, 2542–2561, 1971.
- KATSUMATA, M. and L.R. SYKES, Seismicity and tectonics of the Western Pacific: Izu-Mariana Caroline and Ryukyu-Taiwan regions, *J. Geophys. Res.*, **74**, 5923–5948, 1969.
- KAULA, W.M., A tectonic classification of the main features of the earth's gravity field, *J. Geophys. Res.*, **74**, 4807–4826, 1969.
- KOBAYASHI, K. and M. NAKADA, Magnetic anomalies and tectonic evolution of the Shikoku inter-arc basin, this issue, 391–402, 1978.
- NAKAMURA, K., Preliminary estimate of global volcanic production rate, Proc. U.S.-Jpn. Coop. Sci. Semin., pp. 273–285, 1974.
- O'CONNEL, R.J., On the scale of mantle convection, *Tectonophysics*, **38**, 119–136, 1977.
- OXBURGH, E.R. and E.M. PARMENTIER, Compositional and density stratification in oceanic lithosphere-causes and consequences, *J. Geol. Soc. Lond.*, **133**, 343–355, 1977.
- PARKER, R.L. and D.W. OLDENBURG, A thermal model of oceanic ridges, *Nature*, **242**, 137–139, 1973.
- RAMBERG, H., Instability of layered systems in the field of gravity, *Phys. Earth Planet. Inter.*, **1**, 427–474, 1968.
- RICHTER, F.M., On the driving mechanism of plate tectonics, *Tectonophysics*, **38**, 61–88, 1977.
- RINGWOOD, A.E., Petrogenesis in island arc systems, in *Island Arcs, Deep Sea Trenches and Back-Arc Basins*, pp. 311–324, Am. Geophys. Union, Washington, D.C., 1977.
- SEGAWA, J. and Y. TOMODA, Gravity measurements near Japan and study of the upper mantle beneath the oceanic trench-marginal sea transition zones, in *The Geophysics of the Pacific Ocean Basin and its Margin*, pp. 35–54, Am. Geophys. Union, Washington, D.C., 1976.
- SYKES, L.R. and M.L. SBAR, Intraplate earthquakes, lithospheric stresses and the driving mechanism of plate tectonics, *Nature*, **245**, 298–302, 1973.
- TOKSÖZ, M.N., N.H. SLEEP, and A.T. SMITH, Evolution of the downgoing lithosphere and the mechanisms of deep focus earthquakes, *Geophys. J. R. Astr. Soc.*, **35**, 285–310, 1973.
- TOKSÖZ, M.N. and B. PETER, Formation and evolution of marginal basins and continental plateaus, in *Island Arcs, Deep Sea Trenches and Back-Arc Basins*, pp. 379–393, Am. Geophys. Union, Washington, D.C., 1977.
- TURCOTTE, D.L. and E.R. OXBURGH, Mantle convection and the new global tectonics, in *Annual Review of Fluid Mechanics*. Vol. 4, pp. 33–68, Annual Reviews Inc., Palo Alto, Cal., 1972.
- UMINO, N. and A. HASEGAWA, On the two-layered structure of deep seismic plane in northeastern Japan arc, *Zisin. (J. Seismol. Soc. Jpn.)*, **28**, 125–139, 1975 (in Japanese).
- UTSU, T., Seismological evidence for anomalous structure of island arcs with special reference to the Japanese region, *Rev. Geophys. Space Phys.*, **9**, 839–890, 1971.
- UYEDA, S., Some basic problems in the trench-arc-back arc system, in *Island Arcs, Deep Sea Trenches and Back-Arc Basins*, pp. 1–14, Am. Geophys. Union, Washington, D.C., 1977.
- UYEDA, S. and H. KANAMORI, Origin of back-arc basins and arc tectonics, *Kagaku (Science)*, **48**, 91–102, 1978 (in Japanese).
- WATANABE, T., M.G. LANGSETH, and R.N. ANDERSON, Heat flow in back-arc basins of the Western Pacific, in *Island Arcs, Deep Sea Trenches and Back-Arc Basins*, pp. 137–161, Am. Geophys. Union, Washington, D.C., 1977.
- WATTS, A.B. and M. TALWANI, Gravity anomalies seaward of deep-sea trenches and their tectonic implications, *Geophys. J. R. Astr. Soc.*, **36**, 57–90, 1974.
- YOSHII, T., Upper-mantle structure beneath the north Pacific and the marginal seas, *J. Phys. Earth*, **21**, 313–328, 1973.
- YOSHII, T., Y. KONO, and K. ITO, Thickening of the oceanic lithosphere, in *The Geophysics of the Pacific Ocean Basin and its Margin*, pp. 423–430, Am. Geophys. Union, Washington, D.C., 1976.

BASIC TYPES OF INTERNAL DEFORMATION OF THE CONTINENTAL PLATE AT ARC-ARC JUNCTIONS

Kunihiko SHIMAZAKI, Teruyuki KATO, and Ken'ichiro YAMASHINA

Earthquake Research Institute, University of Tokyo, Tokyo, Japan

(Received July 6, 1978; Revised October 30, 1978)

Near the junction of two arc systems, the state of stress within the earth's crust often appears to differ from the regional trend. The internal deformation of the continental plate at arc-arc junctions is probably controlled by geometrical configurations and the forces acting on the plate edges. If forces acting on the two neighbouring plate boundaries which intersect at a junction are not parallel to each other, convergence (or divergence) or shearing would take place at the junction. At a plate edge, four types of force (or displacement) can be assumed, whose direction is constrained by the strike of the edge. Thus four types of deformation can be expected within the continental plate near an arc-arc junction. One of these four basic types appears to be dominant in the real earth, probably because of the limitation on possible combinations of force (or displacement) types acting on the two neighbouring plate boundaries. The anomaly in the state of stress found near the junctions of the Kurile and Japan arcs and of the Aleutian and Kamchatka arcs may be related to a shearing force acting on the obliquely converging plate boundaries.

1. Introduction

The plate tectonic hypothesis basically assumes an absence or near absence of deformation within plates. While this assumption seems to be a good working hypothesis for many purposes, deformation within plates has begun to arouse considerable attention on the part of seismologists (e.g. SYKES and SBAR, 1973; FORSYTH, 1975; SHIMAZAKI, 1976; STEIN and OKAL, 1978; SYKES, 1978). The study of intraplate deformation promises to provide an important clue to a better understanding of global tectonics as well as facilitating the assessment of seismic risk for nuclear power plants, high dams, and other crucial constructions. Among various interesting aspects, this paper discusses only the deformation within the continental plate near an arc-arc junction, where the state of stress often appears to be different from the regional trend. Anomalies in the state of stress can be found north of the junction of the Aleutian and Kamchatka arcs, northwest of the Kurile-Japan arc-arc junction, near the point of acute bending of the Nazca-South American plate boundary, and possibly northeast of the intersection of the Himalaya and Burma arcs. Although explanations which are essentially the same as those described in the following were suggested for a few specific cases (MOLNAR *et al.*, 1973; CORMIER, 1975; STAUDER, 1975), no systematic description of the possible types of internal deformation of the continental plate at an arc-arc junction has previously been made.

The first part of this paper is devoted to a brief review of the anomalous state of stress at arc-arc junctions. Then, we will derive four basic types of intraplate deformation at junctions, assuming four possible types of force (or displacement) at the plate edges. If the forces acting on the two neighbouring plate boundaries are not parallel to each other, convergence (or divergence) or shearing will take place at the junction. This is the basic

idea of this paper. For the sake of simplicity, we restrict ourselves to a two-dimensional problem: only horizontal forces (or displacements) will be considered at plate edges. Because of this restriction, features probably related to the three-dimensional nature of arc-arc junctions will not be discussed in this paper. Among these are the negative isostatic gravity anomaly and Quaternary subsidence found near the intersections of the Kurile and Japan arcs and of the Japan and Izu arcs (HESS, 1948; SUGIMURA and UYEDA, 1973).

2. Anomalous State of Stress at Arc-Arc Junctions

In this section, several examples of anomalies in the state of stress found at arc-arc junctions will be shown. We do not attempt to examine every arc-arc junction for anomalies; only those junctions where pertinent data are available will be discussed.

2.1. The Kurile-Japan arc-arc junction

Northwest of the Kurile-Japan arc-arc junction, the earth's crust is contracting roughly NNE-SSW, or perpendicular to the bisector of the junction, while in the surrounding

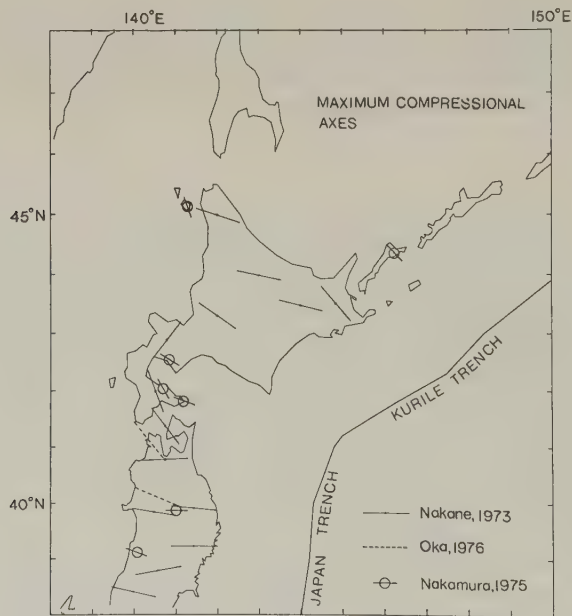


Fig. 1. Local axes of maximum compression (contraction). The thin solid lines with dots indicate strikes of the local axes of maximum contraction obtained by NAKANE (1973), on the basis of repeated triangulation surveys. The broken lines show the trend of maximum compression axes estimated from in-situ stress measurements (ITO *et al.*, 1976). The bars on circles indicate trends of the axes of maximum compression obtained by NAKAMURA (1975) mainly on the basis of the distribution of monogenetic craters and fissures of fissure-eruption volcanoes.

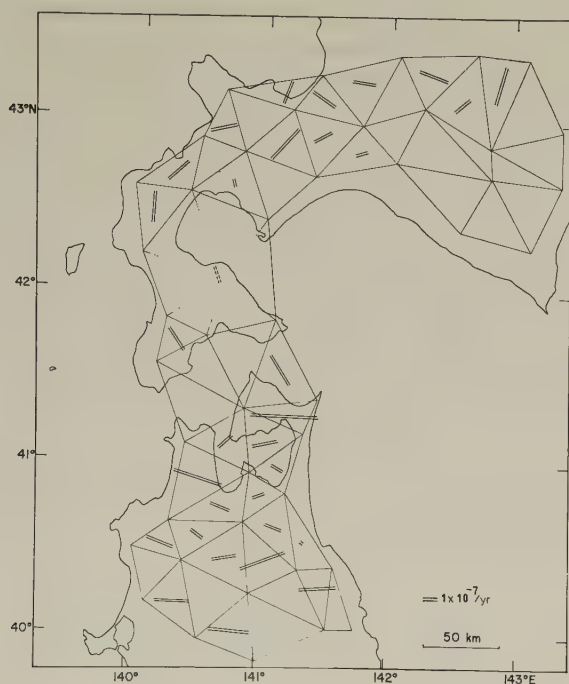


Fig. 2. Trends of maximum contraction axis calculated from each triangle and from one hexagon (after Nakane, personal communication). The strike of the double lines shows the trend of the maximum contraction axis and the length of the double lines is proportional to the horizontal shear velocity. Data from triangles which show large closing errors are excluded.

regions the crust is contracting E-W or ESE-WNW. These results were obtained by NAKANE (1973) who estimated local maximum contraction axes throughout Japan on the basis of repeated first order triangulation surveys using FRANK's (1966) method. Comparing the results of the second survey in 1948–1968 with those of the first survey in 1893–1909, he obtained the directions of the maximum contraction axis with an accuracy of 5° – 15° by averaging results of 4–14 triangles. One exception is the local axis around 42.0°N , 140.5°E (Figs. 1 and 2) which is directly calculated from the triangulation data of one hexagon (Nakane, personal communication, 1978). Triangulation data in areas which are apparently affected by large earthquakes are not used. The maximum contraction axes whose directions are shown by the thin solid lines with dots in Fig. 1 can be considered to represent stationary, or secular tectonic strain. Behind the Japan trench, the axes strike nearly E-W; west of the junction of the Kurile and Japan trenches, the axis starts to gradually rotate clockwise and becomes roughly normal to the bisector of the junction, then the trend of the axis rather abruptly assumes a more or less ESE-WNW direction behind the Kurile trench.

If each axis represented deformation within one triangle, such an abrupt change in the direction of the principal axis (roughly 90°) could be regarded as due to some error-

neous movement of one triangulation point connecting two geodetic triangles. But, this is not the case here; as mentioned earlier, all trends except one represent an average of 4–14 trends. Trends of maximum contraction axis calculated from each triangle are shown in Fig. 2. Trends of the axes of neighbouring triangles are mostly coherent and the state of stress gradually changes in space. The existence of an anomaly is apparent northwest of the junction of the Kurile and Japan trenches. Most of the geodetic triangles shown at the eastern end of Fig. 2 are apparently effected by co-seismic deformation associated with the 1952 Tokachi-Oki earthquake of magnitude 8.1 (NAKANE, 1973). The principal contraction axes from those effected triangles are not shown in Fig. 2. North-south contraction around 43°N , 143°E might also reflect the co-seismic change.

The maximum compression axes shown by the broken lines in Fig. 1 are after Oka, who conducted two in-situ stress measurements in a bore-hole in this region by the over-coring method (see Ito *et al.*, 1976). He found nearly horizontal maximum compressive axes (plunging less than 10°) consistent with Nakane's result. Also shown in Fig. 1 by the bars on circles are trends of the axis of maximum compression estimated mainly from the overall distribution of monogenetic craters and fissures of fissure-eruption volcanoes (NAKAMURA, 1975; Nakamura, personal communication). The details and the principle

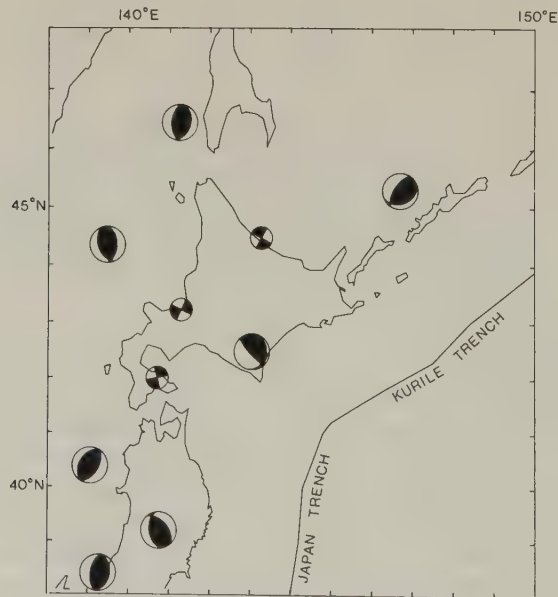


Fig. 3. Fault plane solutions for intraplate earthquakes in northeast Japan. The large circles correspond to large shocks with magnitudes in the range 6.2 to 7.5 (FUKAO and FURUMOTO, 1975; STAUDER and BOLLINGER, 1964; MIKUMO, 1974; ABE, 1975; STAUDER and MUALCHIN, 1976). The small circles correspond to small events (MORIYA, 1976). The shaded areas in each focal mechanism diagram indicate the quadrants of compression first motion of the lower focal hemisphere (equal area projection).

of the procedure to estimate the maximum compressional axis can be found in NAKAMURA (1977), who regards flank eruptions of polygenetic volcanoes as large-scale hydraulic fracturing by magma repeated over a long period of time. His results rather surprisingly agree with Nakane's despite the different time scales represented, except for one trend at Usu volcano ($42^{\circ}32'N$, $140^{\circ}50'E$). The trend differs by roughly 80° from the geodetically estimated one shown in Fig. 1. However, the trend of the maximum contraction axis derived from a geodetic triangle surrounding Usu volcano is closer to this trend (see Fig. 2); the trend at Usu volcano itself might represent strain of some localized nature.

The magnitude of horizontal shear strain rate in this anomalous area northwest of the junction, $1-2 \times 10^{-7}/\text{year}$, is roughly as large as that in other areas behind trenches (NAKANE, 1973; see also Fig. 2). Those areas behind trenches are considered to be strongly strained by the underthrusting Pacific plate (MOGI, 1970; SHIMAZAKI, 1974). The relatively high strain rate in the area northwest of the junction has not previously been explained. In the following section, we will suggest that stress concentration may occur near the arc-arc junction.

Fault plane solutions for intraplate earthquakes in this region are compatible with the local directions of the maximum compression axis shown in Figs. 1 and 2 and are shown in Fig. 3. The areas which are not shaded in each focal mechanism diagram indicate the quadrants of rarefaction first motion of the lower focal hemisphere (equal area projection). The P-axis, which corresponds to the axis of maximum compression in a homogeneous material, lies in the quadrant of rarefaction first motion and bisects the two nodal planes. The large circles indicate fault plane solutions for large earthquakes with magnitude ranging from 6.2 to 7.5 (FUKAO and FURUMOTO, 1975; STAUDER and BOLLINGER, 1964; MIKUMO, 1974; ABE, 1975; STAUDER and MUALCHIN, 1976). The small circles indicate fault plane solutions for small earthquakes ($M=4.0, 5.2$) and one composite solution (the southernmost one of the three) for smaller events (MORIYA, 1976). Most of the solutions represent more or less E-W trending compression. Two solutions in the anomalous area indicate that the axis of maximum compression rotates there by 60° to 90° . One of the two solutions around $43^{\circ}N$, $141^{\circ}E$ is different from what is expected from Fig. 1, but consistent with the local principal axis calculated from the geodetic triangle containing the event (Fig. 2). The solution probably represents tectonic stress of a localized nature.

2.2 The Aleutian-Kamchatka arc-arc junction

An interesting feature of the seismicity of the junction of the Aleutian and Kamchatka arcs is that the fairly active area extends 100 to 200 km north of the junction along the eastern coast of Kamchatka. Two large earthquakes occurred in this area during the past 40 years; one with magnitude 6.8 in 1945 and the other with magnitude 7.3 in 1969 (CORMIER, 1975). ZOBIN and SIMBIREVA (1977) presented fault plane solutions for 91 earthquakes and discussed the heterogeneity of the stress field in this region. In Fig. 4 are shown fault plane solutions for probable intraplate earthquakes obtained by Zobin and Simbireva or by Cormier. The attached numbers starting with Z correspond to earthquake numbers in Table 1 of ZOBIN and SIMBIREVA (1977) and those starting with C correspond to earthquake numbers in Table 2 of CORMIER (1975). All the earthquakes are no deeper than 33 km, except one earthquake numbered Z63 which is 30–50 km deep. Both CORMIER (1975) and ZOBIN and SIMBIREVA (1977) conclude that the compressive stress north of the junction is nearly horizontal and normal to the eastern coast of Kam-

chatka, or roughly perpendicular to the bisector of the junction, although a few poorly constrained solutions may appear to contradict this conclusion. The inferred state of stress north of the junction is quite different from that in other areas shown in Fig. 4 where the maximum compressional axis lies more or less N-S. Cormier suggests that compression normal to the eastern coast of Kamchatka north of the junction may be due to crustal extension in the Kamchatka Basin behind the western end of the Aleutian arc. He also suggests the possibility that this anomaly results from the abrupt change in the strike of the plate boundary at the arc-arc junction.

2.3 *The bend of the Nazca-South American plate boundary near the Peru-Ecuador border*

Near the border of Peru and Ecuador, the boundary between the Nazca and South American plates bends acutely and shows a westward convex arcuate structure. Near the bend, STAUDER (1975) found an anomalous fault plane solution which represents N-S compression, while other solutions in Fig. 5 correspond to horizontal E-W compression. All the fault plane solutions except the northernmost one in the figure are taken from Fig. 6 of STAUDER (1975). All the earthquakes discussed here are shallower than 65 km and considered as intraplate events; the anomalous events near the bend is 25 km deep. The numbers shown in the figure indicate water depth in kilometers. Although the foredeep of the Andes becomes shallower north of the bend, the Nazca plate is considered to be subducting beneath South American plate in this region on the basis of various geophysical measurements (e.g. MEISSNAR *et al.*, 1976). A fault plane solution for an intraplate earthquake behind this arc north of the bend (the northernmost one in Fig. 5) indicates E-W compression, as do those east and southeast of the bend. First motion data for this solution are shown in the Appendix.

STAUDER (1975) suggests that the anomalous state of stress found near the bend is a result of the difference in the direction of subduction of the oceanic plate along the sharply bending boundary of the continental plate. It is also interesting to note that near the bend the maximum compression axis strikes roughly normal to the bisector of the corner of the continental plate.

2.4 *The Himalaya-Burma arc-arc junction*

The eastern Himalayas, a southward convex arc extending E-W, intersect the Burma arc which extends roughly N-S and is convex westward; the intersection of the two arcs represents the northeastern corner of the Indian plate. MOLNAR *et al.*, (1973) found that northeast of the junction of the two arcs three events, including the great "Assam earthquake," represent normal faulting. They suggest that the Indian plate, which pushes north into the Himalayas, stretches the region northeast of the corner of the plate, and thus causes normal faulting. However, BEN-MENACHEM *et al.* (1974) found that various seismological data of the great Assam earthquake are more compatible with right-lateral strike-slip faulting on a fault dipping ENE than normal faulting. Also, the other normal faulting in the vicinity of Kan Tzu is interpreted as representing local extensional stress field resulted from an offset of two segments of the Kang Ting strike-slip fault (TAPPONNIER and MOLNAR, 1977). Nevertheless, the fault plane solution for an event which occurred at the northeastern end of the Hsia Kuan graben system in southwest China shows predominantly normal faulting (TAPPONNIER and MOLNAR, 1977). Although the tectonics in this region are apparently complicated, the Yunnan grabens

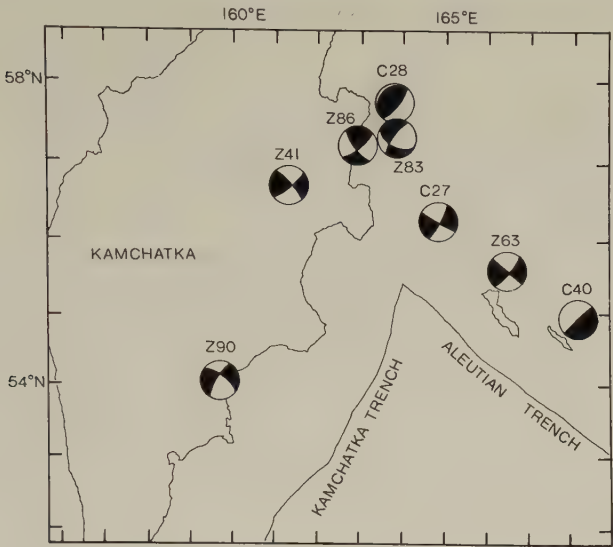


Fig. 4. Fault plane solutions near the junction of the Aleutian and Kamchatka arcs. The attached numbers starting with Z correspond to earthquake numbers in Table 1 of ZOBIN and SIMBIREVA (1977) and those starting with C correspond to event numbers in Table 2 of CORMIER (1975). For focal mechanism diagrams see the caption of Fig. 3.

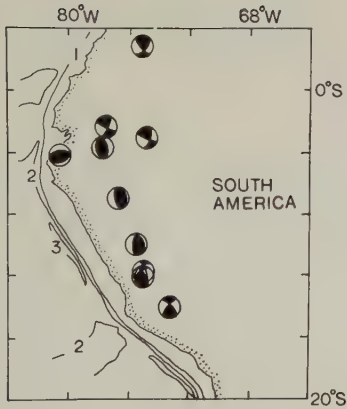


Fig. 5. Fault plane solutions for intraplate earthquakes occurring within the South American plate. First motion data of the solution shown at the top are given in the Appendix. All other solutions are obtained by STAUDER (1975). For focal mechanism diagrams see the caption of Fig. 3.

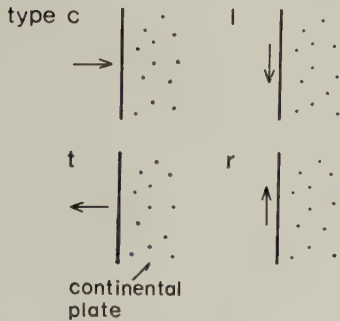


Fig. 6. Four displacement (force) types.

Table 1. Relationship between displacement (or force) types and deformation types.

Displacement (force) type	β	γ	Deformation type	
c and c	$\pi/2$	$\pi/2$	Pure type	$C, 0 < \alpha < \pi/2; T, \pi/2 < \alpha < \pi$
t and t	$3\pi/2$	$3\pi/2$		$T, 0 < \alpha < \pi/2; C, \pi/2 < \alpha < \pi$
c and t^*	$\pi/2$	$3\pi/2$		SR
t and c	$3\pi/2$	$\pi/2$		SL
l and r	0	0	Mixed type	C
r and l	π	π		T
l and l	0	π		$SL, 0 < \alpha < \pi/2; SR, \pi/2 < \alpha < \pi$
r and r	π	0		$SR, 0 < \alpha < \pi/2; SL, \pi/2 < \alpha < \pi$
c and r	$\pi/2$	0		SR and $C, 0 < \alpha < 3\pi/4; SL$ and $T, 3\pi/4 < \alpha < \pi$
c and l	$\pi/2$	π		SL and $C, 0 < \alpha < \pi/4; SR$ and $T, \pi/4 < \alpha < \pi$
r and c	π	$\pi/2$		SR and $C, 0 < \alpha < \pi/4; SL$ and $T, \pi/4 < \alpha < \pi$
l and c	0	$\pi/2$		SL and $C, 0 < \alpha < 3\pi/4; SR$ and $T, 3\pi/4 < \alpha < \pi$
t and r	$3\pi/2$	0		SR and $T, 0 < \alpha < \pi/4; SL$ and $C, \pi/4 < \alpha < \pi$
t and l	$3\pi/2$	π		SL and $T, 0 < \alpha < 3\pi/4; SR$ and $C, 3\pi/4 < \alpha < \pi$
r and t	π	$3\pi/2$		SR and $T, 0 < \alpha < 3\pi/4; SL$ and $C, 3\pi/4 < \alpha < \pi$
l and t	0	$3\pi/2$		SL and $T, 0 < \alpha < \pi/4; SR$ and $C, \pi/4 < \alpha < \pi$

* This indicates that type c displacement occurs (or force acts) on the upper edge and type t on the lower edge.

Table 2. Physically realizable combinations of types l and r .

r and l^*	when $0 < \alpha < \pi/4$
r and l, l and l, r and r	$\pi/4 < \alpha < \pi/2$
l and r, l and l, r and r	$\pi/2 < \alpha < 3\pi/4$
l and r	$3\pi/4 < \alpha < \pi$

* This indicates that type r displacement occurs (or force acts) on the upper edge and type l on the lower edge.

together with this normal faulting might partly reflect an extensional stress field related to the junction of the Himalaya and Burma arcs.

2.5 Southwest Japan

ICHIKAWA (1965, 1970) presented fault plane solutions for earthquakes near the junction of the Izu-Bonin and southwest Japan arcs and the southwest Japan and Ryukyu arcs, which suggest that the earthquake-generating stress systems are different from those in the surrounding regions. He suggested that these anomalies may constitute an important feature of arc-arc junctions. Later studies revealed that fault plane solutions for crustal earthquakes in southwest Japan roughly represent E-W compression while those for subcrustal shocks represent more or less N-S compression (e.g. SHIONO, 1973). The most recent work on the tectonics of the Izu Peninsula at the junction of the Izu-Bonin and southwest Japan arcs (SOMERVILLE, 1978) presents evidence for two stress domains in the *crust* having contrasting orientations resulting from the collision between the Philippine Sea plate and the Eurasian plate. The suggested anomalies at these two arc-arc junctions might be partly explained by the above mentioned complications. The problem of intra-plate deformation at these arc-arc junctions need further investigation and will not be discussed in this paper.

3. Types of Intraplate Deformation

The most fundamental aspects entailed in the behavior of intraplate deformation at an arc-arc junction are probably geometrical configuration and the forces acting on the plate edges. We will assume that horizontal forces are more important than vertical forces. Vertical forces are probably predominant along arcs where the Wadati-Benioff zone is steeply dipping. However, no anomaly in stress orientation has yet been reported at the junction of two steeply-dipping Wadati-Benioff zones, such as the Izu-Mariana arc-arc junction. Accordingly, in the following analysis, we will treat only horizontal forces and consider a flat plate with two straight edges meeting at an angle 2α as a model of the continental plate near an arc-arc junction (see Fig. 7). The following analysis could be modified to take account of the complications of the real earth. However this is not done because the basic principles would then become obscure. First we will intuitively treat displacement boundary conditions and later we will discuss stress boundary conditions.

We assume the following four fundamental types of displacement occurring (or forces acting) on plate edges (Fig. 6):

- 1) contraction (or compression) normal to the edge (hereafter called type c);
- 2) extension (or tension) normal to the edge (type t);
- 3) left-lateral shear parallel to the edge (type l);
- 4) right-lateral shear parallel to the edge (type r).

A type c boundary condition might prevail at arcs because plates are converging there. However, in some island arcs, extension is observed to occur normal to the arc (KARIG, 1970). ELSASSER (1969) proposed a 'suction' mechanism, equivalent to type t , caused by the retreat of the oceanic slab. Type l or r seems to be acting where plates are obliquely converging. Uyeda points out that lateral motion within the continental plate should be expected along an obliquely converging arc if the oceanic plate underthrusts normal to the arc (MATSUDA and UYEDA, 1971). He suggests that this motion accentuates the arcuate shape of island arcs, once a chain of arcs starts to form. The oblique motion of the Philippine Sea plate relative to the Eurasian plate is suggested to be decoupled between the underthrusting and the lateral motion along the boundary (FITCH, 1972; SHIMAZAKI, 1976). The suggested lateral motion corresponds to displacement type l or r . Generally we do not expect the displacement to be exclusively one of the four types. The actual situation may lie somewhere between types c and l (or r) or between types t and l (or r). Displacements (or forces) in any direction can be expressed as a linear combination of c (or t) and l (or r).

The angles between the strikes of the two plate edges and the displacements occurring (or forces acting) on the edges are denoted by β and γ as shown in Fig. 7. If a displace-

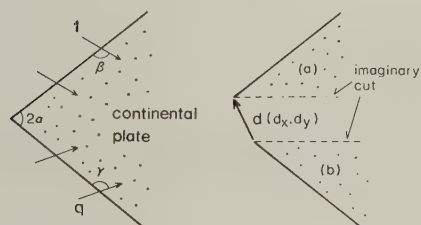


Fig. 7. Forces acting (or displacement occurring) on plate edges.

ment with the same magnitude occurs uniformly in the same direction on both edges, i.e. $2\alpha + \beta + \gamma = 2\pi$, a lateral rigid body motion takes place and no anomaly would be found. Therefore, any displacement components on the two edges which are parallel and also have the same magnitude can be neglected in the following discussion.

Let us assume that a certain type of displacement with unit magnitude occurs uniformly on one edge and another (or the same) type of displacement with magnitude q occurs on the other edge. Then we can derive two orthogonal displacements:

$$d_x = -\cos(\alpha + \beta) + q \cos(\alpha + \gamma)$$

$$d_y = -\sin(\alpha + \beta) - q \sin(\alpha + \gamma).$$

If we were to cut the continental plate along the bisector of the junction into two segments (Fig. 7), these two orthogonal displacements would indicate the displacement of segment (a) relative to segment (b). These parameters enable us to determine the polarity of each of the two fundamental displacement systems, contraction or extension, and left or right lateral shear. These four displacement systems, and their associated deformation modes, are illustrated in Fig. 8 and summarized below:

- a) contractional horizontal displacement occurring normal to the bisector of the junction (hereafter called type *C*);
- b) extensional horizontal displacement occurring normal to the bisector (type *T*);
- c) right-lateral shear horizontal displacement occurring parallel to the bisector (type *SR*, strike-slip);
- d) a mirror image of type *SR* (type *SL*).

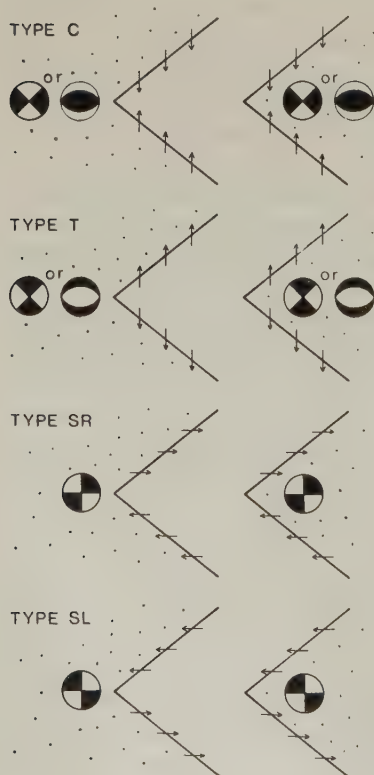


Fig. 8. Four basic types of intraplate deformation at arc-arc junctions. The stippled area indicates the continental plate. The resultant deformation is indicated by focal mechanism diagrams.

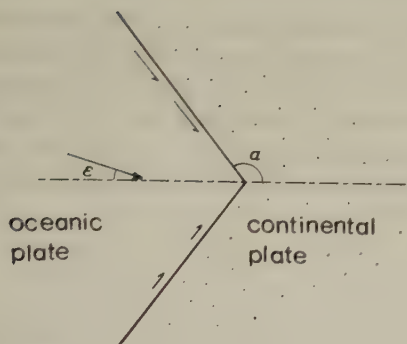


Fig. 9. Motion of the oceanic plate relative to the continental plate. The half arrows indicate type l or r force acting (or displacement occurring) on the obliquely converging plate boundaries.

The absolute value of d_x shows the strength of type SR when d_x is positive and that of type SL when d_x is negative. Similarly, the absolute value of d_y shows the strength of type T when d_y is positive and that of type C when d_y is negative. All the combinations of displacement types occurring on the two neighbouring edges are tabulated in Table 1 on the assumption of $q = 1$. These examples give us a qualitative idea of the relation between displacement types and deformation types. For certain combinations of displacement types, only one type of deformation takes place (pure type). But for other combinations, two types of deformation are expected to occur together (mixed type).

Apparently, some combinations of displacement types are unrealistic. If we assume that displacement (or force) types l and r are purely the result of the decoupling of an oblique convergence, as mentioned earlier, then certain combinations of types l and r become physically unrealizable. Let us denote by ε the angle between the strike of the bisector of a junction and the motion direction of the oceanic plate relative to the continental plate as shown in Fig. 9. The assumption that plates are converging at arcs requires

$$-\alpha < \varepsilon < \alpha \quad \text{when } 0 < \alpha < \pi/2$$

and

$$-\pi + \alpha < \varepsilon < \pi - \alpha \quad \text{when } \pi/2 < \alpha < \pi.$$

If the relative motion is completely decoupled, displacement occurring on the upper edge is proportional to $\cos e$ ($e = \pi - \varepsilon - \alpha$) and that on the lower edge is proportional to $\cos f$ ($f = \alpha - \varepsilon$). The sign of the parameters $\cos e$ and $\cos f$ indicates the polarity of the displacement; if $\cos e$ and $\cos f$ are positive (negative), type l (type r) is expected on the edge. Possible combinations of displacement types for different values of α can be easily obtained from the following equation:

$$e = f + \pi - 2\alpha.$$

It is obvious that only those combinations which are listed in Table 2 are physically realizable.

All the above arguments are based on displacement boundary conditions. For stress boundary conditions, the problem can be analytically formulated by making use of the Mellin transform (Sneddon, 1951). Sneddon's expression is generalized and the state of stress within a thin elastic wedge is calculated in a separate paper (Kato *et al.*, 1978), with the following results. (1) The above argument based on an intuitive geometrical consideration can also apply to cases of stress boundary conditions, unless those components of stress which have the same strength and act uniformly in the same direc-

tion on the both edges are predominant. In other words, if those stress components acting on the edge which are shown in Fig. 7 are weak compared with the prevailing uniform stress, then the expected anomalous state of stress will be masked. (2) Shear stress acting on edges produces a large stress concentration at the intersection. It is concluded that the above classification of anomalous intraplate deformation and relationships between force types and deformation types can hold for cases of stress boundary conditions when an anomaly exists at the junction.

4. Discussion

According to the classification given in the preceding section, three of the four examples of anomalous intraplate deformation at arc-arc junctions can be classified as type *C*. Those examples are at the Kurile-Japan arc-arc junction, at the Aleutian-Kamchatka arc-arc junction, and near the bend of the Nazca-South American plate boundary.

At a concave continental plate boundary, pure type *C* deformation can be expected for a combination of displacement (or force) types *t* and *t* or *l* and *r*. According to the present kinematic model of plate motions (e.g. MINSTER *et al.*, 1974), oblique convergence between the Eurasian and Pacific plates can be expected along the western Aleutian arc, and to a somewhat smaller extent, along the Kurile arc near northeast Japan. It is most likely that type *r* displacement occurs along these arcs and results in type *C* deformation at the junctions. An alternative would be that type *t* displacement occurs along those arcs. One possible arc where type *t* displacement occurs would be the western Aleutian arc; CORMIER (1975) suggests an extension of Kamchatka Basin behind the western end of the Aleutian arc. However, we prefer the former explanation to the latter, because a remarkable stress concentration takes place at a junction if shear stress acts on the plate edges (KATO *et al.*, 1978). The anomalous states of stress found near the junction of the Kurile and Japan arcs and of the Aleutian and Kamchatka arcs are probably related to a shearing force acting at the obliquely converging plate boundaries.

At a convex continental plate boundary, pure type *C* deformation can be expected for a combination of displacement types *c* and *c*, because a combination of types *l* and *r* is found to be physically unrealizable in the preceding section. Accordingly, we suggest that the anomaly found near the acute bend of the Nazca-South American plate boundary is due to normal compressive forces acting on both parts of the boundary north and south of the bend.

The anomalous intraplate deformation near the junction of the Himalaya and Burma arcs, although evidence for its existence is somewhat tenuous, can be classified as type *T*. The only physically realizable combination of displacement types for pure type *T* deformation at a concave continental plate boundary is *c* and *c*. According to MOLNAR *et al.* (1973), the Indian plate is pushing north along the Himalaya arc. The pushing (type *c* force) could result in normal faulting near the junction of the Himalaya and Burma arcs.

It appears that no 'strike-slip' deformation (neither type *SR* nor *SL*) takes place in the real earth. One possible exception might be the junction of the Aleutian trench and the Queen Charlotte Islands transform fault, although strictly speaking this is not an arc-arc junction and the problem of the plate boundary connection in this region remains unresolved. The most significant and interesting tectonic feature in this region is the Denali fault system, a northward-convex arcuate active fault more than 2,000 km long consisting of primarily right-lateral strike-slip fault segments (e.g. BROGAN *et al.*, 1975).

The northward bending of the fault system occurs north of the eastern end of the Aleutian trench, which may be assumed to be the northeastern corner of the Pacific plate. The bending of the right-lateral strike-slip fault indicates a rotation of the maximum compression axis near the corner of the Pacific plate, as clearly shown by NAKAMURA *et al.* (1977). Two fault plane solutions obtained by GEDNEY (1970) north of the Denali fault system are consistent with the rotation of the maximum compressive axis. A right-lateral shear force appears to act perpendicular to the bisector of the junction. This case can be classified as type *SL* deformation (see Fig. 8). However, the Denali fault system itself is considered as an active transform fault (e.g. GEDNEY, 1970; PACKER *et al.*, 1975); until the plate boundary is unambiguously defined elsewhere, the above discussion must be considered as speculative.

Arcs are characteristically arcuate and occur in chains. At an arc-arc junction, the continental plate is usually concave and oblique convergence of the plate tends to bring about a combination of force types *l* and *r*, thus resulting in type *C* deformation. This speculation partly explains the predominance of type *C* deformation in the earth. It is also interesting to notice that type *c* force is suggested at continental collision boundaries and at arcs where the dip of the Wadati-Benioff zone is unusually shallow.

5. Conclusions

It is shown that an anomalous state of stress can be expected at an arc-arc junction where the directions of the forces acting on the two intersecting plate boundaries are different, being constrained in some manner by the strike of the boundaries. Four basic types of internal deformation are derived by assuming four types of force acting (or displacement occurring) at plate edges. All possible combinations of force (or displacement) type are related to resultant deformation types, although some of the combinations are suggested to be physically unrealizable.

The anomalous state of stress found northwest of the junction of the Kurile and Japan arcs and that found north of the Aleutian-Kamchatka arc-arc junction can be classified as type *C* deformation (compression normal to the bisector of the junction). These anomalies may be related to a shearing force acting on the obliquely converging plate boundaries. The anomaly found east of the acute bend of the Nazca-South American plate boundary near the Peru-Ecuador border is also classified as type *C* and may be due to a pushing force acting normal to the two segments of the convex boundary of the continental plate. Some tenuous evidence may suggest an anomaly in the state of stress northeast of the junction of the Himalaya and Burma arcs.

We wish to express our gratitude to Dr. Paul Somerville, and Prof. S. Uyeda for critically reviewing the manuscript. We also wish to thank Dr. K. Nakane for supplying us with some unpublished data, Prof. K. Nakamura for his helpful suggestions, Lynn Sykes, Seth Stein, and Emile Okal for making their work available prior to publication, and Profs. K. Kasahara, and S. Asano for their encouragement. Mrs. K. Noguchi helped us to arrange the manuscript.

APPENDIX

First motion data for the Colombian earthquake of February 9, 1967 are shown in Fig. A-1. Forty-three initial motions of P waves were read on long-period seismograms at WWSSN stations. Dip direction (ϕ) and dip angle (δ) of the two nodal planes are: $\phi_1 = \text{N}130^\circ\text{E}$, $\delta_1 = 57^\circ$, $\phi = \text{N}228^\circ\text{E}$, $\delta = 75^\circ$.

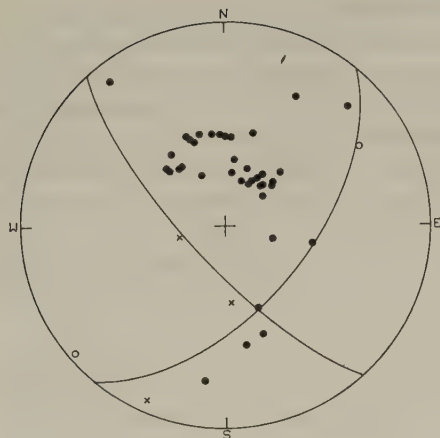


Fig. A-1. Equal area projection (lower hemisphere) of the first motion data for the Colombian earthquake of February 9, 1967. The solid circles represent compressional first motions, the open circles indicate rarefactional first motions, and the crosses show arrivals with nodal character.

REFERENCES

- ABE, K., Re-examination of the fault model for the Niigata earthquake of 1964, *J. Phys. Earth*, **23**, 349–366, 1975.
- BEN-MENACHEM, A., E. ABOODI, and R. SCHILD, The source of the great Assam earthquake—An interplate wedge motion, *Phys. Earth Planet. Inter.*, **9**, 265–289, 1974.
- BROGAN, G.E., L.S. CLUFF, M.K. KORRINGA, and D.B. SLEMMONS, Active faults of Alaska, *Tectonophysics*, **29**, 73–85, 1975.
- CORMIER, V.F., Tectonics near the junction of the Aleutian and Kuril-Kamchatka arcs and a mechanism for middle Tertiary magmatism in the Kamchatka Basin, *Geol. Soc. Am. Bull.*, **86**, 433–453, 1975.
- ELSASSER, W.M., Convection and stress propagation in the upper mantle, in *The Application of Modern Physics to the Earth and Planetary Interiors*, edited by S.K. Runcorn, pp. 223–246, Wiley, New York, 1969.
- FITCH, T.J., Plate convergence, transcurrent faults, and internal deformation adjacent to southeast Asia and the Western Pacific, *J. Geophys. Res.*, **77**, 4432–4460, 1972.
- FORSYTH, D.W., Fault plane solutions and tectonics of the South Atlantic and Scotia Sea, *J. Geophys. Res.*, **80**, 1429–1443, 1975.
- FRANK, F.C., Deduction of earth strains from survey data, *Bull. Seismol. Soc. Am.*, **50**, 35–42, 1966.
- FUKAO, Y. and M. FURUMOTO, Mechanism of large earthquakes along the eastern margin of the Japan Sea, *Tectonophysics*, **25**, 247–266, 1975.
- GEDNEY, L., Tectonic stresses in Southern Alaska in relationship to regional seismicity and the new global tectonics, *Bull. Seismol. Soc. Am.*, **60**, 1789–1802, 1970.
- HESS, H.H., Major structural features of the western north Pacific, an interpretation of H.O. 5485, bathymetric chart, Korea to New Guinea, *Geol. Soc. Am. Bull.*, **59**, 417–446, 1948.
- ICHIKAWA, M., The mechanism of earthquakes occurring in Central and Southwestern Japan, and some related problems, *Pap. Meteorol. Geophys.*, **16**, 104–156, 1965.
- ICHIKAWA, M., Seismic activities at the junction of Izu-Mariana and Southwestern Honshu arcs, *Geophys. Mag.*, **35**, 55–69, 1970.
- ITO, H., Y. OKA, and K. HUZITA, The Japanese islands in contraction, *Kagaku (Science)*, **46**, 745–754, 1976 (in Japanese).
- KARIG, D.E., Ridges and basins of the Tonga-Kermadec island arc system, *J. Geophys. Res.*, **75**, 239–254, 1970.
- KATO, T., K. SHIMAZAKI, and K. YAMASHINA, State of stress within a thin elastic wedge: A model of internal deformation of the continental plate at an arc-arc junction, in preparation, 1978.
- MATSUDA, T. and S. UYEDA, On the Pacific-type orogeny and its model-extension of the paired belts concept and possible origin of marginal seas, *Tectonophysics*, **11**, 5–27, 1971.
- MEISSNAR, R.O., E.R. FLUEH, F. STIBANE, and E. BERG, Dynamics of the active plate boundary in southwest Colombia according to recent geophysical measurements, *Tectonophysics*, **35**, 115–136, 1976.
- MIKUMO, T., Some considerations on the faulting mechanism of the southwestern Akita earthquake of October 16, 1970, *J. Phys. Earth*, **22**, 87–108, 1974.

- MINSTER, J.B., T.H. JORDAN, P. MOLNAR, and E. HAINES, Numerical modelling of instantaneous plate tectonics, *Geophys. J.*, **36**, 541–576, 1974.
- MOGI, K., Recent horizontal deformation of the earth's crust and tectonic activity in Japan, *Bull. Earthq. Res. Inst., Tokyo Univ.*, **48**, 413–430, 1970.
- MOLNAR, P., T.J. FITCH, and F.T. WU, Fault plane solutions of shallow earthquakes and contemporary tectonics in Asia, *Earth Planet. Sci. Lett.*, **19**, 101–112, 1973.
- MORIYA, T., Microearthquake surveys in the northern, central and southwestern parts of Hokkaido, in *Symp. on Subterranean Structure in and around Hokkaido and Its Tectonic Implication*, pp. 70–83, Hokkaido Univ., Sapporo, 1976 (in Japanese).
- NAKAMURA, K., Volcano structure and possible mechanical correlation between volcanic eruptions and earthquakes, *Bull. Volcanol. Soc. Jpn.*, **20**, 229–240, 1975 (in Japanese).
- NAKAMURA, K., Volcanoes as possible indicators of tectonic stress orientation—Principle and proposal, *J. Volcanol. Geotherm. Res.*, **2**, 1–16, 1977.
- NAKAMURA, K., K.H. JACOB, and J.N. DAVIES, Volcanoes as possible indicators of tectonic stress orientation—Aleutians and Alaska, *Pageoph.*, **115**, 87–112, 1977.
- NAKANE, K., Horizontal tectonic strain in Japan (I), (II), *J. Geod. Soc. Jpn.*, **19**, 190–199, 200–208, 1973 (in Japanese).
- PACKER, D.R., G.E. BROGAN, and D.B. STONE, New data on plate tectonics of Alaska, *Tectonophysics*, **29**, 87–102, 1975.
- SHIMAZAKI, K., Pre-seismic crustal deformation caused by an underthrusting oceanic plate, in eastern Hokkaido, Japan, *Phys. Earth Planet. Inter.*, **8**, 148–157, 1974.
- SHIMAZAKI, K., Intra-plate seismicity gap along the Median Tectonic Line and oblique plate convergence in southwest Japan, *Tectonophysics*, **31**, 139–156, 1976.
- SHIONO, K., Focal mechanism of small earthquakes in the Kii peninsula, Kii channel and Shikoku, southwest Japan and some problems related to the plate tectonics, *J. Geosci. Osaka City Univ.*, **16**, 69–91, 1973.
- SNEDDON, I.N., *Fourier Transforms*, 542 pp., McGraw-Hill, New York, 1951.
- SOMERVILLE, P., The accommodation of plate collision by tectonic deformation in the Izu block, Japan, *Bull. Earthq. Res. Inst., Univ. Tokyo*, **53**, 1978 (in press).
- STAUDER, W., Subduction of the Nazca plate under Peru as evidenced by focal mechanisms and by seismicity, *J. Geophys. Res.*, **80**, 1053–1064, 1975.
- STAUDER, W. and G.A. BOLLINGER, The S wave project for focal mechanism studies, earthquakes of 1962, *Bull. Seismol. Soc. Am.*, **54**, 2199–2208, 1964.
- STAUDER, W. and L. MUALCHIN, Fault motion in the larger earthquakes of the Kurile-Kamchatka arc and of the Kurile-Hokkaido corner, *J. Geophys. Res.*, **81**, 297–308, 1976.
- STEIN, S. and E.A. OKAL, Seismicity and tectonics of the Ninetyeast Ridge area: Evidence for internal deformation of the Indian plate, *J. Geophys. Res.*, **83**, 2233–2245, 1978.
- SUGIMURA, A. and S. UYEDA, *Island Arcs: Japan and Its Environs*, 247 pp., Elsevier, Amsterdam, 1973.
- SYKES, L.R., Intra-plate seismicity, reactivation of pre-existing zones of weakness, alkaline magmatism, and other tectonism post-dating continental fragmentation, *Rev. Geophys. Space Phys.*, **16**, 621–688, 1978.
- SYKES, L.R. and M.L. SBAR, Intraplate earthquakes, stresses in the lithosphere and the driving mechanism of plate tectonics, *Nature*, **245**, 298–302, 1973.
- TAPPONNIER, P. and P. MOLNAR, Active faulting and tectonics in China, *J. Geophys. Res.*, **82**, 2905–2930, 1977.
- ZOBIN, V.M. and I.G. SIMBIREVA, Focal mechanism of earthquakes in Kamchatka-Commander region and heterogeneities of the active seismic zone, *Pageoph.*, **115**, 283–299, 1977.

FAULT PATTERNS IN OUTER TRENCH WALLS AND THEIR TECTONIC SIGNIFICANCE†

G.M. JONES*¹, T.W.C. HILDE*², G.F. SHARMAN*³, and D.C. AGNEW*⁴

*¹ *Department of Geophysics*, *² *Department of Oceanography and Geophysics*, *³ *Department of Oceanography, Texas A & M University, College Station, Texas, U.S.A.*

*⁴ *Institute of Geophysics and Planetary Physics, University of California at San Diego, La Jolla, California, U.S.A.*

(Received August 4, 1978; Revised October 3, 1978)

The mechanical behavior of a plate entering a trench has been investigated through comparison between the amount of faulting present in the outer trench wall and the maximum bending stress, as inferred from fitting bathymetry data seaward of the trench axis to the theoretical deflection curve for the bending of an elastic plate. Out of 20 circum-Pacific trench profiles examined, 16 satisfy a quantitative test for elastic behavior seaward of the trench axis and exhibit a consistent relationship between maximum inferred bending stress and the roughness of topography on the outer trench wall. This result, in conjunction with the distribution of earthquake focal mechanisms within the subducting plate, is consistent with a model of an 80 km thick lithospheric plate having an elastic core approximately 30 km thick, outside of which brittle failure occurs.

1. Introduction

The shape of the ocean floor adjacent to the outer wall of many trenches exhibits a characteristic topographic bulge that can be attributed to the flexure of the subducting lithospheric plate. The shape of this outer topographic high has been successfully modeled using thin plate theory for a number of different plate rheologies, including elastic (HANKS, 1971; WATTS and TALWANI, 1974; CALDWELL *et al.*, 1976); elastic-perfectly plastic (MCADOO *et al.*, 1977; FORSYTH and CHAPPLE, 1978); and viscous (DEBREMAECKER, 1977). The shape of this feature can also be explained as a result of viscous flow within the lower part of the lithosphere during subduction (MELOSH, 1978). A range of applied stresses have also been considered, including vertical and horizontal stresses applied at or near the trench axis (HANKS, 1971; WATTS and TALWANI, 1974; MCADOO *et al.*, 1977) and a bending moment applied to the downgoing slab (PARSONS and MOLNAR, 1976).

The fact that the theoretical deflection curve for a bending lithospheric plate is similar for a wide range of rheologies and applied stresses complicates theoretical investigations of the mechanical behavior of the lithosphere at trenches, since bathymetric data alone is not sufficient to discriminate between the various models. It is therefore necessary to seek additional properties of the models that are more sensitive to such differences.

In this paper we use elastic theory for the bending of a thin lithospheric plate to investigate the relationship between maximum apparent bending stress within the subducting plate and the occurrence of faulting on the outer wall of a number of trenches in the Pacific Ocean. We find that the theoretical deflection curve for an elastic plate fits the

† Contribution of the Texas A & M University Geodynamics Research Program, No. 4.

bathymetric data in a large number of cases and that for these profiles there is a consistent relationship between the roughness of the outer trench wall, as defined by the root-mean square (RMS) deviation of topography from a smooth profile, and the maximum bending stress. This result indicates that the major fault patterns in outer trench walls are directly related to the subduction process and in conjunction with seismic focal mechanisms beneath the outer rise, suggests that these faults may be the surface expression of a zone of brittle failure extending to depths of 25 km or more within the oceanic plate.

2. Faults

The work of LUDWIG *et al.* (1966) revealed that a distinctive pattern of faulting exists on the outer wall of the Japan and Northern Bonin Trenches. Using seismic reflection data they mapped a series of grabens and step faults that they interpreted as normal faults caused by tensional forces induced in the convex side of the bent oceanic plate. They concluded that the plate is depressed by the load of the island margin. Additional seismic reflection profiles across the Japan Trench off Northern Honshu were reported on by HILDE and RAFF (1970). They likewise concluded that the seaward trench wall was broken by normal faults forming graben and horst structures due to bending of the oceanic plate into the subduction zone. They noted that the throw of the faults increased towards the trench axis and that apparent reverse offset occurs on some of the faults near and beneath the trench axis (Fig. 1). Although there is clear evidence for a highly faulted oceanic plate, Hilde and Raff were able to map the magnetic lineations associated with the oceanic plate 120 km shoreward of the trench axis. The faulting apparently has not destroyed the continuity of the plate.

Other trench studies have revealed that similar fault patterns exist in the outer walls of most trenches. FISHER and ENGEL (1969) and RAITT *et al.* (1955) recorded bathymetric profiles across the Tonga Trench which show evenly spaced grabens on the seaward trench wall between the outer high and the trench axis. As with the Japan Trench, the throw is clearly greater on the faults nearer the trench axis. This fault pattern is also well developed in the seaward wall of the Philippine Trench (FISHER and HESS, 1963). Bathymetric profiles across the Southern Mariana Trench show this fault pattern (FISHER, 1974), as do seismic reflection profiles across the Mariana Trench in the vicinity of Challenger Deep recorded during a 1973 National Taiwan University expedition by R/V CHIU LIEN.

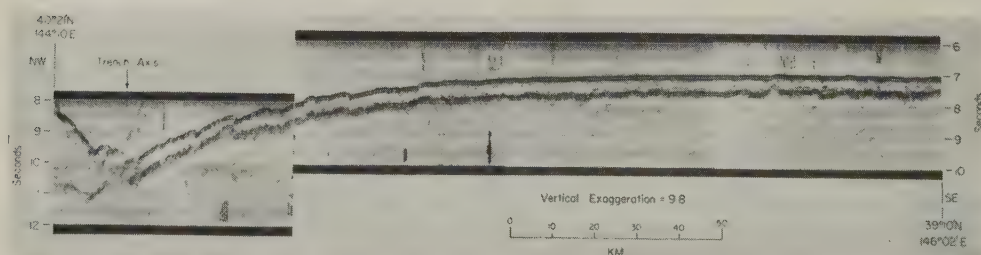


Fig. 1. Seismic reflection profile across the Japan Trench off northern Honshu recorded by R/V *Silas Bent* (HILDE and RAFF, 1970). Note uniform ~400 m sediment thickness overlying oceanic basement, faults confined to subducting plate in the outer trench wall, beneath trench axis and shoreward slope, and the unfaulted ocean basin seaward of the trench. Vertical scale is two-way travel time in seconds.

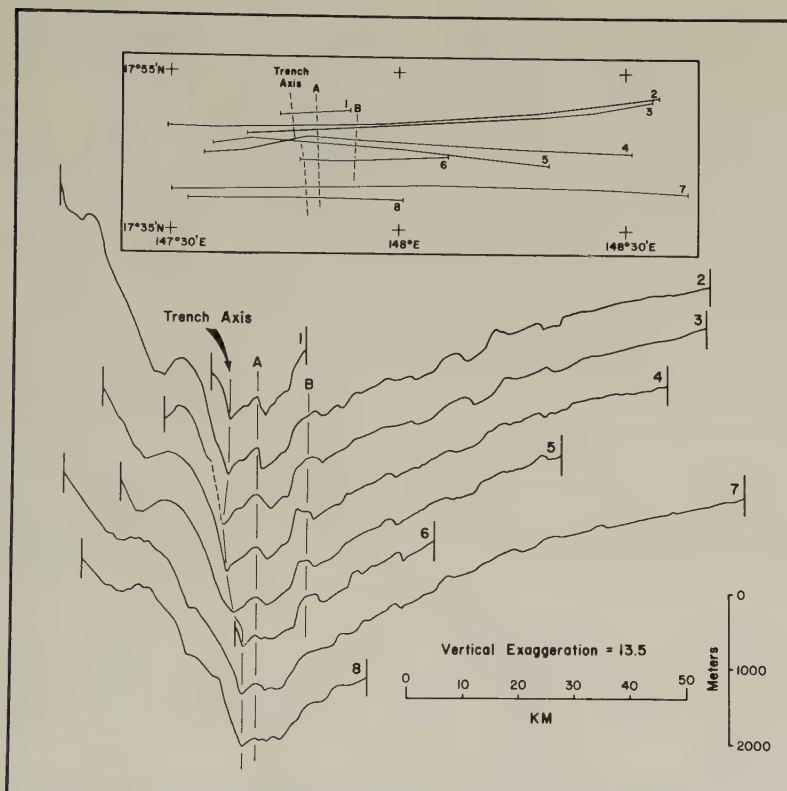


Fig. 2. Closely spaced bathymetric profiles across the Mariana Trench, collected by R/V *Kana Keoki* during 1976–77 IPOD site surveys, showing the horst and graben fault structures in the seaward trench wall. Data provided by Donald Hussong, Hawaii Institute of Geophysics.

BRACEY and ANDREWS (1974) also recorded reflection profiles across the Southern Mariana Trench which reveals this fault structure. This same fault pattern is particularly well developed on the outer wall of the Northern Mariana Trench (Fig. 2).

In all of the above trenches there is a common and distinctive fault pattern which is unique to the outer trench walls. It is easily distinguished in cases like the Japan Trench where the upper surface of the oceanic plate in the ocean basin outside of the trench is smooth (Fig. 1). Where the ocean basin beyond a trench displays rough and irregular relief it is sometimes difficult to recognize faults that may have originated in the seaward trench walls. In these cases, the seaward trench slopes have highly irregular surfaces which could be of the same origin as the rough seafloor of the nearby ocean basins and be displayed on the outer trench slope due only to plate convergence. The Middle America Trench (FISHER, 1961; FISHER and HESS, 1963) is an example. The great relief of the northern Middle America Trench is likely associated with topography which originated at the nearby East Pacific Rise. However, profiles across the southern Middle America Trench, where the adjacent basin is relatively smooth, display a faulted seaward trench wall with at least some graben and horst structures. In the case of the Peru-Chile Trench

COULBOURN (1977) was able to distinguish between outer trench slope faults and original high relief seafloor evident in the adjacent ocean basin. The faulted nature of the Peru-Chile Trench outer wall is also evident in the data of FISHER and RAITT (1962) and HAYES (1966). The Aleutian Trench also appears to have a faulted outer wall along its central and western segments (HAYES and EWING, 1970). The adjoining Pacific Ocean basin is rough in the west and is smooth in the east where there is a thick sediment cover. Seismic reflection profiles across the extreme eastern Aleutian Trench do not show an obvious fault pattern in the outer trench wall (VON HUENE, 1972). Although it may not be possible to recognize a unique pattern of faulting in every case, a greater degree of seafloor roughness than in the adjoining basins can be attributed to faulting associated with the downward bending of the oceanic plate into the subduction zone.

In several trenches faulting of the outer wall may not be obvious due to either surrounding structural complexities or lack of data. However, at least some normal faults and graben structures are evident in the outer walls of the Manila Trench (LUDWIG *et al.*, 1967); the Puerto Rico Trench (BOWIN *et al.*, 1966); the New Britain, New Hebrides, Solomons, and possibly also the Yap and Palau Trenches (FISHER, 1974); and the Kuril Trench. Due to the rough seafloor of the West Philippine Sea Basin it is difficult to recognize faults which may be unique to the outer wall of the Ryukyu Trench (WAGEMAN *et al.*, 1970). There appears to be little or no faulting associated with the outer wall of the Indonesian Trench (FISHER, 1964). However, some outer trench wall faulting is evident in the trenches of the complex Eastern Indonesian Archipelago (HAMILTON, 1977). The outer slope of Nankai Trough exhibits no obvious fault pattern (HILDE *et al.*, 1969; LUDWIG *et al.*, 1973). For worldwide trench profile compilations see FISHER (1974), HAYES and EWING (1970) and KARIG and SHARMAN (1975).

Where closely spaced survey lines have been run across trenches the faults in the seaward walls have been found to strike in a parallel to subparallel direction to the trench axis. Japan Trench DSDP site survey results reveal that the faults strike N20°W, about 30° from the strike of the Japan Trench axis (HONZA, 1978). Honza concludes that the faults formed due to bending of the plate but because the faults are parallel to the direction of spreading that formed the ocean crust, they may indicate a preferential weakness of the crust parallel to the spreading direction. COULBOURN (1977) found that the outer wall faults of the Peru-Chile Trench were predominantly parallel to sub-parallel with the trench axis and concluded that they developed on the outer trench slope due to bending of the plate but followed the structural grain of the oceanic plate as originally developed as the East Pacific Rise. These faults are perpendicular to the direction of spreading that formed the plate.

A preliminary examination of bathymetric data from the R/V KANA KEOKI DSDP site surveys of the Mariana Trench shows that the faults in the seaward trench wall are more nearly parallel to the trench axis in this case (Fig. 2). Low amplitude magnetic lineations have been mapped in the basin just east of the Mariana Trench that strike NE-SW (HUSSONG, 1978), the same direction as the Japanese lineations to the north (HILDE *et al.*, 1976). If these are spreading reversal lineations then the faults along this portion of the Mariana Trench are neither parallel nor perpendicular to the spreading that formed the plate, but diagonal. At present there is probably insufficient data on the strike of outer trench slope faults with which to reach conclusions about preferential directions of crustal strength.

The faults we are concerned with here are unique to the seaward slopes of trenches,

i.e. to the upper portion of the plate being subducted. Common topographic features of the shoreward trench slopes are considerably different and are related to either tectonic accretion or erosion at the front of arcs (KARIG and SHARMAN, 1975; SEELY *et al.*, 1974; SCHOLL *et al.*, 1977). The fault pattern of the seaward trench slopes can be characterized as consisting of normal faults having a strike that is parallel to sub-parallel to the trench axis, often forming graben and horst topography, and having increased and sometimes reverse throw towards the trench axis. Earthquake focal mechanism studies have established the tensional nature of faulting associated with this region of subducting plates (STAUDER, 1968; ISACKS *et al.*, 1968; ISACKS *et al.*, 1969; ISACKS and MOLNAR, 1971). In the several cases where the fault pattern is uncomplicated by other structures, the grabens are typically spaced 5–10 km apart with individual faults having vertical displacement which ranges from 100 to 200 m near the outer topographic high to 400–800 m near the trench axis. The extensive occurrence of these faults, their common characteristics and their confinement to outer trench walls lead us to conclude that they are a general feature of trench tectonics and originate at the outer topographic high due to tensional stresses in the upper part of the oceanic plate as it bends into the subduction zone. They occur in both curved and straight trenches and are therefore likely related only to the vertical bending of the plate.

3. Theory of Method

The theoretical deflection curve for the two-dimensional bending of a thin elastic plate supported by a buoyant fluid is given by (CALDWELL *et al.*, 1976)

$$w' = A \exp(-ax') \sin ax' \quad (1)$$

where w' is the deflection in the vertical (y') direction relative to the origin O' (Fig. 3), x' is the horizontal coordinate and the parameters A and a are constant.

The amplitude, W_b , of the outer topographic bulge and its distance, X_b , from the origin O' , are given by

$$W_b = A \sin\left(\frac{\pi}{4}\right) \exp\left(-\frac{\pi}{4}\right) \quad (2a)$$

$$X_b = \frac{\pi}{4a} \quad (2b)$$

The parameter a is related to the flexural rigidity, D , of the plate through the relation

$$D = \frac{(\rho_m - \rho_w)g}{4a^4} \quad (3)$$

where ρ_m and ρ_w are the densities of the underlying mantle and overlying water, respectively, and g is the acceleration of gravity.

We also have

$$D = \frac{Eh^3}{12(1-\sigma^2)} \quad (4)$$

where E =Young's modulus; h =elastic plate thickness and σ =Poisson's ratio. In the following, we take $E=6.5 \times 10^{11}$ dyn/cm²; $\sigma=0.25$; $(\rho_m - \rho_w)g=2.3 \times 10^3$ dyn/cm³.

Equation (1) may be written in terms of the generalized coordinates x, y (Fig. 3) as

$$w = A \exp(-a(x-C)) \sin(a(x-C)) + B \quad (5)$$

where C and B are additional constants defined in Fig. 3. The form of Eq. (5) provides greater flexibility than Eq. (1) in fitting observed trench profiles.

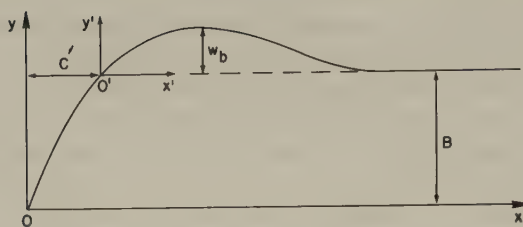


Fig. 3. Elastic trench profile and coordinates used in the least squares fitting procedure. The fitted curve does not necessarily pass through the origin O as shown here.

CALDWELL *et al.* (1976) and Agnew and Sharman (unpublished work) have shown that the form of the theoretical deflection curve is insensitive to horizontal loading forces less than 10 kbar which are therefore neglected in this analysis.

The variation of bending stress τ_{xx} (positive for tension) and shearing stress τ_{xy} within the plate are given by (FILONENKO-BORODICH, 1965)

$$\tau_{xx} = \frac{-Ez}{(1-\sigma^2)} \frac{d^2w}{dx^2} \quad (6a)$$

$$\tau_{xy} = \frac{E \left(z^2 - \frac{h^2}{4} \right)}{2(1-\sigma^2)} \frac{d^3w}{dx^3} \quad (6b)$$

where z is the perpendicular distance (positive upwards) from the neutral plane of the plate.

Using (5) in (6a) and (6b) we obtain

$$\tau_{xx} = \frac{2Aa^2}{(1-\sigma^2)} Ez \exp(-a(x-C)) \cos a(x-C) \quad (7a)$$

$$\tau_{xy} = \frac{Aa^3E}{(1-\sigma^2)} \left(z^2 - \frac{h^2}{4} \right) \exp(-a(x-C)) [\cos a(x-C) + \sin a(x-C)]. \quad (7b)$$

The stress component τ_{yy} is negligible compared to the values of τ_{xx} and τ_{xy} (FILONENKO-BORODICH, 1965).

The magnitude and directions of the principal deviatoric stresses and maximum shear stress along various planes within the plate calculated using Eqs. (7a) and (7b) are shown for a typical profile in Fig. 4.

The stresses reach large values (5–10 kbar) near the upper and lower boundaries of the plate in the region of the outer trench wall. These large values have been cited (DEBREMAECKER, 1977) as evidence against elastic plate models since they are unlikely to be sustained by lithospheric material, particularly near the upper boundary where the maximum principal stress is extensional. Figure 4 demonstrates, however, that even in the region of the outer trench wall and topographic high the plate retains a central core in which stresses remain small and which may possibly be supported elastically. This being the case, the overall deflection of the plate may be described by a theoretical curve of the form (5), even in the region of the outer trench wall. This is in contrast to the elastic-perfectly plastic case (McADOO *et al.*, 1977) in which the deflection between the trench

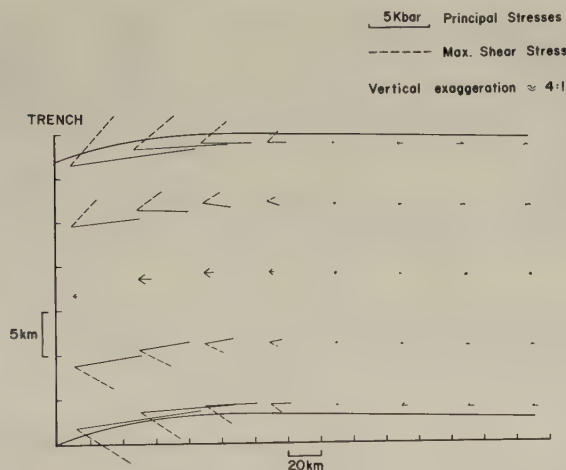


Fig. 4. Orientation and relative magnitude of the principal deviatoric stress and maximum shear stress along various planes within a bending plate. The maximum principal stress is extensional along the upper half of the plate and compressional in the lower half. Note that the stresses remain small near the neutral plane of the plate even beneath the region of the outer trench wall.

and the outer topographic high is influenced by the plastic response of the lithosphere. These two cases may be distinguished by a test described below. It is also possible that the upper part of the plate behaves elastically and that the outer rise is caused by viscous forces developed in the lower lithosphere (MELOSH, 1978). Although in this case (5) is no longer strictly valid, our estimates of the bending stress obtained by fitting it to the observed profile should not be significantly different because of the general applicability of (6a).

The existence of high angle normal faults in the outer walls of trenches (Figs. 1 and 2) and the occurrence of earthquakes within the oceanic plate seaward of trenches (FORSYTH and CHAPPLE, 1978) indicates that brittle failure also accompanies the plate deformation. The throw and dip of the faults and the variation of focal mechanisms of earthquakes at different depths within the oceanic plate (FORSYTH and CHAPPLE, 1978) are consistent with the distribution of stresses shown in Fig. 4, thus suggesting that these fracture events are directly related to the bending of the plate. In order to examine this hypothesis further, we compare the extent of faulting in the outer trench wall of different trenches with the stresses inferred from fitting the different topographic profiles to a theoretical elastic deflection curve.

4. Analysis of Data

We analyzed 20 trench bathymetry profiles obtained in digitized form from the Scripps Institution of Oceanography Geophysical Data Center. In all cases the bathymetric data were projected normal to the trench axis. The locations of the trench profiles used and original source of data are given in Fig. 5.

Table 1. Profile parameters.

Profile number	Profile name	Best fitting parameters					RMS residual for outer trench wall (km)		
		a (km ⁻¹)	A (km)	B (km)	C (km)	D (dyn cm) $\times 10^{30}$	h (km)	S (kbar)	(i) (ii)
1	Bonin Bent 2-2	0.0142	1.99	3.09	56.1	1.4 \pm 0.6	29 \pm 4	12.5 \pm 2.5	0.210 0.161
2	Bonin Japanyon 4	0.0100	2.54	2.92	61.8	5.7 \pm 2.0	46 \pm 7	12.2 \pm 1.0	0.247 0.183
3	Bonin Hunt 1-4	0.0133	1.77	3.19	58.8	1.9 \pm 0.7	32 \pm 5	10.7 \pm 1.3	0.305 0.211
4	Mariana Scan 5	0.0177	1.33	3.84	66.6	0.6 \pm 0.4	22 \pm 5	9.7 \pm 1.8	0.252 0.127
5	Aleutian Seemap 13-4	0.0117	1.69	1.57	48.5	3.1 \pm 1.0	38 \pm 5	9.3 \pm 0.7	0.212 0.119
6	Bonin Aries 7	0.0145	1.44	3.23	63.2	1.3 \pm 0.5	28 \pm 4	9.2 \pm 1.5	0.307 0.298
7	Bonin Hunt 3-2	0.0147	1.40	2.27	58.1	1.2 \pm 0.3	28 \pm 3	9.0 \pm 1.0	0.232 0.229
8	Bonin Bent 1-3	0.0159	1.29	2.99	59.7	0.9 \pm 0.6	25 \pm 5	8.8 \pm 0.8	0.201 0.202
9	Bonin Antipode 3	0.0194	1.09	2.62	58.0	0.4 \pm 0.2	19 \pm 3	8.5 \pm 1.3	0.190 0.189
10	Manila Shell Drake	0.0121	1.40	0.56	24.7	2.7 \pm 2.0	36 \pm 8	7.9 \pm 2.0	0.050 0.042
11	Japan Bent 1-1	0.0068	1.92	1.35	66.4	26.9 \pm 6.0	78 \pm 8	7.4 \pm 0.9	0.129 0.123
12	Kuril Zetes 2-1	0.0212	0.83	1.75	43.9	0.3 \pm 0.2	17 \pm 6	6.8 \pm 1.5	0.134 0.113
13	Kuril Zetes 2-6	0.0177	0.81	2.09	62.4	0.6 \pm 0.2	22 \pm 3	5.9 \pm 0.6	0.059 0.050
14	Manila Maury	0.0177	0.74	0.73	35.4	0.6 \pm 0.5	22 \pm 8	5.4 \pm 1.5	0.064 0.045
15	Middle America Iguana 4-2	0.0221	0.40	1.58	62.1	0.3 \pm 0.2	16 \pm 6	3.4 \pm 0.6	0.114 0.101
16	Middle America Iguana 2	0.0230	0.33	1.75	71.3	0.2 \pm 0.2	15 \pm 6	2.9 \pm 0.5	0.167 0.103
17	Aleutian Seemap 13-2	0.0078	2.13	1.44	44.1	15.6 \pm 7.0	65 \pm 10	9.0 \pm 2.0	0.285 0.090
18	Japan Bent 1-2	0.0076	2.06	1.00	36.2	17.3 \pm 5.0	67 \pm 7	8.6 \pm 1.0	0.131 0.043
19	Japan Hunt 1-3	0.0072	1.35	1.23	58.4	21.2 \pm 8.0	72 \pm 15	5.4 \pm 1.0	0.131 0.055
20	Tonga Oceanographer 7001	0.0221	0.56	3.99	78.9	0.3 \pm 0.2	16 \pm 5	4.7 \pm 1.5	0.328 0.159

a, A, B, C : best fitting profile parameters from Eq. (5).

D : flexural rigidity.

h : effective elastic thickness.

S : maximum bending stress.

(i): outer trench wall residual for theoretical elastic curve.

(ii): outer trench wall residual for quadratic curve.

Profiles 17-20 did not satisfy the test for elastic behavior beneath the outer trench wall and are therefore omitted from Fig. 7.

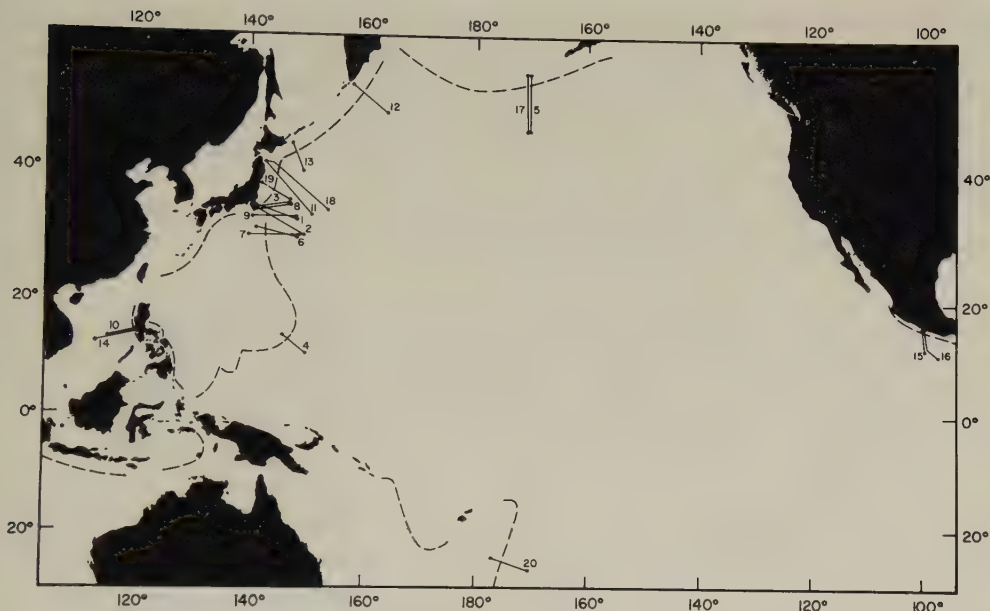


Fig. 5. Location of bathymetric profiles used in this study. Profiles 1, 3, 7, 8, 10, 11, 14, 18 and 19 were collected by the U.S. Naval Oceanographic Office; profiles 2, 4, 6, 9, 12, 13, 15 and 16 by Scripps Institution of Oceanography; and profiles 5, 17 and 20 by the National Oceanographic and Atmospheric Administration.

For each profile, the ocean floor topography seaward of the trench axis (taken as the origin O in Fig. 3) was fitted by a least squares iterative procedure to a theoretical curve of the form (5) for the bending of an elastic plate. We did not make sediment corrections at this stage for reasons discussed below. Selected bathymetric profiles and best fitting curves are shown in Fig. 6(a). The best-fitting parameters a , A , B , C for each profile were then used to estimate the inferred flexural rigidity, D , of the plate; its effective elastic thickness, h ; and the maximum apparent bending stress, S (Table 1).

In order to investigate the correlation between faulting in the outer trench wall and maximum bending stress within the subducting plate, it is necessary to construct a quantitative measure of the amount of faulting and examine how well the theoretical elastic deflection curve fits the trench profile in the vicinity of the outer trench wall. We also need to estimate the uncertainty in our estimate of the maximum bending stress.

Figure 1 shows the results of a seismic reflection survey across the Japan Trench (HILDE and RAFF, 1970). This profile is typical of others we have examined and shows that offsets in the basement beneath the outer trench wall caused by high angle faults are consistently reflected in the topography of the overlying sediment column. Furthermore, the roughness of the topography in this region is dominated by the relative vertical offsets of basement blocks. A convenient measure of the amount of faulting present in the outer trench wall is therefore the RMS deviation of seafloor topography from a smooth best-fitting curve.

We initially tried fitting for each profile the shape of the outer trench wall to a curve of the form (5), but found that this part of the profile did not sufficiently constrain the

least squares iterative procedure, thus leading to the development of instabilities. Instead, we therefore fitted the ocean floor topography between the trench axis and the distance C in Fig. 3 to a quadratic curve of the form $w=ax+b-cx^2$ where a , b and c are constants chosen directly by least squares, and used the RMS residual between the fitted curve and the actual topography as a measure of the amount of basement faulting in this region (Table 1, last column).

This quadratic curve was also used to examine how well the theoretical elastic deflection curve fitted the profiles in the region of the outer trench wall. If the subducting

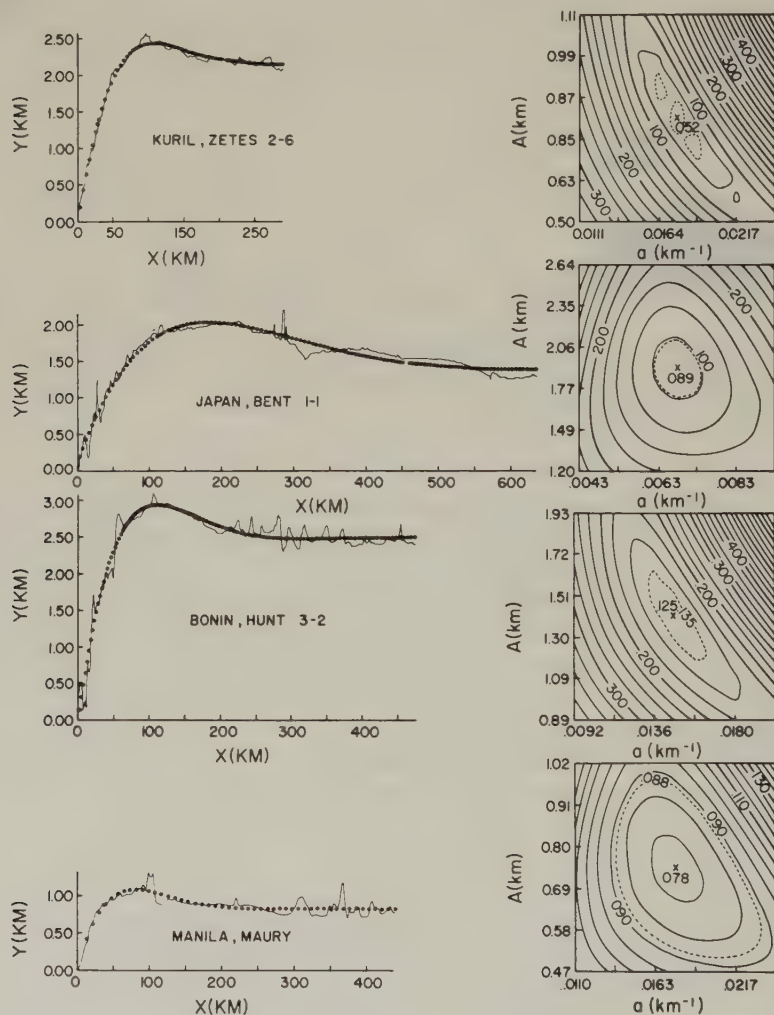


Fig. 6(a). Selected bathymetric profiles and corresponding best-fitting curves for the bending of an elastic plate. Contour maps to the right of each profile show the variation in kilometers of RMS residual differences between the fitted curve and the actual topography as parameters a and A are varied. The dashed contour has the value $[\text{RMS (minimum)} + 0.01]$ and was used to estimate the uncertainty in the value of the maximum bending stress, as discussed in the text.

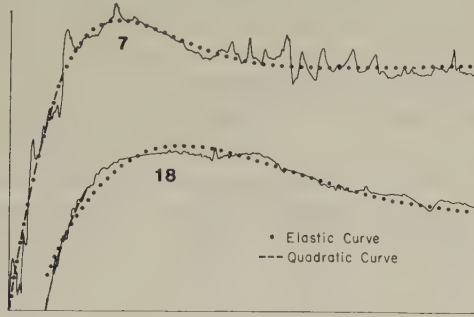


Fig. 6(b). Fitted elastic deflection and quadratic curves for profiles 7 and 18, illustrating the use of the quadratic curve to test the quality of the elastic fit along the outer trench wall. See text for details.

plate behaves elastically along its length, then the theoretical deflection curve should closely approximate the quadratic curve along the outer trench wall.

Figure 6(b) shows examples of the best-fitting elastic deflection and quadratic curves for profiles 7 and 18. For the upper profile, the two curves coincide closely along the outer trench wall and their RMS residuals are in good agreement (Table 1). In this case, we conclude that elastic deformation may be dominant even in the region of the outer trench wall. For the lower profile, on the other hand, the fitted elastic deformation curve differs significantly from the quadratic curve seaward of the trench resulting in large differences in the RMS values for the two curves in this region. Since the elastic curve fits the topography seaward of the rise equally well for the two profiles, we conclude that the lower profile reflects a possible deviation from elastic behavior in the bending plate between the outer rise and the trench axis.

As a quantitative test for elastic behavior beneath the outer trench wall, we therefore compared the RMS residual for both quadratic and theoretical elastic curves between the trench axis and distance C for each profile and only retained those profiles for which the difference in the RMS values was less than a factor of two. Out of 20 profiles examined, 16 passed this test and were used in the subsequent analysis (Table 1). For the rejected profiles, it is possible that an elastic rheology no longer describes the behavior of the plate as it enters the trench and that some other deformation mechanism, such as plastic flow (McAdoo *et al.*, 1977) is dominant. However, the fact that three out of four of the rejected profiles occur in regions where other profiles fit the elastic curve makes it more likely that these particular profiles gave spurious results.

For the acceptable profiles, maximum apparent bending stresses lie in the range 3–13 kbar (Table 1), and occur beneath the outer trench wall at a distance of $\pm h/2$ from the neutral plane of the plate. Although it is unlikely that the plate material can elastically support these large stresses, particularly in the upper part of the plate where the (deviatoric) maximum principal stress is extensional, the occurrence of normal fault earthquakes to a depth of 25 km beneath the outer trench wall of subducting plates and the existence of thrust events at depth of 45–50 km (FORSYTH and CHAPPLE, 1978) is consistent with a model of an 80 km thick lithospheric plate composed of an elastic core of approximately 30 km thickness embedded in a region in which brittle failure occurs. With the exception

of profiles seaward of the Japanese Trench, inferred elastic thicknesses lie in the range 20–40 km (Table 1), thus suggesting that these values may reflect variations in the average thickness of the elastic core within the bending plate. The maximum bending stresses derived using elastic plate theory may therefore reflect relative differences in the stresses experienced by the subducting plate. It has already been noted that the orientation of faults in the basement beneath the outer trench wall are also consistent with the pattern of stresses inferred for the bending of an elastic plate, thus suggesting that the region of extensional brittle failure may extend from depths of 25 km or so to the surface.

5. Confidence Limits for Maximum Bending Stresses

Before comparing the amount of faulting present in the outer trench wall with the inferred maximum bending stress for different profiles, it is necessary to assign confidence limits to our estimates of the bending stress in each case.

The least squares estimates of the parameters a , A , B , C , in Eq. (5) are subject to uncertainty for several reasons. In the first place the bathymetric profiles used to fit the theoretical elastic deformation curve may contain errors. Secondly, variations in sediment thickness along the profiles have not been taken into account. Since corrections for sediment unloading are more uncertain than the bathymetric data, it is preferable to use the uncorrected bathymetric profiles as the initial data base, sediment corrections for each profile then being incorporated into the estimation of confidence limits for the bending stress.

The procedure followed was to vary parameters a and A , which are related to the wavelength and amplitude, respectively, of the outer topographic bulge, in 7.5% increments about their best-fitting values for each profile. The RMS residual difference between the actual topography and the theoretical deflection curve was then calculated for each pair of values (a , A). The values of the parameters B and C were held fixed during this process. Contour maps of RMS residual differences were then constructed, expressed as functions of a and A (Fig. 6(a)). For some profiles, the contours are closely spaced and concentric about the minimum value, indicating that in these cases the best-fitting values of a and A are well constrained, since a small change in these quantities produces a significant deterioration in the quality of the fit to the observed data. In other cases, the contours are more widely spaced or elongate leading to greater uncertainty in the estimates of a and A .

To estimate the uncertainty in the maximum bending stress, we assume that the bathymetric data has an RMS error of 10 m and therefore the best fitting RMS residual is uncertain by this amount. The contour value [RMS (minimum) + 0.01] encloses a certain subset of the pairs of values (a , A) (Fig. 6(a)) that can be related to a corresponding set of values of maximum bending stress through Eq. (7a). Half the difference between the maximum and minimum values of bending stress within this set was used as a measure of the uncertainty in the maximum bending stress (Table 1). The uncertainty in our estimates of effective elastic thickness and flexural rigidity were calculated using the limiting values of a and Eqs. (3) and (4).

To correct for variations in sediment thickness, including the effect of isostatic unloading, we used available seismic profiles in the vicinity of the topographic profiles and the following densities; $\rho_{\text{water}} = 1.0 \text{ g/cm}^3$, $\rho_{\text{sediment}} = 1.6 \text{ g/cm}^3$, $\rho_{\text{mantle}} = 3.4 \text{ g/cm}^3$. For the profiles we examined, the main effect of the sediment corrections is to reduce the

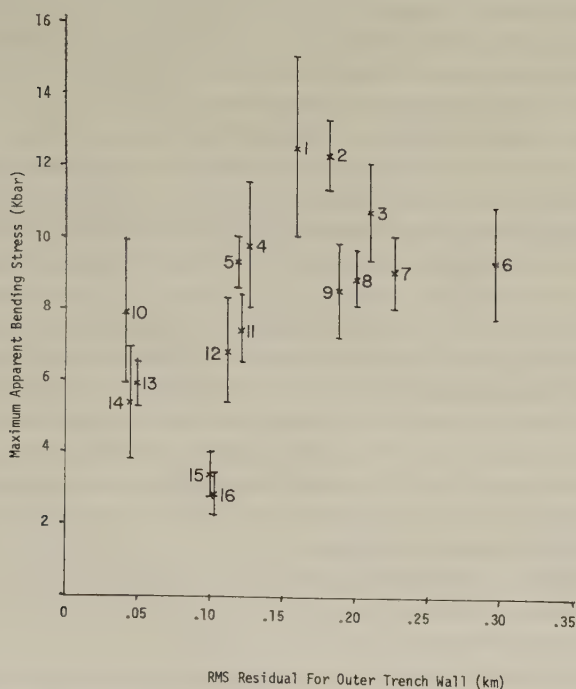


Fig. 7. Relationship of maximum apparent bending stress to the RMS residual (or degree of faulting) of the quadratic curve for the outer trench wall.

amplitude of the outer topographic high, since sediment thicknesses generally decrease seaward of the rise. These corrections lie in the range of 50–150 m and are comparable to the uncertainty in the amplitude of the outer topographic bulge associated with the possible range of values of the parameter A discussed above. Sediment corrections do not therefore invalidate our previous results although they indicate that the maximum elastic bending stresses may have been overestimated.

The final graph of RMS residuals for the outer trench wall versus maximum bending stress, including error bars, is shown in Fig. 7.

6. Discussion

Figure 7 shows that, in general for the profiles we examined, a consistent relationship exists between the amount of faulting present on the outer trench wall and the maximum elastic bending stress. Profiles with large inferred bending stresses systematically exhibit the greatest amount of faulting on the outer trench wall. This observation supports the hypothesis that these faults are a direct result of the subduction process.

Several other features revealed by Fig. 7 and Table 1 deserve comment: (1) With the exception of the profile from the Tonga-Kermadec Trench, at least one profile from each of the trenches examined fits a theoretical deflection curve of the form (5). Since Eq. (5) does not include the effect of a horizontal compressive stress, this result is in contrast to that of WATTS and TALWANI (1974), who concluded that a horizontal compressive stress

of several kbar acting on the oceanic plate was required to explain the topography and gravity anomalies seaward of the Aleutian, Kuril, Japan and Northern Bonin Trenches. The discrepancy may be explained if the downgoing plate is acted upon by a vertical stress landward of the trench axis, rather than at the trench axis, as WATTS and TALWANI (1974) supposed. However, Table 1 does show that inferred bending stresses within the oceanic plate are generally larger seaward of the Bonin Trench than for the other trenches examined. (2) The flexural rigidity and elastic thickness inferred for the plate seaward of the Japan Trench are significantly larger than in the case of the other trenches. These larger values arise because of the greater wavelength of the outer topographic high in this region (Fig. 6(a)). The reason why the oceanic plate seaward of the Japanese arc should apparently behave differently from the region seaward of the adjacent Kuril and Bonin arcs is not yet clear and is being investigated further. (3) Inferred bending stresses within the plate seaward of the Middle America Trench (profiles 15 and 16) are smaller than expected from the amount of faulting in the outer trench wall and the trend set by the other profiles (Fig. 7). This may in part result from the neglect of age corrections for these profiles. Lithosphere being subducted into the Middle America Trench is young (< 50 my; PITMAN *et al.*, 1974) and therefore part of the change in ocean floor depth along these profiles is due to cooling of the lithosphere (SCLATER *et al.*, 1971). Since the seafloor becomes progressively older towards the trench axis, corrections for age would effectively increase the amplitude of the outer rise, leading to larger inferred bending stresses within the downgoing plate than those actually obtained.

The elastic plate model provides a reasonable explanation for the existence beneath island arcs at depths greater than 70 km or so of a double-planed Wadati-Benioff Zone in which earthquake focal mechanisms on the upper plane are compressional whereas those on the lower plane are extensional (HASEGAWA and TAKAGI, 1978; ENGBAHL and SCHOLZ, 1978), in contrast to the case beneath the outer trench wall (FORSYTH and CHAPPLE, 1978). A possible explanation is that elastic energy is stored in the core of the plate as it bends into the trench and is released as the plate unbends at greater depths (ENGBAHL and SCHOLZ, 1978). In order for the unbending to take place, the applied stresses that caused the bending in the first place must be absent or greatly diminished. This in turn suggests that the bending stresses within the subducting plate are caused by interaction with the overriding plate at shallow depth, or by the dynamics of flow within the lower lithosphere as suggested by MELOSH (1978).

The tectonic processes and structural features developed due to the interaction of the two plates at the trench axis and along the upper portion of the subduction zone are probably greatly influenced by the faulted, irregular upper surface of the subducting plate. Where the faults strike in a direction sub-parallel to the trench axis, as in the Japan Trench, offsets in the trench axis are found where the faults intersect the base of the shoreward trench slope (HONZA, 1978). Abrupt changes in depth along the axis of a trench can also be explained by the faults on the subducting plate intersecting with the trench axis. A profile of the Japan Trench axis (SUGIMURA and UYEDA, 1973) reveals several abrupt depth changes, many of which are of about the same magnitude as the vertical displacement on the faults. The horst and graben relief may not always be obvious along a trench axis due to turbidite sedimentation and slumping off the shoreward slope. However, where these fault blocks are sub-parallel to the trench they can be expected to restrict lateral sediment transport along a trench axis and cause the ponding of sediments at varying depths that has been observed along many trench axes.

Along the 20 km length of the North Mariana Trench crossed by the profiles in Fig. 2 the trench axis is offset abruptly while the strike of the faults on subducting plate is not. At this location the faults are essentially parallel to the trench axis and changes of trend along the axis are apparently not directly related to the intersection of the fault blocks with the shoreward slope. A more gentle lower slope on the shoreward trench wall south of profile 5 is interpreted as due to slumping or possibly accretion of oceanic sediments to the base of the shoreward slope. A corresponding eastward offset of the trench axis south of profile 5, with more of fault block A being covered, indicates that the slumping or accretion has resulted in a migration of the trench axis to the east relative to that segment to the north.

The preliminary result of *Glomar Challenger* drilling on the shoreward flank of the Japan Trench during DSDP legs 56 and 57 (SCIENTIFIC PARTY, 1978 a, b) and on the shoreward slope of the Mariana Trench during leg 60 (Donald Hussong, personal communication) indicates that accretionary structures composed of ocean basin sediments were not encountered. These results provide serious limitations on the general application of the recently advanced accretionary models of KARIG (1974), KARIG and SHARMAN (1975), SEELY *et al.* (1974) and others. If ocean basin sediments do not make up a significant portion of the structures beneath the continental shelf and slope between the islands and trench axes of the Japan and Mariana arcs then it must be assumed that they have been carried down the subduction zone. Horst and graben fault structures are well developed in the subducting plate in both of these cases. We suggest that these structures may be a major determining factor in accretionary wedge development. Where they are well developed a large portion of the oceanic sediment may be compacted into the grabens of the subducting plate and carried down the subduction zone. Where they are absent or poorly developed a correspondingly greater portion of the oceanic sediment may be scraped off the subducting plate and directly added to the overriding plate resulting in development of a more extensive accretionary prism. The relationship of faults on the subducting plate to the subduction process is being examined in greater detail by one of the authors (Hilde, in preparation).

In conclusion, we find that the occurrence and magnitude of faulting in the subducting plate in the region of the outer topographic high and seaward trench slope can be used to derive information about the distribution and nature of stresses within the plate. The amount of faulting is directly related to the amount of bending stress. The direction and magnitude of the principal stresses within the subducting plate are consistent with the bending model of a thin elastic plate as applied to a central core 20 to 40 km thick with brittle failure of the upper portion of the plate due to tensional stress, and compressional stress in the lower portion of the plate. We suggest that bending of the plate is due to stress developed at shallow depths and that the faulting produced by the bending has a major influence on the subduction and island arc development processes.

We are grateful to Dr. D. Hussong for providing the R/V *Kana Keoki* Mariana Trench profiles and to Mr. Stuart Smith for providing the digitized bathymetry profiles. Illustrations were drafted by Jay B. Carlton.

REFERENCES

- BOWIN, C.O., A.J. NALWALK, and J.B. HERSEY, Serpentinized peridotite from the north wall of the Puerto Rico Trench, *Geol. Soc. Am. Bull.*, **77**, 257-270, 1966.

- BRACEY, D.R. and J.E. ANDREWS, West Caroline Ridge: Relic Island Arc? *Mar. Geophys. Res.*, **2**, 111–125, 1974.
- CALDWELL, J.C., W.F. HAXBY, D.E. KARIG, and D.L. TURCOTTE, On the applicability of a universal elastic trench profile, *Earth Planet. Sci. Lett.*, **31**, 239–246, 1976.
- COULBOURN, W.T., Tectonics and sediments of the Peru-Chile Trench and Continental margin at the Arica bight, Ph. D. Dissertation, University of Hawaii, 1977.
- DEBREMAECKER, J.C., Is the oceanic lithosphere elastic or viscous? *J. Geophys. Res.*, **82**, 2001–2004, 1977.
- ENGDAHL, E.R. and C.H. SCHOLZ, Double-planned Benioff Zones beneath island arcs: An unbending of the lithosphere (abstr.), Int. Geodyn. Conf., March, Tokyo, p. 22, 1978.
- FILONENKO-BORODICH, M., *Theory of Elasticity*, Chap. 10, Dover Publications, New York, 1965.
- FISHER, R.L., Middle America Trench: Topography and structure, *Geol. Soc. Am. Bull.*, **72**, 703–720, 1961.
- FISHER, R.L., Preliminary results of expeditions Monsoon and Lusiad, 1960–1963, Scripps Inst. of Ocean. Ref. 64-19, 1964.
- FISHER, R.L., Pacific-type continental margins, in *Continental Margins*, edited by C. Burk and C. Drake, pp. 25–41, Springer-Verlag, New York, 1974.
- FISHER, R.L. and C.G. ENGEL, Ultramafic and basaltic rocks dredged from the nearshore flank of the Tonga Trench, *Geol. Soc. Am. Bull.*, **80**, 1373–1378, 1969.
- FISHER, R.L. and H.H. HESS, Trenches, in *The Sea*, Vol. 3, edited by M.N. Hill, pp. 411–436, Interscience, New York, 1963.
- FISHER, R.L. and R.W. RAITT, Topography and Structure of the Peru-Chile Trench, *Deep-Sea Res.*, **9**, 423–443, 1962.
- FORSYTH, D. and W. CHAPPLE, A mechanical model of the Oceanic lithosphere consistent with seismological constraints (abstr.), *EOS, Trans. Am. Geophys. Union*, **59**, 372, 1978.
- HAMILTON, W., Subduction in the Indonesian region, in *M. Ewing Series 1*, edited by M. Talwani and W.G. Pitman, III, pp. 15–31, Am. Geophys. Union, Washington, D.C., 1977.
- HANKS, T.C., The Kuril Trench-Hokkaido Rise system: Large shallow earthquakes and simple models of deformation, *Geophys. J. R. Astr. Soc.*, **23**, 173–189, 1971.
- HASEGAWA, A.N. and A. TAKAGI, Double-planned deep seismic zone beneath the North Eastern Japan Arc (abstr.), pp. 44–45, Int. Geodyn. Conf., March, Tokyo, 1978.
- HAYES, E.E., Ageophysical investigation of the Peru-Chile Trench, *Mar. Geol.*, **4**, 309–351, 1966.
- HAYES, D.E. and M. EWING, Pacific boundary structure, in *The Sea*, Vol. 4, edited by A.E. Maxwell, Part 2, pp. 29–72, John Wiley & Sons, Inc. New York, 1970.
- HILDE, T.W.C. and A.D. RAFF, Evidence of oceanic crust beneath the shoreward slope of the Japan trench from magnetic and seismic reflection data (abstr.), *EOS, Trans. Am. Geophys. Union*, **51**, 330, 1970.
- HILDE, T.W.C., N. ISEZAKI, and J.M. WAGEMAN, Mesozoic sea-floor spreading in the North Pacific, *Geophys. Monogr. No. 19*, pp. 205–226, Am. Geophys. Union, Washington, D.C., 1976.
- HILDE, T.W.C., J.H. WAGEMAN, and W.T. HAMMOND, The structure of Tosa terrace and Nankai trough off southeastern Japan, *Deep-Sea Res.*, **16**, 67–76, 1969.
- HONZA, E., Basic framework of the island arc systems in the NW Pacific margin (abstr.), Int. Geodyn. Conf., March, Tokyo, p. 54, 1978.
- HUSSONG, D.M., Tectonic implications of the crustal structure of the Mariana Island arc system near 18°N Latitude (abstr.), Int. Geodyn. Conf., March, Tokyo, pp. 60–61, 1978.
- ISACKS, B. and P. MOLNAR, Distribution of stresses in the descending lithosphere from a global survey of focal mechanism solutions of mantle earthquakes, *Rev. Geophys. Space Phys.*, **9**, 103–174, 1971.
- ISACKS, B., J. OLIVER, and L.R. SYKES, Seismology and the new global tectonics, *J. Geophys. Res.*, **73**, 5855–5899, 1968.
- ISACKS, B., L.R. SYKES, and J. OLIVER, Focal mechanisms of deep and shallow earthquakes in the Tonga-Kermadec region and the tectonics of island arcs, *Geol. Soc. Am. Bull.*, **80**, 1443–1470, 1969.
- KARIG, D.E., Evolution of arc systems in the Western Pacific, *Annu. Rev. Earth Planet. Sci.*, **2**, 51–75, 1974.
- KARIG, D.E. and G.F. SHARMAN, III, Subduction and accretion in trenches, *Geol. Soc. Am. Bull.*, **86**, 377–389, 1975.
- LUDWIG, W.J., N. DEN, and S. MURAUCHI, Seismic reflection measurements of Southwest Japan Margin, *J. Geophys. Res.*, **78**, 2508–2516, 1973.
- LUDWIG, W.J., D.E. HAYES, and J.I. EWING, 1967, The Manila Trench and West Luzon Trough. I. Bathymetry and sediment distribution, *Deep-Sea Res.*, **14**, 533–544, 1967.
- LUDWIG, W.J., J.I. EWING, S. MURAUCHI, N. DEN, S. ASANO, H. HOTTA, M. HAYAKAWA, T. ASANUMA, K. ICHIKAWA, and I. NAGURCHI, Sediments and structure of the Japan Trench, *J. Geophys. Res.*, **71**, 2121–2137, 1966.
- McADOO, D.C., D.L. TURCOTTE, and J.G. CALDWELL, The analysis of an elastic-perfectly plastic lithosphere entering a trench under both transverse and horizontal bending (abstr.), *EOS, Trans. Am. Geophys. Union*, **58**, 498, 1977.

- MELOSH, H.J., Dynamic support of the outer rise, *Geophys. Res. Lett.*, **5**, 321–324, 1978.
- PARSONS, B. and P. MOLNAR, The origin of outer topographic rises associated with trenches, *Geophys. J. R. Astr. Soc.*, **45**, 707–712, 1976.
- PITMAN, W.C., III, R.L. LARSON, and E.M. HERRON, Age of the ocean basins determined from magnetic anomaly lineations, G.S.A. Map and Chart Series, MC-6, 1974.
- RAITT, R.W., R.L. FISHER, and R.G. MASON, Tonga Trench, in *Crust of the Earth*, GSA Special Paper, Vol. 62, pp. 237–254, 1955.
- SCHOLL, D.W., M.S. MARLOW, and A.K. COOPER, Sediment subduction and offscraping at Pacific Margins, in *M. Ewing Series 1*, edited by M. Talwani and W.G. Pitman, III, pp. 199–210, Am. Geophys. Union, Washington, D.C., 1977.
- SCIENTIFIC PARTY, Transects begun: Near the Japan Trench, Report on DSDP Glomar Challenger Leg 56, *Geotimes*, March, 22–26, 1978a.
- SCIENTIFIC PARTY, Japan Trench transected, Report on DSDP Glomar Challenger Leg 57, *Geotimes*, April, 16–21, 1978b.
- SCLATER, J.G., R.N. ANDERSON, and M.L. BELL, The elevation of ridges and the evolution of the Central eastern Pacific, *J. Geophys. Res.*, **76**, 7888–7915, 1971.
- SEELY, D., P. VAIL, and G. WALTON, Trench slope model, in *Continental Margins*, edited by C. Burk and C. Drake, pp. 249–261, Springer-Verlag, New York, 1974.
- STAUDER, W., Tensional character of earthquake foci beneath the Aleutian trench with relation to sea-floor spreading, *J. Geophys. Res.*, **73**, 7693–7702, 1968.
- SUGIMURA, A. and S. UYEDA, Island Arcs: Japan and Its Environs, p. 247, Elsevier, Amsterdam, 1973.
- VON HUENE, R., Structure of the continental margin and tectonism at the eastern Aleutian trench, *Geol. Soc. Am. Bull.*, **83**, 3613–3626, 1972.
- WAGEMAN, J.M., T.W.C. HILDE, and K.O. EMERY, Structural framework of East China Sea and Yellow Sea, *Am. Assoc. Pet. Geol. Bull.*, **54**, 1611–1643, 1970.
- WATTS, A.B. and M. TALWANI, Gravity anomalies seaward of deep-sea trenches and their tectonic implications, *Geophys. J.R. Astr. Soc.*, **26**, 57–90, 1974.

MOTION OF THE PACIFIC PLATE AND FORMATION OF MARGINAL BASINS: ASYMMETRIC FLOW INDUCTION

R.C. BOSTROM

Geophysics AK 50, University of Washington, Seattle, Washington, U.S.A.

(Received May 23, 1978; Revised October 9, 1978)

We have examined agencies inducing flow in the sub-Pacific mantle. The capable agencies are buoyancy forces (causing convection), and passage of the tidal bulge. Bulge passage induces rotational flow dimensionally identical to that induced by buoyancy, and interacting with it. The stress imposed by bulge passage is additive across the width of the sub-Pacific flow cell, in the fashion that the buoyancy stress is additive in thickness. Each stress builds thus to values in excess of 10^8 dyn/cm², overcoming the flow resistance provided by mantle viscosity. The tidal flow contribution favors the development of the west limb of convection cells, because these represent rotational flow in the tidal direction. East limbs are inhibited.

Under these forces the Pacific plate has developed as the cool, rigid surface of mantle convection surfacing in the eastern Pacific, and foundering at the western margin. The west, co-tidal limb of the East Pacific Rise now extends clear across the Pacific. The counter-tidal east limb is dwindling through its replacement by the extending west limb of the Atlantic spreading center, bearing the Americas plates.

The unbroken line of gravity highs at the western Pacific margin marks excess material accumulating where the west limb of the East Pacific Rise encounters the less mobile Asian continental mass. Material added to the asthenosphere causes disruption of the Asia margin, secondary sea-floor spreading, and the formation of arc-bounded basins. At the termination of the east, counter-tidal limb (overlain by the Cocos and Nazca plates) this process is not operative. Marginal basins, if they form, are destroyed along the Andean orogenic front by the westward-advancing Americas plates.

1. *The Problem*

The Pacific lithosphere plate, 7,000 km wide but only one hundredth as thick, seems to move intact towards eastern Asia and Australasia. What causes this motion?

The only agency which seems capable of thus rafting the plate without deformation is convection in the mantle. Observation shows that convection is in fact associated with the motion of the Pacific plate. Material is seen to reach surface at the crest of the East Pacific Rise, and to return to the planetary interior in zones of subduction at the west Pacific margin.

However buoyancy convection possesses a cell structure which seems to preclude the development of a cell spanning the width of the Pacific Ocean; even if convection embraces the entire mantle, the pattern should be that of smaller cells, breaking up the Pacific plate into several. Further difficulties exist. Theoretical and numerical models of convection (see for instance MCKENZIE *et al.*, 1974) indicate that under unforced thermal convection upflow limbs should be the site of positive gravity anomalies, downflow limbs of negative. The gravity geoid (Fig. 1) shows that the observed anomalies in no way

agree with the models. The Pacific-Antarctic and East Pacific Rise is marked randomly by highs and by lows. At best a secondary relationship (SCLATER *et al.*, 1975) can be distinguished between gravity anomalies and the world rift system. On the contrary, the subduction zones marking downflow at the west Pacific margin are the site uniquely of gravity highs, the opposite of the relation to be expected under thermal convection. Deep seismicity, marking downflow, occurs world-wide only in the context of gravity highs.

To obviate such difficulties it has been suggested that the lithosphere plates move on small-scale convection in the asthenosphere. As has however been pointed out, such models cannot account for the net flow of material. The drift of plates represents uni-directional material flow at variance with that imparted by a random thermal process.

With respect to buoyancy forces, it has been pointed out (FORSYTH and UYEDA, 1975) that the forces acting on the down-going slab are greater than any others. It has been suggested that cooled, dense, foundering lithosphere (ELSASSER, 1966) draws plates after it. McKENZIE (1969) however has pointed out that not all plates are attached to sinking slabs. It seems implausible that such a frail object as the Pacific plate can be pulled or pushed from either end without disruption.

The basic problem is one of energy supply and the stress required to overcome resistance of the mantle to flow. It has frequently been concluded (see for example McKENZIE, 1972) that thermal convection, only, can supply energy sufficient to drive plates. Nevertheless, two non-thermal energy sources are of sufficient magnitude. These are: the creation of buoyancy by differentiation of mantle material (hence the release of gravitational energy); and the dissipation of Earth rotational energy by tides. Of these, differentiation buoyancy has earlier been identified (RINGWOOD, 1973). It may well play a part in driving convection, but explains no more effectively than does thermal buoyancy the geometry of plate motion. Both types of buoyancy create forces having limited lateral extent, resulting in the well-recognized limitations on cell size.

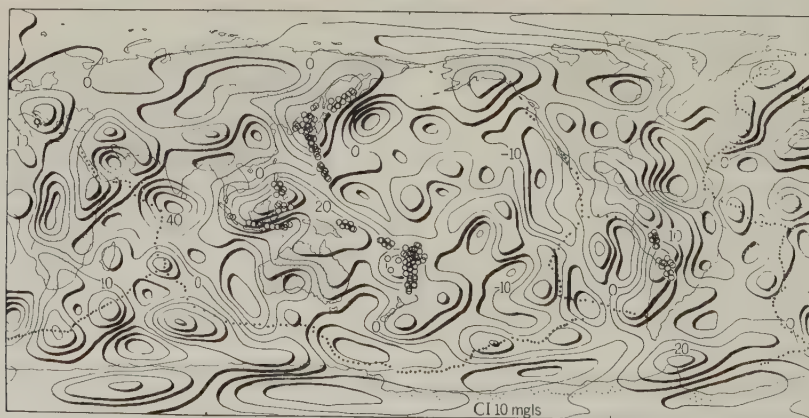


Fig. 1. Gravity geoid, after GAPOSCHKIN (1974), and incidence of deep ($h > 300$ km) hypocenters, recorded by WWSSN 1961–1967 (BARAZANGI and DORMAN, 1969). Reference ellipsoid, $f=1/299.67$; terms to 18th degree and order. Small black circles indicate axis of sea floor spreading; circles do not represent individual epicenters. To eliminate uncertain events, magnitude of deep hypocenters is not less than 5. Contour interval, 10 mGal.

Accordingly, in what follows we have examined the effect of tidal bulge passage on mantle in convection, and this specifically in regard to the Pacific plate. A companion paper (BOSTROM, 1978a) considers the flow processes responsible for the orogenesis at the eastern Pacific margin.

2. *Observed Pacific Plate Motion*

The seismicity of the Pacific region played a formative part in the concept of plate tectonics. MCKENZIE and PARKER (1967) noted the magnetic pattern and seismic characteristics of the sea floor spreading and consumption centers of the North Pacific, and concluded that "these observations are explained if the sea floor spreads as a rigid plate and interacts with other plates in seismically active regions which also show recent tectonic activity." The westward or northwestward motion of the Pacific plate apparent at that time from focal mechanism studies has been confirmed by later observations. The latter furthermore have been interpreted to suggest that the lithosphere at the west Pacific margin plunges into the asthenosphere and lower mantle as a slab (OLIVER and ISACKS, 1967; ISACKS *et al.*, 1969).

One line of evidence is now held as to the motion of the Pacific plate relative to the mantle (rather than to other plates). This is the trace of mantle magma sources or hot spots on the lithosphere plate (WILSON, 1965, 1973). MINSTER *et al.* (1974) believe that mantle sources may be immobile relative to each other.

The combined evidence suggests that the Pacific lithosphere plate forms at a rate of about 10 cm per year at the crest of the East Pacific Rise; moves across the Pacific Ocean where it encroaches on the eastern flank of Asia and Australasia in a belt of convergence; and reenters the planetary interior in subduction zones extending from the Kermadec region, north of New Zealand, to Kamchatka.

Deep seismicity ($h > 300$ km) is confined to low and intermediate latitudes, suggesting that deep subduction is similarly restricted. As KAULA (1970) has pointed out, the gravity relationship (Fig. 1) displays that a mass deficiency drawing material towards the west Pacific margin does not exist; material is crowded into the subduction region, where it is reassimilated in the mantle, by an external force system.

3. *Vorticity Induction under Tidal Bulge Passage*

A connection has been sought for some time (DARWIN, 1879; EDDINGTON, 1923; SHAW, 1970; JOLY, 1926; JEFFREYS, 1926; MOORE, 1973; DEHLINGER, 1971; DANES, 1973; JORDAN, 1974) between geotectonics and the action of tides. The connection has been obscured because usually the stress imposed by the weak, secondary retarding torque has been taken to be the only tide stress inducing cumulative deformation (DARWIN, 1879; JEFFREYS, 1929; JORDAN, 1974). The stresses caused by tidal bulge formation are 10^8 times more intense, but have been thought to entirely reverse through time, thus not result in cumulative deformation.

However the tidal bulge does not form in place, but by the passage of a wave around the Earth, namely by the addition of simple shear always in one direction. Inevitably, the real Earth is not perfectly elastic. In consequence the tidal wave is not irrotational as commonly assumed, and imposes cumulative rotational strain or vorticity. The mechanism is as follows:

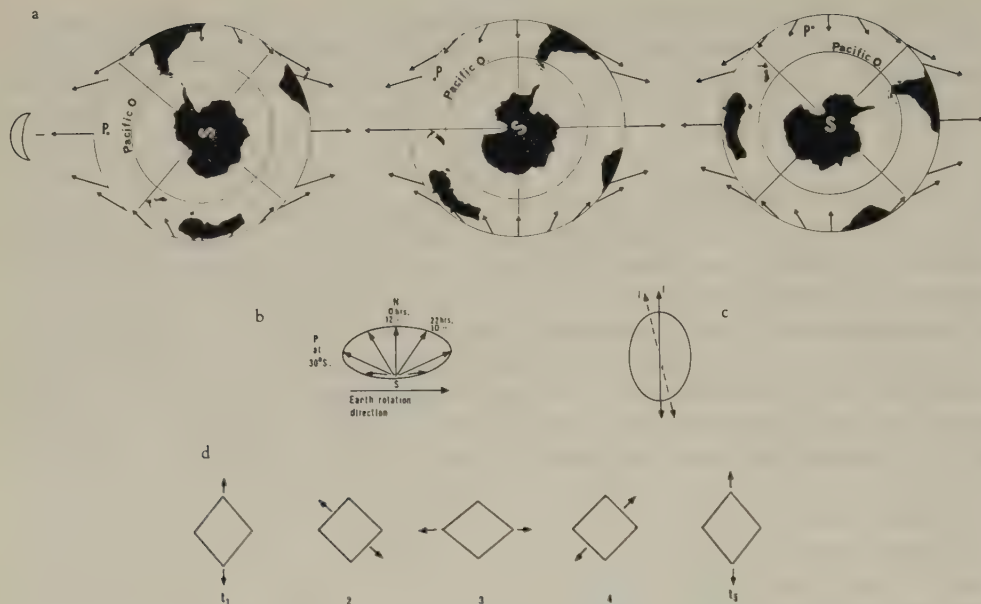


Fig. 2. (a) Tide-generating force in Equator plane. At a fixed point on Earth the direction rotates without reversal. (b) Displacement of particle at point P (point of arrow), in horizontal plane, at 30°S. Particle is displaced a few centimeters twice daily around ellipse, always in same (counterclockwise) direction without reversal. (c) Instantaneous stress axes i constantly lead axes of finite strain ellipsoid, f . (d) Resulting distortion of elastic rhomboidal element. In response to rotating stress axes, strain progression is via incremental simple shears. Distortion is non-cumulative. Material consists of predominant, perfectly elastic fraction and commingled minor fraction imperfectly elastic, see Fig. 3.

The bulge advances as a result of the Earth rotating in the tide-raising potential field of itself plus the Moon (Fig. 2). At a fixed point in the Earth, the tide-raising force, hence the imposed strain field, does not oscillate back and forth; it rotates, always in one direction. The elastic fraction of mantle material does not experience cumulative strain (Fig. 2(d)).

Intermingled with the elastic fraction is the anelastic fraction. In consequence of its presence (Fig. 3), the observed tidal bulge slightly lags in time the overhead passage of the Moon or Sun. The phase lag describes the anelastic bulge. The anelastic bulge is the bulge which would remain if tidal forces were instantaneously withdrawn. Its parameters are the difference in magnitude and direction of the principal axes between those of the observed and the equilibrium or elastic bulge.

The simple shear (pure shear plus rotation, cf. LOVE, 1944) in the elastic portion of the material (representing almost all of the observed displacement of a few tens of centimeters under the bodily tides) incorporates a rotation amounting to $\tan^{-1}(\epsilon_1 - \epsilon_2)$ where ϵ is the strain, i.e. about 2.9×10^{-6} degrees. The rotation embodied in the anelastic portion is even more minute; but is cumulative, rather than self-cancelling through time.

The anelastic, bodily tidal phase displacement in the real Earth is difficult to observe, due to the gross disturbing effect of the water tides. In the case of M_2 , a large, unknown part of the observed phase lag represents elastic deformation resulting from water dis-

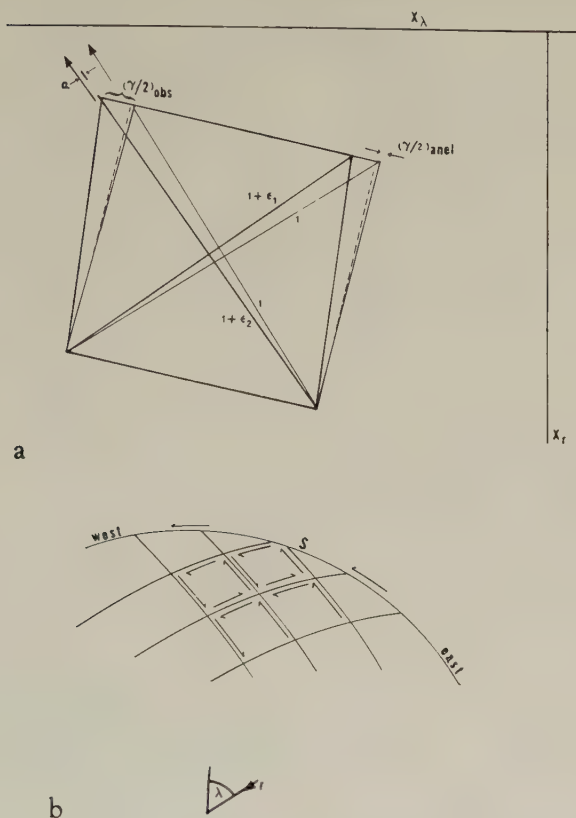


Fig. 3. (a) Distortion of imperfectly elastic volume element. Sides of rhombus rotate through small angle $(\gamma/2)_{\text{obs}} = 1/2 (\epsilon_1 - \epsilon_2) \approx 5 \times 10^{-8}$ rad. Stress axes rotate in counterclockwise direction. The direction of principal strain axes lags overhead position of Moon and Sun by the small angle $\alpha \approx 0.5^\circ$. $(\gamma/2)_{\text{anel}}$, the anelastic rotation of particle lines in the material (dash line), is small fraction of $(\gamma/2)_{\text{obs}}$; but is cumulative. In terms of the observed magnitude of ϵ_1 , ϵ_2 and phase lag α , $(\dot{\gamma})_{\text{anel}} \approx 2.5 \times 10^{-8}$ rad/year, entailing westward displacement of the surface relative to base of mantle of 7.3 cm/year. (b) Deformation mode of continuous medium under rotational strain $(\gamma)_{\text{anel}}$. Volume elements within surface S rotate as shown against the viscous resistance of the mantle. The cumulative deformation represents rotational flow (cf. LAMB, 1932) or vorticity, $\zeta = (\partial u_\lambda / \partial x_r - \partial u_r / \partial x_\lambda)$ where u is velocity. Circulation is in direction shown (counterclockwise) under bulge passage, and in the west limb of convection cells.

Table 1. Phase of diurnal solid-Earth tide (DUCARME and MELCHIOR, 1977).

Station	Location						Phase of O_1 (α_{01})	Mean square error
	Latitude			Longitude				
Brussels-Uccle	50	48	N	04	22	E	-0.20°	0.34
Helwan-Cairo	29	51	N	31	20	E	-2.05	0.75
New Delhi	28	38	N	77	11	E	-0.61	0.69
Bangkok-Latprao	13	48	N	100	36	E	-1.50	0.54
Kuala Lumpur	3	07	N	101	39	E	-13.86	1.22
Hong Kong	22	18	N	114	10	E	-4.61	0.83
Baguio	16	24	N	120	34	E	-7.40	0.77
Bandung	6	54	S	107	38	E	+11.04	1.63
Port Moresby	9	25	S	147	09	E	+0.03	0.81
Canberra	35	19	S	149	00	E	-0.96	0.61
Perth	31	59	S	116	13	E	+2.54	0.35
Hobart	42	55	S	149	19	E	-2.25	0.25
Lauder	45	02	S	169	41	E	-1.54	0.46
Suva-Vunikawai	18	03	S	178	28	E	+2.39	1.19

—, phase lag; +, phase lead. The above observations were made using gravimeters calibrated at the base station (Brussels) for not less than 4 months.

placement in the marine tides. MELCHIOR (1974) has pointed out that the remaining, anelastic portion of α observed may be measured in terms of the phase displacement of the bodily diurnal tide O_1 . In respect to O_1 , water displacement is small. The gravimetric phase lag, which in western Europe is -0.2° to -0.4° , is a fraction of the phase lag of the actual bulge. A global profile of O_1 is now partly complete (DUCARME and MELCHIOR, 1977) (Table 1). It is already apparent that α_{grav} is small, between -0.2° and -0.5° in stable regions; but that this angle is large, ranging from -14° to $+23^\circ$ in actively orogenic regions, notably the west Pacific margin. Its variation is inexplicable in terms of water displacement.

The imposed cumulative rotational strain represents the induction of rotational flow or vorticity of the form shown in Fig. 3(b). The generation of vorticity by a "collapsing deformed surface" has already been demonstrated by McKENZIE (1968, his Eq. (3.10)). In the present case the collapsing surface is represented by the westward-sweeping tidal bulge. The state of present information therefore is that the observed anelastic phase lag is sufficient, in itself, to account for the greater part of the observed motion of the Pacific plate.

4. Convection under Buoyancy and Bulge Passage

Vorticity likewise is induced by buoyancy, resulting in convection if certain conditions are met. The driving force in buoyancy convection and the forces opposing it are represented by the flow equation

$$\bar{g}\rho\phi(T-T_0)=\eta\nabla^2\bar{u}-\nabla P \quad (1)$$

in which ρ is the density, ϕ the coefficient of thermal expansion, T , T_0 the temperature at different locations, η the dynamic viscosity, \bar{u} the velocity and P pressure (cf. McKENZIE *et al.*, 1974, their Eq. (10)).

In comparison,

$$\nabla\tau_a+\rho(\bar{u}\cdot\nabla)\bar{u}=\eta\nabla^2\bar{u}-\nabla P \quad (2)$$

describes the forces driving and opposing flow induced by tidal bulge passage. In (2) the buoyancy stress is replaced by

$$\tau_\alpha = \tau_{\text{equil}} \tan \alpha,$$

in which the first R.H. term represents the equilibrium (symmetric) stresses in bulge formation. The magnitude of τ_α accordingly is a few tens of dyn/cm², based on the value 0.2° of the lag angle α and the value 10⁴ dyn/cm² (TAKEUCHI, 1951) of the stress differences in bulge formation.

In respect to both (1) and (2), taking the curl of both sides eliminates P ; but vorticity remains. The reason in the case of (2) is that shears are present acting always in the same sense, as the bulge stress axes constantly lead those of the finite strain ellipsoid. In both cases, the flow represents the continual induction of rotational flow and its dissipation under viscous friction.

It is not possible to solve the Rayleigh equations of convection for the real Earth due to the unknown relationship between T , P and η , far less to reach simultaneous solutions of (1) and (2). However it is possible to discern the contribution of each to the flow. The distribution of the torques due to buoyancy and to bulge passage is compared in Fig. 4. The usual means of solution of the Rayleigh equations of convection (by exchange of variables) obscures the origin of the large stresses generated in thermal convection. The primary stress between volume elements

$$\tau_{\text{buoy}} = \Delta T \phi \rho \bar{g}$$

is minute. If for instance the lateral thermal gradient in the mantle were as great as

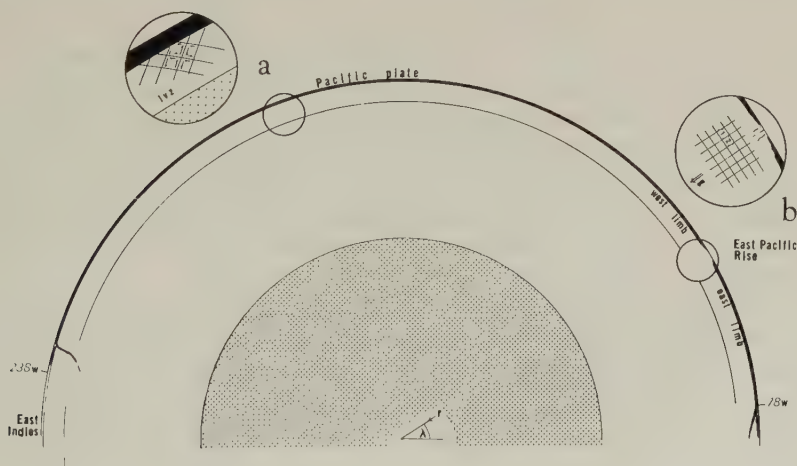


Fig. 4. Comparison of flow under bulge passage and flow under thermal buoyancy: Buoyancy torques (b) represent difference in gravitational attraction on neighboring volume elements 1, 2, etc., hence act only where there is present a horizontal gradient in the density. Primary stress acts only in the vertical. For Rayleigh numbers specified by mantle viscosity and thermal gradient, Pacific plate would be underlain by multiple flow cells, breaking it up. In contrast, flow under bulge passage (a) is induced by torques acting uniformly, at all points clear across Pacific. The flow induced by bulge passage is of mode identical to that representing the west limb of convection cells; and opposite to that in east limbs. Under either or both forcings stems, stresses sum to values $> 10^8$ dyn/cm², according with orogenesis and seismicity of west Pacific margin.

100°C/500 km, $\rho=3.5$ g/cm³ and $\phi=2 \times 10^{-5}/^\circ\text{C}$, τ_{buoy} is only 1.4×10^{-7} dyn/cm². The large stresses in buoyancy convection arise because of its organized, cellular form. Once flow commences, the buoyancy of volume elements forming a cell is cooperatively through stress transmission.

For the same reason the velocity in convection varies (TOZER, 1967) as $1/3 \kappa/d R^{1/2}$ (κ thermal diffusivity), where the Rayleigh number R is a function of the fourth power of the layer thickness, d . Stress in a layer d thick of material having a viscosity ν , attains at its maximum (KNOPOFF, 1964) the value

$$\tau_{\text{max}} = (\pi/\sqrt{2}) (\rho \nu u_{\text{max}}/d).$$

Typically, for whole-mantle convection, $\nu=10^{22}$ P, u_{max} as indicated by plate motion 8 cm/year, $\rho=4.0$ g/cm³. $d=2.9 \times 10^8$ cm, τ_{max} is 1.3×10^8 dyn/cm².

In the case of the tidal torques, Eq. (2), identical conditions apply. Under flow, the stress acting at a point beneath the Pacific plate is additive to that developed at similar points across the whole width of the plate, which acts as a stress transmitter in respect to the highly coherent bulge stress. The horizontal limb in the case of tidal vorticity induction is the analog of the vertical limb in buoyancy convection. The buoyancy force acts only where there is present a horizontal gradient in the density, the physical reason why it is difficult to model cells having the width of the Pacific Ocean, one third the circumference of the Earth. However tidal vorticity induction acts ubiquitously and in phase across this great distance. Based on the plate width, the stress thus developed assuming that the anelastic phase lag α is 0.2° is (plate width) times τ_α , namely several times 10^8 dyn/cm², comparable with or greater than the stress developed in buoyancy convection. The direction of the flow under vorticity induction, representing the tidal contribution to the convection (Fig. 5), is that of the observed motion of the Pacific plate.

The observed phase angle α describes dissipation in the mantle as a whole. The viscosity distribution in the mantle requires that the flow responsible for the dissipation is concentrated in the asthenosphere, in the fashion described by TAKEUCHI and SAKATA (1970). If the base of the lithosphere is the site of a layer of partial melting or lubrication as deduced by ANDERSON and SAMMIS (1970), flow must be concentrated within it. In this case, in a sense, the lithosphere slides or works its way over the more slowly flowing lower part of the asthenosphere.

Measured in terms of the dissipation as a function of α , the tidal contribution to the flow is independent of assumed values of the mantle viscosity.

The phase-derived dissipation if α_{grav} is -0.5° is (MELCHIOR, 1974) 8.5×10^{26} erg/year. The flow must accord with the flow resistance of the mantle in respect to tide stresses, next examined.

5. Tide-Effective Viscosity

Determinations of the viscosity of the mantle with respect to surface loads (O'CONNELL, 1971; CATHLES, 1971) indicate that its value is between 10^{21} and 10^{23} P. In this case the elastic quality factor Q of Earth in respect to elastic tides has a value of millions (OROWAN, 1967) and the dissipation is negligible. Q in respect to the decay of seismic waves and eigenvibrations (ANDERSON and KOVACH, 1964; SMITH, 1972) is less by a factor of thousands, namely about 650. On this basis dissipation in respect to the oscillatory part of bodily tidal deformation is 10^{26} erg/year or less. Estimates of the displacement in re-

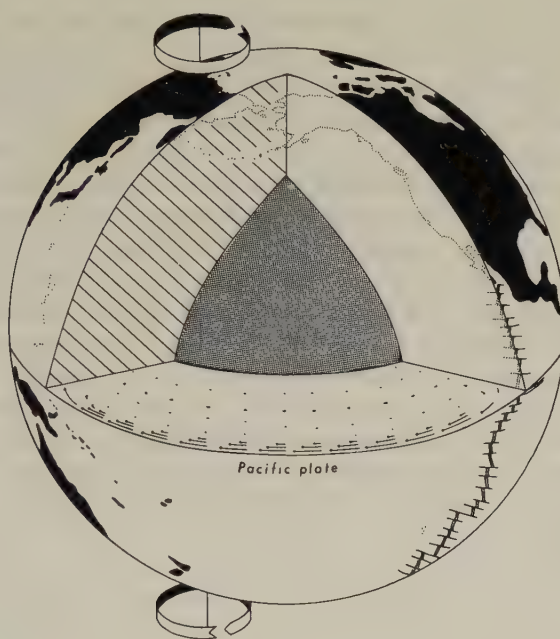


Fig. 5. Form of the circulation contribution under tidal vorticity, shown as stream lines. The viscosity gradient is very steep. In consequence the flow must be concentrated in the asthenosphere in the manner found by TAKEUCHI and SAKATA (1970). Return flow is slow, in the thick lower mantle. In sum, as much material is displaced east as west. Note flow is under internal torques; the crust is not "towed around over a fluid layer" by an external force system, which as JEFFREYS (1929) has pointed out would catastrophically reduce the Earth's rotation. The rings describe the sense of the vorticity vector. Vorticity is induced ubiquitously and continuously, with rotation of bulge-stress axes. Circulation causing west displacement of surface is fostered in low latitudes, thus the west limbs of convection cells are fostered. With increase in latitude, due to the angle made by the vorticity vector to the Earth's surface, clockwise circulation is fostered in the north hemisphere, and vice versa. Note switch at Equator of the polarity of the transforms.

sponse to tides assuming perfect elasticity (TAKEUCHI, 1951; TAKEUCHI and SAITO, 1962) yield Love numbers close to those observed.

The answer to the question of why the lag-determined dissipation is several times 10^{26} erg/year is twofold.

Firstly, (*supra*) under a flow regime of large cells, bulge passage imposes steady stress which is additive across cell-wide segments of the mantle. The stress thus developed, $>10^8$ dyn/cm², is comparable to or greater than that developed by buoyancy convection.

It is therefore able to account for mantle flow and ultimately for orogenesis, either in its own right or in conjunction with buoyancy forces.

Secondly, the stress-strain relationship in respect to the processes comprising "flow" in the Earth is extraordinarily non-linear. The tide stress is imposed (Fig. 6) on mantle already stressed to the point of failure by the convection. Mantle convection comprises multifarious processes of material and energy transference. These include not only high-temperature creep, but fracture, fractionation including vulcanicity, and phase transition. CARTER (1976) has shown that in respect to flow in rock materials the strain rate is related to the stress raised to the power 2 to 9. The investigations of KLEIN (1976) and MAUK and JOHNSTON (1973) suggest that seismicity and vulcanicity are non-linear in the extreme, to the extent of being triggered phenomena. With respect to viscosity the ice-loading of continents or the imposition of a stationary load do not impose stress in the mode of a bulge sweeping across the sub-oceanic asthenosphere. The latter imposes strain on a mantle already stressed to the yield point under convection; and does so in precisely the mode (rotational flow) in which it is pre-stressed. An example of the effect to be expected at the west Pacific margin is illustrated in the next section of this paper.

5.1 Energy expenditure

The energy dissipated in the Earth including the seas is known from the acceleration of the Moon (JEFFREYS, 1921; MULLER, 1976) to lie between 8 and 15×10^{26} erg/year. This is larger than the flux required to drive convection and orogenesis. The tidal dissipation has several times been attributed almost wholly to the seas. Internal dissipation as in the mantle would then be small.

HENDERSHOTT (1972) has quantified the total dissipation in terms of the observed ocean tides. Gauge-observed water tides are used to determine the deformation of the sea floor, assuming perfect elasticity. Integrated over the oceans, the work done by M_2 is found to be 9.6×10^{26} erg/year, explaining the acceleration of the Moon.

LAMBECK (1975; p. 2923) has compared Hendershott's tidal dissipation rate for M_2 with the orbitally derived measure of the dissipation. As the difference is small he concludes that little dissipation is effected in the solid Earth. However Hendershott's formu-

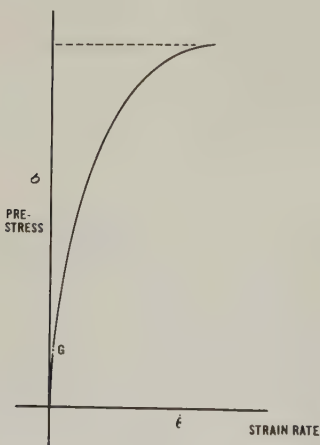


Fig. 6. Viscosity $\eta = \sigma / \dot{\epsilon}$ with respect to superimposed stress in pre-stressed, non-linear material. In metastable regions of the mantle, such as those (Fig. 7) in subduction, material is pre-stressed (dotted line) to point of failure in yield, fracture and compression; superimposed stress $\delta\sigma$ as by tides results in large deformation. Effective viscosity (slope of curve) is small. On the contrary, in stable regions locally stressed such as Fennoscandia by ice loading (G), effective viscosity is high.

lation by intention includes no dissipation terms, in respect either to the seas or the solid Earth. The phase displacement in the observed water tide upon which the computation is based is assumed to be due to dissipation "somewhere" outside the boundary of the computation. His formulation thus makes no statement as to whether the phase displacement in the motion of the seas and sea floor is due to dissipation in the seas or in the solid Earth (for instance, the thick sub-oceanic asthenosphere). The elastic Love number used in the computation is insignificantly different from the anelastic number appropriate if all dissipation were to take place in the solid Earth.

Extra-terrestrial data such as the acceleration of artificial satellites cannot separate the phase lag due to dissipation in the sea and underlying floor. The seas and lossy part of the asthenosphere are coincident and their spatial spectra the same. To effect the separation MILLER (1966) measured the flux of tidal energy into shallow seas, where almost all the marine dissipation takes place. The flux thus measured is between 4.4 and 5.5×10^{26} erg/year. This accounts for about half only of the astronomically-detected dissipation, but accords with the large value of the dissipation in the solid Earth indicated by the lag in O_1 . It accords also with the large value of the quality factor Q , $Q=34$, derived by Hendershott. To account for the dissipation entirely in terms of marine processes, the value of Q_{marine} (MUNK and MACDONALD, 1960, p. 213) must be about 2.6; see also NEWTON (1972, 1973, 1976).

We therefore are inclined to conclude that about half the dissipation astronomically measured, namely between 4 and 7.5×10^{26} erg/year, is available to drive or modulate flow processes in the mantle.

6. *Structure of Pacific Margin*

The margin of the Pacific basin was at one time regarded as tectonically uniform; hence the Pacific "ring of fire." Marginal structure is now seen to vary strongly from region to region. The west margin consists of minor ocean basins outlined by island arcs and underlain by Benioff zones. Benioff zone features (the tectonic trench, the Meinesz gravity strip, sub-lithosphere seismicity) are absent in the Canada/United States portion of the Pacific rim with the exception of Alaska. The Andean sector is sublain by a Benioff zone, but this region is devoid of marginal basins. As pointed out by DICKINSON (1978) and others, the Pacific basin is remarkably asymmetric. The west Pacific is the site of a continuous string of marginal basins. In the east these are absent. The Pacific plate, representing the west limb of the East Pacific Rise axis of sea floor spreading, occupies most of the ocean floor. The east limb is one fifth this size.

6.1 *Flow regime, west margin*

Seismologic evidence (ISACKS and MOLNAR, 1969) and the geologic record indicate that the west Pacific margin, the most active region of the planet, is the site of large-scale foundering of lithosphere. In terms of convection, this represents the return to the planetary interior of material which originally upwelled to form new lithosphere at the crest of the East Pacific Rise, 6,000 km to the east. Theory, laboratory and seismologic evidence (RINGWOOD, 1973; AHRENS, 1972; JOHNSTON, 1969) require that as material under surface conditions passes into regions of high pressure and temperature its minerals transform into dense phases, to the accompaniment of energy transference. In flow the process represents

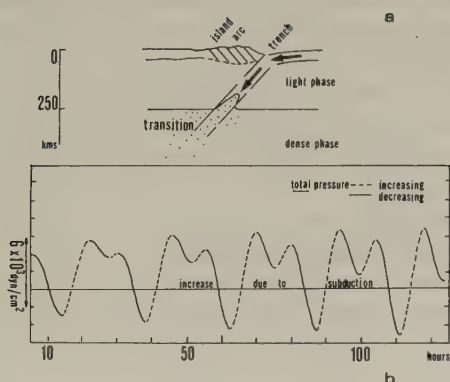


Fig. 7. (a) Creation of metastable material in subduction region. As material founders minerals such as olivine change phase to dense, high-pressure form. Transition takes place in over-pressured, metastable zone. Probability of transition to dense form increases to 100% at base of metastable zone, and transition is complete. Transition surface is complicated and may be concave upward or downward dependent upon whether slope of equilibrium curve is positive or negative. (b) Regime in metastable zone. At typical foundering rate 5 cm/year, the hydrostatic pressure change ($+5.5 \times 10^{-4} \text{ dyn/cm}^2/\text{sec}$) is represented by the slope of the almost horizontal line. The pressure change due to tidal gravity disturbance is about one thousand times this rate. The oscillatory curve represents the total pressure change in transition region under tides. Over a period of many cycles, transition must take place predominantly when the total pressure is rising (dashed line), rather than falling. Note that process cannot operate in stable regions, where metastable material is not continuously created by convection.

volumetric or bulk viscosity, because the released energy becomes locally unavailable and the deformation (compression) is irrecoverable.

The flow regime in this region is illustrated in Fig. 7. Mineral species such as olivine, stable near surface, experience transition into high-density forms at depth. Within the down-flowing limb, iso-phase surfaces may be convex upward or downward, dependent upon the sign of the curve describing the conditions of transition. Laboratory and seismologic evidence (AKIMOTO and FUJISAWA, 1966; RINGWOOD, 1973; JOHNSTON, 1969) indicate that phase transitions are numerous and overlapping, and extend to the lower mantle.

Putting aside at first the effect of tides, foundering causes the increase through time of both pressure and density. On the average the pressure increase due to the downward flow component, if the latter is 5 cm/year and the density 3.5 g/cm^3 , is $5.4 \times 10^{-4} \text{ dyn/cm}^2/\text{sec}$.

Upon this slow secular increase is superimposed the rapid, much larger, but oscillatory pressure variation due to the tidal disturbance in gravity. Assuming the latter typically to be 0.1 mGal, the tidal pressure variation is

$$h\rho\Delta g$$

where h is depth of the volume element. The rate is $2.6 \times 10^{-1} \text{ dyn/cm}^2/\text{sec}$ at a depth 350 km. Locally, water-loading increases this variation by an order of magnitude (ZSCHAU, 1977). The pressure change due to the tidal gravity cycle is thus hundreds to thousands of times greater than the pressure increase in the same length of time under foundering. The total pressure actually decreases in the negative part of the tide cycle, Fig. 7(b).

Within the metastable, over-pressured material continually created under foundering, it seems inevitable that phase transition preponderantly takes place when the total pressure is increasing; and not when it is decreasing. Conversely, with respect to its bulk viscosity

the material of the mantle must respond elastically to the tidal pressure variation in regions where upflow or downflow is not present (not creating material at the metastable point or point of failure in volume). It seems no coincidence that large tidal phase lags are typical of the west Pacific region. Thus for instance the lag in the diurnal bodily tide, little affected by water displacement, is -7° at Manila (Table 1).

In regions such as the west Pacific margin, where the resistance of the material in volume to the tidal pressure variation has been overcome by foundering and metastability prevails, volumetric viscosity must be a dominant loss mechanism. Apparently, the advance in the convection must be modulated significantly by the tidal pressure variation. GRIGGS (1972) has pointed out that the energy released by the foundering lithosphere is very large, of the order 10% of the Earth's total heat efflux, i.e. about 10% of 10^{28} erg/year. Thus even a minor modulation of the advance in the convection (such for instance that 60% is accomplished during pressure-rise times versus 40% during the remaining half of any time interval) could by itself account for the entire "missing" fraction of the tidal energy dissipation.

Analogous tidal modulation, of phase decompression and partial melting, must take place in upflow regions such as the axis of the sea floor spreading system. KLEIN (1976) has demonstrated synchronization of tide stress and seismicity in the portions he has examined, namely the north segment of the East Pacific Rise and the north half of the mid-Atlantic Ridge. In upflow regions the advance in convection takes place during tidal pressure minima.

6.2 *Formation of marginal basins*

As in his discovery of mantle plumes (WILSON, 1965a), transforms, and plates (WILSON 1965b), WILSON (1973) has pointed to the significance of relative motion in the formation of marginal basins. It seems to matter profoundly, in plate convergence, which plate is more nearly stationary relative to the mantle. If for instance a continental plate is fixed and oceanic plates encroach upon it, island arcs will form, enclosing marginal basins.

This circumstance becomes more comprehensible when considered alongside the fact (NELSON and TEMPLE, 1972) that, world-wide, subduction zones facing east differ from those facing west. As pointed out by UYEDA and KANAMORI (1978), if the motion of the mantle relative to the lithosphere is eastward, the east-west asymmetry is explicable. In terms of the tidal contribution to vorticity, the subduction zones at the west Pacific margin benefit from the tidal contribution, and from induction across the trans-oceanic expanse of the Pacific plate. Not coincidentally, the downgoing slab assumes a steep angle, and is in places overridden or overturned. At the east or Andean margin, on the contrary, we are dealing with the weak, counter-tidal east limb of the East Pacific Rise. This bucks tidal vorticity induction, and is rapidly being supplanted (BOSTROM, 1978a) by the west, co-tidal limb of the mid-Atlantic spreading center. The slope of the Benioff zone is less, the volume of material foundering is less, the continental plate is overriding the oceanic for buoyancy reasons, and no marginal basins are present.

It is possible to account for these phenomena simultaneously if we allow tidal vorticity induction across the expanse of thick asthenosphere underlying the Pacific basin. By now the west limb of the East Pacific Rise is grossly extended relative to the east limb; and the larger the west limb becomes, the greater the induction. An increasing volume of material is being carried to the terminus of the west limb, the east flank of the

Asian continent. The accumulation of material at the west Pacific margin, marked by the string of geoidal highs (Fig. 1), is subject to intense negative buoyancy, and founders. Mineral phases in equilibrium under shallow conditions cannot be in equilibrium at depth. Their transition and the role of entrained volatiles is the subject of active petrologic research (FEDORCHENKO and PISKUNOV, 1978; YODER, 1978; WYLLIE, 1978). Necessarily a fraction of the material separates upward. Material is added to the asthenosphere, resulting in secondary sea floor spreading and the formation of the arc-bounded basins described by KARIG *et al.* (1973) and others.

It is to be expected, and found to be the case, that at the terminus of the weak, counter-tidal east limb of the East Pacific Rise, basin formation will itself be weak. Basins, if they form, will be overridden and incorporated (DALZIEL, 1978) in the advancing west edge of the west limb of the Atlantic spreading center, namely the Andean margin of South America.

Basin formation and tectonic activity is latitude-dependent, as is to be expected under tidal vorticity induction. The tropical west Pacific margin is the site of the greatest geoidal high on the planet, and accounts for more than 80% of seismicity, deep, intermediate and shallow. Deep seismicity ($h > 300$ km) decreases with latitude (BOSTROM, 1973) and disappears altogether towards the poles. The fragmentation of the east Asian margin and the increasing "oceanicity" of the marginal basins is likewise latitude-dependent. The floor of the Sea of Okhotsk in the north is thought largely to consist of altered and foundering continental material (KROPOTKIN, 1978; YANSHIN, 1978). The oldest rocks in Japan formed when Japan was attached to the Asian mainland, the Sea of Japan having developed and widened since. Since Oligocene times the tectonics of Japan has changed as indicated by the development of the Fossa Magna, as a result of the alteration in the subduction regime and the opening of the Philippine Sea to the south. This coincided with the destruction in the northern hemisphere (BOSTROM, 1978 a,b) of the east limb of the East Pacific Rise, now overridden by the Californias. Co-tidal vorticity now characterizes the upper mantle continuously without a break from the middle of the Atlantic, across North America and the entire width of the Pacific, to the shores of Japan.

The Pacific plate is at its widest at the Equator, at this latitude extending furthest east and furthest west. The structure of the intensely active Indonesian region has already been attributed (KROPOTKIN and SHAKVARSTOVA, 1965; KROPOTKIN, 1978) to the fragmentation of the southeast portion of the Asian continent. With increasing latitude southward, seismic activity and subduction gradually decrease. Deep seismicity, associated with the entry of material into the deep mantle, ceases at the latitude of New Zealand.

The latitude dependence of the spreading at the crest of the East Pacific Rise, the symmetry of the Pacific basin about the Equator, and its east-west asymmetry, are shown in Fig. 8.

7. *Historical Development of the Circulation*

It seems at first curious, if the circulation is marshalled by tidal bulge passage, that mantle circulation is not ubiquitously co-tidal, and has not been thus patterned since convection commenced. The reason may lie in the re-setting of the circulation pattern by a supercessive force.

It has been postulated elsewhere (BOSTROM, 1978b) that the circulation in the mantle

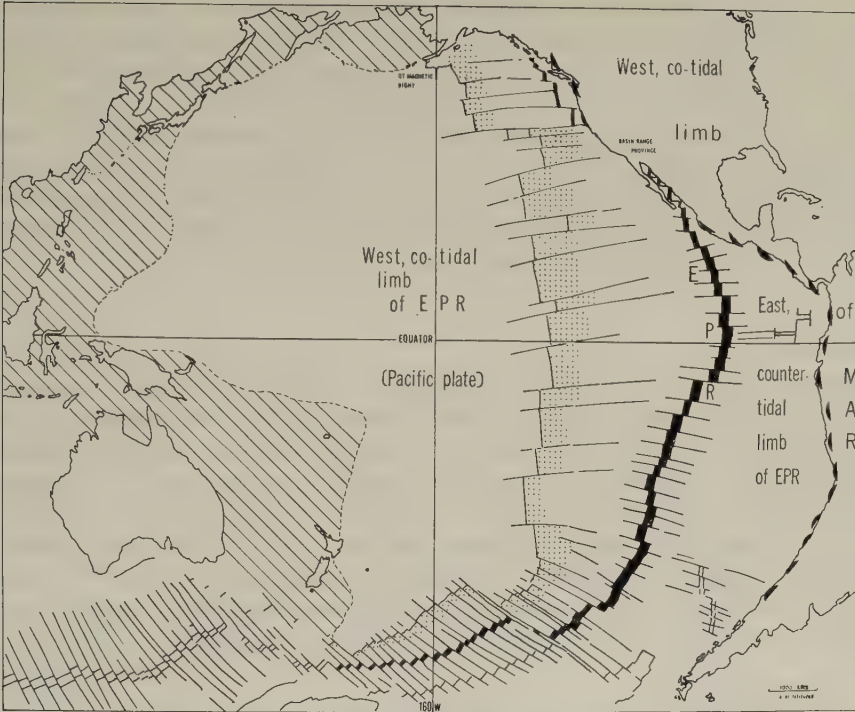


Fig. 8. Pacific plate, representing surface of the west limb of the East Pacific Rise (EPR; Pleistocene at crest, *black*). The east-west spreading rate, indicated by distance to Paleocene/Eocene boundary (*stippled*), is symmetrical about Equator. The spreading maximum coincides with the Equatorial maximum in vorticity induction. The grossly extended west limb of the EPR forms most of the Pacific basin. The counter-tidal east limb is being replaced by the extending west limb of the mid-Atlantic spreading center (MAR) bearing the Americas plates. The sense of the transforms reverses at the Equator, to predominantly sinistral in the south hemisphere. Departure from north-south symmetry is mainly due to the excess of continental lithosphere in the north hemisphere; the North America plate has overridden the crest of the EPR. The convergence of N America and Siberia has caused the development of the Bering Sea marginal basin. We attribute the development of the basins flanking the west Pacific margin (*hatched*) to convergence between the co-tidal west limb of the EPR and the less mobile continental material of Australasia and eastern Asia. As a result of differentiation material is added to the asthenosphere, causing the disruption of the continental margin, sea floor spreading, and the formation of back-arc basins. At the east Pacific margin, on the contrary, the west limb of the Atlantic spreading center is overriding and extinguishing the east limb of the EPR. Data: HEEZEN and FORNARI (1976). Scale identical at all latitudes, $1: 10^8 \times 1.5$.

is determined by the interplay of two factors. The first is the marshalling effect of tidal bulge passage on buoyancy convection. The second factor stems from the fact that in a convective Earth, Goldreich-Toomre wandering of the Earth about the space-fixed pole of rotation (GOLDREICH and TOOMRE, 1969) is inevitable. The manner in which the bulge of rotation migrates is by adjustment of the sea-floor spreading pattern so as to effect the necessary mass transfer (SILLING, 1978).

We therefore suppose that tidal ordering of the convection becomes dominant during

periods such as the post-Paleozoic period of minimal pole wander. The present cycle in the Pacific hemisphere was initiated in the early Mesozoic. The pattern inherited at that time was the result of the period of pole wander occurring during the Paleozoic, extending into the Mesozoic. Thus the post-Paleozoic geological record in the Pacific basin and rim (see for instance LARSON and CHASE, 1972; BOSTROM, 1977; SUZUKI *et al.*, 1978) describes gradual marshalling of the flow pattern in the mantle, culminating in the highly ordered present pattern and concentration of activity at the west margin. World-wide, hot-spot traces unequivocally describe the present predominance of westward lithosphere motion in low latitudes (BOSTROM, 1978b).

8. Conclusions

The Pacific plate is the cool, rigid surface of mantle convection surfacing in the eastern Pacific, and foundering at the west Pacific margin. The convection represents vorticity (rotational flow) induced jointly by thermal buoyancy and the passage of the M_2 tidal bulge. Thermal convection, which would by itself produce small random flow cells, is marshalled by the highly coherent bulge stress.

The west limb of the East Pacific Rise, representing co-tidal vorticity, now extends clear across the Pacific basin. The counter-tidal east limb, underlying the Nazca, Cocos and small Juan de Fuca plates, is being replaced by the extending west limb of the Atlantic spreading center, fronted by the Andean orogenic belt.

8.1 Marginal basins

Material accumulates at the west margin of the Pacific as a result of the convergence between the co-tidal, active west limb of the EPR and less mobile material which forms the east margin of Asia. The accumulation is marked by an unbroken line of gravity highs, coincident with deep seismicity. Deep-seated differentiation results in the addition of material to the asthenosphere. This causes the disruption of the continental margin, localized sea floor spreading, and the formation of arc-bounded basins.

At the east Pacific margin this mechanism is not operative, because the co-tidal west limb of the Atlantic spreading axis (bearing the Americas plates) is overriding and extinguishing the counter-tidal east limb of the EPR.

8.2 Stress, strain, and energy flux

The stress driving the convection is supplied by thermal buoyancy and the continuously rotating bulge stress axes. The elemental shear stresses contributed by each of these agencies are minute. However in large flow cells the buoyancy stress is cooperative and additive vertically through great thicknesses of the mantle, resulting in regional stresses of the order 10^8 dyn/cm², and the stress concentrations at plate edges observed in seismicity. Analogously, the bulge stress is additive horizontally across the width of plates; the larger the plate, the larger the induced stress. Across the Pacific plate the bulge stress sums to values greater than the buoyancy stress.

The resulting strain and flow in the mantle is enhanced by the grossly non-linear relation between stress and strain. The latter includes processes of fracture, fractionation and compression. Thus in a subduction region such as the west Pacific margin, continuously-renewed volumes of material exist in an over-pressured state through downflow. The tidal pressure increment, larger than that in downflow, must effect the transition to

dense phases, modulating the convection. In mantle continuously pre-stressed to the point of failure in shear or volume, the tide-effective viscosity thus is small.

The geologic phenomena suggest that thermal buoyancy and the rotating bulge stress contribute about equally to the convection. The energy flux required in toto is about 10^{27} erg/year (mean viscosity 10^{22} P; mean plate motion, 3 cm/year). Of this the phase lag in the diurnal bodily tides suggests that about 5×10^{26} erg/year is contributed by tidal dissipation. This value accords with the dissipation required to explain the lunar acceleration, but not found in the seas. Based on this reasoning, sea floor spreading is passive, the response to forced convection rate-limited by the rate at which buoyancy is created.

8.3 Data status

The magnitude and phase of the bodily tides (Table 1) varies greatly from one region to another. Besides revealing the large dissipation, the variation has revealed the inadequacy of our station coverage. It would be of value from the geotectonic point of view to extend the observations initiated by DUCARME and MELCHIOR (1977) to a much larger number of stations. To do so, it is necessary to use instruments (gravity meters) calibrated as to their individual phase delay through side by side running at a base station (DUCARME, 1975). It would also be worth using the technique used by KLEIN (1976) in the east Pacific to identify correlations between tide stress and seismicity at the west Pacific margin. Into the bargain, such correlations might eventually prove valuable in forecasting periods of enhanced seismicity.

Note Added in Press: Tidal Dissipation in the Seas and Solid Earth

The recent important paper by LAMBECK (K. LAMBECK, *Phil. Trans. Roy. Soc. Lond., A*, **287**, 545–594, 1977) reviews data as to the energy expenditure in tidal action. The conclusion is reported, in the abstract, that “dissipation occurs almost exclusively in the oceans and neither the solid Earth nor the Moon are important energy sinks.”

This is based upon finding that an estimate of work done on the oceans by body forces and the heaving sea floor matches the dissipation required to account for the acceleration of the Earth and Moon. The work done on the world ocean is represented as:

$$\begin{aligned} \langle \overline{W} \rangle &= \rho_w (1 + k_2) \int_S \langle U_{lm} d\xi / dt \rangle dS && \text{term 1} \\ &+ \rho h_2 \int_S \langle \xi dU_{lm} / dt \rangle dS && 2 \\ &+ \rho_w \int_S \langle \nabla_S \cdot [u D \psi] \rangle dS, && 3 \end{aligned}$$

in which: ρ_w and ρ are the density of water and sea floor; h and k are the elastic Love numbers; U is the potential of the direct tide raising potential; ξ is the geocentric sea-surface tide; u is the horizontal velocity of tidal currents; D is the ocean depth; ψ is the total tidal potential; and integration is over the ocean-covered part of the Earth.

In evaluating $\langle \overline{W} \rangle$, term 3 is discarded on the assumption that the boundary of the region of integration is impermeable. Dissipation in the solid Earth also is precluded, through the use of the elastic Love numbers.

These assumptions make it possible to reach a solution solely on the record of coastal marine tide gauges. However, *ipso facto* they preclude our reaching conclusions as to the site of dissipation. The equation contains no dissipation terms. Dissipation is assumed

to take place somewhere, but the phase of the ocean tides upon which the computation is based may be attributed to dissipation in the waters, in the solid Earth, or in both.

In point of fact investigations extending over many decades, cited by Lambeck, have failed to find dissipation in the seas capable of explaining the observed phase of M_2 . Observations not cited, such as those by DUCARME and MELCHIOR (1977) of the phase lag in bodily O_1 , suggest that a large part of the dissipation takes place in the solid Earth. They require, furthermore, that dissipation also occurs in the sub-continental third of the Earth, arbitrarily excluded in the equation by the range S of the integration.

External observations such as those of the flight of satellites, alone or in conjunction with coastal tide gauge records, cannot distinguish whether the phase of the marine tides is determined by dissipation in the seas or subjacent sea floor (asthenosphere).

The estimate of the work $\langle \overline{W} \rangle$ done on the oceans arrived at as shown tallies with the observed acceleration of the Moon. However estimates arrived at on the basis of equally unrealistic assumptions, such as that the Earth is rigid (PEKERIS and ACCAD, 1969), also tally.

The unwelcome fact remains that computations, no matter how intricate, based upon the assumption that dissipation in the Earth is nil cannot measure the dissipation in the solid Earth. Regretfully, therefore, we find it not possible to concur with the conclusion cited at the head of this note.

REFERENCES

- AHRENS, T.J., The state of mantle minerals, *Tectonophysics*, **13**, 189–219, 1972.
- AKIMOTO, S. and H. FUJISAWA, Olivine-spinel transition in system Mg_2SiO_4 - Fe_2SiO_4 at 800°C, *Earth Planet. Sci. Lett.*, **1**, 237–340, 1966.
- ANDERSON, D.L. and R.L. KOVACH, Attenuation in the mantle, *Natl. Acad. Sci. Proc.*, **51**, 168–172, 1964.
- ANDERSON, D.L. and C. SAMMIS, Partial melting in the upper mantle, *Phys. Earth Planet. Inter.*, **3**, 41–50, 1970.
- BARAZANGI, M. and J. DORMAN, World seismicity map, 1961–1967, *Bull. Seismol. Soc. Am.*, **59**, 369–380, 1969.
- BOSTROM, R.C., Arrangement of convection in the Earth by lunar gravity, *Phil. Trans. Roy. Soc. Lond., A*, **274**, 397–407, 1973.
- BOSTROM, R.C., An increasing tidal couple, Proc. 8th Int. Symp. Earth Tides, I.U.G.G., Bonn, 1977 (in press).
- BOSTROM, R.C., Formation of the Cordillera; flow processes in the sub-Pacific mantle, *Pac. Geol.*, **15**, 1978a (in press).
- BOSTROM, R.C., Tectonics of the tidal, convective Earth, II, *Mod. Geol.*, **6**, 185–197, 1978b.
- CARTER, H.L., Steady state flow of rocks, *Rev. Geophys. Space Phys.*, **14**, 301–360, 1976.
- CATHLES, L.M., III, The viscosity of the Earth's mantle, Ph. D. Thesis, Princeton University, University Microfilm, Ann Arbor, 1971.
- DALZIEL, I.W.D., The early Cretaceous marginal basin in the southern Andes and the Andean orogeny; a review, Abstr. of Papers, Int. Geodyn. Conf., I.U.G.G., Tokyo, p. 20, 1978.
- DANES, Z.F., Mainstream mantle convection: A geologic analysis of plate motion: Discussion, *Am. Assoc. Pet. Geol. Bull.*, **57**, 410–411, 1973.
- DARWIN, G.H., Problems connected with the tides of a viscous spheroid, *Phil. Trans. R. Soc. Lond.*, **170**, Part II, 539–593, 1879.
- DEHLINGER, P., Tidal Friction and plate tectonics, Symp. Ocean. Floor Spreading, I.U.G.G., Int. Meet., Moscow, List of Abstr., Vol. 4, 34, 1971.
- DICKINSON, W., Keynote address to Int. Geodyn. Conf., Tokyo, 13 March, 1978.
- DUCARME, B., A fundamental station for trans-world tidal gravity profiles, *Phys. Earth Planet. Inter.*, **11**, 119–127, 1975.
- DUCARME, B. and P. MELCHIOR, Tidal gravity profiles in western Europe, Asia, Australia, New Zealand and Pacific Islands, *Bull. D'Obs.*, Vol. iv, Fasc. 4, Obs. Roy. de Belg., 1–106, 1977.
- EDDINGTON, Sir A., The borderland of astronomy and geology, *Nature*, **111**, 18, 1923.
- ELSASSER, W.M., Thermal structure of the upper mantle and convection, in *Advances in Earth Science—Int. Conf.*, pp. 461–502, M.I.T. Press, Cambridge, Mass., 1966.

- FEDORCHENKO, V.I. and B.N. PISKUNOV, Volcanic associations in an ocean-island arc—marginal sea zone: Types, correlations, geological problems, *Abstr. of Papers, Int. Geodyn. Symp., I.U.G.G., Tokyo*, pp. 24–25, 1978.
- FORSYTH, D. and S. UYEDA, On the relative importance of the driving forces of plate motion, *Geophys. J. R. Astr. Soc.*, **43**, 163–200, 1975.
- GAPOSCHKIN, E.M., Earth's gravity field to the 18 degree, *J. Geophys. Res.*, **79**, 5377–5411, 1974.
- GOLDREICH, P. and A. TOOMRE, Some remarks on polar wandering, *J. Geophys. Res.*, **74**, 2555–2567, 1969.
- GRIGGS, D.T., The sinking lithosphere and the focal mechanism of deep earthquakes, in *The Nature of the Solid Earth*, edited by E.C. Robertson, pp. 361–384, McGraw-Hill, New York, 1972.
- HEEZEN, B.C. and D.J. FORNARI, Pacific Ocean, in *Geological World Atlas*, edited by G. Choubert, 1/10 m, UNESCO, Paris, 1976.
- HENDERSHOTT, M.C., The effects of solid-Earth deformation on global ocean tides, *Geophys. J. R. Astr. Soc.*, **29**, 389–402, 1972.
- ISACKS, B. and P. MOLNAR, Mantle earthquake mechanisms and the sinking of the lithosphere, *Nature*, **223**, 1121–1124, 1969.
- ISACKS, B., L.R. SYKES, and J. OLIVER, Focal mechanisms of deep and shallow earthquakes in the Tonga-Kermadec region and the tectonics of island arcs, *Bull. Geol. Soc. Am.*, **80**, 1443–1470, 1969.
- JEFFREYS, H., Tidal Friction in shallow seas, *Phil. Trans. R. Soc. Lond., A*, **221**, 239–264, 1921.
- JEFFREYS, H., On Prof. Joly's theory of earth history, *Phil. Mag.*, Ser. 7, **1**, 923–931, 1926.
- JEFFREYS, H., *The Earth*, 2nd Ed., p. 322, Cambridge University Press, Cambridge, 1929.
- JOHNSTON, L., Array measurements of P velocities in the lower mantle, *Bull. Seismol. Soc. Am.*, **59**, 973–1008, 1969.
- JOLY, J., The movements of the Earth's surface crust, *Phil. Mag.*, Ser. 6, **45**, 1167–1188, 1926.
- JORDAN, T.H., Some comments on tidal drag as a mechanism for driving plate motions, *J. Geophys. Res.*, **79**, 2141–2142, 1974.
- KARIG, D., J.C. INGLE, A.H. BOUMA, H. ELLIS, N. HAILE, I. KOIZUMI, I.D. MACGREGOR, C. MOORE, H. UJIE, T. WATANABE, S.M. WHITE, M. YASUI, and H. YI LING, Origin of the west Philippine Basin, *Nature*, **246**, 458–461, 1973.
- KAULA, W.M., Earth's gravity field: Relation to global tectonics, *Science*, **3949**, 982–985, 1970.
- KLEIN, F.W., Earthquake swarms and the semidiurnal solid-earth tide, *Geophys. J. R. Astr. Soc.*, **45**, 245–295, 1976.
- KNOPOFF, L., The convection current hypothesis, *Rev. Geophys.*, **2**, 89–122, 1964.
- KROPOTKIN, P.N. and K. SHAKVARSTOVA, Geological structure of the circum-Pacific mobile belt, *Trudi Geol. Sci.*, **134**, p. 366, Akad. Nauk, USSR, 1965.
- KROPOTKIN, P.N., The crustal structure and origin of the basins of the Sea of Okhotsk and the Japan Sea, *Abstr. of Papers, Int. Geodyn. Conf., I.U.G.G., Tokyo*, 1978, pp. 92–93, 1978.
- LAMB, Sir H., *Hydrodynamics*, 6th Ed., Cambridge University Press, Sec. 31, Cambridge, 1932.
- LAMBECK, K., Effects of tidal dissipation on the Moon's orbit and the Earth's rotation, *J. Geophys. Res.*, **80**, 2917–2925, 1975.
- LARSON, R.L. and C.G. CHASE, Late Mesozoic evolution of the Pacific Ocean, *Geol. Soc. Am. Bull.*, **83**, 3627–3644, 1972.
- LOVE, A.E.H., *A Treatise on the Mathematical Theory of Elasticity*, pp. 34–36, Dover, New York, 1944.
- MAUK, F.I. and M.J.S. JOHNSTON, On the triggering of volcanic eruptions by earth tides, *J. Geophys. Res.*, **78**, 3356–3362, 1973.
- McKENZIE, D.P., The influence of the boundary conditions and rotation on convection in the Earth's mantle, *Geophys. J. R. Astr. Soc.*, **15**, 457–500, 1968.
- McKENZIE, D.L., SPECULATIONS on the consequences and causes of plate motions, *Geophys. J. R. Astr. Soc.*, **18**, 1–32, 1969.
- McKENZIE, D.P., Plate Tectonics, in *The Nature of the Solid Earth*, edited by E.C. Robertson, pp. 323–360, McGraw-Hill, New York, 1972.
- McKENZIE, D.P. and R.L. PARKER, The North Pacific: An example of tectonics on a sphere, *Nature*, **216**, 1276–1280, 1967.
- McKENZIE, D.P., J.M. ROBERTS, and N.O. WEISS, Convection in the earth's mantle; towards a numerical simulation, *J. Fluid Mech.*, **62**, 465–538, 1974.
- MELCHIOR, P., Earth tides, *Geophys. Surv.*, **1**, 275–303, 1974.
- MILLER, G.R., Flux of tidal energy out of the deep oceans, *J. Geophys. Res.*, **71**, 2485–2489, 1966.
- MINSTER, J.B., T.H. JORDAN, P. MOLNAR, and E. HAINES, Numerical modelling of plate tectonics, *Geophys. J. R. Astr. Soc.*, **36**, 541–576, 1974.
- MOORE, G.W., Westward tidal lag as the driving force of plate tectonics, *Geology*, **1**, 99–100, 1973.

- MULLER, P.M., Determination of the cosmological rate of change of G and the tidal accelerations of Earth and Moon from ancient and modern astronomical data, Rep. JPL 46-36, Calif. Inst. Technol. Pasadena, pp. 1-24, 1976.
- MUNK, W.H. and G.J.F. MACDONALD, *The Rotation of the Earth*, p. 218, Cambridge University Press, Cambridge, 1960.
- NELSON, T.H. and P.G. TEMPLE, Mainstream mantle convection: A geologic analysis of plate motion, *Bull. Am. Assoc. Pet. Geol.*, **56**, 226-246, 1972.
- NEWTON, R.R., Astronomical evidence concerning non-gravitational forces in the Earth-Moon system, *Astrophys. Space Sci.*, **16**, 179-200, 1972.
- NEWTON, R.R., The historical acceleration of the Earth, *Geophys. Surv.*, **1**, 123-145, 1973.
- NEWTON, R.R., *Ancient Planetary Observations*, Vol. 5, pp. 4-6, Johns Hopkins University Press, Rockville, Maryland, 1976.
- O'CONNELL, R.J., Pleistocene glaciation and the viscosity of the lower mantle, *Geophys. J. R. Astr. Soc.*, **23**, 299-327, 1971.
- OLIVER, J. and B. ISACKS, Deep earthquake zones, anomalous structure in the upper mantle, and the lithosphere, *J. Geophys. Res.*, **72**, 4259-4275, 1967.
- OROWAN, E., Seismic damping and creep in the mantle, *Geophys. J. R. Astr. Soc.*, **14**, 191-218, 1967.
- PEKERIS, C.L., and Y. ACCAD, Solution of Laplace's equations for the M_2 tide in the world oceans, *Phil. Trans. R. Soc. Lond., A*, **265**, 413-436, 1969.
- RINGWOOD, A.E., Phase transformation and their bearing on the dynamics of the mantle, *Fortschr. Mineral.*, **50**, 113-139, 1973.
- SCLATER, J.G., L.A. LAWVER, and B. PARSONS, Comparison of long-wave length residual elevation and free air gravity anomalies in the North Atlantic and possible implications for the thickness of the lithospheric plate, *J. Geophys. Res.*, **80**, 1031-1052, 1975.
- SHAW, H.R., Earth tides, global heat flow, and tectonics, *Science*, **168**, 1084-1087, 1970.
- SILLING, R.M., Polar wandering and bulge migration in a convective Earth, *EOS, Trans. Am. Geophys. Union*, **59** (4), 388, 1978.
- SMITH, S.W., The anelasticity of the mantle, *Tectonophysics*, **13**, 601-622, 1972.
- SUZUKI, Y., K. KODAMA, and T. MITSUNASHI, The formation of intermediate-deep earthquake zone in relation to the geologic development of east Asia since Mesozoic, Abstr. with Papers, Int. Geodyn. Conf., I.U.G.G., Tokyo, 1978.
- TAKEUCHI, H., On the earth tide in the compressible earth of varying density and elasticity, *J. Fac. Sci. Univ. Tokyo*, Sec. II, Vol. VII, Part II, 1-153, 1951.
- TAKEUCHI, H. and M. SAITO, Static deformations and free oscillations of a model Earth, *J. Geophys. Res.*, **67**, 1141-1154, 1962.
- TAKEUCHI, H. and S. SAKATA, Convection in a mantle with variable viscosity, *J. Geophys. Res.*, **75**, 921-927, 1970.
- TOZER, D.C., Towards a theory of thermal convection in the mantle, in *The Earth's Mantle*, chapter 11, edited by T.F. Gaskell, Academic Press, London, 1967.
- UYEDA, S. and KANAMORI, H., Origin of back-arc basins and tectonics, Abstr. of Papers, Int. Geodyn. Conf., I.U.G.G., Tokyo, p. 168, 1978.
- WILSON, J.T., Evidence from islands suggesting movement in the Earth, *Phil. Trans. R. Soc. Lond., A*, **258**, 145-165, 1965a.
- WILSON, J.T., A new class of faults and their bearing on continental drift, *Nature*, **207**, 1965b.
- WILSON, J.T., Mantle plumes and plate motion, *Tectonophysics*, **19**, 149-164, 1973.
- WYLLIE, P.J., H_2O and CO_2 in magma generation in subduction zones, Abstr. of Papers, Int. Geodyn. Conf., I.U.G.G., Tokyo, p. 346, 1978.
- YANSHIN, A.L., History and mechanism of the formation of the deep-water marginal seas basins of the Far East of the USSR, Abstr. of Papers, Int. Geodyn. Conf., I.U.G.G., Tokyo, pp. 184-185, 1978.
- YODER, H.S., Basic magma generation and aggregation, Abstr. of Papers, Int. Geodyn. Conf., I.U.G.G., Tokyo, pp. 4-5, 1978.
- ZSCHAU, J., Phase shifts of tidal sea load deformations in the Earth's surface, Proc. 8th Int. Symp. Earth Tides, Bonn, Sept. 14-19, 1977.

THE RELATIONSHIP BETWEEN VOLCANIC ISLAND GENESIS AND THE INDO-AUSTRALIAN PACIFIC PLATE MARGINS IN THE EASTERN OUTER ISLANDS, SOLOMON ISLANDS, SOUTH-WEST PACIFIC

G. Wyn HUGHES

*Geological Division, Ministry of Natural Resources,
Honiara, Solomon Islands*

(Received April 19, 1978; Revised October 6, 1978)

The Eastern Outer Islands form a group of small islands situated in the south-west Pacific Ocean, to the south-east of the main Solomon Islands chain, and to the north of the New Hebrides chain.

They are founded upon the northern part of the submarine Fiji Plateau and flanked by deep sea trenches on the western, northern and eastern sides, but by an east-west trending fracture zone on the southern side. Two south-easterly trending island chains can be recognized, the western chain includes the islands of Tinakula, Nendö, Vanikolo and Utupua, and the eastern chain includes the islands of the Duff Group, Anuta and Fatutaka. The island of Tikopia is situated midway between both chains. The Torres and Vitiaz Trenches form the western and eastern flanks respectively of the north Fiji Plateau, which is itself bordered to the west and east respectively by the Indo-Australian and Pacific lithospheric plates. A westerly extension of the Vitiaz Trench, known as the Cape Johnson Trough, forms the northern boundary. The south side of the region is delimited by the Hazel Holme Fracture Zone.

Volcanic rocks within the group range from picrite basalts, through basalts and andesites, to dacites. Mafic lavas predominate in the older islands of the western chain, two islands of the eastern chain and in samples dredged from the Vitiaz Trench. More sialic lavas are exposed in two islands of the eastern chain, the isolated island of Tikopia and also in the active volcanic island of Tinakula.

Petrologic, petrochemical, seismic and heat flow evidence suggests that the Eastern Outer Islands represent two, discrete south-easterly trending island arcs, each associated with the adjacent trench. The sequence of volcanic episodes can be best explained in terms of plate tectonics, in which the islands of the western chain were produced during two episodes of volcanic activity associated with an easterly inclined Torres subduction zone. Late Oligocene to early Miocene subduction produced the island of Nendö, but the islands of Utupua, Vanikolo and Tinakula were produced during the late Pliocene to Recent. The westerly-dipping Vitiaz subduction zone is postulated as a source from which the east facing Duffs-Anuta-Fatutaka island arc was produced during the Middle Miocene to late Pliocene.

1. *Introduction and Geological Setting*

The Solomon Islands form part of a discontinuous chain of islands which extend south-eastwards from New Guinea to Tonga, in the south-west Pacific Ocean.

The Eastern Outer Islands comprise a group of small, scattered islands which are situated approximately 450 km east of the main Solomon Islands chain, and approximately

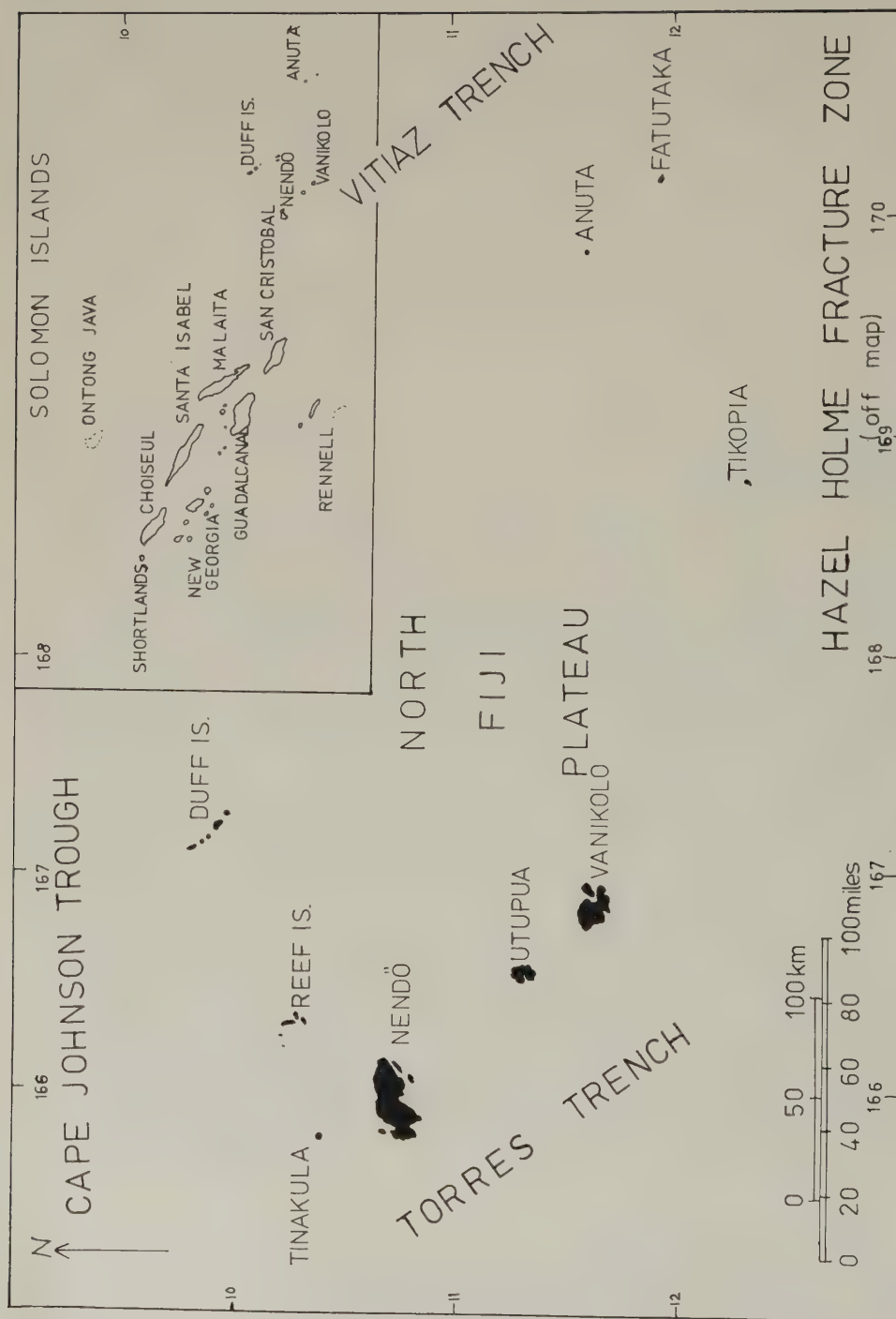


Fig. 1. Locality diagram for the Eastern Outer Islands (E.O.I.) Group, Solomon Islands.

130 km north of the New Hebrides. They were mapped geologically between 1968 and 1973 by the Geological Division of the Ministry of Natural Resources (then Geological Survey).

Tinakula, Nendö, Utupua and Vanikolo islands form a well-defined south-east trending chain in the west of the Group (Fig. 1). To the north-east of Nendö lie the Reef Islands. The Duff Islands, Anuta and Fatutaka form a poorly defined south-east trending chain in the east of the Group, and the isolated island of Tikopia is situated midway between both island chains. Volcanic cones are well preserved on the islands of Vanikolo, Utupua and Tikopia, as well as on the active volcano of Tinakula.

Eight of the nine islands and island groups are volcanogenic and range in age from late Oligocene to Recent; the Reef Islands have a biogenic origin, but are considered to have a volcanogenic base. Tinakula is the only active volcanic island in the Group while Nendö is the only island in the Group which is composed of both volcanic and sedimentary rocks.

2. Summary of the Geology

Nendö island contains a late Oligocene to early Miocene volcanic pile which was faulted and partly submerged during the Middle Miocene to late Pliocene. The lavas are commonly labradorite augite basalts with a variable porphyritic mode in which some horizons contain olivine phenocrysts and others, orthopyroxene. Radiometric dating on a sample from this basal lava succession gives an age of 26 my (HUGHES *et al.*, in press).

An episode of volcanism in the Middle Pliocene gave submarine lavas which lie upon a sequence of calcareous volcanoclastic sediments which contain planktonic foraminifera of Middle Pliocene age (HUGHES, 1977). The lavas consist typically of zoned sodic bytownite and augite phenocrysts in a groundmass of andesine and augite microlites. Glass horizons are common within these lavas.

Utupua lies 65 km south-east of Nendö, and consists of a cone with a low-lying central crater of an extinct volcano. The rocks include inter-bedded ankaramitic porphyritic augite and olivine lavas with poorly porphyritic volcanoclastics, both of which have been intruded by dykes. The lava flows have red weathered upper surfaces which are indicative of subaerial deposition.

Vanikolo is a highly dissected volcanic complex formed of four coalesced volcanoes and includes porphyritic olivine augite basaltic lavas, volcanoclastics, sheet intrusions and dykes. Pillowed lavas are exposed on the coast, and probably represent the distal portions of subaerially erupted lava which flowed into the sea. The preservation of the Utupuan and Vanikolo volcanic forms suggest a possible Plio-Pleistocene age.

The Duff Islands are a chain of nine small islands situated about 145 km north-east of Nendö. The islands are formed of andesitic lavas, andesitic pyroclastic deposits and basaltic dykes. Agglomerates are common and grade into tuff beds, some of which are stratified. Most of the lava flows are massive but a few show pillowed structure.

Unlike Utupua and Vanikolo, no volcanic cone is preserved which suggests that the islands probably represent the uplifted remnants of an older, shallow submarine volcano of possible early Pliocene age.

Anuta is situated in the extreme eastern part of the Group. It is an eroded remnant of a once more extensive volcanic mass which remains as a shallow, submerged platform now around the island, and which resembles a flat-topped seamount in bathymetric pro-

file. The volcanic rocks include olivine and labradorite-phyric basaltic andesite lavas and lamprobolite-oligoclase, and augite oligoclase agglomerates.

Fatutaka is situated 35 km south-east of Anuta, and remains as an even smaller sub-aerial remnant of a once larger volcano. It is composed of labradoritic olivine basaltic andesite lavas with some agglomerates. Radiometric datings on two samples by JEZEK *et al.* (1977) give a reliable age of 2.2 my and an uncertain age of 12.5 my.

Tikopia is a small island definite Pleistocene age dated as 80,000 years B.P. by FRYER (1974). It is an extinct volcano, the central part of which has been enlarged by central collapse to form a pit crater whose south side has been breached. A slightly saline crater lake now occupies the centre of the island. The volcano is composite, with lava dominant over volcanoclastic material. The lavas are oligoclase augite andesites, but labradoritic olivine clasts dominate the agglomerates.

Tinakula is the only active volcano in the Group, and commenced eruption at least as early as 1595 (MARKHAM, 1904). The island has a subcircular outline, the slopes of which rise at an angle of 30° to the summit at 851 m. The composite cone consists of subaerial hypersthene andesitic lava and pyroclastic flows with olivine basalt clasts which have been intruded by labradoritic dolerite dykes. Fumerolic activity is continuous, but lava and pyroclastic flows are periodic.

Samples have only been collected from the *Vitiaz Trench*, in the east by FRYER (1974). These lava samples were dredged from the south-west wall, and all four samples show evidence of low grade metamorphism.

To summarise, five stages of volcanism can be recognized:

- 1) The earliest evidence of volcanism in the Group is that provided by the Oligocene lavas of Nendö.
- 2) A second stage is shown by Middle Miocene to early Pliocene lavas on Anuta and Fatutaka in the east of the Group.
- 3) Middle Pliocene volcanism represents the third stage, in which the Anuta-Fatutaka volcanism extended north-westerly to form the Duff Islands. Volcanism recommenced in the west by this time, as evidenced by the alkali basalt lavas on Nendö.
- 4) During the late Pliocene to Pleistocene, volcanism in the east ceased, with the late Fatutaka lavas dated at 2.2 my. Utupua and Vanikolo were produced in the west by a fourth stage of volcanism, which includes Tikopia at 80,000 years, in the central part of the area.
- 5) The final volcanic stage is that of the present day, in which Tinakula became, and still is, active.

The Eastern Outer Islands are situated upon a north-west extension of the submarine Fiji Plateau which lies beneath an average water depth of 3,600 m (MAMMERICKX *et al.*, 1971) (Fig. 2). This is bounded on the west side by the New Hebrides or Torres Trench, situated 95 km off the west coasts of Nendö, Utupua and Vanikolo. The trench is a narrow, elongate oceanic depression with a maximum depth of 6,955 m, and extends discontinuously southwards to the New Hebrides.

The north eastern limit of the area is marked by the south-east trending Vitiaz Trench, situated 270 km north east of Anuta, and with a maximum depth of 6,150 m. To the north, the area is limited by a shallower westerly extension of the Vitiaz Trench known as the Cape Johnson Trough, while the southern limit to the area is the Hazel Holme Fracture Zone, which extends eastwards from Espiritu Santo in the northern New Hebrides.

Individual islands in the group rise steeply from the floor of the Plateau and, with the



Fig. 2. Simplified bathymetric map of the Eastern Outer Islands region (MAMMERICKX *et al.*, 1971).

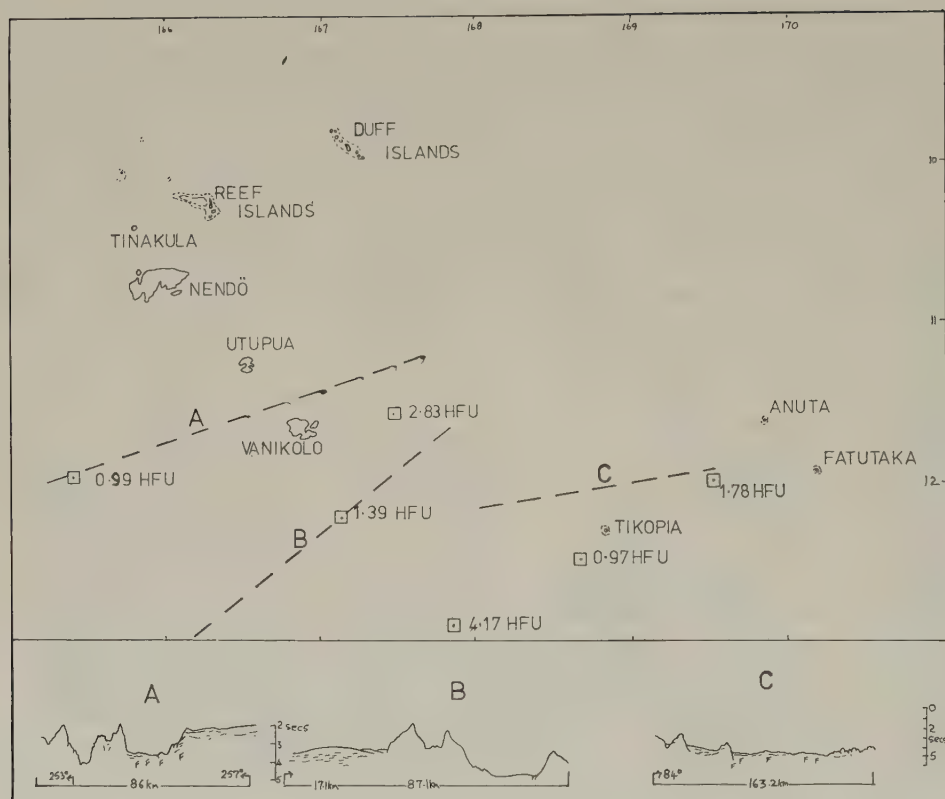


Fig. 3. Seismic reflection profiles and heat flow measurements (Luyendyk *et al.*, 1974; MACDONALD, 1973).

exception of Tinakula and Nendö, are not inter-connected by any well-defined submarine ridges. The Duff Islands are situated upon the crest of a single submarine ridge. Seismic reflection profiles carried out by LUYENDYK *et al.* (1974) (Fig. 3) reveal a rugged submarine relief along the western chain, especially in the vicinity of the Torres Trench.

The central part of the north Fiji Plateau (3rd profile) has a comparatively low relief, with sedimentary rocks disturbed only by minor faulting. The rather lobate features to the east possibly represent tightly folded sedimentary rocks resulting from compressional forces associated with the Vitiaz Trench.

This paper introduces the concept of two periodically active, converging subduction zones associated with the Torres and Vitiaz Trenches respectively, and combines previously unpublished geological data with geophysical data already published.

Rocks of basaltic composition have been analysed from all islands in the group, and include those rocks dredged from the Vitiaz Trench by FRYER (1974). Andesitic rocks display a more selective distribution, however, are found only on Tinakula, the Duffs, Tikopia and Anuta.

2.1 The basalts

Tholeiitic, high alumina and alkali basalts are recognized by their silica-alkali-

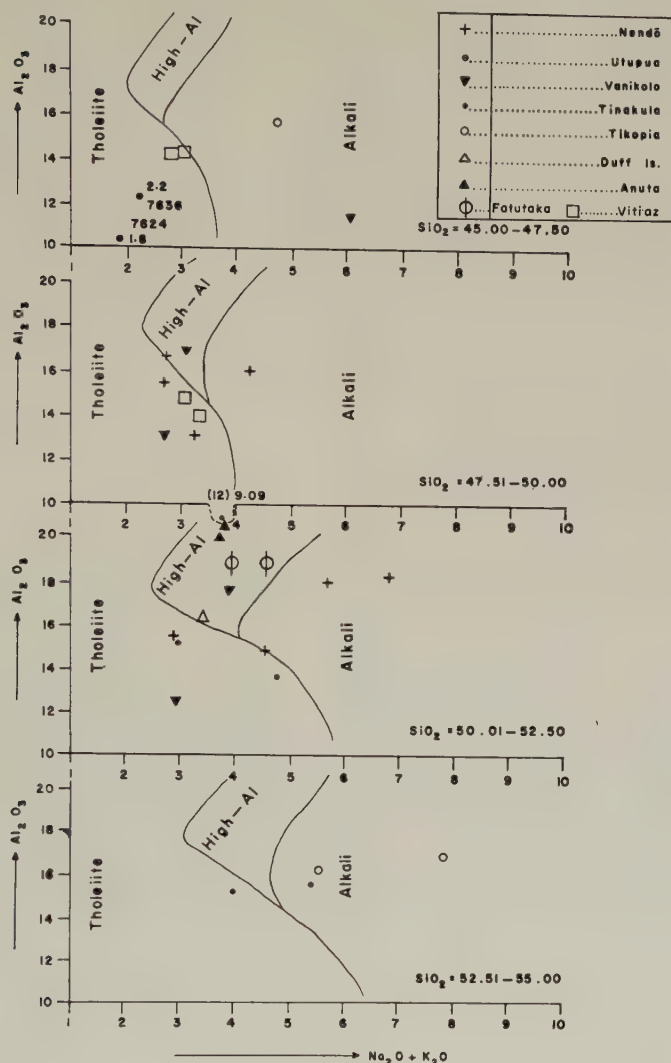


Fig. 4. KUNO's (1960) variation diagram for classification of the basaltic rocks from the Group.

alumina content on KUNO's (1960) variation diagram (Fig. 4). Two basaltic chemical compositions from the Duff Islands cannot be accommodated on Kuno's variation diagram however, and include a picrite basalt which is too low in silica, and a dyke rock which is too low in alumina.

Fourteen rocks fall into the field of tholeiitic basalt, ten of which come from the western island chain, the remaining four come from the Vitiaz Trench.

Nine rocks are here included within the alkali basalt type, and include six from the western chain and three from Tikopia. Whereas high alumina basalts are found exclusively in the Duffs, Anuta and Fatutaka samples, they are found with other basalt types on

Nendö and Vanikolo. All four basalt samples from Anuta and Fatutaka are notably high in alumina and exceed 19.20% Al_2O_3 .

2.2 The andesites

Andesites have not been found on Nendö, Utupua, nor Vanikolo, but have been found among rocks from the other islands. They are grouped as low-silica and high-silica andesites and dacites, following DICKINSON (1968)

Low-silica andesites contain between 55 and 60% silica, and include one from Tinakula and two from the Duff Islands.

High-silica andesites contain between 60 and 65% silica and include one from Tinakula, two from Tikopia and one from Anuta.

Dacitic rocks contain more than 65% silica, and include two from the Duff Islands, one from Tikopia and one from Anuta.

The distribution of analysed basaltic, andesitic and dacitic rock types in each island (Fig. 5) suggests a broad double trend in which predominantly tholeiitic basalts are found in the western chain of islands and also in the samples collected from the Vitiaz Trench. In the eastern chain and Tikopia, however, high alumina and alkali basalts are common, together with andesites and dacites. This pattern favours a situation in which both the Torres and Vitiaz subduction zones have contributed magmas at increasing stages of differentiation.

Figure 6 shows the relative variations in the range of weight per cent silica and average total iron in all analysed rocks, together with highest potash values in andesites. Islands of the western chain with the exception of Tinakula, together with Fatutaka and Vitiaz Trench samples show lowest silica range but highest total iron values. These proportions are reversed in the Duffs, Anuta, Tikopia and Tinakula, where highest silica range and lowest total iron values are found. Potash in the andesitic rocks displays higher values from the Duffs and Tikopia.

The overall pattern is one in which less mafic rocks are found in Tikopia in the central part of the region, and in the Duffs, both of which are situated almost mid-way between both trenches.

Three natural clusters are apparent on the AFM diagram (Fig. 7). One cluster indicates a trend towards magnesia enrichment, and includes samples from Nendö, Utupua and Vanikolo from the western chain with Anuta, Fatutaka and the Vitiaz Trench from the eastern chain.

The second cluster is a continuation of the first and shows a trend towards high alkali enrichment. Samples from Tikopia, the Duffs and Anuta are included within this suite.

Samples from Tinakula alone form the third cluster which shows a trend towards iron enrichment.

The most significant feature evident in the AFM diagram is that samples from the western chain, with the exception of Tinakula, plot within the same cluster as a number of samples from the eastern chain, and this coincidence is considered to suggest a similar petrogenesis. The trend towards alkali enrichment in some of the Duff Island, Anuta and Tikopia samples probably represents differentiation of the parent magma along the Vitiaz subduction zone.

The Tinakula samples exhibit a trend which originates in a parent magma which is common to most other islands in the Group, but which has become enriched in iron.

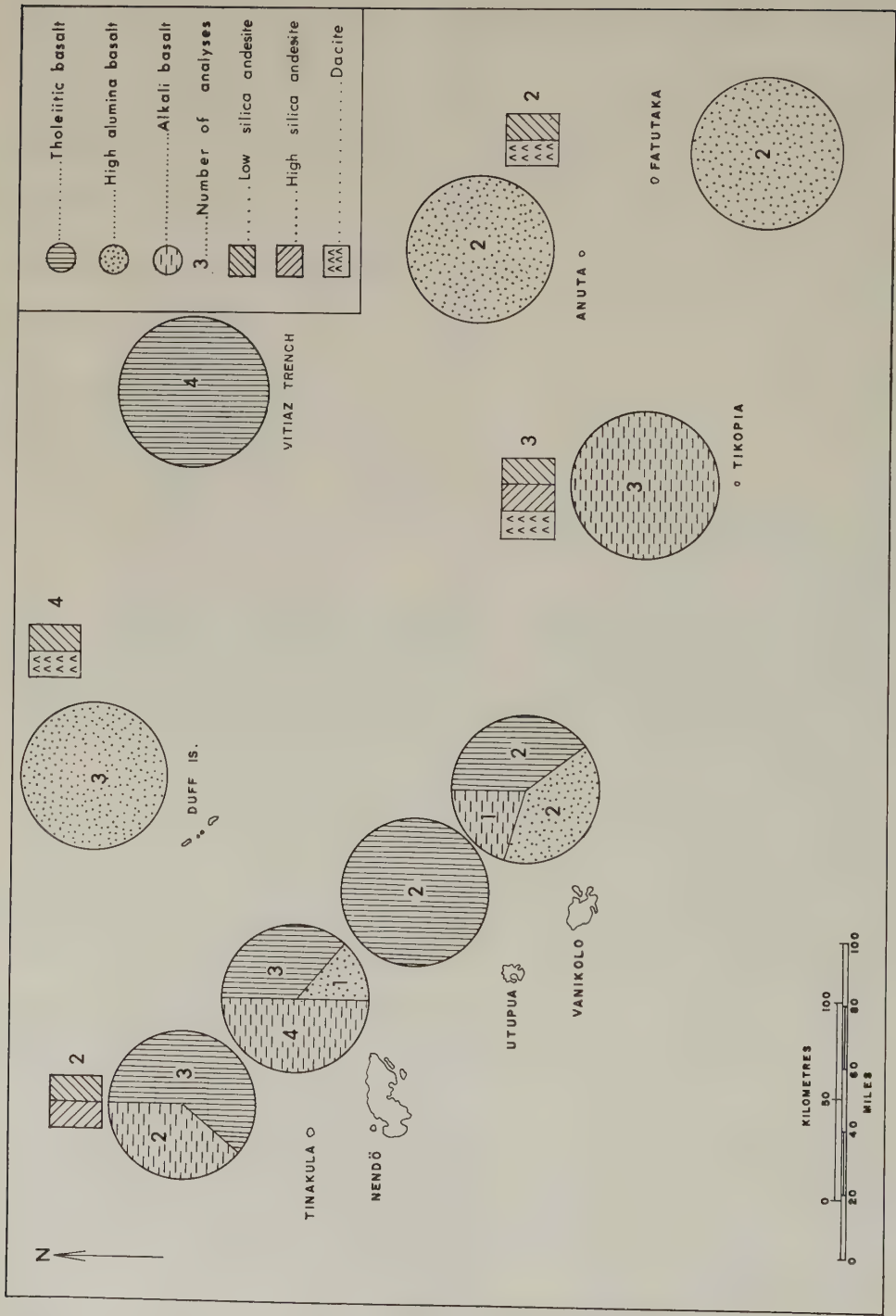


Fig. 5. Distribution of analysed basaltic, andesitic and dacitic rock types in each island.

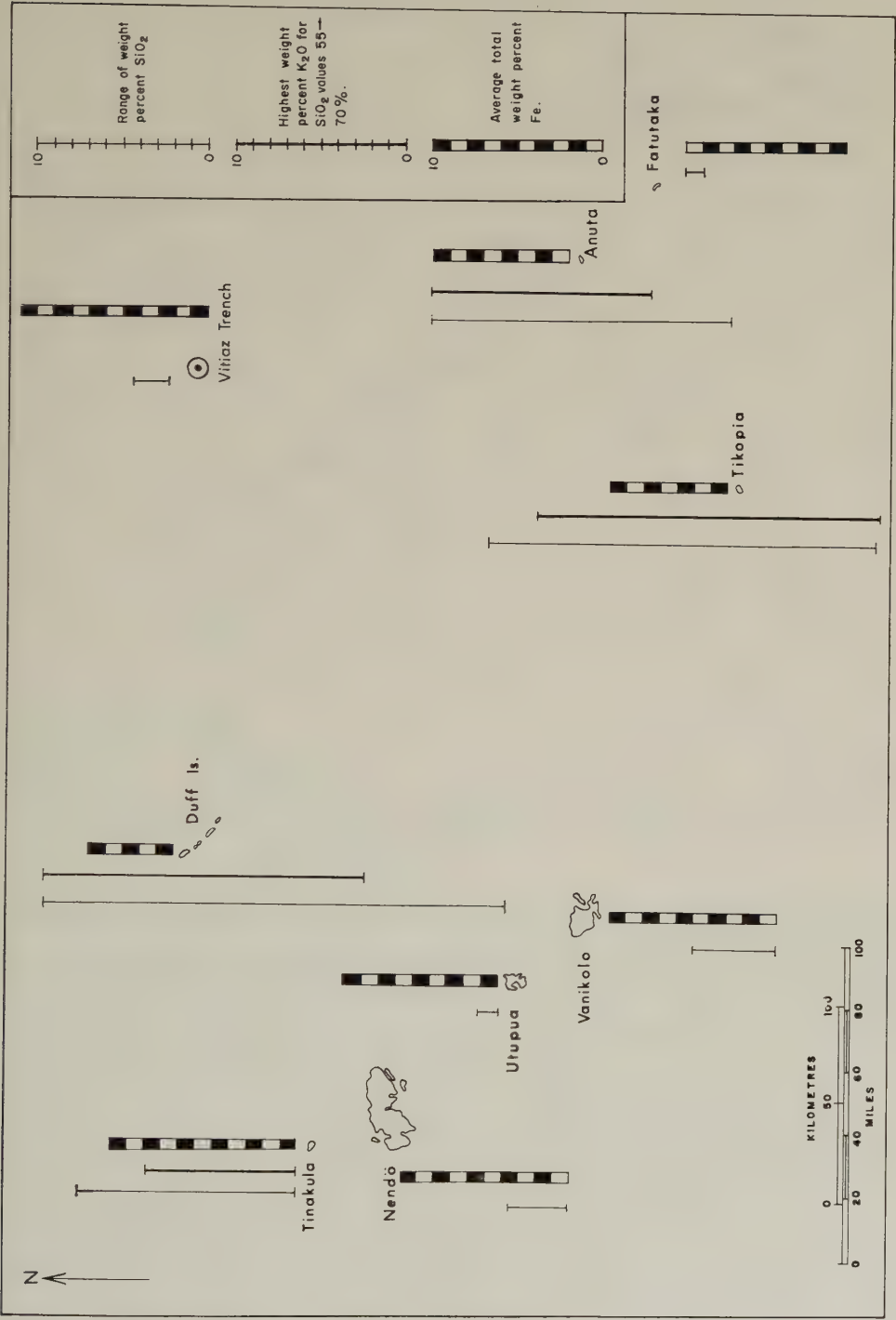


Fig. 6. Relative variations in the range of weight per cent silica, and average total iron in all analysed rocks, together with highest potash values in andesites, E.O.I. Group.

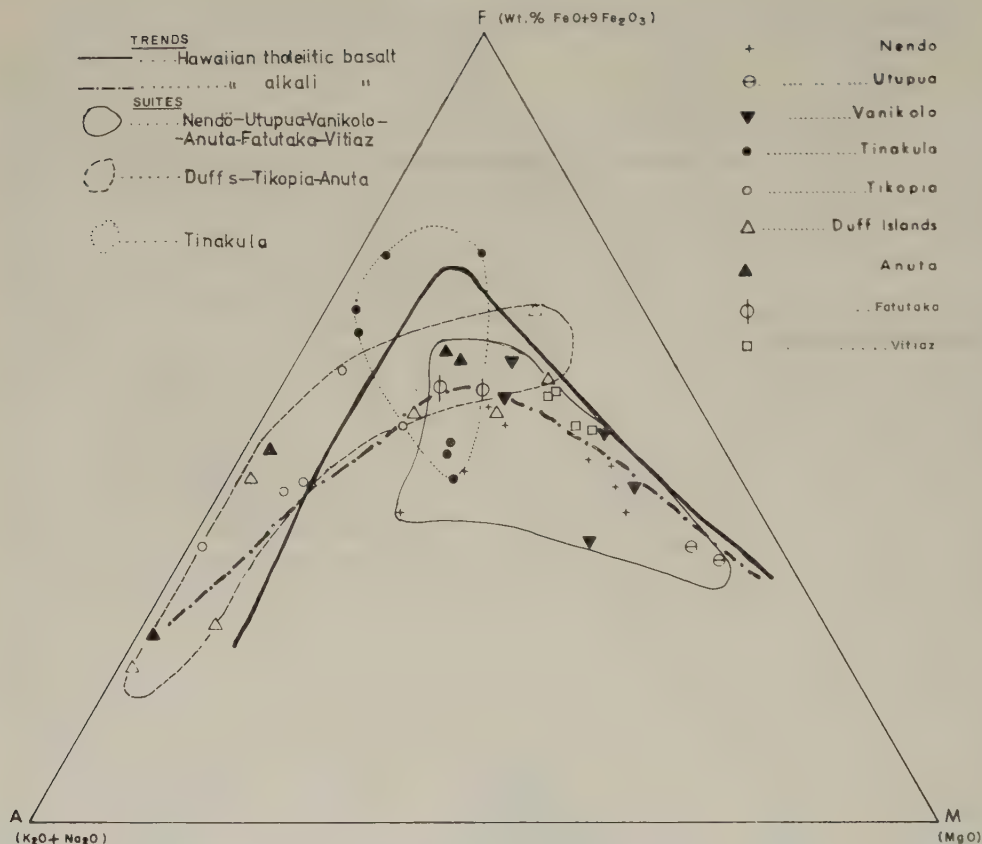


Fig. 7. AFM diagram illustrating calculated positions of all available analyses from islands in the E.O.I. Group.

Iron enrichment of rocks close to the Trench is attributed to early crystallization of olivine rather than magnetite (OSBORN, 1962).

Seismic data (Fig. 8) from the Eastern Outer Islands region clearly illustrate an increase in epicentre depth in relation to lateral distance north-eastwards away from the Torres Trench. This inclined plane of seismicity is considered to represent the inclined zone along which the oceanic floor lying south-west of Santa Cruz is being currently subducted in a north-easterly direction.

There are limited seismic data for the central part of the area except for a few deep epicentres situated south of Tikopia, and considered by Kroenke (personal communication) to represent a detached fragment of lithospheric material.

There is little seismic activity in the vicinity of the Vitiaz Trench, and available data indicate only one shallow epicentre in 1971 situated approximately 200 km north of Anuta. This evidence suggests that the Vitiaz Trench is a fossil trench associated with a subduction zone which recently became inactive.

Seismic velocities are high and LUYENDYK *et al.* (1974) suggest that the north Fiji Plateau consists of old oceanic lithosphere.



Fig. 8. Seismic data for the Eastern Outer Islands (D. Tuni, Seismological Division, Ministry of Natural Resources, Honiara, Solomon Islands).

Heat flow measurements north of the Hazel Holme Fracture Zone are generally lower than those to the south (MACDONALD, 1973) (Fig. 3).

The low heat within the Torres Trench is probably the result of depression of the isotherms by the downgoing slab of lithosphere combined with rapid sedimentation. The higher measurements from stations between Vanikolo and Tikopia are attributed to subduction beneath and behind the island arc. The low heat flow near Anuta agrees with the trend of decreasing heat flow with further distance away from the active Nendö-Vanikolo arc, but there is no evidence to suggest that subduction is currently taking place beneath and behind the Anuta-Fatutaka arc.

Magnetic trends are northerly, south of the fracture zone, but almost east-west in the north, as would be expected if the northern area was originally part of the Pacific Plate, and thus have an extrapolated late Cretaceous age.

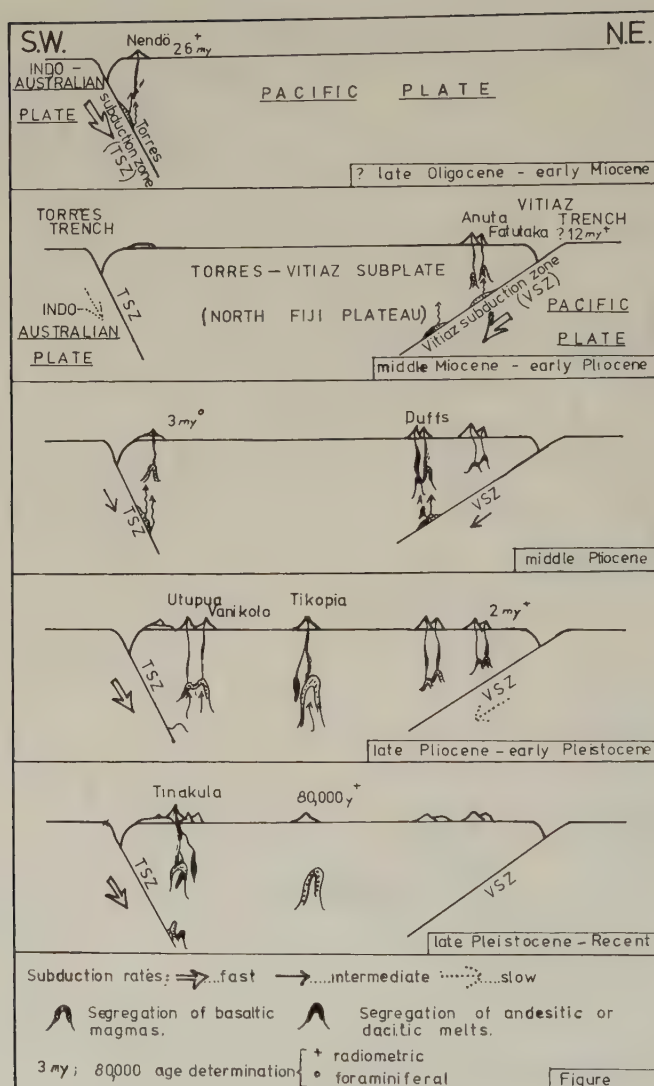


Fig. 9. Diagrams to illustrate a model depicting stages in the geological evolution of the E.O.I. Group.

3. Summary of Volcanic Stages

The five stages of volcanism described earlier can now be explained in terms of the petrochemical and geophysical evidence (Fig. 9).

Stage 1. The Oligocene to Lower Miocene tholeiitic basalts of Nendö provide the earliest evidence of volcanism within the group and have been radiometrically dated as 25 my old. This volcanic episode is linked to subduction of the Indo-Australian Plate beneath the western Pacific Plate, associated with the Torres Trench. GREENBAUM *et al.* (1975) have also described Oligocene to early Miocene volcanics from the Torres group

and CARNEY and MACFARLANE (in press) also suggest that easterly subduction at this time produced the western volcanic belt of the New Hebrides.

Stage 2. The Middle Miocene saw a new period of volcanism, which was situated in the eastern part, as evidenced by the 12.5 my old lavas on Fatutaka. This stage is attributed to the initiation of a new, westerly dipping subduction zone associated with the Vitiaz Trench, and which caused a simultaneous decline in Torres subductive activity. This caused part of the western Pacific Plate to be detached, and so form the north Fiji Plateau or Torres-Vitiaz subplate. Both Anuta and Fatutaka are considered to have been produced at this time, but unlike Nendö, tholeiitic lavas were not produced, and the presence of high alumina basalts and basaltic andesites is attributed to deeper melting (GREEN and RINGWOOD, 1968) or possibly more prolonged fractionation down a shallower subduction zone than that associated with the Torres Trench.

Stage 3. In the Middle Pliocene, evidence that the Torres subduction zone became active again is provided by the alkali basalt flows on Nendö which lie within sedimentary rocks which contain planktonic foraminifera of Middle Pliocene age. The Vitiaz subduction zone was still active, and probably produced the Duff Island high alumina basalt, with high silica andesite and dacite volcanism at this time.

Stage 4. This stage ranges from the late Pliocene to Pleistocene, in which the final stage of volcanism in the east is dated at 2.2 my on Fatutaka lavas. The reduction in Vitiaz subduction was compensated by strong volcanism, and renewed subduction, associated with the Torres Trench in the west. The basaltic volcanoes of Utupua and Vanikolo were produced close to the Torres Trench. The alkali basalts, low- and high-silica andesites with dacites, on Tikopia, and dated at 80,000 years by FRYER (1974) are evidence for extreme differentiation of the parent magma beneath the central part of the area. Tikopia is situated midway between both trenches, but evidence for its association with Torres subduction is the coincidence of simultaneous volcanism with Utupua and Vanikolo, and suggests that the Torres subduction zone was probably involved in its genesis.

Stage 5. This stage includes the present day, when volcanic activity is restricted to the island of Tinakula. Low- and high-silica andesitic lavas with tholeiitic and alkali basalt clasts are produced. The active easterly dipping seismic zone associated with the Torres Trench provides little doubt that Tinakula magmas are derived from melting along the Torres subduction zone. The present attitude of the Torres seismic zone has been examined by WEST WOOD (1970) whose results produce an angle of 60° for the seismic plane, which dips towards the north-east at N 70° E.

The active volcanoes of the southern Banks Islands, described by MALLICK and ASH (1975) are also considered to belong to this recent stage of volcanism.

4. Conclusions

1) Eastern Outer Islands are situated upon an interarc basin which is bordered by two recently active subduction zones.

2) Transfer of subduction from an original easterly direction to a later westerly direction and a final return to a presently active easterly direction was probably caused by differential rates of seafloor spreading in both the Indo-Australian and Pacific Plates. Another possible cause for cessation of westerly subduction may have been the approach of an unusually thickened portion of oceanic crust, similar to that of the Ontong Java Plateau; this mass may have effectively blocked, or choked, the Vitiaz subduction process.

3) Petrologic and petrochemical variations can be explained in terms of two main trends, each of which is related to partial melting of a common parent magma associated with subduction beneath the western and eastern island arcs respectively. Both trends, of decreasing maficity of lavas converge towards the central part of the area. Differentiation of the magma within asthenospheric diapirs, rising from the subduction zone, is considered to be responsible for the variation of lava types within most islands. The petrochemical variations agree well with the model suggested by the bathymetric and geophysical data.

4) Compressional stresses were also relieved by anticlockwise rotation of the Vitiaz arc, resulting in oblique subduction. This was eventually replaced by strike-slip faulting which sheared off the subducted plate. The Cape Johnson Trough probably represents a westerly extension of this shear zone.

5) Geophysical evidence does not provide evidence for crustal spreading but rather that the Eastern Outer Islands are rooted in a detached segment of Pacific floor of possible late Cretaceous age, and which is considerably older than that to the south of the Hazel Holme Fracture Zone.

6) The Torres and Vitiaz trenches are so far apart in the study area that the stages involved in the development of the Eastern Outer Island Group, combined with the model of two converging subduction zones, may possibly be used to reconcile models envisaged for both the main Solomons chain and also for the New Hebrides Group. Theories regarding the evolution of the Torres and Vitiaz island arcs have now therefore been combined to form a unified history for this part of the northern Fiji Plateau.

REFERENCES

- CARNEY, J.N. and A. MACFARLANE, Implications of a possible correlation between the late Tertiary geology of the New Hebrides and Fiji, (in press).
- DICKINSON, W.R., Circum-Pacific andesite types. *J. Geophys. Res.*, **73**, 2261–2269, 1968.
- FRYER, P., Petrology of some volcanic rocks from the Northern Fiji Plateau, *Geol. Soc. Am. Bull.*, **85**, 1717–1720, 1974.
- GREEN, D.H. and A.E. RINGWOOD, Genesis of the calc-alkaline igneous rock suite. *Contr. Mineral. Petrol.*, **18**, 105–162, 1968.
- GREENBAUM, D., D.I.J. MALLICK, and N.W. RADFORD, The geology of the Torres Islands. *Reg. Rep. New Hebrides Geol. Surv.*, 1–46, 1975.
- HUGHES, G.W. The geology and foraminiferal micropalaontology of the Lungga and Itina basin areas, W. Guadalcanal, Solomon Islands, Ph. D. Thesis, Univ. of Wales, 1977.
- HUGHES, G.W., P.M. CRAIG, and R.A. DENNIS, The geology of the Eastern Outer Islands, *Bull. 4, Sol. Is. Geol. Divn., Min. Natl. Res. Honiara*, (in press).
- JEZEK, P.A., W.B. BRYAN, S.E. HAGGERTY, and H.P. JOHNSON, Petrography, petrology and tectonic implications of Mitre Island, northern Fiji Plateau, *Marine Geol.*, **24**, 123–148, 1977.
- KUNO, H. High alumina basalt, *J. Petrol.*, **1**, 121–145, 1960.
- LUYENDYK, B.P., W.B. BRYAN, and P.A. JEZEK, Shallow structure of the New Hebrides Island Arc, *Geol. Soc. Am. Bull.*, **85**, 1287–1300, 1974.
- MACDONALD, K.C., Heat flow and plate boundaries in Melanesia, *J. Geophys. Res.*, **78**, 2537–2546, 1973.
- MALLICK, D.I.J. and R.P. ASH, Geology of the Southern Banks Islands, *Reg. Rep. New Hebrides Geol. Surv.*, 1–33, 1975.
- MAMMERICKX, J., T.E. CHASE, S.M. SMITH, and I.L. TAYLOR, *Map, Bathymetry of the South Pacific*, Calif. Scripps Inst. of Oceanography, 1971.
- MARKHAM, C.R. The voyages of Pedro Fernandez de Quiros, 1595–1606, *Hakluyt Soc. (London)*, **11**, 14–15, 1904.
- OSBORN, E.F., Reaction series for subalkaline igneous rocks based on different oxygen pressure conditions, *Am. Mineral.*, **47**, 211–226, 1962.
- WESTWOOD, J.V.B., Seismicity of the Solomon and Santa Cruz Islands, southwest Pacific, *J. Geol. Soc. Aust.*, **17**, 87–92, 1970.

UPPER MANTLE VELOCITY STRUCTURE IN THE NEW HEBRIDES ISLAND ARC REGION

K.L. KAILA and V.G. KRISHNA

National Geophysical Research Institute, Hyderabad, India

(Received April 25, 1978; Revised August 8, 1978)

Upper mantle velocity structure in the New Hebrides island arc region has been determined to a depth of 240 km from the analysis of P and S wave travel times of 39 deep earthquakes using KAILA's (1969) analytical method. The present analysis reveals a linear increase of P wave velocity from 8.06 km/sec at a 40-km depth to 8.19 km/sec at a 240-km depth with a gradient of only 0.06 ± 0.01 km/sec per 100 km. For S waves also, the velocity increases linearly from 4.55 km/sec at a 40-km depth to 4.64 km/sec at a depth of 220-km with a gradient of only 0.04 ± 0.02 km/sec per 100 km. The velocity gradients for P and S waves, from 40 to 240 km depth in the upper mantle beneath the New Hebrides arc are found to be extremely small as compared to those at similar depths in the adjacent Tonga-Kermadec-New Zealand region. Consequently, the P and S velocities, to a depth of 240 km, beneath the New Hebrides arc are found to be about 6% lower, on the average, than those in the Tonga-Kermadec-New Zealand region. This velocity difference is attributed primarily to very high upper mantle temperatures in the New Hebrides region which may be about 1,000°C higher than those in the Tonga-Kermadec-New Zealand region. An alternative explanation based on existence of high temperatures in this region is also presented which explains deep seismic activity at 600 km depth in the New Hebrides region without invoking the concept of a detached lithospheric slab proposed by some of the earlier workers.

1. Introduction

The New Hebrides island arc region in the southwest Pacific forms a belt of great seismic activity to intermediate depths extending from 10°S, 166°E to 24°S, 172°E and a belt of active volcanism is also associated with it. The intermediate depth earthquakes in this region occur along the northeasternly dipping New Hebrides seismic zone which appears as a plane dipping at about 30° at shallow depths and about 70° at intermediate depths (PASCAL *et al.*, 1973). There is a remarkable gap in seismic activity between depths of about 300–600 km in this region. Deep focus earthquakes with depths greater than 600 km are concentrated mainly in a region northeast of the New Hebrides arc although a very few deep earthquakes have also occurred in the southern part of the New Hebrides arc. However, the deep earthquake activity in this region is very limited. BARAZANGI *et al.* (1973) studied the seismic wave propagation beneath the New Hebrides island arc and interpreted the gap in seismic activity between deep and intermediate depth earthquakes at the northern part of the arc as corresponding to a gap in the lithospheric slab descending beneath the arc. They interpreted the deep earthquakes occurring in the northeastern region of the arc as representing a detached piece of lithosphere. PASCAL *et al.* (1973) found that the observed travel time residuals along the New Hebrides arc can be explained by P travel times computed for a velocity model which includes a 6% higher velocity relative to a normal mantle inside a dipping lithospheric slab 300 km deep, a 6%

higher velocity inside a detached slab at a depth of 600 km, and a 4% lower velocity in the wedge of the mantle above the inclined seismic zone. However, these are only the estimates of relative differences of the velocity structure in different parts of the upper mantle and the actual velocity structure as a function of depth, for P and S waves, is not well known in the New Hebrides island arc region. In the present study, we have determined the upper mantle velocity structure to a depth of 240 km in the inclined seismic zone beneath the New Hebrides island arc region from the analysis of P and S wave travel times. The resulting velocity functions for P and S waves are compared with those determined by KAILA and KRISHNA (1978) for the Tonga-Kermadec-New Zealand region and also with the velocity functions for various regions of the earth determined by other workers. The gross differences in the velocity structure between the New Hebrides island arc and

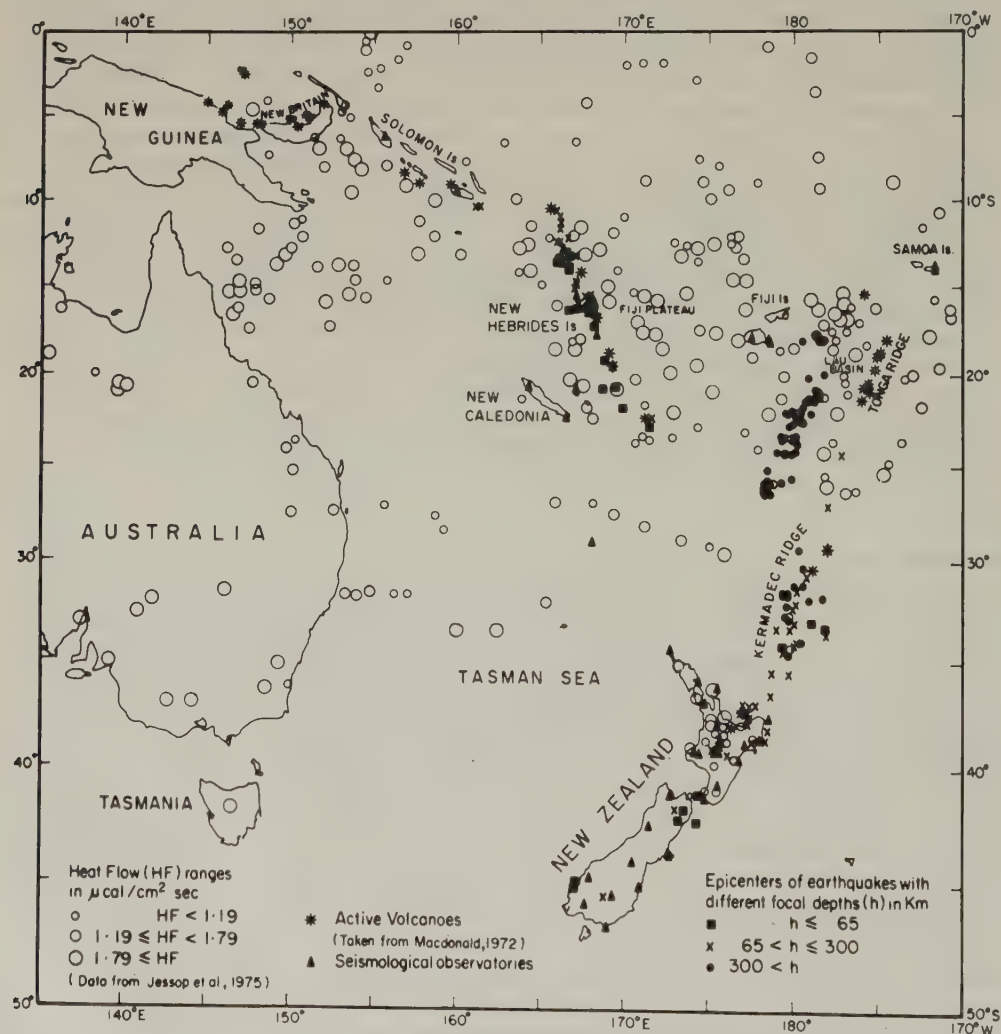


Fig. 1. Map of the southwest Pacific region showing the seismicological observatories and epicenters of earthquakes in the New Hebrides region used in the present study. Epicenters of earthquakes used by KAILA and KRISHNA (1978) for determining the upper mantle velocity structure in the Tonga-Kermadec-New Zealand region are also shown.

Table 1. Earthquake epicentral data.

Earth- quake No.	Date	Time			Epicenter		Focal depth (km)
		(h)	(m)	(s)	Latitude (deg)	Longitude (deg)	
1	Mar. 4, 1964	03	17	23.6	20.67S	168.59E	36
	Nov. 20, 1961	11	44	21.0	21.81S	169.88E	36
3	Oct. 21, 1964	10	08	46.7	14.10S	166.70E	37
4	Feb. 7, 1964	23	12	52.8	19.24S	168.70E	38
5	Sept. 16, 1963	20	05	23.0	13.39S	166.53E	40
6	Nov. 3, 1964	17	07	41.8	22.80S	171.50E	41
7	June 6, 1964	02	14	11.0	16.20S	167.10E	41
8	Jan. 27, 1964	05	06	59.7	13.04S	166.60E	41
9	Sept. 6, 1960	14	03	01.0	20.57S	169.35E	44
10	Aug. 10, 1964	14	44	40.8	14.00S	166.70E	44
11	Feb. 18, 1964	01	31	18.7	16.32S	166.74E	50
12	Jan. 22, 1964	23	59	45.3	13.64S	165.96E	50
13	June 10, 1964	11	53	31.0	17.16S	168.10E	52
14	Dec. 24, 1963	11	18	15.0	13.17S	166.72E	53
15	Nov. 6, 1961	05	28	26.0	13.38S	166.14E	63
16	Apr. 17, 1964	14	44	21.3	16.19S	167.50E	66
17	Dec. 28, 1961	23	55	54.0	12.38S	166.16E	69
18	June 22, 1964	03	03	38.1	10.34S	161.11E	74
19	Nov. 11, 1962	16	09	58.0	12.88S	166.41E	75
20	Aug. 22, 1961	08	59	32.0	13.49S	166.46E	79
21	Aug. 9, 1964	05	30	47.5	10.27S	161.30E	86
22	Apr. 28, 1964	15	11	33.2	12.44S	166.01E	87
23	Mar. 27, 1964	08	01	31.0	11.55S	166.20E	96
24	Nov. 21, 1964	06	19	16.0	14.85S	167.24E	97
25	July 2, 1962	08	32	42.0	10.58S	165.99E	98
26	Apr. 3, 1964	19	08	16.5	15.03S	167.04E	99
27	May 2, 1964	10	55	59.4	14.84S	167.23E	102
28	July 15, 1964	08	24	53.6	11.34S	166.24E	103
29	May 22, 1962	08	06	38.0	12.24S	166.66E	121
30	Oct. 5, 1964	13	12	13.9	22.36S	171.65E	130
31	June 26, 1964	05	20	04.2	15.68S	167.79E	135
32	July 11, 1964	17	32	16.7	15.54S	167.68E	140
33	Oct. 24, 1964	22	06	07.8	16.00S	167.20E	141
34	Oct. 21, 1961	17	34	34.0	10.91S	166.19E	164
35	May 27, 1964	00	54	50.8	15.52S	167.99E	166
36	July 16, 1962	09	25	58.0	13.16S	167.07E	204
37	Dec. 5, 1961	13	02	37.0	16.35S	167.85E	205
38	Apr. 19, 1962	22	15	24.0	15.92S	167.92E	223
39	Sept. 1, 1962	04	52	14.0	15.81S	168.11E	238

the Tonga-Kermadec-New Zealand region are interpreted in terms of large lateral temperature variations prevailing even at great depths in the mantle beneath the two oppositely dipping seismic regions. Probable physical and thermal properties of the upper mantle in the New Hebrides region are discussed which provide an alternative explanation for the existence of deep seismic activity at 600 km depth that has been interpreted by some of the workers (BARAZANGI *et al.*, 1973; PASCAL *et al.*, 1973) as an evidence for a detached piece of lithospheric slab.

2. Data Analysis and Results

Thirty-nine shallow and intermediate depth earthquakes are selected in the seismic

region of the New Hebrides for determining the upper mantle velocity structure in the inclined seismic zone beneath this region. P and S wave travel times and epicentral distances (Δ) are taken from the bulletins of the International Seismological Summary (ISS) for the period 1960–1963 and from the bulletins of the International Seismological Center (ISC) for the year 1964. The epicenters of all the earthquakes in the New Hebrides region used in the present study along with the seismograph stations are shown in Fig. 1. The epicentral data for all the earthquakes is also given in Table 1.

For obtaining the velocities at various depths in the seismic zone beneath New Hebrides island arc, we have analysed the P and S wave travel times of all the earthquakes listed in Table 1 by making use of KAILA's (1969) analytical method. The epicentral distance limits Δ_1 and Δ_2 , between which $p(=\partial T/\partial \Delta)$ is considered to remain stationary, are however not determined from the data for various earthquakes used in the present study. Instead, we have made use of the Δ_1 and Δ_2 curves plotted as functions of focal depth given by KAILA *et al.* (1971, Fig. 9 for P waves and 1974, Fig. 7 for S waves) for obtaining the Δ_1 and Δ_2 limits in each case, because in our opinion these estimates of Δ_1 and Δ_2 for various focal depths are quite accurate within the error limits and that they do not affect significantly the final velocity estimates. The travel time data available between the two limits is fitted by a least squares line in each case which yields the apparent $p(=\partial T/\partial \Delta)$ and the $a(=T-p\Delta)$ values with their standard deviations. The least squares fits

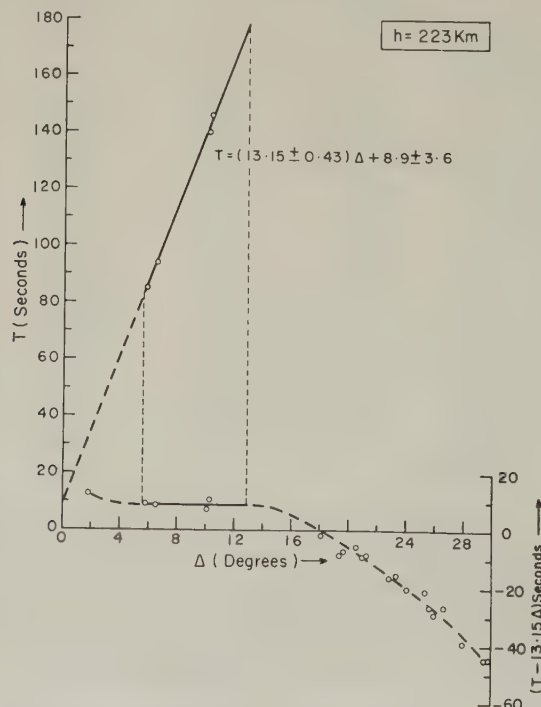


Fig. 2. P wave travel time curve T versus Δ for earthquake with focal depth 223 km between the limits Δ_1 and Δ_2 of epicentral distance. Reduced travel time curve $(T - p\Delta)$ versus Δ is also shown where $p = \partial T / \partial \Delta$ at the inflection point.

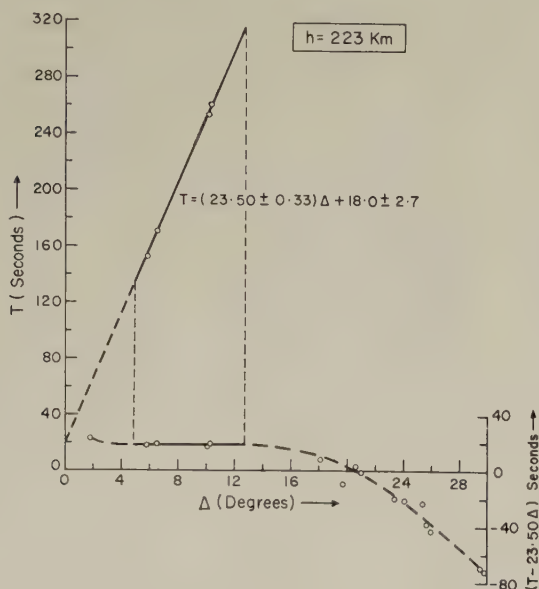


Fig. 3. S wave travel time curve T versus Δ for earthquake with focal depth 223 km between the limits Δ_1 and Δ_2 of epicentral distance. Reduced travel time curve $(T - p\Delta)$ versus Δ is also shown where $p = \partial T / \partial \Delta$ at the inflection point.

obtained for $T-\Delta$ points between the Δ_1 and Δ_2 limits for one specimen earthquake with focal depth 223 km are shown in Figs. 2 and 3 for P and S waves respectively. In the same figures are also shown the plots $(T - p\Delta)$ versus Δ . Using the apparent p values, the true velocities and their standard deviations are computed for each focal depth analysed. It may be mentioned here that the method of analysis adopted in the present study has the greatest advantage that we are able to determine the velocity for P and S waves at the hypocenter of each earthquake thus avoiding completely the effect of the travel path to different stations. Since all the earthquake hypocenters used in the present study are in the inclined seismic zone, the final velocity function resulting on the basis of all these velocity estimates will represent precisely the velocity structure in the inclined seismic zone beneath the New Hebrides island arc. The final results obtained for the p values and velocities with their standard deviations are given in Table 2 for both P and S waves.

The true velocities and the a values thus obtained at various depths are plotted as parts (a) and (b) respectively in Fig. 4 for P waves and in Fig. 5 for S waves. In these figures the velocity-depth and the a value-depth points are shown by circles and the truncated horizontal bars with them indicate the standard deviations of the plotted points. The velocity-depth points and the a value depth points, for both P and S waves, are fitted by straight lines using the method of least squares and are shown by thick lines in Figs. 4 and 5. The broken lines bounding these straight line fits represent the 95% confidence limits of the slopes in each case.

The velocity functions thus determined in the New Hebrides region reveal very small linear increase of velocity with depth for both P and S waves (Figs. 4a and 5a respectively). The velocity for P waves determined as 8.06 km/sec at a 40 km depth increases linearly to 8.19 km/sec at a depth of 240 km with a mild velocity gradient of only 0.06 ± 0.01 km/sec

Table 2. P and S wave true velocities V_P and V_S respectively as functions of depth (h) for the New Hebrides region as determined in the present study.

Earth-quake No.	h (km)	P waves			S waves		
		p (apparent) (sec/deg)	V_P (km/sec)	a_P (sec)	p (apparent) (sec/deg)	V_S (km/sec)	a_S (sec)
1	36	14.04 ± 0.51	7.91 ± 0.29	1.9 ± 1.8	—	—	—
2	36	—	—	—	25.03 ± 2.41	4.44 ± 0.43	11.9 ± 10.6
3	37	13.45 ± 0.44	8.25 ± 0.27	7.7 ± 3.1	—	—	—
4	38	13.73 ± 0.13	8.09 ± 0.08	5.1 ± 0.5	—	—	—
5	40	13.88 ± 0.49	8.00 ± 0.28	4.8 ± 3.2	—	—	—
6	41	14.06 ± 0.37	7.89 ± 0.21	4.1 ± 2.4	—	—	—
7	41	13.74 ± 0.34	8.08 ± 0.20	4.6 ± 2.0	25.77 ± 1.3	4.31 ± 0.23	—
8	41	13.63 ± 0.49	8.14 ± 0.29	6.7 ± 3.2	—	—	—
9	44	14.05 ± 0.30	7.90 ± 0.17	3.6 ± 1.7	—	—	—
10	44	—	—	—	23.41 ± 0.82	4.74 ± 0.17	15.7 ± 5.5
11	50	13.77 ± 0.42	8.05 ± 0.25	2.9 ± 1.9	—	—	—
12	50	13.65 ± 0.46	8.12 ± 0.28	4.1 ± 3.3	—	—	—
13	52	13.38 ± 0.41	8.28 ± 0.26	8.1 ± 2.6	—	—	—
14	53	13.93 ± 0.30	7.95 ± 0.17	4.1 ± 2.0	—	—	—
15	63	—	—	—	24.35 ± 1.02	4.54 ± 0.19	15.5 ± 7.3
16	66	13.29 ± 0.70	8.32 ± 0.44	6.6 ± 3.8	—	—	—
17	69	13.23 ± 0.16	8.35 ± 0.10	—	—	—	—
18	74	13.67 ± 0.10	8.08 ± 0.06	5.4 ± 1.0	—	—	—
19	75	13.57 ± 0.35	8.13 ± 0.21	5.4 ± 2.6	—	—	—
20	79	13.31 ± 0.49	8.29 ± 0.31	7.6 ± 3.5	—	—	—
21	86	14.10 ± 0.26	7.82 ± 0.15	—	—	—	—
22	87	—	—	—	24.10 ± 0.16	4.57 ± 0.03	11.6 ± 1.2
23	96	13.97 ± 0.49	7.88 ± 0.28	—	—	—	—
24	97	—	—	—	23.34 ± 1.29	4.71 ± 0.26	13.1 ± 7.6
25	98	13.70 ± 0.58	8.03 ± 0.34	5.3 ± 5.3	23.69 ± 1.0	4.64 ± 0.22	10.8 ± 8.8
26	99	14.13 ± 0.18	7.78 ± 0.10	2.0 ± 1.4	—	—	—
27	102	—	—	—	23.39 ± 0.72	4.70 ± 0.15	14.3 ± 4.3
28	103	13.13 ± 0.29	8.37 ± 0.19	9.1 ± 2.3	24.01 ± 0.37	4.58 ± 0.07	11.2 ± 2.6
29	121	13.28 ± 0.49	8.25 ± 0.31	7.9 ± 4.0	—	—	—
30	130	13.31 ± 0.63	8.22 ± 0.39	8.3 ± 4.6	—	—	—
31	135	13.80 ± 0.61	7.92 ± 0.35	5.1 ± 3.6	—	—	—
32	140	13.72 ± 0.45	7.96 ± 0.27	4.4 ± 3.2	—	—	—
33	141	13.53 ± 0.51	8.07 ± 0.31	7.2 ± 4.0	—	—	—
34	164	13.37 ± 0.03	8.14 ± 0.02	7.5 ± 0.3	—	—	—
35	166	13.46 ± 0.08	8.08 ± 0.05	6.7 ± 0.6	23.42 ± 0.95	4.64 ± 0.19	17.3 ± 7.4
36	204	13.41 ± 0.33	8.06 ± 0.20	6.0 ± 3.1	—	—	—
37	205	—	—	—	23.78 ± 1.45	4.55 ± 0.28	17.1 ± 12.0
38	223	13.15 ± 0.43	8.19 ± 0.28	8.9 ± 3.6	23.50 ± 0.33	4.59 ± 0.07	18.0 ± 2.7
39	238	12.76 ± 0.26	8.43 ± 0.18	12.4 ± 2.2	—	—	—

per 100 km. On the other hand the S wave velocity from 40 to 220 km depth, increases linearly from 4.55 km/sec to 4.64 km/sec again with a very mild velocity gradient for S waves of only 0.04 ± 0.02 km/sec per 100 km.

3. Discussion

Upper mantle velocity structure for P and S waves in the New Hebrides island arc region as determined in the present study and shown as parts (a) and (b) in Fig. 6 is compared with the upper mantle velocity structure in the Tonga-Kermadec-New Zealand region determined by KAILA and KRISHNA (1978). Upper mantle velocity structure in

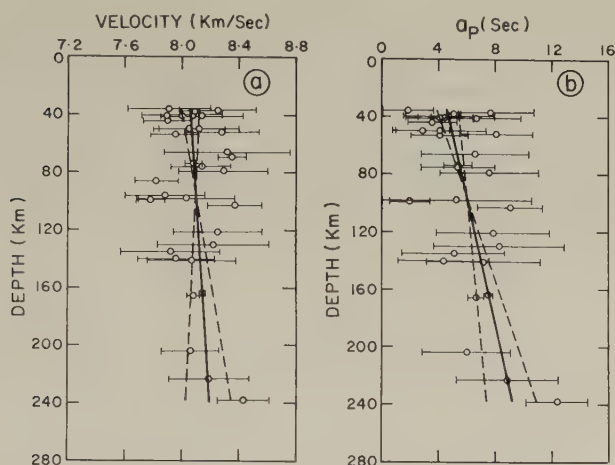


Fig. 4. (a) P wave velocity versus depth curve for the New Hebrides region. (b) $a_P (= T - p\Delta)$, at the inflection point, versus depth as a calibration curve for earthquake focal depth determination from P wave data in the New Hebrides region. In both figures — are the least squares fits obtained for the plotted points shown by \circ and --- are the 95% confidence limits of their slopes. Truncated horizontal bars represent the standard deviations in the velocity and a_P values.

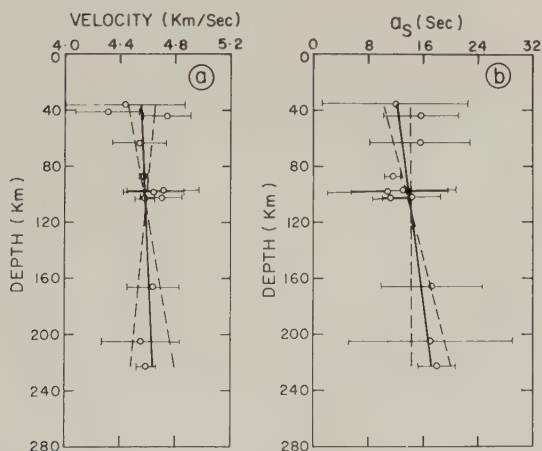


Fig. 5. (a) S wave velocity versus depth curve for the New Hebrides region. (b) $a_S (= T - p\Delta)$, at the inflection point, versus depth as a calibration curve for earthquake focal depth determination from S wave data in the New Hebrides region. In both figures — are the least squares fits obtained for the plotted points shown by \circ and --- are the 95% confidence limits of their slopes. Truncated horizontal bars represent the standard deviations in the velocity and a_S values.

other regions of the earth due to KAILA *et al.* (1971, 1974), JEFFREYS (1939), SIMPSON *et al.* (1974) for P waves and HELMBERGER and ENGEN (1974) for S waves are also included in these figures for comparison. The P and S velocities at the top of the mantle in the New Hebrides seismic region as determined in the present study are 8.06 and 4.55 km/sec respectively. SHOR *et al.* (1971) from seismic refraction studies in the Melanesian Borderland along profile CD south of New Hebrides island and New Caledonia found P_n velocities of 7.8 km/sec under the Fiji plateau, and 7.7 to 8.0 km/sec under the Norfolk ridge. Our P velocity value of 8.06 km/sec at 40 km depth in the New Hebrides region is quite consistent with these findings.

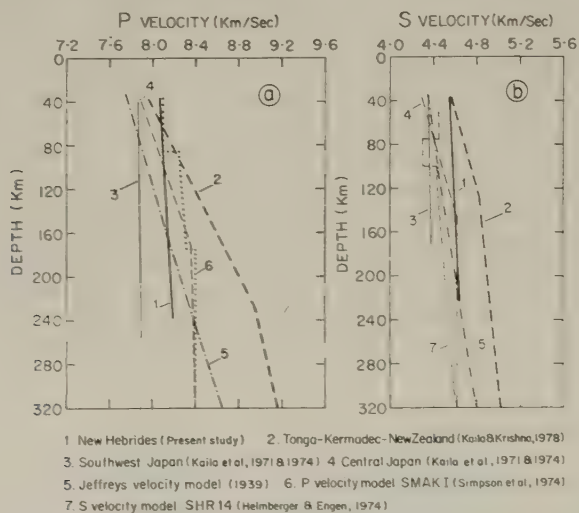


Fig. 6. (a) P wave and (b) S wave velocity functions in the New Hebrides island arc region as determined in the present study alongwith velocity models for other regions of the Earth.

The most remarkable feature that can be noticed from Fig. 6 is the gross differences in the velocity structure between the two oppositely dipping inclined seismic zones, beneath the New Hebrides island arc and the Tonga-Kermadec-New Zealand regions. It can be seen from Fig. 6 that although P and S velocities at the top of the mantle in the New Hebrides region are comparable with the P and S velocities at the top of the mantle in the Tonga-Kermadec-New Zealand region, with increasing depth the velocity functions in the two regions show increasing divergence, the velocities in the Tonga-Kermadec-New Zealand region being substantially larger. At a depth of 240 km, the P velocity in the Tonga-Kermadec-New Zealand region is about 10% higher than that in the New Hebrides region at the same depth. Similarly, at a depth of 220 km, the S velocity in the Tonga-Kermadec-New Zealand region is also 6 to 7% higher than that in the New Hebrides region at a similar depth. We attribute this gross difference in the velocity structure between these two seismic regions of the southwest Pacific to large lateral temperature differences in the upper mantle extending to considerable depths. The velocities of both P and S waves are strongly affected by changes in pressure, temperature and chemical and mineralogical composition which may possibly extend to great depths. Inside the

earth both temperature and pressure increase with depth. The temperature gradient may be highly variable from place to place whereas the pressure gradient can be considered to be almost constant over various regions. The degree of compositional variation and its likely effect on the velocity structure in the two adjacent New Hebrides and the Tonga-Kermadec-New Zealand regions can be safely assumed to be negligible, the velocities in the uppermost mantle in the two regions being almost similar. Therefore the only possible explanation that can satisfactorily account for the gross difference in the velocity structure in the two regions, in our opinion, is the temperature differences prevailing in the upper mantle. The measurements of high temperature and pressure derivatives of elastic constants for a number of compounds appropriate for geophysical considerations as reported by ANDERSON *et al.* (1968) indicate that a temperature contrast of the order of 1,000°C is needed to account for a 6% difference in the observed P velocities. Since, in the depth range from 40 to 240 km, the average P velocity difference between the New Hebrides and the Tonga-Kermadec-New Zealand regions is also about 6%, we therefore infer that there may be a temperature difference of about 1,000°C between these two regions in this depth range. At a depth of 240 km, the temperature contrast required may be even much larger between the two regions to produce the observed 10% P velocity contrast at the pressures prevailing at that depth. However, it is quite possible that this temperature excess in the New Hebrides region, may cause a partial melting which would also decrease the velocity. KANAMORI (1968) found that a 2% partial melting would cause about 1% velocity decrease using the equation $V = V_0(1 - 0.58c)$ given by HASHIN (1962), where V is the P velocity in a material having a liquid inclusion of concentration c and V_0 is the velocity for $c=0$. Thus some component of the velocity contrast between the two regions, the New Hebrides and the Tonga-Kermadec-New Zealand may be also attributable to partial melting in the New Hebrides region and consequently the temperature contrast between the two regions may be somewhat smaller. It is therefore these high temperatures in the New Hebrides region which are primarily controlling the velocity gradients and thus keeping the P velocities more or less constant to a depth of 240 km.

Let us now investigate whether these large lateral temperature variations in the upper mantle between the New Hebrides and the Tonga-Kermadec-New Zealand regions will in any way correlate with the observed heat flow in the two regions. In Fig. 1, we have also shown the heat flow observations in the southwest Pacific region compiled by JESSOP *et al.* (1976). We have, however, classified the heat flow values only into 3 ranges as shown in Fig. 1, instead of 5 ranges given by JESSOP *et al.* (1976). It can be seen from Fig. 1 that the average observed heat flow value in the eastern north island of New Zealand and in the Tonga-Kermadec deep earthquake zone is much smaller than that in the New Hebrides seismic zone. Thus the distribution of the observed heat flow in the two regions is also quite consistent with our idea that the temperatures in the New Hebrides region are much larger than those in the Tonga-Kermadec-New Zealand region. These high temperatures in the New Hebrides region may also imply that the mantle material in this region down to at least 240 km is probably in a partially molten state and the chain of active volcanoes also nicely correlates with this idea (see Fig. 1).

In Fig. 6 we have also shown the P and S velocity functions for the southwest and central Japan regions determined by KAILA *et al.* (1971 and 1974). It is very interesting to note that the difference in the velocity structures between the southwest Japan and the central Japan regions is quite similar to that found by us between the New Hebrides and the Tonga-Kermadec-New Zealand regions. The velocity in the southwest Japan region

almost remains constant to the depth studied, about 255 km for P waves and about 170 km for S waves. On the other hand, although the velocities at the top of the mantle in the southwest and central Japan regions are comparable, the velocities of both P and S waves in the central Japan region increase with high velocity gradients in this depth range. Thus the velocity functions in the southwest and central Japan regions also show increased divergence with increasing depths. In our opinion, these velocity anomalies are also caused by only large lateral temperature contrasts between the southwest and the central Japan regions. KAILA *et al.* (1971, 1974) interpreted the constant P and S velocities in the upper mantle beneath the southwest Japan region as due to relatively high volcanic activity and probable existence of large magma chamber extending to about 250 km depth beneath southwest Japan.

If we compare the velocity structure in the New Hebrides and the southwest Japan regions we can find that although the velocities remain constant in both the regions, the velocities in the southwest Japan region are about 3% lower for P waves and about 4% lower for S waves than those in the New Hebrides region. This may imply that the temperature at the top of the mantle beneath the New Hebrides may be smaller than that in the southwest Japan region. However, the temperature gradients in the two regions may be comparable because the velocities remain almost constant upto about 240 km. Of course, we cannot rule out the possibility that some component of the observed velocity anomaly between these two regions, the New Hebrides (in the southwest Pacific) and the southwest Japan may be also due to some compositional change, the two regions being so wide apart. However, the compositional change, even if it exists to some extent in the uppermost mantle immediately below Moho, may not be able to account for the observed velocity anomaly at large depth, which can be only explained by temperature differences between the two regions.

JEFFREYS (1939) velocity curves for both P and S waves are also shown in Fig. 6. The P velocities in the New Hebrides region to a depth of about 160 km are found to be comparatively higher and they are somewhat lower between 160 to 240 km than those given by JEFFREYS (1939). On the other hand, the S velocities are also relatively higher in the New Hebrides region than those given by JEFFREYS (1939) throughout the depth range of 220 km studied. The P velocity model SMAK I for northeastern Australia given by SIMPSON *et al.* (1974) also reveals very small velocity gradient comparable with the P velocity gradient for the New Hebrides region determined in the present study. It may be mentioned here, that the source region involved in deriving the SMAK I model is New Guinea, New Britain and Solomon islands region which is also an active volcanic region and a region of high heat flow (see Fig. 1) as the New Hebrides region. These observations again substantiate our idea that the temperatures may be considerably higher in these regions therefore the velocity gradients in both the regions are very small. In fact the mantle material in the entire region, beneath the New Hebrides, Solomon islands, New Britain and the New Guinea regions may be in a partially molten state as evidenced by intense volcanism and high observed heat flow in these regions. Therefore, the velocity gradients in these regions are extremely small. However, since some correction to remove the source effect to some extent, is applied by SIMPSON *et al.* (1974) the SMAK I model is therefore revealing somewhat higher velocities than our P velocity curve for the New Hebrides region in the depth range from 90 to 240 km. BROOKS (1962) determined P velocities to a depth of 500 km in the New Guinea-Solomon Islands region from the analysis of travel times using GUTENBERG's (1953) graphical method, and presented evidence

for the existence of a low velocity zone in the region. According to him, the minimum velocity reached may be as low as 7.6 km/sec at a depth of about 150 km and the decrease in velocity in that region is much more pronounced than reported by other workers and that shadow zones for the arrival of direct P waves exist in the area. The S velocity model SHR 14, given by HELMBERGER and ENGEN (1974), applicable for the western United States has a low velocity layer between depths of 80 to 100 km and it reveals somewhat lower velocities than our S velocity curve for the New Hebrides region.

DUBOIS *et al.* (1973) from the study of P and S times from shallow earthquakes between the New Hebrides and Fiji found that in the centre of the Fiji plateau the velocities for P and S waves in the uppermost mantle are 7.70 and 4.30 km/sec respectively. They have also found that along the seismically active margins of the plateau P velocities are only 7.30–7.40 km/sec. According to DUBOIS *et al.* (1973) the zone of low velocity beneath the Fiji plateau has its boundaries which seem to coincide with a high seismic wave attenuation zone that exists in the uppermost mantle between the Fiji and the New Hebrides islands. BARAZANGI *et al.* (1974) studied P and S seismic waves produced by hundreds of earthquakes located along the New Hebrides, Fiji plateau, Solomon, New Britain and New Guinea seismic zones and recorded at stations in Fiji, New Hebrides and New Caledonia. They found significant variations in the amplitudes and frequencies of the waves. Their data defined zones of anomalously high seismic wave attenuation in the uppermost mantle beneath the Fiji plateau and the Woodlark basin south of the Solomon islands. BARAZANGI and ISACKS (1971) also mapped in detail a zone of anomalously high seismic wave attenuation under the Lau basin. All these areas are also the sites of variable but generally high heat flow (SCLATTER *et al.*, 1972; MACDONALD *et al.*, 1973) and low seismic wave velocities (DUBOIS *et al.*, 1973; AGGARWAL *et al.*, 1972; SHOR *et al.*, 1971, FURUMOTO *et al.*, 1970). All these results suggest that hot and probably partially melted upper mantle material exists beneath these areas. It is also evident from our Fig. 1 that the observed heat flow in the Fiji plateau and other anomalous regions is considerably higher. BARAZANGI *et al.* (1974) also found that the high attenuation zone extends to depths of at least 300 km beneath the Fiji plateau. This implies that the temperatures of the mantle material beneath the Fiji plateau to a depth of about 300 km are relatively much higher than those in the surrounding mantle. It is quite possible that, the high temperatures probably prevailing to great depths of about 300 km beneath the Fiji plateau are even affecting the northeasternly dipping New Hebrides seismic zone to a considerable extent and that the temperatures in the dipping seismic zone are also very high. That is why the velocity gradients of P and S waves in the New Hebrides seismic zone as determined by us are extremely small thus the P and S velocities are also much lower in the New Hebrides region as compared to those in the Tonga-Kermadec-New Zealand region at comparable depths.

BARAZANGI *et al.* (1973) studied the seismic wave propagation in the mantle beneath the New Hebrides island arc and presented evidence for the detachment of lithospheric slabs in the upper mantle beneath the New Hebrides arc. They interpreted the remarkable gap in the seismic activity between deep and intermediate depth earthquakes at the northern part of the arc as due to a gap in the lithospheric slab descending beneath the arc, and the deep earthquakes as due to a detached piece of lithosphere. They found that predominantly low frequency (about 0.5 Hz) S waves are recorded at PVC and LNR stations in the New Hebrides from the deep earthquakes north of 15°S. New Hebrides deep earthquakes located at the western part of the deep zone produced attenuated, low

frequency S waves at PVC. The ray paths pass just beneath the dipping seismic zone. BARAZANGI *et al.* (1973) found that frequencies greater than 1 Hz are absent and the amplitude of the S phase is generally less than that of P phase. As OLIVER and ISACKS (1967) and BARAZANGI and ISACKS (1971) showed, this can be explained by a transmission through an attenuating low Q zone. BARAZANGI *et al.* (1973) also found that in contrast, S waves recorded at NIU station on the Tonga island arc from Tongan deep earthquakes have predominant frequencies of 3–4 Hz and the amplitude of S are generally larger than those of P. They interpreted the observation of low frequency S waves at PVC and LNR to be mainly the result of attenuation along the path. According to them the attenuation is chiefly below 300 km. BARAZANGI *et al.* (1973), on the basis of all these observations, suggested that there is absence of lithospheric slab material between depths of about 300 and 600 km, and the deep earthquakes of New Hebrides therefore represent a detached slab in the upper mantle. In our opinion, the very high temperatures reached at about 300 km depth in the surrounding mantle have probably affected the New Hebrides seismic zone to such an extent that the material in the seismic zone also has lost its strength substantially and no stresses can be accumulated in it. FARBEROV and GORELCHIK (1971) studied the focal distribution of subcrustal earthquakes and the dynamic features of seismic wave propagation under some volcanic areas of Kamchatka. They found that under active volcanoes there are aseismic areas of anomalous attenuation of seismic waves. As one of many possibilities, they suggested the presence of low viscosity zones under volcanoes in which there are no concentration of sufficient stresses to generate earthquakes and that these zones extend down to the focal layer. Since the volcanic activity in the New Hebrides region is also quite extensive the large temperatures there might have also reduced the viscosity of the mantle material at depths considerably. Thus beyond the depth of about 300 km there seems to be a gap in the seismic activity in this region. Again at depths greater than 600 km, due to increased pressure, built up by the usual pressure gradient, the material in the seismic zone might have recovered the necessary strength again to accumulate the stresses and therefore there are earthquakes occurring at these depths. Therefore, if we view the properties of the seismic zone in the light of this argument there is no necessity to imagine a gap in the lithospheric slab between depths of 300–600 km and a detached piece of lithosphere at about 600 km depth. The lithospheric slab in the New Hebrides may as well be continuing down to the usual depth of its penetration, i.e., probably the 650 km velocity discontinuity in the mantle. It may be only because of the anomalously high temperatures attained at depths beyond about 300 km, that the seismic activity is not continuing between 300–600 km depths. This does not necessarily mean that there is a gap in the lithospheric slab itself. The gap according to us, is only the change in the physical properties of the lithospheric slab but not its existence as such.

BARAZANGI *et al.* (1973) found that one of the three deep earthquakes occurred south of 15°S at about 18°S and 173°E produced large amplitude, high frequency S waves at PVC station in the New Hebrides. According to them this observation is quite clear and may imply the continuity of descending slab in the southern part of the New Hebrides arc. ISACKS and MOLNAR (1971) suggested that the gaps in seismic activity as a function of depth can be explained by two models. In the first the stress inside a continuous slab varies from downdip extension at intermediate depths to downdip compression at greater depths, and thus is near zero between these depths. In the second a piece of descending lithosphere breaks off, sinks into the upper mantle and leaves a gap between the piece and the plate

to which it was attached. SYKES (1966) studied the seismic activity versus depth for several island arcs. He found that in all island arcs studied the activity decreases in the upper 100 to 200 km approximately exponentially as a function of depth with a decay constant of about 100 km. ISACKS *et al.* (1968) found that there is an approximate correlation of the decrease in seismic activity versus depth with a similar general decrease in seismic velocities, Q and viscosity in the upper 150 km. They stated that these effects may be related to a decrease in the difference between the temperature and local melting temperature.

ISACKS *et al.* (1968) have plotted in their Fig. 12 the annual number of earthquakes per 25 km depth intervals as function of depth for several island arcs, the data being taken by them from SYKES (1966) and from KATSUMATA (1967) for the Japan region. If we scrutinize these curves carefully, we can find that there is either a broad minimum between depths of about 200 to 400 km or there are some gaps in certain depth ranges. We can notice broad minima for the Japan and the Tonga-Fiji-Kermadec regions in almost the same depth range where the P velocity functions reveal reduced velocity gradients in these regions (KAILA *et al.*, 1971; KAILA and KRISHNA, 1978). In our opinion, this is a nice correlation between the zones of less seismic activity and zones of reduced velocity gradients. Both these phenomenon can be easily explained by means of very high temperatures and/or temperature gradients in these depth ranges. Therefore, it is also quite possible that in a region like the New Hebrides which is surrounded by anomalously hot regions of the mantle there may be actual gap in the seismic activity in certain depth range like 300–600 km. In our opinion, this gap in the seismic activity however, does not necessarily mean a gap in the lithospheric slab. The slab may be actually continuing right to its maximum depth of penetration which may be the 650 km seismic discontinuity with variable physical properties throughout its length as explained above.

4. Conclusions

From the present study of the travel times of P and S waves in the New Hebrides island arc region we can make the following conclusions regarding the upper mantle structure in that region.

- 1) The P and S velocities are almost constant in the upper mantle to a depth of about 240 km. These velocities, although are comparable at the top of the mantle, they are however, much lower, by as much as 10% for P waves and 6–7% for S waves at a depth of about 240 km as compared to those at similar depths in the Tonga-Kermadec-New Zealand region. A temperature contrast of about 1,000°C between these two regions is needed to account for these velocity anomalies on the average.

- 2) The lower velocities observed in the New Hebrides seismic zone, are primarily due to anomalously high temperatures prevailing even at great depths in the upper mantle surrounding the New Hebrides region. In fact, the mantle material in the entire region beneath the New Hebrides, Solomon islands, New Britain and New Guinea regions may be in a partially molten state as revealed by very mild velocity gradients, high heat flow and intense volcanism in these regions.

- 3) The remarkable gap in the seismic activity observed in the New Hebrides region between depths of 300–600 km need not necessarily mean a gap in the lithospheric slab descending beneath the New Hebrides island arc. It is only due to the anomalously high temperature, prevailing in this region that the descending slab also has probably lost its

strength considerably and therefore cannot take sufficient stresses to accumulate and subsequently release through the earthquakes. At depths of about 600 km again the material in the slab has probably recovered its strength and therefore there are deep earthquakes at these depths. Therefore, we conclude that the lithospheric slab descending beneath the New Hebrides region is not broken between 300–600 km depth and may be continuing with varying physical and thermal properties right to the maximum depth of its penetration which may extend up to the 650-km seismic discontinuity.

We are grateful to Dr. Hari Narain, Director, National Geophysical Research Institute for providing all the facilities to carry out this research work and for his permission to publish this paper. Our thanks are also due to Mr. G. Khandekar for his help in the data collection and some computations. Preparation of the tracings of various drawings by Mr. P.J. Vijayanandam is duly acknowledged.

REFERENCES

- AGGARWAL, Y.P., M. BARAZANGI, and B. ISACKS, P and S travel times in the Tonga-Fiji region: A zone of low velocity in the uppermost mantle behind the Tonga island arc, *J. Geophys. Res.*, **77**, 6427–6434, 1972.
- ANDERSON, O.L., E. SCHREIBER, R.C. LIEBERMANN, and N. SOGA, Some elastic constraint data on minerals relevant to geophysics, *Rev. Geophys.*, **6**, 491–524, 1968.
- BARAZANGI, M. and B. ISACKS, Lateral variations of seismic wave attenuation in the upper mantle above the inclined earthquake zone of the Tonga island arc: Deep anomaly in the upper mantle, *J. Geophys. Res.*, **76**, 8493–8516, 1971.
- BARAZANGI, M., B.L. ISACKS, J. OLIVER, J. DUBOIS, and G. PASCAL, Descent of lithosphere beneath New Hebrides, Tonga-Fiji and New Zealand: Evidence for detached slabs, *Nature*, **242**, 98–101, 1973.
- BARAZANGI, M., B. ISACKS, J. DUBOIS, and G. PASCAL, Seismic wave attenuation in the upper mantle beneath the southwest Pacific, *Tectonophysics*, **24**, 1–12, 1974.
- BROOKS, J.A., Seismic wave velocities in the New Guinea-Solomon Islands region, in *The Crust of the Pacific Basin*, *Geophys. Monogr.*, **6**, 2–10, 1962.
- DUBOIS, J., G. PASCAL, M. BARAZANGI, B.L. ISACKS, and J. OLIVER, Travel times of seismic waves between the New Hebrides and Fiji islands: A zone of low velocity beneath the Fiji plateau, *J. Geophys. Res.*, **78**, 3431–3436, 1973.
- FARBEROV, A.I. and V.I. GORELCHIK, Anomalous seismic effect under volcanoes and some features of deep seated structure of volcanic areas, *Bull. Volcanol.*, **35**, 212–224, 1971.
- FURUMOTO, A., D. HUSSONG, J. CAMPBELL, G. SUTTON, A. MALAHOFF, J. ROSE, and G. WOOLLARD, Crustal and upper mantle structure of the Solomon islands as revealed by seismic refraction survey of November–December, 1966, *Pac. Sci.*, **24**, 315, 1970.
- GUTENBERG, B., Wave velocities at depths between 50 and 600 kilometers, *Bull. Seismol. Soc. Am.*, **43**, 223–232, 1953.
- HASHIN, Z., The elastic moduli of heterogeneous materials, *J. Appl. Mech.*, **29**, 143–150, 1962.
- HELMBERGER, D.V. and G.R. ENGEN, Upper mantle shear structure, *J. Geophys. Res.*, **79**, 4017–4028, 1974.
- ISACKS, B. and P. MOLNAR, Distribution of stresses in the descending lithosphere from a global survey of focal mechanism solutions of mantle earthquakes, *Rev. Geophys. Space Phys.*, **9**, 103–174, 1971.
- ISACKS, B., J. OLIVER, and L.R. SYKES, Seismology and the new global tectonics, *J. Geophys. Res.*, **73**, 5855–5899, 1968.
- JEFFREYS, H., The times of P, S, and SKS and the velocities of P and S, monthly notices, *Roy. Astron. Soc. Geophys.*, **4** (Suppl.), 498–533, 1939.
- JESSOP, A.M., M.A. HOBART, and J.G. SCLATER, Terrestrial heat flow data, Map produced by P.J. Grim, National Geophysical and Solar-Terrestrial Data Center, (U.S.A.), 1976.
- KAILA, K.L., A new analytical method for finding the upper mantle velocity structure from P and S wave travel times of deep earthquakes, *Bull. Seismol. Soc. Am.*, **59**, 755–769, 1969.
- KAILA, K.L. and V.G. KRISHNA, Upper mantle velocity structure in the Tonga-Kermadec island arc region, Paper presented at the International Geodynamics Conference, March 13–17, Tokyo, Japan, 1978.
- KAILA, K.L., V.G. KRISHNA, and Hari NARAIN, Upper mantle P wave velocity structure in the Japan region from travel time studies of deep earthquakes using a new analytical method, *Bull. Seismol. Soc. Am.*, **61**, 1549–1570, 1971.
- KAILA, K.L., V.G. KRISHNA, and Hari NARAIN, Upper mantle shear wave velocity structure in the Japan region, *Bull. Seismol. Soc. Am.*, **64**, 355–374, 1974.

- KANAMORI, H., Travel times to Japanese stations from Longshot and their geophysical implications, *Bull. Earthq. Res. Inst. Tokyo Univ.*, **46**, 841–859, 1968.
- KATSUMATA, M., Seismic activities in and near Japan 3: Seismic activities versus depth, *J. Seismol. Soc. Jpn.*, **20**, 75, 1967 (in Japanese).
- MACDONALD, G.A., *Volcanoes*, Prentice-Hall, Englewood Cliffs, New Jersey, 1972.
- MACDONALD, K., B. LUYENDYK, and W. BRYAN, Heat flow and plate boundaries in Melanesia, *J. Geophys. Res.*, **78**, 2537–2546, 1973.
- OLIVER, J. and B. ISACKS, Deep earthquake zones, anomalous structures in the upper mantle, and the lithosphere, *J. Geophys. Res.*, **72**, 4259–4275, 1967.
- PASCAL, G., J. DUBOIS, M. BARAZANGI, B.L. ISACKS, and J. OLIVER, Seismic velocity anomalies beneath the New Hebrides island arc: Evidence for a detached slab in the upper mantle, *J. Geophys. Res.*, **78**, 6998–7004, 1973.
- SCLATER, J., U. RITTER, and F. DIXON, Heat flow in the southwestern Pacific, *J. Geophys. Res.*, **77**, 5697–5704, 1972.
- SHOR, G., H. KIRK, and H. MENARD, Crustal structure of the Melanesian area, *J. Geophys. Res.*, **76**, 2562–2586, 1971.
- SIMPSON, D.W., R.F. MEREU, and D.W. KING, An array study of P-wave velocities in the upper mantle transition zone beneath northeastern Australia, *Bull. Seismol. Soc. Am.*, **64**, 1757–1788, 1974.
- SYKES, L.R., The seismicity and deep structure of island arcs, *J. Geophys. Res.*, **71**, 2981–3006, 1966.

UPPER MANTLE VELOCITY STRUCTURE IN THE TONGA-KERMADEC ISLAND ARC REGION

K.L. KAILA and V.G. KRISHNA

National Geophysical Research Institute, Hyderabad, India

(Received April 25, 1978; Revised August 8, 1978)

Upper mantle velocity structure in the Tonga-Kermadec island arc region has been studied in great detail to a depth of 665 km from the analysis of P and S wave travel times of 130 deep earthquakes using KAILA's (1969) analytical method. The velocity function for P waves determined from the present study reveals a velocity of 7.97 km/sec at a 40-km depth which increases linearly, with a high velocity gradient of 0.52 ± 0.02 km/sec per 100 km, to 8.96 km/sec at a depth of 230 km. From 230 km downwards, the velocity increases with a considerably smaller gradient of 0.23 ± 0.02 km/sec per 100 km, reaching a value of 9.37 km/sec at a depth of 410 km. At this transition depth of 410 km, there is a first order velocity discontinuity—the velocity increasing from 9.37 to 9.85 km/sec. In the depth range from 410 to 600 km, the P velocity gradient is found to be extremely small, velocity increasing only to a value of 9.90 km/sec at a depth of 600 km. At this depth of 600 km there is again a first order velocity discontinuity—the velocity increasing from 9.90 to 10.64 km/sec. Below 600 km depth, P velocity increases linearly from 10.64 to 10.72 km/sec at a depth of 660 km.

The S velocity function, determined to a depth of 665 km, also reveals similar features as the P velocity function. However, a decrease in the S velocity gradient is found to occur at a smaller depth of only 130 km. The S velocity determined as 4.58 km/sec at a 40-km depth increases linearly with a gradient of 0.28 ± 0.02 km/sec per 100 km, to 4.83 km/sec at a depth of 130 km. From 130 to 410 km depth S velocity is found to increase linearly from 4.83 to 5.11 km/sec with a low velocity gradient of only 0.10 ± 0.01 km/sec per 100 km. At the transition depth of 410 km there is a first order velocity discontinuity for S waves—the velocity increasing from 5.11 to 5.32 km/sec. Below 410 km depth the S velocity gradient is also extremely small, velocity increasing only to a value of 5.39 km/sec at a depth of 600 km. At this depth of 600 km, there is again a first order velocity discontinuity for S waves—the velocity increasing from 5.39 to 6.21 km/sec. Below 600 km depth, S velocity again increases linearly from 6.21 to 6.34 km/sec at a depth of 665 km. The decrease in the velocity gradient at a depth of 230 km for P waves and 130 km for S waves is interpreted as a second order low velocity channel in the upper mantle beneath the Tonga-Kermadec-New Zealand region.

The P and S velocities in the Tonga-Kermadec-New Zealand region are about 6% higher, on the average, than those in the adjacent New Hebrides island arc region to a depth of at least 240 km. These velocities are also much higher, by about 3 to 6%, than those in the Japan region to a depth of almost 600 km; and also substantially higher than those in the northeastern Australia, the western United States and those for the average upper mantle structure valid for the Pacific ocean basin and its surroundings. It is thus found that the P and S velocities in the inclined seismic zone beneath the Tonga-Kermadec-New Zealand region are probably the highest in the Pacific region and that these velocity differences are prevailing almost to a depth of about 600 km. These differences of about 6% in the velocities can be explained primarily by differences in temperatures of the upper mantle material of the order of 1,000°C. It is therefore inferred that the mantle material in the

inclined seismic zone beneath the Tonga-Kermadec-New Zealand region is relatively much colder than that in the Circum-Pacific region.

1. Introduction

There have been several studies during recent years showing evidence for large lateral variations of seismic wave velocities and attenuation in the upper mantle beneath the Tonga-Kermadec island arc region of the southwest Pacific. OLIVER and ISACKS (1967) observed anomalies in both the velocities and attenuation of seismic energy in the upper mantle beneath the Tonga island arc, but focussed their attention primarily upon the more obvious and prominent effects of attenuation. On the basis of their observations of the amplitudes and predominant frequencies of shear waves, they inferred an anomalous low attenuation (high Q) zone in the upper mantle near the inclined seismic zone. They proposed a model in which the Tonga-Kermadec island arc results from the downgoing motion of a plate of lithosphere that would be more rigid and cooler than the surrounding upper mantle material. Such a model in which a lithospheric plate descends into the mantle beneath an island arc provides the simplest explanation for both the anomalous velocities and the anomalous attenuation. According to this model (OLIVER and ISACKS, 1967; MCKENZIE, 1969; OXBURGH and TURCOTTE, 1970; MINEAR and TOKSOZ, 1970) the high velocities are simply the result of low temperatures in the slab relative to those in the surrounding mantle. MITRONOVAS and ISACKS (1971) observed that the travel times for the P waves from deep earthquakes that go beneath and through the inclined seismic zone of the Tonga island arc are 5 ± 1 sec less than the travel times of waves going through the aseismic and apparently normal mantle beneath the Fiji islands. A less precisely determined difference in the travel times of S waves according to them is about 10 to 12 sec. From this study of travel time residuals of P and S waves, they inferred that, on the average, the P and S velocities near the inclined seismic zone are about 6 to 7% higher than those for comparable parts of aseismic normal mantle. They interpreted these differences in velocities in terms of differences in temperature of the upper mantle material of the order of $1,000^{\circ}\text{C}$. Although these and similar other estimates of the velocity contrasts between the inclined seismic zone and the aseismic surrounding mantle are available to a reasonable degree of accuracy, however, the actual velocity structure as a function of depth neither in the inclined seismic zone nor in the surrounding mantle is known very precisely in the Tonga-Kermadec island arc region.

The velocities of seismic body waves P and S are the most fundamental physical parameters of the earth's mantle measurable to a high degree of accuracy and as such their variation with depth can be used to infer various other physical properties such as temperature, elastic parameters, density and chemical composition (BIRCH, 1952, 1961, 1964; ANDERSON, 1966, 1967; BULLEN and HADDON, 1967; BURDICK and ANDERSON, 1975; KAILA and KRISHNA, 1976). Further, knowledge of the accurate velocity distribution with depth in a seismic region is also very essential for a precise location of earthquakes in the region.

In the present study, we have determined the detailed upper mantle velocity structure for P and S waves to a depth of about 660 km in the inclined seismic zone beneath the Tonga-Kermadec island arc and the New Zealand region from the analysis of P and S wave travel times using KAILA's (1969) method. The velocity functions determined for P and S waves in the present study are compared with those determined by KAILA and

KRISHNA (1978) for the adjacent New Hebrides seismic zone where the velocities as well as the velocity gradients for P and S waves are found to be much smaller to a depth of about 240 km. The P and S velocity functions determined in the present study for the Tonga-Kermadec-New Zealand region are also compared with velocity models derived by other workers for various other regions of the earth and it is found that the seismic velocities in the lithospheric slab descending beneath the Tonga-Kermadec island arc are probably the highest. Attempts are also made in this paper to explain these anomalously high velocities within the inclined seismic zone in the Tonga-Kermadec-New Zealand region in terms of temperature differences probably prevailing even at great depths.

2. Sources of Data

For the period 1957 to 1973, 130 shallow, intermediate and deep earthquakes are selected in the seismic zones of Tonga-Kermadec island arc and the New Zealand regions. Most of the shallow and intermediate depth earthquakes are selected either from the New Zealand seismic zone or towards northeast of the north island; because there is sufficiently good network of seismograph stations throughout New Zealand which can provide travel time data in the required distance ranges from the shallow and intermediate depth earthquakes to obtain reliable velocity estimates at the hypocenters of the earthquakes. On the other hand shallow and intermediate earthquakes located on the trench side of the Tonga-Kermadec islands do not provide sufficient travel time data in the required distance range for velocity determination and therefore they could not be used in the present study. However, deep earthquakes in the seismic zone beneath the Tonga-Kermadec island arc provide sufficiently good number of travel time observations in the required distance ranges to determine the velocities at the hypocenters and so they are also selected for the present study. The North Island of New Zealand overlies a zone of intermediate depth earthquakes, down to a depth of about 350 km, that forms the southern extension of the Tonga-Kermadec zone (HAMILTON and GALE, 1968, 1969; MOONEY and HATHERTON, 1969; HATHERTON, 1970). Travel time residuals reviewed by MITRONOVAS and ISACKS (1971) also suggest that the Tonga-Kermadec high-velocity slab extends south to include the north island and perhaps even the south island of New Zealand. Therefore, we are justified to use shallow and intermediate depth earthquakes in the seismic zone of New Zealand along with the deep earthquakes of the Tonga-Kermadec seismic zone to derive the velocity function, in the depth range from 40 to 660 km, applicable to the inclined seismic zone beneath the Tonga-Kermadec island arc and the New Zealand region.

P and S wave travel times and epicentral distances (Δ) are taken from the bulletins of the International Seismological Summary (ISS) for the period 1957–1963 and from the bulletins of the International Seismological Center (ISC) for the period 1964–1973 for various earthquakes. Figure 1 shows the epicenters of the earthquakes in the Tonga-Kermadec island arc and the New Zealand seismic regions which are used in the present study, along with the seismograph stations. The epicentral data of these earthquakes is also given in Table 1.

3. Data Analysis and Results

For determining the upper mantle velocity structure in the seismic zone beneath the

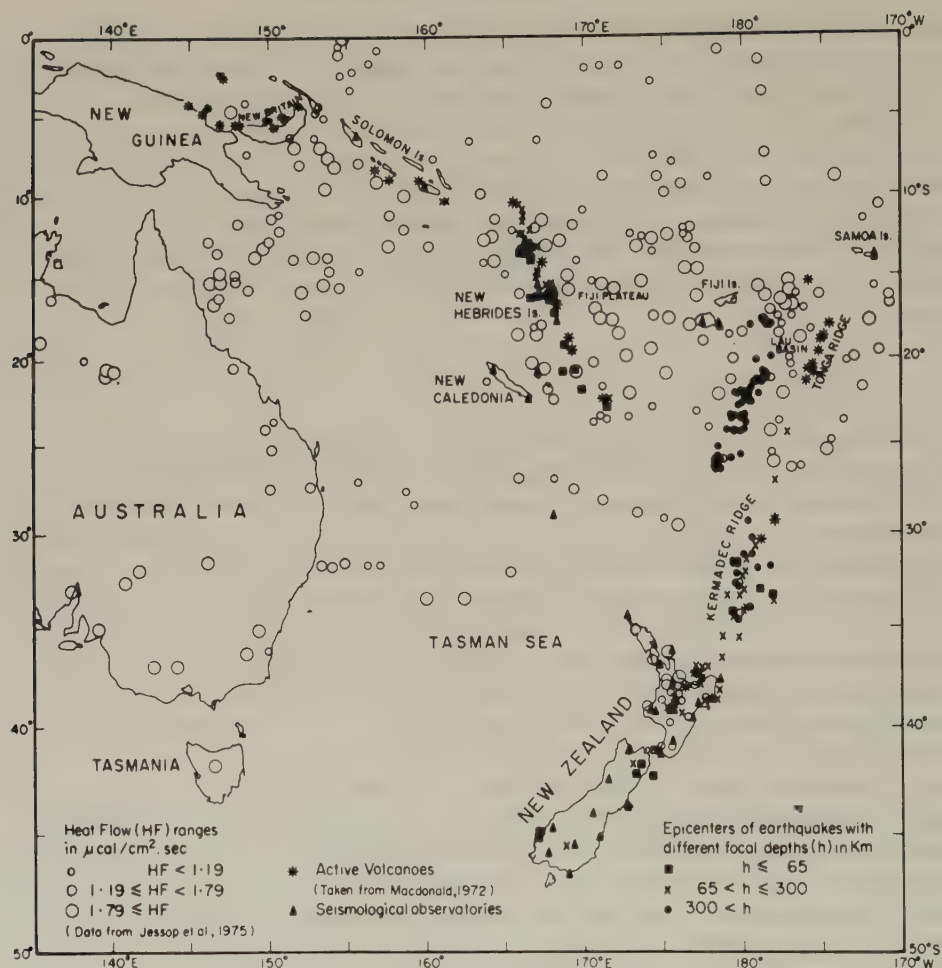


Fig. 1. Map of the southwest Pacific region showing the seismological observatories and epicenters of earthquakes in the Tonga-Kermadec-New Zealand region used in the present study. Epicenters of earthquakes used by KAILA and KRISHNA (1978) for determining the upper mantle velocity structure in the New Hebrides island arc region are also shown.

Tonga-Kermadec island arc region we have analysed the P and S wave travel times of all the earthquakes listed in Table 1 by making use of KAILA's (1969) analytical method. The epicentral distance limits Δ_1 and Δ_2 , between which $p(=\partial T/\partial \Delta)$ remains almost constant, are however not determined for various earthquakes in the present study. Instead, we have made use of the curves for Δ_1 and Δ_2 as functions of focal depth given by KAILA *et al.* (1971 paper, Fig. 9 for P waves and 1974 paper, Fig. 7 for S waves) to determine the Δ_1 and Δ_2 limits for various depths, because, in our opinion these estimates of Δ_1 and Δ_2 are quite reasonable within the accuracy of their determination and are not likely to change much from region to region. The travel time data available between the two limits is fitted by a least squares line in each case, which yielded the apparent $p(=\partial T/\partial \Delta)$ and the $a(=T-p\Delta)$ values with their standard deviations. The least squares fits obtained for $T-\Delta$ points between Δ_1 and Δ_2 for three specimen earthquakes with focal depths of

Table 1. Earthquake epicentral data.

Earth- quake No.	Date	Time			Epicenter		Focal depth (km)
		(h)	(m)	(s)	Latitude (deg)	Longitude (deg)	
1	2	3			4	5	6
1	Apr. 15, 1964	15	02	26.9	45.23S	167.00E	38
2	May 22, 1959	06	57	10.0	41.10S	174.38E	41
3	Jan. 9, 1964	21	47	11.3	42.34S	174.30E	44
4	May 8, 1964	11	47	12.6	41.69S	173.51E	48
5	Feb. 21, 1960	00	46	57.0	42.21S	173.16E	49
6	Aug. 15, 1964	19	37	56.9	44.88S	167.12E	52
7	Dec. 19, 1964	06	41	24.3	32.99S	179.00W	54
8	Aug. 24, 1964	13	32	02.4	33.29S	178.20W	60
9	Dec. 27, 1964	08	21	09.9	34.20S	179.30E	63
10	July 21, 1964	10	33	38.2	37.94S	177.40E	67
11	Nov. 5, 1964	12	16	20.1	38.74S	177.60E	75
12	Apr. 12, 1964	11	10	53.0	34.02S	179.79W	75
13	Sept. 22, 1958	19	05	53.0	33.67S	178.07W	77
14	Nov. 20, 1964	21	20	19.5	39.30S	176.08E	80
15	Feb. 12, 1964	20	39	06.8	41.69S	173.00E	80
16	May 25, 1964	17	40	22.7	37.60S	177.50E	87
17	May 20, 1964	06	06	22.3	35.50S	179.70E	101
18	Oct. 4, 1964	16	43	32.7	38.60S	178.40E	104
19	June 24, 1964	11	37	58.0	45.50S	168.80E	106
20	June 20, 1964	02	32	27.6	36.50S	178.70E	112
21	May 24, 1964	22	22	27.3	36.95S	177.81E	146
22	Apr. 14, 1964	04	32	15.5	38.20S	176.50E	147
23	Nov. 11, 1964	11	19	18.1	24.36S	177.16W	148
24	July 26, 1961	09	19	06.0	37.42S	177.04E	149
25	June 27, 1959	19	04	39.0	33.42S	179.84E	151
26	Dec. 10, 1964	11	39	13.9	38.52S	175.63E	157
27	Feb. 9, 1957	13	29	25.0	34.23S	179.91W	164
28	July 14, 1957	06	23	59.0	27.07S	177.99W	173
29	Mar. 3, 1964	03	57	02.6	33.06S	179.90W	193
30	Nov. 1, 1964	22	12	43.2	37.60S	177.40E	203
31	Oct. 27, 1964	00	40	46.5	37.00S	177.50E	215
32	Aug. 5, 1964	11	06	01.4	32.22S	179.80W	216
33	Mar. 27, 1960	23	28	26.0	39.01S	175.23E	224
34	Nov. 20, 1964	08	53	25.0	35.40S	178.70E	228
35	Feb. 7, 1958	01	10	58.0	31.45S	179.69W	229
36	June 12, 1960	06	58	15.0	30.69S	179.20W	254
37	Feb. 22, 1964	01	47	36.4	37.37S	176.78E	263
38	Oct. 6, 1958	00	47	25.0	32.42S	179.96E	263
39	Dec. 10, 1958	07	03	01.0	36.92S	177.02E	274
40	July 27, 1964	08	47	07.5	34.50S	179.40E	280
41	July 22, 1964	00	07	41.1	33.40S	179.00E	300
42	June 10, 1964	08	54	41.7	31.24S	179.40W	328
43	May 17, 1963	07	33	14.0	31.90S	179.06W	333
44	Dec. 12, 1964	19	03	19.1	34.04S	179.50W	346
45	Sept. 21, 1964	18	10	54.7	30.28S	179.38W	350
46	Apr. 11, 1964	21	21	52.9	34.60S	179.70E	360
47	Feb. 24, 1964	16	18	20.6	31.84S	178.30W	368
48	Apr. 8, 1959	01	23	29.0	32.66S	179.47E	389
49	June 18, 1961	13	55	17.0	31.49S	179.69E	397
50	June 21, 1964	03	32	58.9	31.20S	179.90W	410
51	July 3, 1958	06	27	49.0	29.42S	179.57W	410
52	Sept. 5, 1964	02	17	16.7	32.20S	179.61E	422
53	Nov. 24, 1964	14	48	51.3	24.20S	179.78W	447

Table 1 (Continued)

Earth- quake No.	Date	Time			Epicenter		Focal depth (km)
		(h)	(m)	(s)	Latitude (deg)	Longitude (deg)	
1	2	3			4	5	6
54	Sept. 28, 1963	06	58	13.0	31.68S	179.66E	460
55	July 7, 1964	07	39	04.7	23.58S	179.83W	462
56	Nov. 11, 1971	08	09	40.6	25.62S	179.92E	472
57	Mar. 10, 1960	05	00	25.0	31.50S	179.27E	477
58	Oct. 15, 1964	11	05	14.4	32.94S	179.70E	480
59	Jan. 30, 1959	18	09	55.0	31.64S	179.38E	486
60	July 17, 1964	04	55	00.8	24.34S	179.52E	504
61	March 27, 1964	20	22	09.6	23.74S	179.99E	506
62	Feb. 3, 1964	20	05	47.5	23.30S	179.84W	512
63	Aug. 4, 1963	23	54	15.0	17.66S	178.93W	517
64	Nov. 2, 1965	00	49	13.2	23.78S	179.69W	518
65	Aug. 28, 1964	14	42	16.7	24.27S	179.88E	523
66	Sept. 27, 1961	06	34	03.0	17.55S	178.64W	524
67	Dec. 30, 1964	21	30	57.3	23.33S	179.82W	528
68	Apr. 10, 1971	01	22	16.5	21.22S	178.76W	531
69	June 2, 1965	05	12	59.3	23.53S	179.99E	538
70	Apr. 16, 1964	11	45	37.6	23.64S	179.96E	538
71	Aug. 20, 1961	05	04	14.0	17.96S	178.50W	538
72	Sept. 19, 1971	10	00	19.1	21.23S	178.50W	539
73	Aug. 6, 1964	17	03	32.2	22.64S	179.36W	544
74	Jan. 19, 1960	09	15	05.0	23.41S	179.64E	545
75	Mar. 31, 1964	17	04	39.4	17.70S	178.77W	546
76	Dec. 5, 1964	05	14	41.4	20.90S	178.49W	548
77	Oct. 10, 1961	03	44	40.0	22.82S	179.84E	549
78	Nov. 1, 1965	18	03	09.7	24.18S	179.02E	550
79	July 26, 1964	06	28	32.7	23.43S	180.00W	553
80	Aug. 25, 1963	12	18	12.0	17.58S	178.73W	557
81	Dec. 6, 1967	05	03	40.9	21.26S	178.75W	558
82	Dec. 11, 1963	02	31	21.0	17.88S	178.69W	558
83	May 28, 1971	17	58	24.3	23.58S	179.25E	564
84	Dec. 7, 1963	04	07	54.0	22.11S	179.46W	564
85	Aug. 3, 1958	01	06	28.0	22.10S	179.00W	567
86	Mar. 27, 1972	11	12	28.2	17.89S	178.54W	573
87	Feb. 15, 1971	07	51	02.0	25.20S	178.41E	574
88	Aug. 28, 1964	04	35	29.2	19.85S	178.15W	576
89	Nov. 4, 1969	23	40	19.9	22.14S	179.57W	577
90	Feb. 18, 1969	20	43	14.0	17.94S	178.53W	577
91	Dec. 28, 1964	16	16	08.7	22.13S	179.62W	577
92	Oct. 21, 1961	11	43	43.0	17.91S	178.51W	578
93	Apr. 29, 1965	09	44	36.9	22.10S	179.71E	579
94	Feb. 10, 1964	09	56	45.8	20.97S	178.53W	582
95	Mar. 10, 1965	15	53	40.2	21.98S	179.60E	583
96	Oct. 27, 1963	08	45	44.0	17.99S	178.41W	583
97	Jan. 24, 1969	02	33	03.4	21.87S	179.54W	587
98	Nov. 22, 1964	02	38	30.7	17.80S	178.62W	587
99	July 15, 1968	04	12	26.4	18.01S	178.49W	589
100	Dec. 9, 1961	19	49	43.0	21.89S	179.93E	590
101	June 18, 1968	06	42	21.3	21.72S	179.43W	593
102	Nov. 24, 1969	21	31	18.1	18.01S	178.40W	597
103	Oct. 12, 1968	19	17	39.7	20.79S	178.68W	597
104	Nov. 13, 1964	15	15	29.0	18.11S	178.33W	597
105	Feb. 19, 1964	09	58	39.6	25.82S	179.33E	600
106	June 23, 1967	14	38	35.4	21.40S	179.29W	600
107	Jan. 14, 1968	08	01	27.5	22.43S	179.58W	602

Table 1 (Continued)

Earth- quake No.	Date	Time			Epicenter		Focal depth (km)
		(h)	(m)	(s)	Latitude (deg)	Longitude (deg)	
1	2	3			4	5	6
108	Sept. 21, 1964	04	23	18.9	21.96S	179.46W	603
109	Apr. 12, 1971	21	00	36.8	17.92S	178.17W	606
110	June 8, 1964	02	26	46.0	22.05S	179.60W	606
111	June 12, 1964	18	12	16.5	26.53S	178.57E	600
112	July 23, 1960	07	31	42.0	21.34S	179.23W	602
113	Feb. 15, 1966	22	14	44.2	26.53S	178.30E	605
114	May 29, 1964	18	42	19.3	26.20S	178.35E	606
115	May 29, 1964	19	01	56.7	26.13S	178.31E	609
116	Feb. 15, 1966	22	34	06.6	26.50S	178.29E	609
117	Apr. 24, 1972	02	04	24.7	21.36S	179.34W	613
118	Oct. 25, 1964	12	08	53.2	21.68S	179.37W	617
119	May 29, 1964	18	35	02.3	26.11S	178.30E	617
120	Feb. 3, 1969	07	51	24.9	25.87S	178.23E	618
121	Oct. 3, 1964	17	02	44.0	18.13S	178.48W	618
122	Mar. 19, 1964	04	45	51.9	21.96S	179.62E	627
123	Apr. 9, 1961	09	21	31.0	25.98S	178.25E	628
124	Feb. 3, 1969	08	13	45.0	25.85S	178.26E	629
125	June 2, 1965	14	45	56.1	18.00S	179.38W	636
126	Aug. 16, 1968	11	34	15.8	21.23S	179.14W	637
127	Sept. 21, 1973	19	28	28.7	26.15S	178.33E	643
128	Feb. 20, 1962	10	07	27.0	25.95S	178.29E	660
129	Feb. 3, 1969	08	18	15.6	25.84S	178.36E	665
130	Mar. 20, 1963	04	43	12.0	20.11S	179.05W	668

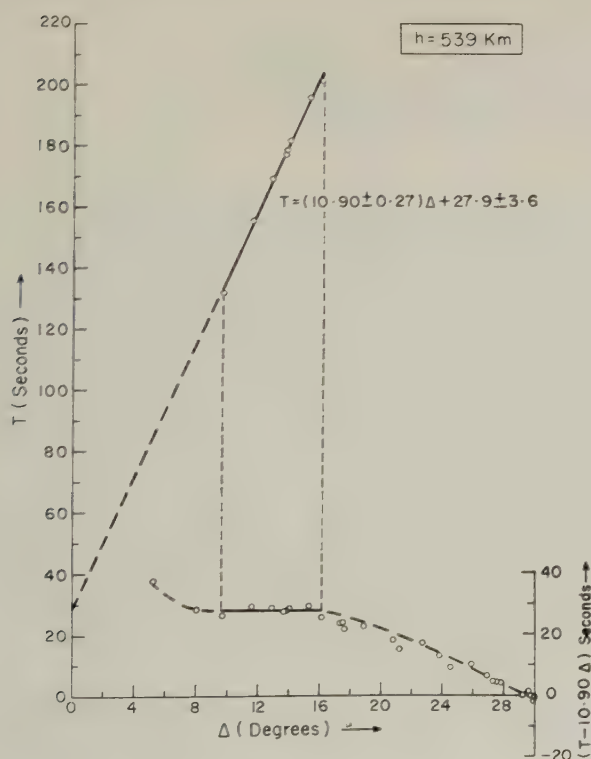


Fig. 2. P wave travel time curve T versus Δ for earthquake with focal depth 539 km between the limits Δ_1 and Δ_2 of epicentral distance. Reduced travel time curve $(T - p\Delta)$ versus Δ is also shown where $p = \partial T / \partial \Delta$ at the inflection point.

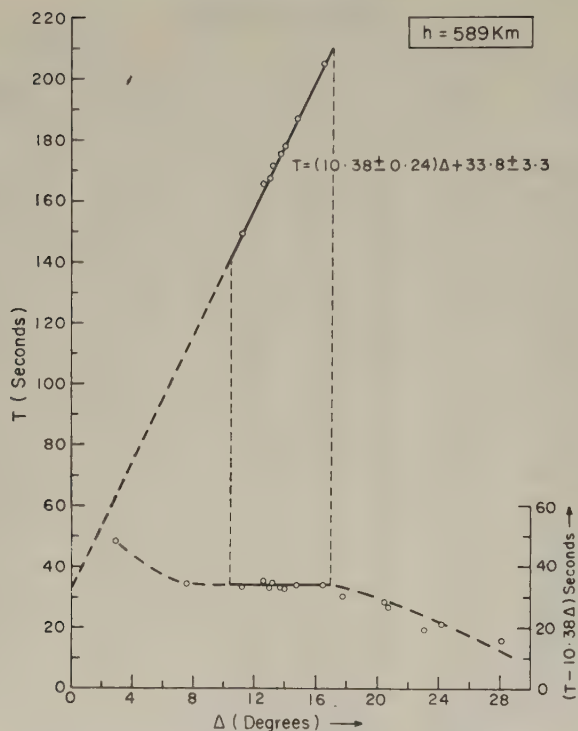


Fig. 3. P wave travel time curve T versus Δ for earthquake with focal depth 589 km between the limits Δ_1 and Δ_2 of epicentral distance. Reduced travel time curve $(T - p\Delta)$ versus Δ is also shown where $p = \partial T / \partial \Delta$ at the inflection point.

539, 589 and 637 km for P waves and one specimen earthquake with focal depth of 609 km for S waves are shown in Figs. 2 to 5 respectively. In the same figures are also shown the plots of $(T - p\Delta)$ versus Δ . Using the apparent p values, the true velocities with their standard deviations are computed for each focal depth studied. It may be mentioned here that the method of analysis adopted in the present study has the greatest advantage that we are able to determine the velocity at the hypocenter of each earthquake studied and the effect of the travel path of the waves is almost negligible. The final results obtained for the p values and velocities with their standard deviations are given in Table 2 for both P and S waves.

The true velocities thus obtained at various depths are plotted in Fig. 6 for P waves and in Fig. 7 for S waves. In these figures, the velocity depth points are shown by circles and the truncated horizontal bars with them indicate the standard deviations of those velocity values. The velocity depth points for P waves are fitted by least squares by various straight line segments in different depth ranges as shown by thick lines in Fig. 6. The broken lines bounding these straight line fits in different depth ranges represent the 95% confidence limits of their slopes.

The velocity function for P waves thus determined for the Tonga-Kermadec-New Zealand seismic zone reveals a velocity of 7.97 km/sec at a 40-km depth which increases

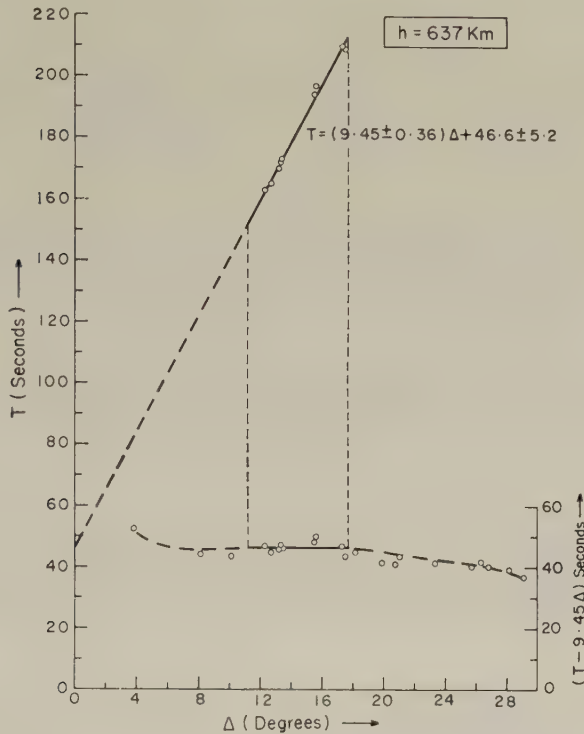


Fig. 4. P wave travel time curve T versus Δ for earthquake with focal depth 637 km between the limits Δ_1 and Δ_2 of epicentral distance. Reduced travel time curve $(T - p\Delta)$ versus Δ is also shown where $p = \partial T / \partial \Delta$ at the inflection point.

linearly, with a high velocity gradient of $0.52 \pm 0.02 \text{ km/sec per } 100 \text{ km}$, to 8.96 km/sec at a depth of 230 km. At this depth of 230 km, there is a decrease in the P velocity gradient, which decreases to $0.23 \pm 0.02 \text{ km/sec per } 100 \text{ km}$, but the velocity still increasing linearly and attaining a value of 9.37 km/sec at a depth of 410 km. At this transition depth of 410 km, there is a first order velocity discontinuity—the velocity increasing from 9.37 to 9.85 km/sec . In the depth range from 410 to 600 km, the P velocity gradient is found to be extremely small, velocity increasing only to a value of 9.90 km/sec at a depth of 600 km. At this depth of 600 km there is again a first order velocity discontinuity—the velocity increasing from 9.90 to 10.64 km/sec . Below 600 km depth, P velocity increases linearly from 10.64 to 10.72 km/sec at a depth of 660 km. The above model of the P velocity function shown in Fig. 6 gave a χ^2 value of about 78 on 96 degrees of freedom which corresponds to a probability of 0.90–0.95 and therefore it is an acceptable model.

The velocity depth points for S waves are also fitted, by using least squares method, by various straight line segments in different depth ranges as shown by thick lines in Fig. 7. The broken lines bounding these straight line fits in different depth ranges represent the 95% confidence limits of their slopes. The S velocity function, determined to a depth of 665 km, also reveals similar features as the P velocity function. However, a decrease in the S velocity gradient is found to occur at a smaller depth of only 130 km. The S velocity

Table 2. P and S wave true velocities V_P and V_S respectively as functions of depth (h) for the Tonga-Kermadec-New Zealand region as determined in the present study.

Earth-quake No.	h (km)	P waves				S waves			
		p (apparent) (sec/deg)	V_P (km/sec)	p (true) (sec/deg)	a_p (sec)	p (apparent) (sec/deg)	V_S (km/sec)	p (true) (sec/deg)	a_s (sec)
1	2	3	4	5	6	7	8	9	10
1	38	14.08±0.49	7.88±0.27	14.09±0.49	4.8±2.7	24.46±0.23	4.54±0.04	24.48±0.23	—
2	41	14.00±0.51	7.93±0.29	14.01±0.51	4.2±1.7	24.99±0.47	4.44±0.08	25.02±0.47	—
3	44	13.63±0.53	8.14±0.32	13.66±0.53	5.8±2.1	24.64±0.77	4.50±0.14	24.68±0.77	9.4±3.1
4	48	13.71±0.57	8.09±0.34	13.74±0.57	5.7±2.3	23.97±0.53	4.62±0.10	24.02±0.53	—
5	49	13.81±0.50	8.03±0.29	13.84±0.50	4.1±2.1	24.70±0.27	4.49±0.38	24.76±2.07	—
6	52	13.80±0.15	8.03±0.09	13.84±0.15	5.4±1.2	23.94±0.25	4.63±0.05	24.01±0.25	—
7	54	13.40±0.51	8.26±0.32	13.45±0.51	8.7±3.6	25.50±0.61	4.34±0.10	25.58±0.61	—
8	60	—	—	—	—	23.77±1.62	4.65±0.32	23.87±1.62	15.4±9.4
9	63	13.84±0.80	7.99±0.46	13.90±0.80	5.1±3.8	—	—	—	—
10	67	—	—	—	—	22.57±1.01	4.90±0.22	22.69±1.01	15.9±4.9
11	75	13.35±0.11	8.26±0.07	13.44±0.11	5.1±0.5	23.33±0.88	4.73±0.18	23.48±0.88	11.5±3.6
12	75	—	—	—	—	22.10±1.00	4.99±0.23	22.25±1.00	24.1±6.6
13	77	—	—	—	—	21.67±2.34	5.09±0.55	21.83±2.34	29.9±17.8
14	80	—	—	—	—	23.74±1.20	4.65±0.24	23.91±1.20	11.5±7.5
15	80	—	—	—	—	24.84±1.11	4.44±0.20	25.03±1.11	—
16	87	13.63±0.18	8.08±0.11	13.74±0.18	3.7±1.4	23.78±0.64	4.63±0.13	23.98±0.64	11.3±3.3
17	101	13.57±0.26	8.10±0.16	13.72±0.26	7.4±1.7	22.64±0.98	4.85±0.21	22.88±0.98	24.8±8.5
18	104	—	—	—	—	22.87±0.69	4.80±0.15	23.13±0.69	15.1±3.9
19	106	—	—	—	—	23.50±0.59	4.67±0.12	23.77±0.59	12.7±3.6
20	112	—	—	—	—	22.33±1.09	4.91±0.24	22.61±1.09	27.5±5.9
21	146	—	—	—	—	21.08±1.06	5.18±0.27	21.46±1.06	22.4±7.0
22	147	—	—	—	—	23.08±0.34	4.73±0.07	23.50±0.34	—
23	148	13.00±0.10	8.39±0.06	13.24±0.10	10.3±0.9	—	—	—	—
24	149	12.50±0.52	8.73±0.37	12.73±0.52	9.9±4.0	23.42±0.94	4.66±0.19	23.86±0.94	9.6±6.9
25	151	12.84±0.47	8.49±0.32	13.08±0.47	9.0±4.2	21.00±1.15	5.19±0.29	21.40±1.15	94.5±9.4
26	157	—	—	—	—	24.48±0.98	4.45±0.18	24.97±0.98	—
27	164	12.94±0.42	8.41±0.28	13.21±0.42	9.0±3.8	21.90±1.08	4.97±0.25	22.37±1.08	27.8±8.6
28	173	13.00±0.82	8.36±0.54	13.29±0.82	13.0±9.2	—	—	—	—
29	193	12.00±0.38	9.03±0.30	12.31±0.38	15.8±2.5	—	—	—	—
30	203	—	—	—	—	22.04±0.49	4.91±0.11	22.65±0.49	22.5±3.1

1	2	3	4	5	6	7	8	9
31	215	—	—	—	—	23.16±0.62	4.66±0.13	23.84±0.62
32	216	—	—	—	—	21.56±1.16	5.00±0.28	22.20±1.16
33	224	—	—	—	—	21.83±0.25	4.94±0.06	22.51±0.25
34	228	—	—	—	—	21.74±0.74	4.95±0.17	22.43±0.74
35	229	11.79±0.49	9.13±0.39	12.17±0.49	20.9±4.4	—	—	—
36	254	12.21±0.71	8.78±0.53	12.65±0.71	17.1±7.0	22.46±2.05	4.77±0.45	23.27±2.05
37	263	12.02±0.27	8.91±0.21	12.47±0.27	16.7±2.4	—	—	—
38	263	11.83±0.34	9.05±0.27	12.28±0.34	18.9±3.3	20.30±0.62	5.28±0.17	21.06±0.62
39	274	—	—	—	—	20.61±0.31	—	—
40	280	—	—	—	—	21.96±0.95	4.86±0.22	22.85±0.95
41	300	11.91±0.43	8.94±0.34	12.43±0.43	18.5±3.7	21.17±0.65	5.03±0.16	22.11±0.65
42	328	11.21±0.72	9.45±0.64	11.76±0.72	25.5±6.2	19.96±1.24	5.31±0.35	20.94±1.24
43	333	11.56±0.04	9.16±0.03	12.13±0.04	22.7±0.3	—	—	—
44	346	—	—	—	—	22.13±0.23	—	—
45	350	11.82±0.49	8.93±0.39	12.44±0.49	19.8±5.2	—	—	35.0±2.4
46	360	—	—	—	—	22.30±0.84	4.73±0.19	—
47	368	11.26±0.38	9.35±0.34	11.88±0.38	25.3±3.2	20.91±0.30	5.03±0.08	22.08±0.30
48	389	11.12±0.33	9.43±0.29	11.79±0.33	25.2±3.6	19.25±0.65	5.45±0.19	—
49	397	11.16±0.10	9.38±0.09	11.84±0.10	25.1±1.1	21.47±1.10	4.88±0.27	22.78±1.10
50	410	11.08±0.24	9.43±0.22	11.78±0.24	27.9±2.4	20.43±1.14	5.12±0.30	21.72±1.14
51	410	10.21±0.11	10.23±0.11	10.86±0.11	37.8±1.1	18.63±0.49	5.61±0.16	19.81±0.49
52	422	—	—	—	—	20.12±1.77	5.18±0.49	21.43±1.77
53	447	10.86±0.61	9.56±0.57	11.62±0.61	29.5±8.5	18.80±1.38	5.51±0.43	20.16±1.38
54	460	10.33±0.31	10.03±0.32	11.08±0.31	33.9±3.5	—	—	—
55	462	10.46±0.73	9.90±0.74	11.22±0.73	37.1±9.9	20.06±1.45	5.15±0.40	21.55±1.45
56	472	10.41±0.33	9.93±0.34	11.18±0.33	36.4±4.3	19.10±0.34	5.41±0.10	20.53±0.34
57	477	—	—	—	—	20.49±0.96	5.04±0.09	—
58	480	—	—	—	—	18.98±0.96	5.43±0.30	20.44±0.96
59	486	10.99±0.26	9.39±0.24	11.84±0.26	26.0±3.2	19.57±2.07	5.26±0.60	21.14±2.07
60	504	—	—	—	—	—	—	—
61	506	10.10±0.64	10.18±0.70	10.92±0.64	38.3±8.9	—	—	—
62	512	10.90±0.34	9.42±0.32	11.79±0.34	27.9±4.8	—	—	—
63	517	10.25±0.08	10.01±0.08	11.10±0.08	37.4±1.0	—	—	—
64	518	10.45±0.53	9.81±0.54	11.32±0.53	33.8±7.4	—	—	—
65	523	9.91±0.35	10.35±0.40	10.74±0.35	41.4±4.9	—	—	—

Table 2 (Continued)

Earth- quake No.	h (km)	P waves				S waves			
		\dot{p} (apparent) (sec/deg)	V_p (km/sec)	\dot{p} (true) (sec/deg)	a_p (sec)	\dot{p} (apparent) (sec/deg)	V_s (km/sec)	\dot{p} (true) (sec/deg)	a_s (sec)
1	2	3	4	5	6	7	8	9	10
66	524	10.21 \pm 0.04	10.04 \pm 0.05	—	—	—	—	—	—
67	528	10.52 \pm 0.60	9.74 \pm 0.60	11.41 \pm 0.60	32.1 \pm 8.1	—	—	—	—
68	531	10.76 \pm 0.41	9.52 \pm 0.40	11.67 \pm 0.41	30.3 \pm 5.6	—	—	—	—
69	538	10.20 \pm 0.62	10.02 \pm 0.66	11.09 \pm 0.62	35.9 \pm 8.5	20.16 \pm 2.58	5.07 \pm 0.71	—	—
70	538	10.60 \pm 0.69	9.65 \pm 0.68	11.52 \pm 0.69	31.3 \pm 9.9	—	—	—	—
71	538	10.16 \pm 0.24	10.06 \pm 0.26	11.04 \pm 0.24	37.0 \pm 3.1	—	—	—	—
72	539	10.90 \pm 0.27	9.38 \pm 0.25	11.84 \pm 0.27	27.9 \pm 3.6	—	—	—	—
73	544	10.39 \pm 0.53	9.83 \pm 0.55	11.30 \pm 0.53	33.5 \pm 7.5	—	—	—	—
74	545	10.10 \pm 0.43	10.11 \pm 0.47	10.99 \pm 0.43	38.3 \pm 6.1	—	—	—	—
75	546	10.08 \pm 0.43	10.13 \pm 0.47	10.97 \pm 0.43	38.1 \pm 6.2	—	—	—	—
76	548	10.55 \pm 0.18	9.67 \pm 0.18	11.49 \pm 0.18	32.3 \pm 2.6	—	—	—	—
77	549	10.17 \pm 0.60	10.03 \pm 0.64	11.07 \pm 0.60	37.0 \pm 8.2	17.90 \pm 1.02	5.70 \pm 0.35	19.49 \pm 1.02	79.2 \pm 13.5
78	550	—	—	—	—	—	—	—	—
79	553	10.03 \pm 0.17	10.17 \pm 0.18	10.93 \pm 0.17	38.5 \pm 2.2	—	—	—	—
80	557	10.44 \pm 0.30	9.76 \pm 0.31	11.39 \pm 0.30	34.4 \pm 4.2	—	—	—	—
81	558	10.70 \pm 0.51	9.52 \pm 0.49	11.67 \pm 0.51	30.3 \pm 7.3	—	—	—	—
82	558	10.26 \pm 0.28	9.93 \pm 0.30	11.19 \pm 0.28	35.5 \pm 4.1	—	—	—	—
83	564	10.02 \pm 0.31	10.16 \pm 0.35	10.93 \pm 0.31	39.2 \pm 4.1	—	—	—	—
84	564	10.64 \pm 0.38	9.57 \pm 0.38	11.61 \pm 0.38	30.6 \pm 5.4	—	—	—	—
85	567	10.60 \pm 0.69	9.60 \pm 0.68	11.58 \pm 0.69	31.7 \pm 9.7	—	—	—	—
86	573	10.38 \pm 0.38	9.79 \pm 0.39	11.35 \pm 0.38	33.7 \pm 5.4	—	—	—	—
87	574	—	—	—	—	17.70 \pm 1.66	5.74 \pm 0.59	19.35 \pm 1.66	79.5 \pm 21.5
88	576	10.27 \pm 0.29	9.89 \pm 0.31	11.23 \pm 0.29	35.6 \pm 4.3	18.36 \pm 0.18	—	20.08 \pm 0.18	—
89	577	10.20 \pm 0.39	9.96 \pm 0.42	11.15 \pm 0.39	36.8 \pm 5.4	—	—	—	—
90	577	10.26 \pm 0.27	9.90 \pm 0.29	11.23 \pm 0.27	35.8 \pm 3.7	20.05 \pm 2.51	5.07 \pm 0.69	—	—
91	577	9.94 \pm 0.56	10.22 \pm 0.63	10.87 \pm 0.56	39.6 \pm 7.9	—	—	—	—
92	578	—	—	—	—	18.88 \pm 1.93	5.38 \pm 0.60	20.66 \pm 1.93	66.1 \pm 25.1
93	579	10.10 \pm 0.47	10.06 \pm 0.52	11.05 \pm 0.47	37.7 \pm 6.6	—	—	—	—
94	582	10.36 \pm 0.54	9.79 \pm 0.56	11.34 \pm 0.54	34.3 \pm 7.9	—	—	—	—
95	583	10.38 \pm 0.44	9.78 \pm 0.46	11.36 \pm 0.44	34.4 \pm 5.9	—	—	—	—
96	583	10.34 \pm 0.38	9.81 \pm 0.40	11.32 \pm 0.38	33.9 \pm 5.6	—	—	—	—
97	587	9.90 \pm 0.30	10.24 \pm 0.34	10.85 \pm 0.30	40.4 \pm 4.1	—	—	—	—

1	2	3	4	5	6	7	8	9	10
98	587	10.16±0.26	9.98±0.28	11.13±0.26	37.2±3.8	—	—	—	—
99	589	10.38±0.24	9.76±0.24	11.38±0.24	33.8±3.3	18.90±1.68	5.36±0.52	20.72±1.68	65.4±22.3
100	590	10.00±0.44	10.14±0.49	10.96±0.44	39.0±6.2	—	—	—	—
101	593	10.73±0.33	9.44±0.32	11.77±0.33	29.7±4.3	—	—	—	—
102	597	10.54±0.21	9.60±0.21	11.57±0.21	31.7±2.9	—	—	—	—
103	597	10.03±0.23	10.10±0.26	11.00±0.23	39.3±3.5	17.60±1.12	5.75±0.40	19.32±1.12	82.5±15.2
104	597	9.83±0.17	10.30±0.19	10.79±0.17	41.3±2.4	—	—	—	—
105	600	9.91±0.31	10.20±0.35	10.89±0.31	39.4±4.0	—	—	—	—
106	600	9.69±0.38	10.44±0.45	10.64±0.38	44.4±5.4	—	—	—	—
107	602	10.39±0.44	9.73±0.45	11.41±0.44	33.9±6.1	—	—	—	—
108	603	9.87±0.30	10.24±0.34	10.84±0.30	40.2±4.2	—	—	—	—
109	606	10.67±0.32	9.47±0.31	11.74±0.32	30.0±4.2	19.74±1.75	5.12±0.50	—	53.8±23.6
110	606	10.08±0.48	10.02±0.52	11.09±0.48	36.8±6.6	—	—	—	—
111	600	9.43±0.45	10.72±0.56	10.36±0.45	46.2±6.0	16.13±1.91	6.27±0.81	17.72±1.91	98.5±24.4
112	602	9.49±0.48	10.65±0.59	10.43±0.48	47.2±7.3	—	—	—	—
113	605	9.47±0.47	10.67±0.58	10.41±0.47	45.1±6.5	—	—	—	—
114	606	9.47±0.37	10.67±0.46	10.41±0.37	45.8±5.2	—	—	—	—
115	609	9.46±0.26	10.67±0.32	10.41±0.26	45.4±3.6	—	—	—	—
116	609	—	—	—	—	16.42±1.13	6.15±0.47	18.06±1.13	94.8±15.2
117	613	9.55±0.42	10.57±0.51	10.51±0.42	46.4±6.2	—	—	—	—
118	617	9.52±0.24	10.59±0.30	10.49±0.24	46.0±3.5	—	—	—	—
119	617	9.43±0.41	10.70±0.51	10.39±0.41	45.6±5.5	16.20±1.90	6.23±0.81	17.85±1.90	97.6±24.8
120	618	—	—	—	—	15.85±0.61	6.36±0.27	17.46±0.61	102.0±8.1
121	618	9.51±0.47	10.61±0.58	10.47±0.47	45.3±6.9	16.37±0.86	6.16±0.36	18.03±0.86	99.4±11.9
122	627	9.45±0.32	10.66±0.39	10.42±0.32	45.4±4.5	—	—	—	—
123	628	9.28±0.47	10.84±0.60	10.25±0.47	47.3±6.4	—	—	—	—
124	629	9.43±0.46	10.67±0.58	10.41±0.46	45.8±6.2	—	—	—	—
125	636	9.53±0.70	10.55±0.86	10.53±0.70	46.3±9.2	—	—	—	—
126	637	9.45±0.36	10.63±0.44	10.45±0.36	46.6±5.2	—	—	—	—
127	643	—	—	—	—	15.92±1.05	6.31±0.46	17.62±1.05	101.3±13.7
128	660	9.26±0.38	10.81±0.49	10.28±0.38	47.2±5.5	—	—	—	—
129	665	—	—	—	—	15.77±0.93	6.34±0.41	17.52±0.93	103.1±12.3
130	668	9.59±0.11	—	—	46.2±1.6	—	—	—	—

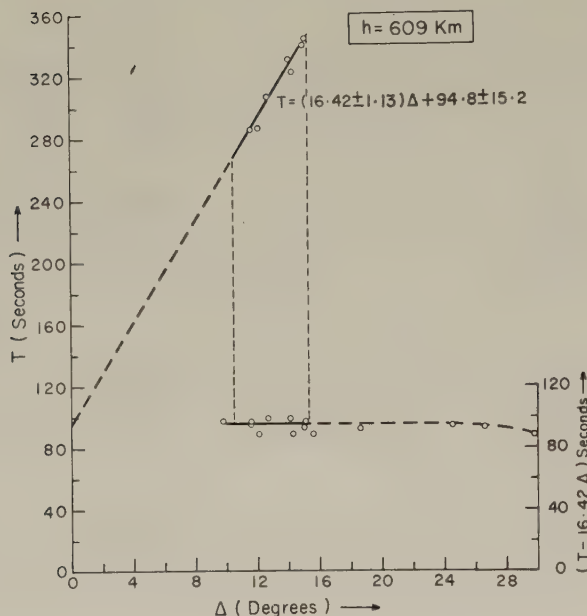


Fig. 5. S wave travel time curve T versus Δ for earthquake with focal depth 609 km between the limits Δ_1 and Δ_2 of epicentral distance. Reduced travel time curve $(T - p\Delta)$ versus Δ is also shown where $p = \partial T / \partial \Delta$ at the inflection point.

determined as 4.58 km/sec at a 40 km depth increases linearly, with a gradient of 0.28 ± 0.02 km/sec per 100 km, to 4.83 km/sec at a depth of 130 km. From 130 to 410 km depth S velocity is found to increase linearly from 4.83 to 5.11 km/sec with a low velocity gradient of only 0.10 ± 0.01 km/sec per 100 km. At this transition depth of 410 km there is a first order velocity discontinuity for S waves the velocity increasing from 5.11 to 5.32 km/sec. Below 410 km depth the S velocity gradient is also extremely small, velocity increasing only to a value of 5.39 km/sec at a depth of 600 km. At this depth of 600 km there is again a first order velocity discontinuity for S waves—the velocity increasing from 5.39 to 6.21 km/sec. Below 600 km depth, S velocity increases linearly from 6.21 to 6.34 km/sec at a depth of 665 km. The above model of S velocity function shown in Fig. 7 gave a χ^2 value of about 66 on 63 degrees of freedom which corresponds to a probability of 0.25–0.75 and therefore it is an acceptable model.

The discontinuities at 410 and 600 km are also revealed by the p_{true} versus depth plots for both P and S waves (Figs. 8 and 9). $a (= T - p\Delta)$ values in the neighbourhood of the inflection point have been plotted versus depth in Fig. 10 for P waves and in Fig. 11 for S waves. Straight line fits are made in different depth ranges by least squares method for the plotted points which are shown by thick lines in Figs. 10 and 11. Both a_P and a_S curves also show clearly the presence of first order discontinuities at depths of 410 and 600 km. These a_P and/or a_S calibration curves are also useful for earthquake focal depth determination in the Tonga-Kermadec arc and the New Zealand regions.

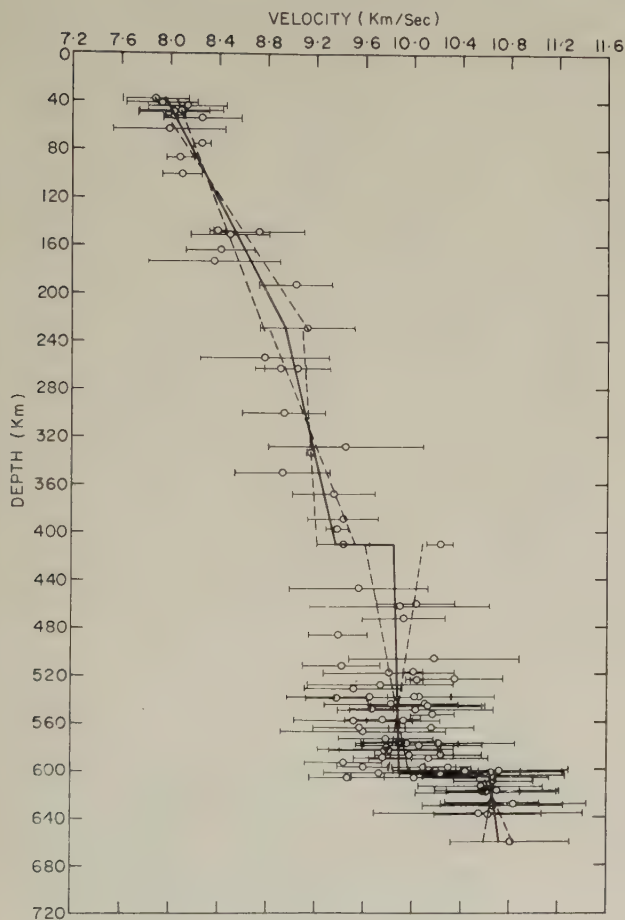


Fig. 6. P wave velocity versus depth curve for the Tonga-Kermadec-New Zealand region. — are the least squares fits obtained for the velocity depth points shown by \circ in different depth ranges and --- are the 95% confidence limits of their slopes. Truncated horizontal bars represent the standard deviations in the velocity values.

4. Discussion

Upper mantle P wave velocity structure in the Tonga-Kermadec-New Zealand region as determined in the present study is compared with the P velocity structure for the New Hebrides region determined by KAILA and KRISHNA (1978) in Fig. 12. Upper mantle P velocity structures for other regions of the earth due to KAILA *et al.* (1971) for Japan, JEFFREYS (1939), JOHNSON (1969) and SIMPSON *et al.* (1974), have also been included in the same figure for comparison. Upper mantle S wave velocity structure in the Tonga-Kermadec-New Zealand region as determined in the present study is also compared with the S velocity structure for the New Hebrides region determined by KAILA and KRISHNA (1978) in Fig. 13. In the same figure are also shown, for comparison, S velocity structures for other regions of the earth due to KAILA *et al.* (1974) for Japan, JEFFREYS (1939) and HELMBERGER and ENGEN (1974). The P and S velocities at the top of the mantle in the New Zealand region, as determined in the present study, are 7.97 and 4.58 km/sec respectively. SHOR *et al.* (1971) from seismic refraction studies in the Melanesian Borderland along a profile GH across the Kermadec ridge found P_n velocities of 7.8 and 8.1 km/sec

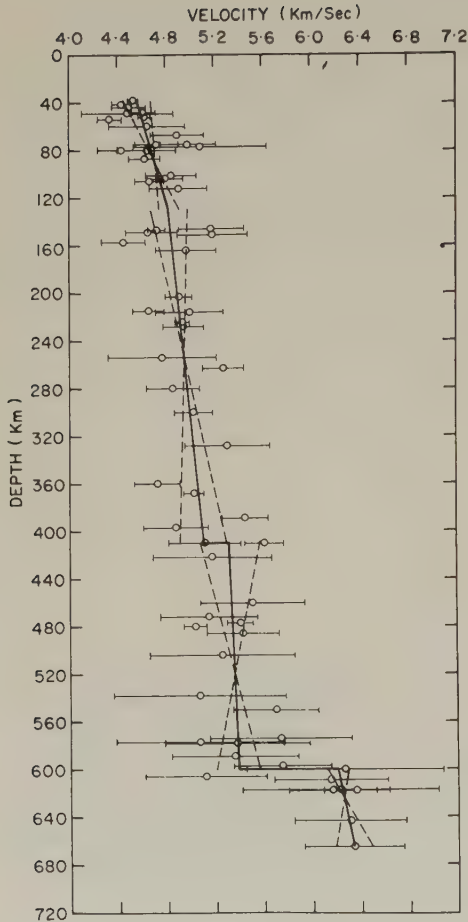


Fig. 7. S wave velocity versus depth curve for the Tonga-Kermadec-New Zealand region. — are the least squares fits obtained for the velocity depth points shown by \circ in different depth ranges and --- are the 95% confidence limits of their slopes. Truncated horizontal bars represent the standard deviations in the velocity values.

under the Kermadec trench and the Kermadec ridge respectively. These velocity values are quite consistent with our P velocity value of 7.97 km/sec. HAMILTON (1966) also determined the P_n and S_n velocities for the New Zealand region as 8.13 ± 0.05 and 4.72 ± 0.03 km/sec respectively based on the data out to 10° distance from 15 earthquakes of the Fiordland earthquake sequence of 1960.

It can be seen from Figs. 12 and 13, that the P and S velocities to a depth of at least 240 km in the Tonga-Kermadec-New Zealand region are about 6% higher, on the average (about 10% higher at a depth of 240 km for P waves and about 7% higher at a depth of 220 km for S waves) than those in the adjacent New Hebrides island arc region although the velocities are comparable in both the regions at the top of the mantle both for P and S waves. In our opinion, these large differences in the velocities are primarily due to the differences in the temperature prevailing at depths in the two regions. The measurements of high temperature and pressure derivatives of elastic constants for a number of compounds appropriate for geophysical considerations as reported by ANDERSON *et al.* (1968), indicate that a temperature contrast of the order of $1,000^\circ\text{C}$ is needed to account for a 6%

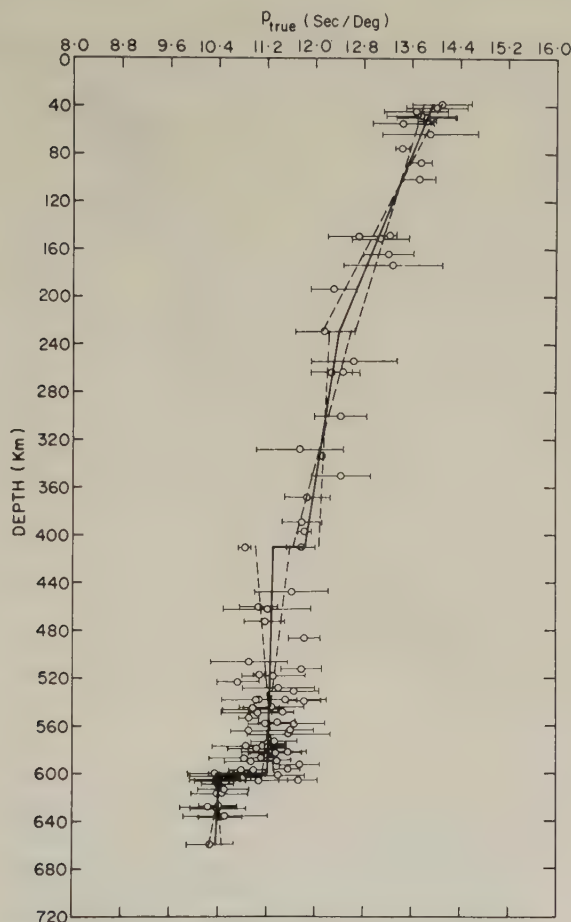


Fig. 8. For P waves $p_{\text{true}} (= \partial T / \partial \Delta)$ versus depth curve for the Tonga-Kermadec-New Zealand region. — are the least squares fits obtained for the p_{true} depth points shown by \circ in different depth ranges and --- are the 95% confidence limits of their slopes. Truncated horizontal bars represent the standard deviations in the p values.

difference in the observed P velocities. The S velocity difference observed in the two regions will, however, require a somewhat smaller temperature contrast. Therefore, the temperatures in the upper mantle beneath the Tonga-Kermadec-New Zealand region are about $1,000^{\circ}\text{C}$ lower than those at comparable depths in the New Hebrides region. Further, it is also possible that this temperature excess in the New Hebrides region, may cause a partial melting which would also decrease the velocity. KANAMORI (1968) found that a 2% partial melting would cause about 1% velocity decrease using the equation $V = V_0(1 - 0.58c)$ given by HASHIN (1962), where V is the P velocity in a material having a liquid inclusion of concentration c and V_0 is the velocity for $c=0$. Thus the actual temperature difference in the two regions, the New Hebrides and the Tonga-Kermadec-New Zealand may be somewhat less than $1,000^{\circ}\text{C}$.

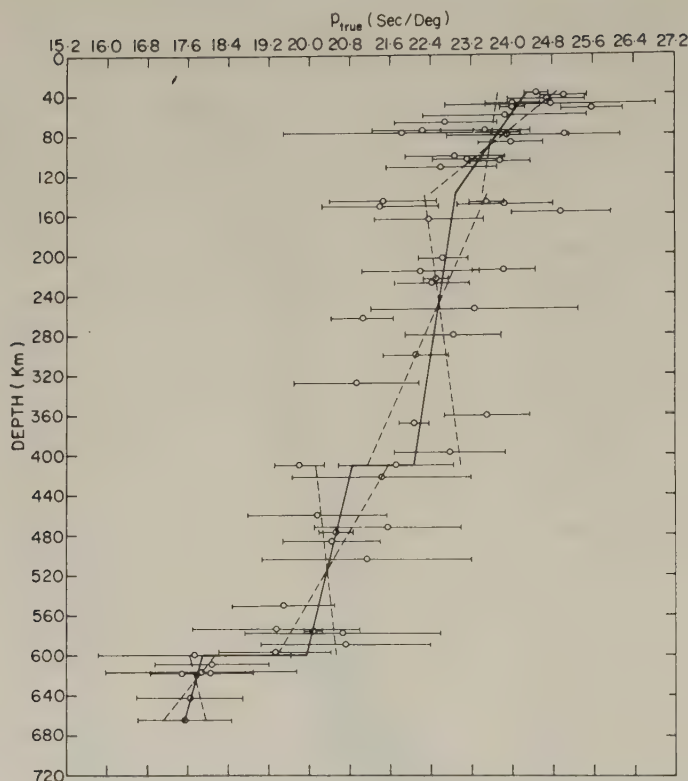


Fig. 9. For S waves $p_{true} (= \partial T / \partial D)$ versus depth curve for the Tonga-Kermadec-New Zealand region. — are the least squares fits obtained for the p_{true} depth points shown by \circ in different depth ranges and --- are the 95% confidence limits of their slopes. Truncated horizontal bars represent the standard deviations in the p values.

In Fig. 1 we have also shown the heat flow observations in the southwest Pacific region compiled by JESSOP *et al.* (1976). We have however, classified the heat flow values only into 3 ranges as shown in Fig. 1 instead of 5 ranges as given by JESSOP *et al.* (1976). It can be seen from Fig. 1 that the average heat flow value in the eastern north island of New Zealand and in the Tonga-Kermadec deep earthquake zone is much smaller than that in the New Hebrides seismic zone. Thus the distribution of heat flow in the two regions is also quite consistent with our idea that the temperatures in the New Hebrides region may be higher than those in the Tonga-Kermadec-New Zealand region. This is precisely the reason why the velocity gradients for P and S waves in the New Hebrides region are extremely small. On the other hand the velocity gradients in the Tonga-Kermadec-New Zealand region are much higher at similar depths for both P and S waves.

The velocity functions for P and S waves in the Tonga-Kermadec-New Zealand region as determined in the present study are also found to reveal much higher velocities than those found in the Japan region by KAILA *et al.* (1971, 1974) as can be seen from Figs. 12 and 13. The P velocities determined in the present study are found on the average, to be about 3% higher in the depth range 40–200 km, 6–7% higher in the depth range

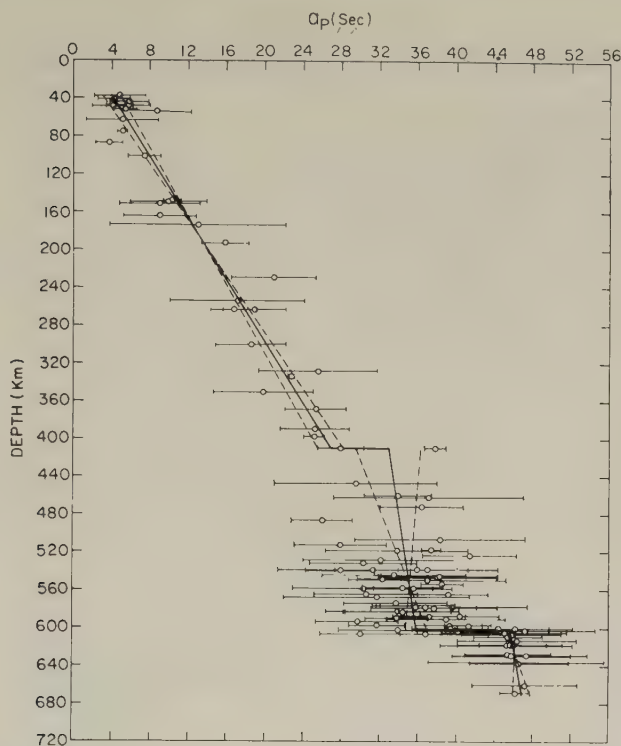


Fig. 10. $a_p (=T-p\Delta)$, at the inflection point, versus depth as a calibration curve for earthquake focal depth determination from P wave data in the Tonga-Kermadec-New Zealand region. — are the least squares fits obtained for the a_p -depth points shown by \circ in different depth ranges and --- are the 95% confidence limits of their slopes. Truncated horizontal bars represent the standard deviations in the a_p values.

200–400 km and again about 3% higher from 400–550 km depth as compared to those in the central Japan region in the corresponding depth ranges. The P velocity in the southwest Japan almost remains constant to a depth of about 255 km thus showing even much lower velocities to that depth. Similarly, the S velocities in the Tonga-Kermadec island arc region as determined in the present study are also found to be 6–7% higher, on the average, throughout the depth range of about 600 km than those in the central Japan region. Again it can be seen that the S velocity in the southwest Japan also remains constant at least to the depth of 170 km studied (KAILA *et al.*, 1974) thus revealing much lower velocities to the depth of 170 km as compared to the S velocities in the Tonga-Kermadec-New Zealand region, New Hebrides region and the central Japan region. However there is an interesting similarity which can be seen from Figs. 12 and 13 as regards the velocity anomalies in the southwest Pacific region and in the Japan region. The velocities in the southwest and central Japan regions are although comparable in the top of the mantle; since the velocity gradient for P and S waves in the southwest Japan are almost close to zero, there are large differences in the velocities at depths in both the re-

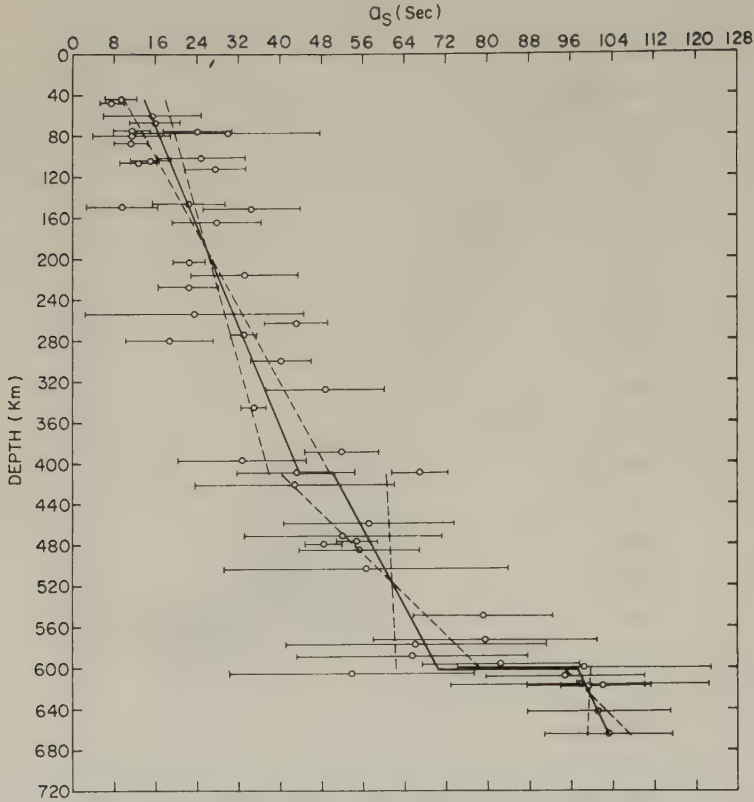


Fig. 11. $a_s (= T - p\Delta)$, at the inflection point, versus depth as a calibration curve for earthquake focal depth determination from S wave data in the Tonga-Kermadec-New Zealand region. — are the least squares fits obtained for the a_s -depth points shown by \circ in different depth ranges and --- are the 95% confidence limits of their slopes. Truncated horizontal bars represent the standard deviations in the a_s values.

gions. A similar situation can also be seen in the southwest Pacific region; the velocities at depths in the New Hebrides and the Tonga-Kermadec regions show larger and larger differences because the velocity gradients of P and S waves in the New Hebrides region are also close to zero. These velocity anomalies in the Japan as well as the southwest Pacific region can be attributed primarily due to the lateral temperature variations prevailing between the southwest and central Japan regions on the one hand and between the New Hebrides and the Tonga-Kermadec regions, on the other. The effects of the compositional variations will be almost negligible between the two sets of regions, the uppermost mantle, velocities being almost similar. On the other hand, the major differences in the velocity structure between the Japan and the southwest Pacific regions although can be attributed primarily due to variations in the thermal structure of the mantle beneath them, however, we cannot rule out the possibility that some component of these velocity anomalies may be also due to some compositional variations. The extent to which compositional variations will affect the velocities in these regions will, of course, be very

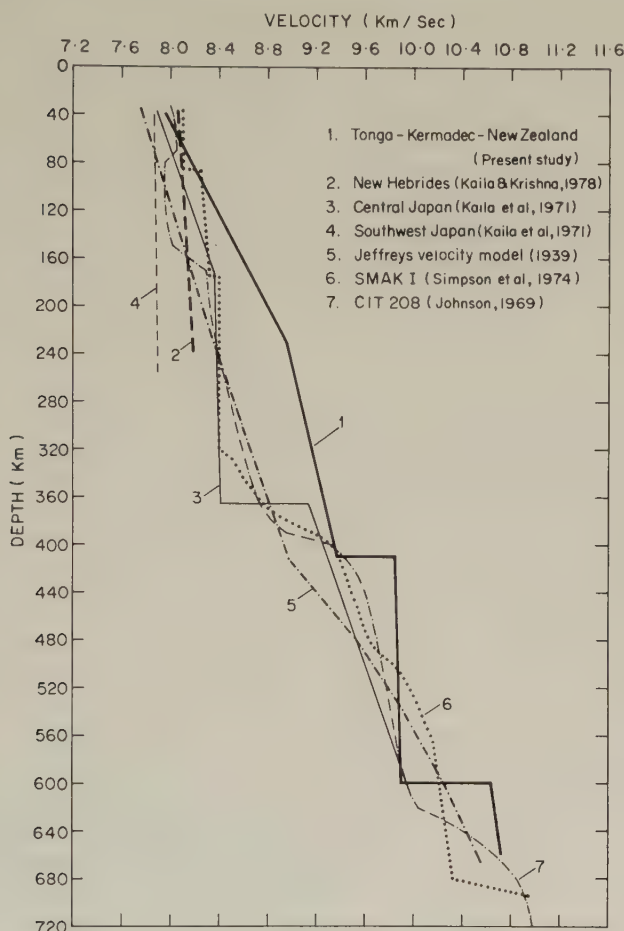


Fig. 12. P wave velocity function for the inclined seismic zone beneath the Tonga-Kermadec-New Zealand region as determined in the present study along with velocity models for other regions of the Earth.

limited and therefore only the temperature differences will account for these velocity anomalies to a great extent.

We can however find from Figs. 12 and 13, that qualitatively the velocity functions reveal very similar features in the Japan and the Tonga-Kermadec-New Zealand regions. A second order low velocity layer, i.e., a decrease in the velocity gradient is found to occur at a depth of 230 km for P waves and 130 km for S waves in the Tonga-Kermadec-New Zealand region also as in the Japan region. In our opinion, this decrease in the velocity gradients for both P and S waves within the inclined seismic zone may be due to the effect of high temperatures at those depths. These high temperatures at depths in the inclined seismic zone might have been resulted due to the influence of the surrounding asthenosphere layer where the temperatures may be anomalously high. BARAZANGI and ISACKS (1971) from a detailed study of the variations of predominant frequencies of P and S waves

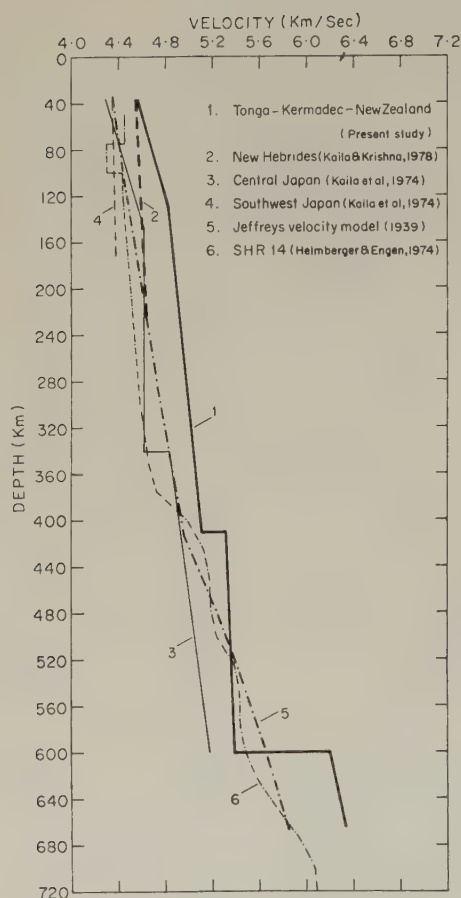


Fig. 13. S wave velocity function for the inclined seismic zone beneath the Tonga-Kermadec-New Zealand region as determined in the present study along with velocity models for other regions of the Earth.

that traverse the wedge of mantle above the inclined seismic zone of intermediate and deep earthquakes of Tonga found that the material present throughout the prism of the mantle above depths of about 150 to 300 km above the inclined seismic zone is of anomalously high attenuation. According to them, the data implies an anomalous increase in attenuation in the asthenosphere near the inclined seismic zone, Q may be as small as 50 for P waves and less than 20 for S waves. The high attenuation at depths in the asthenosphere may be because of anomalously high temperatures at those depths. These high temperatures are even affecting the material in the inclined seismic zone thus reducing the P and S wave velocity gradients considerably. At a depth of 410 km there is a first velocity discontinuity for P and S waves in the Tonga-Kermadec-New Zealand region whereas this discontinuity is found to occur at a depth of 365 km for P waves and 340 km for S waves in the Japan region. The only difference that can be seen is that the P velocity gradient between 410 to 600 km depth is very small in the Tonga-Kermadec-New Zealand region, whereas in this depth range the P wave velocity gradient in the Japan region is much higher. However the P velocities in the Tonga-Kermadec-New Zealand region are much higher in this depth range about 3% higher, on the average, than in the Japan

region whereas at about 600 km depth, the velocity in both the regions is almost the same. This suggests that probably the temperature difference in the two regions is prevailing up to about 600 km depth and beyond this depth the temperatures in the two regions may be almost comparable. CIT 208 P wave velocity model given by JOHNSON (1969) applicable as an average for the Pacific ocean basin and its immediate surroundings is also shown in Fig. 12 for comparison with our P velocity curve. This model has a low velocity layer between depths of 70 and 150 km and regions of rapid increase of velocity starting at depths of 390 and 620 km. The velocities given by CIT 208 model are substantially lower than those given by our P velocity curve thus showing that the velocities in the Tonga-Kermadec-New Zealand seismic region are much higher than the average values for the Pacific region. Therefore we can safely conclude that the mantle material beneath the Tonga-Kermadec-New Zealand seismic region is relatively colder (and denser) than the surrounding upper mantle material and as such the velocities are very high in this region. FITCH (1975), MITRONOVAS and ISACKS (1971), PASCAL *et al.* (1973) and UTSU (1967) have also reported that the inhomogeneity in the upper mantle structure is probably due to a relatively cold (hence denser) oceanic lithosphere which has been thrust downward in these regions and that there may be an average velocity contrast of 5–10%.

JEFFREYS (1939) velocity curves for both P and S waves also reveal about 6% lower velocities on the average, to a depth of about 500 km as compared to our P and S velocity curves for the Tonga-Kermadec-New Zealand region again showing that the velocities in this region are higher than average. The shear velocity model SHR 14 given by HELMBERGER and ENGEN (1974) for the Western United States is also shown in Fig. 13 for comparison with our S velocity curve. The S velocity model SHR 14 also shows regions of rapid velocity gradients at depths of 375 to 425 km and around 500 km. However the S velocities given by SHR 14 model, especially to depths of 400 km, are substantially lower by about 8–10% than those given by our S velocity curve. This shows that the velocities in the Western United States are also much lower than those in the Tonga-Kermadec-New Zealand regions and as such the temperatures in the Western United States are probably much higher as compared to Tonga-Kermadec island arc region.

The P velocity model SMAK I for northeastern Australia given by SIMPSON *et al.* (1974) is shown in Fig. 12 for comparison. According to them, it has a low gradient in velocity up to about 300 km, a gradual increase in velocity between 300 and 400 km a minor zone of high velocity gradient near 520 km, a low gradient in velocity from 550 to 680 km and an abrupt increase in velocity near 680 km. It can be seen from Fig. 12 that our P velocity model reveals two sharp first order velocity discontinuities corresponding to the probable phase transformations of the mantle material at 410 and 600 km depths, whereas, SMAK I model shows a rapid increase of velocity between about 360–400 km depth and an abrupt increase of velocity at a depth of about 680 km. However, an overall comparison of SMAK I model with our P velocity curve shows that the velocities in the Tonga-Kermadec-New Zealand region in the depth range from 100 to at least 400 km are substantially higher than those in the northeastern Australia. This fact again supports our idea that there are large temperature differences prevailing even at great depths in the upper mantle beneath various regions. It can be seen from Fig. 12 that SMAK I model for northeast Australia is much closer to the P velocity curve for the nearby New Hebrides region given by KAILA and KRISHNA (1978). The velocity gradients in both the regions in shallower part are extremely small. It may be mentioned here that the source region involved in deriving the SMAK I model is New Guinea, New Britain and Solomon islands region,

where there are a number of active volcanoes as can be seen from Fig. 1. Same is true of the New Hebrides region where there are number of active volcanoes as shown in Fig. 1. The heat flow in these two regions is also quite high. All these observations suggest that probably the temperatures prevailing in these regions at depths are much higher than those in the Tonga-Kermadec-New Zealand region. The high temperatures prevailing at depths in the regions of New Hebrides, New Guinea, New Britain and Solomon islands are thus controlling the velocity gradients to a great extent and keeping the velocities almost constant to large depths of 200–300 km because most probably the mantle material there may be in a partially molten state. On the other hand the temperatures beneath the Tonga-Kermadec-New Zealand region seem to be less than the temperatures in those regions by as much as $1,000^{\circ}\text{C}$ and therefore the P and S velocities and their gradients in this region, as determined in the present study, are much higher.

ROBINSON (1976) from the study of the relative travel time residuals for P waves at stations in the north island of New Zealand from 5 deep focus events in the Banda sea region found that the upper mantle velocity along paths to stations in the east of the north island should be higher than that along paths to the more western stations. He has explained this difference as due to higher than normal velocities in the oceanic lithosphere which is underthrust to depths of 350 km beneath the north island. After correction for crustal structure, he attributed an average difference in travel time of about 2.5 sec which can arise due to an average P wave velocity about 11% higher than in the surrounding mantle. According to Robinson this is only a rough estimate, which may be on the higher side, the actual difference may be substantially lower. However, the velocity in the underthrust lithosphere is found to be much higher than that in the surrounding mantle. Our P and S velocity functions also reveal much higher velocities in the Tonga-Kermadec-New Zealand seismic region which are quite consistent with these findings.

BARAZANGI and ISACKS (1971) mapped in detail a zone of anomalously high seismic wave attenuation under the Lau basin, an interarc basin located west of or behind the Tonga island arc. High attenuation, or low Q , is often associated with low seismic wave velocities, and together they probably indicate anomalies in temperature or degree of partial melting in the mantle. Quantitative estimates of these thermal anomalies are more reliably determined from velocity data than from attenuation data, although observed effects of attenuation are the most prominent. AGGARWAL *et al.* (1972) reported extremely low compressional wave velocities of about 7.1 km/sec in the uppermost mantle beneath most of the Lau basin. The large difference of about 10–12% between P wave velocities beneath the Lau basin and those found by us in the present study beneath New Zealand probably requires partial melting in the upper mantle beneath the Lau basin. It can be seen from our Fig. 1 that the heat flow in the region of the Lau basin is comparatively much higher on the average than that found in the north island, especially in the eastern north island, of the New Zealand. Therefore, in our opinion, the high attenuation of the seismic energy and very low velocities found in the Lau basin are mainly due to very high temperatures prevailing there which is also evident from the very high heat flow values there. The velocities of P and S waves although are normal at the top of the mantle, they are much higher at depths in the New Zealand region. These differences again substantiate our view that large temperature differences are mainly responsible for these velocity anomalies.

5. Conclusions

From the present study of the upper mantle velocity structure in the Tonga-Kermadec-New Zealand region from travel time data of P and S waves we can make the following conclusions.

1) The P and S wave velocities in the inclined seismic zone beneath Tonga-Kermadec-New Zealand region are about 6% higher than those in the adjacent New Hebrides seismic zone. The difference between them is almost negligible at the top of the mantle but is quite high about 10% at a depth of 240 km for P waves and about 7% at a depth of 220 km for S waves.

2) There are two first order velocity discontinuities at depths of 410 and 600 km for both P and S waves.

3) The velocities for P and S waves in the Tonga-Kermadec-New Zealand region are also much higher (about 3 to 6%) than those in the Japan region to a depth of 600 km. These velocities are also substantially higher than those for the average upper mantle structure valid for the Pacific ocean basin and its surroundings.

4) The P and S wave velocities in the inclined seismic zone beneath the Tonga-Kermadec-New Zealand region are the highest in the Pacific region. All these velocity anomalies, however, seem to exist only to a depth of about 600 km in the mantle and beyond that depth the differences get gradually minimized.

5) Large velocity differences of the order of 6% can arise due to temperature differences of the order of 1,000°C. Such large lateral temperature differences may exist in the upper mantle up to a depth of about 600 km.

6) There is a decrease in the P and S velocity gradients at a depth of 230 km for P waves and 130 km for S waves which is presumed to be due to existence of high temperatures at those depth ranges. This decrease in the P and S wave velocity gradients can be interpreted as the second order low velocity channel.

We are grateful to Dr. Hari Narain, Director, National Geophysical Research Institute for providing all the facilities to carry out this research work and for his kind permission to publish this paper. Our thanks are also due to Mr. G. Khandekar for his help in the data collection and some computations. Preparation of the tracings of various drawings by Mr. P.J. Vijayanandam is duly acknowledged.

REFERENCES

- AGGARWAL, Y.P., M. BARAZANGI, and B. ISACKS, P and S travel times in the Tonga-Fiji region: A zone of low velocity in the uppermost mantle behind the Tonga island arc, *J. Geophys. Res.*, **77**, 6427-6434, 1972.
- ANDERSON, D.L., Recent evidence concerning the structure and composition of the Earth's mantle, in *Physics and Chemistry of the Earth*, Vol. 6, edited by L.H. Ahrens, Frank Press, S.K. Runcorn, and H.C. Vrey, Pergamon Press, New York, 1966.
- ANDERSON, D.L., Phase changes in the upper mantle, *Science*, **157**, 1165-1173, 1967.
- ANDERSON, O.L., E. SCHREIBER, R.C. LIEBERMANN, and N. SOGA, Some elastic constant data on minerals relevant to geophysics, *Rev. Geophys.*, **6**, 491-524, 1968.
- BARAZANGI, M. and B. ISACKS, Lateral variations of seismic wave attenuation in the upper mantle above the inclined earthquake zone of the Tonga island arc: Deep anomaly in the upper mantle, *J. Geophys. Res.*, **76**, 8493-8516, 1971.
- BIRCH, F., Elasticity and constitution of the Earth's interior, *J. Geophys. Res.*, **57**, 227-286, 1952.
- BIRCH, F., Composition of the Earth's mantle, *Geophys. J.R. Astr. Soc.*, **4**, 295-311, 1961.
- BIRCH, F., Density and composition of mantle and core, *J. Geophys. Res.*, **69**, 4377-4388, 1964.
- BULLEN, K.E. and R.A.W. HADDON, Earth models based on compressibility theory, *Phys. Earth Planet. Inter.*, **1**, 1-13, 1967.

- BURDICK, L. and D.L. ANDERSON, Interpretation of velocity profiles of the mantle, *J. Geophys. Res.*, **80**, 1070–1074, 1975.
- FITCH, T.J., Compressional velocity in source regions of deep earthquakes: An application of the master earthquake technique, *Earth Pldnet. Sci. Lett.*, **26**, 156–166, 1975.
- HAMILTON, R.M., The Fiordland earthquake sequence of 1960 and seismic velocities beneath New Zealand, *N.Z.J. Geol. Geophys.*, **9**, 224–238, 1966.
- HAMILTON, R.M. and A.W. GALE, Seismicity and structure of North Island, New Zealand, *J. Geophys. Res.*, **73**, 3859–3876, 1968.
- HAMILTON, R.M. and A.W. GALE, Thickness of the mantle seismic zone beneath the North Island of New Zealand, *J. Geophys. Res.*, **74**, 1608–1613, 1969.
- HASHIN, Z., The elastic moduli of heterogeneous materials, *J. Appl. Mech.*, **29**, 143–150, 1962.
- HATHERTON, T., Gravity, seismicity, and tectonics of the North Island, New Zealand, *N.Z.J. Geol. Geophys.*, **13**, 126–144, 1970.
- HELMBERGER, D.V. and G.R. ENGEN, Upper mantle shear structure, *J. Geophys. Res.*, **79**, 4017–4028, 1974.
- JEFFREYS, H., The times of P, S, and SKS and the velocities of P and S, monthly notices, *Roy. Astron. Soc. Geophys.*, **4** (Suppl.), 498–533, 1939.
- JESSOP, A.M., M.A. HOBART, and J.G. SCLATER, Terrestrial heat flow data, Map produced by P.J. Grim, National Geophysical and Solar-Terrestrial Data Center, U.S.A., 1976.
- JOHNSON, L.R., Array measurements of P velocities in the lower mantle, *Bull. Seismol. Soc. Am.*, **59**, 973–1008, 1969.
- KAILA, K.L., A new analytical method for finding the upper mantle velocity structure from P and S wave travel times of deep earthquakes, *Bull. Seismol. Soc. Am.*, **59**, 755–769, 1969.
- KAILA, K.L. and V.G. KRISHNA, Nature of the 400-km discontinuity in the Earth's mantle, *Geophys. J. R. Astr. Soc.*, **46**, 185–188, 1976.
- KAILA, K.L. and V.G. KRISHNA, Upper mantle velocity structure in the New Hebrides island arc region, Paper presented at the International Geodynamics Conference, March 13–17, Tokyo, Japan, 1978.
- KAILA, K.L., V.G. KRISHNA, and Hari NARAIN, Upper mantle P wave velocity structure in the Japan region from travel time studies of deep earthquakes using a new analytical method, *Bull. Seismol. Soc. Am.*, **61**, 1549–1570, 1971.
- KAILA, K.L., V.G. KRISHNA, and Hari NARAIN, Upper mantle shear wave velocity structure in the Japan region, *Bull. Seismol. Soc. Am.*, **64**, 355–374, 1974.
- KANAMORI, H., Travel times to Japanese stations from Longshot and their geophysical implications, *Bull. Earthq. Res. Inst. Tokyo Univ.*, **46**, 841–859, 1968.
- MACDONALD, G.A., *Volcanoes*, Prentice-Hall, Englewood Cliffs, New Jersey, 1972.
- McKENZIE, D.P., Speculations on the consequences and causes of plate motions, *Geophys. J.*, **18**, 1–32, 1969.
- MINER, J.W. and M.N. TOKSOZ, Thermal regime of a downgoing slab and new global tectonics, *J. Geophys. Res.*, **75**, 1397–1419, 1970.
- MITRONOVAS, W. and B.L. ISACKS, Seismic velocity anomalies in the upper mantle beneath the Tonga-Kermadec island arc, *J. Geophys. Res.*, **76**, 7154–7180, 1971.
- MOONEY, H.M. and T. HATHERTON, Upper mantle inhomogeneity beneath New Zealand, *EOS, Trans. Am. Geophys. Union*, **50**, 246, 1969 (abstr.).
- OLIVER, J. and B. ISACKS, Deep earthquake zones, anomalous structures in the upper mantle, and the lithosphere, *J. Geophys. Res.*, **72**, 4259–4275, 1967.
- OXBURGH, E.R. and D.L. TURCOTTE, Thermal structure of island arcs, *Bull. Geol. Soc. Am.*, **81**, 1665–1688, 1970.
- PASCAL, G., J. DUBOIS, M. BARAZANGI, B.L. ISACKS, and J. OLIVER, Seismic velocity anomaly beneath the New Hebrides island arc: Evidence for a detached slab in the upper mantle, *J. Geophys. Res.*, **78**, 6998–7004, 1973.
- ROBINSON, R., Relative teleseismic travel time residuals, North Island, New Zealand, and their relation to upper mantle structure, *Tectonophysics*, **31**, T41–T48, 1976.
- SHOR, G.G., Jr., H.K. KIRK, and H.W. MENARD, Crustal structure of the Melanesian area, *J. Geophys. Res.*, **76**, 2562–2586, 1971.
- SIMPSON, D.W., R.F. MEREAU, and D.W. KING, An array study of P-wave velocities in the upper mantle transition zone beneath northeastern Australia, *Bull. Seismol. Soc. Am.*, **64**, 1757–1788, 1974.
- UTSU, T., Anomalies in seismic wave velocity and attenuation associated with a deep earthquake zone, I, *J. Fac. Sci., Hokkaido Univ.*, Ser. VII, **3**, 1–25, 1967.

MORPHOLOGY AND STRUCTURE OF THE SOUTHERN PART OF THE NEW HEBRIDES ISLAND ARC SYSTEM

J. DANIEL

Office de la Recherche Scientifique et Technique Outre-Mer, Noumea Cedex, Nouvelle Calédonie

(Received May 25, 1978; Revised September 22, 1978)

A morphological study of the Southern part of the New Hebrides island arc system makes it possible to define the different structural units:

- 1) An accretionary prism with a constant width of approximately 75 km does exist;
- 2) The morphology of this prism varies rapidly along the arc and is linked, firstly to the morphology and structure of the upper part of the dipping plate and, secondly to the presence of volcanic island acting as sediment sources;
- 3) The island arc and its connecting structural features such as troughs at the rear of the arc, are disrupted by transversal discontinuities, the largest of which could be related to fractures of the oceanic crust of the dipping plate.

1. Introduction

The New Hebrides island arc (Figs. 1 and 2), stretching across roughly 1,500 km of the South-West Pacific, is a part of the Indo-Australian and Pacific plates boundary. As opposed to the majority of the peripacific arcs, the dip, as defined by seismicity, faces east towards the ocean; more precisely, the North Loyalty Plateau (Fig. 2) underthrusts the North Fiji Plateau, the origin and the nature of which still remains a subject of conjecture.

The New Hebrides island arc (Fig. 2) is divided into three belts (MITCHELL and WARDEN, 1971): "a western belt comprising Espiritu Santo and Malekula, an eastern belt consisting of Maewo and Pentecost and a central chain which includes all the active and most of the recently extinct volcanoes." The activity of this volcanic belt (Santa Cruz, Banks, Aoba, Ambrym, Epi, Erromango, Tanna) is related to the present subduction, the origin of which is traced back to 7–8 my (DUGAS *et al.*, 1977). The western and eastern belts were formed previously during Oligocene and Miocene and were probably related to subductions involving possible changes of polarity (CARNEY and MACFARLANE, 1977).

In consequence, the northern and central parts of the arc are morphologically complex, whereas the southern part is far more straight forward. This is apparently due to the sole Pliocene-actual subduction in existence. Furthermore the topography of the oceanic crust which makes up the upper part of the dipping plate is so uneven in the northern and central parts that the depth is less than 2,000 m at the level of Torres Islands and the trench disappears at the level of Espiritu Santo and Malekula islands. Consequently it was decided to study the southern part of the arc between the islands of Efate and Tanna. The profiles shown (Figs. 3 and 5) were recorded during AUSTRADEC

* AUSTRADEC group is an association of CEPM (Comité d'Etudes Pétrolières Marines), CNEXO (Centre National pour l'Exploitation des Océans), IFP (Institut Français du Pétrole), and ORSTOM (Office de la Recherche Scientifique et Technique Outre-Mer).

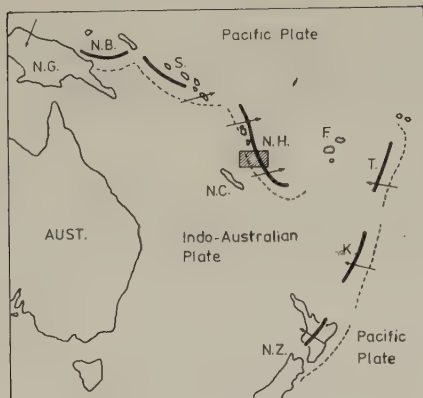


Fig. 1. Subduction zones and island arcs of the South-West Pacific. Dark lines are islands arcs; broken lines are the axis of the trenches. Arrows show underthrusting directions determined from focal mechanisms (from JOHNSON and MOLNAR, 1972). NG, New Guinea; NB, New Britain; S, Solomon; NH, New Hebrides; NC, New Caledonia; F, Fiji; T, Tonga; K, Kermadec; NZ, New Zealand; AUS, Australia.

(AUSTRALDEC group*) and EVA (ORSTOM) cruises of R.V. "Coriolis" and "Le Noroit," R.V. "CHAIN" 800 and 900 (Woodhole Oceanographic Institute), H.M.A.S. "KIMBLA" (ORSTOM and the University New South Wales) and G.C. 30 of R.V. "Glomar Challenger (DSDP)."

The most important morphological features are, firstly, the trench, particularly its inner slope, and secondly the troughs at the rear of the arc.

2. Morphology of the Trench

The morphology of the trenches associated with the subduction zones were studied by several authors especially following the conception of the accretionary prism (DICKINSON, 1973; KARIG, 1974; KARIG and SHARMAN, 1975). The terminology used in this paper is taken from these authors.

The inner wall of a trench can be divided into two sections:

- 1) The lower slope, between the axis of the trench and the trench slope break;
- 2) The upper slope, between the trench slope break and the upper slope discontinuity.

The upper slope discontinuity marks the tectonic boundary between the accretionary prism and the frontal arc.

KARIG and SHARMAN (1975) assumed three principal configurations of the accretionary prism, according to the type of accreted material and its subsequent morphology:

- 1) The simplest type represented by the Tonga and Mariana island arc systems characterizes the trenches accreting high density and high velocity material;
- 2) In the second type represented by Sumatra, Java and Luzon, the trench slope break is made up of a sedimentary ridge caused by the sediment feed at the base of the slope;
- 3) In the third type, represented by Eastern Aleutian, Japan and Middle America arcs, sediments from the frontal arc fill the upper slope and form a broad continental shelf.

According to KARIG and SHARMAN (1975), the inner slope of the New Hebrides island arc system represents the initial stage of the first type of configuration. Nevertheless, DUGAS *et al.* (1977) and RAVENNE *et al.* (1977), in their general description of the arc, showed that the different morphostructural units were clearly distinguishable, and stressed

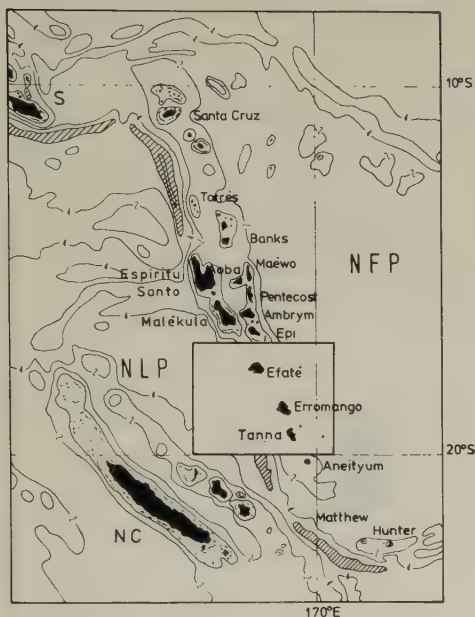


Fig. 2. New Hebrides island arc. Submarine contours are in km. The axis of the trench is shown by hachured area inside of the 6 km isobath. NC, New Caledonia; S, Solomon; NLP, North Loyalty Plateau; NFP, North Fiji Plateau.

the differences between the northern part, the central part (where the trench disappears) and the southern part. Furthermore, in this southern part, it was shown (DANIEL, 1978) that the morphology of the inner slope varied considerably over short distances.

A bathymetric chart substantiating these variations was drawn up in this southern part (Fig. 3) through several profiles interspaced at 10–15 km.

2.1 Outer wall of the trench

The outer wall of the trench is formed by the North Loyalty Plateau. The depth of this plateau is always approximately 4,500 m. However, as can be seen on profile G.C. 30 (Figs. 3 and 4), it appears that a deepening exists in the north which confirms the older age in the north shown by magnetic anomalies (LAPOUILLE, 1978).

The outer slope of the trench itself (Fig. 5) has varied configurations: faulted and extremely steep on the CHAIN profile, it becomes more subdued on profile AUS 113, then becomes faulted on profile EVA 201 and finally becomes infinitely more subdued in the south. On the whole, however, the slope is steeper in the northern part of the studied area. The appearance of the slope is qualified both by thickness of the sediments: in the south the thickness is greater and the slope is more subdued, and by the configuration of the basement itself.

2.2 Trench

It is clear from the bathymetric chart (Fig. 3) that the curve of the trench axis is slightly arched. It would be necessary to know more precisely the termination of the trench in North-West Efaté so as to pinpoint the extend of this curve. Furthermore, as pointed out on the 5,000 m isobath the trench tends to widen in the South.

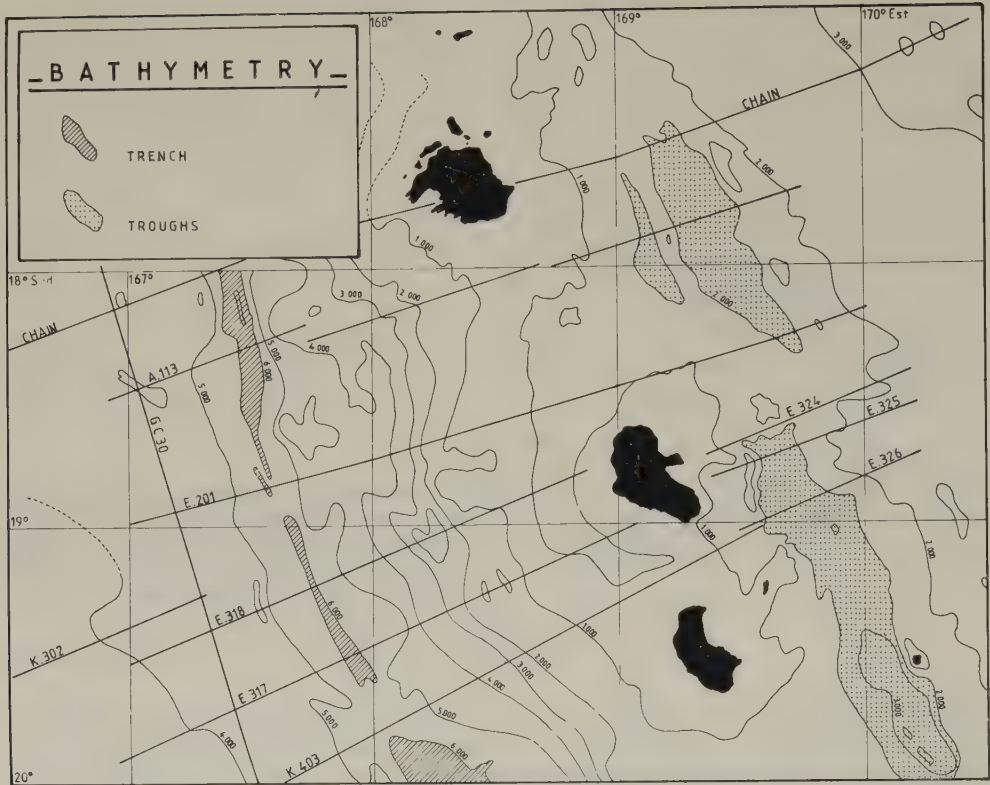


Fig. 3. Bathymetry and localisation of the profiles.

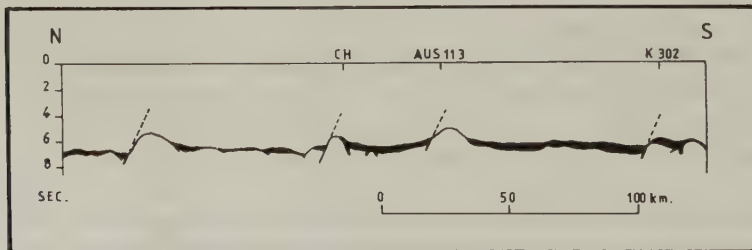


Fig. 4. G.C. 30 (Glomar Challenger) profile on the North Loyalty Plateau.

2.3 Inner wall of the trench

From the 6 profiles shown on Fig. 5, it can be seen that the inner slope varies considerably from one profile to another although the width of the accretionary prism (between the axis of the trench and the upper slope discontinuity) remains virtually constant at approximately 75 km. Four types of inner slopes can be determined by grouping them in twos (Fig. 6).

Group A. These refer to the slopes observed in the northern part of the studied area: both flanks of the trench are fairly steep and the configuration of the upper slope differs

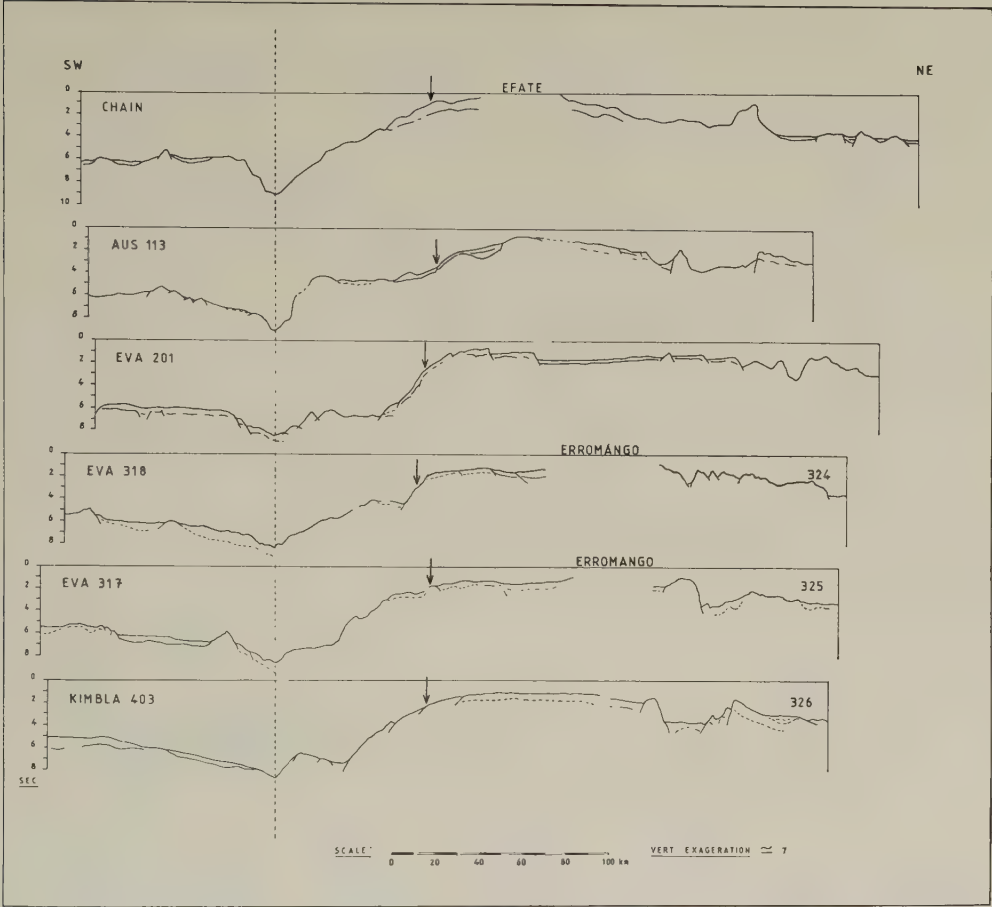


Fig. 5. Bathymetric and seismic reflection profiles across the New Hebrides island arc. Profiles are normalized to the trench axis (broken line). Arrows show the upper slope discontinuity.

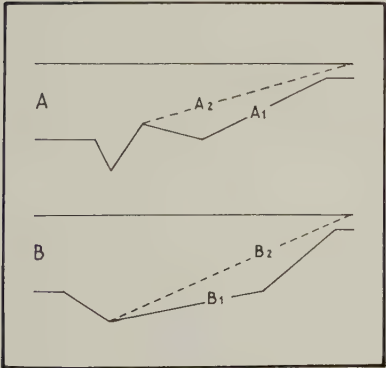


Fig. 6. Sketch of different types of inner slope of the trench observed in the studied area.

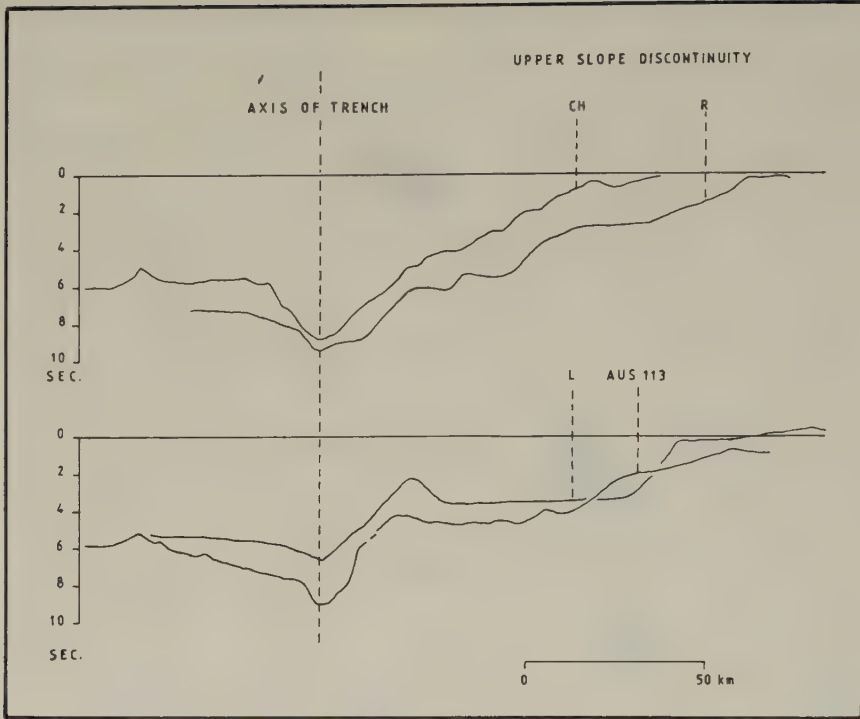


Fig. 7. Comparative bathymetric profiles across inner trench slopes of the New Hebrides [CH (Chain) and AUS (Austradec) 113], Ryukyu (R) and West Luzon (L) (from KARIG and SHARMAN, 1975).

according to whether or not there is a neighbouring island to serve as a source of sedimentation.

Type A1: shown on profile AUS 113; the lower slope is steep and the upper slope is more subdued.

Type A2: shown on the CHAIN profile is a more developed form than the previous one: the upper slope has been modified by sediments from the island of Efate.

Group B. These are the slopes observed in the south: both flanks of the trench slope are gentle, and, as in the previous case, the upper slope may be modified by sediments from the arc.

Type B1: shown on profile EVA 201. The trench slope break between the lower and upper slopes is clearly defined.

Type B2: shown on profile EVA 317. The slope is straightened out by sediments from the island of Erromango.

Therefore, a wide variety of inner slope forms can be seen to exist over roughly 220 km. For reasons of comparison, it is also useful to note (Fig. 7) that on neighbouring profiles such as CHAIN and AUS 113, where the distance is less than 50 km, the inner slopes are very similar to those observed on slightly older arcs with wider accretionary prisms which, according to KARIG and SHARMAN (1975), are characteristic of two different types of accretion. In our interpretation, within both morphological groups A and B, type 2 is derived from type 1 according to the extent of sedimentation from the arc.

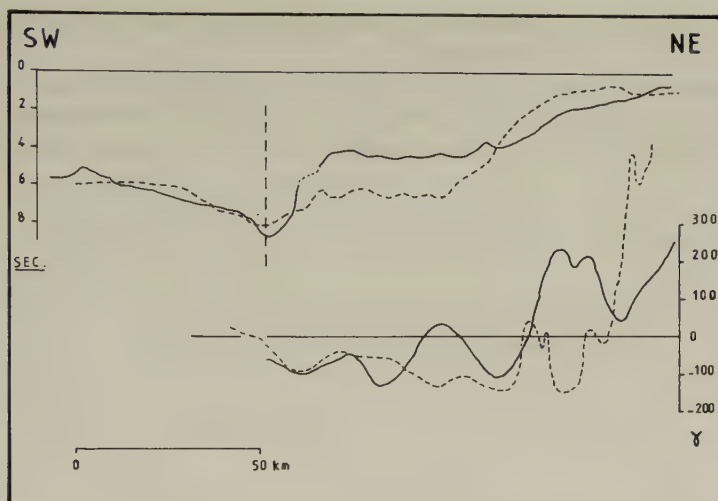


Fig. 8. Comparative magnetic anomalies and bathymetric profiles AUS 113 (solid lines) and EVA 201 (broken lines).

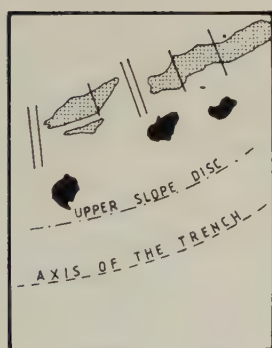


Fig. 9. Relative positions of the troughs at the rear of the New Hebrides island arc, the trench and the upper slope discontinuity. Double lines show major fractures.

According to our observations, there is a link between the inner and the outer flanks of the trench and therefore a tendency to symmetry. One is tempted to deduce that the form of the outer flank determines the inner flank. However, is this merely a question of morphology or, as observed by KARIG and SHARMAN (1975) is there a difference in the type of accreted material? Magnetic anomalies along AUS 113 and EVA 201 profiles (Fig. 8), morphologically very different, are not different enough to permit definite conclusions to be drawn concerning a change of the nature of accreted material.

3. Morphology of the Troughs at the Rear of the Arc

The troughs at the rear of the New Hebrides island arc, discovered during the Coriolis cruises (PUECH and REICHENFELD, 1969) were described as "en echelon inter-arc basins" (KARIG and MAMMERICKX, 1972), or extensional fault troughs (LUYENDYK *et al.*, 1974) and as tectonic troughs (DUBOIS *et al.*, 1975, 1978). The latter authors presented a de-

tailed study of the troughs for all the New Hebrides arc and conclude that their formation must be originated in the asthenosphere.

The bathymetric chart (Fig. 3) pinpoints the position of these troughs and one can particularly see (Fig. 9) that the northernmost trough is clearly discontinued at both ends, probably on major fractures. The fracture which shifts the trough at the island of Er-

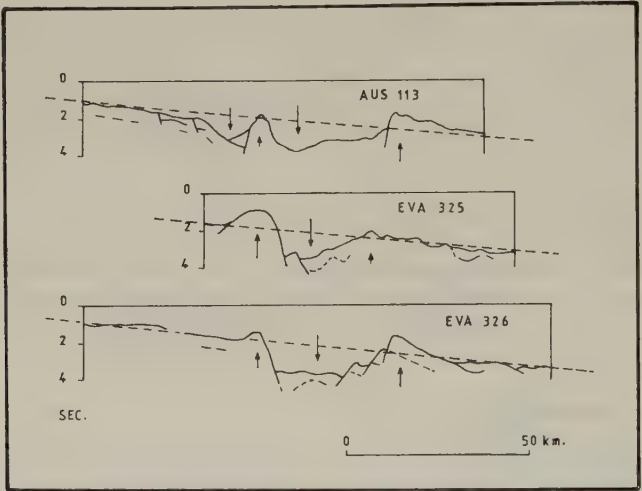


Fig. 10. Morphology of the troughs at the rear of the New Hebrides island arc. The intensity of vertical movement is proportional to the length of the arrows.

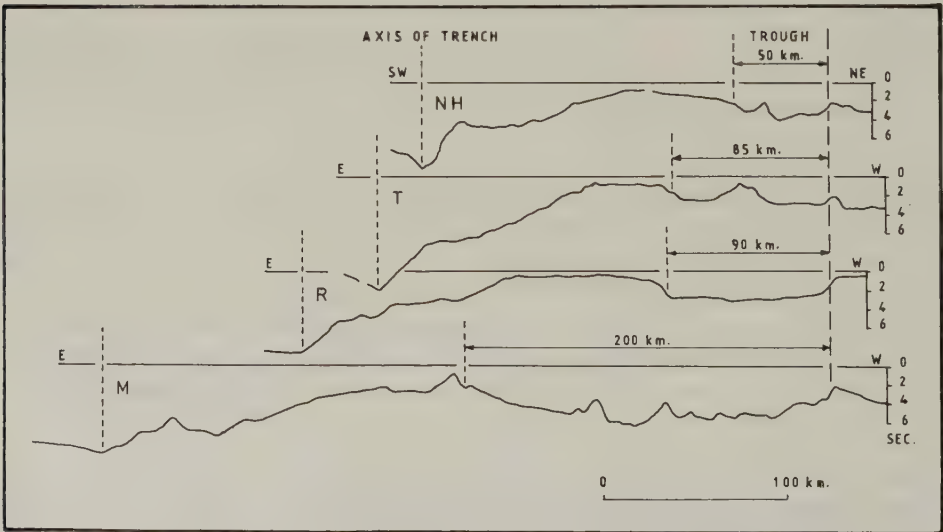


Fig. 11. Comparative widths and positions with respect to the trench axis of the trough at the rear of the New Hebrides island arc (NH) and similar structures on Tonga (T), Ryukyu (R), and Marianna (M) island arcs.

romango is furthermore located in the extension of one of the irregularities observed on the dipping plate (on profile G.C. 30 at K 302, Figs. 3 and 4).

As observed by DUBOIS *et al.* (1975, 1978), the form of the troughs varies considerably. It is noted (Fig. 10) that the downthrow faults are, accordingly, roughly defined on one side or the other of the troughs. Despite these variations in the detailed configuration, the general form suggests (Fig. 10) a formation by vertical movements. The variations in the intensity of positive and negative vertical movements of horsts and grabens are sufficient to modify the form.

One can attempt to compare these troughs to equivalent structures on other arcs. Profiles of the Fig. 11 show morphologies which are comparable, without having necessarily the same origin. The troughs of Ryukyu and Mariana island arcs are inferred to have an origin similar to that of the troughs of the New Hebrides (DUBOIS *et al.*, 1975, 1978) but to be at different stage of development. For the Tonga island arc it must be noted that the profile presented is not representative of the whole of the arc (J. DUPONT, personal communication).

4. Conclusions

The morphological study of the southern part of the New Hebrides island arc allowed us to pinpoint the various structural units and propose some assumptions which need to be substantiated by other methods.

- 1) There is an accretionary prism with a constant width of approximately 75 km.
- 2) The morphology of this accretionary prism varies extremely rapidly along the arc and is controlled, firstly, by the morphology of the dipping plate and secondly by the existence of sources of sediments on the arc.
- 3) The arc and its connecting structural features, such as the troughs situated at its rear, show transversal discontinuities.
- 4) Major discontinuities of the arc could be related to those of the oceanic crust of the dipping plate.

REFERENCES

- CARNEY, J.N. and A. MACFARLANE, Volcanotectonics events and pre-Pliocene crustal extension in the New Hebrides, in *Geodynamics in South-West Pacific*, pp. 91–104, Technip Ed., Paris, 1977.
- DANIEL, J., Phénomène de subduction et existence du prisme d'accrétion: enseignement de l'arc des Nouvelles-Hébrides, *C.R. Acad. Sci. Paris, D*, **286**, 1755–1758, 1978.
- DANIEL, J., C. JOUANNIC, B. LARUE, and J. RECY, Interpretation of d'Entrecasteaux zone (North of New Caledonia), in *Geodynamics in South-West Pacific*, pp. 117–124, Technip Ed., Paris, 1977.
- DICKINSON, W.R., Widths of modern arc-trench gaps proportional to post-duration of igneous activity in associated magmatic arcs, *J. Geophys. Res.*, **78**, 3376–3389, 1973.
- DUBOIS, J., F. DUGAS, A. LAPOUILLE, and R. LOUAT, Fossés d'effondrement en arrière de l'arc des Nouvelles Hébrides. Mécanismes proposés, *Rev. Géo. Phys. Geol. Dyn.*, **XVII**, (1), 73–94, 1975.
- DUBOIS, J., F. DUGAS, A. LAPOUILLE, and R. LOUAT, The troughs at the rear of the New Hebrides island arc. Possible mechanisms, *Can. J. Earth Sci.*, **15**, 351–360, 1978.
- DUGAS, F., J. DUBOIS, A. LAPOUILLE, R. LOUAT, and C. RAVENNE, Structural characteristics and tectonics of an active island arc: the New Hebrides, in *Geodynamics in South-West Pacific*, pp. 79–89, Technip Ed., Paris, 1977.
- JOHNSON, T. and P. MOLNAR, Focal mechanisms and plate tectonics of the Southwest Pacific, *J. Geophys. Res.*, **77**, 5000–5032, 1972.
- KARIG, D.E., Evolution of Arc Systems in the Western Pacific, *Annu. Rev. Earth Planet. Sci.*, **2**, 51–75, 1974.
- KARIG, D.E. and J. MAMMERICKX, Tectonic framework of the New Hebrides island arc, *Mar. Geol.*, **12**, 187–205, 1972.

- KARIG, D.E. and G.F. SHARMAN, Subduction and accretion in trenches, *Geol. Soc. Am. Bull.*, **86**, 377–389, 1975.
- LAPOUILLE, A. Southern New Hebrides basin and western South Fiji basin as single marginal basin, *Aus. Soc. Expl. Geophys. Bull.*, **9**, 130–133, 1978.
- LUYENDYK, B.P., W.B. BRYAN, and P.A. JEZEK, Shallow structure of the New Hebrides arc, *Geol. Soc. Am. Bull.*, **85**, 1287–1300, 1974.
- MITCHELL, A.H.G. and A.J. WARDEN, Geological evolution of the New Hebrides island arc, *J. Geol. Soc.*, **127**, 501–529, 1971.
- PUECH, J.L. and C. REICHENFELD, Etudes bathymétriques dans la région des îles Erromango, Tanna et Anatom (Nouvelles Hébrides du Sud), *C.R. Acad. Sci. Paris*, **268**, 1259–1261, 1969.
- RAVENNE, C., G. PASCAL, J. DUBOIS, F. DUGAS, and L. MONTADERT, Model of a young intra-oceanic arc: The New Hebrides Island arc, in *Geodynamics in South-West Pacific*, pp. 63–77, Technip Ed., Paris, 1977.

PALAEOMAGNETIC EVIDENCE FOR THE ROTATION OF SERAM, INDONESIA

N.S. HAILE*

Department of Geology, University of Malaya, Kuala Lumpur, Malaysia

(Received May 16, 1978; Revised September 8, 1978)

Upper Triassic shale from central Seram gives a direction of magnetization ($D=82$, $I=23$) which (assuming, as seems probable, that it was acquired before folding, and during a period of reversed magnetization) indicates Seram lay in $12 \pm 7^\circ\text{S}$ latitude and has rotated anticlockwise 98° since the late Triassic. The equivalent (south) palaeomagnetic pole is at 8°N , 207°E .

Pillow basalt of late Miocene age, from Kelang Island, west Seram has a magnetic vector $D=106$, $I=9$, indicating extrusion in 5°S latitude, and anticlockwise rotation of 74° . The equivalent (south) palaeomagnetic pole is at 16°S , 214°E .

These results, although only of a reconnaissance nature, are consistent with the postulations of various authors that Seram has rotated anticlockwise in late Cainozoic.

1. Introduction

During the course of an expedition to the Banda Arc, east Indonesia, in 1976, the writer made collections of orientated samples (cores and hand-specimens) for palaeomagnetic measurements. Accessible exposures of rocks suitable for palaeomagnetic research are rare in the Banda Arcs; many of the rocks are metamorphosed, and large sections of the coastlines are built of raised Quaternary coral reefs, so few sites could be sampled. Results recorded here are from Triassic shale in the central section of the south coast of the Main Island of Seram, and late Miocene basaltic lavas from Kelang Island, immediately west of Seram. The only other available palaeomagnetic results from the Banda Arc (CHAMALAUN, 1977), indicates that Timor (or at least the "autochthonous" part of it) may have been part of the Australian plate in the Upper Permian, and since then has rotated 21° anticlockwise.

2. Triassic Shale

The shale sampled is exposed in the Punala stream above the Yapui tributary (Fig. 2). The shale is grey, in part sandy, and in the section sampled strikes 118° and dips southwest at 49° to 60° . The several exposures sampled represent about 10 m of strata. These rocks were mapped by Rutten in 1917–1919, and his map of the stream and his detailed field notes published by GERMERAAD (1946, pp. 23, 97–98). The strata belong to an extensive outcrop of what Germeraad calls "The Normal Triassic" consisting of shale, graywacke, conglomerate, marls and limestone. From shale in the Punala stream collected by Rutten, KRUMBECK (1923) identified *Halobia deningeri* Krumbeck and *Halobia* sp. nov., indicating Upper Triassic, probably Carnian.

* Present address: 53, Nyewood Lane, Bognor Regis, Sussex PO21 25Q, England.



Fig. 1. Map showing the Banda Arcs, with position of Seram and Kelang.

3. Basaltic Lava

The lavas were sampled from coastal exposures on the southwest cape of Kelang Island, west of the Main Island of Seram (see Figs. 1 and 2). There basaltic lava flows, mostly pillowed, some massive, form cliffs up to 30 m high.

The pillow lavas appear to be rather flat-lying with locally an impression of dips to the west of 27° to 60° . Some non-pillowed flows show dips of 35° to the east. The samples represent a number of flows, at least four, and possibly more. The lavas appear to pass up into tuff agglomerates and be part of volcanic formation which extends to a summit towards the southeast corner of the island, in the upper part of which large-scale vertical columnar jointing can be seen from the sea. Because of this vertical jointing, I consider the dips on the lava flows to be primary, and not due to tectonic tilting or folding, which is confirmed palaeomagnetically (see below). The pillowed lavas probably represent the part of lava flows which flowed into the sea, and have subsequently emerged due to the tectonic uplift which affected most of the Banda Arcs in the Quaternary.

Age of the lavas. Radiometric dating of the lavas by the K/Ar method indicates a late Miocene age of 7.6 ± 1.4 Ma (BECKINSALE and NAKAPADUNGRAT, 1979).

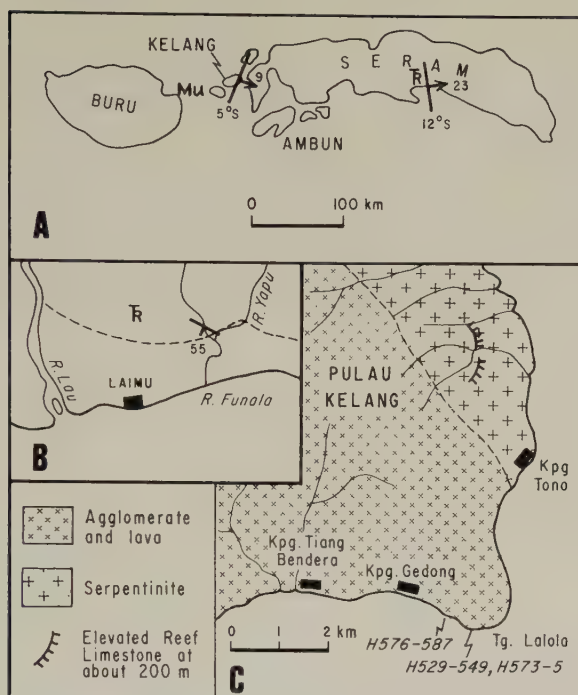


Fig. 2. A, Seram showing Punalá site (TR, Upper Triassic) and Kelang site (Mu, Upper Miocene) with palaeomagnetic vectors and interpreted palaeolatitudes; B, Punalá site, with dip of strata; C, Kelang site.

Table 1. Direction of magnetization of Triassic shale and Cainozoic basalt from Seram (after cleaning).

Triassic shale, Punala River					Late Miocene basalt, Kelang Island					
Sample number	Field position		Corrected for tilt		Sample number	Field position		Sample number	Field position	
	D	I	D	I		D	I		D	I
H461	61	−15	68	35	H530	104	2	H548	157	9
H462	77	−14	83	26	H531	105	8	H549	127	7
H463	63	−29	61	22	H532	105	−1	H573	351	30
H464	44	−29	44	29	H533	97	8	H574	109	11
H465	94	2	107	22	H534	99	11	H576	108	4
H466	68	−17	73	29	H535	101	11	H577	113	11
H469	197	13	193	−47	H536	80	0	H578	112	7
H470	75	−15	89	25	H537	80	4	H579	108	9
H471	86	−43	118	12	H538	103	7	H580	100	7
H472	92	−25	83	8	H539	101	5	H581	99	9
H474	72	−5	86	36	H540	106	13	H582	109	12
H475	90	−26	80	2	H541	124	14	H583	94	12
H480	156	−23	134	−71	H542	105	5	H584	107	12
					H543	107	8	H585	113	26
					H544	102	1	H586	109	8
					H545	98	18	H587	110	12
					H546	89	6			
					H547	115	16			

"Field position" means with respect to horizontal; "corrected for tilt" with respect to bedding plane. D=declination east of north; I=inclination, positive downwards, negative upwards. H469, H480, H573 omitted from the mean, as clearly aberrant.

4. Palaeomagnetic Results

Orientated core samples 25 mm in diameter were drilled in the field, and later measured on a DIGICO complete results spinner magnetometer in the Department of Geology, University of Malaya, with results shown in Table 1.

Triassic shale. Initial intensities range from 0.1 to 0.38 mA m⁻¹. All samples were thermally demagnetized stepwise. The magnetization of the shale is poorly to moderately stable. Of the 23 samples collected, 13 which showed Briden indexes (BRIDEN, 1972) more than 0.75 at all temperatures above 100°C were selected, with results shown in Table 1 and Fig. 3.

Miocene basalt. Initial intensities range from 1,000 to 9,000 mA m⁻¹, falling on AF cleaning to 40–100 mA m⁻¹ at 90 mT, with the direction of magnetization showing little change. Pilot specimens were demagnetized stepwise by AF, and from the results the rest of cleaned at 20 or 60 mT. Results are shown in Table 1 and Fig. 3.

The palaeomagnetic directions show increased scatter if correction for the apparent dips of the lava flows is made, and this, together with the stable nature of the magnetization, indicates that the directions represent a primary thermal remanent magnetism acquired on cooling, and that the dips are original, and not due to tectonic tilting. If so the directions of the magnetic vectors uncorrected for tilt (field position) represent the direction of the magnetic field at the time of extrusion of the lavas. Not much difference in the mean is obtained by first meaning the samples from each flow (where separate flows can be differentiated), and as the total number of flows represented by the samples is uncertain, the mean of the 33 samples has been given (Table 2).

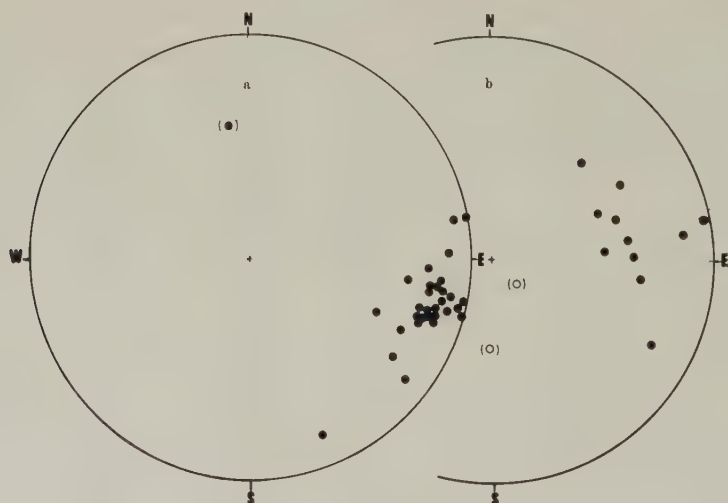


Fig. 3. Stereographic projections showing the cleaned directions of magnetization for (a) Kelang Miocene basalt, inclination relative to horizontal (b) Seram Triassic shale, inclination relative to bedding plane. Directions in parentheses omitted from the mean. Solid symbols on lower hemisphere, open symbols on upper hemisphere.

Table 2. Mean direction of magnetization of Triassic shale and Late Miocene pillow basalt from Seram.

		<i>n</i>	T°/B	<i>D</i>	<i>I</i>	<i>R</i>	<i>k</i>	α_{95}
Triassic shale, cleaned	Field position	11	200–300 °C	78	–19	10.3687	15.8	11.8
	Corrected for tilt	11	200–300 °C	82	23	10.2863	14.0	12.6
Cainozoic	Field position	33	20–60 mT	106	9	32.0314	33.6	4.3

n, No. of samples; *D*, declination east of true north; *I*, inclination, position downwards; *R*, resultant of the *n* unit vectors; *k*, precision parameter; α_{95} , radius of circle of 95% confidence about the mean; T°/B , demagnetizing field in °C or mT.

5. Significance of the Results

Seram forms part of the double island arc—the Banda arcs—which extends northeast from Timor and curves through a tight semi-circle at its eastern end. Seram lies on the northern side of the arcs, and forms part of the outer arc, composed of sedimentary, igneous, and metamorphic rocks including Palaeozoic and Mesozoic formations, whereas the inner arc is of islands formed by young volcanoes, many still active.

A Benioff zone extends along at least part of the arc (STOIBER and CARR, 1971), and its geometry, in such a tightly looped arc system, poses problems of space and movement of the underthrusting plate. It has been suggested that the northern arm of the arc is now less active (ANONYMOUS, 1974, p. 42). The tight curvature of the arc has led to the suggestion that the northern arm has rotated anticlockwise by a large amount. CAREY (1938; 1958, pp. 280–287, Fig. 51; 1963, Figs. 11, 31) suggested an anticlockwise rotation of about 180° for both Seram and Buru based on an expanding-Earth model. His more recent reconstruction (1976, Fig. 79) involves an anticlockwise rotation of about 110°. Other hypotheses also envisage anticlockwise rotation of the arc in late Cainozoic times, either combined with considerable northward motion, together with Australia, and with subduction of a broad intervening orogenic belt (AUDLEY-CHARLES *et al.*, 1972; CARTER *et al.*, 1976), or with more of a westward motion connected with the westward impingement of New Guinea, carried on the Pacific Plate (MOBERLY, 1972). CARTER *et al.* (1976) suggest that the situation is even more complex, in that Seram (with the other islands of the outer Banda Arc) is composed of elements formed along the southern margin of Sundaland during the late Palaeozoic and Mesozoic, onto which elements formed along the Australian margin were thrust in early Cainozoic. In their reconstruction of the early Mesozoic continental margin of Australia, AUDLEY-CHARLES *et al.* (1975) showed the islands of the outer Banda Arcs including Seram forming part of the continental shelf and slope of northern Australia, with Seram in the same position relative to Australia as it occupies today, but rotated nearly 180° clockwise.

The “palaeocontinental” map for latest Triassic of SMITH and BRIDEN (1977, Map 12) also shows Seram in its present position relative to Australia but rotated about 45° clockwise (see Fig. 4). The Audley-Charles and Smith/Briden reconstructions involve a palaeolatitude of 23° or more for Seram in the Triassic.

Triassic results. The Triassic palaeomagnetic results, from rocks with rather low stability, and without the possibility of a fold test, should be treated with caution. Nevertheless, the reasonably good grouping, and wide divergence of the declination from that of

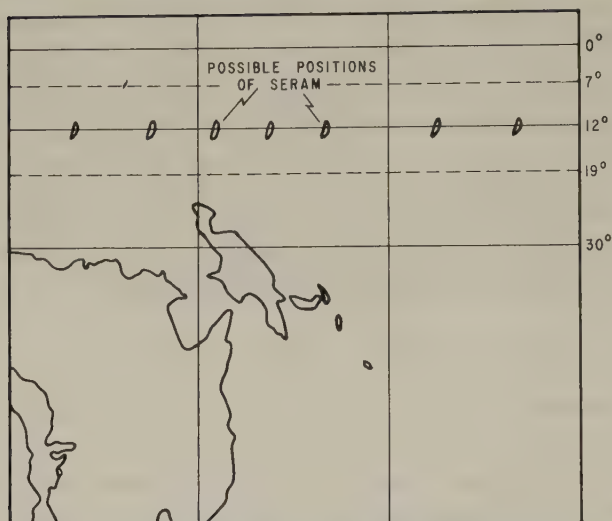


Fig. 4. Position of Australian Continent in latest Triassic, according to Smith and Briden, with position(s) and attitude of Seram. If the Triassic site gives a valid palaeomagnetic direction (see text for discussion), Seram could have lain at any longitude along between 7° and 19°S, to satisfy the palaeomagnetic data.

Table 3. Possible interpretation of the Triassic palaeomagnetic data.

Time of acquisition of magnetization	Polarity	Inclination (degrees)	Equivalent palaeolatitude	Rotation since time of magnetizations
1. Triassic, before folding	A. Normal	23	12°N	82° clockwise
	B. Reversed	23	12°N	98° anticlockwise
2. After folding (late Mesozoic, or Cainozoic)	A. Normal	-19	10°S	82° clockwise
	B. Reversed	19	10°N	98° anticlockwise

Possibility 1B seems most likely. See text for discussion.

the present field indicate that the magnetization was acquired before rotation of Seram into its present position. Assuming that the directions represent a true palaeomagnetic direction (i.e. an average of the earth's magnetic field at some time), the possibilities are that the magnetization was acquired either before folding (presumably at or soon after deposition in the Triassic), or after folding (in the later Mesozoic or the Cainozoic). The various possibilities are shown in Table 3. From the configuration of the Banda Arc it seems most probable that Seram has rotated anticlockwise, and moved north, and so possibility 1B is most likely, namely that the rocks acquired their magnetization before folding, were formed in 12 (± 7)°S latitude, and have since rotated 98° anticlockwise and moved north some 9° to their present position. On this assumption, a palaeomagnetic south pole at 8°N, 207°E can be calculated, widely divergent from the palaeomagnetic Mesozoic pole for Australia at 48°S, 151°E (McELHINNY, 1973, p 228). The palaeolatitude of 12°S is lower than the 23° or so which would be expected if Seram had been adjacent to the Australian plate in the Triassic, but in view of the substantial colatitude

Table 4. Palaeomagnetic (south) pole position for Seram (mean of virtual geomagnetic poles).

Location	Age	Site co-ordinates		Pole co-ordinates		<i>n</i>	<i>K</i>	<i>A</i> ₉₅
		Lat.	Long.	Lat.	Long.			
Punala River	U. Triassic*	3.3°S	129.1°E	8°N	207°E	11	15.2	12.0
Kelang Island	? Cainozoic	3.2°S	127.8°E	16°S	214°E	34	37.0	4.0

n, No. of samples; *K*, precision parameter; *A*₉₅ circle of 95% confidence about mean pole position. After cleaning and correction for tilt. Polar errors: Triassic shale *dp*=7.1, *dm*=13.4; Cainozoic basalt *dp*=2.2, *dm*=4.3.

* Assuming magnetization was acquired before folding, during a reversed magnetic epoch.

error (*dp*) of 7°, and the other uncertainties, the results should not be taken as disproving a close relation to Australia, as is shown by some authors. However, since Seram has clearly moved independently of the Australian plate since the Triassic, there seems no particular reason why it should have been connected to Australia in the early Mesozoic, as is shown, for example, by SMITH and BRIDEN (1977, Map 9).

Miocene results. The results from the Miocene basalts of Kelang are less equivocal. On the assumption that these rocks have not been significantly tilted since their extrusion (evidence for which is discussed above), and that rotation of Seram has been anticlockwise, the lavas were intruded during a reversed magnetic epoch, at about 5°S latitude (present latitude 3.2°S). Subsequently they have rotated anticlockwise by 74°. A palaeomagnetic pole, almost certainly a south pole, at 16°S, 214°E is defined (Table 4).

This fits well with the model of AUDLEY-CHARLES *et al.* (1972, Fig. 5), which involves an anticlockwise rotation of Seram of some 70° since the Middle Pliocene, combined with some north-northwest translational movements.

6. Conclusions

The data together indicate anticlockwise rotation of Seram of 98° since the late Triassic; 74° of this rotation was accomplished since the extrusion of the pillow lavas, probably in late Miocene.

This suggests that the tight curvature of the Banda Arc is probably secondarily acquired, rather than a primary feature, if we assume that the southern part of the arc has not rotated so much, for which the only palaeomagnetic evidence is that of Chamalaun, noted above. It is desirable that these preliminary results be augmented by further work designed to provide a partial apparent polar wandering curve for Timor and Seram.

The field work was made possible by the excellent planning and logistics of the Geological Survey of Indonesia (GSI) under the leadership of Drs H.M.S. Hartono, with Encik Suwarno Darsopajitno organizing local transport. Encik M. Suparman (GSI) and Encik D. Krishnan (University of Malaya) made up, with myself, the palaeomagnetic field team. The participation of the University of Malaya team was made possible by the active support of the Vice-Chancellor, Prof. A. Ungku Aziz, and by financial assistance from CCOP (of UN/ESCAP), PETRONAS, and Exxon Geology Fund.

The writer was assisted in the laboratory measurements by Encik Lee Tiew Hong.

REFERENCES

ANONYMOUS, Metallogenesis, hydrocarbons, and tectonic patterns in Eastern Asia UNDP/CCOP Bangkok, 1974.

- AUDLEY-CHARLES, M.G., D.J. CARTER, and D.J. MILSOM, Tectonic development of eastern Indonesia in relation to Gondwanaland dispersal, *Nature Phys. Sci.*, **239**, 35–39, 1972.
- AUDLEY-CHARLES, M.G., D.J. CARTER, and A.J. BARBER, Stratigraphic basis for tectonic interpretations of the outer Banda Arc, Eastern Indonesia, *Proc. Indonesian Petrol. Assoc.*, 3rd Annu. Conv. (June 1974), 1975.
- BECKINSALE, R.D. and S. NAKAPADUNGRAT, A late Miocene K-Ar age for the lavas of Pulau Kelang, Seram, Indonesia, *J. Phys. Earth*, this issue, S 199–S 201, 1978.
- BRIDEN, J.C., A stability index of remanent magnetism *J. Geophys. Res.*, **77**, 1401–1405, 1972.
- CAREY, S.W., Tectonic evolution of New Guinea and Melanesia, D.Sc. Thesis, University of Sydney, 1938.
- CAREY, S.W., A tectonic approach to continental drift, in *Symp. Continental Drift*, Hobart, pp. 177–355, 1958.
- CAREY, S.W., The asymmetry of the earth, *Aust. Jour. Sci.*, **25**, 369–383, 479–488, 1963.
- CAREY, S.W., The expanding earth, in *Developments in Geotectonics*, Vol. 10, Elsevier, 1976.
- CARTER, D.J., M.G. AUDLEY-CHARLES, and A.J. BARBER, Stratigraphical analysis of island arc-continental margin collision in eastern Indonesia, *J. Geol. Soc. Lond.*, **132**, 179–198, 1976.
- CHAMALAUN, F., Palaeomagnetic evidence for the relative positions of Timor and Australia in the Permian, *Earth Planet. Sci. Lett.*, **34**, 107–112, 1977.
- GERMERAAD, J.H., Geology of Central Ceram. Geological petrographical and paleontological results of explorations carried out in 1917–1919 in Ceram by C. Rutten and W. Hotz, 3 Ser. Geology, No. 2, Thesis, Utrecht, 1946.
- KRUMBECK, L., Brachiopoda, Lamellibranchiata, und Gastropoda aus der oberen Trias der Insel Seran (Mittel-Seran), *Palaeontographica*, **4**, 1923.
- McELHINNY, M.W., *Palaeomagnetism and Plate Tectonics*, Cambridge University Press, Cambridge, 1973.
- MOBERLY, R., Origin of lithosphere behind island arcs, with reference to the western Pacific, *Geol. Soc. Am. Mem.*, **132**, 35–55, 1972.
- SMITH, A.G. and J.C. BRIDEN, *Mesozoic and Cenozoic Paleogeographical Maps*, Cambridge University Press, 1977.
- STOIBER, R.E. and M.J. CARR, Lithospheric plates, Benioff zones, and volcanoes, *Bull. Geol. Soc. Am.*, **82**, 515–522, 1971.

A LATE MIOCENE K-Ar AGE FOR THE LAVAS OF PULAU KELANG, SERAM, INDONESIA

R.D. BECKINSALE and S. NAKAPADUNGRAT*

Institute of Geological Sciences, London, U.K.

(Received September 8, 1978)

K-Ar determinations for ten samples of the basaltic lavas of Pulau Kelang, Seram (for which palaeomagnetic measurements indicate a reversed palaeomagnetic pole at 16°S, 214°E) yield a mean age of 7.6 ± 1.4 Ma. Direct evidence for the age of the lavas is lacking. This K-Ar date confirms a previous inference based on young topographic features of the island that the lavas are of late Cainozoic age and allows a more precise stratigraphic assignment to the Upper Miocene.

1. Introduction

K-Ar age determinations for ten samples of the basaltic pillow lavas of Pulau Kelang, Seram, East Indonesia, are reported below. This study is part of a project undertaken to establish a temporal and palaeomagnetic framework within which to interpret palaeomagnetic studies in North Sumatra in terms of the movements and extents of the tectonic plates in S.E. Asia. Palaeomagnetic measurements and the field occurrence of the lavas of Pulau Kelang have been reported by HAILE (1978) who concluded that they yield a magnetic vector indicating extrusion in latitude 5°S, an anticlockwise rotation of Seram of 74° since the extrusion of the lavas and a palaeomagnetic (south) pole of 16°S, 214°E. Although HAILE (1978) inferred a late Cainozoic age for the lavas from young topographic features of the island, direct evidence for the age of these lavas is lacking. It is evident that a radiometric age would enhance the significance of the palaeomagnetic data in terms of both a pole reversal timetable and the geological history of S.E. Asia.

2. Analytical Methods and Results

Rock and core samples used for palaeomagnetic studies were provided by Professor N.S. Haile and the sample localities are given in his paper (HAILE, 1978). Each sample was crushed and sieved to a powder with a grain size between 60 and 80 mesh. Potassium contents were determined in replicate by flame photometry using an internal lithium standard. Argon was determined by standard methods involving extraction of argon from the sample powder by fusion in vacuo and analysis by mass spectrometric isotopic dilution using a ^{38}Ar spike. The results are set out in Table 1. The argon analyses proved difficult because of extremely high contents of atmospheric argon in most of the samples. The argon analysed in most cases consisted of more than 95% atmospheric contamination. It is well known that high levels of atmospheric contamination yield K-Ar ages with very large analytical errors (see e.g. DALRYMPLE and LANPHERE, 1969) and we have ignored the analyses in Table 1 in which the atmospheric argon content is greater than 97.5%.

* Permanent address: Department of Mineral Resources, Rama VI Road, Bangkok, Thailand.

Table 1

Sample No.	Mean K (%)	Radiogenic ^{40}Ar		Age ⁺ and error (2 standard deviation) in Ma
		nl/g	%	
H 530	0.458	0.0834	2.7	4.7 ± 1.2
H 531	0.309	0.1271	4.1	10.6 ± 3.8
H 534	0.363	0.0954	3.2	6.8 ± 2.3
H 539	0.458	0.1024	3.2	5.8 ± 1.5
H 549	0.446	0.1141	4.5	6.6 ± 1.3
H 573	0.413	0.0489	2.1	$3.0 \pm 1.9^*$
H 575	0.454	0.1680	5.5	9.5 ± 3.1
H 584	0.438	0.0226	0.8	$1.3 \pm 1.1^*$
UM 8509	0.350	0.1235	4.9	9.1 ± 1.8
UM 8539	0.757	0.1935	18.8	7.4 ± 1.6 { 6.6 ± 1.1 8.2 ± 1.0
UM 8539	0.757	0.2407	12.3	
Overall mean				7.6 ± 1.4 Ma (error 2SE)

⁺ Decay constants as recommended by IUGS Subcommittee on Geochronology (STEIGER and JAGER, 1977).

* Excluded.

(i.e. radiogenic ^{40}Ar less than 2.5%) because in these cases the analytical errors associated with the ages rise to more than 60% of the calculated age values. The $^{40}\text{Ar}/^{36}\text{Ar}$ ratio of atmospheric argon was determined frequently during the course of these analyses and appropriate corrections to measured isotope ratios were made for mass spectrometric discrimination. The data remaining in Table 1 (after excluding the analyses with more than 97.5% atmospheric argon) give a mean age of 7.6 ± 1.4 Ma after first averaging the two results for sample number UM 8539. The quoted error is two standard errors. It is important to note that the only sample which yields a reasonable content of radiogenic ^{40}Ar is UM 8539 with about 85% atmospheric contamination. The two K-Ar ages for this sample yield a mean value of 7.4 ± 1.6 Ma. It is also important to note that within errors there is no correlation between the calculated K-Ar age and potassium content and thus no evidence for the presence of significant amounts of excess ^{40}Ar which could produce spuriously old ages.

3. Conclusions

The lack of evidence for the presence of excess ^{40}Ar and the concordance between the overall mean of the more reliable data in Table 1 and the average age for sample number UM 8539 which is the most reliable result from an analytical point of view suggest that the mean age of 7.6 ± 1.4 Ma is a valid measurement of the date of (rapid) cooling of the pillow lavas after extrusion. According to the Geological Society Phanerozoic time-scale 1964* and allowing for the use of new values for the decay constants of ^{40}K the stratigraphic assignment of this age would be within the range Lower Pliocene to Upper Miocene. However on the more recent Cainozoic time scale of BERGGREN (1972) and BERGGREN and VAN COUVERING (1974) the Pliocene-Miocene boundary is placed at 5 Ma and within errors the lavas of Pulau Kelang lie entirely within the late Miocene.

We are grateful to Professor N.S. Haile for providing samples from Pulau Kelang, Director Institute of Geological Sciences for permission to publish this paper, and Dr. J.V. Hepworth, Head of Asia Unit, Overseas Division, Institute of Geological Sciences for his encouragement.

* *Quart. J. Geol. Soc. Lond.*, 120s.

REFERENCES

- BERGGREN, W.A., A Cenozoic time-scale: Some implications for regional geology and paleobiography, *Lethaia*, **5**, 195-215, 1972.
- BERGGREN, W.A. and J. VAN COUVERING, The late Neogene, biostratigraphy, biochronology, and paleoclimatology of the last 15 million years in marine and continental sediments, *Paleogeol. Paleocol. Paleoclimatol.*, **16**, 1-216, 1974.
- DALRYMPLE, G.B. and M.A. LANPHERE, *Potassium Argon Dating*, W.H. Freeman and Co., XIV+258, pp. 1969.
- HAILE, N.S., Palaeomagnetic evidence for the rotation of Seram, Indonesia, this issue, S 191-S 198, 1978.
- STEIGER, R.H. and E. JAGER, Subcommittee on geochronology: Convention on the use of decay constants in geo- and cosmochemistry, *Earth Planet. Sci. Lett.*, **36**, 359-362, 1977.

A SURVEY OF PALEOMAGNETIC DATA ON MEXICO

Surendra PAL

*Instituto de Geofísica, Universidad Nacional Autónoma
de México, México 20, D.F., Mexico*

(Received June 10, 1978; Revised August 22, 1978)

A compilation is given of all the pole positions either calculated from or given in several paleomagnetic studies carried out so far on Mexican regions. These are compared with the paleomagnetic data from North America (N.A.). The results (Oligocene data) clearly show the presence of relative tectonic movements of the Western Cordillera. The data for Recent to Miocene age seem to be consistent with N.A. data except Pliocene pole positions for Baja California which is taken as an evidence of movement of Baja California relative to Mexico or North America. The Mesozoic pole positions are also considered to show the possibility of tectonic instability of Mexico relative to 'stable' North America. Practically no work has been done so far on older rocks (Pre-Mesozoic) of Mexico.

1. Introduction

As paleomagnetism can contribute significantly to the understanding of the tectonic evolution of Mexico, an effort is made in this work to analyze the significance of all the paleomagnetic data available on Mexican rocks. One such attempt was earlier made by PAL and URRUTIA (1977) and the possibility of relative movements of Mexican regions with respect to 'stable' North America was pointed out. Since then, the author has been able to get access to more paleomagnetic data (unpublished as well as published) which warrants their reexamination.

2. Compilation of Data

The locations sampled for different paleomagnetic studies are shown in Fig. 1. Paleomagnetic data on Mexico has been summarized in Table 1. When an original reference did not include pole positions, these have been calculated from the magnetization directions reported by their authors. Pole classification has been done using the criteria of IRVING *et al.* (1976a). The data on pole positions from North America has been compiled in Appendix I for easy reference. Mean pole positions computed using selected data are given in Table 2. The analysis of the implications of paleomagnetic data from Mexico will be presented in the following.

3. Implications of Data

The Quaternary poles for Mexico are from rocks of the so-called Mexican Volcanic Belt (MVB), except one pole (M 12.1) which is from Baja California. If one plots these poles on a conventional stereographic projection, one can see (Fig. 2) that the pole for Baja California lies apart from other poles and its oval of confidence (dp , dm) hardly intersects the circle of confidence of the Mexico's Quaternary poles (MVB). However, the Baja



Fig. 1. A map showing locations of the areas where paleomagnetic studies have been carried out. 1, Valley of Mexico (M 12.2–12.6, 11.21, 11.22, 11.41, 11.62); 2, Huasteca, Hidalgo (M 11.1); 3, Santiago, Jalisco (M 11.2, 11.23, 11.42); 4, NE Jalisco (M 11.61); 5, San Felipe, Baja California (M 12.1, 11.3); 6, Tepalcates-Navios, Durango (M 11.63–11.66); 7, near Tampico, Tamaulipas (Mendez shale: M 10.1); 8, Saltillo, Coahuila (M 10.2); 9, Cd. Victoria, Tamps. (M 9.1, 8.11); 10, Cuesta La Murella, Coah. (M 9.2); 11, Cintalapa, Chiapas (M 9.3); and 12, Gómez-Palacios, Durango (M 8.1).

California Quaternary pole may not represent a paleomagnetic pole position but simply a virtual geomagnetic pole, so that the discordance mentioned above may not have any tectonic significance. STRANGWAY *et al.* (1971) have concluded that this pole position (M 12.1) obtained from muds of Recent age is close to that of the present magnetic pole and that at the 95% level there is no significant difference between the direction of magnetization recorded in these Recent muds and the direction of the local magnetic field. On the other hand the mean Quaternary pole for Mexico does seem to represent a paleomagnetic pole and is not significantly different from the mean Quaternary pole position for North America (Table 2). This suggests that no discernible tectonic movement of the MVB (relative to North America) can be deduced during the Quaternary.

Paleomagnetic information on Pliocene rocks from Mexico is rather poor. Nevertheless the Pliocene pole from Baja California (M 11.3) is significantly different from the other two Pliocene poles from Mexico. STRANGWAY *et al.* (1971) discussed the tectonic implications of the Baja California Pliocene pole. Tectonic movement of the collection sites seems to be required no matter whether one compares this pole position with Mexico's or North America's mean Pliocene poles.

Mio-Pliocene data from Mexico is also meager and somewhat scattered. The mean

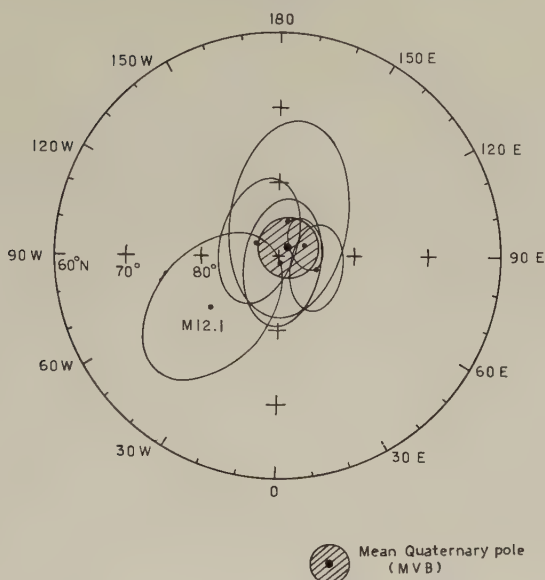


Fig. 2. A comparison of Baja California Quaternary pole (M 12.1) with Mexico's Quaternary mean pole. Note that the data are plotted on polar stereographic projection north of 60°N latitude in this as well as all the other figures.

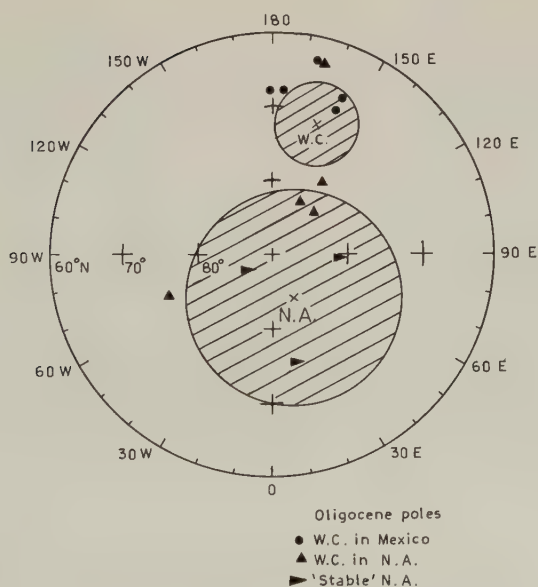


Fig. 3. A comparison of Western Cordillera Oligocene poles with the 'stable' N.A. Oligocene data (mean poles and circles of a_{95} are also plotted).

Table 1. Pole positions from Mexico.

Pole No.	Rock unit and location	Age (my)	Si(Sa)	Stab.	Pole position				Pole class	Ref.	
					λ'	ϕ'	$d\phi$	a_{95}			
<i>Quaternary</i>											
M 12.1	Laguna Salada, Baja California (31N, 115W)	Recent	16 (16)	a	79N	310E	8 11	8	A	STRANGWAY <i>et al.</i> (1971)	
M 12.2	Sediments, Tlapacoya, Mexico (19.3N, 98.9W)	Late Quaternary	57 (57)	a	86N	116E	2 3	2	A	LIDICOAT <i>et al.</i> (1974)	
M 12.3	Sierra de Chichinautzin, Valley of Mexico (19N, 99W)	Quaternary	49 (316)	a	85N	76E	3 6	4	A**	MOOSER <i>et al.</i> (1974)	
M 12.4	Sierra de Chichinautzin, Valley of Mexico (19.2N, 99W)	Quaternary	15 (155)	a	87N	239E	5 8	7	A**	HERRERO and PAL (1977)	
M 12.5	Iztacchuatl volcanics, Valley of Mexico (19.6N, 99W)	Quaternary	35 (232)	a	89N	34E	5 9	—	A**	STEELE (1971)	
M 12.6	Sierras Nevada and Río Frío, Valley of Mexico (19.7N, 99W)	Quaternary	20 (134)	a	85N	163E	8 14	10	A**	MOOSER <i>et al.</i> (1974)	
<i>Tertiary</i>											
M 11.1	Huasteca, Hgo. (21N, 98.7W)	Late Pliocene	22 (66)	a	82N	244E	20 30	—	B	ROBIN and BOBER (1975)	
M 11.2	Santiago, Jalisco (20.8N, 103.3W)	Pliocene (5)	3 (24)	a	75N	184E	26 43	—	B	WATKINS <i>et al.</i> (1971)	
M 11.3	Cañón Rojo and San Felipe, B. California (31N, 115W)	Pliocene	42 (61)	a	53N	335E	8 13	10	A	STRANGWAY <i>et al.</i> (1971)	
M 11.21	Sierra Cruces, Valley of Mexico (19.3N, 99.6W)	Mio-Pliocene	15 (97)	a	84N	261E	7 11	—	A	MOOSER <i>et al.</i> (1974)	
M 11.22	Sierras Nevada and Río Frío, Valley of Mexico (19.7N, 99W)	Mio-Pliocene	9 (55)	a	72N	319E	21 32	—	B	MOOSER <i>et al.</i> (1974)	
M 11.23	Santiago, Jalisco (20.8N, 103.3W)	Mio-Pliocene (7)	7 (69)	a	80N	159E	9 15	—	A**	WATKINS <i>et al.</i> (1971)	
M 11.41	Sierra Guadalupe, Valley of Mexico (19.6N, 99.1W)	Miocene	15 (81)	a	79N	164E	12 21	—	A	MOOSER <i>et al.</i> (1974)	
M 11.42	Santiago, Jalisco (20.8N, 103.3W)	Miocene (9)	4 (45)	a	81N	137E	14 24	—	A	WATKINS <i>et al.</i> (1971)	
M 11.61	Volcanics, NE Jalisco (20.7N, 102.3W)	Oligocene-Early Pliocene	7 (48)	a	68N	181E	7 12	10	A**	URRUTIA and PAL (1977)	
M 11.62	Sierra Guadalupe and Valle Volcanics, Valley of Mexico (19.6N, 99.1W)	Late Oligocene	8 (50)	a	80N	177E	12 21	—	A**	MOOSER <i>et al.</i> (1974)	
M 11.63	Tepecates-Navios + Cd. Durango ignimbrites, Durango (24N, 105W)	Oligocene (23.5)	6 (64)	a	68N	176E	9 16	—	A**	NAIRN <i>et al.</i> (1975)	

M 11.64	Tepalcates-Navios + Cd. Durango ignimbrites, Durango (24N, 105W)	Oligocene (27)	16 (144)	a, t	69N	156E	7	12	11	A**	GUERRERO (1976)
M 11.65	Tepalcates-Navios ignimbrites, Durango (23.9N, 104.8W)	Oligocene (28)	8 (84)	a, t	67N	156E	11	20	—	A	GUERRERO (1973)
M 11.66	Tepalcates-Navios + Cd. Durango ignimbrites, Durango (24N, 105W)	Oligocene (30)	13 (114)	a	63N	167E	7	12	—	A**	NAIRN <i>et al.</i> (1975)
<i>Mesozoic</i>											
M 10.1	Mendez shale, Tamaulipas (22.3N, 98.2W)	Late Cretaceous (Maestrichtian)	— (275)	t	78N	139E	3	6	5	A	KEATING (1975)
M 10.2	Sierra Gujardo and Cerro Huerto, Saltillo, Coah. (25.4N, 101W)	Cretaceous	19 (—)	t	58N	169E	—	—	8	A	NAIRN (1976)
M 9.1	El Huizachal, Cd. Victoria, Tamps. (23.8N, 99.1W)	Jurassic	— (14)	t	76N	71E	10	20	19	A	NAIRN (1976)
M 9.2	Cuesta La Murella, Coahuila (26.5N, 101.3W)	?Jurassic	— (29)	t	61N	155E	4	6	6	A	NAIRN (1976)
M 9.3	Cintalapa, Chiapas (16.8N, 93.7W)	Late Jurassic	— (89)	t	70N	160E	2	3	3	A	GUERRERO and HELSEY (1974, 1976)
M 8.1	Los Cerritos Colorados, Gómez-Palacios, Durango (25.6N, 103.5W)	Triassic	14 (—)	a, t	76N	119E	5	9	8	A	NAIRN (1976)
M 8.11	Caballeros Canyon, Cd. Victoria, Tamps. (23.8N, 99.1W)	Mesozoic	— (30)	t	35N	354E	—	—	—	B	NAIRN (1976)

Pole No.: M stands for Mexico, 12, Quaternary; 11, Tertiary; 10, Cretaceous; 9, Jurassic; 8, Triassic. Rock unit and location: include mean latitude and longitude of the sampling sites. Age (my): radiometric dates are given in parentheses when available. Si (Sa): number of sites (number of samples or specimens) used in each study. Stab.: stability tests carried out are indicated by a, alternating field demagnetization; t, thermal demagnetization. Pole position: λ' , latitude; ϕ' , longitude; δp and dm , semiaxes of the oval of confidence about the pole position at the 95% probability level; a_{95} , radius of the circle of confidence around the estimated mean at the 95% probability level. Pole class: this is based on certain "minimum" reliability criteria, the letter A (or B) indicates that the result does (or does not) fulfill these criteria which consist in that the result should be based on observations from 10 or more separately oriented samples and that δp and dm should be less than 25°. A result is flagged by stars (* or **) if it is based on samples collected from five or more collecting localities, and if at least some of the samples have been subjected to thermal or alternating field demagnetization or leaching by acid, or if it is based on three or more independent results from the same rock unit. More details of pole classification can be found in IRVING *et al.* (1976a). Ref.: reference to the original work is given in this column. M 12.2 was calculated from the data on the directions of magnetization available in the written version of the talk (unpublished) of LINDICOAR *et al.* (1974). M 12.5 pole is the one given by IRVING *et al.* (1976a) and not that given by STEELE (1971) who reports 89N, 4E as the mean pole. The valley of Mexico poles have been calculated from the magnetization directions given by MOOSER *et al.* (1974) and are not taken from the compilation of IRVING *et al.* (1976a). M 11.2 and M 11.42 have been obtained by splitting the paleomagnetic data for two presumably different age groups reported by WATKINS *et al.* (1971). M 10.1 (mean pole) has been calculated from the data of KEATING (1975; Table 2). The sites with $a_{95} > 25^\circ$ have not been included in the mean.

Table 2. Comparison of mean poles from Mexico and North America.

Age	Mexico					North America					
	No. poles used	Poles not used	Pole position			No. poles used	Poles not used	Pole position			
			λ'	ϕ'	a_{95}			λ'	ϕ'	a_{95}	K
<i>Cenozoic</i>											
Quaternary Pliocene	5	M 12.1	88N	128E	4	14	—	84N	77E	7	37
	2	M 11.3	80N	204E	29	7	11 283 11 283, 12 99	87N 85N	22E 76E	9 4	43 242
Mio-Pliocene Miocene	3	—	85N	283E	22	3	—	87N	220E	9	202
	2	—	80N	152E	11	24	—	90N	169E	4	70
Oligocene	6	—	69N	170E	5	16	Early Mio. Late Mio.	88N 86N	281E 107E	4 8	105
	5 (W.C., Mexico)	—	67N	167E	5	9	—	86N	158E	9	36
	4 (W.C., Mexico)	M 11.61	67N	166E	5	8	11 238	86N	145E	10	33
	10 (W.C.)	—	74N	167E	7	5 (W.C., N.A.)	—	81N	167E	14	32
	9 (W.C.)	14.121	71N	163E	5	4 (W.C., N.A.)	14.121	77N	154E	11	73
Eocene	—	—	74N	167E	7	4	W.C.	88N	22E	13	52
	—	—	71N	163E	5	3	W.C., 11 238	84N	26E	15	64
Late Cretaceous	—	—	—	—	—	6	—	81N	177E	9	54
	5	—	—	—	—	5	10 188, 10 212, 10 118, 10 183	69N	185E	6	148
Early Cretaceous	—	—	—	—	—	6	10 161	67N	187E	4	273
	4	—	—	—	—	4	10 161, 10 73, 10 17	68N	188E	7	189
Jurassic-Cret. Late Jurassic Mid-Jurassic Early Jurassic	6	—	—	—	—	6	—	70N	262E	31	6
	5	—	—	—	—	5	—	78N	141E	17	21
	3	—	—	—	—	3	—	86N	98E	24	28
	3	—	—	—	—	3	—	78N	80E	23	29

poles from Mexico and North America for this age again are not significantly different. This is also true for the Miocene poles. Thus with the present data significant tectonic movements of Mexico relative to North America cannot be deduced as far back as the Miocene times. However, the picture becomes interesting when we consider the Oligocene data.

The Oligocene poles from Mexico form a coherent group. From a paleomagnetic study of Tertiary igneous rocks from NE Jalisco, Mexico, URRUTIA and PAL (1977) pointed out the possibility that the sampling sites of Mexico have undergone a rotation since the rocks were magnetized. The results presented by URRUTIA and PAL (1977) on the mean Oligocene poles were such that the mean pole for Mexico fell outside the a_{95} of mean pole for North America and vice versa. The two a_{95} circles, however, did intersect.

GUERRERO (1973, 1976) obtained pole positions from Oligocene ignimbrites and observed that these positions did not agree with the N.A. poles of similar ages. GUERRERO (1973) observed three reversals (four polarity periods) in an ignimbrite sequence (180 m thick). He also obtained a Rb-Sr isochron age on some selected samples. Although the pole position obtained in this study (M 11.65) did not agree with Tertiary poles of North America, GUERRERO (1973) deferred from giving any tectonic implications at this stage until more data could be obtained on more rock units from this area. Later GUERRERO (1976) carried out a more detailed study of the ignimbrite sequences and observed at least five reversals (six polarity periods) in a composite magnetostratigraphic section. The mean position (M 11.64) obtained was still divergent and was considered by GUERRERO (1976) to be due to the fact that secular variation has not been completely averaged out for the number of flows analyzed and the span of time they represent. It is quite intriguing that on one hand he calls the changes in the direction of magnetization as 'true' reversals (he uses them to deny correlation, at least in time, of some volcanic units) and on the other interprets the pole position as a virtual pole where the secular variation is still present. It can be seen from his data that the opposite directions of magnetization are true reversals (not simply 'excursions'). If this is the case, one might wonder why so many polarity transitions observed in the sequence are not sufficient to average out the secular variation of the geomagnetic field.

NAIRN *et al.* (1975) also reported a paleomagnetic and geochronologic (K-Ar) study of the Oligocene ignimbrites from the Western Cordillera. They did not calculate pole positions but only gave the data on cleaned remanent magnetization. URRUTIA and PAL (1976) computed mean pole positions (M 11.63 and 11.66) for two age-groups and used them as a possible evidence of tectonic rotation of Mexico.

Another study on Oligocene rocks from Mexico was that of the Valley of Mexico by MOOSER *et al.* (1974). Pole positions were not given by them but have been computed from their data. In the absence of radiometric dates there seems to be considerable uncertainty about the age assignment in this area and the sites assigned to Late Oligocene might actually be Early Miocene (F. Mooser, personal communication, 1977).

Now if we examine the paleomagnetic data from North America (N.A.), small differences between poles from areas situated on Western Cordillera and those from other areas in N.A. can be noticed. The poles from Western Cordillera (including those from W.C. in Mexico) form a fairly well-defined group. The mean pole is significantly different from the mean Oligocene pole from 'stable' North America as the a_{95} circles do not intersect (Fig. 3). This can be taken as an evidence of tectonic mobility of Western Cordillera in the past.

No paleomagnetic data are available for the Eocene or Paleocene of Mexico. Future attempts to get pole positions of such ages should prove helpful in testing movements of Mexico relative to 'stable' North America.

During the Mesozoic, most of the paleomagnetic results are from sedimentary rocks. The pole position M 10.1 for the Late Cretaceous is based on the data given by KEATING (1975). She observed that the pole position based upon polarity zones is significantly different from other North American pole positions and explained this difference as due to the presence of a component of the present earth's field and not to the rotation of Mexico relative to North America. The evidence for the presence of an appreciable amount of a secondary magnetization in cleaned specimens so as to cause an anomalous pole position is not clear from the intensity data of normal and reversed samples given by KEATING (1975) since the samples with normal directions of magnetization have similar intensities as samples with reverse magnetization. Further the mean directions of normal and reverse magnetizations are about 180° apart and no systematic deviation from this parallelism is found. Thus the explanation given by KEATING (1975) for the anomalous pole position may not be totally satisfactory. This pole position is plotted in Fig. 4 and compared with Late Cretaceous data on N.A.

The pole position (M 9.3) given by GUERRERO and HELSLEY (1974, 1976) warrants further study. There is uncertainty as to what formation was sampled for that study (PAL and URRUTIA, 1977). The details of this study were given by GUERRERO (1976) who assigned this pole position to Late Jurassic and showed it to agree with the pole determined for the upper part of the Morrison Formation in Colorado, U.S.A. The age assigned to Mexico's pole (M 9.3) is based upon palynological analysis of some samples collected from this area. The samples yielded a few specimens of *Cicatricosisporites* sp. GUERRERO (1976) states that this particular species although common since the Early Cretaceous has also been reported in Tithonian strata. Therefore this is obviously not

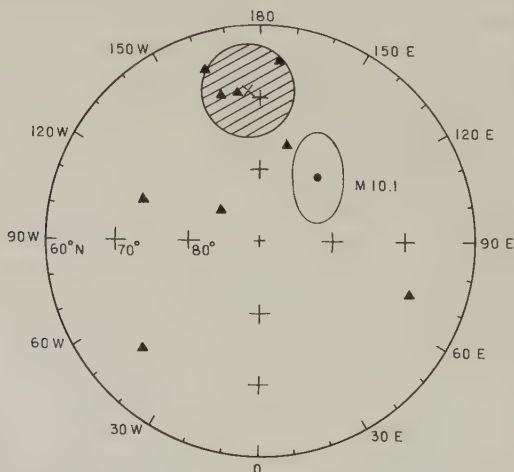


Fig. 4. A comparison of Mexico's Late Cretaceous pole (M 10.1) with the N.A. Late Cretaceous data (see Table 2 for mean poles).

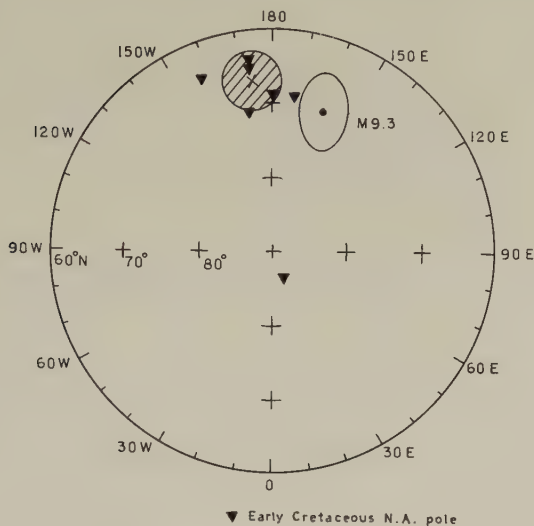


Fig. 5. Mexico's Late Jurassic (?) or Early Cretaceous (?) pole (M 9.3) as compared with N.A.'s Early Cretaceous mean pole.

convincing evidence that the age is really Late Jurassic rather than Early Cretaceous. ALENCASTER (1977) has recently reviewed the paleontological status of this area. She admits that although there is evidence of the Late Jurassic age in San Ricardo Formation, the existence of Early Cretaceous cannot be denied. GUERRERO (1976) argued "Granted that it may be somewhat fortuitous within the resolution of the paleomagnetic methods, the agreement with the results of the upper Morrison Formation is remarkable. This agreement itself may be indicative that indeed the age of the San Ricardo is comparable to that of the Morrison, at least in the area of this work." However, a comparison with Early Cretaceous mean N.A. pole does not exclude the possibility of tectonic movement of the collection site relative to the 'stable' North America (Fig. 5). The arguments of magnetostratigraphy are also not sufficient to assign unambiguously a Late Jurassic age to this pole (M 9.3). It should also be pointed out that there is a considerable spread in the Jurassic data of North America (Table 2 and Appendix I) which makes it rather difficult to use it for tectonic interpretations.

The problem of the data and its interpretation given by NAIRN (1976) has been discussed by PAL and URRUTIA (1978) and NAIRN (1978). The arguments are not sufficient to prove the tectonic stability of Mexican areas studied by NAIRN (1976). Further the pole positions by NAIRN (1976) and GUERRERO (1976) for the Jurassic are not consistent among themselves.

The conclusion drawn from this survey is that the sampling sites of Mexico have been tectonically disturbed and have suffered movements relative to North America. This is also true for the Western Cordillera of Mexico and possibly for that of North America.

The author is grateful to S.K. Banerjee (Univ. of Minnesota), W.D. MacDonald (State Univ. of New York at Binghamton), R. Scandone (Osservatorio Vesuviano, Napoli), K. Kobayashi (Ocean Research Institute, Tokyo) and the reviewer of the Journal for reading the manuscript and making helpful comments for its improvement. N. Figueroa is thanked for the patience of typing the manuscript at different stages.

Appendix I. Pole Positions from North America (Excluding Alaska and Mexico).

Pole No.	Rock unit and location	Age (my)	Si(Sa)	Stab.	Pole position			Pole class	Ref.
					λ'	ϕ'	$d\phi$		
<i>Quaternary</i>									
12 264	Aiyansh flow, British Columbia, Canada (55.2N, 129.1W)	Recent	22 (119)	a	82N	292E	1 1	—	A**
12 231	High Cascade lavas, Oregon, U.S.A. (44.3N, 121.9W)	Recent	9 (92)	a	76N	50E	5 7	—	A**
14.002	Leaside Till, Ontario, Canada (43.7N, 79.2W)	Recent	6 (24)	a	73N	192E	9 11	—	A*
14.003	Sunnybrook Till, Ontario, Canada (43.7N, 79.2W)	Recent	9 (34)	a	72N	84E	9 14	—	A*
14.004	Port Stanley Till, Ontario, Canada (42.5N, 82.0W)	Recent	7 (58)	a	75N	73E	3 4	—	A**
15.001	St. Joseph Till, Lake Huron, Canada (43.5N, 81.6W)	Recent	31 (140)	a	71N	97E	6 9	—	A**
15.002	Varved clays, Walkerton, Canada (44.2N, 81.2W)	Recent	— (39)	a	66N	92E	3 4	—	A
NA 13.3	Suttle Lake lavas, Oregon, U.S.A. (44N, 122W)	Pleistocene	19 (—)	a	88N	272E	—	—	—
12 136	Valles Caldera volcanics, New Mexico, U.S.A. (35.9N, 106.5W)	Quaternary (1.1)	22 (70)	a	83N	83E	5 7	—	A**
12 160	Wilson Creek Formation, Calif., U.S.A. (38N, 119W)	Quaternary	60 (—)	a	82N	59E	4 6	—	A**
12 115	Louistown lavas, Calif., U.S.A. (39.4N, 120W)	Quaternary (1.45)	23 (138)	a	67N	357E	7 11	9	A**
12 47	New England glacial varves, U.S.A. (43N, 73W)	Quaternary	11 (999)	n	79N	128E	9 13	—	A
12 69	Pleistocene silts, Canada and U.S.A. (41N, 84W)	Quaternary	11 (—)	n	87N	166E	22 22	—	A
<i>Tertiary</i>									
12 99	Norris volcanics, Montana, U.S.A. (45.6N, 111.7W)	Pliocene to Early Pleistocene	1 (12)	a	64N	294E	9 10	—	A*
14.058	Curtis Ranch (normal), San Pedro Val., Arizona, U.S.A. (32.5N, 110.5W)	Pliocene to Pleistocene	29 (—)	a	86N	29E	5 7	—	A
									McElhinny and Cowley (1977)

14.059		Curtis Ranch (reversed), San Pedro Val., Arizona, U.S.A. (32.5N, 110.5W)	Pliocene to Pleistocene	28 (—)	a	78N	38E	5	8	—	A	McELHINNY and COWLEY (1977)
11	664	St. David Formation, Arizona, U.S.A. (36N, 110W)	Pliocene (2.15)	57 (171)	a	79N	47E	5	8	—	A*	
11	671	Mt. Edziza lavas, British Columbia, Canada (57.5N, 130W)	Pliocene (3)	84 (354)	a	89N	328E	6	7	—	A**	
11	216	Lavas, Arizona, U.S.A. (35.2N, 111.6W)	Middle Pliocene	7 (34)	a	88N	101E	—	—	19	A**	
NA	12.5	Lavas and baked sediments, New Mexico and Arizona, U.S.A. (35.2N, 111.6W)	Pliocene (4)	24 (111)	a, t	85N	109E	10	14	—	A**	McELHINNY (1973)
11	217	Lavas, New Mexico, U.S.A. (36.4N, 105.7W)	Pliocene (4)	16 (116)	a	85N	91E	9	13	—	A**	
11	501	Somona volcanics, Calif., U.S.A. (38.6N, 122.5W)	Pliocene (4.1)	14 (90)	n, a	79N	83E	—	—	9	A**	
11	283	Lousetown neogene lavas, Calif., U.S.A. (39.4N, 120W)	Pliocene (6.8)	32 (192)	a	16N	204E	3	4	3	A**	
11	320	Brown basaltic dykes, British Columbia, Canada (52.5N, 127.5W)	Post-Late Miocene	9 (36)	a	82N	248E	15	17	—	A**	
11	107	Basalts, Yukon and British Columbia, Canada (61N, 134W)	Miocene to Pliocene	— (48)	n	85N	150E	5	6	—	A	
11	105	Payette Formation, Idaho, U.S.A. (43N, 115W)	Miocene to Pliocene	— (13)	n	89N	316E	3	5	—	A*	
11	104	Ellensburg Formation, Washing- ton, U.S.A. (46N, 120W)	Miocene (10.1)	— (23)	n	85N	245E	13	15	—	A*	
11	232	Cariboo plateau basalt, British Columbia, Canada (51.8N, 121.8W)	Miocene (11.5)	48 (251)	a	84N	220E	5	5	—	A**	
11	231	Gabbroic plug, British Colum- bia, Canada (51.5N, 121.2W)	Miocene (11.5)	17 (70)	a	85N	213E	5	6	—	A**	
11	584	Columbia R. Lavas, Idaho, U.S.A. (46.3N, 116.6W)	Miocene (14)	10 (20)	a	82N	210E	—	—	—	A	
11	585	Columbia R. Lavas, Washing- ton, U.S.A. (46.5N, 117W)	Miocene (14)	9 (18)	a	83N	160E	—	—	—	A	
11	586	Columbia R. Lavas, Washing- ton, U.S.A. (46.1N, 117.2W)	Miocene (14)	28 (56)	a	81N	312E	—	—	—	A	
11	587	Columbia R. Lavas, Oregon, U.S.A. (45.6N, 117.6W)	Miocene (14)	19 (38)	a	87N	123E	—	—	—	A	

Appendix I (Continued)

Pole No.	Rock unit and location	Age (my)	Si(Sa)	Stab.	Pole position			Pole class	Ref.
					λ'	ϕ'	$\frac{dp}{dm}$		
11 588	Columbia R. Lavas, Oregon, U.S.A. (40N, 116.6W)	Miocene (14)	32 (64)	a	82N	18E	—	—	A
11 589	Columbia R. Lavas, Oregon, U.S.A. (45.3N, 121.2W)	Miocene (14)	17 (34)	a	83N	41E	—	—	A
11 590	Columbia R. Lavas, Oregon, U.S.A. (44.8N, 120.9W)	Miocene (14)	6 (12)	a	88N	183E	—	—	A
11 591	Columbia R. Lavas, Oregon, U.S.A. (44.5N, 119.6W)	Miocene (14.5)	14 (20)	a	85N	353E	—	—	A
11 583	Columbia R. Lavas, Snake River, Wash., U.S.A. (46.5N, 117.2W)	Miocene (14.5)	19 (38)	a	78N	168E	—	—	A
11 594	Columbia + Owyhee + Steens basalts, U.S.A. (45N, 118W)	Miocene (14.5)	212 (528)	a	88N	301E	—	—	5 A**
11 103	Neroly Formation, Calif., U.S.A. (37.5N, 122W)	Miocene (15.5)	3 (29)	a, t	85N	318E	3	4	A*
11 592	Owyhee Ridge basalts, Oregon, U.S.A. (43.6N, 117.2W)	Miocene (14.5)	14 (28)	a	72N	312E	—	—	A
11 593	Steens Mt. basalts, Oregon, U.S.A. (42.6N, 118.6W)	Miocene (14.5)	44 (200)	a	81N	311E	—	—	A
14.108	Peach Springs Tuff and flows, Arizona, U.S.A. (35.5N, 113.4W)	Miocene (16.9)	15 (—)	a	84N	34E	8	13	A
15.023	Mount Barr Complex, British Columbia, Canada (49.3N, 121.5W)	Miocene (18)	5 (22)	a	72N	274E	13	15	— A**
11 567	Grotto and Snoqualmie batholiths, Washington, U.S.A. (48N, 122W)	Miocene (20.9)	7 (65)	a	86N	208E	4	6	— A**
11 361	Basalt flows, Colorado, U.S.A. (39.8N, 106.7W)	Miocene (22.8)	17 (35)	a	82N	131E	15	21	— A**
11 441	Ash flows sheets, Nevada, U.S.A. (37.8N, 114.4W)	Miocene (23.8)	5 (98)	a	78N	105E	11	17	10 A
11 147	Abert Rim basalts, Oregon, U.S.A. (42.6N, 120.2W)	Miocene (24)	16 (98)	a	80N	62E	6	6	— A
NA 12.9	Ignimbrites, Nevada, U.S.A. (38.5N, 115W)	Miocene (24)	8 (98)	a, t	73N	142E	17	17	— A
									McELHINNY (1973)
									McELHINNY and COWLEY (1977)
									McELHINNY and COWLEY (1978)

NA 12.3	Lovejoy basalt, California, U.S.A. (40N, 121W)	Miocene (24)	13 (158)	a, t	76N	74E	25	—	A	McElhinny (1973)
(11 A)	SE Arizona volcanics, U.S.A.	Oligocene (27.5)	-- (—)	—	75N	11E	—	—	—	STRANGWAY <i>et al.</i> (1971)
11 440	Ash flows sheets, Nevada, U.S.A. (39.1N, 115.8W)	Oligocene to (28) Early Miocene	54 (500)	a	82N	135E	15	22	20	A
(11 UNOC)	Volcanics, Utah+Nevada+Oregon+Calif., U.S.A.	Oligocene (29.5)	67 (—)	—	78N	146E	—	—	6	A**
11 312	Marys peak sill, Oregon, U.S.A. (44.5N, 123.6W)	Middle Oligocene (29.6)	24 (200)	a	63N	164E	6	10	—	A**
14.121	Needles Range Formation, Utah, U.S.A. (38.5N, 113W)	Oligocene (29.7)	5 (103)	a	75N	291E	14	22	—	A
11 579	San Juan mts. volc., Colorado, U.S.A. (37.5N, 106.5W)	Oligocene (30)	23 (167)	a	86N	298E	8	11	—	A**
11 454	Bull hill volc., Texas, U.S.A. (29.3N, 103.3W)	Oligocene (31.3)	20 (—)	a	81N	89E	—	—	—	A**
14.122	Ash flow sheets, Nevada and Utah, U.S.A. (39N, 116W)	Oligocene (32)	10 (461)	a	82N	151E	17	23	—	A
11 238	Spanish peak dyke, Colorado, U.S.A. (37.3N, 104.5W)	Late Eocene to Early Oligocene	6 (39)	a	81N	211E	16	20	—	A**
11 229	Western cascade series, California, U.S.A. (42N, 122.3W)	Late Eocene to Early Miocene	24 (96)	a	80N	292E	—	—	8	A**
15.029	Hope Complex, British Columbia, Canada (49.3N, 121.5W)	Eocene to Oligocene (38)	5 (21)	a	88N	208E	5	6	—	A**
11 665	East Sooke gabbro, Vancouver Is., Canada (48.4N, 123.6W)	Eocene (39)	29 (145)	a	70N	151E	5	7	—	A**
11 597	Mistastin lake structure, Canada (55.9N, 63.4W)	Eocene (40)	10 (73)	a	86N	118E	3	3	—	A**
11 573	Monterey intrusives, Virginia, Canada (38.4N, 79.6W)	Eocene (42)	6 (36)	a	87N	51E	10	13	—	A**
11 657	Twin sisters dunite, Washington, U.S.A. (48.7N, 121.5W)	Eocene (45.5)	17 (89)	a	28N	297E	6	8	—	A**
11 576	Kasiks + Quotton plutons, Canada (54.3N, 129.5W)	Eocene (46)	9 (31)	a	76N	216E	7	7	—	A**
11 687	Green river Formation, Colorado, U.S.A. (40N, 108.4W)	Eocene (47)	4 (55)	a	19N	225E	8	11	—	A*

Appendix I (Continued)

Pole No.	Rock unit and location	Age (my)	Si (Sa)	Pole position				Pole class	Ref.
				λ'	ϕ'	$d\phi$	dm	a_{95}	
11 98	Siletz river volcanics, Oregon, U.S.A. (45N, 123.5W)	Eocene	8 (57) t	37N	311E	7	10	—	A**
11 101	Green river Formation, Wyoming, U.S.A. (41.5N, 109.5W)	Eocene	— (19) n	85N	192E	8	9	—	A*
11 165	Intrusive + baked rock, Colorado, U.S.A. (40N, 105.3W)	Paleocene or Eocene	3 (15) a	68N	189E	18	23	—	A*
11 97	Duchesne river Formation, Utah, U.S.A. (40N, 110W)	Tertiary	— (24) n	83N	261E	6	8	—	A
<i>Cretaceous</i>									
10 50	Volc. + sediments, Montana, U.S.A. (46N, 112W)	Late Cretaceous or Early Tertiary	10 (—) a	71N	204E	6	8	—	A**
10 48	Sappington basic dyke, Montana, U.S.A. (45.8N, 111.7W)	Late Cretaceous or younger	1 (13) a	53N	273E	7	7	—	A*
10 90	Boulder batholith, Montana, U.S.A. (46N, 112.5W)	Late Cretaceous (73)	— (15) —	76N	164E	—	—	—	A
10 188	Boulder batholith, Montana, U.S.A. (46N, 112.5W)	Late Cretaceous (73)	27 (300) a	73N	249E	12	13	—	A**
10 212	Ecstall pluton, British Columbia, Canada (54.2N, 130W)	Late Cretaceous (75)	7 (35) a	68N	313E	13	16	—	A**
10 216	Niobrara Formation, Wyoming, U.S.A. (42N, 105W)	Late Cretaceous (76.5)	3 (46) a	65N	174E	—	—	6	A*
10 28	Sierra Nevada Pluton, California, U.S.A. (38N, 120W)	Late Cretaceous (85)	14 (80) n, a	69N	195E	—	—	10	A**
10 118	Stevens Pass granite, Washington, U.S.A. (48.6N, 121W)	Late Cretaceous (85)	4 (37) a	68N	71E	—	—	14	A*
10 183	Howe Sound plutons, British Columbia, Canada (48.8N, 123.2W)	Late Cretaceous (94)	17 (68) a	83N	231E	10	13	—	A**
10 222	Elkhora mts. volc., Montana, U.S.A. (46N, 112W)	Late Cretaceous	13 (—) a	69N	189E	7	10	—	A**

10	71	Mesaverde group, Utah, U.S.A. (41N, 109W)	Late Cretaceous	45 (—)	n, t	65N	198E	19	22	—	A**
10	73	Alkalic rocks, Arkansas, U.S.A. (34.5N, 92.8W)	Early to Late Cretaceous (98)	19 (47)	a	65N	187E	9	13	—	A**
10	17	Isachen Diabase, NWT, Canada (78.7N, 103.7W)	Early to Late Cretaceous	10 (20)	a	69N	180E	14	14	—	A**
10	11	Monteregian Hills, Quebec, Canada (45.5N, 73W)	Early Cretaceous (111)	8 (49)	n	65N	203E	—	—	—	A
10	72	Monteregian Hills, Quebec, Canada (45.3N, 72.8W)	Early Cretaceous (111)	32 (147)	a	71N	189E	2	3	—	A**
10	12	Mount Megantic, Quebec, Canada (45.5N, 71W)	Early Cretaceous (115)	1 (12)	a	69N	172E	7	10	—	A
10	161	Southern Calif. batholith, U.S.A. (33.5N, 117W)	Early Cretaceous (121)	18 (110)	a	86N	23E	5	7	—	A**
10	35	Mt. Ascutney gabbro, Vermont, U.S.A. (43.4N, 72.5W)	Early Cretaceous (130)	2 (24)	a	64N	187E	18	22	14	A*
<i>Jurassic</i>											
10	66	Franciscan Peridotite, California, U.S.A. (37.4N, 121.5W)	Late Jurassic to Late Cretaceous	6 (41)	a	56N	310E	4	6	—	A**
10	67	Franciscan dunite, California, U.S.A. (37.4N, 121.5W)	Late Jurassic to Late Cretaceous	5 (18)	a	66N	228E	11	12	—	A**
10	78	Franciscan Formation, California, U.S.A. (38N, 122.5W)	Late Jurassic to Early Cretaceous	25 (127)	n	29N	316E	7	11	—	A**
10	30	Bucks batholith, Sierra Nevada, Calif. U.S.A. (39.9N, 121.3W)	Late Jurassic to Early Cretaceous (135.5)	9 (116)	a	58N	195E	8	10	8	A**
10	256	Buck + Guadalupe intrusives combined, Sierra Nevada, Calif., U.S.A. (38.7N, 120.7W)	Late Jurassic to Early Cretaceous (136)	13 (142)	a	54N	174E	—	—	10	A
10	86	Andesitic dykes, British Columbia, Canada (52.5N, 127.5W)	Mid-Jurassic to Late Cretaceous	11 (—)	a	68N	288E	18	20	—	A**
9	154	Topley intrusions, Endako, British Columbia, Canada (54N, 125W)	Late Jurassic (139)	13 (50)	a	70N	129E	11	14	—	A**

Appendix I (Continued)

Pole No.	Rock unit and location	Age (my)	Stab.	Pole position				Pole class	Ref.
				λ'	ϕ'	dp	dm	a_{95}	
9 177	Lower Morrison Formation, Colorado, U.S.A. (38.1N, 108.2W)	Late Jurassic (143.5)	32 (32) t	68N	162E	4	5	—	A**
9 176	Upper Morrison Formation, Colorado, U.S.A. (38.1N, 108.2W)	Late Jurassic (143.5)	68 (68) t	61N	142E	4	7	—	A**
9 169	Carmel Formation, Utah, U.S.A. (39N, 110W)	Late Jurassic (154)	1 (12) —	76N	307E	15	18	—	A
9 135	Carmel Foundation, Utah, U.S.A. (38.6N, 110.7W)	Late Jurassic (154)	1 (42) t	81N	82E	7	10	—	A*
9 137	Summerville Formation, Utah, U.S.A. (39.9N, 110.1W)	Mid- to Late Jurassic (Upper Oxfordian)	1 (40) t	70N	86E	6	9	—	A*
9 104	Island intrusive, British Columbia, Canada (49.6N, 125.5W)	Mid-Jurassic (159)	17 (65) a	79N	240E	10	11	—	A**
9 170	Navajo sandstone normal, Utah, U.S.A. (39N, 110W)	Mid-Jurassic (164)	1 (176) t	87N	36E	3	4	—	A*
9 72	White mountain Series, New Hampshire, U.S.A. (44N, 71W)	Early Jurassic (180)	12 (130) a	86N	127E	5	6	6	A**
8 253	Kayenta Formation, Utah, U.S.A. (37N, 111.5W)	Early Jurassic (182.25)	4 (39) n	83N	39E	—	—	—	A
15.073	Navajo sandstone reversed, Utah, U.S.A. (38.5N, 109.5W)	Early Jurassic	25 (100) t	46N	65E	7	17	—	A**
8 263	Kayenta Formation, U.S.A. (39N, 110W)	Lowermost Jurassic	1 (13) —	61N	83E	5	10	—	A
									McELHINNY and COWLEY (1978)

The explanation of the captions is the same as that given in the footnote of Table 1 with the only difference that Pole No. here is the one given by compilers and Ref. in most cases is only that of the compilers (where reference to the original work can be found). The poles not referenced here are taken from the compilation of IRVING *et al.* (1976a, b). Most of them can also be found in the compilations of McELHINNY and COWLEY (1977, 1978). The poles obviously classified as B-class poles are excluded from the list.

REFERENCES

- ALENCASTER, G., Moluscos y Braquiópodos del Jurásico Superior de Chiapas, Univ. Natl. Autón. México, Inst. Geología, *Revista*, **1**, 151–166, 1977.
- GROMMÉ, C.S. and E.H. MCKEE, Mid-tertiary paleomagnetic pole from volcanic rocks in the Western United States, (Abstr.), *EOS, Trans. Am. Geophys. Union*, **52**, 187, 1971.
- GUERRERO, J., Paleomagnetismo y relaciones $^{87}\text{Sr}/^{86}\text{Sr}$ en ignimbritas del área Tepalcates-Navios, Durango, Reunión Anu. Unión Geofís. Mexicana, Progr., (Abstr.), pp. 33–34, 1973.
- GUERRERO, G.J., Contribution to paleomagnetism and Rb-Sr geochronology, Ph. D. Thesis, Univ. of Texas at Dallas, p. 131, 1976.
- GUERRERO, J.C. and C.E. HELSLEY, Paleomagnetic evidence for Post-Jurassic tectonic stability of South Eastern Mexico, (Abstr.), *EOS, Trans. Am. Geophys. Union*, **56**, 1110, 1974.
- GUERRERO, J.C. and C.E. HELSLEY, Paleomagnetismo y evolución tectónica Post-Jurásica de la Península de Yucatán, México, III Congr. Latinoamericano de Geología, (Abstr.), p. 56, 1976.
- HERRERO, B.E. and S. PAL, Paleomagnetic study of Sierra de Chichinautzin, Mexico, *Geofís. Int.*, **17**, 1977 (in press).
- IRVING, E., E. TANCZYK, and J. HASTIE, Catalogue of paleomagnetic directions and poles, V issue, Cenozoic results 1927–1975, Geomag. Ser., No. 10, p. 87, Ottawa, Canada, 1976a.
- IRVING, E.E., TANCZYK, and J. HASTIE, Catalogue of paleomagnetic directions and poles, IV issue, Mesozoic results 1954–1975 and results from seamounts, Geomag. Ser., No. 6, p. 70, Ottawa, Canada, 1976b.
- KEATING, B.H., Magnetostratigraphy and biostratigraphy of the Late Cretaceous and problems associated with paleomagnetic study of DSDP core material, M.S. Thesis, Univ. of Texas at Dallas, 1975.
- LIDDICOAT, J.C., R.S. COE, P.W. LAMBERT, and S. VALASTRO, Jr., Dating Mexican archeological sites using a possible Late Quaternary geomagnetic field excursion, Geol. Soc. Am. Annu. Meet., Miami, 1974.
- MC ELHINNY, M.W., *Paleomagnetism and Plate Tectonics*, p. 358, Cambridge Univ. Press, Cambridge, U.K., 1973.
- MC ELHINNY, M.W. and J.A. COWLEY, Paleomagnetic directions and pole positions—XIV. Pole numbers 14/1 to 14/574, *Geophys. J. R. Astr. Soc.*, **49**, 313–356, 1977.
- MC ELHINNY, M.W. and J.A. COWLEY, Paleomagnetic directions and pole positions—XV. Pole numbers 15/1 to 15/232, *Geophys. J. R. Astr. Soc.*, **52**, 259–276, 1978.
- MOOSER, F., A.E.M. NAIRN, and J.F.W. NEGENDANK, Paleomagnetic investigations of the Tertiary and Quaternary igneous rocks. VIII. A paleomagnetic and petrologic study of volcanics of the Valley of Mexico, *Sond. Geol. Rundschau*, **63**, 451–483, 1974.
- NAIRN, A.E.M., A paleomagnetic study of certain Mesozoic formations in Northern Mexico, *Phys. Earth Planet. Inter.*, **13**, 47–56, 1976.
- NAIRN, A.E.M., A paleomagnetic study of certain Mesozoic formations in Northern Mexico—Reply, *Phys. Earth Planet. Inter.*, **16**, 287, 1978.
- NAIRN, A.E.M., J.F.W. NEGENDANK, H.C. NOLTIMIER, and T.J. SCHMITT, Paleomagnetic investigations of the Tertiary and Quaternary igneous rocks. X. The ignimbrites and lava units west of Durango, Mexico, *Neues Jahrb. Geol. Paleontol., Monatsh.*, **11**, 664–678, 1975.
- PAL, S. and J.F. URRUTIA, Paleomagnetism, geochronology and geochemistry of some igneous rocks from Mexico and their tectonic implications, Proc. IV Int. Gondwana Symp., Calcutta, 1977 (in press).
- PAL, S. and J.F. URRUTIA, Comments on “A paleomagnetic study of certain Mesozoic Formations in Northern Mexico,” *Phys. Earth Planet. Inter.*, **16**, 285–286, 1978.
- ROBIN, C. and C. BOBIER, Las fases de vulcanismo de Tlachinol (Hidalgo) según datos paleomagnéticos y geoquímicos, *Bol. Inst. Geol. U.N.A.M.*, **95**, 49–85, 1975.
- STEELE, W.K., Paleomagnetic directions from the Iztaccihuatl volcano, Mexico, *Earth Planet. Sci. Lett.*, **11**, 211–218, 1971.
- STRANGWAY, D.W., B.E. MCMAHON, T.R. WALKER, and E.E. LARSON, Anomalous Pliocene paleomagnetic pole positions from Baja California, *Earth Planet. Sci. Lett.*, **13**, 161–166, 1971.
- URRUTIA, F.J. and S. PAL, Further paleomagnetic evidence for a possible tectonic rotation of Mexico, *Geofís. Int.*, **16**, 255–259, 1976.
- URRUTIA, F.J. and S. PAL, Paleomagnetic data from Tertiary igneous rocks, North-East Jalisco, *Earth Planet. Sci. Lett.*, **36**, 202–206, 1977.
- WATKINS, N.D., B.M. GUNN, A.K. BAKSI, D. YORK, and J. ADE-HALL, Paleomagnetism, geochemistry and potassium-argon ages of the Rio Grande de Santiago volcanics, Central Mexico, *Geol. Soc. Am. Bull.*, **82**, 1955–1968, 1971.

SOUTHEAST ASIAN TIN GRANITOIDS OF CONTRASTING TECTONIC SETTING

Charles S. HUTCHISON

*Department of Geology, University of Malaya,
Kuala Lumpur, Malaysia*

(Received June 22, 1978; Revised September 29, 1978)

The three major tin granitoid belts are, from west to east:

a) Western: From Phuket to Tenasserim. The tin deposits are associated with high-level Cretaceous adamellite, granite and pegmatite. The mineralization extends over a wide vertical extent.

b) Main Range: From Bangka to South Thailand. The tin deposits are associated with deep-seated large-microcline granite and adamellite of late Carboniferous and late Triassic age. The mineralization is confined to the roof zones of the batholith.

c) Eastern: From Billiton to Pahang-Trengganu. The tin-tungsten deposits are associated with adamellite to granite of Permian to mid Triassic high-level plutons. Mineralization extends over a wide vertical extent and there is an important Fe-Sn association.

Only the Eastern Belt can be classified as Circum-Pacific type. It represents an epizonal volcano-plutonic arc characterized by plutonic rocks ranging from gabbro, through tonalite, granodiotite, adamellite to granite. Rhyolitic ignimbritic volcanic rocks are important.

The Western Belt has some of the Eastern Belt characteristics, but lacks the range of plutonic rocks, and volcanic rocks are absent. However, the Tertiary opening of the Andaman Sea requires that the Burmese-Indonesian volcanic arc formerly was adjacent to the adamellite-granite belt.

The Main Range Belt is interpreted as resulting from crustal anatexis of the leading edge of the western craton as it attempted to subduct beneath the Eastern volcano-plutonic arc following the late Triassic closure of the central marginal basin.

1. Introduction

The strong contrast between the Main Range and the Eastern Belt of Peninsular Malaysia has been documented by HUTCHISON (1977). The contrasts were further amplified in respect of the character of the tin mineralization, and associated iron, by HUTCHISON and TAYLOR (1978) and TAYLOR and HUTCHISON (1978), who also focused attention to the distinct character of the third major S.E. Asian tin belt of Phuket-Tenasserim.

A forthcoming review of the stratigraphic and tectonic evolution of the whole Southeast Asian region (HUTCHISON, 1979), highlights a Paleozoic marginal basin extending southwards from Laos, through Thailand and the length of Peninsular Malaysia, separating the Main Range from the Eastern Massif. A major divergence from this interpretation (MITCHELL, 1977) proposes that the marginal basin was the main Tethys Sea and that the massifs to the west and east were formerly connected with Gondwanaland and Eurasia respectively.

A minor narrow granitoid belt within this marginal basin has been referred to as the Central Belt (HUTCHISON, 1977). It has no known tin association.

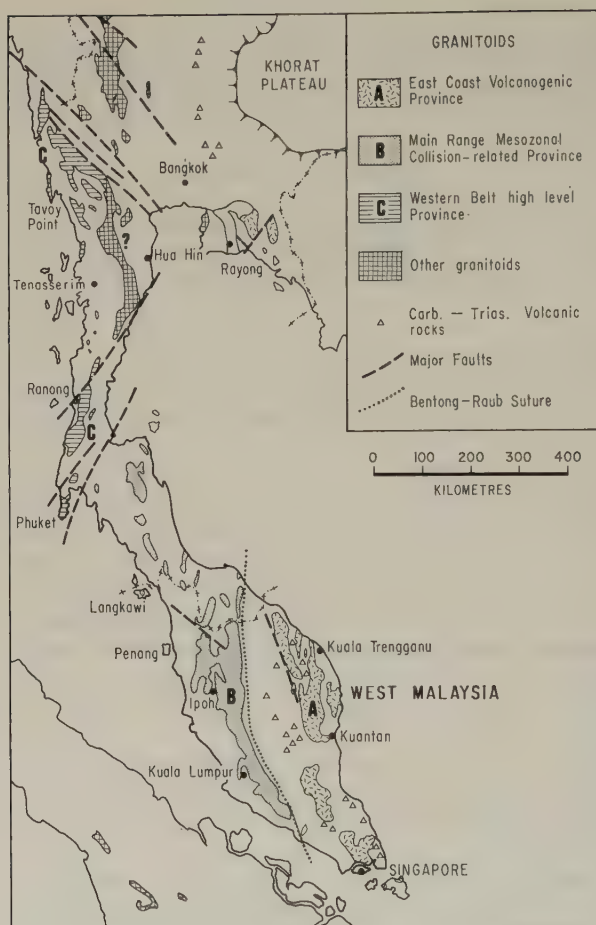


Fig. 1. The three major tin granitoid belts of Southeast Asia, after HUTCHISON and TAYLOR (1978). The central marginal basin separates the Main Range from the Eastern Massif and itself contains a narrow tin-barren granitoid belt which is not shown.

This paper attempts a possible tectonic evolution for the region based on the petrological characteristics of the three main tin belt granitoids. It is a revision of that of HUTCHISON (1973a) in the light of new data.

2. The Tin Granitoid Belts

The three major belts are shown on Fig. 1. The northern part of the Eastern Belt (A) is fault bounded on the west, but the southern part in Singapore and south Peninsular Malaysia occupies a region of low topography and poor exposure. Its western boundary is unknown, but appears offset westwards with respect to the northern part (Fig. 1). The Eastern Massif has all the characteristics of a volcano-plutonic arc (HUTCHISON, 1977),

including a wide range of plutonic rocks from gabbro to granite, and coeval acid to intermediate volcanic and pyroclastic rocks. In this respect, it is of Circum-Pacific character, with close similarity to the Andes (PITCHER, 1978).

The Main Range Belt (Fig. 1, B) is of highly differentiated granite characterised by large megacrysts of maximum microcline. Finer grained varieties also occur locally. Its eastern border is represented by a narrow zone of eastwards dipping crumpled melange-like argillite containing discontinuous blocks of serpentinite, overlain locally by redbeds. This tectonic line has been referred to as the Bentong-Raub Suture (HUTCHISON, 1975), and from recent drilling south of Malacca (KHOO, 1978), it is now known to run out into the Straits of Malacca, and not to continue southwards to Singapore as formerly believed.

Southwards extension of these two belts is badly known, but in Indonesia the tin deposit characteristics indicate that Billiton belongs to the Eastern Massif, and Bangka to the Main Range Massif (HUTCHISON and TAYLOR, 1978).

Northwards extension is also badly known. Extension through the Gulf of Thailand can be inferred by important N-S trending horst and graben structures (WOLLANDS and HAW, 1976).

The Western Belt (Fig. 1, C) is apparently strongly fault-bounded, and extends northwards from Phuket into Burma. The eastwards extent of this belt is not yet defined.

Very little is known about the other tin granites shown in Fig. 1. They occur in West Central Sumatra and North Thailand.

The central marginal basin of Peninsular Malaysia, which includes the minor Central tin-barren granitoid belt, probably continues northwards through Thailand, as documented by a similar Carboniferous to Triassic succession, including contemporaneous volcanic activity (HUTCHISON, 1979). However, instead of the eastern margin being formed by the Eastern massif, it is formed by the Mesozoic continental basin of the Khorat Plateau. The western margin is similarly delimited by an ophiolite belt through Lampang and Houei Sai (HUTCHISON, 1975), similar to the Bentong-Raub Line of Peninsular Malaysia.

2.1 Eastern Tin Belt

The properties of the Eastern Belt are summarized in Table 1, after HUTCHISON and TAYLOR (1978). Radiometric data are from BIGNELL and SNELLING (1977). A general description of the granitoids was given by RAJAH *et al.* (1977). As stressed by HUTCHISON (1977), the concordance of the Rb: Sr and the K: Ar dates amplifies the tectonic stability of this massif. Mineralized quartz hydrothermal veins extend far into the thermally metamorphosed country rocks.

2.2 Main Range Tin Belt

The properties of the Main Range Massif are summarized in Table 1. As stressed by HUTCHISON (1977) the strongly discordant Rb: Sr and K: Ar dates have been taken to mean strong post tectonic uplift. The greenschist facies country rock envelope, together with the maximum microcline of the granitoids, indicate deep seated crystallization in which the volatiles were not permitted to escape and accumulated in the roof zones of the batholiths. The lodes were therefore impounded or closely confined to the roof zones. Post crystallization uplift is indicated by shear zones and young K: Ar dates.

2.3 Western Tin Belt

The properties of the Western Belt are summarized in Table 1, from GARSON *et al.*

Table 1. Summary of the properties of the

Western: Phuket-Tenasserim	
Plutonic rocks	Hornblende adamellite, biotite granite, muscovite-biotite granite, pegmatite
Volcanic rocks	Apparently absent. The Burmese and Sumatran volcanic arc may be coeval
Granitoid texture	Equigranular to porphyritic, medium to coarse
Colour	Pale grey or pink
Femic minerals	Biotite, hornblende, muscovite, ilmenite
Alkali feldspar	Orthoclase to intermediate microcline, 2V not measured
Level of emplacement	High level granitoid plutons with well-developed thermal aureoles containing cordierite and andalusite
Age, Rb : Sr	115 \pm 7 Ma Early Cretaceous
Age, K : Ar	57 \pm 5 Ma
Initial ⁸⁷ Sr/ ⁸⁶ Sr	0.707
Crystallization index	4 to 18
K ₂ O weight % average	5.6
K ₂ O/Na ₂ O average	2.14
Rb/Sr average	3.4
Tin occurrence	Hydrothermal quartz stockworks up to 2 km long. Tin associated with lithium and tantalum in pegmatites
Tin associations	Sn-Li-Ta-W
Post-granitoid dykes	Basaltic dykes common
Other features	Hot springs are common. Placers abundant

(1975), and as shown by HUTCHISON (1979) the tectonic setting for the southern end at Phuket appears to continue into south Burma. This is the only belt in which major pegmatites occur and they contain significant cassiterite (TAYLOR and HUTCHISON, 1978). An unusual feature of the Phuket area is the presence of diamonds in the stanniferous placers. Their primary source is unknown. Radiometric dating of this belt is from GARSON *et al.* (1975) and BIGNELL (1972). Another curious feature is that this belt appears to be strongly fault-bounded (Fig. 1) and the extent of the granites appears to coincide closely with the predominantly Carboniferous Phuket Group and analogous Mergui Formation (HUTCHISON, 1979). A further feature is its similarity with the Eastern Belt in that the granitoids are high level with well-developed thermal aureoles, but with a complete absence of coeval volcanic rocks and of tonalite and gabbro. As will be shown below, it is possible in a pre-Andaman Sea reconstruction, to consider a juxtaposition of the Burmese and Sumatran volcanic arc immediately to the west of this plutonic arc.

3. Proposal for Tectonic Evolution

From a regional stratigraphical review (HUTCHISON, 1979) and from the gravity survey of the Peninsula (RYALL, 1976), it can be deduced that Burma east of the Shan Scarp,

Southeast Asia tin granitoid belts.

Main Range: Kinta-Bangka	Eastern: Trengganu-Billiton
Large-microcline biotite granite, and adamellite. Minor pegmatite. Tourmaline-muscovite marginal phases	Granite, granodiorite, tonalite, and gabbro Muscovite only in marginal phases
No volcanic association known. Ignimbrite and microgranodiorite down faulted against the granite east of the Genting Highlands	Coeval Carbo-Permian-Triassic rhyolitic to andesitic lavas and pyroclastic rocks
Generally coarse with large microcline megacrysts. Finer grained modifications in margin zones	Equigranular to microporphyritic, medium to coarse
Pale grey	Pale grey or pink
Biotite, muscovite in greisen, ilmenite	Biotite, hornblende locally important, ilmenite
Always Maximum microcline, 2V 70° to 90°	Orthoclase to intermediate microcline, 2V 50° to 70°
Deep-seated batholiths in greenschist facies rocks. Slight increase in dynamothermal grade towards contact, but no cordierite and no andalusite	Volcanogenic high level plutons with well-developed thermal aureoles containing andalusite and cordierite
Maxima at 200, 230, 280	Maxima at 220, 250
Late Carboniferous to late Triassic	Permian to Triassic
80 to 200 Ma	220 to 250 Ma
Carboniferous 0.711 Triassic 0.710	Permian 0.710 Triassic 0.708
0 to 14	0 to 25 (excluding the gabbro)
5.0	4.1 (excluding the gabbro)
1.7	1.3 (excluding the gabbro)
10.0 increasing westwards	2.7 (excluding the gabbro)
Impounded ore bodies at granite margins	Vertically extensive hydrothermal vein deposits in overlying country rocks. Skarn and bedded lodes
Tin in greisen margins and in hydrothermal stockworks of limited extent	
Sn-Cu-Pb-Sb Sn-Ca	Sn-Fe Sn-Cu
Sn-W Sn-Nb Sn-As-Fe	
Basaltic dykes generally absent	Basaltic dykes are common
Abundant placer deposits	Placers rare, lode mining important
Hot springs are common	Hot springs absent

Peninsular and northwest Thailand as far east as Chiang Mai, and Peninsular Malaysia west of the Bentong-Raub Suture, are underlain by Precambrian continental crust. The central marginal basin occupies a positive gravity anomaly, and is therefore underlain by oceanic crust covered by a thin late Paleozoic to Mesozoic sedimentary blanket. The Eastern massif, like the Main Range, is underlain by continental crust but of lesser thickness, as shown by a slightly lesser negative gravity (RYALL, 1976). These constraints allow a reconstruction along the lines of HUTCHISON (1973a).

3.1 Carboniferous

The eastern massif is shown attached to its former craton and the central marginal basin is beginning by rifting behind the volcanic arc. This model allows for some of the Carboniferous granites of the Main Range in a back arc setting.

The craton is unknown, and has been speculated by STAUFFER (1973), after reviewing all other literature suggestions, to be North Africa. However, it now seems that the craton is to be found in Tibet, as suggested earlier by CRAWFORD (1973). The palaeomagnetic evidence is compelling, for the Malay Peninsula lay at 15° N during the late Palaeozoic (McELHINNY *et al.*, 1974) and between the Permo-Triassic and the Cretaceous, it rotated 70° clockwise, whilst maintaining much the same palaeolatitude. On the other

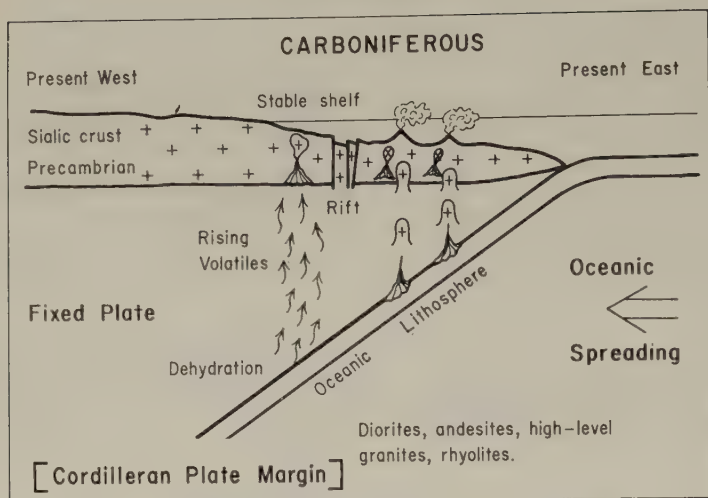


Fig. 2. Diagrammatic tectonic cross section to explain the volcano-plutonic eastern arc and the beginnings of the marginal basin. The pattern of sedimentation requires a western craton. Palaeomagnetic data indicate that the Peninsula did not maintain its present N-S orientation nor its present latitude throughout the Phanerozoic.

hand, recent palaeomagnetic data (MOLNAR and CHEN, 1978) indicate that southern Tibet had a palaeolatitude of 8° N in the late Cretaceous, and has been progressively displaced northwards to its present 30° N position as the Asian Continent was compressed by the Indian collision. The implication is that India began colliding with mainland Asia before 38 Ma ago. Whereas the part of Asia west of the Sagaing and Shan Scarp Fault has been displaced northwards at least 22° , the Malay Peninsula rebounded south-eastwards by about 12° ; a total displacement from its cratonic attachment of no less than 34° of latitude.

3.2 Permian

Throughout the Carboniferous and the Permian, the central marginal basin continued to develop as the Eastern Massif drifted away from its ancestral craton (Fig. 3). Marine sedimentation, intercalated with rhyolitic and andesitic volcanic and pyroclastic rocks, continued into the early mid Triassic (GOBBETT, 1973 a, b). A narrow marginal basin which is receiving active sedimentation as well as simultaneously spreading, must have a linear zone of high heat flow overlying the spreading axis. This zone can now be identified as a narrow belt of high grade metamorphic rocks extending from the Taku Schist in north Kelantan, southwards to Gunung Benom and Gunung Ledang (HUTCHISON, 1973 b, p. 255).

Sedimentation overlapped onto the Eastern Massif, which was largely inundated, but the sea shoaled towards the east (HUTCHISON, 1979).

Marginal seas appear to have a limited life, and the rifted continental margin cannot continue oceanwards indefinitely because the mantle convection cell beneath the marginal basin is of minor importance compared with that of the main ocean. This is well illustrated by the number of extinct marginal basins to be found in Southeast Asia at the present time.

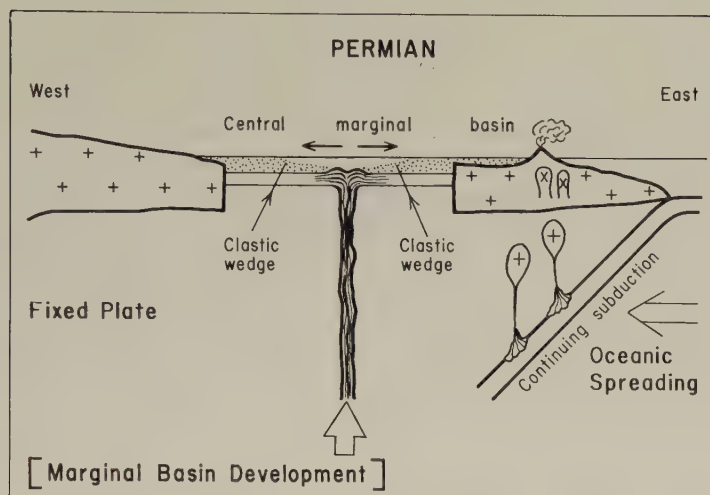


Fig. 3. The marginal basin reached its maximum development in the Permian. The Eastern Massif has a complete suite of plutonic rocks from gabbro to granite, and coeval volcanic rocks from andesite to rhyolite.

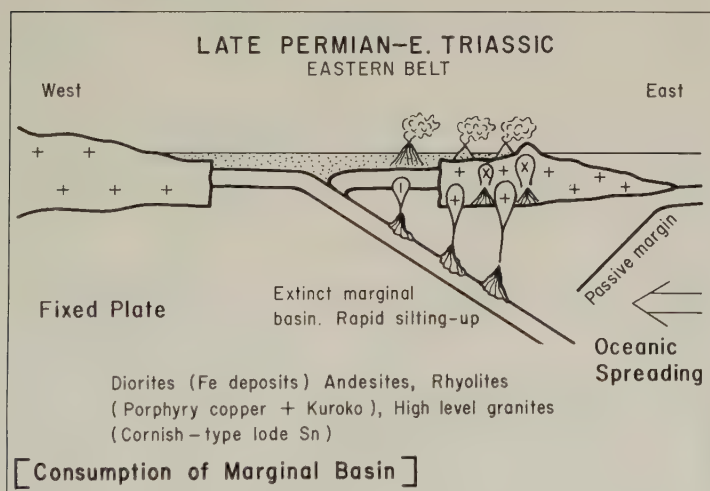


Fig. 4. Extinction of the marginal basin spreading axis, followed by flipping of the subduction polarity, leads to consumption of the marginal basin and rapid shoaling of its seas.

Subduction-related magmatism resulted in dioritic plutons within the Eastern Massif, closely associated with contact iron deposits (HUTCHISON and TAYLOR, 1978). Rising isotherms, because of the subduction-related activity, caused partial melting of the sialic basement of the Eastern Massif giving rise to granitoids. The tin and tungsten deposits associated with these granitoids is considered to have their source in the sialic basement, rifted from the main cratonic continental plate.

3.3 Late Permian-early Triassic

Upon extinction of spreading, it appears to be natural for the polarity of subduction

to flip, so that the old marginal basin lithosphere is consumed (Fig. 4). This proposed mechanism is based on the present activity in the Philippines, in which the old extinct South China Sea lithosphere is being consumed along the Manila Trench, with the result that the northern Philippine islands are now approaching the mainland. But in the southern Philippines, subduction of the Pacific Plate continues along the Philippine Trench (MURPHY, 1973). Thus the Philippine islands are being torn apart by a central transform fault. Such complex activity in marginal basins and island arcs can be considered to have taken place in the past. The Eastern Massif of the Malay Peninsula appears to be torn into two parts, the southern part extending farther westwards than the northern part (Fig. 1).

The model (Fig. 4) is supported by the change throughout the marginal basin from shallow marine to estuarine and continental by the late Triassic (BURTON, 1973). Although the Eastern Massif was almost entirely emergent, the estuarine Jurong Formation overlapped towards the east.

The change of subduction polarity ensured continuing volcanic and plutonic activity, but any regularity of zonation has been confused by the flipping.

3.4 Late Triassic

As the marginal basin lithosphere continues to be consumed, the overlying sediments are folded and uplifted and marine conditions are replaced entirely by estuarine and continental. A redded facies is now widely developed throughout the region (BURTON, 1973; HUTCHISON, 1979).

Eventually the Eastern Massif, with its buffer of folded marginal basin sediments, collided with and over-rode the eastern margin of the craton (Fig. 5). I take this collision to be the main mechanism for the major late Triassic Southeast Asian orogeny.

The crustal thickening over the region of the Main Range, coupled with under-

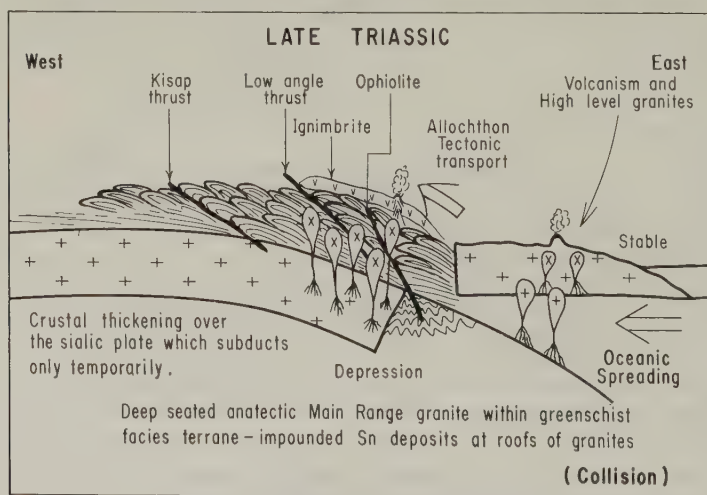


Fig. 5. Continuing contraction of the marginal basin results in collision of the Eastern island arc and its buffer of folded marginal basin sediments with the craton. Crustal thickening resulting from westwards allochthonous overthrusting of the marginal basin sediments and partial subduction of the western craton result in the anatectic deep-seated Main Range Granite.

thrusting of the western plate, resulted in an increase of the geotherms leading to the anatexis formation of the highly differentiated Main Range Granite. Its deep-seated nature resulted from the inability of the wet anatexis magma to rise high in the folded greenschist facies pile. The main cratonic Western Massif could not continue to subduct, so that the welding of the Eastern Massif resulted in cratonization of the whole region, and active subduction thereafter jumped farther oceanwards. The whole Southeast Asian region became the large continental mass of Sundaland, characterised by extensive continental Jurassic redbeds.

The tin deposits were impounded within the roof zone of the Main Range granite because the hydrothermal tin-bearing solutions were unable to escape upwards through the unfractured greenschist facies overburden. The tin had its source in the sialic basement which was once continuous with that of the Eastern Belt. The dramatically different styles of mineralization between the two belts therefore reflects the radically different tectonic histories which caused remobilization of the tin.

3.5 Late Mesozoic-Cenozoic

A complete history cannot yet be written for this complex region. The only approach is to work back from the present.

The present configuration of the Andaman Sea (Fig. 6) includes E-N-E trending spreading axes connected by N-S transform faults. The analysed seismicity indicates N-S directed extension (EGUCHI *et al.*, 1978).



Fig. 6. The present and pre-Miocene Andaman Sea configuration. Before the marginal sea opened by N-S extension, the Burmese and Sumatran volcanic arcs must have been continuous and adjacent to the Cretaceous Phuket-Tenasserim granitic arc.

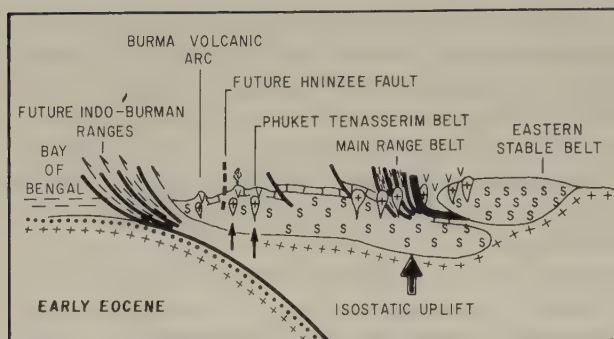


Fig. 7. Diagrammatic tectonic cross-section across Fig. 6 before the opening of the Andaman Sea (after MITCHELL, 1977).

If the Andaman Sea is closed back (Fig. 6), then the Burmese and Sumatran volcanic arcs are continuous and parallel to the Cretaceous plutonic arc of Phuket-Tenasserim. The Andaman Sea has been estimated to begin its opening 10 to 20 Ma ago (EGUCHI *et al.*, 1978). This reconstruction allows the Burmese-Sumatran volcanic arc and the back-arc Cretaceous plutonic belt to be related to Indian Ocean subduction from the present west, as shown diagrammatically on Fig. 7 (after MITCHELL, 1977). Attractive though this reconstruction is, the perfect separation of the andesitic volcanic arc from the granitic plutonic arc is enigmatic and implies that a definite answer has not yet been obtained.

To probe back beyond this is fraught with difficulty. The cratonic hinterland of the Malay Peninsula is considered to have rifted away by the Miocene, and indeed to have been away by the Cretaceous, if the granites of Phuket-Tenasserim, with ages of 115 Ma (Table 1), are to be accepted. Then, what caused the separation of the Peninsula from its craton? If we seek the answer in the collision of India with Eurasia, the timing is unsuitable. The palaeomagnetic data discussed in MOLNAR and CHEN (1978) suggest a collision of India with Tibet at about 8° N at least before 38 Ma. But this collision age cannot be extended back to much more than about 60 Ma, when the northern part of Greater India had just reached the equator (MOLNAR and TAPPONIER, 1975).

The search for the sequence of events is frustrated by such complexities as:

- 1) Collision of the Indian Ocean mid-oceanic ridge with the Sumatran Trench in the mid to late Miocene (EGUCHI *et al.*, 1978).
- 2) The possible late Cenozoic clockwise rotation of Sumatra (NINKOVICH, 1976).
- 3) The 50° anticlockwise rotation and 15° of latitude southwards drift of the Malay Peninsula since the mid Cretaceous (HAILE *et al.*, 1977).

4. Epilogue

Tin mineralization is closely associated with K_2O - and SiO_2 -rich granites in three distinct belts. The epizonal granitoid belts are of Permian to Triassic age in the Eastern Massif and of Cretaceous age in the Western. Only the Eastern Massif has the complete characteristics of a volcano-plutonic arc of Circum-Pacific type. The Main Range Belt of highly differentiated maximum microcline granite, of predominantly late Triassic age, also includes some late Carboniferous granite. It has none of the characters of a volcano-

plutonic arc and is considered to have resulted from collision of the Eastern Massif island arc with its ancestral craton as the separating marginal basin was consumed by subduction. The deep-seated anatectic granites are characterized by hydrothermal tin deposits impounded close to the granite-greenschist contact. The western Belt granites are related in some way to Indian Ocean margin tectonics, but the evolution of this region is extremely complex.

Thus, in the region of Southeast Asia, tin is genetically associated with granites of dramatically different age and tectonic setting. As argued by HUTCHISON and CHAKRABORTY (1978), tin deposits result from polycyclic events in the older continental crust. The three tin belts may be unified only in one respect, that they are derived from a continental basement which already contained unevenly distributed tin concentrations. Tin-bearing granite magma was remobilized from these sources at various times and by dramatically different tectonic processes which caused partial melting of the older basement.

I am grateful to the University of Malaya and the Inter-Union Commission on Geodynamics for financial support to attend the conference. Ms. Zaimah binti Ahamad Saleh typed the manuscript. Mr. Roslin bin Ismail and Mr. Ching Yu Hay drew the figures from my sketches.

REFERENCES

- BIGNELL, J.D., The geochronology of the Malayan granites, Dr. Phil. Thesis, University of Oxford, 1972.
- BIGNELL, J.D. and N.J. SNELLING, Geochronology of Malayan granites. *Overseas Geol. Min. Resour.*, **47**, 1–72, 1977.
- BURTON, C.K., Mesozoic, in *Geology of the Malay Peninsula*, edited by D.J. Gobbett and C.S. Hutchison, pp. 97–141, John Wiley-Interscience, New York, 1973.
- CRAWFORD, A.R., A displaced Tibetan Massif as a possible source of some Malay Rocks, *Geol. Mag.*, **109**, 483–489, 1973.
- EGUCHI, T., S. UYEDA, and T. MAKI, Seismotectonics and tectonic history of the Andaman Sea, *Tectonophysics*, 1978 (in press).
- GARSON, M.S., B. YOUNG, A.H.G. MITCHELL, and B.A.R. TAIT, 1975. The Geology of the tin belt in Peninsular Thailand around Phuket, Phangnga and Takuapa, Inst. Geol. Sci. Lond. Overseas Mem., **1**, 112 pp. + map.
- GOBBETT, D.J., Carboniferous and Permian correlations in Southeast Asia, *Geol. Soc. Malaysia Bull.*, **6**, 131–142, 1973a.
- GOBBETT, D.J., Upper Palaeozoic, in *Geology of the Malay Peninsula*, edited by D.J. Gobbett and C.S. Hutchison, pp. 61–95, John Wiley-Interscience, New York, 1973b.
- HAILE, N.S., M.W. McELHINNY, and I. McDUGALL, Palaeomagnetic data and radiometric ages from the Cretaceous of West Kalimantan (Borneo), and their significance in interpreting regional structure, *J. Geol. Soc. Lond.*, **133**, 133–144, 1977.
- HUTCHISON, C.S., Tectonic evolution of Sundaland: A Phanerozoic Synthesis, *Geol. Soc. Malaysia Bull.*, **6**, 61–86, 1973a.
- HUTCHISON, C.S., Metamorphism, in *Geology of the Malay Peninsula*, edited by D.J. Gobbett and C.S. Hutchison, pp. 253–303, John Wiley-Interscience, New York, 1973b.
- HUTCHISON, C.S., Ophiolite in Southeast Asia, *Geol. Soc. Am. Bull.*, **86**, 797–806, 1975.
- HUTCHISON, C.S., Granite emplacement and tectonic subdivision of Peninsular Malaysia, *Geol. Soc. Malaysia Bull.*, **9**, 187–207, 1977.
- HUTCHISON, C.S., Southeast Asia, in *The Indian Ocean Basin and Margins*, edited by A.E.M. Nairn, F.G. Stehli, and M. Churkin, Plenum Press, New York, 1979 (in press).
- HUTCHISON, C.S. and K.R. CHAKRABORTY, Tin: A mantle or crustal source? (extended abstract in *Commonwealth Geological Liason Office Newsletter*, July 1978, 8–10), *Geol. Soc. Malaysia Bull.*, **11**, 1978 (in press).
- HUTCHISON, C.S. and D. TAYLOR, Metallogensis in SE Asia, *J. Geol. Soc. Lond.*, **135**, 407–428, 1978.
- KHOO, K.K., Serpentinite occurrence at Telok Mas, Malacca, *Geol. Soc. Malaysia Newslett.*, **4**, 1–5, 1978.
- McELHINNY, M.W., N.S. HAILE, and A.R. CRAWFORD, Palaeomagnetic evidence shows Malay Peninsula was not a part of Gondwanaland, *Nature*, **252**, 641–645, 1974.

- MITCHELL, A.H.G., Tectonic settings for emplacement of Southeast Asian tin granites, *Geol. Soc. Malaysia Bull.*, **9**, 123–140, 1977.
- MOLNAR, P. and CHEN Wang-Ping, Evidence of large Cainozoic crustal shortening of Asia, *Nature*, **273**, 218–220, 1978.
- MOLNAR, P. and P. TAPPONIER, Cenozoic tectonics of Asia: Effects of a continental collision, *Science*, **189**, 419–426, 1975.
- MURPHY, R.W., Diversity of Island Arcs: Japan, Philippines, Northern Moluccas, *Aust. Petrol. Exp. Assoc. J.*, **13**, 19–25, 1973.
- NINKOVICH, D., Late Cenozoic clockwise rotation of Sumatra, *Earth Planet. Sci. Lett.*, **29**, 269–275, 1976.
- PITCHER, W.S., The anatomy of a batholith, *J. Geol. Soc. Lond.*, **135**, 157–182, 1978.
- RAJAH, S.S., F. CHAND, and D.S. SINGH, The granitoids and mineralization of the Eastern Belt of Peninsular Malaysia, *Geol. Soc. Malaysia Bull.*, **9**, 209–232, 1977.
- RYALL, P.J., Gravity traverse of Peninsular Malaysia—Preliminary results, *Geol. Soc. Malaysia, Ipoh Meet. Abstr.*, Dec. 1976, 1976.
- STAUFFER, P.H., Malaya and Southeast Asia in the pattern of continental drift, *Geol. Soc. Malaysia Bull.*, **7**, 89–138, 1973.
- TAYLOR, D. and C.S. HUTCHISON, Patterns of Mineralization in Southeast Asia, their relationship to broad-scale geological features and the relevance of plate-tectonic concepts to their understanding, *Proc. XI Comm. Min. and Metall. Congr. Hong Kong, Inst. Min. and Metall. Lond.*, Paper 68, 15 pp. 1978.
- WOOLLANDS, M.A. and D. HAW, Tertiary stratigraphy and sedimentation in the Gulf of Thailand, Southeast Asia Petrol. Exp. Soc. Offshore S. E. Asia Conf., Feb. 1976, Paper 7, 1976.

SEISMICITY, GRAVITY AND TECTONICS IN THE ANDAMAN SEA

R.K. VERMA, Manoj MUKHOPADHYAY, and N.C. BHUIN

*Department of Applied Geophysics, Indian School
of Mines, Dhanbad, India*

(Received June 19, 1978; Revised October 15, 1978)

An analysis of the available bathymetric, gravity and seismicity data of the Andaman Sea that lies between the latitudes 4° to 16°N and longitudes 91° to 97°E has been carried out. A seismicity map of the Andaman Sea has been prepared using all available data for the period 1916–1975. The epicentral distribution parallels the structural lineation of the Andaman Arc showing larger activity under the Andaman Basin. An inclined seismic zone extending at least up to a depth of 150 km is found to be present underneath the Andaman Basin. The seismic zone dips towards the continental side, attaining its deepest part not right below the axis of the negative gravity anomalies, but is rather deflected further east towards the volcanic islands. For a more complete understanding of plate motions in Andaman Sea area, all available focal mechanism solutions incorporating 12 new ones have been analysed. It is observed that normal, thrust as well as strike-slip faulting take place in the area. The direction of seismic slip vectors for thrust-type solutions is generally eastward over the areas of outer sedimentary arc. In the southern part of the Andaman Sea, the direction of seismic slip vectors is towards south. Over the southeastern part of the Andaman Sea, in continuation of the Semangko Fault (rift) of Sumatra, strike-slip mechanism predominates. This gives a clear evidence of the continuation of the Semangko Fault beyond Sumatra underneath the Andaman Sea up to 9°N . The results obtained through the focal mechanism studies further suggest that thrust faulting is prevalent between 30 to 90 km depth under the Andaman Sea. Normal faulting prevails at shallow as well as at greater depths (more than 90 km). The transcurrent type of movement appears to affect a considerable thickness of the lithosphere in the area, at least up to a depth of 150 km. On the basis of these results it is suggested that an active subduction zone is present underneath the Andaman Basin. The present structural form as well as seismicity of the Andaman and the west-Indonesian Arc seems to have resulted as a result of subduction of the Indian Plate at the continental margin of the SE-Asian Plate.

1. Introduction

The Andaman-Nicobar Group of islands and the associated Andaman Sea form a part of the north-south trending Tertiary Folded Belt, in continuation of the Arakan Folded Belt of Burma towards the north and islands approximately between 4° to 16°N and 91° to 97°E . Geology and bathymetry of the area has been studied by RODOLFO (1966, 1969), who has made an attempt to reconstruct the geologic history of the area, and WEEKS *et al.* (1967), who have delineated major segments of the island arc system including fore deep, outer sedimentary arc, inner volcanic arc and back deep through a distance of about 1,100 km. Gravity and magnetic fields and their relationship to surface features has been studied by PETER *et al.* (1966). They have suggested the continuation of the structural trend of the Barisan Ranges of Sumatra into the Andaman Sea up to 10°N .

Detailed seismicity of the area has not so far been studied. SANTO (1969) briefly discussed the seismicity of the area and presented a seismic section across the structural trend of the area. Focal mechanism solutions for few earthquakes have been given by RITSEMA and VELDKAMP (1960) as well as by FITCH (1970, 1972).

In this paper an analysis of the results of the gravity field, seismicity and 32 focal mechanism solutions (12 solutions added from the present studies) from the area mentioned above is presented in terms of plate tectonics model taking into account the geological and tectonic history of evolution of the area.

2. *Geological and Tectonic History of the Area*

According to RODOLFO (1969), the sedimentation in the Andaman Sea started sometime during the Late Cretaceous. The oldest rocks in the Andaman Sea are of this age. Following a period of sedimentation in troughs and basins, an episode of orogeny commenced in the Oligocene and resulted in the formation of the Arakan-Yoma Mountains and the Andaman-Nicobar Ridge. Late Miocene dilational movements formed the Andaman Basin.

The orogenic forces which started during the Late Pliocene times have continued till Recent. In Burma, the orogeny has been marked by volcanism in Mt. Popa-Pegu Yoma trend as well as the Shan Scarp. Similar orogenic forces working in the Andaman Basin have resulted in the formation of Narcondam and Barren Group of volcanoes.

The dominant structural features in the area are related to the Indonesian Arc. This arc consists primarily of a double arc with a recognised inner arc characterised by volcanic activity and a younger outer sedimentary arc. The volcanic trend is well defined in central Burma and can be traced across the Irrawaddy Delta through Narcondam and Barren Islands, the Invisible Banks and then into Sumatra where it manifests itself in the form of Barisan Ranges. These ranges have been elevated during Plio-Pleistocene times (VAN BEMMELEN, 1949). The mountains are split up longitudinally by a well-known fault known as the Semangko Fault, a graben or a rift valley extending along the full length of Sumatra. This rift valley probably developed as a post-elevation collapse feature (WEEKS *et al.*, 1967). In northern Sumatra the trend of the fault zone is identified by Atjeh graben which extends offshore into the Andaman Sea (PETER *et al.*, 1966). Prominent features of the arc are shown in Fig. 1.

The sedimentary oil producing basins of Sumatra and Burma are interconnected through the Andaman Sea which forms a trough like structure. According to KRISHNAN (1960), the Andaman Sea probably acquired its present status during Cretaceous times. West of the sedimentary trough lies the Tertiary Folded Belt or outer Island Arc which can be traced from the Arakan Yoma in the north through Andaman, Nicobar Islands, Simeulue Islands, and Mentawai Islands west of Sumatra.

West of the outer Island Arc (Indonesian Islands) is the fore deep or the trench which on the south is called the "Java Trench." This trench does not seem to extend north of 3° N and is not present west of Andaman and Nicobar Islands.

Major topographic features of the area are shown in Fig. 2, after RODOLFO (1966). The Tertiary Folded Belt comprising the Andaman, Nicobar and other islands clearly shows up as a topographic high. The Andaman Basin reaches an average depth of about 3,000 m below sea level. The Invisible Banks, Barren and Narcondam Islands, also show up as topographic highs.

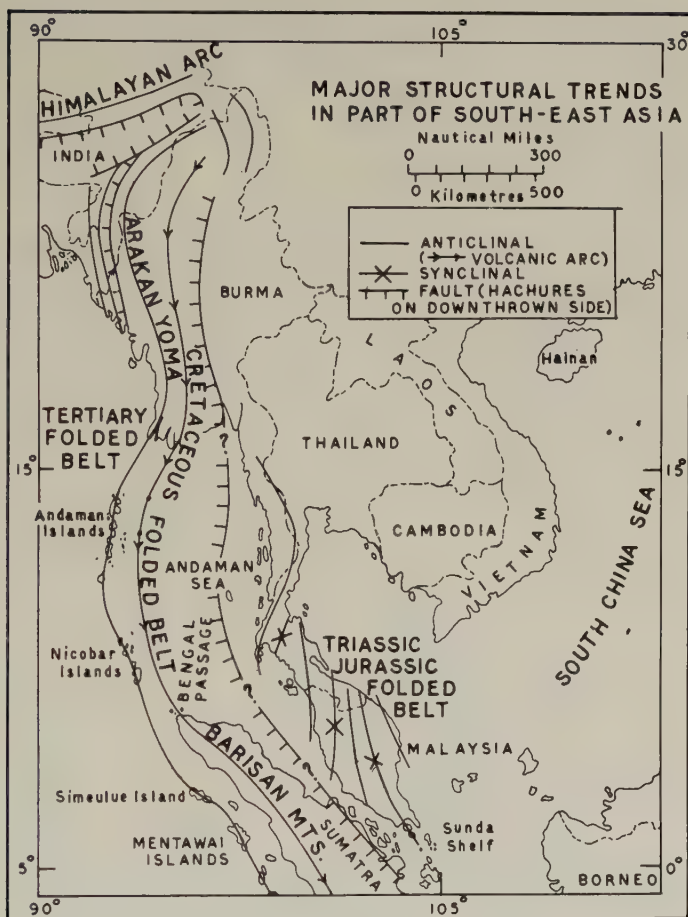


Fig. 1. Prominent structural features of the Andaman Arc depicting the sites for various orogenic belts traced from Burma on the north to Sumatra on the south through the Andaman Sea (after WEEKS *et al.*, 1967).

Volcanic activity in the inner arc during the period Tertiary to historic times is shown in Fig. 3.

3. Free-Air Anomaly Map

The distribution of free-air anomalies in the area (after PETER *et al.*, 1966) is shown in Fig. 4. The free-air anomalies are seen to be strongly positive along the volcanic arc extending from Barisan Ranges of Sumatra through Invisible Banks, Narcondam and Barren Islands. These are also positive over Mergui Archipelago and to the west of Andaman-Nicobar Island Arc. The largest positive anomalies (of the order of +50 to +100 mgals) are found over the Invisible Banks, Narcondam and Barren Islands. In between these volcanic islands and the sedimentary arc (Andaman and Nicobar Islands) the anomalies are seen to be strongly negative being of the order of -100 to -150 mgals, con-

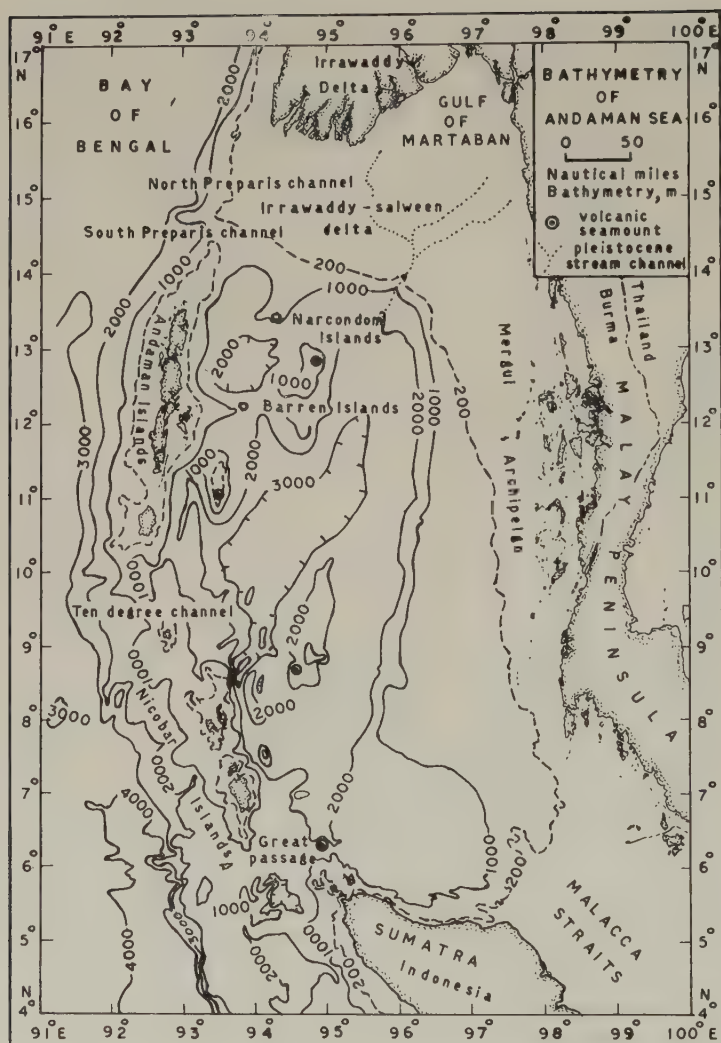


Fig. 2. Prominent topographic features in the Andaman Sea showing the Andaman Group of islands as a major bathymetric rise extended in north-south direction forming the Andaman sedimentary arc. Note that the major part of the Andaman Basin has depths of the order of 3 km (after RODOLFO, 1966).

finned within a relatively narrow zone which extends in N-S direction for about 1,000 km, following the arcuate pattern of the Andaman Arc. The distribution of these anomalies suggests large abnormalities so far as mass distribution with depth is concerned. The outer sedimentary arc also has negative anomalies as compared to the inner volcanic arc.

4. Seismicity Map of the Area

Seismicity map of the area lying between 4° to 16° N and 91° to 97° E for the period 1916–1975 is shown in Fig. 5. The source of data has been the reports of I.S.S., Bull.

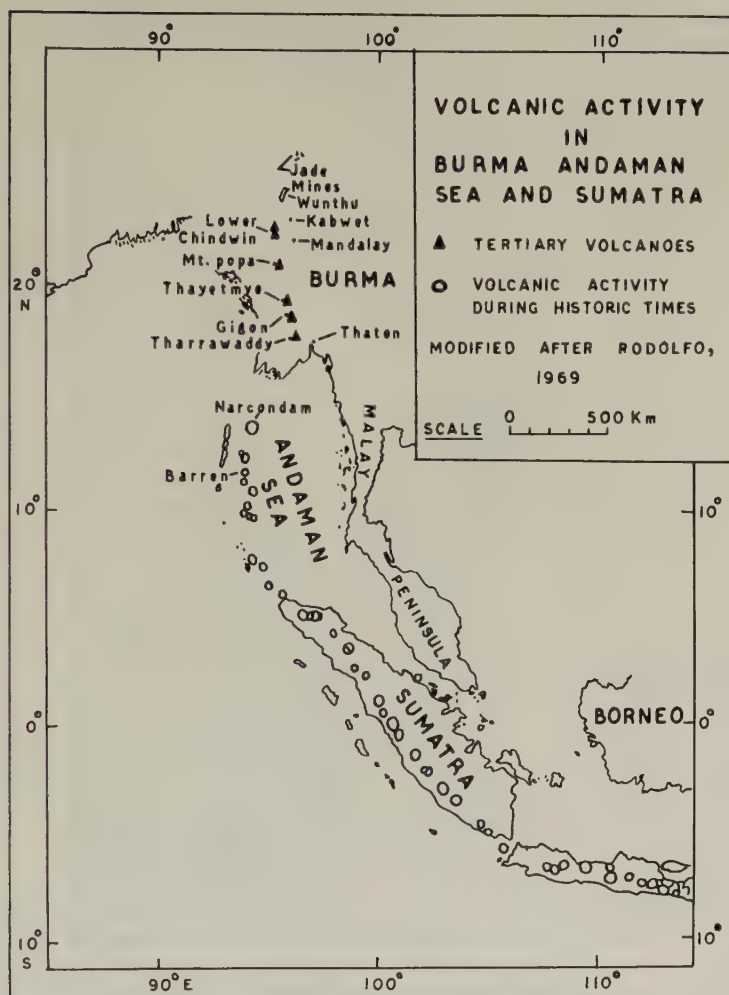


Fig. 3. Volcanicity in the Andaman Sea. Sites for volcanism arc traced from Burma on the north to Sumatra on the south (after RODOLFO, 1969). Refer to discussion in text for association of strong positive free-air anomalies with the chain of volcanic islands.

I.S.C., and reports from India Meteorological Department, as well as P.D.E. Bulletins issued by NOAA. The seismicity shows a well-defined pattern almost parallel to the structural trend of the area. Most of the earthquakes in the area originate from shallow depths. However, the epicenters become deeper (exceeding 100 km) towards the eastern side, close to the above-mentioned volcanic arc. It is evident that the whole of Andaman Basin is seismically very active, the seismic zone dipping towards the continental side to the east. The seismicity, however, is confined within a zone of about 4° , longitudinally.

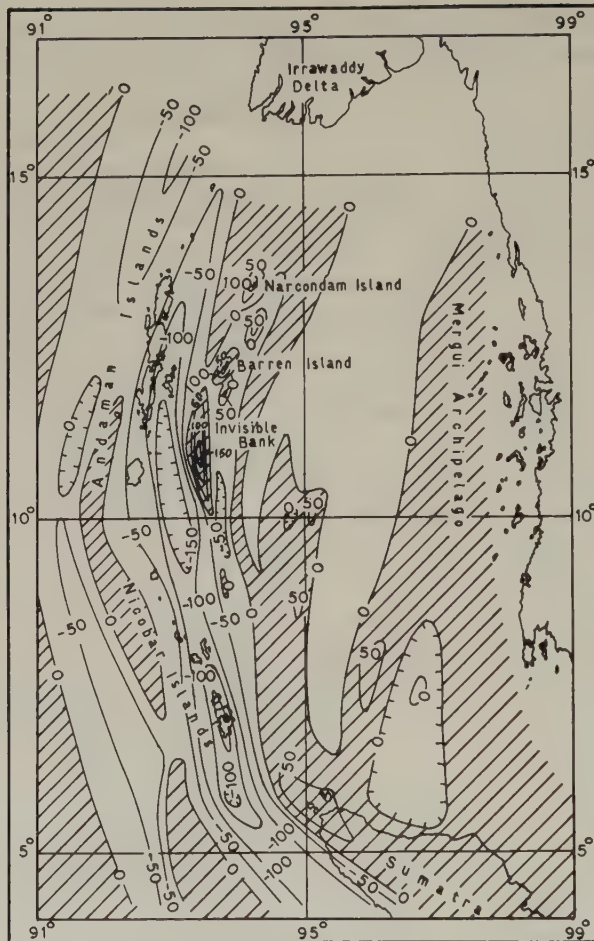


Fig. 4. Principal zones of free-air anomalies in the Andaman Sea (contour interval 50 mgal), after PETER *et al.* (1966). Note the pronounced zone of narrow-cum-elongated negative free-air anomalies immediately to the east of Andaman islands extending over the full length of the Andaman Sea in north-south direction. The anomalies have little correspondence with bathymetry.

5. Focal Mechanism Solutions

The mechanism of release of seismic energy by the earthquakes throws a considerable light on the nature of tectonic forces active in the area. Focal mechanism solutions for few earthquakes have been studied earlier by RITSEMA and VELDKAMP (1960) and FITCH (1970, 1972). Twelve new focal mechanism solutions were determined for earthquakes which occurred during the period 1961–1972. The solutions were determined using P-wave first motion directions reported in the I.S.S. and the I.S.C. Bulletins. First motion

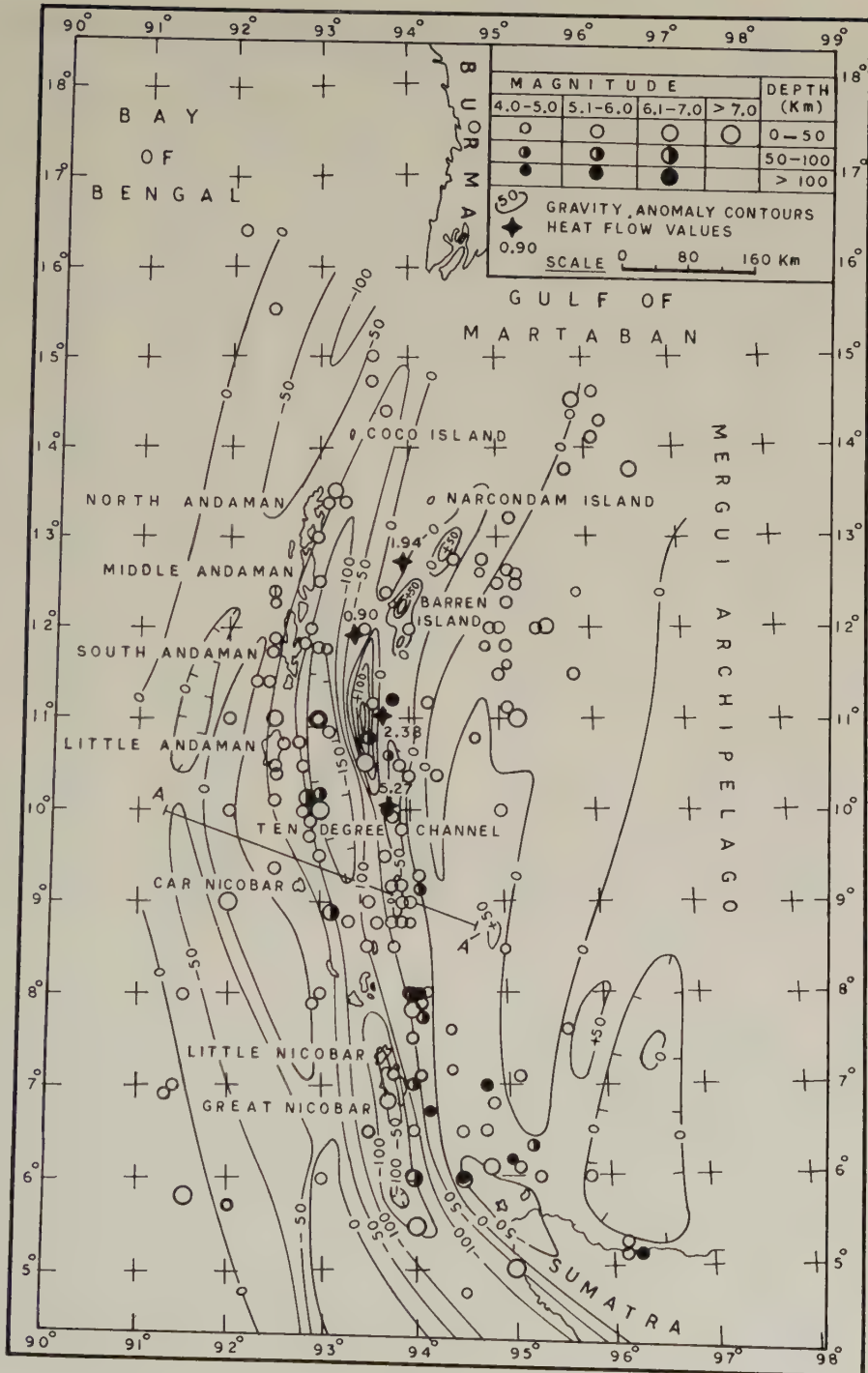


Fig. 5. The seismic activity in the Andaman Sea for the period 1916-1975. The free-air anomalies are also shown in the figure. A larger concentration of seismic activity under the Andaman Basin can be clearly seen. Also note the deepening of earthquake foci eastward towards the continental side.

Table 1. Parameters of earthquake mechanism solutions

Event No.	Date	Origin time (G.M.T.)	Epicenter		Depth (km) and magnitude	1st pole	
			Lat. (°N)	Long. (°E)		Az.	Pl.
1	Jul. 28, 1964	21 : 38 : 42.4	14.3	96.2	22, 5.9	141	50
2	Sep. 15, 1964	15 : 29 : 38.8	8.9	93.1	89, 6.3	51	20
3	Sep. 6, 1967	07 : 30 : 11.0	14.8	93.6	36, 5.5	286	14
4	Apr. 2, 1964	01 : 11 : 48.6	5.8	95.5	65, 5.6	240	4
5	Apr. 3, 1964	04 : 12 : 39.7	4.0	96.6	51, 5.8	234	24
6	Nov. 30, 1964	12 : 27 : 37.9	6.8	94.8	24, 5.7	236	0
7	Apr. 12, 1967	04 : 51 : 41.8	5.3	96.5	63, 6.1	8	62
8	Jun. 15, 1964	00 : 05 : 36.1	5.3	96.8	71, 5.3	350	50
9	Aug. 21, 1967	07 : 33 : 1.6	3.6	95.8	40, 6.1	23	12
10	Jul. 2, 1967	07 : 03 : 54.0	8.7	93.8	44, 5.7	351	0
11	Jul. 11, 1961	09 : 31 : 45.0	7.88	93.07	51, —	234	21
12	May 26, 1962	19 : 44 : 23.0	6.58	94.53	94, —	195	40
13	Nov. 16, 1962	21 : 10 : 0.0	13.58	92.93	33, 6.25	140	71
14	Dec. 12, 1962	22 : 56 : 44.0	4.01	94.56	149, —	205	26
15	Sep. 16, 1964	01 : 26 : 26.6	10.71	92.81	40, 5.7	174	64
16	Feb. 14, 1967	01 : 36 : 04.0	13.75	96.47	13, 5.6	350	21
17	Oct. 6, 1968	07 : 42 : 26.5	9.9	93.6	124, 5.0	244	30
18	May 6, 1970	15 : 21 : 55.0	9.81	92.91	32, 5.3	280	60
19	Jun. 5, 1971	01 : 38 : 01.0	9.4	92.5	25, 5.3	90	82
20	Nov. 5, 1971	22 : 11 : 15.0	10.1	92.9	53, 5.9	147	67
21	Feb. 4, 1972	15 : 20 : 07.0	7.95	94.03	89, 5.2	327	65
22	Nov. 25, 1935	10 : 03 : 02.0	5.5	94.0	S, 6.5	264	54
23	Aug. 23, 1936	21 : 12 : 13.0	6.0	95.0	40, 7.3	26	25
24	Aug. 4, 1937	23 : 35 : 22.0	6.0	94.5	120, 6.0	68	7
25	Jun. 26, 1941	11 : 52 : 00	12.5	92.5	65, 8.1	146	5
26	May 9, 1949	13 : 36 : 18.0	5.0	95.0	S, 6.7	125	57
27	May 17, 1955	14 : 49 : 49.0	6.5	94.0	S, 7.25	116	14
28	Aug. 12, 1971	04 : 17 : 03.0	12.50	95.08	19.7, 5.3	78	2
29	Nov. 13, 1972	23 : 34 : 11.80	12.44	95.23	24.1, 5.0	74	4
30	Mar. 28, 1971	08 : 23 : 21.50	12.12	95.22	22.2, 5.2	0	3
31	Mar. 29, 1971	17 : 55 : 43.0	11.16	95.11	16.5, 5.1	98	9
32	Jul. 9, 1973	16 : 19 : 46.70	10.66	92.59	43.8, 5.6	45	4

S indicates shallow focal depth of the event.

directions were plotted on an equal area projection of the lower hemisphere using the (i , d) tables of NUTTLI (1969). A double couple source mechanism was assumed. EGUCHI *et al.* (1978) have reported the results of 5 new mechanism solutions. The results of all the solution parameters (in all 32 solutions) are listed in Table 1, and are schematically illustrated in Fig. 6. The main points brought out by these results are discussed below. It may be seen from Table 1 and Fig. 6 that normal, thrust as well as strike-slip faulting take place in the area. Over the western sedimentary arc, characterized by relatively shallow seismicity, mostly thrust as well as normal faulting prevails. The transcurrent faulting prevails over the eastern and southeastern parts of the Andaman Sea.

Thrust mechanisms. Out of a total 32 mechanisms, 10 relatively shallow-focus mechanisms (up to a depth of about 90 km) discussed in this paper indicate thrust faulting (mechanisms 2, 7, 8, 9, 13, 15, 18, 21, 25 and 26). Mechanisms 2, 9, 13, 15, 18, 25 and 26 are for the earthquake events located over the western sedimentary arc, and mechanism 7, 8 and 21 are for earthquake events located to the east of the axis of the

of Andaman region (azimuth and plunge in degrees).

2nd pole		<i>P</i> axes		<i>T</i> axes		Type of faulting	References
Az.	Pl.	Az.	Pl.	Az.	Pl.		
352	34	45	71	160	7	Normal	FITCH (1970)
168	52	204	17	88	52	Thrust	FITCH (1970)
106	75	286	59	106	31	Normal	FITCH (1970)
331	0	196	3	285	3	Strike slip	FITCH (1972)
88	62	208	65	66	19	Normal	Present study
326	0	191	0	281	0	Strike slip	FITCH (1972)
188	28	8	17	188	73	Thrust	FITCH (1972)
214	30	16	11	264	65	Thrust	FITCH (1972)
203	78	203	33	23	57	Thrust	FITCH (1972)
261	15	215	10	307	10	Strike slip	FITCH (1972)
110	55	197	56	75	19	Strike slip	Present study
339	43	260	71	357	3	Normal	Present study
298	17	123	26	288	63	Thrust	Present study
25	64	205	71	25	19	Normal	Present study
354	26	174	19	354	71	Thrust	Present study
147	69	5	66	164	24	Normal	Present study
106	54	200	64	82	14	Normal	Present study
100	30	280	15	100	75	Thrust	Present study
270	8	90	37	270	53	Normal	Present study
277	16	111	28	251	58	Normal	Present study
147	25	327	20	147	70	Thrust	Present study
135	25	174	62	295	15	Normal	RITSEMA and VELDKAMP (1960)
133	31	170	5	78	42	Transcurrent	RITSEMA and VELDKAMP (1960)
161	20	113	19	205	9	Transcurrent	RITSEMA and VELDKAMP (1960)
326	85	326	40	146	50	Thrust	RITSEMA and VELDKAMP (1960)
21	9	176	29	51	44	Thrust	RITSEMA and VELDKAMP (1960)
207	2	71	8	162	12	Transcurrent	RITSEMA and VELDKAMP (1960)
347	17	34	13	300	12	Strike slip	EGUCHI <i>et al.</i> (1978)
297	4	30	12	297	4	Strike slip	EGUCHI <i>et al.</i> (1978)
90	0	45	2	315	2	Strike slip	EGUCHI <i>et al.</i> (1978)
190	11	236	1	144	15	Strike slip	EGUCHI <i>et al.</i> (1978)
137	25	182	12	86	22	Strike slip	EGUCHI <i>et al.</i> (1978)

central negative gravity anomaly zone discussed earlier. One of the nodal planes suggestive of the fault plane is generally oriented in north-south direction in the central part of the outer sedimentary arc but this orientation changes to northeast and northwest in the northern and southern extremities conforming with the arcuate trend of the arc. This change in orientation of the nodal plane from north to south can be clearly seen in Fig. 6. In solution 13 located immediately to the north of the North Andaman Island, both the nodal planes are in northeastern direction. In solution 18 near the Ten Degree Channel, both the nodal planes are in north-south direction. With gradual passage of latitudinal distance towards south, this orientation of nodal planes changes to northwest or WNW near Sumatra on the far south (see solutions 2, 26, 7, 8, 9 etc. in Fig. 6). The near parallelism of the nodal plane with the arcuate trend of the sedimentary arc over the full length of the Andaman Sea over a distance of 1,000 km suggests it to be the fault plane. The only exception being the solution 15 for an earthquake event located near Little Andaman Island, in which both the nodal planes are in east-west direction, which is orthogonal to

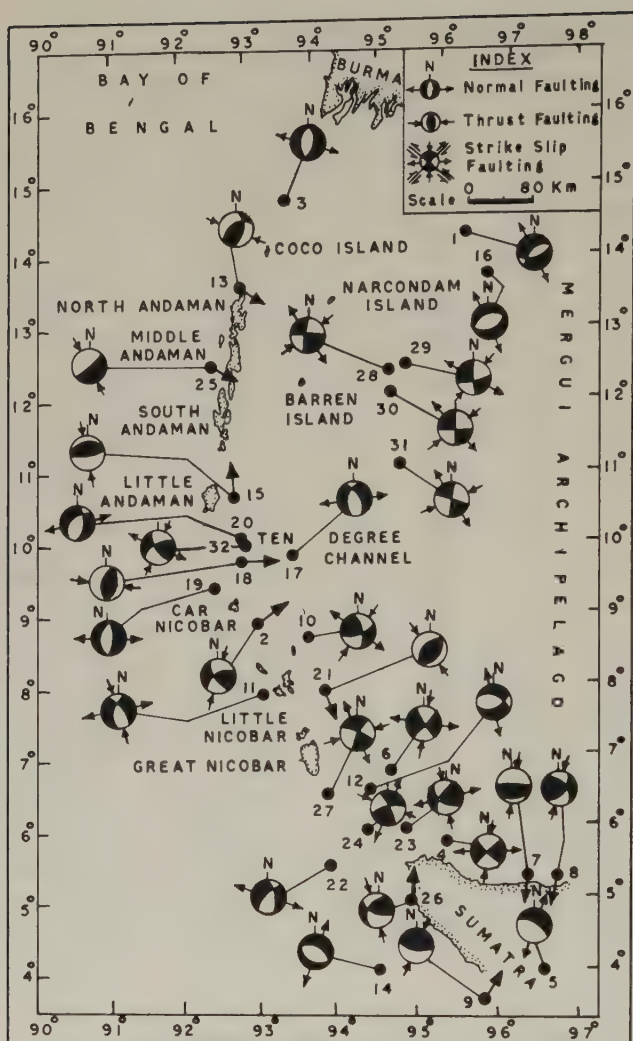


Fig. 6. Schematic orientation of the nodal planes for the 32 focal mechanism solutions considered in the present work. The numbers refer to the earthquake events for which solution parameters are listed in Table 1. Direction of seismic slip vector for thrust type mechanism solutions is marked by thick arrows.

the general structural trend of the outer arc. Obviously, few more solutions would be necessary to establish that faults orthogonal to the outer arc are also existing in the area, if at all.

Normal mechanisms. The mechanism solutions 1, 3, 5, 12, 14, 16, 17, 19, 20 and 22 indicate normal faulting in the area. Normal mechanisms are found for shallow as well as sub-crustal (as deep as 149 km) shocks. In general, one nodal plane in the solutions suggestive of normal mechanisms nearly parallels the local trend of the outer arc. So-

solutions 3, 5, 14 and 19 for earthquake events located under the outer arc suggest pure normal mechanisms, whereas other solutions have got some amount of strike-slip components. The near parallelism of the nodal planes of these solutions with the outer arc suggests them to be fault planes in their respective areas.

The normal mechanism solutions (Nos. 1 and 16) are observed at the northeastern corner of the Andaman Sea. These two solutions are for earthquake events located at the continental slope (about 1,000 m), near Malayan Peninsula. Another mechanism solution suggestive of normal faulting (solution 17) is located near the Ten Degree Channel. The orientation of extensional stress axis in southern 17 is analogous to that found from the solutions belonging to the outer Island Arc which is in east-west direction. However, near the locations of solutions 1 and 16, the extensional stress axis is found to be in NW-SE direction (near 14° N, 96° E). It may be observed from Fig. 5 that there is a curious gap in seismic activity between this place to the Coco Island further west. Another interesting feature being the near orthogonality of the T axis found from these two solutions (1 and 16) to that of the strike direction of the volcanic islands (e.g., Barren and Narcondam Islands etc.) and their associated gravity anomaly pattern. It is felt that these normal mechanism solutions and derived direction of extensional stress is a normal consequence of plate consumption on the inner side of the Island Arc.

Transcurrent mechanisms. Over the southeastern part of the Andaman Sea, in continuation of the Semangko Fault of Sumatra, strike-slip mechanism predominates (solutions 4, 6, 10, 11, 23, 24 and 27). This is a clear evidence of the continuation of the Semangko Fault beyond Sumatra underneath the Andaman Sea up to 9° N. It also suggests that the tectonic forces which were responsible for the creation of Semangko Fault during Tertiary times are still very active.

EGUCHI *et al.* (1978) have determined five focal mechanism solutions for earthquake events located near the Ten Degree Channel and in the north eastern part of the Andaman Sea. All the five solutions (Nos. 28, 29, 30, 31 and 32), whose solution parameters are listed in Table 1, suggest pure strike-slip mechanisms. Event 32 is located near the Ten Degree Channel. This solution in conjunction with other strike-slip mechanism solutions belonging to the southeastern Andaman Sea offers a few interesting inferences to be drawn. These being: (a) the Semangko Fault possibly extends northward beyond Sumatra up to as far as Ten Degree Channel continuing underneath the Andaman Sea, (b) the fault zone almost parallels the outer sedimentary arc formed by the Andaman Group of islands up to this distance. This calls for a close interrelationship between the formation of the sedimentary arc and the active fault zone, (c) the negative free-air gravity anomalies immediately to the east of the sedimentary arc discussed earlier area associated with the fault zone. The anomalies may be partly related to the sediments accumulated in the fault zone. But, since the negative anomalies also encompass the sedimentary arc, and the free-air anomalies over the postulated fault zone and over the Andaman Basin show somewhat inverse relationship with bathymetry, one is led to conclude that the free-air anomalies are due to deeper mass distribution. The earthquake events for which mechanism solutions are discussed above have focal depths ranging up to 120 km (see Table 1). In other words, the fault zone, characterized by strike-slip faulting is a deep-seated fracture zone extending through the major part of the lithosphere. (d) Another interesting feature of the outer Island Arc and the fault zone is the presence of ophiolites in the Andaman Islands. Through a detailed study of stratigraphy and plate motions associated with upper Mesozoic to Pliocene ophiolite nappes of the Pacific, Indian and Mediterranean, BROOKFIELD

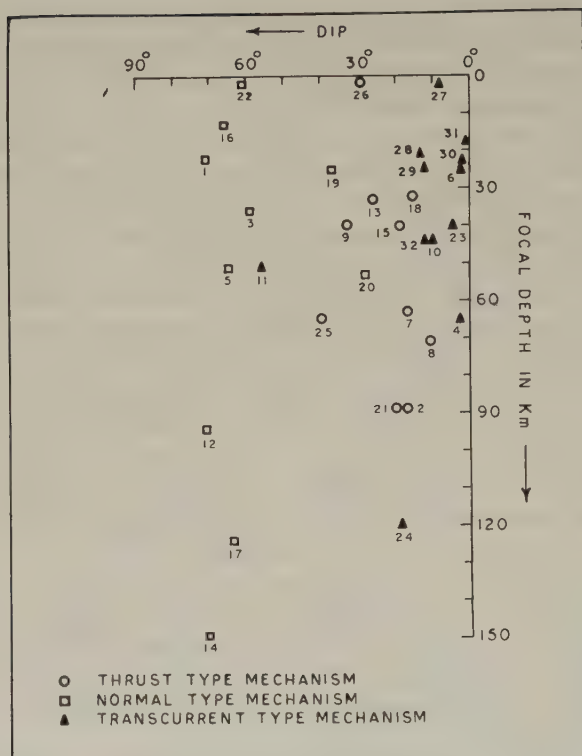


Fig. 7. A plot of dip of P axis with focal depth for the focal mechanism solutions listed in Table 1.

(1977) has shown that the transcurrent faulting during changes in relative plate motions is the major cause of initial ophiolite nappe emplacement (see discussion on ophiolite nappes of the Andaman Islands in Brookfield's paper). All these suggest that the negative gravity anomalies, the transcurrent motion in the fault zone, the presence of ophiolites, the outer Island Arc and inner volcanic arc are all related to plate motions under the Andaman Sea.

A plot of the dip of P axis obtained through focal mechanism studies with focal depth is shown in Fig. 7. It may be noted that the transcurrent type of faulting takes place at shallow as well as deeper levels up to a depth of about 120 km. The P axes for these solutions dip at 10° to 20° . Thrust faulting takes place up to a depth of about 90 km and the dip of P axes for these vary from 15° to 40° . Normal faulting takes place up to a depth of about 150 km and the dip of P axes for these varies from 60° to 80° .

The shallow nature of P axes over the outer zone of Island Arc is typical of conditions prevailing at the outer part of the subduction zones. These results further suggest that practically all the three mechanisms of faulting are active in the area and are at present prevailing over a considerable part of the lithosphere.

An analysis of the gravity and seismicity data along the Profile AA' (location shown in Fig. 5) is presented in Fig. 8. Keeping in view the geological history of the area, the

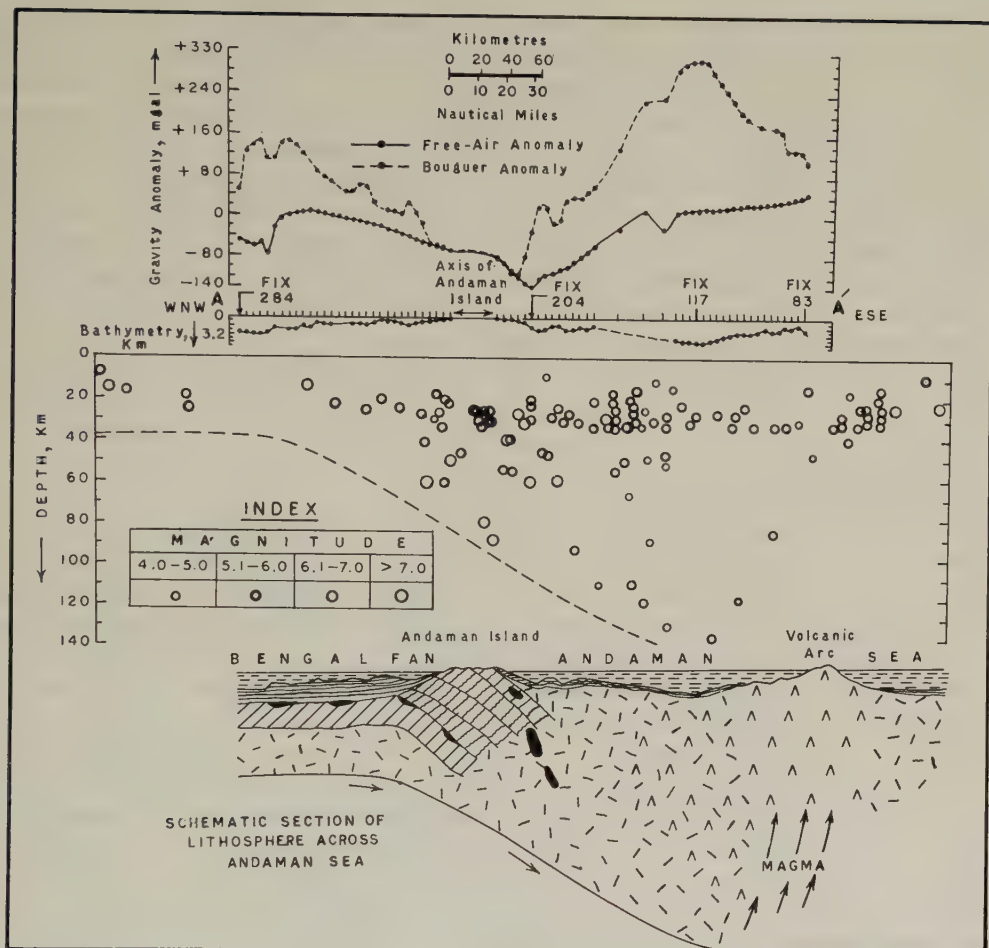


Fig. 8. Free-air gravity anomalies, bathymetry, Bouguer anomalies and epicentral distribution in a vertical section along the Profile AA'. The location of the profile is shown in Fig. 5. A schematic representation of the subducting lithosphere under the Andaman Sea is also shown in the figure.

evidence from gravity, seismicity and the nature of focal mechanism solutions, a model for the present day conditions prevailing in the lithosphere is suggested. For purposes of plotting the seismicity, the locations of earthquake foci (between 6° and 12° N) were projected along the profile.

It is clear from the figure that the depth of foci increases towards the east and reaches a maximum close to the inner volcanic arc. The distribution of earthquake foci does not seem to be related to the narrow belt of strong negative free-air anomalies prevailing close to the Andaman Group of islands. The prevailing anomalies also do not seem to have any correlation with the observed bathymetry. The strong negative anomalies close to the sedimentary arc suggest, abnormal mass distribution resulting in departure from isostatic conditions at least locally. Over the deepest part of the Andaman Sea, the free-air anomalies show inverse relationship with bathymetry. Strong positive gravity anomaly

lies over the inner volcanic arc, and a bias toward positive gravity field over major part of the Andaman Basin may be attributed to large scale submarine volcanism under the Andaman Basin. The deepest part of the inclined seismic zone is attained not right below the axis of the negative gravity anomalies, but is rather deflected east towards the Andaman Basin (over which a positive gravity bias is noted). The model suggests the existence of a subduction zone underneath the Andaman Sea. As a result of this subduction, thrusting, normal faulting as well as strike-slip faulting is taking place at depth. It is also suggested that as a result of relative movement of the lithosphere, magma has been created in the past (perhaps is also being created at present) in the upper mantle. The movement of this magma along faults has been manifested in the form of several volcanic features such as the Invisible Banks, the Narcondam and Barren Islands etc.

The present day seismic evidence suggests that these processes are continuing at present.

6. *Inferred Tectonic Movements*

For a more complete understanding of plate motion in Andaman Sea region, one has to take into consideration the history of evolution of the Indian Ocean apart from the history of evolution of the Andaman Sea. A great deal of evidence obtained from magnetic anomalies (LE PICHON and HEIRTZLER, 1968; MCKENZIE and SCLATER, 1968) has shown that the Indian Ocean has been evolved as a result of drift of the Indian Landmass towards the north. As a result of this movement, the Indian Plate has collided with the Burmese part of the Asian Plate towards the east and the Tibetan part towards the north. From the analysis of seismicity and gravity data for the northern Burma, VERMA *et al.* (1976) have suggested that an active subduction zone exists at present underneath the Arakan Yoma and the Irrawady Basin in Burma. However, apart from subduction, large scale strike-slip movements in the lithosphere seem to be taking place in the entire eastern belt extending from Himalaya to Indonesia. Thus it appears that along the eastern margin of the Indian Plate, probably a substantial part of subduction is transforming into transcurrent motion.

To illustrate this point further, the sense of transcurrent motion derived through the focal mechanism studies considered in the present work was plotted for the individual solutions which are shown in Fig. 9. In addition to the results discussed above, the results obtained for earthquakes located over inland of Burma (VERMA *et al.*, 1977) to the north of the present area have also been included and are shown in Fig. 9. VERMA *et al.* (1977) have reported strike-slip as well as thrust mechanism solutions for earthquakes located in Burma. The direction of thrusting deduced for all the thrust mechanism solutions reported for the Andaman Sea and northern Burma is also shown in the figure. It may be observed from this figure that transcurrent motions are taking place right from the Eastern Himalayan Syntaxis on the extreme north to Sumatra on the far south, across the full length of the Irrawaddy Basin of Burma and the Andaman Sea. It is interesting to observe that the zone affected by transcurrent motions is relatively narrow in width but widespread in north-south direction over a distance of about 2,500 km. This zone of transcurrent motion is currently undergoing right-lateral motion as suggested by the focal mechanism studies. On the far south in Sumatra, earthquakes of the right lateral shear motion type are known to occur along the Semangko Fault trending NW-SE (KATILI and HEHUWAT, 1967).

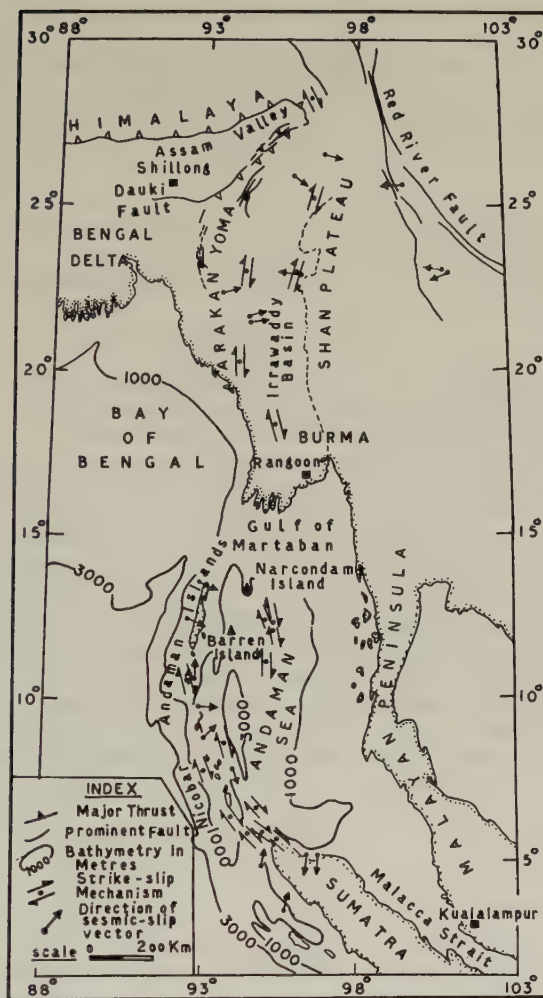


Fig. 9. Sense of transcurrent motion deduced from focal mechanism solutions for earthquake events studied from Andaman Sea and inland Burma. The direction of seismic slip vector for thrust mechanism solutions are also shown in the figure. The results for Burmese earthquakes are after VERMA *et al.* (1977).

It may be further observed from this figure that the direction of seismic slip vectors for various thrust mechanism solutions (shown in Figs. 6 and 7) are in the direction of the northeast in the southern part of the area, it swings towards east in the central part following the arcuate trend of the islands, and then turns towards east-southeast in the northern part (north of 12°). This suggests that the plate margin itself may be taking an arcuate shape in this area.

REFERENCES

- BROOKFIELD, N.E., The emplacement of giant ophiolite appes. I. Mesozoic-Cenozoic examples, *Tectonophysics*, **37**, 247–303, 1977.

- EGUCHI, T., S. UYEDA, and T. MAKI, Seismotectonic history of the Andaman Sea, *Tectonophysics*, 1978 (in press).
- FITCH, T.J., Earthquake mechanisms in the Himalayan, Burmese, and Andaman regions and continental tectonics in central Asia, *J. Geophys. Res.*, **75**, 2699–2709, 1970.
- FITCH, T.J., Plate convergence, transcurrent faults, and internal deformation adjacent to southeast Asia and Western Pacific, *J. Geophys. Res.*, **77**, 4432–4461, 1972.
- KATILI, J.A. and F. HEHUWAT, On the occurrence of large transcurrent faults in Sumatra, Indonesia, *J. Geosci. Osaka City Univ.*, **10**, 5–15, 1967.
- KRISHNAN, M.S., *Geology of India and Burma*, 4th Ed., pp. 604–606, Higginbothams, Madras, 1960.
- LE PICHON, X. and J.R. HEIRTZLER, Magnetic anomalies in the Indian Ocean and sea-floor spreading continents, *J. Geophys. Res.*, **73**, 2101–2118, 1968.
- McKENZIE, D.P. and J.C. SCLATER, Heat Flow inside the island arcs of the Northwestern Pacific, *J. Geophys. Res.*, **73**, 3137–3179, 1968.
- NUTTLI, O.W., Table of angles of incidence of P-waves at focus, calculated from 1968 P-tables, *Earthq. Notes*, **40**, 21–25, 1969.
- PETER, G., L.A. WEEKS, and R.E. BURNS, A reconnaissance geophysical survey in the Andaman Sea and across the Andaman-Nicobar island arc, *J. Geophys. Res.*, **71**, 495–509, 1966.
- RITSEMA, A.R. and J. VELDKAMP, Fault plane mechanisms of Southeast Asian earthquakes, *Mededelingen En Verhandelingen*, **76**, 63–85, 1960.
- RODOLFO, K.S., Marine sedimentation off the Irrawaddy River, Burma, *Prog. Geol. Soc. Am. Annu. Meet.*, San Francisco, pp. 179–180, 1966 (Abstr.).
- RODOLFO, K.S., Bathymetry and marine geology of the Andaman basin, and tectonic implications for Southeast Asia, *Geol. Soc. Am. Bull.*, **80**, 1203–1230, 1969.
- SANTO, T., Regional study on the characteristic seismicity of the world. II. From Burma down to Java, *Bull. Earthq. Res. Inst.*, **47**, 1049–1061, 1969.
- VAN BEMMELEN, R.W., *The Geology of Indonesia*, Vol. 1 pp. 732–757, The Hague Govt. Printing Office, 1949.
- VERMA, R.K., M. MUKHOPADHYAY, and M.S. AHLUWALIA, Earthquake mechanisms and tectonic features of Northern Burma, *Tectonophysics*, **32**, 387–399, 1976.
- VERMA, R.K., M. MUKHOPADHYAY, and A.K. NAG, Seismicity and tectonics in South China and Burma, *Tectonophysics*, 1979 (in press).
- WEEKS, L.A., R.N. HARBISON, and G. PETER, Island arc system in Andaman Sea, *Am. Assoc. Pet. Geol. Bull.*, **51**, 1803–1815, 1967.

FOCAL MECHANISMS AND TECTONICS IN THE TAIWAN-PHILIPPINE REGION

T. SENO and K. KURITA

Geophysical Institute, Faculty of Science, University of Tokyo, Tokyo, Japan

(Received June 10, 1978; Revised September 1, 1978)

Seismic activity and focal mechanisms in the vicinity of Taiwan and the Philippines are studied to elucidate the tectonics in this complex region. Epicentral distribution and vertical profiles of earthquake foci support the idea that the entire Philippines is not a part of the Eurasian plate, but another block of lithosphere and the relative motion between the Philippine Sea and the Eurasian plates is shared by the subduction along the two boundaries, west and east of the Philippines. Thrust type of mechanisms are the dominant mode of deformation along the eastern margin of the Philippines; in contrast, no thrust type of solutions are obtained along the western margin of this islands. Between Taiwan and Luzon, mode of plate consumption is most complex. Seismic activity is mostly shallow and diffuse in a 200 km wide zone. Reverse faultings along the eastern margin of Taiwan, strike-slip faultings off the southeastern coast of Taiwan, and normal faultings between the Manila trench and the North-Luzon trough are the major mode of deformation. We believe that the region between Taiwan and Luzon constitutes a left-lateral shear zone due to the gradual transition of site of plate consumption from eastern margin of Taiwan to east Luzon. Subduction under the west-facing Luzon arc in this region is likely to be ending now; this might be causing the opening of the sedimentary wedge behind the Manila trench. Normal faultings in this study probably indicate the initial phase or prespreading phase of opening of the area behind the Manila trench.

1. Introduction

The 23 focal mechanism solutions presented in this study are from almost all the shallow focus earthquakes occurring during the period from 1970 to 1975 in the vicinity of Taiwan and the Philippines. These solutions are based on the WWSSN long period records. Although they show that all types of mechanism solutions are found in this complex region, each district of the region has a dominant mode of deformation. These focal mechanisms and distribution of recent seismicity are useful for elucidating the tectonic features in the Taiwan-Philippine region.

The region concerned is made complex by the Manila trench-Luzon trough system to the west, the Philippine-Mindanao trench system to the east, the geologically active fault system in the Philippine archipelago, and the arc-continent collision at Taiwan (Fig. 1, LUDWIG *et al.*, 1967; HAYES and LUDWIG, 1967; KATSUMATA and SYKES, 1969; LUDWIG, 1970; WU, 1970, 1978; FITCH, 1970, 1972; CHAI, 1972; BIQ, 1972; KARIG, 1973; MURPHY, 1973; SENO, 1977; BOWIN *et al.*, 1978). As was pointed out by KATSUMATA and SYKES (1969), it is impossible to describe the slip vectors of shallow earthquakes in the entire Ryukyu-Taiwan-Philippine region by only one pole of rotation between two plates. Blank arrows in Fig. 1 indicate the direction of convergence of the Philippine Sea plate with respect to Eurasia (SENO, 1977). It can be seen that the slip directions of

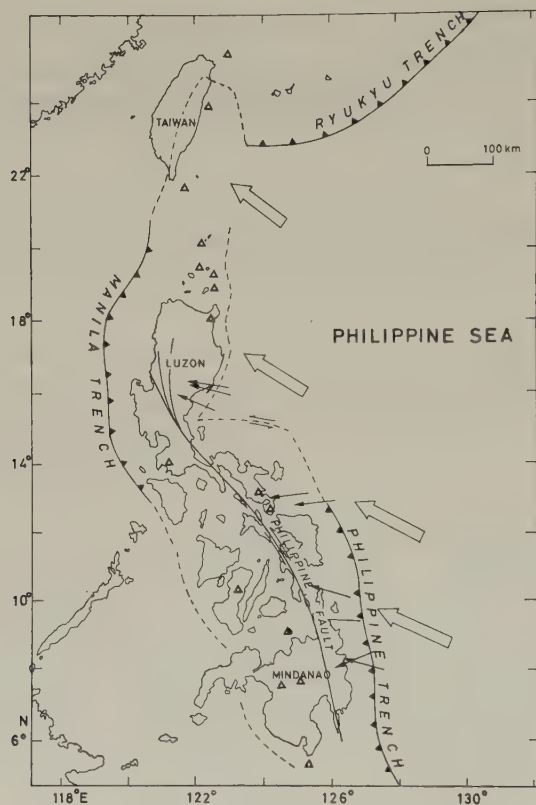


Fig. 1. Tectonic elements in the vicinity of Taiwan and the Philippines. The inferred boundary of the Philippine block (SENO, 1977) is indicated by the line of trench axis and by the broken line. Triangles show the active volcanic centers. Slip vectors of shallow earthquakes along the eastern margin of the Philippines (FITCH, 1972) are indicated by the thin arrows, and the direction of the relative motion between the Philippine Sea and Eurasia (SENO, 1977) are indicated by the blank arrows.

shallow events along the eastern margin of the Philippines (thin arrows in Fig. 1) deviate in a counterclockwise sense from the computed ones. This implies that the Philippines is not a part of the Eurasian plate but forms another block of lithosphere (SENO, 1977). We herein call this block of lithosphere the Philippine block; the inferred boundary of this block (SENO, 1977) is indicated in Fig. 1. The southwestern portion of the boundary, speculative when inferred, is evidenced by the existence of subduction zones which border the islands from the Sulu and Celebes basins (MURPHY, 1975; HAMILTON, 1977). The relative motion between the Philippine Sea and the Eurasian plates may be shared by the motion along the west and east sides of the block (SENO, 1977). The main purpose of this present study is to refine and correct this earlier investigation and delineate tectonic features in this complex region on the basis of seismicity and focal mechanisms.

2. Seismicity

Figures 2 and 3 show the spatial distribution of shallow focus and intermediate and

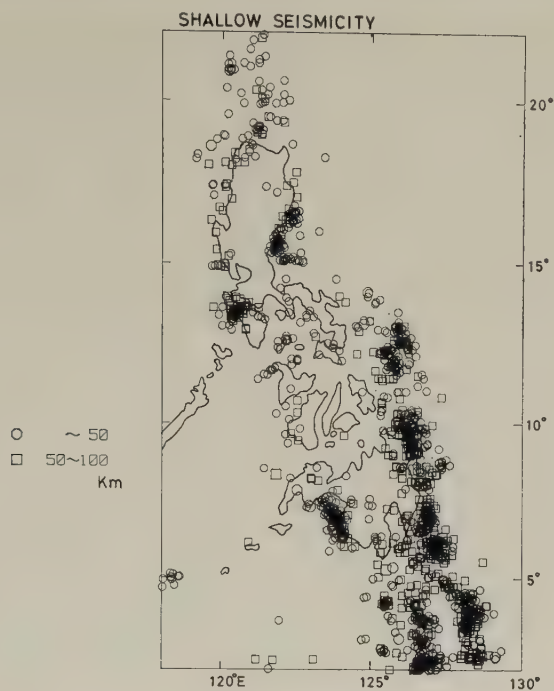


Fig. 2. Epicentral distribution of recent (1964–1976) shallow focus earthquakes ($m_b \geq 5.0$, depths ≤ 100 km) based on the USGS data.

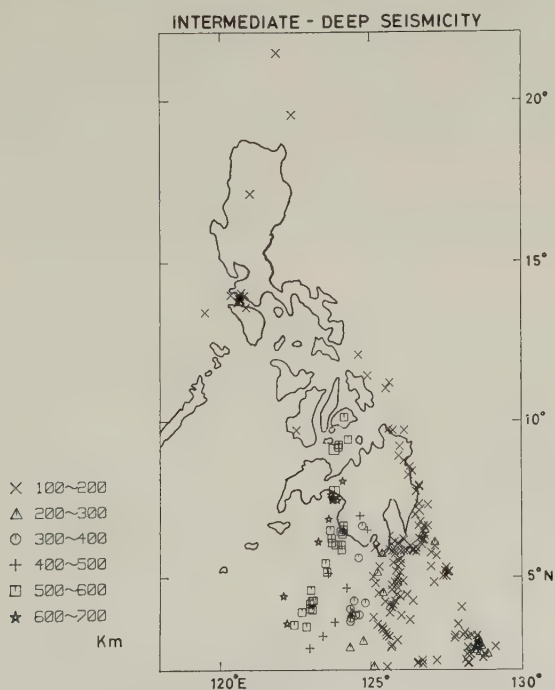


Fig. 3. Epicentral distribution of recent (1964–1976) intermediate and deep focus earthquakes ($m_b \geq 5.0$, depths > 100 km) based on the USGS data.

deep focus epicenters, respectively, based on the USGS data, occurring during the period from 1964 to 1976 in the area of the present study. Nearly all the shallow activity in the vicinity of the Philippines is confined to a narrow zone around the Philippine archipelago (Fig. 2). North of Luzon, the activity is diffuse in a 200 km wide zone. South of Mindanao, there are two zones of activity extending in a SSE direction to the west and northeast of Halmahera. Deep focus epicenters are distributed under the area from north of Mindanao to the Celebes Sea (Fig. 3); their depths are up to 650 km. This deep activity disappears abruptly at about 10°N north of Mindanao. South of Mindanao, as will be shown later, the deep activity can be joined with the zone of shallow activity extending to the west of Halmahera. The shallow activity along the Philippine trench continues to the zone of activity at the northeast of Halmahera (Fig. 2), as does the topography of the trench, and not to the zone at the west of Halmahera, thus we can say that the Benioff zone under the Celebes Sea, which extends northward to the north of Mindanao, is the subducted lithosphere which had existed at the west of Halmahera, contrary to the view of FITCH (1970) who considered this slab as the subducted Philippine Sea plate. This point will be discussed later (Fig. 4). Then, it can be said that the seismic activity around the Philippines which indicates the present relative motion of the Philippine block with respect to the adjacent basins is mostly shallower than 200 km. We call the shallow activity along the west and east margin of the Philippines the western and eastern seismic zone, respectively. The western seismic zone may continue farther southward to the north of Sulawesi as inferred from the embryonic subduction zone there (HAMILTON, 1974, 1977; SILVER and MOORE, 1978).

Profiles of earthquake foci may provide us with some characteristic features of subduction along the Philippine block. Figure 4 shows the vertical profiles of earthquake foci along the latitudinal lines south of 22°N . In section A (22° – 18°N), activity is mostly shallower than 100 km and diffuse in a zone wider than 200 km. In section B (18° – 15°N), two seismic zones, eastern one and western one, appear. The western one, less active than the eastern one, appears to dip eastward. In section C (15° – 12°N), the eastern zone shifts to the east according to the swing of the topography of Luzon. This zone is dipping to the west and the western one to the east. In this section, we can also see the activity between the two zones; this inland activity may be associated with the Philippine fault system. In section D (12° – 10°N), we can also see the two inclined seismic

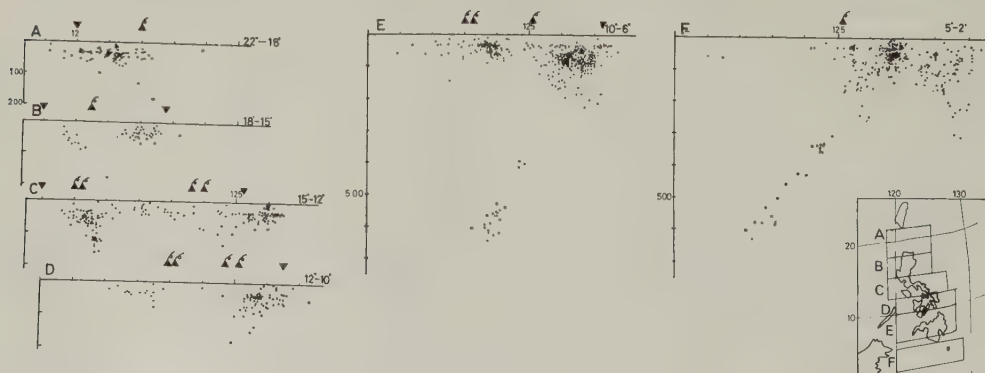


Fig. 4. Profiles of the seismicity around the Philippines. The foci are projected onto vertical planes along the latitudinal lines.

zones, though the western one is not very active. In section E (10° – 6° N), deep activity whose depth is from 350 to 650 km suddenly appears. At a first glance, this activity appears to join with the eastern zone of shallow activity. We, however, do not take this view as will be seen in the next profile. In section F (5° – 2° N), we can see two zones of shallow activity which are corresponding to the two seismic zones extending to the west and northeast of Halmahera in Fig. 2. The eastern seismic zone, which appears to dip steeply in the deeper part, is the continuation of the shallow activity along the Philippine trench as can be seen in Fig. 2. The westerly dipping slab-like zone in this profile can be joined with the western zone of shallow activity and not with the eastern one. Thus, also in section E, the deep activity, which is the northward continuation of the deep activity in section F, cannot be joined with the shallow activity along the Philippine trench. This leads us to conclude that the westerly dipping deep activity under the Philippines indicates the subducted slab which had existed at the west of Halmahera and not the subducted Philippine Sea plate.

In these profiles, active volcanic centers are also shown. Their distribution appears to be associated with the distribution of the Benioff zones, though more close examination of chemical composition of volcanic products may be needed to correlate the volcanic activity with the plate subduction (e.g., HATHERTON and DICKINSON, 1969).

Seismic activity along the geologically active Philippine fault system in the archipelago is not distinct in Figs. 2 and 4. We do not agree with the view of FITCH (1972), MURPHY (1973), and HAMILTON (1977), that this fault system plays an important role in the interplate deformation between the Philippine Sea and Eurasia, as was discussed by SENO (1977).

Depth of seismic zone may provide important information on the rate of plate subduction; we plot the deepest point of the eastern and western seismic zones around the Philippines versus latitude (Fig. 5). It should be noted that we do not use the deep activity under the Philippines in this plot. The depth of eastern seismic zone shoals to the north surprisingly linearly. If the difference in depth of the seismic zone is due to the difference in rate of plate convergence, we can locate the pole of rotation of the Philip-

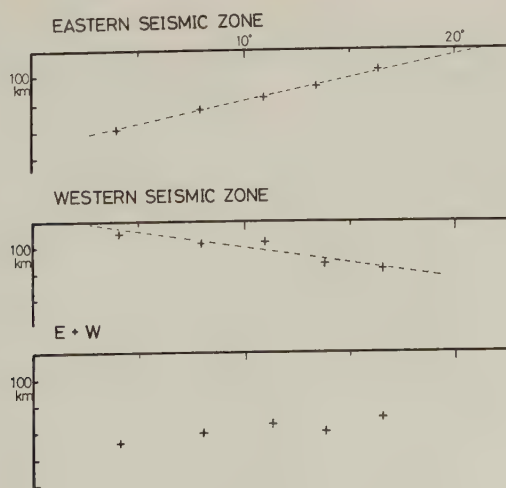


Fig. 5. Distribution of seismic activity with depth as a function of latitude.

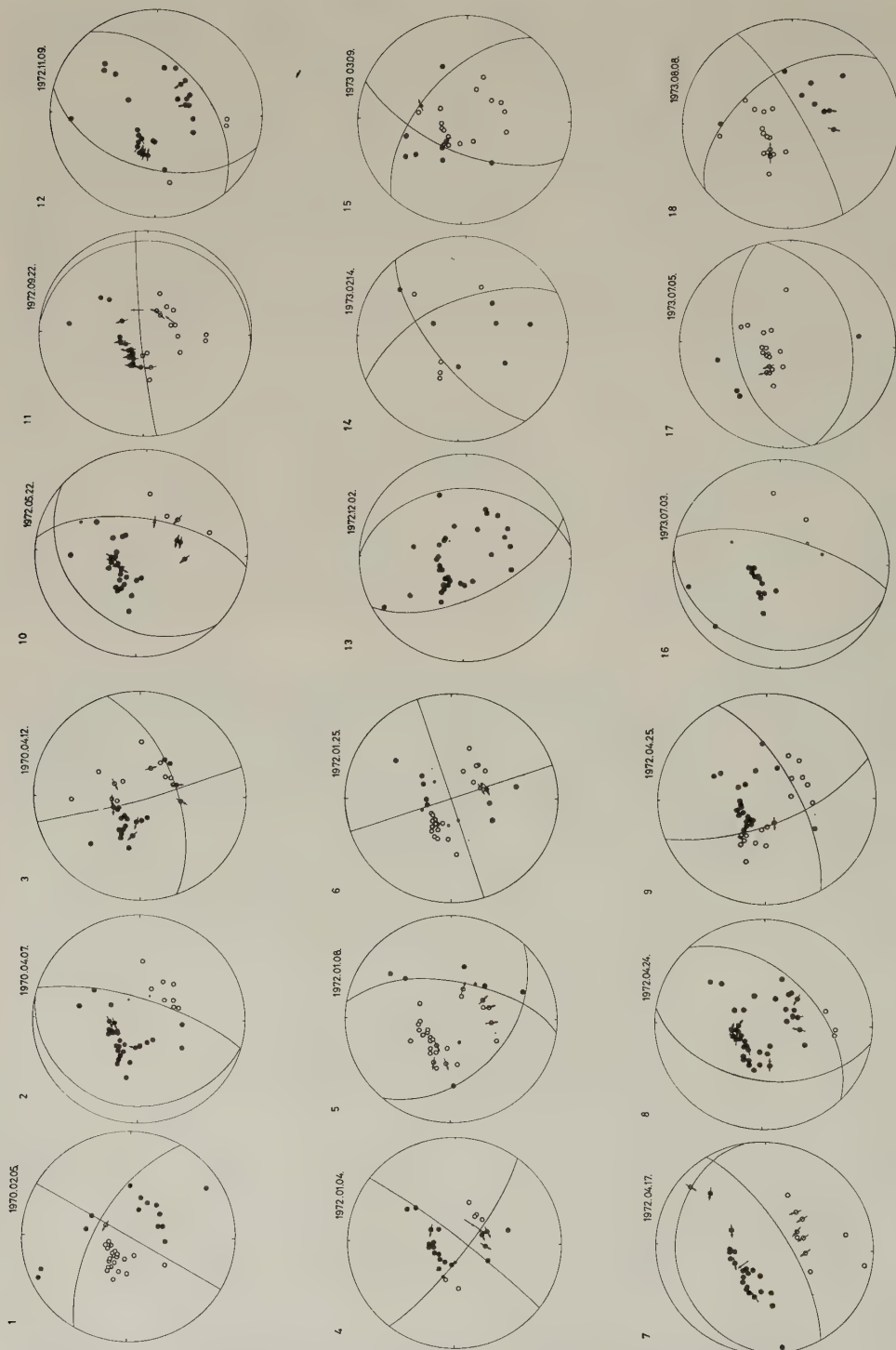


Fig. 6

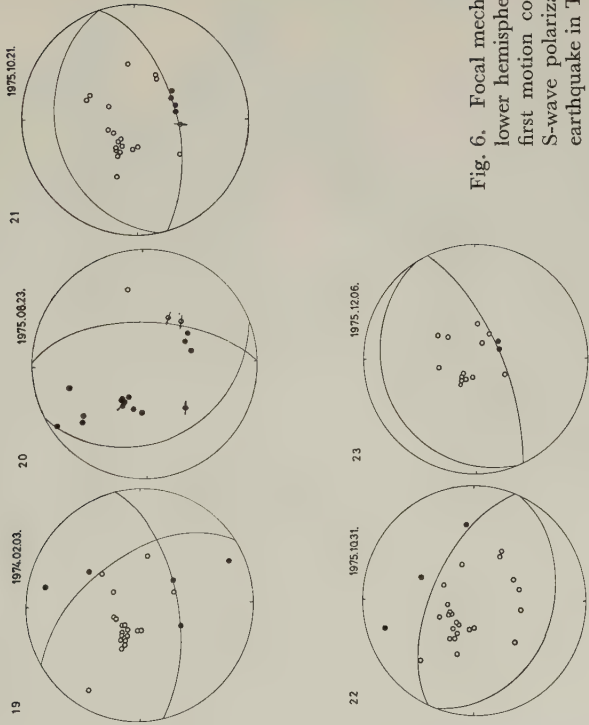


Fig. 6. Focal mechanism solutions presented as equal area projections of the lower hemisphere of the focal sphere. Closed and open circles represent first motion compressions and dilatations respectively. Arrows indicate S-wave polarization directions. Number beside each subfigure denotes earthquake in Table 1 and in Figs. 7 and 8.

pine Sea plate relative to the Philippine block at about 21°N . This pole position is consistent with the slip directions of the shallow events along the eastern seismic zone (see Fig. 1 and also SENO, 1977). The western seismic zone being less active than the eastern one, the depth-latitude relation had to be inferred. But, it appears to shoal to the south. The arithmetic sum of the depths of the two seismic zones is almost constant (250–350 km), but it looks to shoal to the north slightly. It is interesting to note that the deepest point of the Ryukyu seismic zone is 250 km (KATSUMATA and SYKES, 1969). Thus the difference in depth between the Ryukyu and Philippine seismic zones is consistent with the convergence rate of the Philippine Sea plate with respect to the Eurasian plate, if and only if we take the arithmetic sum of the depths of the two seismic zones around the Philippines. This supports the idea that the both boundaries of the Philippine block share the relative motion between the plates.

Between Taiwan and Luzon is a hiatus of subduction zone; we discuss the mode of deformation in this area in a later section.

3. Focal Mechanisms

The 23 focal mechanisms presented in Fig. 6 are from shallow focus earthquakes occurring during the period from January 1970 to December 1975. The events that yielded reliable focal mechanism solutions were selected from a list of all shallow events reported to the USGS. Nearly all the focal mechanisms came from the events with body-wave

Table 1. Parameters for Taiwan-Philippine shallow earthquakes from 1970 to 1975.

Solutions	Date	Location		Depth (km)	Pole 1		Pole 2		P Axis		T Axis		B Axis		Rank*
					AZ	PL	AZ	PL	AZ	PL	AZ	PL	AZ	PL	
1	Feb. 5, 1970	12.58N	122.09E	8	119	0	209	24	257	16	160	17	30	66	C
2	Apr. 7, 1970	15.78N	121.71E	40	106	74	286	16	106	29	286	61	15	0	B
3	Apr. 12, 1970	15.08N	122.01E	25	73	2	341	28	32	23	294	16	169	61	A
4	Jan. 4, 1972	22.50N	122.07E	6	36	10	307	4	82	4	351	10	194	79	A
5	Jan. 8, 1972	20.95N	120.26E	36	42	44	278	30	326	58	71	10	168	31	A
6	Jan. 25, 1972	22.56N	122.37E	29	72	0	162	0	117	0	207	0	0	90	A
7	Apr. 17, 1972	24.10N	122.44E	48	173	70	327	18	154	27	314	62	60	8	A
8	Apr. 24, 1972	23.60N	121.55E	29	99	44	315	40	116	1	22	0	209	19	B
9	Apr. 25, 1972	13.38N	120.34E	38	71	20	332	24	293	2	23	31	196	59	A
10	May 22, 1972	16.66N	122.19E	36	131	58	277	27	109	16	244	67	15	16	A
11	Sept. 22, 1972	22.37N	121.16E	8	173	4	285	79	184	48	344	40	82	10	A
12	Nov. 9, 1972	23.87N	121.61E	22	106	44	321	40	124	2	27	72	214	17	A
13	Dec. 2, 1972	6.41N	126.62E	73	64	32	299	42	271	4	10	58	176	30	C
14	Feb. 14, 1973	22.27N	121.52E	42	140	21	242	30	283	4	189	37	18	52	A
15	Mar. 9, 1973	6.32N	127.38E	25	112	25	221	32	163	45	256	6	354	45	A
16	July 3, 1973	12.27N	125.32E	47	284	20	104	70	104	25	284	65	14	0	B
17	July 5, 1973	13.18N	124.65E	18	164	40	344	50	164	85	344	5	74	0	C
19	Feb. 3, 1974	18.93N	120.13E	21	238	35	348	27	297	47	201	5	105	42	A
20	Aug. 23, 1975	10.04N	125.86E	68	67	58	272	30	81	14	300	71	175	11	C
21	Oct. 21, 1975	11.65N	121.58E	26	164	60	344	30	344	75	164	15	74	0	B
22	Oct. 31, 1975	12.47N	126.01E	48	22	60	202	30	202	75	22	15	115	0	C
23	Dec. 6, 1975	17.42N	119.68E	19	156	72	336	18	336	63	156	27	66	0	B

Data for the epicentral location and depth are from the Bulletins of the International Seismological Centre. AZ denotes azimuth, PL plunge.

* Rank represents the reliability of the solutions: A denotes the case that both of the nodal planes are constrained with little arbitrariness, B the case that one of the nodal planes is constrained well, and C the case that both of the nodal planes have large arbitrariness.

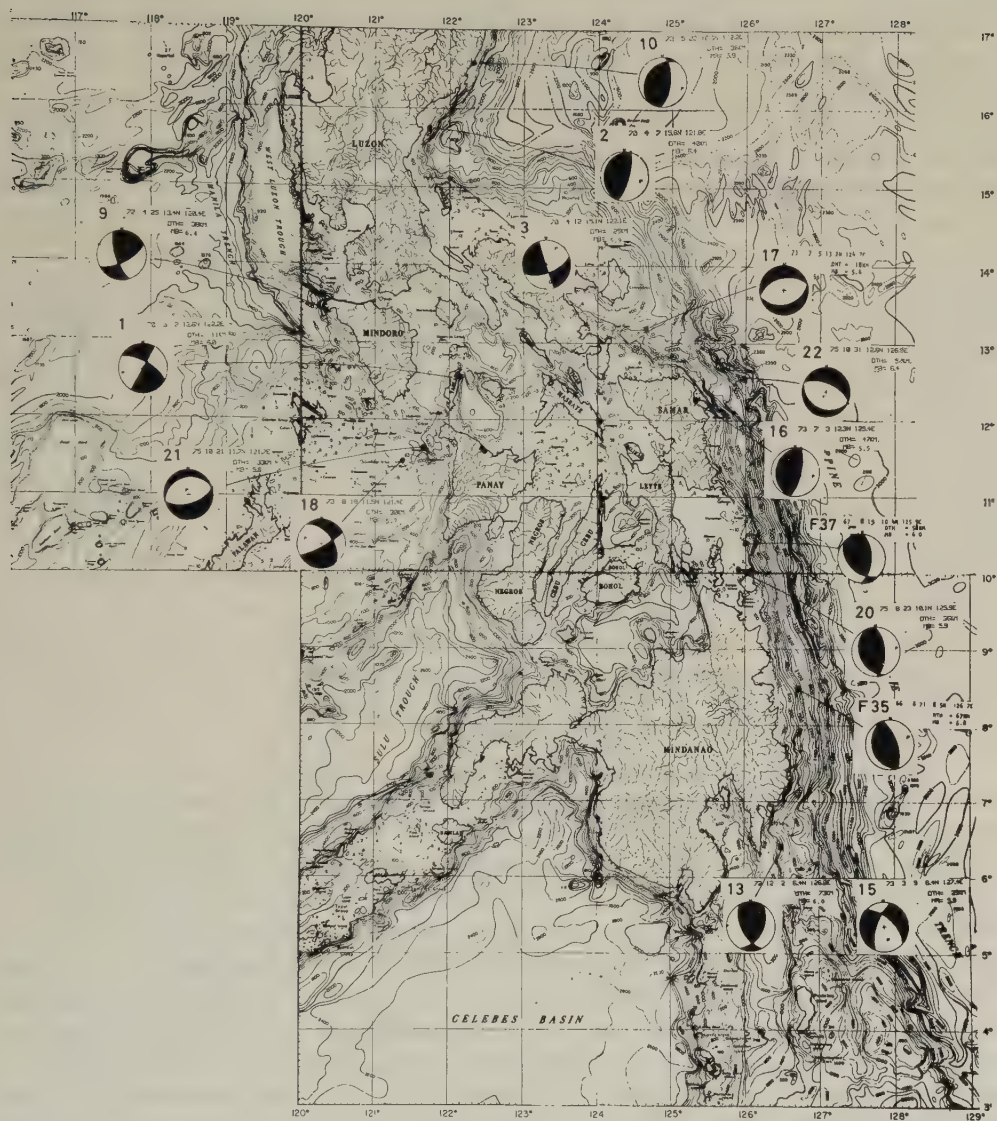


Fig. 7. Compilation of focal mechanism solutions south of 17°N. Number attached with the solution denotes earthquake in Table 1. Solutions F 35 and F 37 are from FIRCH (1970).

magnitude greater than 5.6. The mechanisms are shown as equal area projections of the lower hemisphere of the focal sphere; their parameters are presented in Table 1. To determine the nodal planes of the mechanisms, we used the first motion of long-period P-wave and the polarization angle of long-period S-wave recorded by the seismographs of WWSSN. In some cases, P-wave data are not sufficient to determine nodal planes; in some of such cases, S-wave data were used effectively to determine the nodal planes using the computer program written by HIRASAWA (1970). Mechanism solutions are ranked according to the reliability of their nodal plane solutions (Table 1, see foot notes).

In Fig. 7, mechanism solutions in the area south of 17°N are plotted on the bathymetric chart (U.S. NAVAL OCEANOGRAPHIC OFFICE, 1969). Two solutions in the earlier period by FITCH (1970) are also incorporated into this figure (F35 and F37).

Along the Philippine trench, thrust type of mechanisms are obtained under the landward slope of the trench and the edge of the continental shelf (Nos. 16, 20, F35, F37). Two normal faultings are distributed at the trench axis (Nos. 15, 22) and one at the axis of a canyon extending from the southernmost Luzon to the trench (No. 17). Farther north, along the eastern margin of Luzon are found two thrust type solutions (Nos. 2, 10). Topography of the trench does not develop well there; however, a steep submarine scarp and a shallow trough extend along the east coast of Luzon, and join with the Philippine trench at about 13°N . We believe that this scarp and trough represent an incipient stage of subduction zone as is suggested by KARIG (1973). One strike-slip faulting is obtained where the scarp along the east Luzon swings to the east (No. 3). The aftershock distribution of this event is elongated in an E-W direction; this indicates that the E-W trending nodal plane is a slip plane. The E-W trending scarp must play a role of transform fault here as was pointed out by KARIG (1973); this event can be interpreted to indicate a sinistral shear motion along this transform boundary.

Thrust type solutions along the eastern margin of the Philippines are consistent with underthrusting of the Philippine Sea plate beneath the islands from the east. As was mentioned earlier, the slip direction of these shallow events deviates from the NW-SE direction of the relative motion between the Philippine Sea and the Eurasian plates. The difference in the sense of motion implies that the Philippine block is moving to the northwest with respect to Eurasia (SENO, 1977).

In contrast to the eastern margin of the Philippines, no thrusts are obtained along the western margin of the islands. Three strike-slip faultings and one normal faulting are obtained from Mindoro to Panay (Nos. 1, 9, 18 and No. 21). Though we can see an inclined seismic zone here (Fig. 4), it is not easy to conclude that these events represent the interplate deformation between the Philippine block and the adjacent basins. If these events are interpreted to indicate interplate deformation, the northwestward trending nodal planes of the strike-slip faultings are consistent with the northwestward migration of the Philippine block with respect to Eurasia. It is, however, also possible to interpret these events as indicating the intraplate deformation caused by the E-W compressional tectonic force due to the subduction of the Philippine Sea plate under the islands from the east. Seismic activity along the western margin of the Philippines is less active than along the eastern margin (Fig. 2) and no thrust type of mechanisms are obtained there; this may provide a line of evidence for the idea that the subduction of the marginal basins under the Philippine block from the west is now ceasing and arc polarity reversal is currently taking place from the western boundary to the eastern one (e.g., BOWIN *et al.*, 1978). This point will be discussed later.

South of Panay, no focal mechanism solution was obtained for the period treated in this study. However, a large earthquake ($M_s=7.8$) occurred on August 16, 1976 in the region of Moro gulf, northern Celebes Sea, south of Mindanao. Focal mechanism of this event indicates an eastward subduction of the Celebes basin under the Mindanao (STEWART and COHN, 1977). The relative motion of the Celebes basin to Mindanao does not necessarily coincide with the one inferred between the Philippine block and Eurasia. This implies that the Celebes basin is likely to be detached from Eurasia.



Fig. 8. Compilation of focal mechanism solutions north of 17°N . Number attached with the solution denotes earthquake in Table 1. Solutions KS3 and KS10 are from KATSUMATA and SYKES (1969).

The idea of dormant arcs in the marginal basins of southeast Asia (MURPHY, 1975; HAMILTON, 1977) supports this possibility.

In Fig. 8, the focal mechanism solutions south of 17°N are plotted on the bathymetric chart. Two solutions of the events in the earlier period by KATSUMATA and SYKES (1969) are also incorporated into this figure (KS3, KS10). Main features of mode of deformation in this area are as follows: a thrusting between the Ryukyus and Taiwan (No. 7), high angle reverse faultings along the east margin of Taiwan (Nos. 8, 12), strike-slip faultings off southeast Taiwan (Nos. 4, 6, 14), and normal faultings in the area between the Manila trench and the North Luzon trough (Nos. 5, 11, 19, 23, KS3, KS10). During the period before 1970, large events of strike-slip faultings occurred at the junction between Taiwan and the Ryukyus, of which tectonic significance has been in dispute (WU, 1970, 1978; SUDO, 1972). The most prominent features of the present focal mechanisms, which differ from the earlier investigations (KATSUMATA and SYKES, 1969; WU, 1970; SUDO, 1972), are the normal faultings in the area between the Manila trench and the North Luzon trough and the strike-slip faultings off southeast Taiwan.

The region from the junction between Ryukyu arc and Taiwan to north Luzon is one

of the most complex parts of the Philippine Sea-Eurasian plate boundary (KARIG, 1973; MURPHY, 1973; BIQ, 1972; CHAI, 1972; SENO, 1977; BOWIN *et al.*, 1978). Taiwan is a hiatus of subduction zone and has been a place of collision between the west-facing Luzon arc and the continent of Asia since Pliocene time (CHAI, 1972; KARIG, 1973; BOWIN *et al.*, 1978; WU, 1978). The Ryukyu island arc changes its trend in the vicinity of Taiwan and abuts against the crustal block of northeast Taiwan (Fig. 9, BOWIN *et al.*, 1978, Fig. 1). South of Taiwan, there are the west-facing Luzon arc, the Manila trench and the North Luzon trough (forearc basin), and the volcanic islands. The portion between the Manila trench and the North Luzon trough is a topographic bulge interpreted as an accretionary wedge (BOWIN *et al.*, 1978). The events of normal faultings are distributed under this sedimentary wedge. Their epicenters (International Seismological Centre) are located certainly eastward of the trench axis within the error of epicentral determination (Fig. 8) and their focal depths are ranging from 8 to 42 km. Thus these normal fault type of mechanisms present a quite difficult problem of why the extensional feature is possible under the accretionary wedge of subduction zone. We shall discuss this problem later.

Though distribution of epicenters in the vicinity of Taiwan is not presented in this study, recent study of seismic activity (TSAI *et al.*, 1978) and the earlier investigations (WU, 1970; HSU, 1971; SUDO, 1972; KATSUMATA and SYKES, 1969) show that the activity is mainly along the east margin of Taiwan and at the junction between Taiwan and the Ryukyus. The latter activity is most intense and presents a northward dipping tongue-like slab whose depth is up to 140 km (TSAI *et al.*, 1978). A thrust type of event at the Ryukyu-Taiwan junction (No. 7, Fig. 8) probably indicates underthrusting of the Philippine block under Asia. The activity along the east Taiwan is shallow, mostly within 40 km depth, and confined in an area that has a 100–200 km width in the E-W direction; this seismic area is truncated by the Longitudinal Valley fault at the west end (TSAI *et al.*, 1978). Reverse faultings along the eastern margin of Taiwan (Nos. 8, 12) show that dip-slip motion occurs along the Longitudinal Valley fault in addition to the sinistral shear motion as evidenced geologically and seismologically (ALLEN, 1962; HSU, 1962; KANEKO, 1970).

Between southern Taiwan and north Luzon, seismic activity is shallow and makes a diffuse zone of 100–200 km width in the E-W direction (Fig. 2, and TSAI *et al.*, 1978). Here we cannot apply the idea of double arc such as discussed in the area south of 17°N; we recall that the pole of rotation of the Philippine Sea plate with respect to the Philippine block is located at about 21°N, thus the eastern boundary of the Philippine block must vanish at the north of Luzon. We propose a model for plate consumption in this area as illustrated in Fig. 9. We agree with the view that arc polarity reversal, probably in response to collision at Taiwan, is now taking place between the west-facing Luzon arc and the new subduction boundary along the east margin of Luzon (KARIG, 1973; KARIG and WAGEMAN, 1975; BOWIN *et al.*, 1978). This new subduction boundary is likely to extend farther north along the Palau ridge (Fig. 8) from the west margin of Luzon, because a free-air gravity anomaly low and/or a topographic feature which indicate an embryonic subduction zone continues to about 19°30'N along the Palau ridge (BOWIN *et al.*, 1978) and because the pole of rotation of the Philippine Sea plate relative to the Philippine block is located at about 21°N. The rate of subduction along this boundary must taper off to the north and probably ends at about 21°N. Therefore, the extent of interplate deformation along the eastern margin of Taiwan must taper off to the south in response to the gradual increase of the rate of plate consumption to the south along the east Luzon

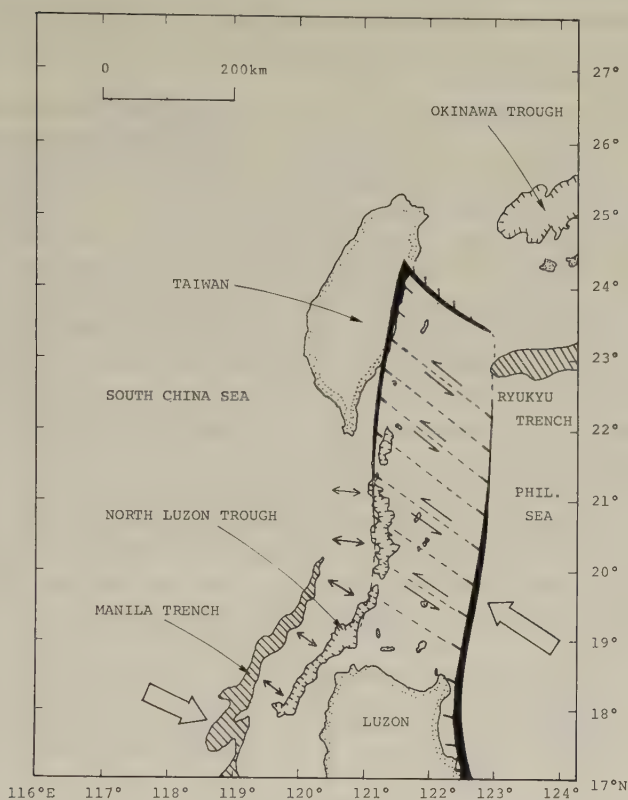


Fig. 9. Model for plate consumption in the region between Taiwan and Luzon. Thickness of the lines along the eastern margins of Taiwan and Luzon shows the relative rate of plate convergence along these boundaries.

subduction zone. This is schematically illustrated in Fig. 9. Some extent of plate consumption is probably taking place along the Manila trench in this area. We, however, believe that the subduction along the west-facing Luzon arc in this portion is now ending because the collision at Taiwan hinders the subduction of the south China basin under the Luzon arc as suggested by BOWIN *et al.* (1978). Thus the major portion of interplate deformation in this area is described by the gradual southward decrease of plate consumption along the eastern margin of Taiwan and, in contrast, by the gradual increase along the east margin of Luzon. This configuration would produce a left-lateral shear in a NW-SE direction between Taiwan and Luzon (Fig. 9). This type of interplate deformation is termed as 'transform belt' by ISHIBASHI (1978) who presented a similar type of deformation in the Izu peninsula at the northernmost part of the Philippine Sea-Eurasian plate boundary.

Now the mysterious features of seismic activity and focal mechanisms between Taiwan and Luzon may be understood as follows. The diffuse activity between southern Taiwan and north of Luzon is interpreted as indicating the activity due to the shear zone in this region. Three strike-slip events off the southeast Taiwan (Nos. 4, 6, 14) are with north-westward striking nodal planes consistent with the left-lateral shear motion of the trans-

form belt. Segmented ridge and trough system north of Luzon also indicates a left-lateral shear in a NW-SE direction (Fig. 8), contrary to the KARIG's (1973) interpretation of left-lateral shear in a NE-SW direction.

The tectonic stress regime along the Manila trench is likely to be turning to extension from compression in response to the cessation of subduction along this boundary; this would make the opening of the portion between the Manila trench and the North Luzon trough. Normal faultings (Nos. 5, 11, 19, 23, KS3, KS10) may indicate the incipient phase of spreading in this portion. Seismic profiles in east-west cross-section of this region show vertical faults between the accretionary bulge and the trough sediment which indicates the uplift of the bulge relative to the trough sediment (R.N. Anderson, personal communication, 1978). Thus the region from the bulge to the trough forms a horst-graben structure, which may indicate an original uplifting phase of opening (R.N. Anderson, personal communication, 1978). Three heat flow measurements at the northernmost corner of the Manila trench (ANDERSON *et al.*, 1977) show the values from 1.8 to 2.6, which are abnormally high compared with that associated with trench. This also supports the speculation that this is a region of incipient spreading. Normal fault type of mechanisms presented in this study may provide an important piece of evidence for the initial or pre-spreading phase of opening of marginal basin due to the change of mode of plate consumption. Reconnaissance of this region is amply warranted because of its importance to elucidate the diverse behaviour of consuming plate boundary.

We wish to thank S. Uyeda and C.O. Bowin for their critical review of the manuscript. We also wish to thank T. Eguchi for assistance of plotting epicenters and line drawings utilizing computer and R.N. Anderson, Y.B. Tsai, and G.S. Stewart for offering us their data before publication. We benefited with discussion with R.N. Anderson, F.T. Wu, H. Mizutani, Y. Matsubara, R.W. Murphy, and K. Ishibashi.

REFERENCES

- ALLEN, C.R., Circum-Pacific faulting in the Philippine-Taiwan region, *J. Geophys. Res.*, **67**, 4795-4812, 1962.
- ANDERSON, R.N., M.G. LANGSETH, and D.E. HAYES, A geophysical atlas east and southeast Asian Seas, Lamont-Doherty Geol. Observatory, 1977.
- BIQ, C.C., Dual trench structure in the Taiwan-Luzon region, *Geol. Soc. China, Proc.*, **15**, 65-75, 1972.
- BOWIN, C., R.S. LU, C.S. LEE, and H. SCHOUTEN, Plate convergence and accretion in the Taiwan-Luzon region, *Bull. Am. Assoc. Petr. Geol.*, **62**, 1645-1672, 1978.
- CHAI, B.H.T., Structure and tectonic evolution of Taiwan, *Am. J. Sci.*, **272**, 389-422, 1972.
- FITCH, T.J., Earthquake mechanisms and island arc tectonics in the Indonesian-Philippine region, *Bull. Seismol. Soc. Am.*, **60**, 565-591, 1970.
- FITCH, T.J., Plate convergence, transcurrent faults, and internal deformation adjacent to southeast Asia and the western Pacific, *J. Geophys. Res.*, **77**, 4432-4460, 1972.
- HAMILTON, W., Earthquake map of the Indonesian region, U.S. Geol. Surv. Misc. Geol. Inv. Map I-875-C, 1974.
- HAMILTON, W., Subduction in the Indonesian region, *Am. Geophys. Union, Maurice Ewing Ser.*, **1**, 15-30, 1977.
- HATHERTON, T. and W.R. DICKINSON, The relationship between Andesitic Volcanism and seismicity in Indonesia, the Lesser Antilles, and other islands arcs, *J. Geophys. Res.*, **74**, 5301-5310, 1969.
- HAYES, D.E. and W.J. LUDWIG, The Manila trench and West Luzon trough. II. Gravity and magnetic measurements, *Deep-Sea Res.*, **14**, 545-560, 1967.
- HIRASAWA, T., Focal mechanism determination from S-wave observations of different quality, *J. Phys. Earth*, **18**, 285-294, 1970.
- HSU, M.T., Seismicity of Taiwan and some related problems, *Bull. Int. Seismol. Earthq. Eng.*, **8**, 41-160, 1971.
- HSU, T.L., Recent faulting in the Longitudinal Valley of eastern Taiwan, *Mem. Geol. Soc. China*, **1**, 95-102, 1962.
- ISHIBASHI, K., Plate convergence around the Izu collision zone, central Japan: Development of a new subduction boundary with a temporary transform belt, *Int. Geodyn. Conf. Tokyo (abstr.)*, 1978.

- KANEKO, S., Transcurrent buckling and some notes on neotectonics in Taiwan, *J. Geol. Soc. Jpn.*, **76**, 215–222, 1970.
- KARIG, D.E., Plate convergence between the Philippines and the Ryukyu islands, *Mar. Geol.*, **14**, 153–168, 1973.
- KARIG, D.E. and J.M. WAGEMAN, Structure and sediment distribution in the northwest corner of the west Philippine Basin, *Init. Rep. D. S. D. P.*, **31**, 615–620, 1975.
- KATSUMATA, M. and L.R. SYKES, Seismicity and tectonics of the western Pacific: Izu-Mariana-Caroline and Ryukyu-Taiwan regions, *J. Geophys. Res.*, **74**, 5923–5948, 1969.
- LUDWIG, W.J., The Manila trench and West Luzon trough. III. Seismic-refraction measurements, *Deep-Sea Res.*, **17**, 553–571, 1970.
- LUDWIG, W.J., D.E. HAYES, and J.I. EWING, The Manila trench and West Luzon trough. I. Bathymetry and sediment distribution, *Deep-Sea Res.*, **14**, 533–544, 1967.
- MURPHY, R.W., The Manila trench-West Taiwan Foldbelt: A flipped subduction zone, *Geol. Soc. Malaysia*, **6**, 27–42, 1973.
- MURPHY, R.W., Tertiary basins of Southeast Asia, *S. E. Asia Pet. Explor. Soc. Proc.*, **2**, 1–36, 1975.
- SENO, T., The instantaneous rotation vector of the Philippine Sea plate relative to the Eurasian plate, *Tectonophysics*, **42**, 209–226, 1977.
- SILVER, E.A. and J.C. MOORE, The Molucca Sea collision zone, Indonesia, *J. Geophys. Res.*, **83**, 1681–1691, 1978.
- STEWART, G.S. and S.N. COHN, The August 16, 1976 Mindanao, Philippine Earthquake, ($M_s=7.8$)—Evidence for a subduction zone south of Mindanao, *EOS, Trans. Am. Geophys. Union*, **58**, 1194, 1977.
- SUDO, K., The focal process of the Taiwan-Oki Earthquake of March 12, 1966, *J. Phys. Earth*, **20**, 147–164, 1972.
- TSAI, Y.B., T.L. TENG, J.M. CHIU, and H.L. LIU, Tectonic implications of recent seismicity in Taiwan area, Preprint, 1978.
- U.S. NAVAL OCEANOGRAPHIC OFFICE, *Bathymetric Atlas of the Northwestern Pacific Ocean*, compiled by T.E.C. Chase and H.W. Menard, 1969.
- WU, F.T., Focal mechanisms and tectonics in the vicinity of Taiwan, *Bull. Seismol. Soc. Am.*, **60**, 2045–2056, 1970.
- WU, F.T., Recent tectonics of Taiwan, *Geodynamics of the Western Pacific*, This issue, 1978.

RECENT TECTONICS OF TAIWAN

Francis T. Wu

*Department of Geological Sciences, State University of New York,
Binghamton, New York, U.S.A.*

(Received June 27, 1978; Revised September 29, 1978)

Taiwan represents a very young arc-continental margin collision zone in a long subduction boundary. The collision started in Late Pliocene and is still vigorously taking place. Off coast of NE Taiwan a northward subducting slab, extending west at depth to northern Taiwan, can clearly be defined; although most parts of Taiwan have been rising steadily at about 5 mm/year for the last 8,500 years, northern Taiwan has had periods with no uplift. The intensity of the collision decreases toward the south off the island, and an east-dipping subduction zone can be delineated there. Thus Taiwan can be viewed as a transform zone in between two subduction zones with quite different geometries.

Seismically Taiwan is much more active than its neighbors, the Ryukyus and Luzon. Large earthquakes reveal the nature of the intense on-going intra-plate deformation; on land, EW compression or left-lateral shear occur along NNE faults and right-lateral shear occur along nearly EW faults; offshore to the southeast of Taiwan, left-lateral shear along NNW or NW faults and thrusts in several directions coexist; to the northeast, the focal mechanisms agree well with other subduction zones. The Ryukyus are terminated at about 123° E by a number of NNE striking right-lateral faults. Focal mechanisms to the southeast of Taiwan are consistent with a tectonic stress direction of $S46^{\circ}$ E to $S76^{\circ}$ E and plunging at -2° to 15° .

1. Introduction

The tectonics of Taiwan presents several points of interest. First, Taiwan is an anomalous member of the Ryukyu-Taiwan-Luzon-Philippine arc chain; whereas Ryukyu, Luzon and Philippines can be interpreted in terms of subduction of lithosphere albeit with complications in the case of Luzon-Philippines (FITCH, 1972), Taiwan represents a hiatus in a long subduction boundary; no systematic active andesitic volcanism along the trend of the Island and no recognizable bathymetric features exist in the vicinity of the Island that are usually associated with island arcs. Although a plate boundary here can be clearly defined in terms of a transition from oceanic crust to continent-like crust and other geological features indicating the past activities along this boundary, this boundary is not the only active feature and current intense shallow crustal deformation in this area extends to both sides of this boundary for more than 100 km. Secondly, the orogeny that produced a rather impressive mountain range (attaining a maximum height of 4,000 m), started sometime in Late Pliocene (CHAI, 1972; CHOU, 1973), increased its intensity throughout Pleistocene and is probably in the most active stage at present (LI, 1976); the incipience of the anomalous situation described above and the emergence of Taiwan were apparently concomitant and the present day tectonics is related closely to the orogeny that produced the Island.

The atypical nature of Taiwan as a member of an island arc chain has been recognized by many geologists. BIG noticed the apparently reversed convexity, the presence of nega-

tive Bouguer anomaly over the Island and positive anomaly in the eastern part of the Island (BIQ, 1960, 1971) and concluded that Taiwan had been a continent-facing arc from Miocene to Pliocene and has undergone a transition to block tectonics since Pleistocene (BIQ, 1971) but it may not yet have reached a steady state (BIQ, 1972). On the other hand, JUAN and WANG (1971) and JUAN (1975) considered Taiwan a coastal range of the mainland Asia originally and had subsequently accreted ocean-ward by successively retreating subduction. While BIQ (1964) hypothesized an east-dipping subduction zone under the Coastal Range, JUAN (1975) proposed the rotation of a west-dipping subduction zone into a vertical zone in Early Pliocene. CHAI (1972) was among the first to propose that the Coastal Range represents a former west-facing arc, i.e., with an east-dipping Benioff zone, and the westward migration of the trench line (with respect to the Asian continent) led eventually to the collision of the arc with the miogeosyncline on the margin of the Asian continent, whence the formation of the Island. KARIG (1973) considered Ryukyu, the Philippines together with Taiwan and reached similar conclusions.

Due to a paucity of data, the polarity of the Bashi-Northern Luzon arc has not been ascertained (KATSUMATA and SYKES, 1969; LUDWIG, 1970); but a short nascent subduction, perhaps west-dipping, may exist on the east side of Luzon (FITCH, 1972; BOWIN *et al.*, 1978). With more seismic data since 1968, we can now be quite sure that the Bashi-Northern Luzon arc is indeed east-dipping as suspected. On the other hand, the west-dipping Ryukyu arc has always been recognized (KATSUMATA and SYKES, 1969 among others). Thus between these two oppositely directed arcs Taiwan can, in a broad sense, be viewed as a transform zone. At present, this transform is accomplished by movements along definable boundaries and a substantial amount of intra-plate deformation under the ocean floor and on land.

Recently new data relevant to the interpretation of the tectonics of Taiwan have been accumulated rapidly. A newly established seismic network of 20 telemetered stations has been providing good location data for events down to magnitude 2 on the island and in the vicinity; a few detailed microearthquake surveys are now available mapping out active faults; and using local and teleseismic network data crustal and mantle structure in the vicinity of Taiwan have been determined (LU, 1976). In addition, a new geological map has recently been published (HO, 1974) and more geological data have been analyzed (see for example JUAN, 1975 for a partial bibliography). Also of great importance is the acquisition of marine geological data in the seas around Taiwan (BOWIN *et al.*, 1978; R.S. Lu, personal communication, 1978).

In the present paper, we shall attempt to analyze the pattern of crustal movements on Taiwan and in its vicinity based on seismological as well as geological data, and from there we hope to understand the tectonics since Late Pliocene, when the Island as we now know came into being, by extrapolation. It should be remarked here that in most of the works cited, a two-dimensional interpretation of the tectonics was made, however there are clear variations in the north-south direction and they should be explained.

2. Geology

Most of the surface geological data have recently been compiled into a new geologic map for the Island (HO, 1974); its explanatory text provides a comprehensive survey of the geological literature on Taiwan (HO, 1975). In Fig. 1, we have presented a simplified version of it. Several detailed descriptions of the geology of Taiwan written pre-

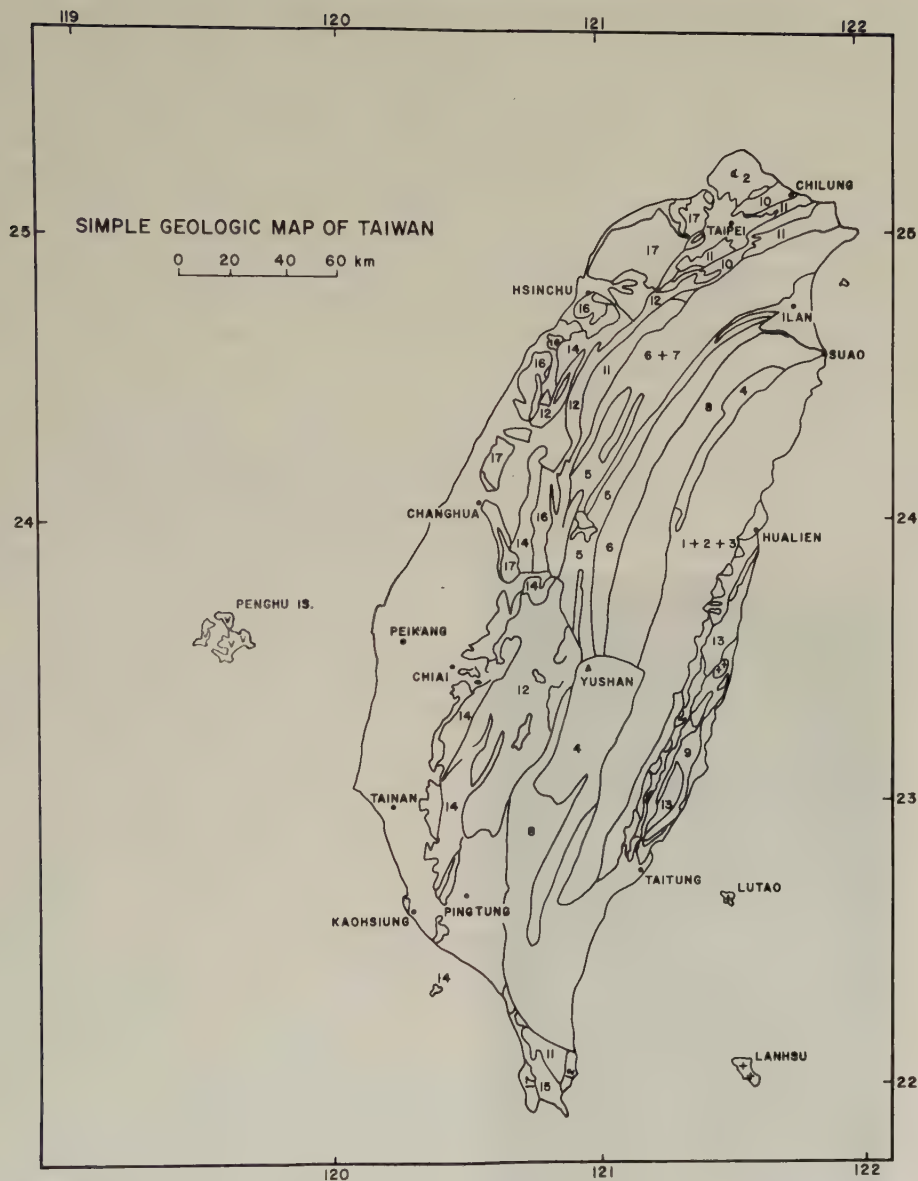


Fig. 1. Simple geologic map of Taiwan. The numbers in the figure refer to the following rock units: 1+2+3, Late Paleozoic to Mesozoic metamorphics; 4, Eocene; 5, Eocene to Oligocene; 6+7, Oligocene to Miocene; 8, Miocene; 9+10, Early Miocene; 11, Middle Miocene; 12, Late Miocene; 13, Late Miocene to Pliocene; 14, Pliocene; 15 and 16, Pliocene and Pleistocene; 17, Pleistocene; blank, Holocene Alluvium. Major cities and off-shore islands are named.

vious to the publication of this map are still valid to a large extent (Ho, 1967; CHAI, 1972; among others). In this section, we shall merely outline aspects of geology of Taiwan that will be relevant to our discussions later.

Physiographically, four provinces can be distinguished on Taiwan. These are, from

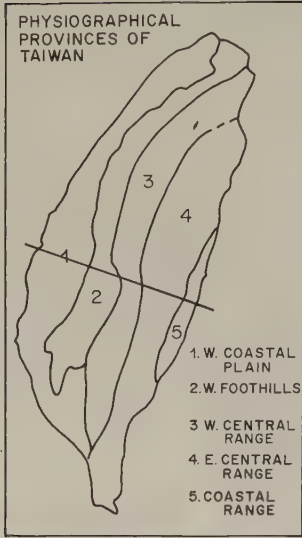


Fig. 2. Physiographical provinces of Taiwan. The line indicates the position of the profile in Fig. 4.

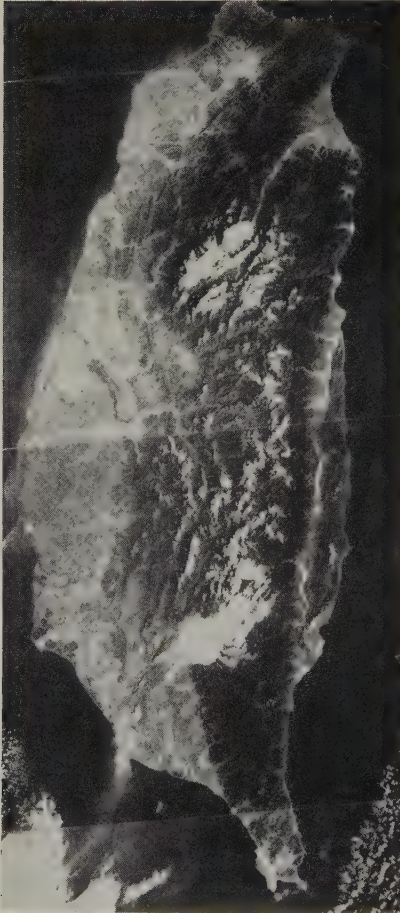


Fig. 3. LANDSAT 1 band 5 image. Notice the prominent Longitudinal Valley of Taiwan and several N-S faults. Compare this figure to Fig. 15.

east to west, the Coastal Range, the Central Range, the Foothills and the Coastal Plain (Fig. 2). The division of the provinces can be seen clearly on the LANDSAT (ERTS) image of Taiwan (Fig. 3).

The Coastal and the Central Ranges are separated by a striking feature, the Longitudinal Valley (Figs. 1, 2 and 3). The floor of the Valley is about 200 m above the sea level and has a width of 5 to 7 km. On the eastern side of this Valley the Coastal Range trends about N20°E and attains a maximum height of about 1,600 m. On the western side, the Central Range is parallel to the Coastal Range in the central and southern parts; toward the north however, it gradually turns to assume a northeastern trend. The ascent from the sea level to the respectable height of 4,000 m in the Central Range is achieved in a distance of not more than 35 km. The descent toward the west from the ridgeline is much slower; a belt of relatively low hills, the Foothills, separates the high mountains from the western Coastal Plains.

The oldest rocks crop out on the eastern side of the Central Mountains (Fig. 1): they are strongly deformed and metamorphosed and are probably Late Paleozoic to Mesozoic in age, based on a few Permian fossils. The rocks include graphite schists, quartz schists, marble, injection gneiss and paragneiss. Age dates are not yet available for most of these rocks, and, as a consequence, the Pre-Tertiary history is not clear. Some geologists believe that these rocks were metamorphosed during a Mesozoic orogeny (Biq, 1971).

A sequence of slates, phylites, quartzite, locally with irregular bodies of graphite and carbonaceous shale form the record of Eocene and Oligocene; these rocks crop out either directly to the west of the Late Paleozoic-Mesozoic metamorphic sequence or to the west of the metamorphosed Miocene strata (Fig. 1).

The Miocene rocks on the western side of the Longitudinal Valley appear very extensively in the eastern Foothills, and also in thrust blocks on the western side of the Central Mountains (Fig. 1). Miocene rocks in the Central Ranges are generally metamorphosed and they include black schists, phylites and slightly metamorphosed shales. The Miocene rocks in the Foothills and in the thrust blocks have been studied in greater details. In general they consist of alternating sandstone and shale beds; in the northern part of the Island, they are quite often coal bearing but no coal seams are found to the south of an east-west line going through Peikang (Fig. 1), near the crest of the so-called "Peikang Basement High" (MENG, 1967), and shale beds dominate in the southern part of the Island.

Pliocene rocks in the western Foothills are composed of shale, siltstone, and thin lithic greywacke in the lower part and fine to coarse grained lithic greywacke with shale in the upper part. The upper part is deemed a flysch type of deposit and the commencement of deposition of this layer is considered the beginning of the present phase of the Taiwan Orogeny (Biq, 1966; see later discussion).

Pleistocene rocks in the western part of the Island consist of two distinct facies; Early Pleistocene is represented by alternating lithic greywacke and shale, much like that of the upper formation of the Pliocene sequence, and the upper unit of the Pleistocene sequence is a thick conglomerate unit consisting mainly of boulders of Paleocene quartzite and other rocks, representing post or syn-tectonic Molasse.

East of the Longitudinal Valley the oldest rocks exposed belong to Miocene. Early Miocene andesitic agglomerates are widely distributed. They tend to form mountain ridges. Mid-Miocene and Early Pliocene rocks consist of a thick sequence (~3,000 m) of shale, siltstone, ill-sorted sandstones, and conglomerates. Late Pliocene rocks in the southern Coastal Range appear as a *mélange* composed of serpentinite, basalts, andesites,

agglomerate, limestone and sandstone (Ho, 1978). Rocks of similar nature also appear in the southern tip of the Island; although the rocks there are not as well understood as the Coastal mélange. A series of conglomerates forms the upper Pleistocene and Holocene outcrops.

As we have mentioned above that in the Coastal Range there are Miocene (K/Ar age of 17–22 my) andesites. These are the only extensive Pre-Pleistocene volcanics on the Island. The two islands to the southeast of Taiwan, Lanyu and Lutaotao are also composed of Miocene and Pliocene andesites (Ho, 1975). Judging from magnetic- and gravity-anomaly trends in the ocean (Lu *et al.*, 1977; Bowin *et al.*, 1978), these islands may link up with the andesites in the Coastal Range. In the Miocene strata of northwestern Taiwan, limited basaltic rocks and tuffs are present: the basalts occur as fissure flow or sills. Large exotic blocks of ultrabasics, serpentinites and basalts are found in the Coastal Range mélange. The age of these rocks is not clear.

A series of basaltic, andesitic, and dacitic extrusions forms a group of volcanoes, agglomerates and small intrusions in northern Taiwan (Fig. 1). Although no age dates for them are yet available, based on the inter-fingering relation with the Pleistocene conglomerates (Ho, 1968), and the uniform normal polarization of the paleomagnetic poles (Hsu *et al.*, 1966) we can give it a maximum age of 800,000 years.

It is generally agreed that the Coastal Range represents a compressed former island arc system that existed since early Miocene (Chai, 1972). During Miocene, the area west of the arc was probably a sedimentary basin not unlike the present continental shelf of Asia. The sense of subduction has been a subject of controversy; Jahn (1972) postulated an east facing arc, but later authors argued strongly for a west facing arc starting from Early Miocene (Chai, 1972; Karig, 1973). Because of the continued counterclockwise rotation of the Philippine Sea Plate, with respect to the Eurasian Plate, the trench moved westward relatively to the Asian mainland. During Miocene, as the island arc approached the continental margin, the crust near the continental margin was progressively depressed. Since the trench was apparently not parallel to the continental margin, the northern part of the depositional basin was on the continental shelf (north and northeast of the present Peikang Basement High) and the southern part was in the ocean basin; due to the thinner crust of the ocean basin, the depression was more pronounced. Such deposition and deepening continued—perhaps more vigorously—through Early Pliocene. The sources for the sediments during Miocene and Early Pliocene are mainly from the west-northwest, namely, in the area presently occupied by the Taiwan Strait (Chou, 1973).

The cessation of subduction in the vicinity of Taiwan and the collision of the island arc with the continental shelf occurred most probably in Late Pliocene. At that time, the source of sediments in the Taiwan depositional basin (both the southern and northern parts) switched from a western one to an eastern one signalling the rise of the Central Mountains. The deposition of the Pleistocene conglomerate probably represent the peak of the orogeny (Wu and Lu, 1976), although as we shall see later, the tectonics in and around Taiwan is still at a very active stage.

3. Crust and Upper Mantle Structures

The recently established telemetered seismographic network, the microearthquake surveys in various areas (e.g., Tsai and Liu, 1977) and gravity surveys in the Plains as well as along newly opened cross-island highways all provide data that allow us to determine

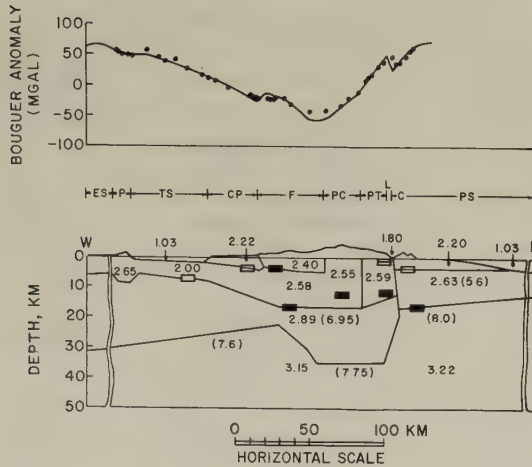


Fig. 4. Crustal structure cross-section going through Chiayi and the mid-section of the Coastal Range based on Bouguer gravity and refracted seismic phases. The numbers are densities in g/cm^3 and seismic P velocities (in parenthesis) in km/sec .

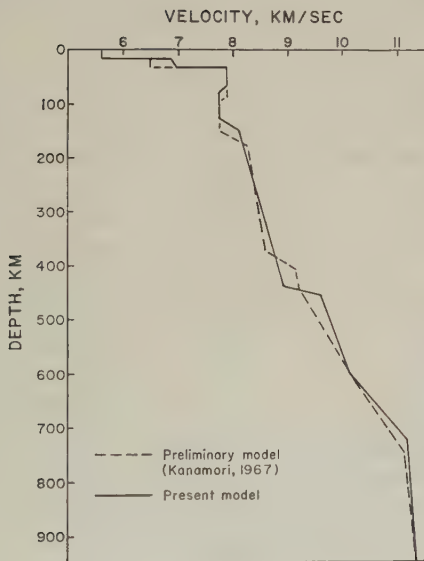


Fig. 5. Upper mantle structure determined by network $dt/d\Delta$ data compared to that under Japan (KANAMORI, 1967).

the crustal structure under and upper mantle structure around Taiwan. The present results were derived from data up to mid-1975, incorporating shallow (<7 km) reflection and refraction as well as deep well data; the details of data source and methods used can be found in Lu (1976).

Figure 4 shows the crustal structure based on gravity and seismic data. The rectangular boxes indicate seismically determined horizons. The line of profile is shown in Fig. 2 including the Peikang Basement High in western Taiwan and the middle section of the Coastal Range. The most prominent feature in this interpretation is the discontinuity

Table 1. Historical seismicity (1644–1900) ($M > 6$).

Year-Month-Date	Locations affected	Nature of damage	Int.	Mag.	Remarks
1644-7-30	S. Taiwan	Tsunami in Anping Citadel wall damaged Liquefaction of lowlands	IX-X	7	
1654-12-14	Anping*	Felt aftershocks lasted for 7 weeks			
1655	Anping	Three weeks of aftershocks Liquefaction Citadel wall cracked	VIII	6.5	
1661-2-15	Tainan Yuchin Sanhua	Many houses collapsed Ships in harbor rocked Wave breaks like clouds (Tsunami) Aftershocks lasted for 6 weeks Ground fissures	IX-X	7	
1686-5-12	Chiayi Tainan Fengshan	Houses destroyed and damaged	VII- VIII	6	
1694-4-24 5.23 (unsure)	N. Taiwan	Part of the Taipei basin subsided	IX	6.5	
1715-10-11	Chiayi Fengshan Tainan	Houses collapsed	VII	6	
1720-10-31	Tainan	Houses destroyed	IX-X	6.5-7	
1721-01-05	Chiayi Fengshan	Surface faulting Liquefaction Aftershocks lasted for 10 days	VIII	6	
1736-1-30	Changhua Chiayi Tainan Fengshan	Twin shocks Destroyed many houses	VIII	6	
1792-8-7	Tainan Chiayi Changhua Fengshan Tanshui	Meitznkeng fault activated Foreshock on prev. day Seiches Extensive liquefaction Intense shaking, houses destroyed. Followed by fire Ground cracks	X-XI	7.5	
1711-10-22	Chiayi Tainan Fengshan Tanshui	Buildings destroyed	XIII	6	
1815-7-11	Ilan Tanshui Taipei Miaoli	Liquefaction Houses destroyed	VIII	6.5	
1839-6-27	Chiayi Tainan Fengshan	12 foreshocks felt in Chiayi Chiayi completely destroyed Limited in area	IX	6.5	

Tble. 1 (Continued)

Year-Month-Date	Locations affected	Nature of damage	Int.	Mag.	Remarks
1845-2	Changhua	Houses destroyed (4,200)	VII	5.5-6	
1848-12-3	Changhua Chiayi Lukang	Liquefaction Town of Changhua completely destroyed	IX	6.5	
1862-6-7	Chiayi Tainan Tanshui	Liquefaction Ground fissures	X	7	
1867-12-18	Keelung Chinshan	10 m Tsunami in Keelung harbor Liquefaction Ground cracks	IX	7	Probably offshore
1882-12-9	Anping Tainan Chiayi	Houses and citadel walls destroyed and damaged	VII- VIII	6	Probably between Penghu and Tainan

* Historical name of Taiwan harbor, where population concentrated.

beneath the Longitudinal Valley and the Coastal Range. The velocities under the Coastal Range do not correspond to any particular known type of crusts. The top layer probably represents a sedimentary (Mio-Pliocene) layer; the second layer velocity is within the range of that for a Pacific "transition layer" (SHOR *et al.*, 1970). But the third layer in the "average" Pacific structure with velocity of about 6.8 km/sec is missing. This layer may be actually absent, but it is likely that either the refraction line is not well covered enough to detect that layer or the layer is fractured badly so that no distinctive discontinuity in velocity can be found.

The velocity structure under the main part of the Island is very similar to that of a continental crust; the mantle velocity of 7.75 km/sec is typical of a tectonically active region such as Basin and Range Province of western U.S. (HEALY and WARREN, 1968). Such value is also prevalent for the mantle under Japan (JAPANESE RESEARCH GROUP FOR EXPLOSION SEISMOLOGY, 1978).

Figure 5 shows a preliminary upper mantle structure in the area around Taiwan by inverting a $dT/d\Delta$ curve derived from the telemetered network data with earthquakes located in Japan and Ryukyu to the northeast and Luzon and Philippines to the south. The details of data and methods used can be found in LU (1976). The upper part of the structure is fairly similar to that of KANAMORI (1967), but the "400 km" and "600 km" discontinuities are somewhat sharper.

4. Seismicity

There are several different sources of Taiwan seismicity data and depending on the nature of the data, they can be used in assessing the levels of activity for different regions, the activeness of a fault or mapping faults.

In Fig. 6(a) and (b), we have shown the damage areas of large historical earthquakes and the epicenters of large ($M > 6$) earthquakes since 1900 (LEE *et al.*, 1978) respectively. For the historical earthquakes, we determined the approximate intensities and magnitudes based on a collection of descriptions of the earthquakes in various ancient documents

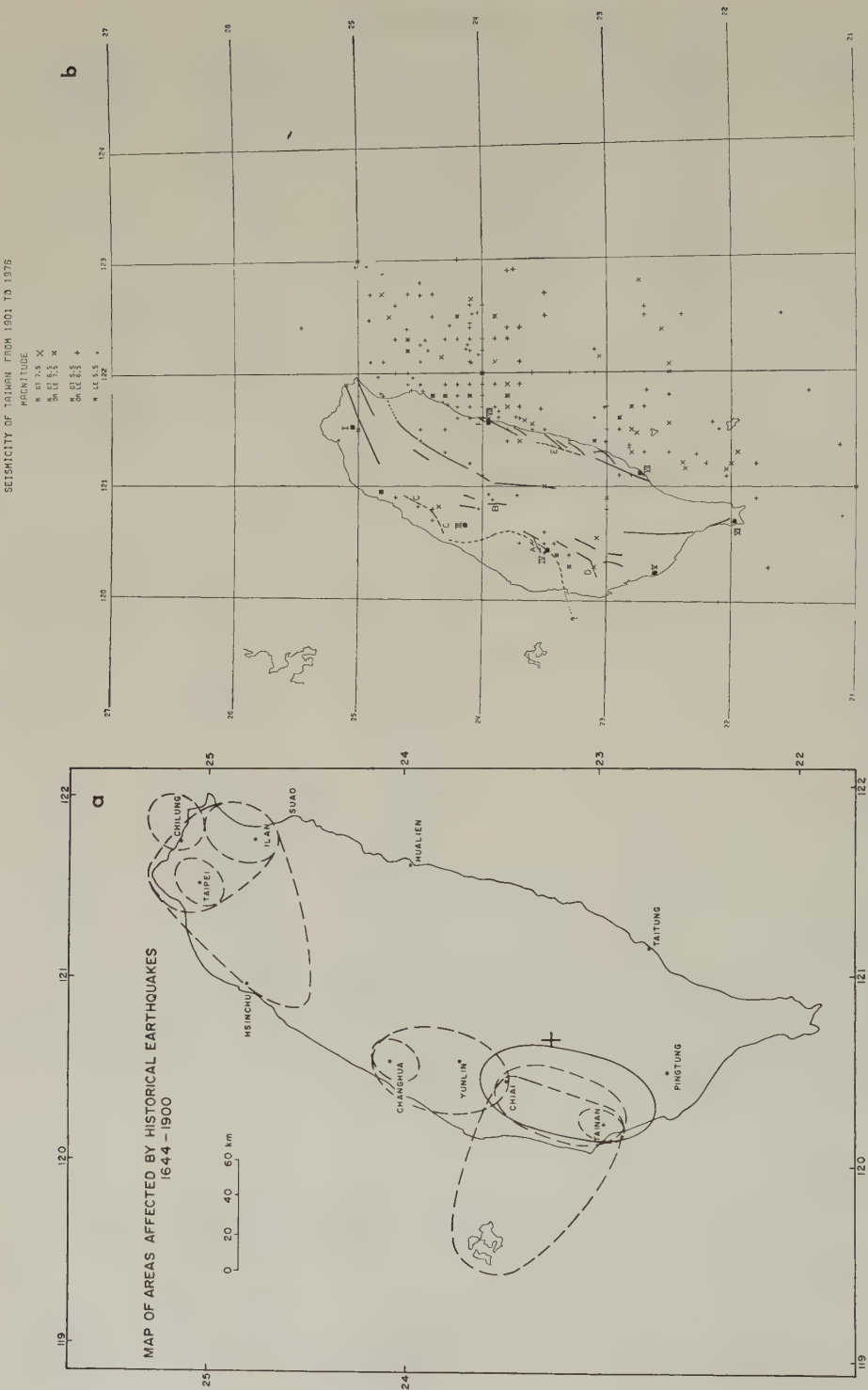


Fig. 6(a). Areas affected by historical earthquakes in the period 1644-1900.
Fig. 6(b). Instrumentally determined large ($M > 6$) earthquakes from 1900 to 1976.

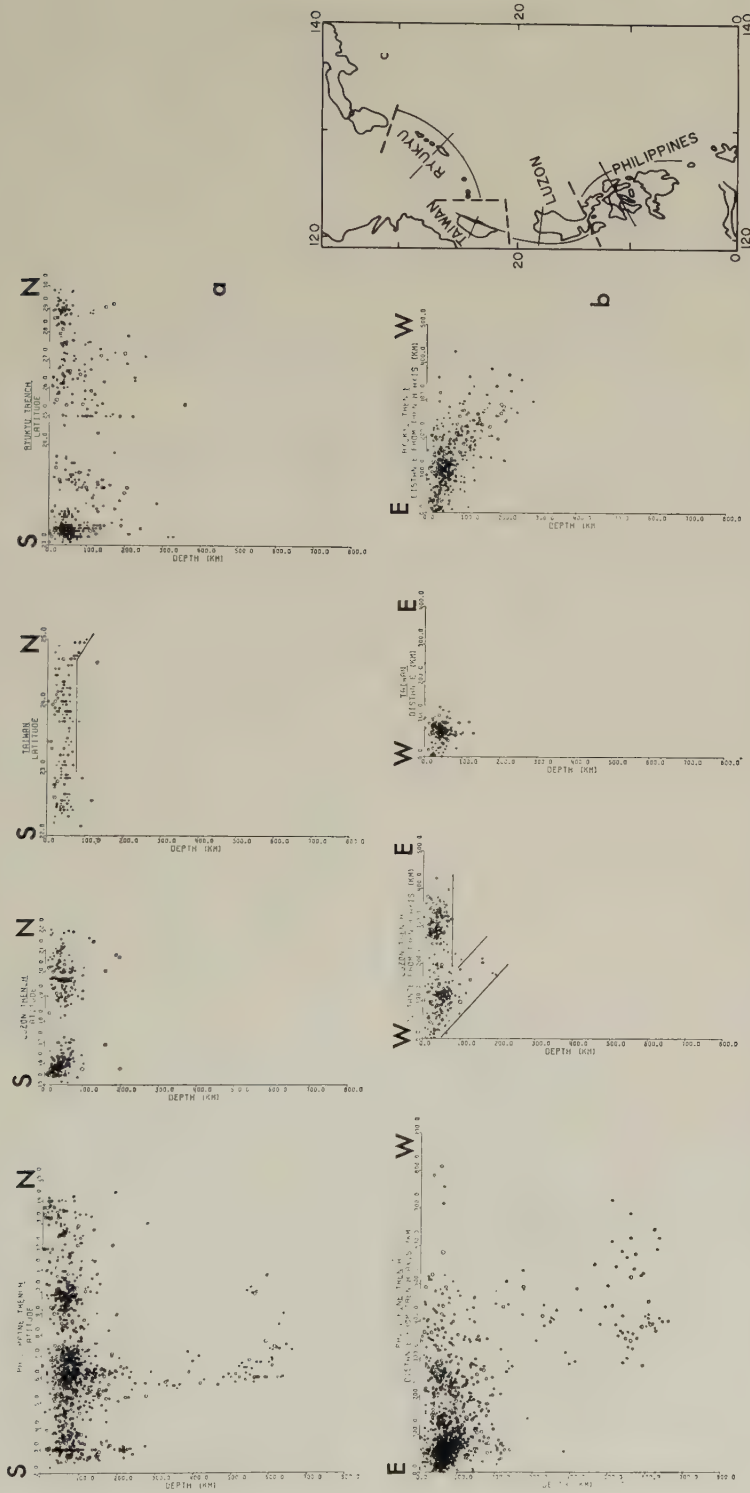


Fig. 7(a). Seismicity profiles parallel to the Philippines, Luzon, Taiwan and the Ryukyu (world-wide data from 1963 to 1974).
Fig. 7(b). Seismicity profiles perpendicular to the trenches or the main structural trend (in case of Taiwan).
Fig. 7(c). Definition of the regions; lines indicate the position of 0 ("trench") in 7(b) and direction of profiles each region.

(FANG, 1968): in Table 1, we have listed the earthquakes parameters, their associated phenomena and the cities affected. The concentration of epicenters in western Taiwan is obviously related to the distribution of Han population; the aborigines who lived in the high mountain ranges in eastern Taiwan did not keep written records. It is likely that some of the epicenters should actually be located in the Foothills. This is made evident in Fig. 6(b); here eastern Taiwan is seen to be more active. In Fig. 6(b), northern Taiwan is shown to be relatively inactive but a few earthquakes occurred in historical time; the large damage area and relatively light damage imply that the depths of these events are fairly large (perhaps 100–200 km). In Fig. 6 and in all subsequent seismicity figures, we have also plotted what we regard as active faults; these are either earthquake faults or geomorphically very prominent linear structures and geologically mapped faults. We shall refer to them in a later section, together with the possible significance of the historical seismicity.

To elucidate the nature of plate activity in the vicinity of Taiwan, we use the 1962–1974 hypocenters as contained in the Earthquake Data File (available from NOAA, U.S. Department of Commerce in Boulder, Colorado, USA).

In Fig. 7(a), we have plotted profiles parallel to Taiwan and the neighboring arcs and in Fig. 7(b) seismicity in profiles perpendicular to the island arcs are plotted. The regional definitions and the orientation of profiles for Fig. 7(b) are shown in Fig. 7(c). Toward the south end of the Philippines, the maximum depth of foci reaches 650 km; however, it becomes shallower going north, there are some gaps, but they may only be apparent ones resulting from a short time window for the data. The decrease in depth toward the north is however real and may be related to the change of rate of subduction of the Philippine Sea Plate (Wu, 1972). In the perpendicular profile, because of the superposition of the Sulu and the Philippines arc that have their Benioff zones dipping differently, the thickness of the seismic zone is rather larger than usual. In Luzon, the maximum depth of foci is about 250 km and the profile perpendicular to the Manila Trench shows in general a deepening of foci from the Manila Trench area toward the east. This is consistent with normal fault mechanisms associated with earthquakes along the Manila Trench (SENO and KURITA, 1978). Therefore, going from the Philippines to Luzon we have a change of polarity of subduction; this point has been observed by FITCH (1972) and KATSUMATA and SYKES (1969) and others. There is a section of trench on the eastern side of Luzon, where thrust faulting has been found to occur. FITCH (1972) and others have hypothesized that a nascent west-dipping subduction has started there.

Going further north toward Taiwan, the foci becomes shallower and underneath Taiwan, between the latitudes of 23°N and 24.2°N , along the whole length of the Coastal Range, there are only earthquakes shallower than 70 km; deepening of foci occur at both ends of this section. This phenomenon can also be seen from Fig. 8, a plot of seismicity with the sizes of the symbols proportional to the depths rather than the magnitude, as is commonly done. It is also clear that shallow seismicity along the Manila Trench terminates at about 21°N , a large earthquake with normal fault mechanism occurred there in 1972; between that point and Pingtung Plain (Fig. 1) there is evidently a gap. Recent local Taiwan network data show that small earthquakes do exist south of the Pingtung Plain (Y.B. Tsai, personal communication, 1978); but whether they do continue to the Manila Trench is not yet known. Northeast of Taiwan the foci deepen toward the north and merge into the earthquakes easily identified with the Ryukyu island-arc. The area

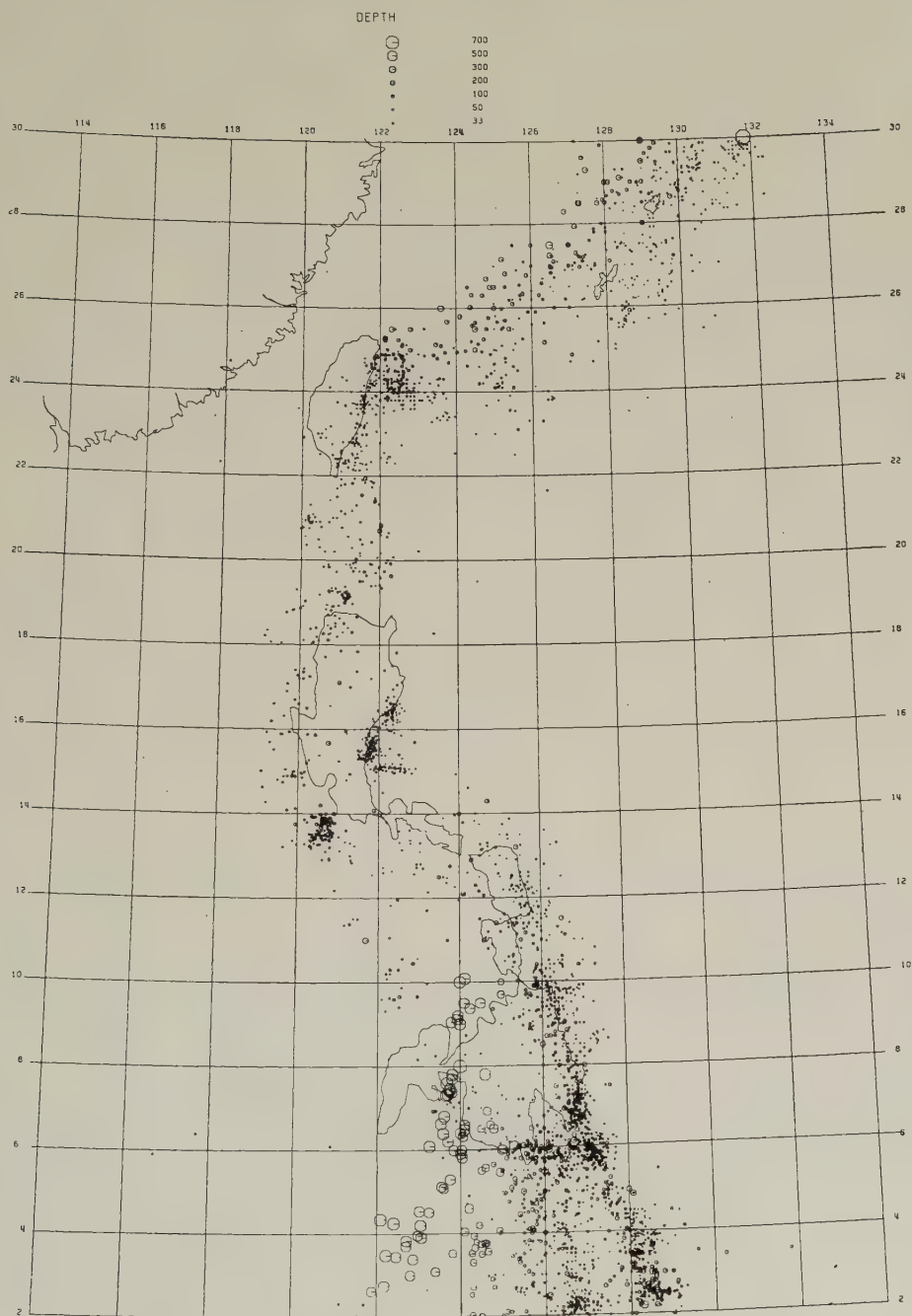
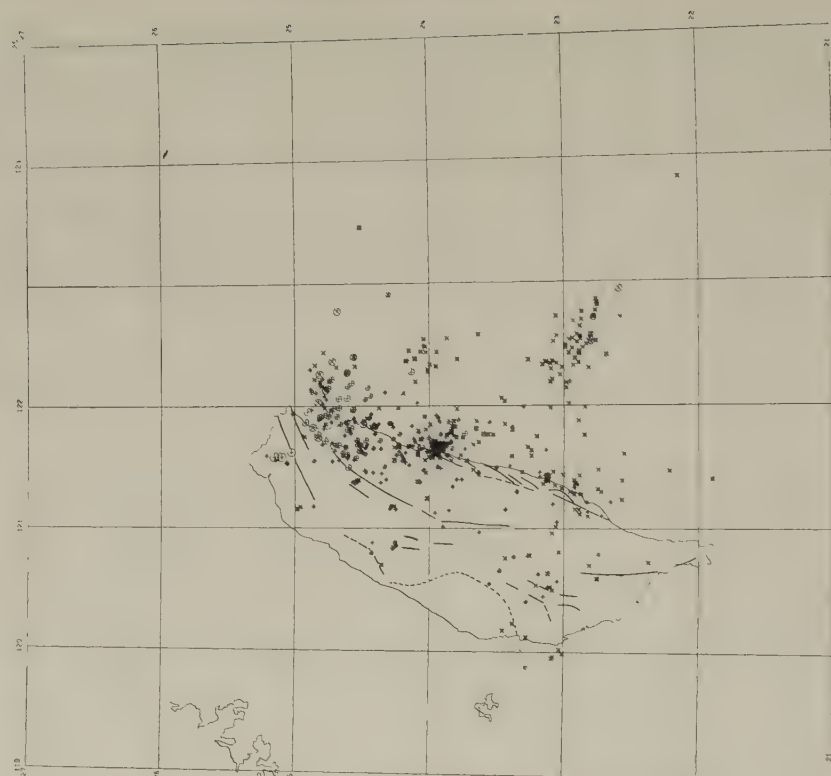
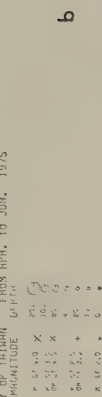
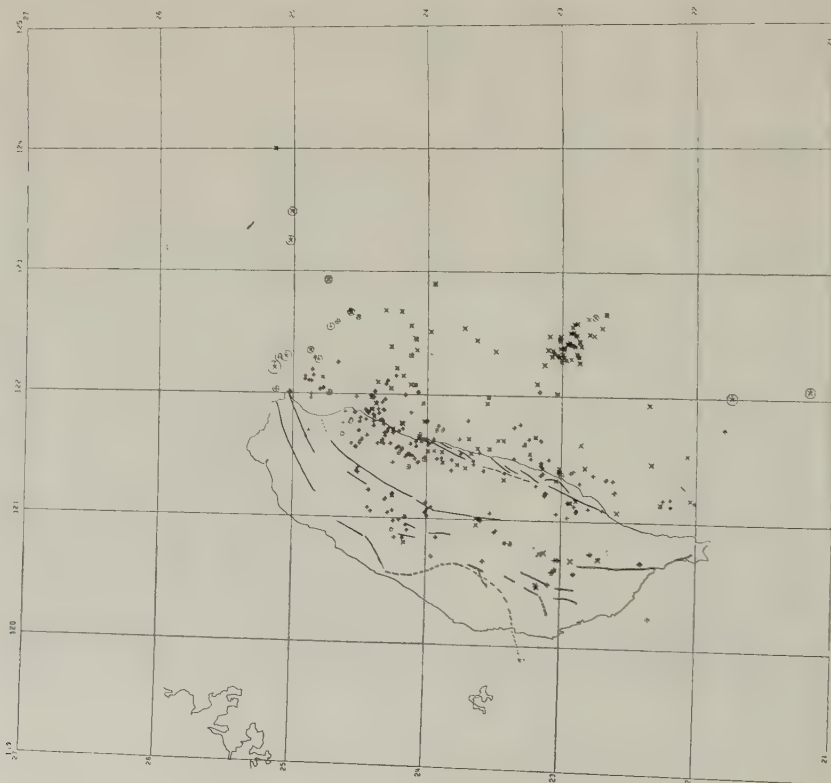
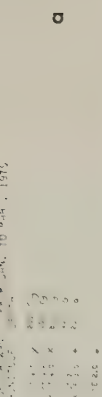
SEISMICITY OF TAIWAN, RYUKYU, AND PHILIPPINE
FROM 1901 TO 1974

Fig. 8. Seismicity along the western margin of the Philippine Sea plate in map view.

SELF-MILICIA OF TAIWAN FROM APR. TO JUN. 1975



20. *Journal of the American Statistical Association*, 1975,



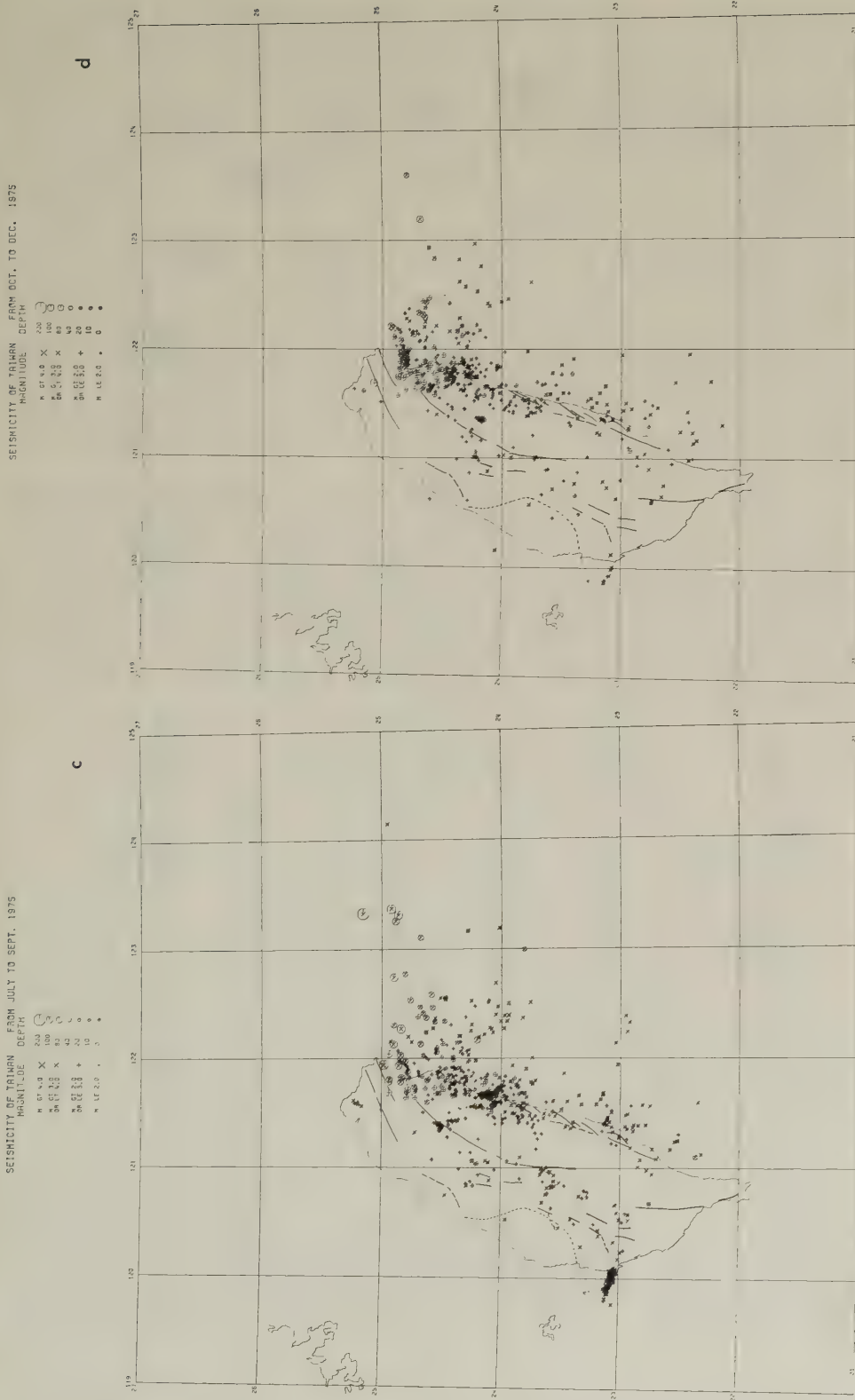


Fig. 9(a)-(d). Quaterly seismicity map of Taiwan (1975) based on a local network of 20 stations. Note that there are two symbols with each point. The circle denote the depth, the larger the deeper, and the size of the crosses is proportional to magnitude. Here it is clear that deeper earthquakes can be found in northern Taiwan and also northeast of the island.

northeast of Taiwan is noticeably more active than its nearby regions (Fig. 8), but basically it shows a north-dipping Benioff zone. It is sometimes asserted that, at present, the Benioff zone under Taiwan dips to the east or becomes vertical (LEE, 1962; JUAN, 1975; BIRD and DEWEY, 1970); from our study, it is evident that there simply is no intermediate earthquakes below the central section of Taiwan and that the deeper earthquakes to the north and to the south are associated with two Benioff zones with quite contrasting directions of dip. In this particular instance, if a cross section near Taiwan such as that in Fig. 7(b) is used, the conclusions can be misleading.

Figure 9(a)–(d) present seismicity maps based on 12 months (of 1975) data from the 22 stations telemetered network that is now in full operation in Taiwan. Several active faults shown as thick lines on land can be correlated with the location of the epicenters. The correlation will be discussed further in the section on active and inactive faults.

One interesting feature that emerges from Fig. 9 is that small but deeper earthquakes are found to occur under northern Taiwan, under the young but dormant Andesitic volcanoes. These hypocenters demonstrate that at present the Benioff zone may extend to that region. With the young age of the overlying volcanics, we may argue that the Benioff zone under it is established only recently.

Microearthquake surveys in various parts of the Island (TSAI *et al.*, 1974, 1975; LIAW *et al.*, 1973, 1974; LU, 1974) show that shallow small earthquakes are quite common. In most cases, the seismicity does not correlate well with known faults. In one area (near Tsengwen reservoir of southwest Taiwan, see LIAW *et al.*, 1974 and WU *et al.*, 1978) the density of foci decreases sharply below 8 km. It is conceivable that the high fluid pressure in the strata in Tsengwen area (S.L. Chang, personal communication, 1978) and also in other areas in the foothills (SUPPE and WITTKKE, 1977) is responsible for the microearthquake seismicity.

Table 2. Focal mechanism solutions.

Date	Origin time	Lat.	Long.	Plane 1 Az, Pi	Plane 2 Az, Pi	Dep (km)	P Az, Pi	T Az, Pi	Type	No.
130263	085004.5	24.33	122.14	169,61	349,29	67	169,16	349,74	T*	1
180164	120435.3	23.09	120.58	105,48	272,42	18	99,5	190,8	T	2
261164	102105.8	24.92	122.03	27,8	207,82	17	27,53	207,37	N	3
260465	221542.0	21.0	120.68	98,76	278,14	29	278,59	98,31	N	4
170565	171932.8	22.41	121.26	14,4	106,32	80	155,20	55,26	SS	5
120366	163119.9	24.24	122.67	24,0	294,37	42	242,50	346,25	SS	6
230366	000433.4	23.86	122.97	22,12	290,10	40	70,1	336,16	SS	7
050566	142122.3	24.33	122.50	28,7	298,8	53	72,1	343,11	SS	8
010766	055038.0	24.86	122.56	32,30	160,48	102	189,10	86,59	T	9
251067	005923.2	24.43	122.25	76,31	282,46	73	267,15	47,21	T	10
260268	105015.0	22.76	121.47	290,50	130,40	8	302,6	185,69	T	11
141170	075820.0	22.82	121.36	82,50	250,40	26	75,5	165,83	T	12
040172	031650.7	22.50	122.07	290,30	53,42	6	85,5	346,57	T	13
250172	020624.0	22.56	122.37	71,0	161,0	29	116,0	26,0	SS	14
080172	052753.7	20.95	120.26	160,40	295,34	36	249,76	136,10	N	15
170472	104944.4	24.10	122.44	320,10	140,80	48	140,35	320,55	T	16
240472	095721.2	23.60	121.55	130,40	339,48	29	247,2	340,68	T	17
220972	195727.4	22.37	121.16	6,5	265,70	8	203,40	355,45	T	18
091172	184113.0	23.87	121.61	18,50	160,44	22	175,10	87,22	T	19
230375	073236.5	22.74	122.80	148,7	237,3	21	103,5	193,5	SS	20
230575	160149.2	22.70	122.57	140,0	230,5	6	95,4	185,4	SS	21

*KATSUMATA and SYKES (1969).



Fig. 10. Summary of focal mechanisms of large earthquakes ($M > 6$) from 1963 to 1975, superposed on bathymetry in the vicinity of Taiwan. The numbers beside the mechanisms correspond to those in Table 2.

5. Focal Mechanism Solutions

Two sources of data are available for focal mechanism solutions in this work. They are (1) world-wide Standard Seismograph stations plus the local Taiwan network of fifteen stations equipped with relatively old instruments (such as Wiecherts and Omori's), for

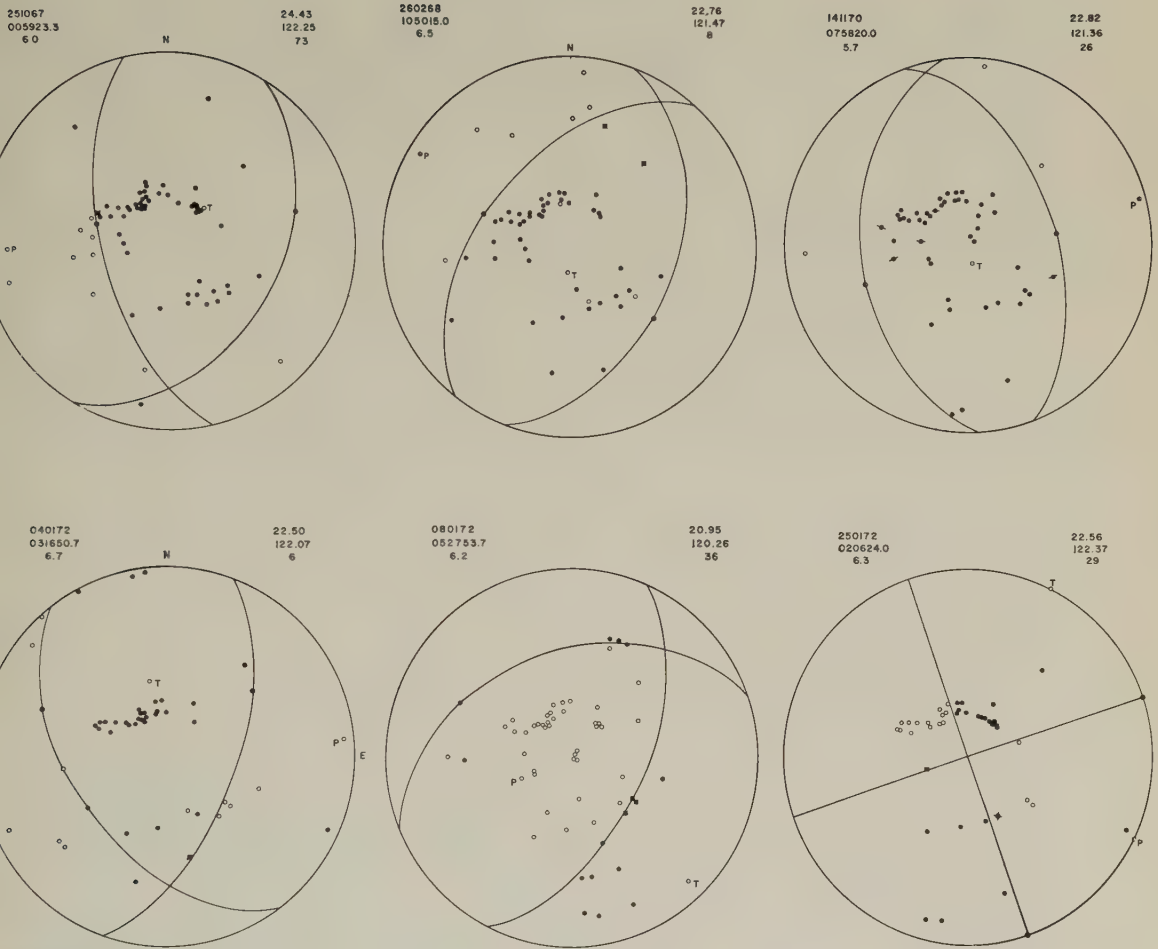


Fig. 11. New focal

events with $m_b > 5.8$ in the period of 1963 to 1975, and (2) microearthquake data for small events in the period of January 1973 to December 1974.

Some of the solutions in the vicinity of Taiwan, utilizing the WWNSS data have already been published (KATSUMATA and SYKES, 1969; WU, 1970; SUDO, 1972). In Table 2 we have listed the previously published solutions as well as new data. It should be pointed out that 1972 is an important year in earthquake data for Taiwan, in that several mechanisms cleared up what had previously been only a conjecture. In Fig. 10, we have presented the data both in terms of interpreted slip vectors (in case of thrust faults), horizontal projections of pressure or tension axes (in case of 45° thrusts or normal faults) or displacement vectors (when the solution indicates strike-slip faulting). The new solutions themselves are presented in Fig. 11.

Earthquakes 6, 7 and 8 represent a distinct group at the junction of Ryukyu and Taiwan. WU (1970) has inferred them to be right-lateral strike-slip fault(s) based on bathy-



mechanism solutions.

metry. Subsequently, results from a reconnaissance cruise in that area by R/V Hunt (WAGEMAN *et al.*, 1970) found right-lateral displacement in the shallow sediments; it is possible that these observations are related. Recently, more ocean bottom reflection data have been accumulated and a north-south zone of disturbed sediments and troughs have been found in the epicentral area of those earthquakes and indicate that a north-south structure underneath (LU *et al.*, 1977). SUDO (1972) on the other hand, believes that these earthquakes are associated with the extension of the left-lateral Central Philippine Basin Fault (HESS, 1946), which is apparently an inactive feature at present and has been interpreted, based on magnetic profiles as ancient ridges (UYEDA and BEN-AVRAHAM, 1972). SUDO (1972) used G-wave radiation pattern from the March 12, 1966 event (No. 6 in Table 2) to support his conclusion. By using more stations for a similar study, we have found a dominant lobe of G-wave radiation pattern in the N 20°E direction (Fig. 12); this maximum represents the direction of growth of the fault, which is not probably parallel

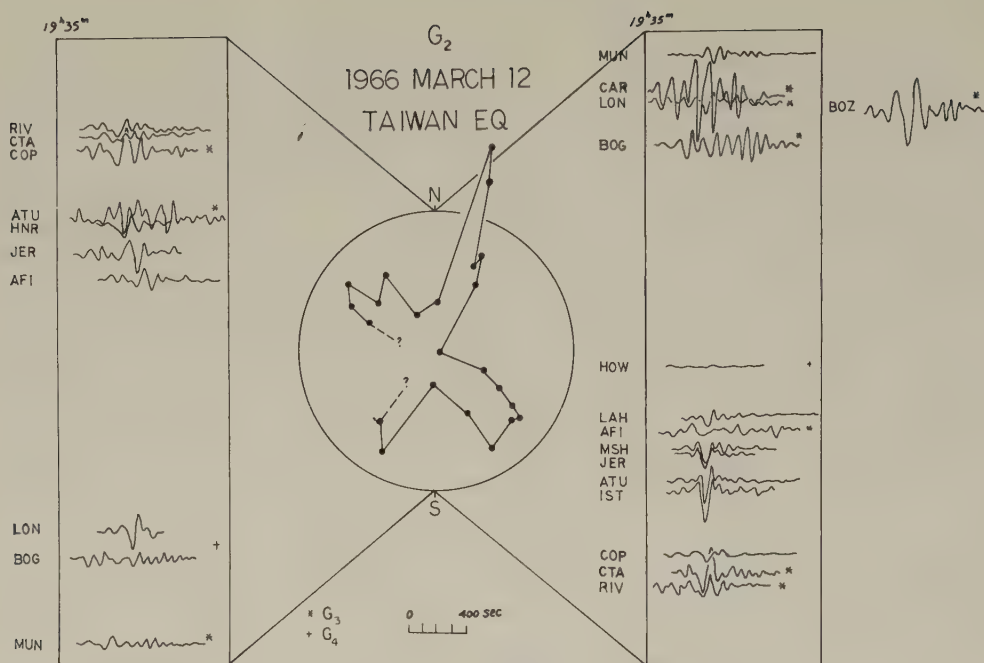


Fig. 12. G-wave radiation pattern of March 12, 1966 Taiwan earthquake.

to the strike. Although the epicenter is located toward the north side of the aftershock zone, normally implying that the rupture had propagated southward, the observed radiation pattern could have resulted from a complex rupture process with the final pattern consistent with that of a northeastward propagating fault—the long period P waves of this earthquake indicate that more than three events occurred in a series.

Earthquakes 2, 10, 11, 12, 13 and 17 have thrust solutions. The fault planes for these solutions strike approximately north-south (event 17 shows NW-SE planes) and the dips of these planes range from 35° to 45° . Solutions 2 and 17 are for events on land. Solution 2 is without doubt associated with the east-dipping Chukou Fault (Fig. 1) although no fault break was observed in the field. Solution 17 belongs to an event immediately east of the Coastal Range and a thrust-type fault break was observed after the earthquake (Lu *et al.*, 1976) in the Coastal Range.

Solutions 11 and 12 are in the vicinity of each other and are consistent; but events 10 and 13 occurred in the vicinity of other earthquakes that show an entirely different solution. Thus event 13 is next to event 14 that shows a pure strike slip mechanism; event 10 is located among events 8, 1 and 16, and these represent strike-slip fault (No. 8), and shallow thrusts (Nos. 1 and 16). At first this phenomenon may appear out-of-order, but this may reflect only that this region is populated by numerous faults or weaknesses oriented in various directions and under the current stress system the motions along these faults are controlled by the stress field and the orientation and/or the characteristics of the fault plane. For example, considering events 13 and 14, representing a thrust fault and a strike-slip fault, respectively, it is reasonable that it is not mechanically advantageous to have thrust motion taking place along the fault plane of a nearly vertical strike-slip fault, so that short-

ening has to take place elsewhere, while the reason that no strike-slip motion took place along the fault plane for the 45° thrust is that the thrust plane may be highly irregular along the strike as to inhibit horizontal strike-slip motion along it. In the next section, we shall try to find the directions of tectonic stress that is consistent with these fault plane solutions.

Events 14, 20 and 21 are all very well-defined strike-slip solutions. The two events in 1975 (20 and 21) have a large number of aftershocks recorded by the local network (Fig. 9(a) and (b)). The long axis of the aftershock zone coincide with the strikes of the NW-SE plane and are therefore deduced to be left-lateral strike-slip faults.

Event 3 is outside of the Ilan-Lotung Plain and has a normal fault solution. Interestingly enough, this solution agrees well with the composite solution of a microearthquake swarm in this area (C.C. Feng, personal communication, 1975). This solution indicates the dominance of N-S tension in this area and may be important in explaining the subsidence of the EW aligned Ilan-Lotung Plain. More will be said on the subject in later discussion.

Events 1, 16 and 19 have shallow thrust or high angle thrust solutions and they are consistent with other island arc situations, where subduction is inferred. Event 9 in an intermediate depth earthquake representing down-dip tension.

Events 4 and 15 are very important events. We have seen that Manila Trench as a submarine topographical feature terminates at about 21°N ; event 15 is located very close to that point and the normal fault mechanism is consistent with that found by STAUDER (1968) below the Aleutian Trench. Event 4, on the other hand, is located on the ridge south of Taiwan; it may have the same origin as event 15. Event 15 strengthens the argument that the Manila Trench is still active and the eastward subduction under Luzon is still taking place.

Many microearthquake surveys have been conducted in areas where seismicity data are required for planning or designing purposes. An extensive survey in the Longitudinal Valley, however, was conducted purely for geological reasons (Lu, 1976). These data have become an important supplement of seismicity in land areas where large earthquakes are infrequent. Due to the small number of stations used for each earthquake, it is not possible to obtain a solution for each event. Assuming that the focal mechanisms for a group of small events narrowly limited in space and time remain the same, then we can combine data from many earthquakes to obtain a composite solution. Such solutions are not as dependable as those from one large earthquake in the region both due to the spatial incoherence and the difficulty in ascertaining the takeoff angle when the crustal structure is not known in detail.

Figure 13 presents a summary of the available composite microearthquake focal mechanism solutions. The actual solutions are included in a series of papers and reports by TSAI *et al.* (1974, 1975), LIAW *et al.* (1973, 1974), and Lu (1976). The quality of the solutions varies from good to very poor, depending on the location and number of stations, the number of earthquakes, accuracy of hypocenter determination, etc.

Solution E (Fig. 13) agrees well with solution 2 of Table 2 and Fig. 11 in being a thrust; Solution C agrees with the NE trending right-lateral surface faulting in that region during the 1935 Hsinchu earthquake (ALLEN, 1962). Solution H implies a fault almost perpendicular to the main fault (Lanyang Fault) in that region; Solution A together with aftershock data led Lu (1976) to conclude that the NNW plane is the fault plane and left-

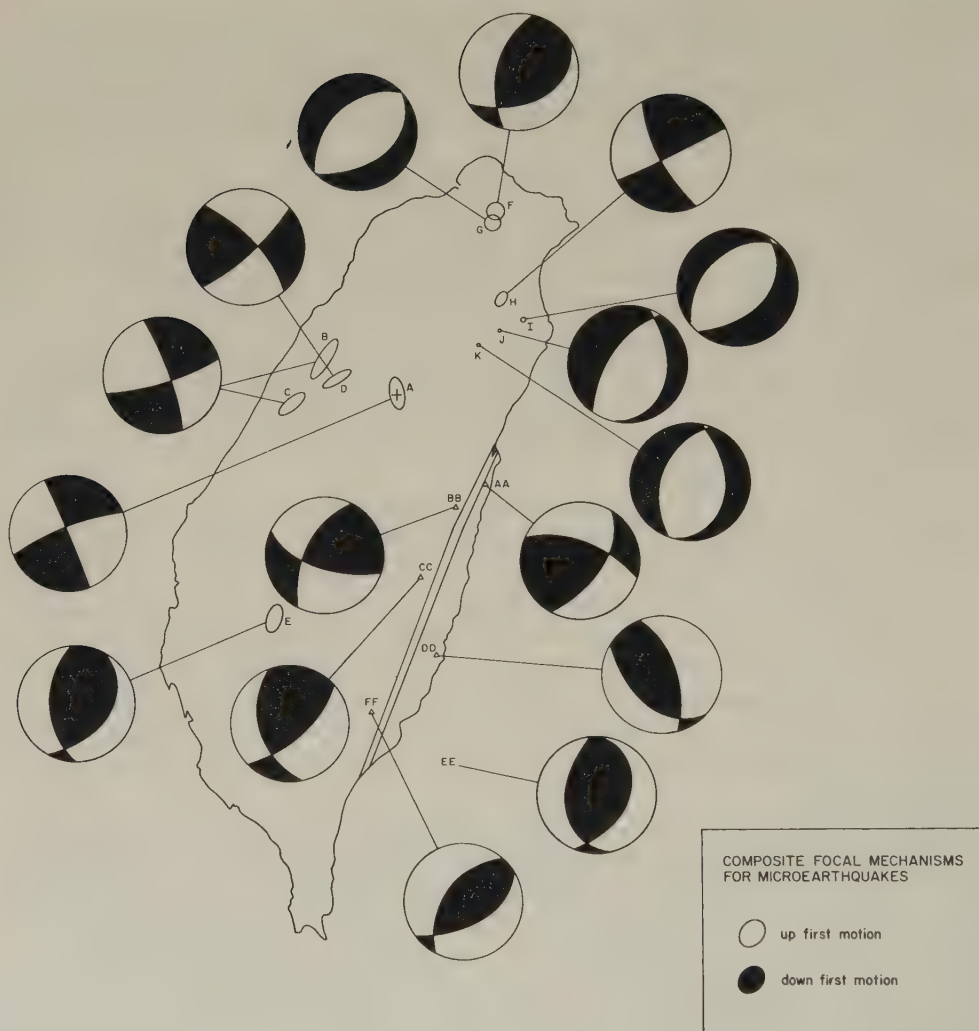


Fig. 13. Summary of composite microearthquake focal mechanism solutions. Note the characteristics of solutions. Note the characteristics of solutions in northeastern Taiwan as compared to that for solution in the rest of the island.

lateral motion took place. The juxtaposition of thrust and normal solutions in the Tatun volcanoes region (Solutions F and G) is not easily explained. The events in or around the Longitudinal Valley (Lu, 1976) produce both thrust and partially strike-slip solutions; those with significant strike-slip components are consistent with an NNE striking left-lateral fault.

6. Tectonic Stress in the Vicinity of Taiwan

As McKENZIE (1969) pointed out, individual focal mechanism solutions only put very mild constraints on the direction, not to mention the magnitude, of the earthquake-gener-

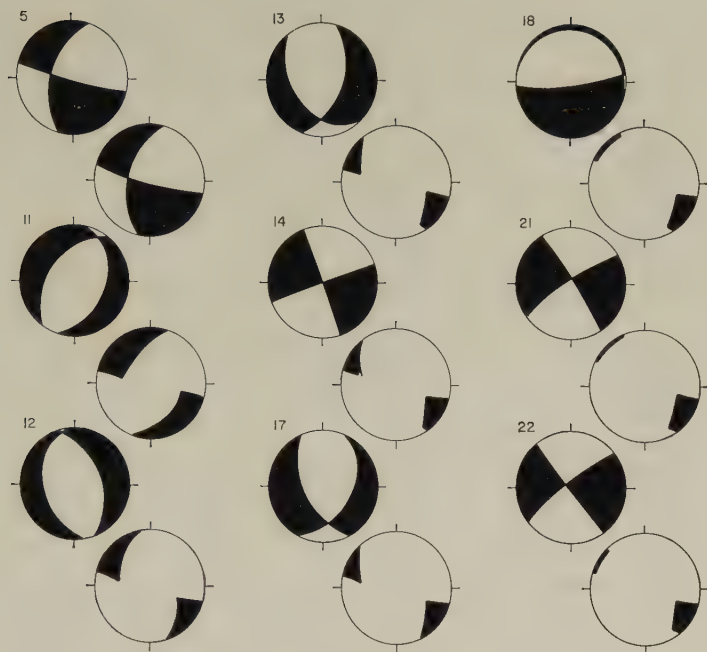


Fig. 14. Successive superposition of regions of admissible P axes to obtain a small region for P axes that satisfies all solutions. There are nine pairs of circles; the one on the left is the focal mechanism solution with region of admissible P as shaded areas; the one on the right represents the superposition of the shaded regions of the present and previous solutions.

ating stresses. Depending on the strength of the fault, the exact location of the true P axis, for example, can be somewhere in the quadrant with downward first motion. In particular, if the strength of the fault is 0, then P can be located anywhere in that quadrant. When we have a number of focal mechanism solutions for a region that is tectonically homogeneous, i.e., no major change in crustal structure, and no major plate boundary crossing the area, and these solutions are sufficiently different, then we may find a region of P common to all solutions.

Figure 14 presents the result of such a superposition using nine solutions located to the southeast of Taiwan. The dark areas represent the area of P; the numbered circle represents the original solution and the circle to the lower right represents the result of successive superposition. We see that as more and more solutions are superposed, the common P region shrinks. The final result indicates that the tectonic stress to the southeast of Taiwan has a direction of $S46^{\circ}E$ to $S76^{\circ}E$ with a plunge between -2° and 15° .

Elsewhere, Wu (1978) has explored the further possibility imposing a reasonable failure criteria on faulting and thereby estimating the order of magnitude of tectonic stress. Using the same focal mechanism solutions and a combination of dehydration-related data (MURREL and ISMAIL, 1976), we have arrived at a tectonic stress of about 2 kbar.

Table 3. Active faults in Taiwan.

No.*	Name	Remarks**
1	Taipei	II, IV, VI, VII, I (1694?)
2	Chuchin	IV, VI
3	Median	II, IV, VI
4	Chuchin	IV, VI
5	Chihhu-Tuntzuchio	I (1935), II
6	Chelungpu	I (1917), III, IV, V
7	Shuilikeng	III, VI
8	Shuilikeng	III, VI
9	Yichu	I (Inferred by the many earthquakes in the vicinity), VII, VIII
9a	Meitzakeng	I (1792 (?), 1906), II, IV, VII, VIII
10	Chuko	I (1964, may be others)
11	Chutouchi	IV, VI, VII, VIII
12	Hsinhua	I (1946), III, VII
13	Chukon	IV, VI
14	Chutouchi	IV, VI, VII, VIII
15	Chaochou	II, VI, VII
16	Longitudinal Valley	I (1951), II, III, IV, V, VI
17	Longitudinal Valley	I (1951), II, III, IV, VI

* Refers to numbers in Fig. 15.

** Roman numerals refer to the following criteria used in judging the fault as being active: I, historical earthquake (date) occurred in the vicinity; II, mapped by microearthquake survey; III, quaternary movements inferred; IV, geologically mapped; V, geodetic movement measured across the fault; VI, prominent on LANDSAT image; VII, mapped by reflection seismic method; VIII, encountered in borehole.

7. Active Faults and Recent Uplifts

In Fig. 15, we have shown what we judge to be active faults, and the basis of judgement is listed in Table 3.

One of the most discussed features of Taiwan is the Eastern Longitudinal Valley (Hsu, 1962; ALLEN, 1962; BIQ, 1965, 1971; YORK, 1976). It is no doubt one of the most important structural elements of Taiwan. It separates the Paleozoic-Mesozoic metamorphic rocks from the Post-Miocene island-arc-associated sedimentary and volcanic rocks. However, due to the rapid erosion rate and the thick alluvium cover in the Longitudinal Valley, exposures of actual fault contact is rare (Hsu, 1962; YORK, 1976). Consequently, the exact nature of the boundary is still being discussed.

Fault breaks associated with two earthquakes in 1951 proved that at least the part of the eastern side of the northern part of the Valley is fault-bounded and there are both strike-slip and dip-slip components along a high angled east-dipping plane (Hsu, 1962). Hsu (1962) reported on a segment of fault scarp on the eastern side of the Longitudinal Valley that has only thrust motion on it. YORK (1976) observed a thrust contact further south, and he postulated that one segment of a fault contact on the western side of the southern Longitudinal Valley is actually the continuation of the fault that broke during the 1951 earthquakes. Unfortunately, in 1951 the quality of the seismic stations around the world or in Taiwan was not yet good enough for dependable focal mechanism and since the establishment of WWNSS only one large earthquake occurred in the vicinity of the Longitudinal Valley (mechanism No. 17), and the solution shows a pure thrust.

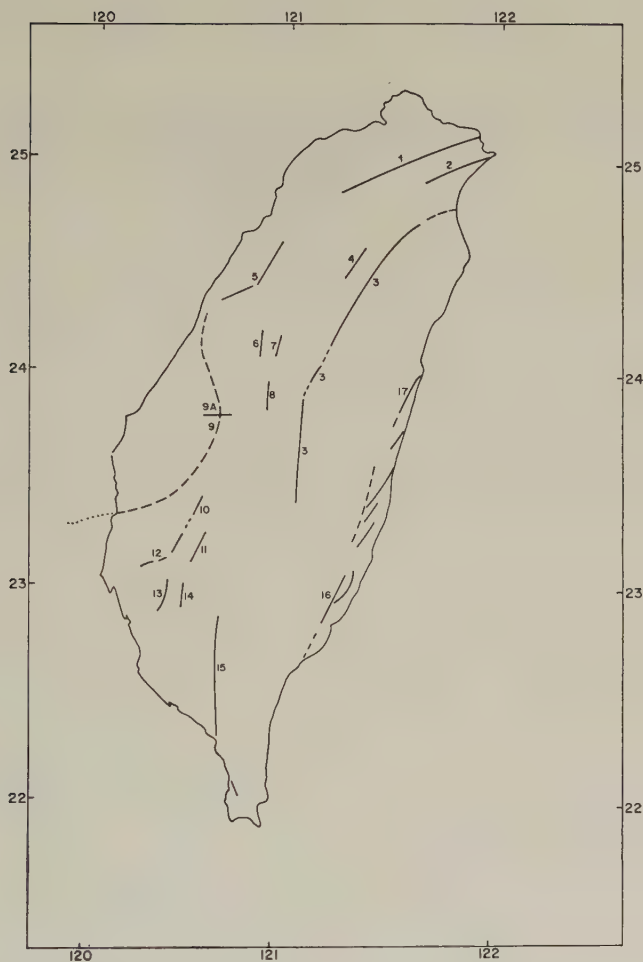


Fig. 15. Active faults of Taiwan. The criteria for judging them to be active are listed in Table 3.

Biq discussed the tectonics of the Longitudinal Valley in some detail. He accepted Hsu's (1962) description of the eastern side of the Longitudinal Valley; however, facing the difficulty of explaining the uplifting of two rock groups of very different ages, and the condition that at some time during Late-Pliocene the Pre-Tertiary rocks on the Central Range side and the Post-Miocene rocks on the Coastal Range side were coeval, he proposed a Central Range Fault on the western side of the Longitudinal Valley, a west-dipping thrust that would allow the Central Range to rise to the present height. YEN (1965) reported the observation of a fenster on the western side of the Longitudinal Valley, that revealed the sole of such a thrust; the condition of the outcrop however, does not allow exact determination of the nature of the contact. Recent seismicity data (Fig. 16) west of the Longitudinal Valley do not indicate the existence of such a fault; the data seem to show an east dipping boundary marking the more active eastern side from the less active west, but

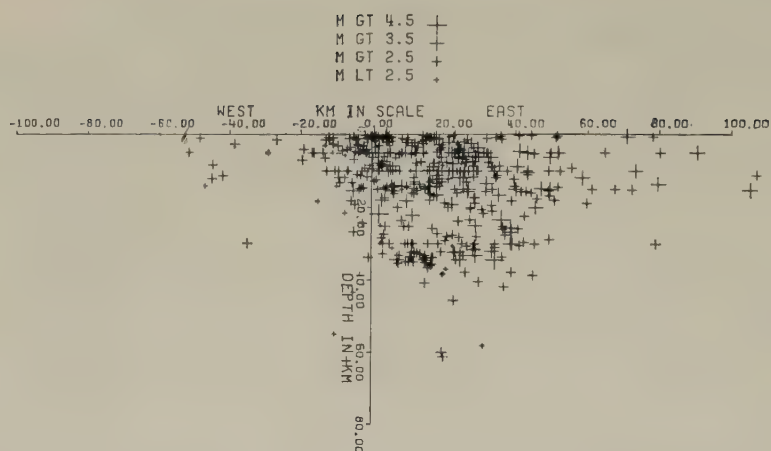


Fig. 16. Local network seismicity data between 22.8°N and 24°N plotted in a profile perpendicular to the Longitudinal Valley. Note the absence of events deeper than about 60 km.

whether this boundary is a fault or not has to be clarified in the future. Thus, although Biq's reconstruction is logical, it has not received direct confirmation from actual observation.

The structural trend of the Coastal Range is also that for the rest of the Island; most of the through-going faults run north-northeast, except north of latitude $24^{\circ}30'\text{N}$, where the faults as well as the strikes of the folds start to turn eastward. In general, those faults that separate the major stratigraphic units are most probably deep thrusts with a left-lateral component and the myriads of low angle thrusts within the Miocene and Pliocene strata in the Foothills are gravity sliding planes (Biq, 1966).

Judging from the historical seismicity, the $M > 6$ earthquakes from 1900 to 1976 (Fig. 6(b)) and the recent telemetered network data, the Median Fault (Fig. 15), is still active. Judged from the stratigraphic offset and the NWW-ESE orientation of the compression axis southeast of Taiwan, this fault should have a thrust component; however, one composite solution from a group of small earthquakes along the fault near the latitude of 24°N yield a normal fault mechanism with E-W tension axis (Lu, 1976). It is interesting that near the coastal area, along the northeastern extension of this fault which was recently mapped by a microearthquake survey (Tsai *et al.*, 1975) the composite solution obtained is similar to that of an earlier large earthquake in the same region (No. 3 in Fig. 10): they both indicate normal faulting (C.C. Feng of CERC, personal communication, 1975). Although in this case the tension axis turns to N-S. This conclusion perhaps is not surprising in that this region is along the extension of the Okinawa Trough, a tensional feature, and that the Ilan-Lotung Plain is one of two areas in Taiwan that are undergoing relatively slow uplifting compared to the rest of the Island. A hinge action may take place somewhere south of 24°N .

The Median Fault is apparently offset by a (geologically inferred) east-west fault in the Central Range which was inferred from stratigraphic data and has not been directly observed (Ho, 1975). The southern section of the Median Fault is named Chao Chou Fault (CHIANG, 1971). It is also a thrust fault and is shown to be active by telemetered

network data (Fig. 9), but no large historical earthquake is known to be associated with it.

On the western side of Taiwan, there are several faults that were associated with earthquakes. These are of two types: (1) NEE-SWW trending the right-lateral faults and (2) NNE-SSW trending thrust faults (Fig. 4). The 1935 earthquake, for example, was reported to have created both types; although whether these two faults (Fig. 4) were created during one continuous process or were two separate events cannot be assured. A combined fault length of about 50 km (NAKAMURA, 1936) can quite conceivably be produced by an $M=7.1$ earthquake. The 1941 Taiwan earthquake fault and the 1964 Tainan-Chiayi earthquake fault (also called the Chukou Fault) form another such pair; the 1964 earthquake however, did not show surface faulting, and the nature of the associated faulting is deduced from the focal mechanism solution (No. 2 in Fig. 9). The 1906 Chiayi earthquake was associated with an NEE-SWW right-lateral strike-slip fault (OMORI, 1907). An earthquake in 1792 (Table 1) near Chiayi probably occurred along the same fault, one person was reported to have fallen into a crack near Meitzukang (FANG, 1968). For an earthquake in 1917 in central Taiwan, no report on surface faulting had been found, but a leveling line across one of the major faults in the area showed a 15 cm maximum increase in elevation over the fault (IMAMURA, 1935).

A number of $M>6$ historical earthquakes cannot easily be correlated with exposed faults, but the estimated epicenters seem to line up in the vicinity of the Yichu marginal fault surrounding the Peikang basement high (MENG, 1967 and Fig. 15). The nature of faulting associated with earthquakes in this region has to be resolved in the future.

The gravity sliding faults are generally thought to be inactive, because they are not connected to deep-seated fractures. However, insofar as they are weak-zones, if they happen to overlie active unexposed faults or as the region is being strained they could be reactivated; the total displacement may not amount to much in this case.

That Taiwan and its vicinity is tectonically very active can also be judged from the rate of uplifted coastal terraces. LI *et al.* (1978) have recently dated by the C^{14} method a number of new coral samples from the eastern side of the Coastal Range and around the Hengchun Peninsula; by adding these new terrace age data to data published by LIN (1969) and TAIRA (1975), the uplifting rates of the Coastal Range, the Hengchun Peninsula and northern tip of the island have been determined. Figure 17(a) shows the unreduced data set and the sea level data as determined by MORNER (1976).

Figure 17(b), (c) and (d) show the rate of uplift of eastern, southern (including southwestern) and northern Taiwan respectively. While eastern and southern Taiwan have a rate of about 5 mm/year, northern Taiwan underwent an episodic history for the last 8,000 years. We shall discuss the significance of these rates in the next section.

8. Plate Boundaries Near Taiwan

Taiwan represents an unique situation in the Circum-Pacific tectonics. For most of the cases where oceanic plate is subducting at the continental margin, the island arcs created on the non-subducting side are relatively low in topography and the highs are the isolated volcanic peaks. Taiwan, however, is composed mainly of miogeosynclinal sediments and they have been subjected to extraordinary compression to become high mountains.

Currently the region is seismically very active and it is difficult to define a single

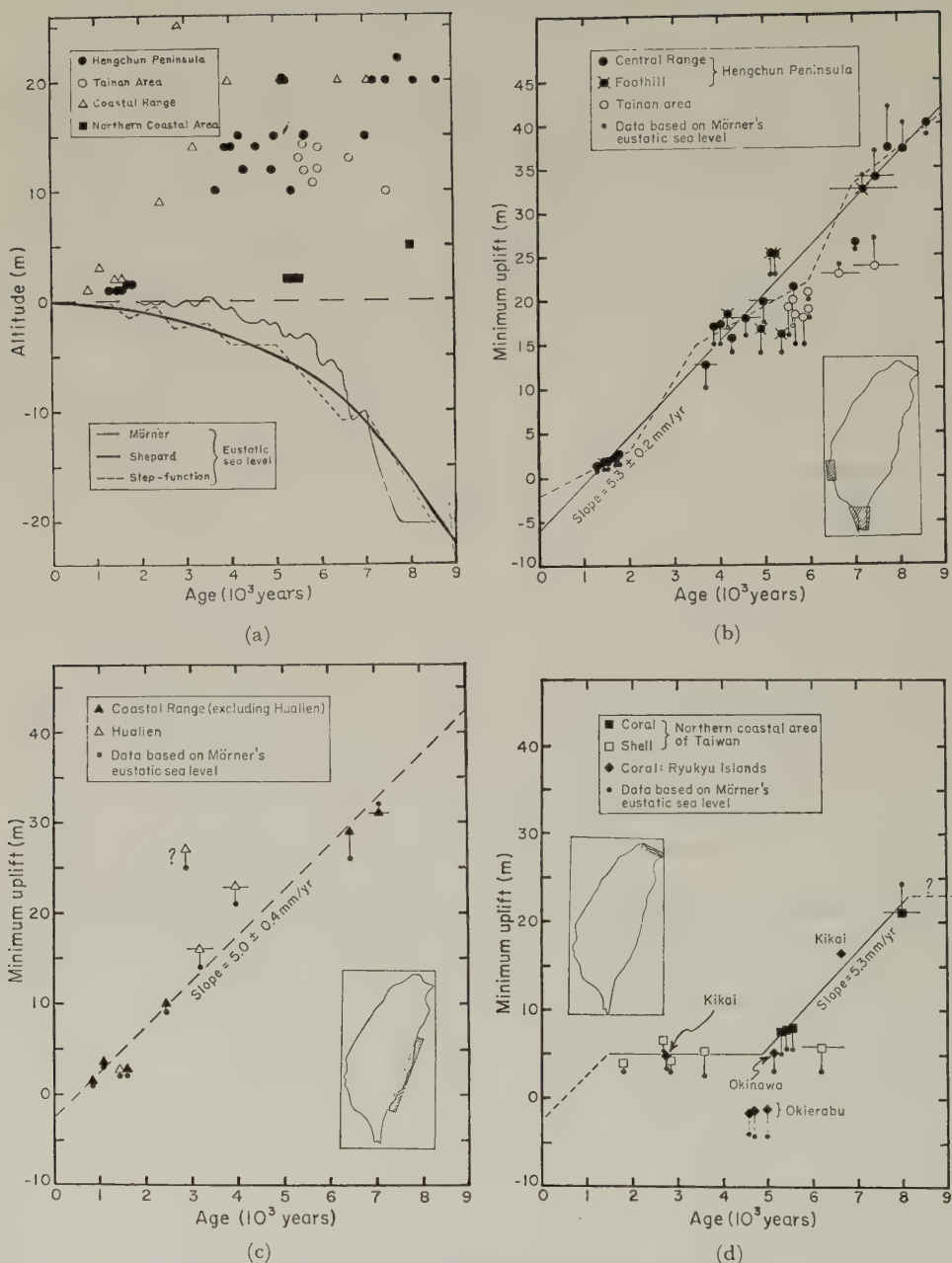


Fig. 17. (a) C^{14} dates and altitudes of the raised coral reef samples. Bottom half presents the sea level change curves (PENG *et al.*, 1977). (b) Minimum uplift (= altitude of coral reef + eustatic sea level relative the present sea level) vs. the age of samples from Hengchung Peninsula and Taiwan area. The dotted line represents a proposed step-wise rise of the Hengchung Peninsula. (c) Minimum uplift vs. age for eastern coast of Taiwan. (d) Minimum uplift vs. age for northern coastal area and the Ryukyu Islands.

continuous plate boundary based on seismicity alone. On the contrary, shallow earthquakes reveal a complex deformation pattern in a belt about 300 km wide; unlike a typical island-arc environment, where earthquake focal mechanisms have dominantly linear distribution patterns, where Benioff zone can be clearly defined and where bathymetric features correlate well with this distribution, in the vicinity of Taiwan, there is no clear display of either focal mechanism patterns nor trenches, ridges or interarc basins.

By combining all the available data however, we can define a boundary composed of several segments that are quite different in characteristics. Not all segments are typical boundaries of plates as commonly described.

It is clear that Ryukyu arc terminates about 100–120 km east of Taiwan. Not only the Ryukyu Trench stops there, but the presence of large strike-slip faults and the sudden increase in seismicity toward Taiwan all indicate the presence of a major boundary there. To the west of this boundary, a subduction zone similar to the Ryukyus exists; but judging by the offset in the E-W bathymetric ridge in the vicinity of 24°N , 122.8°E (Fig. 10), and the offset in the accretion lens as marked by the -100 m gal free-air anomaly (Bowin *et al.*, 1978), this subduction is displaced to the north, relative to the Ryukyus. Further to the west, this subduction boundary connects to the thrust-left-lateral Longitudinal Valley fault zone. This fault zone is not a simple transform fault, but a collision boundary with a transform component. It is very difficult to define a plate boundary between 21°N and 22.8°N ; here we have a hint of a subduction zone with deeper earthquakes under the offshore volcanic islands to the southeast of Taiwan, but there is an apparent lack of $M > 4$ shallow earthquakes along the extension of the Manila Trench; perhaps subduction is now halted and collision is taking place involving a broad zone of deformation.

In Fig. 18, we have sketched the nature of the plate boundary in the Ryukyu-Taiwan-Luzon areas as it is understood.

The kinematics of the right-lateral fault that terminates Ryukyu is not entirely clear. KARIG (1973) considers its formation to be a consequence of the opening of the Okinawa Trough. The difficulty with this explanation is that the Okinawa Trough evidently extends all the way to the Ilan Plain as shown by the focal mechanism and other data, and thus, if back arc basins do imply active spreading, there is no significant differential spreading between the Okinawa Trough behind the Ryukyus and its westward extension. Also, since the faults, as indicated by the focal depth of earthquakes are at depths of 50 km or so (Table 2), it is probable that only the subducting plates are involved; according to Karig's hypothesis, the upper plates are the ones in differential motion.

There is a possible alternative explanation. Because of the complex geometry and the changes in the nature of the plate boundaries near Taiwan, the tectonics here cannot be accounted for fully by purely rigid plate motions. Consider the generally north-westward motion of the Philippine Sea Plate here (Wu, 1972; FITCH, 1972; SENO, 1977), the northward component of this motion can proceed quite expectedly through subduction, the westward component is practically halted by the collision. This collision results in intense intraplate deformation near Taiwan; on the island the mountain building is vigorously taking place and in the ocean the plate is undergoing E-W compression and left-lateral strike-slip fault along NW planes before subduction. Both the compression and the strike-slip faulting would cause a congestion; as there is no prominent topography in the ocean immediately east of Taiwan, the rate of subduction northeast of Taiwan, west of longitude 122.7°E must be higher than that east of 122.7°E ; thus, there is a differential motion along 122.7°E and the sense should be right-lateral.

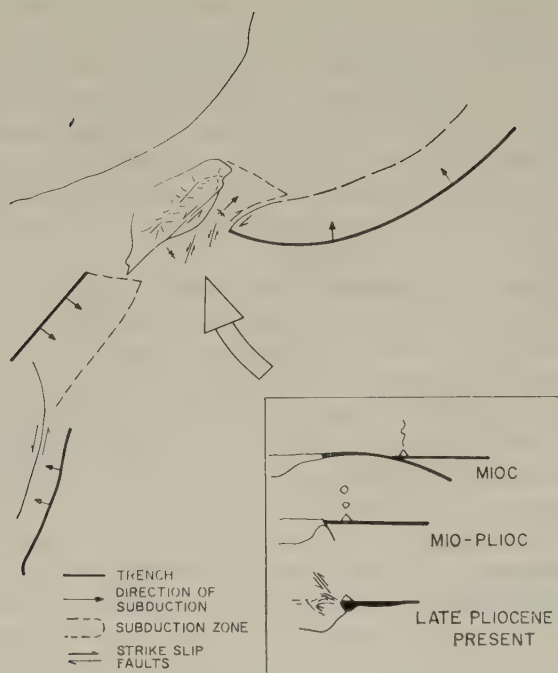


Fig. 18. Schematic plate boundaries and subduction zones in the vicinity of Taiwan.

The subduction zone and the strike-slip faults between Taiwan and the Ryukyus evidently are developed only recently, perhaps within 2 mybp; the absence of volcanic islands and wellformed interarc basins over this zone may be the result of this young age. As the subducted lithosphere is a part of the Philippine Sea Plate, the westerly component of the motion vector of the plate, the deeper part of this zone moves west. This motion is somewhat restricted, because the top of the zone is practically stopped by the collision. This western extension reaches under the northern extremity of Taiwan, and is obviously responsible for the andesitic volcanism there.

The collision-transform boundary is perhaps not as sharp as it is sometimes thought to be. Even though the Longitudinal Valley Fault is considered to be the main plate boundary, with the continuous distribution of foci east of the Coastal Range, this boundary can best be viewed as a boundary zone of tens of kilometers wide. The recently published triangulation data across the northern part of the Longitudinal Valley (CHEN, 1974) indicates a left-lateral displacement rate of more than 6 cm/year, a value close to the rate of motion of the Philippine Sea Plate towards the north in this area; but it could also be reflecting, to a large part, displacement associated with the 1951 earthquake.

The right angle junction of the collision-transform and the subduction boundaries near Hualien has some interesting implications. For example, on the bathymetric map (Fig. 10), there is a rather prominent depression near 24°N and 122°E , and on the free-air gravity map of BOWIN *et al.* (1978) there is a corresponding low. It is tempting to conclude that these features are related to a nascent subduction zone. But the right angle

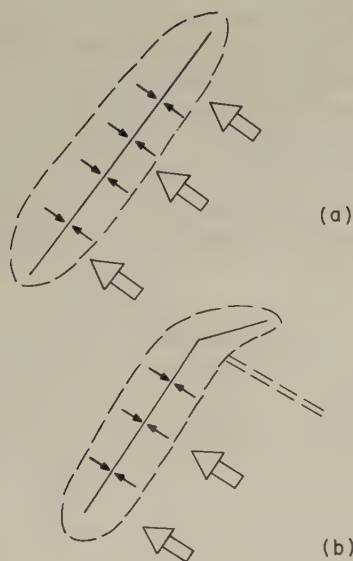


Fig. 19. Mechanism for the bending of northern Taiwan in Pleistocene.

junction of boundaries described above implies that in the vicinity of the bathymetric and free-air gravity low, the subducting plate is reaching deeper level, and while this plate is moving west and compressing Taiwan, the upper plate is not being pushed and may be decoupled from the subducting plate; thus a north-south tension feature develops. This trough is quite persistent; the high rate of sedimentation from a recently raised Taiwan has not been able to bury it.

This junction can also explain the bending of northern Taiwan toward the east as schematically shown in Fig. 19. As can be expected from the uplifting and mountain building in Taiwan, collision must have been taking place along the whole island in the early orogenic history. The commencement of the northward subduction sometime during perhaps Pleistocene causes the northern part of Taiwan to lose compression from then on, while the shortening of the rest of Taiwan is taking place; bending results from this differential compression. The modern revelation of this lack of compression in northern Taiwan is the episodic uplift of the northern coast against the steady uplift of the rest of the island in the last 8,000 years. It is also recorded in the change in fold axes orientation in the metamorphic complex near Suao (TAN, 1978).

With the normal fault type of earthquakes located in or near the Manila Trench south of 21°N and the apparently east dipping Benioff zone under the Bashi Strait and Luzon a more typical subduction plate boundary can be defined. Although complications do exist on the eastern side of Luzon, where a new subduction boundary may be forming.

9. Discussion

Taiwan is a remarkably young and active island. The present rate of uplift of Taiwan is one of the highest in the world and the seismicity is also high. Although the tectonics is not simple, the extrapolation back in time can perhaps be accomplished because of the relatively short geological history it involves.

The present orogeny of Taiwan began in Late Pliocene. That was the time when the sediments in the western Taiwan basin switched from a northwestern source to an eastern one (CHOU, 1973). Collision of the island arc with the continental shelf occurred probably at that time or may be earlier. The extensive Late Miocene to Early Pliocene sediments accumulated in the trench were raised, deformed and eroded and some were redeposited in the southern part of the trench as it was probably still deep. At the same time, the Central Mountains were gradually formed; as the slope increased, some of the sediments were redeposited in the western Taiwan basin, and some of the Miocene and earlier sediments, some not yet fully consolidated, slid off or were pushed off the slope to form part of the western foothills.

Sometime in the Pleistocene, the northward subduction near Taiwan started. The commencement time of this event can be estimated as follows: assume a maximum depth of the subduction zone to be 130 km (Fig. 7(a) and TSAI *et al.*, 1977), a lithosphere of about 50 km (TSAI *et al.*, 1977) and an average subduction rate of about 5 cm/year (SENO, 1977), then the time it takes to develop the part of the subduction zone under the lithosphere is

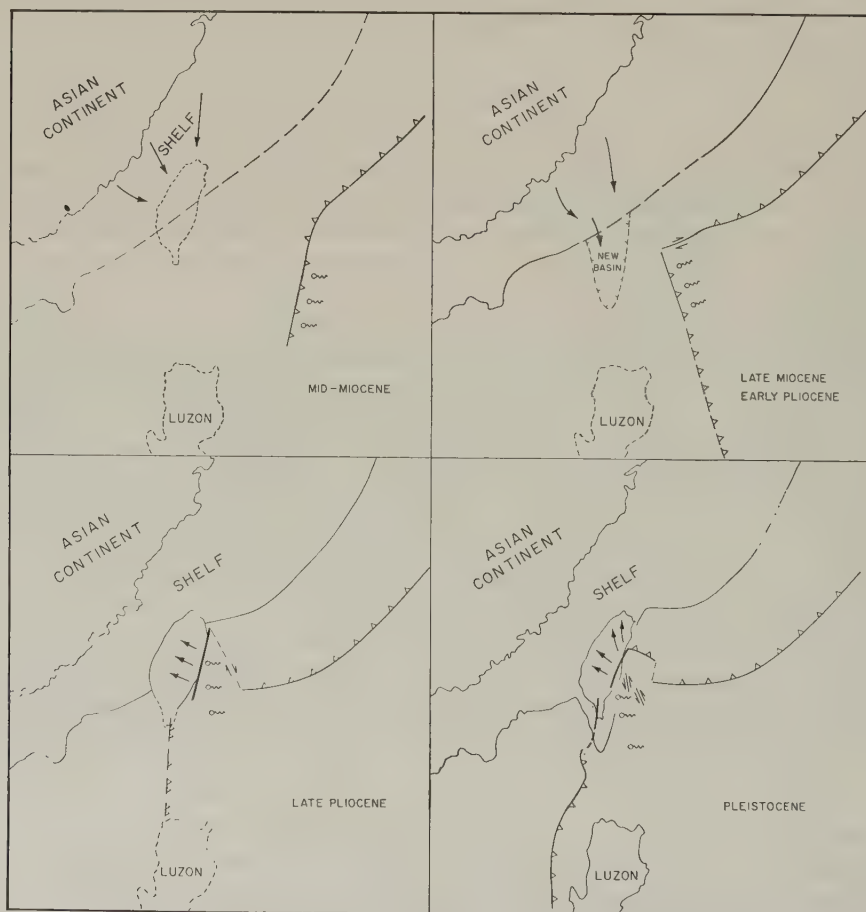


Fig. 20. Schematic time history from Miocene to present for Taiwan and its vicinity. Dotted outlines are used for location only.

about 1.6 my. This corresponds also to the commencement time of the bending of Taiwan.

It is more difficult to reconstruct the sequence of events prior to the collision. Certainly northern Taiwan, north of the Peikang Basement High had been a depositional basin on the continental shelf continuously since early Tertiary. The southern Taiwan basin however, did not receive much sediments until after the Late Miocene, and it was a basin beyond the edge of the shelf. It is quite possible that the Late Miocene "marine transgression" of the northern as well as the southern basins was a result of the advance of the island arc toward the continental shelf, whereby the shelf and the surrounding area was depressed.

Although the idea of an arc, more or less parallel to the long axis of Taiwan, moving toward Taiwan during Miocene and Early Pliocene and eventually colliding with Taiwan is widely accepted (CHAI, 1972; KARIG, 1973; BOWIN *et al.*, 1978), there is still a controversy as to the polarity of the arc. JAHN (1972) and recently Chen (J.C. Chen, personal communication, 1978) favored the subduction toward the west under the continental shelf while CHAI (1972), KARIG (1973) and others favored the subduction toward the east under the Philippine Sea. For sure, the subduction could not be toward the west just before the collision, otherwise we would expect to find traces of volcanic expressions associated with the subduction in the Central Mountains. Also it is much easier to explain the kinematics of a westward drifting arc with an east-dipping subduction zone; with the clockwise rotation of the Philippine Sea Plate (with respect to the Asian continent) an east dipping subduction zone will be pushed toward the west. An east dipping zone is consistent also with the plate boundary south of Taiwan.

Throughout the course of my work on this paper, I have benefited from discussions with many colleagues. I would like to thank Dr. C.C. Biq, C.P. Lu and Y.B. Tsai especially for sending me their preprints or providing assistance in data gathering.

This research is supported by NSF grants EAR76-14457 and INT76-20073. Part of this work was done during a research leave from SUNY-Binghamton during 1975.

REFERENCES

- ALLEN, C.R., Circum-Pacific Faulting in the Philippine-Taiwan Region, *J. Geophys. Res.*, **67**, 4795-4812, 1962.
- BIQ, C.C., Circumpacific tectonics in Taiwan, Report Int. Geol. Congr., XXI Session, Part XVIII, pp. 203-214, 1960.
- BIQ, C.C., Taiwan and Alps: An attempt at comparison of island and mountain arcs, Proc. of Sec. II, XXII Int. Geol. India, 1964, pp. 220-238, 1964.
- BIQ, C.C., The East Taiwan Rift, *Petrol. Geol. Taiwan*, No. 4, 93-106, 1965.
- BIQ, C.C., Tectonic styles and structural levels in Taiwan, *Proc. Geol. Soc. of China*, No. 9, 3-9, 1966.
- BIQ, C.C., Some aspects of post-orogenic block tectonics in Taiwan, Recent Crustal Movements, *R. Soc. N. Z. Bull.*, **9**, 19-24, 1971.
- BIQ, C.C., Transcurrent buckling, transform faulting and transpression: Their relevance in eastern Taiwan kinematics, *Petrol. Geol. Taiwan*, No. 10, 1-10, 1972.
- BOWIN, C., R.S. LU, C.S. LEE, and H. SCHOUTEN, Plate convergence and accretion in the Taiwan-Luzon Region, *Am. Assoc. Pet. Geol.*, 1978 (in press).
- CHAI, B.H.T., Structure and tectonic evolution of Taiwan, *Am. J. Sci.*, **272**, 389-422, 1972.
- CHEN, C.Y., Verification of the north-northeastward movement of the Coastal Range, Eastern Taiwan, by retriangulation, *Bull. Geol. Surv. Taiwan*, No. 24, 119-124, 1974.
- CUOU, J.T., Sedimentology and paleogeography of the upper Cenozoic system of Taiwan, *Proc. Geol. Soc. China*, No. 16, 111-144, 1973.
- DEWEY, J.F. and J.M. BIRD, Mountain belts and the new global tectonics, *J. Geophys. Res.*, **75**, 2625-2647, 1970.
- FANG, H., A review of records on earthquakes in Taiwan before the 20th Century, Collected papers of H. Fang, Taiwan, pp. 693-737, 1968 (in Chinese).

- FITCH, T.J., Plate convergence, transcurrent faulting and internal deformation adjacent to Southeast Asia and Western Pacific, *J. Geophys. Res.*, **77**, 4432-4460, 1972.
- HEALY, J.H. and D.H. WARREN, *Explosion Seismic Studies in North American*, Am. Geophys. Union Geophys. Monogr., No. 13, pp. 208-220, 1968.
- HES, H.H., Major structural features of the western North Pacific: An interpretation of H.O. 5485 Bathymetry Chart, Korea to New Guinea, *Geol. Soc. Am. Bull.*, **59**, 417-446, 1946.
- HO, C.S., Structural evolution and major tectonic forms of Taiwan, *Proc. Geol. Soc. China*, No. 10, 3-24, 1967.
- HO, C.S., Some stratigraphic-structural problems of the Linkon Terrace in northern Taiwan, *Proc. Geol. Soc. China*, No. 12, 65-80, 1968.
- HO, C.S. (ed.), *Geologic Map of Taiwan*, Ministry of Economic Affairs, Republic of China, Taipei, Taiwan, 1974.
- HO, C.S., *An Introduction to the Geology of Taiwan: Explanatory Text of the Geologic Map of Taiwan*, 153p., Ministry of Economic Affairs, Taipei, Taiwan, 1975.
- HO, C.S., Mélanges in the Neogene sequence of Taiwan, Mem. No. 2, pp. 85-96, Geol. Soc. of China, Taipei, Taiwan, 1978.
- HSU, T.L., Recent faulting in the Longitudinal Valley of eastern Taiwan, *Mem. Geol. Soc. China*, No. 1, 95-102, 1962.
- HSU, I.-Chi, J. KIENZLE, L. SIHARON, and S.S. SUN, Paleomagnetic Investigation of Taiwan aqueous rocks, *Bull. Geol. Surv. Taiwan*, No. 17, 27-81, 1966.
- IMAMURA, A., Publications of the Earthquake investigation comm. in foreign languages, No. 25, Tokyo, 1935.
- JAHN, B.M., Reinterpretation of geologic evolution of the Coastal Range, eastern Taiwan, *Geol. Soc. Am. Bull.*, **83**, 241-248, 1972.
- JAPANESE RESEARCH GROUP FOR EXPLOSION SEISMOLOGY, Regionality of crust and upper mantle structure around Japan as derived from big explosions at sea (abstr.), Int. Geodyn. Conf., Tokyo, 1978.
- JUAN, V.C., Tectonic evolution of Taiwan, *Tectonophysics*, **26**, 197-212, 1975.
- JUAN, V.C. and Y. WANG, Taiwan in relation with the tectonic framework of the western Pacific, *Acta Oceanogr. Taiwan.*, No. 1, 1-13, 1971.
- KANAMORI, H., Upper mantle structure from apparent velocities of P waves recorded at Wakayama Micro-earthquake Observatory, *Bull. Earthq. Res. Inst.*, **45**, 657-678, 1967.
- KARIG, D.E., Plate convergence between the Philippines and the Ryukyu Islands, *Marine Geology*, **14**, 153-168, 1973.
- KATSUMATA, M. and L.R. SYKES, Seismicity and tectonics of the western Pacific: Izu-Mariana-Caroline and Ryukyu-Taiwan regions, *J. Geophys. Res.*, **74**, 5923-5948, 1969.
- LEE, C.N., Distribution of earthquake foci in the Taiwan region and its tectonic significance, *Proc. Geol. Soc. China*, No. 5, 109-118, 1962.
- LEE, W.H.K., F.T. WU, and S.C. WANG, A catalog of instrumentally determined earthquakes in China ($M > 6$) compiled from various sources, *Bull. Seismol. Soc. Am.*, **68**, 383-398, 1978.
- LI, Y.H., Denudation of Taiwan Island since the Pliocene epoch, *Geology*, **4**, 105-107, 1976.
- LIAW, H.B., J.P. YANG, and Y.B. TSAI, A preliminary report on the microearthquake studies of the Chiayi-Tainan area, from April 1 to April 27, 1973, Report of Inst. of Physics, Academia Sinica, Taipei, Taiwan, 1973.
- LIAW, H.B., J.P. YANG, and Y.B. TSAI, A progress report on the microearthquake studies of the Chiayi-Tainan area, from June 1 to July 26, 1973, Report of Inst. of Physics, Academia Sinica, Taipei, Taiwan, 1974.
- LIN, C.C., Holocene geology of Taiwan, *Acta Geol. Taiwan.*, No. 13, 83-126, 1969.
- LU, C.P., Implications from aftershocks of Tachien earthquake of 24 December, 1973, Annual Report of the Institute of Physics, Academia Sinica, 1973, pp. 326-343, 1974.
- LU, C.P., Tectonics, crustal and mantle structures of Taiwan, Ph. D. dissertation, State University of New York at Binghamton, 1976.
- LU, R.S., C.S. LEE, and S.Y. KUO, An isopach map for the offshore area of Taiwan and Luzon, *Acta Oceanogr. Taiwan.*, No. 7, 1-9, 1977.
- LUDWIG, W.J., The Manila Trench and West Luzon Trough. III. Seismic refraction measurements, *Deep Sea Res.*, **17**, 553-571, 1970.
- MCKENZIE, D.P., The relation between fault plane solutions for earthquakes and the directions of the principal stresses, *Bull. Seismol. Soc. Am.*, **59**, 591-601, 1969.
- MENG, C.Y., The structural development of the southern half of western Taiwan, *Proc. Geol. Soc. China*, No. 10, 77-82, 1967.
- MORNER, A., Eustasy and geoid changes, *J. Geol.*, **84**, 123-151, 1976.
- MURREL, S.A.F. and I.A.W. ISMAIL, The effect of decomposition of hydrous minerals on the mechanical properties of rocks at high pressures and temperatures, *Tectonophysics*, **31**, 207-258, 1976.
- NAKAMURA, D., Report on the Hsinchu-Taichung earthquake of April 21, 1935, Taipei Observatory, 1936.

- OMORI, F., Preliminary note on the Formosa earthquake of March 17, 1906, *Imp. Earthq. Inv. Comm. Bull.*, 53-69, 1907.
- PENG, T.H., Y.H. LI, and E.T. WU, Tectonic uplift rates of the Taiwan island since the Early Holocene, No. 2, pp. 57-69, *Mem. Geol. Soc. of China, Taipei, Taiwan*, 1977.
- SENO, T. and K. KURITA, Focal mechanisms and tectonics in the Taiwan-Philippine region (abstr.), *Int. Geodyn. Conf. Tokyo*, 1978.
- SENO, T., The instantaneous rotation vector of the Philippine Sea plate relative to the Eurasian plate, *Tectonophysics*, **42**, 209-226, 1977.
- SHOR, G.G., Jr., H.W. MENARD, and R.W. RAITT, *Structure of the Pacific Basin, The Sea*, Vol. 4, edited by Maxwell, Part II, pp. 3-28, Wiley-Interscience, 1970.
- STAUDER, W., Tensional characters of earthquake foci beneath the Aleutian Trench with relation to sea-floor spreading, *J. Geophys. Res.*, **73**, 7693-7701, 1968.
- SUDO, K., The focal process of the Taiwan-Oki earthquake of March 12, 1966, *J. Phys. Earth*, **20**, 147-164, 1972.
- SUPPE, J. and J.H. WITTKE, Abnormal pore-fluid pressures in relation to Stratigraphy and structure in the active fold-and-thrust belt of Northwestern Taiwan, *Petrol. Geol. Taiwan*, No. 14, 11-24, 1977.
- TAIRA, K., Holocene crustal movements in Taiwan as indicated by radiocarbon dating of marine fossils and driftwood, *Tectonophysics*, **28**, 71-75, 1975.
- TAN, L.P., Pleistocene eastward bending of the Taiwan arc, *Mem. Geol. Soc. China*, No. 2, 1978 (in press).
- TSAI, Y.B., M.T. HSU, Y.M. HSIUNG, and H.P. LEUNG, Earthquake studies along the mid-section of the North-South superhighway, Report published by the Earthquake Study Group, Inst. of Physics, Academia Sinica, 1974.
- TSAI, Y.B., C.C. FENG, J.M. CHIU, and H.B. LIAW, Correlation between microearthquakes and geologic faults in the Hsintien-Ilan Area, *Petrol. Geol. Taiwan*, No. 12, 149-167, 1975.
- TSAI, Y.B. and H.L. LIU, Spatial correlation between hot springs and microearthquakes in Taiwan, *Petrol. Geol. Taiwan*, No. 14, 263-277, 1977.
- UYEDA, S. and Z. BEN-AVRAHAM, Origin and development of the Philippine Sea, *Nature, Phys. Sci.*, **240**, 176-178, 1972.
- WAGEMAN, J.M., T.W.C. HILDE, and K.O. EMERY, Structural framework of the East China Sea and Yellow Sea, *Am. Assoc. Petrol. Geol. Bull.*, **54**, 1641-1643, 1970.
- WU, F.T., Focal mechanisms and tectonics of Taiwan, *Bull. Seismol. Soc. Am.*, **60**, 2045-2056, 1970.
- WU, F.T., The Philippine Sea Plate: A sinking towel? *Tectonophysics*, **14**, 81-86, 1972.
- WU, F.T., Focal mechanisms and tectonic stresses, 1978 (in preparation).
- WU, F.T. and C.P. LU, Recent tectonics of Taiwan, *Bull. Geol. Surv. Taiwan*, No. 25, 97-111, 1976 (in Chinese).
- WU, F.T., Y.H. YEH, and Y.B. TSAI, Seismicity in the Tsengwen Reservoir Area, Taiwan, *Bull. Seism. Soc. Am.*, 1979 (in press).
- YEN, T.P., A thrust fault near Juisui, eastern Taiwan, *Proc. Geol. Soc. China*, No. 8, 97-99, 1965.
- YORK, J.E., Neotectonics of eastern Taiwan, *EOS, Trans. Am. Geophys. Union*, **56**, 353, 1976.

TECTONICS OF THE RYUKYU ISLAND ARC

Koshiro KIZAKI

Geological Laboratory, University of the Ryukyus, Naha, Japan

(Received June 14, 1978; Revised August 26, 1978)

The geological and structural contrast between the north and central Ryukyus and the south Ryukyus has been significant since the Late Mesozoic. The difference seems to correspond to that of the nature of the Philippine Sea floor facing the Ryukyus, i.e. the Daito Ridges and Amami plateau to the north and deeper basin to the south. The north and central Ryukyus were a separate tectonic unit from the south Ryukyus from the Late Mesozoic to Middle Tertiary. Subsequently they have united to form an island arc as the island groups shifted southeastwards with different rates in the Late Tertiary to Quaternary.

1. Introduction

The Ryukyu islands are a typical island arc, 1,200 km long, lying between Kyushu and Taiwan at the northwestern Pacific margin. They are composed of the Ryukyu Trench on the Pacific side, a row of islands, a volcanic belt and the Okinawa Trough on the continental margin. The islands are divided morphologically as well as geologically into three groups: the north Ryukyu Osumi islands, the central Ryukyu Amami and Okinawa islands, and the south Ryukyu Miyako and Yaeyama islands. They are separated by the Tokara Channel and the Miyako Depression, which represent strike-slip fault zones.

The structural framework of the islands was studied by KONISHI(1965). His structural zonation paralleled the zonation of the pre-Miocene basement complex of Southwest Honshu: the Ryukyu islands were interpreted as the southwestern continuation of Outer Zone of Southwest Japan modified into an echelon configuration by the left-lateral transcurrent dislocations of the Tokara Channel and the Miyako Depression. NAKAGAWA (1974) correlated the island arc system of the Ryukyu islands with that of Northeast Japan. In this paper, the author attempts to discuss the island arc system from a different point of view. Recent investigations verified that the geological and structural discontinuity of the north-central Ryukyus and south Ryukyu is significant. The geological and structural histories of both island groups are quite different throughout the period of Mesozoic to Miocene. Thereafter, the island groups united into a single island arc.

2. Basement of the Islands

The basement rocks of central Ryukyu are composed of Late Paleozoic eugeosynclinal sediments, including slate, chert, limestone and diabasic green rocks, whereas the Yaeyama metamorphic rocks-phyllite, black schists and green schists including the glaucophane schist facies rocks—are seen only in south Ryukyu.

The Late Paleozoic eugeosynclinal sediments are correlated to the Upper Paleozoic groups of Kyushu and Shikoku to the north and also to those of Taiwan to the south. The structural trend of the basement group is not necessarily parallel to the general trend of the



Fig. 1. Structural trend of the Paleozoic group in the Ryukyu Islands.

island arc but is more or less diverse (Fig. 1). The variation of the fold axes of the Paleozoic group seems to have resulted from the later dislocations than the deformations of the Mesozoic orogeny.

The Yaeyama metamorphic rocks are constructed mainly of two fold systems with different orientations. The principal fold, which trends in NW-SE direction, has a wavelength of several kilometers and is clearly oblique to the trend of the island arc. The preferred orientation of minerals is parallel to the fold axis. A minor fold with EW axes is superimposed on the principal fold. Shear zones and faults are well developed parallel to the minor fold. Blocks of the metamorphic rocks crop out locally through the Lower Miocene sandstone formation along the EW faults. It seems therefore that the EW faulting was activated parallel to the island arc in the Middle to Late Miocene.

Paleomagnetic study of the Eocene volcanic rocks reveals a clockwise rotation of 40° of the Yaeyama islands (south Ryukyu) resulting in the present NW-SE trend of the metamorphic rocks (SASAJIMA, 1977). The original trend, therefore, should be in east-west direction parallel to the present direction of the island arc.

Radiometric ages of the Yaeyama metamorphic rocks are 174 my (K-Ar method), 195 my (Rb-Sr method) (SHIBATA *et al.*, 1968, 1972). The Sambagawa metamorphic rocks representing facies similar to the Yaeyama metamorphics, have ages of 82–102 my, which are much younger than the Yaeyama rocks. But the Sangun metamorphic rocks indicate similar ages of 159–175 my. Both Sambagawa and Sangun rocks are from Honshu, Shikoku and Kyushu. The green schist of the Tananao belt of Taiwan is re-

ported to have much younger ages of 82–14 my (YEN, 1975). The Yaeyama metamorphic rocks then seem to be correlated to the Sangun rocks so far as the radiometric ages are concerned. The original sedimentary rocks are considered to be of the Late Paleozoic age but no fossils have yet been found from the metamorphic rocks.

3. *The Shimanto Belt*

The terrane of the Shimanto supergroup of Late Mesozoic to Early Tertiary age continues southwards to the north-central Ryukyus from Kyushu, Shikoku and Honshu where the supergroup signifies the geosynclinal sediments in the outer belt of Southwest Japan on the Pacific side. The upper horizon of the supergroup in central Ryukyu is composed of thick and coarse sandstones containing Eocene nummulites. The distribution of the supergroup is limited to the north-central Ryukyus, whereas calcareous littoral sediments intercalated with andesite and pyroclastic rocks of Eocene age are seen in south Ryukyu (SHIRAO *et al.*, 1976). The Shimanto supergroup of the north-central Ryukyus is severely deformed to form isoclinal folds and SE-verging thrust faults. It is also slightly metamorphosed to black and green phyllites and partly to green schists.

The Eocene formation of south Ryukyu shows different sedimentation facies from that of the northern islands and no deformation and metamorphism except mere tilting and later faulting. The area of south Ryukyu has therefore been a part of stable land mass since the Eocene sedimentation. KONISHI (1965) stated that the Eocene basin of south Ryukyu formed an inner stable zone against the Shimanto belt, which formed the outer mobile zone of the islands arc. Accordingly, the islands of south Ryukyu have had to shift more rapidly southwards so as to form the present Ryukyu island arc.

4. *Miocene and Eocene Volcanism*

The inner zone of the north-central Ryukyus represents a line of recent volcanic islands, some of which are still active forming a present volcanic front. The basement of the volcanoes is constructed usually of volcanic and pyroclastic rocks of Miocene to Pliocene age which are altered to show greenish color by hydrothermal solution. Thus, they are collectively called "Green Tuff Volcanics" of Neogene age similar to those in the main Japanese islands. Marine geological investigations demonstrated that the volcanic and pyroclastic rocks are distributed in a 100 km wide zone in the inner zone and the Okinawa Trough of the north-central Ryukyus, but not of south Ryukyu (HONZA, 1977).

Pyroclastic rocks and andesite flows are found conformably within the Eocene littoral sediments in south Ryukyu (SHIRAO *et al.*, 1976). Their occurrence seems to be similar to that of the "Green tuff" rocks, but the age is quite different. Moreover, the pyroxene andesites of south Ryukyu show a lower alkali-lime index (58.3) than those from the Miocene andesites (61.8) of the north-central Ryukyus (MATSUMOTO, 1964). The Eocene volcanism cannot be traced to Taiwan but might be correlated with that of the Philippines. Here again, the contrast of volcanism in age and character is remarkable between the north-central Ryukyus and south Ryukyu (Fig. 2).

5. *Distribution of the Yaeyama Group*

The Yaeyama group, distributed in the Yaeyama islands of south Ryukyu, the northern part of Taiwan and the Senkaku islands, is composed mainly of sandstone with

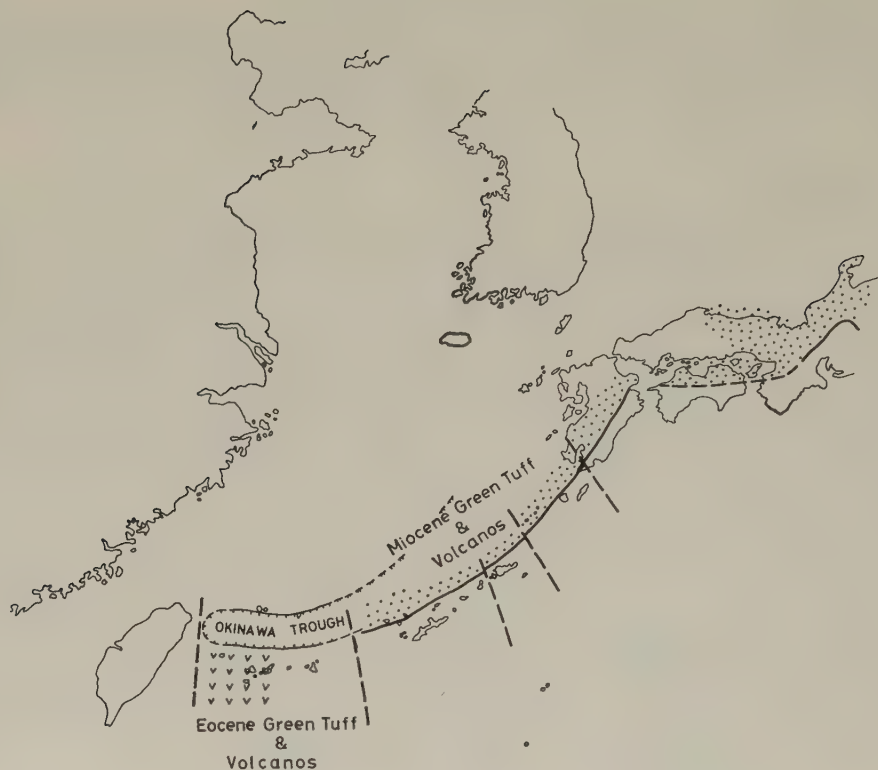


Fig. 2. "Green Tuff Volcanism" in Miocene and Eocene.

intercalations of mudstone and is characterized by coal beds, cross laminae and trace fossils signifying littoral sediments.

Palynological investigation reveals the age of the sediments to be the Lower Miocene (TAKAHASHI and MATSUMOTO, 1964). The group is correlated with the Lower Miocene series of Taiwan and northern Kyushu by the heavy mineral assemblage also (OBARA and MATSUMOTO, 1964). The mineral composition is of zircon, tourmaline, garnet, and often associated with rutile, staurolite and monazite. These minerals are probably supplied from granite and gneiss, which are never found in the neighbouring islands nor Taiwan, but are abundant in the southeast coastal area of China. Therefore, the geological development of south Ryukyu should be interpreted in connection with the geology of the southeast China.

The Yaeyama group is slightly tilted structurally and faulted. This again shows that the Yaeyama islands and their environs have been in stable conditions since Early Miocene.

6. *The Shimajiri Basin*

It is not until the Latest Miocene during the deposition of the Shimajiri group, that the north-central Ryukyus and south Ryukyu formed a common basin throughout the Ryukyu islands.

The sediments of the group, which are composed mainly of siltstone interbedded sand-

Table 1. Marine geological and structural contrast of the north-central Ryukyu to south Ryukyu around the Ryukyu islands after HONZA (1977).

	North-central Ryukyu	South Ryukyu
Okinawa Trough	Tokara volcanic belt	None
	Neogene volcanism	None
	1,000 m at the deepest area	2,200 m at the deepest area
	Amami Trough at the eastern margin	None
	Minor fault group at the western edge	None
	Thick turbidite	Thin and less
Fore-arc slope	Neogene Shimajiri group	Quaternary and Neogene Shimajiri group
	Small frontal slope swell	Big swell zone at the frontal slope edge
Ryukyu Trench	Rough morphology of inner trench slope	Smooth inner trench slope
	V valley and disturbed morphology at the bottom of the Trench	Flat bottom and turbidite

stone and tuff in the upper part, range from the Upper Miocene to the Lower Pleistocene according to the investigation of foraminiferas (LEROY, 1964; NATORI *et al.*, 1972; UJIE and OKI, 1974).

The lower portion of the group shows a deep water paleoenvironment, indicating relative rise of sea level during the Uppermost Miocene to Pliocene. Then rapid regression occurred during deposition of the upper horizon of the group on the basis of benthonic foraminiferas as well as molluscan fossils (LEROY, 1964; NODA, 1976).

Southeastward shift of the basin occurred during the Shimajiri stage accompanied by basement arching. The Ryukyu island arc formed in association with the uplift of the Shimajiri group along the arc, simultaneous with the formation of the Okinawa Trough and probably the Ryukyu Trench. This was at the end of the Lower Pleistocene.

7. Marine Geological Results

Marine geological research has been carried out around the Ryukyu islands by the Hakurei Maru of the Geological Survey of Japan (HONZA, 1977). Honza stressed that significant differences in the marine geology are observed between the southern part of Ryukyu (south Ryukyu) and the northern part of Ryukyu (north-central Ryukyus). The contrast of the geology and structure of the sea floor between the south and north-central Ryukyus around the Ryukyu islands is shown in Table 1. It is particularly apparent in the difference of the nature of the Philippine Sea floor facing the north-central and south Ryukyu.

8. Tectonic Unification of the Islands

From the above considerations, it may be concluded that the geology and tectonics of south Ryukyu differ from those of the north-central Ryukyus. The metamorphism of the Yaeyama metamorphic rocks had completed by the end of the Jurassic time and the



Fig. 3. Distribution of the Shimanto supergroup which shows an oroclinal bend at the southwestern coast of Kyushu resulted from the Kyushu western marginal shear (K.W.M.S.).

region thereafter has been in stable conditions, whereas in the north-central Ryukyus eugeosynclinal stage has continued until the end of the Paleogene and the Early Miocene age partly.

The ENE-WSW trend of the Shimanto supergroup changes almost sixty degrees to the south at the western coast of Kyushu which is called "Hokusatsu Bend" (Fig. 3). This oroclinal bend was produced by the Kyushu western marginal shear (KIZAKI, 1978) with the left-lateral shift in the Middle Miocene age after the completion of the main folding stage associated with thrust faulting. The clockwise rotation of south Ryukyu, mentioned earlier, occurred in the Oligocene time.

In Taiwan, the formations including the Lower Miocene sediments are bent to the east at the northeastern edge of the island where a right-lateral shearing of probable Middle Miocene age has been reported (YEN, 1975).

It is therefore probable that the southeastward shift of the Ryukyu proto-islands culminated in the Middle Miocene and continued thereafter, protruding relatively to the southeast between Kyushu and Taiwan. At that time the Tokara Channel and Miyako Depression were also activated as left-lateral faults. From these facts, it may be inferred that the Ryukyu islands have been shifted differentially southeastwards particularly since the Middle Miocene associated with strike-slip faults to form the modern island arc in the Plio-Pleistocene time. Prior to the Middle Miocene, the north-central Ryukyus and south Ryukyu had experienced different geological and structural histories.

I am very grateful to Dr. R.W. Murphy of Esso Exploration, Inc. and Professor S. Uyeda of Tokyo University for their critical review of the manuscript. Financial support for this work was provided by the Grant-in-Aid for co-operative Research issued from the Ministry of Education (No. 234050).

REFERENCES

- HONZA, E., An island arc activity in the Ryukyu arc and its difference in the northern and southern parts of the arc, *Mar. Sci.*, **9**, 607-611, 1977.
- KIZAKI, K., Kyushu western marginal shear and its significance, *Earth Sci.*, 1979 (in press).
- KONISHI, K., Geotectonic framework of the Ryukyu Islands (Nansei-shoto), *J. Geol. Soc. Jpn.*, **71**, 437-457, 1965.
- LEROY, L.W., Smaller foraminifera from the Late Tertiary of Southern Okinawa, *USGS. Prof. Paper*, 454-F, pp. 1-58, 1964.
- MATSUMOTO, Y., Volcanic rocks of Iriomote-jima, Yaeyama Islands, *Rep. Kyushu Univ. Exp. to the Yaeyama Islands, Ryukyus*, No. 2, 57-72, 1964.
- NAKAGAWA, H., The problems on the geological structure of the Ryukyu Islands (Part 1), *GDP News Lett.*, *II-1-(1)*, *Struct. Geol.*, No. 2, 87-92, 1974.
- NATORI, H., M. FUKUDA, and M. ISHIDA, The late Cenozoic stratigraphy by planktonic foraminiferal species in Okinawa and Miyazaki, *J. Jpn. Assoc. Pet. Tech.*, **37**, 48-53, 1972.
- NODA, H., Preliminary notes on the bathyal Molluscan fossils from the Shinzato formation, Okinawa-jima, Okinawa Prefecture, southwestern Japan, *Ann. Rep., Inst. Geosci., Univ. Tsukuba*, No. 2, 40-41, 1976.
- OBARA, J. and Y. Matsumoto, Heavy mineral assemblage of sandstones from the Yaeyama group of Iriomote-jima, the Yaeyama Islands, *Rep. Kyushu Univ. Exp. to the Yaeyama Islands, Ryukyus*, No. 2, 47-56, 1964.
- SASAJIMA, S., Paleomagnetism of the Eocene Series in the Ryukyu Islands and Southwest Honshu, with special references to the Philippine Sea Plate, *Mar. Sci.*, **9**, 19-26, 1977.
- SHIBATA, K., K. Konishi, and T. NOZAWA, K-Ar ages of muscovite from the crystalline schist of the northern Ishigaki-shima, Ryukyu Islands, *Bull. Geol. Surv. Jpn.*, **19**, 529-533, 1968.
- SHIBATA, K., R.K. WANLERS, H. KANO, T. YOSHIDA, T. NOZAWA, S. IGI, and K. KONISHI, Rb-Sr ages of several so-called basement rocks in the Japanese Islands, *Bull. Geol. Surv. Jpn.*, **23**, 505-510, 1972.
- SHIRAO, M., N. DOI, and H. NAKAGAWA, Geology of Ishigaki-jima in the Ryukyu Islands, *Geol. Stud. Ryukyu Isl.*, **1**, 21-33, 1976.
- TAKAHASHI, K. and Y. MATSUMOTO, Palynological study of the Yaeyama group of Iriomote-jima, the Yaeyama Islands, *Rep. Kyushu Univ. Exp. to the Yaeyama Islands, Ryukyus*, No. 2, 35-46, 1964.
- UJIE, H. and K. OKI, Uppermost Miocene-Lower Pleistocene planktonic foraminifera from the Shimajiri group of Miyako-jima, Ryukyu Islands. *Mem. Natl. Sci. Mus. Tokyo*, **7**, 31-58, 1974.
- YEN, T.P., Lithostratigraphy and geologic structure of Taiwan, *Geol. Paleontol. S. E. Asia*, **15**, 303-323, 1975.

EXPLOSION SEISMIC STUDIES IN SOUTH KYUSHU ESPECIALLY AROUND THE SAKURAJIMA VOLCANO

Koji ONO,* Kosuke ITO,* Isao HASEGAWA,* Kanenori ICHIKAWA,* Susumu IIZUKA,**
Toshiki KAKUTA,*** and Hiroyoshi SUZUKI****

* *Geological Survey of Japan, Kawasaki, Japan*

** *Tokai University, Shimizu, Japan*

*** *Kagoshima University, Kagoshima, Japan*

**** *National Research Center for Disaster Prevention,
Sakura-mura, Ibaraki, Japan*

(Received June 19, 1978; Revised October 13, 1978)

A series of seismological observations of explosions from 1972 to 1977 has been worked out to study underground structure and possible anomaly of wave propagation beneath and around the Sakurajima Volcano and the Aira Caldera as well as regional structure of south Kyushu. Results described in this report are summarized as follows:

1. Name, velocity and bottom depth of the identified layers are, L-1, 3.7–3.8 km/sec, 0.7–1.8 km; L-2, 4.7–4.9 km/sec, 3.3–5.6 km; L-3, 5.6–6.1 km/sec, 22 km; L-4, 7.0 km/sec, (40 km); L-5, (7.8 km/sec).

2. Two fan-shooting observations revealed following anomalies of wave propagation.

1) A large attenuation of the amplitude of seismic waves occurs under the Sakurajima Volcano and the Aira Caldera.

2) Wave velocity is likely to decrease under the Sakurajima Volcano.

3) These anomalies of wave propagation occurs at the 6 km/sec layer.

1. Introduction

South Kyushu, where a large volume of magma has erupted in the late Quaternary time, is one of the most active volcanic fields in Japan. Active volcanoes and calderas are aligned along the Kagoshima Bay and its extension to the north and south. The Kagoshima Bay has been thought to be a graben probably of a volcanotectonic origin from the following informations; the topography on land and sea bottom (ONO, 1974), the depth of the pre-Neogene basement as revealed by drill-hole data (HAYASAKA and OKI, 1971), thick sedimentary fills and negative Bouguer anomaly along the axis of the bay (CHUJO and MURAKAMI, 1976) and many pyroclastic units possibly centered in or near the bay (ARAMAKI and UI, 1976). The Sakurajima Volcano is an active andesite volcano, located at the south margin of the Aira Caldera which occupies the northernmost part of the Kagoshima Bay. The Aira Caldera was formed about 22,000 years ago following eruption of a large amount, nearly 40 km³, of rhyolite magma (ARAMAKI and UI, 1966).

Although efforts to clarify the structure of the earth's crust and upper mantle in and around Japan by the Research Group for Explosion Seismology has been continued since 1950, practically no work had been done in the Kyushu area before our group initiated this work. A series of observations for explosions were carried out every year from 1972 to 1977 except 1976 around two volcanoes, the Sakurajima Volcano and the Aira Caldera. The objective of the study was to probe into the underground structures beneath the active volcanic area as well as the regional structure of south Kyushu. The work is a part of the

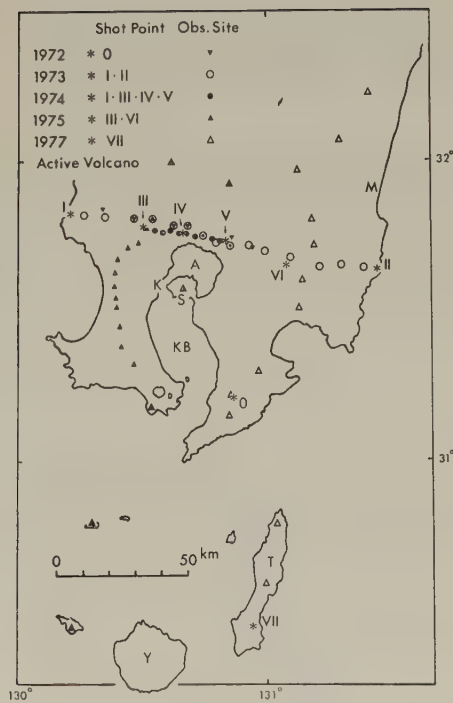


Fig. 1. Location of shot points and observation sites. Some observation sites are not shown to avoid too much complication. A, Aira Caldera; S, Sakura-jima Volcano; KB, Kagoshima Bay; T, Tanegashima Island; Y, Yaku-shima Island; K, Kagoshima City; M, Miyazaki City.

Table 1. List of observations.

Year	Date	Shot point	Charge amount (kg)	<i>d</i> (km)	Number of observation sites	Method
1972	8.9	SP.0	507.0	56-85	9	Fan-shooting
	8.13	SP.0	544.5			
1973	8.22	SP.I	405.0	0-119	15	Refraction
	8.22	SP.II	504.0			
	8.28	SP.I	486.0			
	8.29	SP.II	121.5			
1974	8.22	SP.III	297.0	0-34	11	Refraction
	8.22	SP.V	300.5			
	8.24	SP.IV	146.25			
	8.24	SP.I	395.0			
1975	8.12	SP.III	301.5	0-51	12	Refraction
	8.12	SP.VI	501.5	54-70		Fan-shooting
1977	8.9	SP.VII	967.5	0-202	12	Refraction

Japanese Geodynamics Project. The earlier part of this work was already reported elsewhere by ONO *et al.* (1977).

The locations of the shot points and the observation sites are shown in Fig. 1 and the data are listed in Table 1.

2. Regional Crustal Structure of the South Kyushu

Refraction seismic observation spanning 119 km across the south Kyushu was done in 1973. The observation line was designed to take as longer span on land as possible in an E-W direction, to traverse the major structural trend in the region and at the same time to run across the northern extension of the Kagoshima Bay, which is a possible graben structure as stated already.

The result of this observation was reported by Ono *et al.* (1977) in detail and is summarized as follows. Two shot points are located at both ends of the observation line; SP. I at the west and SP. II at the east. Three velocity layers are identified near both ends (Table 2). Velocities of the third layer, which constitutes the main part of the upper crust, are determined as 6.1 km/sec in the western portion and 5.6 km/sec in the eastern portion respectively but the base of this layer was not detected. Remarkable increase of delay time was observed at the observation sites to the north of the Kagoshima Bay and could be interpreted due either to slower velocity or deeper boundary of velocity layers there. A graben model, 16 to 19 km in width and 0.7 km downthrow with a little tilt to the east, well accounts for this increase of delay time.

To know the structure of the lower crust and the uppermost mantle, a longer-spanned refraction seismic observation was done in 1977 along a N-S trending observation line, which spans 202 km from the shot point SP. VII near the southern end of Tanega-shima Island to the north of Miyazaki City (Fig. 1). This observation line was designed parallel to the general structural trend and to detect the boundaries of the upper crust, the lower crust and the uppermost mantle.

Seismic record sections of this observation are shown in Fig. 2. Onsets of signals are not clear for some distant observation sites by the noise due to an unexpected storm. Travel time curve from these records is shown in Fig. 3.

Although this is a one-way observation, we assume a structure of horizontal plane boundaries to derive four velocity layers as shown in Fig. 3. Assumption of horizontal structure in the N-S profile is supported by the regional Bouguer anomaly (TOMODA, 1973). The velocities of 5.9 km/sec and of 7.0 km/sec are identified well in Fig. 3, however, data points near the shot point are not enough to determine the shallow structure. Since the apparent velocity of 5.9 km/sec corresponds to that of the third layer in previous observation in this region in 1973 and in 1975, the 5.9 km/sec layer is assumed to be the third layer along this observation line. Then the velocities of upper two layers are assumed to be

Table 2. List of velocity layers in south Kyushu.

	1973				1977	
	Near SP. I		Near SP. II		V_p (km/sec)	Depth of bottom (km)
	V_p (km/sec)	Depth of bottom (km)	V_p (km/sec)	Depth of bottom (km)		
Layer 1	3.7	0.9	3.8	1.5	3.8	0.7
Layer 2	4.9	3.3	4.8	5.6	4.7	4.8
Layer 3	6.1	?	5.6	?	5.9	22
Layer 4					7.0	40
Layer 5					(7.8)	?

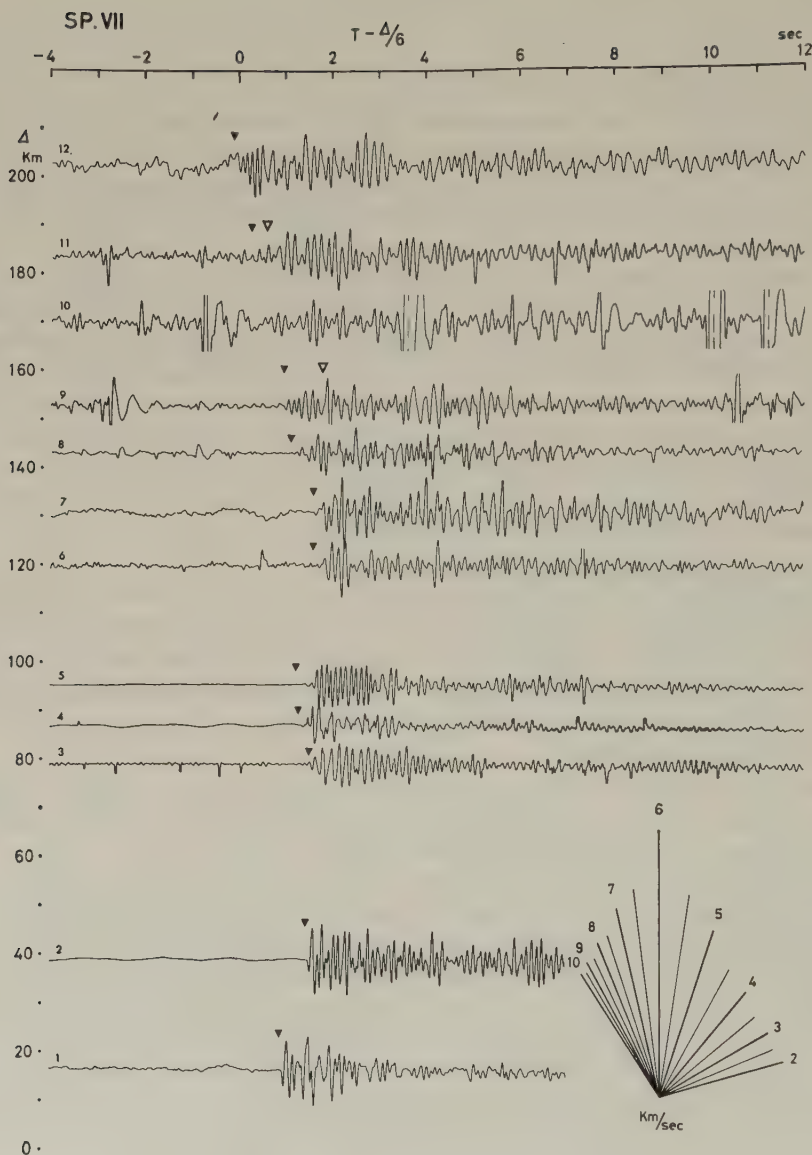


Fig. 2. Seismic record sections of the refraction observation of 1977. Solid inverted-triangles mark the onsets of signals and open inverted-triangles mark the read later phases.

represented by the average values of respective layers obtained in the former observations and determined as shown in Fig. 4.

The fourth layer is the lower crust having a well-defined velocity of 7.0 km/sec. A velocity layer faster than 7 km/sec is not found as first arrivals but later-phase information suggests probable existence of 7.8 km/sec layer as shown in Figs. 2 and 3. The calculated depth of the boundary between Layers 4 and 5, that is Moho, is 40 km which is much deeper than former estimations; 32 km by gravity (KANAMORI, 1963) and 24 km by phase

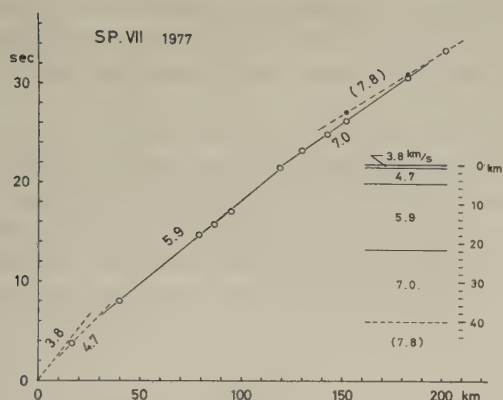


Fig. 3

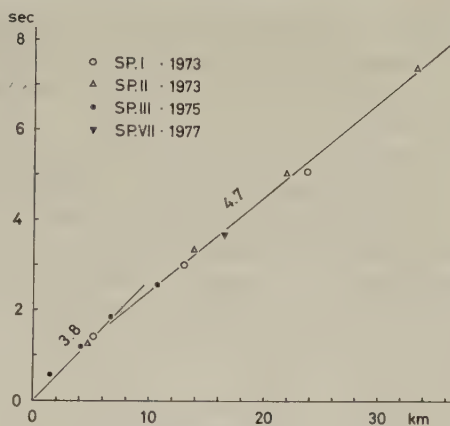


Fig. 4

Fig. 3. Travel time curve of the refraction observation of 1977 and derived structure assuming all layers are horizontal. For the shallow structure see the text and Fig. 4. Later phase informations of distant sites are shown by small solid circles and a broken line.

Fig. 4. Travel time curve of the refraction observations in 1973, 1975 and 1977. The data only for the layers, the velocity of which are slower than 6 km/sec, are shown.

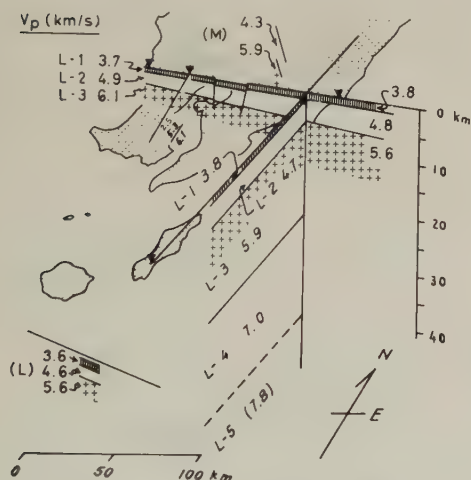


Fig. 5. Schematic fence diagram of the south Kyushu region. Structures obtained by the refraction observation in 1975 (see Fig. 10), by MIYAZAKI *et al.* (1977) shown as (M) and by LUDWIG *et al.* (1973) shown as (L) are included.

velocity of Rayleigh wave (KAMINUMA, 1966). Since the onset of the first arrival may be obliterated by noise in distant stations, where the quality of the record is low, true onset might be earlier than the read one and Moho might be shallower than the obtained depth.

A schematic fence diagram compiled for this region, including the data of a N-S section by the one-way refraction observation from SP. III (Fig. 10), those near the Kiri-shima Volcano by MIYAZAKI *et al.* (1978) and on an E-W section south of Yaku-shima Island by LUDWIG *et al.* (1973), is shown in Fig. 5.

Main parts of Layers 1 and 2 probably correspond to folded Mesozoic and Paleozoic formations of the Outer Zone of the Southwest Japan, but the uppermost part of Layer 1 near SP. II is the westernmost portion of the thick sedimentary basin, of which axis is located in Hyuga-nada off the east coast of Kyushu, and is overlying on older rocks. Layer 3 probably corresponds to the pre-Cambrian crystalline basement which extends from the Chinese continent through Tunghai Shelf (WAGEMAN *et al.*, 1970). Underlying

of older, metamorphic or igneous rocks is suggested by the presence of xenolithic inclusion in Neogene granitic plutons in south Kyushu (NOZAWA, 1977) and by Sr isotopic data (YANAGI *et al.*, 1971). Layer 4 represents the lower crust but no more definite information is available.

The velocity of Layer 5, P_n velocity, is 7.8 km/sec which is faster than 7.5 km/sec beneath Northeastern Japan (RESEARCH GROUP FOR EXPLOSION SEISMOLOGY, 1977). Recently MASUDA *et al.* (1978) reported that the P_n velocity of 7.5 km/sec is for the western part of northeast Honshu, west of the volcanic front, while that of 7.8 km/sec is for the eastern part of the region, between the volcanic front and the ocean, where the tectonic location is very similar to the area along our observation line of 1977 on the oceanic side of the volcanic front in south Kyushu.

3. Fan-Shooting Observation across the Sakurajima Volcano and the Aira Caldera

Two fan-shooting observations which are designed nearly perpendicular to each other

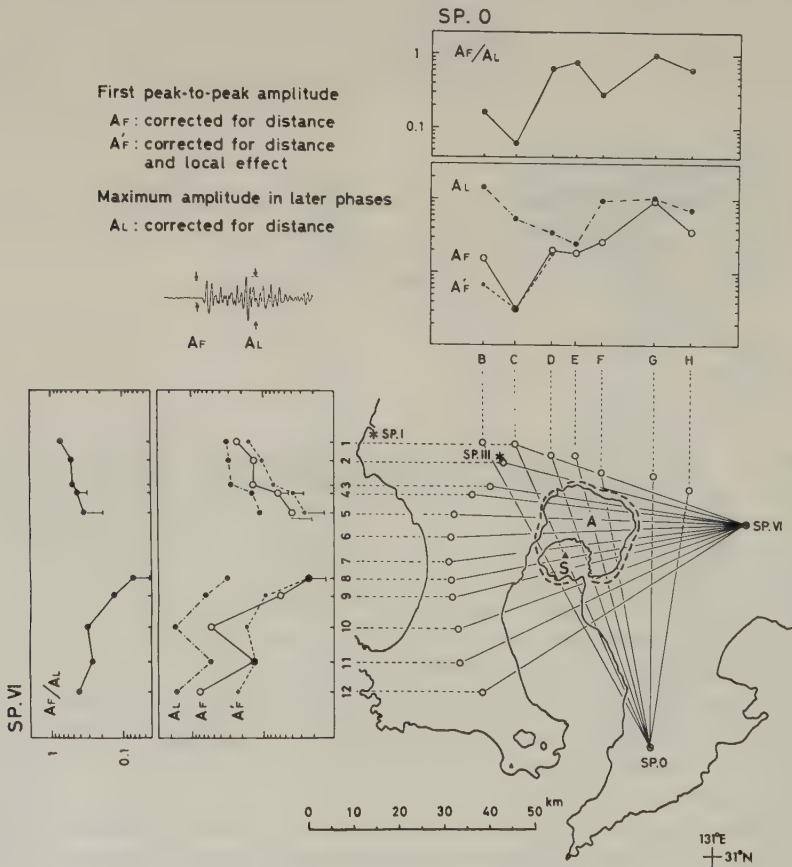


Fig. 6. Relative amplitudes A_F , A'_F and A_L observed at each site of the fan shootings from SP. 0 and from SP. VI shown in arbitrary scales and the ratio A_F/A_L . For Sites 4, 5 and 8, values may be less than those marked by circles but not as low as the lower ends of the bars under the circles.

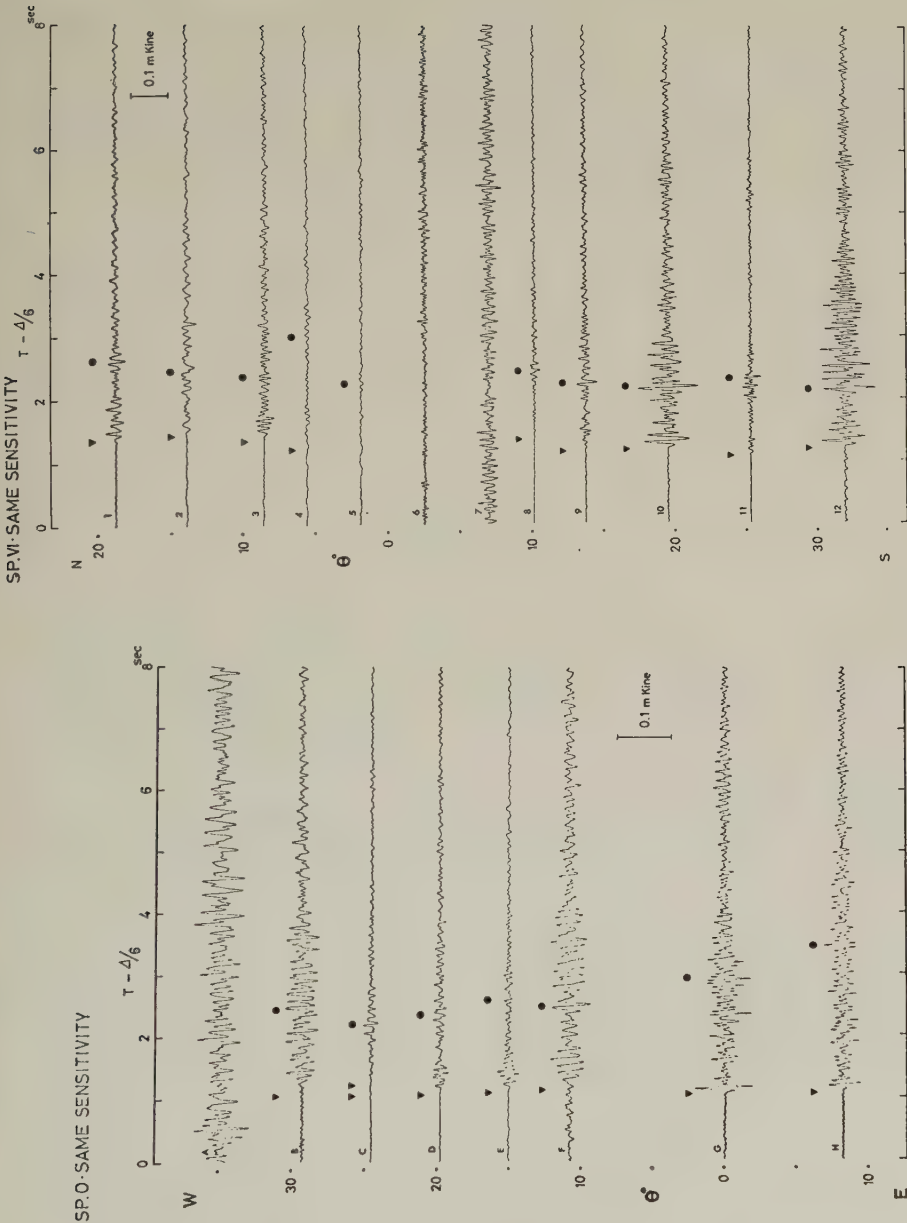


Fig. 7

Fig. 7. Seismic record sections of the fan-shooting observation for SP. 0 in 1972. Inverted triangles mark the first arrivals and solid circles mark the maximum amplitudes in later phases. Signals can not be detected in the record of Site A due to high noise level.

Fig. 8. Seismic record sections of the fan-shooting observation for SP. VI in 1975. Symbols are the same as those in Fig. 7. Signals are not detected or not clear enough to mark the specific position in the records at Site 5 to 7 due to small S/N ratios.

Fig. 8

in direction and cover the areas of the Sakurajima Volcano and the Aira Caldera, were carried out in 1972 and in 1975 (Fig. 6). Sites C of 1972 and 8 of 1975 are located right on the other side of the Sakurajima Volcano relative to the shot points and E and F of 1972 and 5 to 7 of 1975 are on the other side of the central portion of the Aira Caldera. Seismic record sections of these observations are shown as Figs. 7 and 8.

The relative amplitudes of the first peak-to-peak, which are corrected for distance, are shown as A_F in Fig. 6. The correction was made on the basis that the amplitude decreases as the second power of distance from the shot point. Although the first peak-to-peak amplitude were not detected or not measured at some observation sites due to higher noise levels or smaller signals, a general tendency that the amplitude becomes smaller at sites located on the other side of the volcanoes relative to the shot points, is evident.

Sites B, C, D and E of the fan shooting of 1972 from SP. 0 were used also for the observations in refraction method of 1973 from SP. I and SP. II. Similarly, all sites, 1 to 12, of the fan shooting of 1975 from SP. VI were used for the one-way refraction observation for SP. III, located near the north end of the observation line. So, the correction of local effect near the observation sites can be made by comparing the amplitudes of fan shooting with the amplitudes of refraction method, both observed at the same sites and corrected* for distance in the same fashion. The spatial anomaly of amplitude remains after this correction of local effect (A'_F in Fig. 6). The minimum of the amplitudes A_F or A'_F is located at Site C, right on the other side of the Sakurajima Volcano, for SP. 0. For SP. VI, the minimum, though not definitely located, lies between Site 4 to Site 8. The first arrivals at these sites should be waves passed through the 6 km/sec layer if we take account the path and the structure of this region derived from the refraction observation in 1973, 1975 and 1977 (Fig. 5). It is concluded that anomaly is not due to local cause but due to some cause along the paths between the shot points and the observation sites. Since those anomalously smaller amplitudes are observed at sites where ray paths passed across the areas of the Sakurajima Volcano and the Aira Caldera and waves of the first arrivals passed through the 6 km/sec layer, the decrease of amplitude occurs most likely in the 6 km/sec layer under these volcanoes.

The amplitudes of later phases of these records vary in accordance with the amplitudes of the earliest phases at most sites with some exceptions. The maximum amplitudes in later phases (A_L : solid circles in Figs. 7 and 8) and the ratios A_F/A_L are shown in Fig. 6. It is noted that the ratios A_F/A_L are small at Site C of 1972 and Site 8 of 1975, both located at right on the other side of the Sakurajima Volcano. The first arrivals at these sites are waves passed through the 6 km/sec layer and the later phases treated here are likely to represent the refraction of the adjacent layer above the 6 km/sec layer considering the path and the structure of this region. Then, the smaller ratios A_F/A_L at these sites probably mean that attenuation in the adjacent layer above the 6 km/sec layer is not as conspicuous as in the 6 km/sec layer.

Travel times of the two fan-shooting observations, which are reduced to 6 km/sec, are shown as open circles in Fig. 9. The reading accuracy of travel time is within 0.02 sec. As for the observation of 1972 for SP. 0, travel time anomaly is not found except at Site C. The first arrival time at Site C is not decisive due to small S/N ratio. It can be read in two ways as shown by two open circles, tied by a bar, in Fig. 9. The lower one is

* The correction was not made for Site E because the amplitude was not calibrated there in 1973.

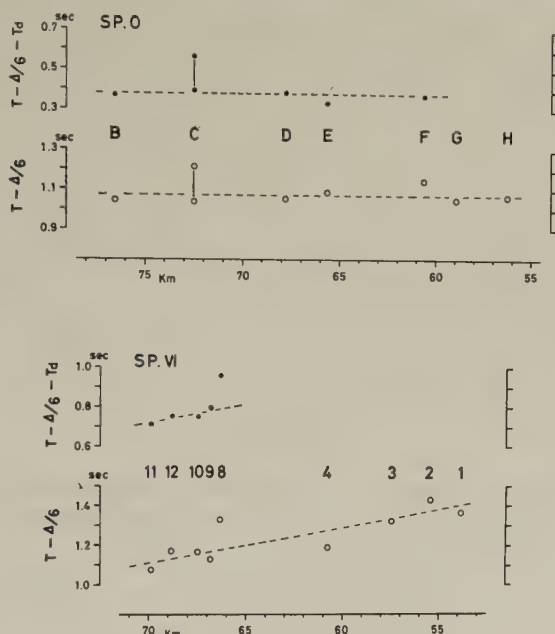


Fig. 9. Travel times reduced to $\Delta/6$ and those corrected for delay times at the observation sites for fan-shooting observations of 1972 (top) and 1975 (bottom).

close to the broken line which represents the apparent velocity and the other is about 0.2 sec later than the former. In the case of 1975 for SP. VI, the first arrival time at Site 8 is delayed by about 0.2 sec than the apparent velocity determined by the travel times of other sites (bottom of Fig. 9).

It should be examined if this delay of travel time at Site 8 and possibly at Site C is due to some anomalous, low-velocity space between the shot point and the observation sites or due to the underground structure near the observation sites. The travel time at the fan-shooting observation, T_f , is expressed as

$$T_f = T_s + \frac{\Delta}{V} + T_o$$

where T_s and T_o are delay times at the shot point and the observation site respectively, Δ is the distance between the shot point and the observation site, and V is the velocity of the refractor. In order to detect a possible anomaly in the velocity, delay times, T_s and T_o , should be determined. T_s is assumed to be equal for all the sites for one shot regardless of azimuthal directions. The delay times T_o at some Sites B, C, D and E of 1972 were obtained in the refraction observation of 1973 (ONO *et al.*, 1977). For Site F of 1972, the delay time of a site of 1973, where is 300 m distant from the former, was used. The delay times at the sites of 1975 are derived by the one-way refraction observation for SP. III (Fig. 10), assuming that the true velocity* of the refractor is 6.0 km/sec. The delay time, however, can be obtained only for Sites 5 to 12, where the first arrival from the re-

* The difference between real and assumed velocities is not critical here to detect an anomaly in velocity.

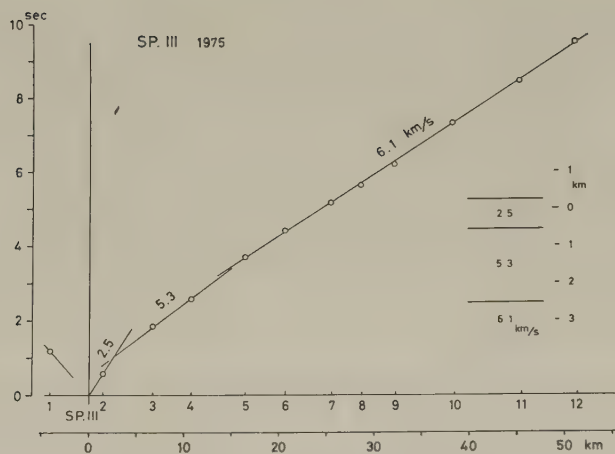


Fig. 10. Travel time curve of the refraction observation of 1975 and derived structure assuming all layers are horizontal.

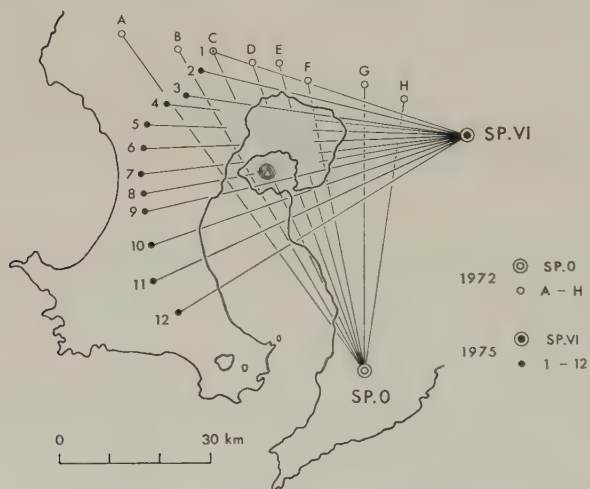


Fig. 11. Area of anomalous wave propagation around the Sakurajima Volcano and the Aira Caldera (see the text).

fractor is observed. The travel times after subtraction of delay times are shown as solid circles in Fig. 9. The delay at Site 8, and possibly at Site C, is more clearly seen.

The records at Site C and Site 8 are characterized also by very small A_F , A'_F and A_F/A_L as previously stated. The intersection of the ray paths to Site C and Site 8 coincides to the Sakurajima Volcano.

KAMO *et al.* (1977) found from the results of observation of natural earthquakes at sites located around the Aira Caldera that S-waves were more attenuated than P-waves when the seismic waves passed beneath the caldera or the Sakurajima Volcano while decrease in velocity was not detected.

These results are summarized as follows:

1. A large wave attenuation occurs under the Sakurajima Volcano and the Aira Caldera. S-wave is more attenuated than P-wave (KAMO *et al.*, 1977).

2. Wave velocity is likely to be decreased under the Sakurajima Volcano.

3. Anomalies of wave propagation occur at the 6 km/sec layer.

The physical state causing these anomalies is not definitely determined yet. Areal distribution of anomalies is shown in Fig. 11. The edge of the anomalous area is not definite because the anomalies are not very critical but rather gradual. The dotted area around the Sakurajima Volcano and in the Aira Caldera is likely to be more shattered than the surrounding region but we can not tell if liquid magma exists there or not. The state in the small striped area under the Sakurajima Volcano is something different from that under the Aira Caldera causing more attenuation and velocity decrease.

We are grateful to the local government and people who helped us in many ways during the operations.

REFERENCES

- ARAMAKI, S. and T. UI, Aira and Ata pyroclastic flows and related calderas, and depressions in southern Kyushu, Japan, *Bull. Volcanol.*, **29**, 29–48, 1966.
- ARAMAKI, S. and T. UI, Pyroclastic deposits in southern Kyushu—A correlation by the Ca-Mg-Fe ratios of the phenocrystic minerals, *Bull. Earthq. Res. Inst.*, **51**, 151–182, 1976 (in Japanese).
- CHUJO, J. and F. MURAKAMI, The geophysical preliminary surveys of Kagoshima bay, *Bull. Geol. Surv. Jpn.*, **27**, 807–824, 1976 (in Japanese).
- HAYASAKA, K. and K. OKI, Geological consideration on the subsurface data from the deep wells drilled in Kagoshima City, south Kyushu, Japan, *Rep. Fac. Sci., Kagoshima Univ., Earth Sci. and Biology*, No. 4, 15–29, 1971 (in Japanese).
- KAMINUMA, K., The crust and upper mantle structure in Japan. II. Crustal structure in Japan from the phase velocity of Rayleigh waves, *Bull. Earthq. Res. Inst.*, **44**, 495–510, 1966.
- KAMO, K., K. NISHI, T. FURUSAWA, J. AKAMATSU, S. KIKUCHI, H. ONO, Y. SUDO, A. TAKAGI, T. UMINO, S. HORI, Y. SATO, and T. KAKUTA, Seismic activity and detection of abnormal propagation of seismic wave around the Aira caldera, in *The Second Concentrated and Co-ordinated Observations on the Activity of the Sakurajima Volcano*, pp. 13–20, Sakurajima Volc. Observatory, Disaster Prevent. Res. Inst., Kyoto Univ., Kagoshima, 1977 (in Japanese).
- KANAMORI, H., Study on the crust-mantle structure in Japan, Pt. 2, Interpretation of the results obtained by seismic refraction studies in connection with the study of gravity and laboratory experiments, *Bull. Earthq. Res. Inst.*, **41**, 781–799 (1963).
- LUDWIG, W.J., S. MURAUCHI, N. DEN, P. BUHL, H. HOTTA, M. EWING, T. ASANUMA, T. YOSHII, and N. SAKAJIRI, Structure of East China Sea-West Philippine Sea Margin off southern Kyushu, Japan, *J. Geophys. Res.*, **78**, 2526–2536, 1973.
- MASUDA, T., K. GOTO, S. HORIUCHI, and S. HORI, Pn-velocity beneath the inland northeast Japan, *Abstr. Seismol. Soc. Jpn.*, No. 1, 175, 1978 (in Japanese).
- MIYAZAKI, T., M. YAMAGUCHI, F. MASUTANI, and H. TERAOKA, P-wave velocity structure beneath the Kirishima Volcanoes, *Bull. Volcanol. Soc. Jpn.*, **23**, 215–225, 1978 (in Japanese).
- NOZAWA, T., Pre-Silurian basement in *Geology and Mineral Resources of Japan*, 3rd ed., Vol. 1, pp. 18–19, Geological Survey of Japan, Kawasaki, Japan, 1977.
- ONO, K., Geology and explosion seismic study around the volcanic belt in south Kyushu, *Kaiyokagaku*, **6**, 684–689, 1974 (in Japanese).
- ONO, K., K. ITO, S. IZUKA, I. HASEGAWA, T. HIROSHIMA, T. KAKUTA, K. ICHIKAWA, and H. SUZUKI, Explosion seismic studies near and around Sakurajima Volcano, in *Volcanism of Island Arcs*, edited by S.A. Fedotov and P.I. Tokarev pp. 43–54, Nauka, Moscow, 1977 (in Russian).
- RESEARCH GROUP FOR EXPLOSION SEISMOLOGY, Regionality of the upper mantle around Northeastern Japan as derived from explosion seismic observations and its seismological implications, *Tectonophysics*, **37**, 117–130, 1977.
- TOMODA, Y., *Maps of Free Air and Bouguer Gravity Anomalies in and around Japan*, Univ. of Tokyo Press, Tokyo, 1973.
- WAGEMAN, J.M., T.W.C. HILDE, and K.O. EMERY, Structural framework of East China Sea and Yellow Sea, *Am. Assoc. Petrol. Geol.*, **54**, 1611–1643, 1970.
- YANAGI, T., M. YAMAGUCHI, and T. NOZAWA, Rb-Sr whole rock ages of the granites of Minami-oshima and Amami-oshima, southwest Japan, *Mem. Fac. Sci., Kyushu Univ.*, Ser. D, **21**, 163–175, 1971.

TWO TYPES OF ACCRETIONARY FOLD BELTS IN CENTRAL JAPAN

Yujiro OGAWA* and Kazutoshi HORIUCHI

Department of Earth Sciences, Nihon University, Sakurajosui, Tokyo, Japan

(Received May 31, 1978; Revised September 8, 1978)

Sedimentary and structural characteristics in two types of accretionary fold belts in central Japan are introduced and the tectonic significance are discussed. The Shimanto Fold Belt, grown up from the Cretaceous arc-trench gap and trench slope sediments, has the collisional features of large scale folds. The fold styles in the belt are differently developed in inner and outer parts. The former is characterized by a series of shear folds and the latter is by a series of lens folds. This difference may be caused chiefly by the different geothermal gradients of the area. The Miocene Miura Basin is influenced by lateral compression of strike slip field at the time of sedimentation. The development of the basin was related to the strike slip motion at the plate boundary between the Philippine Sea and Asian Plates.

1. Introduction

The accretionary fold belts in Southwest Japan were considered to be the products of the Japanese or Pacific type orogenic movements (KOBAYASHI, 1941; YEHARA, 1953; MATSUMOTO, 1967). The origin of the belts, especially of the Shimanto Fold Belt, has recently been discussed on the basis of subduction tectonics (KANMERA, 1976; DICKINSON, 1977). Although structural profiles were obtained for some areas (KIMURA and TOKUYAMA, 1971; KIMURA, 1974; SUZUKI, 1975; KANMERA and SAKAI, 1975), detailed internal fold structures and characteristics of deformation have not yet been fully elucidated. Sometimes the structural characteristics observed in the fold belts are interpreted by oneway polarity shown by slice or imbricate structures, but as shown in the following they could much more reasonably be explained by collision or in some cases lateral slip tectonics in central Japan.

Two types of accretionary fold belts differing in tectonic features are discriminated in both sides of the Fossa Magna in central Japan. The one developed from the Cretaceous Shimanto Geosyncline in the Akaishi and Kanto Mountains, and the other from the late Miocene Miura Basin in the Miura Peninsula (Fig. 1). The tectonics in both the belts may be interpreted as a result of successive migration of geosynclines and accretion of fold belts to the major cordillera of Japan. The Miocene basin developed in connection with the development of a triple junction.

In this paper we treat with the accretionary fold belts. The sedimentation and structures are briefly described and the characteristics of the small structures are considered in view of the differential series of fold styles and the application of plate tectonics.

* Present address: Department of Geology, Kyushu University, Hakozaki, Fukuoka 812, Japan.

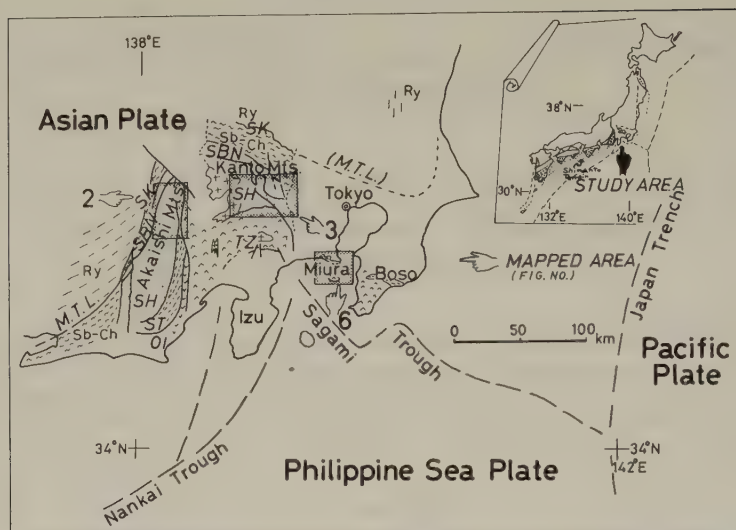


Fig. 1. Index map. Fold belts from inner are as follows: SK, Sakawa Fold Belt (including Ry, Ryoke Zone; Sb-Ch, Sambagawa-Chichibu Zone); SBN, Sambosan; SH, Shimanto (s.s.); ST, Setogawa; OI, Oigawa; TZ, Tanzawa; M.T.L., Median Tectonic Line.

2. Tectonic Setting

The Japanese Islands have not a few evidence for the welding of eugeosynclinal materials deposited in marginal basins or forearc areas together with microcontinent crust to the Asian Continent. The history involves subduction and collision around the marginal areas of western Asian Continent. The welding occurred during the late Paleozoic and Mesozoic two big orogenic movements of Akiyoshi and Sakawa series (KOBAYASHI, 1941; KIMURA, 1974; OGAWA, 1978). The welding during the orogenesis finally resulted in the building of the Eo-Japan Cordillera in Jurassic (KOBAYASHI, 1941), and the last apparent paired metamorphic belts of Ryoke and Sambagawa emerged in Cretaceous during the displacement of the Median Tectonic Line. Since that time several fold belts have accreted intermittently outward to this cordillera. They are divided from inner to outer as follows; the Sambosan Fold Belt (mainly of Triassic sediments including from Carboniferous to Jurassic), Shimanto (s.s.) (Cretaceous sediments), Setogawa or Nakamura (Paleogene sediments) and Oigawa-Tanzawa-Miura (Neogene sediments) (KIMURA and TOKUYAMA, 1971). Each fold belt represents an orogenic belt with a metamorphic core. The sediments except in the Tanzawa are composed of a large amount of terrigenous clastics, such as turbidite, sandstone and mudstone, and interbedded conglomerate, limestone, chert and rhyolitic tuff. Although the intercalated layers, i.e. conglomerate, limestone, chert and tuff generally constitute rather small proportions of the sedimentary pile, they locally develop to a large extent. A few layers of basaltic rocks are also interbedded in specific, generally in the lower horizons. In some areas sediments are thought to be sedimentary mélangé or olistostrome (KANMERA, 1977).

In order to elucidate the sedimentation and tectonics in the fold belts, therefore, it is considered desirable to analyze thoroughly the subduction zone between continental and

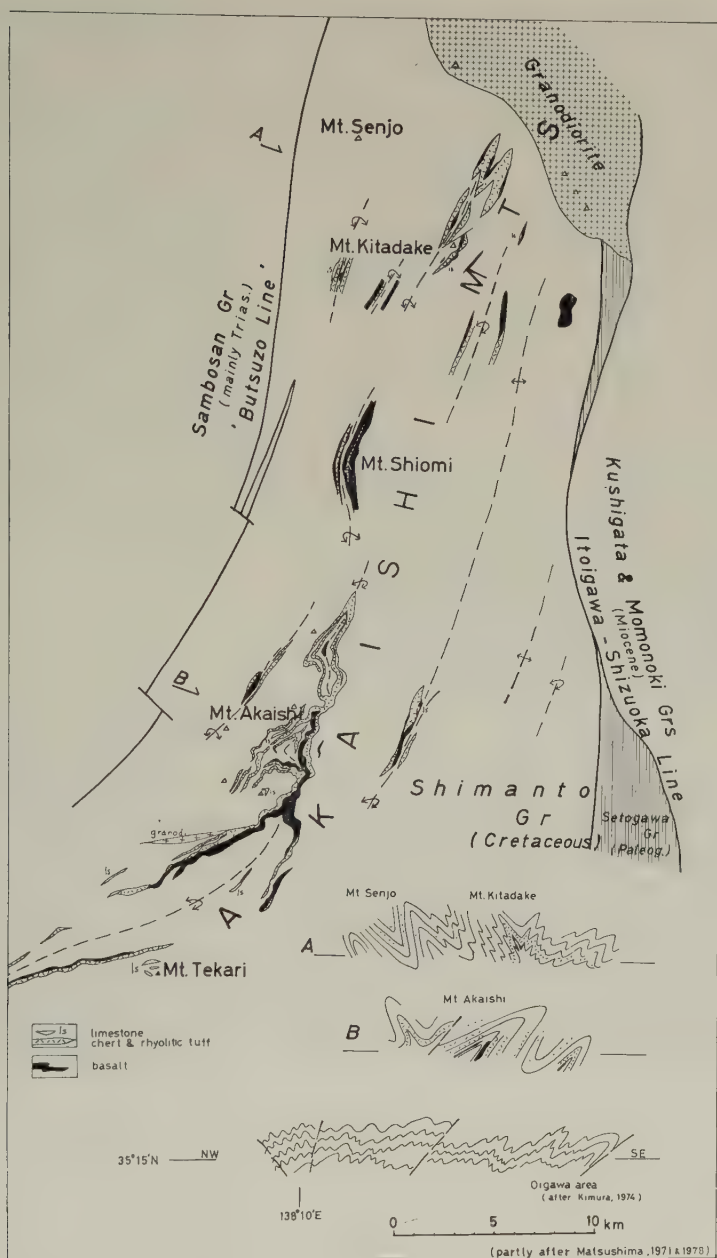


Fig. 2. Sketch map of the northern part of the Shimanto Group in the Akaishi Mountains. Rock distribution and cross section (B) around Mt. Akaishi are based on MATSUSHIMA (1972, 1978).

oceanic plates. The interaction of the plate motions in western Pacific should affect all the processes which take place in the destructive plate boundary.

A change in the motion of the plates occurred in late Paleogene (UYEDA and MIYASHIRO, 1974). After the change, the Pacific Plate has been moving westward and subducting in the same direction as it does today. As a result of this change in the plate motion, the site of active volcanism and sedimentation shifted or jumped to newer zones which ran in N-S direction across the Japanese Islands. The Fossa Magna is the intersection between the old and new deformation zone along plate boundaries. The fold belts older than Paleogene bend convexly innerward on the both sides of the Fossa Magna and turned again concavely in the east (Fig. 1). The Neogene Oigawa-Tanzawa-Miura Fold Belt was welded to the outermost part of these fold belts. The Izu Peninsula is said to be the collisional bar to the central part of Japan (MATSUDA, 1978), and the Miura Basin corresponds to the eastern flank of the major eugeosynclinal area affected by strike slip tectonism in late Miocene.

3. *Shimanto Fold Belt in the Akaishi and Kanto Mountains*

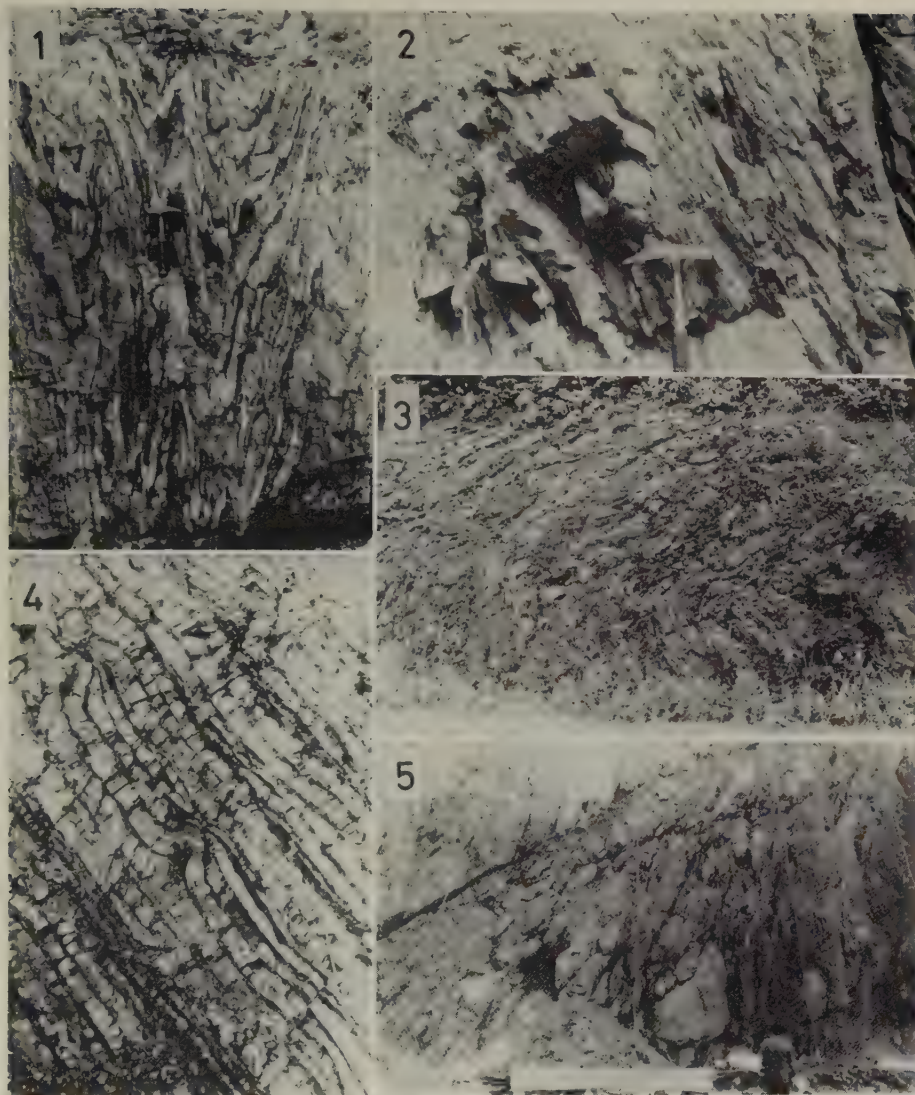
The Shimanto Fold Belt (s.s.) occupies the inner half of the so-called Shimanto Terrain, where Cretaceous and Paleogene geosynclines occurred. The Shimanto Group (s.s.), composed of Cretaceous (partly Jurassic) marine sediments, is in contact with the north Sambosan Group by a low angle thrust called the Butsuzo Line. The Sambosan Group contains Carboniferous to Jurassic clastic sediments with locally large amounts of limestone and chert besides basaltic and rhyolitic rocks. Permian and Triassic limestone is characteristically developed on the outer margin of the geosyncline.

The Shimanto Group is made of turbidite, sandstone, mudstone, slump deposits and a small amount of limestone, chert and rhyolitic tuff in several horizons. Basaltic rocks are distributed in the lower and middle horizons usually accompanying rhyolitic tuff and chert. Metamorphic grade reaches as high as pumpellyite or greenschist facies. No blueschist is found.

3.1 *Akaishi Mountains*

The group in the mountains forms north-south trending anticlinoria bent convexly southeastward. The eastern anticlinoria in the vicinity of the Oigawa River area were structurally traced by KIMURA and TOKUYAMA (1971). Turbidite-rich sediments make many folds within mostly horizontal enveloping surfaces (Fig. 2). The sediments are several thousands meters thick. Structures in the western anticlinoria, on the other hand, are characterized by large-scale recumbent folds, like mushroom folds, which have been analyzed by the precise mapping by MATSUSHIMA (1972, 1978) (Fig. 2). Strata in the core are nearly horizontal around Mt. Akaishi. This large scale folding corresponds to the major core of the whole belt. The general structure diverges upward with opposite-vergence folds, namely west vergence in the west and east vergence in the east. Small scale folds are rarely developed in the limbs of the large scale folds unlike in the eastern flank of the Oigawa River area.

The small structures in these areas are very significant, especially the fold styles (See Fig. 9 as for the fold styles). In the lowest horizon in the core part of the western anticlinoria, flow folds made of crystalline schist or phyllite are developed (Pl. I-1). Crenulation cleavages of later stage are sporadically developed in the west and east. In the west



Pl. I. 1. Flow folds at the eastern foot of Mt. Kitadake. Alternated beds of chert, rhyolitic tuff and mudstone in the Shimanto Group, thermally metamorphosed. 2. A part of shear folds to the west of Mt. Akaishi, Shimanto Group. Slaty cleavages obliquely cut the bedding plane. Left-hand is upward. 3. Lens folds with lenticular bodies of sandstone in alternated beds of mudstone and sandstone, Shimanto Group at Senzu, Oigawa River area. 4. A part of flexial-slip folds, Shimanto Group at the south of Senzu, Oigawa River area. 5. Slump deposits with sandstone fragments. Ogochi Group at the south of the Okutama Lake.

shear folds characterized by slaty cleavages are common (Pl. I-2). On the other hand lens folds are the dominant structure in the east, where bedding slip usually occurs (Pl. I-3). Lens structure developed from small conjugate faults in the brittle layers and extreme slip along bedding and/or fault planes. In the upper horizons, weakly developed slaty cleavages without bedding slip are observed in the west, while flexural-slip folds with

remarkable bedding slip predominate in the east (Pl. I-4). To summarize, fold styles in the west are series of shear folds and those in the east are series of lens folds (Figs. 5 and 9).

3.2 Kanto Mountains

The Shimanto Group in the Kanto Mountains is divided into the north Ogochi and south Kobotoke Groups. Each group constitutes the respective fold belt. The two are in contact with the Itsukaichi-Kawakami Line (Fig. 3). There are no distinct Paleogene sediments in the Kanto Mountains unlike in the other Shimanto Terrain in Southwest Japan.

The Ogochi Group is distributed on the south of the Sambosan Group under the low angle thrust fault, the Butsuzo Line. The group is composed of a large amount of muddy slump deposits containing lenses or fragments of basaltic to rhyolitic volcanic rocks, chert, limestone and conglomerate. Some of them are interpreted not as layers in situ but as allochthonous slump deposits (Pl. I-5). Some possibly Jurassic indicating fossils are found in the limestone of this group (FUJIMOTO and SUZUKI, 1969). These rocks are covered by quartz-feldspathic sandstone and sandy sediments which yield an Upper Cretaceous pelecypod *Inoceramus* sp. (NISHIMIYA, 1976). The large-scale structures of the group are not clearly determined, but generally vergence of folds is northward in the north and south-



Fig. 3. Sketch map of the Ogochi and Kobotoke Groups in the Kanto Mountains. Data in the Sambosan and Ogochi Groups are after UCHIDA (1978).

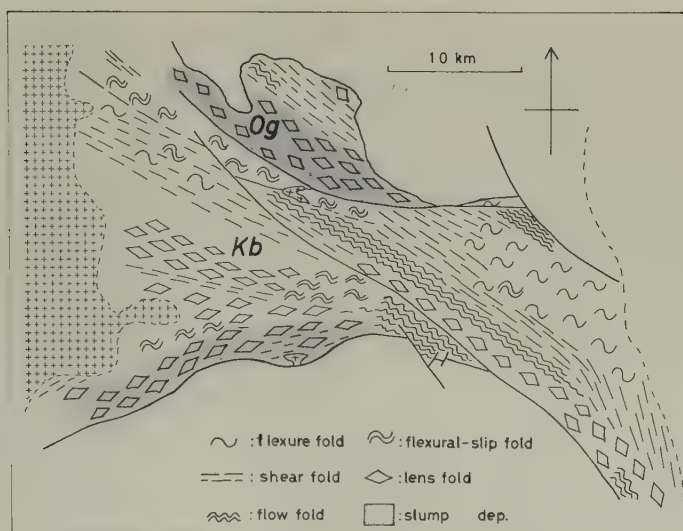


Fig. 4. Distribution of fold styles in the Ogochi (Og) and Kobotoke (Kb) Groups.

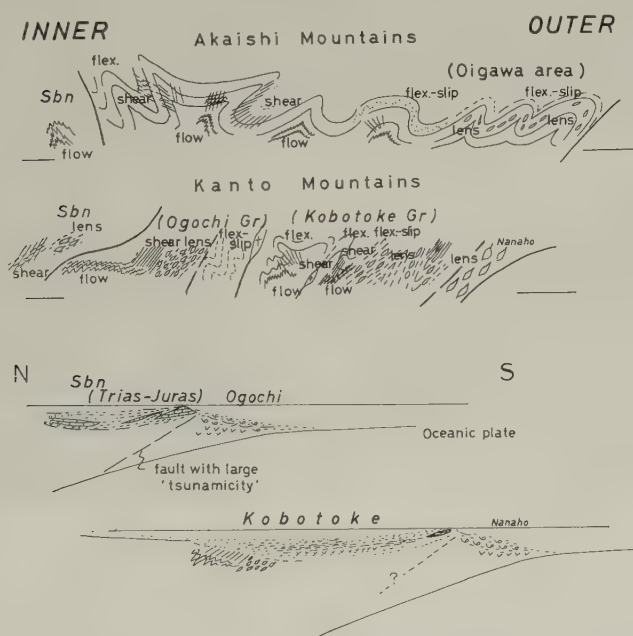
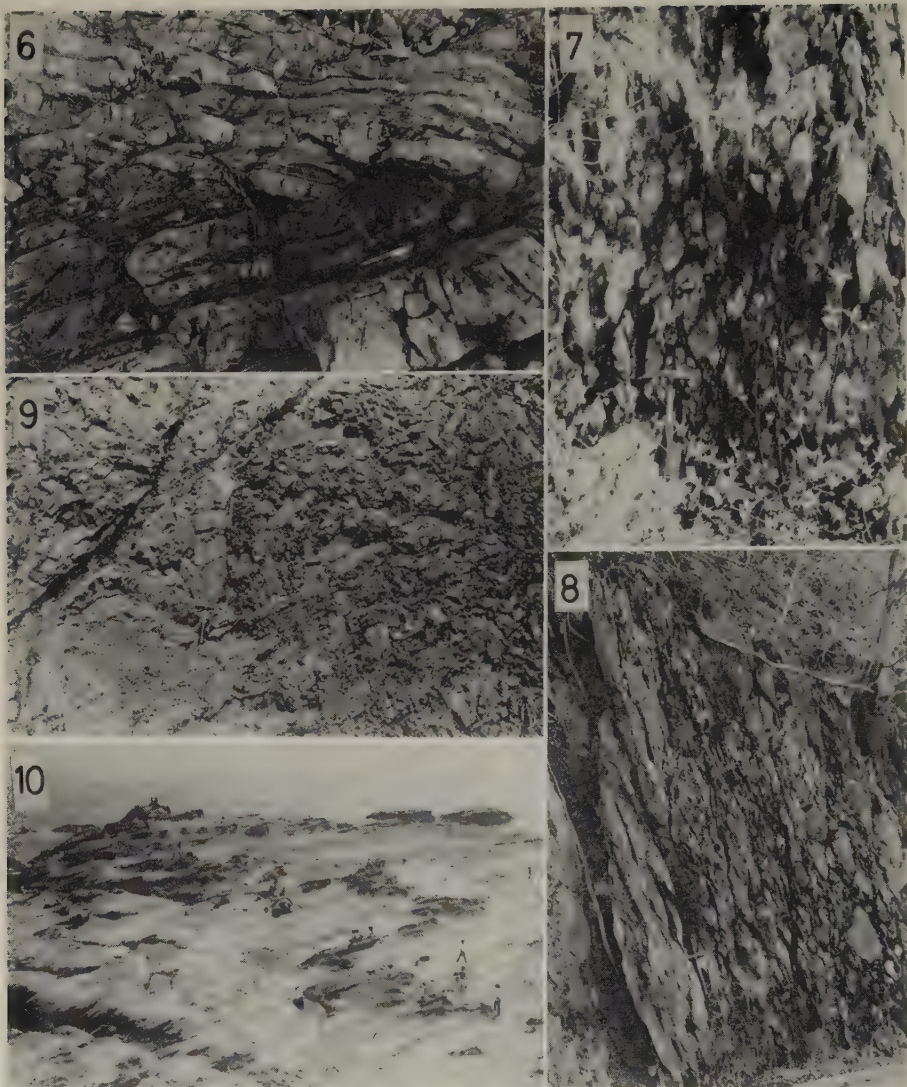


Fig. 5. Cross sections and distribution of fold styles in the Shimanto Fold Belt in the Akaishi and Kanto Mountains, and brief sketches of the status in Jurassic-early Cretaceous (above) and in late Cretaceous (below) in the Kanto Mountains.

ward in the south. Strata form tight folds of several hundred meters scale, but slice or imbricate structures such as reported in Kyushu by KANMERA and SAKAI (1975) have not yet been observed.

In the Ogochi Group, schistose rocks showing flow folds are distributed in the lowest



Pl. II. 6. A shear fold with scarce bedding slip. Slaty cleavages and microfolds developed in the muddy part. Kobotoke Group, at Wadamukai, west of Itsukaichi. 7. A part of lens folds in the alternating beds of sandstone and mudstone in the Kobotoke Group at the north of Nanaho, Otsuki. 8. A part of lens folds in alternating beds of mudstone and sandstone in the Kobotoke Group at the north of Nanaho, Otsuki. 9. Flexural-slip folds in the alternating beds of sandstone and mudstone. Slaty cleavages scarcely developed in mudstone. Kobotoke Group, at the west of Kosuge. 10. Thrust faults displace the scoriaceous layer (dark). Misaki Formation at Kenzaki, southernmost part of the Miura Peninsula.

horizon around Otaki, Chichibu district, and upward in the north of Ogochi, shear folds made of slaty cleavages and phyllitic planes are well developed. The slump deposits which occupy the southern part of the group are more or less sheared to form lens structures. There is no regular slate plane. In the upper part to south flexural-slip folds with remarkable bedding slip are observed. Therefore it is summarized that in the north a

series of shear folds predominates while in the south series of lens folds predominates (Figs. 4 and 5).

The Kobotoke Group, south of the Ogochi, is composed mainly of sandstone and mudstone with turbidite. Sandy deltaic aprons are developed in the northeastern part of the group. An Upper Cretaceous ammonite has been found in float in the middle horizon (MATSUMOTO *et al.*, 1973). Basaltic rocks are intercalated in the lower sandstone in the middle part. Slump deposits are distributed with dacitic tuff and chert along the southern margin of the group. Strata are deformed in steeply dipping to overturned or recumbent folds of various scales. The enveloping surfaces in the order of one kilometer across are gently undulating (Fig. 3). As for the large scale folds, those in the north show north vergence and those in the south have south vergence. One anticline in the middle part shows south vergence in the west and is twisted to east to show north vergence (Fig. 3). Along the river south of Motojuku, typical mushroom folds on the scale of several hundred meters are observed (B-B' in Fig. 3). Gently dipping strata are rather widely developed in the central part of the folds.

Small structures in the Kobotoke Group are developed differently from north to south. In the north folds are characterized by a series of shear folds and in the south by a series of lens folds, though several intermediate types are observed in places. Flow folds are developed in the cores of anticlines or synclines. In the northernmost and some middle parts, muddy sediments are deformed with development of slaty cleavage or phyllitic planes. Bedding slip is rarely observed in the alternating beds of sandstone and mudstone, which contains slaty cleavage (Pl. II-6). There are some examples of recumbent folds without bedding slip and with slaty cleavages in mudstone. This is the intermediate type between flexure folds and shear folds. In the south, on the other hand, lens folds are typically developed. The muddy sediments are usually sheared by irregularly developed shear planes. The sandstone layers in the alternating beds of sandstone and mudstone are strongly deformed into lenticular bodies (Pl. II-7, 8). Lens folds gradually convert to the style of flow folds to north, and then change into flexural-slip folds further to the north (Pl. II-9). To the north slaty cleavages are developed in mudstone and flexural slip and flexure folds in the alternating beds of sandstone and mudstone at the same outcrop. Gradual changes from lens to flow, and flow to shear or flexure folding occur in the north-south section (Figs. 4 and 5).

4. Miura Fold Belt in the Miura Peninsula

The distributions of the Miura Basin is outlined by the upper Oligocene-lower Miocene Hayama Group (Fig. 6). This basin was filled with the Upper Miocene Misaki and Hatsuse Formations of the Miura Group, which conformably or unconformably overlies the Hayama Group or Yabe Formation (AKAMINE *et al.*, 1956; KIMURA, M., 1971). The Misaki and Hatsuse Formations are composed of considerable amounts of scoria, pumice and tuffaceous siltstone. They are free from any continent-derived material such as quartzose sediments. The volcanoclastic material such as scoriaceous or pumiceous turbidite decrease to north. They were supplied chiefly from south or west, probably from the volcanic islands situated around the present Izu Peninsula.

The strata in the Miura Basin are generally gently undulated into some nose or dome-basin structures (Fig. 6), but some intense folds show south vergence. Strata are not compacted hard, nor have they suffered from significant metamorphism, but they are deformed

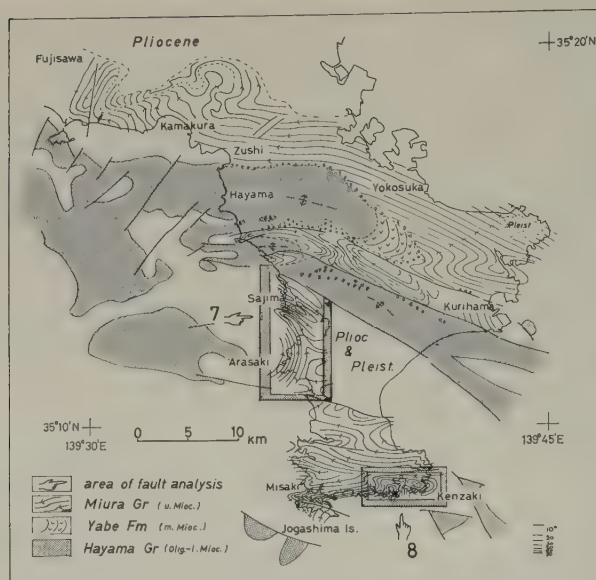


Fig. 6. Sketch map of the Neogene sediments in the Miura Peninsula. Data in the southern part partly after ABE (1978), in the middle-east after MITSUNASHI and YAZAKI (1968), and in the north after Ogawa (unpublished data, 1976) and IIZUKA (1978). Distribution of the Hayama Group mainly after GEOLOGICAL SURVEY OF JAPAN (1976). Strata dip right side of the arrows.

by various types of small faults. Especially in the Misaki Formation, which is composed mostly of turbidite of tuffaceous siltstone and scoriaceous sandstone or conglomerate, many small scale faults are developed together with slump and slide deposits (Pl. II-10). The tectonic and sedimentary structures indicate that they were developed immediately after deposition. Two main stages of the formation of faults are recognized.

The first is characterized by thrust faults, and the second by normal-strike slip faults. The two are developed in the area where bedding planes are variable. The principal stress axes of each type deduced from the conjugate sets of shear planes trend systematically in view of the large fold patterns (Figs. 7 and 8). As for the first stage, the stress axes are converted to the original stage of the formation of faults by rotating of the bedding planes to the horizontal as shown in the figures, since they are assumed to have developed when the strata were still horizontal. As shown in Figs. 7 and 8, the maximum compressive principal stress axes tend to parallel the present strike of the bedding planes (=marked in the projection), and the minimum stress axes were nearly vertical. This indicates that the stress field at the formation of the thrust faults are compressional, related to the shearing at the beginning of the doming in the basin.

In the second stage, faults of mainly normal and strike slip types were developed. Conical type faults are occasionally developed. Usually the compressive stress trends normal to the axes of syncline and anticline and the minimum axes parallel the axial direction. Therefore the normal compression to the axis of the folds during the development of the folds is inferred.

These two types of faults are developed rather continuously considering the nature and succession of the development. The folds related to the formation of the faults may

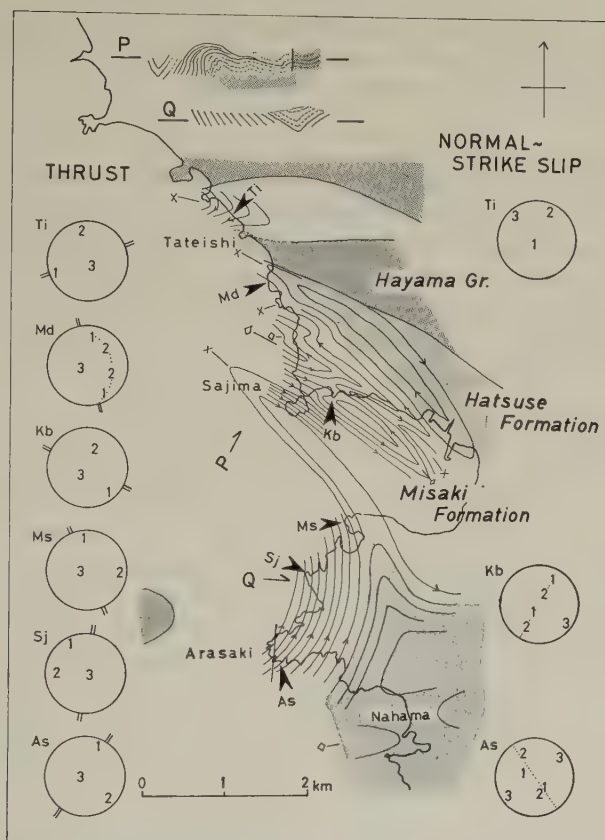


Fig. 7. Structural map in the Sajima-Arasaki area. 1, 2 and 3 in the projections indicate the maximum, intermediate and minimum principal compressive stress axes respectively deduced from conjugate sets of shear planes. Data around Sajima after UENO (1974). Lower-hemisphere equal area projection on a horizontal plane. = mark indicates the direction of a strike of bed.

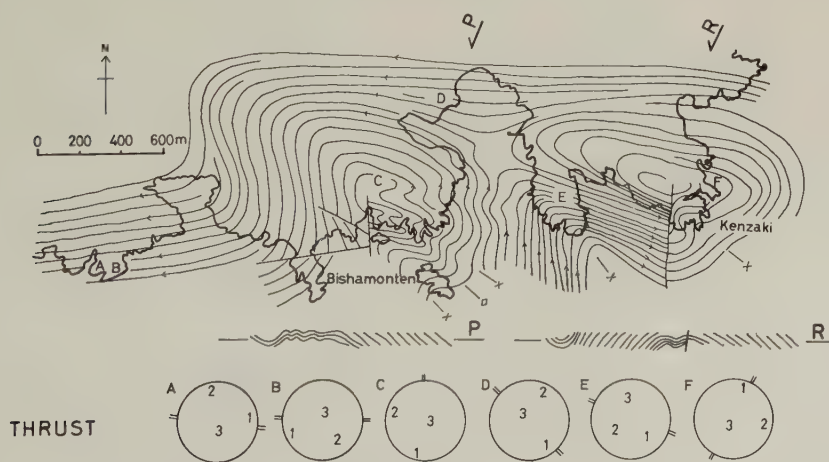


Fig. 8. Structural map in the Kenzaki-Bishamonten area. Explanations are the same as in Fig. 7.

have been influenced both by the lateral shearing within the basin and by the relative uplift of the basement, since the anticlines of the Misaki Formation coincide with the distribution of the substrata Hayama Group.

5. *Tectonic Significance of the Cretaceous Shimanto Geosyncline and the Miura Basin*

As mentioned above there are two types of accretionary fold belts in central Japan. One is the Shimanto and the other is the Miura. The former developed in and around the area of arc trench gap and trench slope and its tectonics could be explained by subduction tectonics. The tectonics of the latter is explained by the compressive shearing on transform type plate boundary.

5.1 *Shimanto Fold Belt*

The Shimanto Fold Belt in the two areas shows particular internal fold patterns. The folds in the core of the belt are characterized by upward diverging of opposite-vergence folds, namely the inner folds show inner vergence and the outer folds outer vergence. The enveloping surfaces in the flank of the fold belts are almost horizontal. It has been postulated that the axial planes were twisted and dragged laterally in the late-stage upheaval of the mountains (MATSUSHIMA, 1973). But the cleavage planes do not show any significant rotation. The large scale folds observed in the core part of the mountain are of the principal folding stage. Lateral drag might have occurred during the deformation of the western part of the Fossa Magna, the left lateral slip since Paleogene (TOKUYAMA and HANDA, 1978). In the Kii Peninsula, SUZUKI (1975) reported some mushroom folds in the Paleogene Muro Group in the outer half of the Shimanto Terrain. There are, however, no other examples of such folds in the Shimanto Terrain. These folds might be the specific style in the area of the Akaishi and Kanto Mountains and other parts where particular collisional tectonism occurred. At least in these areas fold patterns could not be explained by oneway polarity of lateral compression but rather well be explained by collisional compression within the geosyncline. In the both sides of the Fossa Magna, the microcontinent Izu Peninsula collided against the Japanese Islands and the collisional features also occurred in these regions in the Neogene sediments (MATSUDA, 1978).

There is another problem on the tectonics of the Shimanto Geosyncline: the basaltic magmatism. The basaltic rocks in the Akaishi Mountains are lava, partly with pillow structures, and hyaloclastites. They are intercalated between muddy sediments in the lower horizon. Some basaltic rocks developed in the innermost and outermost parts of the Shimanto Terrain in Shikoku are regarded as fragments scraped from oceanic crust itself (SUZUKI *et al.*, 1978; Hada, personal communication, 1978). But layers in the central part of the Shimanto Fold Belt in the Akaishi and Kanto Mountains are distributed widely (Figs. 2 and 3) not as fragments and are conformably intercalated within clastic sediments. The sediments under the basaltic layers in the central part of the Kobotoke Group are quartz-feldspathic. These are not explained by scraping of the oceanic crust derived from beyond the trench.

As far as is known at present, there is no sedimentary basin in the forearc area containing basaltic volcanism. It should be noted that the basaltic rocks discussed are relatively thin, and are intercalated as one or a few layers in restricted horizons. The volume generally attains 5% and partly 10% at most. We do not interpret the Shimanto Geosyncline to be a so-called big eugeosyncline, but interpret that the basin is 'non-eugeo-

synclinal' and is characterized by a temporary basaltic volcanism. The volcanism may be attributed to a short extensional stage at the beginning of the arc-trench gap. At that stage rhyolitic or dacitic volcanism and sedimentation of chert and limestone also occurred in the area.

The slump deposits in some parts of the groups, including various kinds of rocks fragments such as chert, limestone, basaltic rocks as well as dominant sandstone, may be *mélange* deposits on the trench slope. Figure 5 shows hypothetical sections for the Jurassic-Cretaceous status in the Kanto Mountains, where, in Triassic and partly Jurassic, the Sambosan Group rested in the arc-trench gap with big limestone masses on the trench slope break or basement high. The large faults thrust outward under the trench slope break, probably corresponding to faults with large *tsunamicity* (FUKAO, 1978), become the Butsuzo Line afterward. In the next stage the sedimentary area prograded outward and the Kobotoke Group were widely deposited as arc trench gap sediments.

The shift of the sedimentary area is attributed to a jump of subduction of the oceanic plate (KIMURA and TOKUYAMA, 1971). The slump deposits on the southernmost area of the Kobotoke Group around Nanaho correspond to trench-slope sediments.

5.2 Significance of the divergent development of the fold styles

As mentioned above, fold styles are differently distributed in the inner and outer parts in the Shimanto Fold Belt. Series of shear folds are characteristically developed in the inner side and series of lens folds in the outer. The shear folds are characterized by slaty cleavages, which were formed under relatively steady state flow in the rocks. On the other hand the lens folds are characterized by fault planes, which were formed by stick slip of brittle deformation. Generally flexure folds without bedding slip are developed in the upper horizon of the shear folds, and flexural-slip folds with remarkable bedding slip do occur in the upper horizon of the lens folds (Figs. 5 and 9). The steady state flow and stick slip may be differently developed under the different ductility contrast (UEMURA, 1978). The tectonic levels are chiefly influenced by mean ductility, and ductility con-

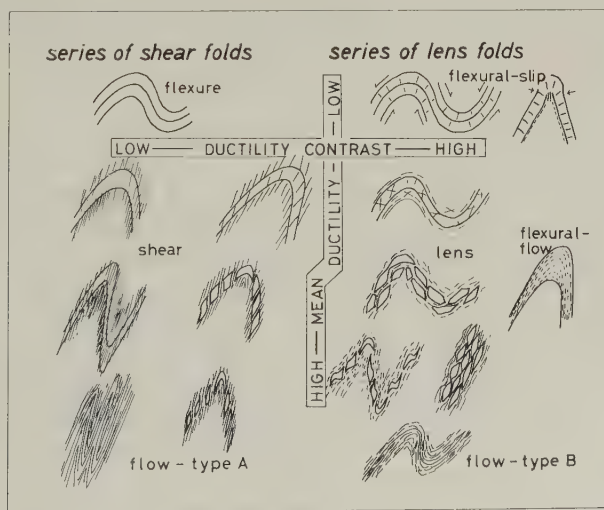


Fig. 9. Fold styles in different series. Basically after KIMURA (1968).

trast is generally variable according to the homogeneity within the rocks and to the condition outside, especially temperature.

As for the similar rocks type like the alternating beds of turbidite, the relative difference in the outside condition can be compared (KIMURA, 1968; OGAWA, 1978). The steady state flow occurs under higher temperatures when confining pressure are constant (HANDIN and HAGER, 1958). In these considerations it will be supposed that in the Shimanto Fold Belt the inner part which is characterized by series of shear folds was situated in the area of much higher geothermal gradient than the outer part which is characterized by the series of lens folds.

The lateral variation of the value of the geothermal gradient was first introduced to the trench and island arc area by TAKEUCHI and UYEDA (1965) and was further discussed in view of the origin of paired metamorphism by MATSUDA *et al.* (1967), MATSUDA and UYEDA (1971), MIYASHIRO (1972) and others. But it does also realize in the mid-depths around the arc trench gap area of the Cretaceous geosyncline in central Japan. The small scale orogenic belt of the Shimanto Fold Belt may have the similar condition of the paired metamorphism.

5.3 Miura Fold Belt

The Miura Basin in upper Miocene corresponds to the flank of the Tanzawa Eugeosyncline, where a vast extent of submarine basaltic to dacitic volcanism occurred throughout Miocene, and a collisional Alpine type mini-orogenic belt occurred in late Tertiary and Quaternary (SEKI *et al.*, 1969; MATSUDA, 1978). The sediments in the Miura Basin were derived chiefly from the volcanic region around Izu, southern extension of the Tanzawa. The Shirahama Group in Izu, equivalent to the Misaki and Hatsuse Formations in Miura, is not structurally deformed, but the Misaki Formation is both sedimentarily and structurally deformed in complex fashion. Small faults originated from differential compressive stress under low confining pressure just after sedimentation. The first stage of the faulting was during lateral compression at the beginning of folding, and the second stage was during the maximum development of the folding. The fold patterns as a whole represent a strike slip stress field. The basin was strongly affected by shearing similar to the present Sagami Trough as the boundary between the Philippine Sea and Pacific Plates. The fault on the trough has right lateral strike slip movement with a thrust component (ANDO, 1974). This movement is characterized by the plate motion to the northwest side of the triple junction of Japan, which is situated about 200 km southeast of the Miura Peninsula (Fig. 1). On the Plate of Philippine Sea, the Izu Peninsula moves northward to collide the central part of Japan (MATSUDA, 1978). The lateral movement around the region may be traced back at least to the sedimentation stage of the Misaki Formation, about 12 mybp (after the geomagnetic correlation by NIITSUMA, 1978). It is said that the Shikoku Basin began to spread westward at 40, 27 or 22 mybp (KOBAYASHI and ISEZAKI, 1975; WATTS and WEISSEL, 1975; TOMODA *et al.*, 1975). This roughly coincides with the change of the plate system around Japan and with the beginning of the opening of the Sea of Japan (HORIKOSHI, 1975). These tectonic movements intersected around the southern Fossa Magna area and the sedimentary and structural complexities occurred on both sides of the Fossa Magna and Miura Basin. Thus collisional and strike slip tectonics in these area are interpreted in relation to regional tectonics.

6. Summary

Tectonics in the Shimanto and Miura Fold Belts in central Japan is discussed in view of the sedimentation and deformation on the plate boundaries.

Shimanto Fold Belt in the Akaishi and Kanto Mountains grown up from the Cretaceous Shimanto Geosyncline. The development is summarized as follows:

1) Sediments are composed of trench slope slump deposits in the lower and inner part and by arc-trench gap ones in the outer and upper part. This set of position and rock facies migrated outward intermittently.

2) Basaltic rocks are included as slump fragments in the trench slope deposits but those in the arc-trench gap ones are not fragments but layers in situ. They may have been extruded at the extensional stage of the basin.

3) Fold styles in the inner and outer are characterized by the series of shear and lens folds respectively. This difference is attributed to different geothermal gradients in the area. This is similar to the origin of the paired metamorphism in arc-trench area.

4) Large scale fold patterns are of upward diverging vergence, like of mushroom folds. This suggests that they are formed by collisional tectonics, not by oneway slicing.

Miura Fold Belt grown up from the Miocene Miura Basin, and the development is summarized as follows:

1) Sediments are mostly volcanoclastics derived from the outer oceanic side not from the inner continental side. They are deposited on the right laterally slipped area along the plate boundary between the Asian and Philippine Sea Plates.

2) The fault systems indicate that they were formed by lateral slip and compressive stress in the basin.

We are grateful to Professor Fukutaro Hori of Nihon University for his interest and stimulus through the study. We also thank Professor Toshio Kimura of University of Tokyo for his field guide and discussions. Professor Kazuo Kobayashi and the staff of Ocean Research Institute of University of Tokyo are appreciated for their discussions. Messrs. Nobuyuki Matsushima, Tsutomu Hiraki, Kazuo Uchida and Keiichi Endo are acknowledged for the guidance in the field survey. The manuscript has been reviewed by Dr. Richard W. Murphy of Exxon Production Research Company, Houston, Texas and we thank him for the constructive help in its improvement. Expenses of this study were partly paid by Grants in Aid for Scientific Research from Nihon University and Ministry of Education of Japan.

REFERENCES

- ABE, N., Stratigraphy and geologic structures in the southern part of the Miura Peninsula (MS), 58pp. Nihon Univ., 1978.
- AKAMINE, H., S. IWAI, K. KOIKE, Y. NARUSE, S. OGOSE, M. OMORI, Y. SEKI, K. SUZUKI, and K. WATANABE, Geology of the Miura Peninsula, *Chikyu-Kagaku (Earth Sci.)*, **30**, 1-8, 1956.
- ANDO, M., Seismo-tectonics of the 1923 Kanto Earthquake, *J. Phys. Earth*, **22**, 263-277, 1974.
- DICKINSON, W.R., Subduction tectonics in Japan, *EOS, Trans. Am. Geophys. Union*, **58**, 948-952, 1977.
- FUKAO, Y., Slip process along the lithospheric interface in island arcs, this issue, 1978.
- FUJIMOTO, H. and M. SUZUKI, Geology of the basin of the River Obora-gawa, a tributary of the River Arakawa *Bull. Chichibu Mus. Nat. Hist.*, **15**, 1-18, 1969.
- GEOLOGICAL SURVEY OF JAPAN (ed.), Geological Map of Tokyo Bay and adjacent areas (1: 100,000), 1976.
- HANDIN, J. and R.V. HAGER, Jr., Experimental deformation of sedimentary rocks under confining pressure: Tests at high temperature, *Am. Assoc. Pet. Geol. Bull.*, **42**, 2892-2934, 1958.
- HORIKOSHI, E., Genesis of Kuroko-stage deposits from the tectonical point of view, *Bull. Volc. Soc. Jpn., Sec. Ser.*, **20**, 341-353, 1975.
- IIZUKA, M., On the geology in the northern part of the Miura Peninsula (MS), Nihon Univ., 23pp., 1978.
- KANMERA, K., Correlation between the geosynclinal sediments of past and present, I and II, *Kagaku (Science)*, **46**, 284-291, 371-378, 1976.

- KANMERA, K., General aspects and recognition of olistostromes in the geosynclinal sequence, in *Progress of the Study on the Geologic Developments of the Japanese Islands*, Assoc. Geol. Collab. Jpn. Monogr. No. 20, pp. 145–159, 1977.
- KANMERA, K. and S. SAKAI, On the correlation of the past geosynclines of the Shimanto, *GDP Rept. II-1-(1)*, No. 3, pp. 55–64, 1975.
- KIMURA, M., Crustal model in the South Kanto region, *Chishitsu News (Geol. News)*, **204**, 1–10, 1971.
- KIMURA, T., Some folded structures and their distribution in Japan, *Jpn. J. Geol. Geogr.*, **39**, 1–26, 1968.
- KIMURA, T., The ancient continental margin of Japan, in *The Geology of Continental Margins*, edited by C.A. Burk and C.L. Drake, pp. 817–829, Springer, New York, 1974.
- KIMURA, T. and A. TOKUYAMA, Geosynclinal prism and tectonics in Japan, *Geol. Soc. Jpn. Mem.*, **6**, 9–20, 1971.
- KOBAYASHI, K. and N. ISEZAKI, Magnetic anomalies in the Sea of Japan and the Shikoku Basin: Possible tectonic implications, in *The Geophysics of the Pacific Ocean and its Margin*, edited by G.H. Sutton, M.H. Manghnani, and R. Moberly, Geophys. Monogr. Ser. Vol. 19, pp. 235–251, 1976.
- KOBAYASHI, T., The Sakawa Orogenic Cycles and its bearing on the origin of the Japanese Islands, *J. Fac. Sci., Univ. Tokyo, Sec. 2*, 219–578, 1941.
- MATSUDA, T., Collision of the Izu-Bonin arc with the central Honshu-Cenozoic tectonics of the Fossa Magna, Japan, this issue, S 409–S 421, 1978.
- MATSUDA, T., K. NAKAMURA, and A. SUGIMURA, Late Cenozoic orogeny in Japan, *Tectonophysics*, **4**, 349–366, 1967.
- MATSUDA, T. and S. UYEDA, On the Pacific-type orogeny and its model of the paired belts concept and possible origin of marginal seas, *Tectonophysics*, **11**, 5–27, 1971.
- MATSUMOTO, T., Fundamental problems in the circum-Pacific orogenesis, *Tectonophysics*, **4**, 595–613, 1967.
- MATSUMOTO, T., H. OTSUKA, and K. OKI, Cretaceous fossils from the Shimanto belt of Kagoshima Prefecture, *J. Geol. Soc. Jpn.*, **79**, 703–704, 1973.
- MATSUMISHIMA, N. (ed.), Geological Map of Shimoina (1: 100,000), Editorial Committee of History of Shimoina, Nagano Prefecture, 1972.
- MATSUMISHIMA, N., The Median Tectonic Line in the Akaishi Mountains, in *Median Tectonic Line*, edited by R. Sugiyama, pp. 9–27, Tokai Univ. Press, Tokyo, 1973.
- MATSUMISHIMA, N., Geology of the Southern Alps of Japan—Geologic structure of the Shimanto Belt in the Akaishi Mountains, *J. Nat. Sci., Shimoina Educ. Soc. (Geol.)*, **1**, 119–134, 1978.
- MITSUMASHI, K. and K. YAZAKI (eds.), Geological Map of the Oil and Gas Field, 6, Miura Peninsula (1: 25,000), Geological Survey of Japan, 1968.
- MIYASHIRO, A., Pressure and temperature conditions and tectonic significance of regional and ocean-floor metamorphism, *Tectonophysics*, **13**, 141–159, 1972.
- NIITSUMA, N., Magnetic stratigraphy of the Japanese Neogene and the development of the island arcs of Japan, this issue, S 367–S 378, 1978.
- NISHIMIYA, K., Discovery of *Inoceramus* from the Kobotoke group, Kosugemura, Yamanashi Prefecture, *J. Geol. Soc. Jpn.*, **82**, 795–796, 1976.
- OGAWA, Y., Structural characteristics and tectonisms around the microcontinent in the outer margin of the Paleozoic-Mesozoic geosyncline of Japan, *Tectonophysics*, **47**, 295–310, 1978.
- SEKI, Y., Y. OKI, T. MATSUDA, K. MIKAMI, and K. OKUMURA, Metamorphism in the Tanzawa Mountains, central Japan, *J. Assoc. Jpn. Min. Pet. Econ. Geol.*, **61**, 1–25, 50–75, 1969.
- SUZUKI, H., Deformed structures and deformational history of the Paleogene Muro flysch nepton in southwest Japan, in *Concept of Geosyncline*, Assoc. Geol. Collab. Jpn. Monogr. No. 19, pp. 167–177, 1975.
- SUZUKI, T., S. HADA, T. SAKAMOTO, and H. NAKAGAWA, Origin of the green-rocks in the Shimanto belt, Abstr. 85th Annu. Meet., Geol. Soc. Jpn., p. 286, 1978.
- TAKEUCHI, H. and S. UYEDA, A possibility of present-day regional metamorphism, *Tectonophysics*, **2**, 59–68, 1965.
- TOKUYAMA, A. and K. HANDA, Structural framework and recent crustal movements of the Fossa Magna, *J. Geogr., Tokyo Geogr. Soc.*, **87**, 68–81, 1978.
- TOMODA, Y., K. KOBAYASHI, J. SEGAWA, M. NOMURA, K. KIMURA, and T. SAKI, Linear magnetic anomalies in the Shikoku basin, northeastern Philippine Sea, *J. Geomag. Geoelectr.*, **27**, 47–56, 1975.
- UEMURA, T., Deformational facies and series, Abstr. 85th Annu. Meet., Geol. Soc. Jpn., p. 391, 1978.
- UENO, M., Geologic structure in the Sajima area, Miura Peninsula (MS), Nihon Univ., 35 pp., 1974.
- UYEDA, S. and A. MIYASHIRO, Plate tectonic model and Japanese Islands: A synthesis, *Geol. Soc. Am. Bull.*, **85**, 1159–1170, 1974.
- WATTS, A.B. and J.K. WEISSEL, Tectonic history of the Shikoku marginal basin, *Earth Planet. Sci. Lett.*, **25**, 239–250, 1975.
- YEHARA, S., Geotectonics of the Pacific concerning the Japanese Islands. II, *J. Geol. Soc. Jpn.*, **59**, 510–526, 1953.

PERMIAN AND TRIASSIC SEDIMENTARY HISTORY OF THE HONSHU GEOSYNCLINE IN THE TAMBA BELT, SOUTHWEST JAPAN

Daikichiro SHIMIZU,* Nobuhiro IMOTO,** and Makoto MUSASHINO**

**Department of Geology, Faculty of Science, Kyoto University, Kyoto, Japan*

***Department of Geology, Kyoto University of Education, Kyoto, Japan*

(Received July 7, 1978; Revised September 18, 1978)

The Honshu Geosyncline of middle Paleozoic to early Mesozoic age suffered a strong diastrophism in late Permian to early Triassic as shown by many stratigraphic breaks in the Maizuru and other Belts of Southwest Japan. This geosyncline survived through the Triassic Period in the Tamba and other Belts. The Tamba Belt had many troughs, submarine volcanism and also some tectonic lands. Abundant detrital materials had been supplied from both northern uplifting land, and southern tectonic lands. Detailed nature of sediments and their facies distribution and paleogeography of the middle to late Triassic Period are discussed.

1. Introduction

The Honshu Geosyncline (middle Paleozoic to early Mesozoic) of Japan is represented by extensive distribution of thick formations in the southwest Japan. In its upper formations, two distinct facies have been noticed, namely calcareous facies and non-calcareous facies of the same age. The former facies is typically exposed as the Akiyoshi and other plateaus in the inner side of the southwest Japan, where the formations are composed of several hundred meter thick limestone sequence (Fig. 1) of middle Carboniferous to middle Permian age. These limestone facies have been shown to be a reef complex constructed on the top of seamounts of early Carboniferous (OTA, 1968; OKIMURA, 1975). On the other hand, the latter non-calcareous facies is distributed in a wider area than these limestone reefs. The non-calcareous facies is composed of thick clastic rocks, bedded cherts and submarine volcanics with rare limestone lentiles. This facies is several thousand meters in thickness, and represents a region of deeper water depth and rather rapid subsidence than the limestone facies of the same age. The limestone areas were buried by clastic rocks in the late Permian, and then changed to positive areas in the Triassic Period. Together with these areas, the wide region of the Chugoku and the Hida Belts were uplifted in the Triassic. At the same time, some regions continued to subside in the Triassic, namely, the Tamba Belt, the Ryoke Belt and others.

The Tamba Belt has many exposures of Permian and Triassic formations characteristic to eugeosyncline. The writers and their colleagues (TAMBA BELT RESEARCH GROUP) studied this Belt around Kyoto, with the purpose of clarifying its stratigraphy, sedimentary characteristics, and geologic structures. They also planned to reconstruct the paleogeography of this Belt and adjacent regions in the Permian and the Triassic Periods. In the following, several features of eugeosynclinal facies of the Belt are described, and tectonic status and paleogeography are mentioned.

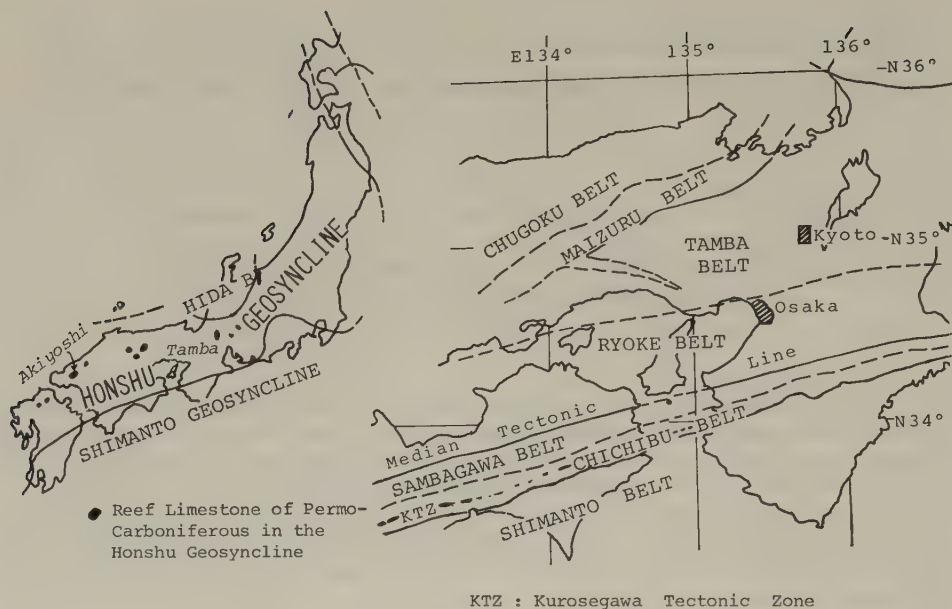


Fig. 1. Index map.



Fig. 2. Distribution of the Triassic coarser clastic rocks (dotted area) and paleocurrent direction (arrows) in the Tamba Belt at the northern hills of Kyoto City (Complied from data of TAMBA BELT RES. GROUP, 1971; and MUSASHINO and NAKAMURA, 1976).

2. Geosynclinal Formations of the Tamba Belt

Paleozoic and Mesozoic formations of the Tamba Belt are composed of clastic rocks, bedded cherts and submarine volcanics (so-called Schalstein) with small lentiles of limestone. The geological age of the Tamba Group is determined by fusuline and conodont fossils as middle Carboniferous to late Triassic.

Clastic rocks. Clastic rocks are slate-shale, sandstone and rare conglomerate, and they show sometimes turbidite sequences. Sandstone is contained in the upper and middle formations of the Tamba Group (SAKAGUCHI, 1961). The rock is generally poorly

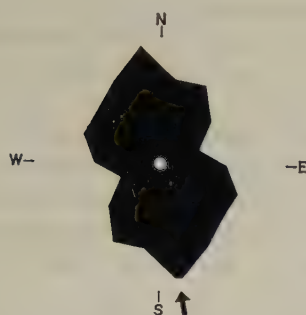


Fig. 3. Distribution diagram of long axis directions of sand grains, sandstone bed of the Tamba Group, at the northern hills of Kyoto City (MUSASHINO and NAKAMURA, 1976). Arrow indicates paleocurrent direction determined from sole marking of the same bed.

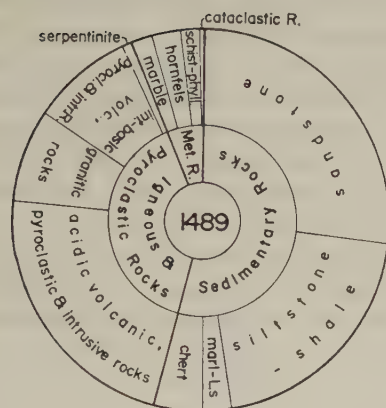


Fig. 4. Rock species of pebbles of a conglomerate of the Tamba Group, in the northern hills of Kyoto City. 1489 pebbles are examined. (MUSASHINO and NAKAMURA, 1976).

sorted and the grains are angular with many lithic fragments. The lithology corresponds to greywacke. The strata of sandstone occasionally show typical turbidite sequence, having grading, cross- and parallel laminations, and accompany pelitic layers on the top of the beds. Sole markings are sometimes observed in the turbidite sequences. Many kinds of flute cast and load cast are found. The flute casts show paleocurrent direction from South-SSE to North-NNW (TAMBA BELT RES. GROUP, 1971, 1974; MUSASHINO and NAKAMURA, 1976) (Fig. 2). Grain orientation of sand in turbidite layers shows the same direction as that of sole markings (Fig. 3).

A few conglomerate beds are intercalated in sandstone and shale formations of the upper to middle part of the Group. They are usually so-called muddy conglomerate and poorly sorted. The size of pebbles varies from cobble to granule. Statistic analysis of lithology of pebbles shows that clastic sedimentary rocks are most common, and chert pebbles are rather rare (Fig. 4). The point to be noted is abundance of acidic volcanics and pyroclastics. They are rhyolitic and dacitic rocks and tuffites, and welded structures is frequently observed. Granitic rocks are also included. These facts indicate an intensive acidic igneous activity on a vast land area prior to the eugeosynclinal stage to the south of the Tamba Belt (SHIMIZU *et al.*, 1974). Orthoquartzitic pebbles are found in conglomerate, and can be correlated to the Precambrian rocks of Asian continent (may be southern extension of the continent). The materials of the beds including conglomerate were supplied from the south and/or southeast judging from the sole markings which are the same

as those of sandstone beds. From these sedimentary features of clastic rocks, the existence of some uplifting land masses of various rocks is estimated to the south of the Tamba Belt. These land masses may have existed as tectonic land in the eugeosynclinal basin during the Permian to late Triassic Period.

Chert. There are three types of cherts, namely bedded, massive and nodular, in the Belt. Among them, bedded cherts are most predominant. Bedded cherts are the type showing rhythmical alternation of siliceous layers a few to 10 cm in thickness and thin clay films. Etching procedure by dilute HF solution is very convenient for the observation of siliceous layers. By examination using this procedure, the following characteristics have been clarified.

Siliceous layers are mainly composed of organic remnants, such as radiolarian tests and sponge spicules, and frequently include conodont fossils. Some kinds of sedimentary structures, namely grading, parallel and cross laminations, cut and fill structure and orderly arrangements of sponge spicules or radiolarian spines are observed (IMOTO and SAITO, 1973; IMOTO and FUKUTOMI, 1975). An example showing the relationship between the current direction obtained from cross-lamination and orderly arrangement of sponge spicules is cited in Fig. 5 (TAMBA BELT RES. GROUP, 1974). Also a sole marking concluded to be a flow mark was discovered at the central part of the Tamba Belt. Figure 6 shows a sketch of surface cut along the flow direction (IMOTO *et al.*, 1974).

The above-mentioned sedimentary structures clearly show that organic remnants composing the siliceous layers of bedded cherts have been deposited under the influence of current including the siliceous turbidity currents (NISBET and PRICE, 1974; IMOTO and

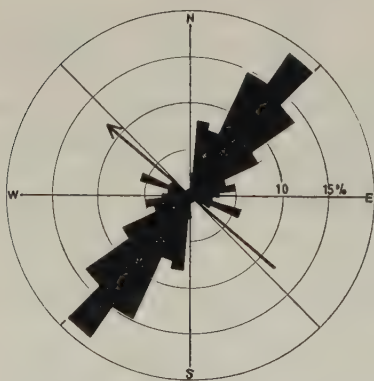


Fig. 5. Preferred orientation of sponge spicules on a lamination of chert layer (measured 122 spicules). Arrow indicates paleocurrent direction assumed from cross lamination in chert layer. (TAMBA BELT RES. GROUP, 1974).

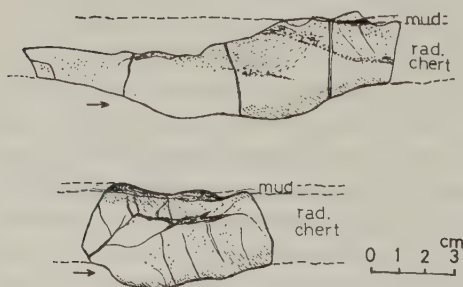


Fig. 6. Longitudinal cross cut section of sole marks (flute mould) of bedded chert layers in the Tamba Belt. Arrows indicate paleocurrent direction determined by sole markings, and show fine coincidence between sole markings and cross laminations in the layer (IMOTO *et al.*, 1974).

FUKUTOMI, 1975). The mode of occurrences and the sedimentary structures of the bedded cherts clearly differ from them of radiolarian oozes of the present ocean bottom (IMOTO and FUKUTOMI, 1975).

Submarine volcanism. Greenstone formations of the Tamba Group were studied by OKAICHI and others (1975). Their observation clarified that the so-called "Schalstein" beds are accumulation of basaltic lavas and pyroclastics. The occurrences and characteristics of thick green stone formations of the Tamba Group are as follows. The formations are divided into many pillow lava layers. Each pillow lava layers has thickness of 15–30 m, and is composed of several parts, namely, massive lava part, pillow lava part, hyaloclastite part and associated pelitic layers in ascending order. In the pillow lava part, the size of pillow blocks becomes gradually smaller from the lower part to the upper part. Two thick greenstone formations are extensively distributed in the Tamba Belt. They are called the lower f-formation and the upper h-formation (TAMBA BELT RES. GROUP, 1971, 1974). OKAICHI and others (1975) discriminated the two formations by the difference in their minerals and occurrences. The lower f-formation contains small limestone lentiles. On the other hand, the upper h-formation has manganese and silica ores in common but no limestone lentiles. The h-formation is associated with a bedded chert formation in the upper horizon at each exposures. The horizons and ages of two formations are determined by fossils. The lower f-formation is early to middle Permian in age, judging from many fusuline fossils contained in the limestone lentiles (TAMBA BELT RES. GROUP, 1974). The upper h-formation is estimated as early to middle Triassic by conodont fossils found in or near the horizons of the formation. The two formations can also be discriminated by composition and optics of minerals (OKAICHI *et al.*, 1975).

The submarine volcanic activity of the Permian and Triassic Periods in the Tamba Belt has some centers of eruption. They were estimated by the change in thickness and composition of pillow lava sequences. The thickness of formation gradually diminishes from several hundreds of meters or one thousand meters to several tens of meters within a distance of several or 10 km. The site of submarine volcanism seems to show some linear arrangement along the direction of the Maizuru Belt, and also in another direction oblique to the former direction (Fig. 7). They may correspond to some lineaments in the eugeosynclinal through in the Belt. Sites of volcanic eruptions might shift in the ages of the Permian and the Triassic Periods.

3. *Paleogeography*

Facies distribution. The Tamba Belt was an eugeosynclinal basin throughout the Triassic Periods. As shown in Fig. 7, sediments of the middle to late Triassic Period of this Belt are distributed in a characteristic east-west trend. In the northern region of the Belt, coarser clastic beds (sand-shale alternation with turbidite sequences) extend along the border of the Maizuru Belt and in a more eastern region. YOSHIDA (1977) estimated that they were supplied from the north by turbidity currents. They originated on or near the shelf of the Maizuru Belt and carried into the Tamba Belt, forming sedimentary prism at the foot of the shelf. The coarser clastic materials of the region diminish southwards in size and amount and gradually change into shale facies associated with abundant cherts. The more southern middle region of the Belt is a chert-shale facies region of the same time. These beds intercalate with some dolomitic layers in the chert beds.

In the southern part of the Tamba Belt, coarser clastic facies occupy dominantly two

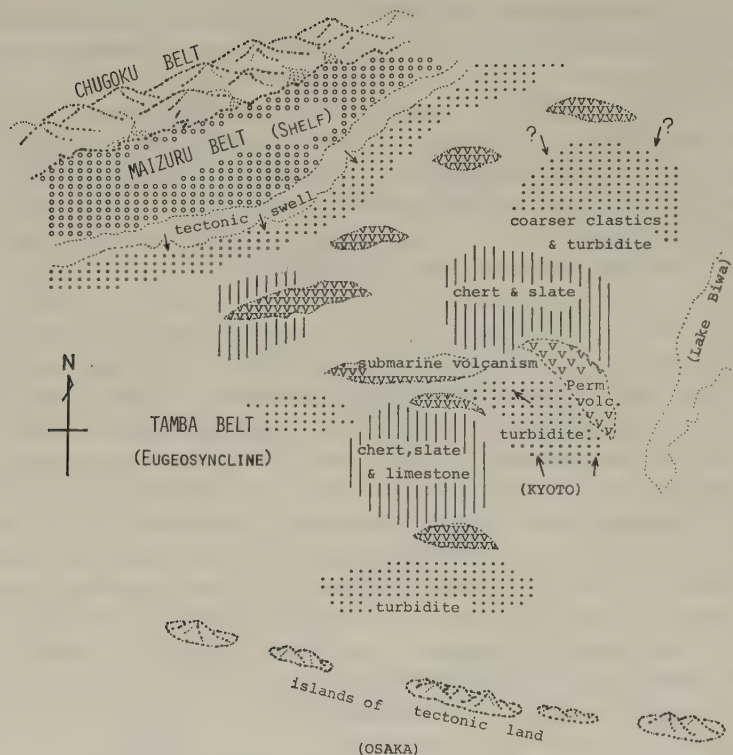


Fig. 7. Paleogeography and facies distribution of the Maizuru and the Tamba Belts in the middle to late Triassic Period.

areas, namely, the northern hills and the western hills of Kyoto City. In the northern hills, thick beds of sandstone and shale form a synclinal structure of NW-SE trend (Fig. 2, TAMBA BELT RES. GROUP, 1971). Turbidite sequences in these beds have many sedimentary structures described in the previous section, and show distinct paleocurrent direction of SE to NW and/or south to north as shown in Fig. 2. The thickness of formation is variable, that is, the formation is thickest in the axial part of the syncline and gradually diminishes in thickness to lateral wing part of the syncline. The variation of the thickness may represent the original difference of sedimentation rate or subsidence rate at the time of sedimentation.

In contrast to the coarser clastic formations, slate and chert facies of the Triassic age is widely distributed in the north-western hills of Kyoto, where the Triassic formations are represented by alternation of slate and bedded chert beds and sometimes intercalate thin limestone layers. This region must be a rather distal area of clastic materials and an area with less subsidence in the middle to late Triassic Period. It is to be noted that in some case these two facies divided by areas of greenstone of the same age. Submarine volcanism of basaltic lava formed seamounts topography and might have restricted supply of coarser clastic materials in this region. The older Permian seamount might also have retained their topography in the Triassic time. The areal arrangement of facies is shown in Fig. 7.

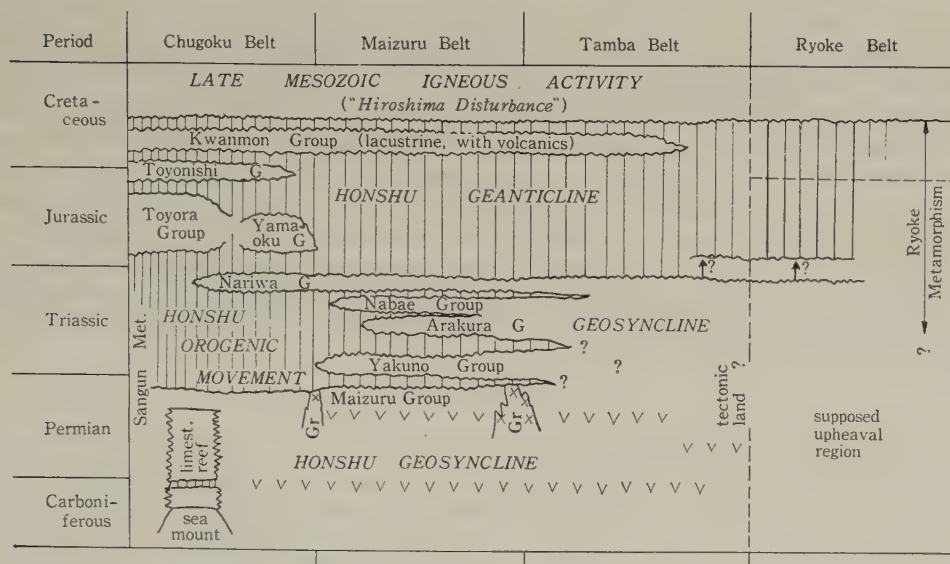


Fig. 8. Tectonic evolution of the Tamba Belt and adjacent regions in the late Paleozoic and Mesozoic Era (TAMBA BELT RES. GROUP, 1975)

The Maizuru Belt and the Tamba Belt. The Maizuru Belt was a typical field of the Honshu Orogenic Movement in the late Permian to Triassic Periods. As described by NAKAZAWA (1958), this Belt formed a shelf area during the Triassic Period, and accumulated thick neritic sediments, namely, the Yakuno Group of early to middle Triassic age, and the Arakura formation and the Nabae Group of the late Triassic Period (Fig. 8). These formations and Groups are divided by numerous unconformities. Stratigraphic evidence shows that repeated transgression and regression of this neritic sea covered a wide area of the Maizuru and the Chugoku Belt.

In the entire Permian and the Triassic Periods, the Tamba Belt persisted as an eugeosynclinal basin. In the Tamba Group, the lower to middle Permian and the middle to upper Triassic horizons are clearly recognized by many fossils. On the other hand, upper Permian and lower Triassic fossils are scarcely found in the Belt (NAKAZAWA and SHIMIZU, 1955). But no stratigraphic break is found in the Tamba Group. This Belt continued to subside in the Honshu Geosyncline throughout the Triassic Periods (Fig. 8).

Triassic sedimentary facies show some contrasts between various Belts, that is neritic shallow sea facies in the Maizuru and the Chugoku Belts and typically eugeosynclinal facies in the Tamba Belt. Triassic clastic materials supplied from both the uplifting northern land, and the southern tectonic lands (probably islands) and filled the eugeosynclinal trough of the Tamba Belt. Areal arrangement of lands and basins and sedimentary facies are shown in Fig. 7.

Paleogeographic reconstruction. The trend of paleogeography and submarine topography is parallel or subparallel with the main direction of the Honshu Geosyncline. They may have originated in the basement structure of the geosynclinal trough. The paleogeographic existence of troughs, tectonic lands and submarine volcanics is also estimated in the outside of the southwest Japan. The Kurosegawa tectonic zone of the Chichibu Belt

survived as island of tectonic land composed of various ancient rocks in the Permian and the Triassic Periods. These tectonic lands supplied abundant materials to the eugeo-synclinal trough of the Chichibu Belt (HADA, 1974). As mentioned above, eugeosynclinal sea of the Triassic Period of the southwest Japan was a system of borderland, shelf, troughs (with various rates of subsidence), sea mounts, tectonic lands with tectonic swells, and formed biaxial (inner and outer) geosynclinal basin. We have no information as to the southern end of the Honshu Geosyncline, but it can be estimated that some land mass ancestral to Kuroshio Paleoland existed at the Permian and the Triassic Periods. The paleogeography of Permian and Triassic of the southwest Japan thus can be compared with that of the topography and tectonic status of the present marginal sea like the north-western part of the Philippine Sea.

REFERENCES

- HADA, S., Construction and evolution of the intrageosynclinal tectonic lands in the Chichibu Belt of western Shikoku, Japan, *J. Geosci., Osaka City Univ.*, **17**, 1–52, 1974.
- IMOTO, N. and Y. SARRO, Scanning electron microscopy of chert, *Bull. Natl. Sci. Mus.*, **16**, 397–400, 1973.
- IMOTO, N., D. Shimizu, T. Shiki, and Y. Yoshida, Sole markings observed in bedded cherts from the Tamba Belt, Japan, *Mem. Kyoto Univ. Educ.*, Ser. B, **44**, 19–26, 1974 (in Japanese with English abstract).
- IMOTO, N. and M. FUKUTOMI, Genesis of bedded cherts in the Tamba Belt, southwest Japan, *Assoc. Geol. Collab. Jpn. Monogr.*, No. 19, 35–42, 1975 (in Japanese with English abstract).
- MUSASHINO, M. and M. NAKAMURA, Sandstone and conglomerate of Kuriyasha-dani in the Kumogahata area, the northern part of Kyoto City, *Mem. Kyoto Univ. Educ.*, Ser. B, **49**, 25–40, 1976 (in Japanese with English abstract).
- NAKAZAWA, K., The triassic system in the Maizuru zone, southwest Japan, *Mem. Coll. Sci., Univ. Kyoto*, Ser. B, **24**, 265–313, 1958.
- NAKAZAWA, K. and D. SHIMIZU, Discovery of Glyptophiceras from Hyogo Prefecture, Japan, *Trans. Proc. Palaeontol. Soc. Jpn. N.S.*, **17**, 13–18, 1955.
- NISBET, E.G. and I. PRICE, Siliceous turbidites: Bedded cherts as redeposited, ocean ridge-derived sediments, *Spec. Publ. Int. Assoc. Sediment.*, **1**, 351–366, 1974.
- OKAICHI, M. *et al.*, The mode of occurrence of pillow lavas in the Tamba Belt, southwest Japan, *Assoc. Geol. Collab. Jpn. Monogr.*, No. 19, 25–34, 1975 (in Japanese with English abstract).
- OKIMURA, Y., Geosynclinal development of the northern part of the Chugoku Belt based on facies analysis of the limestone groups, *Assoc. Geol. Collab. Jpn. Monogr.*, No. 19, 49–56, 1975 (in Japanese with English abstract).
- OTA, M., The Akiyoshi Limestone Group: A geosynclinal reef complex, *Bull. Akiyoshidai Sci. Mus.*, **5**, 1–44, 31 plates., 1968 (in Japanese with English abstract).
- SAKAGUCHI, S., Stratigraphy and palaeontology of the south Tamba district, Part I, Stratigraphy, *Mem. Osaka Gakugei Univ.*, Ser. B, **10**, 35–76, 1961.
- SHIMIZU, D. *et al.*, Pre-Tamba rhyolites—Pre-Permian acidic magmatism represented by conglomerates of paleozoic formations in the Tamba Belt, *Bull. Magma Genesis in Time and Space, Tokyo*, **2**, 55–59, 1974 (in Japanese).
- TAMBA BELT RESEARCH GROUP, The paleozoic system in the Tamba Belt. II. The paleozoic strata of the southern part of Keihoku-cho, Kitakuwada-gun, Kyoto Prefecture, *Chikyu Kagaku (Earth Science)*, **25**, 211–218, 1971 (in Japanese with English abstract).
- TAMBA BELT RESEARCH GROUP, Paleozoic system in the Tamba Belt. III. Paleozoic strata of Omori and Kumogahata district in the northern part of Kyoto City, Kyoto Prefecture, *Chikyu Kagaku (Earth Science)*, **28**, 57–63, 1974 (in Japanese with English abstract).
- TAMBA BELT RESEARCH GROUP, Geosynclinal facies of the Tamba Belt, southwest Japan, *Assoc. Geol. Collab. Jpn. Monogr.*, No. 19, 13–23, 1975 (in Japanese with English abstract).
- YOSHIDA, S., Triassic formations in the northern part of the Tamba Belt, report of Research group for Honshu Geosyncline, southwest Japan, Kyoto, Vol. 2, pp. 45–52, 1977 (in Japanese).

THERMAL STRUCTURE OF THE SANBAGAWA METAMORPHIC BELT IN CENTRAL SHIKOKU

Shohei BANNO,*¹ Toshio HIGASHINO,*² Masayuki OTSUKI,*³
Tetsumaru ITAYA,*⁴ and Takashi NAKAJIMA*⁵

*¹ *Department of Earth Sciences, Kanazawa University, Kanazawa, Japan*

*² *Hakusan Nature Conservation Center, Ishikawa, Japan*

*³ *Geological Institute, University of Tokyo, Tokyo, Japan*

*⁴ *Department Petrol. Min. Econ. Geol., Tohoku University, Sendai, Japan*

*⁵ *Department of Earth Sciences, Nagoya University, Nagoya, Japan*

(Received July 17, 1978; Revised September 18, 1978)

A detailed metamorphic zonal mapping is being in progress on the Sanbagawa metamorphic belt in central Shikoku. The mapping is based upon the distribution of index minerals, garnet and biotite in pelitic schists, and on the sliding equilibrium among silicate and oxide minerals. The distribution of mineral zones has revealed a peculiar thermal structure of the metamorphic complex that the highest-grade rocks occur in the middle of apparent stratigraphy. A large scale recumbent fold, with south vergency and extending for more than 20 km, is postulated as a possible structural interpretation.

It is concluded, as the most probable model we could imagine at the moment, that before the maximum temperature of metamorphism was reached, the Sanbagawa schists had been metamorphosed in more or less normal thermal regime that the temperature had increased downwards. Then a large scale recumbent fold took place, separating the higher-grade rocks from the heat source and bringing them in between the lower-grade ones. This recumbent fold was accompanied by the start of the uplift of the whole metamorphic complex, while continuing metamorphic reactions with decreasing temperature and pressure.

The fact that the Sanbagawa belt is overturned suggests that a very distinctive crustal shortening took place in the present day Sanbagawa terrain in the Mesozoic time, and that the present day distribution of pre-Tertiary geologic units in the outer zone of the southwestern Japan can hardly be in situ.

1. Introduction

The Sanbagawa metamorphic belt is an intermediate high pressure metamorphic belt, which extends from the Kanto Mountains, northwest of Tokyo, to eastern Kyushu for about 800 km. The basic scheme of the petrology of the belt has been established until mid 1960's, through the works of SEKI (1958), MIYASHIRO and BANNO (1958), MIYASHIRO (1961), IWASAKI (1963), BANNO (1964), KANEHIRA (1967), ERNST *et al.* (1970) and others. In the last several years, we have been engaged in the petrological works on the Sanbagawa schists in central Shikoku, where, thanks to steep topography, we enjoy good exposure of bedrock geology. Our main concern has been the phase petrology of this typical intermediate high pressure metamorphic terrain, and the basic scheme obtained before 1970 has been re-examined by extensive use of electron-probe microanalysis of rock-forming minerals. We feel it still, but probably always, premature to depart from petrology and discuss its geological implications, but we intend to summarize our present view herein, if only to reveal the problems lying ahead of us.

After a brief review of the geology and petrology of the Sanbagawa belt in central Shikoku, a tentative scheme of the thermal structure, by which, following MIYASHIRO (1961), we mean the distribution of metamorphic temperature in the present day metamorphic complex, will be presented.

2. Outline of Geology

In central Shikoku, the Sanbagawa belt is about 40 km wide. The northern border of the belt is the Median Line, by which the schists terrain is separated from the Cretaceous Izumi group. To the south, the Sanbagawa belt is separated from the Chichibu belt, which is composed of Carboniferous to Triassic formations (as to the Triassic refer to MATSUDA, 1978), by the green rock complex customarily called the "Mikabu complex" or by the faults chosen to fit the tastes of individual authors. The boundary to the Chichibu terrain is in any case not clearly defined. No distinctive break has been recognized in mineral facies of the two belts, and in many places, no break in the degree of the development of schistosity as well.

The geology of the Sanbagawa belt is best summarized in HARA *et al.* (1977) and that of the Chichibu belt in TAKEDA *et al.* (1977). The Chichibu terrain, especially its northern part, suffered the Sanbagawa metamorphism. The notion that the Chichibu terrain is a "prehnite-pumpellyite facies terrain" adopted in "Metamorphic facies map of Japan" by HASHIMOTO *et al.* (1970), who include one of the present authors (S.B.), probably has to be modified. However, in this paper we will concentrate on the Sanbagawa belt, and treat the Chichibu belt as its lower-grade areas.

Figures 1 and 2 are lithologic and mineral zone maps of the Sanbagawa belt in central Shikoku. The predominant rock-types of the Sanbagawa belt are pelitic, psammitic and basic schists.

Based upon the mapping of marker beds and analysis of structural elements, a large



Fig. 1. Geological sketch map of the Sanbagawa belt in central Shikoku.

scale recumbent anticline with south vergency has been proposed by many authors (HIDE, 1954; HIDE *et al.*, 1956; KAWACHI, 1968; ERNST *et al.*, 1970; HARA *et al.*, 1977), but the location and significance of the axial plane, recumbent syncline and thrust faults are still in dispute. We have also proposed a recumbent fold based upon the zonal mapping (KURATA and BANNO, 1974; HIGASHINO, 1975), but the location of the anticline is a little different from the other proposals. After the metamorphic facies is reviewed, we will present our view on the structure of the Sanbagawa belt.

3. Metamorphic Zonation

We have succeeded to define five isograds in the Sanbagawa terrain in central Shikoku. They are as follows in the ascending order of metamorphic grade.

1) Disappearance of pumpellyite associated with epidote, chlorite and actinolite in basic schists (NAKAJIMA *et al.*, 1977).

2) Appearance of garnet associated with chlorite in pelitic schists (KURATA and BANNO, 1974; HIGASHINO, 1975).

3) Disappearance of glaucophane (crossite) associated with hematite, epidote and chlorite and the formation of Fe_2O_3 -rich subcalcic hornblende (barroisite) in basic schists (Otsuki and Banno, in preparation).

4) Disappearance of actinolite associated with epidote and chlorite in Fe_2O_3 -poor basic schists (OTSUKI, 1977).

5) Appearance of biotite associated with chlorite, phengite and garnet in pelitic schists (KURATA and BANNO, 1974; HIGASHINO, 1975, cf. Fig. 3).

This is the area where isograd mapping of BANNO (1964) and ERNST *et al.* (1970)

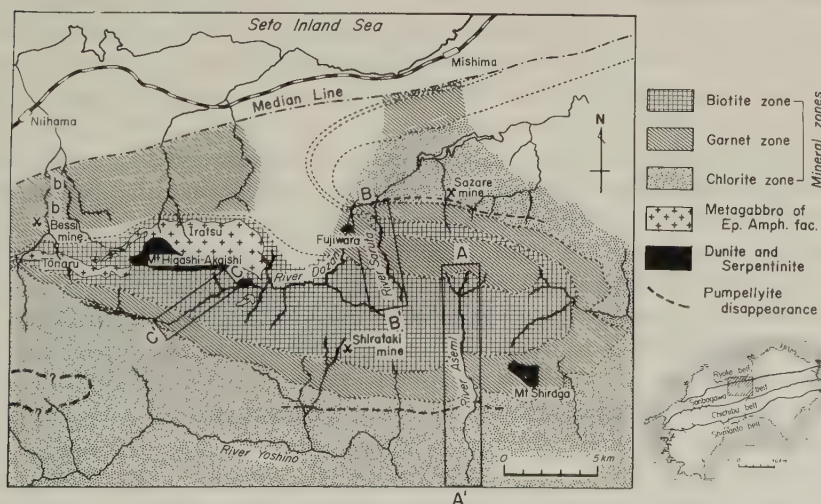


Fig. 2. Mineral zones of the Sanbagawa belt in central Shikoku. The mark "b" denotes the area where biotite schists occur but not fully studied if they define the biotite zone or not.



Fig. 3. Distribution of index minerals in the southeastern part of the mapped area. The letters denotes the rivers. DZ, Dozan; SR, Saruta; TC, Tachikawa; SM, Shimokawa; AS, Asemi; NM, Namekawa.

was performed. Although essential scheme in their papers is underwritten by recent works, a few important points have to be corrected. First, Banno's zone E, as the zone of sodic oligoclase should be abandoned because later detailed works have revealed that plagioclase is not sodic oligoclase, but albite (ERNST *et al.*, 1970; BANNO *et al.*, 1976). The pumpellyite-disappearance line should be located on the higher temperature side than postulated by Banno, and Ernst *et al.*, to conform with the observation made by HIDE (1973). This reduces the areas of their zone B and zone I, respectively. The chemical reactions to define the isograds are described in the papers quoted for individual isograds.

All the isograds mentioned above are based upon continuous reactions, and hence cannot be mapped only upon the distribution of index minerals. The pelitic schists are fairly isochemical and hence the garnet (2) and biotite (5) isograds, especially the latter, are reliable (BANNO, 1977). An example of the accuracy of locating these isograds may be inspected in Fig. 3, which shows the distribution of mineral assemblages of the pelitic schists in the southeastern part of Figs. 1 and 2. The mineral zone map in Fig. 2 is mainly based upon the paragenesis in the pelitic schists primarily because they are the most predominant rock-types. Other isograds are based upon the paragenesis in basic schists, but because of the facts that the basic schists are common but their distribution is not uniform as well as that they are far from being isochemical, we need laborious chemical works to define them. The disappearance line of pumpellyite (3) is thus shown only in the areas where detailed petrographic works have been done. The isograd (4) is not hard to locate, because hematite + alkali amphibole, and hematite + subcalcic hornblende assemblages are easily distinguished from each other, but it is not very useful in mapping as it is located in the garnet zone, which is rather narrow. The actinolite disappearance line (4) also seems to be in the garnet zone.

The mapped area includes the Bessi area of BANNO (1964), and the major difference between his and present results lies in the rejection of his zone E and the question of the evaluation of the sporadic occurrence of biotite in the northern part of the Bessi area, i.e., whether or not his zone D or biotite zone is as wide as has been postulated by him. The latter question is not yet solved and must await further chemical works on solid solution minerals. The following gives an approximate correlation of metamorphic zones proposed in the past and the present works:

BANNO (1964)	ERNST <i>et al.</i> (1970)	This paper
zone A		lower chlorite zone, pumpellyite-actinolite zone
zone B	zone I	higher chlorite zone, above pumpellyite disappearance line
zone C	zone II	garnet zone
zone D	zone III	biotite zone, lower-grade
zone E		biotite zone, higher-grade

As seen in Fig. 2, a vast area is assigned to the chlorite zone, and its subdivision is urgent. The pumpellyite disappearance line serves to this purpose to some extent. The work in progress by one of us, Itaya, has revealed that the basal spacing $d(002)$ of graphitic materials becomes shorter with the grade, with rapid change of its value from 3.6 to 3.5 Å within the pumpellyite-actinolite zone defined for basic schists, thereby demonstrating the possibility of subdividing the chlorite zone by this empirical, in the sense that it is reaction rate controlled, parameter.

4. Thermometry by Continuous Reaction

The zonal mapping based upon the mineral assemblages does not speak, by definition, the temperature difference within individual zones. Sliding equilibrium of continuous reactions makes it possible to treat the temperature not only as a discontinuous quantity, being measured only at the isograds, but also as a continuous quantity, being measured at any place if only rocks with suitable bulk compositions are exposed. The main difficulty of using sliding equilibrium as a thermometer lies not only on the laborious works required to analyze coexisting minerals in fine-grained rocks, but also on the chemical heterogeneity of minerals and limited range of equilibrium domains. The chemical heterogeneity of the minerals of the Sanbagawa schists and its genesis has been discussed by many authors: BANNO (1965), BANNO and KURATA (1972) and HIGASHINO (1975) on garnet; KURATA (1972) on chlorite; TORIUMI (1972) and NAKAJIMA *et al.* (1977) on epidote; TORIUMI (1975), IWASAKI (1975), WATANABE (1977), and Otsuki and Banno (in preparation) on amphiboles; Itaya and Banno (in preparation) and Itaya and Otsuki (in preparation) on opaque minerals. The heterogeneity of some minerals (zoned garnet, epidote) is due to the remnant of equilibrium state preceding the maximum temperature of metamorphism, but some others (chlorite, amphibole, ilmenite) mainly represent the equilibration continued after the maximum temperature. NAKAJIMA *et al.* (1977) have considered that the heterogeneity of epidote in the pumpellyite-actinolite zone corresponds to the temperature fluctuation of about 40°C. When the heterogeneity is represented by regular zonal structure, as in garnet and amphibole, it is possible to eliminate the effect of earlier or later stage recrystallization to some extent and restore the equilibrium state at the time of the maximum temperature.

The sliding equilibria we can use in distinguishing the relative temperature of metamorphism within mineral zones are as follows:

1) The assemblage albite + quartz + clinozoisite + phengite + garnet + chlorite + biotite + hornblende is common in a higher-grade part of the biotite zone. It is a divariant assemblage (BANNO, 1977) and for a small area such as central Shikoku, the pressure of metamorphism may not differ much and hence the relative temperature can be measured by the composition of one of the constituents. The $\text{Mg}/(\text{Mg} + \text{Fe}^{2+})$ ratio of chlorite is sensitive to temperature and easy to handle, and then the thermal axis in the biotite is estimated by this parameter.

2) The Fe^{2+} —Mg and Mn— Fe^{2+} partitionings between garnet and chlorite are also temperature sensitive. They can be used to confirm the relative temperature in the biotite and garnet zones (KURATA and BANNO, 1974; HIGASHINO, 1975).

3) The composition of amphibole in the assemblage amphibole + albite + quartz + hematite + chlorite + phengite, is trivariant. In the garnet and biotite zones (defined for pelitic schists), amphibole with this assemblage is subcalcic hornblende and in the garnet zone, subcalcic amphibole and alkali amphibole coexist defining a divariant assemblage.

Otsuki and Banno (in preparation) have concluded that the Al_2O_3 content (corrected for excess components) in calcic and subcalcic amphibole in the trivariant assemblage is a sensitive parameter of relative temperature, being able to distinguish the lower- and higher-grade parts of the biotite zone by the sliding equilibria in the basic schists. Thus, the subdivision of the biotite zone into lower- and higher-grades was supported by the mineralogy of both the pelitic and basic schists.

The composition of alkali amphibole associated with the assemblage in question is also sensitive to the temperature. Hosotani and Banno (in preparation) have shown that chlorite zone, including a higher-temperature part of the pumpellyite-actinolite zone, can be distinguished into three based upon the alkali amphibole coexisting with hematite.

4) The assemblage quartz + albite + phengite + epidote + chlorite + actinolite + pumpellyite is common in basic schists of a lower-grade part of the chlorite zone, which is referred as the pumpellyite-actinolite zone herein. The assemblage is trivariant, and hence by fixing the $\text{Fe}^{2+}/(\text{Fe}^{2+} + \text{Mg})$ ratio of chlorite, this assemblage becomes divariant and serves as a thermometer. NAKAJIMA *et al.* (1977) and the work of Nakajima being in progress have shown that $\text{Fe}^{3+}/(\text{Fe}^{3+} + \text{Al})$ ratios of epidote and associated pumpellyite are good thermometers by which we can distinguish two or three areas of different grade within the pumpellyite-actinolite zone.

The mapping based upon the sliding equilibrium has been done only on some selected areas. The mineralogy of garnet, chlorite and biotite in pelitic schists has been most extensively studied in the Shiragayama and Sazare areas, southeast of the mapped area, the pumpellyite decomposition reaction in the Shiragayama and Shirataki areas, and the amphibole mineralogy in the Shiragayama and Bessi areas. The graphite mineralogy is being nearly completed in the Shiragayama area and is in progress in the Bessi and other areas.

5. Thermal Structure

The thermal structure of the Sanbagawa belt in central Shikoku is best understood along the section to pass the Saruta river in the Sazare area and the Asemi river in the

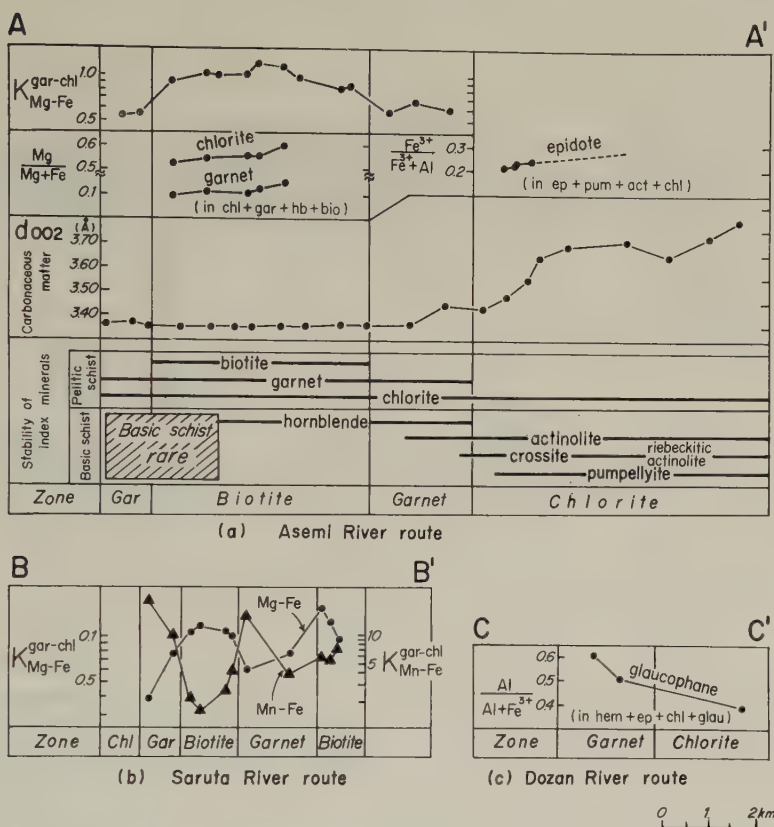


Fig. 4. Mineral paragenesis in some selected area. The paragenesis and the chemistry of solid solution minerals are plotted on lines parallel to the major routes shown in Fig. 2. A-A', Asemi river; B-B', Saruta river; C-C', Dozan river (Bessi area).

Shiragayama area, where we have been concentrating petrographic works. Figure 4 summarizes the paragenesis and mineralogy of the schists along this section, along with that of the Bessi (Dozan river route) area. Figure 5 are cross sections along this route. In addition to the data on the surface exposures summarized in Fig. 4, the data on the drill cores of S-2 deep drilling of the MINERAL EXPLORATION CORP. (1969), which penetrated 2,000 m from the Ojoin formation to the middle member of the Minawa formation, are used to construct the diagram. The most important feature of the thermal structure of this area is that the maximum temperature or thermal axis lies in the middle of the apparent stratigraphy, from which the metamorphic grade decreases both up- and downwards. Further, using the sliding equilibrium, we have confirmed that this trend is real even in individual mineral zones. Thus, at least from the high-grade part of the pumpellyite-actinolite zone to the highest-grade of the Sanbagawa belt so far known, the biotite zone, the temperature changes gradually. The accuracy of distinguishing the metamorphic temperature differs for different equilibria. The alkali amphibole composition in hematite-epidote-alkali amphibole (and some other excess phases) assemblage is the most

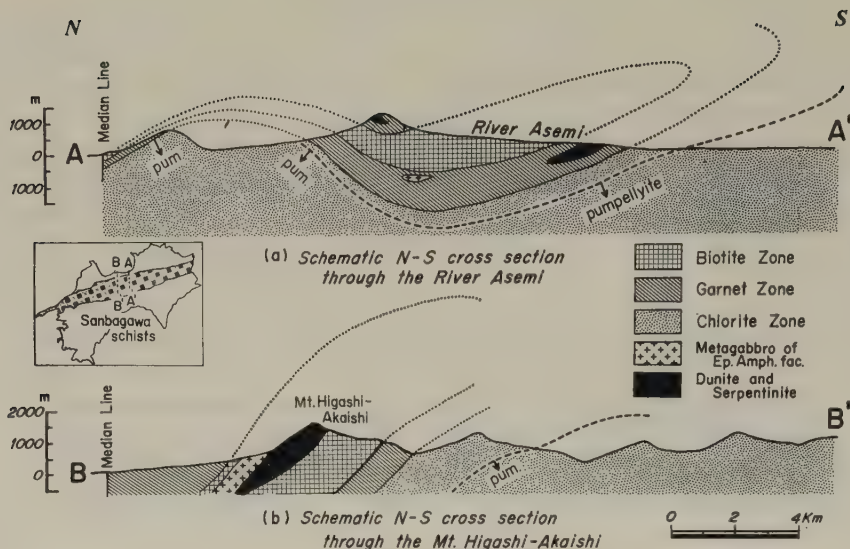


Fig. 5. North-south cross sections of the Sanbagawa belt. A-A', Saruta-Asemi rivers section; B-B', Bessi section passing through Mt. Higashi-Akaishi.

temperature sensitive in our experience, being able to distinguish the temperature difference of two localities, being 100 m apart normal to the isotherm, if only basic schists with appropriate bulk compositions are exposed. It is possible, or rather probable that later deformation of the schists as represented by isoclinal folds and thrust faults (HARA *et al.*, 1977; KAWACHI, 1968) disturbed monotonous temperature gradient, but the scale of such a disturbance is smaller than the accuracy of detecting the temperature difference by sliding equilibrium. From the thermal axis, the temperature of metamorphism decreases monotonously downwards, but we have as yet not detected its another reversal, i.e., temperature trough or syncline, in the study area. We expect that if the trough exists it should be in the pumpellyite-actinolite zone, or in terms of lithological classification, in the Koboke or Kawaguchi formations on the following reasons. First, it is obvious that the trend we have established cannot be extrapolated to much depth. Second, the thermal structure within this zone awaits much of future study and we still do not know its details, but if the thermal trough exists, the fact that a vast area is undelain by nearly isothermal rocks can be explained.

6. Discussion

6.1 Thermal structure

The question then arises is what is the heat source of the overturned temperature distribution. If the present day structure retains largely that at the time of metamorphic recrystallization, we need heat sources in the middle of the biotite zone. Spontaneous heat flow within the crust of the earth cannot explain the thermal axis in the middle of the pile of sedimentary sequence. TAKASU (1978) has insisted that the complex of the epidote amphibolite, being the metamorphosed layered gabbro, is the heat source, but the meta-gabbro had passed the granulite facies metamorphism before they suffered the Sanbagawa metamorphism (YOKOYAMA and MORI, 1975; YOKOYAMA, 1976; BANNO *et al.*, 1976), and

hence it could have not been in molten state at the time of its intrusion into the Sanbagawa schists. The same argument applies to the idea of YOSHIDA (1977), who has insisted that the dunite, which is associated with metagabbro, intruded the Sanbagawa schists in the state of crystal mush. However, it still is possible that the metagabbro-dunite complex intruded the Sanbagawa schists retained the granulite facies temperature and gave some thermal effects to the neighbouring low-grade schists. Even though we did not perform the heat balance calculation, as we did not think it necessary, it is hard to believe that the metagabbro-dunite complex that forms large masses only in the Bessi area, northwest of the study area, and only a few small masses of metagabbro have been recognized in the southeastern part. In the drill hole, S-2, metagabbro measures only 30 m thick and in the Asemi valley, where the biotite zone is about 500 m thick, a few small masses again measuring less than 30 m thick are exposed, but not on the river bed and bank of the Asemi river itself. Their quantity is so small to ascribe the thermal high to their heat effect.

If the overturned thermal structure in central Shikoku cannot be ascribed to the intrusion of the heat sources, its explanation has to be sought in the deformation history. The only idea we could think of is a large scale recumbent fold, probably related to nappe formation, in which the high-grade rocks occupy the axial part. This explanation assumes that at the stage of the major metamorphic recrystallization, the metamorphic temperature increased downwards, as normally expected for metamorphic complex, and later deformation, the recumbent fold, brought the higher-grade rocks in between the lower-grade ones. As the phase study alone cannot determine the vergency of such a fold, we follow KAWACHI (1968) and HARA *et al.* (1977) among others, who concluded that vergency is southwards. The cross sections in Fig. 5 are drawn on this view. We postulate that the axis of the recumbent anticline is in the biotite zone, and that of the syncline, which is not yet confirmed, in the pumpellyite-actinolite zone. This interpretation is not consistent, to confess the truth, with those based upon structural analysis, which postulates the recumbent axis in the overlying garnet zone and the syncline axis somewhere around the garnet zone (KAWACHI, 1968; HARA *et al.*, 1977). Our view is based upon the fact that no significant break in metamorphic grade, expected by the geological conclusions, has been detected in the Saruta and Asemi river sections. Far more complicated models may explain the discrepancy, but as yet not concretely proposed. Among the models to be seriously considered are plural deformations, and the recumbent fold of the metamorphic complex originally metamorphosed in the overturned thermal regime. The latter model assumes that the higher-grade rocks, having been located on the hanging wall side of the lower-grade ones, were brought in between the latter. We will not discuss this model simply because we are not ready to do so.

6.2 Retrograde metamorphism

Detailed petrographic works on the constituent minerals of the Sanbagawa schists have revealed that the retrograde metamorphism affected the Sanbagawa schists more seriously than hitherto considered. Although we are not ready to fully discuss the status of the retrograde metamorphism, the data at hand suggest that it was accompanied by the decrease of pressure. This is most clearly demonstrated in the replacement of garnet by chlorite and by biotite in particular and the formation of actinolite around the prograde hornblende in hematite-bearing basic schists (Otsuki and Banno, in preparation). In

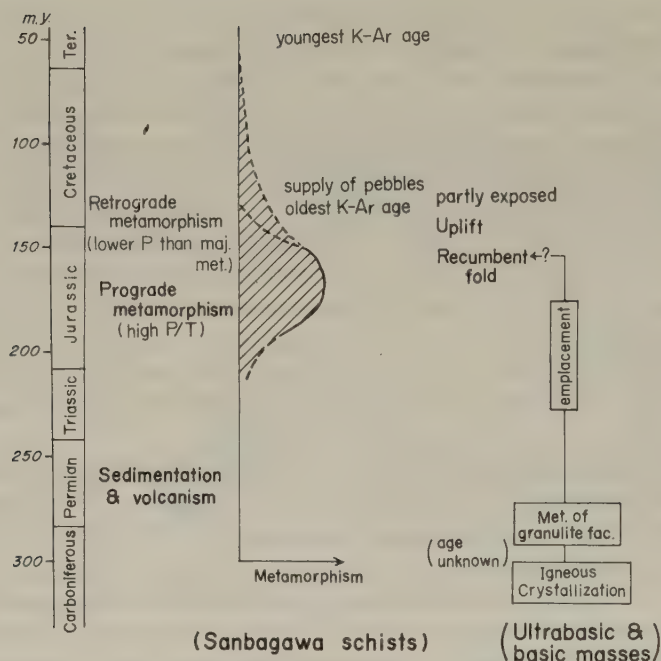


Fig. 6. Schematic representation of the time sequence of the Sanbagawa metamorphism. Subject to change without notice.

the latter case, if the retrograde recrystallization took place at the same pressure as the prograde one, we expect crossite around the hornblende.

At the time of the regional recumbent fold, the higher-grade rocks were separated from the heat source and started to cool down. We therefore consider that the retrograde metamorphism started at the time of the recumbent fold. It follows that the recumbent fold was accompanied by the pressure decrease or uplift of the metamorphic complex, by which the complex was still sufficiently hot to keep the metamorphic reaction going with decreasing temperature and pressure. A tentative scheme of the time sequence of the Sanbagawa metamorphism is illustrated in Fig. 6.

6.3 Implication to the geology of the southwestern Japan

We have concluded that the overturned thermal structure in central Shikoku was formed by the deformation that took place after the maximum temperature was reached. Often quoted generalized pictures of the Sanbagawa belt that the higher-grade rocks occur at structurally higher positions, or that the grade of metamorphism increases northwards, or towards the Median Line, are not unreasonable, but are secondary features that do not offer direct support to the idea that the metamorphism took place in overturned thermal regime expected in the subduction zone. Such an idea may be true for some other metamorphic terrains, namely the Franciscan, or may ultimately be proven valid even for the Sanbagawa schists, but it does not lie on the logical extension of our present understanding of the thermal structure of the Sanbagawa belt.

In central Shikoku, the overturned structure can be traced for more than 20 km from north to south, or parallel to the vergency. It follows that the major part of the Sanbagawa terrain in central Shikoku, or possibly in whole Shikoku island, is overturned. As is seen in Fig. 5, the root zone of the metamorphic complex should have been located on the north of the present day Median Line. Therefore, a vast area between the Ryoke and Sanbagawa belt was lost by Mesozoic tectonic movements. The present day geographical relations between the Ryoke and Sanbagawa metamorphic belts could hardly be the essentially in situ relations.

As to the Chichibu terrain on the south of the Sanbagawa belt, we are as yet not succeeded in metamorphic zonal mapping. However, this terrain, or at least a part of it, is the lower-grade equivalent of the Sanbagawa metamorphic belt. Therefore, there is few reason to deny to extend the essential scheme of the structures of the Sanbagawa belt, i.e., strong lateral movement, to the Chichibu belt. Most probably, the whole terrains from the Median Line to the Kurosegawa zone suffered strong deformation resulting in the north-south crustal shortening, and we are observing a very much telescoped geology in the outer zone of the southwestern Japan.

REFERENCES

- BANNO, S., Petrologic studies on Sanbagawa crystalline schists in the Bessi-Ino district, central Sikoku, Japan, *J. Fac. Sci. Univ. Tokyo*, Sec. 2, **15**, 203-319, 1964.
- BANNO, S., Notes on rock-forming minerals. 34. Zonal structure of pyralspite garnet in Sanbagawa schists in the Bessi area, Sikoku, *J. Geol. Soc. Jpn.*, **71**, 185-188, 1965.
- BANNO, S., Mineral facies of the Sanbagawa metamorphic belt, in *Sambagawa Belt*, edited by K. Hide, pp. 97-106, Hiroshima University Press, Hiroshima, 1977 (in Japanese with English abstract).
- BANNO, S. and H. KURATA, Distribution of Ca in zoned garnet of low-grade pelitic schists, *J. Geol. Soc. Jpn.*, **78**, 507-512, 1972.
- BANNO, S., K. YOKOYAMA, O. IWATA, and S. TERASHIMA, Genesis of epidote amphibolite masses in the Sanbagawa metamorphic belt of central Shikoku, *J. Geol. Soc. Jpn.*, **82**, 199-210, 1976 (in Japanese with English abstract).
- ERNST, W.G., Y. SEKI, H. ONUKI, and M. GILBERT, Comparative study of low-grade metamorphism in California Coast Ranges and the outer metamorphic belt of Japan, *Mem. Geol. Soc. Am.*, **124**, 276, 1970.
- HARA, I., K. HIDE, K. TAKEDA, E. TSUKUTA, M. TOKUDA, and T. SHIOTA, Tectonic movement of the Sambagawa belt, in *Sambagawa Belt*, edited by K. Hide, pp. 307-390, Hiroshima University Press, Hiroshima, 1977 (in Japanese with English abstract).
- HASHIMOTO, M., S. IGI, Y. SEKI, S. BANNO, and G. KOJIMA, Metamorphic Facies Map of Japan, *Geol. Surv. Jpn.*, 1970.
- HIDE, K., Geological structure of the Shirataki mining district, Kochi Prefecture, *Geol. Rep. Hiroshima Univ.*, **4**, 47-83, 1954 (in Japanese with English abstract).
- HIDE, K., Finding and significance of pumpellyite in the main Greenschist member of the Minawa formation in the Bessi and Shirataki districts, Sanbagawa metamorphic belt in central Sikoku, Commem. Volume of Prof. K. Umegaki, pp. 77-87, 1973 (in Japanese with English abstract).
- HIDE, K., G. YOSHINO, and G. KOJIMA, Preliminary report on the geologic structure of the Besshi-spotted schists zone, *J. Geol. Soc. Jpn.*, **62**, 574-584, 1956 (in Japanese with English abstract).
- HIGASHINO, T., Biotite zone of Sanbagawa metamorphic terrain in the Shiragayama area, central Shikoku, Japan, *J. Geol. Soc. Jpn.*, **81**, 653-670, 1975 (in Japanese with English abstract).
- IWASAKI, M., Metamorphic rocks of the Kotu-Bizan area, eastern Shikoku, *J. Fac. Sci. Univ. Tokyo*, Sec. 2, **15**, 1-90, 1963.
- IWASAKI, M., Metamorphic zonal mapping and mineral paragenesis, Abstr. Symp. on Kinetics and Physical Conditions of the Formation of Rock-Forming Minerals, pp. 15-21, 1975.
- KANEHIRA, K., Sanbagawa crystalline schists in the Iimori district, Kii Peninsula, *Jpn. J. Geol. Geogr.*, **38**, 101-115, 1967.
- KAWACHI, Y., Large-scale overturned structure in the Sambagawa metamorphic zone in central Shikoku, Japan, *J. Geol. Soc. Jpn.*, **74**, 607-616, 1968.
- KURATA, H., Local chemical heterogeneity of chlorites in Sanbagawa pelitic schists from Sazare area, central Shikoku, *J. Geol. Soc. Jpn.*, **78**, 653-657, 1972.

- KURATA, H. and S. BANNO, Low-grade progressive metamorphism of pelitic schists of the Sazare area, Sanbagawa metamorphic terrain in central Shikoku, Japan, *J. Petrol.*, **15**, 361–382, 1974.
- MATSUDA, T., Discovery of the Middle-Late Triassic conodonts genus *Metaplygnathus* from calcareous schist of the Sambagawa southern marginal belt in central Shikoku, *J. Geol. Soc. Jpn.*, **84**, 331–333, 1978 (in Japanese with English abstract),
- MINERAL EXPLORATION CORP., Report of Detailed Survey of the Shiragayama Region, Mineral Explor. Corp., 1969 (in Japanese with English abstract).
- MIYASHIRO, A., Evolution of metamorphic belts, *J. Petrol.*, **2**, 277–311, 1961.
- MIYASHIRO, A. and S. BANNO, Nature of glaucophanitic metamorphism, *Am. J. Sci.*, **256**, 97–110, 1958.
- NAKAJIMA, T., S. BANNO, and T. SUZUKI, Reactions leading to the disappearance of pumpellyite in low-grade metamorphic rocks of the Sanbagawa metamorphic belt in central Shikoku, Japan, *J. Petrol.*, **18**, 263–284, 1977.
- OTSUKI, M., Progressive metamorphism of basic schists of the Asemi river area, Sanbagawa metamorphic terrain in central Shikoku, MS. M. Sc. Thesis, Kanazawa University, 1977.
- SEKI, Y., Glaucophanitic regional metamorphism in the Kanto mountains, central Japan, *Jpn. J. Geol. Geogr.*, **29**, 233–258, 1958.
- TAKASU, A., On the lithology of the Tonaru amphibolite intruded the Sanbagawa schists in the Bessi area, Shikoku, Abstr. 85th Annu. Conv. Geol. Soc. Jpn., p. 34, 1978 (in Japanese).
- TAKEDA, K., E. TSUKUDA, M. TOKUDA, and I. HARA, Structural relationships between the Sambagawa and the Chichibu belts, in *Sambagawa Belt*, edited by K. Hide, pp. 107–152, Hiroshima University Press, Hiroshima, 1977 (in Japanese with English abstract).
- TORIUMI, M., Microprobe study of zoned epidote in the Sambagawa rocks from the Kanto mountains, *J. Geol. Soc. Jpn.*, **78**, 545–548, 1972.
- TORIUMI, M., Petrological study of the Sambagawa metamorphic rocks, the Kanto mountains, central Japan, *Bull. Univ. Museum, Univ. Tokyo*, No. 9, 1975.
- YOKOYAMA, K., Finding of plagioclase-bearing granulite from the Iratsu epidote amphibole mass in central Shikoku, *J. Geol. Soc. Jpn.*, **82**, 549–551, 1976.
- YOKOYAMA, K. and T. MORI, Spinel-garnet-two pyroxene rock from the Iratsu epidote amphibolite mass, central Shikoku, *J. Geol. Soc. Jpn.*, **81**, 29–37, 1975.
- YOSHIDA, T., Petrology of the Bessi intrusive complex, (Abstr.), *J. Jpn. Assoc. Petrol. Mineral. Econ. Geol.*, **72**, 126–127, 1977 (in Japanese).
- WATANABE, T., Metamorphism of the Sambagawa and Chichibu belt in the Oshika district, Nagano Prefecture, central Japan, *J. Fac. Sci. Hokkaido Univ.*, Ser. IV, **17**, 629–694, 1977.

SHIMANTO GEOSYNCLINE AND KUROSHIO PALEOLAND

T. HARATA,* K. HISATOMI,** F. KUMON,** K. NAKAZAWA,**
M. TATEISHI,** H. SUZUKI,*** and T. TOKUOKA**

* *Department of Earth Science, Faculty of Education,
Wakayama University, Wakayama, Japan*

** *Department of Geology and Mineralogy, Faculty of Science,
Kyoto University, Kyoto, Japan*

*** *Faculty of Technology, Dôshisha University, Kyoto, Japan*

(Received June 16, 1978; Revised August 7, 1978)

The late Mesozoic to early Neogene geosyncline in the Outer zone of Southwest Japan has been studied in detail in the Kii Peninsula by the Research Group for the Shimanto Geosyncline. The existence of the Kuroshio Paleoland to the south of the geosyncline was inferred by various sedimentologic evidences. The Shimanto belt in the Kii Peninsula is divided from north to south into three zones of Cretaceous, Eocene and Oligocene to lower Miocene. In these belts thick geosynclinal sediments were accumulated showing coarsening upward. The southward migration of the basin occurred in Cretaceous/Eocene, Eocene/Oligocene, and in early Miocene. In the present paper the reconstruction of paleogeography of the Shimanto geosyncline was attempted and the Kuroshio Paleoland was discussed in relation to the geohistory of the Philippine Sea. In spite of the detailed geologic survey in the Kii Peninsula there is no evidence of large exotic blocks nor tectonic mélanges, and this does not support the plate tectonic model of the Pacific-type orogeny for the Shimanto belt.

1. Introduction

The Shimanto belt was a geosynclinal area throughout the late Mesozoic to early Neogene. The Shimanto belt had long been an area of *terra incognita* because of monotonous and thick clastic sequences (mostly composed of sandstones and mudstones), complicated geologic structure, and of being barren of fossils. Geologic mapping of the Shimanto terrain in the Kii Peninsula has been done in the last decade by the Research Group for the Shimanto Geosyncline. The existence of a former land mass (Kuroshio Paleoland) to the south of the geosyncline was inferred by them in 1970. The Kuroshio Paleoland existed up to the early Neogene and was submerged thereafter to an oceanic depth. This hypothesis was based mainly on paleotransportation analysis, indicating the supply of clastic materials not only from the continental side but also from the Pacific Ocean side. It was also inferred from the frequency and size distribution of exotic clasts of orthoquartzite of probably Precambrian age in the Shimanto belt. The present writers describe briefly the Shimanto supergroup in the Kii Peninsula and discuss the Kuroshio Paleoland and its bearing in the development of the Shimanto geosyncline. The Kuroshio Paleoland must have an important meaning in relation to the geologic development of the Philippine Sea and that of the Western Pacific region.

2. The Shimanto Supergroup in the Kii Peninsula

The Shimanto belt contacts northward with the Chichibu belt, which consists of

middle to upper Paleozoic and Mesozoic strata, along the Butsuzo tectonic line. It is divided into three zones from north to south, i.e., the Hidakagawa (Cretaceous), the Otonashigawa (probably Eocene) and the Muro (Oligocene to lower Miocene) groups. These were already reported by HARATA (1965), TOKUOKA (1967, 1970), KISHU SHIMANTO RESEARCH GROUP (1970, 1975, 1977), HATENASHI RESEARCH GROUP (1975), SUZUKI (1975) and TATEISHI (1978). A generalized geologic map is shown in Fig. 1.

Hidakagawa group (KISHU SHIMANTO RESEARCH GROUP, 1975, 1977). The Hidakagawa group attains 12,000 m in thickness and is divided into three formations. Its geologic age is assigned roughly as Cretaceous (mainly upper Cretaceous). There is little fossil evidence in the Kii Peninsula.

The lower (Nyunokawa) formation,* 2,200 m in thickness, is composed of shales and muddy flysch in the lower part, and of normal to sandy flysch and thick-bedded sandstones in the upper part. The Nyunokawa conglomerates of 400 m thick are intercalated

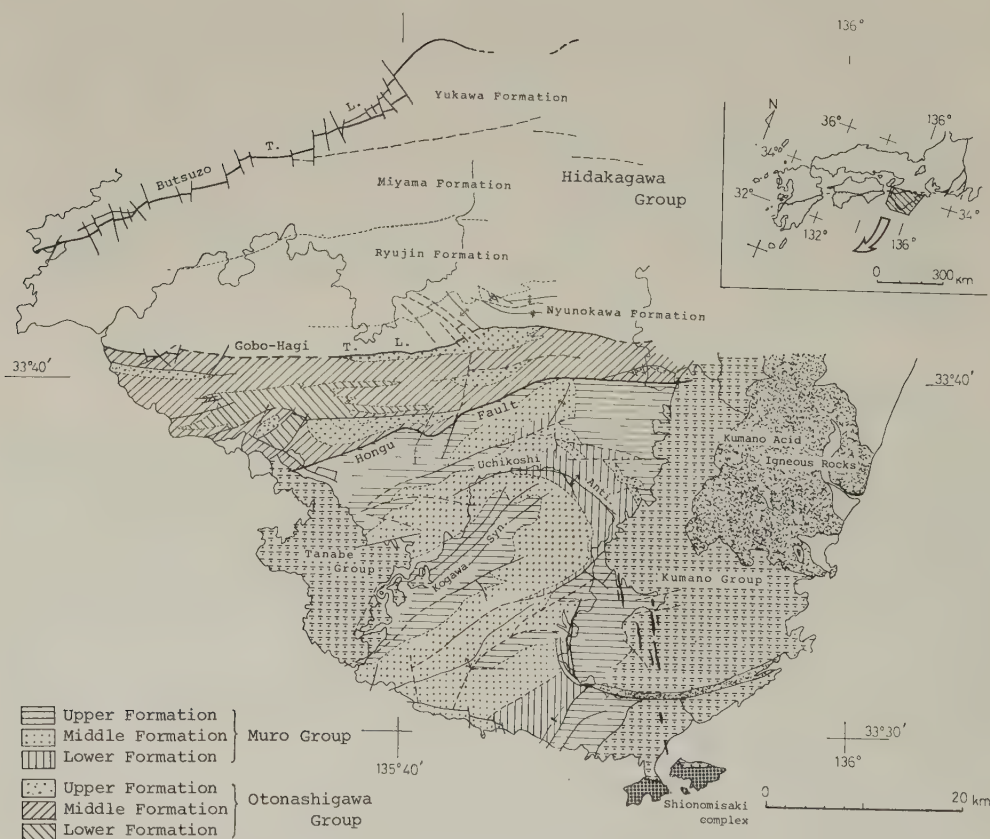


Fig. 1. Generalized geologic map of the Shimanto terrain in the Kii Peninsula, South-west Japan. The Kumano and the Tanabe groups of the late early to middle Miocene overlies unconformably the Shimanto supergroup in the east and west, respectively. (The data are mainly based on KISHU SHIMANTO RESEARCH GROUP, 1975 and 1977.)

* In Fig. 1, the Yukawa formation in the north is shown as the correlative of the lower formation.

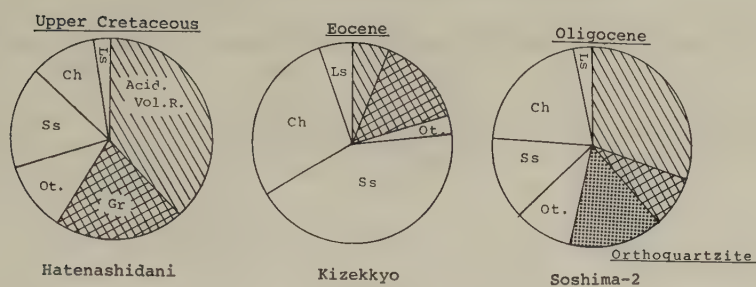


Fig. 2. Representative compositions of conglomerates. These conglomerates are thought to have been supplied from the Kuroshio Paleoland.

in the top of the formation. The clasts are pebbles, cobbles and sometimes boulders, consisting of acidic volcanics (mostly rhyolite), granite, sandstone, chert, etc., among which acidic volcanic rocks are most abundant (Fig. 2).

The middle (Ryujin) formation, 3,000 m in thickness, is characterized by predominant shale and muddy flysch, occasionally accompanied with sandy flysch. Greenstones yielded by submarine volcanism and rhyolitic tuffs supplied by subaerial volcanic activity are sometimes intercalated in the formation. A large body of greenstone with pillow structures is located in the eastern part of the Hidakagawa zone (SHIIDA *et al.*, 1971).

The upper (Miyama) formation, 7,000 to 7,500 m thick, is composed of massive sandstones and sandy flysch. Several greenstone layers of less than several tens of meters are intercalated in shaly parts. These are sometimes accompanied by radiolarian cherts.

It is somewhat difficult to find sole markings due to severe tectonic deformation. However, current markings can be found in the Hidakagawa group. The sediments of the lower formation were mostly transported by lateral currents from SE to NW, while those of the middle formation by longitudinal currents from E to W. In the upper formation lateral currents from N to S are found in addition to eastern longitudinal currents.

Otonashigawa group (HATENASHI RESEARCH GROUP, 1975). The Otonashigawa group attains to more than 1,600 m in thickness. Its geologic age may be assigned to the Eocene although no reliable fossil evidence has been obtained in the Kii Peninsula. The lower half is rich in mudstones and muddy flysch, while the upper half is rich in sandstones and sandy flysch, comprising a coarsening upward sequence as a whole. In the southern part of the belt the Kizekkyo conglomerates, about 100 m in thickness are intercalated in the uppermost part of the group. The clasts are of pebble to cobble, sometimes boulder size, composed of sandstone, chert, granite, etc. (Fig. 2). Current markings are well developed. The longitudinal currents from E to W are dominant in the lower half, while lateral ones from S to N, which are accompanied with proximal facies, are found in the upper half of the southern part.

Muro group (KISHU SHIMANTO RESEARCH GROUP, 1975). The Muro group, 7,500 to 9,000 m thick, is divided into the lower, middle and upper formations. The geologic age can be assigned to the Oligocene to early Miocene by molluscan fossils. The lower part (1,200 m) is composed mainly of mudstones and muddy flysch, and the middle part (2,500 to 3,000 m thick) is composed predominantly of sandy flysch and thick-bedded massive sandstones intercalated with several conglomerates. The upper part (3,000 to 4,000 m thick) consists mainly of mudstones and various types of flysch. Conglomerates with

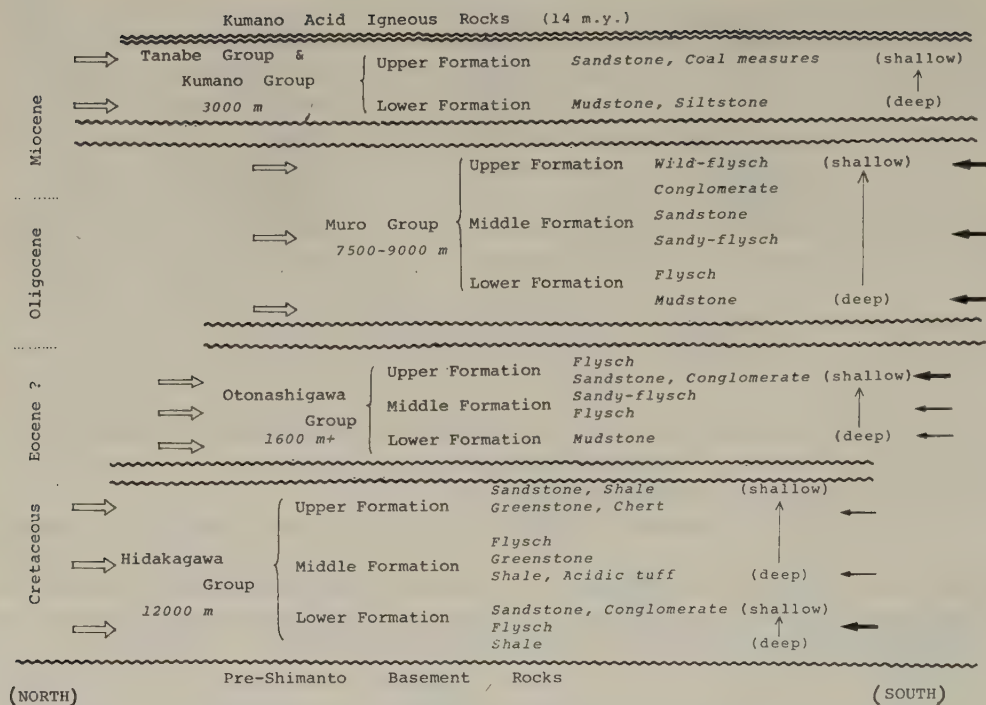


Fig. 3. Schematic illustration of the development of the Shimanto geosyncline in the Kii Peninsula. Arrow indicates a direction of sediment supply.

sandy matrix, muddy conglomerates and angular-fragment bearing mudstones are intercalated in the upper part.

The conglomerates with sandy matrix in the middle and upper parts contain abundant clasts of rhyolite, and subordinate ones of chert, sandstone, granite, and orthoquartzite (Fig. 2). The occurrence of orthoquartzite clasts, which were precisely described by TOKUOKA (1970), is limited to the area south of the Uchikoshi anticline in the Muro zone. Typical flysch facies are well developed and a number of sole markings are found in the Muro group. The paleocurrents in the zone are variable as a whole. However, it is likely that the main currents are longitudinal from E to W or from ENE to WSW but lateral ones from the north and south are also frequent. There are found channel structures in the southern coastal area in the Kii Peninsula. Careful observation of channel walls and paleocurrent analyses of the filling sediments by means of sole markings and grain fabrics of conglomerates and thick-bedded sandstones led to a conclusion that the channels were excavated by south current and filling materials were transported from the same direction (TATEISHI, 1978).

The development of the Shimanto geosyncline in the Kii Peninsula is schematically shown in Fig. 3. There are several cycles of upward coarsening megasequences in the Shimanto supergroup, that is, two cycles in the Hidakagawa group and each one cycle in the Otonashigawa and Muro groups respectively. These sequences reflect the change of sedimentary environment from deep to shallow, suggesting gradual filling-up of the sedimentary basins. Furthermore it is likely in the Shimanto belt in the Kii Peninsula that,

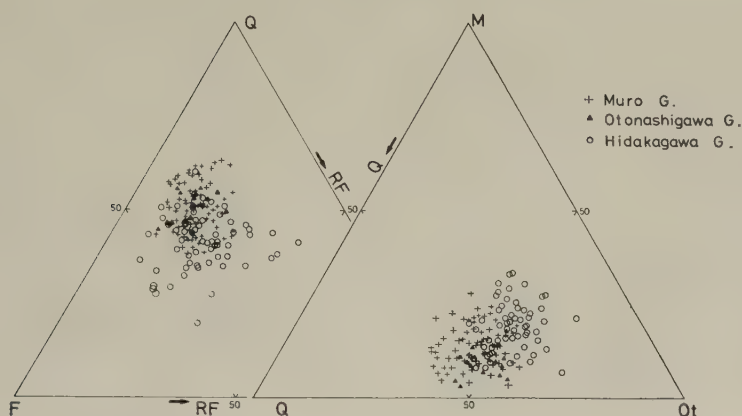


Fig. 4. Properties of massive and thick-bedded sandstones in the Shimanto supergroup in the Kii Peninsula. Q, quartz; F, feldspar; RF, rock fragments; M, matrix; Ot, the others except quartz and matrix.

after filling up the basin of the Hidakagawa belt, the depositional axis migrated southward to the Otonashigawa belt. Similar southward basin migration can also be deduced from the Otonashigawa to the Muro basins. In addition to the migration of the basins, there are found some changes in sedimentary sequences. Muddy facies, sometimes accompanied with greenstones and cherts, are dominant in the Hidakagawa group, while sandy facies prevail in the Otonashigawa group. Sandy facies dominate in the Muro group, frequently accompanied by conglomerates. Moreover, there are some differences in the properties of massive and thick-bedded sandstones among these groups (Fig. 4). These observations may reflect the change of the sedimentary environment of the Shimanto supergroup from eugeosyncline to miogeosyncline. Terrigenous materials were supplied from both sides of the basins as shown by arrows in Fig. 3.

3. Paleogeographic Reconstruction of the Shimanto Geosyncline

Paleogeographic reconstruction of the Shimanto geosyncline was attempted on the basis of facies analysis (especially distribution of conglomerates and massive sandstones), paleocurrent analysis by sole markings and grain fabrics of sandstone and conglomerate, channel structure analysis in proximal turbidites, and the occurrence of exotic clasts of orthoquartzite. Hypothetical paleogeographic maps of three stages in the Shimanto geosyncline are offered in Fig. 5. The paleogeography of the early Miocene is added in the same figure, the data of which are adopted from K. Hisatomi and the Hatenashi Research Group. The Kii Peninsula is meridionally extended by one and half times considering the shortening of each belt after deposition.

Hidakagawa stage (late Cretaceous). The longitudinal currents were dominant in the axial part, by which sediments of distal turbidite and/or shale were transported. In the eastern part there is found a submarine (basic) volcano which forms a mound. Acidic tuffs, which may have been derived partly from acidic volcanic activity on the Kuroshio



Fig. 5. Paleogeography of the Shimanto geosyncline in the province of the Kii Peninsula. The basin in each stage of the geosyncline situated between two land areas (Asiatic Continent in the north and Kuroshio Paleoland in the south), from which clastic materials were supplied through submarine channels. The successive southward migration of the basin is noticeable.

Paleoland, are frequently intercalated in the sequence. In the southern part of the basin proximal turbidites (thick-bedded sandstone and conglomerate) were frequently transported from the Kuroshio Paleoland forming a deep-sea fan and channel system. Similar fans and channel systems existed in the northern part. In the northern shelf area there were two troughs represented by the Izumi and Sotoizumi groups. The northern land area was a part of the Asiatic Continent, where acidic volcanism and plutonism were occurring quite extensively.

Otonashigawa stage (Eocene). After the filling of the basin of the Hidakagawa stage, the axis of depositional site shifted slightly southward. Longitudinal currents from E to W were dominant throughout the basin. Submarine (basic) volcanism is inferred somewhere outside the Kii Peninsula, from which volcanic materials were supplied to the basin in small quantity. A deep-sea fan developed in the southern part of the basin, which is interpreted from the presence of proximal facies of the Kizekkyo conglomerates and sandstones. There were similar deep-sea fans in the northern part of the basin.

Muro stage (Oligo-Miocene). After the filling of the former basin, the succeeding one was born to the south. Eastern longitudinal currents were still dominant in the basin. However, an upheaval zone was formed along the axial part (Uchikoshi anticline) of the basin at a later stage to yield complicated paleocurrents. Terrigenous materials were supplied from the south by submarine channels in the southern part of the basin, while those of the northern part were supplied from the northern land area. In the south there are found many exotic gravels of orthoquartzite and slump deposits, all of which were transported from the south.

Kumano and Tanabe stage (late early Miocene). After the filling of the Muro basin, a great tectonic movement occurred, changing the Shimanto geosyncline to the land area. Simultaneously the Kuroshio Paleoland which had supplied vast materials to the geosyncline subsided beneath the area. The new basin of the Kumano and Tanabe groups was formed upon the Shimanto belt. These groups overlie the severely folded and faulted strata of the Shimanto supergroup with pronounced clinounconformity. Terrigenous materials were supplied from the northern land area and were deposited on the submarine shelf and slope. Recent investigation around Cape Shionomisaki area, the southern end of the peninsula, by Y. Miyake and K. Hisatomi reveals volcano-plutonic activity of basic to acid composition early in this stage. They concluded that the igneous complex formed tectonically upheaved submarine ridge which trapped the sediments. It is highly probable that a remnant of the Kuroshio Paleoland constituted this ridge.

4. *The Kuroshio Paleoland and Its Bearing in the Development of the Shimanto Geosyncline*

The existence of the Kuroshio Paleoland can be inferred from various geologic evidences. It must have been located in the area now occupied by the continental slope off the Kii Peninsula, although no direct evidence has been obtained there. Pre-Shimanto basement rocks (sandstones, cherts, etc.) are inferred from the study on the Kuroshio Paleoland, from which a large amount of volcanic materials were supplied to the geosyncline. As shown in Fig. 6, the upheaval and erosional movements progressed on the Kuroshio Paleoland in accordance with the depression and deposition in the Shimanto geosyncline. In the later (Muro) stage erosion of the Precambrian basement of the paleoland was suggested by the presence of orthoquartzite gravels very similar to those of Sinian age. The submergence of the paleoland occurred finally in the early Miocene.

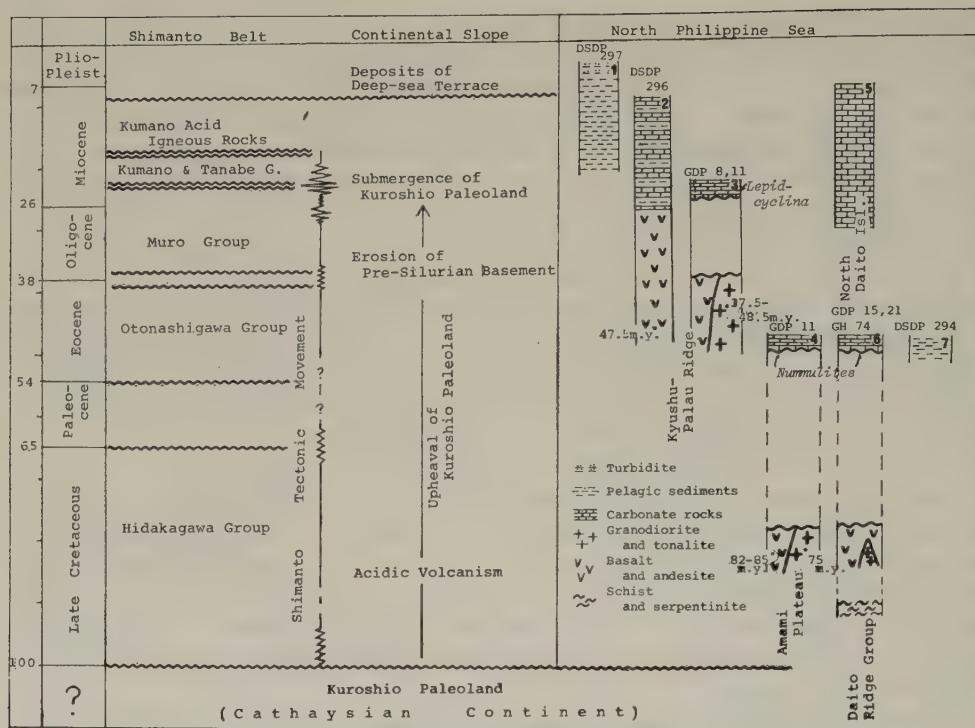


Fig. 6. The geohistory of the Shimanto geosyncline and Kuroshio Paleoland and their relation to that of the Philippine Sea. 1, KARIG *et al.* (1975); 2, KARIG *et al.* (1975), OZIMA *et al.* (1977); 3, MIZUNO *et al.* (1977a), MIZUNO *et al.* (1977b), SHIBATA and OKUDA (1975), SHIBATA *et al.* (1977), SHIKI *et al.* (1975); 4, KONDA *et al.* (1977), MATSUDA *et al.* (1975), MIZUNO *et al.* (1976), MIZUNO *et al.* (1977b), SHIKI *et al.* (1975); 5, HANZAWA (1940–41); 6, MIZUNO and KONDA (1977), MIZUNO *et al.* (1976), MIZUNO *et al.* (1977b), SHIKI *et al.* (1975), YUASA and WATANABE (1977); 7, KARIG *et al.* (1975).

As shown in the reconstruction (Fig. 4), the depositional site of the Shimanto geosyncline can never have been a trench facing to ocean, but was an inner-arc basin or arc-trench gap. No pelagic sediments are found in the Shimanto belt in the Kii Peninsula. An environment shallower than deeper bathyal or abyssal is preferred for the Shimanto geosyncline. In spite of the detailed geologic survey in the Kii Peninsula there is no evidence of large exotic blocks due to gravity sliding nor tectonic mélanges and long distance thrusting. This does not support the plate tectonic model of the Pacific-type orogeny proposed for the outer (Shimanto) belt of Southwest Japan by SUGIMURA and UYEDA (1973).

As to the birth and development of the Philippine Sea there must have been an intimate relation to the geohistory of the Shimanto geosyncline, including the Kuroshio Paleoland. Late Cretaceous/Eocene, Eocene/Oligocene, early Miocene and late Middle Miocene crustal movements are known in the Shimanto terrain. Similarly, the presence of late Cretaceous/Eocene, Eocene/early Miocene and middle Miocene hiatuses have been revealed by DSDP and GDP explorations in the Philippine Sea (Fig. 6). These events

indicate considerable vertical movements and subaerial erosion at least in plateau and ridge areas.

From the sedimentological view point the Kuroshio Paleoland was as large as the present Japanese Islands. There is no evidence of the paleoland prior to late Cretaceous. However, the presence of orthoquartzites very similar to that of the Sinian in the Asian Continent suggests that the paleoland extended further south to the present Philippine Sea in the late Precambrian. There remains a large gap in the geologic record since then. Several scientists (LIU, 1959; LIU *et al.*, 1973; MINATO *et al.*, 1965; etc.) suggested that the "Cathaysian Continent" extended to the Philippine Sea in late Precambrian and Paleozoic time. These considerations should be taken into account in reconstructing the birth and development of the Philippine Sea.

REFERENCES

- HANZAWA, S., Micropalaeontological studies of drill cores from a deep well in Kita-Daito-Zima (North Borodino Island), *Jubilee Publ. Com. Prof. Yabe 60th Birth*, **2**, 755–802, 1940–41.
- HARATA, T., Some directional structures in the Flysch-like beds of the Shimanto Terrain in the Kii Peninsula, Southwest Japan, *Mem. Coll. Sci., Univ. Kyoto*, Ser. B, **32**, 103–176, 1965.
- HATENASHI RESEARCH GROUP, The stratigraphy and geologic structure of the Otonashigawa-Mura group in the Kii Peninsula, Southwest Japan, *Assoc. Geol. Collab. Jpn. Monogr.*, No. 19, 157–166, 1975 (in Japanese with English abstract).
- KARIG, D.E. *et al.* (eds.), *Initial Reports of the Deep Sea Drilling Project, Leg 31*, U. S. Government Printing Office, Washington, D.C., 1975.
- KISHU SHIMANTO RESEARCH GROUP, Sedimentological and paleontological studies of the Muro group at the southern coastal region of the Kii Peninsula—The study of the Shimanto Terrain in the Kii Peninsula, Southwest Japan (Part 4), *Mem. Fac. Educ., Wakayama Univ., Natural Sci.*, **20**, 75–102, 1970 (in Japanese with English abstract).
- KISHU SHIMANTO RESEARCH GROUP, The development of the Shimanto geosyncline, *Assoc. Geol. Collab. Jpn. Monogr.*, No. 19, 143–156, 1975 (in Japanese with English abstract).
- KISHU SHIMANTO RESEARCH GROUP, The Hidakagawa group in the Southern part of the Ryujin village, Wakayama Prefecture—The Study of the Shimanto Terrain in the Kii Peninsula, Southwest Japan (Part 8), *Earth Sci.*, **31**, 250–262, 1977 (in Japanese with English abstract).
- KONDA, I., K. MATSUOKA, A. NISHIMURA, and T. OHNO, *Nummulites boninensis* HANZAWA from the Amami Plateau in the northern margin of the Philippine Sea, *Trans. Proc. Palaeontol. Soc. Jpn., N. S.*, **106**, 61–70, 1977.
- LIU Hung-Yun (ed.), *Paleogeographic maps of China*, 69pp., Science Press, Peking, China, 1959.
- LIU Hung-Yun, SHA CHING-AN, and HU SHIN-LING, The Sinian system in Southern China, *Sci. Sin.*, **16**, 266–278, 1973.
- MATSUDA, J., K. SAITO, and S. ZASHU, K-Ar age and Sr isotope of rocks of manganese nodule nuclei from Amami Plateau, West Philippine Sea, in *Geological Problems of the Philippine Sea*, edited by K. Nakazawa *et al.*, 99–101, 1975 (in Japanese).
- MINATO, M., M. GORAI, and M. HUNAHASHI (eds.), *The Geologic Development of the Japanese Islands*, 442 pp., Tsukiji Shokan, Tokyo, 1965.
- MIZUNO, A. and I. KONDA, Eocene larger foraminifers from the sea floor near Oki-Daito-Shima Island (GH74-7-167), *Bull. Geol. Surv. Jpn.*, **28**, 639–651, 1977.
- MIZUNO, A., Y. OKUDA, and K. TAMAKI, Some problems on the geology of the Daito Ridges Region and its origin, *Geol. Stud. Ryukyu Isl.*, **1**, 177–198, 1976 (in Japanese with English abstract).
- MIZUNO, A., K. SHIBATA, S. UCHIUMI, M. YUASA, Y. OKUDA, M. NOHARA, and Y. KINOSHITA, Granodiorite from the Minami-koho Seamount on the Kyushu-Palau Ridge and its K-Ar age, *Bull. Geol. Surv. Jpn.*, **28**, 507–511, 1977a (in Japanese with English abstract).
- MIZUNO, A., T. SHIKI, and H. AOKI, Dredged rock and piston and gravity core data from the Daito Ridge and the Kyushu-Palau Ridge in the North Philippine Sea, *Geol. Stud. Ryukyu Isl.*, **2**, 107–119, 1977b.
- OZIMA, M., I. KANEOKA, and H. UJIE, ^{40}Ar - ^{39}Ar age of rocks and the development mode of the Philippine Sea, *Nature*, **267**, 816–818, 1977.
- SHIBATA, K. and Y. OKUDA, K-Ar age of a granite fragment dredged from the 2nd Komahashi Seamount, *Bull. Geol. Surv. Jpn.*, **26**, 71–72, 1975 (in Japanese with English abstract).

- SHIBATA, K., A. MIZUNO, M. YUASA, S. UCHIUMI, and T. NAKAGAWA, Further K-Ar dating of tonalite dredged from the Komahashi-Daini Seamount, *Bull. Geol. Surv. Jpn.*, **28**, 503–506, 1977.
- SHIIDA, I., K. SUWA, R. SUGISAKI, T. TANAKA, and H. SHOZAKI, Greenstones of the Cretaceous Hidakagawa Belt of the Shimanto Terrain in the Totsukawa area, Nara Prefecture, Central Japan, *Geol. Soc. Jpn., Mem.*, **6**, 137–149, 1971 (in Japanese with English abstract).
- SHIKI, T., T. TOKUOKA, H. AOKI, Y. MISAWA, I. KONDA, and S. NISHIDA, GDP cruise in the Philippine Sea, with special reference to the bottom sampling in GDP-8 and -11, in *Geological Problems of the Philippine Sea*, edited by K. Nakazawa *et al.*, pp. 67–74, 1975 (in Japanese).
- SUGIMURA, A. and S. UEDA, *Island arcs: Japan and Its Environs*, 246 pp., Elsevier, Amsterdam, 1973.
- SUZUKI, H., Deformed structures and deformational history of the Paleogene Muro Flysch Nepton in Southwest Japan, *Assoc. Geol. Collab. Jpn. Monogr.*, No. 19, 167–177, 1975 (in Japanese with English abstract).
- TATEISHI, M., Sedimentology and basin analysis of the Paleogene Muro Group in the Kii Peninsula, Southwest Japan, *Mem. Fac. Sci., Kyoto Univ., Ser. Geol. and Mineral.*, **45**, 187–232, 1978.
- TOKUOKA, T., The Shimanto Terrain in the Kii Peninsula, Southwest Japan—With special reference to its geologic development viewed from coarser clastic sediments, *Mem. Fac. Sci., Kyoto Univ., Ser. Geol. and Mineral.*, **34**, 35–74, 1967.
- TOKUOKA, T., Orthoquartzitic gravels in the Paleogene Muro Group, Southwest Japan, *Mem. Fac. Sci., Kyoto Univ., Ser. Geol. and Mineral.*, **37**, 113–132, 1970.
- YUASA, M. and T. WATANABE, Pre-Cenozoic metamorphic rocks from the Daito Ridge in the northern Philippine Sea, *J. Jpn. Assoc. Min. Pet. Econ. Geol.*, **72**, 241–251, 1977.

MAGNETIC STRATIGRAPHY OF THE JAPANESE NEOGENE AND THE DEVELOPMENT OF THE ISLAND ARCS OF JAPAN

Nobuaki NIITSUMA

Institute of Geoscience, Shizuoka University, Shizuoka, Japan

(Received June 19, 1978; Revised September 11, 1978)

Detailed correlation and chronology of the Neogene and Quaternary marine sediments in the Japanese island arc area have been established by the application of magnetostratigraphic methods supplemented by microbiostratigraphic data. The sedimentation rates of several sedimentary sequences show a similar pattern among the studied areas, and two drastic synchronous changes in the rates of sedimentation are recognized. Thus the Japanese Neogene and Quaternary can be divided into three major time intervals, named I, II, and III in increasing age. The boundaries between these three intervals are 4.7 mybp (base of the Gilbert Epoch; magnetic anomaly 3) and 10.4 mybp (Epoch 9; magnetic anomaly 5). The geographic distribution of the land area during the time interval I and II was similar to the present; however, in the time interval III, it is completely different but similar to the present Bonin-Mariana arc area. It has been documented by Hawaiian hot spots and spreading features on the East Pacific Rise that the plate motion in the Pacific Ocean area has also changed drastically. The time interval I is the period of high rate of sedimentation (several hundreds cm/1,000 years) and moderately increasing plate motion; the time interval II extremely low rate of sedimentation (less than several cm/1,000 years) and slow plate motion, and at the same time land areas were expanded; the time interval III moderate rate of sedimentation (several tens cm/1,000 years) and high rate of plate motion, and land areas were reduced. These drastic changes can be explained by the "cyclic evolutionary model", originally proposed by Kanamori, and Forsyth and Uyeda's slab-pulling driving force of the oceanic plate motion as follows. The drastic change from the time interval III to II is ascribable to detachment of the down-going slab from the ocean plate. The reduction in plate motion may also be triggered by the detachment, which releases the ocean plate from the down pulling force. The high rate of sedimentation in the time interval I is resulted from the steepening in the topographic relief and the increase in the amplitude of tectonic deformation, which should be related with the horizontal compressional stress caused by the coupling between the continental and oceanic lithospheres.

1. Introduction

The island arc systems, now found mainly along the continental margins around the Pacific, are particularly important areas to understand the geodynamics of the world. It has been conclusively documented that the oceanic lithosphere bends and descends into the mantle at the island arc system. In the theory of plate tectonics, lithospheric subduction is one of the major tectonic processes related to the formation and evolution of island arcs. There is a diversity of topography, seismicity, Wadati-Benioff zones, volcanism, gravity anomalies, stress fields, etc., in the island arc systems. It is almost certain that the degree of mechanical coupling between the oceanic and continental lithospheres varies among different island arcs, and the coupling may play an essential role in the diversity of the systems (KANAMORI, 1977).

There are two kinds of model which have been proposed to explain the diversity and evolution of island arc systems:

1) Stationary subduction model—inter-plate coupling is controlled by relative movement of both plates, and the relative movement is quasi-stationary or does not have any special trend of change;

2) Non-stationary subduction model—inter-plate coupling changes with evolutionary stages of plate subduction (the evolutionary model of KANAMORI, 1971, 1977; and KOBAYASHI and ISEZAKI, 1976).

If some changes in the tectonic features of an island arc system during geologic time are found, they may provide us with some constraints on the island arc models. For such an investigation, the Japanese island arcs area is most suitable because of the existence of ample geologic and geophysical data. Unraveling the geological records and determining the trends in tectonic features requires knowledge of the precise chronology of relevant geological events, which can be compared with the history of the oceanic plate motion. For this purpose, the magnetic stratigraphy is the most useful method because:

1) magnetic stratigraphy can be used on a global scale;

2) magnetostratigraphic patterns can be directly correlated with ocean magnetic anomaly patterns, which show the spreading history of an ocean plate.

In this article, the magnetic stratigraphy of Japanese Neogene and Quaternary sediments and the tectonic evolution of the Japanese island arcs during the last 15 million years are discussed, referring to the mechanism of Pacific plate motion.

2. Magnetic Stratigraphy of Japanese Neogene and Quaternary Sequences

Japanese Neogene and Quaternary rocks have been investigated paleomagnetically since MATUYAMA (1929) recognized periodic change in the polarity of the geomagnetic field. KAWAI (1951) applied paleomagnetic methods to sedimentary rocks, and reported several horizons in which remanent magnetization had reversed polarity. NAKAGAWA *et al.* (1969) first applied the combined magneto- and biostratigraphic techniques to sedimentary sequences, and found that a correlation of the sedimentary sections with the deep-sea bottom sediments was possible. As the next step, magneto- and biostratigraphic in-

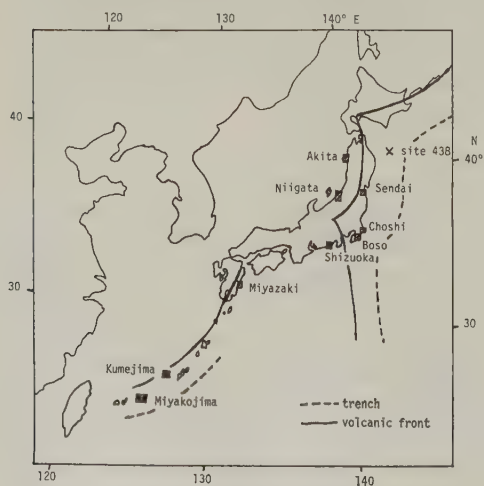


Fig. 1. Index map of investigated areas in the Japanese island arc system.

vestigations on Japanese Neogene and Quaternary sediments outcropping in the Akita, Sendai, Niigata, Choshi, Boso, Shizuoka, Miyazaki, Kumejima, and Miyakojima areas have been made by the author and his colleagues (NIITSUMA, 1970, 1976; KIMURA, 1974; NAKAGAWA and NIITSUMA, 1977; NAKAGAWA *et al.*, 1975, 1977; NITOBE, 1977). Figure 1 shows the examined areas, which are widely distributed in the Northeastern Japanese arc, Southwestern Japan, and the Ryukyu arc.

Figure 2 is an example of magneto- and biostratigraphy in the Boso area, central Japan. The vertical axis corresponds to the thickness of the sedimentary sequence, and the columns show lithostratigraphic classification (Formation), geologic columnar section marked with the horizons of key tuff layers, intensity of remanent magnetization after cleaning with alternating field and thermal demagnetization methods, latitude of virtual geomagnetic pole position (VGP) calculated from the direction of remanent magnetization, geomagnetic polarity determined by the latitude of VGP, and magnetostratigraphic classification (Magnetozone). On the right-hand side of this figure, the alphabetically nominated horizons correspond to the microbiostratigraphic data, which are shown in the figure caption. The Boso area has a sequence of several thousands meters thick continuous marine sediments, which is probably one of the thickest Neogene successions in the world of which geology, paleontology, sedimentology, and tephra-stratigraphy have been well studied.

The magnetostratigraphic sequence can be correlated with the standard normal and reversed geomagnetic polarity pattern, supplemented with the ocean magnetic anomalies (Fig. 3), using the microbiostratigraphic datums which are shown as the alphabetic nominations in Fig. 2 and beside the left column in Fig. 3. Those microbiostratigraphic datums have been calibrated to the standard magnetostratigraphic scale (RYAN *et al.*, 1974; SARTO *et al.*, 1975; TAKAYANAGI *et al.*, 1978), as shown the alphabetic nominations beside the right column in Fig. 3. This correlation makes it possible to calibrate the sedimentary sequence to the absolute age. The 5,500 m thick sedimentary sequence in the Boso area is defined to be deposited for the last 16 my, and a one-third of the duration corresponds to the remarkably thin part of the sequence (80 m in thickness; magnetozones of BS-H and BS-I) as shown by the correlation line in Fig. 3. This fact shows the existence of drastic changes in the rate of sedimentation in this area, and in this part of the sequence, the rate of sedimentation is extremely low. Using the calibration, the rate of sedimentation can be calculated as shown in Fig. 5. In this part (4.7 to 10.4 mybp), the sedimentation rate is ranged from 1.0 to 10 cm/1,000 years and increasing in the rate appears in the upper horizons of this part. Above this part, the sedimentation rate is ranged from several tens to several hundreds cm/1,000 years. Below this part, the rate is almost constant, ranged from 20 to 40 cm/1,000 years.

Based on the geologic sequence in the Boso area and these changes in sedimentation rates, the author proposes the following geochronologic classification of tectonic evolution: i.e. the time intervals I, II and III (increasing in age). The boundaries between these three time intervals are 4.7 mybp (basal part of the Gilbert Epoch; magnetic anomaly 3) and 10.4 mybp (Epoch 9; magnetic anomaly 5).

The same kind of magnetostratigraphy in other areas has also been established. Figure 4 shows magnetostratigraphic correlation with supplemented microbiostratigraphic data. Based on this correlation, the rate of sedimentation of those sections can also be calculated as shown in Fig. 5. It can be seen that the previously mentioned drastic change in sedimentation rates occurred not only in the Boso area but also in the other areas.

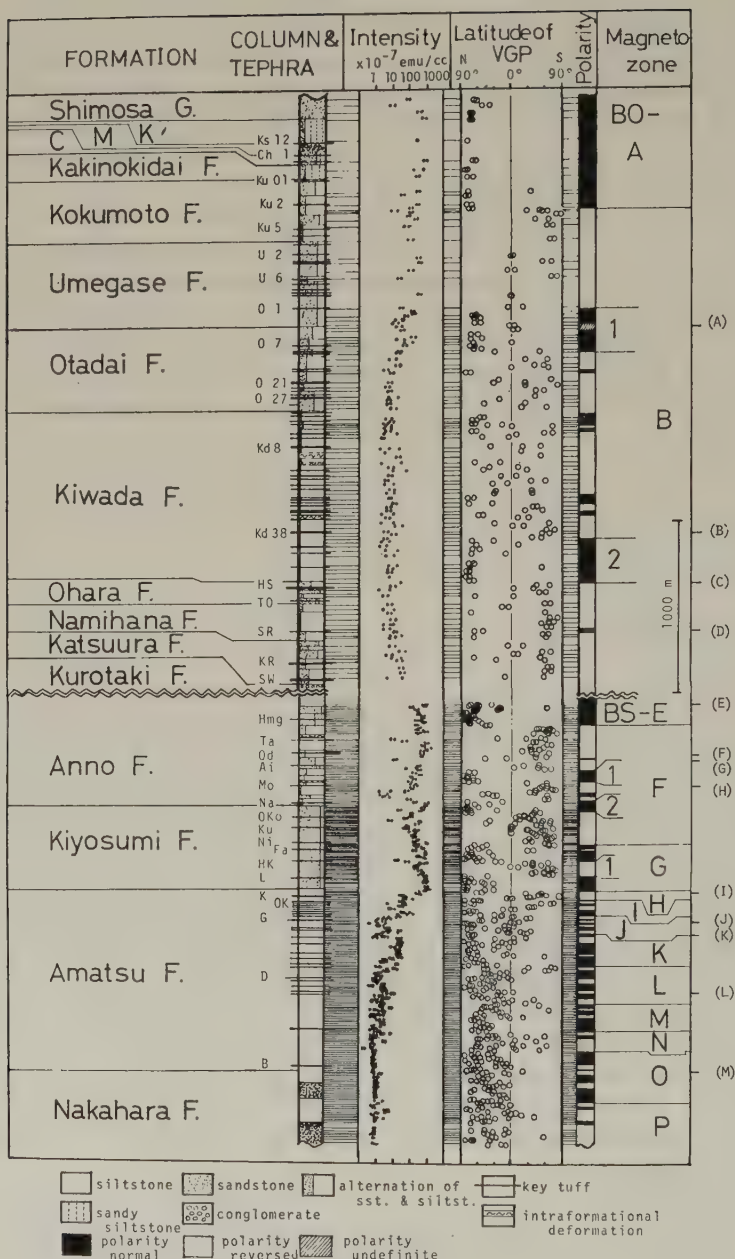


Fig. 2. Magnetostratigraphy of Neogene and Pleistocene sedimentary sequence in the Boso area and selected microfossil events (NIITSUMA, 1976; NAKAGAWA and NIITSUMA, 1977; NAKAGAWA *et al.*, 1977; TAKAYAMA, 1973, 1976; ODA, 1975. A, Lowest occurrence of *Gephyrocapsa oceanica*; B, highest occurrence of *Discoaster* spp. and coiling change of *Pulleniatina* from left to right; C, lowest occurrence of *Globorotalia truncatulinoides*; D, coiling change of *Pulleniatina* from right to left; E, highest occurrence of *Sphaeroidinella* spp.; F, coiling change of *Pulleniatina* from left to right; G, highest occurrence of *Globorotalia margaritae*; H, highest occurrence of *Globigerina nepenthes*; I, lowest occurrence of *Pulleniatina primalis*; J, lowest occurrence of *Globorotalia acostaensis*; K, highest occurrence of *Discoaster* cf. *hamatus*; L, lowest occurrence of *Globigerina nepenthes*; M, lowest occurrence of *Orbulina suturalis*.

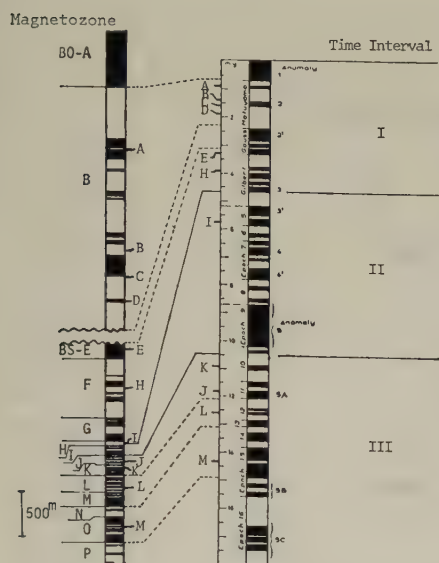


Fig. 3. Magnetostratigraphic correlation with the standard polarity pattern, supplemented with the ocean magnetic anomalies (RYAN *et al.*, 1974), and geochronologic classification of tectonic evolution in the Boso area.

Additional to these results, similar changes in sedimentation rate are found in DSDP site 438 (leg 57) taken from the inner trench slope of the northern part of the Japan trench system (VON HUENE *et al.*, 1978). It can be suspected that these drastic changes in sedimentation rates have some implications in the tectonic evolution of the Japanese island arcs.

3. Tectonic Evolution of the Japanese Island Arcs in the Last 15 my

In this section, the tectonic evolution of the Japanese island arcs in the last 15 my is discussed, based on the precise chronology and geochronologic classification by magnetostratigraphy mentioned above. The geologic character of the sedimentary sequences in the Japanese island arcs is mentioned below for each time interval:

Time interval I (0 to 4.7 my). The sedimentation rate is high (several hundreds cm/1,000 years) in the coastal plain area and intramontane basins. Distribution of marine sediments is limited to the coastal area.

Time interval II (4.7 to 10.4 my). In the coastal areas such as the Boso, Akita, Niigata and Shizuoka areas, the sedimentation of marine sediments occurred and the rate of sedimentation is extremely low (less than several cm/1,000 years). In the inland area, a large amount of terrestrial pyroclastic deposits is supplied by dacitic volcanism, and the distribution of this volcanism is limited to the zone of the present Backbone Ranges (KITAMURA and ONUKI, 1973).

Time interval III (10.4 to 16 my). This time interval is characterized by intermediate sedimentation rates, the widest distribution of marine sediments (KITAMURA and ONUKI, 1973), and the Kuroko deposits which are believed to be created by submarine volcanic activity (HORIKOSHI, 1976).

Figure 6 shows the paleogeographic maps for these time intervals. Since the early stage of time interval I, the distribution of land area is similar to the present (Fig. 6(a)). In the time interval II (Fig. 6(b)), also, it has a similar pattern except in the Ryukyu arc (NAKAGAWA *et al.*, 1977). In time interval III, it has a quite different pattern from the

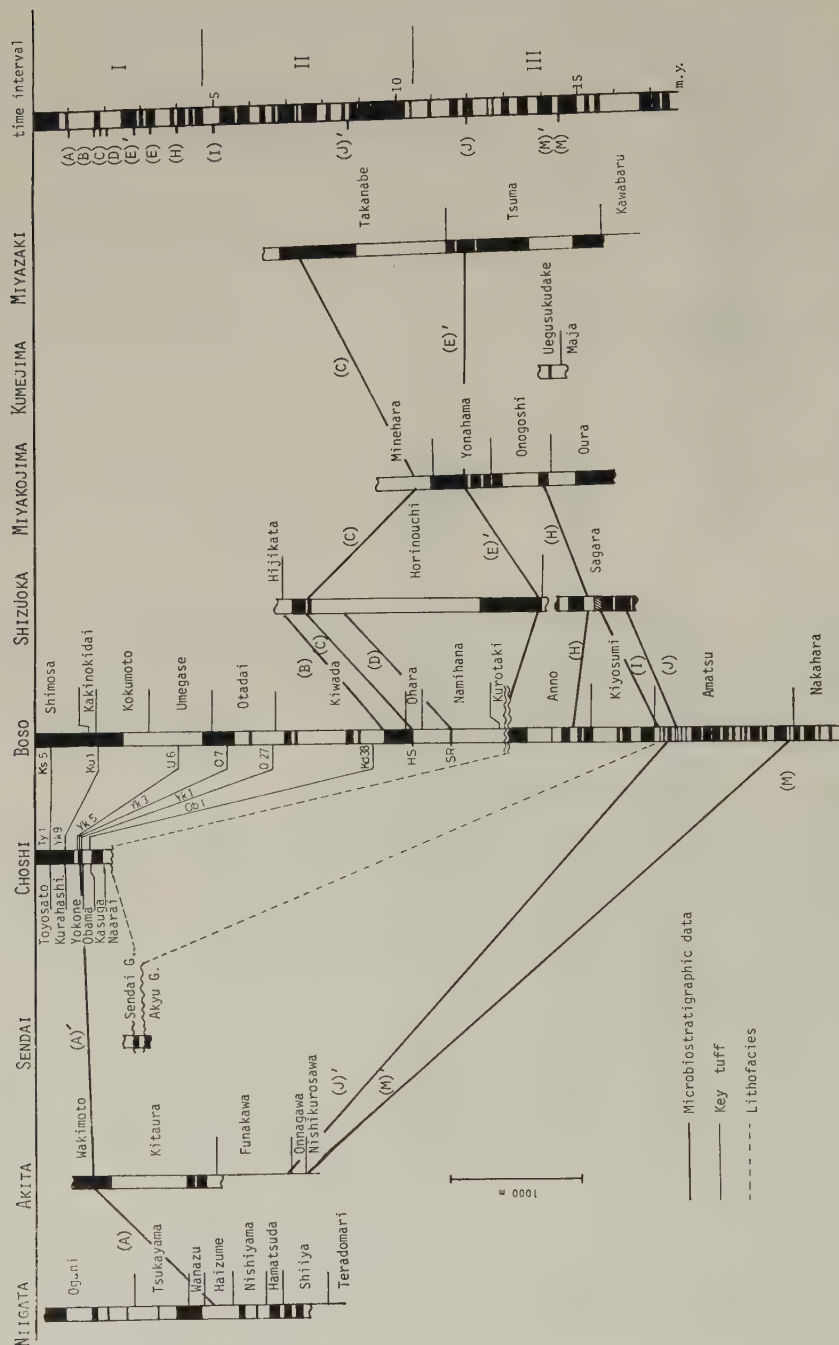


Fig. 4. Magnetostratigraphic correlation of Neogene and Pleistocene sedimentary sequences with supplemented biostratigraphic data (NAKAGAWA *et al.*, 1977; SAITO and MAYA, 1973; SAITO and BURCKLE, 1977; UJIRÉ and HARU, 1975) in the Japanese island arc area. A, highest occurrence of *Miocena elliptica*; E', lowest occurrence of *Globorotalia tosaensis*; J', coexistence of *Ommatartus antepenultimus* and *O. penultimus*; M', existence of *Globorotalia peripheroronda*, *G. birnagene*, *G. denseconnexa*, and *Globigerina praebulloides pseudociperoensis*; A-M, see figure caption of Fig. 3.

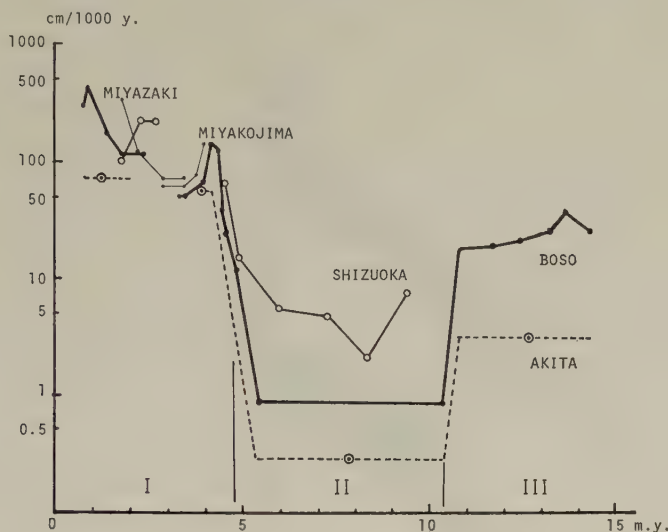


Fig. 5. Changes in rate of sedimentation of Neogene and Pleistocene sedimentary sequence and geochronologic classification of tectonic evolution in the Japanese island arc area.

present (Fig. 6(c)). The volcanic activity is marked in Fig. 6 by crosses (\times). In time interval II, volcanism is characterized by terrestrial dacitic activity. In the later part of time interval III, volcanism is characterized by basalt and dolerite extrusion (KONDA, 1974). The extrusion is assumed to have occurred under tensional conditions (KOBAYASHI and NAKAMURA, 1978). The paleogeographic features in time interval III are rather similar to those of the Bonin-Mariana island arc system where the island arc consists mainly of non-volcanic islands such as Ogasawara and the Saipan islands, and the submarine volcanic activity occurring.

4. The Condition of the Lithospheric Plate under the Northeastern Japanese Island Arc and the Cyclic Evolutionary Model

In the present Northeastern Japanese island arc system, the continental and the oceanic lithospheres are nearly completely decoupled so that no major thrust earthquake can occur along the interface, according to KANAMORI (1977). Because of the reduced coupling, the tensional force caused by the gravitational pull of the denser downgoing lithosphere may be transmitted to the oceanic lithosphere and may cause a large intra-plate normal fault earthquake. The 1933 Sanriku Earthquake is interpreted as a lithospheric normal-fault which cuts through the entire thickness of the lithosphere (KANAMORI, 1977).

On the basis of the seismological results, UYEDA and KANAMORI (1978) estimated that the subduction type in the Northeastern Japanese island arc system is an intermediate one between the two end members. The end members are named the Chile and Mariana types. In the Chile type, the coupling between the lithosphere of ocean and continent is strongest and the width of the contact zone is very large, so that when slippage occurs it results in a really major earthquake. This type is also characterized by the shallow angle



Fig. 6. Paleogeographic maps of the Japanese island arc area in the each tectonic evolutionary time interval.

of the Wadati-Benioff zone and the lack of deep earthquakes below 200 km. In the Mariana type, the coupling is weakest, and decoupling and detaching may occur. This type is characterized by the steep angle of the Wadati-Benioff zone and by an active back arc basin.

KANAMORI (1971, 1977) presented an interesting explanation for these features in terms of gradual decoupling at the interface zone between the landward and subducting plates. The Mariana type corresponds to the last stage of the evolutionary trend.

KOBAYASHI and ISEZAKI (1976) modified the original Kanamori's model to be more consistent with geophysical observations such as magnetic anomalies, thickness of sediment cover and age of the marginal sea floor. The modification is based upon the assumption that subduction always starts at the boundary between the continental and oceanic lithospheres. (In the case of the original model, the oceanic plate, having lost the mechanical support of the opposing continental lithosphere, may start sinking from the leading edge.) When this process is completed, the detached slab of oceanic lithosphere sinks down to the deeper asthenosphere, and the new cycle will repeat by renewed subduction.

The observations of the spatial distribution of earthquake hypocenters in the North-eastern Japanese arc system suggest that the Wadati-Benioff zone reaches 550 km in depth

and has 30° inclination (ISHIDA, 1970). Using these values, the length of the Wadati-Benioff zone can be calculated as 1100 km. If we use the average moving rate of the Pacific plate of 10 cm/year, estimated by Hawaiian hot spot data (JACKSON, 1976), it can be calculated that 1,000 km plate slab needs only 10 my for sinking. This could be interpreted to mean that the present lithospheric plate under the Northeastern Japanese island arc system started to sink about 10 mybp. From this, we can examine the two kinds of subduction models, stationary and non-stationary, using the relationship between subducting slab and tectonic evolution of the island arc system in the last 15 my.

If we use the modified Kanamori's model, called the "cyclic evolutionary model" in this article (Fig. 7), we should find the geologic events corresponding to the beginning of the present cycle and previous cycle in the last 15 my, based on the chronologic data. Using the above-mentioned geologic and paleogeographic evidence, we can say that the present status goes back to the time interval II. It seems that the present cycle of plate subduction started in the early part of the time interval II, 10 mybp. This estimated age agrees well with the possible starting time of sinking of the present plate under the island arc system. Before the beginning of this cycle in the time interval II, the island arc system should be in the last stage of the previous cycle, similar to the Mariana type. It has already been noticed that the paleogeographic map of the time interval III shows a similar pattern of land area distribution to the Bonin-Mariana arc. Because of the consistency with the chronologic and paleogeographic data, we can conclude that the "cyclic evolutionary model" is able to explain the process of oceanic lithospheric subduction.

Figure 7 illustrates the simplified cycle of the "cyclic evolutionary model," referring to the development of the Northeastern Japanese island arc system. In this figure, (e) shows the present status of the Northeastern Japanese island arc system. In (a) (early time interval III), we appear to have a configuration similar to a slightly later development of the situation shown in (e). The subductive slab increases in length and the gravitational down-going force increases. This affects the decreasing land area in the island arc system. Because the bending portion is pulled toward the oceanic side, the back arc area is under a tensional stress field, by the suction force between continental and subductive slab (ELSASSER, 1971). The inclination of the slab increases to 45° or 50° . This stage corresponds to the present Izu arc. In (b), the slab becomes heavier and its inclination increases up to 90° . The main part of island arc subsides below sea level. The bent portion of the slab moves toward the ocean, and because the relative position of the trench and island arc is kept more or less constant by the suction force, the back arc basin opening, which occurred under tensional stress field, is associated with extrusion of igneous rocks and Kuroko deposits. This stage corresponds to the present Mariana arc, and the later stage of the time interval III of the Northeastern Japanese arc. In (c), the down-going slab is detached from the oceanic lithosphere. The island arc system is released from the heavy lithospheric slab, isostatic rebound should occur and also release from the horizontal stress. A new cycle is initiated and the oceanic lithosphere begins to subduct between continental and oceanic lithospheres. This stage corresponds to the early part of the time interval II. In this stage (d), the oceanic lithosphere underthrusts beneath the continental lithosphere and is opposed by the latter. Because of its strength, the oceanic lithosphere is unlikely to bend and low-angle (10° to 20°) thrusting occurs. The stress in the oceanic and continental lithospheres is compressive. At this stage, caused by the strong coupling between the continent and oceanic lithospheres, major earthquakes occur. This stage corresponds to the present Chile area and to the later stage of the time interval

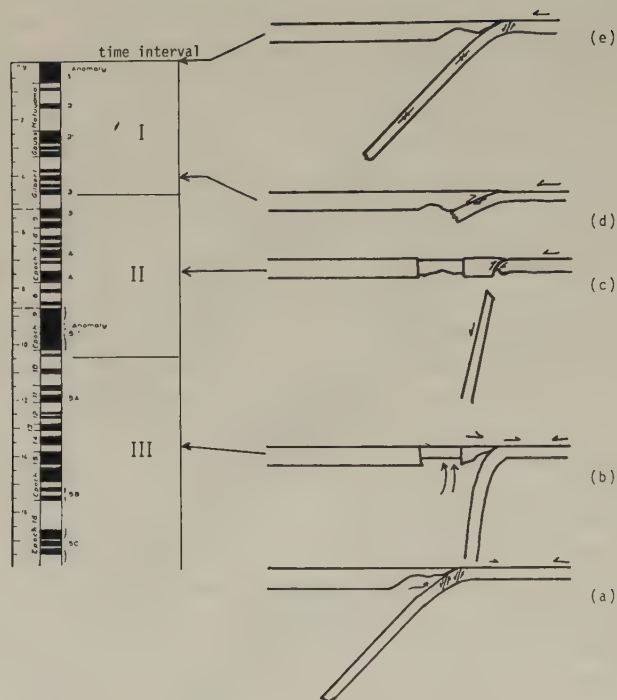


Fig. 7. Schematic "cyclic evolutionary model" for the plate subduction in Northeastern Japanese island arc system and geochronologic classification of tectonic evolution.

II and early part of the time interval I.

5. Discussion and Conclusions

The relationship between the sedimentation rate in the Japanese sedimentary basins and the lithospheric condition under the Japanese arcs may be controlled by three factors. These are: supply of sediments, horizontal stress, and isostatic balance. The supply of sediments is estimated to be mainly controlled by the width and topographic relief of the land area. The horizontal compressional stress would affect the island arc to make its topographic relief steep and to increase the amplitude of tectonic deformation. It would make the depressed area a deeper sedimentary trap and the uplifted area a higher source of sediments. In the compressional stage such as the time interval I, the rate of sedimentation should be high in the basins and coastal areas. This deduction agrees well with the above-mentioned rate of sedimentation. After the detachment of a dense lithospheric slab under an island arc system, isostatic rebound would be expected, and the land area should be more extensive and the amplitude of topographic relief should decrease, due to decrease of horizontal stress. The sedimentation rate should be made lower. The extremely low rate of sedimentation in time interval II can be explained by this process.

According to FORSYTH and UYEDA (1975), the motive force of plate motion is mainly caused by the subsidence of an oceanic lithospheric slab. If we follow this scheme, we

should find the influence of cyclic evolutionary trends of plate subduction on the plate motion and ocean floor spreading. We can monitor the motion of oceanic plates by the position of volcanic islands created by the activity of hot spots. In the Hawaiian hot spot chain, the rate of volcanic progression has been smoothly accelerating in the last 4 my (JACKSON, 1976). The acceleration is consistent with the existence of Northeastern Japan-Izu-Bonin-Mariana Arcs in which the inter-plate friction decreases with the evolutionary trend.

The spreading feature at the mid-oceanic ridge can be demonstrated by the ocean magnetic anomaly pattern correlating with the geomagnetic polarity reversal history. In the East Pacific area where the Pacific plate is being created, a fossil spreading center has been found by HERRON (1972). Because it is estimated that this center stopped spreading at 10 mybp (corresponding to anomaly 5), the East Pacific region must have had two spreading centers prior to 10 mybp. This age corresponds to the boundary between time interval II and III, when the new cycle of subduction started. Because the early stage of the evolutionary cycle can be compared to the Chile type subduction in which inter-plate coupling is strongest, the pulling force for plate motion should have been decreased at the subduction area. The decrease in the pull of the Pacific plate was able to close the fossil spreading center and to decrease the total spreading rate.

In conclusion, the rate of sedimentation deduced from magnetostratigraphy is a very useful parameter in reconstructing past tectonic conditions. Using the sedimentation rate data, the Japanese Neogene and Quaternary can be divided into three major time intervals. The features of tectonic evolution and paleogeography in each time interval are consistent with the "cyclic evolutionary model," originally proposed by KANAMORI (1971, 1977) to explain the process of oceanic lithospheric subduction. The pulling force of plate motion at the subduction area, represented by FORSYTH and UYEDA (1975), seems to control the Pacific plate motion because of the correspondence between the plate motion and cyclic evolutionary trend of plate subduction.

Grateful thanks are expressed to Professors Hakuyu Okada, Shizuo Yoshida of Shizuoka University, and Professor John H. McD. Whitaker of Leicester University for discussion and critical reading of the manuscript, and to Professors Nobu Kitamura, Hisao Nakagawa, and Drs. Toyosaburo Sakai, Kenshiro Otsuki of Tohoku University, and Professor Asahiko Taira of Kochi University for valuable suggestions. Acknowledgements are also due to Dr. Kenichi Manabe of Fukushima University and Mr. Kazuo Yoshida of Tohoku University for discussion and magnetostratigraphic information in the Sendai and Boso areas.

REFERENCES

- ELSASSER, W.M., Sea-floor spreading as thermal convection, *J. Geophys. Res.*, **76**, 1101-1112, 1971.
FORSYTH, D. and S. UYEDA, On the relative importance of driving forces of plate motion, *Geophys. J. R. Astr. Soc.*, **43**, 163-200, 1975.
HERRON, E.M., Sea-floor spreading and the Cenozoic history of the East Central Pacific, *Geol. Soc. Am. Bull.*, **83**, 1671-1692, 1972.
HORIKOSHI, E., Development of Late Caenozoic petrogenic provinces and metallogeny in Northeast Japan, *Geol. Assoc. Can. Spec. Pap.*, **14**, 121-142, 1976.
ISHIDA, M., Seismicity and travel-time anomaly in and around Japan, *Bull. Earthq. Res. Inst. Tokyo Univ.*, **48**, 1023-1051, 1970.
JACKSON, E.D., Linear volcanic chains on the Pacific plate, *Am. Geophys. Union, Geophys. Monogr.*, No. 19, 319-335, 1976.
KANAMORI, H., Great earthquakes at island arcs and the lithosphere, *Tectonophysics*, **12**, 187-198, 1971.
KANAMORI, H., Seismic and aseismic slip along subduction zones and their tectonic implications, in *Island Arcs, Deep Sea Trenches and Back-Arc Basins*, pp. 163-174, Am. Geophys. Union, Washington, D.C., 1977.
KAWAI, N., Magnetic polarization of Tertiary rocks in Japan, *J. Geophys. Res.*, **56**, 73-79, 1951.

- KIMURA, K., Magnetic stratigraphy of the Late Cenozoic sedimentary sections in Boso Peninsula, Niigata area, and Oga Peninsula, Japan, *J. Geol. Soc. Jpn.*, **80**, 579–592, 1974.
- KITAMURA, N. and Y. ONUKI, Geological and crustal sections of the A-zone, Northeast Japan, in *The Crust and Upper Mantle of Japanese Area (Part II)*, edited by M. Gorai and S. Igi, pp. 38–60, Geol. Surv. Jpr., Kawasaki, 1973.
- KOBAYASHI, K. and N. ISEZAKI, Magnetic anomalies in Japan Sea and Shikoku Basin and their possible tectonic implication, *Am. Geophys. Union, Geophys. Monogr.*, No. 19, 235–251, 1976.
- KOBAYASHI, Y. and K. NAKAMURA, Restoration of tectonic stress field of Tertiary Southwest Japan by means of dikes, *Abstr. Int. Geodyn. Conf.*, pp. 86–87, 1978.
- KONDA, T., Bimodal volcanism in the Northeast Japan arc, *J. Geol. Soc. Jpn.*, **80**, 81–89, 1974.
- MATUYAMA, M., On the direction of magnetization of basalt in Japan, Työsen and Manchuria, *Proc. Jpn. Acad.*, **5**, 203–205, 1929.
- NAKAGAWA, H., N. NIITSUMA, and I. HAYASAKA, Late Cenozoic geomagnetic chronology of the Boso Peninsula, *J. Geol. Soc. Jpn.*, **75**, 267–280, 1969.
- NAKAGAWA, H., N. NIITSUMA, K. KIMURA, and T. SAKAI, Magnetic stratigraphy of Late Cenozoic stages in Italy and their correlatives in Japan, in *Late Neogene Epoch Boundaries*, edited by T. Saito and L.H. Burckle, Micropaleont. Press, pp. 64–70, New York, 1975.
- NAKAGAWA, H. and N. NIITSUMA, Magnetostratigraphy of the Late Cenozoic of the Boso Peninsula, Central Japan, *Quatern. Res.*, **7**, 294–301, 1977.
- NAKAGAWA, H., N. KITAMURA, Y. TAKAYANAGI, T. SAKAI, M. ODA, K. ASANO, N. NIITSUMA, T. TAKAYAMA, Y. MATOBA, and H. KITAZATO, Magnetostratigraphic correlation of Neogene and Pleistocene between the Japanese Islands, Central Pacific, and Mediterranean regions, *Proc. 1st Int. Congr. Pacific Neogene Stratigraphy*, pp. 285–310, 1977.
- NIITSUMA, N., Some magnetic stratigraphic problems in Japan and Italy, *J. Mar. Geol.*, **6**, 99–112, 1970.
- NIITSUMA, N., Magnetic stratigraphy of the Boso Peninsula, *J. Geol. Soc. Jpn.*, **82**, 163–181, 1976.
- NITOME, T., Magnetic and pollen stratigraphy of the Uonuma Group in Niigata Prefecture, North Central Japan, *Quatern. Res.*, **7**, 302–315, 1977.
- ODA, M., A chronological interpretation of the paleomagnetic polarity records of the Upper Cenozoic of the Boso Peninsula based upon planktonic foraminifera, *J. Geol. Soc. Jpn.*, **81**, 645–647, 1975.
- RYAN, W.B.F., M.B. CITA, M. Dreyfus RAWSON, L.H. BURCKLE, and T. SAITO, A paleomagnetic assignment to Neogene stage boundaries and the development of isochronous datum planes between the Mediterranean, the Pacific and Indian oceans in order to investigate the response of the world ocean of the Mediterranean “salinity crisis,” *Riv. Ital. Pal.*, **80**, 631–638, 1974.
- SAITO, T. and S. MAIYA, Planktonic foraminifera of the Nishikurosawa Formation, Northeast Honshu, Japan, *Trans. Proc. Palaeontol. Soc. Jpn.*, *N.S.*, **91**, 113–125, 1973.
- SAITO, T., L.H. BURCKLE, and J.D. HAYS, Late Miocene to Pleistocene biostratigraphy of equatorial Pacific Sediments, *Micropaleontol. Spec. Publ.*, **1**, 226–244, 1975.
- SAITO, T. and L.H. BURCKLE, Occurrence of silicoflagellate *Mesocena elliptica*: Further evidence on the age of the Wakimoto Formation, Oga Peninsula, Japan and the recognition of the Jaramillo Event, *J. Geol. Soc. Jpn.*, **83**, 181–186, 1977.
- TAKAYAMA, T., On the distribution of calcareous nannoplankton in the youngest Cenozoic of Japan, *Mem. Geol. Soc. Jpn.*, **8**, 45–63, 1973.
- TAKAYAMA, T., Calcareous nannoplankton in the Plio-Pleistocene sections of Calabria, A Preliminary Report, 2nd Symp., N/Q Boundary, IGCP, Bologna, Rep., pp. 115–122, 1977.
- TAKAYANAGI, Y., T. TAKAYAMA, T. SAKAI, M. ODA, and M. KATO, Late Cenozoic micropaleontological events in equatorial Pacific sediments, in *Professor Bandy Memorial Volume*, edited by R.L. Kolpack, 1978 (in press).
- UJIE, H. and S. HARIU, Early Pliocene to late Middle Miocene planktonic foraminifera from the type section on the Sagara Group, central Japan, *Bull. Natl. Sci. Mus. Tokyo*, Ser. C, **1**, 83–92, 1975.
- UYEDA, S. and H. KANAMORI, Origin of back-arc basins and arc tectonics, *Abstr. Int. Geodyn. Conf.*, p. 168, 1978.
- VON HUENE, R. and SCIENTISTS ABOARD GLOMAR CHALLENGER FOR LEG 57, Japan trench transected, *Geotimes*, **23** (4), 16–21, 1978.

REGIONAL CHARACTERISTICS AND THEIR GEODYNAMIC IMPLICATIONS OF LATE QUATERNARY TECTONIC MOVEMENT DEDUCED FROM DEFORMED FORMER SHORELINES IN JAPAN

Yoko Ota* and Torao YOSHIKAWA**

* *Department of Geography, Yokohama National University, Yokohama, Japan*

** *Department of Geography, University of Tokyo, Tokyo, Japan*

(Received June 19, 1978; Revised September 8, 1978)

In the Japanese coastal area, deformation patterns deduced from the height of former shorelines are classified into four types, A, B, C and D, each reflecting different response of tectonic regions to island arc movements. Each area has been progressively and acceleratedly deformed in a same pattern during the late Quaternary. Maximum rate of average uplift is 1.5 m/1,000 years for the Last Interglacial terrace and 4 m/1,000 years for the Holocene terrace.

The landward tilting, type D, on the Pacific coast of Southwest Japan has been associated with great earthquakes occurring below the inner slope of the Nankai Trough. Type D area is separated from upwarping mountains by hinge lines along which subsidence has accumulated. Tectonic basins filled with younger sediments on the continental slopes are assumed to be depressed zones along the former hinge lines. Ages of deformed shorelines suggest that until the early Pleistocene seismic deformation had affected only the continental slopes and later propagated onto the coastal area in the late Pleistocene at the latest, resulting in the intensification of deformation of former shorelines. In contrast, type C deformation has predominated on the Pacific coast of Northeast Japan, which are 200 km distant from the Japan Trench and seem to be still located landward of hinge lines of seismic crustal movement.

1. Introduction

Height analysis of the former shorelines preserved on marine terraces as "shoreline angles" offers the best data for estimating the pattern and rate of tectonic deformation in coastal areas in the late Quaternary. It has almost the same accuracy as re-levelling of bench marks, if age estimation and correlation of terraces as well as height measurement are satisfactory done. The authors have collected data of former shorelines in collaboration with members of Research Group for Quaternary Tectonics as a part of the Japanese Geodynamics Project to deduce the characteristics of late Quaternary tectonic movement in Japan.

The purpose of this paper is to analyse the areal distribution and deformation types of the height of the former shorelines on the two prominent marine terraces, the late Pleistocene "S" terrace (Ota, 1975) and the Holocene terrace, with special reference to the pattern of seismic deformation, and to discuss the temporal sequence of deformation pattern and the rate of uplift. Attention is paid to the cause of differentiation of deformation types and its tectonic implication in Northeast Japan and Southwest Japan, both facing the trenches with different distance, however.

2. Late Quaternary Tectonic Movement Deduced from Deformed Shorelines

The S and younger Holocene terraces are almost continuously developed around the Japanese Islands and are useful as marker surfaces to deduce late Quaternary tectonic movements. Radiometric age of the S terrace in Kanto is estimated at 120,000–130,000 Y.B.P. by the fission track method from a tephra layer which covers the marine terrace (MACHIDA, 1975), and at about 120,000 Y.B.P. by the Th230 or Pa231 method from the raised coral reef complex of Kikai-jima, Ryukyu Islands (KONISHI *et al.*, 1974). The S terrace, therefore, represent a high sea level of the Last Interglacial stage and are correlated with Barbados III (MESOLELLA *et al.*, 1969) and the stage VII of New Guinea (CHAPPELL, 1974).

Some parts of the Holocene terraces are of depositional surfaces containing woods, shell beds or fossil corals and represent the main stage of the latest transgression. Numerous C14 dates from the Holocene terrace show that the transgression culminated 5,500–6,500 Y.B.P. (YONEKURA, 1975; Ota *et al.*, 1978).

Heights of former shorelines of the S terraces were measured by barometric survey and those of the Holocene terrace by levelling with a handlevel or an autolevel. Height data were corrected to the height above mean sea level.

2.1 Height distribution of the S terrace and its deformation pattern

Areal height distribution of the S terrace is summarized in Fig. 1. Isobases are drawn to show the pattern of deformation in some areas investigated in detail (OTA and NARUSE, 1977). Height data in 14 areas are also listed in Table 1. From Fig. 1 and Table 1 it is obvious that the S terrace ranges from 10 to 200 m in height, indicating a great amount of differential uplift. Data are not enough in Hokkaido, Seto Inland Sea and Kyushu, however.

Deformation pattern of former shorelines of the S terrace are classified into four types (OTA, 1975). Type A is warping with small wavelength of 20–30 km, parallel to the coastline (areas 1–4). The undulation of this type clearly corresponds to the present topographic features. Upwarping predominates along the foot of mountains and peninsulas and downwarping in intervening plains. This type is observed on the Japan Sea coast of Northeast Japan where the S terrace is 10–105 m high.

Type B is tilting of small blocks, 10–30 km long, and are found only in the western area of the Japan Sea coast (areas 5–8). Noto Peninsula (area 6), which tilts southward from 110 to 15 m high as a whole, is subdivided into nine small blocks tilting southward. Sado Island (area 5) also consists of three tilted blocks (OTA *et al.*, 1976).

Type C is very gentle undulation with wavelength larger than 100 km and predominates in the piedmont areas of Kitakami and Abukuma Mountains (areas 9 and 10) on the Pacific coast of Northeast Japan. Height differences of the S terrace in these areas ranges from 40 to 100 m, smaller than in the other types, however.

Type D is notable landward tilting of coastal zones 30–50 km wide. The Pacific coastal area from south Kanto to south Shikoku is characterized by the deformation of this type. The Ryukyu Islands, where the S terrace is higher closer to the Ryukyu Trench, have also been deformed in this type (Ota, unpublished). Differential uplift in type D is the most distinguished among all the types of deformation. The height of the S terrace in these areas reaches about 200 m.

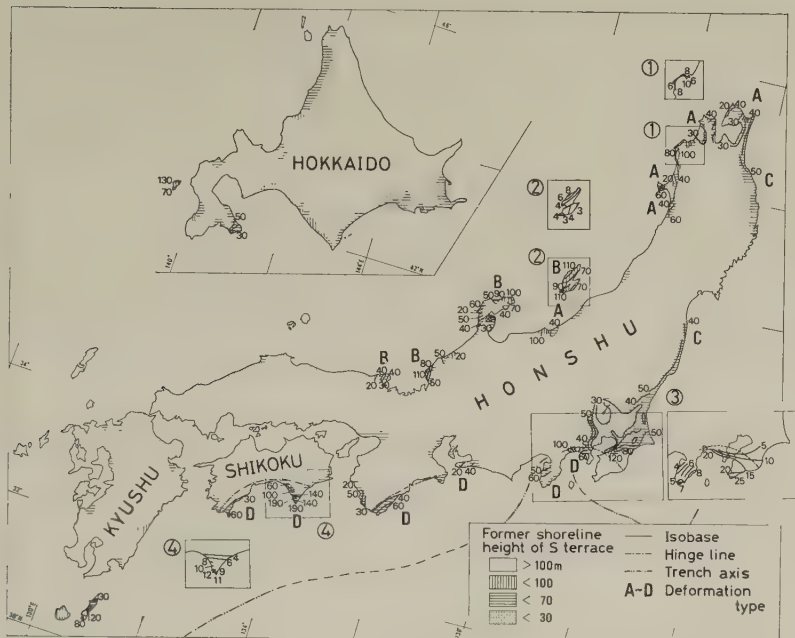


Fig. 1. Height and deformation pattern of S terrace (after Ota and NARUSE, 1977). Insets 1-4 show the deformation of Holocene terrace in area 2 (Inset 1), area 5 (Inset 2), areas 11 and 12 (Inset 3) and area 13 (Inset 4). Data source is indicated in Table 1.

Table 1. Rate of uplift estimated from height of former shorelines.

Area number, locality and type of deformation		Last Interglacial (130,000 Y.B.P.)		Holocene (6,000 Y.B.P.)	
		I	II	I	II
1. Tsugaru Peninsula	A	20-50 (1)	0.4		
2. Shirakami Mts.	A	40-100 (1)	0.7	5-10 (5)	1.3
3. Oga Peninsula	A	40-90 (1)	0.7		
4. Noshiro Plain	A	20-60 (1)	0.4		
5. Sado Island	B	40-120 (1)	0.9	2-9 (5)	1.2
6. Noto Peninsula	B	15-110 (1)	0.8		
7. Nyu Mountains	B	30-115 (1)	0.9	5-8 (5)	1.0
8. Tango Peninsula	B	15-50 (1)	0.4		
9. Kitakami Mts.	C	40-100 (2, 5)	0.7		
10. Abukuma Mts.	C	40-60 (1)	0.4		
11. Boso Peninsula	D			5-25 (6, 7)	3.8
12. Oiso Hills	D	20-160 (3)	1.2	10-26 (6)	4.0
13. Muroto Peninsula	D	40-195 (4)	1.5	3-13 (8)	1.8
14. Ryukyu Islands	D	20-200 (5)	1.5	5-13 (9)	1.8

I, height (m); II, maximum rate of average uplift (m/1,000 year).

Data source: (1) Ota, 1975; (2) YONEKURA, 1966; (3) MACHIDA, 1973; (4) YOSHIKAWA *et al.*, 1964; (5) Ota, unpubl.; (6) YONEKURA, 1975; (7) MATSUDA *et al.*, 1978; (8) KANAYA, 1978; (9) Ota *et al.*, 1978.

2.2 Height distribution and deformation pattern of the Holocene terrace

The Holocene terrace is normally less than 7–8 m high and attains 26 m in maximum (Table 1). This shows that a marked differential uplift occurred also after the formation of the Holocene terrace as did after the S terrace formation. Increasing yet insufficient number of data do not allow us to show the areal distribution of height in all the area of the Japanese Islands. Thus, a few examples are indicated in the insets of Fig. 1 to show the deformation pattern of the Holocene terrace.

Warping of small wavelength of type A in Shirakami Mountains (area 2) is shown in Fig. 1-1, and tilting of small blocks of type B in Sado Island (area 5) in Fig. 1-2. Landward tilting of type D is clearly seen in south Kanto (areas 11 and 12, Fig. 1-3) and in Muroto Peninsula (area 13, Fig. 1-4). The Holocene terrace of the Ryukyu Islands shows the same pattern of deformation as the S terrace.

2.3 Uniform sequence of uplift pattern in the late Quaternary and its relation to seismic crustal deformation in historic times

The pattern of deformation of the terraces higher (older) than the S terrace is similar to that of the S terrace, but the older terrace is everywhere more deformed than the S terrace (OTA, 1975). Similar relation is also observed between the S and younger Holocene terraces. It is concluded, therefore, that each area has been progressively deformed in a certain consistent pattern throughout the late Quaternary. This is interpreted as accumulating process of coseismic deformation observed in historic times in type D area (YOSHIKAWA, 1970; YONEKURA 1975; MATSUDA *et al.*, 1978), as well as in types A and B areas as explained below.

In type A areas, short wave length warping of Shirakami Mountains has positive relation to the coseismic uplift in 1704 and 1793 earthquakes (NAKATA *et al.*, 1976). As for type B areas, an example of accumulated coseismic deformation is the progressively northwardtilted flight of terraces in Ogi Peninsula, Sado Island, which was affected by coseismic tilting in 1802 (OTA *et al.*, 1976). It is also noticed that the smaller scale deformation of types A and B on the Japan Sea coast seems to be caused by earthquakes of smaller magnitude than those on the Pacific coast.

2.4 Rate of uplift

Average rates of uplift during the two different times, since the formation of the S and the Holocene terraces are calculated under the assumption that sea level of the Last Interglacial (about 130,000 Y.B.P.) and about 6,000 Y.B.P. were 6 and 2 m above present sea level respectively (OTA and NARUSE, 1977). The maximum values of average rate of uplift in 14 areas are listed in Table 1. The rate of uplift since the formation of the S terrace ranges between 0.4 and 0.9 m/1,000 years for areas of types A, B and C, but in the southern tip of Muroto Peninsula and Kikai-jima, which show type D deformation, it is about 1.5 m/1,000 years. The uplift rates since the formation of the Holocene terrace are higher than those of the S terrace and more than 1 m/1,000 years in areas of A and B types, and the maximum rate attaining to 4 m/1,000 years in type D area. It is suggested, therefore, that in the late Quaternary each coastal area of Japan has been progressively and acceleratedly deformed in a consistent pattern, and type D area has been most active in terms of vertical deformation.

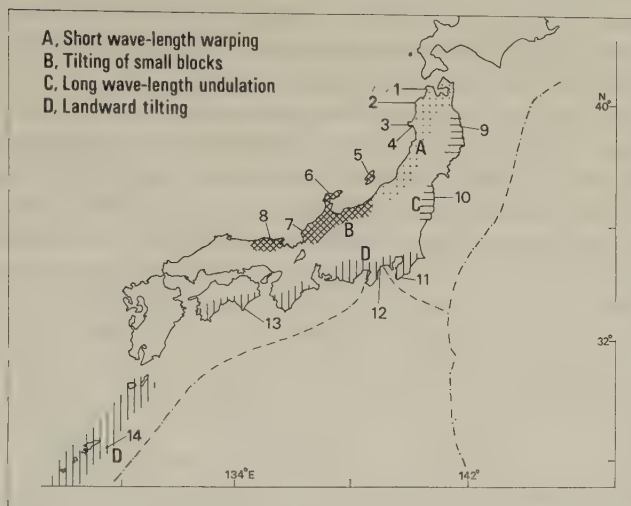


Fig. 2. Distribution of deformation types deduced from height of former shorelines (after OTA, 1975). Numbers are referred to area numbers in Table 1.

3. Difference in Type of Late Quaternary Crustal Deformation between the Pacific Coasts of Northeast and Southwest Japan

Japanese coastal areas are divided into four tectonic regions characterized by different types of late Quaternary crustal deformation, as shown in Fig. 2. Each tectonic region has experienced persistently single type of crustal deformation in the late Quaternary, which depends on its geological structure and location in the island arc system, as was analysed by one of the present authors (OTA, 1975). In this chapter, the difference of deformation type in the late Quaternary between the Pacific coasts of Northeast and Southwest Japan is discussed from a geodynamic point of view.

3.1 Characteristics of late Quaternary crustal deformation on the Pacific coast of Shikoku

The type D area, that is, the Pacific coasts of Southwest Japan and the Kanto district, has repeatedly experienced severe earthquakes associated with acute crustal deformation in recent times, for example, the 1923 Kanto earthquake, the 1944 Tonankai earthquake and the 1946 Nankai earthquake. The recent coseismic crustal deformation in Shikoku, a part of the area, has been of the pattern that tips of promontories were uplifted and inland areas subsided, which is very similar to that of the late Quaternary tectonic movement detected from the deformation of former shorelines. On the other hand, recent interseismic secular crustal deformation revealed by precise levellings is of the pattern reverse to the coseismic one in that mountains are upwarped and coastal areas subside. A hinge line of the co- and interseismic crustal movement is clearly recognized running nearly parallel to the south coast (Fig. 3). The hinge line coincides with the axis of notable subsidence associated with the 1946 Nankai earthquake. At the time of this earthquake, coastal areas to the south of the hinge line where marine terraces descend north- or northwestward were uplifted tilting north- or northwestward. But, during the interseismic period from 1897 to 1937, the main part of the Shikoku Mountains was broadly upwarped

and the southern coastal area was steeply downwarped. The hinge line is located along the southern margin of the broadly upwarped area. The interseismic secular crustal deformation seems to have acted at an almost uniform rate.

In the southern part of Shikoku, great earthquakes associated with characteristic crustal deformation similar in pattern to the recent coseismic one have occurred at intervals of 100 to 150 years in historic times. If the rate of tectonic movement in an interseismic period of about 100 years was as nearly uniform as in the recent one, crustal deformation resulting from co- and interseismic tectonic activities in a seismic cycle of about 120 years on an average could be estimated from the results of precise levellings as follows (YOSHIKAWA, 1970):

- 1) A depressed zone is formed along the hinge line of co- and interseismic crustal deformation.
- 2) The coastal area to the south of the hinge line is uplifted tilting north- or northwestward.
- 3) In the area to the north of the hinge line, the mountains are upwarped.

Such a resultant crustal deformation is very similar in pattern to the late Quaternary crustal movement deduced from the present topographic features of each area. Drowned valleys are developed very well on the coasts along the hinge line where subsidence has predominated. Height of marine terraces tilting north- or northwestward to the south of the hinge line and that of the mountains on its northern side have positive correlations with the resultant crustal deformation (YOSHIKAWA, 1970). These marine terraces were inferred to have been formed and displaced due to the late Quaternary eustatic changes in sea level and the recurrence of the above-mentioned co- and interseismic tectonic activities at least for the past 250,000 years (YOSHIKAWA *et al.*, 1964).

3.2 The distribution of hinge lines on the Pacific coast of Southwest Japan

In the regions other than Shikoku of the type D area, too, coseismic crustal deformation has been similar in pattern to that in Shikoku and depressed zones along hinge lines can be found, as shown in Fig. 3. The hinge line in the southern part of Kii Peninsula (YONE-

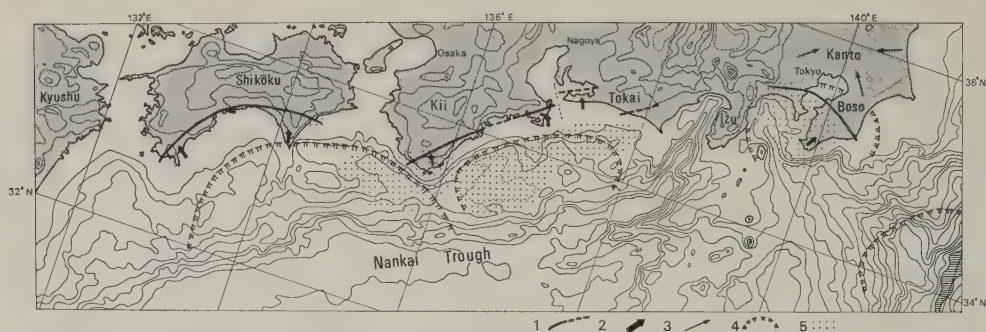


Fig. 3. Distribution of seismic deformation areas on and submarine topography off the Pacific coast of Southwest Japan (after YOSHIKAWA, 1974). Contours and bathymetric curves are drawn at intervals of 500 m, among which broken ones show depressions and the hatched part is deeper than 9,000 m. 1, hinge lines of recent crustal deformation; 2, tilt directions of marine terraces in seismic deformation areas; 3, tilt directions of upland surfaces in the Kanto tectonic basin; 4, tsunami source areas associated with recent great earthquakes (HATORI, 1966); 5, aftershock areas in a day after recent great earthquakes (MOGI, 1968).

KURA, 1968) extends to its southeast coast indented by well-developed drowned valleys, and in Shima Peninsula late Quaternary marine terraces are lowest and drowned valleys are best developed on its further northeastward extension.

In Atsumi Peninsula, an upland composed mainly of early to middle Pleistocene formations which were derived from the northern mountains tilts northward and its southern margin is bordered by sea cliff (ISHIKAWA and OTA, 1967). Mikawa Bay is a depressed zone located at the northern margin of this tilted block, offset a little left-laterally to the depressed zone of Shima Peninsula. This offset may have been caused by recent activities of the northwest-trending sinistral fault at the mouth of Ise Bay inferred from the geological structure of Paleozoic and Mesozoic rocks in both peninsulas (OTUKA, 1928). In the Tokai coastal region, depressed zones have migrated westward since the late Miocene in its eastern part and eastnortheast-trending elongate updoming and intervening depressions in the late Quaternary are arranged en echelon (TSUCHI, 1968, 1970; YONEKURA, 1975). The southeastern margin of the westernmost updomed area was displaced in the nearly similar pattern to the tip of Muroto Promontory, Shikoku, during the period before and after the 1944 Tonankai earthquake (GEODETIC DIVISION AND CRUSTAL ACTIVITY RESEARCH OFFICE, 1970). The updomed areas composed of thick late Cenozoic formations may have been formed by landward tilting of basement rocks similar in pattern to those in Shikoku and Kii Peninsula.

A hinge line of recent co- and interseismic crustal deformation is found in the southern part of the Kanto district (DAMBARA and HIROBE, 1964; GEODETIC DIVISION AND CRUSTAL ACTIVITY RESEARCH OFFICE, 1969, 1973). On the north coast of Sagami Bay, terraces along the hinge line are lower than those on both sides (MACHIDA, 1973). But, in Boso Peninsula, northeastward tilting Holocene terraces on the coast abruptly decrease the gradient on the hinge line, changing its direction to northwest so as to correspond to that of the Kanto tectonic basin.

3.3 Change of pattern of crustal deformation on the Pacific coast of Southwest Japan

From the above-mentioned facts it has been clarified that on the Pacific coast of the type D area the coastal areas to the south of the hinge lines have been uplifted tilting landward and along the hinge lines depressed zones have been formed in the late Quaternary, whereas in the areas landward of the hinge lines the mountains have been upwarped and the tectonic basins have subsided progressively. Such late Quaternary tectonic movement is very similar in pattern to crustal deformation resulting from the co- and interseismic tectonic activities, and is inferred to have acted since a time after the deposition of middle Pleistocene formations and before the formation of the highest landward-tilting marine terraces in the late Quaternary.

Generally speaking, the large scale topographic features of the Japanese Islands (HAGIWARA, 1967) are nearly concordant with the long wavelength pattern of crustal deformation during the Quaternary (YOSHIKAWA, 1971). This means that the broad tectonic relief of the Japanese Islands has mostly been formed during the Quaternary. But in the type D area promontories to the south of the hinge lines protrude seaward beyond the 0 m isopleth of the long wavelength topography (HAGIWARA, 1967). This suggests that the promontories have been affected by crustal movement of a certain pattern different from the broad upwarping of the Japanese Islands in the Quaternary. Because in the coastal areas to the south of the hinge lines the late Quaternary marine terraces descend landward quite reversely to the broad upwarping in the Quaternary, while the mountains decrease

their height seaward, it is inferred that the coastal areas to the south of the hinge lines had also been upwarded tilting seaward before the highest marine terraces were formed, and that since then the pattern of tectonic movement in these areas had changed so that marine terraces have been tilted landward. Such a change of the pattern of tectonic movement probably occurred in the late or middle Pleistocene and was caused by the recurrence of seismic activities. Since then, the areas to the south of the hinge lines have been deformed in similar patterns to the recent coseismic crustal deformation. From this point of view, the areas seaward of the hinge lines may be called the seismic deformation areas. They are 100 to 150 km long and are arranged en echelon along the Pacific coast of the type D area.

3.4 Features of submarine landforms off the Pacific coast of Southwest Japan

About 100 km off the Pacific coast of the type D area the Nankai Trough runs nearly parallel to the outline of the coast and the Sagami Trough extends from northwest to southeast off the south coast of the Kanto district (Fig. 3). Off the seismic crustal deformation areas, submarine terraces are developed well on the continental slopes descending to the troughs. These terraces are bordered on both sides by submarine rises located at intervals of about 100 km, which are submarine extensions of promontories on the coast. Their landward margins are generally parallel to the hinge lines and are often a little deeper than their trench-side margins.

The seismic sounding (YOSHII *et al.*, 1973; LUDWIG *et al.*, 1973) clarified that the submarine terraces off the south coast of Shikoku and Kii Peninsula were tectonic basins filled with younger sediments about 1,000 m thick, and that the continental slopes off the submarine terraces were cut by step faults. Aftershock areas and tsunami source areas of recent great earthquakes, which are considered to be submarine parts of seismic deformation areas, extend on the continental slopes, coinciding very well with the submarine terraces off the coast of Shikoku and Kii Peninsula (HATORI, 1966; MOGI, 1968).

The submarine trough about 1,500 m deep south of the Kii Strait is also a northward tilting tectonic basin formed in the early to middle Pleistocene (INOUCHI *et al.*, 1978). Its inner scarp runs nearly along the eastward extension of the hinge line in southern Shikoku and bounds the tsunami source area associated with the 1946 Nankai earthquake.

From these facts, the submarine terraces and trough are considered to be landward tilted blocks of seismo-tectonic origin, of which the inner depressed parts were filled with sediments. The areal dimension and features of the submarine terraces are nearly similar to those of a tectonic basin, about 50 km wide and 1,000 m deep, which would have been formed when the recent subsidence along the present hinge line in Shikoku would have lasted uniformly for about 500,000 years.

From these considerations it may be concluded that the submarine terraces too are included into seismic deformation areas, and that their inner margins are also probably hinge lines of co- and interseismic crustal deformation, along which subsidence has predominated.

3.5 Cause of the change in pattern of crustal deformation on the Pacific coast of Southwest Japan

Recent great earthquakes that occurred beneath the inner slopes of the Nankai and Sagami Troughs were caused by underthrusting along the plate boundary (FIRCH and SCHOLZ, 1971; ANDO, 1974, 1975), and the associated landward tilting of the coastal areas

was a result of elastic rebound, whereas in the interseismic periods mountains were upwarped and coastal areas subsided by compressional stress (MOGI, 1970).

From the above-mentioned considerations the cause of the change in pattern of crustal deformation on the Pacific coast of the type D area is interpreted as follows;

The mountains including those to the south of the hinge lines had been upwarped under a compressional state and seismic crustal rebound had acted only on the submarine terraces, forming tectonic basins along former hinge lines located at their inner margins, throughout the early and middle Pleistocene, and probably in the late Pleistocene seismic deformation areas abruptly expanded landward and hinge lines discontinuously migrated onto the coast about 50 km northwestward. Consequently, the pattern of crustal deformation in the coastal areas changed and landward tilting by elastic rebound of former shorelines commenced less than 500,000 years ago, because the subsidence along the present hinge lines and landward tilting have not yet developed so well as in the submarine tectonic basins filled with sediments. The discontinuous expansion of seismic deformation areas and migration of hinge lines may be caused by the progressive underthrusting of the Philippine sea plate, probably controlled by the structure and physical properties of the upper crust of the region. From the present rate of plate convergence, it is estimated that underthrusting will proceed about 30 to 50 km in the future 1,000,000 years and may cause a further discontinuous landward expansion of seismic deformation areas and landward migration of hinge lines probably at an interval of this order of time.

The Japanese Islands have been broadly upwarped under a compressional state due to plate convergence, as was still detected from the present interseismic crustal deformation, and seismic crustal deformation of the type D area is a byproduct of such a broad upwarping.

3.6 Characteristics of the late Quaternary crustal deformation on the Pacific coast of Northeast Japan

Marine terraces along the Pacific coast of the type C area have been very gently warped with a wavelength of about 100 km, corresponding to each mountain unit, and nowhere have been tilted landward. At times of recent great earthquakes, this coast has been frequently attacked by gigantic tsunamis, but has not experienced any acute crustal deformation (YONEKURA, 1972). These earthquakes occurred mainly beneath the inner slope of the Japan Trench running about 200 km offshore from the coast and their epicenters were located more offshore than those in Southwest Japan. From these facts it is inferred that seismic crustal deformation which caused gigantic tsunamis has not yet affected the Pacific coast but only the continental slope in the type C area, because the areal dimension of seismic deformation areas associated with great earthquakes is estimated at about 100 km in diameter.

Off the Pacific coast of Northeast Japan too are recognized submarine terraces at three levels from 1,000 to 2,500 m deep. These terraces are also tectonic basins bordered by elevations of basement rocks on their outer margins and filled with younger sediments (NAKAJIMA, 1973). These submarine terraces are similar in dimension and geological structure to those in Southwest Japan. But the formers are located more offshore than the latters. Their surface generally dips seaward and sediment fills are thinner in Northeast Japan than in Southwest Japan. Epicenters of recent great earthquakes were chiefly located on the outer slopes of these submarine terraces descending to the trench.

From these facts the submarine terraces off the Pacific coast of Northeast Japan might

be also considered to be seismic deformation areas of recent great earthquakes, not developed so well as those in Southwest Japan, and the seismic deformation areas seem to have not yet expanded onto the coast. The Pacific coastal area of Northeast Japan is, therefore, still located landward of the hinge lines of co- and interseismic crustal movement and has been deformed in a pattern similar to that in the area landward of the present hinge lines in the type D area.

4. Concluding Remark

Coastal areas of the Japanese Islands are divided into four tectonic regions from the types of late Quaternary crustal deformation. Each region has been deformed progressively and acceleratedly in its own characteristic type through the late Quaternary. Such regional characteristics of crustal deformation reflect the difference in the responses of these regions to island arc tectonics.

The difference in type of late Quaternary crustal deformation between the Pacific coasts of Northeast and Southwest Japan is caused by the difference in the distance from trenches and the location of seismic deformation areas. On the Pacific coast of Northeast Japan distant from the Japan Trench, the crustal deformation associated with great earthquakes occurring beneath the inner slope of the trench has not yet affected the coastal area and the seismic deformation areas extend only on the continental slope still now. Therefore, the coastal area has been deformed in the pattern of broad upwarping. In contrast, the Pacific coast of Southwest Japan is not only located close to the Nankai Trough, but seismic deformation areas which had previously extended on the continental slope expanded onto the coast in the late Quaternary at the latest, and, therefore, has since been deformed in the pattern of landward tilting.

This study was financially supported by the special research funds for the Geodynamics Project and the grant-in-aid for fundamental scientific research provided by the Japanese Ministry of Education.

REFERENCES

- ANDO, M., Seismotectonics of the 1923 Kanto earthquake, *J. Phys. Earth*, **22**, 263–277, 1974.
- ANDO, M., Possibility of a major earthquake in the Tokai district, Japan and its pre-estimated seismotectonic effects, *Tectonophysics*, **25**, 69–85, 1975.
- CHAPPELL, J., Geology of coral terraces, Huon Peninsula, New Guinea: A study of Quaternary tectonic movements and sea-level changes, *Am. Geol. Soc. Bull.*, **85**, 553–570, 1974.
- DAMBARA, T. and M. HIROBE, Vertical movements of Japan during the past 60 years: II. Southern part of the Kanto district, *J. Geod. Soc. Jpn.*, **10**, 61–70, 1964 (in Japanese with English abstract).
- FITCH, T.J. and C.H. SCHOLZ, Mechanism of underthrusting in Southwest Japan: A model of convergent plate interactions, *J. Geophys. Res.*, **76**, 7260–7292, 1971.
- GEODETIC DIVISION AND CRUSTAL ACTIVITY RESEARCH OFFICE, GEOGRAPHICAL SURVEY INSTITUTE, Crustal activity in Boso and Miura Peninsulas, *Rep. Coord. Comm. Earthq. Predict.*, **1**, 25–33, 1969 (in Japanese).
- GEODETIC DIVISION AND CRUSTAL ACTIVITY RESEARCH OFFICE, GEOGRAPHICAL SURVEY INSTITUTE, Vertical movements in Tokai district, *Rep. Coord. Comm. Earthq. Predict.*, **2**, 49–53, 1970 (in Japanese).
- GEODETIC DIVISION AND CRUSTAL ACTIVITY RESEARCH OFFICE, GEOGRAPHICAL SURVEY INSTITUTE, Vertical movements in south Kanto district, *Rep. Coord. Comm. Earthq. Predict.*, **10**, 24–29, 1973 (in Japanese).
- HAGIWARA, Y., Analyses of gravity values in Japan, *Bull. Earthq. Res. Inst.*, **45**, 1091–1228, 1967.
- HATORI, T., Vertical displacement in a tsunami source area and the topography of the sea bottom, *Bull. Earthq. Res. Inst. Univ. Tokyo*, **44**, 1449–1464, 1966.
- INOUE, Y., Y. OKUDA, and F. YOSHIDA, On the age of formation of upper continental slope configuration in the south of the Kii Strait, *J. Geol. Soc. Jpn.*, **84**, 91–93, 1978 (in Japanese).
- ISHIKAWA, K. and Y. Ota, Upwarping movement during the Quaternary in the Atsumi Peninsula, central Japan, *Daiyonki-Kenkyu (The Quaternary Research)*, **6**, 89–92, 1967 (in Japanese with English abstract).

- KANAYA, A., Holocene marine terrace and crustal movement of the Muroto Peninsula, Japan, *Geogr. Rev. Jpn.*, **51**, 451-463, 1978 (in Japanese).
- KONISHI, K., A. OMURA, and O. NAKAMICHI, Radiometric coral ages and sea level records from the late Quaternary reef complexes of the Ryukyu Islands, *Proc. 2nd Int. Coral Reef Symp.*, pp. 595-613, 1974.
- LUDWIG, W.J., N. DEN, and S. MURAUCHI, Seismic reflection measurements of Southwest Japan margin, *J. Geophys. Res.*, **78**, 2508-2516, 1973.
- MACHIDA, H., Tephrochronology of coastal terraces and their tectonic deformation in south Kanto, *J. Geogr. Tokyo*, **82**, 53-76, 1973 (in Japanese with English abstract).
- MACHIDA, H., Pleistocene sea level of South Kanto, Japan, analysed by tephrochronology, *Quatern. Stud., R. Soc. N. Z. Bull.*, **13**, 215-222, 1975.
- MATSUDA, T., Y. OTA, M. ANDO, and N. YONEKURA, Fault mechanism and recurrence time of major earthquakes in the southern Kanto district, Japan, as deduced from coastal terrace data, *Geol. Soc. Am. Bull.*, **89**, 1610-1618, 1978.
- MESOLELLA, K.J., R.K. MATTHEWS, W.S. BROEKER, and D.L. THURBER, The astronomical theory of climatic changes: Barbados data, *J. Geol.*, **77**, 250-274, 1969.
- MOGI, K., Development of afterschock areas of great earthquakes, *Bull. Earthq. Res. Inst.*, **46**, 175-203, 1968.
- MOGI, K., Recent horizontal deformation of the earth's crust and tectonic activity in Japan (1), *Bull. Earthq. Res. Inst. Univ. Tokyo*, **48**, 413-430, 1970.
- NAKAJIMA, T., Submarine topography off the southern part of Sanriku district, *J. Geogr. Tokyo*, **82**, 136-147, 1973.
- NAKATA, T., T. IMAIZUMI, and H. MATSUMOTO, Late Quaternary tectonic movements on the Nishi-tsugaru coast, with reference to seismic crustal deformation, *Sci. Rep. Tohoku Univ.*, 7th Ser., **26**, 101-112, 1976.
- OTA, Y., Late Quaternary vertical movement in Japan estimated from deformed shorelines, *Quatern. Stud., R. Soc. N. Z. Bull.*, **13**, 231-239, 1975.
- OTA, Y., T. MATSUDA, and K. NAGANUMA, Tilted marine terraces of the Ogi Peninsula, Sado Island, central Japan, related to the Ogi earthquake of 1802, *Zisin (J. Seismol. Soc. Jpn.)*, 2nd Ser., **29**, 55-70, 1976 (in Japanese with English abstract).
- OTA, Y. and Y. NARUSE, Marine terraces in the Circum-Pacific area with special reference to the crustal movement and sea-level change, *Kagaku (Science)*, **47**, 281-292, 1977 (in Japanese).
- OTA, Y., H. MACHIDA, N. HORI, K. KONISHI, and A. OMURA, Holocene raised coral reefs of Kikai-jima (Ryukyu Islands): An approach to Holocene sea level study, *Geogr. Rev. Jpn.*, **51**, 109-130, 1978 (in Japanese with English abstract).
- OTUKA, Y., Major faults inferred from geology and landforms in the Ise-Shima district, *Geogr. Rev. Jpn.*, **4**, 649-670, 1928 (in Japanese).
- TSUCHI, R., Crustal movements deduced from the deformation of dissected fans, with reference to those in the Tokai region, *Daiyonki-Kenkyu (The Quaternary Research)*, **7**, 225-234, 1968 (in Japanese with English abstract).
- TSUCHI, R., Quaternary tectonic map of the Tokai region, the Pacific coast of central Japan, *Rep. Fac. Sci. Shizuoka Univ.*, **5**, 103-114, 1970.
- YONEKURA, N., Geomorphological Development of the northern Rikuchu coastal region, northeastern Japan, *Geogr. Rev. Jpn.*, **39**, 311-323, 1966 (in Japanese with English abstract).
- YONEKURA, N., Geomorphic development and mode of crustal movement on the south coast of the Kii Peninsula, southwestern Japan, *J. Geogr. Tokyo*, **77**, 1-23, 1968 (in Japanese with English abstract).
- YONEKURA, N., A review of seismic crustal deformations in and near Japan, *Bull. Dept. Geogr. Univ. Tokyo*, **4**, 17-50, 1972.
- YONEKURA, N., Quaternary tectonic movements in the outer arc of Southwest Japan with special reference to seismic crustal deformation, *Bull. Dept. Geogr. Univ. Tokyo*, **7**, 19-71, 1975.
- YOSHII, T., W.J. LUDWIG, N. DEN, S. MURAUCHI, M. EWING, H. HOTTA, P. BUHL, T. ASANUMA, and N. SAKAJIRI, Structure of Southwest Japan margin off Shikoku, *J. Geophys. Res.*, **78**, 2517-2525, 1973.
- YOSHIKAWA, T., On the relation between Quaternary tectonic movement and seismic crustal deformation in Japan, *Bull. Dept. Geogr. Univ. Tokyo*, **2**, 1-24, 1970.
- YOSHIKAWA, T., Prof. N. Yamasaki's contribution to tectonic geomorphology, *Geogr. Rev. Jpn.*, **44**, 552-564, 1971 (in Japanese with English abstract).
- YOSHIKAWA, T., Seismic crustal movement and its relation to the displacement of coastal terrace surfaces, *Kaiyo-Kagaku (Marine Sciences Monthly)*, **6**, 671-676, 1974 (in Japanese with English abstract).
- YOSHIKAWA, T., S. KAIZUKA, and Y. OTA, Crustal movement in the late Quaternary revealed with coastal terraces on the southeast coast of Shikoku, southwest Japan, *J. Geod. Soc. Jpn.*, **10**, 116-122, 1964.

MAGNETIC ANOMALIES AND TECTONIC EVOLUTION OF THE SHIKOKU INTER-ARC BASIN

Kazuo KOBAYASHI and Masao NAKADA

Ocean Research Institute, University of Tokyo, Nakano, Tokyo, Japan

(Received June 30, 1978; Revised October 15, 1978)

Detailed analysis of magnetic anomalies has revealed a clear pattern of symmetric lineations in the Shikoku Inter-arc Basin, northern Philippine Sea. Amplitudes of anomalies are in general a few hundred nanotesla (gammas, peak to peak), which are moderate compared to those of the normal ocean basins accreted from the mid-oceanic ridges and are relatively larger than those of some other inter-arc basins such as the Parece Vela Basin, Mariana Trough and West Philippine Basin. Correlation of anomalies is usually so good that age identification can be convincingly performed except for the axial irregular zone. Mode of opening derived from the distribution of magnetic anomalies as well as the topographic features provides the evolutionary history of the Shikoku Basin in the following manner:

- 1) The Kyushu-Palau and Shichito-Iwojima Ridges began rifting at their northern end at about 30 mybp. The rifting propagated towards south at a speed of about 10 cm/year.
- 2) After the whole basin was rifted at about 25 mybp, it continued to open symmetrically from the central spreading axis at a half rate of nearly 4 cm/year until about 22 mybp.
- 3) In the latest stage of opening the spreading became slower and even irregular. The spreading axis jumped in some parts of the basin. A chain of seamounts was formed and widespread off-ridge intrusions occurred in the eastern portion of the basin.

1. Introduction

The Shikoku Basin south off the Island of Shikoku, southwestern Japan is one of the most typical inter-arc basins ever recognized in the world ocean. It is bordered by the N-S trending Shichito-Iwojima Ridge (active island arc) on the east and by the NWN-SES trending Kyushu-Palau Ridge (remnant arc) on the west. Its northern boundary is the Nankai Trough at which floor of the basin sinks under the Shikoku continental crust (Fig. 1).

The crust of the Shikoku Basin is oceanic in its seismological structure (MURAUCHI *et al.*, 1968) and characterized by existence of linear magnetic anomalies trending nearly parallel to those of the marginal ridges, as first pointed out by TOMODA *et al.* (1968, 1975). WATTS and WEISSEL (1975) postulated a correlation of these magnetic anomalies and discussed a tectonic history of this basin. KOBAYASHI and ISEZAKI (1976) summarized geophysical and geological data available at that time and proposed a model of evolution of the inter-arc basins. However, some problems remained unsolved mostly because of lack of very detailed survey in this area of the sea.

Under the aegis of the Geodynamics Project of Japan the total magnetic forces and water depths in the Shikoku Basin have been extensively measured together with seismic reflection profiling along more than twenty parallel tracks crossing the basin roughly vertical to its axis with spacings of 5 to 10 nautical miles. KOBAYASHI and NAKADA (1977)

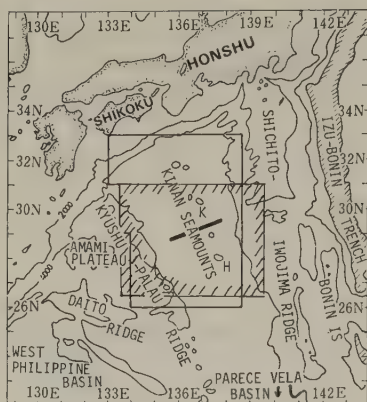


Fig. 1. Index map of the surveyed area. Contours are 2,000 and 4,000 m, based upon bathymetric chart 6302 prepared by Hydrographic Department, Maritime Safety Agency of Japan. Square denotes area for which magnetic anomaly profiles are compiled (Fig. 4). Shaded zone indicates area for detailed bathymetric map reproduced in Fig. 2. Solid line indicates a track for seismic reflection profiling shown in Fig. 3. H, Hakuho Seamount; K, Daini-Kinan Seamount.

published a map of magnetic anomaly profiles of this basin using these results along with available data previously collected by other cruises. All tracks surveyed after 1972 were controlled by the satellite navigation fixes and the accuracy of position is usually better than 1 nautical mile. Detailed bathymetric maps were also drawn with results of these cruises. The basin between 27°N and 33°N in latitude was particularly well surveyed.

In this article we will present an identification of magnetic anomalies based upon these newly obtained results. Magnetic structure of the eastern part of the basin, particularly around the Kinan Seamount Chain can be properly understood with our detailed magnetic and bathymetric maps. Some tectonic implications of the results to the evolutionary history of the Shikoku Basin are then postulated.

2. Topographic Features of the Shikoku Basin

Figure 2 represents a topographic map of the basin between $27^{\circ}40'\text{N}$ and $30^{\circ}40'\text{N}$ which was contoured by ourselves using bathymetric data along the ships' tracks the same as used for magnetic analysis. Addition of other results would not substantially change the topography of the basin, as density of the data used for this mapping is sufficiently high. In contrast topography of the Kyushu-Palau and Shichito-Iwojima Ridges in this map is only provisional and should be greatly modified by more detailed survey and collection of additional reliable information.

General topography of this basin clearly indicates a lineated feature trending nearly parallel to the trend of the Kyushu-Palau Ridge. Parallel ridge and trough sequences are distinctly recognized in the basin having an average water depth of about 4,500 m. Maximum water depth of troughs exceeds 5,500 m, while the crests of ridges are shallower than 4,000 m. It is thus implied that this basin was formed under an extensional stress perpendicular to its linear trend, as postulated by KARIG (1971a, b) with the Parece Vela Basin and the Mariana Trough.

Distribution of sediments revealed by seismic reflection profiling along the same survey tracks has been published by MURAUCHI and ASANUMA (1977). Thickness of sediment cover decreases towards the south and generally amounts to 300 to 500 m in the central zone of the basin except for small sediment ponds. There exist thick sediment wedges on both margins of the basin. A multichannel seismic profile between $29^{\circ}29'\text{N}$,

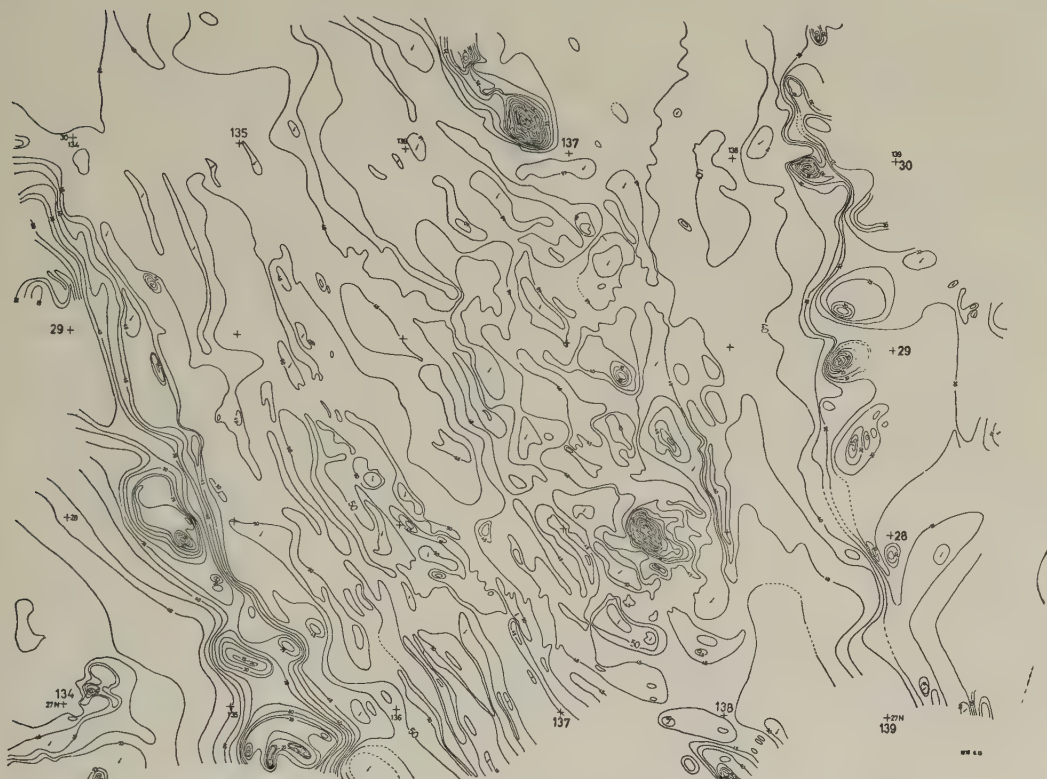


Fig. 2. A detailed topography of the Shikoku Basin between 27°40'N and 30°40'N. Contour interval: 2,500 m.

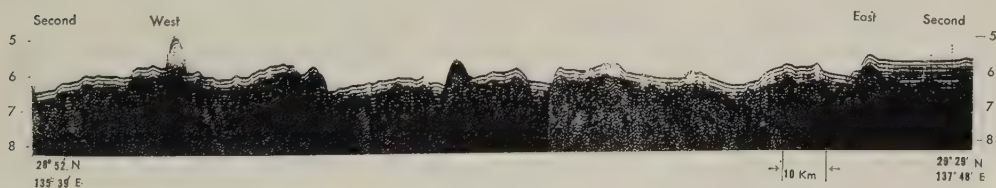


Fig. 3. Seismic reflection profile of the Shikoku Basin nearly perpendicular to the basin axis. Survey by Kaiyo-Maru of the Japan Petroleum Exploration Co., Ltd. (IPOD-JAPAN, 1977). Unprocessed record.

137°49'E and 28°52'N, 135°40'E (IPOD-JAPAN, 1977) shows that the sediment structure in the central zone of the basin is generally concordant with the morphology of acoustic basement so that study of bottom topography alone would reveal tectonic patterns of the basin formation. No evidence of the present tectonic activity of the basin is seen in the profile (Fig. 3), although apparently deformed sediment reflectors in the lower levels of layer one above the acoustic basement may possibly indicate some tectonic movement after the formation of the basin.

A chain of seamounts called the Kinan Seamount Chain occurs in the eastern part of the central zone in the basin, as seen in Fig. 2 and other topographic maps. Some of the

KAZUO KOBAYASHI AND MASAO NAKADA,
Ocean Research Institute
University of Tokyo
1977

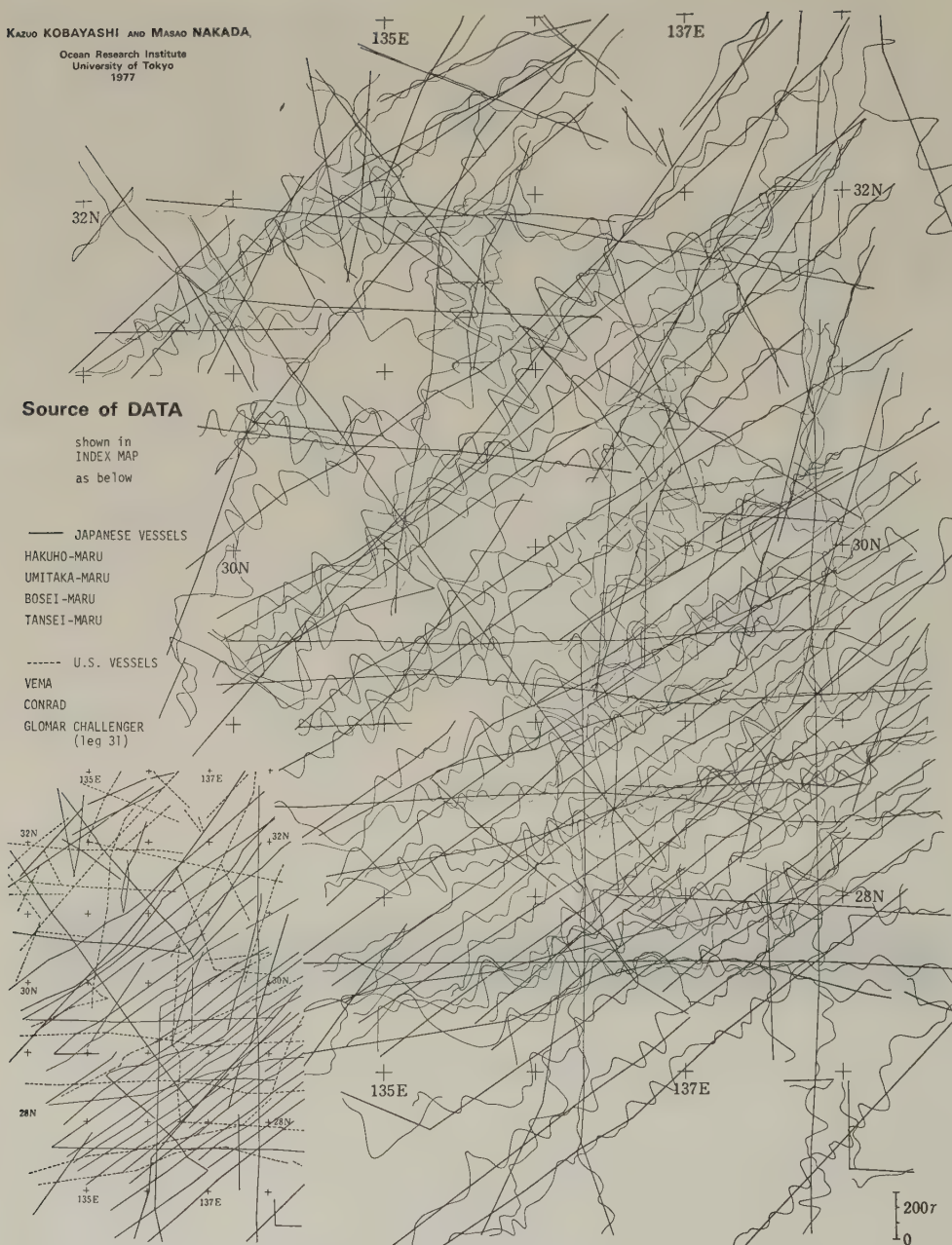


Fig. 4. Magnetic anomaly profiles in the Shikoku Basin used for the present analysis (Kobayashi and Nakada, 1977).

seamounts, for example, one located at $30^{\circ}15'N$, $136^{\circ}40'E$: Daini-Kinan Seamount and one at $28^{\circ}00'N$, $137^{\circ}40'E$: Hakuho Seamount (tentative name) are as large as those occurring in the Mid-Pacific seamount region. Apparently the seamounts in the Shikoku Basin compose a chain roughly parallel to the trend of the basin but the topographic highs are not so continuous as those in the mid-oceanic ridges. Each seamount is separated from the adjacent ones by deep moats to form segmented alignment of topographic highs. Their crests are not located on the geometric axis of symmetry of the basin but are appreciably off-centered towards the eastern margin.

A large boulder of pillow basalt was collected by dredge haul from the crestral area of the Hakuho Seamount. Chemical and mineralogical composition of the rock indicates that it is quite similar to that of the abyssal tholeiites (TOKUYAMA and FUJIOKA, 1976) and different from rocks derived from hot spots and island-arc volcanoes. The origin of the Kinan Seamount Chain should therefore be explained as a specific stage of seafloor spreading in the Shikoku Basin. Fossils of nannoplankton contained in the ferromanganese coating and vesicles of the rock sample have been identified to be of late Middle Miocene (12–14 mybp), which provides the minimum age limit of eruptions at the Hakuho Seamount (Uchio, private communication).

3. Magnetic Lineations

Our magnetic analysis wholly relies upon a recently published 1/1,000,000 map of magnetic anomaly profiles of the Shikoku Basin (KOBAYASHI and NAKADA, 1977, Fig. 4). As the spacing of two adjacent profiles is generally less than 10 nautical miles which is much shorter than wavelengths of the local magnetic anomalies, profile to profile correlation of magnetic anomalies can convincingly be done.

Figure 5 shows six selected profiles of anomalies projected on a line perpendicular to the trend of the basin. Their correlation with a model profile simulated using standard polarity time scale (BLAKELY, 1974; LABRECQUE *et al.*, 1977) between 18.5 and 27 mybp is also shown on an assumption of two-limb symmetric spreading. Correlation is generally satisfactory. Characteristic shapes of anomaly 6, 6A and 6B can be identified on both sides of the basin.

In the southwestern portion of the surveyed area the lineation pattern and age identification proposed by WATTS and WEISSEL (1975) seem to be the most acceptable. In

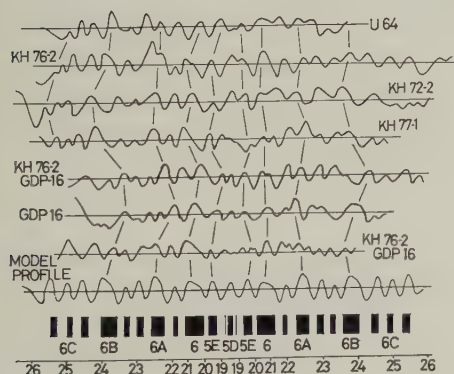


Fig. 5. Selected profiles of magnetic anomalies and their correlation with a model profile. Profiles are projected at azimuth of 62° . Magnetic layer is assumed in depths between 5 and 7 km. Magnetic time scale and anomaly numbers are according to HEIRTZLER *et al.* (1968), BLAKELY (1974) and LABRECQUE *et al.* (1977).

this article we further extended it towards north with additional data. No fracture zones offsetting these lineations can be recognized. Magnetic anomalies in the eastern portion of the basin are somewhat irregular but still correlatable in the areas where magnetic observations on sufficiently close survey tracks are available. Correlation of anomalies without offsets seems to be also possible in this zone.

The most complex is the east-central zone surrounding a chain of seamounts and associated moats. In addition to localized magnetic anomalies caused by topography of seamounts, magnetic lineations seem to be disrupted in some places in this zone. A detailed survey was carried out in a $1^{\circ} \times 1^{\circ}$ rectangular area surrounding the Hakuho Seamount. A couple of positive and negative circular anomalies is superimposed on the linear magnetic anomalies around the crest of the seamount. If this couple of positive and negative anomaly circles is due to magnetization of the seamount, overall direction of magnetization of this seamount is reversed with moderate inclination. The reversed polarity of rock is quite likely to occur because the crest of seamount is situated in a linear strip of negative magnetic anomaly.

Correlation of adjacent linear anomalies appears to be still possible, if the survey is so much in detail. Magnetic lineations in an area surrounding the seamount are segmented by right-lateral faults trending NE-SW. Amount of offset is about 20 to 30 km. The same size of offset can be found in the basement topography near the seamount. It must be noted that neither magnetic nor topographic offset is extended to the marginal zones of the basin. The faults are truncated at the boundaries between the central zone and both margins defined by linear anomalies.

Figure 6 represents aerial distribution of magnetic isochrons in the Shikoku Basin thus postulated. This pattern differs from the previously proposed ones in a point that

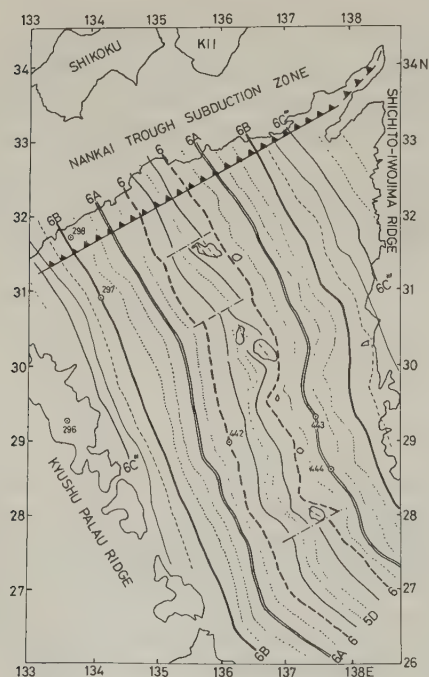


Fig. 6. Magnetic isochrons in the Shikoku Basin.

the fractures are existent only in the central zone. Anomalies on both margins can be smoothly correlated and seem to be symmetric in respect to the geographic axis of symmetry of this basin, as far as the proposed identification of anomaly is valid. T.-C. Shih postulated similar patterns of fracture zones (private communication, 1977), although his identification of anomalies is different from that proposed here.

According to the present identification of anomalies anomaly 6' (approximately 22 mybp) is the boundary between undisrupted margins and fractured center. In the fractured center anomalies are hardly identifiable and appear to be asymmetric. Assuming that there existed no hiatus in opening of the basin, the youngest isochron may be anomaly 5D (17 mybp) or 5C (16 mybp). Presumed axis of symmetry for these anomalies is, in some parts, off-centered from the geometrical axis of the basin. Tectonic significance of this catastrophic jump of spreading axis in the inter-arc basin will be discussed in a later section of this paper.

In both margins of the Shikoku Basin anomalies 7 to 6C pinch out in succession from north to south, as WATTS and WEISSEL (1975) pointed out with the western margin only. We confirmed that the same configuration of anomalies occur in the eastern margin as well. Such a pattern of anomalies indicates that the basin began opening at its northern end and the rifting propagated longitudinally from north to south with a rate of approximately 10 cm/year.

Except for these margins and fractured center, rate of spreading are quite uniform on both sides of the axis. Distances of identifiable anomalies from the geometrical axis of the basin versus magnetic ages of anomalies are shown in Fig. 7. Half spreading rates are 4 to 6 cm/year between 26 and 22 mybp and decrease to about a half (2–3 cm/year)

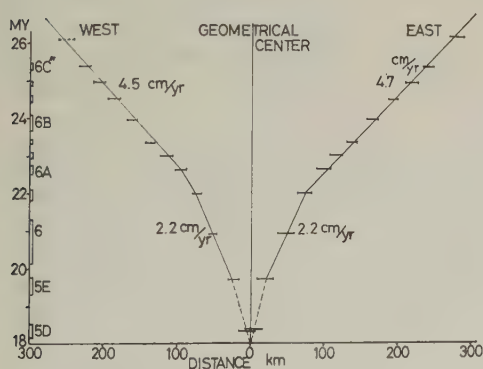


Fig. 7. Magnetic ages versus distance from the geometrical axis of the basin.

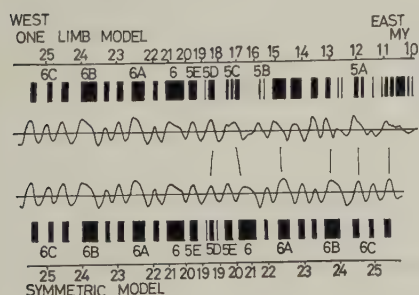


Fig. 8. Comparison of the symmetric spreading model with the one-limb opening model.

in the later stage. Rates after 18 mybp (anomaly 5E) seem to be variable with time and space.

Spreading rates in the southern portion (around 27°N) are nearly equal to those in the northern part of the basin within a statistical fluctuation. This result indicates that separation of two ridges is essentially a parallel movement relative to each other. On a sphere such a motion is equivalent to a rotation around a pole 90 degree far from the sites.

4. *Alternative Models for Opening of the Shikoku Basin*

WATTS and WEISSEL (1975) once postulated a one-limb spreading model to explain the magnetic lineations in the Shikoku Basin. Simulated anomalies based upon the one-limb model are reproduced and compared with those calculated from the present model in Fig. 8. Apparently correlation of simulated anomalies with observed ones appears to be also good in one-limb model, since the pattern of magnetic reversals between 18 and 11 mybp is, just by chance, similar to the mirror image of the reversal pattern occurring between 26 and 18 mybp. It is hard to judge which model is better fitted to the observed pattern by anomalies alone.

Paleontological age of the lowest recovered sediments obtained at the DSDP site 442, leg 58 (21 my) is quite consistent with the present models, regardless whether the spreading is symmetric or one-limbed, since the site is located in the western part of the basin (DSDP SCIENTIFIC STAFF, LEG 58, 1978; KLEIN *et al.*, 1978). On the contrary age of sediments above the acoustic basement at DSDP sites 443 and 444 are 14 to 17 mybp which is apparently discrepant with magnetic ages of the symmetric model. It appears to be agreeable with the one-limb model age. However, the recovered sediments are only those above intrusive sills at the latter two sites and cannot provide the spreading ages. At site 442 sediments interbedded between sills and pillow basalts were collected and supplied for the paleontological dating which showed 3 to 5 my time difference between sediments above the pillow basalts and intrusive sills.

Major difficulties of the one-limb model are: (1) Axial zone with irregular anomalies and rugged topography cannot be reasonably explained; (2) A rectangular area in the northeastern corner cannot be regarded as a rifting wedge, which could be interpreted in the symmetric model as described above. The basement ages of DSDP sites 449 and 450 drilled on the western and eastern parts of the Parece Vela Basin indicated validity of the symmetric spreading model (DSDP SCIENTIFIC STAFF, LEG 59, 1978). Ages of sites 53 and 54 located on the eastern part of the basin are also consistent with the spreading of the Parece Vela Basin in harmony with the opening of the Shikoku Basin. It is therefore the most reasonable to assume that the opening of the Shikoku Basin was symmetric and synchronous with the Parece Vela Basin situated in its southern extension.

Some other models of spreading may be possible if we assume asymmetric opening but they will be disregarded hereafter because of this reasoning.

5. *Evolutionary History of the Basin and Its Tectonic Implications*

Age identification of magnetic anomalies as shown in Fig. 6 indicates that the Shikoku Basin opened through three different stages; (1) rifting between the Kyushu-Palau and Shichito-Iwojima Ridges, (2) parallel spreading of the Shikoku Basin, (3) more irregular opening, formation of seamounts and post-spreading intrusion.

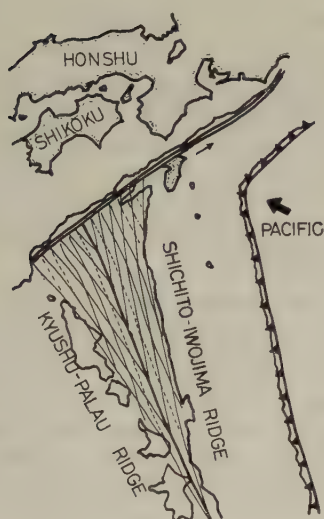


Fig. 9. Schematic illustration of propagation of rifting in the Shikoku Basin in a shape of a wedge front.

Rifting began at approximately 30 mybp from the northern boundary of the ridges at which the present Nankai Trough subduction zone intersects with the ridges and the basin. The rifting propagated towards south in a shape like a wedge front (Fig. 9). Such a shape of the rigid matters is unstable, as an infinite stress may be concentrated at the acute-angle wedge to cause propagation of rifting. The anomaly ages show the speed of southward propagation was approximately 10 cm/year. Similar growth of rifting in the initial stage of break-up of plate has been postulated with the South Atlantic (WRIGHT, 1968; BURKE, 1976), the Gulf of Aden (McKENZIE *et al.*, 1970) and the African Rift Valley (MAASHA and MOLNAR, 1972).

At about 25 mybp the rifting reached a latitude of 25°N . The Parece Vela Basin was very likely to start rifting from its south end, although no distinct magnetic evidence is available there due to low latitude of the basin. The rifting of both basins got together probably around 25°N .

It must be noted here that the rifting of the Shikoku Basin (and possibly the Parece Vela Basin as well) began about 10 my after the Pacific plate changed its direction of motion. Prior to 42 mybp the Pacific plate moved northwards in a direction nearly parallel to the trend of the Kyushu-Palau, Shichito-Iwojima Ridges so that no subduction occurred along the ridges. Great amount of subduction possibly proceeded along the southwestern Japan and caused opening of the Japan back-arc basin in this stage of plate motion.

After the Kyushu-Palau and Shichito-Iwojima Ridges were completely rifted, two ridges were separated further by parallel spreading of the Shikoku Basin. Rate of opening was nearly 4 cm/year (half rate) which is intermediate between that of the East Pacific Rise and that of the Mid-Atlantic and Mid-Indian Ridges. The spreading axis was not offset by transform faults but linear and continuous. Magnetic lineations formed in this stage are symmetric and most recognizable.

Spreading became more irregular at about 22 mybp (magnetic anomaly 6'). Spreading rate decreased to nearly a half of the previous value. Because magnetic anomalies are generally disrupted in this zone, it is rather difficult to identify their ages. Neverthe-

less, offsets of magnetic lineations are clearly recognized. If the spreading is still symmetric, equivalent amount of offsets of the accreting axis associated with transform faults should be assumed. Such a transition of axis configuration implies a jump of spreading axis at about 22 mybp. Similar discontinuous jumps of spreading center have been suggested with the northeastern Pacific (HARRISON and SCLATER, 1972; SHIH and MOLNAR, 1975), the east-central Pacific (ANDERSON and SCLATER, 1972; HERRON, 1972; HANDSCHUMACHER, 1976), Galapagos area (HEY and VOGT, 1977) and the Atlantic north of Iceland (JOHNSON and HEEZEN, 1967; VOGT *et al.*, 1970). Local migration of spreading center has also been postulated (BLAKELY, 1975).

It seems reasonable to assume the second jump of the spreading axis in the Shikoku Basin to cause seamounts and moats in the central zone. Detailed examination of topography indicates that the seamounts and moats were formed under an extensional stress perpendicular to the trend of the basin in a similar manner to the formation of general microtopography of the basin. Origin of the seamount chain is, therefore, closely related to spreading of the basin rather than to hot spots or orogenic activity. A lack of the mirror images of the seamount topography in the western side of the basin indicates that the spreading axis producing the seamount chain should have existed on the seamounts themselves in the latest stage of spreading.

It is very likely that such jumps and the irregular behavior of spreading axis have caused complex stress in the older rigid oceanic lithosphere, particularly in the trenchward (eastern) side of the basin. At some spots where stress was extraordinarily concentrated, local cracks may have been generated to cause intrusions of magma forming sheets or sills. Sites 442, 443 and 444 of DSDP Leg 58 in the Shikoku Basin revealed occurrence of many post-spreading intrusions at periods (14 to 17 mybp) slightly after the spreading ceased (KLEIN *et al.*, 1978). The result of drilling appears to be quite consistent with the present explanation of the evolutionary history of the basin.

Magnetization of the post-spreading intrusives takes a part as a noise in the observed magnetic anomalies. Thermal and chemical influence of the intrusive rocks on the previously seated materials may also disturb the original magnetic lineations recorded in the regularly accreted oceanic crust. Less remarkable linearity in the eastern portion of the Shikoku Basin can be explained by greater degree of off-ridge activity compared to the normal ocean and the western part of this basin.

Sudden decrease in spreading rate and abnormal behavior of the accreting axis in the late stage of opening in the Shikoku Basin may possibly be attributable to the distance of the axis too far from the down-going slab which supplies magma and heat to the spreading axis. At 22 mybp the geometrical axis of the basin was situated at a distance of about 500 km from the trench. If the subduction angle was 45° as observed with usual subduction zone such as the Japan and Kuril trenches, the upper surface of sinking lithosphere was 500 km deep beneath the spreading axis. Distances exceeding this amount may be too large to supply magma and heat unless a special channel of magma or heat conduit exists.

In the Mariana Trough the pattern of spreading appears to be more irregular than in the Shikoku Basin or other similar inter-arc basins throughout the whole basin of the "trough," although it is young and may be still opening (KARIG *et al.*, 1978). Difference between the Mariana Trough and the Shikoku Basin is that the subduction angle along the Mariana Trough is very steep and its accreting axis is already far from the source of magma and heat.

REFERENCES

- ANDERSON, R.N. and J.G. SCLATER, Topography and evolution of the East Pacific Rise between 5°S and 20°S, *Earth Planet. Sci. Lett.*, **14**, 433–441, 1972.
- BLAKELY, R.J., Geomagnetic reversals and crustal spreading rates during the Miocene, *J. Geophys. Res.*, **79**, 2979–2985, 1974.
- BLAKELY, R.J., Evidence of local migration of a spreading center, *Geology*, **3**, 35–38, 1975.
- BURKE, K., Development of graben associated with the initial ruptures of the Atlantic Ocean, *Tectonophysics*, **36**, 93–112, 1976.
- DSDP SCIENTIFIC STAFF, LEG 58, Philippine Sea drilled, *Geotimes*, **23** (5), 23–25, 1978.
- DSDP SCIENTIFIC STAFF, LEG 59, In the Philippine Sea, questions answered, *Geotimes*, **23** (7), 20–23, 1978.
- HANDSCHUMACHER, D.W., Post-Eocene plate tectonics of the Eastern Pacific, in *The Geophysics of the Pacific Ocean Basin and Its Margins*, Geophys. Monogr. No. 19, pp. 177–202, Am. Geophys. Union, Washington, D.C., 1976.
- HARRISON, C.G.A. and J.G. SCLATER, Origin of the disturbed magnetic zone between the Murray and Molokai fracture zones, *Earth Planet. Sci. Lett.*, **14**, 419–427, 1972.
- HEIRTZLER, J.R., G.O. DICKSON, E.M. HERRON, W.C. PITMAN, III, and X. LEPICHON, Marine magnetic anomalies, geomagnetic field reversals and motions of ocean floor and continents, *J. Geophys. Res.*, **73**, 2119–2136, 1968.
- HERRON, E.M., Sea-floor spreading and the Cenozoic history of the east-central Pacific, *Geol. Soc. Am. Bull.*, **83**, 1671–1692, 1972.
- HEY, R. and P.R. VOGT, Spreading center jumps and sub-axial asthenosphere flow near the Galapagos hot-spot, *Tectonophysics*, **37**, 41–52, 1977.
- IPOD-JAPAN, Multichannel seismic reflection data across the Shikoku Basin and the Daito Ridges, 1976 (Part 1), in *IPOD-Japan Basic Data Series*, No. 1, 17pp., Ocean Resarch Inst., Univ. Tokyo, 1977.
- JOHNSON, G.L. and B.C. HEEZEN, The morphology and evaluation of the Norwegian-Greenland Sea, *Deep-Sea Res.*, **14**, 755–771, 1967.
- KARIG, D.E., Structural history of the Mariana island arc system, *Geol. Soc. Am. Bull.*, **82**, 323–344, 1971a.
- KARIG, D.E., Origin and development of marginal basins in the Western Pacific, *J. Geophys. Res.*, **76**, 2542–2561, 1971b.
- KARIG, D.E., R.N. ANDERSON, and L.D. BIBEE, Characteristics of back arc spreading in the Mariana Trough, *J. Geophys. Res.*, **83**, 1213–1225, 1978.
- KLEIN, G.D., K. KOBAYASHI, H. CHAMLEY, D.M. CURTIS, H.J.B. DICK, D.J. ECHOLS, D.M. FOUNTAIN, H. KINOSHITA, N.G. MARSH, A. MIZUNO, G.V. NISTERENKO, H. OKADA, J.R. SLOAN, D.M. WAPLES, and S.M. WHITE, Off-ridge volcanism and seafloor spreading in the Shikoku Basin, *Nature*, **273**, 746–748, 1978.
- KOBAYASHI, K. and N. ISEZAKI, Magnetic anomalies in the Sea of Japan and the Shikoku Basin: Possible tectonic implications, in *The Geophysics of the Pacific Ocean Basin and Its Margins*, Geophys. Monogr. No. 19, pp. 235–251, Am. Geophys. Union, Washington, D.C., 1976.
- KOBAYASHI, K. and M. NAKADA, Local magnetic anomaly profiles, Shikoku Basin, Northwestern Pacific Ocean, *Contr. Geodyn. Proj. Japan*, 77–2, 1977.
- LABRECQUE, J.L., D.V. KENT, and S.C. CANDE, Revised magnetic polarity time scale for Late Cretaceous and Cenozoic time, *Geology*, **5**, 330–335, 1977.
- MAASHA, N. and P. MOLNAR, Earthquake fault parameters and tectonics in Africa, *J. Geophys. Res.*, **77**, 5731–5743, 1972.
- MCKENZIE, D.P., D. DAVIES, and P. MOLNAR, Plate tectonics of the Red Sea and East Africa, *Nature*, **226**, 243–245, 1970.
- MURAUCHI, S. and T. ASANUMA, *Seismic Reflection Profiles in the Western Pacific, 1965–74*, 232 pp., University of Tokyo press, Tokyo, 1977.
- MURAUCHI, S., N. DEN, S. ASANO, H. HOTTA, T. YOSHII, T. ASANUMA, K. HAGIWARA, K. ICHIKAWA, T. SATO, W.J. LUDWIG, J. EWING, N.T. EDGAR, and R.E. HOUTZ, Crustal structure of the Philippine Sea, *J. Geophys. Res.*, **73**, 3143–3171, 1968.
- SHIH, J. and P.T. MOLNAR, Analysis and implications of the sequence of ridge jumps that eliminated the Surveyor transform fault, *J. Geophys. Res.*, **80**, 4815–4822, 1975.
- TOKUYAMA, E. and K. FUJIOKA, The petrologic study on basalt from Kinan Seamount and DSDP site 54, *Mar. Sci. Month.*, **8**, 184–191, 1976 (in Japanese with English abstract).
- TOMODA, Y., K. OZAWA, and J. SEGAWA, Measurement of gravity and magnetic force on board a cruising vessel, *Bull. Ocean Res. Inst., Univ. Tokyo*, **3**, 1–70, 1968.

- TOMODA, Y., K. KOBAYASHI, J. SEGAWA, M. NOMURA, K. KIMURA, and T. SAKI, Linear magnetic anomalies in the Shikoku Basin, northwestern Philippine Sea, *J. Geomag. Geoelectr.*, **28**, 47-56, 1975.
- VOGT, P.R., N.A. OSTENSO, and G.L. JOHNSON, Magnetic and bathymetric data bearing on sea floor spreading north of Iceland, *J. Geophys. Res.*, **75**, 903-920, 1970.
- WATTS, A.B. and J.K. WEISSEL, Tectonic history of the Shikoku marginal basin, *Earth Planet. Sci. Lett.*, **25**, 239-250, 1975.
- WRIGHT, J.B., South Atlantic continental drift and the Benue trough, *Tectonophysics*, **6**, 301-316, 1968.

A COMPILATION OF MAGNETIC DATA IN THE NORTHWESTERN PACIFIC AND IN THE NORTH PHILIPPINE SEA

Nobuhiro ISEZAKI* and Hiroyuki MIKI**

*Department of Earth Sciences, Faculty of Science, and

**Graduate School, Kobe University, Kobe, Japan

(Received June 10, 1978; Revised September 22, 1978)

Magnetic data obtained during the period of the Geodynamics Project by various institutions are compiled and a new distribution map of magnetic anomaly lineations is proposed for the northwestern Pacific Basin and in the north Philippine Sea.

1. *Magnetic Anomaly Lineations in the Northwestern Pacific Basin*

Magnetic anomaly lineations in the northwestern Pacific Basin were reported by UYEDA *et al.* (1967), LARSON and CHASE (1972), ISEZAKI (1973) and HILDE *et al.* (1976). We have recompiled these existing magnetic data with those obtained during the Japanese Geodynamics Project as shown Figs. 1 and 2. Some features of the magnetic lineations shown in Fig. 2 are apparently different from those by HILDE *et al.* (1976) which are shown in Fig. 3. In the area off the Japan trench (35° – 42° N, 144° – 150° E), the strike of lineations of anomalies M6 to M15 is ENE (oblique to the strike of the Kuril trench) in Fig. 2, while it is almost NE, just parallel to the strike of the Kuril trench in Fig. 3. The three long lineations are recognized parallel to the Kuril trench off the Kuril trench (149° – 158° E) in Fig. 2 but there is none of such lineations in Fig. 3. In the area off the Bonin trench (27° – 32° N, 144° – 152° E), there is the abrupt change of the strike of lineations, that is, ENE in the north of 32° N latitude and NE in the south as shown in Fig. 2 (ISEZAKI, 1976), while in Fig. 3 this feature is very vague. HILDE *et al.* (1976) identified many offsets of lineations and we reexamined these offsets with new available data and came to a conclusion that two offsets in Fig. 3, one whose northern end is at the Kuril trench, 155° E and whose southern end at the Shatzky Rise, 160° E, and the other whose northern end is at the southern end of the Shatzky Rise, 158° E and whose southern end at 26° N, 155° E, do not exist, and the further detail magnetic surveys should be necessary to identify confidently many other offsets in Fig. 3, especially in the area off the Japan trench.

2. *Magnetic Anomaly Lineations in the North Philippine Sea*

Magnetic anomaly lineations in the Shikoku Basin in the northern part of the Philippine Sea, have been studied by TOMODA *et al.* (1975), WATTS and WEISSEL (1975), KOBAYASHI and ISEZAKI (1976) and WATTS *et al.* (1977). We compiled magnetic data obtained during the Geodynamics Project period and obtained one of possible interpretations of lineations as shown in Fig. 4. The characteristic feature of this tentative lineations is that

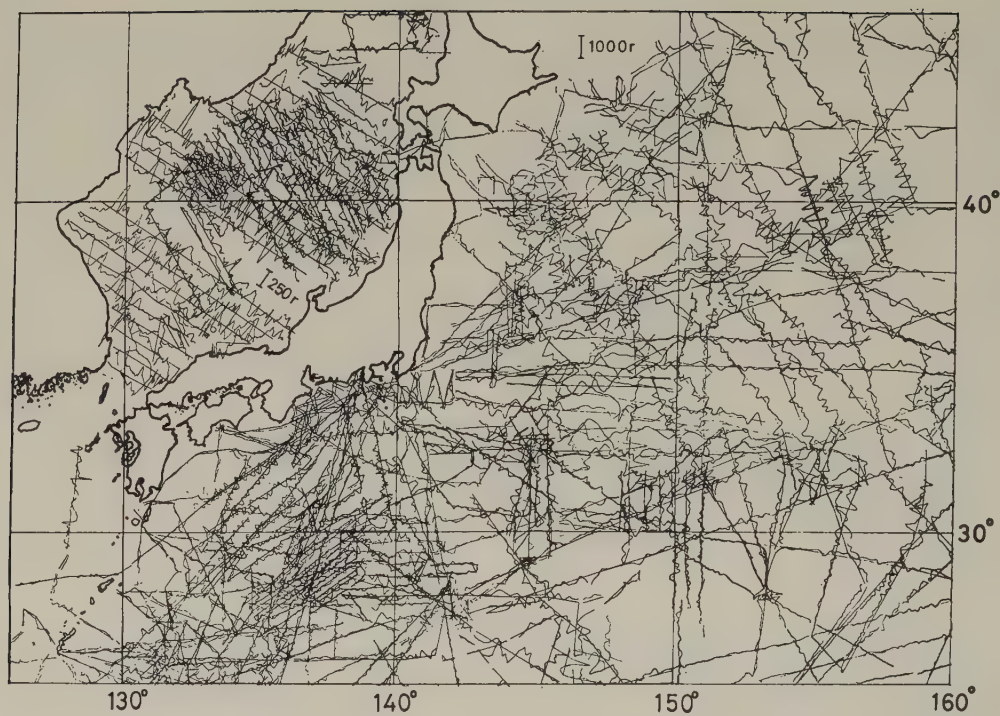


Fig. 1

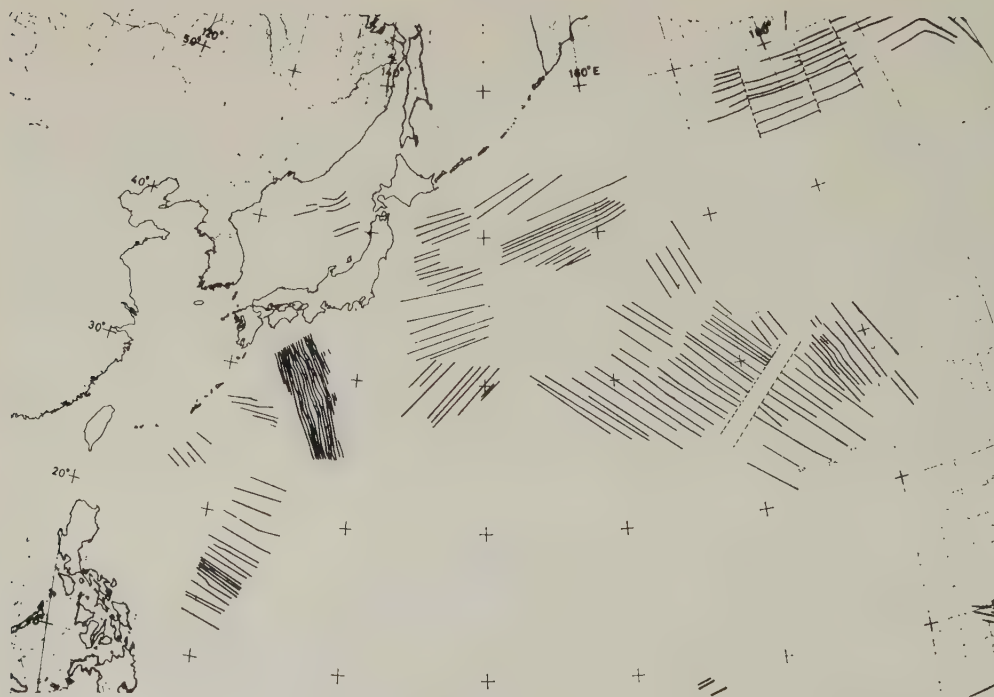


Fig. 2

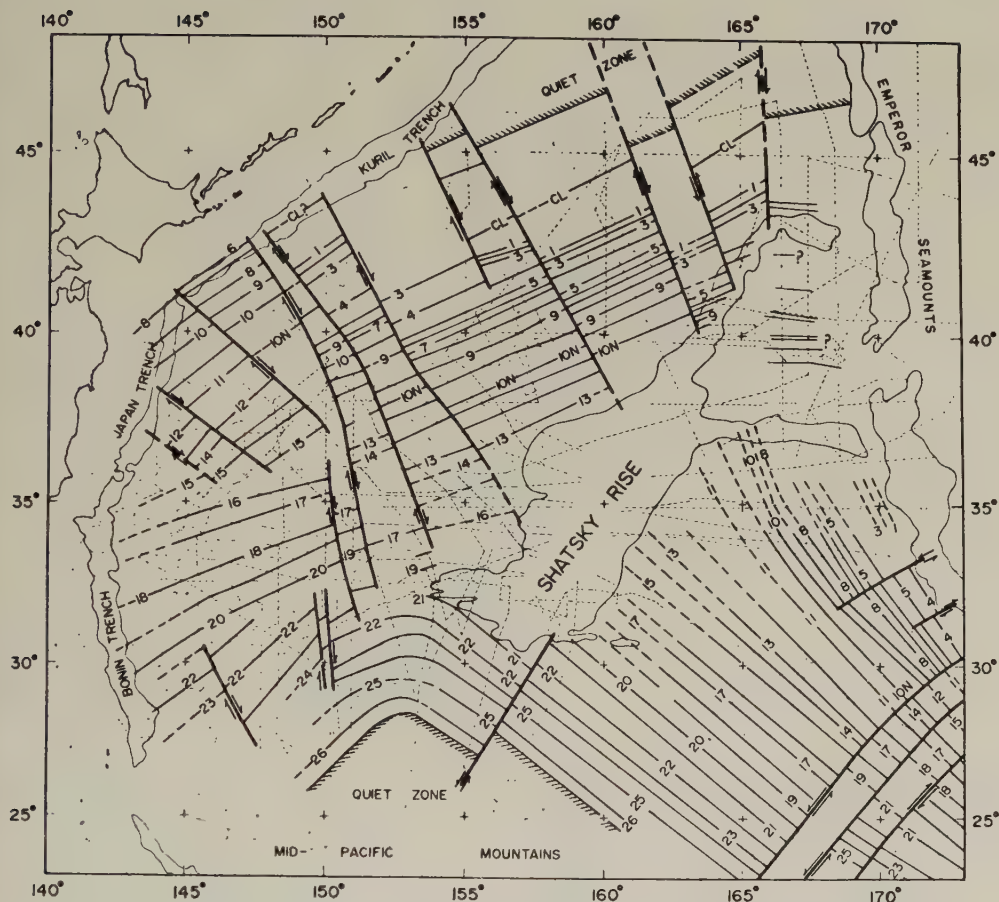


Fig. 3. Geomagnetic total intensity anomaly lineations from HILDE *et al.* (1976).

the lineations have no clear offset and appear to extend further south, at least to 25°N latitude.

We found lineations which run east-west in the area between the Amami plateau and the Daito ridge. Details are shown in Fig. 5.

Fig. 1. Distribution of magnetic data. Magnetic anomaly profiles are projected on the shiptracks. North side is positive. Notice that the scale of the amplitude of anomaly in the Japan Sea is about three times as large as in other seas.

Fig. 2. Geomagnetic total intensity anomaly lineations in the northwestern Pacific basin. Solid lines represent the lineated positive anomalies.

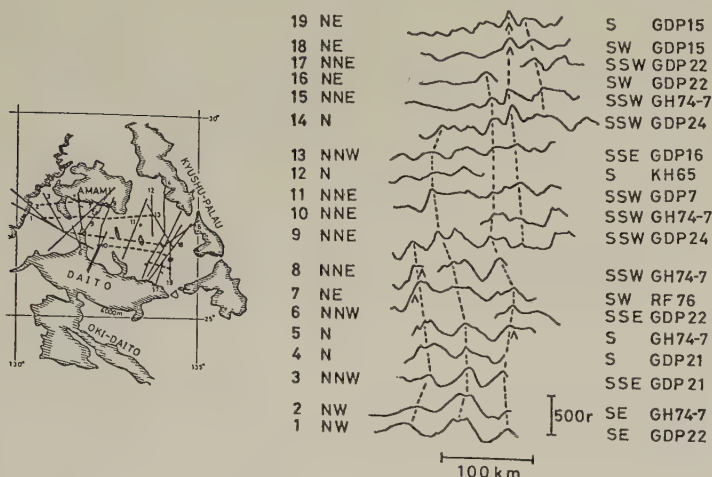


Fig. 5. Geomagnetic total intensity anomaly lineations and profiles in the Amami plateau and the Daito ridge area. The solid lines are track lines and the broken lines represent lineations. Δ indicates a seamount.

A part of this work was done in the Japanese Geodynamics Project when one of authors, N. Isezaki, was at the Meteorological College of Japan Meteorological Agency, and he wishes to express his thanks to Dr. Nozomu Den who was the chief of the working group.

REFERENCES

- HILDE, T.W.C., N. ISEZAKI, and J.M. WAGEMAN, Mesozoic sea-floor spreading in the north Pacific, in *Geophysics of the Pacific Ocean Basin and Its Margin*, Am. Geophys. Union Monogr. No. 19, pp. 205–226, 1976.
- ISEZAKI, N., Geomagnetic anomalies and tectonics around the Japanese Islands, *Oceanogr. Mag.*, **24**, 107–158, 1973.
- ISEZAKI, N., A preliminary report of magnetic surveys in GDP, Geomagnetic anomaly lineations in the area southwest of Shatzky Rise, *Oceanogr. Mag.*, **27**, 37–41, 1976.
- KOBAYASHI, K. and N. ISEZAKI, Magnetic anomalies in the Sea of Japan and the Shikoku Basin; Possible tectonic implications, in *Geophysics of the Pacific Ocean Basin and Its Margin*, Am. Geophys. Union Monogr. No. 19, pp. 235–253, 1976.
- LARSON, R.L. and C.G. CHASE, Late Mesozoic evolution of the western Pacific Ocean, *Geol. Soc. Am. Bull.*, **83**, 3627–3644, 1972.
- TOMODA, Y., K. KOBAYASHI, J. SEGAWA, M. NOMURA, K. KIMURA, and T. SAKI, Linear magnetic anomalies in the Shikoku Basin, northeastern Philippine Sea, *J. Geomag. Geoelectr.*, **28**, 47–56, 1975.
- UYEDA, S., V. VAQUIER, M. YASUI, J. SCLATER, T. SATO, J. LAWSON, T. WATANABE, F. DIXON, E. SILVER, Y. FUKAO, K. SUDO, M. NISHIKAWA, and T. TANAKA, Results of geomagnetic survey during the cruise of R/V Argo in western Pacific 1966 and the compilation of magnetic charts of the same area, *Bull. Earthq. Res. Inst. Univ. Tokyo*, **45**, 799–824, 1967.
- WATTS, A.B. and J.K. WEISSEL, Tectonic history of the Shikoku marginal basin, *Earth Planet. Sci. Lett.*, **25**, 239–250, 1975.
- WATTS, A.B., J.K. WEISSEL, and R.L. LARSON, Sea-floor spreading in marginal basins of the western Pacific, *Tectonophysics*, **37**, 167–181, 1977.

COLLISION OF THE IZU-BONIN ARC WITH CENTRAL HONSHU: CENOZOIC TECTONICS OF THE FOSSA MAGNA, JAPAN

Tokihiko MATSUDA

Earthquake Research Institute, University of Tokyo, Tokyo, Japan

(Received July 17, 1978; Revised September 11, 1978)

The Izu-Bonin arc joins with Honshu at the Fossa Magna where pre-Miocene terrains bend in a cusp form. The Miocene terrains in the region also have a northward-convex structure north of the Izu Peninsula. Moreover, highly compressive deformation, Quaternary strong uplift and anomalous trajectories of crustal stress axes also characterize this region.

These features of central Honshu at the junction are explained well by assuming that a north-south trending plate boundary has been located off central Honshu since the late Cretaceous. The bend of the terrains was formed for the most part in the early Tertiary by buoyant subduction of aseismic ridges lying along the north-south trending transform fault.

The Izu-Bonin arc, which was developed along this transform fault, has been dragged northward by oblique subduction of the Pacific plate and underwent subduction beneath central Honshu during the late Tertiary. In the early Quaternary, the Izu Block (the Izu Peninsula) of the Izu-Bonin arc collided with central Honshu and is pushing it north-northwestward. It is very likely that the triple junction off central Honshu has been located at its present position relative to Honshu since the late Mesozoic.

1. Introduction

The main geologic terrains of the Japanese Islands bend sharply to form a cusp at the Fossa Magna, central Honshu, where the Izu-Bonin arc joins with it. KOBAYASHI (1941, p. 429) explained the Cretaceous deformation of Honshu at this bend by a difference of resistance or a subaqueous obstacle lying in front of Honshu shifting oceanward at that time. EHARA (1953) ascribed the bend to a north-northwestward pushing of his "Shichito Batholith" against central Honshu since the Miocene. These earlier ideas have been followed by recent analyses from the plate tectonic viewpoint. Uyeda (MATSUDA and UYEDA, 1971) considered the curved Tertiary structure in the South Fossa Magna as a result of pushing of the Izu-Bonin arc. SUGIMURA (1972) delineated the northeastern boundary of the Philippine Sea plate inland north of the Izu Peninsula, in which the northward shift of the Izu Peninsula was estimated at 10–30 km during the past 0.3–0.5 my. KAIZUKA (1975) interpreted the geomorphological features in the region as an effect of northward shift of the Izu-Bonin arc by dragging of the Pacific plate and proposed a narrow plate, "the Izu Inner Bar" moving to the north relative to the Philippine Sea floor. As for the pre-Miocene bending of Honshu, MATSUDA (1976, 1977) attributed it to the buoyant subduction of aseismic ridges beneath central Honshu in the early Tertiary.

This paper outlines the geologic history and structure of the region and attempts to interpret them in terms of the plate tectonic evolution around Japan.

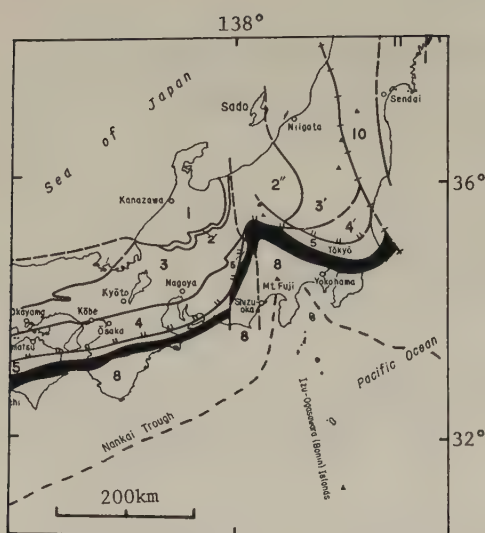


Fig. 1. Central Honshu showing the bend of pre-Miocene terrains (after YOSHIDA, 1975). Solid belt indicates Chichibu belt and Sambosan belt of Paleozoic to early Mesozoic age.

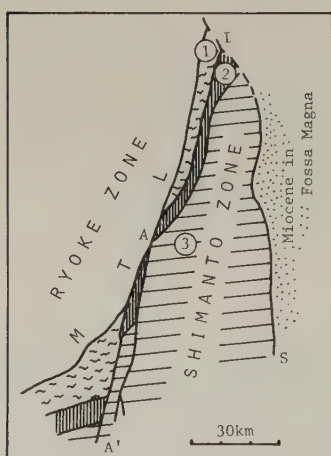


Fig. 2. Left-lateral offset along the Akaishi Tectonic Line (A-A') west of the Akaishi Mountains (after MATSUSHIMA, 1973). For location, see Fig. 4. ①, Sanbagawa zone (Paleozoic); ②, Chichibu zone (Paleozoic to early Mesozoic); ③, Shimanto zone (Cretaceous to early Tertiary); M.T.L., Median Tectonic Line; I-S, Itoigawa-Shizuoka Tectonic Line.

2. Pre-Miocene Bending of Central Honshu

As shown in Fig. 1, pre-Miocene terrains are sharply convex northward in central Honshu. It has been known that the bend structure is associated with a left-lateral fault on its western wing. The left-lateral fault trending north-south to the west of the Akaishi Mountains, called the Akaishi Tectonic Line, offsets the Cretaceous-Paleogene Shimanto and the older terrains about 60 km (KIMURA, 1961; MATSUSHIMA, 1973) as shown in Fig. 2. Since Miocene rocks have not been subjected to significant offset by this fault, the faulting took place mainly before the Miocene. The right-lateral fault trending NW-SE northeast of the Kanto Mountains, called the Kanto Tectonic Line, was postulated to account for more than 100 km of offset of pre-Miocene terrains between the Kanto Mountains and northern Japan (KOBAYASHI, 1941). This tectonic line, or the Kashiwazaki-

Choshi Tectonic Line (Fig. 4) proposed by YAMASHITA (1970), shows no evidence of faulting in the Miocene and later times.

Although the early phase of the bending may have occurred in the Late Mesozoic or Middle Mesozoic (KOBAYASHI, 1941; HAYAMA and YAMADA, 1973; MATSUSHIMA, 1973; HARA and HIDE, 1974), the left-lateral and right-lateral faulting mentioned above imply a contemporaneous northward movement of a block between the two tectonic lines in the early Tertiary, resulting in bending of the terrains. This bending would have been associated with bending of the subduction zone which then existed along the South coast of Honshu. Buoyant subduction proposed by VOGT (1973) seems to be able to explain the bending of the subduction zone and adjacent continental crust.

3. Miocene Subsidence and Metamorphism in the South Fossa Magna

A Miocene sedimentary zone (the South Fossa Magna) lies on the ocean side of the Shimanto zone, where marine volcanic and clastic sediments more than 10 km thick were deposited probably on the ocean floor. These rocks in the South Fossa Magna, together with rocks of the Shimanto zone, have been strongly folded, partly overturned, and thrust-faulted to form west- or north-dipping imbricate structures. In this region, the degree of deformation for Miocene rocks is the highest among the provinces of Japan (MATSUDA *et al.*, 1967). The trend of depositional troughs in this zone and their deformational trend are subparallel or slightly oblique to those of the Shimanto zone and form a northward convex arc around the Izu Peninsula (Fig. 3). One of the most remarkable sedimentary troughs closest to the Izu Peninsula (the Ashigara belt of subsidence) extends to the present Suruga trough to the southwest and the present Sagami trough to the southeast, both troughs being thought to be the present plate boundary between the Philippine Sea plate and the Asian plate (SUGIMURA, 1972). This present tectonic situation of the region as well as the nature of Miocene geosynclinal sedimentation with buried

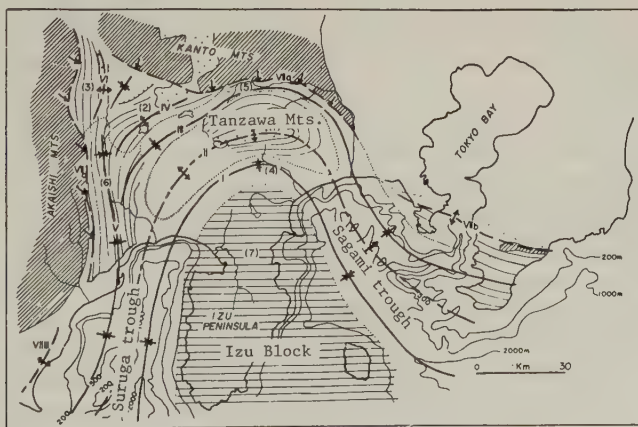


Fig. 3. Curved axes of uplift and subsidence of Miocene terrains in the South Fossa Magna around the Izu Peninsula, central Honshu (MATSUDA, 1962). Horizontal hatch, Izu Block; shaded area, pre-Miocene rocks (Akaishi and Kanto Mountains and Mineoka area in central Boso Peninsula).

metamorphism up to the pumpellyite-prehnite facies in the region seem to indicate that the region was a continuously subsiding basin located along the subducting plate boundary lying off Honshu.

Chrystalline schists of actinolite-greenschist facies and higher grade facies derived from the Miocene formations are exposed in a zone of uplift (the Tanzawa Mountains) in the South Fossa Magna (SEKI *et al.*, 1969). This metamorphism would have been caused by dragging down to depth and shearing of the crust due to the subducting oceanic plate in the Miocene. The nature of the metamorphism, however, is not a high pressure low temperature type. The region was an area of active volcanism and plutonism at that time. High P/T conditions cannot be expected there due to the thermal effect of the magmatism.

The present curved structure of the Miocene sedimentary trough and fold axes (Fig. 3) is inferred to have been formed for the most part not after the deposition (post-Miocene), but before it. The paleocurrent analysis for the middle Miocene turbidites laid down in a north-south trending trough (the Fujigawa area) in the western part of the South Fossa Magna indicates that much coarse debris from the Kanto Mountains came from the east (MATSUDA, 1958). If the present N-S trend of the sedimentary trough was a result of post-depositional anticlockwise rotation, the coarse debris carried from the Kanto Mountains would have to have been brought to the trough from the south at that time, a rather improbable situation. From this and from the small amount of northward indentation of the Izu Block since its collision as mentioned later, it appears that the Miocene sedimentary troughs were developed originally in a sinuous form on the oceanic side of the already-curved pre-Miocene terrains.

4. *The Izu Block and the Miocene Volcanic Front*

The Izu Peninsula area, here called the Izu Block (Fig. 3), is different in structure and history from the main part of the South Fossa Magna (MATSUDA, 1962). After the regional subsidence and deposition in the Miocene, the South Fossa Magna basin north of the Izu Block was differentiated into several belts of uplift and subsidence, the latter having received much coarse debris from the former in late Miocene and Pliocene, while the Izu Block remained stable and was subjected only to block faulting. Overlying the early Miocene volcanics and volcaniclastic sediments, there had accumulated thick late Miocene volcanic piles comprising pillow lavas in the Izu Peninsula. Quaternary subaerial volcanoes rest on them. No coarse clastic materials derived from the older terrains are found. The Izu Block seems to have been a composite volcanic island since the Miocene.

Rocks of the Miocene volcanism in the South Fossa Magna are characterized by a chemical polarity in which alkali content increases westward. In the Tanzawa and Izu areas to the east the rocks are dominantly of tholeiitic suites. In the areas to the west they are dominantly high alumina basalt and alkali olivine basalt. This polarity in chemistry as well as the geographical distribution of the Miocene volcanics indicates that the Miocene volcanism was part of the arc volcanism related to the west-dipping subduction of the Pacific plate beneath the eastern Japan-Izu-Bonin arcs.

It is noteworthy that the Miocene volcanic front of Honshu extends southward smoothly to the eastern margin of the Izu Block, running to the east of the Tanzawa Mountains (Fig. 4). This smooth continuity of the Miocene volcanic front from the main part of Honshu to the Izu Peninsula, and the resemblance in rock appearance and

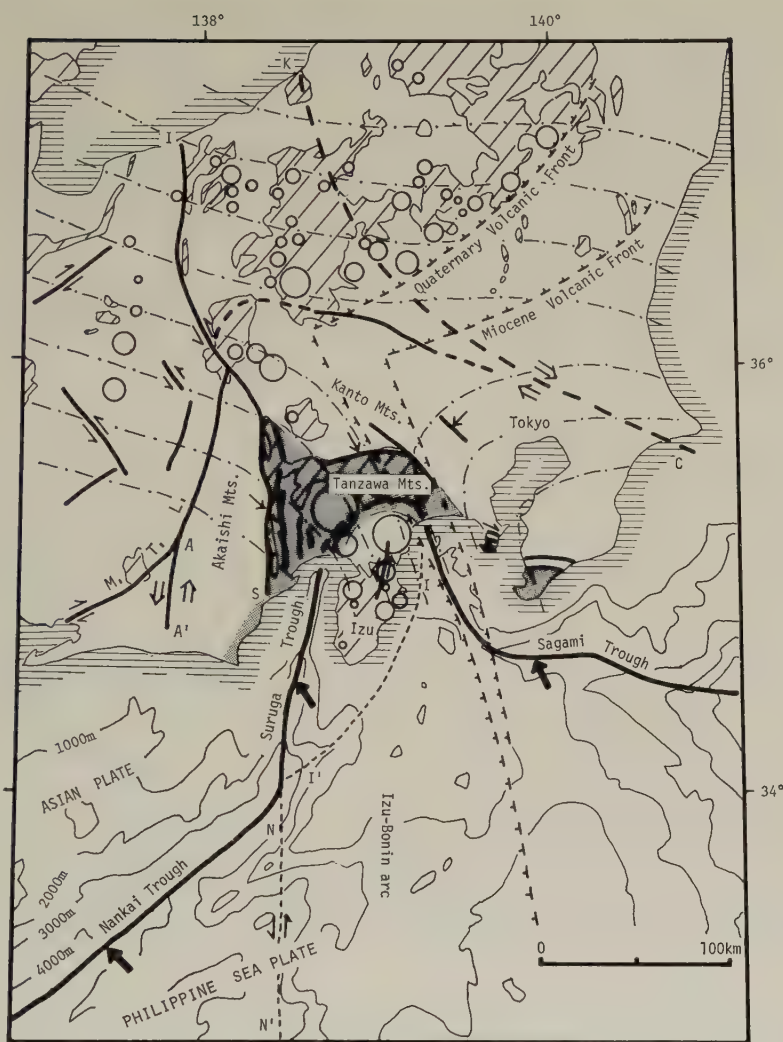


Fig. 4. Tectonic map of central Honshu and the northern part of Izu-Bonin arc, showing highly deformed region, major faults, stress trajectories and volcanic fronts. Stippled area, highly deformed area (South Fossa Magna) in late Tertiary and Quaternary; thin dash and dot lines, trajectories of maximum compressional axes in Quaternary (slightly modified from MATSUDA, 1977); hatched area, Neogene volcanic field (after ISSHIKI *et al.*, 1968); open circles, Quaternary volcanoes; solid thick lines and broken lines, major faults. A-A', Akaishi Tectonic Line; I-S, Itoigawa-Shizuoka Tectonic Line; I-I', Izu Toho Line (ISHIBASHI, 1978); K-C, Kashiwazaki-Choshi Line (YAMASHITA, 1970); M.T.L., Median Tectonic Line; N-N', Nishi-Shichito Fault Zone (MOGI, 1972; KAIZUKA, 1975). Small arrows indicate sense of motion in Quaternary. Open arrows indicate sense of motion in early Tertiary.

in chemical composition between the Tanzawa Mountains and the Izu Block seems to indicate that the Izu Block has been located at the same place relative to the Miocene volcanic front in central Honshu since the Miocene. This inference precludes the hypothesis of eastward migration of the Izu-Mariana arc to its present position from south of Kyushu. If the Izu-Mariana arc came from south of Kyushu, the present fit in position between the Miocene volcanic front in Honshu and that of the present Izu-Bonin arc would have to be regarded as a coincidence. In the following discussion, I assume that the Izu-Bonin arc and the incipient ridges were located originally to the south of central Honshu in the Miocene and earlier periods.

Thus, the South Fossa Magna in the Miocene had a dual character: the area was an active subsiding belt parallel to the Shimanto Belt, and was part of an active volcanic belt parallel to the Izu-Bonin trench.

5. Quaternary Compressional Features

The South Fossa Magna in the Quaternary has strong compressional features with an anomalous orientation of the crustal stress field. As shown in Fig. 4, trajectories of the maximum compressional stress axes of the region distribute in a fan-shape extending from the northern end of the Izu Block. The major faults northwest of the Izu Block, such as the north-south trending Itoigawa-Shizuoka tectonic line and other parallel faults are west-dipping left-lateral reverse faults, while the northwest-southeast trending faults northeast of the Izu Block such as the Sagami trough fault are northeast-dipping right-lateral reverse faults, and the east-west trending Kannawa fault and Ogiyama fault to the north of the Izu Block are north-dipping thrust faults. Since the Pliocene and Quaternary formations are involved in these structures, they are considered to have been formed mostly during the Quaternary.

Another characteristic feature of this region is a strong uplift in the Quaternary. The Akaishi Mountains to the west of the South Fossa Magna are one of the highest mountain ranges in Japan, having been uplifted in the Quaternary (KAIZUKA and MURATA, 1969). Recent uplift of the Akaishi Mountains during the last 60 years, detected by precise leveling, exceeds 4 mm/year (DAMBARA, 1971), which is the highest value observed

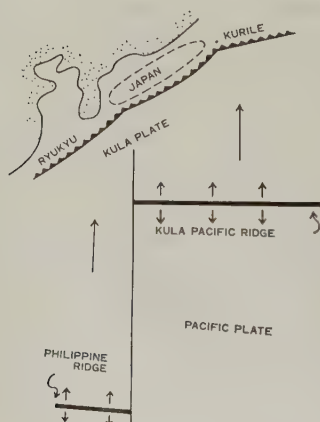


Fig. 5. Plate motion and arrangement at about 100 mybp in the western Pacific after UYEDA and BEN-AVRAHAM (1972).

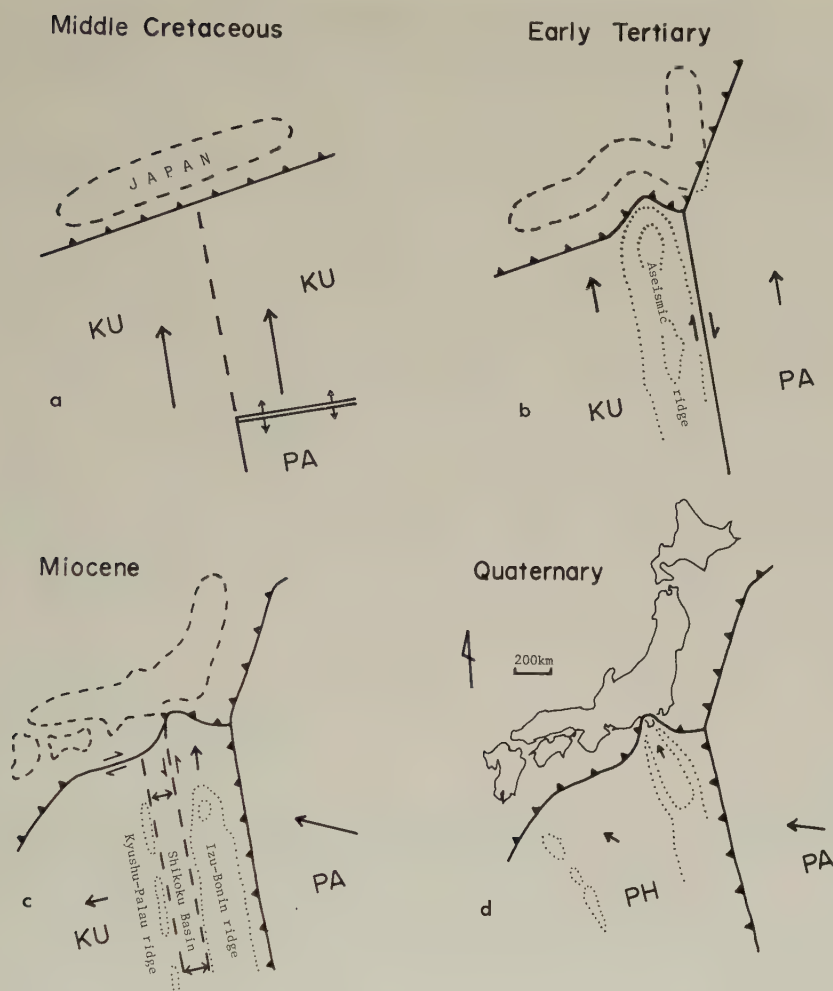


Fig. 6. Plate motion and arrangement around Japan. Middle Cretaceous (a) to Quaternary (d), KU, Kula plate; PA, Pacific plate; PH, Philippine Sea plate.

in Japan. The marine Miocene rocks deposited in the South Fossa Magna have been uplifted as much as 1,500–2,000 m above sea level to form mountains within the South Fossa Magna. Exposures of the Miocene crystalline schist in the Tanzawa Mountains indicate a deep denudation due to strong uplift after the Miocene.

This Quaternary compressive deformation with strong uplift and radial arrangement of the maximum stress trajectories in the region can be interpreted as a result of the collision of the Izu-Bonin arc against central Honshu in the Quaternary.

6. Plate Tectonic Interpretation

For the Late Mesozoic state of oceanic plates, UYEDA and BEN-AVRAHAM (1972) and HILDE *et al.* (1977) have postulated a north-south trending great transform fault in the western Pacific separating the Pacific plate from the Kula plate in the Late Mesozoic

(Fig. 5). This transform fault has played an important role in the tectonic history of central Honshu. Here I assume that the north-south trending transform fault proposed by UYEDA and BEN-AVRAHAM (1972) was located to the south of central Honshu instead of south of Kyushu.

In the middle Cretaceous, the Kula plate was subducting beneath the Japanese Islands (Fig. 6(a)). Active sedimentation and deformation had proceeded in the Shimanto belt lying along a subduction zone (off-Honshu subduction zone) in the Cretaceous to early Tertiary.

After descent of the Kula-Pacific ridge beneath the Japanese arc in the late Cretaceous (UYEDA and MIYASHIRO, 1974), the north-south trending transform fault west of the Pacific plate joined with the off-Honshu subduction zone off central Honshu (Fig. 6(b)). Buoyant subduction (VOGT, 1973; VOGT *et al.*, 1976) of aseismic ridges on the Kula plate lying along the transform fault had resulted in bending of the off-Honshu subduction zone, which contemporaneously caused a bend of the pre-Miocene terrains in Honshu. This bending of Honshu was probably associated with the opening of the Japan Sea (MURAUCHI, 1971) and the anticlockwise rotation (KAWAI *et al.*, 1971) of northern Honshu. The southeastward shift of Honshu associated with the opening of the Japan Sea had encountered the resistance of aseismic ridges south of Honshu, which brought about not only the northward-convex bend of pre-Miocene terrains in central Honshu, but also the anticlockwise rotation of northern Honshu along the Kanto Tectonic line as stated by KOBAYASHI (1941).

Owing to this rotation of northern Honshu, the Mesozoic structure off the Abukuma Mountains in the southern part of northern Honshu was truncated obliquely along the Japan trench by tectonic erosion due to the subducting Pacific plate (MURAUCHI, 1971; SUGIMURA, 1972).

The eastern extension of the zonally arranged, pre-Miocene terrains in central Honshu is hardly traceable into northern Honshu beyond the Tanakura shear zone (OTSUKI and EHIRO, 1978). The deformational history of the eastern half of the off-Honshu subduction zone and northern Honshu would have been more complex than that shown in Fig. 6(b), as described by OTSUKI and EHIRO (1978).

The change in the direction of motion of the Pacific plate 45 my ago from NNW to WNW (CLAGUE and JARRARD, 1973) induced new subduction on the former transform faults (UYEDA and BEN-AVRAHAM, 1972). Thus the Izu-Bonin arc-trench system was born and abutted to the eastern Japan arc-trench system (Fig. 6(c)). Related arc volcanism has occurred since then along the eastern Japan-Izu-Bonin arcs, crossing the former Shimanto zone at the South Fossa Magna. Since the change 45 my ago, the Pacific plate has been subducting obliquely along the Izu-Bonin trench. The oblique subduction of the Pacific plate has dragged the Izu-Bonin arc to the north by incomplete decoupling between them in a manner suggested by Uyeda (MATSUDA and UYEDA, 1971) and FITCH (1972). Consequently, in the Miocene the Izu Block was approaching the South Fossa Magna, where the Izu-Bonin arc was subducting beneath central Honshu, probably accompanied by strong subsidence and deposition. The ultrabasic rocks and oceanic basalts exposed in the Shimanto zone and in the Miocene terrain in the South Fossa Magna region (the Setogawa and Kamogawa areas, TANAKA and NOZAWA, 1977, p. 317) might have been emplaced by this subduction process.

If we assume that about one-fifth of the west-northwest movement of the Pacific plate, about 2 cm/year, served for the northward shift of the Izu-Bonin arc, the Izu Block

was located about 500 km south of Honshu in the early Miocene, namely about halfway between the present position of the Bonin islands and the coast of Honshu.

A fraction of this northward shift of the Izu-Bonin arc might have contributed to pushing and bending of central Honshu. However, the effect of the pushing against central Honshu in the Miocene appears insignificant because the syn-depositional deformation of the sedimentary basin was relatively gentle as compared with the post-depositional (post-Miocene) deformation.

The Shikoku Basin was spreading in the Miocene (WATTS and WEISSEL, 1975, KOBAYASHI and ISEZAKI, 1976). The Izu-Bonin arc was split by Karig's process (KARIG, 1971, 1974) and the western half of the arc migrated westward to form the present Kyushu-Palau ridge (Fig. 6(c)). Although the exact direction of spreading of the Shikoku Basin is not clear, it is inferred that the spreading direction had been nearly parallel to the trend of the Nankai trough, because the late Tertiary tectonism on land in western Japan had been very quiet compared with that in the early Tertiary when subduction was proceeding. The Nankai trough west of the axis of the spreading center was a plate boundary along which right-lateral faulting predominated during the Miocene.

Thus it is likely that the Izu-Bonin arc on the eastern margin of the Shikoku Basin was moving north relative to Honshu by dragging of the Pacific plate, while the western part of the Shikoku Basin was moving to the west by inter-arc spreading. According to the different movements between the two parts of the plate, there would have developed a north-south trending left-lateral shear zone along the western margin of the Izu-Bonin arc. The Nishi-Shichito fault introduced by KAIZUKA (1975), which is a left-lateral Quaternary fault bordering the Izu-Bonin volcanic arc on its western side, would have originated in this way in the Miocene.

The degree of deformation of the Shimanto and Miocene terrains is significantly different between the South Fossa Magna and the coastal regions west of it. The difference is attributable to the difference in relationships with oceanic plate motions between the two regions since the Miocene: The South Fossa Magna region has been a converging plate boundary between Honshu and the Izu-Bonin arc (subduction zone in the Miocene and collision zone in the Quaternary), while regions to the west were located along a transform plate boundary in the Miocene as mentioned above and are not a collision zone in the Quaternary.

In the late Miocene to Pliocene, anomalously thick and coarse conglomerates derived from adjacent belts of uplift were deposited and filled belts of subsidence within the South Fossa Magna. This indicates the growth of the belts of uplift and subsidence north of the Izu Peninsula (Fig. 3), which appears to be a precursory effect of the Quaternary collision of the Izu Block.

In the Quaternary, the Izu Block reached the South Fossa Magna and collided with it. Pushing of the Izu Block against Honshu brought about Quaternary compressional geologic structures, strong regional uplift and fan-shaped stress trajectories of maximum compression in the South Fossa Magna around the Izu Peninsula. Paleogeographically speaking, the collision of the Izu Block with the South Fossa Magna took place in the early Quaternary as inferred from the fact that a deep marine sedimentary trough (the Ashigara trough) had persisted between the South Fossa Magna proper and the Izu Peninsula until the end of the upper Pliocene (MACHIDA *et al.*, 1975) or possibly early Quaternary (HASEGAWA *et al.*, 1975).

The direction of movement of the Izu-Bonin arc relative to Honshu is probably about

north-northwest as inferred from analyses of the inter-plate earthquakes of 1923 (ANDO, 1971) and 1703 (MATSUDA *et al.*, 1978) along the Sagami trough. The trend of maximum pressure axes deduced from intra-plate large earthquakes in the Izu Peninsula (ABE, 1978) and from Quaternary faults (KANEKO, 1964; MATSUDA, 1977) and from intrusive dikes and parasitic cones of volcanoes (NAKAMURA, 1969) in the region also lies between north and northwest.

The northward movement of the Izu-Bonin arc has been absorbed by subduction beneath Honshu along the Sagami and Suruga troughs, but north of the Izu Peninsula between these two troughs, it has caused a northward shift of the colliding edge of the Izu-Bonin Inner arc. The amount of the northward shift of the Izu Block into central Honshu since the collision cannot be estimated precisely because of the lack of reliable data on the converging rate between Honshu and the Philippine Sea plate in this region. If we assume it is 3 cm/year based on the slip rate obtained by KANAMORI (1972), ANDO (1971, 1975), and SENO (1977) from analyses for historic inter-plate great earthquakes along the Sagami trough and the Nankai trough, the colliding head of the Izu Block would have gone into central Honshu about 30 km during the past 1 my. This estimate seems to be the maximum plausible value, because the converging rate may be much smaller as suggested by MATSUDA *et al.* (1978) and because the northward shift has been partly absorbed within the Izu Block by intraplate faulting. Moreover, part of the northward shift of the Izu Block has been consumed by internal deformation of Miocene terrains north of the Izu Peninsula. Thus, only a small fraction of the northward shift of the Izu-Bonin arc in the Quaternary may have served to strengthen the cusp structure of pre-Miocene terrains in central Honshu.

As a consequence of the collision of the Izu Block against central Honshu, a new subduction zone may have begun to develop off the eastern and southern coast of the Izu Peninsula (I-I' in Fig. 4), as discussed by ISHIBASHI (1978).

Occurrence of a westward component in the northward movement of the Izu Block implies that east-west spreading of the Izu-Bonin arc is occurring, provided that the off-Honshu triple junction has remained at its present position relative to Honshu.

7. Conclusion

The interpretation of the tectonics of central Honshu presented in previous sections leads to the conclusion that the present triple junction off central Honshu has remained in the same position relative to central Honshu since the late Cretaceous. In the early Tertiary, earlier than 45 my ago (Fig. 6(b)), the triple junction was TTF(a) type of McKENZIE and MORGAN (1969). If this triple junction was stable and fixed as mentioned above, the trend of the off-Honshu transform fault should have been parallel to the movement of the Pacific plate at the triple junction. The triple junction became a TTT(a) type after the change in motion of the Pacific plate in the Eocene. The triple junction can still be stable and fixed to Honshu, because the northward movement of the Kula plate may have possibly been parallel to the Izu-Bonin trench. During the Miocene, when the Shikoku Basin was spreading, the tendency of westward migration of the triple junction was compensated by inter-arc spreading behind the Izu-Bonin arc, so that the triple junction stayed there. The present submarine topography at the junction of the Japan-Izu-Bonin-Sagami trenches appears to indicate that the triple junction is stable and has remained at the present position at least through the Quaternary. Nevertheless, north-

ward movement of the Izu Block involves a westward component as mentioned previously. These facts imply that spreading with an east-west component has been occurring in the Izu-Bonin ridge.

An alternative hypothesis of the eastward migration of the off-central Honshu triple junction during spreading of the Shikoku Basin in the Miocene has been postulated by many workers (UYEDA and BEN-AVRAHAM, 1972; KOBAYASHI and ISEZAKI, 1976; HILDE *et al.*, 1977; MARSHAK and KARIG, 1977; KANAMORI, 1977), with the exception of MURAUCHI (1971). KIMURA and KOBAYASHI (1975) and MARSHAK and KARIG (1977) interpreted the occurrence of anomalously near-trench igneous activity in the outer zone of southwestern Japan in the Miocene and its eastward decrease in K-A age (NOZAWA, 1968) as an indication of eastward migration of the Izu-Bonin arc-trench system. The igneous activity, ranging from about 20 to 5 my in age, resulted in small, sporadically distributed, acidic volcano-plutonic bodies. However, those rocks seem unlikely to be an earlier product of the arc volcanism related to the eastward-migrating volcanic front of the present northern Japan-Izu-Bonin arc-trench system, because Miocene volcanic activity has been prevailing since early Miocene in the South Fossa Magna, which indicates that the north-south trending volcanic front was already located to the east of the South Fossa Magna at that time. This minor igneous activity in the outer zone west of the South Fossa Magna may be related to a weakened compressional tectonic condition after the cessation of subduction of the Kula plate beneath southwest Japan in the Miocene.

Although the problem of whether the Izu-Bonin arc has been fixed or migrated from south of Kyushu is still unsolved, the unique geologic structure and its history since the late Mesozoic in central Honshu seem to favor a model in which the Izu-Bonin ridge is fixed relative to Honshu since the late Mesozoic.

I am indebted to Professor Seiya Uyeda and Professor Kazuaki Nakamura for helpful discussions. I also thank Dr. Paul Somerville for a critical reading of the manuscript.

REFERENCES

- ABE, K., Dislocations, source dimensions and stresses associated with earthquakes in the Izu Peninsula, Japan, 1978 (in press).
- ANDO, M., A fault-origin model of the great Kanto Earthquake of 1923 as deduced from geodetic data, *Bull. Earthq. Res. Inst.*, **49**, 19–32, 1971.
- ANDO, M., Source mechanisms and tectonic significance of historical earthquakes along the Nankai trough, Japan, *Tectonophysics*, **27**, 119–140, 1975.
- CLAGUE, D.A. and R.D. JARRARD, Tertiary Pacific plate motion deduced from the Hawaiian-Emperor Chain, *Geol. Soc. Am. Bull.*, **84**, 1135–1154, 1973.
- DAMBARA, T., Synthetic vertical movements in Japan during the recent 70 years, *J. Geod. Soc. Jpn.*, **17**, 100–108, 1971.
- EHARA, S., Geotectonics of the Pacific concerning the Japanese Island. 1. The Fossa Magna, the Shichito and the Ogasawara salients, *J. Geol. Soc. Jpn.*, **59**, 173–200, 1953.
- FITCH, T.J., Plate convergence, transcurrent faults, and internal deformation adjacent to southeast Asia and the western Pacific, *J. Geophys. Res.*, **77**, 4432–4460, 1972.
- HARA, I. and K. HIDE, The origin of the Median Tectonic Line, *Kaiyo Kagaku (Marine Sciences)*, **6** (9), 35–40, 1974.
- HASEGAWA, Y., Y. MATSUSHIMA, and T. SHIKAMA, read at Annu. Meet. Palaeontol. Soc. Jpn., 1975.
- HAYAMA, Y. and T. YAMADA, Some considerations on the Median Tectonic Line of the Kashio Phase in the light of the Ryoke plutonic history, in *Median Tectonic Line*, edited by R. Sugiyama, pp. 1–7, Tokai University Press, Tokyo, 1973.
- HILDE, T.W.C., S. UYEDA, and L. KROENKE, Evolution of the western Pacific and its margin, *Tectonophysics*, **38**, 145–165, 1977.
- ISHIBASHI, K., Plate convergence around the Izu collision zone, central Japan: Development of a new subduc-

- tion boundary with a temporary transform belt, Abstr. Int. Geodyn. Conf. on Western Pacific and Magma Genesis, Tokyo, March 13–17, 1978, pp. 66–67, 1978.
- ISSHIKI, N., K. MATSUI, and K. ONO, Volcanoes of Japan, 1 : 2,000,000 Map Ser. 11, Geol. Surv. Jpn., 1968.
- KAIZUKA, S., A tectonic model for the morphology of arc-trench systems, especially for the echelon ridges and mid-arc faults, *Jpn. J. Geol. Geogr.*, **45**, 9–28, 1975.
- KAIZUKA, S. and A. MURATA, The amounts of crustal movements during the Neogene and the Quaternary in Japan, *Geogr. Rep. Tokyo Metrop. Univ.*, **4**, 1–10, 1969.
- KANAMORI, H., Tectonic implications of the 1944 Tonankai and the 1946 Nankaido earthquakes, *Phys. Earth Planet. Inter.*, **5**, 129–139, 1972.
- KANAMORI, H., Seismic and aseismic slip along subduction zones and their tectonic implications, in *Island Arcs, Deep Sea Trenches and Back-Arc Basins*, Maurice Ewing Series 1, pp. 163–174, Am. Geophys. Union, Washington, D.C., 1977.
- KANEKO, S., Tectonic relief in south Kanto, Japan, *Trans. R. Soc. N. Z., Geology*, **13**, 187–204, 1964.
- KARIG, D.E., Origin and development of marginal basins in the western Pacific, *J. Geophys. Res.*, **76**, 2542–2561, 1971.
- KARIG, D.E., Evolution of arc systems in the western Pacific, *Annu. Rev. Earth Planet Sci.*, **2**, 51–75, 1974.
- KAWAI, N., T. NAKAJIMA, and K. HIROOKA, The evolution of the Island arc of Japan and the formation of granites in the circum-Pacific belt, *J. Geomag. Geoelectr.*, **23**, 267–292, 1971.
- KIMURA, T., The Akaishi Tectonic Line, in the eastern part of southwest Japan, *J. Geol. Geogr.*, **32**, 119–136, 1961.
- KIMURA, K. and K. KOBAYASHI, The spreading of the Shikoku Basin and the Japanese islands, Abstr. 82th Annu. Meet. Geol. Soc. Jpn., 1975, p. 49, 1975.
- KOBAYASHI, T., The Sakawa orogenic cycle and its bearing on the origin of the Japanese islands, *J. Fac. Sci., Imp. Univ. Tokyo*, Sec. 2, **5**, 219–578, 1941.
- KOBAYASHI, K. and N. ISEZAKI, Magnetic anomalies in the Sea of Japan and the Shikoku Basin: Possible tectonic implications, *Geophys. Monogr.*, **19**, 235–251, 1976.
- MACHIDA, H., Y. MATSUSHIMA, and I. IMANAGA, Tephrochronological study on eastern foot of Mt. Fuji Volcano—With special reference to geomorphological development accompanied with growth of Mt. Fuji and development of the Kannawa fault, *Daiyonki Kenkyu (Quaternary Research)*, **14**, 77–89, 1975.
- MARSHAK, R.S. and D.E. KARIG, Triple junctions as a cause for anomalously near-trench igneous activity between the trench and volcanic arc, *Geology*, **5**, 233–236, 1977.
- MATSUDA, T., Late Tertiary stratigraphy and development of folding in the upper Fuji River Valley, Yamaguchi Prefecture, central Japan, *J. Geol. Soc. Jpn.*, **64**, 325–343, 1958.
- MATSUDA, T., Crustal deformation and igneous activity in the South Fossa Magna, Japan, *Geophys. Monogr. Am. Geophys. Union*, **6**, 140–150, 1962.
- MATSUDA, T., The peculiarity of the Fossa Magna region in the Honshu arc, *Kaiyo Kagaku (Marine Sciences)*, **8** (9), 20–24, 1976.
- MATSUDA, T., Tertiary and Quaternary tectonism of Japan in relation to plate motions, *Assoc. Geol. Collab. Jpn. Monogr.*, No. 20, 213–225, 1977.
- MATSUDA, T., K. NAKAMURA, and A. SUGIMURA, Late Cenozoic orogeny in Japan, *Tectonophysics*, **4**, 349–366, 1967.
- MATSUDA, T., Y. OTA, M. ANDO, and N. YONEKURA, Fault mechanism and recurrence time of major earthquakes in the southern Kanto district, Japan, as deduced from coastal terrace data, *Geol. Soc. Am. Bull.*, **89**, 1610–1618, 1978.
- MATSUDA, T. and S. UYEDA, On the Pacific-type orogeny and its model—Extension of the paired belts concept and possible origin of marginal seas, *Tectonophysics*, **11**, 5–27, 1971.
- MATSUMURA, N., The Median Tectonic Line in the Akaishi Mountains, in *Median Tectonic Line*, edited by R. Sugiyama, pp. 9–27, Tokai University Press, Tokyo, 1973.
- MCKENZIE, D.P. and W.J. MORGAN, Evolution of triple junctions, *Nature*, **224**, 125–133, 1969.
- MOGI, A., Bathymetry of the Kuroshio Region, in *Kuroshio—Its Physical Aspects*, edited by H. Stommel and K. Yoshida, Chap. 2, pp. 53–80, University of Tokyo Press, Tokyo, 1972.
- MURAUCHI, S., The renewal of island arcs and the tectonics of marginal seas, in *Island Arc and Marginal Sea*, edited by S. Asano and G.B. Udintsev, pp. 39–56, Tokai University Press, Tokyo, 1971.
- NAKAMURA, K., Arrangement of parasitic cones as a possible key to regional stress field, *Bull. Vol. Soc. Jpn.*, **14**, 8–20, 1969.
- NOZAWA, T., Isotope dating data for granitic rocks from the outer zone of Southwest Japan and its extension—Summary in 1968 and a hypothesis of northward migration of igneous activity, *J. Geol. Soc. Jpn.*, **74**, 485–489, 1968.
- OTSUKI, K. and M. Ehiro, Major strike-slip faults and their bearing on spreading in the Japan Sea, this issue, S 537–S 548, 1978.

- SEKI, Y., Y. OKI, T. MATSUDA, K. MIKAMI, and K. OKUMURA, Metamorphism in the Tanzawa Mountains, central Honshu, *J. Jpn. Assoc. Min. Pet. Econ. Geol.*, **61**, 1-24, 50-75, 1969.
- SENO, T., The instantaneous rotation vector of the Philippine Sea Plate relative to the Eurasian plate, *Tectonophysics*, **42**, 209-226, 1977.
- SUGIMURA, A., Plate boundaries near Japan, *Kagaku (Science)*, **42**, 192-202, 1972.
- TANAKA, K. and T. NOZAWA (eds.), *Geology and Mineral Resources of Japan*, **1**, 430 pp., Geol. Surv. Jpn., 1977.
- UYEDA, S. and Z. BEN-AVRAHAM, Origin and development of the Philippine sea, *Nature (Phys. Sci.)*, **40**, 176-178, 1972.
- UYEDA, S. and A. MIYASHIRO, Plate tectonics and the Japanese Islands: A synthesis, *Geol. Soc. Am. Bull.*, **85**, 1159-1170, 1974.
- VOGT, P.R., Subduction and aseismic ridges, *Nature*, **241**, 189-191, 1973.
- VOGT, P.R., A. LOWRIE, D.R. BRACEY, and R.N. HEY, Subduction of aseismic oceanic ridges: Effects on shape, seismicity, and other characteristics of consuming plate boundaries, *Geol. Soc. Am., Spec. Pap.*, **172**, 1-59, 1976.
- WATTS, A.B. and J.K. WEISSEL, Tectonic history of the Shikoku marginal basin, *Earth Planet Sci. Lett.*, **25**, 239-250, 1975.
- YAMASHITA, N., A proposal of the Kashiwazaki-Choshi Tectonic Line, in *Island Arc and Ocean*, pp. 179-191, Tokai University Press, Tokyo, 1970.
- YOSHIDA, T., *An Outline of the Geology of Japan*, pp. 1-61, Geol. Surv. Jpn., 1975.

FLOW UNDER THE ISLAND ARC OF JAPAN AND LATERAL VARIATION OF MAGMA CHEMISTRY OF ISLAND ARC VOLCANOES

Mitsuhiro TORIUMI*

University Museum, University of Tokyo, Tokyo, Japan

(Received May 31, 1978; Revised September 8, 1978)

Dislocation densities of olivine grains in peridotite nodules from Ichinomegata (25 samples), Sannomegata (18 samples), Oki-Dogo (13 samples), Hamada (3 samples) and Takashima (10 samples) were measured for estimating differential stress in the upper mantle. The density was in the range of 10^6 – 10^7 cm^{-2} . The differential stress is estimated as 100–300 bars using KOHLSTEDT and GOETZE's empirical relationship (1974) between the dislocation density and the differential stress. Strain rate is inferred from the geotherm of the island arc and the flow law of olivine single crystal proposed by KOHLSTEDT and GOETZE (1974) and DURHAM and GOETZE (1977). Strain rate in the upper mantle from 30 to 100 km depth is less than 10^{-15} sec^{-1} , but it is nearly constant around 10^{-13} – 10^{-12} sec^{-1} from 100 to 200 km depth.

The convective flow induced by descending oceanic plate is suggested and the velocity of the return flow is estimated to be 5 cm/year. The return flow of the upper mantle toward the trench causes the lateral variation of magma chemistry and the upper mantle materials, if partially molten liquid continuously flows out from the moving upper mantle. The model in this study gives a relation between the horizontal distance from the volcanic front, X , and the concentration ratio of C_r^1/C^1 (C_r^1 ; concentration at volcanic front) as follows;

$$C_r^1/C^1 = \exp(-\beta\phi X/v),$$

in which β and v are the rate of outflow of the liquid per unit volume of the upper mantle and the mean velocity of the return flow, and ϕ is a constant.

1. Introduction

Convective flow of the upper mantle materials under the island arc induced by subducting oceanic plate (SLEEP and TOKSÖZ, 1971) contributes to heat transportation and chemistry of mantle materials. Heat transportation by convective flow gives a great effect on the temperature distribution and, therefore, the state of partial melting in the upper mantle. Convective flow also affects the chemistry of partially molten liquid because of continuous outflow of partially molten liquid from the moving mass. They are important to the magma chemistry of the island arc, the chemistry of the upper mantle materials, and the opening of the Back Arc Basin (SLEEP and TOKSÖZ, 1971).

Actual flow can be demonstrated by measuring the differential stress acting within the upper mantle, which is estimated from the dislocation density or the subgrain size of olivine derived from the upper mantle. The experimental relations between the dislocation density and the differential stress have been obtained by KOHLSTEDT and GOETZE (1974) and

* Present address: Earth Sciences, Faculty of Science, Ehime University, Matsuyama, Ehime, 930 Japan.



Fig. 1. Localities of mantle derived xenoliths.

DURHAM *et al.* (1977), and those between the subgrain size and differential stress also have been proposed by DURHAM *et al.* (1977). Further, decrease of the dislocation density in static annealing has been investigated by GOETZE and KOHLSTEDT (1973), and TORIUMI and KARATO (1978). Combining these data, the differential stress of the upper mantle could be estimated by means of the dislocation density or the subgrain size of the mantle-derived olivine grains.

If we can estimate the differential stress, the strain rate of the upper mantle should be inferred by the geotherm and empirical flow law. Thus, the author intends to discuss the strain rate and flow in the upper mantle beneath the Island Arc of Japan, based on the dislocation density of the mantle-derived olivine in peridotite xenoliths of Japan. Further, he proposes a zone refining model of the upper mantle due to the upward outflow of the partially molten liquid from the moving upper mantle. The model can interpret the lateral variation of magma chemistry of the island arc volcanoes.

2. Brief Descriptions of Peridotite Xenoliths

Xenoliths studied here are from Ichinomegata (25 samples), Sannomegata (18 samples), Oki-Dogo (13 samples), Hamada (3 samples), and Takashima (10 samples). They

are included in alkali basaltic lavas and breccias. Ichinomegata and Sannomegata are located in the Northeast Japan Arc, and Oki-Dogo, Hamada and Takashima are in the Southwest Japan Arc (Fig. 1). The volcanic rocks including the peridotite xenoliths erupted at a time of 0–3 my. Petrology of Ichinomegata peridotite xenoliths has been studied by KUNO and AOKI (1970), AOKI (1973) and TAKAHASHI (1976), and that of Oki-Dogo by TAKAHASHI (1976). Petrological studies of Hamada and Takashima peridotite xenoliths have been carried out by FUJII (1974) and OBATA (1972), respectively.

Most of the xenoliths are amphibolite, granulite, hornblende gabbro, olivine-pyroxene gabbro, spinel lherzolite, hornblende-spinel lherzolite, plagioclase-spinel lherzolite, dunite, wherlite, and websterite. It is important that there is a certain difference between the Northeast Japan Arc (Ichinomegata, and Sannomegata) and the Southwest Japan Arc (Oki-Dogo, Hamada and Takashima). In Ichinomegata and Sannomegata, spinel lherzolite including hornblende is common, but the spinel lherzolite does not contain hornblende at other localities.

Petrological difference in xenoliths at a single locality probably leads to a layered model of the upper mantle. FUJII (1974) and TAKAHASHI (1976) have suggested the layered model of the upper mantle consisting with spinel lherzolite, dunite and pyroxenite layers with ascending order. The upper mantle under Ichinomegata and Sannomegata are also considered to be stratified with spinel lherzolite, wherlite, dunite and pyroxenite layers (Takahashi, personal communication, 1978). The structure of the upper mantle is probably formed through a crystallization differentiation process in the magma reservoir within the upper mantle (FUJII, 1974).

Equilibration temperature of spinel lherzolite has been estimated using orthopyroxene-clinopyroxene, olivine-clinopyroxene, and spinel-olivine geothermometers by FUJII (1974) for Hamada, OBATA (1972) for Takashima, and TAKAHASHI (1976) for Oki-Dogo and Ichinomegata. Most of spinel lherzolite xenoliths show the equilibration temperature of 900–1,000°C but pyroxenite xenoliths show that of 700–900°C. This supports the layered model of the upper mantle mentioned above.

3. Dislocation Structure and Density

TORIUMI and KARATO (1978) have recognized two types of dislocation structure of olivine grains; one is the cellular type (Fig. 2(A)) which consists of network of simple dislocation walls (small angle subboundaries), and the other is the tangled type (Fig. 2(B)) which is composed of tangled dislocations without simple dislocation walls. Simple dislocation walls are usually (100) subboundary (Fig. 2(C)), (010) (Fig. 2(D)), and (001) subboundaries. Most spinel lherzolite xenoliths in Ichinomegata, Sannomegata, and Oki-Dogo contain olivine grains of both types (TORIUMI and KARATO, 1978), but all of dunite and olivine pyroxenite xenoliths of Takashima contain only equigranular grains of olivine with the cellular type dislocation structure. Cumulate group peridotites (FUJII, 1974; TAKAHASHI, 1976) contain few grains of the cellular type olivine.

The cellular type dislocation structure is probably formed in the steady state creep, considering that the structure is similar to the dislocation structures of experimentally deformed MgO (HÜTHER and REPPICH, 1973) and LiF (STREB and REPPICH, 1973) in the steady state creep. Recent works by DURHAM *et al.* (1977) have also pointed out that the steady state dislocation structure of olivine at high temperature creep displays abundant (100) subboundaries which are one type of the dislocation walls in the cellular type dis-

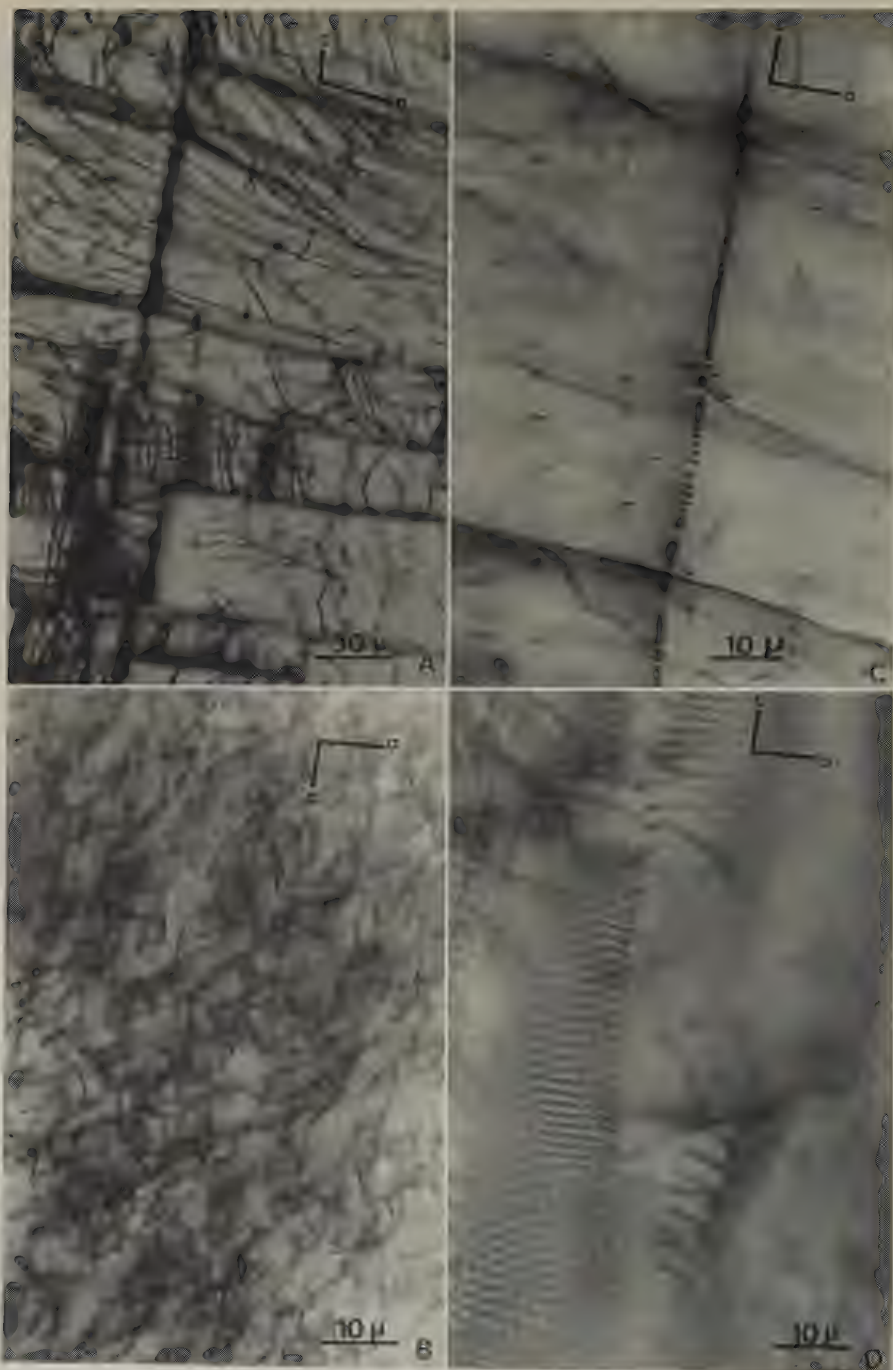


Fig. 2. Dislocation structures of olivine decorated by oxidation-decoration method of KOHLSTEDT and VANDER SANDE (1975). (A) Cellular dislocation structure. (100) and (001) subboundaries (dislocation walls) are recognized as the broadly dark lines. (B) Tangled dislocation structure without subboundary. Dislocations are tangled with each other. (C) (100) simple dislocation wall (small angle subboundary) showing the clear array of dislocation lines. (D) (010) simple network of dislocations (small angle twist boundary).

location structure in this study. On the other hand, the tangled type structure is probably formed in the transient creep, judging from the fact that this structure appears very much alike the transient structure in DURHAM *et al.* (1977). Considering that the uppermost mantle possesses cumulated layers from liquid, the deformation of such layers may be in the transient state.

Taylor's equation $\sigma = \alpha G b \sqrt{\rho}$, in which σ , ρ , G , and b are the differential stress, dislocation density, the rigidity, and the magnitude of the Burger's vector of olivine, respectively, is applied to the steady state creep, but not to the transient creep. This is because the dislocation density changes during transient creep and achieves a constant value in the steady state creep as investigated on olivine single crystals by DURHAM *et al.* (1977).

On the other hand, the subgrain size may provide an indicator of stress as suggested by RALEIGH and KIRBY (1970) and DURHAM *et al.* (1977). The subgrain size is defined by the mean distance between simple dislocation walls (subboundaries). DURHAM *et al.* (1977) have proposed the relation, $d = 45 G b / \sigma$, in which d is the subgrain diameter. As the formation of the simple dislocation walls has been considered to be in the steady state creep (TORIUMI and KARATO, 1978), the relation is also applicable to estimating the stress.

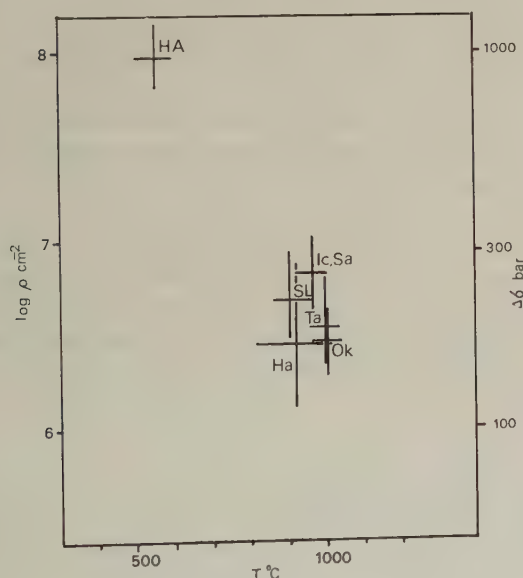


Fig. 3. Observed dislocation density (ρ)-equilibration temperature diagram. Differential stress is estimated from KOHLSTEDT and GOETZE's empirical equation (1974). Ic, Ichinomegata; Sa, Sannomegata; Ta, Takashima; Ok, Oki-Dogo; Ha, Hamada; SL, Salt Lake of Hawaii; HA, Higashi Akaishi dunite mass in Shikoku, Japan (TORIUMI, 1978).

Table 1. Dislocation densities and subgrain sizes of olivine.

Locality	Dislocation density (cm^{-2})	Subgrain size (μm)
Ichinomegata (25)*	$6 \times 10^6 - 2 \times 10^7$	40-70
Sannomegata (18)	$5 \times 10^6 - 1 \times 10^7$	70-100
Oki-Dogo (13)	$2 - 5 \times 10^6$	100-160
Hamada (3)	$1 - 3 \times 10^6$	120-210
Takashima (10)	$2 \times 10^6 - 1 \times 10^7$	60-120
Salt Lake (16)	$4 \times 10^6 - 1 \times 10^7$	40-60

* Number of xenoliths.

The ranges of the dislocation density and the subgrain diameter are listed in Table 1, and are plotted in the temperature-logarithmic dislocation density diagram (Fig. 3). The temperature used are the equilibration ones as stated in the previous section.

The data of spinel lherzolite xenoliths (16 samples) of Salt Lake in Hawaii, of which equilibration temperatures have been estimated by MCGREGOR (1974), are added for reference. The figure shows that the dislocation densities and the differential stress of studied peridotite xenoliths are plotted in the narrow ranges of 10^6 – 10^7 cm⁻² and 100–300 bars, respectively, and they are quite similar to those of other localities studied by GUEGUEN (1977). The samples, however, were derived from different positions of the earth surface and different depths in the upper mantle under the Island Arc of Japan as mentioned above. Therefore, at least in the uppermost mantle the stress is probably constant around 100–300 bars, in other words, the stress gradient in the upper mantle is quite small. The stress is also in the same order as that in the oceanic plate deduced from Salt lake xenoliths (Fig. 3).

4. Strain Rate

Creep equation of the single crystals of olivine and peridotite has been investigated by CARTER and AVELLALLEMENT (1970), KOHLSTEDT and GOETZE (1974), and DURHAM and GOETZE (1977). Their results have indicated the power-law creep equation for the stress in which the power is 2–5. Most reliable data on single crystals of olivine have been proposed by DURHAM and GOETZE (1977), and their results showed the power of 3–4. This value is quite close to that of the WEERTMAN (1968)'s model of steady state creep. They have also clarified that the creep process of olivine single crystals must be governed by the dislocation climb process, because independent slip systems have only three components and this fact is out of the Von Mises's criterion (DURHAM and GOETZE, 1977). Further, the activation energy for the creep process obtained by KOHLSTEDT and GOETZE (1974) is quite close to that for annihilation process controlled by the dislocation climb (TORIUMI and KARATO, 1978). These facts strongly suggest that the steady state creep of olivine single crystal and also polycrystalline aggregates of olivine is mainly controlled by the dislocation climb process as stated by WEERTMAN (1970) and GOETZE and KOHLSTEDT (1973).

The Weertman type creep law becomes,

$$\dot{\epsilon} = A\sigma^3 \exp(-(E_C + PV^*)/RT), \quad (1)$$

in which $\dot{\epsilon}$, σ , E_C , and V^* are strain rate, differential stress, activation energy, and activation volume of creep process, respectively. A is a constant. STOCKER and ASHBY (1973) have given $V^* = 11.40$ cm³/mol, and $E_C = 150$ kcal/mol, but we assume $E_C = 125$ kcal/mol and $V^* = 14$ cm³/mol (KARATO, 1977). The coefficient A is estimated as 20 sec⁻¹ bar⁻³ from the least square fitting of DURHAM and GOETZE's data (1977). The high temperature experiments by KOHLSTEDT and GOETZE (1974) and DURHAM and GOETZE (1977) have been carried out in the H₂-CO₂ gas mixture, and consequently the creep of olivine crystals probably proceeds in somewhat wet conditions. As stated by GRIGGS (1974) on SiO₂ aggregates, the component OH⁻¹ can agitate the glide mobility of dislocations. It still remains as a problem whether the component OH⁻¹ also affects the climb mobility of dislocations, which controls the steady state creep. Climbing of dislocations is made by emitting oxygen or vacancy toward other dislocations or by absorbing one (NABARRO, 1967). Thus, the dislocation climb is governed by diffusion of oxygen. As the diffusivity

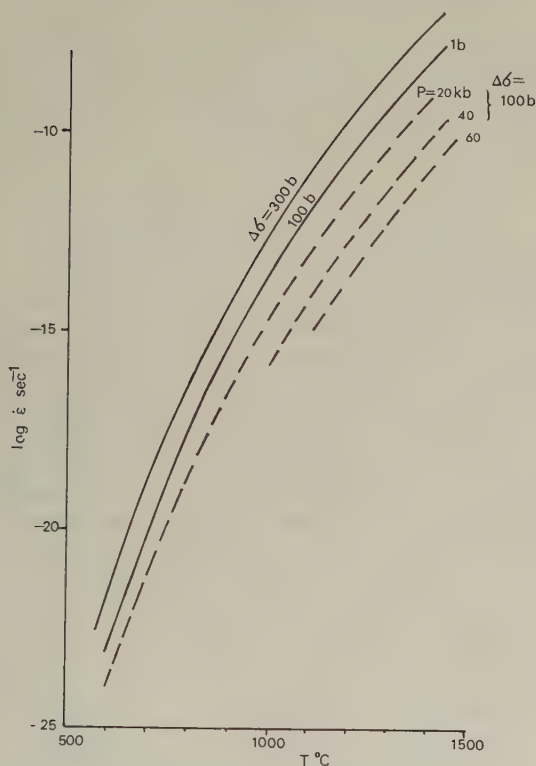


Fig. 4. Isostress curves under various hydrostatic pressures in temperature-strain rate diagram.

of oxygen in crystal probably depends on the concentration of OH^{-1} ion, it is suggested that the climb mobility of dislocations, that is, the creep rate is somewhat affected by presence of that ion. However, as we have no data on creep equation depending upon the content of H_2O in olivine, it is assumed in this paper that the upper mantle materials contain some amounts of H_2O or that the OH^{-1} -dependence of creep equation is negligible.

In Fig. 4, the isostress curves calculated from the creep equation are shown in a temperature versus strain rate diagram for various hydrostatic pressures. In this diagram, we also ignore the Nabarro-Herring and Coble creep which are preceded by oxygen-self diffusion because they are predominant in very low stress and high temperature region (STOCKER and ASHBY, 1973). It is suggested that the strain rate depends mainly on temperature but slightly on stress and pressure within the range of variation of them as shown in Fig. 4.

5. Temperature Distribution under the Island Arc

As stated in the previous sections, the temperature distribution of the upper mantle is quite important for calculating strain rate in the upper mantle. The temperature distribution under island arc has been simulated using some geophysical constraints by HASEBE *et al.* (1970), TOKSÖZ *et al.* (1971) and others. They have weighted on the surface heat flow of the island arc and the temperature distribution on the surface of the descending slab. But, their temperature distributions cannot explain the petrological data on perido-

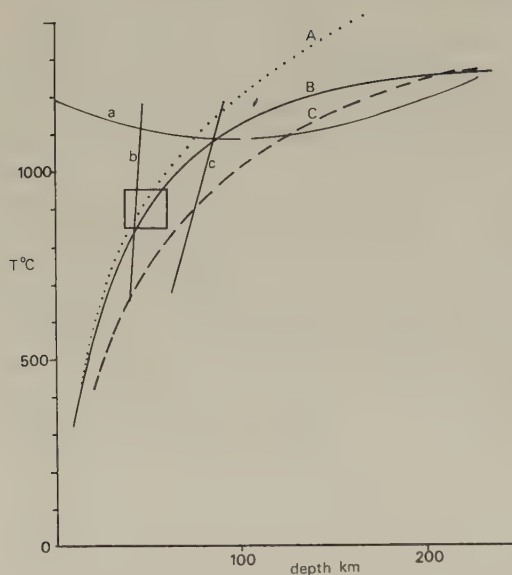


Fig. 5. Temperature distribution under island arc. A, Toksöz *et al.* (1971); B, geotherm used in this paper; C, Hasebe *et al.* (1970). a, wet solidus of peridotite by Kushiro *et al.* (1968); b, boundary between plagioclase and spinel peridotite; c, boundary between spinel and garnet peridotite (Kushiro and Yoder, 1966). Square shows the possible conditions of studied spinel lherzolite xenoliths in Japan.

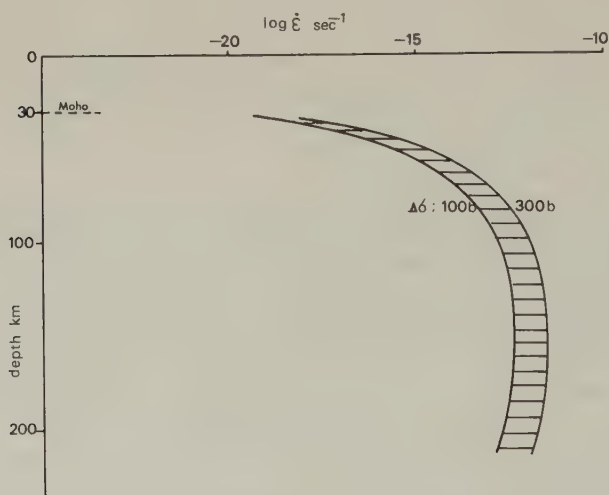


Fig. 6. Strain rate distribution in the upper mantle under the Island Arc of Japan.

tite xenoliths and seismological data. As clarified by OBATA (1972), FUJII (1974) and TAKAHASHI (1976), peridotite xenoliths of the Island Arc of Japan are commonly spinel lherzolite and plagioclase-spinel lherzolite, and their equilibration temperatures are ranging from 900 to 1,000°C. As shown in Fig. 5, these data are deviated toward high temperature regions from the geotherm by HASEBE *et al.* (1970) under the Back Arc region. On the other hand, the geotherm by TOKSÖZ *et al.* (1971) is running across the region much above solidus of wet peridotite (KUSHIRO *et al.*, 1968) below 70 km depth. FUJISAWA (1968) has deduced the temperature of $1,300 \pm 100^\circ\text{C}$ at 375 km depth near Japan, combining the experimental condition of spinel-olivine transition and seismological data.

In this paper, we use a geotherm B in Fig. 5 of which shallower part is close to TOKSÖZ *et al.*'s geotherm (1971) and deeper part to HASEBE *et al.*'s one (1970). This assumption means a high thermal conductivity of the upper mantle compared with that of HASEBE *et al.* (1970) due to rising partially molten liquid. The geotherm B satisfies the surface heat flow of 2.0–3.0 HFU.

6. Strain Rate Distribution in the Upper Mantle

Strain rate distribution in the upper mantle can be estimated under the assumption of negligible effect of partial melting on it. Though a large degree of partial melting, of course, can make the strain rate increase, presence of liquid less than some per cents does not probably increase the strain rate (STOCKER and ASHBY, 1973). In this paper the strain rate of the upper mantle is inferred from the flow law of olivine single crystals proposed by KOHLSTEDT and GOETZE (1974) and DURHAM and GOETZE (1977) as mentioned previously. Figure 6 shows the strain rate as a function of depth. An increase of strain rate from 30 to 100 km depth of the upper mantle is governed almost by the geothermal gradient, but below 100 km depth it is affected by the pressure.

It is important that the strain rate in the upper mantle of 100–200 km depth is relatively uniform around 10^{-13} – 10^{-12} sec $^{-1}$, and it abruptly decreases with decreasing depth. The mantle from 30 to 100 km depth is, therefore, considered as a rigid layer and that below 100 km depth is a soft layer. The corresponding Newtonian viscosity, defined as $\eta = \sigma / \dot{\epsilon}$, of the soft layer is about 10^{15} – 10^{17} poise, and that of the rigid layer is 10^{18} – 10^{28} poise.

Flow velocity can be inferred under the assumption of laminar flow of the upper mantle beneath the Island Arc. The boundary conditions in this study are taken at the Moho surface and the surface of the descending slab as follows:

$$v_X = 0 \text{ at Moho surface } (z = 30 \text{ km}),$$

and

$$v_X = -10 \text{ cm/year at slab surface } (z = 200 \text{ km}).$$

Here, we consider the horizontal velocity (v_X) toward the trench as a function of depth, z . Velocity profile $v_X(z)$ is calculated as follows. The mass balance in the mantle wedge

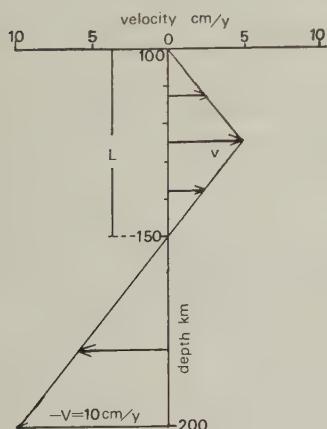


Fig. 7. A simple model of velocity profile at the reference cross section of which depth to the seismic zone is 200 km of the upper mantle of the Island Arc of Japan. The drag flow induced by descending slab is in the range of 150–200 km depth, and the return flow with thickness, L , is in 100–150 km.

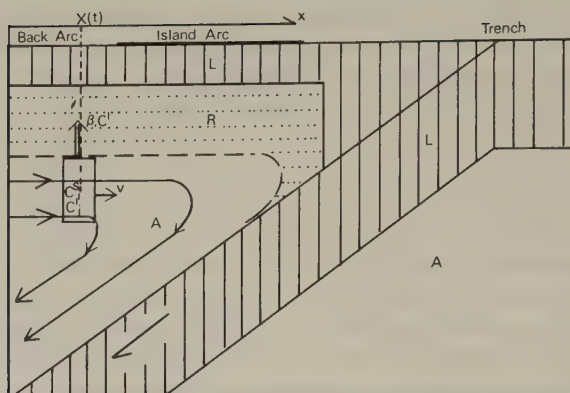


Fig. 8. A model of convective flow in the upper mantle under the Island Arc. L, lithosphere; A, asthenosphere; R, rigid mantle with strain rate less than $10^{-15} \text{ sec}^{-1}$. Other symbols refer in text.

can be considered at a reference cross section of which depth to the slab surface is 200 km (Fig. 7). As stated in the previous sections, the strain rate of the mantle from 30 to 100 km depth is very small, and it is nearly constant around 10^{-13} – $10^{-12} \text{ sec}^{-1}$ from 100 to 200 km depth. Therefore, the velocity gradient of the mantle flow should be assumed to be constant from 100 to 200 km depth. In this case, the drag flow of the mantle by descending slab induces the return flow in the shallower mantle as shown in Fig. 7. If the maximum velocity of the return flow is $v(\text{cm/year})$, and the thickness of the return flow is $L(\text{km})$, we have,

$$2Lv = 10(100 - L) \quad (\text{mass balance}), \quad (2)$$

and

$$2v/L = 10/(100 - L) \quad (\text{constant strain rate}). \quad (3)$$

Combining Eq. (2) with Eq. (3), we obtain

$$L = 50 \text{ km and } v = 5 \text{ cm/year.}$$

At this time, the strain rate becomes $3 \times 10^{-14} \text{ sec}^{-1}$, being quite close to the estimated strain rate in the earlier section.

7. Lateral Variation of Magma Chemistry of the Island Arc Volcanoes

The convective flow of the upper mantle under the Island Arc gives a great effect on chemistry of partially molten liquid and the upper mantle materials. Considering the continuous outflow of partially molten liquid from the moving upper mantle, we can easily expect the zone refining of the upper mantle materials. In this section, the simple model, in which the liquid supply from the deeper mantle into the moving upper mantle is zero, is considered. Rate of the upward outflow of liquid per unit volume of the mantle is $\beta (\text{year}^{-1})$ and the concentrations of a volatile component such as K_2O are C^1 in liquid, and C^s in solid phase (mantle material). It is assumed that the degree of partial melting (α) is constant and very small in the moving upper mantle and the velocity ($v \text{ km/year}$) of the return flow is also constant. Considering $C^1(x; t)$ and $C^s(x; t)$ at the distance, x , toward the trench in the two dimensional model as shown in Fig. 8, the concentrations at $x + \delta x$ becomes $C^1 + \delta C^1$ and $C^s + \delta C^s$ after δt , and volume of the outflow of liquid with

C^1 is $\beta\delta t$. Therefore, we get the following equation of mass balance of the component;

$$\alpha C^1 + (1-\alpha)C^s = \alpha(1-\beta\delta t)(C^1 + \delta C^1) + C^1\beta\delta t + (1-\alpha)(1-\beta\delta t)(C^s + \delta C^s). \quad (4)$$

Assuming the constant concentration ratio $k = C^s/C^1$, Eq. (4) becomes,

$$\delta C^1/C^1 = -\beta\phi\delta t, \quad (5)$$

$$\text{with } \phi = (1-k-\alpha)/(\alpha+k). \quad (6)$$

If α is very small against k , Eq. (5) becomes

$$\phi \doteq (1/k-1). \quad (7)$$

Combining Eq. (5) with $v\delta t = \delta x$, we obtain,

$$\delta C^1/C^1 = -\beta\phi\delta x/v. \quad (8)$$

Integrating Eq. (8), we have,

$$C^1/C_0^1 = \exp(-\beta\phi x/v), \quad (9)$$

In which C_0^1 is a constant.

Therefore, the concentration ratio C_r^1/C^1 , in which C_r^1 is the concentration of the volatile component in the liquid at the volcanic front, becomes,

$$C_r^1/C^1 = \exp(-\beta\phi X/v), \quad (10)$$

where X is the distance from the volcanic front, $x_f - x$.

Consequently, it is suggested that the concentration of a volatile component ($k < 1$) decreases toward the volcanic front in the upper mantle materials and in the partially molten liquid. Applying Eq. (10) to the lateral variation of magma chemistry of the Island Arc volcanism, we must know the rate of upward outflow of liquid and the mean velocity of the return flow of the upper mantle.

According to NAKAMURA (1974) and SUGIMURA (1974), the eruption rate of volcanic rocks is estimated to be 10^{-2} – 10^{-3} km³/year \times 100 km in the Island Arc of Northeast Japan. Taking the width of the Island Arc of Japan as 200 km and the thickness of the return flow as 50 km as discussed in the previous section, the rate of outflow, β , should be approximated as 10^{-8} – 10^{-9} year⁻¹. Consequently, if the mean velocity of the return flow is 10^{-5} km/year, and the concentration ratio, k , is 0.1 for K₂O, the amplification factor, $\beta\phi/v$ is in the order of 10^{-2} – 10^{-3} km⁻¹. Figure 9 shows the theoretical changes of K₂O-content in liquid for various eruption rates.

HATHERTON and DICKINSON (1969) and NIELSON and STOIBER (1973) have suggested that the K₂O-content both in basaltic andesite (SiO₂=55 wt%) and andesite (SiO₂=60 wt%) decreases toward the volcanic front from the Back Arc region. The lateral vari-

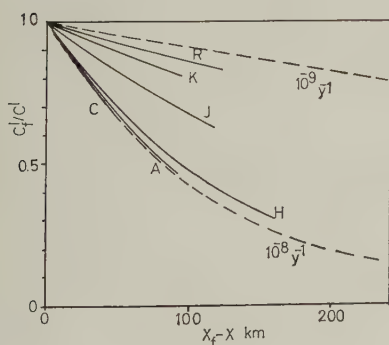


Fig. 9. Theoretical change of K₂O-content in the liquid against the distance from the volcanic front, and the lateral variations of K₂O-content in basaltic andesite (SiO₂=55wt%) of Ryukyus (R), Kurile-Kamchatka (K), Java (J), Central America (C), Aleutian (A) and Northeast Japan (H) (cited from NIELSON and STOIBER (1973)). Abbreviations are follows: C_f^1 ; K₂O-content at the volcanic front, $x_f - x$; distance from the volcanic front.

ations of K_2O -content in basaltic andesite obtained by them are shown in Fig. 9. It is suggested that the range of chemical variation of natural rocks is just in the calculated range, and the theoretical change is quite similar to the lateral variation of magma chemistry of volcanic rocks.

If the lateral change of K_2O -content of the Island Arc volcanism can be interpreted by the zone refining model discussed here, other components such as FeO , Na_2O and Al_2O_3 , of which the ratio, k , is smaller than 1, should be enriched in volcanic rocks with increasing distance from the volcanic front. But, considering that k is close to 1, the amplification factor of such components is less than that of K_2O by a factor of 10 or less. Therefore, the ratio of C_r^1/C^1 of FeO and Na_2O may be less than 0.9 at the distance of 100 km from the volcanic front.

Figure 9 also suggests that the eruption rate of island arcs of Java, Kurile-Kamchatka, and Ryukyu is less than that of island arcs of Central America, Aleutian, and Northeast Japan, if the mean velocity of the return flow of the upper mantle is in the same order.

8. Conclusion

The dislocation densities of olivine grains from Ichinomegata, Sannomegata, Oki-Dogo, Hamada and Takashima are in the range of 10^6 – 10^7 cm^{-2} . The data lead to the following conclusions:

- 1) The actual differential stress of the upper mantle is in the range of 100–300 bars, and it is similar to that of the Pacific Plate deduced from spinel lherzolite xenoliths of Salt Lake of Hawaii.
- 2) The strain rate in the mantle from 30 to 100 km depth is less than 10^{-15} sec^{-1} , and it is constant around 10^{-13} – 10^{-2} sec^{-1} from 100 to 200 km depth.
- 3) Convective flow is inferred and it is composed of drag and return flow induced by descending slab.
- 4) Return flow of the upper mantle causes the lateral change of magma chemistry and upper mantle materials due to continuous upward outflow of the partially molten liquid from the moving upper mantle.

I thank Drs. I. Kushiro, S. Aramaki, Y. Nakamura and S. Karato of University of Tokyo for many discussions. I am also indebted to Drs. T. Fujii, H. Fukuyama and E. Takahashi of University of Tokyo for discussions.

REFERENCES

- AOKI, K., Materials derived from upper mantle—Ejected accidental fragments from Ichinomegata crater, *Kagaku*, **42**, 615–621, 1973 (in Japanese).
- CARTER, N.L. and H.G. AVELLALMANT, High temperature flow of dunite and peridotite, *Geol. Soc. Am. Bull.*, **81**, 2181–2202, 1970.
- DURHAM, W.B. and C. GOETZE, Plastic flow of oriented single crystals of olivine. 1. Mechanical data, *J. Geophys. Res.*, **82**, 5737–5753, 1977.
- DURHAM, W.B., C. GOETZE, and B. BLAKE, Plastic flow of oriented single crystals of olivine. 2. Observation and interpretation of the dislocation structures, *J. Geophys. Res.*, **82**, 5755–5770, 1977.
- FUJII, T., Petrology of Hamada nephelinite and associated ultramafic inclusions, PhD Thesis of University of Tokyo, 1974.
- FUJISAWA, H., Temperature and discontinuities in the transition layer within the earth's mantle. Geophysical application of the olivine-spinel transition in the Mg_2SiO_4 – Fe_2SiO_4 system, *J. Geophys. Res.*, **73**, 3281–3294, 1968.
- GOETZE, C. and D.L. KOHLSTEDT, Laboratory study of dislocation climb and diffusion in olivine, *J. Geophys. Res.*, **78**, 5961–5971, 1973.

- GRIGGS, D.T., A model of hydrolytic weakening in quartz, *J. Geophys. Res.*, **79**, 1653–1661, 1974.
- GUEGUEN, Y., Dislocations in mantle peridotite nodules, *Tectonophysics*, **39**, 231–254, 1977.
- HASEBE, K., N. FUJII, and S. UYEDA, Thermal process under island arcs, *J. Geophys. Res.*, **10**, 1–13, 1970.
- HATHERTON, T. and W.R. DICKINSON, The relationship between andesitic volcanism and seismicity in Indonesia, the Lesser Antilles and other island arcs, *J. Geophys. Res.*, **74**, 5301–5310, 1969.
- HÜTHER, W. and B. REPPICH, Dislocations structure during creep of MgO single crystals, *Phil. Mag.*, **28**, 363–371, 1973.
- KARATO, S., Rheological properties of the materials composing the earth's mantle, PhD Thesis of the University of Tokyo, 1977.
- KOHLSTEDT, D.L. and C. GOETZE, Low stress high temperature creep in olivine single crystals, *J. Geophys. Res.*, **79**, 2045–2051, 1974.
- KOHLSTEDT, D.L. and J.B. VANDER SANDE, An electron microscopy study of naturally occurring oxidation produced precipitates in iron-bearing olivines, *Contrib. Mineral. Petrol.*, **53**, 13–24, 1975.
- KUNO, H. and K. AOKI, Chemistry of ultramafic nodules and their bearing on the origin of basaltic magmas, *Phys. Earth Planet. Inter.*, **3**, 273–301, 1970.
- KUSHIRO, I. and H.S. YODER, Anorthite-forsterite and anorthite-enstatite reactions and their bearing on the basalt-eclogite transformation, *J. Petrol.*, **7**, 337–362, 1966.
- KUSHIRO, I., Y. SYONO, and S. AKIMOTO, Melting of a peridotite at high pressures and high water pressures, *J. Geophys. Res.*, **73**, 6023–6029, 1968.
- MCGREGOR, I.D., The system MgO-Al₂O₃-SiO₂: Solubility of Al₂O₃ in enstatite for spinel and garnet peridotite compositions, *Am. Mineral.*, **59**, 110–119, 1974.
- NABARRO, F.R.N., *Theory of Crystal Dislocations*, 821 pp., Clarendon Press, Oxford, 1967.
- NAKAMURA, K., Preliminary estimate of global volcanic production rate, in *The Utilization of Volcano Energy (Proc. of a U. S.-Japan Coop. Sci. Semin.)*, edited by J.L. Golp and A.S. Furumoto, pp. 273–285, 1974.
- NIELSON, D.R. and R.E. STOIBER, Relationship of potassium content in andesitic lavas and depth to the seismic zone, *J. Geophys. Res.*, **78**, 6887–6892, 1973.
- OBATA, M., Petrography and petrogenesis of ultramafic inclusions from Takashima, northern Kyushu, Japan, Ms. Thesis of Kanazawa University, 1972.
- RALEIGH, C.B. and S.H. KIRBY, Creep in the upper mantle, *Mineral. Soc. Am. Spec. Pap.*, **3**, 113–121, 1970.
- SLEEP, N. and M.N. TOKSOZ, Evolution of magrinal basins, *Nature*, **233**, 548–550, 1971.
- STOCKER, R.L. and M.F. ASHBY, On the rheology of the upper mantle, *Rev. Geophys. Space Phys.*, **11**, 391–426, 1973.
- STREB, G. and B. REPPICH, The steady state deformation and dislocation structure of pure and Mg-doped LiF single crystals. II. Etch-pit studies of dislocation structure, *Phys. Stati. Solidi*, **16a**, 493–505, 1973.
- SUGIMURA, A., Island arcs. in *Physics of the Earth*, edited by Phys. Soc. Japan, Maruzen, pp. 189–222, 1974.
- TAKAHASHI, E., Ultramafic xenoliths of alkali basalt, Oki-Dogo Islands in the Japan Sea, Ms. Thesis of University of Tokyo, 1976.
- TOKSÖZ, M.N., J.W. MINEAR, and B.R. JULIAN, Temperature field and geophysical effects of a downgoing slab, *J. Geophys. Res.*, **76**, 1113–1138, 1971.
- TORIUMI, M., Dislocation structure of olivine in the Mt. Higashi Akaishi dunite mass in the Sambagawa metamorphic terrane of Japan, *J. Geol. Soc. Jpn.*, **84**, 299–308, 1978.
- TORIUMI, M. and S. KARATO, Experimental studies on the recovery process of deformed olivines and the mechanical state of the upper mantle, *Tectonophysics*, **49**, 79–95, 1978.
- WEERTMAN, J., Dislocation climb theory of steady state creep, *Trans. Am. Soc. Met.*, **61**, 681–694, 1968.
- WEERTMAN, J., The creep strength of the earth's mantle, *Rev. Geophys. Space Phys.*, **8**, 145–168, 1970.

SEISMIC ACTIVITY AND PORE PRESSURE ACROSS ISLAND ARCS OF JAPAN

Naoyuki FUJII* and Kei KURITA**

* *Department of Earth Sciences, Kobe University, Kobe Japan*

** *Geophysical Institute, University of Tokyo, Tokyo Japan*

(Received July 17, 1978; Revised November 6, 1978)

Recent seismic researches have revealed the variation of shallow seismic activity across the trench-arc system of Japan, which is characterized by, A) a high activity throughout the crust and upper mantle between trench axis and "aseismic front", B) a low activity between "aseismic-front" and volcanic front, and C) a moderate activity within the upper crust behind volcanic front. This variation of shallow seismicity across the island arc is explained by the effects of pore pressure in the crust, based on laboratory experiments of stick-slip and stable-sliding movements combined with temperature distribution estimated from terrestrial heat flow and thermal model of subducting slab. High pore pressure is expected in the low activity area (region B). Pore pressure is controlled mainly by 1) fluid supply from below (released from subducting oceanic crust), and 2) permeability distribution in the crust and upper mantle. Dehydration process in subducting slab has a great influence on shallow seismic activity.

1. Introduction

Among geophysical and geological observations, the spatial distribution of earthquakes is one of the most direct indications of plate interactions. Recent investigations of precise determination of microearthquake foci in the plate convergence regions have revealed some detailed features of the intraplate shallow seismicity (e.g., OIKE, 1977; TAKAGI *et al.*, 1977), and interplate seismicity such as the double-planed structure of deep seismic zone (TSUMURA, 1973; UMINO and HASEGAWA, 1975; ENGDahl and SCHOLZ, 1977; HASEGAWA *et al.*, 1978).

TAKAGI *et al.* (1977) noted that in the northeast Japan arc, shallow intraplate earthquakes occur behind (i.e., landward of) the volcanic front and are confined in the upper crust having a compressional wave velocity (V_p) of 6.0 km/sec (depths less than 20 km). In the southwestern part of Japan, OIKE (1977) showed that frequency distribution of focal depths has a maximum at 10–15 km and is mostly confined within the V_p —6.0 km/sec layer. YAMASHINA *et al.* (1978) pointed out that a low-seismicity region (frontal arc) between the volcanic front and "aseismic front" (YOSHII, 1975) can be observed in various regions in the circum Pacific trench-arc systems. Since this low activity region has a width of 50–100 km, it is called "aseismic belt." Major seismic activity is concentrated in the prismatic region, which is bounded by "aseismic front" and trench axis. We call this region as "seismic prism." Actually these characteristic features are most distinguishable in the northeastern part of Japan (MOGI, 1967), where is one of the most highly investigated areas through microearthquake and crustal deformation observation network of Tohoku University (TAKAGI *et al.*, 1977), and other geophysical observations as discussed by YOSHII (1978).

A shallow earthquake is considered to be the stick-slip sliding instability on a pre-existing fault (BYERLEE and BRACE, 1969). Although many difficulties and uncertainties still exist in the application of laboratory experiments on stick-slip and stable-sliding phenomena to the real earth (BRACE, 1972), the microearthquake activity in the crust of trench-arc systems can be understood through these phenomena at least qualitatively. The depth-limit of the occurrence of shallow earthquakes of the San Andreas fault have been tried to be explained by the transition from stick-slip to stable-sliding caused by temperature variation (BRACE and BYERLEE, 1970). STESKY and BRACE (1973) suggested that existence of fault gauge or high pore pressure could explain the observed low frictional stresses of the San Andreas fault.

In this paper, we try to explain the vertical and horizontal variation of shallow seismic activity across the trench-arc systems by means of the effects of pore pressure on the stick-slip to stable-sliding transition for pre-existing fault deduced from laboratory experiments. When we consider the temperature distribution and thermal processes beneath island arcs (e.g., HASEBE *et al.*, 1970; ANDERSON *et al.*, 1978), we can infer that variations of pore pressure should be closely related with the water released by the dehydration reaction of subducting oceanic crust (ANDERSON *et al.*, 1976; DELANY and HELGESON, 1978; R.N. Anderson, personal communication, 1978), andesitic volcanisms (e.g., RINGWOOD, 1974; OXBURGH and TURCOTTE, 1976; ANDERSON *et al.*, 1978), and the evolution of frontal arc structure (KARIG, 1974; KARIG and SHARMAN, 1975).

2. Cross Sectional Structure and Shallow Seismicity

Cross sectional distributions (a band about 100 km wide) of released seismic energy and microearthquake foci across the northeastern part of Japan along 39.5°N are shown in Fig. 1a, b, respectively. In estimating seismic energy (E , in erg) by the use of the relation $\log E = 1.5 M + 11.8$, the earthquakes that occurred during 17-year period (1960–1976) with focal depths less than 60 km were selected, whose magnitude (M) were tentatively taken from the Seismological Bulletin of the Japan Meteorological Agency (JMA). The distributions of microearthquake foci (Fig. 1b) were reproduced after TAKAGI *et al.* (1977) in which data were taken over one and a half years from April, 1975 to October, 1976.

As seen in Fig. 1a, b, shallow intraplate earthquakes are distributed behind the volcanic front and clearly separated by "aseismic belt." This belt (hereafter called region B) would correspond to the non-volcanic arc or the frontal arc (KARIG, 1974), and its nature of very low seismic activity throughout the crust and upper mantle is clearly identified both in microearthquake foci distribution for one and a half years and in seismic energy release for 17 years. A thick line segment on the top of Fig. 1b indicates the land area, and the accuracy of the location of earthquakes is quite high, about 2 km in epicenter and less than 3 km in focal depth at least in and near the land area (HASEGAWA *et al.*, 1978).

Figure 2 shows another example of cross sectional structure of seismic activity in western part of Japan (Kyushu). Data were taken from the Seismological Bulletin of the JMA (1960–1976). The distribution of the seismic energy release and the earthquake foci are similar to that in the northeastern Japan, although the accuracy of the determination of earthquake foci are not so good because of the lack of microearthquake observation network.

The crustal structure derived from explosion seismic observation (YOSHII and ASANO, 1972; RESEARCH GROUP FOR EXPLOSION SEISMOLOGY, 1977) are also indicated in Fig. 1b.

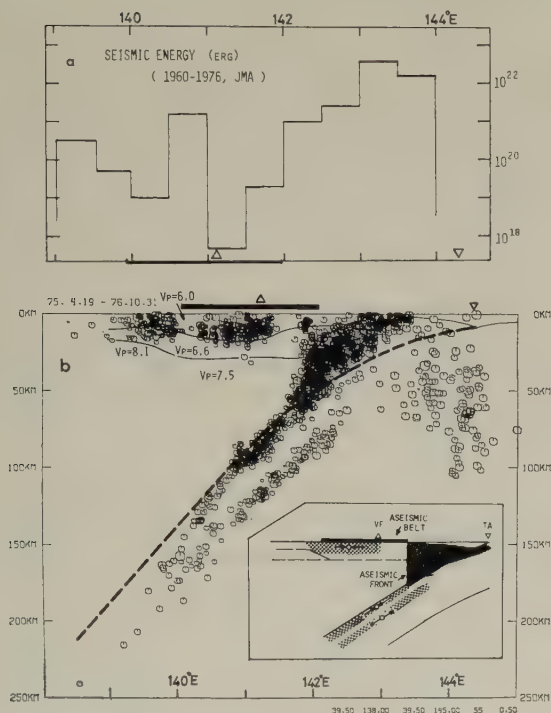


Fig. 1. (a) Cross sectional distributions of released seismic energy along the 1° wide belt at 39.5°N , in units of erg summed over 17 years by $1/2$ degree interval in the northeastern Japan. Magnitude data were taken from the Seismological Bulletin of Japan Meteorological Agency (JMA) during 1960–1976. (b) Cross sectional distribution of microearthquake foci in the same belt as in Fig. 1a from April, 1975 to Oct., 1976 (after TAKAGI *et al.*, 1977). In insert, a schematical explanation of the seismicity and focal mechanism is shown (modified after YOSHII, 1978).

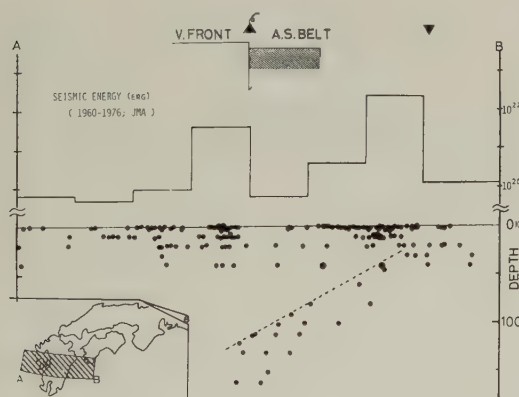


Fig. 2. Cross sectional distributions of released seismic energy (top) and earthquake foci (bottom) across the western part of Japan (Kyushu) based on the JMA data during 1960–1976. Data are taken from the hatched area in the insert.

The concentration of shallow earthquake foci into the $V_p=6.0$ km/sec layer is obvious at least beneath the land area. Shallow foci are distributed behind the volcanic front to the off coast of Japan Sea (hereafter called region C). Shallow seismic activity in the Japan Sea (off Oga peninsula) seems to be extended to the lower crust where the upper crust becomes thin. This may be related to the activity along eastern margin of the Japan Sea (FUKAO and FURUMOTO, 1975).

Major seismic activity is found between the trench and “aseismic front” (hereafter called region A, “seismic prism”). This activity continued to the upper plane of the

double-planed deep seismic zone (HASEGAWA *et al.*, 1978). The boundary between upper lithosphere and subducting Pacific plate is estimated and shown by a broken curve in Fig. 1b. P_n velocity of this region A is 8.1 km/sec and clearly contrasting with that of 7.5 km/sec beneath the Japanese land area. The eastern boundary of this low P_n region coincides with the aseismic front (RESEARCH GROUP FOR EXPLOSION SEISMOLOGY, 1977; YOSHII, 1978). The scattered earthquake foci beneath the trench appear to extend to a depth of 100 km. They may be the aftershocks of the great normal fault event off Sanriku (KANAMORI, 1971). But as the accuracy of hypocentral determination is relatively less in this region, there remains some possibilities of the biasing of hypocenters caused by the lateral heterogeneities in the velocity structure.

Principal stresses projected in this cross section are schematically indicated in the insert in Fig. 1b after YOSHII (1978). East-west compression (mostly thrust fault events) are observed for shallow earthquakes in both region A and C. As pointed out by YOSHII (1978), low-angle thrust fault events along the inferred upper surface of the descending lithosphere occur only ocean side of the aseismic front.

Temperature distribution across the northeastern Japan arc is estimated based on a model developed by HASEBE *et al.* (1970) which satisfies the observations of terrestrial heat flow taking into account of the frictional heating along Wadati-Benioff zone below 60 km depth and penetrative convection heat transfer in the upper mantle wedge. To estimate the temperature at the upper-most mantle beneath region C (volcanic area), petrological model by TAKAHASHI (1978) is also referred to. In Fig. 3, the temperature and velocity structure for the three regions (A, B and C) are schematically indicated. Average values of terrestrial heat flow is shown in the upper diagram of Fig. 3 (after HASEBE *et al.*, 1970).

Note that 500°C isotherm nearly coincides with the lower limit of intraplate shallow seismicity in region C. Temperatures at the depth of 10–20 km are more or less similar in region C and region B, but are significantly lower in region A. Nearly vertical isotherms for temperatures higher than 300°C are dominant feature in "seismic prism." Although precise location of vertical isotherms in this region would vary with model parameters, the high seismic activity could be closely related with the low temperature and low angle thrust fault along the subducting lithosphere.

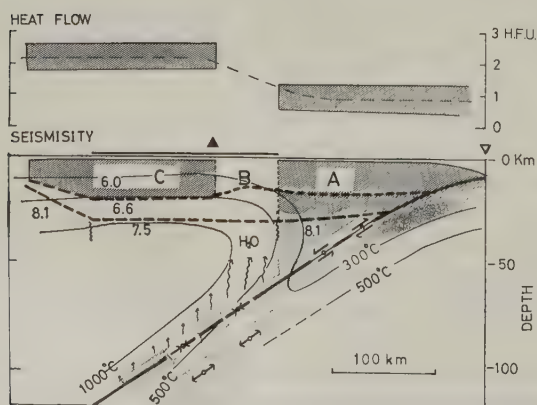


Fig. 3. Cross sectional diagrams of heat flow (top) and structure (bottom) beneath island arcs. Numerals in the bottom figure indicate the values of V_p by RESEARCH GROUP FOR EXPLOSION SEISMOLOGY (1977).

3. Variation of Pore Pressure across Trench-Arc Systems

There are many factors closely related to the observed variation in seismic activity across the trench-arc systems. Among them, followings are likely to be important; 1) the differences of strength due to different types of constituent material, 2) the differences of stress level due to interactions of subducting plate and/or flow law of the crustal rocks, and 3) the variation of effective pressure acting on pre-existing faults.

The first factor seems to be less important if we consider that shallow earthquakes are explained by stick-slip motion of pre-existing fault. STESKY *et al.* (1974) showed no difference existed in the boundary of stick-slip to stable-sliding transition between granite and gabbro, that are considered to be representative rock types of 6.0 km/sec layer and 6.6 km/sec layer respectively. It seems unlikely that this factor alone can explain both the low seismicity in region B and the depth-limit in region C.

The second factor could be a likely source. As subducting slab causes a drag force along Wadati-Benioff zone and a tilting of overlying continental plate wedge toward the trench during interseismic period, local deviatoric tensile stress region appears around volcanic front (SMITH and TOKSÖZ, 1972; BISCHKE, 1974; NEUGEBAUER and BREITMAYER, 1975). YAMASHINA *et al.* (1978) noted that the horizontal contractive strain perpendicular to the trench axis has a local minimum which coincides to aseismic belt (region B) based on a calculation to fit the observed crustal deformation in eastern Hokkaido by SHIMAZAKI (1974). The location and width of the local minimum in contractive horizontal strain depend on the depth and dip angle along which the drag force due to subducting slab is assumed (e.g., SENO, 1978). Since this local minimum becomes less clear with depth gradually, a sharpness of aseismic front throughout the crust and upper mantle and the concentration of seismicity in the upper crust in region C should need additional explanations.

KOBAYASHI (1976) discussed that the constituent material throughout the crust of Japan arc is likely to be granodioritic rocks and flow law of quartz could be applicable to explain the depth-limits of shallow intraplate seismicity. He assumed that the seismically active region corresponds to the region where a shear stress is higher than the critical value estimated from the flow law of granodioritic rocks (represented by quartz) at geological strain rate of $10^{-14} \text{ sec}^{-1}$. Combining the temperature distribution estimated from terrestrial heat flow and a critical shear stress of ≤ 100 bars (i.e., similar to the stress drop from focal mechanism), he concluded that 300°C isotherm would correspond to the depth-limits of shallow intraplate seismicity. It would, however, be difficult to explain the existence of the aseismic belt when we consider the temperature distribution in the belt (Fig. 3).

As a consequence, we suggest that pore pressure in the crust would vary from trench to back arc, that is, the third factor may be responsible for the shallow seismic activity in the plate convergence area. Stick-slip and stable-sliding phenomena are controlled by temperature and effective pressure (confining pressure minus pore pressure) as shown by laboratory experiments on pre-existing faults (STESKY *et al.*, 1974). If we consider that seismically active region corresponds to the region of stick-slip sliding, less active region of similar depth and temperature should have higher pore pressure. Left diagram in Fig. 4 shows stick-slip and stable-sliding regions in the temperature-effective pressure diagram after STESKY *et al.* (1974) and BRACE (1977). Dashed curve with hatches indicates the

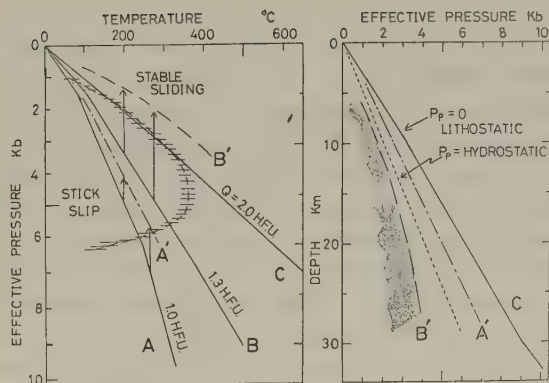


Fig. 4. In the left, stick-slip to stable-sliding transition boundary (a dashed curve with hatches) is shown in the temperature-effective pressure diagram (after STESKY *et al.*, 1974). Solid lines labelled A, B and C indicate representative geotherms corresponding to the regions in Fig. 3. Surface heat flow, Q (1 H.F.U. = 10^{-6} cal/sec-cm²), for each region is also indicated, in which depth scale to the right should be referred to when pore pressure is zero. Since the high pore pressure makes the effective pressure low, the geotherms move upward as indicated by arrows (lines A' and B'). In the right diagram, effective pressure versus depth is shown for various pore pressures (see text).

boundary of stick-slip to stable-sliding transition, and should be regarded as an iso-stress drop curve (experimentally zero stress drop). Depths in the righthand side correspond to the case of zero pore pressure. Solid lines labelled A, B and C show representative temperature distributions within the crust in respective regions estimated from heat flow and appropriate heat generation in the crust. A representative surface heat flow (Q) in each region is also indicated.

If we assume laboratory determined stick-slip to stable-sliding transition actually corresponds to seismically active to inactive boundary, effective pressure in the regions A and B should be lowered to the lines of A' and B', respectively, as shown by arrows in the left diagram in Fig. 4. To the right in Fig. 4, effective pressure with depth thus expected is indicated for each region. The curves with pore pressure (P_p) equal to zero and to the hydrostatic pressure are also shown by solid and dotted lines. Judging from this figure, we can estimate that the pore pressure is highest in region B (aseismic belt) and lowest in region C. It may be expected that P_p is nearly hydrostatic or the ratio of P_p to total pressure (P_t) ranges 0.1 to 0.5 in region A, and $P_p/P_t \geq 0.5$ and ≤ 0.2 for regions B and C respectively.

However, as already pointed out by BRACE (1972) and STESKY and BRACE (1973), many difficulties and uncertainties still exist to apply above assumptions to the actual earthquakes. For example, experimentally determined frictional shear stress and stress drop are higher than those of actual earthquakes (STESKY and BRACE, 1973), acoustic emission is observed even in stable-sliding region (i.e., STESKY, 1975), and fault gauge in actual fault surface in the earth could have influenced on the stick-slip to stable sliding transition boundary (BRACE, 1977).

Although the existence of precise correspondence between the stick-slip phenomenon observed in laboratory experiments and earthquakes is a fundamental problem to be investigated more extensively, our explanation and conclusion would not be affected so much at least in a relative and qualitative sense.

A high seismicity in the upper mantle beneath the seismic wedge could be understood following the idea similar to that of KOBAYASHI (1976). If we consider that mantle is composed of peridotitic rocks, flow law of olivine could be applied to estimate the shear stress. Using the values both for wet and dry olivines with strain rate of 10^{-14} sec⁻¹ (KIRBY, 1977), the estimated shear stress in the upper mantle at the aseismic front (Fig. 3)

is about a few kb and 100 bars for the isotherms of 500°C and 750°C, respectively. Below this temperature, that is, from the aseismic front toward the trench, shear stress becomes high and rocks would become brittle. Aseismic front could be understood this way as far as the upper mantle is concerned.

4. Discussion

At present we have no direct evidence of pore pressure differences in the upper crust of depths 5–20 km. As pointed out by STESKY *et al.* (1974), a high pore pressure region is observed in deep drill holes in California Coast Range and this region seems to correspond to the relatively low seismicity area (BERRY, 1973). The region B (aseismic belt) where we expect relatively high pore pressures, corresponds to non-volcanic frontal arc characterized by high gravity anomaly (YOSHII, 1978) and gradual uplift since Tertiary (e.g., SUGIMURA and UYEDA, 1973). To keep pore pressure high, e.g., higher than hydrostatic, it may need the supply of fluid from below and a low permeable cap rock as known in the geothermal field. Although it is generally or implicitly considered that there would be much of water (and high fluid pressure) in volcanic region (region C) relative to region B (K. Nakamura, personal communication, 1977), it does not always mean that the pore pressure is high when minerals are partially hydrated.

The current petrological view of volcanism of island arcs (e.g., RINGWOOD, 1977) suggests free water released from the subducting slab by dehydration and its interaction with the overlying mantle wedge have great influence of volcanic activity. If we consider the overlying mantle wedge to be peridotitic and in the water-saturated condition ($P_{H_2O} = P_t$), the stability field of the hydrated minerals could be estimated provided that the subducting oceanic crust is hydrous basalt and gabbro and temperature distribution in the wedge is known (DELANY and HELGESON, 1978). Figure 5 shows schematically the mineral stability boundaries for two cases of temperature distributions. We expect that partial melting zone beneath volcanic area (region C) would not extend toward the trench so much and the temperature beneath the frontal arc (region B) would be lower than 1,000°C. Thus, released free water from the subducting oceanic crust could make melt beneath region C, but not beneath region B. As the thermal regime is so complex in this mantle wedge, there could still be two possible cases, 1) no hydrous minerals and 2) talc and presumably chrysotile exist beneath region B. The former (top in Fig. 5) expects that the aseismic front nearly coincides with 750°C isotherm and released water would rise freely through the mantle. The latter (bottom in Fig. 5) expects that the temperature of the aseismic front is 500°C or less. As pointed out by DELANY and HELGESON (1978), the release of water through the dehydration of subducting oceanic crust should be controlled by the rate of heat supply from the ambient mantle or heat generated in this portion such as viscous frictional heating. Although we could not, at the moment, specify the precise depth of complete dehydration reaction in the subducting slab, most probable depth would be some 60 to 100 km in the northeastern Japan when dip angle of subducting plate is about 30° as pointed out by HASEBE *et al.* (1970). It is interesting to note that the aseismic front meets the plate-interface at about 60 km depth and earthquakes with low angle thrust fault mechanism occur only above this depth (YOSHII, 1978).

The newly released water will be highly mobile because the migration of free water would be controlled by permeable flow due to buoyancy effect as suggested by ANDERSON *et al.* (1978). Then we could expect that a large volume of released water would migrate

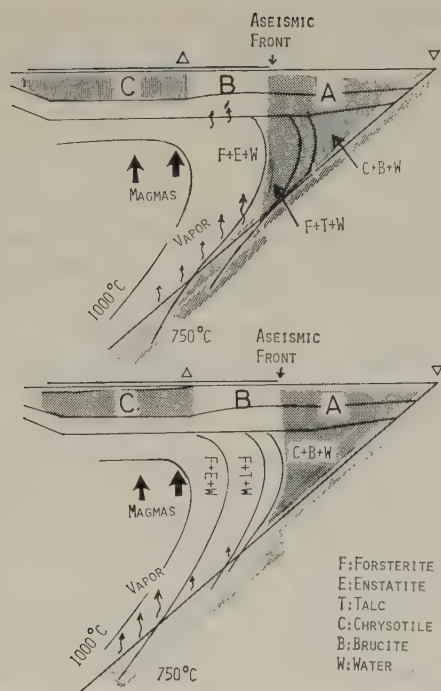


Fig. 5. Mineral stability boundaries for peridotitic mantle in the 'wedge-zone' beneath the arc-trench gap are schematically shown in two cases, when hydrous minerals are unstable (top) and stable (bottom) beneath aseismic belt (region B). Shaded areas indicate seismically active regions as in Fig. 1b.

through the upper mantle beneath region B, and the lower crust of this region would be saturated with water.

As noted in the previous section, the observation that P_n velocity of 8.1 km/sec in the seismic wedge at 30 km depth seems to be incompatible with wet peridotitic mantle model. As far as the water-saturated or hydrous mantle candidate minerals are concerned, $V_p = 8.1$ km/sec could not be explained from experiments. There may be a possibility that released free water could not reach the apex of the mantle wedge beneath the seismic wedge, and this region may be dry and non-hydrous, although we need to explain the generation of blue-schist and greenschist facies metamorphic rocks and serpentine.

In summary, though no direct evidence for high pore pressure in region B can be demonstrated and no quantitative correspondence between stick-slip phenomenon and shallow seismicity, the migration of released water from subducting oceanic crust would have an important role in the mantle wedge and lower crust.

Our conclusion could be tested by 1) precise determination of stress drop variation with depth or across region B, 2) more investigation of fine crustal velocity structure, 3) deep drilling in respective region to estimate average pore pressure, and 4) the investigation of thermal regime in the wedge beneath arc-trench gap taking into account of dynamical processes and influence of fluid phases.

We thank A. Takagi, A. Hasegawa, T. Yoshii, T. Seno and R.N. Anderson for discussions and access to unpublished manuscripts. Critical comments by K. Nakamura, S. Uyeda, T. Hirasawa and Y. Kobayashi were helpful.

We wish to thank T. Asada and A. Takagi for their kind encouragements and to H. Wada for typing the manuscript.

REFERENCES

- ANDERSON, R.N., S. UYEDA, and A. MIYASHIRO, Geophysical and geochemical constraints at converging plate boundaries. Pt. I; Dehydration in the down going slab, *Geophys. J. R. Astr. Soc.*, **44**, 333–357, 1976.
- ANDERSON, R.N., S.E. DELONG, and W.M. SCHWARZ, Geophysical and geochemical constraints at converging plate boundaries. Pt. II; A thermal model for subduction with dehydration in the down going slab, *Tectonophysics*, 1978 (in press).
- BERRY, F.A.F., High fluid potentials in California Coast Ranges and their tectonic significance, *Bull. Am. Assoc. Pet. Geol.*, **57**, 1219–1248, 1973.
- BISCHKE, R.E., A model of convergent plate margins based on the recent tectonics of Shikoku, Japan, *J. Geophys. Res.*, **79**, 4845–4857, 1974.
- BRACE, W.F., Laboratory studies of stick-slip and their application to earthquakes, *Tectonophysics*, **14**, 189–200, 1972.
- BRACE, W.F., Recent laboratory studies of earthquake mechanics and prediction. *J. Phys. Earth*, **25**, Suppl., S185–S202, 1977.
- BRACE, W.F. and J.D. BYERLEE, California earthquakes: Why only shallow focus? *Science*, **168**, 1573–1575, 1970.
- BYERLEE, J.D. and W.F. BRACE, High-pressure mechanical instability in rocks, *Science*, **164**, 713–715, 1969.
- DELANY, J.M. and H.C. HELGESON, Calculation of the thermodynamic consequences of dehydration in subducting oceanic crust to 100 kb and 800°C, *Am. J. Sci.*, **278**, 638–686, 1978.
- ENGDAHL, E.R. and C.H. SCHOLZ, A double Benioff zone beneath the central Aleutians; An unbending of the lithosphere, *Geophys. Res. Lett.*, **4**, 473–476, 1977.
- FUKAO, Y. and M. FURUMOTO, Mechanism of large earthquakes along the eastern margin of the Japan Sea, *Tectonophysics*, **25**, 247–266, 1975.
- HASEBE, K., N. FUJII, and S. UYEDA, Thermal processes under island arcs, *Tectonophysics*, **10**, 335–355, 1970.
- HASEGAWA, A., N. UMINO, and A. TAKAGI, Double-planed structure of the deep seismic zone in the northeastern Japan arc, *Tectonophysics*, **47**, 43–58, 1978.
- KANAMORI, H., Seismological evidence for a lithospheric normal faulting—The Sanriku earthquake of 1933, *Phys. Earth Planet. Inter.*, **6**, 346–359, 1971.
- KARIG, D.E., Evolution of arc systems in the western Pacific, *Ann. Rev. Earth Planet. Sci.*, **2**, 51–75, 1974.
- KARIG, D.E. and G.F. SHARMAN, III, Subduction and accretion in trenches, *Geol. Soc. Am.*, **86**, 377–389, 1975.
- KIRBY, S.H., State of stress in the lithosphere: Inferences from the flow laws of olivine, *Pageoph*, **115**, 245–258, 1977.
- KOBAYASHI, Y., A relationship between the distribution of focal depth of microearthquakes and surface heat flow in the southwestern Japan and central Japan, in *Proceedings of Symposium on Earthquake Prediction in Japan*, Seismol. Soc. Jpn., pp. 184–193, 1976 (in Japanese with English abstract).
- MOGI, K., Regional variation of aftershock activity, *Bull. Earthq. Res. Inst.*, **45**, 711–726, 1967.
- NEUGEBAUER, H.J. and G. BREITMAYER, Dominant creep mechanism and descending lithosphere, *Geophys. J. R. Astr. Soc.*, **43**, 873–895, 1975.
- OIKE, K., Seismic activities and crustal movements at the Yamasaki fault and surrounding regions in the southwest Japan, *J. Phys. Earth*, **25**, Suppl. S31–S41, 1977.
- OSBURGH, E.R. and D.L. TURCOTTE, The physico-chemical behavior of the descending lithosphere, *Tectonophysics*, **32**, 107–128, 1976.
- RESEARCH GROUP FOR EXPLOSION SEISMOLOGY, Regionality of upper mantle around northeastern Japan as derived from explosion seismic observations and its seismological implications, *Tectonophysics*, **37**, 117–130, 1977.
- RINGWOOD, A.E., The petrological evolution of island arc systems, *J. Geol. Soc. Lond.*, **130**, 183–204, 1974.
- RINGWOOD, A.E., Petrogenesis in island arc systems, in *Island Arcs, Deep Sea Trenches and Back-Arc Basins*, edited by M. Talwani and W.C. Pitman, III, pp. 311–324, Am. Geophys. Union, 1977.
- SENO, T., Intraplate seismicity in Tohoku and Hokkaido, northern Japan, and a possibility of a large interplate earthquake off the southern Sanriku coast, *J. Phys. Earth*, 1978 (in press).
- SHIMAZAKI, K., Pre-seismic crustal deformation caused by an under thrusting oceanic plate, in eastern Hokkaido, Japan, *Phys. Earth Planet. Inter.*, **8**, 148–157, 1974.
- SMITH, A.T. and M.N. TOSOF, Stress distribution beneath island arcs, *Geophys. J. R. Astr. Soc.*, **29**, 289–318, 1972.
- STESKY, R.M. and W.F. BRACE, Estimation of frictional stress on the San Andreas fault from laboratory measurements, in *Proceedings of the Conference on Tectonic Problems of the San Andreas Fault System*, edited by R.L. Kovach and A. Nur, pp. 206–214, Stanford Univ. Publ., Stanford, Calif., 1973.
- STESKY, R.M., Acoustic emission during high temperature frictional sliding, *Pageoph*, **113**, 31–43, 1975.

- STESKY, R.M., W.F. BRACE, D.K. RILEY, and P.Y.F. ROBIN, Friction in faulted rock at high temperature and pressure, *Tectonophysics*, **23**, 177–203, 1974.
- SUGIMURA, A. and S. UYEDA, *Island Arcs; Japan and Its Environs*, 247 pp. Elsevier, New York, 1973.
- TAKAGI, A., A. HASEGAWA, and N. UMINO, Seismic activity in the northeastern Japan arc, *J. Phys. Earth*, **25**, Suppl., S95–S104, 1977.
- TAKAHASHI, E., Petrological model of the upper mantle and the lower crust of the island arc: Petrology of mafic and ultra-mafic xenoliths in Cenozoic alkali basalts of the Oki-dogo island in the Japan Sea, in *Physics and Chemistry of Magma Genesis* (Bull. Volcanol., Special issue), 1978 (in press).
- TSUMURA, K., Microearthquake activity in the Kanto District, Publications for the 50th Anniversary of the great Kanto Earthquake in 1923, pp. 63–87, 1973 (in Japanese with English abstract).
- UMINO, N. and A. HASEGAWA, On the two-layered structure of deep seismic plane in northeastern Japan arc, *Zisin* 2, **28**, 125–139, 1975 (in Japanese with English abstract).
- YAMASHINA, K., K. SHIMAZAKI, and T. KATO, Aseismic belt along the frontal arc and plate subduction in Japan, *J. Phys. Earth*, this issue, S 447–S 458, 1978.
- YOSHII, T., Proposal of the “aseismic front,” *Zisin* 2, **28**, 365–367, 1975 (in Japanese).
- YOSHII, T., A detailed cross-section of the deep seismic zone beneath northeastern Honshu, Japan, *Tectonophysics*, 1978 (in press).
- YOSHII, T. and S. ASANO, Time-term analysis of explosion seismic data, *J. Phys. Earth*, **20**, 47–57, 1972.

ASEISMIC BELT ALONG THE FRONTAL ARC AND PLATE SUBDUCTION IN JAPAN

Ken'ichiro YAMASHINA, Kunihiko SHIMAZAKI, and Teruyuki KATO

Earthquake Research Institute, University of Tokyo, Tokyo, Japan

(Received July 6, 1978; Revised October 4, 1978)

Along arcs, a belt-like area can be identified where shallow seismicity within the continental plate is extremely low compared with other parts of the plate margin. Examples are in the Tohoku, Hokkaido, Kurile, Kamchatka, Aleutian, Peru-Chile, New Hebrides and Tonga arcs. The present paper proposes to call this inactive (or less-active) area the "aseismic belt," which seems to be a typical feature of arcs. The aseismic belt is some tens of kilometers wide and is located, generally speaking, along the frontal non-volcanic arc between the volcanic front and the aseismic front. This belt can be explained as a mechanically unstrained area on the basis of a plausible model of plate subduction. Geodetic data and seismological results obtained in Japan are incorporated into this model in the framework of plate tectonics.

1. Introduction

Shallow seismicity in trench-arc regions is characterized by (1) major activity along the trench and (2) minor activity occurring inland. The former is probably directly related to the subduction of the oceanic plate beneath the arc. Great shallow thrust earthquakes occur in this major seismic zone. The continuation of this major activity extends along the Wadati-Benioff zone beneath the arc. The latter minor activity usually takes place within the crust, mostly within the upper crust. In addition to these well-known characteristics, (3) few shallow earthquakes occur in a belt-like area between these two active seismic zones, along the frontal non-volcanic arc.

MOGI (1967) discussed the subsurface mechanical structure of Japan based on the regional variation of seismicity and aftershock activity. He divided the Japan area into five zones parallel to the Japan trench considering (1) the decay rate of aftershock activity, (2) activity of earthquake swarms and (3) the difference in magnitude between the main shock and the largest aftershock (Fig. 1). As this figure shows, inland shallow earthquakes occur along the volcanic region (region 3). The seismically inactive area (region 4) lies between this volcanic region and the highly active regions (1 and 2) along the Japan trench.

YOSHII (1975) noticed that few earthquakes occur within the continental mantle beneath Tohoku, northeast Japan. He interpreted this fact the result of special properties of materials in the mantle. Figures 2 and 3 are cross sections of the distribution of the ISC (International Seismological Center) hypocenters in Tohoku and a model for the subsurface structure proposed by YOSHII (1978), respectively. According to his model, the continental mantle has low- Q (reciprocal of the attenuation constant of elastic waves) and low- V (velocity of elastic waves); this low- Q is responsible for the low seismicity. The eastern end of this wedge-like aseismic mantle is sharply bounded by the highly active region adjacent to the trench. This boundary was named the "aseismic front" by YOSHII

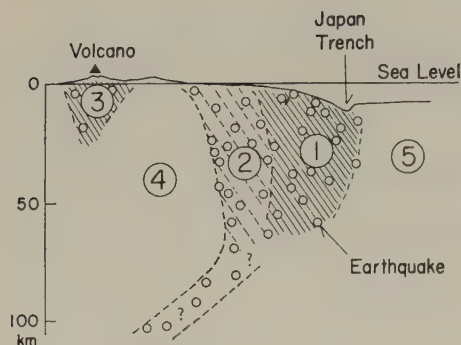


Fig. 1. Schematic vertical section showing the seismic activity and structure across the Japan trench (Mogi, 1967). Shaded areas represent fractured zones. (1) Seismically active and highly fractured. (2) Seismically active, but not fractured. (3) Moderately active and appreciably fractured. (4) No earthquakes occur in this region, which is probably in an unfractured state. (5) Seismically inactive and homogeneous in structure.

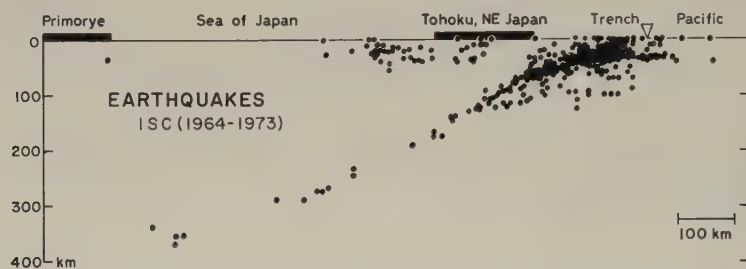


Fig. 2. A cross section of ISC hypocenters along a band 200 km wide across Tohoku, northeast Japan, for the period 1964-1973 (Yoshii, 1978).

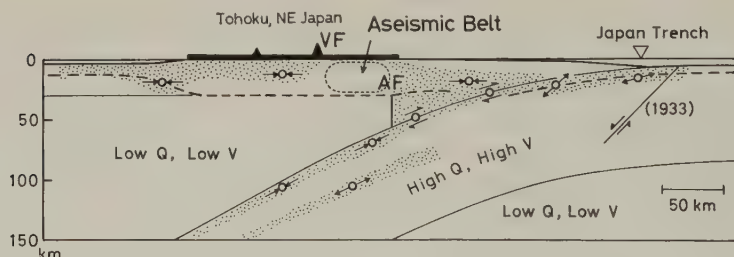


Fig. 3. A schematic cross section of structure slightly modified from Yoshii (1978). Stippled areas indicate the seismically active region with arrows representing the general trend of the earthquake-generating stress system. AF and VF are the aseismic front and the volcanic front, respectively.

(1975). It also bounds, he proposed, the low- Q and low- V mantle from the high- Q and high- V mantle.

The "aseismic front" is defined as a discontinuity in seismicity in the *mantle*. As shown in Figs. 1 and 2, however, it is remarkable that there exists an aseismic zone in the *crust*, too. The existence of the inactive zone in the crust has not previously been noted. The present paper proposes that this inactive zone in the crust, referred to as the "aseismic belt," may constitute a typical feature of arcs. The aseismic belt can be recognized in many trench-arc systems, as will be shown in the following section. A possible explanation for this belt will also be presented in the framework of plate tectonics.

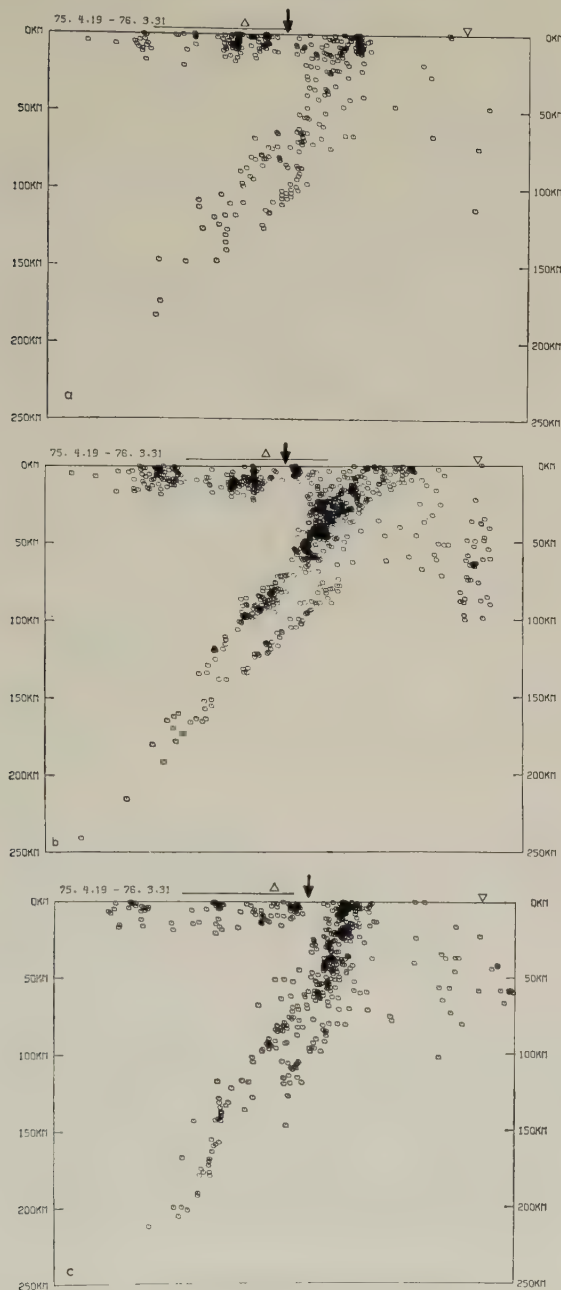


Fig. 4. Focal depth distribution of microearthquakes in Tohoku projected on an east-west section (HASEGAWA *et al.*, 1978). The upper, middle and lower sections correspond to the regions from 38–39°N, 39–40°N and 40–41°N, respectively. Arrows indicate the location of the aseismic belt (39–40°N: the Kitakami Mts.). The triangles and the reverse triangles represent the positions of the volcanic front and the Japan trench, respectively. In these sections, quarry blasts are not eliminated and some of the points within the aseismic belt are known to have been blasts. The figure has a vertical exaggeration of 2.

2. Data

2.1 Tohoku, northeast Japan

A typical example of an aseismic belt occurs in Tohoku as previously shown in Fig. 2. In the recent 10-year interval of 1964–1973, no earthquakes were reported in the Kitakami Mountains, the frontal non-volcanic arc. The width of the inactive zone is about 50 km, about 200–250 km from the trench.

Figure 4 is a cross section of microearthquakes in Tohoku obtained by the network of Tohoku University (HASEGAWA *et al.*, 1978). This network has high detectability and small errors in hypocentral determination. The inactive zone can be identified in this figure, too, bounded by the major off shore and minor inland active zones. This indicates that this area, the Kitakami Mountains, is inactive (or less-active) even microseismically.

In historical times, no damaging earthquakes are known to have definitely occurred in the Kitakami Mountains with the exception of the Oguni earthquake of 1931 ($M=6.1$; USAMI, 1975). This was the only event of magnitude greater than 6 in the last 100 years. This event differs from inland earthquakes in Tohoku in that its fault plane solution shows the *minimum* compressive axis (T axis) lying horizontally in the east-west direction perpendicular to the trench axis (ICHIKAWA, 1971; TAKAGI *et al.*, 1973; YAMASHINA, 1976). However this direction is the general trend of the *maximum* compressive axis (P axis) for shallow inland earthquakes.

The seismic activity of the middle and western parts of Tohoku is in contrast with that of the Kitakami Mountains. Along the Morioka-Shirakawa tectonic line (TSUBOI *et al.*, 1956), which bounds the Kitakami Mountains and the central (Ou) mountains, some damaging earthquakes have occurred, such as the events in 1956 (Shiroishi, $M=6.1$) and 1962 (Kita-Miyagi, $M=6.5$). In this area microearthquakes are most active at present. The active region extends from this line to off the west coast of the district. Recently, major inland earthquakes with magnitude equal to or greater than 7 occurred in the central mountains (the 1896 Rikuu earthquake, $M=7.0$), near the west coast (the 1939 Oga earthquake, $M=7.0$) and under the Japan Sea (the 1964 Niigata earthquake, $M=7.5$).

Another less-active area near the west coast of Tohoku can be distinguished (Fig. 4). It appears to divide the shallow activity of microearthquakes west of the Morioka-Shirakawa line into two groups; one along the central mountains, which corresponds to the volcanic arc, and the other off the Japan Sea coast. However, the present inactivity near the Japan Sea coast might be a temporary rather than an intrinsic and permanent phenomenon, because there were many damaging earthquakes in historical times which caused marked crustal deformation in the coastal region (USAMI, 1975).

2.2 South America

South America is also a region where the aseismic belt is discerned. Sections across South America (Fig. 5) were compiled by ISACKS and BARAZANGI (1977). In the sections of Peru and central Chile no earthquakes have been observed at shallow depths along the Pacific coast, while many inland earthquakes occur beneath and east of the Andean Mountains. The aseismic area is about 100 km in width, and about 150–250 km from the trench. The depths of inland events are as much as 65 km, which is deeper than in

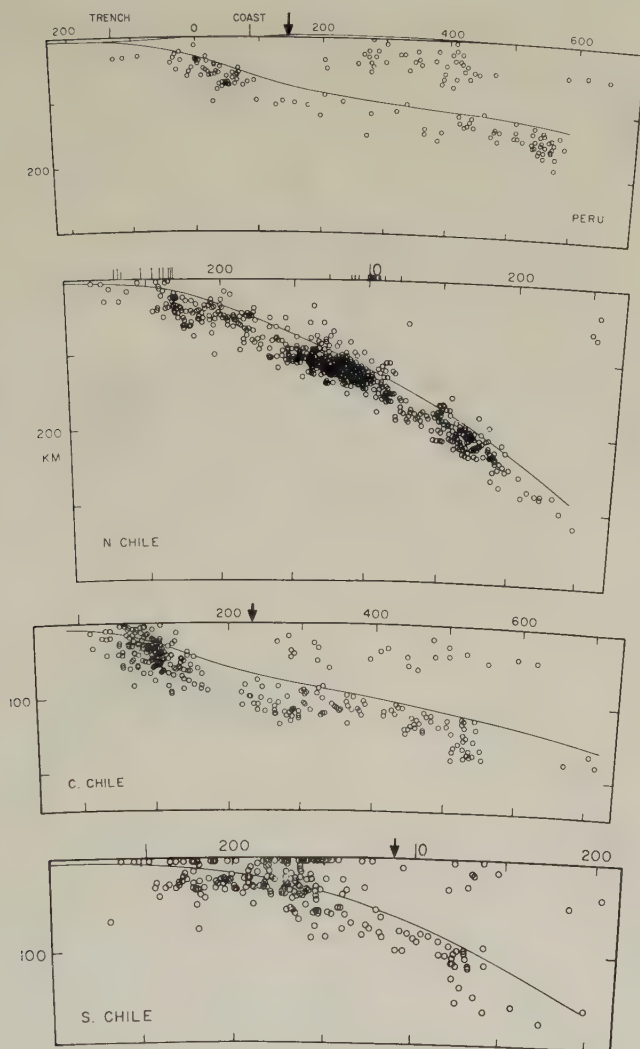


Fig. 5. Cross sections of earthquake hypocenters in the Peru-Chile region for the period 1959–1975 (ISACKS and BARAZANGI, 1977). The projection for volcanoes and trench axes are shown by the long and short vertical lines respectively at the top of each figure. Horizontal and vertical scales are shown in kilometers. Arrows indicate the location of the aseismic belt.

Tohoku although the accuracy of the hypocentral determination is less in South America than in Tohoku. In Peru and central Chile there are no active volcanoes (ISACKS and BARAZANGI, 1977). Therefore the inland active zone does not coincide with the volcanic region in these areas as it does in Tohoku.

In the segments with active volcanoes (northern and southern Chile), the aseismic belt is less clear. In northern Chile, since few events have been observed inland, it is impossible to identify the aseismic belt. In southern Chile, the aseismic belt is not clearly

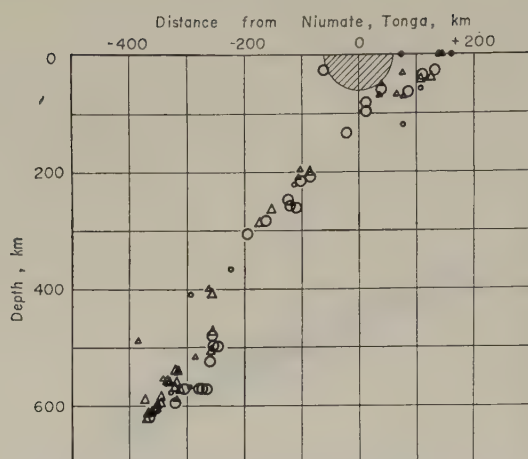


Fig. 6. Earthquake hypocenters projected onto a section along a band 300 km wide oriented perpendicular to the Tonga trench from January 1, 1965, to January 12, 1966 (SYKES *et al.*, 1969). Hatches denote the absence of activity with S-P times less than 6.5 sec at Niuate on the frontal arc.

defined although there seems to be a less-active area about 250 to 350 km from the trench.

2.3 Other regions

The Tonga arc appears to be another example (SYKES *et al.*, 1969). It was pointed out that no earthquakes were observed with S-P times less than 6.5 sec at Niuate station located on the frontal arc, while one earthquake took place in the volcanic arc, suggesting some activity there (Fig. 6). Many events occurred along the Wadati-Benioff zone.

Similar spatial distributions of hypocenters are recognized in southern Hokkaido (MORIYA, 1976), eastern Hokkaido (SHIMAZAKI, 1972), the Kuriles (FEDOTOV *et al.*, 1963), Kamchatka (FEDOTOV, 1968), the Aleutians (ENGDAHL, 1977) and the New Hebrides (ISACKS and BARAZANGI, 1977). Some of them are shown in Fig. 7. In these arcs, inland shallow seismicity is active only along the volcanic arc. Consequently, an inactive area is formed between the volcanic arc and the most active zone near the trench.

When the accuracy of hypocentral location is not good enough to distinguish the activity at shallow depths from that along the Wadati-Benioff zone, or when the inland shallow seismicity is not active enough to be detected by the seismograph network, the existence of the aseismic belt remains unclear. Examples are probably southwest Japan, the Izu-Bonins and Alaska.

3. Discussion

The aseismic belt is defined, in this paper, as a seismically inactive zone in the crust of arcs. It is located, generally speaking, along the oceanward side of the volcanic arc, between the volcanic front (SUGIMURA, 1960) and the aseismic front. It is about 30–100 km in width. This zone corresponds to the area where the depth of the Wadati-Benioff

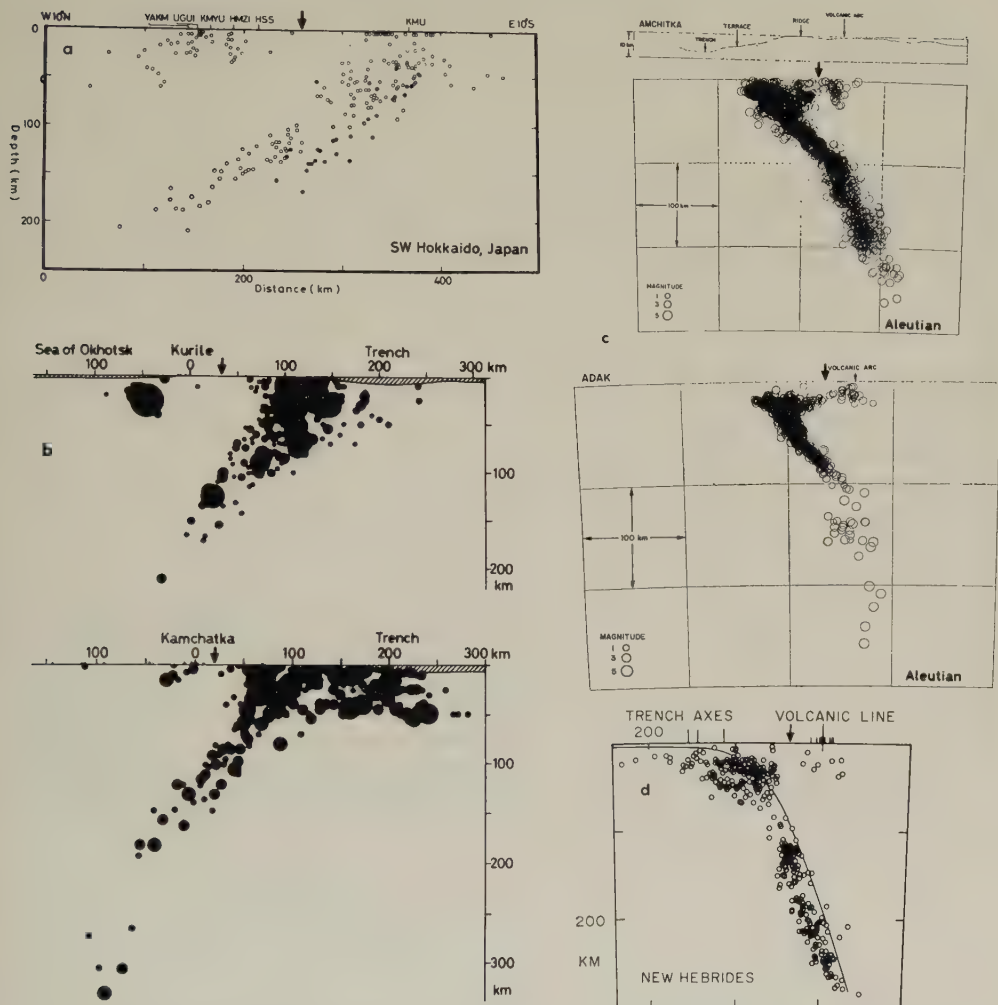


Fig. 7. Cross sections of earthquake hypocenters approximately perpendicular to the trench axis in southern Hokkaido (MORIYA, 1976), the Kuriles (after FEDOTOV *et al.*, 1963), Kamchatka (after FEDOTOV, 1968), the Aleutians (ENGDAHL, 1977) and the New Hebrides (ISACKS and BARAZANGI, 1977). Arrows indicate the location of the aseismic belt. For notations which are not essential to the present discussion, see the original papers.

zone is about 60–100 km. In a double arc system, the aseismic belt may correspond to the frontal non-volcanic arc.

The aseismic belt seems also to be an anomalous region with respect to crustal deformation and the earthquake-generating stress system. The strain (and stress) field in Tohoku shows a contraction trending east-west approximately perpendicular to the trench axis (NAKANE, 1973, for triangulation; ICHIKAWA, 1971, and TAKAGI *et al.*, 1973, for focal mechanisms). In spite of this general trend, east-westward extension has been observed by both a geodimeter traverse survey (GEOGRAPHICAL SURVEY INSTITUTE, 1974) and strain measurements in vaults (ISHII, 1977) in the aseismic belt.

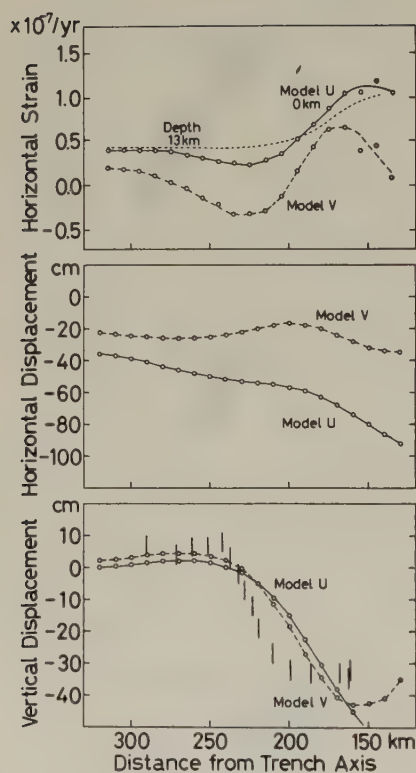


Fig. 8. Computed crustal deformation during interseismic period based on a model of plate subduction which was proposed by SHIMAZAKI (1974) to explain the observations in eastern Hokkaido. The solid and broken curves represent calculations for models U and V, respectively. These models are illustrated in Fig. 10. The dotted curve in the upper figure shows the strain at 13 km depth for model U. The bars in the lower figure indicate the observed vertical displacement with its uncertainty.

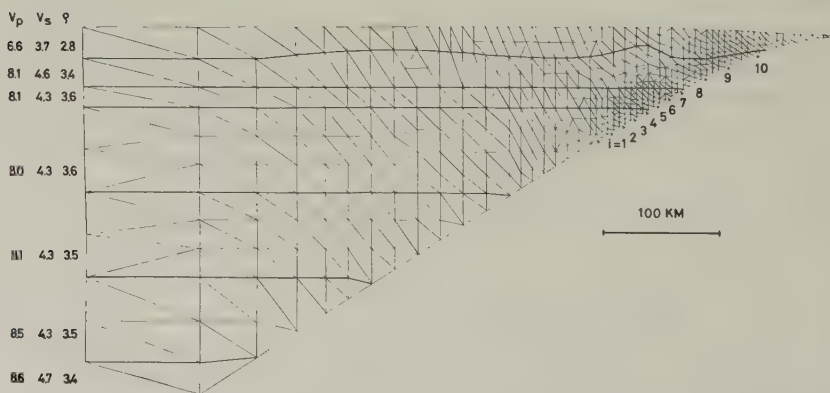


Fig. 9. The finite element grid used to compute the crustal deformation shown in Fig. 8 (SHIMAZAKI, 1974). V_p , V_s and ρ indicate velocities of longitudinal and shear waves in km/sec, and density in g/cm³, respectively.

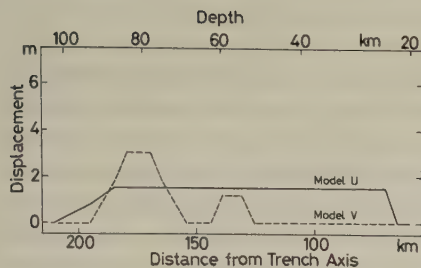


Fig. 10. Tangential displacements of models U and V along the plate interface proposed by SHIMAZAKI (1974) to explain the general features of crustal deformation in eastern Hokkaido during the period 1900–1955.

Figure 8 shows the result of a calculation of crustal strain occurring during the period between interplate great earthquakes. This calculation is based on a mechanical model of plate subduction in eastern Hokkaido proposed by SHIMAZAKI (1974), which will be explained later in this section. The figure shows the predominant horizontal contractive strain perpendicular to the trench axis. Thus the model helps explain the earthquake-generating stress system prevailing along plate margins such as Tohoku. However, note that there is a remarkable feature in the horizontal strain at shallow depths; the horizontal contractive strain has a local minimum along the island arc. Under certain conditions (e.g. model V in Fig. 8) the model even predicts extension perpendicular to the trench axis and suggests an explanation for the anomalous strain (stress) field in the aseismic belt in Tohoku. It is most likely that this unstrained region in the model corresponds to the aseismic belt. Horizontally compressed regions on the oceanic and continental sides of this region would correspond to the major and minor seismic zones, respectively.

The local minimum in horizontal strain is due to a bending of the continental lithosphere. The position of the local minimum and its spatial extent are closely related to the coupling between oceanic and continental plates. SHIMAZAKI (1974) discussed the crustal deformation in eastern Hokkaido with special reference to the predicted earthquake off the southeast coast of Hokkaido, which actually occurred in 1973 (the Nemuro-Oki earthquake, $M=7.4$), presenting a model to explain the general features of crustal deformation during the interseismic period. The continental plate is considered to be compressed and dragged down into the asthenosphere by the underthrusting oceanic plate. The effect of the underthrusting of the oceanic plate on continental plate deformation was approximated by imposing tangential displacements along the interface of the oceanic and continental plates. On the basis of a two-dimensional finite element method for the calculation of static deformation, he obtained two models, one having a nearly uniform, and the other a variable tangential displacement along the interface (models U and V, respectively in Figs. 8 and 10) which both explain the observed vertical deformation. The coupling between the two plates implied from the obtained displacements should disappear at some depth in order to explain the minor inland uplift during the interseismic period along the volcanic arc. The depth of the coupling-decoupling transition is taken as 100 km in his model. Steady state creep movement probably takes place along the lower segment of the interface; the continental plate is no longer dragged down by the oceanic plate beyond this depth. In that case, as has been shown in Fig. 8, the local minimum in horizontal strain appears on the surface in the continental side above the transition point, oceanward of the minor uplift region. The strain is even extensional

in the case of model V, though model U was preferred in eastern Hokkaido on the basis of the horizontal deformation data.

These features of crustal deformation such as the minor uplift occurring during the interseismic period are not unique to eastern Hokkaido. Repeated geodetic surveys conducted throughout the Japanese islands have revealed a typical mode of crustal deformation related to great thrust earthquakes in the major seismic zone along trenches (i.e. interplate earthquakes). The interseismic period is characterized by chronic tilting towards the trench along coastal regions and contraction in the direction approximately perpendicular to the trench axis. The rebound of the continental plate is co-seismic and results in large acute landward tilting and extension of the crust perpendicular to the trench axis, as has been observed several times in Japan. During this cycle of deformation, a minor uplift and a minor subsidence occur inland parallel to the trench axis in the inter- and co-seismic periods, respectively. One example has been shown in Tohoku (DAMBARA, 1974) and another in Shikoku, southwest Japan (GEOGRAPHICAL SURVEY INSTITUTE, 1972). Precise observations of crustal deformation have not been available in most of the other trench-arc systems. However the geodetic data in Japan suggest that the aseismic belt in many arcs could be explained by the coupling and coupling-decoupling transition between continental and oceanic plates.

The existence of the coupling-decoupling transition, and the local minimum in contractive strain, is also supported by the study of focal mechanisms. YOSHII (1978) suggested that such a transition occurs fairly sharply along the plate interface in Tohoku. He found a sharp transition in the earthquake-generating stress system along the interface from nearly horizontal compression in the shallower part to down-dip compression in the deeper part. The transition seems to occur at the aseismic front, that is, the oceanward limit of the low- Q and low- V mantle under the arc. This fact shows that elastic shear strain is not accumulated effectively at the plate interface at the deeper parts beyond the aseismic front. This is also supported by the fact that the depth of the fault planes of interplate great thrust earthquakes usually does not exceed tens of kilometers.

The local minimum in horizontal strain in Fig. 8, however, does not coincide exactly with the aseismic belt in eastern Hokkaido; the calculated unstrained region is located slightly landwards (about 30 km) of the aseismic area. This is probably due to the oversimplified nature of the present subduction model. In fact, the lower part of Fig. 8 shows that the crustal deformation cannot be explained in detail by the present simple models. Detailed discussions will be left for further investigation; inclusions of more appropriate boundary conditions at the plate interface and the effect of anelasticity is obviously a direction in which an attempt to extend the model should be made.

It might be proposed that inland shallow seismicity is active only in the volcanic region, so that the inactive zone which the present paper calls the aseismic belt has no special significance. This might be true to a certain degree as far as the Hokkaido, Kamchatka, Aleutian, New Hebrides and Tonga regions are concerned. But in well-developed arcs such as Japan (Tohoku) and South America, shallow earthquakes do occur not only in the volcanic region but also in a broad area behind the volcanic front. Besides, major inland events usually occur away from the volcanoes. This suggests that the inland shallow activity is not necessarily related only to volcanic phenomena, if at all. It therefore appears that the inactivity of the aseismic belt is significant and its explanation may have an important bearing on our understanding of the subduction process.

BISCHKE (1974) proposes that the arching due to the sinking oceanic plate will induce

a *broad* region of large (deviatoric) tensile stress within the continental plate, which may explain the position of the active volcanic chains. However, his result is in conflict with the geodetic data in Japan which indicates that most areas are contracting perpendicular to the trench axis. One might also argue that the unstrained region shown in the present paper corresponds to that of active volcanism along the volcanic front, because such an unstrained region would appear to permit volcanic eruption. The following facts, however, run counter to this argument. First, the calculation shows that the unstrained region is limited to shallow depths, probably in the upper crust (see Fig. 8). If the volcanism is strongly controlled by the mechanical state at shallow depths, the distribution of volcanoes would be scattered by local irregularities of the crust. This is in conflict with the remarkable linearity of volcanic fronts and the absence of volcanoes on the oceanward side of the volcanic front. The linearity rather suggests that there are some critical conditions for production of magma under island arcs (e.g. SUGIMURA and UYEDA, 1973). Second, many observations in the volcanic arc suggest that the maximum compressive axis is trending horizontally in the general direction perpendicular to the trench axis. They include earthquake-generating stress system (e.g. ICHIKAWA, 1971; TAKAGI *et al.*, 1973; YAMASHINA, 1976), crustal deformation (e.g. NAKANE, 1973) and trends of dikes and distribution of craters in active volcanoes (NAKAMURA, 1977). One exception is in south Kyushu, southwest Japan where the minimum compressive axis of the earthquakes in the volcanic region seems nearly perpendicular to the trench axis (MINAKAMI *et al.*, 1969; NISHI, 1976; YAMASHINA, 1977).

4. Conclusion

There exists a belt-like area where few shallow earthquakes occur along arcs. It is situated in the crust of the continental plate between seismically active areas; the major active area along the trench and the minor one along the volcanic arc. Such a seismically inactive (or less active) area can be identified in many arc systems such as the Tohoku, Hokkaido, Kurile, Kamchatka, Aleutian, Peru-Chile, New Hebrides and Tonga arcs.

This belt is termed the "aseismic belt" in the present paper. It seems to be a typical feature of arcs. It is about 30–100 km in width and corresponds to an area where the Wadati-Benioff zone is about 60–100 km deep. Accordingly the area is located between the volcanic front and the aseismic front, almost coinciding with the frontal non-volcanic arc.

A model of plate subduction, based on a two-dimensional finite element method, shows a remarkable feature in the horizontal strain at shallow depths; the horizontal contractive strain (and stress) perpendicular to the trench axis has a local minimum along the arc. This less-strained area corresponds most likely to the aseismic belt, although detailed analysis is left for further investigation.

We wish to express our gratitude to Dr. Paul Somerville and Professors Kazuaki Nakamura, Seiya Uyeda, and Arata Sugimura for their critical comments on the manuscript. We also wish to thank Professors Toshikatsu Yoshii and Naoyuki Fujii, Dr. Katsuhiko Ishibashi, and Mr. Kei Kurita for their helpful suggestions, and Professors Shuzo Asano and Keichi Kasahara for their encouragement. We are also grateful to the authors of Figs. 1–7 who kindly permitted us to use their figures. Mrs. Kazuko Noguchi helped us to arrange the manuscript.

REFERENCES

- BISCHKE, R.E., A model of convergent plate margins based on the recent tectonics of Shikoku, Japan, *J. Geophys. Res.*, **79**, 4845–4857, 1974.

- DAMBARA, T., Vertical movement near Sakata and Shinjo, *Rep. Coord. Comm. Earthq. Predict.*, **11**, 62–63, 1974 (in Japanese).
- ENGDAHL, E.R., Seismicity and plate subduction in the central Aleutians, in *Maurice Ewing Series 1*, pp. 259–271, Am. Geophys. Union, Washington, D.C., 1977.
- FEDOTOV, S.A., On deep structure, properties of the upper mantle, and volcanism of the Kurile-Kamchatka island arc according to seismic data, in *Geophys. Monogr.*, No. 12, pp. 131–139, Am. Geophys. Union, Washington, D.C., 1968.
- FEDOTOV, S.A., A.M. BAGDASAROVA, I.P. KUZIN, and R.Z. TARAKANOV, On the seismicity and the deep structure of the southern part of the Kurile island arc, *Dokl. Akad. Nauk S.S.S.R.*, **153**, 668–671, 1963 (in Russian).
- GEOGRAPHICAL SURVEY INSTITUTE (Crustal Activity Research Office), Vertical movement in south Shikoku district, *Rep. Coord. Comm. Earthq. Predict.*, **7**, 45–46, 1972 (in Japanese).
- GEOGRAPHICAL SURVEY INSTITUTE (Geodetic Division), G.D.P. traverse survey of high precision in north-eastern part of Japan, *Rep. Coord. Comm. Earthq. Predict.*, **11**, 60–61, 1974 (in Japanese).
- HASEGAWA, A., N. UMINO, and A. TAKAGI, Double-planed structure of the deep seismic zone in the north-eastern Japan arc, *Tectonophysics*, **47**, 43–58, 1978.
- ICHIKAWA, M., Reanalyses of mechanism of earthquakes which occurred in and near Japan, and statistical studies on the nodal plane solutions obtained, 1926–1968, *Geophys. Mag.*, **35**, 207–274, 1971.
- ISACKS, B.L. and M. BARAZANGI, Geometry of Benioff zones: Lateral segmentation and downwards bending of the subducted lithosphere, in *Maurice Ewing Series 1*, pp. 99–114, Am. Geophys. Union, Washington, D.C., 1977.
- ISHII, H., Characteristics of crustal movement observed at wide area, Reports on the Symposium for Earthquake Prediction Study (1976), *Seismol. Soc. Jpn.*, pp. 116–126, 1977 (in Japanese with English abstract).
- MINAKAMI, T., S. HIRAGA, T. MIYAZAKI, and H. TERAOKA, The Ebino earthquake swarm and the seismic activity in the Kirishima volcanoes in 1968–1969. II. Geographical distribution of initial motion and travel time curves along the Kirishima volcanoes, *Bull. Earthq. Res. Inst., Univ. Tokyo*, **47**, 745–767, 1969.
- MOGI, K., Regional variation of aftershock activity, *Bull. Earthq. Res. Inst., Univ. Tokyo*, **45**, 711–726, 1967.
- MORIYA, T., Folded structure of intermediate depth seismic zone and attenuation of seismic waves beneath the arc-junction at southwestern Hokkaido, Symposium on Subterranean Structure in and around Hokkaido and its Tectonic Implication, Hokkaido Univ., pp. 13–27, 1976 (in Japanese with English abstract).
- NAKAMURA, K., Volcanoes as possible indicators of tectonic stress orientation—Principle and proposal, *J. Volcanol. Geotherm. Res.*, **2**, 1–16, 1977.
- NAKANE, K., Horizontal tectonic strain in Japan (I) and (II), *J. Geod. Soc. Jpn.*, **19**, 190–208, 1973 (in Japanese with English abstract).
- NISHI, K., The latest distribution of hypocenters in Sakurajima volcano (abstr.), *Bull. Volcanol. Soc. Jpn.*, **21**, 122, 1976 (in Japanese).
- SHIMAZAKI, K., Focal mechanism of a shock at the northwestern boundary of the Pacific plate: Extensional feature of the oceanic lithosphere and compressional feature of the continental lithosphere, *Phys. Earth Planet. Inter.*, **6**, 397–404, 1972.
- SHIMAZAKI, K., Pre-seismic crustal deformation caused by an underthrusting oceanic plate, in eastern Hokkaido, Japan, *Phys. Earth Planet. Inter.*, **8**, 148–157, 1974.
- SUGIMURA, A., Zonal arrangement of some geophysical and petrological features in Japan and its environs, *J. Fac. Sci., Univ. Tokyo, Sect. 2*, **12**, 133–153, 1960.
- SUGIMURA, A. and S. UYEDA, *Island Arcs: Japan and Its Environs*, 247 pp., Elsevier, Amsterdam, 1973.
- SYKES, L.R., B.L. ISACKS, and J. OLIVER, Spatial distribution of deep and shallow earthquakes of small magnitudes in the Fiji-Tonga region, *Bull. Seismol. Soc. Am.*, **59**, 1093–1113, 1969.
- TAKAGI, A., A. HASEGAWA, and N. UMINO, Focal mechanisms of shallow earthquakes occurred in the Tohoku district, Abstr. Pap. Spring Meet. 1973, *Seismol. Soc. Jpn.*, p. 124, 1973 (in Japanese).
- TSUBOI, C., A. JITSUKAWA, and H. TAJIMA, Gravity survey along the lines of precise levels throughout Japan by means of a WORDON gravimeter. VII. Tohoku district, *Bull. Earthq. Res. Inst., Univ. Tokyo, Suppl. IV*, 311–406, 1956.
- USAMI, T., *Nihon-Higai-Jishin-Soran*, Tokyo University Press, 327 pp., Tokyo, 1975 (in Japanese).
- YAMASHINA, K., The earthquakes of reverse-fault type in Tohoku district, Abstr. Pap. Spring Meet. 1976, *Seismol. Soc. Jpn.*, p. 104, 1976 (in Japanese).
- YAMASHINA, K., The Ebino earthquake swarm of 1968 and the stress field in the Kirishima volcanic area, Kyushu, Japan (abstr.), *Bull. Volcanol. Soc. Jpn.*, **22**, 100, 1977 (in Japanese).
- YOSHII, T., Proposal of the “aseismic front”, *J. Seismol. Soc. Jpn.*, **28**, 365–367, 1975 (in Japanese).
- YOSHII, T., A detailed cross-section of the deep seismic-zone beneath northeastern Honshu, Japan, *Tectonophysics*, 1978 (in press).

TSUNAMICITY OF SANRIKU DEPENDS ON SUBDUCTION TECTONICS

Wm. Mansfield ADAMS

*Hawaii Institute of Geophysics, University of Hawaii,
Honolulu, Hawaii, U.S.A.*

(Received June 5, 1978; Revised September 18, 1978)

The tsunamicity of the Sanriku Coast has been shown to have an anomalous gap in energy, or tsunami magnitude. Furthermore, this gap in magnitude correlates directly with epicentral distance from shore—there also is a gap in the epicenter distribution versus offshore distance. The large tsunamis are generated on the east side of the trench. The gap is for intermediate tsunamis, of which there are none.

These observed features can be explained by considering the spatial distribution of shear stress about a subduction zone. The stress attains maxima at two locations: one is on the upper interface between the mantle and the downgoing slab; the other is within the oceanic lithosphere, at the flexure. The observation rationalizes the observed anomalies of tsunamicity.

1. Background

The tsunamicity of the Sanriku Coast (see Fig. 1) has been shown to differ from that of the rest of Japan (ADAMS, 1972a). In the special case of the Sanriku Coast, there is a gap in the distribution of tsunamis when the number of occurrences is plotted versus tsunami magnitude (see Fig. 2). The anomalous distribution of tsunami energy is probably statistically significant (ADAMS, 1972b).

The idiosyncracies of Northeastern Honshu are anticipated, in a sense, by the tectonic uniqueness of Northern Honshu. The ria-type coastline of Sanriku is not prevalent anywhere else in Japan—or in any trench-facing coast, for that matter. Furthermore, evidence has been presented (ADAMS, 1973) for a zonal lineament traversing the primary arcuate trend on a west-northwest bearing from Sendai (see Fig. 1). (See recent definitions of lineament in O'LEARY *et al.* (1977); see also discussion by ALLUM (1978) and reply by authors.)

First we consider additional evidence for the lineament, and then we consider the energy gap. The lineament was named Margo Vorticis, for reasons set forth in the original paper (ADAMS, 1973). (For a review of the geology of Japan, see UYEDA and MIYASHIRO (1974)).

2. Substantiating Seismic Evidence for the Margo Vorticis Lineament

The Margo Vorticis was revealed initially by various geophysical data; geodetic data were the most significant. All types of geophysical data were examined to determine whether the feature does exist. The strongest evidence was from the horizontal and vertical earth movements (see Fig. 3); magnetic and gravity data were, at best, supporting, and seismicity data did not indicate the proposed lineament at all (see Fig. 1).



Fig. 1. Location map for the Sanriku Coast. Note the ria-type coastline. Dashed line indicates the location of the lineament.

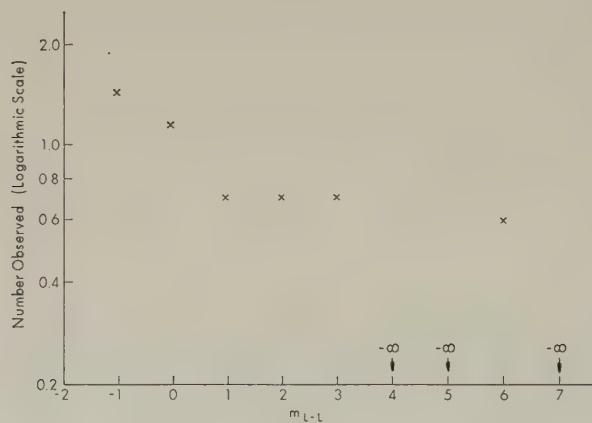


Fig. 2. Number of occurrence of tsunamis off Sanriku (from 1868 to 1968) versus logarithmically linear tsunami magnitude (after Fig. 4 of ADAMS, 1972a).



Fig. 3. Secular horizontal velocity of the surface of Japan. Vectors are in units of meters per quarter century. Data taken from HARADA (1967).

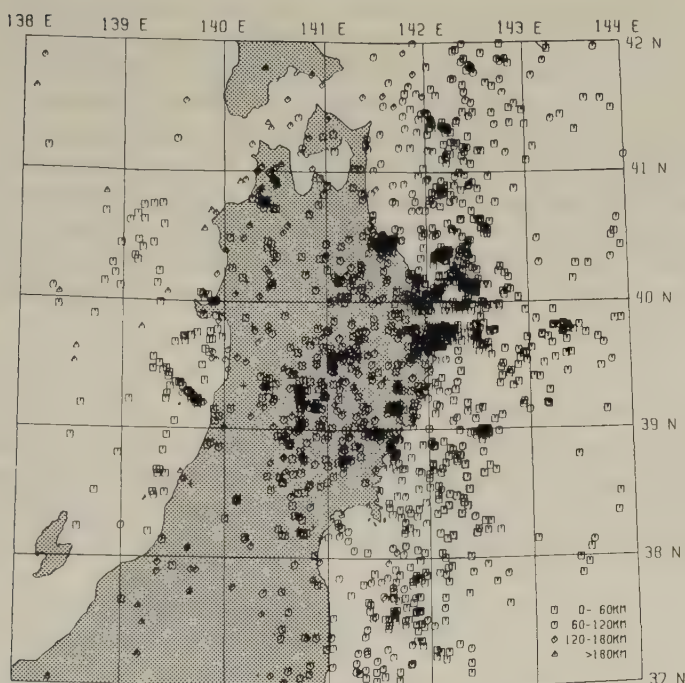


Fig. 4. Distribution of epicenters from Northern Honshu from April 1975 to March 1976 (from HASEGAWA *et al.*, 1977, with permission of the authors). The crosses are the seismographic observatories.

2.1 Seismic data

For the past several years, a seismic network has been operated by Tohoku University in Northern Honshu. The excellent quality of the data permit precise determination of epicenter location for microearthquakes. The epicenter distribution of microearthquakes in the Tohoku District during the period from April 1975 to March 1976 is kindly provided by HASEGAWA *et al.* (1977) in Fig. 4. From these seismicity data, we are able to easily see the NW to SE linear alignment of some of the epicenters in the one-degree area, 39° – 40° N, 139° – 140° E. An extension of this alignment through Sendai encounters a weak cluster of epicenters in the right upper center of the area 37° – 38° N, 141° – 142° E. The hiatus noticeable in the 140° – 141° E segment is probably due to the axis of vulcanism that crosses the proposed lineament there.

The lineation supported by these epicenter clusters is consistent with most of the geophysical data reviewed by ADAMS (1973). It is not exactly congruent with the horizontal-velocity data (see Fig. 3), which would be explained most simply with a line extending due west from Sendai. This discordancy is tentatively interpreted to mean that a zone is involved rather than a single lineament.

2.2 Other geophysical data

The information available on the deep-sea terraces along Eastern Honshu has been set forth by IWABUCHI (1968); his data have been interpreted by KELLEHER and McCANN

(1977) to mean that larger seismic-tsunami sources are spatially related to larger basins and terraces. There is a gap in terraces right at the zone of terraces. They propose that portions of oceanic lithosphere are more buoyant than the average oceanic lithosphere, a condition that leads to two, significantly different, subduction processes.

Other data, such as heat flow or bathymetry, do not disprove the proposed lineament but rather give it marginal, almost intuitive support. Additional work is clearly necessary. The uniqueness of the ria-type coastline for Sanriku is, of course, also supportive. Perhaps most encouraging is that OTSUKI and EHIRO (1978, this issue, pp. S 537-S 555) propose a fault in this zone; at least it is so designated in their Fig. 1. However, they call it the Chokai-Ishinomaki tectonic line. This name has the advantage of being independent of the genesis of the feature.

3. *Tsunamis and Subduction Tectonics*

The hypothesis was set forth by ADAMS and FURUMOTO (1970) for tele-tsunamis in Hawaii that "for large earthquakes, either a very large tsunami is generated or none at all." In fact, "none-at-all" includes small tsunamis, not observed visually but recordable. So the pragmatic result is again that there is a hiatus in energy for tsunamis from a given coastal region.

The efforts to explain tsunamigenic earthquakes in terms of plate tectonics concepts began in earnest with KANAMORI (1972) and ABE (1973), and KANAMORI (1977) recently reviewed some aspects of his model.

Explanation of the binary nature of tsunamis on the Sanriku Coast is accomplished with plate tectonics modeling with the observation that subduction results in two real concentrations of stress (see Fig. 5). One of these stress concentrations is along the interface between the upper surface of the downgoing lithospheric slab and the contiguous mantle; the other is in the oceanic plate itself, at the flexure. These two stress concentrations can rationalize the observed tsunami-energy hiatus. This hiatus can be explained as follows: earthquakes on the interface are of lower magnitude since they occur in rock of higher temperature which ruptures at lower yield strengths. The motion is dip-slip; the oceanic lithosphere moves downward and the hanging wall moves upward. The large dip results in 30% lower vertical-component of motion. We call these interface earthquakes. For the earthquakes on the flexure, the fracturing is caused by both tension and a moment, hence both sides can have an upward component, which results in a monopole rather than a dipole source and thus an efficient source for tsunami generation. This process can be illustrated by considering flexure of an elastic plate, as in Fig. 6. The solid lines show the flexed elastic plate. Let rupture occur at Point A on the suture, the region of greatest tension. The extreme case, in which the rupture propagates completely through the plate, allows the elastic material to resume its original shape (shown by the dashed lines). Point A moves to A₁ and A₂; relative to the center of curvature, there is a large radial component in these motions. Furthermore, initiation of fracture will not relieve the stresses, as in the case of the interface earthquakes, but rather will redistribute the stresses. The situation is shown diagrammatically in Fig. 7. In the upper diagram, pre-fracture, the tension in the volume above the neutral plane is supported along the entire interface AN. The lower diagram illustrates the situation a few seconds after initiation of fracture, said to be co-fracture. Essentially, the same total tension is now distributed across the smaller interface BN, so fracture continues. The "neutral plane"

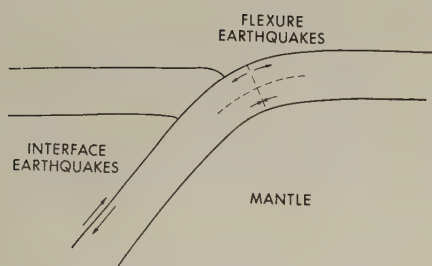


Fig. 5. Cross-section diagram of a subduction zone, showing the two locations of stress concentrations: one at the interface between the upper surface of the down-going slab and the mantle, the other at the flexure in the oceanic lithosphere. Dashed line indicates the neutral plane.

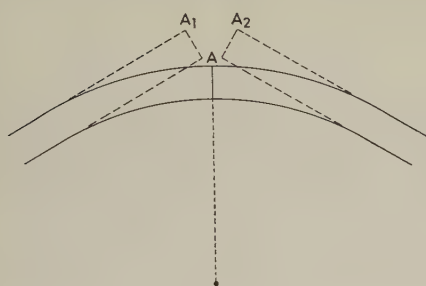


Fig. 6. Diagram showing the type of movement due to fracture that has both sides with a significant upward component. This type of faulting is said to be monopolar: all other types of faulting would be dipolar—one side would have movement in the opposite direction of the other side.

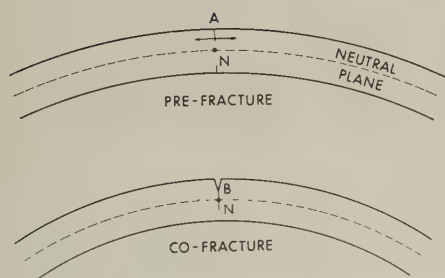


Fig. 7. Cross-sectional diagram showing how the pre-fracture tensional stress field is redistributed during fracture—the co-fracture state—so as to increase the intensity of tension ahead of the tip of the fracture. This may be thought of as the first time step in a time-marching model of the mechanics of rupture.

(see Fig. 5) (JOHNSON, 1970) of the oceanic lithosphere plate migrates toward the mantle, which is to say that the tension ahead of the downward-propagating fracture is increasing. Indeed, levels that were in compression pass into tension and then fracture. The result is that the rupture often passes almost through the lithosphere. Thus the earthquakes at the flexure are always large in energy release, consequently very rare (relative to the time span of a human life) and always large in generation of tsunami energy. Evidence for this is provided by the horst-graben morphology so common on the collision flexure (data from HILDE *et al.*, 1978). Toward the trench axis, the apparent vertical offset on the faults increases. Furthermore, HILDE *et al.* find these features to be consistent with theoretical models of the bending of an elastic plate having stress concentrations in the area of the collision flexure (which they call the "outer topographic high"). HILDE *et al.* (1978) base their work on that of CALDWELL *et al.* (1976), who developed a universal elastic trench profile. Caldwell *et al.* reasoned as follows: since the shape observed is that predicted for an elastic plate, the oceanic lithosphere is therefore behaving elastically. As a corollary, fracturing completely through the lithosphere does not occur at the flexure. Here we will attempt to show that this is a specious argument.

BIOT (1954) has shown that the equations for describing the deformation of visco-elastic media can be derived from those equations describing the deformation of elastic media simply by replacing the elastic parameters by appropriate operators. This means that every shape achieved by an elastic plate can be attained by some appropriate visco-elastic plate. It is faulty to conclude that the assumptions are true because the conclusion is true; that is to say, the agreement between the field observations and the shape taken by an elastic plate does not mean that the assumption of elasticity is correct. Indeed, it is better to argue from the assumptions to the conclusion.

Because the assumption of elasticity is not necessarily true, fracturing completely through the oceanic lithosphere is possible and may occur.

4. Summary

Prompted by empirical evidence showing that the tsunamis off Sanriku fall into two energy groups and two spatial groups, I have examined the possibility of rationalizing these observations using the plate tectonic model of subduction zones. I find that there are two zones of stress concentration; these zones are taken to correspond to the bimodality of tsunamis. (The energy grouping appears to be equivalent to the spatial grouping.)

Estimation of the types of earthquakes to be expected at the two zones of stress concentration leads to differences that correlate satisfactorily with existing observations. Additional observations and further study of historical data are appropriate.

This work has been assisted by discussions with Roy A. Kikuyama, who is working on the numerical and analytical modeling. The author is grateful to the Geodynamics Commission for the financial support that permitted presentation of this work at the Symposium in Tokyo, Japan. Hawaii Institute of Geophysics contribution No. 953.

REFERENCES

- ABE, K., Tsunami and mechanism of great earthquakes, *Phys. Earth Planet. Inter.*, **7**, 143–153, 1973.
- ADAMS, W.M., A hiatus in the energy range of tsunamis generated off Northeastern Honshu, *Bull. IISSE*, **9**, 11–25, 1972a.
- ADAMS, W.M., Statistical significance of the energy gap observed for tsunamis generated off the Sanriku Coast, *Bull. IISSE*, **9**, 137–141, 1972b.
- ADAMS, W.M., Division of Northern Honshu by a lineament traversing the primary arcuate trend, *Bull. IISSE*, **10**, 67–80, 1973.
- ADAMS, W.M. and A.S. FURUMOTO, Features of tsunamigenic earthquakes, in *Tsunamis in the Pacific Ocean*, edited by W.M. Adams, pp. 57–68, East-West Center Press, Honolulu, 1970.
- ALLUM, John A.E., Lineament, linear, lineation: Some proposed new standards for old terms: Discussion and reply, *Bull. Geol. Soc. Am.*, **88**, 159–160, Doc. 80113, 1978.
- BIOT, M.A., Theory of stress-strain relations in anisotropic viscoelasticity and relaxation phenomena, *J. Appl. Phys.*, **25**, 1385–1419, 1954.
- CALDWELL, J.G., W.F. HAXBY, D.E. KARIG, and D.L. TURCOTTE, On the applicability of a universal elastic trench profile, *Earth Planet. Sci. Lett.*, **31**, 239–246, 1976.
- HARADA, T., Precise readjustment of old and new first order triangulation, and result in relation with the destructive earthquakes in Japan, *Bull. Geophys. Surv. Inst.*, **12**, 5–64, 1967.
- HASEGAWA, A., N. UMINO, and A. TAKAGI, Double-planed deep seismic zone of upper mantle structure in the Northeastern Japan arc, available as preprint, 1977.
- HILDE, T.W.C., G.F. SHARMAN, and G.M. JONES, Fault patterns in outer trench walls and their tectonic significance, Abstr. of Papers, Int. Geodyn. Conf. "Western Pacific" and "Magma Genesis," p. 52, 1978.
- IWABUCHI, Y., Topography of trenches east of the Japanese Islands, *J. Geol. Soc. Japan.*, **74**, 37, 1968.
- JOHNSON, A., *Physical Processes in Geology*, 577 pp., see especially p. 226, Freeman, Cooper and Co., San Francisco, 1970.
- KANAMORI, H., Mechanism of tsunami earthquakes, *Phys. Earth Planet. Inter.*, **6**, 346–359, 1972.

- KANAMORI, H., Seismic and aseismic slip along subduction zones and their tectonic implications, in *Island Arcs, Deep-sea Trenches and Back-arc Basins*, edited by M. Talwani and W.C. Pitmann, III, pp. 163–174, Am. Geophys. Union, Washington, D.C., 1977.
- KELLEHER, J. and W. McCANN, Bathymetric highs and the development of convergent plate boundaries, in *Island Arcs, Deep-sea Trenches and Back-arc Basins*, edited by M. Talwani and W.C. Pitmann, III, pp. 115–122, Am. Geophys. Union, Washington, D.C., 1977.
- O'LEARY, E.W., J.D. FRIEDMAN, and J.A. POHN, Lineament, linear, lineation: Some proposed new standards for old terms, *Bull. Geol. Soc. Am.*, **87**, 1463–1469, Doc. 61011; see also discussion in **88**, 159–160, Doc. 80113, 1977.
- OTSUKI, K. and M. EHIRO, Major strike-slip faults and their bearing on spreading in the Japan Sea, this issue, S 537–S 555, 1978.
- UYEDA, S. and A. MIYASHIRO, Plate tectonics and the Japanese Islands: A synthesis, *Geol. Soc. Am. Bull.*, **85**, 1159–1170, 1974.

SEISMIC STUDIES OF THE UPPER MANTLE BENEATH THE ARC-JUNCTION AT HOKKAIDO: FOLDED STRUCTURE OF INTERMEDIATE-DEPTH SEISMIC ZONE AND ATTENUATION OF SEISMIC WAVES

Takeo MORIYA

Department of Geophysics, Faculty of Science, Hokkaido University, Sapporo, Japan

(Received June 30, 1978; Revised September 29, 1978)

Distribution of intermediate and deep earthquake hypocenters beneath the Hokkaido corner, one of the notable arc-junctions in Japan, is investigated. A specially designed projection of the hypocenters is made to demonstrate the configuration of the seismic zone beneath the arc-junction. The configuration is characterized by a peculiar folding in the depth range between 80 and 150 km, which seems to be caused by plastic deformation of the descending lithosphere.

Attenuation of seismic waves of local earthquakes is also studied. Q values for S waves fall in the range between 50 and 200 in the upper mantle beneath Hokkaido. The distribution of Q values shows that the high attenuation zones correspond to the areas of high heat flow.

1. Introduction

The spatial distribution of intermediate and deep earthquakes is useful for confirming the deformation of the descending lithosphere and provides an important clue to the response of materials to the subduction process. Beneath an arc-junction like the Hokkaido corner, the descending lithosphere must be deformed and overlapped due to conservation of the surface area. There are three notable arc-junctions in Japan. These are the Hokkaido corner at the junction of Kurile arc and northeast Honshu, the central part of Honshu near the triple junction of the Pacific plate, Philippin-Sea plate and Honshu, and the Kyushu corner at the junction of Ryukyu arc and southwest Honshu.

The spatial distribution of earthquake hypocenters in and around Japan has been investigated by many authors (e.g., WADATI *et al.*, 1969; KATSUMATA and SYKES, 1969; KATSUMATA, 1970; UTSU, 1971). The more accurate observations have revealed the more detailed structure of deep seismic zone. Beneath the Hokkaido corner, UTSU (1968) showed curved contour lines for deep seismic zone, but UTSU (1974) later modified them to discontinuous contour lines (Fig. 1). To obtain more distinctive structure of the deep seismic zone, highly accurate distribution of hypocenters must be required. The Hokkaido island is a place suitable to observe intermediate and deep earthquakes and to resolve the problem of deformation of the lithosphere beneath the arc-junction because of relatively high seismicity comparing with the other two junctions.

In this paper, the distribution of intermediate and deep earthquakes which occurred in and around Hokkaido is investigated. In addition to the distribution of hypocenters, attenuation of seismic waves of local earthquakes is studied to reveal the regionality of low Q zone in the upper mantle beneath Hokkaido.

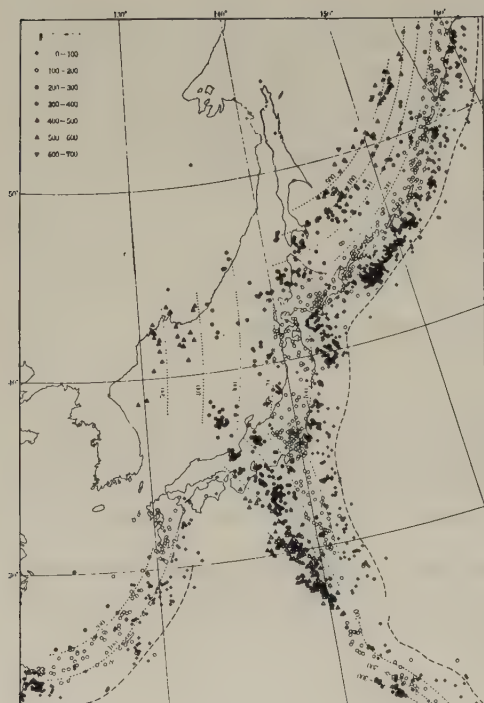


Fig. 1. Map showing epicenters of earthquakes in and around Japan located by ISC (after Utsu, 1974).

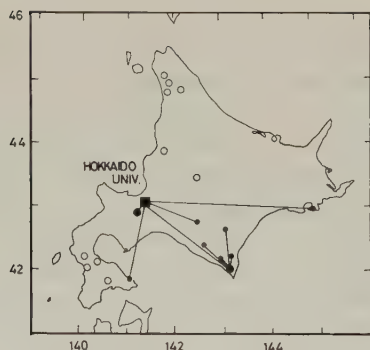


Fig. 2. The seismic network of Hokkaido University. Open circles are the temporary stations and solid circles are the telemetered routine stations.

2. Seismic Network and Method of Hypocenter Determination

The location of observation stations in the routine as well as temporary seismic network used in this study is shown in Fig. 2. The digitized data of the routine stations are telemetered to the observation center of Hokkaido University. At each temporary station, a system of slow speed magnetic tape recording with AC bias is used. The system can observe for two months by a tape of 1,100 m long continuously with very low power consumption of about 1 W. To keep high time resolution, the system has a crystal coded clock and a radio to compensate the clock. Time accuracy is kept better than 0.02 sec at any time.

The temporary network in the southwestern part of Hokkaido was in operation for four months in 1973, and the central and northern parts of Hokkaido have been operated from 1974. The routine observation by telemetered network was begun in July, 1976.

The hypocenters are determined by the following method. First, the origin time t_{oi} is calculated at the i -th station by

$$t_{oi} = t_{pi} - (V_p/V_s - 1)^{-1} t_{(s-p)i}$$

where t_{pi} and $t_{(s-p)i}$ are P-wave arrival and S-P times, respectively and $V_p/V_s = 1.73$ is assumed. The average value of t_{oi} at each station provides the origin time. Then coordinates of hypocenter are calculated by the least squares method to fit t_{pi} to ICHIKAWA-MOCHIZUKI's table (1971). The computer program was designed by SHIBUYA *et al.* (1973).

3. Hypocenter Distribution of Intermediate and Deep Earthquakes

About 200 hypocenters are determined using the routine and temporary observation data during the period, July 1976–November 1977, and about 200 hypocenters which are relocated using JMA (Japan Meteorological Agency) and some of the routine and temporary observation data during the period January 1961–June 1976, are added. Figure 3 shows the epicenter distribution of the earthquakes. Beneath the Hokkaido corner, the deeper seismicity is generally lower and less uniform. A northeast trend of seismicity from west off Hokkaido seems to constitute an edge of the deep seismic zone. Some aseismic regions appear in southwestern and central Hokkaido, and along the coast line of Okhotsk Sea. A clear northwest trending seismic zone appears in northeastern Hokkaido. The nonuniform seismicity suggests that the stress distributes inhomogeneously in the descending lithosphere which is deformed beneath the arc-junction.

Because the seismic zone beneath Hokkaido changes its dip angle and dip direction, and has a relatively low seismicity, vertical and horizontal projection of the hypocenters are not adequate for establishing the configuration of the seismic zone, and another device is required. In this study, specially designed projection is made. In making this projec-

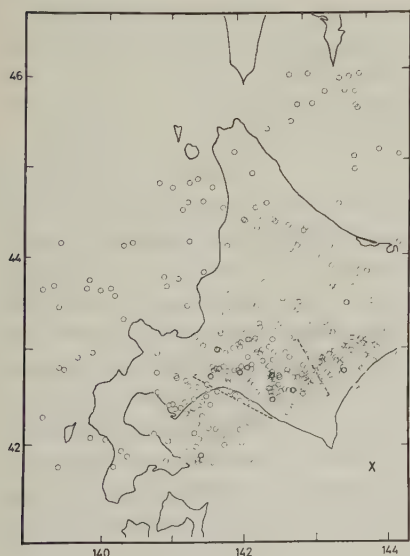


Fig. 3. Epicenters of intermediate and deep earthquakes determined by the seismic network of Hokkaido University or relocated by JMA data. \times indicates the origin for measuring dip angles and azimuths with earthquakes. In the area between two broken lines, the folded seismic zone is situated.

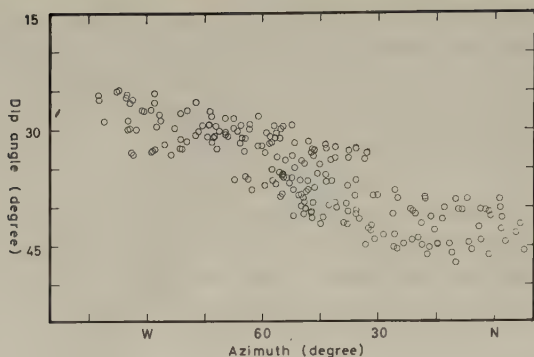


Fig. 4. Distribution of hypocenters of earthquakes on the azimuth-dip plane in a depth range between 80 and 150 km.

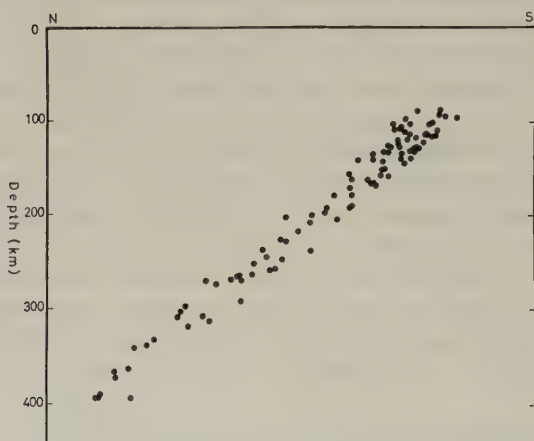


Fig. 5. Distribution of hypocenters of earthquakes projected on the vertical plane in the N-S direction. These occurred in an area northeast of the line directing $N60^{\circ}W$ from the origin, \times in Fig. 3.

tion, a point is placed on the Earth's surface near the junction of the Kurile and Japan trenches. From this point, the hypocenters are projected on the azimuth-dip plane. Then the seismic zone becomes a thin plane. The position of the point is selected (\times in Fig. 3) so that the thickness of the seismic zone on the azimuth-dip plane becomes thinnest. Figure 4 shows the distribution of the hypocenters in the depth range between 80 and 150 km by the projection. A fairly thin continuous seismic zone which has a small scale Z-shaped peculiar folding appears just beneath the junction. If the distribution of hypocenters is nonuniform, the folded seismic zone may be an only apparent feature made by the projection. But the existence of the folding is reliable because hypocenters are located rather uniformly even in the folded seismic zone which corresponds to an area between the lines of $N30^{\circ}W$ and $N60^{\circ}W$ from \times in Fig. 3. It has been predicted that the seismic zone may be deformed notably at the transitional zone between Kurile and

northeast Honshu (ISACKS and MOLNAR, 1971; UTSU, 1971; AOKI, 1974), and existence of the folded seismic zone is significant.

Beneath the Tohoku and Kanto districts, northern and central Honshu, a double planed seismic zone was discovered (TSUMURA, 1973; UMINO and HASEGAWA, 1975). But beneath Hokkaido, double planed seismic zone is not obvious in the present analysis (Fig. 5). It may be suspected that absence of a double planed seismic zone was caused by the low accuracy of hypocenter determination. But UMINO and HASEGAWA (1975) showed that the seismic zone can be separated into two planes even using JMA data of low magnification seismographs. We believe that the time accuracy of the data of Hokkaido University is high enough to distinguish the hypocenters into two planes if they exist. Therefore the absence of double planed seismic zone beneath Hokkaido may be one of the essential characteristics of the arc-junction.

The thickness of the seismic zone in Fig. 5 is about 40 km and almost the same as that of Tohoku District (UMINO and HASEGAWA, 1975). If the thickness of the lithosphere including the seismic zone is about 40 km, it can be understood easily how the folding can be produced by conservation of area at the junction. But the lithosphere has thickness of about 100 km near the Japan trench (YOSHII, 1973). It is quite reasonable that the descending lithosphere keeps its thickness to the depth of 150 km at least. If the whole lithosphere with thickness of 100 km is rigid body and is folding in such a narrow region as shown in Figs. 3 and 4, earthquakes may occur in the whole lithosphere and thickness of seismic zone must become 100 km. Figure 4 shows that there is no difference in thickness of the seismic zone even in the folded zone and that just only the seismic zone with thickness of about 40 km is folding. These suggest that the thickness of rigid part in the lithosphere is about 40 km and that outer parts of the seismic zone in the lithosphere behave as a plastic body. TURCOTTE *et al.* (1978) suggested the existence of plastic behaviour of the lithosphere at the trench.

The focal mechanisms of intermediate earthquakes in the folded seismic zone may be influenced by the development of the folding. Maximum compressional and tensile stresses of these earthquakes are expected to have directions nearly perpendicular to the folding axis. Focal mechanism solutions for earthquakes that occurred in and around Hokkaido, have been obtained by many authors (ICHIKAWA, 1971; ISACKS and MOLNAR, 1971; KOYAMA *et al.*, 1973; SASATANI, 1976). Figure 6 shows distribution of the focal mechanism solutions after SASATANI (1976). In and around the folded seismic zone, the distribution of maximum stress direction appears to be not systematic. Nos. 29 ($h=114$ km), 38 ($h=133$ km) and 51 ($h=147$ km) earthquakes in Fig. 6 having E-W directions of compressional axis, are probably affected by the folding. But Nos. 2 ($h=300$ km) and 47 ($h=169$ km) direct their compressional axes almost parallel to the folding axis. These suggest that development of the folding affect the mechanisms of the earthquakes shallower than 150 km.

Figure 7 shows the distribution of hypocenters deeper than 150 km on the azimuth-dip plane. In this depth range the folded structure disappears. This suggests the existence of lateral tensile stress to smooth the folding. In Fig. 6, Nos. 4 ($h=240$ km), 8 ($h=280$ km), 18 ($h=309$ km), 20 ($h=221$ km), 22 ($h=224$ km) and 36 ($h=238$ km) direct the axes of tension almost perpendicular to the folding axis.

To establish the configuration of deep seismic zone and to understand how the folded seismic zone is smoothed, more data of deep earthquake are required.

There are three notable arc-junctions in Japan. AOKI (1974) investigated P-wave

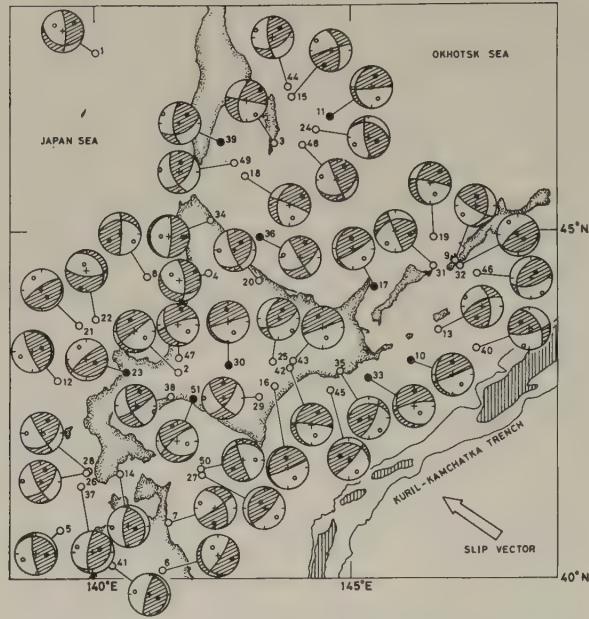


Fig. 6. Focal mechanism solutions of earthquakes that occurred near the Hokkaido corner. In the solution a filled small circle represents the axis of tension and an unfilled small circle the axis of compression (after SASATANI, 1976).

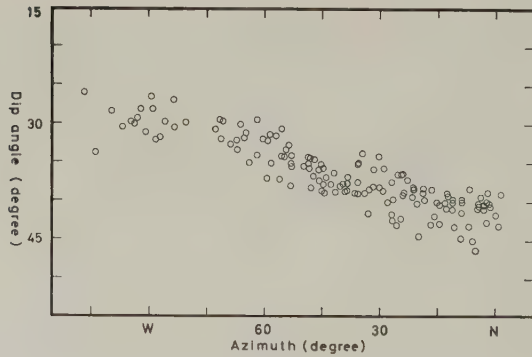


Fig. 7. Distribution of hypocenters of earthquakes on the azimuth-dip plane deeper than 150 km.

travel time anomaly of Cannikin event and concluded that the descending lithosphere separates into two segments and overlapped beneath central Honshu. However, folded seismic zone is not found beneath central Honshu or any other arc-junctions except for the Hokkaido corner.

4. Attenuation of Seismic Waves in the Upper Mantle

A large scale anomalous structure of the upper mantle beneath the island arcs of Japan has been confirmed by UTSU (1966) and UTSU and OKADA (1968) from the evidence of anomalous seismic wave propagation. According to these studies, ratio of Q for high Q to low Q zones in the upper mantle is estimated to be 10. In this section, distribution of Q values for S wave in the low Q wedge beneath the Hokkaido corner using local earthquakes, is described. Q values are determined by using S/P method (SACKS and OKADA, 1974). In this method, the spectra of P and S waves originated from the same source are compared and two assumptions are required to obtain Q values. One is that ratio of Q for P wave to S wave is assumed to be constant. ANDERSON *et al.* (1965) suggested the value of 2.25 for the ratio. The other, the source spectra of P wave and S wave are assumed to be identical.

There are many methods for determination of Q (OKADA, 1977), for example, direct slope method (ASADA and TAKANO, 1963; TAKANO, 1966; OLIVER and ISACKS, 1967), spectral ratio method, comparative path method (UTSU and OKADA, 1968), differential path method, and S/P method. S/P method, though containing some ambiguities, has an advantage for evaluating the regional variation of Q values beneath the island arcs.

Forty earthquakes including several shallow earthquakes are used for the determination of Q values. For spectral analysis, multichannel band-pass filters are used. The electric Q values of the filters are adjusted to be 20. Average amplitudes of P and S waves are measured from filtered records. Time intervals for the averaging are selected to be 0.5 and 1.0 sec for P and S waves respectively. Distribution of the apparent Q values along the paths from hypocenters to stations is shown in Fig. 8. Beneath the central and northern parts of Hokkaido, apparent Q values appear to be 150, while southwestern part,

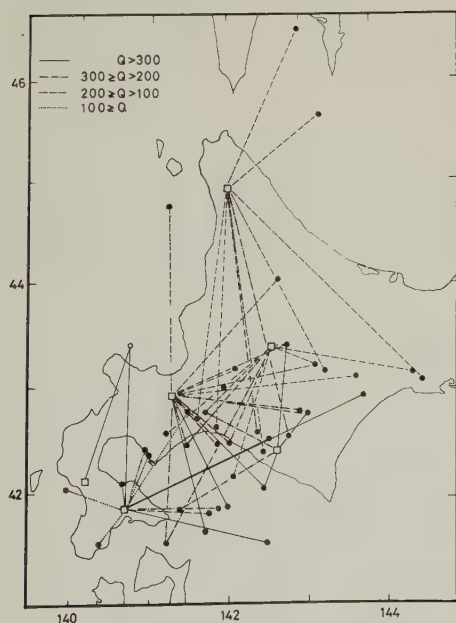


Fig. 8. Distribution of apparent Q values for S waves along the paths from hypocenters to the stations. Open circles denote epicenters of earthquakes shallower than 50 km, and solid circles those in excess of 50 km. Squares indicate locations of the stations.

it is about 70 for intermediate and deep earthquakes. For shallow earthquakes, Q values of about 400 are obtained beneath the southwestern part. To obtain the average Q values in the upper mantle, the effect of Q in the crust must be excluded. Apparent Q and travel time T are expressed simply by

$$T/Q = T_c/Q_c + T_m/Q_m, \quad T = T_c + T_m$$

where T_c , T_m and Q_c , Q_m are travel times and Q values in the crust and upper mantle respectively. Beneath the central and northern part of Hokkaido, Q_m is estimated to be 120 and southwestern part, to be 50. The latter is extremely low and smaller than that of central Honshu obtained by using the same method (SACKS and OKADA, 1974). But this value is almost the same as those beneath the Lau basin, west off the Tonga arc (BARAZANGI and ISACKS, 1971) and northern part of New Zealand (MOONEY, 1970), though different methods were used to estimate Q values.

In the southwestern part of Hokkaido, high heat flow values (2–4 HFU) are observed and high temperature in the upper mantle is estimated, while in the central and northern parts, heat flow values are not so high (1.0–1.5 HFU) (EHARA, 1974). BARAZANGI *et al.* (1975) pointed out that the high attenuation zones correspond to the areas of high heat flow and low seismic wave velocities by using spectral ratios for P and pP phases. And they indicated that the upper mantle beneath the whole Hokkaido is a low attenuation zone, and they could not distinguish such a regional difference in Hokkaido.

Distribution of Q values beneath Hokkaido obtained in this study suggests that high temperature and partial melting in the upper mantle is probably the main cause of the seismic wave attenuation.

The author wishes to thank Professor Hiroshi Okada who read the manuscript. I am indebted to the seismological observatories and Research Center for Earthquake Prediction of Hokkaido University for supplying earthquake data. I also thank Drs. Hiromu Okada and Tohoru Nakajima for many criticisms and suggestions. The numerical calculations were carried out by FACOM-230-60/75 at the Computer Center of Hokkaido University (Problem No. 1001FR0420).

REFERENCES

- ANDERSON, D.L., A. BEN-MENACHEM, and C.B. ARCHAMBEAU, Attenuation of seismic energy in the mantle, *J. Geophys. Res.*, **70**, 1441–1448, 1965.
- AOKI, H., Plate tectonics of arc-junction at central Japan, *J. Phys. Earth*, **22**, 141–161, 1974.
- ASADA, T. and K. TAKANO, Attenuation of short period P wave in the mantle, *J. Phys. Earth*, **11**, 25–34, 1963.
- BARAZANGI, M. and B. ISACKS, Lateral variations of seismic-wave attenuation in the upper mantle above the inclined earthquake zone of the Tonga Island Arc: Deep anomaly in the upper mantle, *J. Geophys. Res.*, **76**, 8493–8516, 1971.
- BARAZANGI, T., W. PENNINGTON, and B. ISACKS, Global study of seismic wave attenuation in the upper mantle behind island arcs using pP waves, *J. Geophys. Res.*, **80**, 1079–1092, 1975.
- EHARA, S., Thermal structure of the crust and upper mantle beneath Hokkaido and its surrounding regions deduced from terrestrial heat flow, *Geophys. Bull. Hokkaido Univ.*, **31**, 33–48, 1974 (in Japanese).
- ICHIKAWA, M., Reanalysis of mechanism of earthquakes which occurred in and near Japan and statistical studies on the solutions obtained, 1926–1968, *Geophys. Mag.*, **35**, 207–274, 1971.
- ICHIKAWA, M. and E. MOCHIZUKI, Travel time tables for local earthquakes in and near Japan, *Pap. Meteorol. Geophys.*, **22**, 229–290, 1971 (in Japanese).
- ISACKS, B. and P. MOLNAR, Distribution of stress in the descending lithosphere from a global survey of focal mechanism solutions of mantle earthquakes, *Rev. Geophys. Space Phys.*, **9**, 103–174, 1971.
- KATSUMATA, M. and L.R. SYKES, Seismicity and tectonics of the western Pacific: Izu-Mariana-Caroline and Ryukyu-Taiwan regions, *J. Geophys. Res.*, **74**, 5923–5948, 1969.
- KATSUMATA, M., Seismicity and some related problems in and near the Japanese islands, *Kenshinjiho (Quart. J. Seismol.)*, **35**, 75–142, 1970 (in Japanese).

- KOYAMA, J., S. HORIUCHI, and T. HIRASAWA, Earthquake generating stresses in North-eastern Japan arc inferred from superposition of the initial motions of P-waves, *Zisin (J. Seismol. Soc. Jpn.)*, Ser. 2, **26**, 241–253, 1973 (in Japanese).
- MOONEY, H.M., Upper mantle inhomogeneity beneath New Zealand: Seismic evidence, *J. Geophys. Res.*, **75**, 285–309, 1970.
- OKADA, H., Fine structure of the upper mantle beneath Japanese island arcs as revealed from body wave analysis, Ph. D. Thesis Hokkaido Univ., 1977.
- OLIVER, J. and B. ISACKS, Deep earthquake zones, anomalous structure in the upper mantle, and the lithosphere, *J. Geophys. Res.*, **72**, 4259–4275, 1967.
- SACKS, I.S. and H. OKADA, A comparison of the anelasticity structure beneath western south America and Japan, *Phys. Earth Planet. Inter.*, **9**, 211–219, 1974.
- SASATANI, T., Mechanism of mantle earthquakes near the junction of the Kurile and the northern Honshu arcs, *J. Phys. Earth*, **24**, 341–354, 1976.
- SHIBUYA, K., Y. MIYASHITA, and K. TSUMURA, The crustal structure of the Kanto district, *Abstr. Meet. Seismol. Soc. Jpn.*, **2**, 225, 1973 (in Japanese).
- TAKANO, K., Attenuation of Short period S waves in the mantle, *Zisin (J. Seismol. Soc. Jpn.)*, Ser. 2, **19**, 246–254, 1966 (in Japanese).
- TSUMURA, K., Microearthquake activity in the Kanto district, Publications for the 50th Anniversary of the Great Kanto Earthquakes, 1923, pp. 67–87, 1973 (in Japanese).
- TURCOTTE, D.L., D.C. McDoo, and J.G. CALDWELL, An elastic-perfectly plastic analysis of the bending of the lithosphere at a trench, *Tectonophysics*, **47**, 193–205, 1978.
- UMINO, T. and A. HASEGAWA, On the two-layered structure of deep seismic plane in northeastern Japan arc, *Zisin (J. Seismol. Soc. Jpn.)*, Ser. 2, **28**, 125–140, 1975 (in Japanese).
- UTSU, T., Regional differences in absorption of seismic waves in the upper mantle as inferred from abnormal distribution of seismic intensities, *J. Fac. Sci. Hokkaido Univ.*, Ser. 7, **2**, 359–374, 1966.
- UTSU, T., Seismic activity in Hokkaido and its vicinity, *Geophys. Bull. Hokkaido Univ.*, **20**, 51–75, 1968 (in Japanese).
- UTSU, T., Anomalous structure of the upper mantle beneath the Japanese islands, *Geophys. Bull. Hokkaido Univ.*, **25**, 99–127, 1971 (in Japanese).
- UTSU, T., Distribution of earthquakes in and near Japan, *Kagaku*, **44**, 739–746, 1974 (in Japanese).
- UTSU, T. and H. OKADA, Anomalies in seismic wave velocity and attenuation associated with a deep earthquake zone (II), *J. Fac. Sci. Hokkaido Univ.*, Ser. 7, **3**, 65–84, 1968.
- YOSHII, T., Upper mantle structure beneath the north Pacific and the marginal seas, *J. Phys. Earth*, **21**, 313–328, 1973.
- WADATI, K., T. HIRONO, and T. YUMURA, On the attenuation of S-waves and structure of upper mantle in the region of Japanese islands, *Pap. Meteorol. Geophys.*, **20**, 49–78, 1969.

SEDIMENTARY PATTERNS IN APPARENT BACK-ARC BASINS: A CASE STUDY OF THE NEOGENE SEQUENCE IN NORTHWESTERN HOKKAIDO, JAPAN

Hakuyu OKADA

Geoscience Institute, Faculty of Science, Shizuoka University, Shizuoka, Japan

(Received June 30, 1978; Revised October 9, 1978)

In northwestern Hokkaido, where the Honshu and Kuril arcs intersect, an enormous pile of Neogene sediments (about 10 km thick) is developed in close relation to the Cenozoic orogenesis. The Kotanbetsu Formation, representing the lower to middle Miocene sequence of these sediments, exceeds 3 km in thickness and is characterized by gravity-flow deposits. The strata are divisible into three major facies: 1) chaotic deposits or olistostrome facies, 2) graded-bed or turbidite facies, and 3) ripple-bed or contourite facies.

The chaotic deposit facies, rather restricted in distribution in the proximal parts of the basin, is further subdivided into three sedimentary types: pebbly mudstone, chaotic breccia, and matrix-deficient conglomerate. The graded-bed and the ripple-bed facies are predominant in the relatively distal parts of the basin. The chaotic deposits were generated by intense tectonic movements of the 'Mesozoic' basement rocks thrust up to towards the west. The graded beds were deposited from turbidity currents, although their current directions are not clearly defined, whilst the ripple beds were formed by southward-flowing contour currents.

These characteristic sediments are comparable in their tectonic position of an apparent back-arc belt to the Onerahi Chaos-Breccia of Northland, New Zealand, related to the Miocene to Pliocene Kaikoura Orogeny. The Kotanbetsu and its equivalents, however, may have been the deposits in basins produced by collision of two continental blocks, known generally as the Hidaka Orogeny, but not in the ancient back-arc belt.

1. Introduction

The structural framework of arc systems and their tectonic development have been studied in some detail in terms of plate tectonics. However, the sediments, an important component of arc systems, are not so well understood. This paper presents an interesting example of the sedimentary features in tectonically active Neogene basins of the present back-arc area in northwestern Hokkaido.

Neogene sedimentary basins in northwestern Hokkaido, which are developed along the western margin of the Hidaka Mountain Range, apparently occupy the present back-arc position. Sediments in these basins attain a tremendous thickness, probably more than 10 km, far thicker than contemporaneous sediments in other areas of Hokkaido (Fig. 1). Neogene sediments in the west of the Hidaka Mountain Range have long been regarded as postorogenic sediments of the so-called Hidaka Orogeny which made the backbone of Hokkaido by the early Miocene (NAGAO, 1938; MINATO *et al.*, 1965), and in this context the Kawabata Formation in central Hokkaido and the Kotanbetsu Formation in the northwestern part are well known, both representing postorogenic sediments. It is interesting to note that serpentinite sandstones occur in the sequence of the Kawabata Formation (OKADA, 1964).

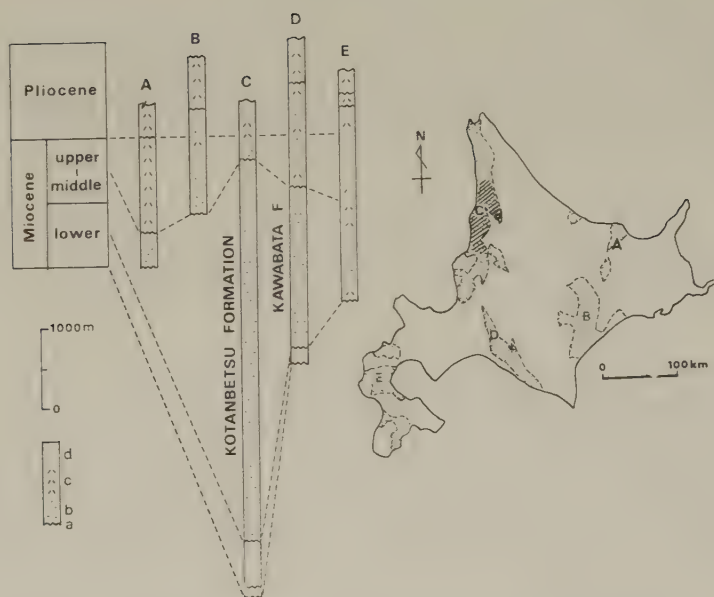


Fig. 1. Index map of Hokkaido showing major outcrops of Neogene sediments (dotted). Hatched are the exposures of the Kotanbetsu Formation, which are enlarged in Fig. 2. Columnar sections (A-E) showing generalized Neogene successions at some representative areas (Letters A-E correspond to those in the index map: A, Abashiri; B, Honbetsu; C, Haboro; D, western part of the Ishikari coal field; E, Setana; modified from MINATO *et al.*, 1965, pp. 262-263). a, unconformity; b, coarse clastics; c, pyroclastics; d, fine clastics.

This paper, aimed at presenting the sedimentary characteristics of apparent back-arc basins, describes the lithofacies of the Kotanbetsu Formation and discusses its tectonic significance.

2. Geologic Setting

Neogene strata, underlain by the Upper Cretaceous and locally by the Paleogene, are excellently exposed in northwestern Hokkaido. They are composed mostly of marine water deposits and partly of brackish to non-marine water ones. The general stratigraphy of the Neogene in the central part (Shosanbetsu and Haboro areas) is summarized in Table 1 according to MATSUNO and KINO (1958) and HATA (1961). The early Pliocene to late Miocene sequence of Table 1 was intensively studied by UJHÉ *et al.* (1977) in order to establish a combined microfossil-paleomagnetic-sedimentologic stratigraphy. Their study indicates that Neogene marine sediments reveal evidence of active arc magmatism at the time of deposition related to active plate motion and a remarkably fast rate of sedimentation.

The early to middle Miocene Kotanbetsu Formation is very different in lithology and thickness from the rest of the Neogene (Fig. 1), as described in the following sections. This formation is most widely developed in northwestern Hokkaido, being accommodated

Table 1. General stratigraphy of the Neogene succession in the central part of northwestern Hokkaido.

Age	Stratigraphic unit*	Lithology	Environment	Thickness (m)
Pliocene	Mochikubetsu Formation	Fine-grained sandstone with pebbly sandstone near its top	Marine	260-350
	Embetsu Formation	Diatomaceous mudstone with a basal, strongly cross-bedded, coarse-grained sandstone	Marine	160-700
Miocene	Kinkomanai F./ Higashino F./ Chiebotsunai F.	Tuffaceous fine- to coarse-grained sandstone with andesitic agglomerate and breccia	Marine to the north and non-marine to the south	50-270
	Kotanbetsu Formation	Chaotic deposits and interbedded mudstone, graded sandstone and graded conglomerate	Marine	>3,000
	Chikubetsu Formation	Upper mudstone with shallow marine molluscs, lower sandstone with coaly shale and basal conglomerate	Shallow marine to brackish water	<450
	Sankebetsu Formation	Lower fine- to medium-grained sandstone and upper tuffaceous sandstone and shale alternation	Marine	<800
	Haboro Formation	Fine- to coarse-grained sandstone interbedded with mudstone, bentonitic tuff, coal and coaly shale	Non-marine	<240
?	Pankezawa Formation	Upper banded andesitic crystal tuff and lower medium- to coarse-grained, massive sandstone	?	<115

* conformable, ~~~~~ unconformable.

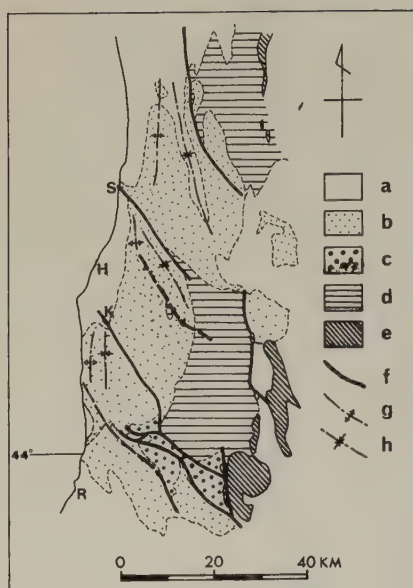


Fig. 2. Geologic map showing the distribution and major structures of the Kotanbetsu Formation (adapted from GEOLOGICAL SURVEY OF JAPAN, 1962, 1965). a, post-Kotanbetsu sequence; b, Kotanbetsu Formation (the Miocene sequence underlying the Kotanbetsu Formation is included); c, Paleogene strata; d, Cretaceous sediments; e, serpentinite masses; f, thrusts; g, anticlinal axis; h, synclinal axis; S, Shosanbetsu; H, Haboro; K, Kotanbetsu; R, Rumoi.

in at least three depositional basins which are separated by major thrusts with an NW-SE trend (Fig. 2; MATSUNO, 1958). These thrusts are regarded as synsedimentary tectonic structures, along which Upper Cretaceous sedimentary rocks are narrowly exposed, sometimes forming dome structures. The Kotanbetsu Formation also forms large-scale fold structures with N-S axes plunging gently northwards. Two major synclines and one major anticline are recognized in the Shosanbetsu area (Fig. 2), the anticline indicating oil seepage at some places along the crest.

3. Sedimentology of the Kotanbetsu Formation

3.1 Lithofacies

The Kotanbetsu Formation, more than 3,000 m thick in the northern basin (Shosanbetsu area; see Fig. 2) is generally characterized by gravity-flow deposits. The formation is divisible fundamentally into three major facies: 1) chaotic deposit facies, 2) graded-bed facies, and 3) ripple-bed facies.

1) *Chaotic deposit facies.* This facies is rather restricted in distribution, mainly near the southern margin of the basin (Fig. 3). The facies may be further subdivided into three sedimentary types: 1a) pebbly mudstone, 1b) chaotic breccia, and 1c) matrix-deficient conglomerate.

1a) The pebbly mudstones are characterized by many pebbles, cobbles, and boulders randomly floating without clast contacts within non-stratified mudstones (Fig. 4). The clasts are generally fairly rounded. One of the pebbly mudstone sequences is about 200 m thick in the proximal part and traceable over 20 km, thinning out distally. The pebbly mudstones show the most extensive distribution of the chaotic deposits.

1b) The chaotic breccias are composed mostly of subangular to angular pebbles, cobbles, and boulders together with blocks of varying sizes from less than 1 cm to more than 20 m in diameter. The clasts show neither sorting effect nor preferred orientation.

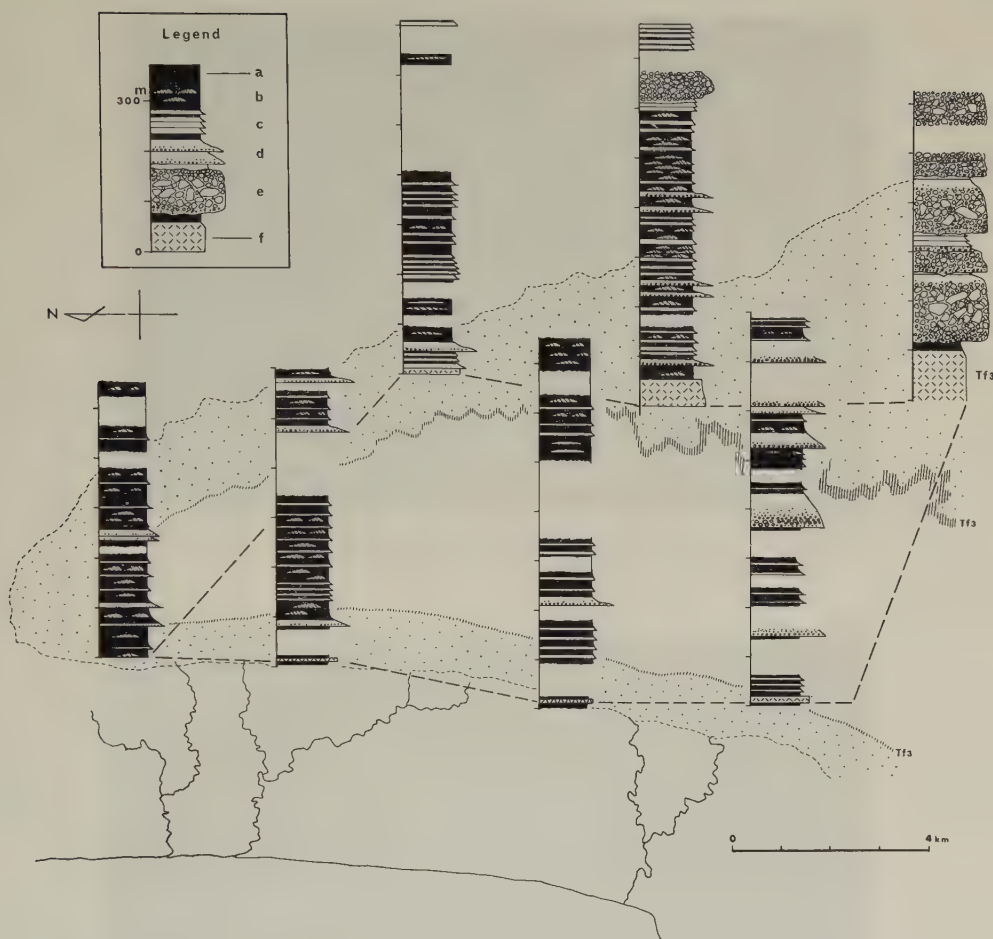


Fig. 3. Columnar sections at some selected localities showing lithofacies changes in the Kotanbetsu Formation above the sequence of a tuff bed tf3 exposed to the northeast of Shosanbetsu (Fig. 2). Note also that the thickness of tf3 decreases northwards. a, claystone; b, ripple beds; c, graded sandstone beds; d, graded conglomerate beds; e, chaotic breccia; f, tuff.

Boulders and blocks consist generally of mudstone and thinly alternating sandstone and shale of 'cannibalistic' origin. Many of the stratified rock clasts show contorted or folded structures, formed during the sliding down of the chaotic breccias. Smaller clasts consist of extrabasinal older sedimentary rocks such as sandstone, slate, chert, marl and limestone, granite, porphyry, basalt, and so on. The matrix of the breccia is either coarse-grained sandstone or claystone, and this forms 10 to 50% of the rock. The chaotic breccias are mostly developed in the southeastern part of the basin, exceeding 50 m in thickness. The occurrence of the chaotic breccias is shown in Fig. 5.

1c) The matrix-deficient conglomerates are composed mainly of sorted, subangular to rounded pebbles and cobbles (Fig. 6). These consist of older (Mesozoic?) sedimentary rocks (mostly sandstone and slate), granite, basalt, rhyolite, porphyry, etc. This kind of deposit is from several meters to some tens of meters in thickness, sometimes reaching more than 100 m.

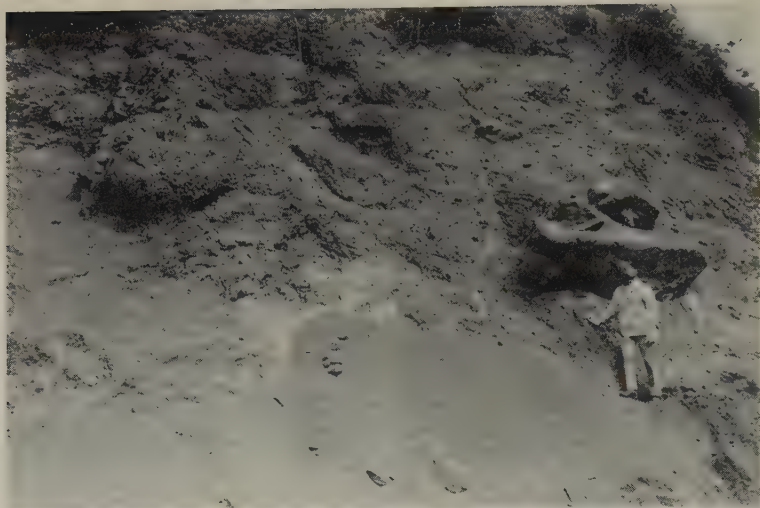


Fig. 4. An exposure of pebbly mudstones, about 16 km east of Haboro. Clasts of varying sizes are embedded in mudstones.

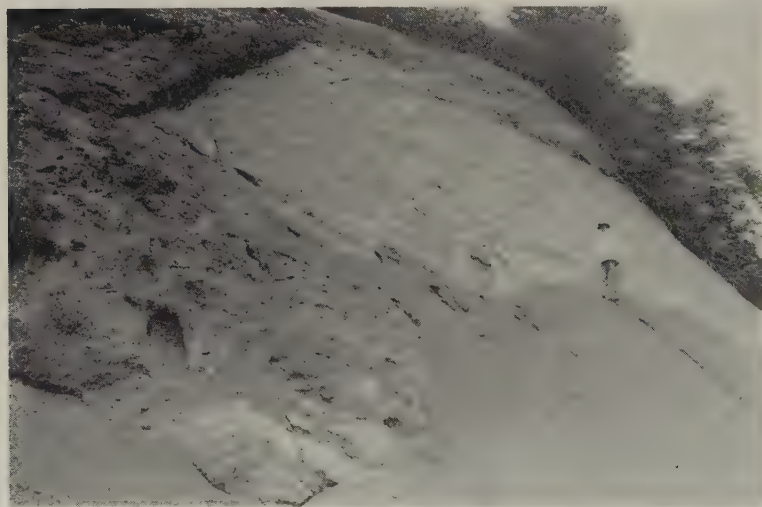


Fig. 5. Chaotic breccias, about 18 km east of Haboro, showing a large block of disrupted beds as large as at least 20 m.

2) *Graded-bed facies*. This facies is characterized by graded sandstone and/or conglomerate beds. It is predominant in more distal parts of the basin than the chaotic deposit facies. Graded sandstone beds are variable in thickness from a few centimeters to 5 m, whereas graded conglomerate beds are usually several meters thick. In many cases, graded conglomerate beds with gradually decreasing particle size change upwards into graded sandstones and finally into mudstones. Graded conglomerate beds almost always show reverse grading over several centimeters from their bases. In graded sandstone



Fig. 6. Matrix-deficient conglomerates in the river bed exposure in the upper course of the Sankebetsu River, about 17 km southeast of Kotanbetsu.

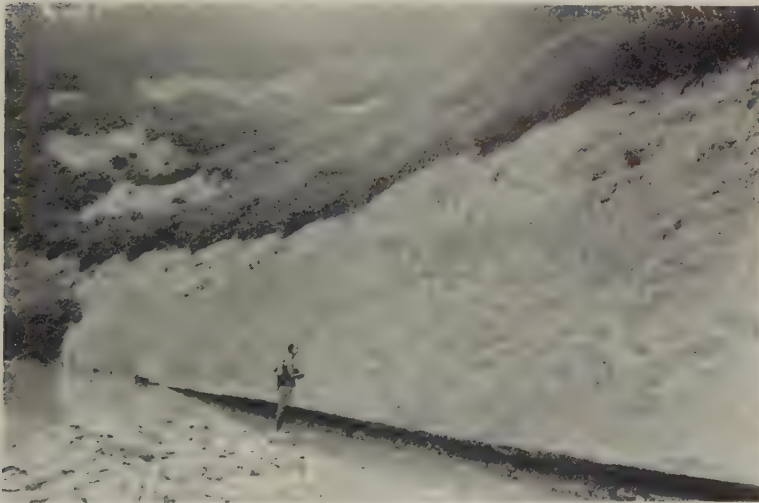


Fig. 7. A very thick graded bed with granule conglomerates at the basal part which are gradually changed upwards into very fine-grained sandstones, showing a clean-cut bottom surface.

beds, Ta, Tb, and Tb-c of the Bouma sequence (BOUMA, 1962) are common as internal structures. Usually the bottom surface of the graded beds is remarkably flat (Fig. 7).

3) *Ripple-bed facies*. This is represented by mudstones frequently intercalated by rippled thin beds of fine- to medium-grained sandstones (Fig. 8). These sandstone beds show some characteristic features: a) both upper and lower surfaces are sharply defined, b) small-scale ripple marks are developed on the surface, c) minor cross-lamination is common as internal structures, d) no graded-bedding is observed at all, e) the thickness of

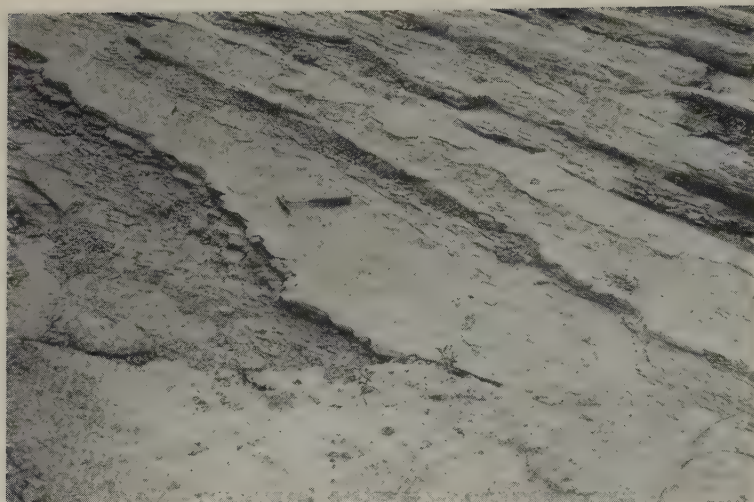


Fig. 8. Typical exposure of the ripple-bed facies in the river bed of the Kotanbetsu River, about 6 km southeast of Kotanbetsu.

beds ranges from 0.5 to 3 cm, and f) the sandstones are deficient in matrix and well sorted in texture. Sometimes a type of ripple-bedding known as flaser-bedding is observed, which shows rippled sand lenses preserved within the mud, with mud streaks in the troughs and on the crests of ripples.

Horizontal and vertical distributions of the lithofacies described above are summarized as follows: the Kotanbetsu Formation as a whole shows that the chaotic breccia facies is developed in the most proximal or southeasternmost part of the basin, the pebbly mudstone and matrix-deficient conglomerate facies are more prominent in the proximal part, the graded bed facies is developed in more distal parts than the chaotic breccia facies, and the rippled bed facies is characteristic of the most distal part or the northernmost area of the basin (Fig. 3).

The vertical succession of the Kotanbetsu Formation generally shows a rhythmic stratigraphic pattern, which is distinguished by a unit sedimentary cycle (in ascending order): graded conglomerate–graded sandstone–mudstone with rippled or graded sandstone beds. The thickness of the unit sedimentary cycles ranges from 20 to 100 m. The mudstone sequence of unit cycles tends to predominate in the more distal areas.

As stated above, the general lithology of the Kotanbetsu Formation shows a gradual predominance of the fine-grained facies northwards or in distal areas. At the same time, not only single beds but also particular stratigraphic sequences decrease their thickness in the same direction (see a tuff bed tf3 in Fig. 3 and the sequence between tuff beds tf2 and 3 in Fig. 9).

3.2 *Paleocurrents*

Paleocurrent analysis was attempted, using sole markings such as flute marks, groove marks, etc. as well as ripple marks and cross-stratification. Sole markings indicate strong westward-flowing currents at the southwesternmost part of the Shosanbetsu basin, but are too poorly developed to show general current directions in the distal areas. On the



Fig. 9. Lithofacies changes of the Kotanbetsu Formation from south (Wuennai River section) to north (Chebotsunai River section) (15 km away) in the Kotanbetsu area in a sequence between Tuff 2 and Tuff 3.

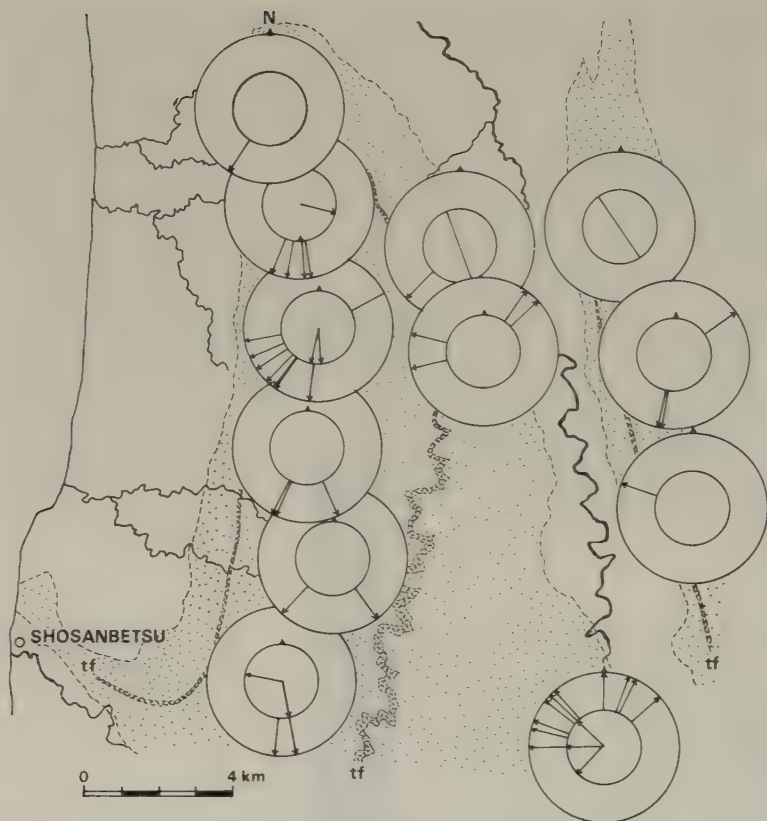


Fig. 10. Map showing paleocurrent directions in the sequence above Tuff 3 in the northern basin of the Kotanbetsu deposits. Outer circle, ripple marks and cross-laminations; inner circle, sole marks.

contrary, ripple marks and cross-laminae show southward movements of bottom waters (Fig. 10).

3.3 Composition

For the conglomerates and breccias, the boulders and blocks are composed mostly of mudstone and stratified sedimentary rocks of 'cannibalistic' origin and partly of Mesozoic (?) sandstones and other sedimentary rocks, while granules, pebbles, and cobbles consist for the most part of Mesozoic (?) sandstone and slate (more than 80%) and partly of limestone, marl, chert (<5%), granite (<15%), porphyritic rocks, rhyolite, andesite, basalt, basic tuff, and others (<3%). Of these components, limestone and granite are relatively concentrated locally.

The sandstones are generally well-sorted, fine- to medium-grained and calcite-cemented. As Fig. 11 shows, major constituents of the sandstones are characterized by the overwhelming amount of lithic fragments derived from sedimentary rocks and igneous rocks as well as by a deficiency of quartz grains. Heavy minerals of the sandstones are characterized by rounded grains of zircon, tourmaline, rutile, and garnet and less worn

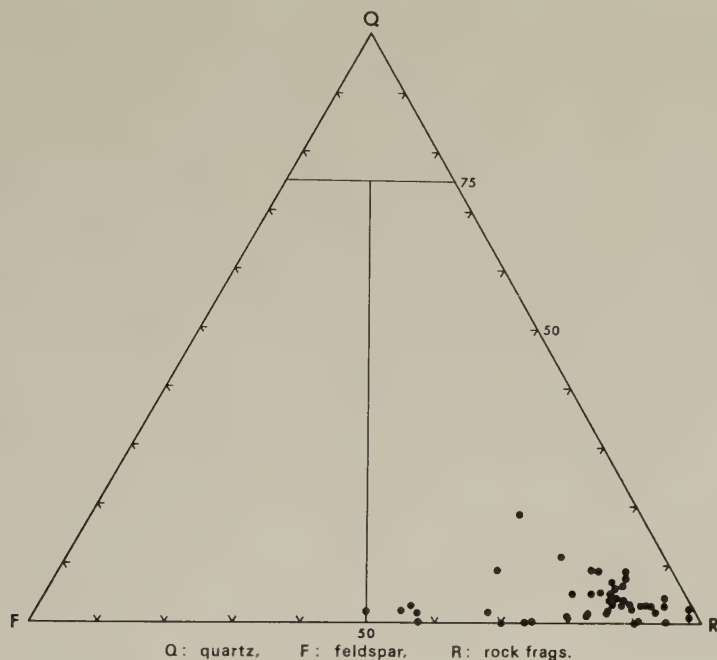


Fig. 11. Ternary diagram showing the composition of the Kotanbetsu sandstones, which are classified as the lithic arenite.

grains of augite, hornblende, epidote, anatase, etc. They suggest that sedimentary rocks and volcanic rocks were important as source rocks.

4. Discussion

During a short time span of the early to middle Miocene, an enormous pile of clastic sediments of the Kotanbetsu Formation was developed under the control of gravity in rapidly subsided basins along the western margin of the meridional Hidaka Mountain Range. The Kotanbetsu sedimentary basin seems originally to have been separated into some minor basins with an N-S direction (MATSUNO, 1958). These minor basins might have been formed through the development of the NW-SE trending faults, along which Mesozoic and Paleogene basement rocks were thrust up to form raised topographic features. Such active tectonic uplifts supplied detritus to the basins, and the cyclic stratigraphy of the Kotanbetsu Formation suggests rhythmic upheavals of these uplifts.

The lithology, geometry of the strata and the paleocurrent system suggest that the clastics of the Kotanbetsu Formation were supplied from the southeast. The sedimentary features summarized in the preceding section lead us to interpret the chaotic breccias as an olistostrome (in the sense of ELTER and TREVISAN, 1973) resulting from intense tectonic movements of the basement rocks thrust up to the west. The matrix-deficient conglomerates are assigned to grain-flow deposits defined by MIDDLETON and HAMPTON (1976). The graded-bed facies represents turbidity-current deposits or turbidites, and the ripple-bed facies implies contour-current deposits or contourites (see BOUMA, 1972). The

turbidity currents may have flowed in the proximal part mainly from the east to the west, but in the distal part it is rather difficult to define general current directions. However, the contourites were formed mainly by southward-flowing bottom currents.

The Kotanbetsu basin, characterized by thick gravity-flow deposits, extends southwards into the contemporaneous Kawabata basin filled up by similar sediments, and further southwards into the Neogene sedimentary basin called the Hidaka Trough (ISHIWADA and OGAWA, 1976) with more than 8 km of sediments. These depressions seem to represent the final stage of a collision of two continents, the western Hokkaido west of the Kamuikotan Belt and the Okhotsk Platform, which took place from the late Cretaceous to the early Miocene, as is advocated by GRAPES (1978). A series of the movements may correspond to the so-called Hidaka Orogeny, as was first argued by HORIKOSHI (1972). Westward upthrusting or overthrusting of basement rocks due to the southwestward movement of the Okhotsk Platform, depressing the eastern margin of the western Hokkaido block, developed these deep Neogene basins, which was most intense during Miocene time. In a sense that these basins apparently occupy the present back-arc belt in terms of arc tectonics (DICKINSON, 1974), the Kotanbetsu deposits are comparable to the Onerahi Chaos-Breccia (KEAR and WATERHOUSE, 1967) of Northland, New Zealand, which is related to the Miocene to Pliocene Kaikoura Orogeny (GRINDLEY, 1974). However, the Kotanbetsu and its related sediments cannot be regarded as representing the back-arc position, because they may have been deposited in basins developed by a collision of two continental blocks.

In addition, it is interesting that the Kotanbetsu and its equivalents are developed at the present arc-junction between the Honshu and Kuril arcs, where the folded seismic zone was recently discovered by MORIYA (1978) beneath the arc junction. In order to understand more fully the original tectonic setting of the present Neogene sedimentary basins, mutual relationships between these facts should be analyzed. It is also obvious that the Kotanbetsu and its equivalent sediments were deposited at a time of intense arc tectonism related to active plate movement in the North Pacific (HILDE *et al.*, 1977; NIITSUMA, 1978, among others).

5. Summary and Conclusions

This sedimentological study was carried out on the middle Miocene Kotanbetsu Formation which is a part of the very thick Neogene sediments in the west of the Hidaka Mountain Range, where the Honshu and Kuril arcs meet. The results of the study are summarized as follows:

The Kotanbetsu Formation, more than 3,000 m thick, was deposited in rapidly subsiding basins in a short time span within the early to middle Miocene, which seem originally to have been divided into some minor basins open to the northwest, arranged en echelon in an N-S direction. They were under active tectonic controls mainly due to thrust movements of basement rocks composed mainly of probably Mesozoic rocks, which provided such characteristic sediments as gravity-flow deposits.

The sediments of the Kotanbetsu Formation are divided into three major facies: 1) chaotic deposit or olistostrome facies, 2) graded-bed or turbidite facies, and 3) ripple-bed or contourite facies. The chaotic deposit facies is further subdivided into three sedimentary types: 1a) pebbly mudstone, 1b) chaotic breccia, and 1c) matrix-deficient conglomerate. The first type shows the most extensive distribution; the second one is

the most characteristic of the chaotic deposits, consisting of granules to boulders and blocks of varying sizes, of both intrabasinal and extrabasinal origins; the last one is characterized by sorted, subangular to rounded cobbles of extrabasinal origin. The chaotic breccias are mostly developed in the proximal (southern) parts of the basin. The graded-bed facies is predominant to the north of the chaotic breccia facies, and the ripple-bed facies is developed in the distal (northern) parts of the basin. The general lithology of the Kotanbetsu Formation shows a gradual predominance of the fine-grained facies northwards or in the distal areas.

The paleocurrent system and other sedimentary features suggest that the clastics were supplied from the southeast: the chaotic breccias were developed in the most proximal parts owing to intense tectonic movements of the basement rocks thrust up westwards. The graded beds were deposited from turbidity currents, though direction of these current flows is not clearly defined owing to a paucity of measurable sole markings. The ripple beds were developed in the mudstone facies by south-flowing contour currents.

The composition of the sediments is characterized by the predominance of clasts from both older and contemporaneous sedimentary rocks together with some igneous rocks.

Although the apparent tectonic position of the Kotanbetsu Formation in the present back-arc belt is similar to that of the Onerahi Chaos-Breccia of Northland, New Zealand, related to the Miocene to Pliocene Kaikoura Orogeny, the Kotanbetsu and its equivalents may have been deposited in basins developed by a collision of two continental blocks, which seems to correspond to the so-called Hidaka Orogeny. Therefore, the Kotanbetsu and its related sediments do not represent the ancient back-arc belt.

I would like to thank Mr. Henk Worries (Union Oil International Los Angeles), Professor Nobu Kitamura (Tohoku University), Professor William R. Dickinson (Stanford University), and Dr. Nobuaki Niitsuma (Shizuoka University) for their encouragement and fruitful discussions. I am indebted to Dr. John H. McD. Whitaker (University of Leicester) for his valuable comments and for reviewing the manuscript. Acknowledgement is due to the Japan Petroleum Exploration Co., Ltd. (Tokyo and Sapporo Offices) for supporting the field work. The study is supported by a Grant-in-Aid for Scientific Researches from the Ministry of Education (Grant No. 246037).

REFERENCES

- BOUMA, A.H., *Sedimentology of Some Flysch Deposits*, 168 pp., Elsevier, Amsterdam, 1962.
- BOUMA, A.H., Recent and ancient turbidites and contourites, *Trans. Gulf Coast Assoc. Geol. Soc.*, **22**, 205–221, 1972.
- DICKINSON, W.R., Sedimentation within and beside ancient and modern magmatic arcs, in *Modern and Ancient Geosynclinal Sedimentation*, Soc. Econ. Paleont. Mineral., Spec. Publ., No. 19, edited by R.H. Dott, Jr. and R.H. Shaver, pp. 230–239, 1974.
- ELTER, P. and L. TREVISAN, Olistostromes in the tectonic evolution of the Northern Apennines, in *Gravity and Tectonics*, edited by K.A. De Jong and R. Scholter, pp. 175–188, Wiley, New York, 1973.
- GEOLOGICAL SURVEY OF JAPAN, Haboro: Geological Map of Japan (Scale 1: 200,000), 1962.
- GEOLOGICAL SURVEY OF JAPAN, Metallic and Non-metallic Mineral Deposits of Hokkaido. IV. Geological Map of Hokkaido (Scale 1: 800,000), 1965.
- GRAPES, R.H., Mesozoic-Cenozoic arc-trench development, Neogene orogeny and the 'Hidaka Belt' anomaly in Hokkaido, in *Plutonism in Relation to Volcanism and Metamorphism*, ICGP 7th Circum Pacific Plutonism Project Meeting, Toyama, pp. 282–296, 1978.
- GRINDLEY, G.W., New Zealand, in *Mesozoic-Cenozoic Orogenic Belts*, edited by A.M. Spencer, pp. 387–416, Geol. Soc. London, London, 1974.
- HORIKOSHI, E., Orogenic belts and plates in Japanese Islands, *Kagaku (Science)*, **42**, 665–673, 1972 (in Japanese).
- HATA, M., Hatsuura: Explanatory text of the geological map of Japan (Scale 1: 50,000), pp. 1–60, Geol. Surv. Japan, Kawasaki, 1961.
- HILDE, T.W.C., S. UYEDA, and L. KROENKE, Evolution of the western Pacific and its margin, *Tectonophysics*, **38**, 145–165, 1977.

- ISHIWADA, Y. and K. OGAWA, Petroleum geology of offshore areas around the Japanese Islands, *U.N. ESCAP, CCOP Tech. Bull.*, **10**, 23–34, 1976.
- KEAR, D. and B.C. WATERHOUSE, Onerahi Chaos-Breccia of Northland, *N.Z. J. Geol. Geophys.*, **10**, 629–646, 1967.
- MATSUNO, K., The depression of the sedimentary basin of the Kotanbetsu Formation, *J. Jpn. Assoc. Pet. Technol.*, **23**, 130–132, 1958.
- MATSUNO, K. and Y. KINO, Chikubetsu-Tanko: Explanatory text of the geological map of Japan (Scale 1 : 50,000), pp. 1–43, Geol. Surv. Japan, Kawasaki, 1960.
- MIDDLETON, G.V. and M.A. HAMPTON, Subaqueous sediment transport and deposition by sediment gravity flows, in *Marine Sediment Transport and Environmental Management*, pp. 197–218, Wiley, New York, 1976.
- MINATO, M., M. GORAI, and M. HUNAHASHI, *The Geologic Development of the Japanese Islands*, 442 pp., Tsukiji Shokan, Tokyo, 1965.
- MORIYA, T., Folded structure of intermediate depth seismic zone and attenuation of seismic waves beneath the arc-junction at Hokkaido corner, *Abstr. Int. Geodyn. Conf.*, pp. 104–105, 1978.
- NAGAO, T., Tertiary orogeny in Hokkaido, *Hokkaido Imp. Univ., Fac. Sci. J.*, Ser. IV, **4**, 23–30, 1938.
- NIITSUMA, N., Magnetic stratigraphy of the Japanese Neogene and the development of the island arcs of Japan, *Abstr. Int. Geodyn. Conf.*, pp. 110–111, 1978.
- OKADA, H., Serpentine sandstones of Hokkaido, *Kyushu Univ., Fac. Sci., Mem.*, Ser. D, **15**, 23–38, 1964.
- UJME, H., T. SAITO, D.V. KENT, P.R. THOMPSON, H. OKADA, G. deV. KLEIN, I. KOIZUMI, H.E. HARPER, JR., and T. SATO, Biostratigraphy, paleomagnetism and sedimentology of Late Cenozoic sediments in north-western Hokkaido, Japan, *Bull. Natl. Sci. Mus.*, Ser. D, **3**, 49–100, 1977.

VELOCITY ANISOTROPY IN THE SEA OF JAPAN AS REVEALED BY BIG EXPLOSIONS

Hiroshi OKADA,*¹ Takeo MORIYA,*¹ Toru MASUDA,*² Takeshi HASEGAWA,*³ Shuzo ASANO,*⁴
Keiji KASAHARA,*⁵ Akira IKAMI,*⁶ Harumi AOKI,*⁶ Yoshimi SASAKI,*⁷
Nobuo HURUKAWA,*⁸ and Kazuo MATSUMURA*⁸

*¹ Faculty of Science, Hokkaido University, Sapporo, Japan

*² Faculty of Science, Tohoku University, Sendai, Japan

*³ Akita Technological College, Akita, Japan

*⁴ Earthquake Research Institute, University of Tokyo, Tokyo, Japan

*⁵ National Research Center for Disaster Prevention, Tokyo, Japan

*⁶ Faculty of Science, Nagoya University, Nagoya, Japan

*⁷ Faculty of Education, Gifu University, Gifu, Japan

*⁸ Disaster Prevention Research Institute, Kyoto, Japan

(Received June 19, 1978; Revised September 18, 1978)

Seismic waves generated by two explosions of dynamite, 5 tons each, in the Sea of Japan off the coast of northern Honshu were observed at more than 100 temporary and permanent seismological stations in the Hokkaido, Honshu, Sado, and Oki islands. A purpose of these measurements was to extend our investigation of lateral variation in Pn velocity which has been found around northeastern Japan in the previous explosion experiments. In fact, a lateral variation in Pn velocity by about 5% was confirmed in regions of the uppermost mantle below the Sea of Japan and the Honshu island, although the boundary where the velocity change takes place was not determined.

The measurements have also revealed an indication that the upper mantle just beneath the Moho interface under the area in the southeastern half of the Sea of Japan is anisotropic with respect to P-wave velocity. The velocity variation in the anisotropy is approximately 0.4 km/sec (i.e., 5%) about a mean velocity of 7.94 km/sec. The direction of the maximum velocity is 141° E of north which corresponds roughly to a direction perpendicular to the general trend of northern Honshu as well as to magnetic lineations.

1. Introduction

Until recently, seismic anisotropy of the uppermost mantle has been revealed in a number of oceanic areas (RAITT *et al.*, 1969; MORRIS *et al.*, 1969; KEEN and TRAMONTINI, 1970; KEEN and BARRETT, 1971) and has been considered as a typical and exclusive property of the upper mantle under the ocean. More recently, explosion-seismic experiments provided an evidence that the seismic anisotropy is also present in the upper mantle under the continent (BAMFORD, 1973, 1976, 1977). Furthermore, in the long-range observations of large explosions, HIRN (1977) presented some evidence of anisotropic propagation of mantle phase beneath the European continent, from which an anisotropic layer was inferred at depths where the lithosphere-asthenosphere transition is supposed to be.

All these measurements provide variations in the mantle P-wave velocity with azimuth, amounting to 3–8% of the mean velocity; the direction of maximum velocity has been obtained to be approximately parallel to the strike of the nearest fracture zones, i.e., perpendicular to the ridge axis or perpendicular to magnetic lineations in the ocean (e.g.,

RAITT *et al.*, 1971) and also to be parallel to the tectonic trend in the continent (e.g., FUCHS, 1977).

The Sea of Japan is a marginal sea with two major structural provinces, separated approximately at $40^{\circ}30'N$ (HILDE and WAGEMAN, 1973). North of this latitude is the large Abyssal Plain of the Japan Basin. South of $40^{\circ}30'N$, ridge and trough topography is predominant, including the Yamato Rise, Tsushima Basin, Yamato Basin, and the ridges and troughs along the continental slope off Honshu; the dominant structural trend of the ridges and troughs is roughly northeast to southwest.

In the Sea of Japan, magnetic surveys have extensively been carried out by YASUI *et al.* (1967) and ISEZAKI *et al.* (1971). Using all the available geomagnetic data in the Sea of Japan, ISEZAKI and UYEDA (1973) established that sublinear magnetic anomalies run subparallel to the general trend of the Japanese islands.

The Sea of Japan is also characterized with high heat flow which indicates that the isotherms are anomalously raised under the Japan Sea bottom (WATANABE, 1972).

From all these features, reflecting the dynamic processes in the crust and upper mantle, it was inferred that some seismic anisotropy would be induced in the upper mantle under the Sea of Japan. In 1976 the Research Group for Explosion Seismology carried out explosion-seismic experiments with two shots in the Sea of Japan off northern Honshu and with observation stations in the Hokkaido, Honshu, Sado, and Oki islands. The main purpose of the experiments was to extend our investigation of the lateral variation in Pn velocity, which had been studied during the preceding few years in the regions from the Honshu island to the Pacific area around the Japan trench. The distribution of the shot points and observation stations in the experiments was suitable for the purpose, but of less ideal for measurements of the anisotropy in the uppermost mantle under the Sea of Japan.

2. Explosions and Observations

Explosives, 5 tons of dynamite for each shot, were fired at a depth of 175 m in the Sea of Japan about 250 km off northern Honshu on July 28 and 30, 1976. The two explosions in the experiments are the fourth and fifth ones in a series of experiments conducted as a part of the Japanese Geodynamics Project, in which "Seiha Maru," a salvage ship of Nippon Salvage Company, was used as the shooting vessel. The shot points will then be referred to as SEIHA-4 and SEIHA-5, respectively. The locations of the shot points are $41^{\circ}31.9'N$ and $137^{\circ}31.1'E$ for SEIHA-4, and $39^{\circ}28.0'N$ and $137^{\circ}03.6'E$ for SEIHA-5, respectively, which were fixed by satellite navigation. The shooting procedure was the same as that in the previous experiments (ASANO *et al.*, 1978; OKADA *et al.*, 1978).

For the two shots Pn arrivals were recorded at 103 temporary and permanent seismological stations in the Hokkaido, Honshu, Sado, and Oki islands. In the experiments an ocean bottom seismometer was also anchored at a point about 160 km east of shot point SEIHA-4, but because of anomalous arrival times the data obtained by the OBS were not used in the analysis.

Figure 1 shows the locations of the shot points and observation stations. Crosses are the shot points and circles, the stations. In the figure, four profiles, P1, P3, P4, and P5 of the seismic refraction surveys by Murauchi *et al.* (JAPANESE NATIONAL COMMITTEE FOR THE UMP, SCIENCE COUNCIL OF JAPAN, 1967) are also shown. The results from these surveys will be referred to later.

Among these stations we selected 27 stations which are located less than 50 km land-

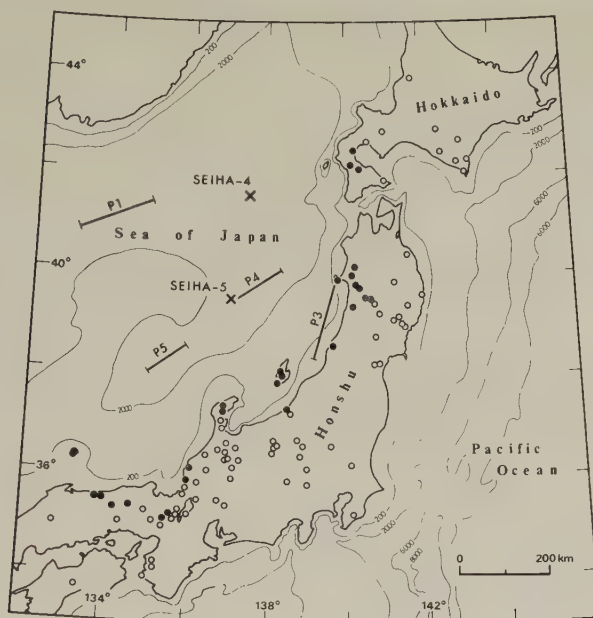


Fig. 1. Shot points and observation stations. Crosses designated by SEIHA-4 and SEIHA-5 represent the shot points; solid circles show the stations at which the data used in the analysis were obtained and open circles show other stations. Segments designated by P1, P3, P4, and P5 are the seismic refraction profiles by Murauchi *et al.* (JAPANESE NATIONAL COMMITTEE FOR THE UMP, SCIENCE COUNCIL OF JAPAN, 1967)

wards from the coastline along the wave paths. The selection of the stations was mainly to focus the present study on data pertinent to the properties of the uppermost mantle beneath the sea. Such data are to be provided by the selected stations because these stations have 30–50 km offset distance of Pn arrivals and more than 80% of the wave paths to these stations are under the Sea of Japan. The selected stations, represented by solid circles in Fig. 1, are distributed in a distance range of 200–750 km with an azimuthal range of 40°–220° E of north, and wave paths from the shot points to the stations are almost uniformly spread out over a nearly semicircular area in the southeastern half of the Sea of Japan.

3. Travel Time Data

The Pn arrivals from the two shots were observed at a total of 44 stations: 18 for SEIHA-4 and 26 for SEIHA-5. Travel times of the arrivals were determined with an accuracy better than 0.1 sec.

Clearly the amount of data was so little that the crust and upper mantle structures could be derived neither beneath the shot points nor beneath the observation stations. For the present purpose, however, it is enough that only the Moho-time terms can be estimated at the shot points and stations. The Moho-time terms at the shot points could

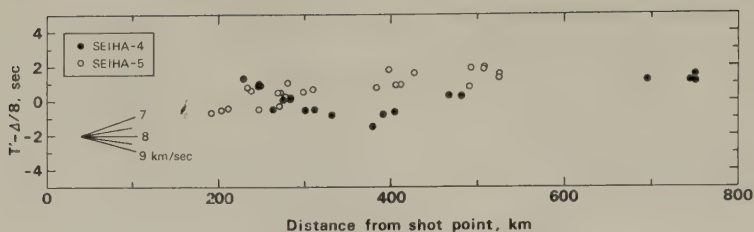


Fig. 2. Reduced mantle travel time plots. Δ is distance from shot point to station.

be estimated on the basis of the crust and upper mantle structures derived by Murauchi *et al.* (JAPANESE NATIONAL COMMITTEE FOR THE UMP, SCIENCE COUNCIL OF JAPAN, 1967) for four refraction profiles P1, P3, P4, and P5 (Fig. 1). The smallest one among the Moho-time terms given by the structures is 3.04 sec at profile P3 located very near the northern Honshu, the largest one 3.81 sec at profile P1 located in the Japan Basin, and the average of all the time terms 3.40 ± 0.34 sec. Throughout the analysis, the average time term is assumed for the Moho-time terms at both shot points.

The Moho-time terms at stations except ones where crustal structures were available were estimated by using the relationship between Moho-time term and Bouguer gravity anomaly obtained by OKADA *et al.* (1978). The relationship will give time terms in which errors are less than 0.33 sec that has little effect on the results to be obtained. The Bouguer gravity anomalies required at stations were provided by the map of Bouguer gravity anomalies in Japan (TOMODA, 1974).

If the Moho-time terms estimated for a shot point and station are subtracted from original travel time of the station, the residual gives a time of propagation taken by waves which propagate from a point under the shot point to a point under the station in the mantle just below the Moho interface. The residual time will be referred to as the mantle travel time for simplicity.

Figure 2 shows the mantle travel times for the two shots plotted against distances with the reduction velocity 8.0 km/sec. As shown in the figure, the mantle travel times are largely scattered between -2 and $+2$ sec with an indication that most arrivals for SEIHA-4 are early relative to those for SEIHA-5 at stations 300 to 500 km distant from shot point. From this figure, it is difficult to find any dependence of travel times on distance. However, it should be noted that a velocity given by a line roughly fitting these travel time plots is 7.9 km/sec which is higher by 5% than the velocity in the topmost mantle under northern Honshu (ASANO *et al.*, 1978). The difference between these velocities should be taken as an evidence for a lateral change in the velocity in the upper mantle below the Sea of Japan and the Honshu island, although the boundary where the velocity change occurs is not determined.

The mantle travel times are plotted again as a function of azimuth in the upper part of Fig. 3, the lower part of the figure being the corresponding distance. As can be seen in the figure, the mantle travel times for both shots are distributed so as to supplement with each other, and as a result the variation of the mantle travel times shows a clear dependence on the azimuth. It may be a question whether the observed azimuthal dependence of the mantle travel time is a spurious one resulting from the distribution of the stations with different distances. However, the question was to some extent answered by con-

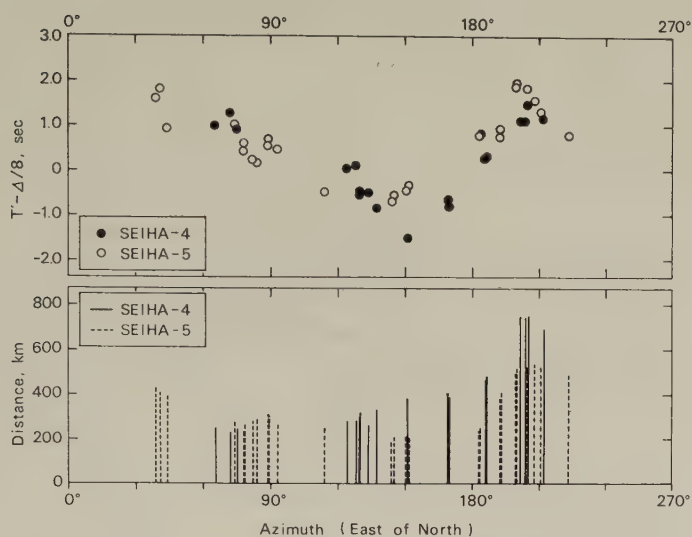


Fig. 3. Reduced mantle travel times and their corresponding distances versus azimuth.

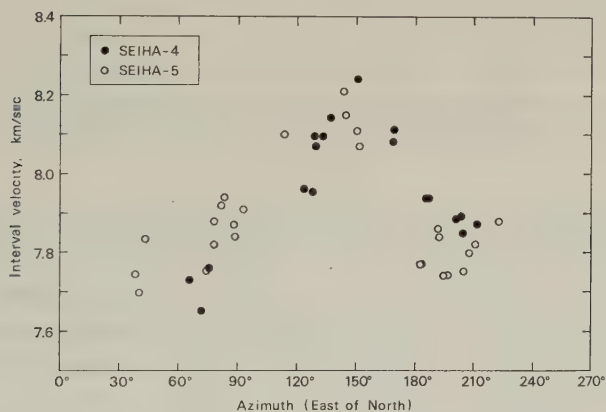


Fig. 4. Pn interval velocities as a function of azimuth.

verting the mantle travel time into Pn interval velocity, with which the Pn phase traveled from a point under the shot point to a point under the station in the upper mantle just below the Moho interface. The Pn interval velocity is the velocity given by dividing the distance between shot point and station by the mantle travel time. Figure 4 shows the Pn interval velocities as a function of azimuth. The interval velocity also has a clear dependence on the azimuth. Figure 5 is a map to show spatial distribution of wave paths along which the interval velocity is either higher or lower than the average interval velocity. The stations in northern Honshu provide an evidence that the azimuthal dependence of the interval velocity is not produced by local effects of certain stations where arrivals are always either early or late. This evidence is also given in Table 1 in which listed are the

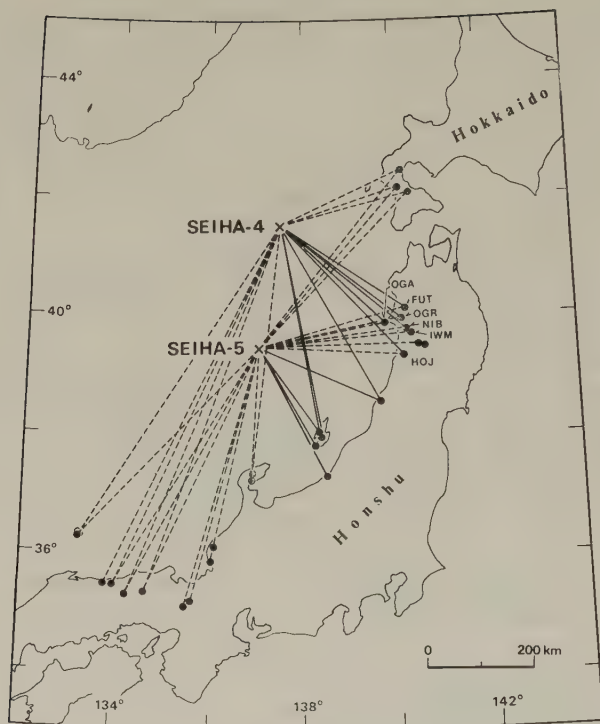


Fig. 5. Map showing spatial distribution of wave paths along which the interval velocity is either higher (solid line) or lower (dotted line) than the average interval velocity 7.95 km/sec.

Table 1. Data on azimuths, distances, reduced mantle travel times, and interval velocities for two shots at stations FUT, OGR, NIB, IWM, OGA, and HOJ in northern Honshu.

Station	SEIHA-4				SEIHA-5			
	Azimuth (°E of N)	Distance (km)	$T' - d/8$ (sec)	Interval velocity (km/sec)	Azimuth (°E of N)	Distance (km)	$T' - d/8$ (sec)	Interval velocity (km/sec)
FUT	124.05	274.68	0.16	7.96	74.41	280.64	1.11	7.76
OGR	128.10	283.64	0.21	7.95	78.46	271.36	0.52	7.88
NIB	129.50	301.36	-0.45	8.10	82.24	277.97	0.35	7.92
IWM	129.69	311.01	-0.35	8.07	83.81	283.96	0.26	7.94
OGA	133.52	263.32	-0.40	8.10	78.39	238.04	0.69	7.82
HOJ	137.23	331.63	-0.73	8.14	93.05	269.89	0.38	7.91

data on azimuths, distances, reduced mantle travel times, and interval velocities for the two shots at 6 stations: FUT, OGR, NIB, IWM, OGA, and HOJ in northern Honshu. Table 1 provides that the interval velocities for SEIHA-4 are higher than the average interval velocity 7.95 km/sec and those for SEIHA-5 lower than the average. While the distance differences at a station for both shots are less than 20%, most differences in the reduced travel time between both shots evidently exceed the errors included in the Moho-time terms at shot point and station. From these data, it may be concluded that the dif-

ference of interval velocities for both shots is not a spurious but actual one and will be attributable to the nature of the uppermost mantle under the area of investigation.

4. Results of Analysis

Among various possibilities to cause the azimuthal dependence of the reduced travel times, or of the interval velocities are lateral variations in Pn velocity and velocity anisotropy in the uppermost mantle under the sea.

In the present paper, we shall try to analyze the data on the assumption that the observed azimuthal variation is due to the velocity anisotropy existing in the uppermost mantle under the Sea of Japan.

According to BACKUS (1965), for a small anisotropy the P-wave velocity V_p may be represented by a constant term and a perturbation term that depends upon azimuth, that is,

$$V_p = c_p + A \cos 2\phi + B \sin 2\phi + C \cos 4\phi + D \sin 4\phi \quad (1)$$

where c_p is the assumed isotropic velocity, and ϕ , the azimuth. In this paper, V_p corresponds to the Pn velocity observed and the azimuth is measured clockwise from the north. If such anisotropy is assumed in the uppermost mantle over which the crust has a gently undulating structure beneath the area of investigation, the theoretical Pn travel time t_{ij} between the i -th shot point and the j -th station may be written as

$$t_{ij} = a_i + a_j + D_{ij}/V_0 + (1/V_0^2)(R_i + R_j - D_{ij}) \cdot (A \cos 2\phi + B \sin 2\phi + C \cos 4\phi + D \sin 4\phi) \quad (2)$$

where V_0 is the velocity averaged over all angle and a 's represent the Moho-time terms corresponding to this velocity of the i -th and j -th area, respectively. D_{ij} is the distance between the shot point and station, and R 's are the offset distances at i -th and j -th area, respectively.

The method to measure the anisotropy based on a set of travel times, Eq. (2), has been developed by RAITT *et al.* (1969) and MORRIS *et al.* (1969). The method is particularly suited to experiments in which large amounts of data are available from uniformly distributed shot points and stations. If least squares analysis is applied to the data, not only the numerical values of A , B , C , and D of Eq. (1), or of Eq. (2), that is, the variation of velocity with azimuth but also the time terms and the averaged mantle velocity will be determined.

In the present experiments, the observations of Pn arrivals were made on a semicircle; furthermore, the amount of data is relatively small so that it is difficult to calculate even the time terms. Therefore, direct application of the method to the data seems to be impractical. In the present analysis, however, not only the Moho-time terms but also the offset distances at the shot points and stations may be taken as known quantities. Of course, the Moho-time terms and the offset distances include errors due to the fact that these quantities have been estimated without taking account of anisotropy in the mantle. Practically the uncertainties were too small to produce serious errors in the solutions. In the calculation, the 4ϕ terms in Eq. (2) were ignored since the coefficients C and D are in general much smaller than the coefficients A and B , and the offset distances at all the stations were assumed to be 43.4 ± 4.6 km that is the average of all the offset distances calculated from the structures. The structures were determined by the past seismic refraction experiments in the Japanese islands. In addition, the offset distances at both shot

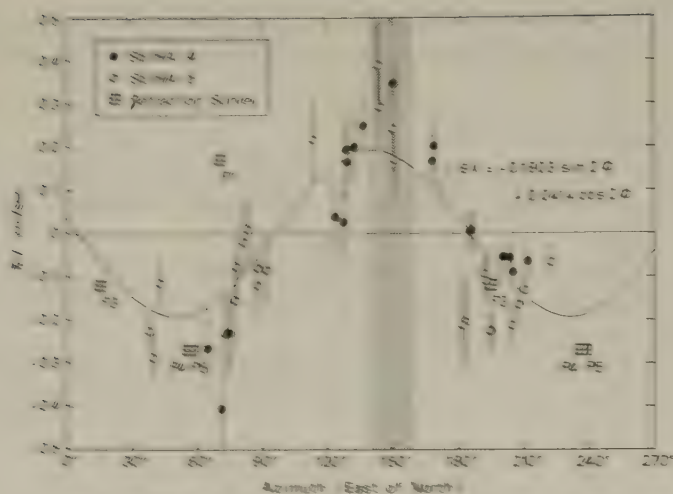


FIG. 5. Velocity anisotropy given as deviations from mean velocity of 7.94 km/sec plotted against azimuth. Filled circles are the values derived from seismic refraction profiles (JAPANESE NATIONAL COMMITTEE FOR THE U.M.P. SCIENCE COUNCIL OF JAPAN, 1967). Shaded portion represents the range within which a direction perpendicular to negative deviations (see text) and (Yoshida, 1972) is obtained. Vertical bars represent errors in velocity which result in ambiguity in the Mohorovičić slope and offset distances at that point and observation stations.

points were also estimated to be 1.44 ± 3.1 km that is the average of all the offset distances estimated from the structures in profiles P1, P4, and P5.

Figure 6 shows a least-squares fit of the velocity anisotropy given as deviations from the mean velocity. In the figure, the refraction results obtained by Murauchi *et al.* (JAPANESE NATIONAL COMMITTEE FOR THE U.M.P. SCIENCE COUNCIL OF JAPAN, 1967) in the Sea of Japan are also shown. The refraction results at each profile is plotted on two azimuths which are different by 180° from each other, because there is uncertainty by 180° in the direction of wave arrival. As can be seen in the figure, the refraction results except for the Japan Basin well supplement the results we obtained. As the Japan Basin has topographic features different from those in the area of the present investigation (HILDE and KAWAMURA, 1974), the directions of anisotropy may be also different in the two areas.

The maximum velocity obtained occurs in a southeast-northwest direction, that is, 141° E of north. The velocity in this direction is 0.4 km/sec greater than the minimum. The difference between the maximum and minimum velocities amounts to about 5%, which is within the range of anisotropy in the uppermost mantle observed to date in the Pacific Ocean. The mean velocity was obtained to be 7.94 km/sec which is lower by 2–4% than those observed in the Pacific Ocean.

Table 2 gives the least-squares regression results for an anisotropic upper mantle as well as an isotropic one. Comparison between the results shows that standard error about the regression for anisotropy is smaller than that for isotropy, and hence allows us to conclude that the anisotropic upper mantle under the Sea of Japan is probably real.

Table 2. Comparison of least-squares regression results of anisotropic upper mantle with those of isotropic one.

Mantle material	Std. error about regression (sec)	Mantle velocity (km/sec)	Anisotropy 2ϕ term (km/sec)	Anisotropy azimuth (max. vel.) ($^{\circ}$ E of N)
Isotropic	1.7006	7.882 ± 0.018		
Anisotropic	0.8060	7.936 ± 0.015	0.195 ± 0.023	141.1 ± 0.2

5. Discussion

For the possibilities to cause the azimuthal dependence of the reduced travel times, or of the interval velocities, the lateral variations in Pn velocity and velocity anisotropy may be considered. The lateral variations in Pn velocity may be produced by such a model that a low velocity material occurs in several regions in the upper mantle. In this model, the low velocity material has to be located at both regions off southwest Honshu and off southwest Hokkaido. A sequence of thin vertical layers with alternating high and low velocities such as dyke injections is a model of the layering anisotropy (KUMAZAWA, 1964; FUCHS, 1977). Based on the model, the dyke has to be oriented perpendicular to the general trend of the Japanese islands, or unlikely large fraction of the dyke material has to be located in the uppermost mantle under the Sea of Japan. However, no evidences to suggest these models have been reported. At the present stage, these models are unlikely to be applicable to our case.

The most favorable model to explain the observed azimuthal dependence of the reduced travel times, or of the Pn interval velocities is the velocity anisotropy due to crystal anisotropy in the upper mantle (DE ROEVER, 1961; HESS, 1964). Although pyroxenes in eclogites show considerable preferred orientation, eclogites in bulk do not show significant anisotropy (KUMAZAWA *et al.*, 1971). On the other hand, olivine grains in peridotitic rocks usually show the pronounced preferred lattice orientation (PHILLIPS, 1938; TURNER, 1942) and the presence of large velocity anisotropy in peridotitic rocks has been confirmed by a number of authors (e.g., CHRISTENSEN, 1966; KASAHARA *et al.*, 1968; KERN, 1978).

If the genetical and evolutionary environments (temperature, stress and the resulting deformation) in the upper mantle are uniform in a region, the pattern of preferential orientation of olivine is expected to be uniform, giving rise to the uniform anisotropy in the region. On the assumption of uniformity in the anisotropy type as well as in the mean velocity in the upper mantle under the Sea of Japan, we have obtained the anisotropy of 5° and the mean Pn velocity of 7.94 km/sec. The degree of anisotropy 5° obtained here is quite reasonable in magnitude for peridotitic rocks and is also the same magnitude as those observed in the upper mantle under the Pacific Ocean (RAITT *et al.*, 1969; MORRIS *et al.*, 1969). However, the mean velocity 7.94 km/sec is lower by $2-4^{\circ}$ than those reported in the Pacific Ocean. This difference raises a question whether the present peridotite model for the upper mantle under the Sea of Japan is adequate or not.

To account for the low mean velocity observed, we have referred to the measurements of velocities of peridotite under the simultaneous action of high temperature and high confining pressure by MATSUSHIMA and AKENI (1977), and KERN (1978). According to their measurements, the low mean velocity may be observed as a velocity of the peridotitic

upper mantle only if temperature at depths in the upper mantle under the Sea of Japan is higher by 200–300°C than that under the Pacific Ocean.

In fact, heat flow measured in the Sea of Japan is anomalously high (YASUI *et al.*, 1968) as indicating that the isotherms are abnormally raised under the sea bottom. Based on the heat flow measured, the temperature difference under the Sea of Japan and the Pacific Ocean at depths just beneath the Moho interface is estimated to be more than 200°C (WATANABE, 1972), which would have yielded the observed low mean velocity.

The direction of the maximum velocity seems to roughly agree with a direction perpendicular to the axis of the northern part of Honshu as well as to the long axes of three main ridges in the Sea of Japan: the Yamato, Oki, and Sado ridges, which are located in the area of investigation.

In Fig. 6, the shaded portion shows the range of azimuth perpendicular to magnetic lineations (ISEZAKI and UYEDA, 1973). As can be seen in the figure, a surprisingly close agreement between the direction of the maximum velocity and that perpendicular to the magnetic lineations can be recognized. Such agreement has been observed also in the northeast Pacific where significant anisotropy has been observed (RAITT *et al.*, 1969; MORRIS *et al.*, 1969).

The present paper is the first to suggest the presence of velocity anisotropy in the uppermost mantle under the Sea of Japan, the marginal sea. Although more detailed measurements might be required to confirm the suggested anisotropy, the result we obtained would be an evidence in favor of the view that the Japan Sea floor evolved through a similar spreading process to that occurring at the midoceanic ridges.

6. Conclusions

Seismic waves generated by two explosions, 5 tons each, in the Sea of Japan off the coast of northern Honshu were observed at more than 100 seismic stations in the Japanese islands. First arrival data obtained at 27 selected stations which are located on the Japan Sea side of Hokkaido and Honshu islands as well as in Sado and Oki islands were analyzed. Although the observations were made only on a semicircular area, the results presented here demonstrate that the anisotropy of Pn velocity is required by the data. The velocity variation is approximately 0.4 km/sec (i.e., 5%) about a mean velocity of 7.94 km/sec, and the direction of the maximum velocity is 141° E of north which agree with a direction perpendicular to magnetic lineations.

The Nippon Salvage Co., Ltd. gave us the opportunity to realize big explosions at sea by the salvage ship, Seiha Maru. Mr. K. Kobayashi, Captain of Seiha Maru, and all her officers and crew provided invaluable cooperation in explosion work. Our hearty thanks are also due to Nippon Yushi Co., Ltd. and Okanishi-Shibuya Maito Co., Ltd. for their cooperation in the explosion work.

We thank the members of the micro-earthquake observatories of universities, who placed their data at our disposal, and the members of the Research Group for Explosion Seismology, who cooperated in the observation program. We would also like to thank Professor M. Kumazawa of Nagoya University for critically reading the manuscript.

Financial aid was granted by the Japanese Geodynamics Project and Earthquake Research Institute. A part of the numerical computation was carried out by FACOM 230-75 at the Hokkaido University Computing Center (Problem No. 1001FO0401).

REFERENCES

- ASANO, S., H. OKADA, T. YOSHII, K. YAMAMOTO, T. HASEGAWA, K. ITO, S. SUZUKI, A. IKAMI, and K. HAMADA, Crust and upper mantle structure beneath Northeastern Honshu, Japan as derived from explosion seismic observations, submitted to *J. Phys. Earth*, 1978.
- BACKUS, G.E., Possible forms of seismic anisotropy of the uppermost mantle under oceans, *J. Geophys. Res.*, **70**, 3429–3439, 1965.
- BAMFORD, D., Refraction data in Western Germany—A time-term interpretation, *Z. Geophys.*, **39**, 907–927, 1973.
- BAMFORD, D., MOZAIC time-term analysis, *Geophys. J. R. Astr. Soc.*, **44**, 433–446, 1976.
- BAMFORD, D., Pn velocity anisotropy in a continental upper mantle, *Geophys. J. R. Astr. Soc.*, **49**, 29–48, 1977.
- CHRISTENSEN, N.I., Elasticity of ultrabasic rocks, *J. Geophys. Res.*, **71**, 5921–5931, 1966.
- DE ROEVER, W.P., Mantelgesteine und Magmen tiefer Herkunft, *Fortschr. Mineral.*, **39**, 96–107, 1961.
- FUCHS, K., Seismic anisotropy of the subcrustal lithosphere as evidence of dynamical processes in the upper mantle, *Geophys. J. R. Astr. Soc.*, **49**, 167–179, 1977.
- HESS, H., Seismic anisotropy of the uppermost mantle under oceans, *Nature*, **203**, 629–631, 1964.
- HILDE, T.W.C. and J.M. WAGEMAN, Structure and origin of the Japan Sea, in *The Western Pacific Island Arcs Marginal Seas Geochemistry*, edited by P.J. Coleman, pp. 415–434, University of Western Australia Press, Nedlands, Western Australia, 1973.
- HIRN, A., Anisotropy in the continental upper mantle: Possible evidence from explosion seismology, *Geophys. J. R. Astr. Soc.*, **49**, 49–58, 1977.
- ISEZAKI, N. and S. UYEDA, Geomagnetic anomaly pattern of the Japan Sea, *Mar. Geophys. Res.*, **2**, 51–59, 1973.
- ISEZAKI, N., K. HATA, and S. UYEDA, Magnetic survey of the Japan Sea (Part 1), *Bull. Earthq. Res. Inst.*, **49**, 77–83, 1971.
- JAPANESE NATIONAL COMMITTEE FOR THE UMP, SCIENCE COUNCIL OF JAPAN, Geophysical and geological data in and around the Japan Arc, in *Japanese National Report for the UMP*, compiled by T. Rikitake, pp. 2–25, the National Committee for the UMP, Science Council of Japan, 1967.
- KASAHARA, J., I. SUZUKI, M. KUMAZAWA, Y. KOBAYASHI, and K. IIDA, Anisotropism of P-wave in dunite, *J. Seismol. Soc. Jpn.*, **21**, 222–228, 1968 (in Japanese).
- KEEN, C. and C. TRAMONTINI, A seismic refraction survey on the Mid-Atlantic Ridge, *Geophys. J. R. Astr. Soc.*, **20**, 473–491, 1970.
- KEEN, C.E. and D.L. BARRETT, A measurement of seismic anisotropy in the Northeast Pacific, *Can. J. Earth Sci.*, **8**, 1056–1064, 1971.
- KERN, H., The effect of high temperature and high confining pressure on compressional wave velocities in quartz-bearing and quartz-free igneous and metamorphic rocks, *Tectonophysics*, **44**, 185–203, 1978.
- KUMAZAWA, M., The elastic constants of rocks in terms of elastic constants of constituent mineral grains, petrofabric and interface structures, *J. Earth Sci. Nagoya Univ.*, **12**, 147–176, 1964.
- KUMAZAWA, M., H. HELMSTAEDT, and K. MASAKI, Elastic properties of eclogite xenoliths from diatremes of the East Colorado Plateau and their implication to the upper mantle structure, *J. Geophys. Res.*, **76**, 1231–1247, 1971.
- MATSUSHIMA, S. and K. AKENI, Elastic wave velocities in the Ichinome-gata ultramafic nodules: Composition of the uppermost mantle, in *High-Pressure Research Applications in Geophysics*, edited by M.H. Manghnani and S. Akimoto, pp. 65–76, Academic Press, New York, 1977.
- MORRIS, G.B., R.W. RAITT, and G.G. SHOR, JR., Velocity anisotropy and delay-time maps of the mantle near Hawaii, *J. Geophys. Res.*, **74**, 4300–4316, 1969.
- OKADA, H., S. ASANO, T. YOSHII, A. IKAMI, S. SUZUKI, T. HASEGAWA, K. YAMAMOTO, K. ITO, and K. HAMADA, Regionality of the upper mantle around northeastern Japan as revealed by big explosions at sea. I. SEIHA-1 explosion experiment, submitted to *J. Phys. Earth*, 1978.
- PHILLIPS, F.C., Mineral orientation in some olivine-rich rocks from Rum and Skye, *Geol. Mag.*, **75**, 130–135, 1938.
- RAITT, R.W., G.G. SHOR, JR., T.J.G. FRANCIS, and G.B. MORRIS, Anisotropy of the Pacific upper mantle, *J. Geophys. Res.*, **74**, 3095–3109, 1969.
- RAITT, R.W., G.G. SHOR, JR., G.B. MORRIS, and H.K. KIRK, Mantle anisotropy in the Pacific Ocean, *Tectonophysics*, **12**, 173–186, 1971.
- TOMODA, Y., *Maps of Free and Bouguer Gravity Anomalies in and around Japan*, University of Tokyo Press, Tokyo, 1974.
- TURNER, F.J., Preferred orientation of olivine crystals in peridotites, with special reference to New Zealand examples, *Trans. R. Soc. N. Z.*, **72**, 280–300, 1942.

- WATANABE, T., Heat flow through the sea floor, in *Kaitai Butsuri*, edited by M. Iwashita, Y. Komaki, M. Hoshino, S. Horibe, and J. Masuzawa, pp. 1–107, Tokai University Press, Tokyo, 1972 (in Japanese).
- YASUI, M., Y. HASHIMOTO, and S. UYEDA, Geomagnetic studies of the Japan Sea—Anomaly pattern in the Japan Sea, *Oceanogr. Mag.*, **19**, 221–231, 1967.
- YASUI, M., T. KISHII, T. WATANABE, and S. UYEDA, Heat flow in the Sea of Japan, in *The Crust and Upper Mantle of the Pacific Areas*, Geophys. Monogr. Ser., No. 12, edited by L. Knopoff, C.L. Drake, and P.J. Hart, pp. 3–16, Am. Geophys. Union, Washington, D.C., 1968.

GEODYNAMICS OF THE NORTH-EASTERN ASIA IN MESOZOIC AND CENOZOIC TIME AND THE NATURE OF VOLCANIC BELTS

L.M. PARFENOV, I.P. VOINOVA, B.A. NATAL'IN, and D.F. SEMENOV

Institute of Tectonics and Geophysics, Khabarovsk, U.S.S.R.

(Received August 30, 1978; Revised November 6, 1978)

Geodynamics and tectonic evolution of the North-Eastern Asia was determined by the establishment of those structural elements in the geological sections which are typical of the modern active continental margins.

The Neogene island arcs on the majority of their strike coincide with the modern ones (the Kuril-Kamchatka) but locally they are broken up (the Western Sakhalin). They are conjugated with the back, front and interarc troughs. The Paleogene island arc occurs, probably, in the northwestern Kamchatka and on the Academy of Sciences uplift in the Sea of Okhotsk. The Early Mesozoic Uda-Murgal island arc marks the southeastern boundary of the ancient Eastern Siberia megablock. Along its southern and northern boundaries the island arc complexes of the same age are distinguished. Position of Eugeo-synclinal zones on the outer side of the island arcs indicates the isolation of the Eastern Siberia megablock from the Bureya-Ehanka, Okhotomorskiy and Chukotka ones the basement of which is composed by the Early Precambrian metamorphic complexes of sialic composition and granitoids. Tectonic movements at the end of Neocomian are expressed in the formation of the Andian type active continental margin with the Okhotsk-Chukotka margin-continental volcanic belt originated on a site of the Uda-Murgal island arc. This process was accompanied by the geometrical changes of the Benioff zone determined by the analysis of K_2O content in volcanites on the base of Dickinson and Hatherton's diagrams — the angle of dip became more gentle, the width along the dip and depth of the magma active part of the Benioff zone were increased. Simultaneously with the development of the Okhotsk-Chukotka volcanic belt there was formed the island arc on the East of the Sikhote-Alin. Owing to the Pre-Senonian movements on a site of this arc the Eastern Sikhote-Alin margin-continental volcanic belt similar to the Okhotsk-Chukotka one originated.

Many of the island arcs and margin-continental volcanic belts occur along the margins of the ancient sialic megablocks. Paleotectonic reconstructions prove the fact that there were significant horizontal displacements of the sialic megablocks causing the crash of the oceanic basins situated between them. The enlargement of the eastern part of the Asian continent took place not only at the expense of the island arcs displacement towards the ocean, but also due to the sialic blocks joining.

Geodynamics and tectonic evolution of the continental margin is revealed by the determination of those structural elements in the geological sections which are typical of the modern and Late Cenozoic geosynclinal systems (island arcs). The most significant attention is paid to the tectonic position and nature of volcanic belts of different types and ages widely distributed in the North East of Asia. They help to reconstruct the former plate boundaries and to determine the kinematics of their movements according to the plate tectonics models. Among them we distinguish: (1) the inner island arcs or volcanic

geanticlines, (2) margin-continental volcanic belts, (3) plateau-basalts coinciding with the margin-continental belts in the space but being the independent formations.

1. Main Tectonic Units

There are Cenozoic geosynclinal and Mesozoic folded geosynclinal systems following each other from the Siberian Platform to the ocean. The Mesozoic systems completed their geosynclinal development at the end of Jurassic–Neocomian (Nevadan) and Cenomanian–Paleogene (Laramide) (Fig. 1).

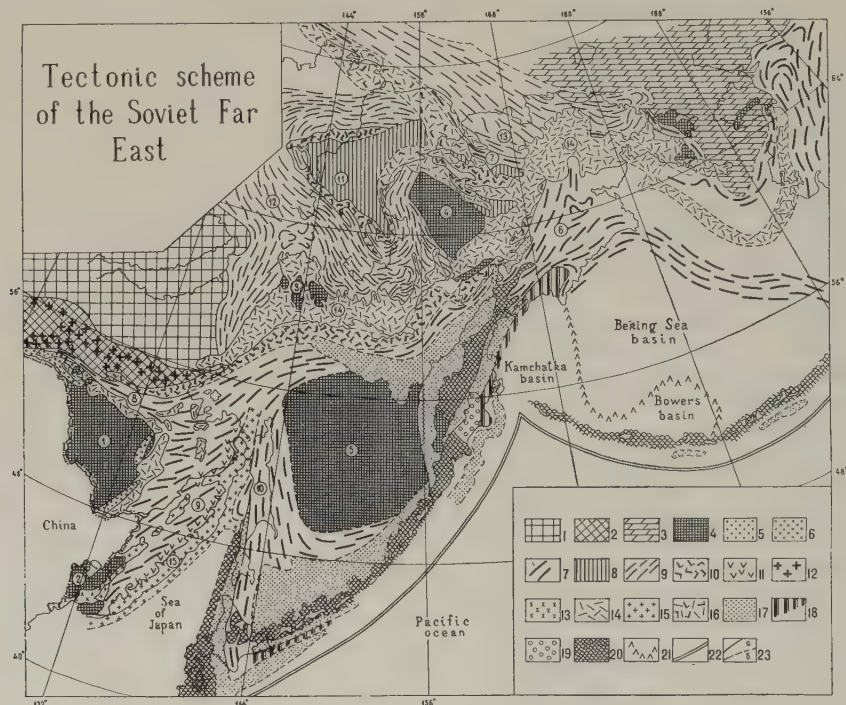


Fig. 1. 1, Siberian Platform; 2, Late Archean–Early Proterozoic (older than 2 by) Stanovoy folded system; 3, Middle Paleozoic Brooks–Vrangel folded system; 4, median massifs and blocks of Early Precambrian rocks in Phanerozoic folded systems; 5 and 6, marginal troughs of the median massifs (5, Paleozoic; 6, Mesozoic); 7 and 8, Mesozoic eugeosynclinal systems (7, type A; 8, type B); 9, Mesozoic miogeosynclinal systems; 10 and 11, Mesozoic island arcs (10, Early Mesozoic; 11, Late Mesozoic); 12, belt of Early Mesozoic granodiorite batholiths; 13 to 15, margin-continental volcanic belts (13, Late Paleozoic; 14, Cretaceous; 15, Senonian–Paleogene); 16, Mesozoic island arcs and margin-continental volcanic belts non-separated; 17 to 22, Cenozoic geosynclinal systems (17, miogeosynclinal zones (back troughs), interarc troughs and troughs on the trench slopes; 18, eugeosynclinal zones; 19, Quaternary volcanic geanticlines (island arcs); 20, Neogene ones; 21, Paleogene ones; 22, abyssal trenches; 23, geological boundaries (a, trustworthy; b, supposed). Figures in circles designate: 1 to 5, median massifs (1, Bureya; 2, Khanka; 3, Okhotsk; 4, Omolon; 5, Okhotomorskiy); 6 to 12, Mesozoic eugeosynclinal systems (6, Koryak; 7, South–Anyuy; 8, Mongolia–Okhotsk; 9, Sikhote–Alin; 10, Eastern Sakhalin; 11, Alazeya–Oloy); 12 and 13, Mesozoic miogeosynclinal systems (12, Yana–Kolyma; 13, Chukotka); 14, Okhotsk–Chukotka volcanic belt; 15, Eastern Sikhote–Alin volcanic belt.

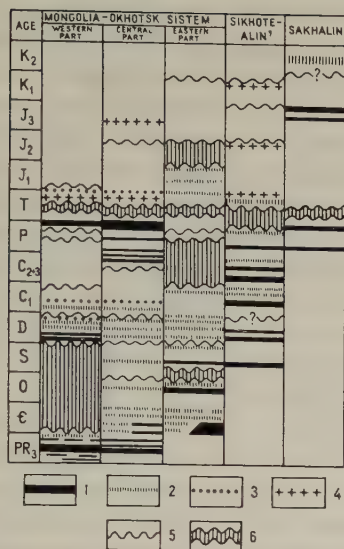


Fig. 2. Correlation scheme of some elements of tectonic activity within the eugeosynclines of type A. 1, tholeiite basalts; 2, alkaline olivine basalts; 3, calc-alkali andesite-basalts and andesites; 4, acid volcanites; 5, unconformities; 6, stratigraphic breaks.

The Mesozoic geosynclinal systems are subdivided into eugeosynclinal systems of types A and B and miogeosynclinal ones.

Eugeosynclinal systems of type A (the Koryak, Sikhote-Alin and others) joining each other form a Circum-oceanic belt. The Mongolia-Okhotsk and South-Anyuy systems that jut into the continent-like narrow strips are the branches of this belt.

The systems are characterized by a long period of their development. They include not only Mesozoic but also Paleozoic and in the Mongolia-Okhotsk system Upper Precambrian sequences (Fig. 2). Some parts of their sections, especially the lower ones, are undoubtedly, the deep-sea formations represented by siliceous and clay-siliceous rock associations with basic volcanites. The more shallow-water accumulations composed, mainly, by greywacke and sometimes arkose occur usually in olistostromes. They are characterized by the intensive and superimposed folding. Unconformities quite often have the similar age along the vast areas and the most distinctly the Late Hercynian ones are expressed by the omission from the section of Low and Middle Triassic.

Eugeosynclinal systems of type B. The Alazeya-Oloy system belonging to this type (TIL'MAN *et al.*, 1975) is characterized by the combination of deep-sea clay-siliceous and shallow-water coastal-marine deposits including the coarse ones with plant detritus at the same stratigraphic levels. Together with basalts there are widely distributed the andesite-basalts, andesites and acid rocks including those with high alkalinity. Late Hercynian movements are well expressed here, like in the above-mentioned systems.

Miogeosynclinal systems (the Yana-Kolyma and Chukotka) border the eugeosynclines towards the continent. They are characterized by a long period of their development which is obviously expressed in the Yana-Kolyma system where the uninterrupted section from Late Precambrian up to Jurassic is observed. There are no distinct discontinuities and unconformities that are typical of the eugeosynclines.

Among the Cenozoic geosynclinal systems there are distinguished the folded structures formed in Paleogene-Neogene time and modern geosynclines.

The median massifs representing the large (300–500 km in diameter) sialic blocks and

being formed in Early Precambrian are the independent tectonic units. The Late Precambrian granulite complexes of the same type as those within the Siberian Platform basement with the age of about 3,500 my compose the Okhotsk and Omolon massifs. Together with the Siberian Platform they form the Early Precambrian Eastern Siberia megablock which is one of the most ancient cores of the Asian continent. The Yana-Kolyma miogeosynclinal system originated above this megablock in the zone of its breaking and thinning. Slightly altered Late Precambrian and younger deposits of the Okhotsk and Omolon massifs have the platform peculiarities. The Bureya and Khanka massifs which are framed by the eugeosynclinal zones compose another ancient sialic megablock (Bureya-Khanka) formed later than the Eastern Siberia one (about 2,000 my). Its basement consists of the Early Precambrian complexes metamorphosed in amphibolitic and less abyssal granulitic facies. The Late Precambrian and sometimes Early Paleozoic complexes are characterized by the increased thickness; they are dislocated and usually metamorphosed from greenschist to epidote-amphibolitic facies. One of the peculiarities of the megablock is the vast distribution of granitoids occupying about 90% of its territory including batholith-like bodies of Late Precambrian Early, Middle and Late Paleozoic and Early Mesozoic age. Similar megablocks are assumed in the Chukotka miogeosynclinal basement and central part of the Sea of Okhotsk. From the paleogeographic point of view the megablocks of this type can be considered as the microcontinents.

The metamorphic complexes known in the Sikhote-Alin, Taygonos peninsula, Kamchatka and other regions (for some of them the Precambrian age is proved) represent, probably, the fragments of the ancient megablocks separated from them during the active continental margin evolution.

2. *Cenozoic Continental Boundaries*

Cenozoic continental boundaries are determined by the position of the island arcs systems.

The modern inner island arcs with the active volcanism are the Greater Kuril ridge extended to the Kamchatka as the Eastern volcanic belt and also the Aleutian Islands. The active volcanos of the Kuril-Kamchatka arc lay on the arc with the radius of 1,884 km. The average quadratic variation of the volcanos of this arc is ± 22 km (FEDOTOV, 1974). The modern volcanic chains coincide with the seismofocal zones which lay on the depth of 120–150 km. Volcanism is absent in the places where the earthquake foci on these depths are not defined, for example, Commander Islands (Fig. 3). The connection of modern volcanos with the seismofocal zone in the Eastern Kamchatka is also proved by the fact that the volcanos coincide with the narrow zone in the focal layer where the sharp decrease of the seismic activity occurs because of the depth change (TOKAREV, 1974).

The Greater Kuril ridge can be considered as the modern volcanic geanticline which divide the back (the South-Okhotsk basin) and front (the abyssal trench with the adjacent parts of the ocean floor) troughs. These troughs occupy accordingly the positions of mio- and eugeosynclinal zones. The outer slope of the arc is complicated by the interarc trough and outer arc uplift devoid of volcanism (the Lower Kuril ridge).

Neogene island arcs originated at the end of Oligocene–beginning of Miocene time are more widespread (Fig. 1). The Neogene and modern arcs coincide within the Greater Kuril ridge and the Southern Kamchatka. Northwards the Neogene arc stretches along the Kamchatka Median ridge separated by the transform fault from its southern



Fig. 3. Modern active tectonic zones. 1, structure contours on the axial surface of the Benioff zone (for the Kuril-Kamchatka arc according to P.Z. Tarakanov, for the Aleutian arc according to V.P. Semakin); 2, areas of crust earthquake epicenters outside the island arcs; 3, transform and strike slip faults; 4, thrusts; 5, zones of modern volcanism; 6, oceanic type crust; 7, direction of the oceanic plate movements.

part. The arcs are traced along the Commander Islands and further eastwards along the Aleutian Islands. The Western Sakhalin arc is supposed to trend along the Moneron, Rebun and Risiri Islands. It lays on the continuation of the Nasau arc of the Japanese Islands and is characterized by the intensive linear positive magnetic and gravity anomalies (PAVLOV and PARFENOV, 1974).

The inner arcs are composed by the complicated sedimentary-igneous rock assemblages of several kilometers thick. Geanticlinal character of the Neogene-Quaternary sequences of the Greater Kuril ridge is determined by the following features (GAVRILOV and SOLOV'YEVA, 1973): relatively small thickness, vast development of the coastal-marine, continental and shallow-water deposits which are altered in the section and lateral direction, a great number of local scours and unconformities. Accumulation conditions of these complexes are mainly determined by the volcanism active during the whole time of their development. Volcanic-terrigenous sedimentation prevails over the chemogenic one. Terrigenous rocks originated almost exceptionally at the expense of the erosion of volcanos and the products of volcanic eruptions. Among them the rudaceous varieties and rocks with detrital fragments of different sizes are widely distributed forming layers and bands which are sharply changed along their strike.

Volcanites constituting about 80% of all the rocks occur in the section and form modern volcanos of different types: separately situated volcanos, linear-type and caldera volcanos. Basic and intermediate rocks are abundant, though the ratio of the rocks of different composition changes as along the arc strike so as along vertical section. Thus, among the Lower Miocene volcanites basic and intermediate rocks constitute 30–50% on the Kunashir Island and up to 80% on the Paramushir. In the younger assemblages basalts constitute 20–25%; andesite-basalts, 35–45%; andesites, 15–19%; dacites and liparites up to 25%; varieties with SiO_2 content $>68\%$ are rare.

Basic and intermediate rocks are represented by lavas, lava breccias, agglomerates and tuff breccias. In the lower part of the section there are pillow lavas and hyaloclastites (PISKUNOV, 1975). Acid rocks are the most widely distributed on the southern islands of the Greater Kuril ridge. They are predominantly made of pumice stones either of the caldera volcanos or small depressions and also lavas of extrusive bodies.

From the petrochemical point of view the great majority of the rocks correspond to the calc-alkaline series with the increased calcium and aluminium content, low alkalinity,

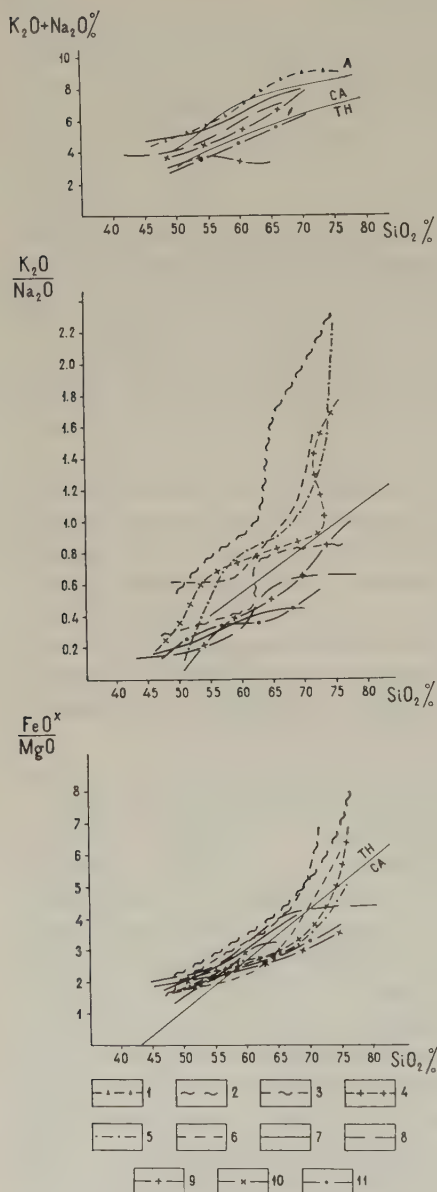


Fig. 4. Variation diagrams of the chemical composition of volcanic assemblages. 1 to 6, Okhotsk-Chukotka belt: 1, belt on the whole (364 analyses); 2, Central Chukotka area (78 analyses); 3, Middle Anadyr area (44 analyses); 4, Okhotsk area (26 analyses); 5, Kuidusunskaya basin (25 analyses); 6, Ul'ya trough (190 analyses). 7 to 10, Uda-Murgal geanticline: 7, Murgal uplift (7 analyses); 8, Central Taygonos area (82 analyses); 9, Koni-P'yagina area (5 analyses); 10, Uda trough (33 analyses); 11, Greater Kuril Islands (366 analyses). Letters designate the fields of volcanic series: TH, tholeiitic; CH, calc-alkali; A, alkaline. Division boundaries of the fields of volcanic series are given on the diagram $K_2O + Na_2O - SiO_2$ after KUNO (1964), on the diagram $FeO^*/MgO - SiO_2$ after MIYASHIRO (1974). $FeO^* = FeO + 0.9 Fe_2O_3$.

especially the K_2O content and strong predominance of Na_2O over K_2O (Fig. 4). In the Lower Miocene assemblages (green tuff complex) the alkali content is slightly increased but within the ranges permissible for the calc-alkaline series. Even in the acid varieties there is no significant alkali increase. The increased K_2O content is observed only in Quaternary andesites of central and northern islands. Basalts are similar to high-alumina tholeiites. The FeO^*/MgO ratio with the SiO_2 increasing rises weakly, thus, the basic varieties are distributed in the field of tholeiite rocks according to Miyashiro's classification (MIYASHIRO, 1974) but acid—in the field of calc-alkaline rocks. This regularity takes

place because of the weak iron accumulation relative to the quick accumulation of silica (significant rate of differentiation).

The back (miogeosynclinal) trough of the Neogene island arc is well expressed in the western Kamchatka. It is composed by the thick (up to 6,000 m) folded relatively deep-sea clay-greywacke and siliceous sequences in the low parts of the section and coastal-marine greywacke and psephites with lignite and clay in the upper parts of the section. The South-Okhotsk basin occupies the similar position relative to the Kuril arc. The thickness of the deposits composing this basin is considered as 5 km according to the Deep Seismic Sounding data (SUVOROV, 1975) and up to 4 km according to the Reflected Seismograph Method data.

The trough between the Greater and Lower ridges of the Kuril Islands characterized by the increased sediments thickness (TUESOV *et al.*, 1975), the Central Kamchatka and other troughs are considered as interarc troughs. Judging from the outcrops of the Cenozoic deposits on the Karagin Island and western bank of the Litke Straits, the Central Kamchatka trough is made of relatively deep-water terrigenous and diatomite flysch sequences of the Miocene age containing the great amount of pyroclastic material (GLADENKOV and GRECHIN, 1969; VLASOV *et al.*, 1977). According to G.M. Vlasov this is the tuffite flysch assemblage originated mainly due to active volcanic processes within the geanticline connected with the trough. On the geanticlinal slopes this assemblage is alternated by the shallow-water tuff flysch-like sequence which is changed landwards by the sedimentary-volcanic complexes of the geanticlines themselves. The existence of the Miocene tuff flysch-like sequence in the South of the Greater Kuril ridge (VLASOV *et al.*, 1977) points to the fact that the tuffite flysch is of great significance in the trough between the Greater and Lower ridges.

Paleogene deposits of the Eastern Kamchatka together with the Middle Miocene ones compose a thick (about 1,000 m) clay-greywacke flysch complex including bands of volcanic and siliceous rocks. Generation of this complex took place in the deep-water trough restricted from the ocean by the uplift in the area of Cretaceous rock outcrops of the Eastern peninsulas. This uplift is indicated by the decreased thickness of the Paleogene and Neogene in this area, occurrence of unconformities in the base of the Paleogene and Neogene, increase of the clastic material size and appearance of Miocenic coastal deposits and even coal bands eastwards (ARSANOV, 1973; SHAPIRO and SELIVERSTOV, 1975). The flysch trough complex is characterized by many features which liken it with the modern turbidites (MARKOVSKIY and SUPRUNENKO, 1972). Numerous subaqueous slump horizons attached to the northwestern slope of the trough indicate the steeply dipping floor and active tectonic processes. This trough should be considered as the analogue of the modern abyssal trenches. Tectonic nature of the Eastern peninsulas is not finally clear. Due to the presence of coastal-marine sediments here they are assumed to belong to islands of the oceanic aseismic range. S.A. Ushakov and others (USHAKOV *et al.*, 1977) pointed out a principal possibility of cutting of volcanic piles on an oceanic floor and their attachment to the island arc.

Along the trough there is a zone (about 25 km wide) of intensive folding represented by the overturned northwestwards dipping isoclinal folds complicated by the numerous thrusts including the gently dipping ones. This is the so called the Bogachev structural zone (SHAPIRO and SELIVERSTOV, 1975). Moving away from this zone the dislocations become essentially simple.

The Western Sakhalin arc is characterized by the wide distribution of the pyroxene

Table 1. Chemical composition of Paleogene and Neogene

Components	Northern Japan			Southern Sakhalin		
	1	2	3	4	5	6
SiO ₂	49.26	52.11	54.47	47.80	53.04	58.19
TiO ₂	0.94	0.97	0.69	0.77	0.97	0.65
Al ₂ O ₃	18.75	17.50	17.56	16.70	16.46	15.23
Fe ₂ O ₃	3.22	3.36	2.98	5.34	5.67	5.17
FeO	7.16	6.96	4.91	5.97	4.08	3.33
MnO	0.17	0.19	0.14	0.09	0.13	0.07
MgO	5.62	4.58	3.72	5.75	2.01	3.12
CaO	10.76	9.64	7.41	11.25	10.15	8.47
Na ₂ O	2.12	2.52	2.97	2.01	2.13	1.93
K ₂ O	0.52	0.70	1.09	0.67	1.18	1.56
H ₂ O ⁺	0.69	0.59	0.72	1.32	0.45	0.82
H ₂ O ⁻	0.72	0.43	0.69	—	—	—
P ₂ O ₅	0.17	0.17	0.15	0.14	0.17	0.09
S	—	—	—	0.27	0.61	0.08
	—	—	—	1.14	2.46	1.25
Sum	100.16	99.92	100.50	99.22	99.51	99.96
Number of analyses	Unknown	Unknown	Unknown	8	6	3

Notes: 1, 4, 7, 9, 12, basalts; 2, 5, 8, 10, 13, andesite-basalts; 3, 6, 11, 14, andesites.

andesites and andesite-basalts together with the highly aluminous tholeiites. Lavas are accompanied by the subvolcanic intrusions of the bipyroxene diorites and gabbrodiorites. There is observed the basic composition of plagioclase, vast distribution of rhombic pyroxenes, quartz occurrence in the andesites, high aluminium and low alkali contents. In addition to these common features the composition of volcanites along the arc undergoes some changes. Northwards the amount of acid products and the alkalinity of basic volcanites increases (Table 1). Back trough of this arc is composed by the Neogene greywacke-clay thick series with opokas, diatomites and ash tuffs and also coarse-grained greywackes with andesite-basalt and trachyandesite lava and tuff horizons. The thickness of these deposits of the Western Sakhalin is about 7,000 m. The Tatar Straits and Sea of Japan can be considered as the young eugeosynclinal zone.

The Paleogene island arc is defined by the outcrops of volcanic rocks in the North-West of Kamchatka along the Penzhina inlet coast. The island arc, probably, continues southwards along the Western Kamchatka shelf to the South of the Midian ridge where the small fields of the Paleogene volcanites are known and then, according to the magnetometric data, to the area of the submarine upland of the U.S.S.R. Academy of Sciences in the Sea of Okhotsk (SHIMARAEV, 1976). According to dragging data there is assumed that the Shirshov Range and laying on its continuation the Bowers Range also represent Paleogene island arc.

3. Mesozoic Continental Boundaries in the Northern Preokhot'ie

In the Northern Preokhot'ie there is distinguished the Uda-Murgal arc which stretches for 2,500 km separating the Mesozoic Circum-oceanic eugeosynclinal belt from the Yana-Kolyma miogeosyncline situated northwards from it (Fig. 1). The sedimentary-volcanic assemblages of the arc crop out on the left bank of the Uda river (the northeastern margin

volcanic rocks of Nasau-Western Sakhalin volcanic geanticline.

Alexandrovsk region of Northern Sakhalin			Northern Preamur'ie		Schmidt peninsula of Northern Sakhalin		
7	8	9	10	11	12	13	14
50.27	55.13	49.6	55.1	57.0	50.18	53.13	58.10
1.23	1.03	1.3	1.1	1.0	0.97	0.99	0.94
18.50	17.52	18.9	17.5	18.6	18.32	18.76	14.91
4.67	5.10	—	—	—	6.41	5.23	4.03
5.68	6.76	—	—	—	2.19	1.33	1.89
0.31	0.09	5.8	3.6	4.1	0.19	0.12	0.08
5.33	2.09	8.6	6.3	7.6	3.27	3.14	3.13
9.22	8.65	3.30	3.39	1.82	7.65	6.77	5.82
2.95	0.77	1.24	2.17	1.32	3.87	3.90	4.02
0.48	0.42	—	—	—	2.56	2.01	1.92
1.80	—	—	—	—	1.31	0.82	0.63
—	—	—	—	—	—	—	—
0.41	1.42	—	—	—	0.64	0.57	0.36
0.03	0.22	—	—	—	0.04	0.04	0.04
1.17	1.40	—	—	—	1.40	3.28	1.55
99.33	100.57	—	—	—	99.73	99.87	100.13
3	1	14	6	1	3	6	7

of the Mongolia-Okhotsk geosynclinal system) (VOINOVA, 1975), the Koni, P'yagina (BELIY and KOTLYAR, 1975) and Taygonos (NEKRASOV *et al.*, 1971) Peninsulas, in the basins of the Penzhina and Anadyr Rivers (BELIY and MILOV, 1973). The age of these assemblages is determined as the Late Triassic-Late Jurassic in the Uda area (GONCHAROV, 1976). On the northeastern slope of the arc its formation continued up to Neocomian. Northwards from the Koni and P'yagina peninsulas the lower part of the arc section consists of Late Permian fossils.

Sedimentary-volcanic assemblages of different regions of the arc are characterized by the common features similar to those of the Neogene-Quaternary Kuril-Kamchatka arc. Volcanites are associated with the coastal-marine and less continental terrigenous rocks, associating with more granulometric coarse varieties. Among the volcanites the basic and intermediate rocks are abundant, acid varieties constitute about 20%. The basic and intermediate rocks are represented by lavas and tuffs including also agglomerates, tuff breccias; acid volcanites are predominantly ash tuffs and also subvolcanic liparite-dacites and dacites.

The volcanites belong to the calc-alkalic series. The basalts are similar to the highly aluminous tholeiites. All these rocks are characterized by the low alkalinity, constant and often very strong predominance of Na_2O over K_2O , increased content of CaO, weak rise of the FeO^*/MgO ratio in the process of differentiation, $\text{CaO} > \text{MgO}$ (Fig. 4).

From the continent the Uda-Murgal arc is conjugated with the back trough which is the most well expressed on its central part from the Gizhigin inlet up to the Ini river basin. Here there is distinguished a thick (about 10,000 m) section of the Upper Permian, Triassic and Jurassic represented, mainly, by the greywacke schist thick series with some andesite lava horizons and wide distribution of the pyroclastics. The main removal of clastic material to the trough took place from the South-West and South, namely, from a land situated within the Okhotsk massif and along the northern coast of the Sea of

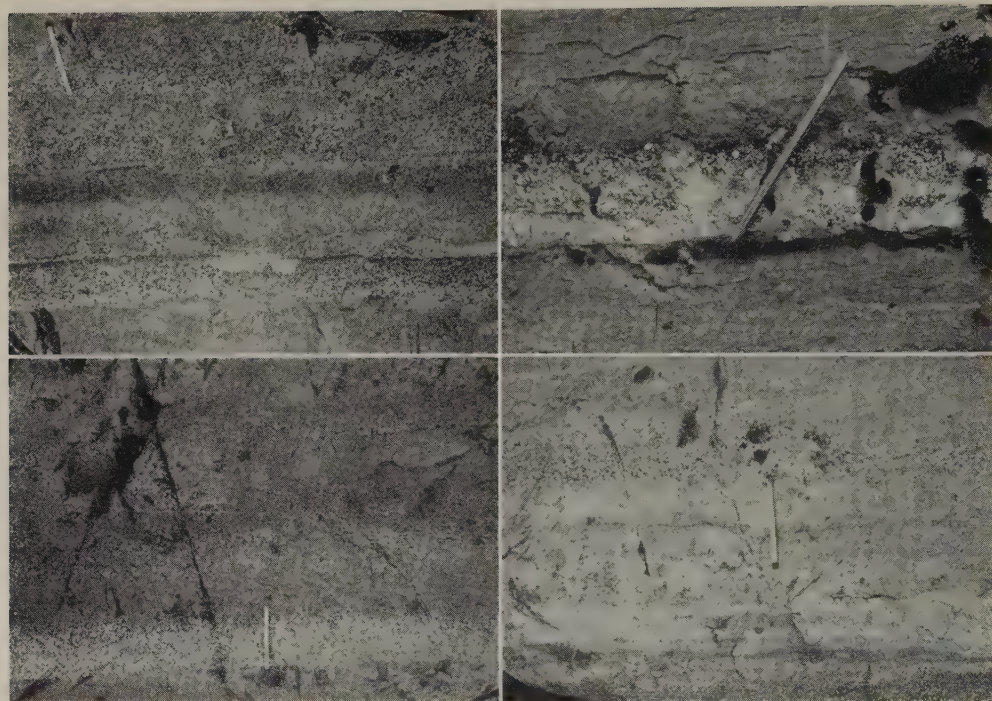


Fig. 5. Early Mesozoic tuff flysch.

Okhotsk (EPSTEIN, 1977). In the clastic material composition the intermediate and rare acid volcanites and pyroclastics are predominant, metamorphic and intrusive rock destructions are also found. In the Lower Jurassic deposits represented mainly by the dark-grey and black aleurolites and argillites with rare organic remains, the submarine rock-slide phenomena are widely distributed (POLUBOTKO *et al.*, 1977). The tuff flysch is a representative assemblage of the trough. It contains the layers rich in the pyroclastic material, dark-grey and black aleurolites (Fig. 5). The thickness of these layers ranges from some millimetres up to 15–20 cm. The peculiar features of these layers are the flat base without any erosion traces and diffused cover, differentiation of the pyroclastic fragments by their sizes in the section of these layers. A tuff flysch generation can be explained by the recurrent supplement of the pyroclastic material to the sedimentary basin from the subaral volcanic eruptions in island arcs and its following accumulation in the aqueous medium.

From the oceanic side the Uda-Murgal arc was accompanied by some basins and uplifts which nowadays are designated by the study of the section of the northwestern Koryak highlands, Kamchatka and Taygonos peninsulas (MIGOVICH, 1972; NEKRASOV, 1976; ZABOROVSKAYA and NEKRASOV, 1977). Here there is supposed a non-volcanic arc which is characterized by the shortened section of Upper Paleozoic, Triassic and Jurassic carbonaceous, volcanic and rudaceous rocks with numerous breaks. The trough defined between this uplift and the Uda-Murgal arc can be compared with the interarc troughs of the modern island arcs. The Permian, Triassic and Jurassic sequences composing the trough crop out in the separated tectonic blocks along its southeastern side. In the most warped part of the trough there is assumed a complete and uninterrupted section with widely distributed terrigenous and sedimentary-volcanic rocks.

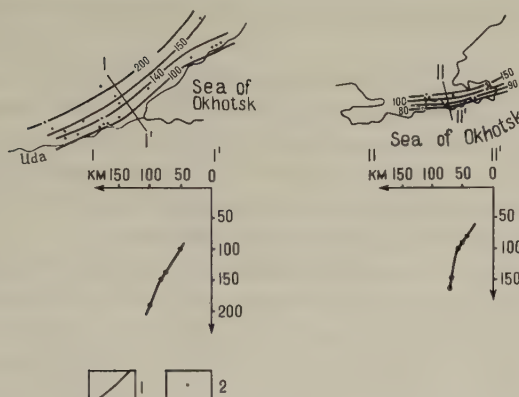


Fig. 6. Benioff paleoseismic zone position of the Uda-Murgal arc.
1, isobaths of the Benioff zone; 2, data points.

The Uda-Murgal arc is supposed to be similar to the Kuril-Kamchatka one and has been accompanied by the Benioff zone. A position of this paleoseismic zone is determined by the belt of the Alpine-type ultrabasites and glaucophane schists which trends from the Pekul'ney Range through the Ust-Bel'skiy Mountains, Aldan Range and Penzhina Range (ALEXANDROV *et al.*, 1975) to the southeastern edge of the Taygonos peninsula (NEKRASOV, 1976), accompanied everywhere by the intensive dislocations, gently-dipping thrusts and serpentinitic melange. According to aeromagnetic data this belt is traced approximately for 100 km to the southwest from the Koni and P'yagina peninsulas.

The Benioff paleoseismic zone position was determined by the K_2O content in the volcanic rocks on the basis of Dickinson and Hatherton's diagrams (DICKINSON and HATHERTON, 1967) for the two parts of the arc: the Uda river basin and Koni and P'yagina peninsulas (Fig. 6).

The continental boundary that is marked by the Uda-Murgal arc retained its position, probably, from the Early Paleozoic time. The Paleozoic sections on its both sides are very different. In the west of the Koryak highland the Late Paleozoic belt of glaucophane schists and ultrabasites stretches parallel to the Early Mesozoic one (DOBRETISOV, 1974). Paleozoic glaucophane schists are found recently in the Mongolia-Okhotsk system.

In the Late Mesozoic time there is designated the Andean type active continental margin the position of which is determined by the Okhotsk-Chukotka margin-continental volcanic belt. The belt composed, mainly, by the continental volcanites and granitoids of the similar age on all its great length (about 3,000 km) is parallel to the inner side of the Circum-oceanic eugeosynclinal belt and the Uda-Murgal geanticline. The belt partially overlaps the Uda-Murgal geanticline (Fig. 1) by its outer (southeastern) edge and by its inner edge superposes discordantly the heterogeneous tectonic elements: the miogeosynclinal systems, massifs, Alazeya-Oloy system and South-Anyuy eugeosynclinal system of type A closed at the beginning of the Early Cretaceous time. The strong orogenic processes occurring within the whole Verchoyano-Chukotka area preceded the belt origination. In the base of the belt there are rudaceous coastal-marine and continental molassa of Late Jurassic-Neocomian age.

On the major northeastern part of the belt the age of its lower layers is determined not older than Albian (BELIY, 1977). According to radiometric data and plant remnants

the lower parts of the belt section on its southwestern flank have Neocomian age (GRINBERG, 1976).

In the longitudinal direction the belt is subdivided into some sections distinguished by the average composition of magmatic rocks and chemical composition of rocks of similar basicity (BELIY, 1969; SHILO *et al.*, 1974; MAP OF MAGMATIC FORMATIONS OF THE U.S.S.R., 1971). These sections are the Central Chukotka and Okhotsk characterized by the wide distribution of acid and intermediate rocks (liparites, dacites) and the Anadyr formed, mainly, by andesite-basalts, basalts and andesites.

At the same time the obvious differentiation across the belt is observed on its large extent (BELIY, 1969; FILATOVA and DVORYANKIN, 1974). The majority of the acid volcanites is confined to the inner (near-continental) belt margin. The plagiogranites and tonalites typical of the outer parts of the belt are replaced by the sodium-potassium granodiorites and granites of the same age in the inner zone (MILOV, 1971; BELIY and MILOV, 1974).

In spite of the distinct longitudinal and transverse differentiation of the belt, its development as a rule, begins with the andesite-basalts, basalts and andesites eruption and only after that the andesite-basalt-liparite and liparite suits originate (USTIEV, 1959, 1965). It is assumed that in the belt development the basic magma of mantle origin was initial, and the appearance of great volumes of acid rocks as volcanic so as intrusive is connected with the sialic crust melting under the heat influence containing in the basaltic magma.

The volcanites of the belt overlie discordantly on the Uda-Murgal arc assemblages essentially differing in composition from the latter as well as from volcanites of any island arc (Fig. 4).

The Okhotsk-Chukotka belt is composed predominantly of the volcanic rocks, terrigenous deposits constitute not more than 20% and form the local parts within its section. Among the belt volcanites the acid ones in contrast with the island arcs occur very often and in some areas they are even predominant (45–70% of the section) including liparites with $\text{SiO}_2 > 70\%$. Basalts constitute 5–6%; andesite-basalts and andesites, 25–55%. The basic and intermediate volcanites are represented by lavas less by tuffs with fine to coarse fragments and sometimes bombs or tuffs with heterogeneous fragments. Among the acid volcanites the ignimbrite type rocks prevail (from the non-coagulated tuffs up to rheoignimbrites). Fine-grained ash tuffs are rare.

The volcanic rocks of the belt especially, ignimbrites compose large volcano-tectonic depressions which exceed in their sizes the negative structural forms of the island arcs. The basic and intermediate lavas form the lava plateau inside of which there is distinguished a great number of necks (paleovents) that proves an areal character of the volcanism.

Among the acid rocks in contrast with those of the island arcs there are always biotite and feldspathic impregnations. In ignimbrites the plagioclase is of increased basicity (up to Na_4O) in lavas it is poor in calcium (albite-oligoclase). Whereas in the island arc volcanites the plagioclase is sufficiently basic (from albite to andesine and sometimes even bytownite), on the Greater Kuril Islands there are even labradorites occurring in dacites. All the belt rocks are characterized by the great melanocratic degree.

Together with the calc-alkalic rocks the subalkalic and alkalic volcanites are widespread (Fig. 4). The alkaline content constitutes in general 9.5–10% and potassium is abundant in their composition. This is distinctly observed in the acid varieties especially in the ignimbrites in which $\text{K}_2\text{O}/\text{Na}_2\text{O}$ ratio is more than 2. In some areas the alkaline amount increases owing to the high Na_2O content. The high alkalinity is exposed in

Table 2. The average composition of magmatic rocks of the Okhotsk-Chukotka belt and Kuril Islands.

Components	The Okhotsk-Chukotka belt (after USTIEV, 1965)	The Kuril Islands (after MARKHININ, 1967)
SiO ₂	65.52	59.26
TiO ₂	0.69	0.75
Al ₂ O ₃	15.74	17.43
Fe ₂ O ₃	2.43	3.47
FeO	3.19	4.18
MnO	0.06	0.13
MgO	2.21	3.47
CaO	4.04	7.24
Na ₂ O	3.24	2.85
K ₂ O	2.88	1.22
Sum total	100.00	100.00

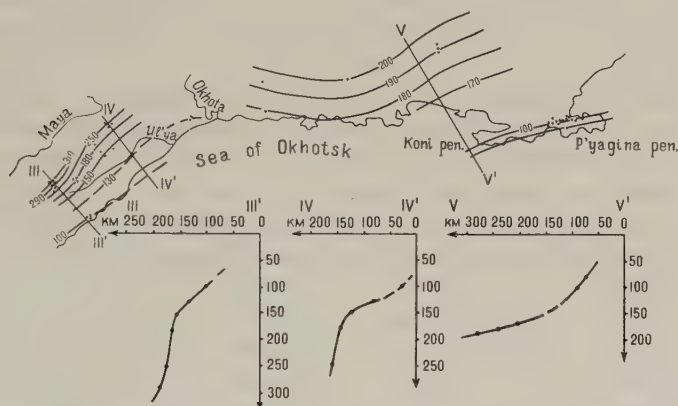


Fig. 7. Benioff paleozoone position of the Okhotsk-Chukotka volcanic belt. The legend is the same as in Fig. 6.

the rock mineralogy by the existence of Ti-impregnations that is of augite, potassic feldspar, analcime. FeO^*/MgO ratio contrary to that of island arc volcanites tends to sharply increase in the acid components of the sequence, that is expressed by the appearance of the increased ferruginization in the dark minerals and existence of the magnetite impregnations. Such tendency is probably explained by the slow increase of SiO_2 content during the differentiation. These correlations between Fe^{2+} , Mg and Si are not typical of the island arc volcanites.

The differences in the average chemical composition of the volcanites of the belt and Kuril Islands are clearly expressed (Table 2).

The Okhotsk-Chukotka belt so as the island arcs is connected with the Benioff zone but with different geometric and, probably, kinematic parameters.

On the whole the Benioff paleozoone determined by the K_2O content in the volcanites of the lower belt strata, mainly, made of andesite-basalts and andesites is more gentle than that of the Uda-Murgal arc (Fig. 7). It is characterized by the complex pattern, that is the vast (120–170 km) gentle area corresponding to the major part of the belt and sharp subsidence within the small distance in the southwestern part of the belt. The surface

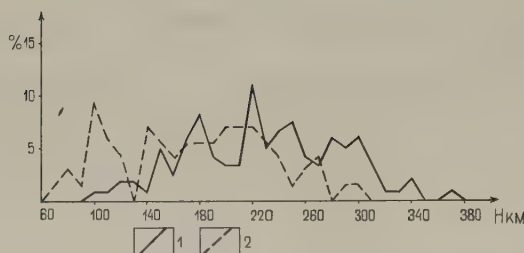


Fig. 8. Depth values up to the supposed Benioff zone for the upper section of the Okhotsk-Chukotka volcanic belt. 1, histogram of the Ul'ya part of the belt; 2, histogram of the Northern Okhotsk part of the belt.

projection of the magmatic active part of the Benioff paleozone is significantly wider (120–200 km) than that of the Uda-Murgal (about 50 km) and Kuril-Kamchatka (about 45 km) arcs.

The analogous calculations for the upper part of the belt section composed by the contrast andesite-basalt-liparite associations show the significant confusion of the depth values (Fig. 8). It is supposed that the received confusion of the depth values and their irregular distribution across the belt strike can be caused by the increase of the K_2O content in the andesite-basalts and andesites due to the crust material contamination. This conclusion is proved by the fact that the histogram of the depth value distribution for the Ul'ya part of the belt is shifted to the area of the greater depths in regard to that of the Northern Okhotsk part of the belt. The Ul'ya part of the belt is situated on the Early Precambrian sialic basement of the Okhotsk massif. The basement of the Northern Okhotsk part of the belt is composed by the dislocated Early Mesozoic assemblages of the Uda-Murgal arc and its back trough; Early Precambrian crystalline complexes are not found there.

From the oceanic side the Okhotsk-Chukotka belt is conjugated with the linear troughs composed by the thick slightly dislocated shale-greywacke series which are synchronous to the belt volcanites. They are the Penzhina Trough, stretching for 500 km, and trough in the northern part of the Sea of Okhotsk which is supposed to exist according to some interpretations of modern seismic data. They can be considered as the interarc troughs or sedimentary terraces. The Penzhina Trough is situated on the place of the Early Mesozoic interarc trough having no significant displacements. The Benioff zone outcrop should be supposed eastwards from the trough. Probably, it coincides with the Mid-Koryak glaucophane-schist and ultrabasite belts of the Early Mesozoic age.

In the Okhotsk-Chukotka belt territory there are widely distributed young basalt sheets. Some investigators consider these basalts as the constituents of the volcanic belt, but these basalts differ sufficiently from the rocks of the belt taking into consideration the occurrence conditions, petrochemical and some other features.

The plateau-basalts are distributed locally but traced on the whole belt strike. They are mostly widespread in the Middle-Anadyr, Ul'ya and Chukotka areas where their thickness reaches 500–1,000 m (BELIY, 1969, 1977; BAKHAREV, 1976). They have been considered as Paleogene because the flora remnants of the underlaying series have been dated as Late Senonian–Danian. The recent discoveries of flora and fauna remnants in these suits of the Okhotsk and Central Chukotka parts of the belt enable to date these suits as

belonging to the first half of the Late Cretaceous and thus, to refer the plateau-basalts to the end of Cenomanian (BELIY, 1977).

In the composition of these volcanites basalt lavas are predominant, tuffs and tuff breccias are subordinate in contrast with the older basalt associations. The more acid rock varieties represented by horizons of ignimbrites, dacites, liparites, trachyliparites, trachytes and subvolcanic bodies of the corresponding composition are constantly found in small quantities. The acid volcanites are distinguished in the different parts of the section but their amount increases upwards in the stratigraphic column.

Fracture-type eruptions were predominant because of the vast basalt distribution, occurrence of flat basalt sheets, rare neck existence and connection with extending fractures. There are observed the contiguous subparallel dike swarms of some meters up to tens of meters wide which can be considered as incurrent channels.

The cenotypal appearance is typical of these rocks on the contrary to the Cretaceous volcanites. Among the lavas there are usually preserved vesicular, slaggy varieties with pores not filled by the secondary minerals whereas the Cretaceous lavas possess amygdaloidal texture. The slaggy varieties often have red-violet colour usual for the sub-aerial lavas. The characteristic feature of the basalts is the existence of olivine in them. The olivine-pyroxene basalts are abundant. Pyroxene-olivine, non-olivine bipyroxene basalts and andesite-basalts are less distributed. Analcime, pseudoleucite, oligoclase basalts, crinites are constantly observed. Olivines and orthopyroxenes of the basalts are highly magnesian (up to 75% of Mg), monoclinic pyroxene is usually represented by the augite, in the Middle-Anadyr region titan-augite is often found, in the Central Chukotka—pigeonite.

The increased alkalinity is the characteristic feature of the chemical composition of basalts (Fig. 9). The rocks of the Ul'ya and Central Chukotka areas possess the highest alkalinity. In these areas the gradual alkali accumulation occurs during the melt differentiation and the most acid varieties have the alkalic features. In the Middle Anadyr

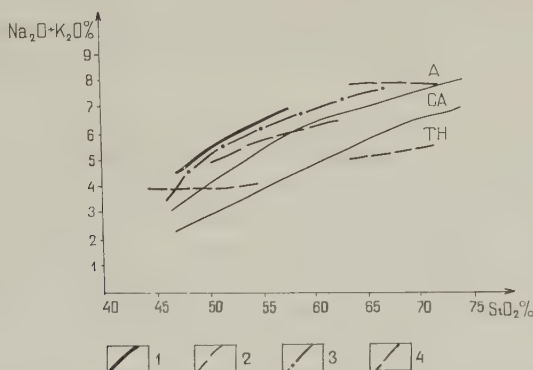


Fig. 9. Chemical composition of the plateau-basalts in the Okhotsk-Chukotka belt. 1, Ul'ya trough; 2, Middle Anadyr area; 3, Central Chukotka area; 4, Eastern Chukotka area. Letters designate the fields of volcanic series: TH, tholeiite; CH, calc-alkali; A, alkaline. Division boundaries of the fields of volcanic series are given according to H. KUNO (1964).

area the alkali accumulation is not observed. There appear the calc-alkaline andesite-basalts. The most potassic part in the alkalic varieties of the basalts is distinguished for the Ul'ya and Central Chukotka areas. Basalts of the Middle Anadyr and Eastern Chukotka areas are sufficiently sodic.

The volcanic assemblages under consideration are referred to the alkaline-olivine basalt association. In contrast with the more ancient volcanic associations of the belt they are characterized by: (1) sufficiently basic composition and slight differentiation; (2) predominance of the alkalic olivine basalts; (3) the higher alkalinity of the rocks; (4) cenotypal appearance; (5) fracture type of eruptions.

The plateau-basalt origination can be connected with the Benioff paleozone extinction and recession eastwards to the ocean. When the compressive stress in the lithosphere disappeared the large linear uplifts began to form on site of the belt and the large extension zone originated causing the eruption of high alkalic homogeneous basalts.

4. *Mesozoic Continental Boundaries in the Sikhote-Alin Region*

In the East of the Sikhote-Alin a Late Mesozoic island arc is distinguished (Fig. 1). Under the continental volcanites of the Eastern Sikhote-Alin belt there are outcrops of the dislocated coastal-marine and continental volcanic-sedimentary assemblages of Albian-Turonian age. They are represented by greywackes with clastic materials of volcanic origin, aleurolites, conglomerates, tuffites, tuffs and andesite lavas up to 2,500 m thick. The Upper Cretaceous sequence of the northwestern edge of the Sakhalin on the Cape Maria seems to belong to the same type. They are made of trachyandesites, andesite-basalts, basalts, trachybasalts, dacites and their tuffs of 2,000 m thick. Southwards in the village Boshnyakovo area the upper part of the Upper Cretaceous complex is composed by the thick series of volcanic conglomerates, breccias, greywackes and gritstones. Petrographic composition of the fragments and facies appearance of the deposits indicates the erosion of predominantly intermediate volcanic thick series. The Late Cretaceous complex of the northern part of the Western Sakhalin mountains is represented largely by the continental coal-bearing deposits with the abundant volcanic clastic material. Facies composition of these assemblages indicates the occurrence of a removal source situated westwards.

The back trough of the assumed arc is distinctly determined on the whole Sikhote-Alin strike westwards from the Eastern Sikhote-Alin volcanic belt. It is composed by the thick (up to 10,000–11,000 m) greywacke-shale complex of Hauterivian-Coniacian age which overlays the more ancient assemblages sometimes accordantly and sometimes with angular and stratigraphic unconformity. In the complex composition there are distinguished the horizons of basic and intermediate lavas and tuffs, rudeaceous rocks the amount of which increases eastwards and in the upper parts of the section. The linear foldings with the southeastwards dip of axial planes are typical.

Eastwards from the arc within the Sakhalin Island there are known the synchronous associations. In the Western Sakhalin the Cretaceous deposits (from Albian to Maastrichtian) are represented by the marine amagmatic greywacke-shale series of 5,000–6,000 m thick which compose the monocline dipping westwards and complicated by the linear folds. The thickness of this complex sharply decreases (up to 1,000–2,000 m) in the Central Sakhalin. The unvolcanic uplift which is assumed to have existed eastwards is particularly proved by the increase of the coarse-grained Upper Cretaceous deposits in

this direction. In the Eastern Sakhalin Mountains the Upper Cretaceous complex is typically eugeosynclinal in which jaspers, spilites and Alpine type ultrabasites are present. The Western Sakhalin trough can be considered as the interarc trough (between the inner volcanic and outer non-volcanic arcs).

The Benioff paleozone of this island arc is assumed to coincide with the Susunay glaucophane-schist belt (DOBRETsov, 1974) which is situated on the Kamuikotan belt continuation of the Hokkaido.

The Eastern Bureya margin-continental volcanic belt comprising the discontinuous fields of granitoids and continental volcanites elongated for 600 km along the eastern margin of the Bureya massif originated in general simultaneously with the above-mentioned island arc (Fig. 1). The calc-alkalic andesites, andesite-dacites and liparites which are conjugated with diorite, granodiorite and granite bodies are abundant in the belt composition. Subalkalic potassic liparites in a form of ignimbrites, tuffs and less lavas compose the larger upper part of the section in the central area of the belt (the Badzhai Range).

The distinct alkalinity increase occurs westwards from the Eastern Bureya belt within the Bureya massif. The volcanic zone situated in the massif developed synchronously with the volcanic belt. They are formed by trachyliparites, trachyandesites, trachydacites, trachyandesite-basalts and subalkalic liparites associated with the alkalic granitoids. The typical combination is that of the contrast by their acidity associations, for example, trachyandesite with trachyliparites. The predominance of the basic and intermediate rocks in the lower parts of the section is also representative.

The above-mentioned data compared with the Okhotsk-Chukotka volcanic belt allow to suppose the connection of the Eastern Bureya belt with the Benioff paleozone. Dislocated shale-greywacke, predominantly, sandstone Apt-Albian series of the western slope of the Sikhote-Alin ridge probably correspond to the interarc trough. But nevertheless, synchronous ophiolite complexes which could mark the Benioff paleozone outcrop are unknown in the Sikhote-Alin. In the axial zone of the Sikhote-Alin the most recent are the ultrabasite blades in the thrust zones cutting the Valanginian sandy-shale suits.

The Eastern Sikhote-Alin volcanic belt stretches for 1,500 km. It is about 300 km wide including its eastern part covered by the Tatar Straits and the Sea of Japan, but obviously mapped according to aeromagnetic and dragging data (Fig. 1). The belt origination took place in Senonian-Paleogenic time.

In the longitudinal direction the belt is subdivided into three sections with the different volcanites composition and associated granitoids (SUKHOV, 1974). In the northern part of the belt the andesite-dacite and granodiorites are prevalent, in the middle part—the andesite-dacite, granodiorites and granites, and in the southern part—andesite-dacites, liparites and granites. Within the central areas of the Sikhote-Alin parallel to the belt there is a chain of volcanic zones which developed in general simultaneously with the belt development. In the northern part of the Sikhote-Alin they are composed by the subalkalic andesites, basalts, andesite-basalts, andesite-dacites, dacites which are followed by the subalkalic potassic liparites and liparite-dacites. In the more southern areas of the Sikhote-Alin the trachyandesites and trachyliparites are abundant. They are accompanied by the intrusive formations represented by the monodiorites, granosyenites and alkalic granites.

It is likely that the tectonic nature of the Eastern Sikhote-Alin belt is similar to that of the Okhotsk-Chukotka belt. The belt formation took place after the active orogenic

movements in the Sikhote-Alin geosyncline which caused the closing of the existing there troughs and were accompanied by folding. The belt superimposes over the former island arc and is accompanied by the trough with thick terrigenous series from the ocean side. The upper parts of the Upper Cretaceous and Paleogene of the Western Sakhalin represented by the thick (up to 5,000 m) marine, partially, (in Eocene) continental greywacke, aleurolite and argillite series can be considered as deposits of that trough. The depth to the Benioff paleozone of the belt has been determined according to the K_2O content in volcanites as 160 km in the eastern, 180 km in the central and 220–230 km in the western parts of the belt (SONENSHEIN *et al.*, 1976). The approximate angle of zone inclination is 21–23°. The young plateau-basalts are distributed in the Eastern Sikhote-Alin belt territory as well as within the Okhotsk-Chukotka belt. They are known as the Kizi suit of Miocene age. In the Sovgavan area the suit is represented by the alternating sheets of basalts, andesite-basalts and andesites and in the upper parts, mainly, by dacites with a total thickness of about 600–700 m. The volcanites are made predominantly of lavas, in the lower part of the section there are agglomerates, tuffs and breccias, olivine, bipyroxene plagioclase basalts and andesite-basalts are mostly widespread. They provide a plagiandesite-basalt assemblage. In the Lower Preamur'ie the Miocene basalts, andesite-basalts of the Kizi suit compose sheets of the shield volcanos. Pyroclastic formations are almost absent. According to petrochemical and petrographic features the basaltoids of this area constitute an alkaline-basalt assemblage.

5. *Tectonic Evolution*

Kinematics of the plate movements in the North-Eastern Asia during Mesozoic and Cenozoic time had been determined by the mid-ocean ridge position in the Pacific Ocean and the spreading rate in them and also by the Eurasia drift as a result of the Atlantic and Indian Ocean opening. But it is hardly acceptable to make a simple vector addition on the Pacific margin of the Eurasia (UYEDA and MIYASHIRO, 1974), because in its inner regions there are known some intensive Mesozoic and Cenozoic dislocations indicating that the Eurasia plate was not a single rigid body at that time. That is why while reconstructing only the semi-quantative estimations of the rates and drift vectors are possible. And as for Mesozoic active boundaries it is impossible to do even such reconstructions because these boundaries are separated from the Pacific plates by the other active margins.

In our reconstructions it is supposed (Fig. 10) that the direction of the plate displacements is perpendicular to the large thrusts and parallel to the shifts and in the whole it should be combined in the general pattern.

During the Mesozoic and Cenozoic time the consequent oceanward displacement of the island arc occurred. The Uda-Murgal Island arc marks the southeastern boundary of the Eastern Siberia megablock from the Late Paleozoic up to Neocomian time. The northern boundary of the Eastern Siberia megablock can be defined by the belt of the Upper Jurassic volcanites, stretching along the South Anyuy eugeosynclinal system and by the volcanic belts of the same age framing the Alazeya-Oloy eugeosynclinal system of type B. The modern data concerning these regions in many cases do not allow us to determine the polarity of some Early Mesozoic island arcs, to reconstruct the ancient microplates there and to recreate their relative displacements. The northern boundary of the megablock is quite different from the linear southeastern one because of the complicated spatial position of the volcanic belts which join each other with great angles. We assume

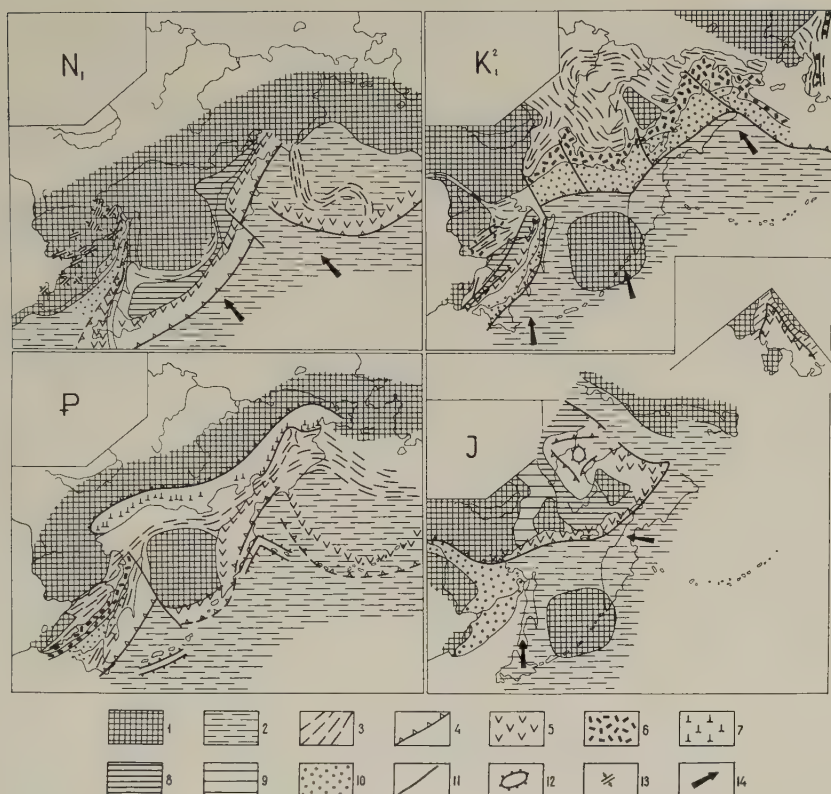


Fig. 10. Paleotectonic schemes. 1, continents and microcontinents; 2, ocean; 3, young folded zones; 4, Benioff zones; 5, volcanic geanticlines (inner island arcs); 6, margin-continental volcanic belts; 7, plateau-basalts; 8 and 9, back troughs (mio-geosynclinal zones) (8, their inner zones; 9, outer zones); 10, shale-greywacke troughs; 11, transform faults; 12, uplifts; 13, rifts; 14, direction of the plate movement.

that in Mesozoic time there was the marginal sea system similar to the modern Soud archipelago. On the place of the South-Anyuy eugeosynclinal system it is supposed a vast oceanic basin in Early Mesozoic time. According to paleomagnetic reconstructions for Jurassic time there is the significant overlapping of the Eurasia and Northern America continents in the apical part of the Boreal sinus (IRWING, 1977) that allows us to assume the sufficient removal of the Chukotka microcontinent from the region disposing southwards from the South-Anyuy system. The attachment of the Chukotka microcontinent to the Eastern Siberia megablock and disappearance of the active continental margin took place at the end of Neocomian. In this time the compound folded structure of the South-Anyuy zone was formed. The rigid structural connections originated between Eurasia and Northern America due to the comparatively narrow Chukotka microcontinent stretched in the sublatitudinal direction.

The southwestern continuation of the Uda-Murgal arc is considered to be the Late Jurassic granodiorite belt of the Stanovoy Region. The belt stretches parallel to the Mongolia-Okhotsk eugeosynclinal system of type A (Fig. 1). The granodiorites should

be considered as the deep analogues of the andesites locally retained in the roof of the plutons (GODZEVICH, 1976). The granodiorite belt defines the southern active margin of the Eastern Siberia megablock.

Paleomagnetic data for the Permian period allow us to suppose the significant width of the oceanic basin occurred on the place of the eastern part of the Mongolia-Okhotsk eugeosynclinal zone. The Siberian Platform in this time was characterized by the high paleolatitudes ($>45^\circ$) (IRWING, 1977). The Japanese Islands rigidly connected with the Bureya-Khanka microcontinent were situated near latitude 30° North (SONENSHEIN, 1976) and according to other values near latitude 20° North (THE GEOLOGICAL DEVELOPMENT OF THE JAPANESE ISLANDS, 1968). Paleomagnetic data for China indicate its position in latitude 10° – 20° North (IRWING, 1977). The rough estimate of the oceanic basin width by longitude constitutes 1,500–2,000 km. In Mesozoic time the basin width was steadily decreasing and the basin was intensively filled with thick flysch series.

After the closing of the Mongolia-Okhotsk system and wedging it by the Bureya-Khanka microcontinent in Apt-Albian an island arc accompanied by the large left strike-slip faults in its back parts was originated along the Sikhote-Alin continental margin (Fig. 10).

At the end of Cretaceous–beginning of Paleogene the geosynclines closing of the Northern Preokhot'ic and Benioff zone wedging by the Okhotomorskiy massif caused the generation of a new seismofocal zone in the region of the Western Kamchatka and, probably, along the southern edge of the Okhotomorskiy massif (Fig. 10).

The Neogene structural elements mostly coincide with the modern ones but sometimes they are separated (Fig. 10). From the point of view of regularities observed in the modern geosynclines it is difficult to explain the nature of some parts of the Western Sakhalin and Kuril-Kamchatka volcanic arcs stretching into the continent far from the points of their conjugation. They could be originated above the faults which are developing in the re-entrant angles of the island arcs. The Northern part of the Western Sakhalin arc can be interpreted in another way. The basin of the Sea of Japan is supposed to be the extension zone. The band of the rift-like Cenozoic basin and alkalic basalt trends along the Ussuri and Amur rivers parallel to this zone. The extension in these zones could be indemnified by the existence of additional Benioff zone westwards from the volcanic uplift traced through the Western Hokkaido, Rishiri, Rebun and Moneron Islands. According to such interpretation the origin of the Sea of Japan which is considered as the Cenozoic eugeosyncline and conjugated with it the Western Sakhalin arc which is excepted from the general regularity of island arcs displacement towards the Pacific, should be connected with the destruction of the continental crust formed earlier.

The oceanwards retreat of the island arcs took place not gradually but it was the sharp displacement from 150 up to 500 km. It was due to the change of the strain fields and wedging of the Benioff zones by the microcontinents. Thus, the new arcs usually originated making great angles with the more ancient structures cutting them and separating the parts of the ocean floor.

The margin-continental volcanic belt (the Okhotsk-Chukotka, Eastern Sakhalin and others) display the great similarity with the active continental boundaries of Andean type (PARFENOV, 1976; SONENSHEIN *et al.*, 1976). Some features prove their regular origination on the site of the former margin of the island arc type volcanic belt. Volcanic belts overlap the island arc complexes slightly shifted towards the continent. The interarc troughs connected with the belts inherit the analogous troughs of the former island arcs.

The volcanic belts are disposed on the consolidated basement after the orogenic movements which embrace the large territory; first of all they are situated in the back of them, namely, the miogeosynclinal zones. This peculiarity, which is not attributed to the island arcs speaks for the significant tectonic activity of the continental plate exceeding that of the submerging oceanic plate. This process could cause the changes of the Benioff zone geometry: decrease of the inclination angle, enlargement of the width along its dip and depth of its magma active part.

The volcanic belts are characterized by their short history (10–30 my). The heterogeneity of the vertical section is typical for them. There are andesite-basalts and andesites at the base and large volumes of acid volcanites in the upper parts of the sections. While the genesis of lower horizons is connected with the Benioff zone, the upper ones are believed to be influenced by the continental crust remelting. The eruptions of high-alkalic plateau-basalts, homogeneous over the vast areas finish the development of the margin-continental volcanic belts. These eruptions are connected with the extension zones on the arches appearing on site of the volcanic belts after the Benioff zone disappears.

Many island arcs and margin-continental volcanic belts are distributed along the ancient sialic megablock boundaries. Their position assumes the large mutual horizontal displacements between the megablocks and separating them are the eugeosynclinal zones. The continental enlargement took place not only at the expense of the island arc displacement towards the ocean, but also owing to the joining of the ancient sialic megablocks originated in the Early Precambrian time into one continental mass.

This paper draws the information from the work of many other geologists. Essential references have been given but many others have been omitted for space requirements. Special thanks for helpfull discussions are in particular due to L.P. Sonenshein, L.P. Karsakov, V.A. Popeko, S.M. Til'man and R.B. Umitbaev. Mrs. Natal'ina I.S. put this paper into English and the authors appreciate very much this hard work.

REFERENCES

- ALEXANDROV, A.A., N.A. BOGDANOV, S.C. BYALOBZHENSKY, M.S. MARKOV, S.M. TIL'MAN, V.E. KHAIN, and A.D. CHEKHOV, New data on the tectonics of the Koryak highland, *Geotectonica*, No. 5, 60–72, 1975 (in Russian).
- ARSANOV, A.S., Paleogeography of the Eastern Kamchatka in Miocene, *Bull., Moscow Soc. Nat., Geol. Ser.*, No. 3, 142–143, 1973 (in Russian).
- BAKHAREV, A.G., Stratigraphy and composition peculiarities of the volcanic assemblages of the Ul'ya superimposed basin, in *Volcanic and Intrusive Assemblages of the Prekhot'ie*, pp. 53–75, Nauka, Novosibirsk, 1976 (in Russian).
- BELIY, V.F., Volcanic belts in the areas of Mesozoic tectogenesis of the Eastern Asia, in *Mesozoic Tectogenesis*, pp. 112–114, Magadan, 1969 (in Russian).
- BELIY, V.F., Okhotsk-Chukotka volcanic belt, Doctor's Thesis, 57 pp., Novosibirsk, 1977 (in Russian).
- BELIY, V.F. and I.N. KOTLYAR, New data on the geology of the western part of the P'yagina peninsula (the inner zone of the Okhotsk-Chukotka volcanic belt), in *Proc. on Geology and Mineral Resources of the North-East of the USSR*, Issue 22, pp. 74–85, Magadan, 1975 (in Russian).
- BELIY, V.F. and A.P. MILOV, Structure and development of the inner zone of the Okhotsk-Chukotka belt in the basin of the Penzhina river, *Sov. Geol.* No. 1, 86–99, 1973 (in Russian).
- BELIY, V.F. and A.P. MILOV, On the petrological zonation of gabbro-granite series in the Okhotsk-Chukotka volcanic belt, *AN SSSR, Izv. Ser. Geol.*, No. 10, 49–57, 1974 (in Russian).
- DICKINSON, W.R. and T. HATHERTON, Andesitic volcanism and seismicity around the Pacific, *Science*, **157**, 801–803, 1967.
- DOBRETSOV, N.L., *Glaucophane-Schist and Eclogite-Glaucophaneschist Complexes of the USSR*, 425 pp., Nauka, Novosibirsk, 1974 (in Russian).
- EPSTEIN, O.G., Removal sources in the origination of the Verkhoysk complex (the southern part of the Yana-Kolyma folded area), in *Proc. on Geology of the North-East of the USSR*, Issue 23, Book I, pp. 110–113, Magadan, 1977 (in Russian).

- FEDOTOV, S.A., On volcanic connection with the Pacific focal layer, mechanism of magma uplifting and proposed position of mantle areas of volcano feeding, in *Geodynamics, Magma Formation and Volcanism*, pp. 9–20, Petropavlovsk-Kamchatskiy, 1974 (in Russian).
- FILATOVA, N.I. and A.I. DOORYAKIN, Volcanic evolution of the central part of the Okhotsk-Chukotka volcanic belt, *AN SSSR Izv. Ser. Geol.*, **N 11**, 51–68, 1974 (in Russian).
- GAVERILOV, V.K. and N.A. SOLOV'YEVA, *Volcanic-Sedimentary Assemblages of the Geanticlinal Uplifts of the Lower and Greater Kuril Islands*, 151 pp., Nauka, Novosibirsk, 1973 (in Russian).
- GLADENKOV, Yu. B. and V.I. GRECHIN, Formation peculiarities of Neogene volcanic-sedimentary series of the Eastern Kamchatka (Karagin Island), *Bull. Moscow Soc. Nat., Geol. Ser.*, No. 5, 72–81, 1969 (in Russian).
- GODZEVICH, B.L., Tectonics of the Stanovoy folded area, in *Tectonics of the East of the Soviet Asia*, pp. 34–55, Vladivostok, 1976 (in Russian).
- GONCHAROV, V.N., New data about the volcanic-sedimentary assemblages age of the Northern Uda trough, in *Tectonics of the North of the Soviet Asia*, pp. 70–72, Vladivostok, 1976 (in Russian).
- GRINBERG, G.A., Volcanic assemblages of the South-Western Okhotsk-Chukotka belt, in *Volcanic and Intrusive Assemblages of the Prekhot'ie*, pp. 4–13, Nauka, Novosibirsk, 1976 (in Russian).
- KUNO, H., Series of igneous rocks, in *Chemistry of the Earth Crust*, VII, pp. 117–121, Nauka, Moscow, 1964 (in Russian).
- IRWING, E., Drift of the major continental blocks since the Devonian, *Nature*, **270**, 304–309, 1977.
- MAP OF MAGMATIC FORMATIONS OF THE USSR, Scale 1 : 2,500,000, Leningrad, 1971 (in Russian).
- MARKOVSKIY, B.A. and O.I. SUPRUNENKO, Comparative characteristics of two types of turbidite formations of the Eastern Kamchatka, *Sov. Geol.*, No. 10, 24–31, 1972 (in Russian).
- MIGOVICH, I.M., Tectonic development of the Penzhina-Anadyr folded zone, Doctor's Thesis, All-Union Geological Institute, Leningrad, 1972 (in Russian).
- MILOV, A.P., On the influence of tectonic conditions to the peculiarities of Late Mesozoic granitoid magmatism of Chukotka, in *Mesozoic Tectogenesis*, pp. 291–295, Magadan, 1971 (in Russian).
- MIRYASHIRO, A., Volcanic rock series in island arc and continental margins, *Am. J. Sci.*, **4**, 321–355, 1974.
- NEKRASOV, G.E., *Tectonics and Magmatism of the Taygonos Peninsula and North-Western Kamchatka*, 157 pp., Nauka, Moscow, 1976 (in Russian).
- NEKRASOV, G.E., N.B. ZABOROVSKAYA, and M.L. GEL'MAN, Tectonics of the zone of mesozoic transition to the structures of the Koryak-Kamchatka folded region on the example of the Taygonos peninsula, in *Mesozoic Tectogenesis*, Magadan, pp. 80–87, 1971 (in Russian).
- PARFENOV, L.M., Tectonic position and the Okhotsk-Chukotka volcanic belt nature, in *Deep-Sea Construction, Magmatism and Metallogeny of the Pacific Volcanic Belts*, 11 pp., Vladivostok, 1976 (in Russian).
- PAVLOV, Yu. A. and L.M. PARFENOV, On the geological nature of Hokkaido-Sakhalin gravitational minimum, *Akad. Nauk SSSR Dokl.*, **217**, 1390–1393, 1974 (in Russian).
- PISKUNOV, B.N., *The Greater Kuril arc Volcanism and Petrology of the High-Aluminiferous Rocks*, 187 pp., Nauka Novosibirsk, 1975 (in Russian).
- POLUBOTKO, I.V., K.V. PARAKETSOV, and Yu.S. REPIN, Jurassic structural facies areas on the North-East of the USSR, in *Proc. on Geology of the North-East of the USSR*, Issue 23, Book I, pp. 42–51, Magadan, 1977 (in Russian).
- SHAPIRO, M.N. and V.A. SELIVERSTOV, Morphology and age of folded structures of the Eastern Kamchatka at the latitude of the Kronotsky peninsula, *Geotectonica*, No. 4, 84–94, 1975 (in Russian).
- SHILO, N.A., V.P. BELIY, and A.A. SIDOROV, Volcanic belts of the Eastern Asia as applied to the problems of tectonics, magmatism and metallogeny, *Geol. Geophys.*, No. 5, 70–88, 1974 (in Russian).
- SHIMARAEV, V.N., Volcanic belts of the East of the Sea of Okhotsk, in *Deep-Sea Structure, Magmatism and Metallogeny of the Pacific Volcanic Belts*, pp. 99–100, Vladivostok, 1976 (in Russian).
- SONENSHIN, L.P., M.I. KUS'MIN, and V.M. MORALEV, *Global Tectonics, Magmatism and Metallogeny*, 231 pp., Nedra, Moscow, 1976 (in Russian).
- SUKHOV, V.I., *Volcanic Assemblages of the South of the Soviet Far East*, 112 pp., Nedra, Moscow, 1974 (in Russian).
- SUVOROV, A.L., *Deep Constructions of the Earth Crust of the South Okhotsk Sector According to Seismic Data*, 103 pp., Nauka, Novosibirsk, 1975 (in Russian).
- THE GEOLOGICAL DEVELOPMENT OF THE JAPANESE ISLANDS (eds. M. Minato, M. Gorai, and M. Hanahashi), 719 pp., Mir, Moscow, 1968 (in Russian).
- TIL'MAN, S.M., S.G. BYALOBZHEVSKY, A.D. CHEKHOV, and L.L. KRASNYY, Specific features in the formation of the continental crust in the North-East of the USSR, *Geotectonica*, No. 6, 15–29, 1975 (in Russian).
- TOKAREV, P.I., Seismic activity of the Kamchatka focal layer and its connection with volcanism, in *Seismicity and Seismic Prediction of the Upper Mantle Peculiarities and Its Connection with Volcanism in Kamchatka*, pp. 166–176, Nauka, Moscow, 1974 (in Russian).

- TUESOV, I.K., M.L. KRASNY, B.I. VASIL'YEV, A.A. KULIKOV, and V.I. MIKHAILOV, Geological structure of the southern member of the Kuril island arc., *Geol. Geophys.*, No. 12, 63-72, 1975 (in Russian).
- USHAKOV, S.A., YU.A. GALUSHKIN, and A.M. GORODNITSKY, Conditions of deep-sea mountains stripping by dragging them under the island arcs. in *Tectonics of the Lithospheric Plates (Energy Sources of the Tectonic Processes and Plate Dynamics)*, pp. 123-127, Moscow, 1977 (in Russian).
- USTIEV, E.K., The Okhotsk tectomagmatic belt and some relating problems, *Sov. Geol.*, No. 3, 3-26, 1959 (in Russian).
- USTIEV, E.K., Composition of primary magmas as exemplified by Cretaceous and Paleogene formations of the Okhotsk volcanic belt, *Akad. Nauk SSSR, Izv. Ser. Geol.*, No. 3, 3-19, 1965 (in Russian).
- UYEDA, S. and A. MIYASHIRO, Plate tectonics and Japanese Islands: A synthesis, *Geol. Soc. Am. Bull.*, **85**, 1159-1170, 1974.
- VLASOV, G.M., O.G. BORISOV, and M.I. POPKOVA, Neogene tuff flysch formation of the Kuril-Kamchatka system and flysch genesis, *Litologia i Poleznie Iskopaniya*, No. 1, 110-124, 1977 (in Russian).
- VOINOVA, I.P., Magmatic assemblages of the Uda volcanic belt, in *Problems of Magmatism and Tectonics of the Far East*, pp. 179-189, Vladivostok, 1975 (in Russian).
- ZABOROVSKAYA, N.B. and G.E. NEKRASOV, Tectonics and magmatism of the transition zone from the Yana-Kolyma mesozoids to the Koryak-Kamchatka folded area, *Geotectonica*, No. 1, 103-117, 1977 (in Russian).

THE CRUSTAL STRUCTURE AND ORIGIN OF THE BASINS OF JAPAN SEA AND SOME OTHER SEAS OF THE CIRCUM-PACIFIC MOBILE BELT

Peter N. KROPOTKIN

*Institute of Geology, Academy of Sciences of
the U.S.S.R., Moscow, U.S.S.R.*

(Received June 5, 1978; Revised September 8, 1978)

The reconstructions of Mesozoic pre-drift arrangement of tectonic units, grounded on the geological and geophysical data and on the fit of continental slope contours, were compiled for the regions of the sea of Japan, the South China sea, the Tasman and Caribbean seas and the Gulf of Mexico. These reconstructions confirm a supposition that the basins of marginal seas were formed by the tension and break of the continental crust. In the deep basins a crust of oceanic type was formed by the sea floor spreading. The tension and rupture of the earth's crust was due in most areas of marginal seas to the drift of island arcs from the continent towards the Pacific, but in other areas (the Gulf of Mexico, the Caribbean and Tasman seas) it was connected with the removal of adjacent large continental blocks (N. and S. Americas, Australia and Antarctica).

An intermittent line of different tectonic structures formed by the tension of earth's crust during the Late Mesozoic and Cenozoic eras stretches from the East Pacific rise to the Gulf of California, then to the Basin and Range Province, depressions of the Pacific coast of Canada and deep basins of the south parts of the Bering sea and the sea of Okhotsk, to the basins of the Japan sea, Okinawa trough, the South China sea, Sulu, Celebes and Banda sea basins and further to the Coral sea and the Tasman sea basins. It is possible that a chain of mantle diapirs beneath these basins (KARIG, 1971) is joined on considerably deep levels by means of a general process involving the uplift of mantle matter within a common belt. Tensional tectonic structures of the Caribbean sea may be identified with a branch of this belt.

Treatment of the mentioned depressions as tension structures of the earth's crust is based on the interpretation of magnetic anomalies due to the sea floor spreading and on the reconstructions of the former arrangement of tectonic units. The reconstructions of this kind are grounded on geological and morphological data concerning the regions of the Japan sea and Tasman sea as well as the region of the Gulf of Mexico and the Caribbean sea (Figs. 1 and 2).

As far back as in 1940s KOBAYASHI (1941) and BUBNOFF (1942) expressed an opinion that deep basins of the Japan sea were formed during the late Mesozoic and Cenozoic times as a result of tension and rupture of the earth's crust related to the drift of Japan towards the Pacific ocean. This assumption was based on the remarkable similarity of the Triassic and Jurassic sedimentary series of the Vladivostok area (U.S.S.R.) and Honshu island of Japan.

A detailed reconstruction of the pre-drift arrangement of structural units in this area was carried out by the author on the ground of geology and morphology and was published

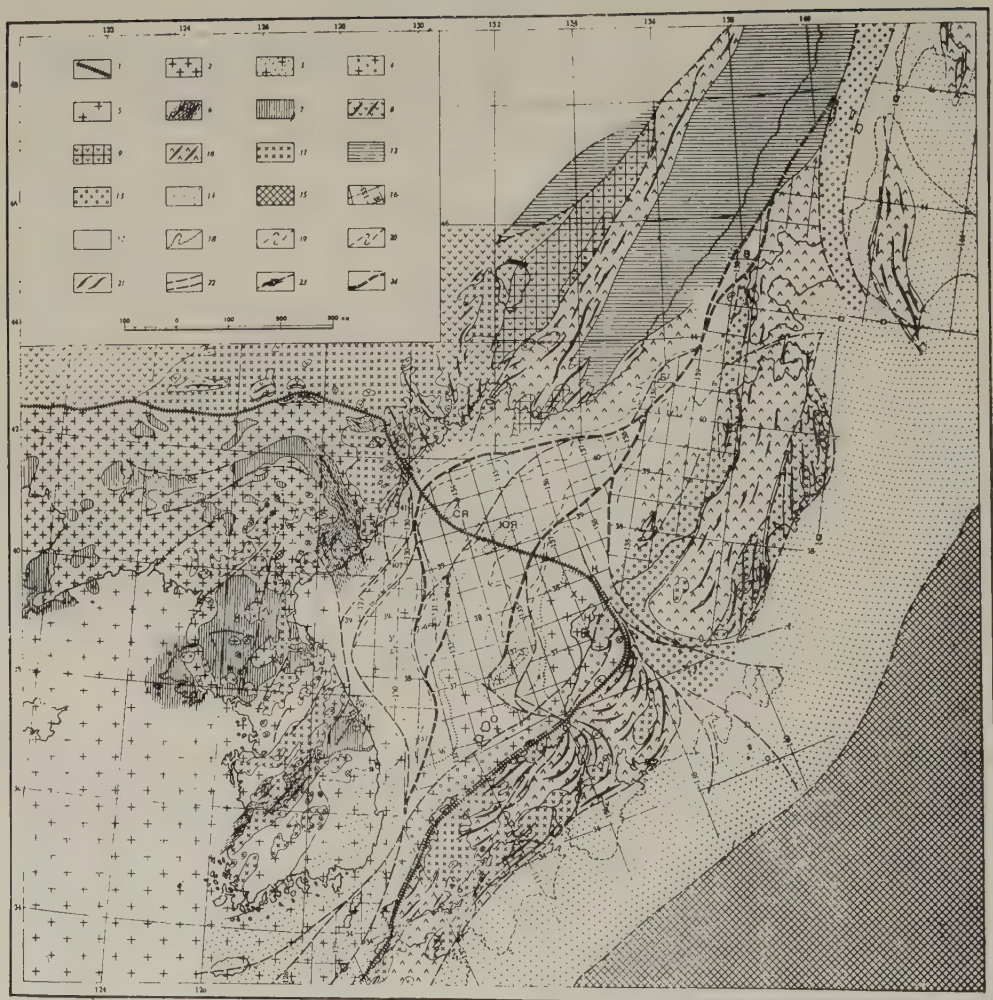


Fig. 1. Paleotectonic map of Korean peninsula, Maritime province of the USSR, Sea of Japan and Japan islands (after KROPOTKIN, 1964). Reconstruction dates to the middle of Mesozoic era. (1-7)—Chinese platform, including: 1, border of the Precambrian platform (craton); 2, Archean and lower Proterozoic basement (in the contours of recent outcrops on the surface); 3, Precambrian basement on the areas covered now by the Jurassic and Cretaceous sediments of Tsushima depression; 4, Precambrian basement supposed in the belt of Shinji geosyncline filled by Tertiary sediments; 5, supposed Precambrian basement under the floor of the sea of Japan and the Yellow sea; 6, Proterozoic folded belt of the Machenrion-Okchhon geosyncline; 7, sedimentary cover of the Precambrian platform (consisting of upper Proterozoic, Cm-O and C₂-T₁; in the Okchhon folded zone only Cm-O and C₂-T₁), shown in the recent contours of extension. For the middle of the Mesozoic era a more wide extension of sedimentary cover is supposed almost on the whole area of the Precambrian platform. (8-11)—Belts of Permian and Early Mesozoic folding and extension of P-J granitoides intrusions, including: 8, belts of Late Hercynian and Early Mesozoic folding consolidated in the middle of Triassic, 9, median mass of Khanka lake and other blocks of earlier consolidation, 10, belts of Late Hercynian and Early Mesozoic folding that have undergone a posterior deformation during the Cretaceous and Tertiary folding, 11, the granitoids of Permian, Triassic and Jurassic age (recent outcrops, partly with extrapolation). (12-14)—Belts of Mesozoic marine geosyncline depressions, including: 12, Mesozoic geosyncline of the Sikhota-Alin range (marine basin, subsidence of syncline areas dur-

in four editions in the U.S.S.R. (KROPOTKIN, 1964, 1971a, 1972; KROPOTKIN and SHAKHVARSTOVA, 1965). Subsequent geophysical survey and dredge works on the steep bottom sections have confirmed this reconstruction (BERSENEV, 1973; PAC. OCEANOL. INST. ACAD. SCI. U.S.S.R., 1977; MELANHOLINA and KOVYLIN, 1976; HILDE and WAGEMAN, 1973).

In our reconstruction (Fig. 1) made for Jurassic time Japan was represented as an almost straight structure located 50–430 km nearer to the continent of Asia than in the recent epoch. A deformation which transformed this structure into a broken arc occurred during considerably later times, as it was confirmed by the study of paleomagnetism of Cretaceous rocks (KAWAI *et al.*, 1969; KIENZLE and SCHARON, 1966). The submarine Yamato rise, the shelf around Oki islands and the Noto peninsula as well as the rises near Utsuryo (Ullindo) island, the Korea plateau and the Bogorov ridge in the north part of the sea of Japan were considered as the fragments of Asia.

The basic foundation of proposed reconstruction is a good fit of contour lines of the northern slope of the Yamato rise and of the continental slope near the coast of Korea and the U.S.S.R. between 130° and 135° E to the west and east of Vladivostok. In this reconstruction the Korea peninsula, Utsuryo island, the western part of Yamato rise and the Oki-Noto shelf form the parts of Precambrian Chinese craton. A Precambrian basement was supposed beneath Tertiary and more ancient sediments in south Korea, near the coast of Honshu island and in the Hida belt. Now this supposition is confirmed: (1) By the dredging of Precambrian granite-gneisses of the age 2,000–2,700 my near the Utsuryo island and on the Krishtofovich rise to the northeast of this island (LELIKOV *et al.*, 1975), (2) by the study of pre-Silurian rocks of southwest and central Japan, in particular the gneiss pebbles in the Permian Kamiaso conglomerate (SHIBATA and ADACHI, 1974; HURLEY *et al.*, 1973).

The study of morphology of the microcontinents in the Atlantic area and in the marginal seas shows that a typical feature of such small blocks of continental crust has a steep slope, roughly corresponding to the line of faults bordering every block. One can determine the contours of a microcontinent by tracing its steepest slopes. In contrast to the slopes of large continental blocks which commonly demonstrate their greatest steepness at the depth level 1,000–1,500 m, one observes usually the deepest slopes of microcontinents at the depth 1,500–2,500 m. Rather flat areas of microcontinents lie often at the depth 400–1,000 m instead of the depth 0–200 m, which is typical for the marginal areas of large blocks of the continental crust.

A detailed study of the bottom relief, seismic profiles and magnetic anomalies confirms the presence of faults (mainly normal faults) bordering and cutting the Yamato rise (SHE-

ing T₃, J and Cr₁, active volcanism); 13, depressions where subsequent Tertiary geosynclines and grabens were developed; 14, Mesozoic geosyncline Shimanto and the depressions of subsequently developed Cenozoic geosyncline of the outer belt of Japan and of the Sakhalin island; 15, Pacific basin (an oceanic tectonic plate); 16, blocks of the Japan sea floor that have a continental crust (B, Vitiaz rise; B, submarine Bogorov range; CЯ, northern bank of the Yamato rise; ЮЯ, southern bank of the Yamato rise; V, Korea plateau and the rise of the Ullindo island; O, the Oki islands shelf, XH, the Hegura island and Noto peninsula shelf). Recent parallels and meridian lines (interval 0.5°) are shown. (17–20)—Schematic recent bottom bathymetry contours, including: 17, 500 m; 18, 1,000 m; 19, 2,000 m; 20, 2,500 m. 21, Strike of folds; 22, faults of different types, 23, strike-slip faults (direction of a posterior displacement is shown; KK, Kanto transcurrent fault); 24, main ruptures of the Earth's crust along which the tension of deep basins of the Sea of Japan took place.

VALDIN, 1974) and submarine plateaus of the southwest part of Japan sea to the east of Korea (KARP *et al.*, 1974; MURAUCHI and ASANUMA, 1970). Using these data and a recent bathymetric map (MAMMERICKX *et al.*, 1976) one can obtain more exact contours of microcontinents by tracing the line of the steepest slopes (of declivity 0.07–0.5) of the submarine rises. Such a refinement does not result in any essential change of the reconstruction given on Fig. 1.

The continental structure of the Yamato rise, Korea plateau and Bogorov ridge is confirmed now by the seismic sounding and other geophysical studies (KOVYLIN and STROEV, 1976; PAC. OCEANOL. INST. ACAD. SCI. U.S.S.R., 1972; KARP *et al.*, 1974).

In northern Korea the margin of the Precambrian craton is bordered by the belt of Late Permian and Triassic folding of NW-SE trend. In our reconstruction this orogenic belt continues over the Yamato rise to the Toyama bay and the Hida mountains. This is in agreement with the NW-SE orientation of magnetic anomalies on the Yamato rise (ISEZAKI and UYEDA, 1973; SHEVALDIN, 1974). The granites with the age of about 200 my dredged on the Yamato rise (UENO *et al.*, 1974) correspond to the granites of the same age in other parts of the mentioned belt, including the Hida zone.

The granites and metamorphic volcanic and sedimentary rocks of Yamato rise have a remarkable similarity to the rocks of Vladivostok area (VASILYEV and MARKEVICH, 1973).

The mean virtual position of Cretaceous pole was obtained by paleomagnetism of the rocks of North Korea (GURARIJ *et al.*, 1966) and South Korea (YASKAWA, 1975) as 69° – 72° N, 178° – 211° E, and of SW Japan as 53° N, 201° E. It follows that southwest part of Japan underwent a clockwise rotation by 20° since Cretaceous period. The reconstruction corresponds to a small southward displacement of SW Japan and its clockwise rotation by 27° relatively to Korea during the drift of Japan towards the Pacific.

The oceanic crust was formed by the spreading of sea bottom in great basins of the north, west and south parts of the sea of Japan and in two rifts: (1) Between north and south parts of the Yamato rise, (2) in the Tatar strait belt (TULINA *et al.*, 1970). The Kilju-Moenchhon graben of NE Korea was formed in connection with the same tension (KROPOTKIN and RO, 1966). The southern prolongation of this graben is distinctly expressed as a rift of meridional direction on the continental slope (at 129.5° E).

The central part of the sea of Okhotsk is a vast region of continental crust. But its thickness was reduced to 20–30 km owing to the formation of rifts and the fragmentation due to the tension of the crust during the Cenozoic era. A meridional graben was formed along the Deriugin basin (western part of the sea). Another depression filled by a still more thick sequence of Cenozoic sediments was formed along the west coast of the Kamchatka peninsula. Some outcrops of basement rocks were found on the rises (Institut Okeanologii rise, Akademii Nauk rise). The tops of these rises are at the depth level 930–1,000 m (UDINTSEV *et al.*, 1976; KRASNYY *et al.*, 1975). This basement represents a region of early Mesozoic and Paleozoic folding and consolidation (so called "Okhotia" median mass).

Due to the isostatic submergence connected with the reduction of the earth's crust thickness, the continental slope appears here on the depth 1,100 m, i.e. considerably deeper than usual, and is observed to 2,000 m downwards to the deep basin of the south part of the sea. Such a peculiarity is analogous to the above mentioned specific feature of the relief concerning the levels of tops and slopes of microcontinents.

The deep basin of southern part of the sea of Okhotsk is built of an oceanic crust formed

by the sea floor spreading due to the drift of the Kurile arc towards the Pacific. On the west side this basin is limited probably by a meridional sinistral wrench-fault.

A reconstruction of the tectonic units in the southeast Asia at the end of Paleozoic and in the Mesozoic era, i.e. before the formation of oceanic crust in the deep (up to 4,500 m) basin of the South China sea, was also published in the cited book (KROPOTKIN and SHAKHVARSTOVA, 1965). This reconstruction is based on the assumption that shallower (200–2,500 m) parts of this basin being a former prolongation of the Asia continent, have a crust of continental type. Near the Vietnam coast between 11° and 17° N, the Precambrian massif of Kon-Thum and almost latitudinal folding belt which consists of Paleozoic, Triassic and Jurassic sedimentary series are cut by a large fault along the continental margin. One can suppose a prolongation of these tectonic structures as well as of the structures of South China into the west and northwest parts of South China sea embracing the Paracel islands, Pratas and Macelesfield banks. This area is evidently a ruptured, disintegrated continental block.

Another block of the same type, measuring $400 \times 1,000$ km, occupies the southern part of the sea. It is limited by the bathymetric contour 2,500 m and consists of the rises of the Spratley and Amboina islands and numerous banks and reefs to the west of the Palawan island and to the north of Borneo. Many of them have flat tops and steep slopes (MAMMERICKX *et al.*, 1976). The corresponding contours of both these blocks fit sufficiently if one assumes that latter one underwent a clockwise rotation by 20° and a drift in the southeast direction together with Luzon island during late Mesozoic and Cenozoic times.

Using the spherical models and geologic and paleomagnetic data I compiled a global reconstruction of all continents at the late Paleozoic-early Mesozoic times (KROPOTKIN, 1964, 1967, 1971b). A fit of continental slopes of the separated parts of Gondwanaland and Laurasia was reached by adjusting of the 2,000 m bathymetric contours. More detailed reconstructions of Atlantic (BULLARD *et al.*, 1965) and Australian-Antarctic (SPROLL and DIETZ, 1969) regions confirm the validity of this reconstruction. In my scheme in contrast to many global reconstructions (for example, BRIDEN *et al.*, 1974) account was already made of the removal of the Chinese craton and Japan to the east relative to the north part of Eurasia during Mesozoic and Cenozoic times (KROPOTKIN, 1971c). The tectonic structures of the Chukotsk peninsula and Alaska were not disrupted in this reconstruction. Their unity should be retained if one takes into account that the Verkhoyansk range geosyncline was considerably wider during the Mesozoic era than the recent folded belt which originated from this geosyncline.

In my global reconstruction (KROPOTKIN, 1964) the deep basin of the Tasman sea was covered by placing the Lord Haw submarine rise near the Australian continent, and the Campbell plateau-near Tasmania and the Antarctic continent. The fold belts of eastern Australia are cut off by the fault on the continental slope at an angle of 40° – 90° to their trend. One must look for their prolongation on the other side of the Tasman basin in the Lord Haw ridge, south extremity of New Zealand and the Campbell and Chatam plateaus (CAREY, 1958; GRIFFITHS, 1971; SUZYUMOV, 1977).

For the explanation of the origin of deep basins of the Japan sea, the sea of Okhotsk, the Bering, South China, Coral seas and Okinawa trough it is sufficient to suppose a drift of an island arc from the continent to the Pacific. But in the case of the Tasman sea basin an account should be made of the break of the adjacent continent and a displacement of its two parts, Australia and Antarctica.

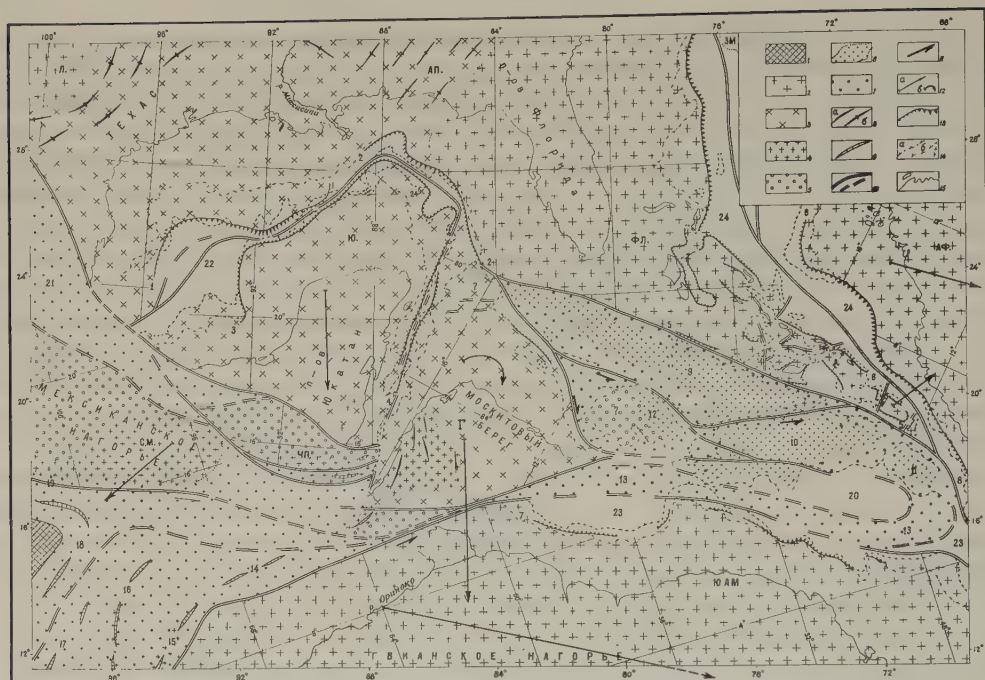


Fig. 2. Paleotectonic reconstruction of the area including the Gulf of Mexico, Central America and the Antilles (after KROPOTKIN and SHAKHVARSTOVA, 1965). A scheme illustrating supposed arrangement of the crustal blocks at the end of Paleozoic and beginning of Mesozoic era. 1, Pacific basin; 2, Precambrian cratons (a) North American craton (Л), (b) the parts of Gondwanaland (Florida platform, African and S. American platforms); 3, areas consolidated owing to the Upper Paleozoic and Early Mesozoic folding; 4, the outcrops and areas where the Precambrian and metamorphic Paleozoic rocks are at shallow depth (the blocks of Yucatan and Honduras massifs, the anticlinoria of the Late Mesozoic and Cenozoic folded belts); 5, the area of gently deformed Mesozoic and Paleogene sedimentary layers over the Paleozoic or Precambrian basement; 6, the crustal blocks of the Greater Antilles islands, further deformed (the recent coast line contours are plotted); 7, areas that similarly to the previous ones (6) became the parts of folded belts and island arcs at posterior times; 8, Paleozoic folding strike (a, established trend; b, supposed trend); 9, Paleozoic geanticlines being the nuclei of consolidation in the Mesozoic and Cenozoic folded belts; 10, main ruptures from which originated the rifts and transcurrent faults; 11, direction of the strike-slip displacement; 12, supposed direction of the displacement (a) and rotation (b) of the crustal blocks during the Mesozoic and Cenozoic areas. The movement relative to the North American platform is shown, the latter is conditionally considered as a stable block; 13, Abrupt and steep continental slopes of the platform recent surface; 14, recent bottom bathymetry contours following approximately along the margins of crustal blocks that have a continental type of structure (a, 1,000 m; b, 2,000 m); 15, contours of the recent coast lines. Letter symbols—The areas of Precambrian (partly Lower Paleozoic) consolidation: АФ, African platform; 3М, the Cape Verde islands block; Л, Llano bend (a part of North American Precambrian platform); ФЛ, Florida platform (including the blocks of Bahama islands and banks); ЮАМ, South American Platform. The areas of Late Paleozoic consolidation: АЛ, the Southern Appalachian belt and its prolongation; Г, the block including Honduras massif and Mosquito and Rosalinde banks; СМ, Southern Sierra Madre massif; ЧП, Chiapas massif; Ю, Yucatan block, including Campeche bank. Steep continental slope lines: 1-1, Sigsbee; 2-2, West Florida; 3-3, Campeche; 4-4, fault slopes that originated the Yucatan basin and Cayman trench; 5-5, the abrupt slopes and faults of the Bahama bank, Silver bank etc.; 6-6, 7-7, 8-8, the fault slopes bordered the primary main rift of Atlantic. Embryonal structure belts of recent tectonic units: 9, Cuba; 10, Haiti island; 11, Puerto-Rico; 12, Jamaica; 13, Lesser Antilles, Trinidad island and Eastern Coastal Cordilleras of Venezuela; 14, Coastal Cordillera of Venezuela; 15, Cordillera Merida; 16, Cordillera Perija; 17, Central Cordillera of Colombia; 18, Panama isthmus arc; 19, Guatemala trench; 20, middle part of Caribbean sea; 21, eastern Mexico; 22, middle part of the Gulf of Mexico; 23, 24, Atlantic ocean.

The rupture and the parting of the Paleozoic continental blocks in the direction roughly parallel to the margins of Circum-Pacific mobile belt was still more important in the case of formation of the basins of the Gulf of Mexico and the north and south parts of the Caribbean sea. A reconstruction of this area based on the analysis of geological structure and on the fit and adjusting of the continental slope contours was compiled for the early Mesozoic time (Fig. 2). The deep basins were formed here mainly by the removal of North America away from South America. This displacement was accompanied by a rupture and fragmentation of the plates consolidated by Paleozoic folding. The blocks of Chiapas, Yucatan, Honduras and other tectonic massifs were formed by this way. The Florida peninsula and Bahamas bank were a part of Precambrian Gondwanaland craton teared off western Africa. South and North Americas on Fig. 2 are drawn together to the extent required for the global reconstruction.

It may be concluded that the sea floor spreading resulting in the generation of marginal seas is not necessarily connected with a subduction of oceanic plates in adjacent areas (as it was supposed according to the Karig's model; KARIG, 1971). Figures 1 and 2 show the initial stages of two different types of the marginal sea formation.

The study of tectonic structures formed by the tension between the continent and island arcs may be useful for the oil prospecting in the grabens and depressions of shelf areas.

REFERENCES

- BERSENEV, I.I., The origin and development of the Japan sea basin, in *Voprosy Geologii dna Japonskogo Moria*'' (Geological Problems of the Bottom of the Japan Sea), pp. 15-35, 149, Academy of Sciences of the USSR, Vladivostok, 1973 (in Russian with English abstract).
- BRIDEN, J.C., G.E. DREWRY, and A.G. SMITH, Phanerozoic equal-area world maps. *J. Geol.*, **82**, 555-574, 1974.
- BUBNOFF, S., Die Tektonik Japans und der Bau des pazifischen Raumes von Ostasien, *Naturwissenschaften*, **30**, H. 38/39, 1942.
- BULLARD, E.C., J.E. EVERETT, and A.G. SMITH, The fit of the continents around the Atlantic. *Philos. Trans. R. Soc. Lond., Ser. A*, **258**, 41-51, 1965.
- CAREY, S.W., The tectonic approach to continental drift. in *Continental Drift (A symposium)*, pp. 177-355, Hobart, 1958.
- GRIFFITHS, J.R., Reconstruction of the south-west Pacific margin of Gondwanaland, *Nature*, **234**, 203-207, 1971.
- GURARIJ, G.Z., P.N. KROPOTKIN, M.A. PEVZNER, Su Von, Ro, and V.M. TRUBIHIN, Paleomagnetic study of the sedimentary rocks of North Korea, *Fizika Zemli (Physics of the Earth)*, No. 11, 128-135, 1966 (in Russian).
- HILDE, T.W.C. and J.M. WAGEMAN, Structure and origin of the Japan sea, in *The Western Pacific*, edited by P.J. Coleman, pp. 415-434. University of Western Australia Press, 1973.
- HURLEY, P.M., H.W. FAIRBAIRN, W.H. PINSON, and J.H. LEE, Middle Precambrian and older apparent age values in basement gneisses of South Korea, and relations with Southwest Japan, *Bull. Geol. Soc. Am.*, **84**, 2299-2304, 1973.
- ISEZAKI, N. and S. UYEDA, Geomagnetic anomaly pattern of the Japan sea, *Mar. Geophys. Res.*, **2**, 51-59, 1973.
- KARIG, D.E., Origin and development of marginal basins in the Western Pacific, *J. Geophys. Res.*, **76**, 2542-2561, 1971.
- KARP, B.Y., E.A. MOURAVOVA, J.V. SHEVALDIN, and V.P. FILATIEV, New data concerning the structure of the earth's crust of SW part of the Japan sea, in *Voprosy geologii i geofiziki okrainnykh morej severo-zapadnoj chasti Tihogo okeana (The Problems of Geology and Geophysics of the Marginal Seas of North-western Part of the Pacific Ocean)*, pp. 145-154, Academy of Sciences of the USSR, Vladivostok, 1974 (in Russian with English abstract).
- KAWAI, N., K. HIROOKA, and T. NAKAJIMA, Paleomagnetic and potassium-argon age informations supporting Cretaceous-Tertiary hypothetic bend of the main island Japan. *Paleogeogr. Palaeoclimatol. Palaeoecol.*, **6**, 277-282, 1969.
- KIENZLE, J. and L.R. SCHARON, Paleomagnetic comparison of Cretaceous rocks from South Korea and late Paleozoic and Mesozoic rocks of Japan, *J. Geomag. Geoelectr.*, **18**, 413-416, 1966.

- KOBAYASHI, T., The Sakawa orogenic cycle and its bearing on the origin of Japanese islands, *J. Fac. Sci., Imp. Univ. Tokyo*, Sec. 2, 5, Part 7, 219–508, 1941.
- KOVYLIN, V.M. and P.A. STROEV, About the origin of the Japan Sea basin (from geophysical data), in *International Geological Congress, XXV Session, Reports of Soviet Geologists. Paleontology, Marine Geology*, pp. 270–276, Nauka, Moscow, 1976 (in Russian with English abstracts).
- KRASNYJ, M.L., V.I. MIKHAILOV, and A.A. KULIKOV, Geological structure of the Akademia Nauk SSSR upland (The Sea of Okhotsk), *Doklady Akad. Nauk SSSR*, **225**, 1389–1392, 1975 (in Russian).
- KROPOTKIN, P.N., Relations between surface and deep structure and a general characteristics of crustal movements, in *Stroenie i razvitie zemnoj kory (Structure and Evolution of the Crust)*, pp. 72–96, Nauka, Moscow, 1964 (in Russian).
- KROPOTKIN, P.N., Mechanism of the Earth's crust movements, *Geotektonika*, No. 5, 25–40, 1967 (in Russian with English abstract).
- KROPOTKIN, P.N., On the age and origin of oceans, in “*Istorija mirovogo okeana*” (*The History of the World Ocean. Geological Structure, Origin, Development*), pp. 46–51, Nauka, Moscow, 1971a (in Russian with English abstract).
- KROPOTKIN, P.N., Paleomagnetism and structure of Eurasia, in *Gondwana System (A symposium)*, Ann. Geol., Departm., Aligarh Muslim Univ., Vol. 5–6, pp. 75–87, Aligarh (India), 1971b.
- KROPOTKIN, P.N., Eurasia as a composite continent, *Tectonophysics*, **12**, 261–266, 1971c.
- KROPOTKIN, P.N., Character of the tectonic processes of the island arcs of the Far East, in *Zemnaja kora ostrovnih dug i dalnevostochnyh morej (The Earth Crust of the Island Arcs and Far East Seas)*, pp. 51–68, Nauka, Moscow, 1972 (in Russian with English abstract).
- KROPOTKIN, P.N. and Ro Su Von, Tectonics of the North-Eastern Korea and South-Western part of the Maritime province, in *Geologicheskoe stroenie severo-vostochnoj Korei i juga Primoria (The Geological Structure of NE Korea and South Part of the Maritime Province)*, pp. 262–298, Nauka, Moscow, 1966.
- KROPOTKIN, P.N. and K.A. SHAKHVARSTOVA, *Geological Structure of the Circum-Pacific Mobile Belt*, pp. 1–368, Nauka, Moscow, 1965 (in Russian with English Contents).
- LELIKOV, E.P., I.I. BERSENEV, Ju. I. BERSENEV, Ju. S. LIPKIN, I.K. PUSHCHIN, E.P. TEREHOV, and V.P. FILATIEV, On the discovery of Early Proterozoic rocks in South-West part of the Japan sea, in *Geologija okrainnyh morej Tihogo okeana (Geology of the Pacific Marginal Seas)*, Trans. Pac. Oceanolog. Inst. Acad. Sci. U.S.S.R., Vol. 7, pp. 15–19, Vladivostok, 1975 (in Russian).
- MAMMERICKX, J., R.L. FISHER, F.J. EMMEL, and S.M. SMITH, Bathymetry of the East and Southeast Asian seas, Scripps Inst. Oceanogr., 1976.
- MELANHOLINA, E.N. and V.M. KOVYLIN, Tectonic structure of the Sea of Japan, *Geotektonika*, No. 4, pp. 72–87, 1976 (in Russian).
- MURAUCHI, S. and T. ASANUMA, Geological studies of the area off San, in district in the Japan sea by means of seismic profiler, *Bull. Natl. Sci. Mus. (Tokyo)*, **13**, 83–90, 1970 (in Japanese with English abstract).
- PAC. OCEANOL. INST. ACAD. SCI. U.S.S.R., *Geofizicheskie issledovaniya v Japonskom more (Geophysical Research in the Japan Sea) (A Symposium)*, pp. 1–72, Vladivostok, 1972 (in Russian).
- PAC. OCEANOL. INST. ACAD. SCI. U.S.S.R., *Geologicheskie issledovaniya v Okrainnyh moriah severo-zapadnoj chasti Tihogo okeana (Geological Research in the Marginal Seas of NW Pacific) (A Symposium)*, pp. 1–171, Vladivostok, 1977 (in Russian).
- SHEVALDIN, Y.V., Magnetic research of the central part of the Japan sea, in *Voprosy geologii i geofiziki okrainnyh morej severo-zapadnoj chasti Tihogo okeana (The Problems of Geology and Geophysics of the Marginal seas of Northwestern Part of the Pacific Ocean)*, pp. 168–174, Academy of Sciences of the USSR, Vladivostok, 1974 (in Russian with English abstract).
- SHIBATA, K. and M. ADACHI, Rb-Sr whole rock ages of Precambrian metamorphic rocks in the Kamiaso conglomerate from central Japan, *Earth Planet. Sci. Lett.*, **21**, 277–287, 1974.
- SPROLL, W.P. and R.S. DIETZ, Morphological continental drift fit of Australia and Antarctica, *Nature*, **222**, 345–348, 1969.
- SUZUMOV, A.E., *The Floor Structure of the South-West Pacific Seas*, pp. 1–76, Nauka, Moscow, 1977 (in Russian with English abstract).
- TULINA, Yu. V., Yu. A. TRESKOVA, S.K. BICKENINA, N.A. NIKONOVA, E.A. STARSHINOVA, E.G. ZHILTSOV, V.I. MIRONOVA, S.M. ZVEREV, I.N. GALKIN, and N.M. MIKHAILOVA, Earth's crust structure of some parts of Japan sea and Tartar strait according to DSS data in *Morskaja geologija i geofizika (Marine Geology and Geophysics)*, Vol. 1, pp. 115–122, Zinatne, Riga, 1970 (in Russian with English abstract).
- UDINTSEV, G.B., A.F. BERESNEV, A.A. GEODEKIAN, Ye. G. MIRLIN, L.A. SAVOSTIN, A.A. SHREIDER, B.V. BARANOV, and A.V. BELIAEV, Preliminary data of the geological-geophysical researches in the Sea of Okhotsk and in the north-eastern part of the Pacific Ocean made by the e/v “Vityaz,” in *Geologo-geofizicheskie issledovaniya zony perekhoda ot Aziatskogo kontinenta k Tihomu okeanu (Geological-geophysical Researches of the Transition Zone from the Asiatic Continent to the Pacific Ocean)*, pp. 19–29, Sovetskoye Radio, Moscow, 1976 (in Russian and English abstract).

- UENO, N., I. KANEOKA, and M. OZIMA, Isotopic ages and strontium isotopic ratios of submarine rocks in the Japan sea, *Geochem. J. (Geochem. Soc. Jpn.)*, **8**, 157-164, 1974.
- VASILYEV, B.I. and P.V. MARKEVICH, On the geological structure of the Yamato bank (the sea of Japan), in *Voprosy geologii dna Japonskogo moria (Geological Problems of the Bottom of the Japan Sea)*, pp. 58-65, 149-150, Academy of Sciences of the USSR, Vladivostok, 1973 (in Russian with English abstract).
- YASKAWA, K., Palaeolatitude and relative position of South-West Japan and Korea in the Cretaceous, *Geophys. J. R. Astr. Soc.*, **43**, 835-846, 1975.

MAJOR STRIKE-SLIP FAULTS AND THEIR BEARING ON SPREADING IN THE JAPAN SEA

Kenshiro OTSUKI and Masayuki EHIRO

Institute of Geology and Paleontology, Tohoku University, Sendai, Japan

(Received May 31, 1978; Revised September 13, 1978)

The authors emphasize the important role of the large scale strike-slip faults in the tectonic history of the circum-Japan Sea region including the origin of the Japan Sea Basins. NE-SW to NNE-SSW trending faults in the region were formed by the intense compression from the south which corresponds to the "pulse" suggested by LARSON and PITMAN (1972). NS to NNW-SSE trending faults in Northeast Japan were formed one after another from east to west by the left-lateral simple shear force induced by the subduction of the peculiar transform fault between the Kula and Tethys plates. Subduction of the seamount chain on the peculiar transform fault formed NW-SE trending faults and the cusp structure in the Kanto region. The subduction of the Kula-Pacific and Tethys ridges produced the acidic igneous activities of the Cretaceous to Paleogene in the Asiatic continental margin. Japan Sea Basins were formed in the Paleogene time by the southward drift of the western part of Japan bounded on the east by the Tanakura shear zone and on the west by the Tsushima fault, both of which had already been formed as left-lateral faults in the Cretaceous time.

1. Introduction

The Japan Sea is one of the typical marginal seas which are intimately related to the island arc and deep sea trench system. It is divided into the Japan Basin, the Yamato Basin, and the Tsushima Basin by the Oki Bank-Yamato Ridge and the Korean Plateau. The Japan Basin has water depths of 3,000 to 3,700 m, Yamato Basin and Tsushima Basin have depths of 2,000 to 2,500 m. The sediment cover on the acoustic basement attains 2.25 km in thickness in the Japan Basin and 1.5 km in the Yamato Basin (HILDE and WAGEMAN, 1973; LUDWIG *et al.*, 1975). The geological age of the sediments ranges probably from the Miocene to Holocene (KARIG *et al.*, 1975). The crust in the Japan Basin is typically oceanic (KOVYLIN and NEPROCHNOV, 1965; MURAUCHI, 1966; VASILKOVSKY *et al.*, 1971; LUDWIG *et al.*, 1975). Also in the Yamato Basin, there is oceanic crust with a layer of 3.5 km/sec material possibly comprising of green tuff. KARIG (1971b) classified the Japan Sea as an inactive marginal basin with high heat flow.

Various opinions have been offered on the origin of the Japan Sea. According to BELOUSSOV and RUDITCH (1961), MINATO *et al.* (1965), BELOUSSOV (1968), and MINATO and HUNAHASHI (1970), the Japan Sea bottom is a former landmass that has subsided to the present depth by crustal foundering or by oceanization. VASILKOVSKY *et al.* (1971) considered that the sea represents a permanent ocean basin. However, a widespread hypothesis regarding this problem is that the Japan Sea is a by-product of the southward drift of the Japanese Islands from the Asiatic continent (MURAUCHI, 1966, 1971; HASEBE *et al.*, 1970; MATSUDA and UYEDA, 1971; HORIKOSHI, 1972; HURLEY *et al.*, 1973; HILDE and WAGEMAN, 1973). UYEDA and MIYASHIRO (1974) have proposed that the Japan Sea

opened up during Cretaceous to Oligocene as a result of collision and subduction of the hypothetical Kula-Pacific ridge. MELANKHOLINA and KOVYLIN (1976) considered by the geological data of land and the Japan Sea bottom that the Japan Sea was formed in the Paleogene.

In this paper, the authors attempt to clarify the evolutionary history of the Japan Sea and its surrounding area with special attention focused on the major strike-slip faults in the circum-Japan Sea region. Plate motions in the western Pacific will be discussed on the basis of the land-based geological data.

2. Major Strike-Slip Faults in the Circum-Japan Sea Region

Recently, many major strike-slip faults have been studied in the Japanese Islands, Korean Peninsula, and Sikhote-Alin Range. The authors consider that they played an important role in the Cretaceous tectonic movements in the region, and also in the southward drift of the Japanese Islands. These faults are classified into three groups by their trends; NS to NNW-SSE, NE-SW to NNE-SSW and NW-SE. Distribution and some characteristics of these faults are shown in Fig. 1 and Fig. 2. Fault name will be often written in the form of "F-fault number" for short.

2.1 NS to NNW-SSE trending faults

2.1.1 Hizume-Kesennuma fault and other faults in the Kitakami belt, Northeast Honshu

EHIRO (1977) studied the NNW-SSE trending faults in the Kitakami belt, especially the Hizume-Kesennuma fault (F-3) in detail and concluded that F-3 is a left-lateral fault with a displacement of about 30 km on the basis of the offset of the Permian formations and of the synclinal structure of the Jurassic and Lower Cretaceous formations.

The left-lateral displacements of the Hitokabe-Iriya fault (F-4) and the Tono-Takada fault (F-2) were estimated to be 5 to 10 km and about 10 km, respectively, judging from the distribution of the Jurassic, Triassic and Permian formations. The Tsuchibuchi-Sakari fault (F-1) was assumed to have a left-lateral displacement of about 20 km from the distribution of the Lower Cretaceous volcanoclastics. The left-lateral displacement of these faults amounts to 70 to 80 km in all. These faults were formed during the period of the Barremian to Early Aptian Oshima Orogenic Movement (KOBAYASHI, 1941).

2.1.2 Futaba and Hatakawa shear zones

To the west of the Kitakami belt, there is the Abukuma belt which is bounded on the west by the Tanakura shear zone (F-10), and on the east by the Futaba and Hatakawa shear zone (F-6, F-7) trending in NS direction. Along F-6 and F-7, granitic mylonites are observed within the width of several hundreds meters or more. The mylonitic foliations trend in NNE-SSW obliquely to the general trend of the shear zones, and have a tendency of becoming parallel to the trend of the shear zones in the more intensely mylonitized parts. Such deformational configuration of mylonites indicates that the displacement along the shear zones is left-lateral in sense (RAMSAY and GRAHAM, 1970). KITAMURA (1963, 1976) studied the northern extension of these shear zones and named it Nyunai-Yakeishidake tectonic line. The pre-Tertiary granitic rocks cropping out to the south of Mt. Yakeishi reported by KITAMURA and KANISAWA (1971) is highly mylonitized, and the deformation features indicate the left-lateral shearing with a NNW-SSE trend.

There is no visible indication of the displacement along F-6 and F-7, but it is possible to estimate the displacement along them to be about 80 and 20 km, respectively, based on

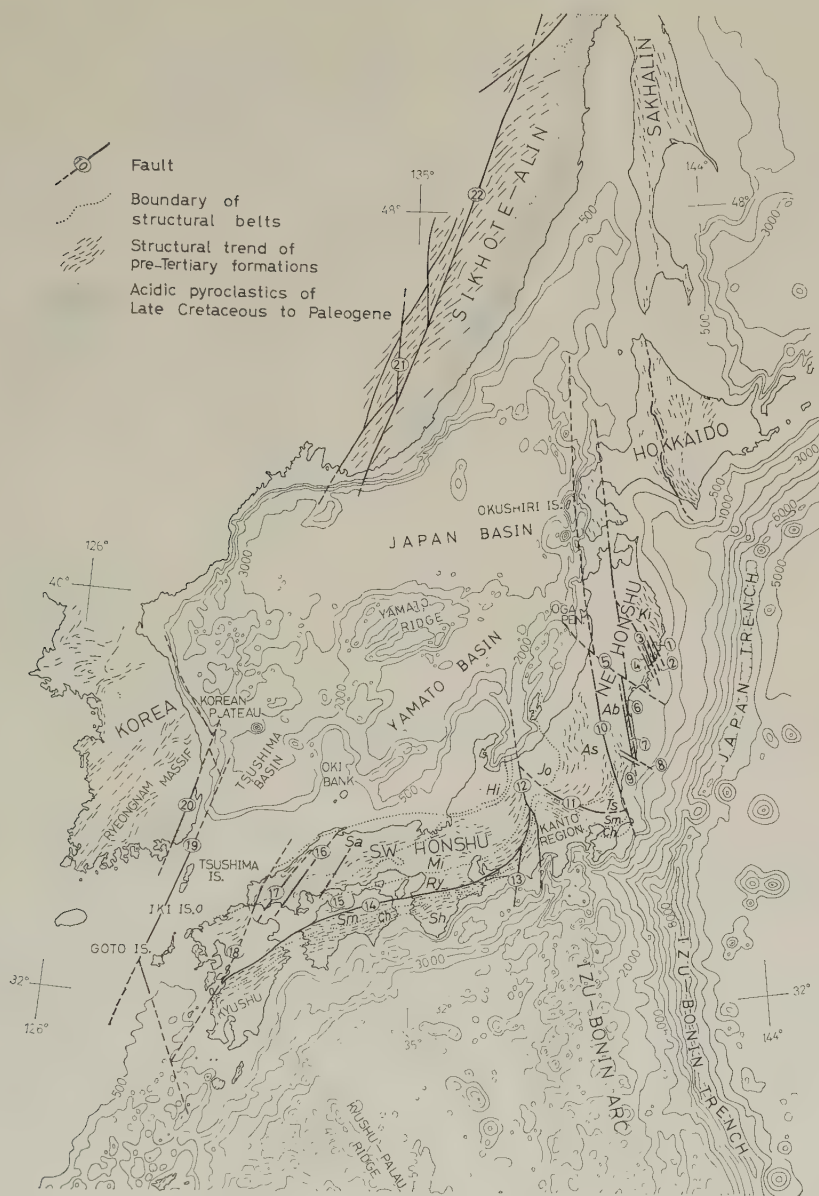


Fig. 1. Structural and physiographic map of the Japanese Islands and the adjacent regions. 1, Tsuchibuchi-Sakari fault; 2, Tono-Takada fault; 3, Hizume-Kesennuma fault; 4, Hitokabe-Iriya fault; 5, Chokai-Ishinomaki tectonic line; 6, Futaba shear zone; 7, Hatakawa shear zone; 8, Futatsuya fault; 9, Yunotake fault; 10, Tanakura shear zone; 11, Kwanto tectonic line; 12, Itoigawa-Shizuoka tectonic line; 13, Akaishi tectonic line; 14, Median tectonic line; 15, C fault; 16, B fault; 17, A fault; 18, Nagato tectonic line; 19, Tsushima fault; 20, Yangsan fault; 21, Fudzino-Iman fault; 22, Central Sikhote-Alin fault. Ki, Kitakami belt; Ab, Abukuma belt; Jo, Joetsu belt; As, Ashio belt; Ts, Tsukuba belt; Hi, Hida belt; Sa, Sangun and Hida marginal structural belts; Mi, Mino and Tanba belts; Ry, Ryoke belt; Sm, Sambagawa belt; Ch, Chichibu belt; Sh, Shimanto belt.

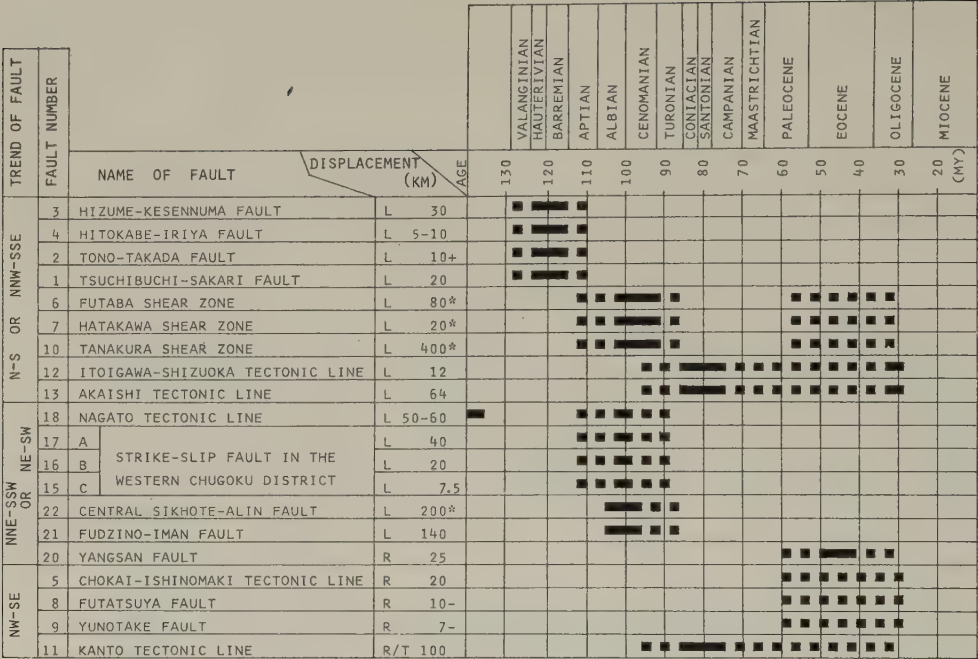


Fig. 2. Displacement and period of activity of the strike-slip faults. R, right-lateral; L, left-lateral. Asterisk denotes the displacement estimated by the relation between the width of shear zone and displacement along fault established by OTSUKI (1978).

the relationship between the width of shear zone and displacement along fault established by OTSUKI (1978).

F-6 and F-7 influenced the Cretaceous granitic rock province (WATANABE *et al.*, 1953, 1955; ONO *et al.*, 1953). K-Ar ages of the Cretaceous granitic rocks in the Kitakami belt range from 110 to 120 my which are about 20 my older than those in the Abukuma belt (KAWANO and UEDA, 1965, 1966a, b, 1967; NOZAWA, 1970, 1975). Most of granitic mylonites along the shear zones show the protoclastic texture, and K-Ar age of 91 my was obtained from one of them (KAWANO and UEDA, 1966a). Moreover, these mylonites suffered brittle shearing after cooling. Accordingly, two stages are distinguished in the activity of the shear zones; in the Middle Cretaceous time and later period.

2.1.3 Tanakura shear zone

The Tanakura shear zone (F-10) is a remarkable tectonic line with a mylonitic and cataclastic shear zone of 2 to 3 km in width. The Paleozoic and Mesozoic tectonic belts (Ashio, Tsukuba and Sambagawa belts) to the west of F-10 are abruptly terminated by this shear zone and cannot be traced further east. Besides, F-10 influenced the provinces of the Cretaceous to Paleogene igneous activities. Namely, the Cretaceous granites in the Abukuma belt are 90 to 100 my in age, and those in the Ashio and Tsukuba belts are younger than the formers by about 25 my (KAWANO and UEDA, 1966a, b, 1967; NOZAWA, 1970, 1975). The Late Cretaceous to Paleogene acidic volcanism occurred intensely in the inner zone of Southwest Japan and the Ashio belt, but it cannot be traced to the east beyond F-10 (TAKAHAMA, 1972; YANAI *et al.*, 1973; OGUCHI *et al.*, 1973). Many geo-

logists (ISHIHARA, 1973; KANAYA and ISHIHARA, 1973; KIKUCHI, 1974; TSUSUE and ISHIHARA, 1974; KANISAWA, 1975; ISHIHARA and TERASHIMA, 1977) clarified that there are remarkable differences in the chemical and mineral composition of the granitic rocks, as well as in the nature of the ores accompanied by the granitic rocks, between the areas on the west and east of F-10.

OTSUKI (1975) concluded that F-10 is a large-scale left-lateral fault on the basis of the pattern of faults in the shear zone. Though no direct indication is observed, the displacement along the shear zone is estimated to be about 400 km from the width of shear zone-displacement relation (OTSUKI, 1978). There is no definite indication of climax of movement in the shear zone, but authors infer that it was reached in the Middle Cretaceous and Paleogene from the fact that F-10 influenced the province of the igneous activities during this period. Two stages are distinguished in the activities of the leftlateral fault movement. In the first stage the mylonitic rocks were formed, and in the second stage they were sheared into fault breccia and clay. Since Miocene, only the vertical and small scale right-lateral movements have occurred along the shear zone.

The northern extension of F-10 has been discussed by many geologists. But the thick Neogene covers prevent them from exact recognition. The authors stand to the opinion of KITAMURA (1963), OGUCHI *et al.* (1973), and YOSHIDA *et al.* (1976) that the northern extension of F-10, not only in the Miocene but also in the Paleogene and Cretaceous, can be traced along the Sagaegawa fault or Oisawa fault, Tachiyazawa fault and to the base of Oga Peninsula. Further extension to the north is traced across the lower reaches of Irakawa River on the Japan Sea coast of Aomori Prefecture, where intensely mylonitized granitic rocks are observed in the Shirakami-dake granitic body (KATADA and OZAWA, 1964; KANO *et al.*, 1966; FUJIMOTO, 1976). The deformation feature of the mylonites indicates left-lateral shear trending in NNW-SSE direction. K-Ar ages of the granitic mylonites are 63 and 93 my (KAWANO and UEDA, 1966b). Further north extension of F-10 is considered to be along the Okushiri Ridge with NS trend which forms the boundary between the Japan Basin and the continental borderland of Northeast Japan, and pass through the eastern side of Okushiri Island to the "Sikhote-Alinsky swell" of ZVEREV and TULINA (1973).

2.1.4 Akaishi and Itoigawa-Shizuoka tectonic lines

Itoigawa-Shizuoka tectonic line (F-12) is a western boundary fault of the Fossa Magna region. It trends roughly in NS, and has about 12 km left-lateral displacement (KAWACHI *et al.*, 1966). The Akaishi tectonic line (F-13) is a left-lateral fault with displacement of about 64 km and its lateral movement occurred within the period between the Cretaceous and Paleogene times (KIMURA, 1959; MATSUSHIMA, 1973). KIMURA (1966) considered that the incipience of F-12 was at nearly same time as the left-lateral fault movement along F-13.

2.2 NE-SW to NNE-SSW trending faults

NE-SW to NNE-SSW trending faults are developed in Southwest Japan, Korean Peninsula, eastern China and Sikhote-Alin Range.

2.2.1 Central Sikhote-Alin fault and Fudzino-Iman fault

In the Sikhote-Alin region, there are major left-lateral faults with NNE-SSW trend, such as the Fudzino-Iman fault (F-21) and the Central Sikhote-Alin fault (F-22). The former has displacement of 120 to 140 km (BERSENEV, 1971). The width of the Central Sikhote-Alin fault is measured about 2 km on the ERTS images. The displacement along

the fault is estimated to be about 200 km on the basis of the width of shear zone-displacement relation (OTSUKI, 1978). BERSENEV (1971) considered them to have been formed in the Late Turonian to Early Senonian; ABLAEV *et al.* (1972), in the Late Albion; MELANKHOLINA and KOVYLIN (1976), in the Middle Senonian to Late Cretaceous.

2.2.2 *Nagato tectonic line and other faults*

In the Chugoku and Kyushu districts, Southwest Japan, there develop NE-SW trending faults. The Nagato tectonic line (F-18) (MATSUMOTO, 1949) is the largest fault among them. NUREKI (1972) hypothetically proposed that the tectonic line left-laterally shifted the southern boundary of the Sangun metamorphic belt by 50 to 60 km. NUREKI (1969) also suggested that three same trending faults (A, B, and C faults; F-17, 16, 15) associated with F-18 have left-lateral displacement of 40, 20, and 7.5 km respectively.

The incipient movement of F-18 was thought to be pre-Jurassic (MURAKAMI, 1971), but it was active also in the Late Jurassic to Early Cretaceous (MATSUMOTO, 1949; SUZUKI, 1971). The appearance of F-15-17 may be in the Middle Cretaceous time judging from their relation to the Ryoke metamorphism and the Cretaceous igneous activity in this region (OKAMURA and KOJIMA, 1951; OKAMURA, 1963; NISHIMURA and NUREKI, 1966; NUREKI, 1966).

2.2.3 *Yangsan fault and Tsushima fault*

The Yangsan fault (F-20) (REEDMAN and UM, 1975) with NNE-SSW trend is located in the southeastern part of the Korean Peninsula associated with other sub-parallel faults (SON *et al.*, 1968). It right-laterally dislocated the Late Cretaceous granitic bodies and the boundary between the Silla Group and the Early to Middle Cretaceous volcanic rocks by 25 km. SON *et al.* (1968) concluded that F-20 originated soon after the consolidation of the Eonyang granite with K-A age of 72 my (LEE and UEDA, 1976) and ended its activity before the deposition of the Miocene formations. It seems to have been active as a normal fault since Miocene. It should be noted that F-20 is a right-lateral fault in spite of its same trend as the left-lateral fault of F-22, and its activity is younger than the other faults trending NNE-SSW to NE-SW. Many faults parallel with F-20 are recognized in the Korean Peninsula by ERTS images. They seem to have similar history as F-20.

Another major fault parallel to F-20 is known along the eastern wall of the Tsushima trough, named "Tsushima fault" (F-19) (MURAUCHI and ASANUMA, 1969). The southern extension of the fault was detected west off Goto Islands (INOUE, 1975). Furthermore, F-19 might extend southward along the Taiwan-Sinzi folded zone (EMERY and NIINO, 1968; EMERY *et al.*, 1969) which was considered to be originated during the Paleogene and Miocene. The authors consider that F-19 and F-18 are the southern extension of F-22, and that F-19 was reactivated in the later period as a right-lateral fault.

2.3 *NW-SE trending faults and the cusp structure in the Kanto region*

In Northeast Honshu, several faults trending NW-SE are developed. They are considered to have originated in the pre-Miocene time. The Chokai-Ishinomaki tectonic line (F-5) is an important fault among them. This tectonic line shifted the northern extension of F-6 and F-7 right-laterally by about 20 km (KITAMURA, 1976).

In the southeastern part of Northeast Honshu, Futatsuya fault (F-8) and Yunotake fault (F-9) are developed. They are assumed to be right-lateral faults which offset F-7 (IWAO and MATSUI, 1961). Accordingly, aforementioned faults are considered to have originated later than the NS trending faults and before the Miocene.

The most important fault of these is the Kanto tectonic line (F-11) (KOBAYASHI,

1941). Structural belts trending in EW direction in Southwest Japan are bent northward in the area to the west of F-12. The equivalents of these structural belts can be recognized also in the Kanto region to the east of F-12 (ISOMI and KAWATA, 1968; YAMASHITA and FUJITA, 1973). In the Kanto region, the structural belts are convex northward. On the other hand, they are convex southward in the area between F-10 and F-11 as shown in Fig. 1. F-11 forms boundary between the northeastern wing of the northward convex structure and the southwestern wing of the southward convex structure. This tectonic line has been considered to represent a large scale right-lateral fault (KOBAYASHI, 1941) and the displacement was estimated to be about 100 km (ISOMI and KAWATA, 1968).

On the basis of the structural analysis on the Sambagawa and Ryoke belts, HARA *et al.* (1977) concluded that the northward convex and bent structures were formed by the northward differential compression which was powerful particularly in the Kanto region. The authors consider that the origin of the southward convex structure is intimately related to a drag resulted from the large scale left-lateral displacement along F-10. It is a difficult problem to date the development of the bent and convex structures. As mentioned already, the left-lateral displacement along F-13 and probably also F-12 occurred in the Middle Cretaceous and Paleogene. Kashio mylonites, which are observed along the Median tectonic line (F-14) in the area of the bent structure, were considered to have been formed contemporaneously with the development of the northward bent and convex structures in the intimate relations to the left-lateral movement along F-13 (HAYAMA and YAMADA, 1973). Lead-alpha ages of the Kashio mylonites are 80 to 100 my (KARAKIDA *et al.*, 1965). The Cretaceous to Paleogene granitic rocks in the inner zone of Southwest Honshu are divided into two groups, younger granites (40 to 75 my) and older granites (75 to 100 my). The former is distributed in the northern area and the latter in the southern area (NOZAWA, 1970, 1975; TERAOKA, 1977). The older granitic bodies appear to take a part of the northward bent structure, but the younger granitic bodies not to be influenced by the bent deformation. Accordingly, the authors consider that the northward bent structure was almost completed during the period from 100 to 75 my.

The Shimonita tectonic line, a part of F-11 (ISHII, 1962), was originated probably during the Heterian (Late Campanian to Maastrichtian) and Paleogene (ARAI *et al.*, 1966). In the area to the northeast of F-11, the structural trends of the Jurassic and Lower Cretaceous Formations are involved in the southward convex structure (SUDO, 1976). The Hauterivian to Turonian formations in the Sanchu graben take a part of the northward convex structure (TAKEI, 1963; SAKA and KOIZUMI, 1977). On the other hand, the geologic structure of the pyroclastics of the Latest Cretaceous Chuzenji acidic rocks (60 to 70 my) appears to be independent of the southward convex structure (YANAI, 1972). Therefore, the authors consider that most part of the bent and convex structures was formed during the Middle and Late Cretaceous, probably in the period from 75 to 100 my, and exaggerated in the later period.

3. Age of the Japan Sea Basins: A Synthesis

Many geologists and geophysicists have discussed about the problem of the origin of the Japan Sea Basins. The authors have compiled available information concerning the problem.

i) The provenance of the arkose sandstones of the Triassic, Berriasian to Valanginian, and Hauterivian to Early Albian formations in the Sikhote-Alin region was thought to

be within the present Japan Sea area where some landmass existed during that time (BERSENEV, 1971).

ii) As mentioned already, it is considered by Russian geologists that the terminal folding in Sikhote-Alin occurred during Middle to Late Cretaceous. Corresponding tectonic movements, the post-Kanmon movements, occurred in the inner zone of Southwest Japan during the Cenomanian (ICHIKAWA *et al.*, 1968). At the same time, NE-SW to NNE-SSW trending left-lateral faults were active in the Sikhote-Alin region and Southwest Japan. This geological evidence shows that strong NS compression governed all over the circum-Japan Sea region.

iii) F-20, along which the Eonyang granite body of 72 my in age was right-laterally shifted, should be taken into consideration in studying the southward drift of Japan.

iv) Acidic volcano-plutonic activity of the Cretaceous to Paleogene age occurred in Sikhote-Alin, the Korean Peninsula, and the inner zone of Southwest Japan. The acidic volcanism continued from 100 to 50 my and peaked at about 90 my or later in Southwest Japan (ICHIKAWA *et al.*, 1968; SUDO, 1977), whereas in Sikhote-Alin, it continued from 80 to 30 my, and peaked at about 60 my (BASKINA and VOLCHANSKAYA, 1972). Acidic plutonism continued from 100 to 40 my and peaked at about 90 and 70 my in Southwest Japan (NOZAWA, 1970, 1975), whereas in Sikhote-Alin it continued from 80 to 50 my and peaked at about 60 my (BASKINA and VOLCHANSKAYA, 1972).

Acidic volcanic rocks which are similar to those in Sikhote-Alin and Southwest Japan were dredged from the Yamato Ridge and some other banks in Japan Sea (SATO and ONO, 1964; HOSHINO and Honma, 1966; IWABUCHI and MOGI, 1973). A huge amount of acidic volcano-plutonic products as those of the Cretaceous and Paleogene in the circum Japan Sea region may require the existence of a thick continental crust. Moreover, marginal structures of the Japan Sea Basins truncate the province of the volcano-plutonic activities as pointed by MELANKHOLINA and KOVYLIN (1976).

Above-mentioned geologic facts from i) to iv) suggest that the Japan Sea Basins originated after the intense igneous activities, namely, after 60 or 50 my.

v) BELYAYEVSKIY and RODNIKOV (1972) pointed out that a 4.8 km/sec layer of about 2 km thick in the Japan Basin and a 3.3 to 4.2 km/sec layer of 3 to 4 km thick in the Tsushima Basin are correlative with the Paleogene and Cretaceous sediments in the Tatar Strait. In the Japan Sea Basins, LUDWIG *et al.* (1975) observed the 3.5 km/sec layer and layer-2 (3.5 to 6.4 km/sec) beneath the Miocene pelagic sediments, and considered that the former represents a wide range of consolidated sediments and volcanics and the latter may be the result of discrete layering with either one-, two-, or three-component layer. These observations indicate that the existence of the pre-Miocene sediments in the Japan Sea Basins is quite probable.

vi) In the northern part of Kyushu, Japan, the Eocene to Oligocene sediments are mainly of non-marine and partly of marine origin. In the Eocene and Oligocene Taishu Group of Tsushima Islands and Katsumoto Group of Iki Island, northward paleocurrents were detected (NAGAHAMA *et al.*, 1966; NAGAHAMA, 1967). The paleocurrent data indicate that there existed already a large sedimentary basin approximately in the same position as the present Tsushima Basin during the Eocene to Oligocene.

vii) VASIL'EV and MARKEVICH (1973) dredged sedimentary rocks with plant fragments from the Yamato Ridge, which were considered to be correlative with the Paleocene to Oligocene sediments of south Sikhote-Alin. From the same area, they also dredged basalts of 22 to 46 my in K-Ar age. The former is significant for interpretation of the

information mentioned in v) and vi). The latter is also an important evidence because the obtained ages are considerably older than those previously known from the Japan Sea floor (UENO *et al.*, 1971) and of the lower Miocene volcanic rocks in the "Green Tuff Region."

The data mentioned in v), vi) and vii) suggest that the sedimentary basins were already formed in the Japan Sea region in Eocene and probably in Paleocene.

viii) In the Japan Basin, undeformed sediments, probably of the Miocene to Holocene (KARIG *et al.*, 1975), cover the acoustic basement with rough topography. LUDWIG *et al.* (1975) concluded from seismic reflection studies that the Japan Sea might have existed essentially in its present form prior to the beginning of the "Green Tuff movement" in the Miocene.

Summerizing all of information mentioned above, there is a strong suggestion that the Japan Sea Basins formed during Paleogene, probably 60 or 50 my to 30 my, and only subsidence predominantly occurred thereafter.

4. Major Strike-Slip Faults, and Their Role on the Drifting of Japanese Islands from the Asiatic Continent

Most popular hypothesis on the origin of the Japan Sea is that the Japan Sea is a by-product of the southward drift of the Japanese Islands relative to the Asiatic continent. Regarding the southward drift of Japan, many investigators seem to agree with anti-clockwise rotation of Northeast Honshu, which occurred from 121 to 114 and from 100 to 92 my, proposed by KAWAI *et al.* (1961, 1969, 1971) on the basis of the paleomagnetic measurements of the Cretaceous granites. However, as already mentioned, the Japan Sea Basins might have formed during the Paleogene and not in the Cretaceous. Also, ENE-WSW trending magnetic lineations and hypothetical spreading centers which are sub-parallel to the structural trend of Southwest Japan have been mapped in the Japan Sea Basins (ISEZAKI and UYEDA, 1973; ISEZAKI, 1975). This evidence seems to be inconsistent with the anti-clockwise rotation, which should be accompanied by fan-shaped magnetic lineations. On the contrary, the magnetic lineation pattern suggests that the western part of Japan has drifted southward without any remarkable rotation of Northeast Honshu. The paleomagnetic data by Kawai and others are in need of re-examination in light of the recent knowledge on block tilting (ITO and TOKIEDA, 1974, 1977) and horizontal rotation of granitic bodies after cooling by the left-lateral faults in Northeast Honshu mentioned in Section 2.

The present authors pay attention to crustal condition of the circum-Japan Sea region at the time just before the formation of the Japan Sea, where many weak planes had been formed in the crust by the Cretaceous fault movements mentioned in Section 2. Regarding the southward drifting of the Japanese Islands, F-10 and F-19 are most important weak planes. The former had already originated in the Cretaceous time as a left-lateral fault and was reactivated as a left-lateral fault before Miocene. The latter might have originated in Cretaceous as a southern extension of F-22 and was reactivated as a large-scale right-lateral fault in the Paleogene time accompanied by the origination of F-20. The reactivation of these faults is nearly same time as the origination of the Japan Sea Basins. Therefore, it is reasonably concluded that the western part of the Japanese Islands has drifted southward, being bounded on the east mainly by the left-lateral fault of F-10 and on the west by the right-lateral fault of F-19, during the period from 60 or 50 to 30 my.

This mode of marginal sea formation is very similar to the "rhombochasm" by CAREY (1958) and to the ideas of RODOLFO (1969).

5. Restoration of the Circum-Japan Sea Region, and the Tectonic History

An attempt is made at restoration of the position of the Japanese Islands to the original state prior to the drifting of Southwest Japan. In the restoration, the displacement along faults is reversed, but folds are not smoothed out because insufficient data are available. The Asiatic continent is fixed. The Japan Sea region is closed to such an extent that the areas deeper than 2,000 m in water depth (probably with oceanic crust) become minimum and the areas shallower than 1,500 m do not overlap. The position of Japan in the Early Cretaceous is shown in Fig. 3, A. Sakhalin and the eastern half of Hokkaido are ten-

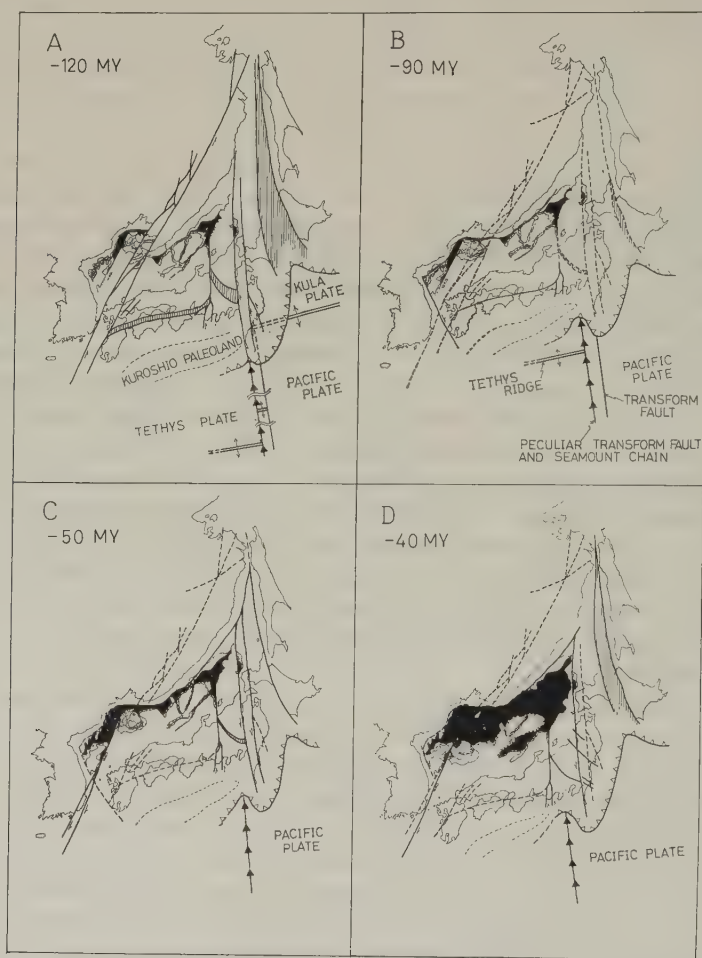


Fig. 3. Reconstruction of the circum-Japan Sea region at 120, 90, 50, and 40 my. Scattering dotted area; the area of 1,500–2,000 m deep at present. Densely dotted area; the area of overlap of fit. Black area; the area of unoverlap of fit. Hatched area; the gap closed by later crustal shortening. Thick line and dashed line; active and inactive fault, respectively, in the successive interval.

tatively fixed more eastward than the present location, so that they do not superposed on the western part of Hokkaido at the stage shown in Fig. 3, C.

The Hida belt, including the Yamato Ridge, existed as a large tectonic landmass which extended southwestward and connected with the Ryeongnam massif of south Korea as inferred by HURLY *et al.* (1973). The Funatsu granites in the Hida belt are correlative with the Deabo granites in Korea (REEDMAN and UM, 1975). In the Sikhote-Alin region, the geosynclinal trough trended NE-SW and opened northeastward. The provenance of arkose sandstone older than the Middle Albian in the Sikhote-Alin region (BERSENEV, 1971) is considered to be the Hida-Ryeongnam belt. Along the southern side of the Hida-Ryeongnam belt, there was a narrow trough in which mainly terrestrial and brackish sediments accumulated. In the western extension of the trough, the Lower Cretaceous Gyeongsang Supergroup in south Korea and Kanmon Group in the western end of the inner zone of Southwest Honshu were deposited in the same basin. The axial zone of Southwest Japan was also an uplifted zone, the eastern extension of which was connected with another uplifted zone, the NE-SW trending Abukuma-Kitakami uplift. This zone, having been situated more oceanward (Fig. 3, A), belonged originally to an unit different from the axial zone of Southwest Japan. The possible western extension of the Abukuma-Kitakami uplifted zone may correspond to the "Kuroshio paleoland" proposed by KISHU SHIMANTO RESEARCH GROUP (1968, 1970, 1975). In the area between the uplifted axial zone of Southwest Japan and the Abukuma-Kitakami-Kuroshio paleoland, the Shimanto geosynclinal trough was developed. Basalts in the Shimanto belt are abyssal tholeiite (SHIIDA *et al.*, 1971; SUGISAKI *et al.*, 1972), and the Lower Cretaceous volcanic rocks in the Kitakami belt belong to the high-alumina rock series (SUGISAKI *et al.*, 1972; KANISAWA, 1974). The distribution pattern of rare earth elements of basalts in the Shimanto belt belongs to solid-type, and that in the Kitakami belt belongs to liquid-type (TANAKA, 1977). Accordingly, if the Shimanto geosynclinal trough was a kind of marginal sea as considered by SUGISAKI *et al.* (1971, 1972), ICHIKAWA *et al.* (1972), and ICHIKAWA (1975), the Kitakami-Abukuma-Kuroshio paleoland might be an island arc.

Four stages of the tectonic movements can be distinguished in the circum-Japan Sea region during Early Cretaceous to Miocene. In Fig. 3, the restoration maps at 120, 90, 50, and 40 my are shown. Main geologic events are arrayed in Fig. 4.

1st stage (130 to 90 my). During the Hauterivian to Barremian, the Oshima Orogenic Movement (KOBAYASHI, 1941) occurred in the Kitakami and Abukuma belts. At the same time, the left-lateral faults originated and were followed by granitic intrusion (120 to 110 my) in the Kitakami belt. After a short while, large-scale left-lateral movements along F-6, F-7, and F-10 and granitic igneous activity (90 to 100 my) occurred in the Abukuma belt. These NS trending faults suggest that the compressional stress in a NW-SE direction or simple shear stress along these faults predominated in Northeast Honshu. Soon after (90 to 75 my), the cusp structure of Kanto region was formed by the differential compression from south.

In the inner zone of Southwest Japan, the post-Kanmon movement proceeded and was accompanied by left-lateral displacement along the NE-SW trending faults. Thrusting along F-14 might have occurred with resulting crustal shortening by few tens kilometers (KOJIMA, 1973). In the Sikhote-Alin region, terminal folding and left-lateral movements along F-21 and F-22 occurred. All of these tectonic movements in Southwest Japan and Sikhote-Alin regions resulted from intensive northward compression. The left-lateral displacement along NS to NNW-SSE and NE-SW to NNE-SSW trending faults sums to a

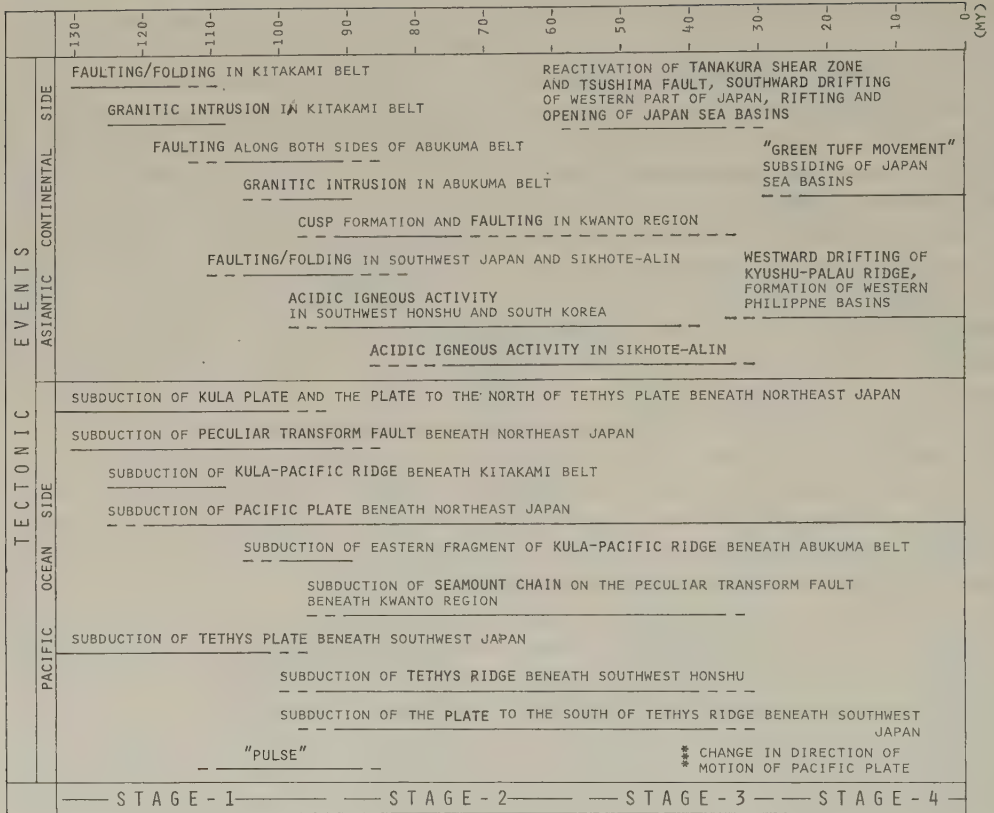


Fig. 4. Tectonic history of the circum-Japan Sea region and related plate motions.

several hundreds kilometer north-northeastward movement of the western half of Hokkaido. It is expected to have resulted in the subduction of the western half of Hokkaido beneath the eastern half of Hokkaido-Sakhalin (Fig. 3, A and B). This subduction might have been accompanied by the right-lateral movement along the consuming zone.

2nd stage (90 to 50 or 60 my). Soon after the tectonic movements in the 1st stage, very intense acidic volcano-plutonic igneous activities occurred in the inner zone of Southwest Japan, south Korea, and Sikhote-Alin regions, as well as in the Yamato Ridge and some other banks in the Japan Sea. In these regions, volcano-tectonic depressions were formed, and huge amounts of acidic pyroclastics filled them and covered the intensely folded basements with pronounced clino-unconformity. The acidic pyroclastics are scarcely folded in these regions, where compressional stress was no longer dominant.

3rd stage (50 or 60 to 30 my). Acidic igneous activities declined in the late phase of the 2nd stage but continued into the early phase of the 3rd stage. Initial rifting may have occurred along the present continental slope on the continental side being accompanied by a few degrees anti-clockwise rotation of the Japanese Islands (Fig. 3, C).

Next, southward drift of the western part of Japan came to its climax. The drifting part was bounded on the west by F-19 and on the east mainly by F-10. F-20 was formed as a right-lateral fault during this stage. With the progress of southward drifting of South-

west Japan, the Japan Sea Basins opened behind it (Fig. 3, D). Some small-scale spreading centers may have originated at the locations as proposed by ISEZAKI (1975). Acidic igneous activity was converted into basic activity, resulting in the formation of oceanic crust. A narrow trough was formed between south Korea and Kyushu, through which clastic sediments were transported into the Japan Sea Basins. In the early stage of the spreading in the Japan Sea Basins, a non-marine environment was predominant as indicated by the Paleogene sediments dredged from the Yamato Ridge with many plant fragments (VASIL'EV and MARKEVICH, 1973). The cusp structure in the Kanto region may have been slightly exaggerated by southward drifting. As a result of the southward drift of Japanese Islands, crustal stretching may be expected between the western and eastern parts of Hokkaido (Fig. 3, D).

4th stage (30 my –). At about 30 my, southward drifting and spreading in the Japan Sea region ceased and another type of tectonic movement ("Green Tuff Movement") began with violent andesitic volcanism along the Japan Sea side of the Japanese Islands. The Japan Sea floor was subsiding continuously, accompanied by the accumulation of thick pelagic sediments and turbidites. The Neogene formations in the inner side of the Japanese Islands and on the Japan Sea continental slope were intensely deformed during the Late Miocene to Quaternary. But in the Japan Sea Basins, neither notable folding nor faulting has occurred since Miocene.

6. *The Configuration and Kinematics of Oceanic Plates Suggested by the Tectonic History of the Continental Margin*

The above-mentioned tectonic history in the circum-Japan Sea region leads us to the better understanding on the configuration and kinematics of the oceanic plates in the Pacific ocean (Figs. 3 and 4).

i) The characteristics of folds and faults in Sikhote-Alin and Southwest Japan strongly suggest a NS to NNW-SSE compressional stress field during the Early to Middle Cretaceous. The same stress field was obtained by MIZUTANI and KANAORI (1976), who studied it in Central Honshu by means of fault analysis. Intense compression is consistent with the moving direction of the Kula and Tethys plates, and corresponds to the "pulse" suggested by LARSON and PITMAN (1972).

ii) Attention should be paid to the cusp structure of the Kanto region, which was concluded by HARA *et al.* (1977) to have been formed by differential compression from the south. VOGT *et al.* (1975) suggested that cusp structures are formed by subduction of aseismic ridges, oceanic plateau or seamount chains. MATSUDA (1976, 1978) proposed that something like a seamount chain existed somewhere about the present Izu-Bonin arc and was subducted beneath the Kanto region since the Middle Cretaceous.

iii) HILDE *et al.* (1977) mapped transform faults trending in NNW-SSE in the western Pacific region. The most important fault among them is postulated to have been located in nearly the same position as the present Kyushu-Palau Ridge. It separated the Tethys and Australo-Antarctic plates from the Kula and Pacific plates. They also suggested that the Kula plate might have moved north considerably faster than the Tethys plate due to the combined velocities of spreading from the ridges to the north and south of the Pacific plate. If their assumption is acceptable, the subduction of this peculiar transform fault might have induced intense simple shear stress in the continental margin that could cause large-scale NS to NNW-SSE trending left-lateral faults. According to HILDE *et al.* (1977),

this peculiar transform fault might have been subducted beneath Kyushu. But no such fault is found there. Concerning the location of the transform fault, Hilde *et al.* followed the idea of UYEDA and BEN-AVRAHAM (1972) and UYEDA and MIYASHIRO (1974), who assumed that the present Kyushu-Palau Ridge was a western half of the arc which was formed by the conversion of the transform fault into a subduction zone. The eastern half of this arc corresponds to the Izu-Mariana arc system which later drifted eastward away from the Kyushu-Palau Ridge by the process proposed by KARIG (1971a, b). However, this idea takes no account of the land-based evidence. The authors prefer to propose another story as follows.

This peculiar transform fault was located along the present Izu-Bonin arc and has been subducted beneath the Kanto region since the Middle Cretaceous (MATSUDA, 1976, 1978). It is quite probable that, unlike the other common transform faults, the transform fault was accompanied by a seamount chain on it, because it was active not only along the segment between the Tethys and Pacific-Phoenix ridges but also along the segment to the north of the Kula-Pacific ridge. Subduction of the transform fault crested by a seamount chain must have formed the cusp structure of the Kanto region.

iv) The left-lateral faults developed mainly in Northeast Honshu (F-1-4, 6, 7, 10) have slightly different directions from those in Southwest Japan and Sikhote-Alin though they originated at nearly the same time. This fact suggests that somewhat different stress field prevailed in Northeast Honshu: i.e. either NW-SE trending compression or simple shear stress parallel to the faults. The former is not consistent with the moving direction of the Pacific plate calculated by LARSON and PITMAN (1972), and the latter is preferably accepted. As mentioned already, the subduction of the peculiar transform fault must have induced simple shear stress toward the continental side. If the transform fault was moving with a westward component at 1 cm/year before it arrived at the position of the present Izu-Bonin arc, it must have been located off the Kitakami massif and subducted beneath it at about 120 my. The simple shear force induced by the subduction of the peculiar transform fault caused the NNW-SSE trending left-lateral faults in the Kitakami belt. Nearly the same time, the subducted Kula-Pacific ridge produced the intermediate to acidic volcanics (Valanginian to Hauterivian) and granitic rocks of 110 to 120 my in the Kitakami belt.

At about 100 my, the transform fault arrived off the Abukuma massif, and formed F-6, F-7, and F-10 one after another from east to west. Nearly the same time granitic activity was produced in the Abukuma belt by subduction of the western fragment of the Kula-Pacific ridge which was left-laterally shifted by another transform fault (Fig. 3, A).

At about 90 my, the peculiar transform fault arrived at the present Izu-Bonin arc. Subduction of the seamount chain on it formed F-11-13 and the Kanto cusp structure. Simple shear force was no longer induced, because the Kula-Pacific ridge had already been subducted. These events are shown in Fig. 3, A and B and Fig. 4.

v) A zone of high positive magnetic anomaly is observed along the area off Northeast Japan landward of the Japan trench. SEGAWA and OSHIMA (1975) proposed the idea that this magnetic anomaly belt is due to the buried Mesozoic volcanic-plutonic front. The present authors suggest that the anomaly may be caused by the fragments of the seamount chain on the peculiar transform fault which were left behind on the continental side of the paleo-Japan trench as it subducted.

vi) UYEDA and MIYASHIRO (1974) thought that the descent of the Kula-Pacific ridge produced the Cretaceous acidic magmatism of east Asia. The present authors consider

that the Cretaceous magmatism in Northeast Honshu was due to the descent of the Kula-Pacific ridge, and that the Late Cretaceous to Paleogene acidic magmatism in Southwest Japan, Korea and Sikhote-Alin regions was caused by the subduction of the Tethys ridge. The subduction of the different oceanic ridges might have resulted in some chemical and mineralogical differences in granitic rocks between the areas to the west and east of the Tanakura shear zone.

vii) As mentioned already, the peculiar transform fault has been located at about the same position as the present Izu-Bonin arc about 90 my. If the Shikoku and Parece Vela Basins were formed by rifting, as inferred by many investigators, the Kyushu-Palau ridge must have drifted westward apart from Izu-Mariana arc system.

The authors thank Prof. N. Kitamura, Prof. H. Nakagawa, and Prof. K. Mori of Tohoku University for kindly going through the manuscript. The authors are indebted to our colleagues in our institute for useful discussions.

REFERENCES

- ABLAEV, A.G., V.P. KONOVALOV, and V.A. KRASILOV, On the age of folding in Sikhote-Alin, *Akad. Nauk SSSR Dokl.*, **207**, 665–668, 1972 (in Russian).
- ARAI, F., Y. HAYAMA, S. HAYASHI, T. HOSOYA, H. IBE, K. KANZAWA, Y. KIZAKI, S. KUBO, T. NAKAJIMA, K. TAKAHASHI, K. TAKEI, K. TOYA, N. YAMASHITA, and K. YOSHIBA, The Shimonita tectonic zone, *Chikyu Kagaku (Earth Sci.)*, No. 83, 8–24, 1966 (in Japanese).
- BASKINA, V.A. and I.K. VOLCHANSKAYA, Age of igneous rocks in eastern Sikhote-Alin (by K-A method), *Akad. Nauk SSSR Dokl.*, **204**, 667–670, 1972 (in Russian).
- BELOUSSOV, V.V., Some problems of development of the earth's crust and upper mantle of oceans, in *The Crust and Upper Mantle of the Pacific Area*, Am. Geophys. Union Monogr. No. 12, 449–459, 1968.
- BELOUSSOV, V.V. and E.M. RUDITCH, Island arc in the development of the earth's structure, especially in the region of Japan and the sea of Okhotsk, *J. Geol.*, **69**, 3–23, 1961.
- BELYAYEVSKIY, N.A. and A.G. RODNIKOV, Crustal structure of the island arcs and Far Eastern seas, 1. The island arcs, *Int. Geol. Rev.*, **14**, 171–184, 1972.
- BERSENEV, I.I., Geological structure of the Sikhote-Alin, in *Island Arc and Marginal Sea*, edited by S. Asano and G.B. Udintsev, pp. 39–56, Tokai University Press, Tokyo, 1971 (in Japanese).
- CAREY, S.W., The tectonic approach to continental drift, in *Continental Drift—A Symposium*, pp. 177–355, Univ. Tasmania, 1958.
- EHRO, M., The Hizume-Kesennuma fault—With special reference to its character and significance on the geologic development, *Tohoku Univ. Inst. Geol. Pal. Contr.*, No. 77, 1–37, 1977 (in Japanese).
- EMERY, K.O. and H. NIINO, Stratigraphy and petroleum prospects of Korea Strait and the East China Sea, *ECAFE, Comm. for Co-ordination of Joint Prospecting for Min. Res. in Asian Offshore Areas, Tech. Bull.*, **1**, 13–27, 1968.
- EMERY, K.O., Y. HAYASHI, T.W.C. HILDE, K. KOBAYASHI, J.H. KOO, C.Y. MENG, H. NIINO, J.H. OSTERHAGEN, L.M. REYNOLDS, J.M. WAGEMAN, C.S. WANG, and S.J. YANG, Geological structure and some water characteristics of the East China Sea and the Yellow Sea, *ECAFF, Comm. for Co-ordination of Joint Prospecting for Min. Res. in Asian Offshore Areas, Tech. Bull.*, **2**, 3–43, 1969.
- FUJIMOTO, S., Tectonic movement of the Shirakami-dake granitic complex in Aomori Prefecture, p. 263, Abstr. Annu. Meet. Geol. Soc. Jpn., 1976 (in Japanese).
- HARA, I., K. HIDE, K. TAKEDA, E. TSUKUDA, M. TOKUTA, and T. SHIOTA, Tectonic movement in the Sambagawa belt, in *The Sambagawa Belt*, edited by K. Hide, pp. 307–390, Hiroshima University Press, Hiroshima, 1977 (in Japanese).
- HASEBE, K., N. FUJII, and S. UYEDA, Thermal processes under island arcs, *Tectonophysics*, **10**, 335–355, 1970.
- HAYAMA, T. and T. YAMADA, Some consideration on the Median tectonic line of the Kashio phase in the light of Ryoke plutonic history, in *Median Tectonic Line*, edited by R. Sugiyama, pp. 1–7, Tokai University Press, Tokyo, 1973 (in Japanese).
- HILDE, T.W.C., S. UYEDA, and L. KROENKE, Evolution of the western Pacific and its margin, *Tectonophysics*, **38**, 145–165, 1977.
- HILDE, T.W.C. and J. WAGEMAN, Structure and origin of the Japan Sea, in *The Western Pacific*, edited P.J. Coleman, pp. 415–434, Crane, Russak and Co., Inc., and University of Western Australia Press, New York, 1973.

- HORIKOSHI, E., Orogenic belts of the Japanese Islands and plate tectonics, *Kagaku (Science)*, **42**, 665–673, 1972 (in Japanese).
- HOSHINO, M. and H. HONMA, Geology of submarine banks in the Japan Sea, *Chikyu Kagaku (Earth Science)*, No. 82, 10–16, 1966 (in Japanese).
- HURLEY, P.M., H.W. FAIRBAIRN, W.H. PINSON, and J.H. LEE, Middle Precambrian and older apparent age values in basement gneisses of South Korea, and relations with Southwest Japan, *Geol. Soc. Am. Bull.*, **84**, 2299–2304, 1973.
- ICHIKAWA, K., Honshu and Shimanto geosynclines in Southwest Japan and plate tectonics, *Assoc. Geol. Collab. Jpn. Monogr.*, No. 19, 241–246, 1975 (in Japanese).
- ICHIKAWA, K., T. MATSUMOTO, and M. IWASAKI, Origin of the Japanese Islands, *Kagaku (Science)*, **42**, 181–191, 1972 (in Japanese).
- ICHIKAWA, K., N. MURAKAMI, A. HASE, and K. WADATSUMI, Late Mesozoic igneous activity in the inner side of Southwest Japan, *Pac. Geol.*, **1**, 97–118, 1968.
- INOUE, E., Goto-nada sea and Tsushima Strait investigations northwestern Kyushu, 1972–1973, Cruise Report No. 2, edited by E. Inoue, 68 pp., Geol. Surv. Jpn., 1975.
- ISEZAKI, N., Possible spreading centers in the Japan Sea, *Mar. Geophys. Res.*, **2**, 265–277, 1975.
- ISEZAKI, N. and S. UYEDA, Geomagnetic anomaly pattern of the Japan Sea, *Mar. Geophys. Res.*, **2**, 51–59, 1973.
- ISHIHARA, S., The Mo-W metallogenic provinces and the related granitic provinces, *Min. Geol.*, **23**, 13–32, 1973 (in Japanese).
- ISHIHARA, S. and S. TERASHIMA, The tin content of the Japanese granitoids and its geological significance on the Cretaceous magmatism, *J. Geol. Soc. Jpn.*, **83**, 657–664, 1977 (in Japanese).
- ISHII, M., Basement of the Kwantow plain, *Jpn. Assoc. Pet. Technol.*, **27**, 615–640, 1962 (in Japanese).
- ISOMI, H. and K. KAWATA, Correlation of the basement rocks on both sides of the Fossa Magna, in *The Fossa Magna*, pp. 4–12, Geol. Soc. Jpn., 1968 (in Japanese).
- ITO, H. and K. TOKIEDA, Tilting of Hokkaido Island and Kitakami mountains deduced from the NRM of Cretaceous granitic rocks, *Rock Magn. Paleogeophys.*, **2**, 54–58, 1974.
- ITO, H. and K. TOKIEDA, Paleomagnetism and chemical composition of Cretaceous granitic rocks, *Rock Magn. Paleogeophys.*, **4**, 118–121, 1977.
- IWABUCHI, Y. and A. MOGI, Summarization of submarine geology in each zone of Japanese Upper Mantle Project, in *The Crust and Upper Mantle of Japanese Area, Part II, Geology and Geochemistry*, directed by I. Kobayashi, pp. 138–162, Jpn. Natl. Comm. for UMP, 1973.
- IWAO, S. and MATSUI, H., Explanatory text of the geological map of Japan, 1/50,000, Taira and Kawamae, p. 103, Geol. Surv. Jpn., 1961 (in Japanese).
- KANAYA, H. and S. ISHIHARA, Regional variation of magnetic susceptibility of the granitic rocks in Japan, *J. Jpn. Assoc. Min. Pet. Econ. Geol.*, **68**, 211–224, 1973 (in Japanese).
- KANISAWA, S., Igneous activity and metamorphic history in the Northeast Japan, *Geol. Soc. Jpn. Mem.*, No. 10, 5–19, 1974. (in Japanese).
- KANISAWA, S., Chemical composition of hornblendes of some Ryoke granites, Central Japan, *J. Jpn. Assoc. Min. Pet. Econ. Geol.*, **70**, 200–211, 1975.
- KANO, H., K. YANAI, M. TSUJI, A. KAWASE, and S. KANISAWA, Structure of some basement granitic masses and their significance in geotectonics of the Green Tuff Region, *Assoc. Geol. Collab. Jpn. Monogr.*, No. 12, 1–15, 1966 (in Japanese).
- KARAKIDA, Y., T. TOMITA, D. GOTTFRIED, T.W. STERN, and H.J. ROSE, Jr., Lead-alpha ages of some granitic rocks, from North Kyushu and Central Japan, *Mem. Fac. Sci. Kyushu Univ.*, Ser. D, Geol., **16**, 249–263, 1965.
- KARIG, D.E., Structural history of the Mariana island arc system, *Geol. Soc. Am. Bull.*, **82**, 323–344, 1971a.
- KARIG, D.E., Origin and development of marginal basins in the western Pacific, *J. Geophys. Res.*, **76**, 2542–2561, 1971b.
- KARIG, D.E., J.C. INGLE, Jr. et al., *Initial Reports of the Deep Sea Drilling Project*, Vol. 31, Site 299–302, pp. 351–468, U.S. Government Printing Office, Washington, 1975.
- KATADA, M. and A. OZAWA, Schistose granites (Shirakami-dake granite) in the southern area of Aomori Prefecture, *Bull. Geol. Surv. Jpn.*, **15**, 87–94, 1964 (in Japanese).
- KAWACHI, Y., T. YAMADA, and Y. YOKOYAMA, Crystalline schists of Yokokawa district (Yokokawa-gawa metamorphic rocks), north of Lake Suwa, Central Japan, *J. Jpn. Assoc. Min. Pet. Econ. Geol.*, **56**, 21–29, 1966 (in Japanese).
- KAWAI, N., K. HIROOKA, and T. NAKAJIMA, Paleomagnetic and potassium-argon age informations supporting Cretaceous Tertiary hypothetical bend of the main island of Japan, *Paleogeogr. Paleoclim. Paleocool.*, **6**, 277–282, 1969.
- KAWAI, N., H. ITO, and S. KUME, Deformation of the Japanese Islands as inferred from rock magnetism, *R. Astr. Soc. Geophys. J.*, **6**, 124–129, 1961.

- KAWAI, N., T. NAKAJIMA, and K. HIROOKA, The evolution of the island arc of Japan and the formation of granites in the circum-Pacific belt, *J. Geomag. Geoelectr.*, **23**, 267–293, 1971.
- KAWANO, Y. and Y. UEDA, K-A dating on the igneous rocks in Japan. II. Granitic rocks in Kitakami massif, *Sci. Rep. Tohoku Univ.*, 3rd Ser., **9**, 199–251, 1965.
- KAWANO, Y. and Y. UEDA, K-A dating on the igneous rocks in Japan. III. Granitic rocks of Abukuma massif, *Sci. Rep. Tohoku Univ.*, 3rd Ser., **9**, 513–523, 1966a.
- KAWANO, Y. and Y. UEDA, K-A dating on the igneous rocks in Japan. IV. Granitic rocks of Backbone Range in northeastern Japan and its western district, *Sci. Rep. Tohoku Univ.*, 3rd Ser., **9**, 525–539, 1966b.
- KAWANO, Y. and Y. UEDA, Periods of the igneous activities of the granitic rocks in Japan by K-A dating method, *Tectonophysics*, **4**, 523–530, 1967.
- KIKUCHI, J., The Japanese Cretaceous granitic province based on Kuno's silica-total alkalis variation diagram, *J. Geol. Soc. Jpn.*, **80**, 251–259, 1974 (in Japanese).
- Kimura, T., A sharp bent of the Median tectonic line—Tectonic significances yielded by lateral faults, *Jpn. J. Geol. Geogr.*, **30**, 215–232, 1959.
- KIMURA, T. Tectonic movements in the southern Fossa Magna, Central Japan, analized by the minor structures in its southwestern area, *Jpn. J. Geol. Geogr.*, **37**, 63–85, 1966.
- KISHU SHIMANTO RESEARCH GROUP, The study of the Shimanto terrain in the Kii Peninsula, Southwest Japan (Part 2), *Chikyu Kagaku (Earth Science)*, **22**, 224–231, 1968 (in Japanese).
- KISHU SHIMANTO RESEARCH GROUP, Sedimentological and paleontological studies of the Muro Group at the southern coastal region of the Kii Peninsula (Part 4), *Bull. Fac. Edu., Wakayama Univ. (Nat. Sci.)*, No. 20, 75–102, 1970 (in Japanese).
- KISHU SHIMANTO RESEARCH GROUP, The development of the Shimanto geosyncline, *Assoc. Geol. Collab. Jpn. Monogr.*, **19**, 143–156, 1975 (in Japanese).
- KITAMURA, N., Tertiary tectonic movements of the Green Tuff region, *Fossils, Pal. Soc. Jpn.*, No. 5, 123–137, 1963 (in Japanese).
- KITAMURA, N., Basement rocks from the Green Tuff region in northeast Japan, in M. Minato's Res. Rep. on the Paleozoic Orogenic Movement in Northeastern Japan, No. 2, pp. 9–20, 1976 (in Japanese).
- KITAMURA, N., and S. KANISAWA, On the pre-Tertiary rocks at the southern foot of Mt. Yakeishidake in the Ou Backbone Range, Northeast Japan, *Tohoku Univ., Inst. Geol. Pal. Contr.*, No. 71, 61–66, 1971 (in Japanese).
- KOBAYASHI, T., The Sakawa orogenic cycle and its bearing on the origin of the Japanese Islands, *J. Fac. Sci. Univ. Tokyo*, Sec. 2, **5**, 219–578, 1941.
- KOJIMA, G., Geological segments lost at the Median tectonic line, in *Median Tectonic Line*, edited by R. Sugiyama, pp. 253–261, Tokai University Press, Tokyo, 1973 (in Japanese).
- KOVYLIN, V.M. and Yu. P. NEPROCHNOV, Structure of the earth's crust and sedimentary layer in the central part of the sea of Japan, *Akad. Nauk SSSR Izv. Ser. Geol.*, No. 4, 10–26, 1965 (in Russian).
- LARSON, R.L. and W.C. PITMAN III, World-wide correlation of Mesozoic magnetic anomalies and its implications, *Geol. Soc. Am. Bull.*, **83**, 3645–3662, 1972.
- LEE, Y.-J. and Y. UEDA, K-Ar dating on granitic rocks from the Eonyang and the northwestern part of Ulsan-quadrangle, Kyeongsang-nam-do, Korea, *J. Korean Inst. Min. Geol.*, **9**, 127–134, 1976 (in Korean).
- LUDWIG, W.J., S. MURAUCHI, and R.E. HOUTZ, Sediments and structure of the Japan Sea, *Geol. Soc. Am. Bull.*, **86**, 651–664, 1975.
- MATSUDA, T., The peculiarity of the Fossa Magna region in the Honshu arc, *Kaiyo Kagaku (Marine Sciences)*, **8**, (9), 20–24, 1976 (in Japanese).
- MATSUDA, T., Collision of the Izu-Bonin arc with central Honshu—Cenozoic tectonics of the Fossa Magna, Japan, this issue, S 409–S 421, 1978.
- MATSUDA, T. and S. UYEDA, On the Pacific-type orogeny and its model—Extension of the paired belts concept and possible origin of marginal seas, *Tectonophysics*, **11**, 5–27, 1971.
- MATSUMOTO, T., The late Mesozoic geological history in the Nagato province, Southwest Japan, *Jpn. J. Geol. Geogr.*, **21**, 235–243, 1949.
- MATSUSHIMA, N., Median tectonic line in the Akaishi mountains, in *Median Tectonic Line*, edited by R. Sugiyama, pp. 9–26, Tokai University Press, Tokyo, 1973 (in Japanese).
- MELANKHOLINA, Ye N. and V.M. KOVYLIN, Tectonics of the sea of Japan, *Geotectonics*, **10**, 273–282, 1976.
- MINATO, M., M. GORAI, and M. HUNAHASHI (eds.), *The Geologic Development of the Japanese Islands*, 442pp., Tsukiji Shokan Co., Ltd., Tokyo, 1965.
- MINATO, M. and M. HUNAHASHI, Origin of the earth's crust and its evolution, *Hokkaido Univ. Fac. Sci. J.*, Ser. 4, **14**, 515–561, 1970.
- MIZUTANI, S. and Y. KANAORI, Genetic process of fault, *Kagaku (Science)*, **46**, 536–544, 1976 (in Japanese).
- MURAKAMI, N., Petrology of the granitic rocks in alpine-type serpentinite from Dai, Nagato tectonic zone, West Chugoku, in *Prof. H. Matsushita Memorial Volume, II*, pp. 57–66, 1971 (in Japanese).

- MURAUCHI, S., Explosion seismology, in *Second Progress Report on the Upper Mantle Project of Japan* (1965–1966), pp. 11–13, Natl. Comm. for UMP, Sci. Council of Japan, 1966.
- MURAUCHI, S., The renewal of island arc and the tectonics of marginal seas, in *Island Arc and Marginal Sea*, edited by S. Asano and G.B. Udintsev, pp. 39–56, Tokai University Press, Tokyo, 1971 (in Japanese).
- MURAUCHI, S. and T. ASANUMA, Studies on the seismic profiler records of sediments on the continental shelf east of the Tsushima Islands, Kyushu, Japan, *Natl. Sci. Mus. Mem.*, **2**, 39–41, 1969 (in Japanese).
- NAGAHAMA, H., Paleocurrent data from the Katsumoto Group, Iki Island, *J. Geol. Soc. Jpn.*, **73**, 124, 1967 (in Japanese).
- NAGAHAMA, H., H. ISOMI, C. ONO, and S. SATO, Dagger blade structure—A new method for detecting line of depositional current of siltstone, *J. Geol. Soc. Jpn.*, **72**, 531–540, 1966.
- NISHIMURA, Y. and T. NUREKI, Geological relations of the “non-metamorphic Paleozoic formations” to the Sangun metamorphic rocks in the Nishiki-cho area, Yamaguchi Prefecture, *J. Geol. Soc. Jpn.*, **72**, 385–398, 1966 (in Japanese).
- NOZAWA, T., Isotopic ages of Late Cretaceous acid rocks in Japanese Islands: Summary and notes in 1970, *J. Geol. Soc. Jpn.*, **76**, 493–518, 1970 (in Japanese).
- NOZAWA, T., Radiometric Age Map of Japan, Granitic Rocks, Geol. Surv. Japan, 1975.
- NUREKI, T., Structural petrology of a thrust shear zone developed between the Sangun metamorphic zone and the Ryoke zone in the eastern part of Yamaguchi Prefecture, *J. Geol. Soc. Jpn.*, **72**, 219–231, 1966 (in Japanese).
- NUREKI, T., Geological relations of the Sangun metamorphic rocks to the “non-metamorphic” Paleozoic formations in the Chugoku province, *Geol. Soc. Jpn. Mem.*, No. 4, 23–39, 1969 (in Japanese).
- NUREKI, T., An idea on the Nagato tectonic zone, in T. Nureki's Res. Rep. on the Studies on the Basement Rocks before the Honshu Orogenic Movements; “Basement Rocks”, No. 2, 10–12, 1972 (in Japanese).
- OGUCHI, T., K. YANAI, and T. INOUE, On the origin of fragments of hornfelses found in the Shiosenomisaki sandstone and conglomerate, Monzen Formation, Oga Peninsula, Northeast Japan, *Geol. Soc. Jpn. Mem.*, No. 9, 45–54, 1973 (in Japanese).
- OKAMURA, Y., The relation between the crystalline schist formations and the non-metamorphic Paleozoic formations in the eastern part of the Sangun zone in Yamaguchi Prefecture, *Geol. Rep. Hiroshima Univ.*, No. 12, 221–234, 1963 (in Japanese).
- OKAMURA, Y. and G. KOJIMA, Geological relations of the Sangun metamorphic rocks to the Ryoke metamorphic rocks in the northern area of Tokuyama, Yamaguchi Prefecture, *J. Geol. Soc. Jpn.*, **57**, 342–343, 1951. (in Japanese).
- ONO, K., T. TOGAWA, I. WATANABE, and H. SHIBATA, Geology of the southern border district of northern Abukuma Plateau—Geology and Petrological studies of Abukuma Plateau (Part 5), *Studies from Geol. Min. Inst. Tokyo Univ. Edu.*, No. 2, 79–89, 1953 (in Japanese).
- OTSUKI, K., Geology of the Tanakura shear zone and adjacent area, *Tohoku Univ., Inst. Geol. Pal. Contr.*, No. 76, 1–71, 1975 (in Japanese).
- OTSUKI, K., On the relationship between the width of shear zone and the displacement along fault, *J. Geol. Soc. Jpn.*, **84**, 661–669, 1978.
- RAMSAY, J.G. and R.H. GRAHAM, Strain variation in shear belts, *Can. J. Earth Sci.*, **7**, 786–813, 1970.
- REEDMAN, A.J. and S.H. UM, *The Geology of Korea*, 139pp., Geol. Min. Inst. Korea, 1975.
- RODOLFO, K.S., Bathymetry and marine geology of the Andaman basin, and tectonic implications for south Asia, *Geol. Soc. Am. Bull.*, **80**, 1203–1230, 1969.
- SAKA, Y. and K. KOIZUMI, Paleocurrent of Turonian Sanyama Formation in the eastern part of the Sanchu graben, Kwanto mountains, Central Japan, *J. Geol. Soc. Jpn.*, **83**, 289–300, 1977 (in Japanese).
- SATO, T. and K. ONO, The submarine geology off San'in district, southern Japan Sea, *J. Geol. Jpn.*, **70**, 434–445, 1964 (in Japanese).
- SEGAWA, J. and S. OSHIMA, Buried Mesozoic volcanic-plutonic fronts of the north-western Pacific island arcs and their tectonic implications, *Nature*, **256**, 15–19, 1975.
- SHIIDA, I., K. SUWA, R. SUGISAKI, T. TANAKA, and H. SHIOZAKI, Greenstones of the Cretaceous Hitakagawa belt of the Shimanto terrain in the Totsukawa area, Nara Prefecture, Central Japan, *Geol. Soc. Jpn. Mem.*, No. 6, 137–149, 1971 (in Japanese).
- SON, C.M., C.H. CHEONG, B.K. KIM, and S.M. LEE, Study of the ages of Mesozoic crustal movements, igneous activities and mineralizations, *Minis. Sci. Tech. Korea*, i–iv+1–31, 1968 (in Korean).
- SUDO, S., Geology of the Katashina area, Gunma Prefecture, Central Japan, *Geol. Soc. Jpn. Mem.*, No. 13, 229–240, 1976 (in Japanese).
- SUDO, S., Some problems on the Late Cretaceous to Paleogene volcano-plutonic activity in Central Japan, *Assoc. Geol. Collab. Jpn. Monogr.*, No. 20, 53–60, 1977 (in Japanese).
- SUGISAKI, R., S. MIZUTANI, M. ADACHI, M. HATTORI, and T. TANAKA, Rifting in the Japanese Late Paleozoic geosyncline, *Nature*, **233**, 30–31, 1971.

- SUGISAKI, R., S. MIZUTANI, H. HATTORI, M. ADACHI, and T. TANAKA, Late Paleozoic geosynclinal basalt and tectonism in the Japanese Islands, *Tectonophysics*, **14**, 35–56, 1972.
- SUZUKI, M., Report of the meeting at the field of Nagato tectonic zone, in T. Nureki's Res. Rep. on the Studies on the Basement Rocks before the Honshu Orogenic Movements; "*Basement Rocks*", No. 1, pp. 10–16, 1971 (in Japanese).
- TAKAHAMA, N., Late Mesozoic volcanic rocks found from Asahi massif, in the northern part of Niigata Prefecture: Asahi rhyolites, *J. Geol. Soc. Jpn.*, **78**, 323–324, 1972 (in Japanese).
- TAKEI, K., Stratigraphy and geological structure of the Cretaceous system in the eastern part of the Sanchu graben, Kwanto mountainland, *J. Geol. Soc. Jpn.*, **69**, 130–146, 1963 (in Japanese).
- TANAKA, T., Rare earth abundances in Japanese Paleozoic geosynclinal basalts and their geological significance, *Bull. Geol. Surv. Jpn.*, **28**, 529–559, 1977 (in Japanese).
- TERAOKA, Y., Cretaceous sedimentary basins in the Ryoke and Sambagawa belts, in *The Sambagawa Belt*, edited by K. Hide, pp. 419–432, Hiroshima University Press, Hiroshima, 1977 (in Japanese).
- TSUSUE, A. and S. ISHIHARA, The iron-titanium oxides in the granitic rocks of Southwest Japan, *Min. Geol.*, **24**, 13–30, 1974 (in Japanese).
- UENO, N., I. KANEOKA, M. OJIMA, S. ZASHU, T. SATO, and Y. IWABUCHI, K-Ar age, Sr isotopic ratio and K/Rb ratio of the volcanic rocks dredged from the Japan Sea, in *Island Arc and Marginal Sea*, edited by S. Asano and G.B. Udintsev, pp. 305–309, Tokai University Press, Tokyo, 1971 (in Japanese).
- UYEDA, S. and Z. BEN-AVRAHAM, Origin and development of the Philippine Sea, *Nature*, **240**, 176–178, 1972.
- UYEDA, S. and A. MIYASHIRO, Plate tectonics and the Japanese Islands: A Synthesis, *Geol. Soc. Am. Bull.*, **85**, 1159–1170, 1974.
- VASIL'EV, B.I. and P.V. MARKEVICH, Result of dredging on the Yamato bank, *Akad. Nauk SSSR Dokl.*, **213**, 1178–1180, 1973 (in Russian).
- VASILKOVSKY, N.P., G.B. UDINTSEV, B.G. KULP, and E.A. MOURAVOVA, Japan Sea—Relict of ocean, in *Island Arc and Marginal Sea*, edited by S. Asano and G.B. Udintsev, pp. 58–64, Tokai University Press, Tokyo, 1971 (in Japanese).
- VOGT, P.R., A. LOWRIE, D.R. BRACEY, and R.N. HEY, Subduction of aseismic ridge: Effects on shape, seismicity, and other characteristics of consuming plate boundaries, *Geol. Soc. Am. Spec. Paper*, **172**, 59 p., 1975.
- WATANABE, I., Y. SOTOZAKI, and M. GORAI, Geology of northeastern border district of northern Abukuma Plateau—Geological and Petrological studies of Abukuma Plateau (Part 4), *Studies from Geol. Min. Inst. Tokyo Univ. Edu.*, No. 2, 69–78, 1953 (in Japanese).
- WATANABE, I., M. GORAI, Y. KURODA, K. ONO, and T. TOGAWA, Igneous activities of the Abukuma Plateau—Geological and Petrological studies of the Abukuma Plateau (Part 9), *Chikyu Kagaku (Earth Science)*, No. 24, 1–11, 1955 (in Japanese).
- YAMASHITA, N. and Y. FUJITA, The Shin'etsu-Bozu Zone, a intersecting of the Honshu and Shichito arcs and the initial stage of the Green Tuff Orogeny, in *The Crust and Upper Mantle of the Japanese Area, Part II, Geology and Geochemistry*, directed by I. Kobayashi, pp. 61–83, Jpn. Natl. Comm. for UMP, 1973.
- YANAI, K., The late Mesozoic acidic igneous rocks of the northern Ashio mountainland, part 1, field geology, *J. Jpn. Assoc. Min. Pet. Econ. Geol.*, **67**, 193–202, 1972 (in Japanese).
- YANAI, K., T. INOUE, and T. OGUCHI, Late Cretaceous Tagawa acidic rocks in the Asahi Mountains, Northeast Japan, *J. Geol. Soc. Jpn.*, **79**, 11–22, 1973 (in Japanese).
- YOSHIDA, T., K. KASAI, and C. AOKI, Geology of the Yamizo mountains and geotectonic situation of the Ashio belt, *Geol. Soc. Jpn. Mem.*, No. 13, 15–24, 1976 (in Japanese).
- ZVEREV, S.M. and Yu. V. TULINA, Peculiarities in the deep structure of the Sakhalin-Hokkaido-Primorye zone, *Tectonophysics*, **20**, 115–127, 1973.

SIGNIFICANT ERUPTIVE ACTIVITIES RELATED TO LARGE INTERPLATE EARTHQUAKES IN THE NORTHWESTERN PACIFIC MARGIN

Masaaki KIMURA

*Department of Marine Sciences, Science and Engineering Division,
University of the Ryukyus, Naha, Japan*

(Received June 13, 1978; Revised October 6, 1978.)

Definite spatial and temporal relations were found between large interplate earthquakes and eruptive activities along the arc systems in the northwestern Pacific margin; Kurile-Kamchatka and Japan areas. A major pattern of the relation between both phenomena reveals that eruptive activity increases during the preseismic stage to the landward of the rupture zone in the direction parallel to the convergent plate motion. Increased eruptive activity had occurred from between 2 to 27 years prior to the large earthquakes. The volcanoes usually cease their activities and sometimes decrease them after seismicity. The intense activity generally migrates to adjacent areas, namely to the landward extension of seismicity gaps. These observations suggest that the eruptive activity is strongly influenced by regional tectonic stresses, and that the accumulated crustal strain may squeeze up magmas. Support for this conclusion was obtained by observing the level change of the magma head at Mihara-yama in Oshima Volcano, Japan. Some of the volcanoes also erupted immediately after the large earthquakes. One explanation for the post-shock eruption may be provided by considering the possible effect of seismic shocks on the catastrophic seismic events. This study may provide an important key for predicting large interplate earthquakes and major eruptions in the arc areas.

1. Introduction

It is a widely accepted idea that most large, shallow earthquakes along island arcs result from a fault motion across the zone of contact between the overthrust and the underthrust plates of the lithosphere. Tectonic strain accumulates in the lithosphere in the preseismic stage and is released by the shock. NAKAMURA (1975) suggests that contractional strain generated by regional crustal stresses around the magma reservoir can squeeze up of magma within an open conduit, causing a summit eruption on one hand and the formation of dike resulting in flank eruptions through the increase of pore pressure on the other hand. If the eruptions are influenced by regional tectonic stresses causing earthquakes, some spatial and temporal relationships between large interplate earthquakes and eruptions can be expected along the island arc systems. In this paper an attempt is made to correlate these events by, from a different angle, looking at the recent data of eruptive activity and seismicity along the typical subduction zone of the northwestern Pacific margin extending from the Kurile-Kamchatka to the northeastern Japan areas. Also the Izu-Bonin area is discussed.

2. Previous Works

A number of researchers have pointed out the relationships that existed between eruptive activity and seismicity since early times. MACGREGOR (1949), for instance, inferring from statistical studies, suggests that a temporal relation exists between the local seismicity and volcanic eruptions in the Caribbean volcanic arc. Such local seismicity was thought to be directly involved in volcanisms. Through his studies around the Japanese and New Hebrides areas, BLOT (1965, 1972) shows that the deep seismicity migrates from a greater depth to a shallower one and finally results in volcanic eruptions (Blot process). On the basis of statistical and worldwide studies, LATTER (1971) states that Blot process would probably be a second phenomenon and that the relationship would be primarily the correlated sequence of seismic and volcanic events resulting from periods of tectonic instability and perhaps increased tensional conditions which affect very wide areas of the earth's surface for periods of several months to several years at a time. On the other hand, many scientists have pointed out that there exists some physical relation between volcanic activity and tectonic seismicity (e.g., TOKAREV, 1971; YOKOYAMA, 1971; KAMINUMA, 1973).

In recent years, observers have noticed that major eruptions of Oshima Volcano, which stands on the Philippine Sea Plate, occurred in the period preceding the great Kanto earthquake of 1923 ($M_s=8.2$) and Boso-Oki earthquake of 1953 ($M_s=8.3$). Although one can't be sure what a physical mechanism connects the volcanic eruptions with the large earthquakes, the remarkable correlation suggests that they are largely governed by a common physical processes (NAKAMURA, 1971, 1975; KANAMORI, 1972; KIMURA, 1973, 1976).

3. Data

3.1 Eruptive activity

The areas treated in the present paper were selected primarily on the basis of available data. The scientific study of volcanoes has been carried out since the eighteenth century in Kamchatka (TOMKEIEFF, 1949; Fedotov, personal communication, 1976) and since the end of the nineteenth century in Japan (SUWA, 1970). Data is based on eruptions occurring in the Kurile-Kamchatka from 1880 to 1976 and in the northeastern Japan from 1880 to 1977. The term 'active volcano' used in this paper refers to a volcano which has erupted during the present century.

The data on eruptions discussed here were taken from the following sources: (1) *the Catalogue of the Active Volcano of the World Including Solfataral Fields*, IAVCEI (International Association of Volcanology and Chemistry of the Earth's Interior); (2) *the Bulletin of Volcanic Eruption*, Volcanological Society of Japan, IAVCEI; (3) *the Event Information Reports*, Center for Short-lived Phenomena, Smithsonian Institution; (4) *the List of the World Active Volcanoes*, Special Issue of Bulletin of Volcanic Eruption; (5) *Science Almanac* (Rikanempyo), Tokyo Astronomical Observatory; (6) published papers on volcanic eruptive activities.

3.2 Seismicity

Large interplate earthquakes (M or $M_s \geq 7.7$) are treated. Estimates of the rupture zones of large interplate earthquakes were taken from the papers by KELLEHER *et al.* (1973) for the Kurile-Kamchatka area and by SENO (1977a, 1978) for the northeastern Japan area. These are supplemented by the reestimations of McCann (personal communication,

1976) for the Kurile-Kamchatka. Special attention is given to the determination of rupture zones of the large interplate earthquakes discussed in Seno's detailed reestimations. The mechanism of many of these earthquakes suggests low-angle thrust faulting and of others suggest strike slip faulting which is consistent with the motion along the circum Pacific belt. In addition to these, the paper will also make a comparison with large intraplate earthquake along the trench; the 1933 Sanriku earthquake ($M=8.3$). The average values of the directions of the slip vector between underthrusting oceanic lithosphere and the overthrusting continental one were used as $N70^{\circ}W$ along the Japan trench and as $N60^{\circ}W$ along the Kurile trench (SENO, 1978).

4. Data Analysis

The volcano has both its own specific active stages, characterized generally by major eruptions and also dormant stages. The major eruption is generally characterized by great intensity of eruption or by lava-flows. In general such major eruptions may last from several weeks to several hundred days (NAKAMURA, 1978), but an active stage may continue for more than several years depending on the volcano. Therefore, the author took ten year intervals for assessing the degree of eruptive activity.

A pattern was designed to represent regional eruptive activities. The author defined the degree of the eruptive activities by the following four grades. Grade 4 is defined by the occurrence of a 'great' eruption or another significant eruption accompanied with lava-flows for a period of 10 years (most active). Grade 3 is assigned if there occur 'medium' or 'small' eruptions for more than 2 years in total during a period of 10 years (more active). Grade 2 is assigned if there occurs small to medium eruption for a period of 10 years. Grade 1 is assigned if there occur no eruptions for a period of 10 years.

Determination of the magnitude of eruption is based on the category of which IAVCEI classifies intensity of eruption into three: little (small) (l), medium (m) and great (g) depending on the volume of erupted material as the follows. $(l) < 1 \times 10^7 \text{ m}^3$, $(m) = 1 \times 10^4 - 10^7 \text{ m}^3$, $(g) > 1 \times 10^7 \text{ m}^3$. The volume of erupted material, however, were not well estimated in eruptions before 1950 and in volcanoes located in unpopulated or sparsely populated areas. Therefore it has been difficult to make an balanced comparison of eruptive activity in an extensive region by using the intensity classification only.

Eruptions accompanying lava-flows are included during a major eruptive activity in general, so they are included in Grade 4 even if the intensity is 'medium.' Thus, significant eruption accompanied by lava-flows or the formation of lava domes are treated as having the same rank in cases in which the magnitude of eruption can not be estimated in old eruptions or in volcanoes isolated from a population.

The spatial and temporal relationship between eruptive activity and seismicity is shown in diagram (e.g., Figs. 1 and 2). Equal grades of activity are shown by contours (Fig. 2). Volcanoes are set from north to south along axis perpendicular to the direction of the relative slip vector between plates at the ordinate in the figure. The interval between volcanoes does not show the real distances because this study emphasizes the relationship between the visual phenomena on eruptive activity and interplate seismicity; the area between volcanoes are not discussed in this paper. The shape of these contours varies according to the way how one takes the time interval, therefore a detailed discussion of the comparison for the shape of contours is meaningless, but it is valid to discuss long-term variation of eruptive activity in broad areas.

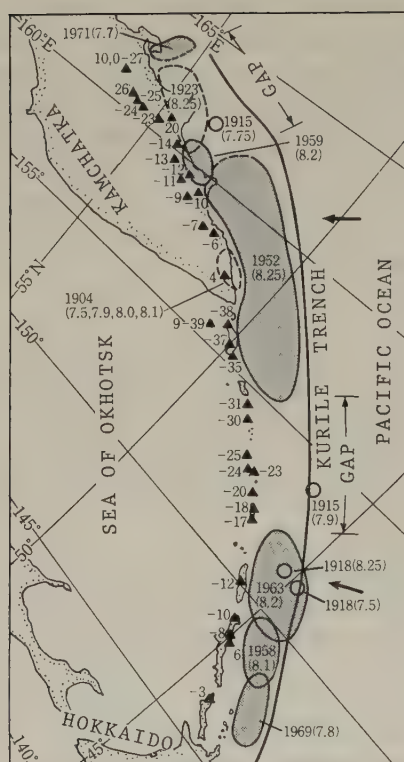


Fig. 1

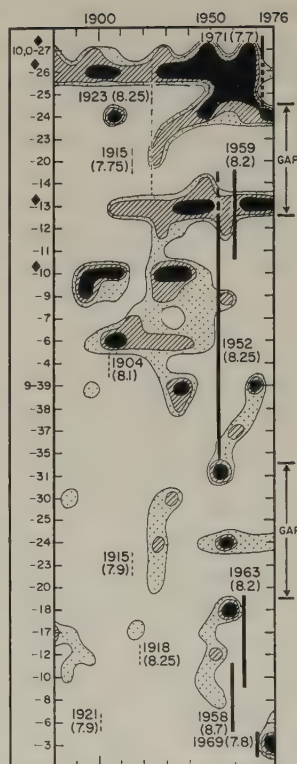


Fig. 2

Fig. 1. The spatial distribution of active volcanoes (closed triangle) and rupture zones of large interplate earthquakes in the Kurile-Kamchatka area. The reference numbers of active volcanoes are common with those in Fig. 2 and they were taken from the *Catalogue of the Active Volcano of the World Including Solfatara Fields*. The arrows show the direction of the slip vector between the oceanic and continental plates. Distribution of the rupture zones was mostly taken from KELLEHER *et al.* (1973). In preparation of this figure assistance was given by W. McCann.

Fig. 2. Relationship between eruptive activity and large interplate earthquakes in the Kurile-Kamchatka area. The numbers put in the left column represent volcanoes shown in Fig. 1. Rhombic symbols represent volcanoes having volcano observatories. The contoured dark areas represent eruptive activity of Grade 4, hatched areas Grade 3, stippled areas Grade 2 and blank areas Grade 1. The thick bars show the large earthquakes. Two thin broken lines show older earthquakes of 1904 and 1923 events and others are ones of which rupture zones have not been determined. The magnitude is shown in the parenthesis.

Elongation of the rupture zone along the axis perpendicular to the direction of the relative slip vector is projected to the volcanic zone parallel to the direction of relative slip vector between plates. And the elongation of the bar in the figure represents how many volcanoes the rupture zone includes in the direction of the relative slip vector. Therefore the lengths of the bars do not show the real length of the rupture zones.

5. Results

5.1 Kurile-Kamchatka

Eight rupture zones of large earthquakes were determined in the Kurile-Kamchatka area (Fig. 1). Two seismicity gaps are recognized in the areas between the ruptures of 1952 and 1963 events, and between those of 1952 and 1971. Increased eruptive activity prior to the six shocks is seen in the landward areas of four rupture zones: except two events of 1904 and 1969 (Fig. 2). Eruptive activity decreases after the shocks.

Significant activity prior to the 1971 shock ($M=7.7$) was recorded in the three volcanoes along the northern Kamchatka Peninsula: Sheveluch (10, 0-27), Kliuchevskoi (10, 0-26) and Bezymiany (10, 0-25). These three volcanoes shown in Fig. 1 appear not to be in the direction of slip vector; however, it is possible that the rupture zone extends to the south as shown by KELLEHER *et al.* (1973). The southern neighbouring volcano Plosky Tolbachik (10, 0-24), which stands in the area landward of the seismicity gap has shown significant eruption since 1975 after the shock of 1971. Eleven volcanoes had increased their activities since the 25 years prior to the 1952 shock. Avachinsky (10, 0-1) and Alaid (9-39) especially showed significant eruptions. A new impetus towards the studies of Kamchatka volcanoes was provided by the eruption of Avachinsky during 1926-27. This eruption prompted the Geological Committee and the Academy of Sciences of the U.S.S.R. to organize a systematic study of Kamchatka volcanoes (TOMKEIEFF, 1949). Then the eruption of 1937-38 was investigated in detail. Three powerful eruptions with lava-flows occurred in 1938. A great amount of andesitic ash was ejected as a result of strong explosive eruption on February 25, 1945. A new island called Taketomi, was born during the eruption of 1933-34 near Alaid Volcano. Later, the island was connected to the main island by a sand bar. As the main summary pattern shows, the eruptive activity landward of the rupture zones had increased prior to the great shocks in the Kurile-Kamchatka area, and after those shocks eruptive activity had increased in the vicinity of the landward extensional areas of seismicity gaps. And then great earthquakes occurred in those gaps. Spatial migration of the pattern of eruptive activity was consistent with that of seismicity.

There also exists another pattern. Volcanoes, Tiatia (9-3) and Karymsky (10, 0-13) erupted after the shock of 1959 ($M=8.2$) and of 1969 ($M=7.8$), respectively.

5.2 Northeastern Japan

SENO (1978) divided the northeastern Japan into some provinces of which the boundaries are parallel to the relative slip vector of plates and are located between rupture zones of large interplate earthquakes (M or $M_s \geq 7.7$) since 1938 event (Fig. 3). Rupture zones of large interplate earthquakes during 1880-1937 are also largely located in those provinces.

Nine rupture zones of interplate earthquakes have been determined since 1880 in the northeastern Japan including the southern Kanto region. Marked correlation between eruptive activity and seismicity are seen in this area, too (Fig. 4). But one can find a somewhat different pattern from that of the Kurile-Kamchatka area by a careful inspection of the figures. At first glance, the distribution pattern of the rupture zones in the northeastern Japan is more complicated and each rupture zone is smaller than that in the Kurile-Kamchatka area, and that the rupture zones are located farther from volcanoes than in the Kurile-Kamchatka area.

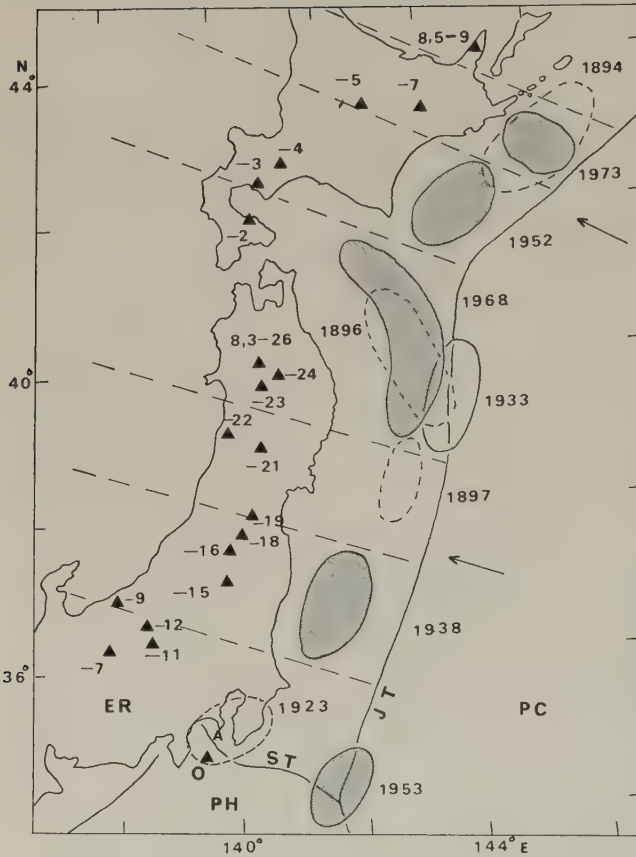


Fig. 3

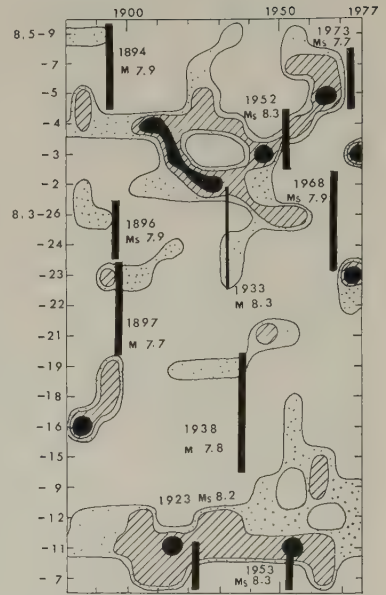


Fig. 4

Fig. 3. The spatial distribution of active volcanoes (triangle) in the northeastern Japan during the period between 1880 to 1977. The shaded areas show the rupture zones of the large interplate earthquakes during the period, and the land area is divided into zone six along the lines parallel to the direction of the slip vectors of the interplate earthquakes (SENO, 1977a, 1978). Open circles drawn by broken lines show older rupture zones of large interplate earthquakes. The open circle with the solid line shows the 1933 Sanriku earthquake. Arrows represent the directions of slip vectors between plates. JT, Japan trench; ST, Sagami trough; ER, Eurasian Plate; PH, Philippine Sea Plate; PC, Pacific Plate; A, Aburatsubo; O, Oshima Volcano.

Fig. 4. Relationship between eruptive activity and the large interplate earthquakes (thick bar) in the northeastern Japan. The thin bar indicates intraplate shock. Pattern symbols are common with those of Fig. 2.

As a result, four out of the nine events were accompanied with eruptive activity of Grade 4, from 3 to 16 years before the great events in preseismic stages. The remaining five shocks may be regarded as showing eruptive increases in preseismic stages although activity is lower than Grade 4. Events showing eruptive activity of Grade 4 succeeded by the large interplate earthquakes are as follows: Mt. Usu (8, 5-3) erupted in 1944 and 1945, forming new volcanic mountain Showa-shinzan. Then the Tokachi-Oki earthquake of $M_s=8.3$ occurred in 1952. Then eruptive activity increase shifted to both areas, north and south from Usu Volcano. At north, Tokachi (8, 5-5) showed strong eruption in 1962

and then the Nemuro-Oki earthquake of $M_s=7.7$ occurred in 1973. In the south, there occurred no major eruptions, but eruptive activity of Akita-yake-yama (8, 3-26) increased, and then the Tokachi-Oki earthquake of $M_s=7.9$ occurred in 1968. After the shock, eruptive activity increased at the neighbouring areas of the rupture zone: the major eruptions of Mt. Usu in the north and Akita-komaga-take in the south. A major eruption occurred at Asama (8, 3-11) in 1913 when the bottom-floor of the summit crater rose up, and then the great Kanto earthquake occurred in 1923. The Boso-Oki earthquake was followed from the significant eruption of Asama Volcano in 1950 when the bottom-floor of the crater also rose up.

Evidence below Grade 4 in eruptive activity shows the relation between eruptive activity and seismicity as follows. The increased activity of Siretoko-iwo-zan (8, 5-9) and Tokati succeeded the large shock of 1894 ($M=7.9$). Then an increase in the eruptive activity of Komaga-take (8, 5-2) and Akita-yake-yama occurred prior to the 1896 shock ($M=7.7$). An increase in the eruptive activity of Akita-komaga-take (8, 3-23) occurred following the 1897 shock. A new fault was generated at the 1897 shock at Akita-komaga-take. Eruptive activity increased at Zao (8, 3-19) resulting in the large shock of the 1938 Fukushima-Oki earthquake ($M_s=7.8$).

In 1929 the great eruption of Komaga-take occurred succeeding the 1933 Sanriku earthquake of $M=8.3$. This eruption may have brought on the 1933 Sanriku earthquake, though it is not an interplate event and is regarded as a normal fault type of a great intra-plate shock in the oceanic lithosphere (KANAMORI, 1971).

In summary, a tendency occurs showing that eruptive activity increases prior to large interplate earthquakes and that the increased eruptive activity migrates to adjacent areas, in the northeastern Japan as well as in the Kurile-Kamchatka area.

6. Summary and Discussions

In total, seventeen large interplate earthquakes were treated in the northwestern Pacific marginal region from the Kamchatka via Kurile to the northeastern Japan. Mostly all the events showed specific spatial and temporal correlation with volcanic activity. The correlation for these events are divided into three patterns according to the preseismic or postseismic events.

In the first case—as the main pattern in the studied area—the following regularity is found. Eruptive activity in the vicinity of a landward direction to a rupture zone increased prior to a large interplate earthquake. The direction is roughly parallel to that of slip vector between the oceanic lithosphere and the continental lithosphere. Activity usually ceased after the shock. However, activity usually increases in the adjacent areas behind the seismicity gaps after the shock. This was the case in fifteen out of the seventeen events (88%). The time of increasing eruptive activity preceding the shocks varies from 2 to 27 years depending on the kind of the shocks (Table 1). Most of these shocks were thrust type, interplate earthquakes.

The second case indicates the increase of eruptive activity following the shocks over the long-term. In general, increases in eruptive activity after the shock occur in the vicinity neighbouring the area landward of the rupture zone and parallel to the direction of the slip vector. However, some cases show increased eruptive activity just landward of the rupture zones. Such cases have been seen in the 1923, 1959 and 1969 shocks in the Kurile-Kamchatka.

Table 1. Examples of the preseismic eruptions and earthquakes showing good correlation between both phenomena.

Catalogue No.	Volcano	Volcanic eruption			→			Earthquake	
		Date of start	Mode of eruption	Distance* (km)	Interval** (Year)	Date	M		
Kurile-Kamchatka	Kliuchevskoi	1896 XII	O ↑ ↗	80	27	1923 II 3	8.25		
	Avachinsky	1926 III 28	O ↑ ↗ ↗ ↗	10	26	1952 XI 4	8.25		
	Kudriav	1946	↑ ?	60	12	1958 XI 6	8.7		
	Karymsky	1935 I	O ↑ ↗	20	24	1959 V 4	8.2		
	Goriashaia	1944 ?	↑	80	19 ?	1963 X 13	8.2		
	Sheveluch	1944	O ↑ △ △	80	27	1971 XII 15	7.7		
Northeast Japan	Siretoko-iwozan	1876 IX 23	O ∞ ↑	120	18	1894 III 22	7.9		
	Akita-yake-yama	1887	↑ ?	220	9	1896 VI 15	Ms 7.9		
	Akita-komaga-take	1890		300	2	1897 VIII 5	7.7		
	Asama	1913	↑ △	150	16	1923 IX 1	Ms 8.2		
	Komaga-take	1929 VI	O ↑ ↗	380	4	1933 III 3***	8.3		
	Zao	1918		130	20	1938 XI 5	Ms 7.8		
	Usu	1943 XII 27	O ↑ △	250	8	1952 III 4	Ms 8.3		
	Asama	1950	↑	320	3	1953 XI 26	Ms 8.3		
	Akita-yake-yama	1948		190	20	1968 V 16	Ms 7.9		
	Tokat	1962 VI	O ∞ ↑	190	11	1973 VI 17	Ms 7.7		

* Distance from a volcano to a rupture zone.
** Time interval from start of an eruption to seismicity.
*** Intraplate earthquake.

Table 2. Examples of the large interplate earthquakes and post-shock eruptions.

Earthquake		→		Volcanic eruption		Mode of eruption
Date	M	Distance (km)	Interval (Day)	Date of start	Catalogue No.	
Kurile Kamchatka 1952 XI 4	8.25	20	1	1952 XI 5	9-35	↑
		50	8	1952 XI 12	9-31	↑
		100	-3 ≤ ≤ 26	1952 XI	10,0-13	↑
		160	26 ≤ ≤ 57	1952 XII	10,0-14	↑
NE Japan 1973 VI 17*	Ms 7.7	140	27	1973 VII 14*	9-3	↑
		310	189	1894 X 17	8,5-4	↑

* Relation between the 1973 Nemuro-Oki earthquake and eruption of Tiatia in 1973 was taken from NAKAMURA (1975).

In addition to the long-term correlations described so far in this paper, some short-term relationships may be recognized between eruptions and interplate earthquakes. That is, some eruptions occur at almost the same time with the shocks, usually immediately after them (Table 2). In the Kurile-Kamchatka area some volcanoes erupted in the same year as the shocks of 1952. Two volcanoes in the vicinity of the southern end of the landward area erupted in the same year as the 1952 shock. It is impressive that one of them, Karpinsky (9-35), exploded in November 5, 1952, just a day after the shock on November 4, 1952; its only eruption record in history. Another volcano, Krenitzyn (9-31), erupted in the vicinity of the southern edge of the rupture zone. Its eruption, too, was the first and only one up to the present time. A major eruption causing a lava-dome started on November 12, 1952, a week after the 1952 shock. Two other volcanoes erupted in the vicinity of the northern edge of the rupture zone of the 1952 shock, though they do not seem to be major eruptions. In the northeastern Japan, a few volcanoes erupted immediately after the shocks. For example, following the earthquake on March 22, 1894, Tarumai (8, 5-4) erupted on October 17, 1894. We found that most of the example occurred in the vicinity at the edge of the landward areas of the rupture zones. Figure 5 shows the short-term, time-space relationship between large interplate earthquakes and postseismic eruptions. This shows that the volcano nearest the rupture zone erupted after seismicity in earlier time and the farthest one erupted at a later time. This suggests that there exists tectonic relation between both phenomena. This means that the eruptions which occurred just after the large interplate earthquakes, may, theoretically, be explained in the following way: the magma chamber is instantaneously compressed by the seismic wave, and as the inner pressure of the conduit increases, the magma is squeezed up to erupt when the magma chamber has reached the critical condition for eruption.

A long-term relationship between eruptions and large interplate earthquakes can also be observed in other areas, such as at Izu-Bonin. Data, however, are less reliable in that area where many volcanoes are located far from the main land and many of these under water. Also, the shock areas of the earthquakes have not yet been fully determined. A great but deep earthquake with a magnitude of 7.9 occurred in the northern area in 1907. The rupture zone has not yet been fully inspected, but the landward terrain of the shock area clearly covers at least two volcanoes, Bayonnaise Rocks and Tori-sima. Before the shock, a new volcanic island was born in the 1896 eruption in the vicinity of Bayonnaise Rocks, and then a violent eruption took place at Tori-sima that destroyed the central summit and killed 125 persons in 1902. Five years after that eruption, in 1907, a great shock occurred, then the eruptive activity in the area ceased. In 1933, a deep and great earthquake of $M=8.0$ occurred again in that vicinity. In this case, Tori-sima erupted severely, causing lava to flow after the shock. As a result, a new summit was formed in 1939, 6 years after the shock. Subsequently, the new volcanic island Myojinsho was formed during 1946-53 around Bayonnaise Rocks from the eruption. After that, activity in the area decreased. Activity has again increased around Bayonnaise Rocks since 1970. In addition to that, new activity has occurred near the Bonin Islands. Nishinoshima-shinto, as it has been named, was formed by the eruption during 1973-74. A deep but great earthquake with a magnitude of 7.8 occurred in the vicinity of those volcanoes on March 7, 1978. A correlation between the shock and volcanic activity in the vicinity had been expected.

The existence of long-term correlation between eruptive activity and large interplate seismicity has been recognized around Pacific areas by the author (KIMURA, 1978a,b).

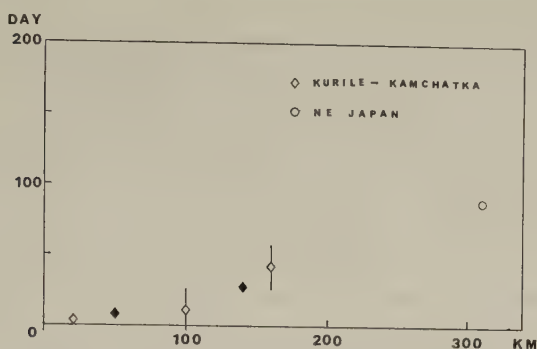


Fig. 5. The post-shock eruption showing short-term relation to large interplate earthquakes. The rhombic symbols represent volcanoes in the Kurile-Kamchatka and the circle does those in the north-eastern Japan, and the closed symbols show major eruptions and the open ones ordinary eruptions. The length of the bar shows the range of the error. Data were taken from Table 2. The ordinate represents the time interval from an eruption to an earthquake, and the abscissa does distance from the volcano to the concerned rupture zone.

For a long period, observations have been made in the vicinity of the Sagami trough area. Previous workers have already suggested a strong correlation between major eruptions of Oshima Volcano and the large interplate earthquakes along the trough (NAKAMURA, 1971; KANAMORI, 1972; KIMURA, 1973). Indeed, 11 years prior to the shock of the 1923 great Kanto earthquake, the bottom-floor (basaltic magma head) of the Mihara-yama's summit crater in Oshima Volcano rose more than 400 m, and a great eruption took place in Mihara-yama during 1912-14. Since then the bottom of the crater had remained at the high level and then went rapidly down after the shock of 1923. A similar change took place at the crater bottom at the time of the 1953 Boso-Oki earthquake (NAKAMURA, 1971). Both shocks occurred along the Sagami trough, which is considered to be the boundary between two plates: the Philippine Sea and Eurasian Plates (Fig. 3). Comparing the level change of the magma head with the vertical crustal movement at Aburatsubo facing the Sagami trough shows that the magma rose when the crustal strain accumulation was at its maximum. In another words, the long-term level change of the bottom is inversely correlated with that of the land of Aburatsubo located on the continental side of the trough (KIMURA, 1976). These findings suggest that the increased compressional crustal stresses caused by the convergent Philippine Sea Plate squeeze up the magma beneath Mihara-yama until an interplate large earthquake occurs to release the strain along the trough. In 1974 the authors observed a 100-m elevation of the crater-floor of Mihara-yama (KIMURA and TOYODA, 1975). This implies that strain was accumulating there after the 1953 Boso-Oki earthquake.

Figure 6 shows the long-term relationship between eruptions and earthquakes in the Kurile-Kamchatka and in northeastern Japan. The most significant eruption was chosen as an indicator of increased eruptive activity preceding a large interplate earthquake. Here again we can see a fairly good time-space correlation. The figure reveals

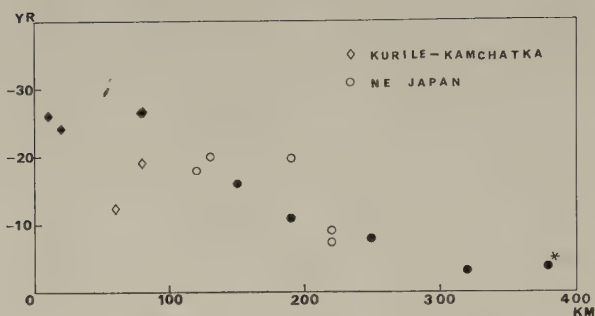


Fig. 6. Eruptions which preceded to the large inter-plate earthquakes in the northwestern Pacific margin. Period shown by years (ordinate) is the interval from the starting time of concerned eruptive activity increase to the occurrence of the large earthquake. Distance shown by kilometers (abscissa) is from the rupture zone to the volcano. Closed rhombuses and circles show the major eruptions and open ones ordinary ones. Data were taken from Table 1. * 1933 Sanriku earthquake.

that when a shock area is located close to a volcano, significant eruptive activity starts early, and when the shock area is farther from the volcano, it starts later. For example, many volcanoes started their major activities between the 12th and 27th year (at the average of the 23rd year) prior to the typical great earthquakes in the Kurile-Kamchatka. On the contrary, many cases show that eruptive activity increases started between the 2nd and 20th year (at the average of the 12th year) prior to the shocks in the northeastern Japan. Such difference may be explained by the fact that the seismicity rupture zones are closer to the concerned volcanoes in the Kurile-Kamchatka than those in the northeastern Japan. If the stress concentration starts at the proposed future rupture zone, then it migrates toward the inside of the continental lithosphere. If this is true, the variation of time-interval from an eruption to an earthquake shows the difference of the migration time of compressive crustal strain from the proposed rupture zone to the volcano. For example, if the volcano is located close to the proposed rupture zone, the needed strain will accumulate in a shorter time. Consequently the major eruption will occur at an earlier time. Therefore, this evidence suggests a tectonical relation between eruptions and earthquakes in the arcs.

Based on the volcanological and seismological data, it has been suggested that the volcanic frontal areas of island arcs in the northwestern Pacific margin are under horizontal compressive stresses in the direction of plate convergence (NAKAMURA, 1977; NAKAMURA *et al.*, 1977). Furthermore, it has been said that such features as a distribution of preseismic and postseismic activities are present which correspond to a mode of strain accumulation in the land area in the southwestern Japan; i.e., the area contracts toward the landward direction of the rupture zone in the direction of the plate motion during the interseismic event (SENO, 1977b). Intraplate earthquakes of a magnitude of 6 or greater started to increase from about 50 years before the occurrence of large interplate earthquakes in the continental lithosphere landward of the rupture zones in the northeastern Japan (SENO, 1978). The long-term distribution of the eruptive activity in the preseismic stages in the

northwestern Pacific margin is consistent with the mode of occurrence of interplate earthquakes in Japan. The contractional strain accumulated during long periods preceeding large interplate earthquakes can cause the squeezing up of magmas and increased eruptive activity in the arcs. The compressive strain will be released by large interplate earthquakes. The eruptive activity ceases or remarkably decreases after the events, due to the stress drop in the continental lithosphere. Increased eruptive activity in the vicinity of the seismicity gaps may be explained by increased crustal contractional stresses after the large earthquakes. Eruptions of Mt. Usu since 1977 may be due to the contractional stress concentration after the 1968 and 1973 shocks in the northeastern Japan. Akita-komaga-take and Tyokai (8, 3-22) also showed significant eruptions after the large shock of the 1968 Sanriku earthquake.

It is also true that some volcanoes erupt after large earthquakes. In the future, detailed research is needed to see if it is possible to explain such an occurrence in terms of the distribution of tectonic stresses that depend on the geographical locations of both events. And the findings of definite relationship between eruptions and earthquakes will be valid for predicting major eruptions and large interplate earthquakes along arcs.

7. Conclusions

1) There are three significant patterns showing a relationship between eruptive activities and the large interplate earthquakes in the northwestern Pacific margin. The first is a long-term relationship showing that eruptive activity increases in the preseismic stages of large earthquakes in directional areas parallel to the relative slip vector of oceanic lithosphere, landward of the shock areas. The increase in eruptive activities begins in an average of about 10 years in the northeastern Japan and in an average of about 20 years in the Kurile-Kamchatka prior to the seismicity. This is the main pattern in the arc areas. In most instances, this case shows that the activity increase occurs at the adjacent areas landward of the seismicity gaps.

2) The second also shows that in the long-term relationship between volcanism and seismicity eruptive activity increases after the shocks, in a few cases. This is the second significant pattern.

3) The third pattern reveals that specific eruptions, which usually are not major ones, occur immediately after the shocks, mostly within a year. One explanation for the postseismic eruptions may be provided by the seismic shocks.

4) The major patterns in the long periods are regarded as reflecting the distribution of regionally accumulated crustal strain which may be generated by the plate motions.

I wish to express my gratitude to Professor L.R. Sykes for his encouragement and discussions. I also thank K.H. Jacob, T.L. Johnson, Y.P. Aggarwal and K.Y. Chun for helpful suggestions at various stages of preparation. I benefited greatly from discussions held with S.A. Fedotov, P.I. Tokarev and S. Nagumo. I am grateful to K. Nakamura for giving me information on the bibliography of the volcanological data over the studied areas. I also thank T. Seno for giving me Japanese seismological data. Thanks are due to W. McCann for providing me with seismological data. His assistance was very useful in writing the manuscript. This paper was critically reviewed by T. Higa and J. Reid. Observations of Mihara-yama's crater were supported by member of Kantoken Jishinyochi-chosa Group (K.J.G.). Most of this work was done while I was at Lamont-Doherty Geological Observatory of Columbia University as a recipient of the visiting researcher award from the Japanese Science and Technology Agency.

REFERENCES

- BLOT, C., Relations entre séismes profonds et les éruption volcaniques au Japon, *Bull. Volcanol.*, **28**, 25–63, 1965 (in French).
- BLOT, C., Volcanism et séismes du manteau supérieur dans l'Archipel des Nouvelles-Hébrides, *Bull. Volcanol.*, **36**, 446–561, 1972 (in French with English abstract).
- KAMINUMA, K., Correlation between volcanic and seismic activities in Kyushu, Japan, *Publ. for the 50th Anniversary of the Great Kanto Earthquake, 1923*, pp. 185–197, Earthquake Res. Inst., Tokyo Univ., 1973 (in Japanese with English abstract).
- KANAMORI, H., Seismological evidence for a lithospheric normal faulting—The Sanriku earthquake of 1933, *Phys. Earth Planet. Inter.*, **4**, 289–300, 1971.
- KANAMORI, H., Relation between tectonic stress, great earthquakes and earthquake swarms, *Tectonophysics*, **14**, 1–12, 1972.
- KELLEHER, J., L.R. SYKES, and J. OLIVER, Possible criteria for predicting earthquake location and their application to major plate boundaries of the Pacific and Caribbean, *J. Geophys. Res.*, **78**, 2537–2585, 1973.
- KIMURA, M., A study for prediction of great earthquakes in and around Sagami Bay, *J. Geogr.*, **82**, 171–188, 1973 (in Japanese with English abstract).
- KIMURA, M. and J. TOYODA, Recent level change of the bottom-floor in the summit crater of Mihara-yama, Oshima Island, Japan, *Bull. Volcanol. Soc. Jpn.*, **20**, 66–78, 1975 (in Japanese with English abstract).
- KIMURA, M., Major magmatic activity as a key to predicting large earthquakes along the Sagami trough, Japan, *Nature*, **260**, 131–133, 1976.
- KIMURA, M., *Relation between Eruptions and Large Earthquakes*, 187 pp., Univ. Tokyo Press, Tokyo, 1978a (in Japanese).
- KIMURA, M., Volcanism and seismicity in the Kyushu and Ryukyu Islands areas, *Geological Studies of the Ryukyu Islands*, Vol. 3, pp. 181–187, 1978b.
- LATTER, J.H., The interdependence of seismic and volcanic phenomena: Some space-time relationship in seismicity and volcanism, *Bull. Volcanol.*, **35**, 127–142, 1971.
- MACGREGOR, A.G., Prediction in relation to seismo-volcanic phenomena in the Caribbean volcanic arc, *Bull. Volcanol.*, **8**, 69–85, 1949.
- NAKAMURA, K., Volcano as a possible indicator of crustal strain, *Bull. Volcanol. Soc. Jpn.*, **16**, 63–71, 1971 (in Japanese with English abstract).
- NAKAMURA, K., Volcano structure and possible mechanical correlation between volcanic eruption and earthquakes, *Bull. Volcanol. Soc. Jpn.*, **20**, 229–240, 1975 (in Japanese with English abstract).
- NAKAMURA, K., Volcanoes as possible indicators of tectonic stress orientation—principle and proposal, *J. Volcanol. Geotherm. Res.*, **2**, 1–16, 1977.
- NAKAMURA, K., *Volcano*, 228pp., Iwanami, Tokyo, 1978 (in Japanese).
- NAKAMURA, K., K.H. JACOB, and J.N. DAVIES, Volcanoes as possible indicators of tectonic stress orientation—Aleutian and Alaska, *Pageoph.*, **115**, 87–112, 1977.
- SENO, T., The instantaneous rotation vector of the Philippine Sea Plate relative to the Eurasian Plate, *Tectonophysics*, **42**, 209–226, 1977a.
- SENO, T., Pattern of intraplate seismicity in southwest Japan before and after great earthquakes, *Tectonophysics*, 1977b (in press).
- SENO, T., Intraplate seismicity in Tohoku and Hokkaido, northern Japan, and a possibility of a large interplate earthquake off the southern Sanriku coast, *J. Phys. Earth*, 1978 (in press).
- SUWA, A., *Eruptions in Japanese Islands*, 221 pp., Kodan-sha, Tokyo, 1970 (in Japanese).
- TOKAREV, P.I., On the focal layer, seismicity and volcanicity of the Kurile-Kamchatka zone, *Bull. Volcanol.*, **35**, 230–242, 1971.
- TOMKEIEFF, S.I., The volcanoes of Kamchatka, *Bull. Volcanol.*, **8**, 87–113, 1949.
- YOKOYAMA, I., Volcanic eruptions triggered by tectonic earthquakes, *Bull. Geophys. Inst., Hokkaido Univ.*, **25**, 129–139, 1971 (in Japanese with English abstract).

A MECHANISM TO EXPLAIN THE EARTHQUAKES AROUND JAPAN BY THE PROCESS OF PARTIAL MELTING

Masami HAYAKAWA and Susumu IIZUKA

Faculty of Marine Science and Technology, Tokai University, Shizuoka, Japan

(Received May 31, 1978; Revised September 13, 1978)

Partial melting at the hypocentral depths (30 to 40 km) is closely related to great earthquakes occurring in comparatively high heat flow zones such as the sea just south off the southwestern Japan. It is obvious from the thermal gradient curves in such high heat flow zones that temperature at the hypocentral depths approaches the melting point of wet peridotite. Under such circumstances the partial melting proceeds by the effect of some pressure decrease or temperature increase associated with the huge tectonic force acting on the rocks. The partial melting will yield some increase in volume. Consequently some stresses will be originated and added to the tectonic forces due to the mantle convection and other origins to trigger earthquakes. Changes in seismic wave velocities owing to the partial melting is calculated in this paper using the Lindemann's equation based upon the Debye's theory of specific heat.

1. *Great Earthquakes in High Heat Flow Zones, and the Possibility of Partial Melting in These Hypocentral Depths*

In the great inter-plate earthquakes off Japan with hypocentral depth of 30–40 km, the subduction of the Pacific plate will act to drag down the margins of the main Japanese islands as part of the overlying plate. These great earthquakes are said to occur in the low heat flow zones. In this paper, we first question if this is always true or not.

To examine this problem, we put the locations of epicentral areas on the heat flow maps (Fig. 1, HAYAKAWA and IIZUKA, 1976). From this figure, it is clear that the great earthquakes have not always taken place only in the low heat flow zones. The Kanto (1923, "A" in Fig. 1), Enshunada (1854, "B"), Tonankai (1944, "C"), Nankaido (1946, "D") and Hyuganada (1968, "E") earthquakes, all of them of the order of $M=8$, took place in comparatively high heat flow zones of 2.0 HFU or more beneath the Philippine Sea just off Japan in the southwestern half of the Japanese islands.

On the other hand, the major earthquakes occurring beneath the Pacific Ocean just off the northeastern half of Japan are located in abnormally low heat flow zones averaging 1.0 HFU. Nevertheless, it is still worthy of note that the depths of hypocenters in this area have been located at depths greater than those of the great earthquakes in the southwestern half of Japan. This means that even in the case of the earthquakes in the low heat flow zones, fairly high temperatures can be expected at the hypocentral depths. However, in this paper the main purpose is to explain the mechanism of the great earthquakes in high heat flow zones, therefore we shall leave this problem to some other chance.

The curves showing the relation of temperature with pressure and the depth are given in Fig. 2 with melting temperature data (HAYAKAWA and IIZUKA, 1976). In this figure M.T. means the melting temperature of wet peridotite, while (M.T.) shows the melting

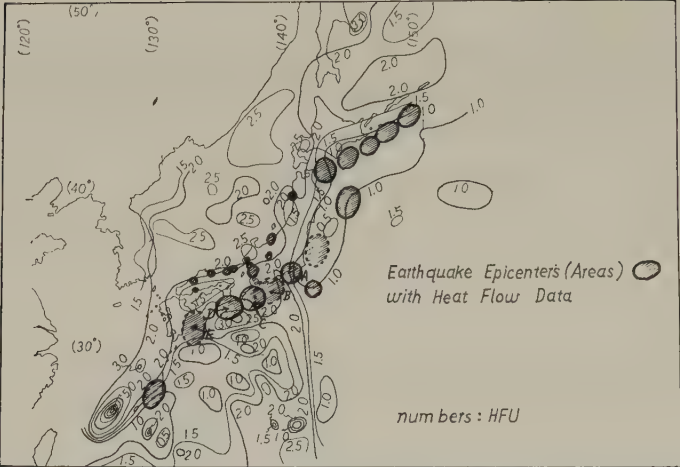


Fig. 1. Locations of epicentral areas on the heat flow maps around Japan. Heat flow data by Uyeda *et al.* are included in Ref. (HAYAKAWA and IZUKA, 1976).

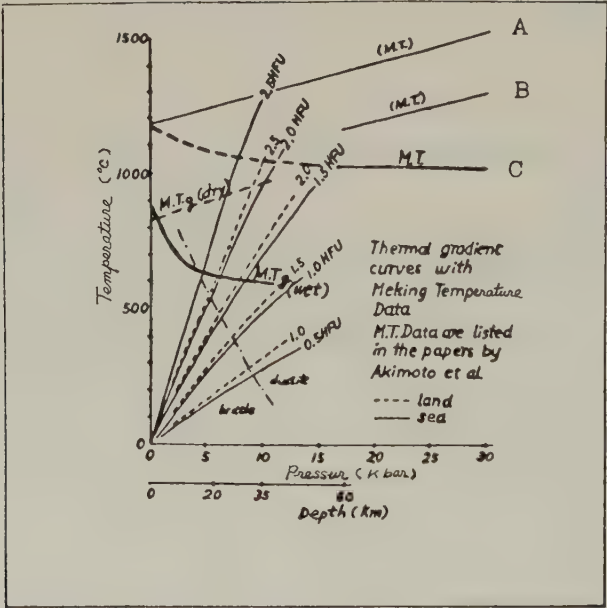


Fig. 2. Curves showing the relations of temperature against pressure and the depth. Melting data are also shown. M.T. data by Akimoto *et al.* are included in Ref. (HAYAKAWA and IZUKA, 1976).

temperature of dry peridotite. In the case of granite, the melting temperature M.T.g is lower than M.T.

Let us consider some examples. In the case of the earthquakes of Kanto, Enshunada, Tonankai, Nankaido and Hyuganada, the depths of hypocenters are roughly 30 km, and the heat flow values recorded on the sea floor are 1.5–2.5 HFU, therefore from the thermal

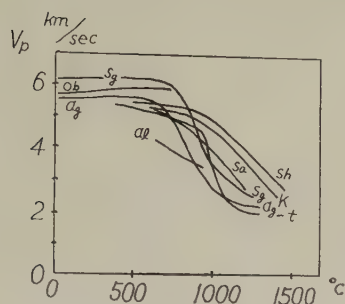


Fig. 3. Change in the longitudinal wave velocity with temperature increase. Refer to Refs. (IDE, 1937; KUMAZAWA *et al.*, 1964; MURASE and SUZUKI, 1966). ag, Asahi glass; t, lava of Volc. Tarumae; sa, lava of Volc. Sakurajima; sh, lava of Volc. Showashinzan; ob, obsidian; sg, silica glass; al, alkali silicate.

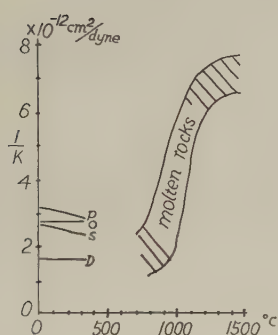


Fig. 4. Relation between the reciprocal of incompressibility and temperature. Refer to Refs. (BIRCH *et al.*, 1942; MURASE and SUZUKI, 1966; MURASE and MCBIRNEY, 1973). p, pyrex glass; o, obsidian; s, silica glass; D, diabase glass.

gradient curves, it is obvious that the temperature in the hypocentral zone will approach the melting points of wet peridotite. Under such circumstances, partial melting will be possible in the hypocentral zone, assuming that there is some pressure decrease or temperature increase due to the existence of the huge force acting on the rocks.

The partial melting will yield some volume increase. Consequently, some stresses will be originated, and such forces will be added to the original forces due to the mantle convection, causing earthquakes to take place. This idea was first presented by T. Matsuzawa (MATSUZAWA, 1964). During the time elapse through dilatancy, partial melting and partial recovery, the velocity of longitudinal and transverse waves and the ratio of these velocities will change.

2. Calculation of Changes in Seismic Wave Velocities Due to the Partial Melting

Let us consider the matters explained above a little more in detail in the following. The changes of seismic wave velocities can be obtained by synthesizing the following experiments. Namely, concerning the change in the longitudinal wave velocity with temperature, there have been many experiments as seen in Fig. 3 (IDE, 1937; KUMAZAWA *et al.*, 1964; MURASE and SUZUKI, 1966). In Fig. 4 (MURASE and SUZUKI, 1966; MURASE and MCBIRNEY, 1973; BIRCH *et al.*, 1942), the reciprocal of incompressibility K is drawn on the ordinate, and the temperature on the abscissa.

Putting the average values from Figs. 3 and 4 into Eq. (1) and by solving the simultaneous equations (1) and (2) assuming density value ρ , the transverse wave velocity can be obtained, as seen in Fig. 5. Consequently the ratio between the longitudinal and transverse wave velocities can be obtained.

$$V_p = \sqrt{\frac{K + \frac{4}{3}\mu}{\rho}}, \quad (1)$$

$$V_s = \sqrt{\frac{\mu}{\rho}}. \quad (2)$$

Above experiments were made under nearly atmospheric pressures. Here, let us look at the relation of seismic wave velocities and pressure under room temperature. One of these experiments is seen in Fig. 6 (NAGUMO, 1962). As the pressure increases, the curves become flat. By taking the velocity increase with pressure into consideration, Fig. 5 can be modified as seen in Fig. 7, applying the dotted line of Fig. 6.

At this stage, let us consider the changes of seismic wave velocities under partial melting. For example, we take here the Green's experiment (Fig. 8, GREEN, 1972). This figure shows the plot of percentage of melt against temperature at approximately 15 kbar for pyrolite composition under anhydrous and hydrous conditions.

Now, it is clear and important that the solidus temperature for each material consisting pyrolite increases as the melt percentage increases. Converting these elements to the response of seismic wave velocities, let us apply here the Lindemann's equation between melting temperature and seismic wave velocities, which is based upon the Debye's theory on specific heat.

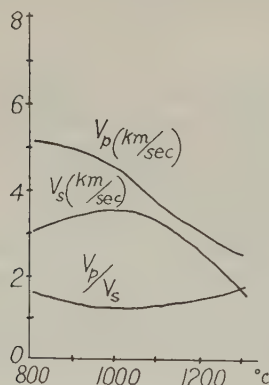


Fig. 5. Change of seismic wave velocities with temperature increase (1), obtained by combining the results of Figs. 3 and 4.

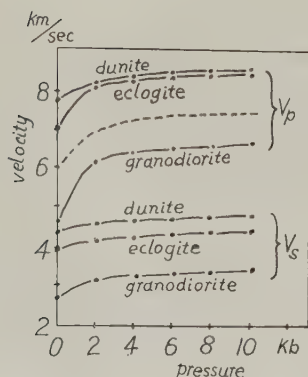


Fig. 6. Change of seismic wave velocities with pressure increase. Refer to Ref. (NAGUMO, 1962).

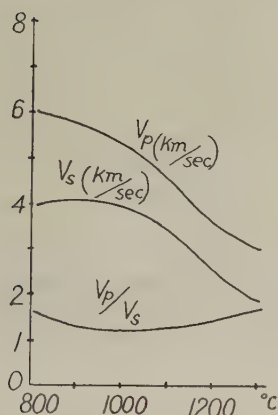


Fig. 7. Change of seismic wave velocities with temperature increase (2), taking the pressure effect into consideration.

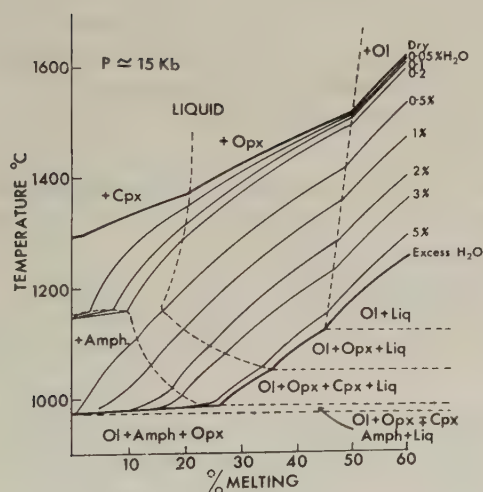


Fig. 8. Temperature increase against the progressive partial melting. Refer to Ref. (GREEN, 1972).

Lindemann's equation:

$$T_m = C \times M \times \frac{1}{\left(\frac{1}{V_p^3} + \frac{2}{V_s^3} \right)^{2/3}}$$

where T_m , C and M are melting temperature, constant and atomic weight of the material, and V_p and V_s are longitudinal and transverse wave velocities, respectively.

It is very clear that when the melting temperature increases, the denominator must decrease. Consequently V_p and V_s must increase. At a glance, it may seem queer that the velocity increases with melting, but after careful consideration, it is found reasonable, because the gradual increase of melting temperature corresponds to the solidus temperature increase for the different materials consisting of pyrolite. Now, applying these results, assuming the ratio of V_p to V_s is maintained, we find that the velocity change with temperature becomes high after the start of the partial melting as the solid lines in Fig. 9.

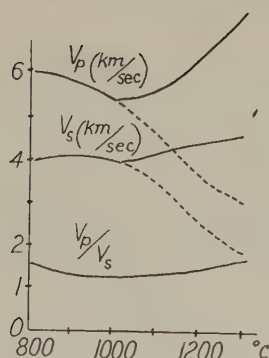


Fig. 9. Change of seismic wave velocities by progressive partial melting, based on the results of Fig. 8. The dotted lines are the same as in Fig. 7.

3. Consideration for the Velocity Change of the Bulk Which Contains the Melt Using Solid-Liquid Mixture Model

However, strictly speaking, in the above calculation, the effect of the seismic wave velocity of the melt was not taken into consideration, therefore let us consider here on the velocity of bulk which contains the melt by using a solid-liquid mixture model.

The total volume V can be written with the following equation,

$$V = V_s + V_l$$

where V_s and V_l are the volumes for solid and liquid parts, respectively. Assuming that all the pores are filled with liquid, the porosity n can be expressed with

$$n = V_l/V.$$

The bulk modulus K and density ρ of this media becomes

$$\frac{1}{K} = \frac{(1-n)}{K_s} + \frac{n}{K_l} \quad (3)$$

and

$$\rho = (1-n)\rho_s + n\rho_l \quad (4)$$

consequently, the longitudinal wave velocities for such mixed model, can be written as follows,

$$V_p = \sqrt{f(\sigma) \frac{K}{\rho}}, \quad V_{ps} = \sqrt{f(\sigma) \frac{K_s}{\rho_s}}, \quad V_{pl} = \sqrt{f(\sigma) \frac{K_l}{\rho_l}} \quad (5)$$

where V_p , V_{ps} , V_{pl} are the longitudinal wave velocities for the total, solid and liquid parts, respectively, and $f(\sigma)$ is written by

$$f(\sigma) = \frac{3(1-\sigma)}{1+\sigma} \quad (\text{GASSMANN, 1951}). \quad (6)$$

From Eqs. (3) and (5), the following equation is obtained,

$$\frac{1}{\rho} \cdot \frac{f(\sigma)}{V_p^2} = \frac{(1-n)}{\rho_s} \cdot \frac{f(\sigma)}{V_{ps}^2} + \frac{n}{\rho_l} \cdot \frac{f(\sigma)}{V_{pl}^2}.$$

In the numerical calculation of this equation, assuming the values of density and Poisson's ratio as

$$\rho_s = 2.9, \quad \rho_l = 2.6, \quad \sigma_s = 1/4, \quad \sigma_l = 1/2$$

then, from Eq. (6), the values for $f(\sigma_s)$ and $f(\sigma_l)$ become as follows

$$f(\sigma_s) = 1.8, \quad f(\sigma_l) = 1$$

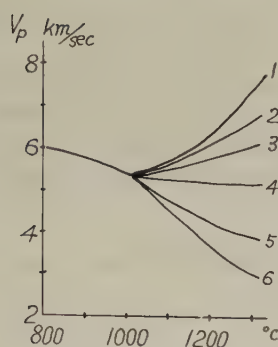


Fig. 10. Modified figure of Fig. 9, when the velocity of melt is taken into consideration. Refer to Ref. (IZUKA and HAYAKAWA, 1978).

consequently, $f(\sigma)$ can take the values between 1 and 1.8.

Under the circumstances before the partial melting starts,

$$n = 0, \text{ namely } f(\sigma) = f(\sigma) = 1.8$$

while for the total melt, $n=1$, namely $f(\sigma) = f(\sigma) = 1$.

Figure 10 shows the results of this calculation, that is the relation of longitudinal wave velocity and melting temperature with progressive partial melting. Curve 1 shows the velocity change in solid part, curves 2–5 show the velocity changes in the partial melting media in the case of $V_p=5, 4, 3, 2$ km/sec, respectively, and curve 6 corresponds to the experimental data as already shown with dotted line in Fig. 9.

This figure shows that the tendency obtained in the solid line of longitudinal wave velocity after partial melting starts in Fig. 9, will not contradict with the case when the velocity of the melt is taken consideration, unless the wave velocity in liquid part is very low as less than 3 km/sec.

4. A Mechanism to Explain the Great Earthquakes in High Heat Flow Zones Applying the Process of Partial Melting

If we suppose here that the area in question was under high temperature but slightly below the melting at the beginning, and the temperature has gradually increased to start the partial melting by diapirism or by the pressure decrease due to the dynamical force, the abscissa in Figs. 9 and 10 may correspond to the time elapse factor.

On the other hand, as the partial melting proceeds, the volume increases unless the rock has excess H_2O . We can, then, estimate the stress increase accompanied by the volume increase, and earthquakes will take place at slightly shallower part than this area. Of course, in this case, the direction of brittle fracture will be affected by the geological structures of the area.

It will be difficult to explain the occurrence of such earthquakes with focal depths of 30–40 km by only the dilatancy mechanism, since there will be some limits to the downward penetration of water. In contrast, the deeper the location of hypocenters, the more significant will be the thermal effect.

Comparing the mechanism of earthquake following the process of partial melting, with the velocity changes explained above, it can be thought as follows. Due to the time elapse, the longitudinal and transverse wave velocities, and the ratio of these velocities

first show the decrease, and then they show the recoveries and then, earthquake takes place at some stage.

We would like to continue this work quantitatively to make clear the mechanism of earthquake occurrences, which are related, in our opinion, not only with the dynamical force due to the plate subduction, but also with the thermodynamical elements, especially the process of partial melting of the uppermost mantle. We are also trying to find the practical field examples to make clear this relation.

We would like to express our thanks to Prof. S. Uyeda and Prof. K. Kobayashi for reading the manuscript and for valuable comments to improve it.

REFERENCES

- BIRCH, F., J.F. SCHAIRER, and H.C. SPICER (ed.), Handbook of physical constants, *Geol. Soc. Am. Spec. Pap.*, **36**, 39 and 87, 1942.
- GASSMANN, F., Elastic waves through a packing of spheres, *Geophysics*, **16**, 4, 1951.
- GREEN, D.H., Magmatic activity as the major process in the chemical evolution of the earth's crust and mantle, *Tectonophysics*, **13**, Upper Mantle Sci. Rep. No. 41, The upper mantle, 47-71, 1972.
- HAYAKAWA, M. and S. IIZUKA, A mechanism to explain the changes in V_p/V_s , *Zisin (J. Seismol. Soc. Jpn.)*, **29**, 339-353, 1976 (in Japanese with English summary).
- IDE, J.M., The velocity of sound in rocks and glasses as a function of temperature, *J. Geol.*, **45**, 689-716, 1937.
- IIZUKA, S. and M. HAYAKAWA, An effect of partial melting on seismic velocity changes, under printing (in Japanese with English summary), *J. Fac. Mar. Sci. Tech. Tokai Univ.*, 1978 (in press).
- KUMAZAWA, M., H. FURUHASHI, and K. IIDA, Seismic wave velocity of silicate melt under high temperature, *Kazan (Bull. Volcanol. Soc. Jpn.)*, **9**, 17-24, 1964 (in Japanese with English summary).
- MATSUZAWA, T., *Study of Earthquakes*, Ch. X, Thermodynamics of Earthquakes (Field Theory of Earthquakes), p. 213, Uno Shoten, Tokyo, 1964.
- MURASE, T. and T. SUZUKI, Ultra-sonic velocity of longitudinal waves in molten rocks, *J. Fac. Sci. Hokkaido Univ.*, Ser. VII, **2**, 273-285, 1966.
- MURASE, T. and A.R. MCBIRNEY, Properties of some common igneous rocks and their melts at high temperatures, *Geol. Soc. Am. Bull.*, **84**, 3563-3592, 1973.
- NAGUMO, S., On the elasticity of solid particle media, *Butsuri-Tankō (J. Soc. Explor. Geophys. Jpn.)*, **15**, 65-71, 194-197, 1962 (in Japanese with English summary).

THE FORMATION OF INTERMEDIATE AND DEEP EARTHQUAKE ZONE IN RELATION TO THE GEOLOGIC DEVELOPMENT OF EAST ASIA SINCE MESOZOIC

Yasumoto SUZUKI, Kisaburo KODAMA, and Takashi MITSUNASHI

Geological Survey of Japan, Tokyo, Japan

(Received July 18, 1978; Revised August 22, 1978)

The intermediate and deep earthquake zone comes into existence under the condition that the continental side upheaves and the oceanic side subsides, judging from the geologic development of East Asia including the Japanese Islands since the Mesozoic age.

The authors try an experiment by F.E.M. to examine the internal condition accompanied by the vertical movement in the deeper part of the earth and explain the geologic development of East Asia including the Japanese Islands and the earthquake zone.

1. Introduction

It has often been pointed out that the geologic development of East Asia was intimately related to that of the Japanese Islands (MINATO *et al.*, 1965). The intermediate and deep earthquake zone runs parallel to the island arcs and dips away from the trench toward the Asiatic continent. The tectonic and igneous activities of East Asia including the Japanese Islands since the Mesozoic took place parallel to the zone. These phenomena suggest that the geologic development of East Asia should be explained in relation to the intermediate and deep earthquake zone.

In this paper the authors propose a model to explain the formation of intermediate and deep earthquake zone in relation to the geologic development of East Asia since the Mesozoic age. They tried an experiment to explain the internal condition accompanied by vertical movement situated at deep place in the lower mantle beneath the region.

2. Geodynamic Process

The paleogeography during the Late Paleozoic period showed that marine geosynclinal environment prevailed on China and its adjacent areas, including the Japanese Islands (MINATO *et al.*, 1965). Then the sea regressed from East Asia toward east and south, and inland basins filled with thick nonmarine clastic sediments deposited there during the Mesozoic period. On the other hand, marine geosynclinal condition existed successively along the outer zone of the Japanese and Rhyukyu Islands. The transitional zone between them was in shallow marine, brackish and fresh water environments.

These movements were accompanied by intense volcanism of andesites, dacites and rhyolites, and intrusion of granitic rocks in the area from the inner zone of the island arcs to the East Asiatic continental region. The geosynclinal region along the outer zone of the island arcs were intruded by basalts and serpentinites.

Similar tectonic and igneous activities were repeated at the those areas throughout the Paleogene age.

In the middle of the Tertiary, intense faulting, which was accompanied by andesitic, dacitic and rhyolitic volcanisms occurred along the island arcs, and then geosynclinal subsidence took place. In the continental region, Neogene and Quaternary basins were formed and filled with nonmarine clastic sediments. Alkali olivine basalts intruded and flowed out on the area from the inner zone of the island arcs to the continental region.

In the Quaternary age, the island arcs began to uplift into mountain ranges and volcanic zones appeared there.

Sedimentary basins which have been formed in the continental region of East Asia since the Mesozoic age are characterized by very large and gentle undulated structures which are steeply inclined and often cut by thrust faults along their margins. On the other hand the island arcs region is marked by steep folds and thrust faults.

As is well known, the intermediate and deep earthquake zones run parallel to the island arcs and dip away from trenches toward the continent. The Mesozoic and Cenozoic crustal movements and igneous activities take place parallel to the earthquake zones, and their width reaches more than 2,000 km (Fig. 1).

These facts show that the earthquake zones have come into existence under the con-

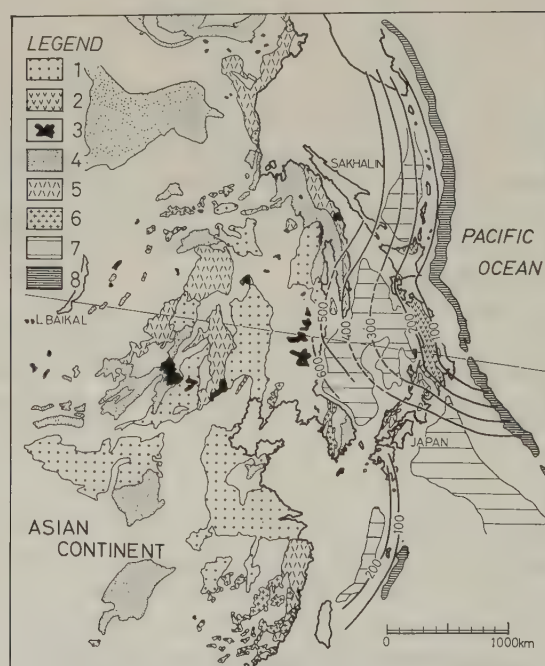


Fig. 1. The outline of geology of East Asia and the isobath lines of the intermediate and deep earthquake zone. 1, Tertiary and Quaternary basins; 2, Tertiary volcanics; 3, Tertiary and Quaternary alkali olivine basalts; 4, Mesozoic basins; 5, Mesozoic and Paleogene volcanics; 6, Mesozoic and Paleogene granites; 7, Marginal sea; 8, Trench.

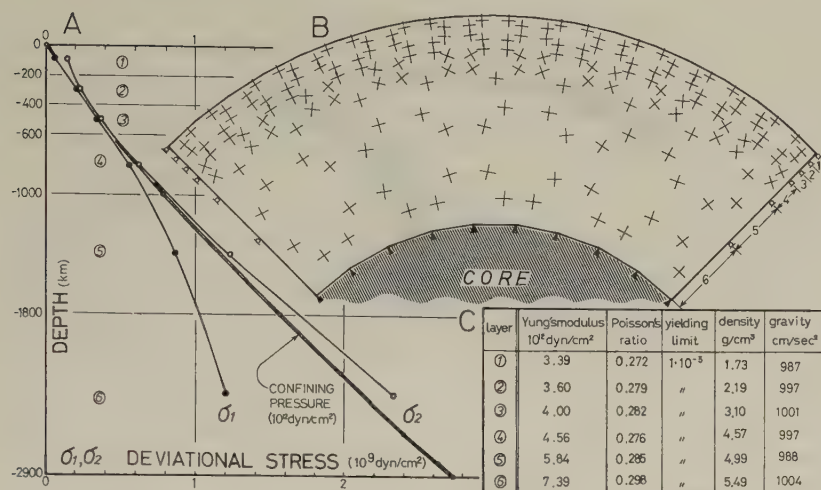


Fig. 2. The initial stress state under the gravity field. A, principal stress value; B, orientations of principal stress; C, physical parameters for layered earth, calculated after BULLEN (1965).

dition of uplift of the continent and subsidence of the ocean. The authors think that its great width is resulted from very deep process in the earth, so they tried to study the internal condition due to uplift and subsidence on the surface of the earth's core.

3. Tectonic Model

According to the geodynamic process mentioned above, the authors modelled crust and mantle by means of two-dimensional plane-strain finite element approximation. The model is perpendicular to the marginal tectonic zone of the Asiatic continent, and a quadrant of the earth with a depth of 2,900 km (Fig. 2).

The crust and mantle are divided into six layers, each of which is assumed to behave as perfect plastic material after a slight elastic deformation. Elastic parameters and yielding limits are given in the table of Fig. 2 after BULLEN (1965).

Non-tectonic initial stresses are obtained when all elements are deformed toward the earth's center by their own weight where displacements at the points on the core's surface are restricted to zero. The directions of maximum compressive stress are horizontal in the shallow part, but vertical in the deeper part of the mantle (Fig. 2). Though the magnitude of deviatoric stress is far less than that of confining pressure, it has important effect upon the applied tectonic stress distributions.

Various kind of vertical deformation are applied on the surface of the core according to the geodynamic process mentioned in the previous section.

4. Numerical Results

Figure 3 shows the deformation of the earth's surface when the surface of the core is displaced up to ± 8 km in vertical direction. Vertical displacement on the earth's surface reach ± 6 km and a wide flexural zone is formed in the mantle. It is noticeable that such

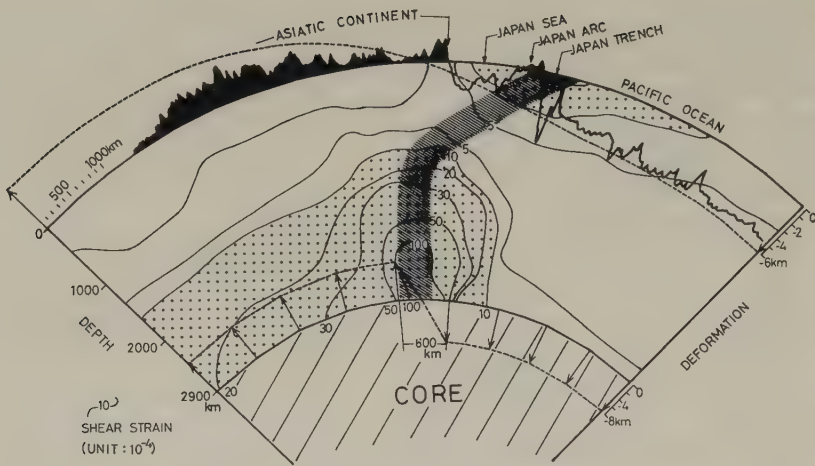


Fig. 3. Deformation and strain distributions.

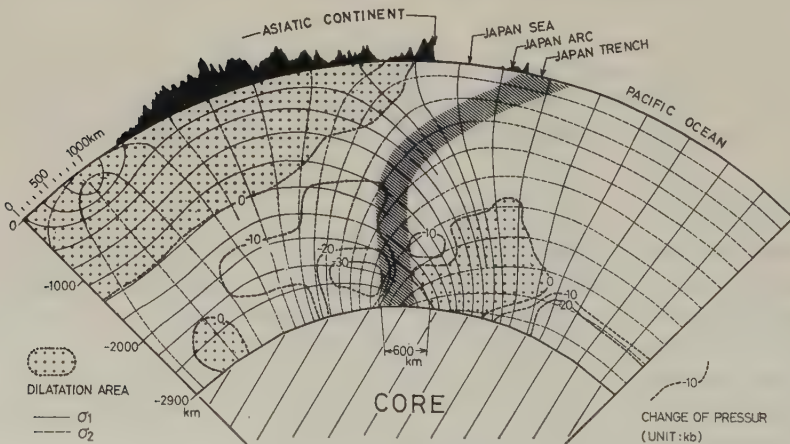


Fig. 4. Principal stress trajectories. Contour lines show the change of mean stress.

a slight displacement on the surface of core gives rise to considerable deformations in the mantle and on the earth's surface.

The distribution of shear strain is also shown in the figure. One of two maxima of shear strain occurs on the step of deformation of the core and the other around the upward concave hinge of the earth's surface, so a continuous shear concentrated zone is defined by connecting the greatest parts of shear strain at each depth (shaded zone in Fig. 3) as pointed out already in the previous paper (KODAMA and SUZUKI, 1977). This zone is nearly vertical in the lower mantle but gently inclined in the shallow part less than 1,000 km in depth. It might correspond to the intermediate and deep earthquake zone.

Three principal stresses are compressive, though the horizontal stresses are reduced near the surface of the uplifted region. Figure 4 shows that the maximum compressive

stresses are horizontal in the subsided region, vertical in the uplifted region, and inclined in the transitional region between them. The maximum compressive stress runs obliquely to the shear zone near the earth's surface, while they are inclined and parallel to the shear zone in the lower part more than 400 km deep. These stress distributions are compared with those deduced from P-wave radiation pattern under the Japanese Islands and their neighbours (ICHIKAWA, 1971).

The change of confining pressure is also shown in Fig. 4. It shows that the progress of vertical deformation is accompanied by the formation of dilatational area under the uplifted region, and increase of confining pressure under the subsiding region. When the surface of the core is uplifted +8 km, dilatational area reaches 1,500 km in depth and pressure decrease amounts to 5 kbar near the convex hinge of the earth's surface.

5. Discussions and Conclusions

As stated above, the strain and stress distribution in the uplifted region are in a striking contrast to those in the subsided area. The uplifted region is characterized by horizontal extension and release of confining pressure. These conditions might result in the formation of large graben and horst structures and intensive volcanic activities near the earth's surface. They are just the geologic phenomena in the marginal region of the Asiatic continent since the Mesozoic age. On the contrary, stable tectonics may be attributed to the increase of confining pressure throughout the subsided region as in the Pacific Ocean.

The topography of the transitional zone, which consists of marginal seas and island arcs, is too complicated to be compared with the corresponding part gently deformed on the model. It may be due to some shallower tectonic conditions caused by the deep process. Figure 5 shows a model in which the boundary displacements are applied at depth of 1,000 km and the width of flexural step is narrowed. Such flexural step may be expected within the shear concentrated zone in the former model at the advanced stage of core's deformation. It might be the case of local deformation such as the island arcs including the marginal sea.

KAULA (1969) showed a map of the earth's gravity anomalies based on a combination of satellite data and terrestrial gravimetry. He examined the relation between tectonic classification and main feature of the earth's gravity and pointed out that dominant gravity positive are markedly associated with recent geologic activity, especially in the trench and island arcs. Kaula considered that these global scale gravity variations were

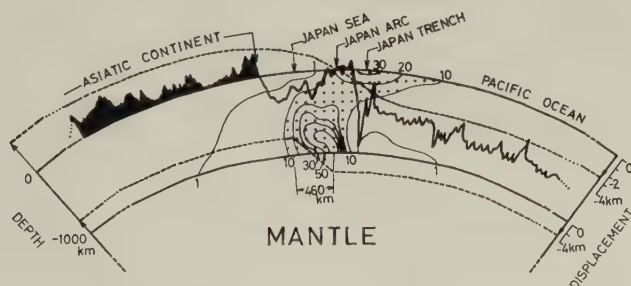


Fig. 5. A modified model to explain the formation of island arcs and marginal sea.

caused by upper mantle density variations which may be due to thermal expansion and contraction, or some lateral transfer of mantle material.

It is noticeable that mild but substantial positive anomalies distribute along the Circum Pacific orogenic belt and gravity deficiency appears in the north west or north east Pacific Ocean in the Kaula's map (Fig. 1 of KAULA, 1969). These worldwide gravity anomalies may be supposed to be caused by the tectonic deformations in the deep part of the lower mantle during long geologic period as the present model.

According to the model, the intermediate and deep earthquake zone correspond to a potential zone where shear strain is the highest at each depth and many fractures are expected to occur. NAGUMO (1972) discussed the high- Q , high- V properties of the deep seismic zone (UTSU, 1971) and explained them by the saturation of the pore/crack space by H_2O and/or magma. The presence of these conditions may be explained reasonably by the present model.

In this paper the authors propose a model in which the formation of intermediate and deep seismic zone and geodynamic process near the earth's surface are explained by simple vertical movement in the deep beneath the lower mantle. It is hoped that this somewhat tentative model will assist in more analytic interpretations of the tectonics of Japanese Islands and adjacent areas.

This paper lacks in the discussion of the cause of deformation of core-mantle boundary. Some convective current or thermal expansion in the outer core may be supposed to result in such boundary deformation, but precise discussions will be done when the relation between the deep tectonic process and surface geology or extent and magnitude of deep deformations are examined more distinctly for the future.

The authors express their sincere thanks to Prof. Yukinori Fujita, Niigata University and Prof. Shozaburo Nagumo, the Earthquake Research Institute, University of Tokyo for offering many valuable suggestions. They extend their thanks to Mrs. Kazunori Kobayashi and Masahiko Tsuboi for numerous calculating works.

REFERENCES

- BULLEN, K.E., *An Introduction to the Theory of Seismology*, 3rd ed., 381 pp., Cambridge University Press, London, 1965.
- ICHIKAWA, M., Reanalyses of mechanism of earthquakes which occurred in and near Japan, and statistical studies on the nodal plane solutions obtained 1926-1968, *Geophys. Mag.*, **35**, 207-274, 1971.
- KAULA, W.M., A tectonic classification of the main features of the earth's gravitational field, *J. Geophys. Res.*, **74**, 4807-4826, 1969.
- KODAMA, K. and Y. SUZUKI, Formation of the deep earthquake zone due to mantle diapirism, *Bull. Geol. Surv. Jpn.*, **28**, 795-810, 1977.
- MINATO, M., M. GORAI, and M. HUNAHASHI (eds.), *The Geologic Development of Japanese Islands*, 442 pp., Tsukiji-Shokan, Tokyo, 1965.
- NAGUMO, S., An interpretation of high- Q , high- V of deep seismic surface, in *Izu-Peninsula*, edited by M. Hoshino and H. Aoki, pp. 305-310, Tokai University Press, Tokyo, 1972.
- UTSU, T., Some characteristics of earthquake occurrence and anomalous structure of the upper mantle in Japan, in *Island Arcs and the Marginal Sea*, edited by S. Asano and G.B. Udintsev, pp. 201-214, Tokai University Press, Tokyo, 1971.

Subject Index

- Abyssal tholeiite, 65, 395
- Accretion, 1, 2, 5, 13, 14, 15, 16
 - accretionary bulge, 262
 - accretionary fold belt, 321, 332
 - accretionary prism, 99, 181, 182, 184
 - accretionary sedimentary wedge, 260
 - continental accretion, 25
- AFM diagram, 131, 134
- Arc-junction, 467, 469, 471, 472, 488
- Arc-arc junction, 69, 70, 73, 74, 76, 77, 78, 80
- Arc magmatism, 11, 12, 13
- Arc polarity reversal, 260
- Arc trench gap, 5, 334, 335, 444
- Arc trench system, 6, 7, 10, 16, 26, 419
- Arc volcanism, 412
- Aseismic belt, 438, 447, 448, 449, 451, 452, 453, 455, 456, 457
- Aseismic front, 437, 439, 440, 443, 447, 448, 452, 456
- Aseismic ridge, 49, 409, 416, 549
- Asthenosphere, 1, 5, 6, 7, 10, 11, 12, 21, 39, 42, 43, 44, 45, 55, 57, 58, 59, 60, 61, 62, 64, 65, 66, 104, 105, 110, 111, 112, 113, 115, 116, 118, 175, 176, 188, 374, 432
- Back-arc basin, 47, 117, 229, 374, 399, 478
- Back-arc belt (region), 433, 477, 488, 489
- Backarc behavior, 5, 7
- Back-arc opening, 51
- Back arc rifting, 31
- Back arc spreading, 5, 6, 12, 32, 42, 55, 56, 65, 66
- Back arc thrusting, 5, 6, 12
- Benioff zone, 39–54, 58, 61–64, 113, 115, 253, 273, 280, 293, 503, 513–523
- Biogeography, 33, 34
- Block faulting, 412
- Bouguer gravity anomaly, 226, 271, 309, 311, 494
- Bouyancy convection, 108, 110, 111, 117
- Bouyancy force, 103, 104
- Bouyancy stress, 118
- Bulge passage, 107
- Calc-alkalic rock series, 13, 508, 514
- Cascadia, 24
- Cascades volcanic arc, 11
- Cathaysian continent, 365
- Collision, 2, 31, 32, 76, 230, 231, 249, 260, 261, 270, 293, 296, 297, 322, 412, 415, 418, 488
 - collisional zone, 265, 417
 - collisional tectonics, 335
 - continental collision, 24, 26, 28, 32, 34, 35, 81
 - crustal collision, 14, 15, 16
- Compression, 62, 70, 72, 73, 74, 77, 81
 - compressional stress, 63, 64, 99, 138
 - compressional wave velocity, 437
 - compressive force, 80
 - compressive stress, 97
- Contourite, 487, 488
- Contraction, 57, 71, 72, 78
- Convection cell, 107, 109, 226
- Convective flow, 423, 432, 434
- Convergence, 105
 - converging rate, 418
 - converging subduction zone, 128
- Cordillera, 12
- Coseismic deformation, 382
- Co-tidal vorticity, 118
- Creep, 425
 - creep movement, 455
 - creep process, 428
 - creep rate, 429
- Crustal thickening, 5, 228
- Cratonic continental plate, 227
- Deep earthquake zone, 172
- Deep-sea drilling project (DSDP), 2, 398, 400
- Deep seismic sounding data, 509
- Dehydration, 57, 437, 438, 443
- Descending lithospheric slab, 400, 429, 431, 432, 467, 472
- Diastrophism, 12
- Differentiation (chemical differentiation), 56, 57, 59, 65, 118, 131, 137, 138
- Dip-angle (of the slab), 55, 59, 61
- Dipping plate, 181
- Dislocation climb process, 428
- Dislocation density, 423, 424, 427, 428, 434
- Dislocation structure, 425, 426
- Double arc, 234
- Double couple source mechanism, 240

- Double (Wadati-)Benioff (deep-seismic) zone, 55, 98, 440, 471
- Double zone, 42, 48
- Down-dip compression, 42, 150,
- Down-dip extension, 43, 48, 150
- Down-dip stress, 40, 41
- Downgoing (lithospheric) slab, 56, 59, 85, 104, 135, 459, 462, 463
- Driving force (of plate motion), 55, 56, 59, 60, 62, 63
- Elastic plate theory, 96
- Excess ^{40}Ar , 200
- Extensional stress field, 62, 64, 74, 76, 77, 78
- Fan-shooting, 315, 316
- Fault block, 99
- Fault Pattern, 85, 86, 87, 89
- Fault plane Solution, 73, 74, 75, 76, 81, 450
- First motion, 81, 82, 238
- Flow velocity, 431
- Flank eruption, 557
- Focal mechanism (solution), 39, 72, 75, 86, 89, 233, 234, 238, 243, 245, 249, 255, 280, 281, 285, 286, 453, 456, 471, 472
- Fossa Magna, 321, 324, 332, 334, 411, 412, 414, 415, 416, 417, 419, 541
- Fracture Zone, 123, 135, 396, 397
- Free-air gravity anomaly, 52, 57, 58, 64, 235, 238, 243, 245, 260, 295
- Frontal arc, 182, 438, 443, 450, 452
- Geodetic triangle, 72, 73
- Geoid, 103
- Geoidal high, 116
- Geomagnetic polarity, 369, 377
- Geosyncline, 503, 504, 505, 521
- Geosynclinal sediment, 31, 411
- Geotherm, 424
 - geothermal gradient, 334, 431
 - geothermometer, 425
- Gondwanaland, 2, 221
- Granitoid belt, 221, 222, 227
- Gravity anomaly, 59, 98, 103, 224, 225, 233, 241, 246, 270, 367, 443, 507
- Gravity-flow deposit, 488
- Gravity sliding fault, 291
- Gravitational differentiation, 60, 66
- Grey wacke, 509, 518, 519, 520
- Green tuff, 304, 545
- G-wave radiation pattern, 283
 - 178, 226, 262, 423, 429, 440, 442, 473, 500, 537
- High attenuation zone, 149
- High Q zone, 156
- Horst and graben structure, 99, 223, 262
- Hot spot, 1, 3, 8, 7, 367, 375, 395
- Hydrothermal solution, 223, 303
- Incipient spreading, 262
- Inclined seismic zone, 140, 156, 157, 175, 176, 179, 233, 246, 252
- In-situ* stress measurement, 72
- Interarc basin, 2, 5, 40, 48, 51, 52, 187, 391, 400
- Interarc spreading, 5, 41
- Interarc trough, 509, 519
- International Seismological Center (I.S.C.), 157
- Interval velocity, 495, 496, 497, 499
- Intra-oceanic arc, 5
- Intraplate deformation, 69, 76, 77, 80, 261, 266
- Intraplate earthquake, 72, 73, 75, 418, 437, 438, 456, 568
- Intraplate faulting, 418
- Island arc, 21, 34, 57, 59, 64, 65, 77, 99, 113, 115, 123, 135, 139, 140, 143, 151, 155, 156, 157, 170, 178, 181, 182, 189, 231, 234, 243, 244, 265, 270, 276, 296, 303, 334, 367, 368, 375, 379, 383, 388, 395, 423, 429, 430, 431, 432, 438, 443, 457, 473, 503, 506, 507, 509, 510, 512, 514, 515, 519, 520, 522, 547
- Island arc volcanism, 424, 432, 433, 434
- Isostasy, 60
 - isostatic adjustment, 52, 57, 59, 65
 - isostatic gravity anomaly, 52, 70
- Joides, 29
- K-Ar age, 199, 200
- Karig's process, 51, 417
- Klamaths, 24
- Kuno's variation diagram, 129
- Kuroko deposit, 375
- Kuroshio Paleoland, 363, 365
- LANDSAT, 268, 269
- Laramide orogeny (deformation), 12, 13, 14, 17
- Laurasia, 2
- Latent heat, 57
- Lithosphere, 1, 5, 6, 7, 10, 14, 21, 43, 44, 55, 56, 57, 59, 60, 62, 63, 64, 66, 85, 91, 98, 103, 104, 105, 110, 113, 115, 134, 135, 139, 149, 150, 156, 176, 178, 228, 233, 243, 244, 245, 246, 249, 250, 265, 296, 367, 373, 374, 400, 432, 455, 459, 462, 463, 464, 467, 471, 557, 559, 563, 568, 569
- Lithospheric slab, 139, 141, 149, 150, 151, 152,

- 157, 375, 376
 Llanoria, 24
 Low grade metamorphism, 126
 Low Q zone, 150, 178, 467, 473
 Low-Q and low-V mantle, 448, 456
 Low velocity channel, 155
 Low velocity layer (zone), 149, 150, 175, 176, 178
 Love number, 111
- Magma chamber (reservoir), 148, 557
 Magnetic anomaly, 33, 51, 57, 183, 187, 246, 270, 371, 374, 377, 391, 394, 395, 396, 398, 399, 400, 403, 405, 407, 492, 527, 529, 550
 Magnetic lineation, 88, 396, 399, 400, 403, 405, 406, 500, 545
 Magnetostratigraphy, 368, 370, 371, 377
 Mantle convection, 55
 Marginal (sea) basin, 1, 2, 5, 55, 56, 57, 59, 63, 64, 65, 66, 103, 113, 115, 116, 117, 118, 221, 223, 225, 226, 228, 231, 262, 322, 374, 492, 500, 520, 529, 533, 537
 Marine transgression, 297
 Melting point (temperature), 57, 151
 Mesosphere, 39, 42, 43, 48, 52
 Metamorphic complex, 355, 506
 Metamorphic grade, 351
 Metamorphism, 10, 31, 352, 353, 354, 412
 Microcontinent, 26
 Mid-ocean ridge, 55, 56, 57, 62, 64, 230, 391, 500
 Moho, 56, 148, 313, 431, 493, 494, 497, 498
 Moho interface, 491, 495, 500
- Negative bouyancy force, 61
 Normal fault, 282, 373, 440
 Normal fault solution, 285
 Normal faulting, 80, 244, 246, 249, 258, 259, 260, 262 290,
- Ocean-floor spreading, 64, 65, 377
 Oceanic crust, 55, 56, 57, 58, 59, 66, 137, 181, 189, 225, 437, 443, 530, 531
 Oceanic plateau, 549
 Off-ridge activity, 400
 Ophiolite, 243, 244
 Ophiolite belt, 223
 Orogeny, 57, 234, 265, 269, 270, 488, 489
 orogenic belt, 1, 2, 3, 29, 32, 34, 59, 64, 108, 334
 orogenic movement, 321, 322, 520, 523
 orogenesis, 112, 477
 Orthoquartzite, 363
 orthoquartzitic pebble, 339
 Outer rise, 86, 94
 Outer-topographic bulge, 89, 96, 97
- Outer-topographic high, 85, 89, 91, 97, 99, 463
 Outer-trench wall, 85, 86, 87, 89, 90, 93, 94, 97, 98
- P wave, 29, 140, 142, 143, 144, 145, 146, 148, 151, 156, 157, 158, 161, 162, 163, 168, 169, 171, 172, 173, 174, 176, 177, 179, 238, 256, 278, 318, 469, 473
 P_n arrival, 492, 493
 P_n velocity, 314, 491, 497, 500
 Pacifica, 21, 24, 26, 27, 28, 29, 30, 33, 34, 35
 Paired metamorphism, 335
 Paleocurrent, 412, 484, 487, 489
 Pal(a)eocontinental map, 195
 Pal(a)eolatitude, 2, 225, 226
 Paleomagnetic data, 26, 34, 203, 226, 230, 552
 Paleomagnetic direction, 25, 194, 211, 225, 530, 545
 Pal(a)eomagnetic pole, 191, 199, 204, 270
 Pal(a)eomagnetic south pole, 196, 197
 Paleopacific, 1, 2, 24
 Pang(a)ea, 1, 2, 3, 28, 31
 Panthalassa, 2
 Partial melting, 61, 115, 171, 431, 432, 474
 Partially molten liquid, 147, 178, 431, 432, 433, 434
 Peridotite xenoliths, 423, 424, 425, 428, 430
 Phase transformation, 62, 114, 177
 Picrite basalt, 123
 Plate,
 plate consumption, 31, 34, 249, 260, 261, 262
 plate convergence, 87, 253, 437, 441, 568
 plate edge, 69, 70, 77, 81
 plate motion, 39, 66, 80, 104, 244, 246, 324, 368, 376, 377, 414, 415, 502, 520, 538, 568, 569
 plate tectonics, 33, 55, 56, 62, 105, 123, 234, 321, 367, 447, 462, 464, 477, 503
 absolute motion of plate, 41, 44, 45, 49, 52
 break-up of plate, 399
 continental plate, 79, 80, 81, 115
 lithospheric plate, 85, 95, 375
 oceanic plate, 77, 86, 87, 88, 89, 91, 98, 115, 333, 367, 368, 415, 417, 423, 428, 455, 456, 523, 533, 549
 Plateau-basalt, 516, 518, 520, 523
 Polar wandering, 197
 Polarity time scale, 395
 Polarity zone, 210
 Pole position, 203, 204, 206, 209, 210, 369
 Pore pressure, 437, 438, 441, 442, 443, 444, 557
 Post-spreading intrusion, 398, 400
 Pulse, 549
- Rayleigh wave, 313

- Remanent magnetization, 368, 369
- Remnant arc, 55, 64
- Retroarc foreland basin, 5
- Reverse fault, 414
- Reverse faulting, 249, 260
- Reversed magnetic epoch, 197
- Reversed magnetization, 191, 210
- Reversed polarity, 209, 368, 396
- Rheology, 85
 - rheological property, 55
- Ridge consumption, 32
- Ridge push, 59, 60, 61, 62, 64, 66
- Rift valley, 234
- Rifting, 24, 32
- Rise trench encounter, 10, 12, 17
- Rotational strain, 105, 106
- Rotating bulge stress, 119
- S seismic wave, 149
- S terrace, 379, 380, 381, 382
- S velocity, 149
- S wave, 139, 140, 142, 143, 144, 145, 146, 148, 149,
 - 150, 151, 156, 157, 158, 162, 163, 168, 170,
 - 172, 173, 174, 175, 176, 178, 179, 255, 256,
 - 318, 319, 467, 473
- Seafloor spreading, 3, 9, 56, 103, 105, 113, 115,
 - 116, 117, 118, 119, 137, 527, 533
- Seamount, 392, 393, 395, 396, 398, 400, 406, 407
- Seamount chain, 549, 550
- Second layer, 273
- Secular variation, 209
- Sedimentation, 135, 234
- Sedimentation rate, 367, 371, 373, 376, 478
- Sedimentary arc, 235, 236, 240, 241, 243
- Sedimentary basin, 270
- Sedimentary wedge, 249
- Seismic activity, 150, 151, 437
- Seismic deformation area, 386, 388
- Seismic prism, 437, 439, 440
- Seismic reflection profiling, 392, 393, 492, 545
- Seismicity, 113, 134, 233, 234, 236, 244, 245, 250,
 - 276, 280, 293
- Shadow zone, 149
- Shear strain, 73, 77
- Shearing force, 80
- Shoreline, 379, 380, 381, 383
- Slip vector, 250, 269
- Slumping, 99
- Sonoma orogeny, 15, 24
- Spinel lherzolite xenoliths, 425, 428, 430, 434
- Spreading, 24, 31, 42, 138, 418, 419
 - spreading axis, 226, 229
 - spreading center, 2, 12, 28, 29, 33, 66, 116, 117,
 - 417, 549
 - spreading process, 500
 - spreading rate, 397, 398, 399, 400
 - spreading ridge, 27
 - jump of spreading axis, 400
 - symmetric spreading, 395, 398
- State of stress, 72, 74, 80, 81
- Strain rate, 428, 429, 431, 432
- Strike-slip fault, 284, 285, 293, 537, 538
- Strike-slip faulting, 246, 249, 259, 282
- Strike-slip mechanism, 233
- Strike-slip motion, 441, 442, 444
- Strike-slip sliding instability, 438
- Subduction, 74, 85, 86, 103, 114, 118, 135, 137,
 - 181, 227, 228, 229, 231, 233, 246, 249, 253,
 - 262, 266, 270, 293, 295, 296, 297, 321, 322,
 - 333, 367, 368, 373, 376, 400, 409, 411, 447,
 - 454, 455, 456, 457, 462, 463, 464, 533, 537,
 - 549, 551
- subduction jump, 14, 16
- subduction-related magmatism, 227
- subduction slab, 11, 61
- subduction zone, 12, 28, 39, 41, 42, 45, 88, 89,
 - 98, 99, 104, 105, 123, 131, 134, 182, 244, 250,
 - 252, 256, 258, 260, 261, 265, 294, 354, 416,
 - 417, 418, 459, 550, 557
- subducting lithosphere, 245, 440
- subducting oceanic crust, 63, 423, 438, 444
- subducting plate, 12, 89, 93, 95, 98, 99, 374,
 - 423, 441
- subducting slab, 265, 437, 441, 443
- subducted plate, 12
- subducted slab, 61, 375
- Submarine volcanism, 246
- Submerged platform, 34
- Suture, 223
- Suture belt, 3, 16, 17
- Suturing, 1, 2
- Tectonic erosion, 416
- Tectonic movement, 203, 204, 211
- Tectonic rotation, 209
- Tectonic stress, 73
- Tensile stress, 457
- Tensional stress, 99
- Thermal bouyancy, 118, 119
- Thermal conductivity, 431
- Thermal convection, 103, 104, 109, 118
- Thermal structure, 350, 351, 352, 353, 354
- Thrust fault, 282, 347, 414, 440, 443
- Thrust faulting, 42, 233, 244
- Thrust-type earthquake, 39, 47
- Thrusting, 246
- Tibet-Himalaya-India orogen, 26

- Tidal bulge, 103, 105, 108
- Tidal bulge passage, 105, 108, 116, 117
- Tidal dissipation, 119
- Tidal dissipation rate, 112
- Tidal vorticity induction, 10, 115, 116
- Time term, 493, 494, 497
- Tin-bearing granite magma, 231
- Tin granitoid, 221, 222
- Topographic bulge, 260
- Transform belt, 261
- Transform fault, 26, 81, 399, 400, 409, 415, 416, 418, 537, 549, 550, 551
- Transition layer, 273
- Travel time, 139, 142, 155, 156, 157, 158, 179, 317, 318, 493, 494, 496, 497, 499
- Travel time curve, 142, 143, 161, 162, 163, 168
- Travel time residual, 178
- Trench, 3, 5, 12, 31, 32, 123
- Trench arc system, 55, 56, 57, 58, 63, 64, 66, 437, 438, 440
- Trench jump, 31, 32
- Trench pull, 59, 62, 66
- Trench slope break, 182
- Trenchline, 39, 40, 42, 43, 44, 47, 49
- Triangulation, 71
- Triple junction, 11, 12, 312, 334, 409, 418, 467
- Tsunami, 459, 462, 464
- Tsunami energy, 463
- Tsunamicity, 333, 459
- Turbidite, 342, 363, 549
- Turbidity current, 340, 477, 487, 488
- Unbending, 48
- Underthrust lithosphere, 178
- Underthrusting, 182, 260, 455
- Underthrusting plate, 195
- Upper mantle, 492, 494, 498, 499, 500
- Velocity anomaly, 151, 173, 178
- Velocity anisotropy, 491, 497, 498, 499, 500
- Velocity discontinuity, 177, 179
- Velocity function, 143, 144, 147, 148, 151, 155, 156, 163, 168, 174, 176
- Velocity structure, 29, 142, 146, 155, 156, 157, 169, 174, 273, 440, 444
- Volatile component, 433
- Volcanic activity, 58, 65, 123, 234
- Volcanic arc, 230, 233, 235, 237, 245, 450, 452, 457
- Volcanic belt, 503, 504, 516, 523
- Volcanic chain, 11
- Volcanic front, 314, 433, 434, 437, 438, 439, 441, 447, 449, 452, 457
- Volcanic island, 181
- Volcaniclastic sediment, 412
- Volcanism, 31, 125, 126, 136, 137, 148, 151
- Volcano-plutonic arc, 221, 222, 226, 230
- Vorticity, 105, 106, 118
- Wadati-Benioff zone, 77, 81, 367, 374, 375, 440, 441, 447, 452, 457
- Westward lithosphere motion, 118

Geographical Index

- Aira caldera, 309, 316, 318, 319
- Alaska-Bering-Yakutia-region, 3, 16
- Aleutian arc, 1, 13, 81
- Aleutian Ridge, 9, 10, 14
- Aleutian trench, 10
- Amami plateau, 405, 406, 407
- Andaman Sea, 224, 229, 230, 233, 234, 237, 238, 239, 240, 241, 243, 245, 246, 247
- Arctic Ocean, 1, 3
- Atlomic Ridge, 115
- Baja California, 203, 204, 205
- Banda Arc, 191, 192, 195, 196, 197
- Basin-and-Range Province, 9, 11, 12
- Bering Sea, 13
- Bering shelf, 1
- Bonin island, 58, 417
- Bonin-Mariana Arc, 367, 373, 375
- Central America, 1
- Central Basin Fault, 285
- Cordilleras, 1, 14, 15, 16
- Daito ridge, 405, 406
- East Pacific Rise, 105, 115, 116
- Emperor-Hawaii elbow, 14
- Emperor-Seamount chain, 1, 3, 7
- Fiji island, 156
- Fiji plateau, 51, 149
- South Fiji Basin, 51
- North Fiji plateau, 123, 128, 134, 137, 181
- Hawaii Ridge, 3, 7
- Hidaka Trough, 488
- Himalaya, 80, 81
- Itogawa-shizuoka tectonic line, 414
- Izu-Bonin arc, 409, 415, 417, 418
- Izu-Bonin Mariana Arc, 46, 377
- Japan Izu Bonin arc, 412
- Izu-Bonin arc trench system, 416
- Izu-Bonin trench, 418
- Izu-Bonin ridge, 419
- Izu Mariana arc, 13, 14, 414
- Izu Peninsula, 409, 411, 412
- Japan Arc, 80, 321, 322, 324, 332, 334, 368, 371, 373, 374, 376, 382, 385, 387, 388, 409, 416, 423, 425, 430, 433, 492, 497, 499, 500, 506, 522, 537, 538, 545, 546, 548, 549
- Japan Basin, 541
- Japan Sea (also see Sea of Japan), 416, 439, 450, 530, 531, 537, 538, 541, 543, 544, 545, 546, 547, 548, 549
- Japan trench, 371, 387, 388, 416, 447, 448, 449, 471, 492, 559
- Java Trench, 234
- Kamchatka arc, 13, 14, 80
- Kamchatka basin, 80
- Kuril Island, 81, 509
- Kuril-Kamchatka arc, 13
- Kurosegawa tectonic zone, 343
- Kuroshio paleoland, 344
- Kyushu-Palau Ridge (Palau-Kyushu), 9, 392, 417, 549, 550
- Lau basin, 149, 178
- Lau-Havre basin, 51
- Malay Peninsula, 223, 225, 228, 230, 243
- Mariana arc, 39, 48, 51, 58, 375
- Mariana trench, 276, 285, 293, 295
- Mariana trough, 51, 400
- Median (Tectonic) Line, 322, 346, 354
- Mexican volcanic belt, 203, 205, 206, 209, 210, 211
- Nankai Trough, 379, 399, 417, 418
- New Caledonia, 146
- New Hebrides, 123, 125, 126, 137, 138, 139, 140, 141, 142, 143, 147, 148, 149, 150, 151, 152, 155, 169, 170, 171, 174, 181, 182, 185, 187, 188, 189
- North Loyalty plateau, 181, 183, 184
- Okhotsk block, 14, 16, 17
- Okhotsk Sea (also see Sea of Okhotsk),
- Okinawa trough, 293, 301, 305, 527, 531
- Ontong-Java platform, 29

- Parece Vela Basin, 392, 398, 399
Philippine, 249, 250, 252, 253, 258
 Philippine block, 252, 256, 258, 260
 Philippine Sea, 1, 9, 14, 39, 41, 45, 47, 48, 116,
 249, 250, 258, 270, 293, 294, 297, 321, 334,
 335, 357, 364, 365, 391, 403, 409, 411, 415, 418,
 467, 558, 567
Ryukyu, 301, 302, 303, 304, 305, 306
Ryukyu Trench, 305
Sagami trough, 411, 414, 418, 567
Sakhalin, 9, 13
Sakurajima Volcano, 309, 316, 318, 319
San Andreas fault, 9, 11, 12, 26, 438
Sanbagawa, 345, 346, 347, 349, 350, 352, 354, 355
Sea of Japan, 4, 9, 116, 491, 492, 493, 494, 498,
 499, 500, 529
Sea of Okhotsk, 4, 13, 116, 503, 506, 516, 527,
 530, 531
Shikoku Basin, 391, 392, 394, 395, 396, 398, 399,
 400, 403, 406, 417, 418, 419
Shimanto (Simanto), 321, 324, 332, 334, 335, 360,
 361, 363
 Shimanto Belt, 13, 257, 414
 Shimanto supergroup, 303, 306
 Shimanto zone, 411
Solomon Island, 123, 124, 138, 149
Suruga trough, 411
Taiwan, 249, 250, 258, 261, 265, 266, 267, 269,
 270, 271, 273, 276, 281, 282, 286, 287, 288,
 289, 290, 291, 293, 295, 296, 297, 303, 306
Tamba Belt, 337, 339, 341
Tamba Group, 343
Tethys Sea, 3, 221
Tonga island, 150, 452
Tonga-Fiji-Kermadec region, 151
Tonga-Kermadec island arc, 49, 155, 156, 157,
 158, 168, 172
Tonga-Kermadec-New Zealand region, 146, 147,
 151, 155, 157, 169, 170, 171, 172, 174, 176,
 177, 178, 179
Torres Trench, 126, 128, 129, 134, 135, 136, 137
Vitiaz Trench, 126, 128, 131, 137, 138
Western Cordillera, 203, 205, 209, 211
Yamato Ridge, 537, 544, 547, 548, 549

AEPS Vol. 1

Special Issue of Journal of Geomagnetism and Geoelectricity (Included in regular issues)

Proceedings of AGU 1976 Fall Annual Meeting, December 1976, San Francisco

ORIGIN OF THERMOREMANENT MAGNETIZATION

Edited by David J. DUNLOP

Contents TRM and Its Variation with Grain Size: A Review (R. DAY)/Single Domain Oxide Particles as a Source of Thermoremanent Magnetization (M.E. EVANS)/Domain Structure of Titanomagnetites and Its Variation with Temperature (H.C. SOFFEL)/The Demagnetization Field of Multidomain Grains (R.T. MERRILL)/The Hunting of the 'Psark' (D.J. DUNLOP)/On the Origin of Stable Remanence in Pseudo-Single Domain Grains (S.K. BANERJEE)/The Preparation, Characterization and Magnetic Properties of Synthetic Analogues of Some Carriers of the Palaeomagnetic Record (J.B. O'DONOVAN and W. O'REILLY)/Reduction of Hematite to Magnetite under Natural and Laboratory Conditions (P.N. SHIVE and J.F. DIEHL)/Characteristics of First Order Shock Induced Magnetic Transitions in Iron and Discrimination from TRM (P. WASILEWSKI)/The Thermoremanence Hypothesis and the Origin of Magnetization in Iron Meteorites (A. BRECHER and L. ALBRIGHT)/Thermal Overprinting of Natural Remanent Magnetization and K/Ar Ages in Metamorphic Rocks (K.L. BUCHAN, G.W. BERGER, M.O. MCWILLIAMS, D. YORK, and D.J. DUNLOP)/Does TRM Occur in Oceanic Layer 2 Basalts? (J.M. HALL)/The Effects of Alteration on the Natural Remanent Magnetization of Three Ophiolite Complexes: Possible Implications for the Oceanic Crust (S. LEVI and S.K. BANERJEE)

212pp. (7 × 10) 1977 \$24.50

AEPS Vol. 2

Supplement Issue of Journal of Physics of the Earth (Not included in regular issues)

Proceedings of the U.S. -Japan Seminar on Theoretical and Experimental Investigations of Earthquake Precursors

EARTHQUAKE PRECURSORS

Edited by C. KISSLINGER and Z. SUZUKI

Contents Earthquake Prediction-Related Research at the Seismological Laboratory, California Institute of Technology, 1974-1976 (J.H. WHITCOMB)/Research on Earthquake Prediction and Related Areas at Columbia University (L.R. SYKES)/Seismic Activities and Crustal Movements the Yamasaki Fault and Surrounding Regions in the Southwest Japan (K. OIKE)/The New Madrid Seismic Zone as a Laboratory for Earthquake Prediction Research (B.J. MITCHELL, W. STAUDER, and C.C. CHENG)/Anomalous Crustal Activity in the Izu Peninsula, Central Honshu (K. TSUMURA)/Recent Seismometrical Works in Japan (S. SUYEHIRO, M. ICHIKAWA, and K. TSUMURA)/Quiet and Violence in Horizontal Movement of the Crust (T. HARADA)/Anomalous Seismic Activity and Earthquake Prediction (H. SEKIYA)/Seismic Activity in the Northeastern Japan Arc (A. TAKAGI, A. HASEGAWA, and N. UMINO)/Observations of Changes in Seismic Wave Velocity in South Kanto District, South of Tokyo, by the Explosion-Seismic Method (T. KAKIMI and I. HASEGAWA)/Some Precursors Prior to Recent Great Earthquakes along the Nankai Trough (H. SATO)/Possibility of Temporal Variations in Earth Tidal Strain Amplitudes Associated with Major Earthquakes (T. MIKUMO, M. KATO, H. DOI, Y. WADA, T. TANAKA, R. SHICHI, and A. YAMAMOTO)/Gravity Changes Associated with Seismic Activities (Y. HAGIWARA)/Geomagnetism in Relation to Tectonic Activities of the Earth's Crust in Japan (N. SUMITOMO)/

Precursory and Coseismic Changes in Ground Resistivity (T. RIKITAKE and Y. YAMAZAKI)/
 Geochemistry as a Tool for Earthquake Prediction (H. WAKITA)/Recent Laboratory
 Studies of Earthquake Mechanics and Prediction (W.F. BRACE)/Dilatancy of Rocks under
 General Triaxial Stress States with Special Reference to Earthquake Precursors (K. MOGI)/
 Possibility of a Great Earthquake in the Tokai District, Central Japan (T. UTSU)/Depth
 Constraints on Dilatancy Induced Velocity Anomalies (K.W. WINKER and A. NUR)/
 Seismological Precursors to a Magnitude 5 Earthquake in the Central Aleutian Islands
 (E.R. ENGDAHL and C. KISSLINGER)/Estimation of Future Destructive Earthquakes from
 Active Faults on Land in Japan (T. MATSUDA)/Some Problems in the Prediction of the
 Nemuro-oki Earthquake (K. ABE)/Responses to Earthquake Prediction in Kawasaki City,
 Japan in 1974 (H. OHTA and K. ABE)/Socioeconomic and Political Consequences of
 Earthquake Prediction (J.E. HAAS and D.S. MILETI)

304 pp. (7×10) 1978 \$32.50

AEPS Vol. 3

Proceedings of the U.S. -Japan Seminar on Rare Gas Abundance and Isotopic Constraints
 on the Origin and Evolution of the Earth's Atmosphere

TERRESTRIAL RARE GASES

Edited by E.C. ALEXANDER, Jr. and M. OZIMA

Contents *EXPERIMENTAL STUDIES* A Mantle Helium Component in Circum-
 Pacific Volcanic Gases: Hakone, the Marianas, and Mt. Lassen (H. CRAIG, J.E. LUPTON,
 and Y. HORIBE)/Nitrogen to Argon Ratio in Volcanic Gases (S. MATSUO, M. SUZUKI, and
 Y. MIZUTANI)/Rare Gas Abundance Pattern of Fumarolic Gases in Japanese Volcanic
 Areas (O. MATSUBAYASHI, S. MATSUO, I. KANEOKA, and M. OZIMA)/A Review: Some
 Recent Advances in Isotope Geochemistry of Light Rare Gases (I.N. TOLSTIKHIN)/Abun-
 dances and Isotopic Compositions of Rare Gases in Granites and Thucholites (P.K.
 KURODA and R.D. SHERRILL)/Rare Gas Isotopic Compositions in Diamonds (N. TAKAOKA
 and M. OZIMA)/Rare Gases in Mantle-Derived Rocks and Minerals (I. KANEOKA, N.
 TAKAOKA, and K. AOKI)/A Comparison of Terrestrial and Meteoritic Noble Gases (O.K.
 MANUEL)/The Composition and History of the Martian Atmosphere (T. OWEN) *THE-*
ORETICAL STUDIES Nuclear Components in the Atmosphere (T.J. BERNATOWICZ
 and F.A. PODOSEK)/Trapped Xenon and Cosmic-Ray Effects in Meteorites, in Lunar
 Sample, and in the Earth's Materials (K. SAKAMOTO)/Classification and Generation of
 Terrestrial Rare Gases (K. SAITO)/Earth-Atmosphere Evolution Model Based on Ar
 Isotopic Data (Y. HAMANO and M. OZIMA)/Terrestrial Potassium and Argon Abundances
 as Limits to Models of Atmospheric Evolution (D.E. FISHER)/On the Ambient Mantle
⁴He/⁴⁰Ar Ratio and the Coherent Model of Degassing of the Earth (D.W. SCHWARTMAN)/
 Earth Degassing Models, and the Heterogenous vs. Homogeneous Mantle (R. HART and
 L. HOGAN)/Lead Isotope Constraints on the Early History of the Earth (R.D. RUSSELL)/
 Matter Accretion into the Solar System (S. HAYAKAWA)

230 pp. (7×10) 1978 \$24.50

AEPS Vol. 4

Special Issue of Journal of Geomagnetism and Geoelectricity

Proceedings of IAGA/IAMAP Joint Assembly, August 1977, Seattle, Washington

AURORAL PROCESSES

Edited by C.T. RUSSELL

Contents *TIMING OF SUBSTORM EVENTS* Pi 2 Micropulsations as Indicators of Substorm Onsets and Intensifications (G. ROSTOKER and J.V. OLSON)/The Use of Ground Magnetograms to Time the Onset of Magnetospheric Substorms (R.L. MCPHERRON)/Substorm Onset in the Magnetotail (A. NISHIDA) *ELECTROMAGNETIC AND ELECTROSTATIC INSTABILITIES ON AURORAL FIELD LINES* A Review of Electrostatic Wave Measurements on Auroral Magnetic Field Lines (M.C. KELLEY)/Diffuse Auroral Precipitation (M. ASHOUR-ABDALLA and C.F. KENNEL)/Electromagnetic Plasma Wave Emissions from the Auroral Field Lines (D.A. GURNETT)/Theory of Electromagnetic Waves on Auroral Field Lines (J.E. MAGGS) *RAPID AURORAL FLUCTUATIONS AND ASSOCIATED PHENOMENON* Observations of Rapid Auroral Fluctuations (T. OGUTI)/Highlights in the Studies of the Relationship of Geomagnetic Field Changes to Auroral Luminosity (W.H. CAMPBELL)/Microburst Precipitation Phenomena (G.K. PAAKS) *MECHANISMS FOR THE FORMATION OF AURORAL STRUCTURE* Observed Microstructure of Auroral Forms (T.N. DAVIS)/Birkeland Currents and Auroral Structure (H.R. ANDERSON)/Relationships between Particle Precipitation and Auroral Forms (J.L. BURCH and J.D. WINNINGHAM)/Photometric Investigation of Precipitating Particle Dynamics (S.B. MENDE)/Generation Mechanisms for Magnetic-Field-Aligned Electric Fields in the Magnetosphere (C.-G. FÄLTHAMMAR)/Review of Auroral Currents and Auroral Arcs (G. ATKINSON)/Acceleration Mechanisms for Auroral Electrons (D.W. SWIFT) Subject Index

280 pp. (7 × 10) 1979 \$ 32.50

AEPS Vol. 5

Special Issue of Journal of Geomagnetism and Geoelectricity

Proceedings of IAGA/IAMAP Joint Assembly, August 1977, Seattle, Washington

TECTONOMAGNETICS AND LOCAL GEOMAGNETIC FIELD VARIATIONS

Edited by M. FULLER, M.J.S. JOHNSTON, and T. YUKUTAKE

Contents Symposium on Tectonomagnetics and Small Scale Secular Variations Held at the IAGA/IAMAP Joint Assembly at Seattle on Tuesday, August 22nd, 1977 (V.A. SHAPIRO and M.J.S. JOHNSTON) / Tectonomagnetic Studies in Tajikistan (Yu. P. SKOVORODKIN, L.S. BEZUGLAYA, and T.V. GUSEVA)/An Attempt to Observe a Seismomagnetic Effect during the Gazly 17th May 1976 Earthquake (V.A. SHAPIRO and K.N. ABDULLABEKOV)/Secular Variation Anomalies and Aseismic Geodynamic in the Urals (V.A. SHAPIRO, A.L. ALEINKOV, A.A. NULMAN, V.A. PYANKOV, and A.V. ZUBKOV)/Geomagnetic Investigations in the Seismoactive Regions of Middle Asia (V.A. SHAPIRO, A.N. PUSHKOV, K.N. ABDULLABEKOV, E.B. BERDALIEV, and M.Yu. MUMINOV)/Local Magnetic Field Variations and Stress Changes Near a Slip Discontinuity on the San Andreas Fault (M.J.S. JOHNSTON)/Geomagnetic Secular Variation Anomalies in the GDR (W. MUNDT)/Noise Reduction Techniques for Use in Determining Local Geomagnetic Field Changes (R.H. WARE and P.L. BENDER)/Local Variations in Magnetic Field, Long-Term Changes in Creep Rate, and Local Earthquakes along the San Andreas Fault in Central California (B.E. SMITH, M.J.S. JOHNSTON, and R.O. BURFORD)/Geomagnetic Induction Study of the Seismically Active Fault along the Southwestern Coast of the Sea of Japan (J. MIYAKOSHI and A. SUZUKI)/Time Dependence of Magnetotelluric Fields in a Tectonically Active Region in Eastern Canada (R.D. KURTZ and E.R. NIBLETT)/Piezomagnetic Response with Depth, Related to Tectonomagnetism as an Earthquake Precursor (R.S. CARMICHAEL)/Magnetic Susceptibility of Magnetite under Hydrostatic Pressure, and Implications for

Tectonomagnetism (A.A. NULMAN, V.A. SHAPIRO, S.I. MAKSIMOVSKIKH, N.A. IVANOV, J. KIM, and R.S. CARMICHAEL)/Effect of Uniaxial Stress upon Remanent Magnetization: Stress Cycling and Domain State Dependence (J. REVOL, R. DAY, and M. FULLER)/On the Measurement of Stress Sensitivity of NRM Using a Cryogenic Magnetometer (T.L. HENYEY, S.J. PIKE, and D.F. PALMER)

150 pp. (7 × 10) 1979 \$ 22.50







W8-BWD-302

